British Journal of Pharmacology

January 1995

Volume 114 Number 2 pages 257–562

British Journal of Pharmacology (1995) 114, 257-258 © 1995 Stockton Press All rights reserved 0007-1188/95 $9.00

SPECIAL REPORT

Increased striatal dopamine efflux *in vivo* following inhibition of cerebral nitric oxide synthase by the novel monosodium salt of 7-nitro indazole

M.T. Silva, S. Rose, J.G. Hindmarsh, G. Aislaitner, J.W. Gorrod, P.K. Moore, [1]P. Jenner & C.D. Marsden

Neurodegenerative Diseases Research Centre, Pharmacology Group, Biomedical Sciences Division, King's College London, Manresa Road, London

The role of nitric oxide (NO) in striatal dopamine release has been controversial. Most NO synthase inhibitors affect more than one isoform of the enzyme and exert vasoconstrictor effects which may also affect striatal dopamine function. We now report on the effect of a soluble monosodium salt of the selective brain NO synthase inhibitor 7-nitro indazole (7-NINA). Using 7-NINA the first study of selective inhibition of the brain isoform of NO synthase on dopamine efflux in rat striatum was undertaken by use of *in vivo* microdialysis. Perfusion with 7-NINA (1 mM) increased striatal dopamine efflux. The effect of 7-NINA was partially antagonized (67%) by co-perfusion with L-arginine (1 mM), the precursor of NO formation *in vivo*. This suggests that 7-NINA induces a competitive inhibition of NO synthase activity. These data show that endogenous NO has an inhibitory effect on striatal dopamine efflux *in vivo*.

Keywords: Nitric oxide synthase; dopamine; microdialysis; 7-nitro indazole; striatum; L-arginine

Introduction Nitric oxide (NO) acts as a neuromodulator in the brain and functions as a retrograde neuronal messenger following N-methyl-D-aspartate (NMDA) receptor stimulation (Hanbauer *et al.*, 1992; Lei *et al.*, 1992). In this capacity, NO may mediate cortico-striatal glutamatergic modulation of striatal dopamine release (Rose *et al.*, 1994a). However, there is confusion over the manner in which NO modulates dopamine release. *In vitro* studies using tissue slices have shown NO to increase dopamine efflux in the striatum (Lonart *et al.*, 1993), whereas *in vivo* microdialysis studies using NO synthase inhibitors or exogenous NO suggest the opposite to be true (Guevara-Guzman *et al.*, 1994; Rose *et al.*, 1994b).

The use of NO donors such as S-nitroso-*N*-acetylpenicillamine, S-nitrosoglutathione and sodium nitroprusside in brain is limited as the carrier molecules (penicillamine, glutathione and ferricyanide respectively) alter striatal neurotransmitter release *in vivo* (Guevara-Guzman *et al.*, 1994). Similarly, the use of NO synthase inhibitors in brain is complicated by their effect on peripheral and cerebral blood flow.

Recently, Moore and colleagues (1993) reported inhibition of neuronal NO synthase activity by 7-nitro indazole (7-NI) with no effect on mean arterial blood pressure. This suggests that 7-NI is a selective inhibitor of neuronal NO synthase so providing a tool with which to study the effects of NO in brain. However, until now the insolubility of 7-NI at concentrations above 100 μM in physiological media has precluded its use in *in vivo* studies of neurotransmitter release. For this reason, we report on the preparation of a more soluble monosodium salt of 7-NI, termed 7-NINA, and on the effect of selective inhibition of brain NO synthase on striatal dopamine release.

Methods *Preparation of monosodium salt of 7-nitroindazole (7-NINA)* 7-NI (1.625 mmol; Lancaster Synthesis Ltd, Morecambe, UK) was dissolved in 20 ml of methanol:chloroform (3:1 v:v). To this was added 3.385 ml of 0.48 M sodium hydroxide (1.625 mmol). The colour of the solution changed immediately from yellow to red. The red solution was evaporated to dryness in a rotary film evaporator at 35°C under reduced pressure. The red solid formed was dissolved in the minimum amount of methanol, filtered and again evaporated to remove water. This procedure was repeated once more with methanol and then twice with diethyl ether. Structure and purity was determined by thin layer chromatography, nuclear magnetic resonance and mass spectroscopy. The resulting salt was shown to be the monosodium salt of 7-NI and the solid was determined to be 96% pure. 7-NINA was prepared freshly every two weeks and stored in a dessicator at 4°C.

Microdialysis procedure Male Wistar rats (280-320 g, Bantin and Kingman, Hull, UK) were anaesthetized with chloral hydrate (500 mg kg^{-1}, i.p.) and anaesthesia was maintained throughout the experiment. Microdialysis probes (3 mm membrane; Hospal AN 69 HF) were implanted into the striatum by standard stereotaxic techniques (coordinates A + 2 mm, L + 3 mm from bregma and V-6.5 mm from dura; Pelligrino *et al.*, 1979). Body temperature was maintained at 37°C with a homeothermic blanket (Harvard Apparatus Ltd, Watford, UK). The microdialysis probes were continuously perfused with artificial CSF (composition, mM: NaCl 138, KCl 5, $CaCl_2$ 1.2, NaH_2PO_4 1, $NaHCO_3$ 10; pH 7.5) at a rate of 2 μl min^{-1}. At least 1 h following implantation, 10 min fractions of dialysate (20 μl) were collected into 0.25 M acetic acid (25 μl). Following a 1 h period to determine basal dopamine efflux, 7-NINA (1 mM), L-arginine (1 mM), or a combination of 7-NINA (1 mM) and L-arginine (1 mM) were included into the artificial CSF for a period of 90 min. Control animals were perfused continuously with artificial CSF. Dialysate samples were analysed for levels of dopamine, 3,4-dihydroxyphenylacetic acid (DOPAC) and homovanillic acid (HVA) by high performance liquid chromatography (h.p.l.c.) with electrochemical detection.

Results Perfusion of rat striatum with 7-NINA immediately increased dopamine efflux to between 203 and 229% of basal and control values (Figure 1a). In the presence of L-arginine, 7-NINA increased striatal dopamine efflux to between 132 and 191% of basal values (Figure 1a), such that total dopamine efflux over the 90 min period of infusion was significantly less (67%) than that produced by 7-NINA alone

[1] Author for correspondence.

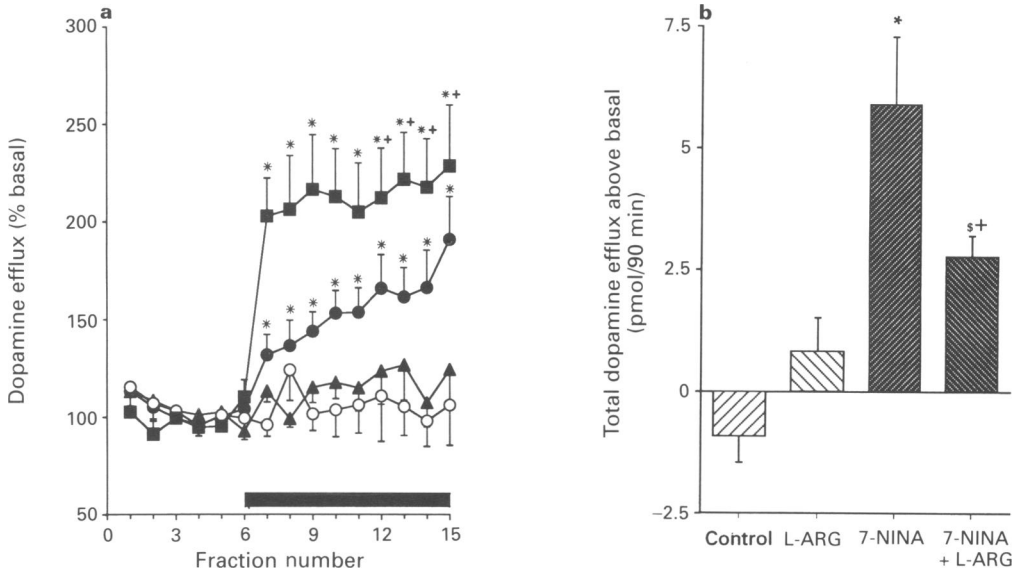


Figure 1 (a) The effect of the monosodium salt of 7-nitro indazole (7-NINA, ■, $n = 8$), 7-NINA plus L-arginine (●, $n = 10$), L-arginine (▲, $n = 9$) and artifical CSF (○, $n = 9$) on dopamine efflux from rat striatum *in vivo*. Results are expressed as % basal efflux ± s.e.mean. $*P < 0.05$ compared to basal dopamine efflux (Dunn's test); $\dagger P < 0.05$ compared to control (Dunn's test). (b) The effect of 7-NINA ($n = 8$), 7-NINA plus L-arginine (L-Arg) ($n = 10$), L-arginine ($n = 9$) and artificial CSF (control, $n = 9$) on total dopamine efflux above basal over the 90 min perfusion period. Results are expressed as mean ± s.e.mean. $*P < 0.05$ compared to artificial CSF (Dunn's test); $\dagger P < 0.05$ compared to L-arginine, $\$P < 0.05$ compared to 7-NINA (Dunn's test).

(Figure 1b). Perfusion with artificial CSF and L-arginine alone did not alter striatal dopamine efflux compared to basal values (Figure 1a and b). DOPAC and HVA levels were unaltered (data not shown).

Discussion The novel monosodium salt of 7-NI, 7-NINA, inhibits cerebellar NO synthase activity *in vitro* with a similar IC_{50} to that reported for 7-NI (Rose *et al.*, 1994b). Inhibition of striatal NO synthase by 7-NINA resulted in increased striatal dopamine efflux which was partially inhibited by L-arginine, the substrate for NO synthase. This inhibition of 7-NINA-induced increased striatal dopamine efflux is consistent with an action as a competitive antagonist of brain NO synthase activity and confirms that 7-NINA exerts its action on dopamine release via the inhibition of NO formation. These data suggest that endogenous NO has an inhibitory influence on striatal dopamine release *in vivo*. This is contrary to the findings of Lonart *et al.* (1993) who reported increased dopamine efflux from striatal slices by donors of NO. However, they are in agreement with Guevara-Guzman *et al.* (1994) who reported decreased dopamine release *in vivo* following local administration of NO donors using microdialysis. The reason for the difference between the *in vitro* and *in vivo* studies is not known. It may be due to an inhibition of NO release following cortical glutamatergic stimulation of striatal NMDA receptors which can occur in the *in vivo* but not the *in vitro* situation (Lei *et al.*, 1992).

In conclusion, for the first time we have shown that selective inhibition of brain NO synthase activity by 7-NINA increases striatal dopamine efflux *in vivo*, suggestig an inhibitory influence of endogenous NO on dopamine release. This may be a direct effect of NMDA-evoked NO on striatal dopaminergic neurones, or mediated by striatal cholinergic or GABAergic interneurones.

This study was supported by the Medical Research Council. M.T.S. holds a M.R.C. Training Fellowship.

References

GUEVARA-GUZMAN, R., EMSON, P.C. & KENDRICK, K.M. (1994). Modulation of in vivo transmitter release by nitric oxide and cyclic GMP. *J. Neurochem.*, **62,** 807–810.

HANBAUER, I., WINK, D., OSAWA, Y., EDELMAN, G.M. & GALLY, J.A. (1992). Role of nitric oxide in NMDA-evoked release of [^{3}H]-dopamine release from striatal slices. *NeuroReport*, **3,** 409–412.

LEI, S.Z., PAN, Z.-H., AGGARWAL, S.K., CHEN, H.-S.V., HARTMAN, J., SUCHER, N.J. & LIPTON, S.A. (1992). Effect of nitric oxide production on the redox modulatory site of the NMDA receptor-channel complex. *Neuron*, **8,** 1087–1099.

LONART, G., CASSELS, K.L. & JOHNSON, K.M. (1993). Nitric oxide induces calcium-dependent [^{3}H]dopamine release from striatal slices. *J. Neurosci. Res.*, **35,** 192–198.

MOORE, P.K., WALLACE, P., GAFFEN, Z., HART, S.L. & BABBEDGE, R.C. (1993). Characterisation of the novel nitric oxide synthase inhibitor 7-nitro indazole and related indazoles: antinociceptive and cardiovascular effects. *Br. J. Pharmacol.*, **110,** 219–224.

PELLIGRINO, L.J., PELLIGRINO, A.S. & CUSHMAN, A.J. (1979). *A Stereotaxic Atlas of the Rat Brain*. New York & London: Plenum Press.

ROSE, S., HINDMARSH, J.G. & JENNER, P. (1994a). Inhibition of nitric oxide synthase enhances NMDA-evoked dopamine released in the intact rat striatum. *Br. J. Pharmacol.*, **111,** 59P.

ROSE, S., HINDMARSH, J.G., SILVA, M.T., PITCHER, A., AISLAITNER, G., MOORE, P.K., GORROD, J.W., JENNER, P. & MARSDEN, C.D. (1994b). The novel monosodium salt of 7-nitro indazole inhibits brain nitric oxide synthase and elevates striatal dopamine efflux *in vivo*. *Br. J. Pharmacol.*, **112,** 506P.

(Received June 20, 1994
Accepted September 15, 1994)

British Journal of Pharmacology (1995) 114, 259-261 © 1995 Stockton Press All rights reserved 0007-1188/95 $9.00

SPECIAL REPORT

Prevention by the tachykinin NK_2 receptor antagonist, SR 48968, of antigen-induced airway hyperresponsiveness in sensitized guinea-pigs

Elisabeth Boichot, Noella Germain, Vincent Lagente & [1]*Charles Advenier

Laboratoire de Pharmacodynamie et de Pharmacologie Moléculaire, Faculté des Sciences Pharmaceutiques et Biologiques, Université de Rennes 1, Rennes, France and *Laboratoire de Pharmacologie Respiratoire, Faculté de Médecine Paris-Ouest, Université Paris V, 15, rue de l'ecole de Medecine, 75006 Paris, France

The involvement of tachykinins in antigen-induced airway hyperresponsiveness (AHR) was characterized pharmacologically in guinea-pigs sensitized to ovalbumin with antagonists of tachykinin NK_1 and NK_2 receptors, namely SR 140333 and SR 48968, respectively. AHR was illustrated by increased sensitivity to bronchoconstriction provoked by aerosolized acetylcholine in anaesthetized, ventilated animals, administrated 48 h after ovalbumin aerosol challenge. SR 48968 (1 mg kg^{-1}, i.p.), when given once 30 min before the antigen challenge, prevented AHR, whereas SR 140333 did not. These findings suggest that the tachykinin NK_2 receptor antagonist, SR 48968, may be useful for investigating mechanisms of tachykinins in the development of airway hyperresponsiveness.

Keywords: Tachykinin NK_1 receptor; tachykinin NK_2 receptor; SR 140333; SR 48968; ovalbumin; aerosol; guinea-pig airway hyperresponsiveness.

Introduction Airway hyperresponsiveness (AHR) is a functional consequence of airway inflammation and is a main feature of asthma. Among the different inflammatory mediators involved, several lines of evidence suggest that tachykinins, such as substance P and neurokinin A might be involved in the pathogenesis of AHR. Indeed, recent studies have reported that exposure of guinea-pigs to an aerosol of either capsaicin, a substance releasing endogenous sensory neuropeptides, or of substance P elicited AHR to exogenous bronchoconstrictor agents (Hsuie *et al.*, 1992; Boichot *et al.*, 1993). Conversely, chronic treatment with high doses (i.p.) of capsaicin which depletes tachykinins from non-adrenergic non-cholinergic nerves, eliminates AHR induced by acute capsaicin or ovalbumin (Matsuse *et al.*, 1991; Hsuie *et al.*, 1992).

The aim of the present study was to investigate the role of tachykinins in the development of AHR and to determine which type of receptor is involved. We have analysed the effects on antigen-induced airway hyperresponsiveness in the sensitized guinea-pig of SR 140333 (Emonds-Alt *et al.*, 1993) and SR 48968 (Emonds-Alt *et al.*, 1992) two non-peptide selective antagonists of tachykinin NK_1 and NK_2 receptors, respectively.

Methods Specific pathogen-free male Hartley guinea-pigs (Charles River, Saint-Aubin-lès-Elboeuf, France) were exposed twice for 30 min to an aerosol (ULTRA-NEB 99, Devilbiss Medical) of ovalbumin (OA) 2 mg ml^{-1} in saline (NaCl, 0.9%), at a 48 h interval in a plexiglass chamber (30 × 50 × 30 cm). Fifteen to 20 days after the initial sensitization procedure, the guinea-pigs were challenged by exposure to five successive solutions of OA of respectively 10 μg ml^{-1}, 100 μg ml^{-1}, 1 mg ml^{-1}, 5 mg ml^{-1} and 10 mg ml^{-1} for 15 min each. The bronchopulmonary reactivity of anaesthetized (urethane, 1.2 g kg^{-1}, i.p.) and ventilated (1 ml laboratory air for 100 g body weight, 60 breaths min^{-1}) guinea-pigs was assessed 48 h after exposure to either OA challenge or saline. Spontaneous breathing was abolished with pancuronium bromide (Pavulon, Organon, France; 2 mg kg^{-1}, i.v.). Airway inflation pressure was evaluated with a pressure transducer (Gould PE 10, Cleveland, Ohio, USA) connected to a lateral port of the ventilator circuit. After a 10 min stabilization period, four successive administrations of ACh aerosol (50, 100, 200 and 500 μg ml^{-1}), generated by a Devilbiss Pulmosonic ultrasonic nebulizer, were given for 1 min each at 10 min intervals. The bronchopulmonary response was monitored constantly and expressed as percentage change over the 100% obtained by clamping the tracheal cannula at the end of the experiment. The following drugs were used: ovalbumin (OA, chicken egg, grade V) and acetylcholine chloride (ACh) (Sigma, St. Louis, MO, U.S.A.). SR 48968 {(S)-*N*-methyl-*N*[4-acetylamino-4-phenylpiperidino-2-(3,4-dichlorophenyl) butyl]benzamide} and SR 140333 ((S)1-{2-[3-(3,4-dichlorophenyl)-1-(3-iso-propoxyphenylacetyl) piperidin-3-yl]ethyl}-4-phenyl-1-azoniabicyclo[2.2.2] octane, chloride) (Sanofi Recherche, Montpellier, France). SR 48968 and SR 140333 were dissolved in saline and injected i.p. at the dose of 1 mg kg^{-1}, 30 min before the ovalbumin challenge.

Results Exposure of sensitized and saline challenged guinea-pigs to successive aerosols of ACh (50– 500 μg ml^{-1}) induced a dose-related bronchopulmonary response which was not modified by either SR 48968 or SR 140333 (1 mg kg^{-1}). In sensitized guinea-pigs that had been challenged with an aerosol of allergen, responses to ACh given 48 h later were augmented compared to those in saline-exposed animals. Hence, the dose-response curve to ACh was significantly shifted to the left ($P < 0.001$), suggesting the development of AHR (Figure 1a and b). Pretreatment of the sensitized guinea-pigs with a single dose of SR 48968 (1 mg kg^{-1}) 30 min before allergen challenge significantly prevented the AHR (Figure 1a). In contrast, pretreatment with SR 140333 (1 mg kg^{-1}) did not modify the significant leftward shift of the dose-response curve to Ach, observed after allergen challenge (Figure 1b).

Discussion Stimulation of NK_2 receptor is involved in bronchoconstriction induced by tachykinins, by substances which release tachykinins from sensory nerves, and by antigen in

[1] Author for correspondence.

sensitized guinea-pigs (Advenier *et al.*, 1992; Bertrand *et al.*, 1993). It has also been suggested that tachykinins are involved in the development of AHR (Hsuie *et al.*, 1992; Boichot *et al.*, 1993). The present finding that the antagonist SR 48968 prevented antigen-induced AHR in sensitized guinea-pigs, an effect which could not be attributed to functional antagonism of acetylcholine-induced bronchoconstriction (Advenier *et al.*, 1992), provides evidence that NK_2 receptor stimulation is involved in the development of AHR. Since the NK_1 receptor antagonist, SR 140333, failed to inhibit the antigen-induced AHR, NK_1 receptor stimulation appears not to be involved. The lack of effect of SR 140333 cannot be attributed to a difference in pharmacokinetic profile since SR 48968 and SR 140333 have comparable time-related dose-effect relationship *in vivo* in the guinea-pig (Emonds-Alt *et al.*, 1992; 1993).

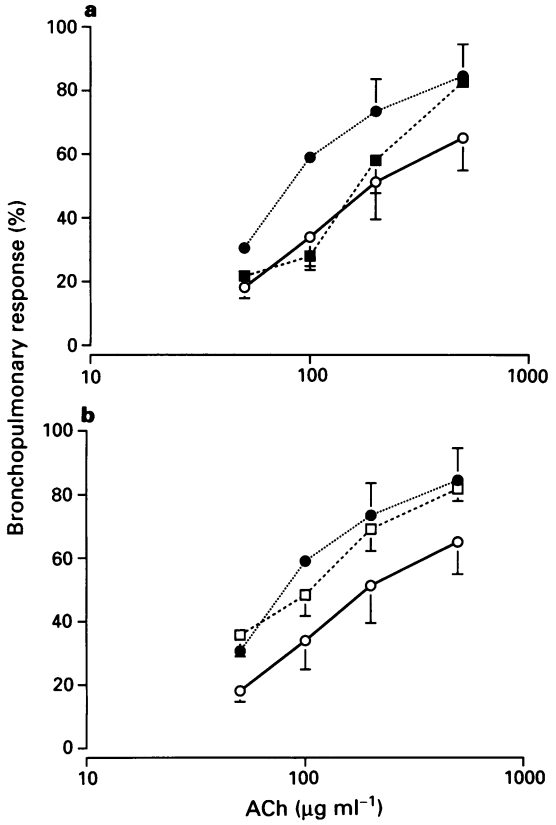


Figure 1 Effect of SR 48968 (a) and SR 140333 (b) on antigen-induced airway hyperresponsiveness to acetylcholine (ACh), 48 h after ovalbumin (OA) challenge. Sensitized guinea-pigs were treated i.p., 30 min before OA exposure, with 1 mg kg^{-1} of SR 48968 or of SR 140333 and the bronchopulmonary responses were assessed 48 h after. The data were compared by two way analysis of variance in order to analyse the whole dose-response curve for each group of guinea pigs. The results are expressed as mean (± s.e. mean) percentages of the maximal bronchopulmonary response obtained by total clamping of the tracheal cannula. Significant differences between saline (○, $n=5$) and OA (●, $n=8$): $P<0.001$. Significant differences between OA (●) and SR 48968 + OA (■, $n=6$): $P<0.01$. No significant differences between SR 48968 + OA (■) and saline (○) or between OA (●) and SR 140333 + OA (□, $n=6$). Significant differences between SR 140333 + OA (□) and saline (○): $P<0.01$.

Although the site of action of SR 48968 is not clear, it is possible that SR 48968 acts to regulate responses of target-cells involved in bronchoconstriction and airway inflammation or on nerve transmission. One of the most important cells involved in the inflammatory process of allergic reactions may be the alveolar macrophage. Indeed, we have previously reported that AHR observed after exposure of guinea-pigs to substance P is associated with an increase in alveolar macrophage activity (Boichot *et al.*, 1993) and an increased responsiveness to NK_2 receptor stimulation of alveolar macrophages from sensitized guinea-pigs has been demonstrated (Brunelleschi *et al.*, 1992). Regarding an effect on nerve transmission, Fischer *et al.* (1994) have recently demonstrated that sensitization of guinea-pigs to ovalbumin induced a 1–5 fold increase of neuropeptide-concentration in lung tissue and also increased two fold the substance P/neurokinin A-immunoreactive neurones in the nodose ganglion 24 h after allergen challenge. Furthermore, in vagal sensory ganglia, these authors observed that the expression of preprotachykinin A mRNA was increased in allergic animals, 12–24 h after allergen challenge.

Finally, Adcock & Garland (1993) have suggested that tachykinins might decrease the threshold for stimulation of sensory nerves endings in the lung as in other inflamed tissues involved in hyperalgesia. In this respect, repeated exposure to sub-threshold doses of neurokinin A leads to an increase in the peripheral hyperalgesia in the rat paw, lasting for more than 4 h and is ten fold more potent than substance P (Nakamura-Craig *et al.*, 1990). Hence, it is possible that SR 48968 may reduce this putative effect on sensory nerves in the airways.

In conclusion, the present data demonstrate the importance of NK_2 receptor stimulation in the development of antigen-induced AHR in sensitized guinea-pigs and suggest that NK_2 receptor antagonists may be useful for investigating mechanisms of bronchopulmonary alterations of allergic reaction and possibly reducing AHR in asthmatic patients.

References

ADCOCK, J.J. & GARLAND, L.G. (1993). The contribution of sensory reflexes and 'hyperalgesia' to airway hyperresponsiveness. In *Airway Hyperresponsiveness: It is really important for Asthma?* ed. Page C.P. & Gardiner, P.J. pp. 234–255. Oxford: Blackwell.

ADVENIER, C., NALINE, E., TOTY, L., BAKDACH, H., EMONDS-ALT, X., VILAIN, P., BRELIÈRE, J.C. & LE FUR, G. (1992). Effects on the isolated human bronchus of SR 48968, a potent and selective non peptide antagonist of the neurokinin A (NK_2) receptors. *Am. Rev. Respir. Dis.*, **146**, 1177–1181.

BERTRAND, C., GEPPETI, P., GRAF, P.D., FORESI, A. & NADEL, J.A. (1993). Involvement of neurogenic inflammation in antigen-induced bronchoconstriction in guinea-pigs. *Am. J. Physiol.*, **265**, L507–L511.

BOICHOT, E., LAGENTE, V., PAUBERT-BRAQUET, M. & FROSSARD, N. (1993). Inhaled substance P induces activation of alveolar macrophages and increases airway responses in the guinea-pig. *Neuropeptides*, **25**, 307–313.

BRUNELLESCHI, S., PARENTI, A., CENI, E., GIOTTI, A. & FANTOZZI, R. (1992). Enhanced responsiveness of ovalbumin-sensitized guinea-pig alveolar macrophages to tachykinins. *Br. J. Pharmacol.*, **107**, 964–969.

EMONDS-ALT, X., DOUTREMEPUICH, J.D., HEAULME, M., NELIAT, G., SANTUCCI, V., STEINBERG, R., VILAIN, P., BICHON, D., DUCOUX, J.P., PROIETTO, V., VAN BROECK, D., SOUBRIÉ, P., LE FUR, G. & BRELIÈRE, J.C. (1993). In vitro and in vivo biological activities of SR 140333, a novel potent non-peptide tachykinin NK_1 receptor antagonist. *Eur. J. Pharmacol.*, **250**, 403–413.

EMONDS-ALT, X., VILAIN, P., GOULAOUIC, P., PROIETTO, V., VAN BROECK, D., ADVENIER, C., NALINE, E., NELIAT, G., LEFUR, G. & BRELIÈRE, J.C. (1992). A potent and selective non-peptide antagonist of the neurokinin A (NK_2) receptor. *Life Sci.*, **50**, PL101–PL106.

FISCHER, A., PHILIPPIN, B., SARIA, A., MCGREGOR, G. & KUMMER, W. (1994). Neuronal plasticity in sensitized and challenged guinea pigs: neuropeptides and neuropeptide gene expression. *Am. J. Respir. Crit. Care Med.*, **149,** A890.

HSUIE, T., GARLAND, A., RAY, D.W., HERSHENSON, M.B., LEFF, A.R. & SOLWAY, J. (1992). Endogenous sensory neuropeptide release enhances nonspecific airway responsiveness in guinea pigs. *Am. Rev. Respir. Dis.*, **146,** 148–153.

MATSUSE, T., THOMSON, R.J., CHEN, X.R., SALARI, H. & SCHELLENBERG, R.R. (1991). Capsaicin inhibits airway hyperresponsiveness but not lipoxygenase activity or eosinophilia after repeated aerosolized antigen in guinea pigs. *Am. Rev. Respir. Dis.*, **144,** 366–372.

NAKAMURA-CRAIG, M. & GILL, B.K. (1990). Possible involvement of neurokinin A, substance P and calcitonin gene-related peptide in peripheral hyperalgesia in the rat. *Br. J. Pharmacol.*, **99,** 288P.

(Received September 23, 1994
Accepted September 28, 1994)

British Journal of Pharmacology (1995) 114, 262–268 © 1995 Stockton Press All rights reserved 0007–1188/95 $9.00

Suppression of VEGF-induced angiogenesis by the protein tyrosine kinase inhibitor, lavendustin A

D.E. Hu & [1]T.-P.D. Fan

Department of Pharmacology, University of Cambridge, Tennis Court Road, Cambridge CB2 1QJ

1 Vascular endothelial growth factor (VEGF) is a heparin-binding angiogenic factor which specifically acts on endothelial cells via distinct membrane-spanning tyrosine kinase receptors. Here we used the rat sponge implant model to test the hypothesis that the angiogenic activity of VEGF can be suppressed by protein tyrosine kinase (PTK) inhibitors.

2 Neovascular responses in subcutaneous sponge implants were determined by measurements of relative sponge blood flow by use of a ^{133}Xe clearance technique, and confirmed by histological studies and morphometric analysis.

3 Daily local administration of 250 ng $VEGF_{165}$ accelerated the rate of ^{133}Xe clearance from the sponges and induced an intense neovascularisation. This $VEGF_{165}$-induced angiogenesis was inhibited by daily co-administration of the selective PTK inhibitor, lavendustin A (10 μg), but not its negative control, lavendustin B (10 μg). Blood flow measurements and morphometric analysis of 8-day-old sponges showed that lavendustin A reduced the ^{133}Xe clearance of VEGF165-treated sponges from 32.9 ± 1.5% to 20.9 ± 1.6% and the total fibrovascular growth area from 62.4 ± 6.1% to 21.6 ± 6.8% ($n = 12$, $P < 0.05$).

4 Co-injection of suramin (3 mg), an inhibitor of heparin-binding growth factors, also suppressed the VEGF165-elicited neovascular response. In contrast, neither lavendustin A nor suramin produced any effect on the basal sponge-induced angiogenesis.

5 When given alone, low doses of VEGF165 (25 ng) or basic fibroblast growth factor (bFGF; 10 ng) did not modify the basal sponge-induced neovascularisation. However, co-administration of these two peptides to a single sponge together caused a significant increase in the rate of ^{133}Xe clearance and angiogenesis similar to that seen with the high dose of VEGF165 (250 ng) acting alone. This VEGF/bFGF neovascular response was also blocked by daily co-administration of lavendustin A (10 μg), suramin (3 mg) or a monoclonal anti-bFGF antibody (DG2, 1 μg), but not lavendustin B (10 μg).

6 These results suggest that selective inhibition of PTK could have therapeutic potential in angiogenic diseases where VEGF plays a dominant role. Furthermore, blockade of the angiogenic activity of VEGF and VEGF/bFGF by suramin reveals an alternative strategy in angiosuppression.

Keywords: Angiogenesis; vascular endothelial cell growth factor (VEGF); protein tyrosine kinase (PTK); lavendustin; suramin

Introduction

Angiogenesis is normally under stringent control and occurs only during embryonic development, the female reproductive cycle and wound repair. In many pathological conditions (e.g., solid tumour, rheumatoid arthritis, diabetic retinopathy and atherosclerosis), the disease itself appears to be driven by persistent unregulated vessel proliferation. Folkman hypothesized in the early 1970s that tumour growth is angiogenesis-dependent and pioneered the idea that an anti-angiogenesis strategy might represent a new therapeutic approach for the treatment of solid tumours (Folkman, 1972). Since the first successful clinical treatment of an angiogenic disease using interferon alpha-2a (White *et al.*, 1989), several natural and synthetic compounds have shown promising therapeutic potentials as angiosuppressants. Some of them are currently undergoing clinical trials for the treatment of cancer (Fan, 1994).

It is now clear that the angiogenic process is tightly controlled by the balance between many positive and negative regulatory signals (Folkman & Klagsbrun, 1987; Folkman & Shing, 1992; Fan & Brem, 1992). However, vascular endothelial growth factor (VEGF) has attracted much attention recently because it is the only angiogenic factor that specifically acts on endothelial cells (Connolly, 1991; Ferrara *et al.*, 1992; Senger *et al.*, 1993). The isolation of VEGF from several tumour cell lines and macrophages has implicated it as a major tumour angiogenesis factor in some human gliomas (Plate *et al.*, 1992) and chronic inflammatory diseases (Senger *et al.*, 1993). Another unique feature of VEGF is that its cell-surface receptors are exclusively expressed in endothelial

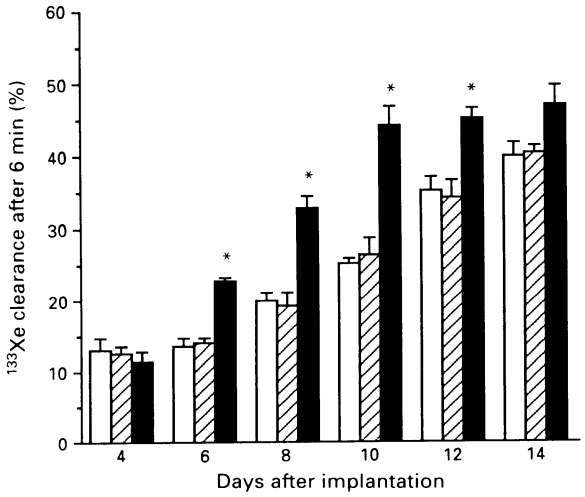


Figure 1 Angiogenesis induced by vascular endothelial growth factor (VEGF). Columns represent sponges treated daily with phosphate-buffered saline (PBS, open columns), 25 ng VEGF (hatched columns) or 250 ng VEGF (solid columns). Data represent the mean ± s.e. $n = 6$. *$P < 0.05$, (VEGF vs PBS).

[1] Author for correspondence.

cells (Millauer *et al.*, 1993; Plate *et al.*, 1993). Thus, VEGF is a promising target for the development of specific angiosuppressive drugs.

Using a rat sponge implant model, we have previously demonstrated that it is possible to block the neovascular responses induced by growth factors/cytokines *in vivo* by their respective neutralising antibodies, receptor antagonists (Hu & Fan, 1993; Fan *et al.*, 1993; Hu *et al.*, 1994), or selective inhibitors of the signal-transduction pathways (Hu & Fan, 1994a). Since the mitogenic and angiogenic activities of VEGF are thought to be mediated by distinct membrane-spanning tyrosine kinase receptors, we predicted that specific inhibitors of protein tyrosine kinase (PTK) should block the biological functions of VEGF *in vivo*. To test this hypothesis, we used a highly potent and specific PTK inhibitor lavendustin A (Onoda *et al.*, 1989; Odell *et al.*, 1991) and showed that it is an effective inhibitor of the angiogenic activity of VEGF.

Suramin is an effective analogue of heparin/heparan sulphate which inhibits the activities of several heparin-binding growth factors such as fibroblast growth factors (FGFs) and platelet-derived growth factor (Myers *et al.*, 1990). Although suramin blocks the growth-stimulating activity of VEGF *in vitro* (Olander *et al.*, 1991), its action against VEGF *in vivo* is unknown. Here we also show that suramin blocks the angiogenic activity of VEGF in the rat sponge model.

Methods

The sponge implant model

Sterile circular polyether sponge discs (5 mm thick, 1.2 cm diameter) with central cannulae (1.3 cm long, 1.4 mm internal diameter) were implanted subcutaneously in male Wistar rats (180–200 g) after induction of neuroleptanalgesia by Hypnorm (0.315 mg ml^{-1} fentanyl citrate and 10 mg ml^{-1} fluanisone; 0.1 ml kg^{-1}, i.m.). Test substances (50 µl) were injected daily into the sponges through the cannulae. To exclude the possible acute effects of the test substances (dilatation or constriction) on the microvasculature, they were given 18–24 h prior to the ^{133}Xe measurements. The neovascular response was assessed as a function of blood flow through the implants by use of a ^{133}Xe clearance technique (Andrade *et al.*, 1987). Briefly, animals were anaesthetized with Hypnorm as before and 10 µl ^{133}Xe in sterile PBS was injected into the sponges through the cannulae. The washout of radioactivity from the implants was monitored with a gamma scintillation detector over a period of 6 min. The clearance value was calculated by the formula % ^{133}Xe clearance = [(initial radioactivity – residual radioactivity at 6 min)/initial radioactivity] × 100%. The use of this technique to assess angiogenesis has been validated by comparison with four other methods, namely, (i) ^{113}Sn microsphere wash-in technique to measure absolute blood flow in the sponges; (ii) the carmine red dye method for measurement of neovasculature; (iii) colorimetric measurement of haemoglobin levels in the implants and (iv) histological and morphometric studies using a computer-assisted image analysis system.

Histology and morphometric analysis of fibrovascular growth areas

The animals were killed by cervical dislocation and sponges dissected out, carefully removing the cannulae and any adherent fat. The samples were then bisected and fixed in formal saline at 4°C for 1 h. Sections (10 µm) were prepared and stained with haematoxylin and eosin (H & E), Masson Trichrome or a specific endothelial cell marker *Bandeiraea simplicifolia* lectin I, isolectin B_4 (BSL-B_4). The specimens were analysed in a 'blind' manner and recorded on Kodak Gold II ASA 200 film. For simplicity, we use the term fibrovascular growth area to describe the tissue growth into a sponge. This is composed of blood vessels and surrounding stroma containing fibroblasts, macrophages, neutrophils and endothelial cells. As reported by Kowalski *et al.* (1992), the area occupied by blood vessels is a consistent percentage of the fibrovascular growth area. Thus, the measurement of fibrovascular growth area provides an accurate index of angiogenesis. To analyse morphometrically fibrovascular growth areas of the sponges, we adopted the axial strip sampling technique as described by Mayhew & Sharma (1984). The H & E-stained sections were observed with a 4 × objective and images relayed to a computer-assisted image analysis system (Seescan, Cambridge, U.K.). By a point counting procedure, using a 96-point square lattice with a field area of 0.66 mm^2, the volume fraction occupied by fibrovascular growth was estimated.

Materials

Recombinant human $VEGF_{165}$ was purchased from R & D Systems, Minneapolis, U.S.A. Lavendustin A and B were purchased from Calbiochem-Novabiochem (UK) Ltd., Nottingham, U.K. Recombinant human basic FGF and the monoclonal antibody to basic FGF, DG2 (Reilly *et al.*, 1989), were gifts from Professor M. Presta, University of Brescia, Brescia, Italy and Dr T.M. Reilly, Du Pont Merck Pharmaceuticals, Wilmington, Delaware, U.S.A., respectively. Other materials were purchased from the following companies: suramin (Imperial Chemical Industries Ltd., Macclesfield, U.K.); polyether foam sheet (R.E. Carpenter & Co., High Wycombe, U.K.); polythene tubings (Portex Ltd., Hythe, U.K.); Hypnorm (Janssen Pharmaceuticals, Oxford, U.K.); ^{133}Xe injection (Medgenix plc, High Wycombe, U.K.) and phosphate buffered saline (PBS) (Sigma Chemical Co. Ltd., Poole, U.K.). Lavendustin A and B were dissolved in dimethyl sulphoxide (DMSO) and then diluted with PBS. The final concentration of DMSO was less than 1.25%. Other solutions were prepared daily in PBS and sterilized by membrane filtration (0.22 µm) before use.

Statistics

Statistical analysis was done using StatView II (Abacus Concepts, Berkeley, CA, U.S.A.) on a Macintosh computer. Statistical significance was tested by analysis of variance (ANOVA) using a multi-comparison significance level for one factor ANOVA of 95% shown in the figures, or by Student's *t* test shown in the table.

Results

Effect of $VEGF_{165}$ on sponge-induced angiogenesis

Daily doses of 250 ng $VEGF_{165}$, the most abundant form of VEGF found *in vivo* (Ferrara *et al.*, 1992), caused a significant enhancement of ^{133}Xe clearance from the sponges as compared to the controls, while lower doses (25 ng) had no apparent effect (Figure 1). Histological studies of sponge sections showed that the cellular infiltration, neovascularisation and connective tissue in the VEGF165-treated sponges were profoundly increased (Figure 2d–2f), as confirmed by a large increase of the fibrovascular growth area (Table 1).

Effect of lavendustin A and B on VEGF-induced angiogenesis

Figure 3 clearly shows that the enhanced ^{133}Xe clearance in $VEGF_{165}$-treated sponges was significantly inhibited by daily co-administration of a selective PTK inhibitor, lavendustin A (10 µg), but not its negative control, lavendustin B (10 µg). Lower doses of lavendustin A and lavendustin B (1 µg) were ineffective. Histological studies of sponge sections showed that the cellular infiltration, neovascularisation and connective tissue in the VEGF-treated sponges were markedly suppressed by lavendustin A (Figure 2g and 2h), as confirmed by

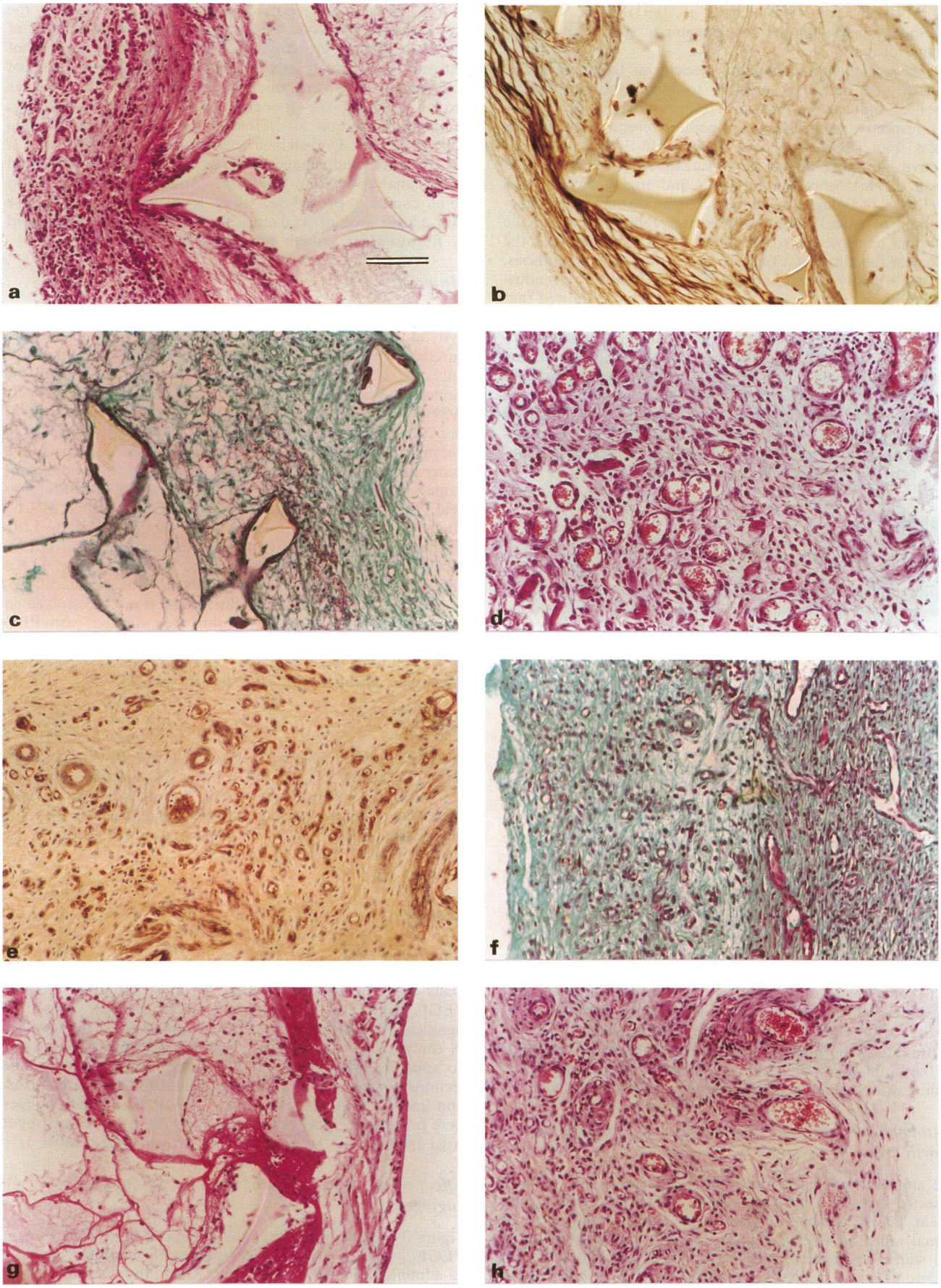
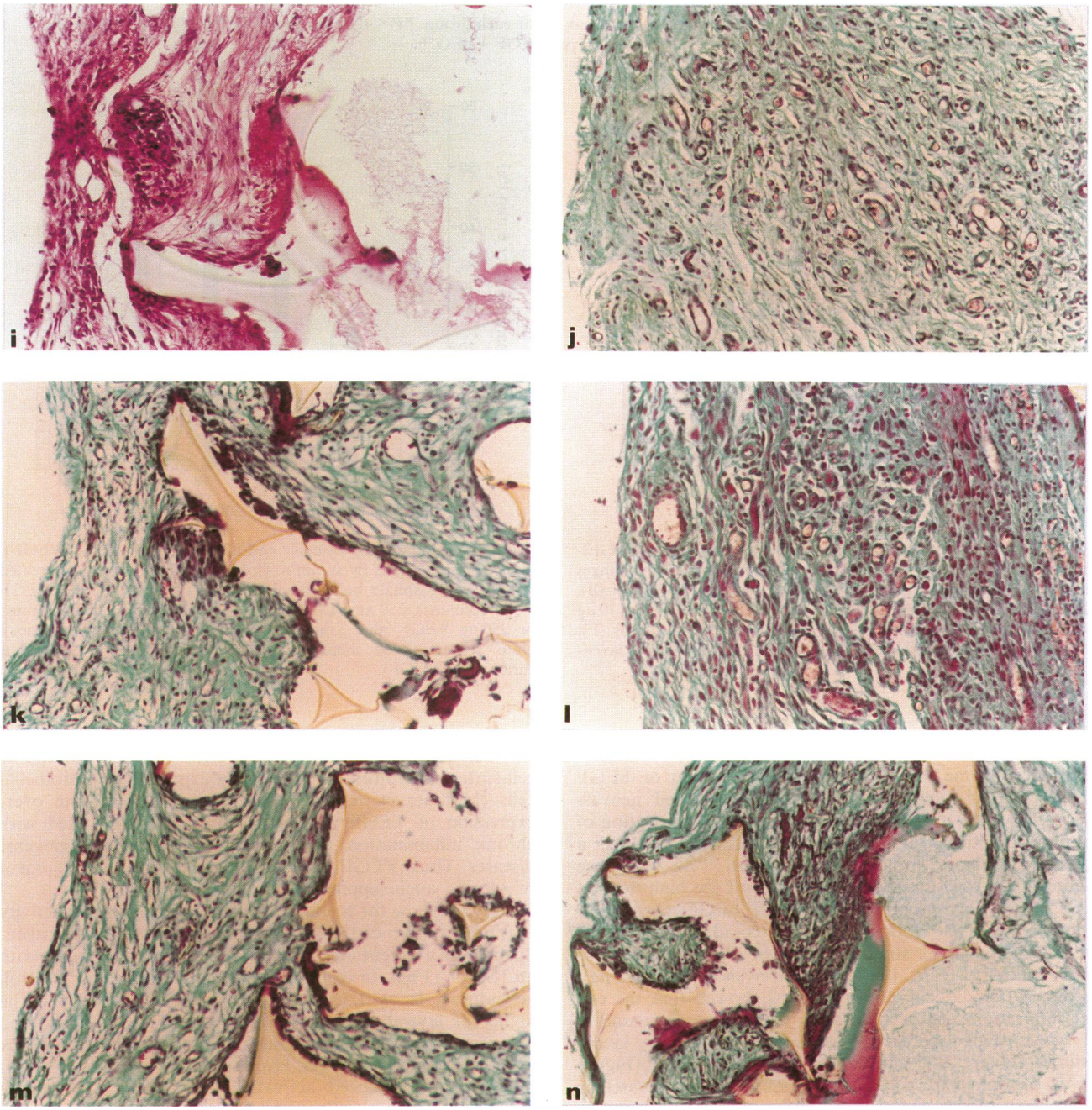


Figure 2 Histological sections of 8-day old sponges illustrating (i) sponge treated with PBS (sections a–c); (ii) the intense neovascular response induced by vascular endothelial growth factor (VEGF) (250 ng day^{-1}, sections d–f); (iii) the inhibition of VEGF-induced angiogenesis by lavendustin A (10 μg day^{-1}, section g), but not by lavendustin B (10 μg day^{-1}, section h); (iv) the inhibition of VEGF-induced angiogenesis by suramin (3 mg day^{-1}, section i), (v) the intense neovascular response induced by a combination of VEGF (25 ng day^{-1}) and bFGF (10 ng day^{-1}, section j); (vi) the inhibition of VEGF/bFGF-induced angiogenesis

a large reduction of the fibrovascular growth area (Table 1). By contrast, neither lavendustin A nor lavendustin B (both at 10 μg) was able to inhibit the basal sponge-induced neovascularisation (data not shown).

Effect of suramin on VEGF-induced angiogenesis

The $VEGF_{165}$-induced neovascular response was inhibited by co-administration of 3 mg suramin, while 1 mg suramin was ineffective (Figure 4). Histological studies of sponge sections showed that the cellular infiltration, neovascularisation and connective tissue in the VEGF-treated sponges were effectively suppressed by suramin (Figure 2i), again confirmed by a large reduction of the fibrovascular growth area (Table 1). In the absence of exogenous peptides, suramin (1 or 3 mg daily) produced no apparent effect on the ^{133}Xe clearance and angiogenesis in control sponges, as confirmed histologically (data not shown).



by lavendustin A (10 μg day^{-1}, section k), suramin (3 mg day^{-1}, section l) or by a monoclonal anti-bFGF antibody (1000 ng day^{-1}, section m), but not by lavendustin B (10 μg day^{-1}, section l). All sections photographed at × 200 magnification. Bar = 100 μm. (a) Sponge treated with PBS (H & E stained); (b) sponge treated with PBS ($BSL\text{-}B_4$ stained); (c) sponge treated with PBS (Masson Trichrome stained); (d) sponge treated with VEGF (H & E stained); (e) sponge treated with VEGF ($BSL\text{-}B_4$ stained); (f) sponge treated with VEGF (Masson Trichrome stained); (g) sponge treated with VEGF plus lavendustin A (H & E stained); (h) sponge treated with VEGF plus lavendustin B (H & E stained); (i) sponge treated with VEGF plus suramin (H & E stained); (j) sponge treated with VEGF plus bFGF (Masson Trichrome stained); (k) sponge treated with VEGF and bFGF plus lavendustin A (Masson Trichrome stained); (l) sponge treated with VEGF and bFGF plus lavendustin B (Masson Trichrome stained); (m) sponge treated with VEGF and bFGF plus suramin (Masson Trichrome stained); (n) sponge treated with VEGF and bFGF plus DG2 (Masson Trichrome stained).

Table 1 Effect of vascular endothelial growth factor on the total fibrovascular growth area (%) of sponge implants

Treatment groups	*Fibrovascular growth area* (%)
Control	19.2 ± 5.3
VEGF (250 ng day^{-1})	67.4 ± 6.0*
VEGF (250 ng) + lavendustin A (10 μg)	21.6 ± 6.8***
VEGF (250 ng) + lavendustin B (10 μg)	62.4 ± 6.1
VEGF (250 ng) + suramin (3 mg)	23.3 ± 6.7**
VEGF (25 ng) + bFGF (10 ng)	61.1 ± 5.9*
VEGF (25 ng) + bFGF (10 ng) + lavendustin A (10 μg)	23.7 ± 6.5****
VEGF (25 ng) + bFGF (10 ng) + lavendustin B (10 μg)	62.9 ± 6.6****
VEGF (25 ng) + bFGF (10 ng) + suramin (3 mg)	22.2 ± 6.3****
VEGF (25 ng) + bFGF (10 ng) + DG2 (1 μg)	24.2 ± 6.9****

Data derived from histological sections of 8-days old sponges, $n = 12$ for each group. *$P < 0.01$ (vs Control); **$P < 0.01$ (vs VEGF); ***$P < 0.05$ (VEGF + lavendustin A vs VEGF); ****$P < 0.01$ (vs VEGF + bFGF).

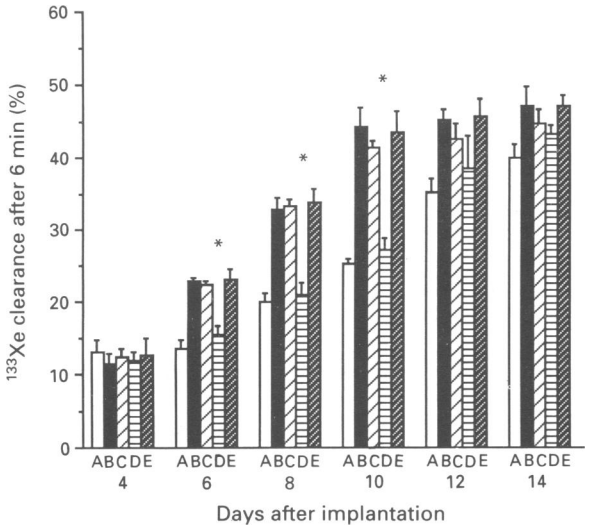


Figure 3 Inhibition of vascular endothelial growth factor (VEGF)-induced angiogenesis by lavendustin A. Columns represent sponges treated daily with phosphate buffered saline (A), 250 ng VEGF (B), 250 ng VEGF plus 1 μg lavendustin A (C), 250 ng VEGF plus 10 μg lavendustin A (D) or 250 ng VEGF plus 10 μg lavendustin B (E). Data represent the mean ± s.e. $n = 6$. *$P < 0.05$, (VEGF plus lavendustin A vs VEGF).

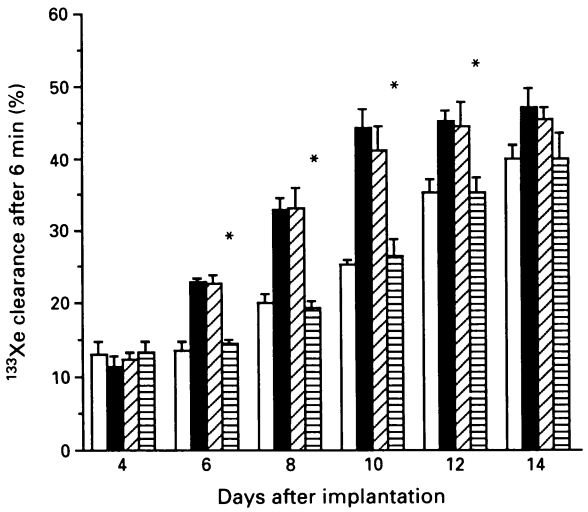


Figure 4 Inhibition of vascular endothelial growth factor (VEGF)-induced angiogenesis by suramin. Columns represent sponges treated daily with phosphate buffered saline (open columns), 250 ng VEGF (solid columns), 250 ng VEGF plus 1 mg suramin (hatched columns) or 250 ng VEGF plus 3 mg suramin (horizontally lined columns). Data represent the mean ± s.e. $n = 6$. *$P < 0.05$ (VEGF plus suramin vs VEGF).

Synergism between VEGF and bFGF

When given alone, low doses of VEGF (25 ng) or bFGF (10 ng) did not modify the basal sponge-induced neovascularisation (data not shown). However, co-administration of these two peptides to a single sponge together caused a significant increase in angiogenesis and ^{133}Xe clearance (Figures 2j and 5) similar to that seen with the high dose of VEGF (250 ng) acting alone. This VEGF/bFGF neovascular response was also blocked by daily co-administration of lavendustin A (10 μg), suramin (3 mg) or a monoclonal anti-bFGF antibody (DG2, 1 μg), but not lavendustin B (10 μg). Histological studies of sponge sections showed that the cellular infiltration, neovascularisation and connective tissue in the VEGF/bFGF-treated sponges were suppressed by lavendustin A (Figure 2k), suramin (Figure 2m) or DG2 (Figure 2n), as confirmed by a large reduction of the fibrovascular growth area (Table 1).

Discussion

VEGF is a highly conserved, multifunctional cytokine expressed and secreted at high levels by activated macrophages and many tumour cells of animal and human origin (Senger *et al.*, 1993). Among the various angiogenic factors identified to date, VEGF is unique because it specifically acts on endothelial cells (Connolly, 1991; Ferrara *et al.*, 1992) and its cell-surface receptors are exclusively expressed in endothelial cells (Millauer *et al.*, 1993; Plate *et al.*, 1993). The overexpression of VEGF and its receptors are associated with chronic inflammation, tumour growth and other angiogenic diseases. Thus, VEGF is a prime target for the development of specific angiosuppressive drugs.

Here we show for the first time that the angiogenic activity of VEGF *in vivo* can be prevented by lavendustin A. Lavendustin A is a potent and selective PTK inhibitor *in vitro*, with an IC_{50} of 11 nM. In contrast, the IC_{50} of its negative control, lavendustin B, is 1.3 μM (Onoda *et al.*, 1989). Thus, the ability of lavendustin A and B to suppress VEGF-induced angiogenesis is entirely consistent with their relative potency as PTK blockers. Recently, lavendustin A has been shown to inhibit antigen-induced activation of PTK and histamine release from mast cells with IC_{50} of 80 μM and 112 μM, respectively (Kawakami *et al.*, 1992). This large discrepancy in the ability of lavendustin A to inhibit PTK enzyme activity in membrane fractions and in intact cells is possibly due to its poor penetration into the cells (Onoda *et al.*,1990). Two other tyrosine kinase inhibitors, herbimycin A (Oikawa *et al.*, 1989) and genistein (Fotsis *et al.*, 1993), have also been shown to inhibit angiogenesis in the chick embryo chorioallantoic membrane and endothelial cell proliferation *in vitro*. Experiments are in progress to assess the inhibitory activities

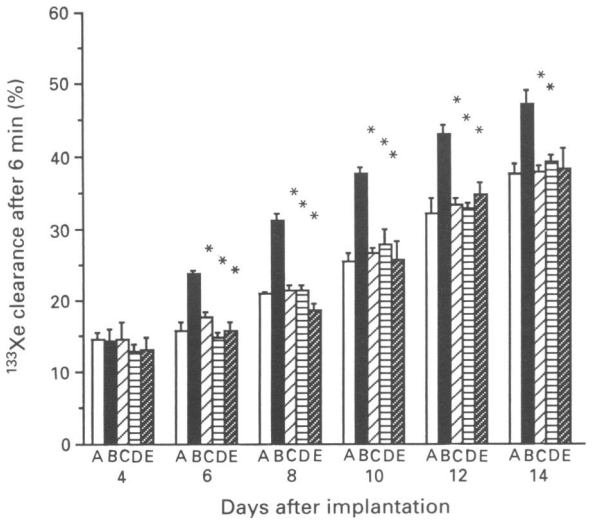


Figure 5 Effects of lavendustin A, suramin and a monoclonal anti-bFGF antibody on the enhanced neovascular response elicited by a combination of vascular endothelial growth factor (VEGF) and bFGF. Columns represent sponges treated daily with phosphate buffered saline (A), 25 ng VEGF and 10 ng bFGF (B), 25 ng VEGF and 10 ng bFGF plus 10 μg lavendustin A (C), 25 ng VEGF and 10 ng bFGF plus 3 mg suramin (D) and 25 ng VEGF and 10 ng bFGF plus 1 μg DG2 (E). Data represent the mean ± s.e. $n = 4-8$. $^*P < 0.05$, (all drug treatment groups vs VEGF and bFGF).

of these compounds on VEGF-induced angiogenesis in the sponge model.

It is important to note that in the absence of exogenous VEGF, lavendustin A did not modify the basal sponge-induced angiogenesis. In a previous report, we showed that the basal sponge-induced angiogenesis was almost completely inhibited by the combination of IL-1 receptor antagonist and neutralising antibodies to bFGF, TNF-α and IL-8 (Hu *et al.*, 1994), suggesting that the interactions between endogenous bFGF, TNF-α, IL-1α and IL-8 are mainly responsible for the neovascularisation elicited by sponges alone. Taken together, these findings strongly suggest that the action of lavendustin A in the present study is directed against VEGF-elicited responses.

Suramin, a polysulphonated naphthylurea, is the prototype of anti-cancer drugs that work by binding growth factors. It inhibits the activities of several heparin-binding growth factors such as transforming growth factor-beta, fibroblast growth factor and platelet-derived growth factor (Coffey *et al.*, 1987; Kopp & Pfeiffer, 1990; Myers *et al.*, 1990). In a rat brain tumour model, suramin inhibits endothelial and tumour cell proliferation (Takano *et al.*, 1993). Our data show that suramin is equally effective against angiogenesis induced by VEGF without any sign of toxicity. Previously, we have shown that the neovascular response induced by bFGF was markedly suppressed by co-administration of 3 mg suramin (Hu & Fan, 1992). In contrast, the angiogenic activity of non-heparin-binding growth factors such as platelet-derived endothelial cell growth factor was resistant to suramin (Fan *et al.*, 1993). In view of the narrow therapeutic window for suramin (La Rocca *et al.*, 1990), we are currently evaluating the anti-angiogenic activity of suramin analogues which are 5 to 10 fold less toxic than suramin (Braddock *et al.*, 1994).

Several other approaches have been used to inhibit VEGF activity. For example, pretreatment with a monoclonal antibody specific for VEGF has been shown to reduce the vascular density and suppress the growth of several human tumours in nude mice, without affecting the growth rate of tumour cells *in vitro* (Kim *et al.*, 1993). Similarly, we have shown that the VEGF-induced neovascular response was neutralised by co-administration of a polyclonal antibody to VEGF (Hu & Fan, 1994a). Two types of VEGF receptors have been identified: Flt and KDR (de Vries *et al.*, 1992; Terman *et al.*, 1992). In a recent study, recombinant human soluble Flt (sFlt) has been shown to bind VEGF with high affinity and inhibit its mitogenic activity for vascular endothelial cells (Kendall & Thomas, 1993). Future work may generate sFlt derivatives as specific high-affinity antagonists of VEGF.

VEGF has been reported to act synergistically with bFGF to stimulate both endothelial cell growth and endothelial cell invasion through collagen gels *in vitro* (Pepper *et al.*, 1992), and on the proliferation and cord formation of bovine capillary endothelial cells within collagen gels (Goto *et al.*, 1993). Here we showed that VEGF acts synergistically with bFGF to enhance neovascularisation *in vivo*. The synergistic effect of VEGF and bFGF was blocked by co-administration of lavendustin A, suramin or a monoclonal anti-bFGF antibody, DG2. These data suggest that in situations where an angiogenic response is elicited by VEGF and bFGF, strategies based on the antagonism of either angiogenic factor could prove feasible.

When given intravenously, bFGF has been reported to dilate blood vessels and decrease arterial blood pressure (Cuevas *et al.*, 1992). However, we did not detect any significant increase in ^{133}Xe clearance when VEGF and/or bFGF were injected intradermally or into the sponges (data not shown). Furthermore, all the test substances were given 18–24 h before the ^{133}Xe measurements to exclude the possible acute effects (dilatation or constriction) on the microvasculature. Thus, the enhanced angiogenesis in sponges treated with VEGF and/or bFGF is not likely to be due to vasodilatation.

We have recently shown that cytokine-induced angiogenesis *in vivo* can be partially prevented by the potent and specific PKC inhibitor calphostin C (Hu & Fan, 1994b; 1995). Here we report that the PTK inhibitor, lavendustin A, can suppress VEGF-induced neovascularisation. Taken together, these data clearly demonstrate that it is possible to down-regulate angiogenesis by inhibitors of signalling pathways. In conclusion, further elucidation of the functions of PKC, PTK and other signalling pathways in angiogenesis will no doubt facilitate the development of enzyme-specific inhibitors that could prove useful in formulating new strategies for the prevention and treatment of angiogenic diseases. Specifically, in angiogenic diseases where VEGF plays a dominant role, we anticipate more potent and permeable derivatives of lavendustin A in combination with VEGF-specific antibodies or soluble VEGF receptors to provide an effective treatment.

This work was supported by The Wellcome Trust.

References

ANDRADE, S.P., FAN, T.-P.D. & LEWIS, G.P. (1987). Quantitative in-vivo studies on angiogenesis in a rat sponge model. *Br. J. Exp. Pathol.*, **68**, 755–766.

BRADDOCK, P.S., HU, D.E., FAN, T.-P.D., STRATFORD, I., HARRIS, A.L. & BICKNELL, R. (1994). A structure-activity analysis of antagonism of the growth factor and angiogenic activity of basic fibroblast growth factor by suramin and related polyanions. *Br. J. Cancer*, **69**, 890–898.

COFFEY, R.J., LEOF, E.B., SHIPLEY, G.D. & MOSES, H.L. (1987). Suramin inhibition of growth factor receptor binding and mitogenicity in AKR-2B cells. *J. Cell Physiol.*, **132**, 143–148.

CONNOLLY, D.T. (1991). Vascular permeability factor: a unique regulator of blood vessel function. *J. Cell. Biochem.*, **47**, 219–223.

CUEVAS, P., CARCELLER, F., ORTEGA, S., ZAZO, M., NIETO, I. & GIMENEZ-GALLEGO, G. (1992). Hypotensive activity of fibroblast growth factor. *Science*, **254,** 1208–1210.

DE VRIES, C., ESCOBEDO, J.A., UENO, H., HOUCK, K., FERRARA, N. & WILLIAMS, L.T. (1992). The *fms*-like tyrosine kinase, a receptor for vascular endothelial growth factor. *Science*, **255,** 989–991.

FAN, T.-P.D. (1994). Angiosuppressive therapy for cancer. *Trends Pharmacol. Sci.*, **15,** 33–36.

FAN, T.-P.D. & BREM, S. (1992). Angiosuppression. In *The Search for New Anti-Cancer Drugs*. pp. 185–229. ed. Waring, M.J. & Ponder, B.A.J. Cancer Biology Series, Vol. 3. Lancaster, U.K.: Kluwer Academic Publishers.

FAN, T.-P.D., HU, D.E., GUARD, S., GRESHAM, G.A. & WATLING, K.J. (1993). Stimulation of angiogenesis by substance P and interleukin-1 in the rat and its inhibition by NK_1 or interleukin-1 receptor antagonists. *Br. J. Pharmacol.*, **110,** 43–49.

FAN, T.-P.D., HU, D.E., MOGHADDAM, A., HARRIS, A.L. & BICKNELL, R. (1993). Comparative studies of the angiogenic activity of platelet-derived endothelial cell growth factor and basic fibroblast growth factor in a rat sponge model. *Br. J. Pharmacol.*, **108,** 228P.

FERRARA, N., HOUCK, K., JAKEMAN, L. & LEUNG, D.W. (1992). Molecular and biological properties of the vascular endothelial growth-factor family of proteins. *Endocr. Rev.*, **13,** 18–32.

FOLKMAN, J. (1972). Anti-angiogenesis: new concept for the therapy of solid tumors. *Ann. Surg.*, **175,** 409–416.

FOLKMAN, J. & KLAGSBRUN, M. (1987). Angiogenic factors. *Science*, **235,** 442–447.

FOLKMAN, J. & SHING, Y. (1992). Angiogenesis. *J. Biol. Chem.*, **267,** 10931–10934.

FOTSIS, T., PEPPER, M., ADLERCREUTZ, H., FLEISCHMANN, G., HASE, T., MONTESANO, R. & SCHWEIGERER, L. (1993). Genistein, a dietary-derived inhibitor of in vitro angiogenesis. *Proc. Natl. Acad. Sci. U.S.A.*, **90,** 2690–2694.

GOTO, F., GOTO, K., WEINDEL, K. & FOLKMAN, J. (1993). Synergistic effects of vascular endothelial growth factor and basic fibroblast growth factor on the proliferation and cord formation of bovine capillary endothelial cells within collagen gels. *Lab. Invest.*, **69,** 508–517.

HU, D.E. & FAN, T.-P.D. (1992). Anti-angiogenic action of suramin and hydrocortisone in rats. *Br. J. Pharmacol.*, **107,** 163P.

HU, D.E. & FAN, T.-P.D. (1993). [Leu^8]des-Arg^9-bradykinin inhibits the synergistic interaction between bradykinin and interleukin-1 in angiogenesis. *Br. J. Pharmacol.*, **109,** 14–17.

HU, D.E. & FAN, T.-P.D. (1994a). Suramin inhibits the angiogenic activity of vascular endothelial growth factor *in vivo*. *Br. J. Pharmacol.*, **112,** 581P.

HU, D.E. & FAN, T.-P.D. (1994b). Involvement of protein kinase C in cytokine-induced angiogenesis in the rat. *Br. J. Pharmacol.*, **111,** 269P.

HU, D.E. & FAN, T.-P.D. (1995). The protein kinase C inhibitor calphostin C prevents cytokine-induced angiogenesis in the rat. *Inflammation*, **19,** (in press).

HU, D.E., HORI, Y., PRESTA, M., GRESHAM, G.A. & FAN, T.-P.D. (1994). Inhibition of angiogenesis by IL-1 receptor antagonist and selected cytokine antibodies. *Inflammation*, **18,** 45–58.

KAWAKAMI, T., INAGAKI, N., TAKEI, M., FUKAMACHI, H., COGGESHALL, K.M., ISHIZAKA, K. & ISHIZAKA, T. (1992). Tyrosine phosphorylation is required for mast cell activation by FcεRI cross-linking. *J. Immunol.*, **148,** 3513–3519.

KENDALL, R.L. & THOMAS, K.A. (1993). Inhibition of vascular endothelial cell growth factor activity by an endogenously encoded soluble receptor. *Proc. Natl. Acad. Sci. U.S.A.*, **90,** 10705–10709.

KIM, K.J., LI, B., WINER, J., ARMANINI, M., GILLETT, N., PHILLIPS, H.S. & FERRARA, N. (1993). Inhibition of vascular endothelial growth factor-induced angiogenesis suppresses tumour growth in vivo. *Nature*, **362,** 841–844.

KOPP, R. & PFEIFFER, A. (1990). Suramin alters phosphoinositide synthesis and inhibits growth factor receptor binding in HT-29 cells. *Cancer Res.*, **50,** 6490–6496.

KOWALSKI, J., KWAN, H.H., PRIONAS, S.T., ALLISON, A.C. & FAJARDO, L.F. (1992). Characterization and applications of the disc angiogenesis system. *Exp. Mol. Path.*, **56,** 1–19.

LA ROCCA, R.V., STEIN, C.A. & MYERS, C.E. (1990). Suramin: prototype of a new generation of antitumour compounds. *Cancer Cells*, **2,** 106–115.

MAYHEW, T.M. & SHARMA, A.K. (1984). Sampling schemes for estimating nerve fibre size. II. methods for nerve trunks of mixed fascicularity. *J. Anat.*, **139,** 45–58.

MILLAUER, B., WIZIGMANN-VOOS, S., SCHNURCH, H., MARTINEZ, R., MOLLER, N.P.H., RISAU, W. & ULLRICH, A. (1993). High affinity VEGF binding and developmental expression suggest Flk-1 as a major regulator of vasculogenesis and angiogenesis. *Cell*, **72,** 835–846.

MYERS, C.E., LA ROCCA, R.V., COOPER, M.R., DANESI, R., JAMISDOW, C.A., STEIN, C.A. & LINEHAN, W.M. (1990). Role of suramin in cancer biology and treatment. In *Molecular Foundations of Oncology*. ed. Broder, S. pp. 419–431. Baltimore: Williams & Wilkins.

ODELL, T.F., KANDEL, E.R. & GRANT, S.G.N. (1991). Long-term potentiation in the hippocampus is blocked by tyrosine kinase inhibitors. *Nature*, **353,** 558–560.

OIKAWA, T., HIROTANI, K., SHIMAMURA, M., ASHINO-FUSE, H. & IWAGUCHI, T. (1989). Powerful antiangiogenic activity of herbimycin A (named angiostatic antibiotic). *J. Antibiotics*, **42,** 1202–1204.

OLANDER, J.V., CONNOLLY, D.T. & DELARCO, J.E. (1991). Specific binding of vascular permeability factor to endothelial cells. *Biochem. Biophys. Res. Commun.*, **175,** 68–76.

ONODA, T., IINUMA, H., SASAKI, Y., HAMADA, M., ISSHIKI, K. & NAGANAWA, H. (1989). Isolation of a novel tyrosine kinase inhibitor, lavendustin A, from *Streptomyces griseolavendus*. *J. Nat. Prod.*, **52,** 1252–1257.

ONODA, T., ISSHIKI, K., TAKEUCHI, T., TATSUTA, K. & NAGANAWA, H. (1990). Inhibition of tyrosine kinase and epidermal growth factor receptor internalization by lavendustin A methyl ester in cultured A431 cells. *Drugs Exp. Clin. Res.*, **16,** 249–253.

PEPPER, M.S., FERRARA, N., ORCI, L. & MONTESANO, R. (1992). Potent synergism between vascular endothelial growth factor and basic fibroblast growth factor in the induction of angiogenesis in vitro. *Biochem. Biophys. Res. Commun.*, **189,** 824–831.

PLATE, K.H., BREIER, G., MILLAUER, B., ULLRICH, A. & RISAU, W. (1993). Up-regulation of vascular endothelial growth factor and its cognate receptors in a rat glioma model of tumor angiogenesis. *Cancer Res.*, **53,** 5822–5827.

PLATE, K.H., BREIER, G.H.A., WEICH, H.A. & RISAU, W. (1992). Vascular endothelial growth factor is a potential tumour angiogenesis factor in human gliomas in vivo. *Nature*, **359,** 845–847.

REILLY, T.M., TAYLOR, D.S., HERBLIN, W.F., THOOLEN, M.J., CHIU, A.T., WATSON, D.W. & TIMMERMANS, P.B.M.W.M. (1989). Monoclonal antibodies directed against basic fibroblast growth factor which inhibit its biological activity in vitro and in vivo. *Biochem. Biophys. Res. Commun.*, **164,** 736–743.

SENGER, D.R., WATER, L.V.D., BROWN, L.F., NAGY, J.A., YEO, N.K.T., YEO, T.K., BERSE, B., JACKMAN, R.W., DVORAK, A.M. & DVORAK, H.F. (1993). Vascular permeability factor (VPF, VEGF) in tumour biology. *Cancer Metastasis Rev.*, **12,** 303–324.

TAKANO, S., GATELY, S., ENGELHARD, H., TSANACLIS, A.M.C., GROSS, J.L., HERBLIN, W.F., EIDSVOOG, K., NEVILLE, M. & BREM, S. (1993). Angiosuppressive and antiproliferative actions of suramin: a growth factor antagonist. In *Growth Factors, Peptides, and Receptors*. ed. Moody, T.W. pp. 255–264. New York: Plenum Press.

TERMAN, B.I., DOUGHER-VERMAZEN, M., CARRION, M.E., DIMITROV, D., ARMELLINO, D.C., GOSPODAROWICZ, D. & BOHLEN, P. (1992). Identification of the KDR tyrosine kinase as a receptor for vascular endothelial-cell growth factor. *Biochem. Biophys. Res. Commun.*, **187,** 1579–1586.

WHITE, C.W., SONDHEIMER, H.M., CROUCH, E.C., WILSON, H. & FAN, L.L. (1989). Treatment of pulmonary hemangiomatosis with recombinant interferon alfa-2a. *N. Engl. J. Med.*, **320,** 1197–1200.

(Received May 23, 1994
Revised September 22, 1994
Accepted September 29, 1994)

British Journal of Pharmacology (1995) 114, 269-274 © 1995 Stockton Press All rights reserved 0007-1188/95 $9.00

5-HT_3 receptor antagonism by anpirtoline, a mixed 5-HT_1 receptor agonist/5-HT_3 receptor antagonist

[1]M. Göthert, *M. Hamon, M. Barann, H. Bönisch, *H. Gozlan, *R. Laguzzi, †P. Metzenauer, †B. Nickel & †I. Szelenyi

Inst. Pharmacol. Toxicol., Univ. Bonn, Reuterstr. 2b, D-53113 Bonn, Germany; *INSERM U288, Fac. Méd. Pitié-Salpétrière, 91 boulevard de l'Hôpital, 75634 Paris Cedex 13, France and †Dept. Pharmacol., ASTA Medica AG, POB 100105, D-60001, Frankfurt/M., Germany

1 The aim of this study was to provide evidence that anpirtoline, which is an agonist at 5-HT_{1B} and 5-HT_{1D} receptors and also displays submicromolar affinity for 5-HT_{1A} recognition sites, in addition, acts as an antagonist at 5-HT_3 receptors.

2 In radioligand binding studies on rat brain cortical membranes, anpirtoline inhibited specific binding of [^{3}H]-(S)-zacopride to 5-HT_3 receptor recognition sites (pK_i: 7.53).

3 In N1E-115 neuroblastoma cells in which [^{14}C]-guanidinium was used as a tool to measure cation influx through the 5-HT_3 receptor channel, the 5-HT-induced influx was concentration-dependently inhibited by anpirtoline. In this respect, anpirtoline mimicked other 5-HT_3 receptor antagonists; the rank order of potency was ondansetron > anpirtoline > metoclopramide.

4 The concentration-response curve for 5-HT as a stimulator of [^{14}C]-guanidinium influx was shifted to the right by anpirtoline (apparent pA_2: 7.78).

5 In urethane-anaesthetized rats, anpirtoline inhibited (at lower potency than zacopride and tropisetron) the 5-HT- or phenylbiguanide-induced bradycardia (Bezold-Jarisch reflex), but did not induce this reflex by itself.

6 Intravenous infusion of cisplatin in the domestic pig caused a consistent emetic response which was antagonized by anpirtoline.

7 It is concluded that anpirtoline, which was previously characterized as a 5-HT_1 receptor agonist also proved to be a 5-HT_3 receptor antagonist in several experimental models and, hence, exhibits a unique pattern of properties at different 5-HT receptors.

Keywords: Anpirtoline; 5-hydroxytryptamine receptors; antiemetic effect; domestic pig; 5-HT_3 receptors; [^{14}C]-guanidinium influx

Introduction

Anpirtoline is a novel drug with antinociceptive and antidepressant-like actions in rodents (Schlicker *et al.*, 1992; Swedberg *et al.*, 1992); furthermore, it has been shown to act as an agonist at 5-HT_{1B} and (at lower potency) 5-HT_{1D} receptors and to display submicromolar affinity not only for 5-HT_{1B} but also for 5-HT_{1A} recognition sites in rat brain membranes (Schlicker *et al.*, 1992). Due to the 5-HT_{1B} and 5-HT_{1D} character of the presynaptic 5-HT autoreceptors in the rat and pig brain, respectively, the drug inhibited the electrically evoked [^{3}H]-5-HT release from the 5-hydroxytryptaminergic nerve terminals contained in superfused cortical slices from these species and it was 22 times more potent in rat than in porcine cortical slices. The antinociceptive and antidepressant-like activities of anpirtoline in rats and mice are probably elicited by its agonist effect at 5-HT_{1A} and 5-HT_{1B} receptors (Schlicker *et al.*, 1992).

In addition to the neuropsychopharmacological properties mentioned so far, anpirtoline exhibited an anxiolytic-like potential: in a mouse light/dark aversion test, it reduced the aversive response of mice (Metzenauer *et al.*, 1992). This test is known to be sensitive to both classical (i.e. benzodiazepines) and novel anxiolytic agents such as 5-HT_{1A} receptor agonists and 5-HT_3 receptor antagonists (Costall *et al.*, 1989). Therefore, the possibility had to be considered that anpirtoline might produce the reduction of aversive response not only by acting as an agonist at 5-HT_{1A} receptors but also by an antagonistic property at 5-HT_3 receptors. The aim of the present investigation was to examine this possibility in classical *in vitro* and *in vivo* models as well as in a newly developed assay for antiemetic properties of drugs in the domestic pig (Szelenyi *et al.*, 1994). A preliminary account of the present data has been given at the 2nd International Symposium on 'Serotonin, from Cell Biology to Therapeutics', Houston 1992 (Szelenyi *et al.*, 1992).

[1] Author for correspondence at Bonn address.

Methods

In vitro *studies*

Radioligand binding assays Adult male Sprague-Dawley rats were killed by decapitation and membranes from pooled entorhinal cortices were prepared as described elsewhere (Bolaños *et al.*, 1990). The membranes were incubated for 30 min at 30°C in 0.025 M Tris-HCl, pH 7.4, supplemented with 154 mM NaCl and 0.6 nM [^{3}H]-(S)-zacopride (specific activity: 83 Ci mmol^{-1}; Synthélabo, Rueil-Malmaison, France); the total volume was 0.5 ml. Nonspecific binding, measured in the presence of a saturating concentration (10 μM) of the 5-HT_3 receptor antagonist, tropisetron, corresponded to 45% of total binding. Further details are given elsewhere (Bolaños *et al.*, 1990).

The inhibition of the specific binding of [^{3}H]-(S)-zacopride by anpirtoline, ondansetron and MDL 72222 was examined with 10 different concentrations of the respective drugs, between 0.1 nM and 10 μM. Calculations of IC_{50} and apparent Hill coefficient values were performed as described by McPherson (1983). The equation of Cheng & Prusoff (1973) was used for converting the IC_{50}s into K_is.

Proteins were determined according to the method of Lowry *et al.* (1951) with bovine serum albumin as the standard.

Effects on 5-HT$_3$ receptor channels Mouse neuroblastoma cells of the clone N1E-115 (Amano *et al.*, 1972) at passage numbers 40–50 were grown in Dulbecco's modified Eagle medium supplemented with 10% foetal calf serum (Gibco; for further details of the composition of the culture medium, see Bönisch *et al.*, 1993). Cells were cultured in a humidified atmosphere containing 5% CO_2 at 37°C in vent flasks (Nunc. 750 ml) and fed every third day. Three days before starting experiments, cells were subcultured in 24-well cell culture clusters (Falcon).

Influx of [^{14}C]-guanidinium was studied under two different ionic conditions (buffer A and buffer B). Both were previously shown to be suitable for such investigations, but each exhibited certain advantages and disadvantages compared with the other (see Results and Discussion). Buffer A (previously used by Reiser & Hamprecht, 1989 and Emerit *et al.*, 1993 in NG 108-15 neuroblastoma cells) was composed as follows (in mM): HEPES 20, NaCl 135, KCl 4.5, $MgCl_2$ 1.0, Na_2HPO_4 2.0 and D-glucose. Buffer B (from Reith, 1990; Bönisch *et al.*, 1993) had the following composition (in mM): HEPES-Tris (pH 7.4) 25, choline chloride 135, KCl 5.4, $MgSO_4$ 0.98 and D-glucose 5.5.

The cells were washed and then preincubated for 20 min (1.5 ml per well) with one of these buffers (20°C) containing either no further drug (control) or the drug under investigation. Subsequently, the cells were incubated for 2 min with the respective buffer (A or B) containing 5 μM [^{14}C]-guanidinium chloride (specific activity 59 mCi mmol^{-1}; CEA) in the absence or presence of the drug under study plus, when relevant, 5-HT as stimulant drug. In the experiments with buffer A, substance P (10 μM) was applied simultaneously with 5-HT (see Reiser *et al.*, 1989; Emerit *et al.*, 1993). After termination of incubation (for details, see Bönisch *et al.*, 1993), the cells were dissolved in 0.5 ml 0.1% Triton X-100 and the [^{14}C]-guanidinium content of this solution was determined by liquid scintillation counting. An aliquot of the cell lysate was used for determination of the protein content according to the method of Lowry *et al.* (1951); the mean protein content per well was 218 ± 38 μg ($n = 68$). All experiments were carried out in duplicate or triplicate.

The apparent pA_2 values for anpirtoline against 5-HT was calculated according to Furchgott (1972).

In vivo *studies*

Bezold Jarisch reflex Adult male Sprague-Dawley rats (250–350 g) were anaesthetized with urethane (1.4 g kg^{-1}, i.p.), and a tracheotomy was performed to insert an endotracheal tube. A catheter (0.3 mm internal diameter) was inserted into the abdominal aorta via the femoral artery in order to record the arterial pressure and heart rate. A femoral vein was exposed and cannulated for i.v. drug administrations. 5-HT or the selective 5-HT$_3$ receptor agonist, phenylbiguanide, was injected at a dose of 30 μg kg^{-1} as a bolus in order to induce bradycardia (Bezold-Jarisch reflex).

Emesis by cisplatin Details of the induction of emesis by cisplatin and the evaluation of antiemetic drugs in the domestic pig have been described elsewhere (Szelenyi *et al.*, 1994). Briefly, 12–15 week-old domestic pigs of either sex (28–40 kg; on average about 30 kg in each of the various treatment groups) were housed in individual boxes of about 10 m^2 with warmed acryl-coated floor. They were maintained under constant environmental conditions (temperature 22 ± 1°C; humidity 50–60%; light/dark-rhythm (12/12 h). They received standardized pellet food for breeding pigs (hemo-Schweinefutter, Hemo, Heilbronn, Germany) twice daily (08 h 00 min and 14 h 00 min). Water was available *ad libitum*. On the day of the experiment (at 09 h 00 min), they were anaesthetized with ketamine 10 mg kg^{-1}, i.m. and xylazine 2 mg kg^{-1}, i.m., and a cannula was inserted into a superficial vein on one of the extremities. Cisplatin was administered intravenously with a total administration time of 15 min. Anpirtoline was given intravenously 15 min prior to cisplatin infusion. After removal of the cannula, the animals were placed in their boxes for recovery from anaesthesia (on an average, 30 min) and for subsequent observation of emesis (during 24 h). Food and water were available *ad libitum*. Emesis was characterized by expulsion of solid and/or liquid material from the gastrointestinal tract (ingested food, gastric juice contaminated by bile, etc.).

Statistical analysis

Results are given as means ± s.e.mean. For comparison of mean values, Student's *t* test was used.

Drugs

Anpirtoline HCl and cisplatin were synthetized by the Department of Chemical Research, ASTA Medica AG, Frankfurt, Germany. In addition, the following drugs were used: tropisetron (formerly ICS 205 930; Sandoz, Basel, Switzerland); ondansetron HCl (Glaxo, Greenford, Middlesex, UK), MDL 72222 (1αH, 3α, 5αH-tropan-3yl-3,5-dichlorobenzoate; Marion Merrell-Dow, Strasbourg, France); zacopride HCl (Synthélabo, Rueil-Malmaison, France, or Research Biochemical Inc., Natick, MA, U.S.A.); 5-hydroxytryptamine creatinine sulphate (5-HT; Merck, Darmstadt, Germany); phenylbiguanide (1-phenylbiguanide; Aldrich, Steinheim, Germany); substance P (SP), metoclopramide, urethane (Sigma, Deisenhofen, Germany). Stock solutions were prepared with dimethylsulphoxide (tropisetron, MDL 72222, metoclopramide) or saline (other drugs); in the case of cisplatin, solution in saline at 70–75°C was followed by gradual cooling to room temperature. The solvents, which were applied in the corresponding control experiments, did not affect the parameters investigated. Ketamine (Ketavet, Parke-Davis, Freiburg, Germany) and xylazine (Rompun, Bayer, Leverkusen, Germany) were used in their commercial form.

Results

Receptor binding studies

Competition experiments with [^{3}H]-(S)-zacopride to label 5-HT$_3$ receptor binding sites in membranes from the rat entorhinal cortex revealed that anpirtoline was a potent inhibitor of the specific binding of the radioligand (Figure 1). The pK_i value of anpirtoline was 7.53 ± 0.13 (Hill coefficient: 0.85 ± 0.10; $n = 3$). Comparison with typical 5-HT$_3$ receptor antagonists indicated that anpirtoline was slightly more potent than MDL 72222 ($pK_i = 7.31 \pm 0.11$; $n = 3$), but less potent than ondansetron ($pK_i = 8.50 \pm 0.09$; $n = 3$; Figure 1).

Effects on 5-HT$_3$ receptor channels

N1E-115 neuroblastoma cells were used to measure [^{14}C]-guanidinium influx through the 5-HT$_3$ receptor channel. When experiments were carried out with buffer A (see Methods), 5-HT induced only a weak influx of [^{14}C]-guanidinium (Reiser & Hamprecht, 1989; Emerit *et al.*, 1993). However, this response was potentiated by substance P (SP), 10 μM, which given alone caused only negligible [^{14}C]-guanidinium influx (Reiser & Hamprecht, 1989; Emerit *et al.*, 1993). Anpirtoline (up to 3 μM), ondansetron (up to 100 nM) and metoclopramide (up to 10 μM) by themselves did not induce [^{14}C]-guanidinium influx, but they caused a

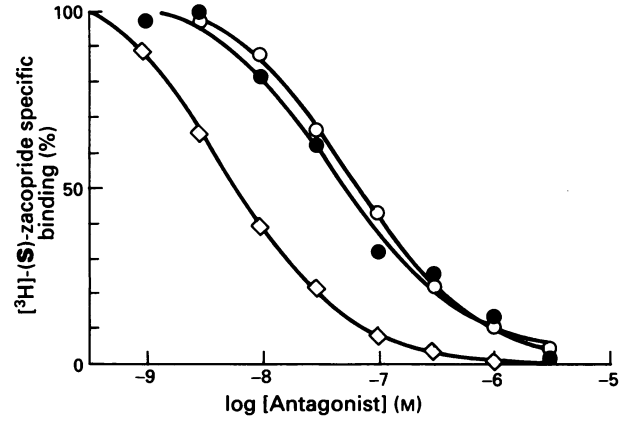


Figure 1 Concentration-dependent inhibition by anpirtoline (●), ondansetron (◇) and MDL 72222 (○) of the specific binding of [^{3}H]-(S)-zacopride (0.6 nM) to 5-HT$_3$ sites in membranes of rat entorhinal cortex. Non-specific binding was determined in the presence of 10 μM tropisetron. Each point is the mean of triplicate determinations in a typical experiment (100% corresponds to 13.2 fmol [^{3}H]-(S)-zacopride specifically bound mg^{-1} membrane protein). This experiment was repeated 3 times for the calculation of pK_i values indicated in the text.

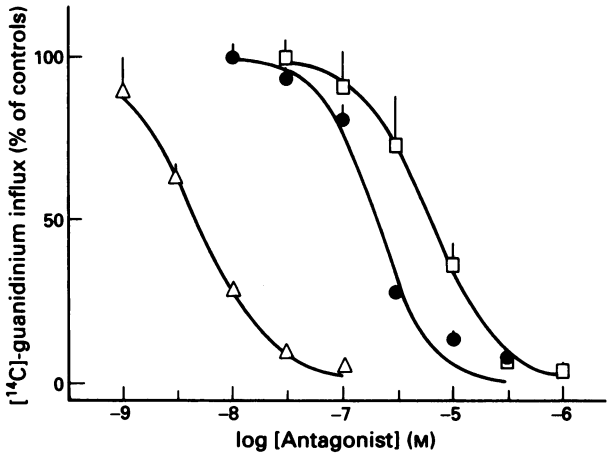


Figure 2 Inhibition of influx of [^{14}C]-guanidinium induced by 5-hydroxytryptamine (5-HT, 10 μM) plus substance P (SP, 10 μM) in N1E-115 cells by anpirtoline (●) in comparison to ondansetron (Δ) and metoclopramide (□). Each antagonist was present for 20 min before and during the 2-min exposure to 5-HT plus SP. The responses are expressed as percentages of the effect elicited by 10 μM 5-HT plus 10 μM SP in parallel control experiments carried out in the absence of antagonists. All experiments were performed with buffer A (see Methods). Each point is the mean with s.e.mean of 3 experiments.

concentration-dependent inhibition of the influx evoked by 10 μM 5-HT plus 10 μM SP (Figure 2). At the highest concentration applied, they virtually abolished evoked influx. The pK_i values for anpirtoline, ondansetron and metoclopramide calculated from the pIC_{50} values (see the concentration-response curves shown in Figure 2) were 7.44 ± 0.23, 9.31 ± 0.06 and 7.21 ± 0.18, respectively. 5-HT applied at increasing concentrations in the presence of 10 μM SP caused a concentration-dependent increase in [^{14}C]-guanidinium influx (Figure 3). The concentration-response curve for 5-HT (EC_{50}: 1.20 ± 0.14 μM) was concentration-dependently shifted to the right by anpirtoline (mean apparent pA_2: 7.78; Figure 3).

In experiments performed with buffer B, 5-HT induced a pronounced [^{14}C]-guanidinium influx even in the absence of SP (Bönisch *et al.*, 1993). This response was resistant to tetrodotoxin but susceptible to blockade by 5-HT$_3$ receptor antagonists at concentrations higher than those required in experiments with buffer A or in experiments on other 5-HT$_3$ receptor models (Bönisch *et al.*, 1993). In agreement with these findings, anpirtoline, ondansetron and metoclopramide concentration-dependently inhibited the 5-HT-induced [^{14}C]-guanidinium influx at lower potency than in the experiments with buffer A (results not shown). The pK_i values (6–8 experiments) for anpirtoline, ondansestron and metoclopramide were 6.60 ± 0.10, 7.38 ± 0.07 and 5.49 ± 0.01, respectively; hence, the rank order of potency of the three compounds was identical to that found with buffer A (see above). In the experiments with buffer B, we also found a rightward shift by anpirtoline (3 μM; 6 experiments) of the concentration-response curve for 5-HT (6 control experiments) as a stimulator of [^{14}C]-guanidinium influx (apparent pA_2: 6.27; result not shown).

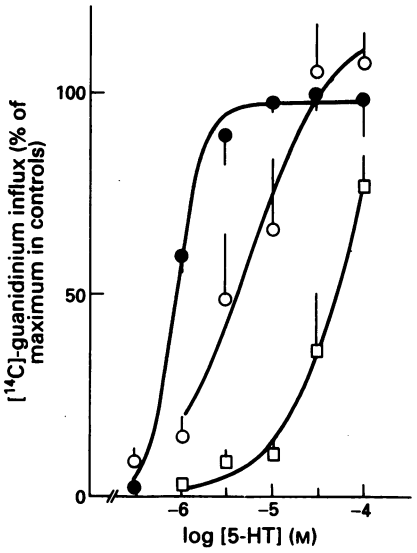


Figure 3 Concentration-response curves for the 5-hydroxytryptamine (5-HT; plus 10 μM substance P, SP)-induced influx of [^{14}C]-guanidinium in N1E-115 cells in the absence (●) or presence of 0.1 μM (○) or 1 μM anpirtoline (□). Anpirtoline was present for 20 min before and during 2-min exposure to 5-HT plus SP. The responses are expressed as percentages of the maximum effect elicited by 30 μM 5-HT plus 10 μM SP) in the absence of anpirtoline. Each point is the mean with s.e.mean of 6 experiments carried out with buffer A (see Methods).

Inhibition of Bezold-Jarisch reflex

Under control conditions, the heart rate of urethane-anaesthetized rats was in the range of 300–350 beats min^{-1}. 5-HT and phenylbiguanide (used as agonists in the laboratories in Paris and Frankfurt/M, respectively) at the submaximally effective dose of 30 μg kg^{-1} induced an immediate decrease in heart rate by 72.4 ± 6.3% (n = 13) and 63.4 ± 7.7% (n = 6), respectively; this effect lasted only for a few seconds. The bradycardia was reproducible when these 5-HT receptor agonists were repeatedly injected (up to five times) at intervals of 10 min (results not shown).

Anpirtoline, zacopride, tropisetron and MDL 72222, given alone did not cause a change in heart rate. However, 5 to 30 min after intravenous injection, all 5-HT$_3$ receptor antagonists dose-dependently inhibited the 5-HT- and/or phenylbiguanide-induced bradycardia (most results not shown; as a representative example, Figure 4 illustrates the decrease of 5-HT-induced bradycardia 5 min after injection of zacopride or anpirtoline). The doses of zacopride and anpirtoline which 5 min after injection induced 50% inhibition of the bradycardic response (ID_{50}) to 5-HT were 0.25 and 13.3 μg kg^{-1}, respectively. When a 15-min interval elapsed between the injection of either zacopride or anpirtoline and that of 5-HT,

the ID_{50} values of the 5-HT$_3$ receptor antagonists were 0.35 and 42.7 $\mu g\,kg^{-1}$, respectively. Anpirtoline also inhibited the phenylbiguanide-induced bradycardia (determined 5, 15 and 30 min after injection; ID_{50}: 3.6, 13.6 and 33.6 $\mu g\,kg^{-1}$, respectively), and this property was shared by tropisetron (ID_{50} determined 15 and 30 min after injection: 2.4 and 2.7 $\mu g\,kg^{-1}$, respectively) and MDL 72222 (ID_{50} determined 5, 15 and 30 min after injection: 28.1, 51.3 and 67.7 $\mu g\,kg^{-1}$, respectively). After 15 min of exposure, the ratios of the potencies of zacopride, tropisetron and MDL 72222 in antagonizing the 5-HT or phenylbiguanide-induced bradycardia related to the corresponding potency of anpirtoline were 0.008, 0.176 and 3.77, respectively.

Antiemetic effect

After cisplatin infusion at a dose of 2 mg kg^{-1} within 15 min in the domestic pig, emesis was induced in all animals. This dose of cisplatin corresponds roughly to the usual therapeutic dose in man. In the control experiments, the average number of vomits was 10.3 per pig within the first 4 h period (Figure 5). In the subsequent 20 h, the emetic response to cisplatin was clearly less: on the average, only about four further vomits were observed (see difference between open and closed circles in Figure 5), yielding a total number of 14.2 vomits during the whole observation period of 24 h.

Anpirtoline which was injected at doses of 1–10 mg per pig (about 0.033–0.33 mg kg^{-1} on the average) produced a dose-dependent inhibition of the cisplatin-evoked emesis in the first 4-h period after infusion of the anticancer drug (Figure 5). In the subsequent 20 h, the number of vomits was not significantly decreased compared to the control experiments: the difference between the open and closed circles in Figure 5 was 3–6 vomits after each dose of anpirtoline investigated. However due to the pronounced antiemetic effect in the first 4 h, anpirtoline 5 and 10 mg significantly decreased the total number of vomits in the whole 24-h period of observation.

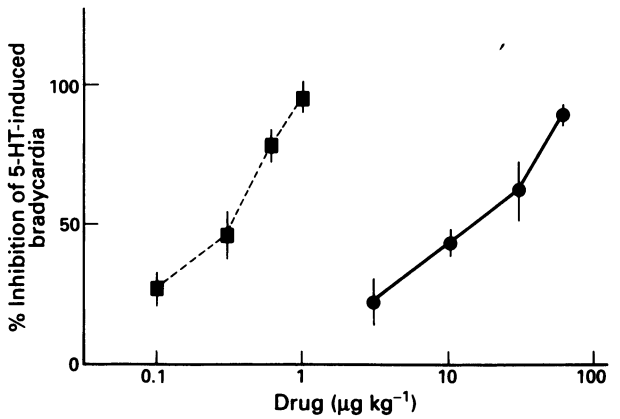


Figure 4 Inhibitory effect of anpirtoline (●) and zacopride (■) on the 5-hydroxytryptamine (5-HT; 30 $\mu g\,kg^{-1}$, i.v.)-induced bradycardia in urethane-anaesthetized rats, determined 5 min after i.v. injection of the respective antagonist. Each point is the mean with s.e.mean of 4–6 experiments.

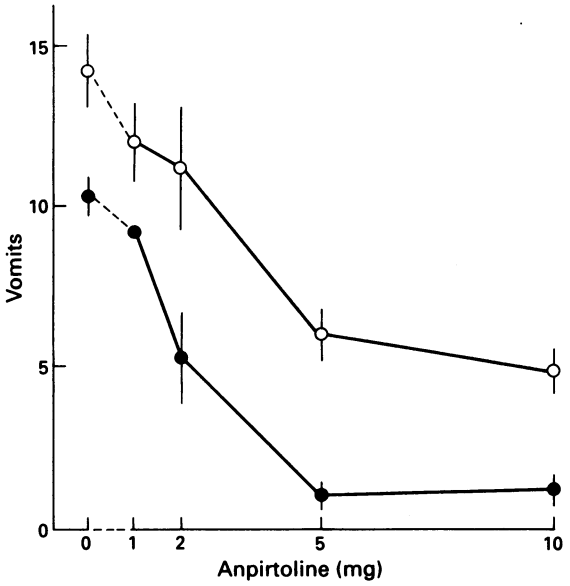


Figure 5 Emesis induced within the first 4 h (●) and 24 h (○) following i.v. infusion of cisplatin and antagonism by anpirtoline. Pigs were treated with the latter drug (i.v. injection) 15 min prior to cisplatin-infusion (2 mg kg^{-1}). The doses of anpirtoline indicated are those per animal (average body weight: 30.2 ± 1.3 kg). Each point represents the mean number of vomits per animal with s.e.mean (3–11 pigs per dose) during the respective observation period. Anpirtoline significantly (at least $P<0.05$, compared to the respective controls) decreased the number of vomits both in the first 4 h (in the dose-range of 2–10 mg) and in the whole 24 h period (at the doses of 5 and 10 mg) after infusion of cisplatin.

Discussion

The present experiments provided evidence that anpirtoline, in addition to its properties as a ligand at 5-HT$_{1A}$, 5-HT$_{1B}$ and 5-HT$_{1D}$ receptors (Schlicker *et al.*, 1992), acts as an antagonist at 5-HT$_3$ receptors. The latter belong to the superfamily of ligand-gated ion channels and they are almost exclusively located on neurones (Kilpatrick *et al.*, 1990; Hoyer, 1990; Maricq *et al.*, 1991). An exception to this rule is the enterochromaffin cell which, at least in the guinea-pig small intestine, also appears to be endowed with 5-HT$_3$ receptors (Gebauer *et al.*, 1993). The antagonistic property of anpirtoline at 5-HT$_3$ receptors can be derived from its abilities (1) to displace at intermediate nanomolar affinity [^{3}H]-S-zacopride from 5-HT$_3$ recognition sites in membranes of rat entorhinal cortex and (2) to counteract specific effects which are known to be mediated by 5-HT$_3$ receptors in classical and newly developed *in vitro* and *in vivo* assay systems. In particular, anpirtoline inhibited the [^{14}C]-guanidinium influx, in N1E-115 neuroblastoma cells (Reiser *et al.*, 1989; Emerit *et al.*, 1993; Bönisch *et al.*, 1993), the Bezold-Jarisch reflex in rats (Fozard, 1984; McQueen & Mir, 1989) and the cisplatin-induced emesis in the domestic pig (in this species, this represents a novel assay for evaluation of antiemetic drugs; Szelenyi *et al.*, 1994). The potency of anpirtoline in these test systems was less than that of zacopride, tropisetron, and ondansetron but higher than that of metoclopramide, and it was in a similar range to that of MDL 72222.

Previously published results of competition experiments using radioligands for the specific labelling of 5-HT$_{1A}$, 5-HT$_{1B}$ and 5-HT$_2$ recognition sites revealed that anpirtoline also bound to these 5-HT receptor types in the rat brain (Schlicker *et al.*, 1992). The drug exhibited the lowest affinity for cortical 5-HT$_2$ sites ($pK_i = 5.83$), its affinity for hippocampal 5-HT$_{1A}$ sites was intermediate ($pK_i = 6.82$), and it had approximately the same high affinity for striatal 5-HT$_{1B}$ sites ($pK_i = 7.55$) as found here for entorhinal cortical 5-HT$_3$ sites ($pK_i = 7.53$).

[^{14}C]-guanidinium is a suitable tool to study cation influx through the 5-HT$_3$ receptor channel in certain cell lines. This has first been shown in experiments with incubation buffer containing 135 mM Na^+ (as buffer A of the present experiments) in NG 108-15 cells by Reiser & Hamprecht (1989) and Emerit *et al.* (1993) and was recently confirmed in N1E-115 cells by Barann *et al.* (1993). Thus, 5-HT receptor agonists induced [^{14}C]-guanidinium influx and 5-HT receptor antagonists counteracted this effect at potencies similar to

those found in other 5-HT$_3$ receptor models. However, as already mentioned above, the disadvantage of this ionic condition was that stimulation with 5-HT had to be carried out in the presence of SP in order to obtain a reliably high [^{14}C]-guanidinium influx (Reiser & Hamprecht, 1989; Emerit *et al.*, 1993; Barann *et al.*, 1993). Conversely, under the ionic conditions applied by Reith (1990) and Bönisch *et al.* (1993), in which Na^+ was omitted and replaced by cholinium$^+$, a reasonably high influx of [^{14}C]-guanidinium could be induced without SP as an auxiliary drug, but the disadvantage was that the potencies of 5-HT receptor agonists and antagonists were 1–1.5 log units lower than in other 5-HT$_3$ receptor models. Under both ionic conditions, the involvement of 5-HT$_3$ receptors was beyond doubt, but the mechanisms underlying the interaction of SP with 5-HT$_3$ receptors and the decrease in potency of 5-HT$_3$ receptor agonists and antagonists by omission of Na^+ are unknown. On the basis of those previous results, one would expect that in the experiments with buffer A containing 135 mM Na^+ and with 5-HT plus SP as a stimulus, the pK_i and pA_2 values of anpirtoline should be in the same range as its affinity for 5-HT$_3$ receptors in entorhinal cortical membranes, whereas in the experiments with buffer B (absence of Na^+ ions and SP), these values should be 1–1.5 log units lower. In fact, this was observed in the present study, indicating that anpirtoline acts as a 5-HT$_3$ receptor antagonist in this 5-HT$_3$ receptor model.

Zacopride, tropisetron, MDL 72222 and anpirtoline, when injected in rats 5–30 min before 5-HT or the preferential 5-HT$_3$ receptor agonist, phenylbiguanide, inhibited the Bezold-Jarisch reflex. This reflex is initiated in the rat by activation of 5-HT$_3$ receptors on vagal afferents projecting the autonomic nuclei in the medulla oblongata (Sanger, 1992); in this brain area, an increased activity of the parasympathetic nerve fibres supplying the sinus node is induced, finally leading to a decrease in heart rate (McQueen & Mir, 1989; Sanger, 1992). Anpirtoline was slightly more potent in inhibiting the phenylbiguanide-induced bradycardia than that evoked by 5-HT, and this may be related to slight differences in the potencies of these agonists. However, the series of experiments with 5-HT and phenylbiguanide resembled each other in that the potency of anpirtoline in antagonizing the response to either agonist declined by a factor of about 3.5 (in detail 3.2 with 5-HT and 3.8, respectively, with phenylbiguanide) from the 5th to the 15th min after injection of anpirtoline. The potency of anpirtoline in antagonizing the response to phenylbiguanide further decreased from the 15th to the 30th min by a factor of 2.5. In contrast, only very slight time-dependent decreases in potency occurred when zacopride, tropisetron and MDL 72222 were applied. These findings suggest that the 5-HT$_3$ receptor antagonistic properties of anpirtoline were of shorter duration than those of the latter drugs.

Investigations carried out in the domestic pig revealed that this species is suitable for evaluating the emetogenic property of anticancer drugs and the ability of certain compounds to counteract this effect (Szelenyi *et al.*, 1994). Evidence has accumulated that 5-HT plays a crucial role in the mechanisms underlying vomiting and nausea induced by anticancer drugs (Fozard, 1987; Andrews *et al.*, 1988; Leslie & Reynolds, 1991; Schwörer *et al.*, 1991; Mitchelson, 1992; Sanger, 1992). The antiemetic properties of selective 5-HT$_3$ receptor antagonists were proved by a large number of experiments with cisplatin and other anti-cancer treatments (Aapro, 1991). In more detail, prevention of cisplatin-induced emesis has been demonstrated using, e.g. tropisetron, granisetron, ondansetron, zacopride and MDL 72222 in ferrets (Costall *et al.*, 1986; 1987; Stables *et al.*, 1987; Sanger, 1992). Investigations in the domestic pig confirmed the antiemetic effect of these 5-HT$_3$ receptor antagonists in these animals treated with a cisplatin dose of 2 mg kg^{-1} (Szelenyi *et al.*, 1994). This dose proved to be most suitable, because it consistently induced emetic responses without other toxic signs in the 24 h following its infusion. In agreement with the 5-HT$_3$ receptor blocking property of anpirtoline (see above), we found in the present investigation in domestic pigs that this drug given in a single dose 15 min prior to cisplatin shared the antiemetic property of other 5-HT$_3$ receptor antagonists. At the doses of 5 and 10 mg, anpirtoline almost abolished vomiting in the first 4 h, whereas it did not decrease the sporadic vomiting in the subsequent 20 h. In the context of this time course, it should be noted that, as a rule, delayed emesis has been found to be resistant to 5-HT$_3$ receptor antagonism (Aapro, 1991). Accordingly, the domestic pig treated with cisplatin may represent an animal model in which delayed emesis can be studied.

In conclusion, evidence has been presented that anpirtoline exhibits a unique pattern of properties at different 5-HT receptors in that it is not only a 5-HT$_1$ receptor agonist (Schlicker *et al.*, 1992), but also acts as a 5-HT$_3$ receptor antagonist. The latter property is responsible for its antiemetic effect and may contribute to the recently demonstrated anxiolytic-like action of the drug (Metzenauer *et al.*, 1992).

This study was supported by a grant of the European Community (Biotechnology programme). The generous gifts of [^{3}H]-(S)-zacopride by L.E.R.S. Synthélabo (Rueil-Malmaison, France) and other drugs by pharmaceutical companies (Synthélabo, Glaxo, Marion Merrell-Dow, Sandoz) are gratefully acknowledged.

References

AAPRO, M.S. (1991). 5-HT$_3$ receptor antagonists. An overview of their present status and future potential in cancer therapy-induced emesis. *Drugs*, **42**, 551–568.

AMANO, T., RICHELSON, E. & NIRENBERG, P.G. (1972). Neurotransmitter synthesis by neuroblastoma clones. *Proc. Natl. Acad. Sci. U.S.A.*, **69**, 258–263.

ANDREWS, P.L.R., RAPEPORT, W.G. & SANGER, G.J. (1988). Neuropharmacology of emesis induced by anti-cancer therapy. *Trends Pharmacol. Sci.*, **9**, 334–341.

BARANN, M., RUPPERT, K., GÖTHERT, M. & BÖNISCH, H. (1993). Influence of buffer conditions on 5-HT$_3$-receptor mediated cation influx in cultured neural cell lines. *Fund. Clin. Pharmacol.*, **7**, 346.

BOLAÑOS, F.J., SCHECHTER, L.E., MIQUEL, M.C., EMERIT, M.B., RUMIGNY, J.F., HAMON, M. & GOZLAN, H. (1990). Common pharmacological and physico-chemical properties of 5-HT$_3$ binding sites in the rat cerebral cortex and NG 108-15 clonal cells. *Biochem. Pharmacol.*, **40**, 1541–1550.

BÖNISCH, H., BARANN, M., GRAUPNER, J. & GÖTHERT, M. (1993). Characterization of 5-HT$_3$ receptors of N1E-115 neuroblastoma cells by use of the influx of the organic cation [^{14}C]-guanidinium. *Br. J. Pharmacol.*, **108**, 436–442.

CHENG, Y.C. & PRUSOFF, W.H. (1973). Relationship between the inhibition constant (K_i) and the concentration of inhibitor which causes 50 percent inhibition (IC_{50}) of an enzymatic reaction. *Biochem. Pharmacol.*, **22**, 3099–3108.

COSTALL, B., DOMENEY, A.M., NAYLOR, R.J. & TATTERSALL, F.D. (1986). 5-Hydroxytryptamine M-receptor antagonism to prevent cisplatin-induced emesis. *Neuropharmacology*, **25**, 957–961.

COSTALL, B., DOMENEY, A.M., NAYLOR, R.J. & TATTERSALL, F.D. (1987). Emesis induced by cisplatin in the ferret as a model for the detection of anti-emetic drugs. *Neuropharmacology*, **26**, 1321–1326.

COSTALL, B., JONES, B.J., KELLY, M.E., NAYLOR, R.J. & TOMKINS, D.M. (1989). Exploration of mice in a black and white test box: validation as a model of anxiety. *Pharmacol. Biochem. Behav.*, **32**, 777–785.

EMERIT, M.B., RIAD, M., FATTACCINI, C.M. & HAMON, M. (1993). Characteristics of [^{14}C]guanidinium accumulation in NG 108-15 cells exposed to 5-HT$_3$ receptor ligands and substance P. *J. Neurochem.*, **40**, 2059–2067.

FOZARD, J.R. (1984). MDL-72222: a potent and highly selective antagonist at neuronal-5-hydroxytryptamine receptors. *Naunyn-Schmied. Arch. Pharmacol.*, **326**, 36–44.

FOZARD, J.R. (1987). 5-HT$_3$ receptors and cytotoxic drug-induced vomiting. *Trends Pharmacol. Sci.*, **8**, 44–45.

FOZARD, J.R. (1990). Agonists and antagonists of 5-HT$_3$ receptors. In *Cardiovascular Pharmacology of 5-Hydroxytryptamine*. ed. Saxena, P.R., Wallis, D.I., Wouters, W. & Bevan, P. pp. 101–115. Dordrecht, Boston, London: Kluwer Academic Publishers.

FURCHGOTT, R.F. (1972). The classification of adrenoceptors (adrenergic receptors). An evaluation from the standpoint of receptor theory. In *Handbook of Experimental Pharmacology*, ed. Blaschko, H. & Muscholl, E. Vol. XXXIII: pp. 283–335. Berlin: Springer Verlag.

GEBAUER, A., MERGER, M. & KILBINGER, H. (1993). Modulation by 5-HT$_3$ and 5-HT$_4$ receptors of the release of 5-hydroxytryptamine from the guinea-pig small intestine. *Naunyn-Schmied. Arch. Pharmacol.*, **347**, 137–140.

HOYER, D. (1990). Serotonin 5-HT$_3$, 5-HT$_4$, and 5-HT-M receptors. *Neuropsychopharmacology*, **3**, 371–383.

KILPATRICK. G.J., BUNCE, K.T. & TYERS, M.B. (1990). 5-HT$_3$ Receptors. *Med. Res. Rev.*, **10**, 441–475.

LESLIE, R.A. & REYNOLDS, D.J.M. (1991). The area postrema and vomiting: how important is serotonin? In *Current Aspects of the Neurosciences*. ed. Osborne, N.N. pp. 79–101. New York: The Macmillan Press.

LOWRY, O.H., ROSEBROUGH, N.J., FARR, A.L. & RANDALL, A.L. (1951). Protein measurement with the folin phenol reagent. *J. Biol. Chem.*, **193**, 265–275.

MARICQ, A.V., PETERSON, A.S., BRAKE, A.J., MYERS, R.M. & JULIUS, D. (1991). Primary structure and functional expression of the 5-HT$_3$ receptor, a serotonin-gated ion channel. *Science*, **254**, 432–437.

MCPHERSON, G.A. (1983). *Kinetics, EBDA, Ligand, Lowry. A Collection of Radioligand Binding Analysis Programs*. Cambridge, U.K.: Elsevier, Biosoft.

MCQUEEN, D.S. & MIR, A.K. (1989). 5-Hydroxytryptamine and cardiopulmonary and carotid body reflex mechanisms. In *The Peripheral Actions of 5-Hydroxytryptamine*. ed. Fozard, J.R. pp. 301–326. Oxford, New York, Tokyo: Oxford University Press.

METZENAUER, P., BARNES, N.M., COSTALL, B., GOZLAND, H., HAMON, M., KELLY, M.E., MURPHY, D.A. & NAYLOR, R.I. (1992). Anxiolytic-like actions of anpirtoline in a mouse light-dark aversion paradigm. *Neuro. Report*, **3**, 527–529.

MINER, W.D., SANGER, G.J. & TURNER, D.H. (1986). Comparison of the effect of BRL 24924, metoclopramide and domperidone on cisplatin-induced emesis in the ferret. *Br. J. Pharmacol.*, **88**, 374P.

MITCHELSON, F. (1992). Pharmacological agents affecting emesis. A review (Part I). *Drugs*, **43**, 295–315.

REISER, G. & HAMPRECHT, B. (1989). Substance P and serotonin act synergistically to activate a cation permeability in a neuronal cell line. *Brain Res.*, **479**, 40–48.

REITH, M.E.A. (1990). ^{14}C-Guanidinium ion influx in Na^+-channel preparations from mouse cerebral cortex. *Eur. J. Pharmacol.*, **188**, 33–41.

SANGER, G.J. (1992). The involvement of 5-HT$_3$ receptors in visceral function. In *Central and Peripheral 5-HT$_3$ receptors*. ed. Hamon, M. pp. 207–255. London: Academic Press.

SCHLICKER, E., WERNER, U., HAMON, M., GOZLAN, H., NICKEL, B., SZELENYI, I. & GÖTHERT, M. (1992). Anpirtoline, a novel, highly potent 5-HT$_{1B}$ receptor agonist with antinociceptive/antidepressant-like actions in rodents. *Br. J. Pharmacol.*, **105**, 732–738.

SCHWÖRER, H., RACKÉ, K. & KILBINGER, H. (1991). Cisplatin increases the release of 5-hydroxytryptamine (5-HT) from the isolated vascularly perfused small intestine of the guinea-pig: involvement of 5-HT$_3$ receptors. *Naunyn-Schmied. Arch. Pharmacol.*, **344**, 143–149.

STABLES, R., ANDREWS, P.L.R., BAILEY, H.E., COSTALL, B., GUNNING, S.J., HAWTHORN, J., NAYLOR, R.J. & TYERS, M.B. (1987). Anti-emetic properties of the 5-HT$_3$ receptor antagonist, GR 38032F. *Cancer Treat. Rev.*, **14**, 333–336.

SWEDBERG, M.D.B., SHANNON, H.E., NICKEL, B. & GOLDBERG, ST.R. (1992). D-16949 (Anpirtoline): a novel serotonergic (5-HT$_{1B}$) psychotherapeutic agent assessed by its discriminative effects in the rat. *J. Pharmacol. Exp. Ther.*, **236**, 1015–1022.

SZELENYI, I., BARANN, M., BÖNISCH, H., GOZLAN, H., HAMON, M., LAGUZZI, R., METZENAUER, P., NICKEL, B. & GÖTHERT, M. (1992). 5-HT$_3$ receptor antagonistic properties of a novel 5-HT$_1$ receptor agonist anpirtoline. Abstracts of the 2nd International Symposium on *Serotonin from Cell Biology to Pharmacology and Therapeutics*, Houston/Texas, 1992, p. 41.

SZELENYI, I., HEROLD, H. & GÖTHERT, M. (1994). Emesis induced in domestic pigs. A new experimental tool for detection of anti-emetic drugs and for evaluation of emetogenic potential of new anticancer agents. *J. Pharmacol. Toxicol. Methods* (in press).

(Received June 13, 1994
Revised September 8, 1994
Accepted September 15, 1994)

British Journal of Pharmacology (1995) 114, 275-282 © 1995 Stockton Press All rights reserved 0007-1188/95 $9.00

Characterization of β_1- and β_3-adrenoceptors in intact brown adipocytes of the rat

François D'Allaire, Claude Atgié, *Pascale Mauriège, Pierre-Michel Simard & Ludwik Jan Bukowiecki

Department of Physiology, Faculty of Medicine, Laval University, G1K 7P4 Québec, (PQ) Canada and *Physical Activity Sciences Laboratory, PEPS, Laval University, G1K 7P4, Québec, (PQ) Canada

1 The binding properties of β_1-, β_2- and β_3-adrenoceptors were determined in isolated brown adipocytes of the rat rather than in membrane preparations from tissue homogenates, because typical brown adipocytes represent only about 40% of the various cells present in brown adipose tissue. Binding characteristics were assessed with the hydrophilic β-adrenoceptor radioligand, (−)-[^{3}H]-CGP 12177. The potent β-antagonist, bupranolol (100 μM) was used to determine nonspecific binding. Characterization was essentially performed by saturation and competition studies.

2 The saturation curve of (−)-[^{3}H]-CGP 12177 was clearly biphasic (Hill coefficient, nH = 0.57 ± 0.11, $P<0.01$) indicating the presence of two different β-adrenoceptor populations of high (K_D = 0.24 ± 0.04 nM) and low (K_D = 80 ± 7 nM) affinity. The low affinity sites were more numerous (B_{max} = 121 000 ± 30 000 sites/cell) than the high affinity sites (B_{max} = 12 000 ± 1 000 sites/cell).

3 (−)-[^{3}H]-CGP 12177 (25 nM) was displaced by adrenaline (Ad), noradrenaline (NA), isoprenaline (Iso), phenylephrine (Phe) and by the new β_3 agonist, CL 316 243 (CL) in a biphasic pattern. The order of potency for (−)-[^{3}H]-CGP 12177 displacement from the small population of high affinity sites (Iso ≫ NA > Ad ≫ CL ≫ Phe was in agreement with a β_1/β_2-classification. In contrast, the potencies of the same agonists for displacing the radioligand from the low affinity binding sites (CL ≫ Iso > NA > Ad ≫ Phe) revealed the presence of a distinct population of adrenoceptors obeying a β_3-classification. 5-HT did not displace (−)-[^{3}H]-CGP 12177 (25 nM) when used at concentrations as high as 0.1 mM.

4 The β-adrenoceptor antagonist, (−)-bupranolol, was more effective than (−)-propranolol for displacing (−)-[^{3}H]-CGP 12177 (25 nM) from the high (K_i = 0.029 ± 0.011 and 0.19 ± 0.07 nM, respectively and low (K_i = 0.27 ± 0.04 μM and 1.6 ± 0.2 μM, respectively) affinity binding sites. The selective β_1-antagonist CGP 20712A efficiently displaced the radioligand from a small population (K_i = 65 ± 19 pM) of binding sites, confirming the presence of β_1-adrenoceptors.

5 To evaluate whether β_2-adrenoceptors could be identified in the population of high affinity binding sites, displacement studies were performed at a low concentration of (−)-[^{3}H]-CGP 12177 (4 nM) that mainly labelled β_1/β_2-adrenoceptors. ICI 118 551 (a selective β_2-antagonist) and procaterol (a selective β_2-agonist) displaced (−)-[^{3}H]-CGP 12177 from its binding sites with very low affinity (K_i = 0.17 ± 0.02 μM and K_i = 11 ± 2 μM respectively).

6 From these observations, we conclude that: (1) two kinds of binding sites with low and high affinities for (−)-[^{3}H]-CGP 12177 can be detected in intact brown adipocytes, (2) there are 10 times more low than high affinity β-adrenoceptors, as determined by saturation or competition curve analysis, (3) the high affinity binding sites mainly correspond to β_1-adrenoceptors, whereas the low affinity sites represent β_3-adrenoceptors, and (4) β_2-adrenoceptors are undetectable.

7 It is suggested that the low affinity β_3-adrenoceptors represent the physiological receptors for noradrenaline secreted from sympathetic nerve endings when the concentration of the neurohormone in the synaptic cleft is very high and/or when the high affinity β_1-adrenoceptors are desensitized by prolonged sympathetic stimulation such as chronic cold exposure.

Keywords: β_1-, β_2-, β_3-adrenoceptors; brown adipose tissue; (−)-[^{3}H]-CGP 12177; CL 316 243; propranolol; bupranolol; catecholamines; CGP 20712A; adipocyte

Introduction

During the last decade, numerous pharmacological studies revealed the presence of atypical or β_3-adrenoceptors in a variety of tissues, and particularly in brown adipose tissue (BAT) (Arch *et al.*, 1984; Arch, 1989; Kaumann, 1989; Lafontan & Berlan, 1993). At present, there is little doubt that β_1-, β_2-, and β_3-adrenoceptors coexist in BAT. As a matter of fact, adrenoceptor mRNAs for β_1-, β_2-, and β_3-adrenoceptors have been identified in BAT (Revelli *et al.*, 1991; Granneman, 1992; Granneman & Lahners, 1992). Studies performed with rat isolated brown adipocytes have demonstrated that β_3-adrenoceptor agonists are as effective as noradrenaline for maximally stimulating thermogenesis (Bukowiecki *et al.*, 1980; 1981; Atgié *et al.*, 1991). However, the physiological function of the three β-adrenoceptor subtypes in mediating the metabolic effects of noradrenaline *in vivo*, still remains to be defined.

The principal goal of the present studies was to characterize the properties of β_1-, β_2-, and β_3-adrenoceptors in intact brown adipocytes. Although the presence of β_3-adrenoceptors has been detected in crude membrane preparations obtained from BAT homogenates (Muzzin *et al.*, 1992), the properties of β_3-adrenoceptors have not yet been determined in intact adipocytes or purified plasma membranes. It is known that typical brown adipocytes represent about 40% of the total cell population in BAT, the other cellular types being

[1] Author for correspondence.

endothelial cells forming the numerous capillaries (50%), pericytes, interstitial stem cells, preadipocytes, protoadipocytes, mast cells etc. (remaining 10%) (Bukowiecki *et al.*, 1986; Géloën *et al.*, 1988; 1990; Goglia *et al.*, 1992). To avoid contamination by other cellular types, it was decided to assess the properties of β-adrenoceptors in intact brown adipocytes using the hydrophilic β-adrenoceptor radioligand, (−)-[^{3}H]-CGP 12177 (Staehelin *et al.*, 1983; Lacasa *et al.*, 1985; 1986; Levin & Sullivan, 1986; Mohell & Dicker, 1989).

Methods

Animals

Female Sprague-Dawley rats weighing 250–300 g were kept at 27°C for at least 2 weeks with a photoperiod of 12L:12D and fed Purina Chow *ad libitum*. Brown adipocytes were isolated, essentially as previously described (Bukowiecki *et al.*, 1981), from pooled interscapular BAT from 3 rats killed at 09 h 00 min. Briefly, cleaned pieces of tissue (about 1 g) were incubated for 15 min in a 2.5 ml Krebs-Ringer-bicarbonate buffer (KRB) (pH 7.4, gassed for 30 min with a 95% O_2:5% CO_2) containing bovine serum albumin (1%), glucose (2.7 mM), HEPES (20 mM) and collagenase (10 mg), with a shaking frequency of 160 cycles per min. At the end of the digestion period, the cells were filtered through a nylon filter (500 μm), diluted in 10 ml of buffer and centrifuged (80 *g*) at room temperature for 5 min. The floating cells were filtered again through a filter (200 μm) and centrifuged following the same procedure. The isolated adipocytes were finally washed twice with 3 ml of KRB and counted in a haemacytometer after trypan blue staining.

Saturation binding experiments

(−)-[^{3}H]-CGP 12177 was chosen for our binding assays because we found, in preliminary experiments, that it had a very low octanolic/aqueous partition coefficient (0.29 ± 0.01) compared to the classical β-adrenoceptor radioligand, [^{125}I]-iodocyanopindolol (24.63 ± 1.30), confirming previous observations (Lafontan *et al.*, 1987). In addition, binding at 25°C was rapid, saturable, proportional to cell concentration, and was not displaced by 0.1 mM phenylephrine (an α-agonist) or 5-hydroxytryptamine (5-HT), confirming previous observations (Levin & Sullivan, 1986; Staehelin *et al.*, 1983; Lacasa *et al.*, 1985; Mauriège *et al.*, 1988). The isolated fat cells were preincubated at 37°C for 15 min in a KRB buffer containing (l^{-1}): glucose 1 g, bovine serum albumin 5.5 g, chloroquine 10 mg (to inhibit ligand uptake and internalization), ascorbic acid 0.1, pargyline 10 mg, catechol 34 mg (to minimize the degradation of catecholamines) and GTP 60 mg (to convert all the β-adrenoceptors into a low affinity state), pH 7.4 (Lafontan *et al.*, 1987; Levitzki, 1986). The cells were then washed with the binding buffer and about $1-1.5 \times 10^5$ cells were incubated 30 min with different concentrations of (−)-[^{3}H]-CGP 12177 ranging from 0.1 to 130 nM in a final volume of 160 μl, essentially as described by Marette *et al.* (1993). However, in this study, we used the potent β-adrenoceptor antagonist, bupranolol (100 μM) (rather than propranolol) to assess nonspecific binding (see below). Incubation was stopped by adding 2 ml of ice-cold NaCl (0.9%) solution and followed by rapid vacuum filtration of the suspension through Whatmann GF/C filters placed on a Millipore manifold. The filters were then washed twice with 10 ml portions of an ice-cold NaCl solution. Radioactivity retained on filters was counted in 4 ml of scintillation liquid (Ecolite, ICN) with a beta counter at 35% efficiency.

Competition binding experiments

Cells ($1-1.5 \times 10^5$) were incubated at 25°C for 30 min with (−)-[^{3}H]-CGP 12177 (4 or 25 nM) in the presence of various agonists and antagonists. The radioligand was used either at a concentration of 4 nM to label preferentially the high affinity binding sites or at a concentration of 25 nM to recruit both the high and low affinity sites. At these concentrations, nonspecific binding assessed with 100 μM bupranolol represented about 13% and 32% of total binding, respectively. The values of nonspecific binding determined by Ligand programme analysis, when nonspecific binding was allowed to float, were similar to those determined with 100 μM bupranolol.

Data analysis

The EBDA programme was used to determine the Hill coefficient (n_H) and to generate a first approximation of the dissociation constant (K_D) (saturation analysis), the inhibition constant (K_i) (competition analysis) and the maximum number of binding sites (B_{max}). Then, the data were analysed by the non-linear curve fitting Ligand programme (Munson & Rodbard, 1980) to determine the final K_D, K_i and B_{max} values. The statistical method based on the 'extra sum of squares' principle (Munson & Rodbard, 1980) given by the Ligand programme was used to determine whether the curves were best fitted by a one- or two-site model. In saturation experiments, the nonspecific binding determined with bupranolol (100 μM) was fixed and all other constants were allowed to float. In competition studies, the K_D of the radioligand for high and low affinity sites were fixed as well as nonspecific binding determined with 100 μM bupranolol. Other constants were allowed to float. The dissociation constant of the different displacing drugs (K_i) were directly given by the Ligand programme. In all tables and figures, values represent means ± s.e. of 3–5 individual experiments performed on separate occasions. The horizontal dotted line in the figures represents the mean value of the nonspecific binding determined with 100 μM bupranolol and the shaded areas correspond to the s.e. ($n = 5$).

Drugs and chemicals

(−)-Noradrenaline bitartrate, (−)-adrenaline bitartrate, 5-HT, phenylephrine, bovine serum albumin (fraction IV) and collagenase (type II) were obtained from Sigma Chemicals Co. (St-Louis, MO, U.S.A.). GTP was purchased from Boehringer Mannheim (Laval, Québec, Canada) and (−)-[^{3}H]-CGP 12177 ((−)-4-(3-*t*-butylamino-2-hydroxypropoxy)-[5,7-^{3}H] benzimidazol-2-1)) (specific activity = 43 Ci mmol^{-1}) was obtained from Amersham (Oakville, Ontario, Canada). (−)-Propranolol and (−)-isoprenaline were purchased from RBI Biochemicals Inc. (Natick, MA, U.S.A.); CL 316 243 (disodium (**R**,**R**)-5-[2-[[2-(3-chlorophenyl)-2-hydroxyethyl]-amino]propyl]-1,3-benzodioxole-2,2-dicarboxylate) and (−)-bupranolol were kindly provided by Dr T.H. Claus (American Cyanamid Company, Lederle Laboratories, Pearl River, NY, U.S.A.) (Bloom *et al.*, 1992) and by Dr M. Lafontan (Université Paul Sabatier, Toulouse, France), respectively. The following compounds were provided as generous gifts: ICI 118 551 (erythro-(±)-1-(7-methyllindane-4-yloxy)-3-isopropylaminobutane-2-olhydrochloride) from ICI Pharmaceuticals (Mississauga, Canada) and CGP 20712A ((±)-(2-(3-carbomoyl-4-trifluormethyl-2-imidazolyl)-phenoxy)-2-propanolmethanesulphonate) from Ciba-Geigy (Mississauga, Canada). Procaterol (OPC-2009) (5-(1-hydroxy-2-isopropylaminobutyl)-8-hydrocarbostyril hydrochloride hemihydrate) (Yabuuchi *et al.*, 1977) was kindly provided by Otsuka Pharmaceuticals (Tokushima, Japan).

Results

Saturation binding studies

Saturation binding experiments with increasing concentrations of (−)-[^{3}H]-CGP 12177 ranging from 0.1 to 130 nM

revealed that the saturation curve was clearly biphasic (Figure 1). The first saturation appeared around 3 nM (see inset of Figure 1). Scatchard plots of the data in Figure 1 were curvilinear indicating that (−)-[^{3}H]-CGP 12177 bound to at least two classes of receptors (Figure 2). EBDA/Ligand analysis clearly indicated that the two-site model was more appropriate than the one-site model ($P<0.01$). Moreover, the Hill coefficient ($n_H = 0.57 \pm 0.11$) confirmed the presence of two different binding sites (Table 1). The low affinity adrenoceptors ($K_D = 80$ nM) were approximately 10 times more numerous than the high affinity adrenoceptors ($K_D = 0.24$ nM).

Competition binding studies with adrenoceptor agonists

Displacement curves were performed with concentrations of (−)-[^{3}H]-CGP 12177 fixed at 25 nM in order to label the high and low affinity binding sites. The capacity of isoprenaline, noradrenaline and adrenaline for displacing (−)-[^{3}H]-CGP 12177 from its binding sites was compared with that of a new selective β_3-agonist, CL 316 243 (Figure 3). All displacement curves of (−)-[^{3}H]-CGP 12177 were best fitted to a two-site model ($P<0.01$) with Hill coefficients smaller than 1 (Tables 2 and 3, Figures 3 and 4). Low concentrations of CL 316 243 (0.1–20 nM) displaced (−)-[^{3}H]-CGP 12177 with high efficiency from a predominant population of binding sites, whereas low concentrations of isoprenaline, noradrenaline or adrenaline displaced the radioligand from a minor population of sites. The results indicated that the major population of β_3-adrenoceptors had a much higher affinity for CL 316 243 than for catecholamines (a difference of 3–4 orders of magnitude), whereas the contrary was observed for the minor population of adrenoceptors. Phenylephrine, an α-adrenoceptor agonist and 5-HT did not displace (−)-[^{3}H]-CGP 12177 (25 nM) even when used at concentrations as high as 0.1 mM (data not shown).

Competition binding studies with an adrenoceptor antagonist

In order to characterize better the high affinity binding sites, competition experiments were performed with the selective β_1-antagonist, CGP 20712A. The displacement curve was biphasic with high (65 ± 19 pM) and low (3.8 ± 0.9 μM) K_is,

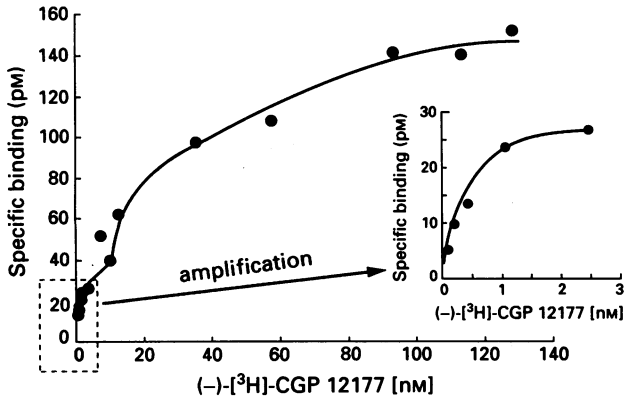


Figure 1 Saturation curve of (−)-[^{3}H]-CGP 12177 specific binding to intact brown adipocytes. Binding assays were performed as described in Methods. The inset amplifies the first saturation of high affinity sites from 0.10 to 2.5 nM of (−)-[^{3}H]-CGP 12177. The graph is from one representative experiment. The Hill coefficient (n_H), the dissociation constants (K_D) of the low and high affinity binding sites and the corresponding number of binding sites (B_{max}) calculated from 5 individual experiments are given in Table 1.

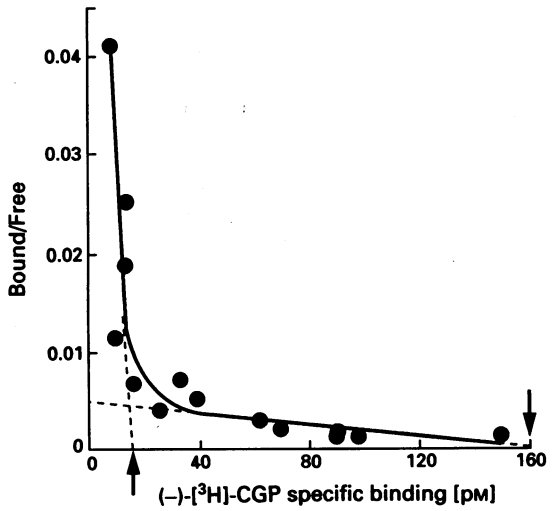


Figure 2 Scatchard analysis of the saturation curve presented in Figure 1. The biphasic plot ($P<0.01$) confirms the presence of at least two distinct populations of high (0.24 ± 0.04 nM) and low (80 ± 7 nM) affinity binding sites ($n = 5$).

Table 1 Pharmacological characteristics of (−)-[^{3}H]-CGP 12177 binding sites in intact rat brown adipocytes

	Dissociation constant K_D (nM)	*Number of sites* B_{max} (× 10^3 sites/cell)
High affinity sites	0.24 ± 0.04	12 ± 1
Low affinity sites	80 ± 7	121 ± 30

Saturation experiments were performed with intact brown adipocytes in a range of concentrations of (−)-[^{3}H]-CGP 12177 from 0.1 to 130 nM. The data were analysed by Scatchard transformation of the saturation curves by the EBDA/Ligand programme to determine the dissociation constant (K_D) and maximal number of binding sites (B_{max}). Values represent the mean ± s.e. of 5 individual experiments. The Hill coefficient (n_H) was 0.57 ± 0.11 ($P<0.01$).

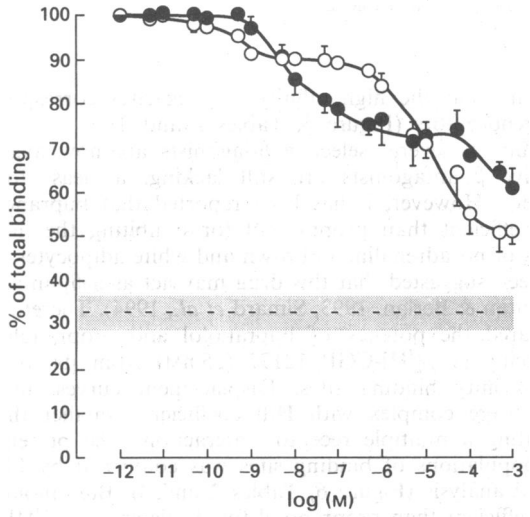


Figure 3 Displacement curves of (−)-[^{3}H]-CGP 12177 (25 nM) by isoprenaline (○) or by the selective β_3-agonist CL 316 243 (●). EBDA/Ligand analysis showed that biphasicity of both curves was statistically significant ($P<0.01$). The Hill coefficient (n_H) of the displacement curves, the inhibition constants (K_i) and the corresponding number of binding sites (B_{max}) are given in Tables 2 and 3. The values represent the mean ± s.e. of 3–5 individual experiments. Symbols without s.e. bars indicate that the s.e. is smaller than the diameter of the circle.

Table 2 Binding characteristics of different β-adrenoceptor drugs for β_1-adrenoceptors in rat intact brown adipocytes

Drugs	Hill coefficients n_H	Binding characteristics: Inhibition constant K_i (nM)	Binding characteristics: Inhibition constant pK_i	Number of sites B_{max} ($\times 10^3$ sites per cell)
Agonists				
Isoprenaline	0.41 ± 0.10 ($P<0.01$)	0.044 ± 0.008	10.4	8.7 ± 2.1
Noradrenaline	0.33 ± 0.10 ($P<0.01$)	0.47 ± 0.16	9.3	12 ± 3
Adrenaline	0.41 ± 0.13 ($P<0.01$)	2.0 ± 0.8	8.6	9.5 ± 1.3
CL 316 243	0.73 ± 0.06 ($P<0.01$)	3600 ± 1300	5.4	10 ± 1
Antagonists				
CGP 20712A	0.37 ± 0.04 ($P<0.01$)	0.065 ± 0.019	10.2	13 ± 3
Bupranolol	0.42 ± 0.11 ($P<0.01$)	0.029 ± 0.011	10.5	13 ± 1
Propranolol	0.46 ± 0.01 ($P<0.01$)	0.19 ± 0.07	9.7	10 ± 1

Competition studies were performed with intact brown adipocytes using a (−)-[^{3}H]-CGP 12177 concentration of 25 nM. Inhibition constants (K_i) and Hill coefficients (n_H) were evaluated by the EBDA/Ligand programme as described under Methods. Values represent the mean ± s.e. of 3–5 individual experiments.

Table 3 Binding characteristics of different β-adrenoceptor drugs for β_3-adrenoceptors in intact rat brown adipocytes

Drugs	Inhibition constant K_i (μM)	Inhibition constant pK_i	Number of sites B_{max} ($\times 10^3$ sites per cell)
Agonists			
CL 316 243	0.015 ± 0.004	7.8	71 ± 12
Isoprenaline	29 ± 10	4.5	131 ± 5
Noradrenaline	56 ± 3	4.2	157 ± 14
Adrenaline	91 ± 10	4.0	225 ± 14
Antagonists			
Bupranolol	0.27 ± 0.04	6.5	51 ± 11
Propranolol	1.6 ± 0.2	5.7	49 ± 5
CGP 20712A	3.8 ± 0.9	5.4	119 ± 21

The experimental conditions and the Hill coefficients were the same as in Table 2.

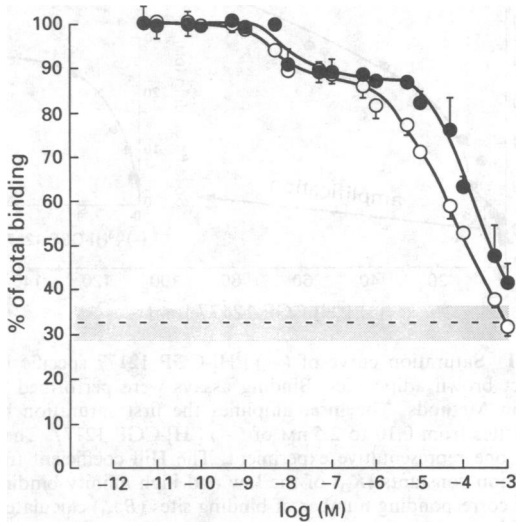


Figure 4 Displacement curves of (−)-[^{3}H]-CGP 12177 (25 nM) by noradrenaline (○) or by adrenaline (●). EBDA/Ligand analysis showed that biphasicity of both curves was statistically significant ($P<0.01$). The Hill coefficient (n_H) of the displacement curves, the inhibition constants (K_i) and the corresponding number of binding sites (B_{max}) are given in Tables 2 and 3. For other details see Figure 3.

attesting that the high affinity binding sites correspond to β_1-adrenoceptors (Figure 5, Tables 2 and 3).

Although several selective β_3-agonists are now available, selective β_3-antagonists are still lacking, at least for the moment. However, it has been reported that bupranolol is more efficient than propranolol for inhibiting the lipolytic effects of noradrenaline in brown and white adipocytes and it has been suggested that this drug may act as a β_3-antagonist (Lafontan & Berlan, 1993; Simard *et al.*, 1994). Therefore, we compared the potency of bupranolol and propranolol for displacing (−)-[^{3}H]-CGP 12177 (25 nM) from its low and high affinity binding sites. Displacement curves, in both cases, were complex with Hill coefficients smaller than 1, indicating a multiple receptor interaction. The presence of two populations of binding sites was confirmed by EBDA-Ligand analysis (Figure 6, Tables 2 and 3). Bupranolol was more efficient than propranolol for displacing (−)-[^{3}H]-CGP 12177 from its high affinity binding sites ($K_i = 0.029 \pm 0.011$ nM and 0.19 ± 0.07 nM, $P<0.01$, unpaired t test). The affinities of bupranolol and propranolol for the second population of adrenoceptors were much lower but bupranolol was still more efficient than propranolol for displacing the radioligand ($K_i = 0.27 \pm 0.04$ μM and 1.6 ± 0.2 μM, $P<0.01$, unpaired t test). Thus, CGP 20712A, bupranolol and propranolol all displaced with high affinity (−)-[^{3}H]-CGP 12177 from the small population of binding sites. However, propranolol and bupranolol generated displacement curves without an apparent transition between the high and low affinity binding sites (Figure 6), whereas the displacement curve obtained with CGP 20712A was clearly biphasic. The higher affinity of CGP 20712A for β_1-adrenoceptors could explain that difference.

Competition studies with selective β_2-adrenoceptor agents

To assess whether β_2-adrenoceptors could be detected in the population of high affinity binding sites, the capacity of two selective β_2-agents, ICI 118 551 (an antagonist) and procaterol (an agonist), for displacing (−)-[^{3}H]-CGP 12177 was evaluated (Figure 7). A reduced concentration of (−)-[^{3}H]-CGP 12177 (4 nM) was used to label preferentially the high

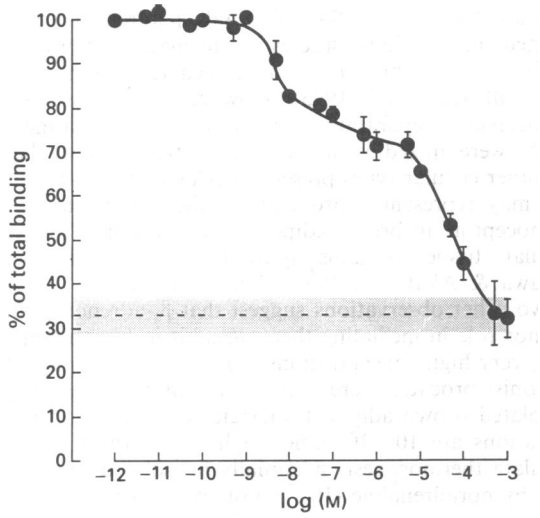


Figure 5 Displacement curve of (−)-[^{3}H]-CGP 12177 (25 nM) by the selective β_1-antagonist, CGP 20712A. EBDA/Ligand analysis showed that the curve was best fitted to a two-site model ($P<0.01$). The Hill coefficient (n_H) of the displacement curves, the inhibition constants (K_i) and the corresponding number of binding sites (B_{max}) are given in Tables 2 and 3. For other details see Figure 3.

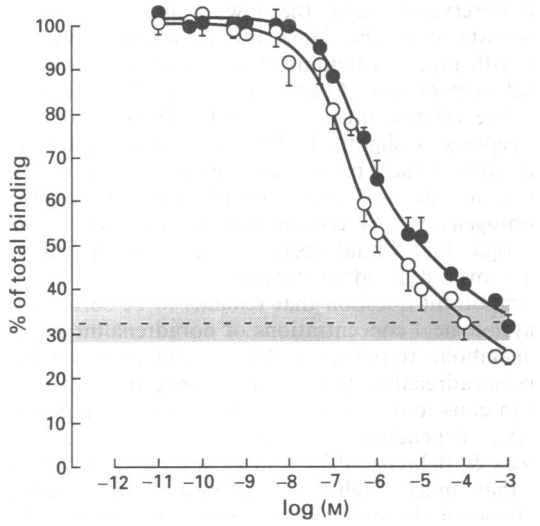


Figure 6 Displacement curve of (−)-[^{3}H]-CGP 12177 (25 nM) by the nonselective β-antagonists propranolol (●) and bupranolol (○). EBDA/Ligand analysis showed that biphasicity of both curves was statistically significant ($P<0.01$). The Hill coefficient (n_H) of the displacement curves, the inhibition constants (K_i) and the corresponding number of binding sites (B_{max}) are given in Tables 2 and 3. For other details see Figure 3.

affinity binding sites (see inset of Figure 1). ICI 118 551 and procaterol displaced (−)-[^{3}H]-CGP 12177 only at very high concentrations with elevated K_i valules (0.17 ± 0.02 μM and 11 ± 2 μM, respectively). Radioligand binding analysis revealed that the displacement curves for both ICI 118 551 and procaterol were best fitted to a one-site model ($P<0.01$). The B_{max} values ($12\,000 \pm 2\,000$ and $22\,000 \pm 4\,000$ sites per cell for procaterol and ICI 118 551) were within the same range of values as the high affinity B_{max} obtained from saturation studies with (−)-[^{3}H]-CGP 12177 (Figures 1, 2 and Table 1). Thus, β_2-adrenoceptors were not detectable.

Discussion

The main objective of the present studies was to characterize the properties of β-adrenoceptors in intact brown adipocytes.

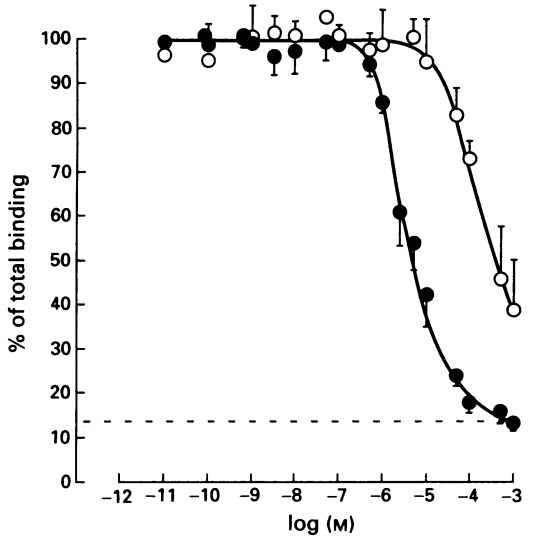


Figure 7 Displacement curve of (−)-[^{3}H]-CGP 12177 (4 nM) by the selective β_2-antagonist, ICI 118 551 (●) and the selective β_2-agonist procaterol (○). EBDA/Ligand analysis showed that the data best fitted to a one-site model ($P<0.01$). The Hill coefficient (n_H) of the displacement curves, the inhibition constants (K_i) and the corresponding number of binding sites (B_{max}) are given in Table 4.

Histological cellular frequency studies have demonstrated that typical brown adipocytes represent about 40% of the total cell population in BAT (Géloën *et al.*, 1988). Endothelial cells forming the numerous capillaries surrounding brown adipocytes occupy another 50%, the remaining 10% being distributed between interstitial stem cells, protoadipocytes, preadipocytes, mast cells etc. It is likely that the distribution of β-adrenoceptors differs among these cellular types and that it changes during BAT growth, cold acclimatization, etc. Vascular tissue contains both β_1- and β_2-adrenoceptors (Aikawa & Akatsuka, 1990; Zink *et al.*, 1993) and may represent a major contaminant in membrane preparations obtained from whole tissue homogenates.

Previous studies, performed with membrane preparations obtained from tissue homogenates, have used radioligands such as (−)-[^{3}H]-dihydroalprenolol or (−)-[^{125}I]-cyanopindolol to determine the properties of β-adrenoceptor-binding sites (Bukowiecki *et al.*, 1978; Dax & Partilla, 1982; Senault *et al.*, 1984; Raasmaja, 1990; Langin *et al.*, 1991; Galitzky *et al.*, 1993b). However, these two radioligands were inadequate for quantifying β-adrenoceptors in intact cells due to their high lipophilicity. Therefore, we chose the highly hydrophilic radioligand (−)-[^{3}H]-CGP 12177 (octanolic/aqueous partition coefficient = 0.29 ± 0.01) to analyses the properties of β-adrenoceptors in intact brown adipocytes. (−)-[^{3}H]-CGP 12177 has been used successfully for quantifying β_1- and β_2-adrenoceptors in intact rat and human adipocytes (Lacasa *et al.*, 1985; 1986; Lafontan *et al.*, 1987; Levin & Sullivan, 1986; Mauriège *et al.*, 1988; Mohell & Dicker, 1989; Marette *et al.*, 1993), but it is the first time that it has been used for characterizing the properties of β_3-adrenoceptors in isolated brown adipocytes. In addition, nonspecific binding was determined with the potent β-antagonist bupranolol (Kaumann, 1989). Bupranolol is 10 times more potent than propranolol for inhibiting the lipolytic effects of β_3-agonists in white (Lafontan & Berlan, 1993) and brown (Simard *et al.*, 1994) adipocytes.

Both saturation (Figures 1 and 2) and competition (Figures 3–7) studies revealed that the low affinity β_3-adrenoceptors predominate over the high affinity β_1-adrenoceptors in brown adipocytes and that β_2-adrenoceptors are undetectable. Adrenoceptor agonists displaced (−)-[^{3}H]-CGP 12177 from its high affinity sites with a potency order typical of β_1-adrenoceptors: isoprenaline≫ noradrenaline>

adrenaline≫CL 316 243≫phenylephrine (Table 2 and Figures 3–6) (Mohell & Nedergaard, 1989). Likewise, the same agents displaced the radioligand from the low affinity sites with a potency order corresponding to β_3-adrenoceptors: CL 316 243≫isoprenaline>noradrenaline>adrenaline≫phenylephrine (Table 3 and Figures 3 and 4) (Fève *et al.*, 1991). Furthermore, the K_D values of the high affinity β_1-adrenoceptors (0.24 nM) and low affinity β_3-adrenoceptors (80 nM) for (−)-[^{3}H]-CGP 12177 (Table 1) were in the same range of values as the corresponding K_D observed in CHO cells expressing the rat β_3-adrenoceptor (Muzzin *et al.*, 1992), in 3T3-F442A adipocytes (Fève *et al.*, 1991), in BAT homogenates (Muzzin *et al.*, 1992), and in garden dormouse white adipocytes (Carpéné *et al.*, 1994).

It may be argued that the K_i values for catecholamines (Table 2) are higher than those previously reported for β_1-adrenoceptors (Levin & Sullivan, 1986; Mohell & Nedergaard, 1989; Raasmaja, 1990). However, most of the past studies have been performed on membranes (and not on cells) and generally used concentrations of displacing drugs ranging from 10^{-9} to 10^{-4} M (and not 10^{-12} to 10^{-4}) in the presence of concentrations of radioligand that bound β_1-, β_2- and probably β_3-adrenoceptors. Under these conditions, the K_i values represent a mean of the K_is for the three β-adrenoceptor subtypes. In fact, we also found, in preliminary experiments, that the K_i value for noradrenaline is in the 10^{-7} M range using *membranes* and [^{125}I]-cyanopindolol (200 pM), but we believe that this is an overestimation for the above reasons.

Noradrenaline displaced (−)-[^{3}H]-CGP 12177 from β_3-adrenoceptors with low affinity (K_i = 56 μM), suggesting that it may stimulate thermogenesis in BAT via both the high (β_1) and low affinity (β_3) receptors. It is clear that the β_3-adrenoceptors will be recruited only at very high noradrenaline concentrations because noradrenaline affinity for β_1-adrenoceptors is several fold greater than for β_3-adrenoceptors (Tables 2 and 3). This marked difference in binding affinities agrees with the difference in noradrenaline capacity for stimulating adenylate cyclase activity, lipolysis or respiration via the high and low affinity receptors (Granneman, 1990; Atgié *et al.*, 1991; 1994; Simard *et al.*, 1994).

It has been reported in functional studies that bupranolol is 10 times more potent than propranolol for inhibiting the lipolytic effects of β_3-agonists (Lafontan & Berlan, 1993; Simard *et al.*, 1994). The displacement curves described in Figure 6 also showed that bupranolol is a better β-antagonist than propranolol. The K_i values of burpanolol and propranolol are comparable to the K_i or pA_2 values reported in literature (Muzzin *et al.*, 1992; Galitzky *et al.*, 1993a).

In order to evaluate further the proportion of β_1- over β_2-adrenoceptors, competition studies were carried out with a β_2-antagonist (ICI 118 551) and a β_2-agonist (procaterol). These experiments revealed that the high affinity β-adrenoceptor binding sites for (−)-[^{3}H]-CGP 12177 mainly represented β_1-adrenoceptors because β_2-selective drugs were not effective in displacing the radioligand from its binding sites (Figure 7 and Table 4). The presence of β_2-adrenoceptors (30–50% of total β-adrenoceptors) was detected in previous studies performed with membranes obtained from whole tissue homogenates (Rothwell *et al.*, 1985; Sillence *et al.*, 1993). However, in the whole tissue homogenate preparations, brown adipocyte plasma membranes were mixed with membranes from endothelial cells and other cellular types present in BAT (Géloën *et al.*, 1988). This may represent a problem for the quantification of β_2-adrenoceptors in brown adipocytes because it is known that vascular tissue contains both β_1- and β_2-adrenoceptors (Aikawa & Akatsuka, 1990; Zink *et al.*, 1993).

Two other observations suggest that β_2-adrenoceptors play a minor role in mediating thermogenesis in brown adipocytes. First, very high concentrations (10^{-5}–10^{-4} M) of the selective β_2-agonist procaterol are required to stimulate thermogenesis in isolated brown adipocytes (Atgié *et al.*, 1994). These concentrations are 10^2–10^3 times higher than those required to stimulate thermogenesis maximally in isolated brown adipocytes by noradrenaline (10^{-7} M) or by the selective β_3-agonist BRL 37344 (10^{-8} M) (Bukowiecki *et al.*, 1980; 1981; Atgié *et al.*, 1991; 1994). Second, the β_2-adrenoceptor antagonist, ICI 118 551, is only a weak inhibitor of the lipolytic or respiratory effects of noradrenaline. Thus, the present binding data as well as our recent respiratory studies suggest that β_2-adrenoceptors are much less important than β_1- or β_2-adrenoceptors for mediating the respiratory effects of noradrenaline in rat brown adipocytes.

The observation that the low affinity β_3-adrenoceptors predominate over the high affinity β_1-adrenoceptors also agrees with previous binding studies performed with unfractionated membranes (Muzzin *et al.*, 1992; Sillence *et al.*, 1993). The relative proportion of β_3-adrenoceptors over β_1-adrenoceptors is slightly higher in the present studies conducted with intact brown adipocytes (Tables 2 and 3). However, as discussed above, membranes prepared from tissue homogenates may contain β_1/β_2-adrenoceptors from vascular origin that would decrease the apparent value of the ratio β_3- over β_1/β_2-adrenoceptors.

An important question that remains to be solved concerns the physiological concentrations of noradrenaline required to elicit metabolic responses in BAT. Cold exposure increases plasma noradrenaline levels from approximately 1 nM (basal values in conscious undisturbed rats at room temperature) to 3–10 nM, depending on the temperature of exposure (Depocas & Behrens, 1978; Liu *et al.*, 1994). However, it is likely that much higher concentrations of noradrenaline occur between the sympathetic nerve varicosities and brown adipocyte plasma membrane, particularly after intensive stress. Unlike white adipose tissue, BAT is densely innervated with sympathetic nerves that run, not only along the capillaries, but also between the individual adipocytes (Cottle *et al.*, 1985). Indirect evidence suggests that concentrations of noradrenaline as high as 100 nM may occur in the synaptic cleft (Depocas *et al.*, 1978). One hundred nanomolar is approximately the noradrenaline concentration that is required to stimulate thermogenesis maximally in isolated brown adipocytes (Bukowiecki *et al.*, 1980; 1981). On the

Table 4 Binding characteristics of different β_2-adrenoceptor agents for high affinity (−)-[^{3}H]-CGP 12177 binding sites in rat intact brown adipocytes

	Binding characteristics			
Drugs	*Hill coefficients* n_H	*Inhibition constant* K_i (μM)	*Inhibition constant* pK_i	*Number of sites* B_{max} (× 10^3 sites per cell)
ICI 118 551	0.99 ± 0.11 ($P<0.01$)	0.17 ± 0.02	6.7	22 ± 2
Procaterol	0.85 ± 0.28 ($P<0.01$)	11 ± 2	4.9	12 ± 2

Competition studies were performed with intact brown adipocytes using a (−)-[^{3}H]-CGP 12177 concentration of 4 nM. Other experimental conditions were the same as in Table 2.

other hand, it is known that β_1-adrenoceptors may be desensitized (internalized or down-regulated) by chronic cold exposure (Bukowiecki *et al.*, 1978) or prolonged exposure to β-agonists (Granneman, 1992). In contrast, β_3-adrenoceptors are particularly resistant to catecholamine-induced desensitization (Granneman, 1992; Carpéné *et al.*, 1993). It should also be pointed out that the affinity of β_3-adrenoceptors for noradrenaline is of the same order of magnitude as the affinity of receptors for neurotransmitters such as acetylcholine (10–100 μM) (Changeux, 1987). All these observations suggest that β_3-adrenoceptors represent the physiological receptors for noradrenaline secreted from sympathetic nerve endings, i.e. when the concentration of the neurohormone in the synaptic cleft is high and/or when the high affinity β_1-adrenoceptors are desensitized by prolonged sympathetic stimulation. In this context, the main role of the high affinity β_1-adrenoceptors would be to mediate the effects of circulating noradrenaline (at low nanomolar levels). Further studies are required to test these hypotheses directly.

This study was supported by a research grant from the Medical Research Council of Canada, a post-doctoral fellowship (C.A.) and two summer fellowships (F.D'A. and P.-M.S.) from the 'Association du Diabète du Québec'. The valuable technical assistance of Fleurette Pérusse is gratefully acknowledged.

References

AIKAWA, J. & AKATSUKA, N. (1990). Vascular smooth muscle relaxation by endothelium-dependent β_1-adrenergic action. *Comp. Biochem. Physiol.*, **97C**, 311–315.

ARCH, J.R.S. (1989). The brown adipocyte beta-receptors. *Proc. Nutr. Soc.*, **48**, 215–223.

ARCH, J.R.S., AINSWORTH, A.T., CAWTHORNE, M.A., PIERCY, V., SENNITT, M.V., THODY, V.E., WILSON, C. & WILSON, S. (1984). Atypical beta-adrenoceptors on brown adipocytes as target for anti-obesity drugs. *Nature*, **309**, 163–165.

ATGIÉ, C., MARETTE, A. & BUKOWIECKI, L.J. (1991). Norepinephrine and BRL 37344 stimulate thermogenesis in rat brown adipose tissue via different receptors. *Int. J. Obesity*, **15S**, 52.

ATGIÉ, C., SIMARD, P.-M., D'ALLAIRE, F. & BUKOWIECKI, L.J. (1994). Relative contribution of β_1- and β_3-adrenoceptors to the regulation of lipolysis and respiration in rat brown adipocytes. *FASEB J.*, **8**, A960.

BLOOM, J.D., DUTIA, M.D., JOHNSON, B.D., WISSNER, A., BURNS, M.G., LARGIS, E.E., DOLAN, J.A. & CLAUS, T.H. (1992). Disodium(R,R)-5-[2-[[2-(3-chlorophenyl)-2-hydroxy-ethyl)-amino]-propyl]-1,3-benzodioxole-2,2-dicarboxylate (CL 316 243): a potent beta-adrenergic agonist virtually specific for the beta$_3$-adrenoceptors; a promising antidiabetic and antiobesity agent. *J. Med. Chem.*, **35**, 3081–3084.

BUCKOWIECKI, L.J., FOLLÉA, N., LUPIEN, J. & PARADIS, A. (1981). Metabolic relationships between lipolysis and respiration in rat brown adipocytes. *J. Biol. Chem.*, **256**, 12840–12848.

BUKOWIECKI, L.J., FOLLÉA, N., PARADIS, A. & COLLET, A.J. (1980). Stereospecific stimulation of brown adipose tissue respiration by caetcholamines via beta-adrenergic receptors. *Am. J. Physiol.*, **238** (Endocrinol. Metab. Vol. 1), E552–E563.

BUKOWIECKI, L.J. FOLLÉA, N., VALLIERES, J. & LEBLANC, J. (1978). β-adrenergic receptors in brown-adipose tissue. Characterization and alterations during acclimation of rats to cold. *Eur. J. Biochem.*, **92**, 189–196.

BUKOWIECKI, L.J., GÉLOËN, A. & COLLET, A.J. (1986). Proliferation and differentiation of brown adipocytes from interstitial cells during cold acclimation. *Am. J. Physiol.*, **250** (Cell Physiol. Vol. 19), C880–C887.

CARPÉNÉ, C., AMBID, L. & LAFONTAN, M. (1994). Predominance of β3-adrenergic component in catecholamine activation of lipolysis in garden dormouse adipocytes. *Am. J. Physiol.*, **266** (Regulatory Integrative Comp. Physiol. Vol. 35), R896–R904.

CARPÉNÉ, C., GALITZKY, J., COLLON, P., ESCLAPEZ, F., DAUZATS, M. & LAFONTAN, M. (1993). Desensitization of beta-1 and beta-2, but not beta-3, adrenoceptor-mediated lipolytic responses of adipocytes after long-term norepinephrine infusion. *J. Pharmacol. Exp. Ther.*, **265**, 237–247.

CHANGEUX, J.-P. (1987). Acetylcholine receptor. In *Encyclopedia of Neuroscience*, ed. Adelman, G. pp. 2–3. Boston: Birkhäusser.

COTTLE, M.K.W., COTTLE, W.H., PÉRUSSE, F. & BUKOWIECKI, L.J. (1985). An imposed glyoxylic acid technique for the histochemical localization of catecholamines in brownadipose tissue. *Histochem. J.*, **17**, 1279–1288.

DAX, E.M. & PARTILLA, J.S. (1982). Adrenergic ligand liposolubility in membranes: direct assessment in a beta-adrenergic binding system. *Mol. Pharmacol.*, **22**, 5–7.

DEPOCAS, F. & BEHRENS, W.A. (1978). Levels of noradrenaline in plasma during thermogenesis induced by cold-exposure or by noradrenaline infusion in warm- and in cold-acclimated rats. *Exp. Suppl.*, **32**, 135–146.

DEPOCAS, F., BEHRENS, W.A. & FOSTER, D.O. (1978). Noradrenaline-induced calorigenesis in warm- and in cold-acclimated rats: the interrelation of dose of noradrenaline, its concentration in arterial plasma, and calorigenic response. *Can. J. Physiol. Pharmacol.*, **56**, 168–174.

FÈVE, B., EMORINE, L.J., LASNIER, F., BLIN, N., BAUDE, B., NAHMIAS, C., STROSBERG, A.D. & PAIRAULT, J. (1991). Atypical β-adrenergic receptor in 3T3-F442A adipocytes. Pharmacological and molecular relationship with the human β_3-adrenergic receptors. *J. Biol. Chem.*, **266**, 20329–20336.

GALITZKY, J., REVERTE, M., CARPÉNÉ, C., LAFONTAN, M. & BERLAN, M. (1993a). β3-Adrenoceptors in dog adipose tissue: studies on their involvement in the lipomobilizing effect of catecholamines. *J. Pharmacol. Exp. Ther.*, **266**, 358–366.

GALITZKY, J., REVERTE, M., PORTILLO, M., CARPÉNÉ, C., LAFONTAN, M. & BERLAN, M. (1993b). Coexistence of β_1-, β_2-, β_3-adrenoceptors in dog fat cells and their differential activation by catecholamines. *Am. J. Physiol.*, **264** (Endocrinol. Metab. Vol. 27), E403–E412.

GÉLOËN, A., COLLET, A.J., GUAY, G. & BUKOWIECKI, L.J. (1988). β-adrenergic stimulation of brown adipocyte proliferation. *Am. J. Physiol.*, **254** (Cell Physiol. Vol. 23), C175–C182.

GÉLOËN, A., COLLET, A.J., GUAY, G. & BUKOWIECKI, L.J. (1990). In vivo differentiation of brown adipocyte in adult mice: an electron microscopic Study. *Am. J. Anatomy*, **188**, 366–372.

GOGLIA, F., GÉLOËN, A., LANNI, A., MINAIRE, Y. & BUKOWIECKI, L.J. (1992). Morphometric-stereologic analysis of brown adipocyte differentiation in adult mice. *Am. J. Physiol.*, **262** (Cell Physiol. Vol. 31), C1018–C1023.

GRANNEMAN, J.G. (1990). Norepinephrine and BRL 37344 stimulate adenylate cyclase by different receptors in rat brown adipose tissue. *J. Pharmacol. Exp. Ther.*, **254**, 508–513.

GRANNEMAN, J.G. (1992). Effects of agonist exposure on the coupling of beta 1 and beta 3 adrenergic receptors to adenylyl cyclase in isolated adipocytes. *J. Pharmacol. Exp. Ther.*, **261**, 638–642.

GRANNEMAN, J.G. & LAHNERS, K.N. (1992). Differential adrenergic regulation of beta 1- and beta 3-adrenoreceptor messenger ribonucleic acids in adipose tissues. *Endocrinology*, **130**, 109–114.

KAUMANN, A.J. (1989). Is there a third heart β-adrenoceptor? *Trends Pharmacol. Sci.*, **10**, 316–320.

LACASA, D., AGLI, B. & GIUDICELLI, Y. (1985). Direct assessment of beta-adrenergic receptors in intact rat adipocytes by binding of [^{3}H]-CGP-12177. Evidence for agonist high affinity complex and for β_1- and β_2-receptors subtypes. *Eur. J. Biochem.*, **146**, 339–346.

LACASA, D., MAURIÈGE, P., LAFONTAN, M., BERLAN, M. & GIUDICELLI, Y. (1986). A reliable assay for β-adrenoceptors in intact isolated human fat cells with a hydrophilic radioligand, [^{3}H]-CGP 12177. *J. Lipid Res.*, **27**, 368–376.

LAFONTAN, M. & BERLAN, M. (1993). Fat cell adrenergic receptors and the control of white and brown fat cell function. *J. Lipid Res.* (Review), **34**, 1057–1091.

LAFONTAN, M., MAURIÈGE, P., DE PERGOLA, G., GALITZKI, J. & BERLAN, M. (1987). Identification and quantification of beta and alpha 2 adrenoceptors on membranes and intact adipocytes. In *Proceeding of the 5th International Congress on Obesity, Recent Advances in Obesity Research: V.* ed. Berry, E.M., Blondheim, S.H., Eliahou, H.E. & Shafrir, E. pp. 212–221. London: John Libbey & Company.

LANGIN, D., PORTILLA, M.P., SAULNIER-BLACHE, J.-S. & LAFONTAN, M. (1991). Coexistence of three β-adrenoceptor subtypes in white fat cells of various mammalian species. *Eur. J. Pharmacol.*, **199**, 291–301.

LEVITZKI, A. (1986). β-adrenergic receptors and their mode of coupling to adenylate cyclase. *Physiol. Rev.*, **66**, 819–854.

LEVIN, B.E. & SULLIVAN, A.C. (1986). Beta-1 receptor is the predominante beta-adrenoceptor on rat brown adipose tissue. *J. Pharmacol. Exp. Ther.*, **236**, 681–688.

LIU, X., PÉRUSSE, F. & BUKOWIECKI, L.J. (1994). Chronic norepinephrine infusion stimulates glucose uptake in white and brown adipose tissues. *Am. J. Physiol.*, **266** (Regulatory Integrative Comp. Physiol. Vol. 35), R914–R920.

MARETTE, A., MAURIÈGE, P., DESPRÉS, J.-P., TULP, O.L. & BUKOWIECKI, L.J. (1993). Norepinephrine- and insulin-resistant glucose transport in brown adipocytes from diabetic SHR/N-cp rats. *Am. J. Physiol.*, **265** (Regulatory Integrative Comp. Physiol. Vol. 34), R577–R583.

MAURIÈGE, P., DE PERGOLA, G., BERLAN, M. & LAFONTAN, M. (1988). Human fat cell beta-adrenergic receptors: beta-agonist dependent lipolytic responses and characterization of beta-adrenergic binding sites on human fat cell membranes with highly selective beta-1-antagonists. *J. Lipid Res.*, **29**, 587–601.

MOHELL, N. & DICKER, A. (1989). The β-adrenergic radioligand [^{3}H] CGP 12177, generally classified as an antagonist, is a thermogenic agonist in brown adipose tissue. *Biochem. J.*, **261**, 401–405.

MOHELL, A. & NEDERGAARD, J. (1989). Comparison of the pharmacological profiles of adrenergic drugs (including BRL-agonists) at [^{3}H]prazosin and [^{3}H] CGP12177 binding sites in brown adipose tissue. *Comp. Biochem. Physiol.*, **94C**, 229–233.

MUNSON, P.J. & RODBARD, D. (1980). Ligand: a versatile computerized approach for characterization of ligand-binding systems. *Anal. Biochem.*, **107**, 220–239.

MUZZIN, P., REVELLI, J.P., FRASER, C.M. & GIACOBINO, J.P. (1992). Radioligand binding studies of the atypical beta 3-adrenergic receptor in rat brown adipose tissue using [^{3}H]-CGP 12177. *FEBS Lett.*, **298**, 162–164.

RAASMAJA, A. (1990). Alpha 1- and beta-adrenergic receptors in brown adipose tissue and the adrenergic regulation of thyroxine 5'-deiodinase. *Acta Physiol. Scand.*, **139** (suppl. 590), 1–64.

REVELLI, J.P., PESCINI, R., MUZZIN, P., SEYDOUX, J., FITZGERALD, M.G., FRASER, C.M. & GIACOBINO, J.P. (1991). Changes in beta 1- and beta 2-adrenergic receptor mRNA levels in brown adipose tissue and heart of hypothyroid rats. *Biochem. J.*, **277**, 625–628.

ROTHWELL, N.J., STOCK, M.J. & SUDERA, D.K. (1985). β-adrenoceptors in rat brown adipose tissues: proportions of β_1- and β_2-subtypes. *Am. J. Physiol.*, **248** (Endocrinol. Metab. Vol. 11), E397–E402.

SENAULT, C., LE COMTE, V. & PORTET, R. (1984). Characteristics of β-adrenergic receptors in isolated cells and in crude membranes of brown adipose tissue. *Biochimie*, **66**, 573–578.

SILLENCE, M.N., MOORE, N.J., PEGG, G.G. & LINDSAY, D.B. (1993). Ligand binding properties of putative β_3-adrenoceptors compared in brown adipose tissue and skeletal muscle membranes. *Br. J. Pharmacol.*, **109**, 1157–1163.

SIMARD, P.M., ATGIÉ, C., MAURIÈGE, P., D'ALLAIRE, F. & BUKOWIECKI, L.J. (1994). Comparison of the lipolytic effects of norepinephrine and BRL 37344 in rat brown and white adipocytes. *Obesity Res.*, **2**, 424–431.

STAEHELIN, M., SIMONS, P., JAEGG, K. & WIGGER, N. (1983). A hydrophilic β-adrenergic receptor radioligand reveals high affinity binding of agonist to intact cells. *J. Biol. Chem.*, **258**, 3496–3502.

YABUUCHI, Y., YAMASHITA, S. & TEI, S.S. (1977). Pharmacological studies of OPC 2009, a newly synthesized β-adrenoceptor stimulant in the bronchomotor and cardiovascular system of the anesthetized dog. *J. Pharmacol. Exp. Ther.*, **202**, 326–336.

ZINK, S., RÖSEN, S., SACKMANN, B. & LEMOINE, H. (1993). Regulation of endothelial permeability by β-adrenoceptor agonists: contribution of β1- and β2-adrenoceptors. *Biochim. Biophys. Acta*, **1178**, 286–298.

(Received June 13, 1994
Revised August 22, 1994
Accepted September 15, 1994)

British Journal of Pharmacology (1995) 114, 283–288 © 1995 Stockton Press All rights reserved 0007–1188/95 $9.00

Local cardiac effects of substance P: roles of acetylcholine and noradrenaline

Hsi Chiao & [1]Robert W. Caldwell

Department of Pharmacology & Toxicology, Medical College of Georgia, Augusta, Georgia 30912-2300, U.S.A.

1 The local cardiac actions of substance P were examined in isolated perfused hearts and atria of the guinea-pig.

2 In both hearts and right atria, substance P caused negative inotropic and chronotropic effects.

3 Atropine (10^{-6} M) or depletion of acetylcholine, by electrical stimulation and hemicholinium-3 perfusion, significantly attenuated the negative inotropic and chronotropic effects of substance P. α- and β-adrenoceptor blockade by nadolol and phentolamine (10^{-6} M each) did not prevent the negative inotropic and chronotropic effects of substance P. This indicates that cholinergic neurones, but not adrenergic neurones, partially mediate the effects of substance P.

4 There was no significant difference in the effects of substance P observed between groups with acetylcholine depletion and with cholinoceptor blockade. This suggests that substance P elicits its effects mainly through release of acetylcholine.

5 These results indicate that substance P has negative inotropic and chronotropic effects in guinea-pig hearts and right atria mediated partly by release of acetylcholine. Substance P also appears to have direct effects on cardiac tissue.

Keywords: Substance P; heart; right atria; local cardiac actions; acetylcholine; noradrenaline

Introduction

There is increasing evidence that certain sensory neurotransmitters not only affect the central nervous system to which the afferent nerves course, but can also be released from peripheral sensory nerve terminals via various stimuli and have local efferent functions, which may have physiological or pathological relevance (Maggi & Meli, 1988). Substance P (SP) immunoreactivity in cardiac nerves has been identified in many species including man (Reinecke *et al.*, 1980; Papka *et al.*, 1981; Weihe *et al.*, 1981, 1984; Wharton *et al.*, 1981; Houghland & Hoover, 1983). The origin of these fibres is believed to be peripheral sensory ganglia since SP immunoreactive cell bodies have been demonstrated in both nodose and dorsal root ganglia (Hökfelt *et al.*, 1975; Katz *et al.*, 1980). In addition, SP immunoreactivity in cardiac nerves is depleted by pretreatment with capsaicin, an ingredient of certain hot peppers which causes depolarization of C-fibre afferents, indicating that SP in heart is located in afferent nerves (Papka *et al.*, 1981; Papka & Urban, 1987). Moreover, the release of SP from guinea-pig heart by capsaicin and bradykinin has been detected by Hoover (1987) and Geppetti *et al.* (1988).

The presence and the release of SP by different stimuli in the heart are consistent with the opinion that SP may be involved in modulating cardiac functions. Some pharmacological studies of SP in guinea-pig isolated right atria (Stanovnik *et al.*, 1986) and in guinea-pig isolated perfused heart (Hoover & Hancock, 1988; Hoover, 1989) have shown that SP has a negative chronotropic effect. However, others have reported differing effects of SP on myocardial contractility. Lundberg *et al.* (1984) observed that the antagonist of SP, [D-Arg[1], D-Pro[2], D-Trp[7,9], Leu[11]]SP, induced a long-lasting stimulation of contractile rate and force in guinea-pig right atria which suggested SP has negative rate and force effects. Some investigators, however, showed in isolated cardiac muscle preparations that SP had no direct effect on myocardial contractility (Burcher *et al.*, 1977). Furthermore, no studies have addressed the mechanisms of the local cardiac actions of SP.

In the present study, we have characterized local cardiac effects of SP in guinea-pig isolated hearts and atria to assess direct and indirect actions. Since SP stimulation of acetylcholine release from cholinergic neurones has been reported in some organs (Yau *et al.*, 1982; Shirakawa *et al.*, 1989; Aizawa *et al.*, 1990) and a role of SP in vascular adrenergic transmission also has been described (Kazushi & Yoshiaki, 1991), our experiments were designed to investigate the possibility that classical neurotransmitters, such as acetylcholine (ACh) and noradrenaline (NA) are involved in the local cardiac actions of SP.

Methods

Langendorff perfused hearts

Male guinea pigs (300–500 g) were decapitated and the hearts were quickly removed and perfused according to a modified Langendorff procedure (Broadley, 1979). The perfusion buffer was a modified Chenoweth-Koelle solution containing (mM): NaCl 120, KCl 5.6, $CaCl_2$ 2.2, $MgCl_2$ $6H_2O$ 2.1, $NaHCO_3$ 19 and dextrose 10. The isolated hearts were cannulated through aorta and perfused at a constant flow of 10 ml min^{-1} which produced a perfusion pressure of about 80–90 mmHg. The perfusion buffer (pH 7.4) was kept at 37°C and gassed with 95% O_2:5% CO_2. A fluid-filled balloon was placed in the left ventricle to monitor the left ventricular developed pressure through a force displacement transducer. Ventricular rate was determined from the left ventricular pressure signal via a cardiotachometer.

Hearts were perfused for ~60 min until stabilization before the administration of drugs. Injections of SP or vehicle were given in a volume of 0.1 ml over 1 min through 27 × G needle into the aortic cannula. Before each dose of SP, stabilization of the heart function was required. Injections of SP were given in order of ascending doses (2.5–187.5 nmol) to construct dose-response curves. Doses were separated by at least 15 min intervals to avoid tachyphylaxis. Some hearts were given only vehicle injections

[1] Author for correspondence.

as control and some hearts were perfused only with buffer without any treatment to observe the influence of time on heart rate and force. Tachyphylaxis to the effects of SP was tested in some hearts by injecting 125 nmol of SP and then the same dose was given again in the same isolated heart preparations after 15 min.

The effects of muscarinic receptor blocker atropine (10^{-6} M) and the adrenoceptor blockers, phentolamine (10^{-6} M) and nadolol (10^{-6} M), were also evaluated on the cardiac responses to SP.

Guinea-pig isolated atria

Guinea-pig hearts were removed and put into ice-cold modified Chenoweth-Koelle buffer. The left and right atria were excised and suspended in water-jacketed organ baths (12 ml) which contained modified Chenoweth-Koelle solution (37°C, pH 7.4) bubbled with 95% O_2:5% CO_2. The atrium was under a passive tension of 0.5 g which was maintained throughout the experiment. The right atria were used to record the changes of spontaneous contractile rate and force by SP, whereas the left atria were paced (3 Hz) to record the changes of contractile force by SP. The electrical stimuli of square wave pulses (5 ms duration) at a voltage approximately double threshold was delivered *via* two platinum electrodes placed adjacent to the left atria by a Grass SD9 stimulator. Some right atria were also placed at a rate above their spontaneous being rate ($\geq$ 3 Hz) to observe the force effects of SP.

For each atrium, an equilibration period of 60 min was allowed before drugs were administered to the bath. During the stabilization period, the Chenoweth-Koelle solution was replaced at 20 min intervals. For the experiments with muscarinic receptor or adrenoceptor blockade, each atrium was then bathed in Chenoweth-Koelle solution with 1 μM atropine or 1 μM each of nadolol and phentolamine, respectively, until new baseline conditions were reached. Concentration-response curves were constructed for SP in both right and left atrial preparations. The concentrations of SP examined were from 3×10^{-10} M to 3×10^{-5} M in order of ascending concentrations. Between each concentration of SP, the atria were washed and allowed to recover baseline values. Concentrations of SP were separated by at least 15 min intervals to avoid tachyphylaxis. Tachyphylaxis to the effects of SP was tested in some right atrial preparations by applying 10^{-6} M SP and then the atria were washed and the same concentration of SP was applied again in the same preparations after 15 min. The role of parasympathetic neurones in the effects of SP was also evaluated in right atrial preparations after depleting ACh in Langendorff heart preparations. Similarly, the role of sympathetic neurones in the effects of SP were evaluated in right atrial preparations after depleting NA by *in vivo* reserpine pretreatment.

The effect of reserpine pretreatment on cardiac sensitivity to exogenous ACh was evaluated in right atrial preparations. Because there were no significant differences of maximum rate responses to ACh between control and reserpine pretreated preparations, the sensitivity was compared using pD_2 values ($-\log EC_{50}$) for ACh. The ability of atropine (10^{-6} M) to block muscarinic receptors was also assessed by comparing the rate effects of exogenous ACh in control and atropine-treated right atria. Similarly, the ability of adrenoceptor blockade by nadolol and phentolamine (10^{-6} M each) was assessed by comparing the rate effects of exogenous isoprenaline in control and treated (nadolol and phentolamine) right atria. The pD_2 values were compared between groups.

Acetylcholine and noradrenaline depletion

For ACh depletion experiments, guinea-pig hearts were isolated and maintained as described for the Langendorff technique. The two vagi were gently isolated near the heart. Perfusion buffer with 2×10^{-5} M hemicholinium-3 (HC-3) was perfused through the hearts. The HC-3 remained in the buffer throughout the experiment in order to prevent the uptake of choline formed from hydrolysis of ACh (Glavinovic, 1988). Cardiac ACh release was enhanced by electrical stimulation of the vagus nerves *via* a Grass SD9 stimulator. Stimulus pulses of 10 ms duration and 6–8 Hz frequency at increasing voltages were delivered through two platinum electrodes to the vagus nerves. Vagus nerve stimulations were monitored by observing decreases of ventricular rate and force which indicated cardiac ACh release. The stimulation intensity started at 10 V and the trains of stimuli lasted 10 s and were separated from each other by 10 s periods of rest. The stimuli were increased by 10 V when there was no effect on ventricular rate and force at the previous voltage. The depletion of ACh was confirmed by observing no rate and force changes by successive vagus nerve electrical stimulations. Then, the right atrium was excised and suspended in an organ bath and the concentration-effect curve was constructed for SP.

Depletion of noradrenaline was carried out by pretreating guinea-pigs with a single dose of reserpine (1 mg kg^{-1}, i.p.) 24 h before the experiment (Rice *et al.*, 1987). The depletion of NA was confirmed by applying different concentrations of tyramine after every atrial experiment. The results with atria that responded to tyramine were discarded.

Data analysis

The effects of SP were expressed as percentage change from baseline. Baseline values were taken 2 min before SP or vehicle applications. Left ventricular developed pressure was measured to estimate left ventricular contractility in Langendorff preparations. In atrial preparations, changes of atrial contractile force were determined as changes in contractile tension. Data are expressed as the mean ± s.e.mean. Statistical analysis of the data was performed by Neuman-Keul's and Scheffe's tests after analysis of covariance (ANCOVA). Values were considered significantly different when $P < 0.05$.

Materials

The following drugs were purchased from Sigma Chemical Company (St. Louis, MO, U.S.A.): atropine, hemicholinium-3, nadolol, phentolamine, substance P, and reserpine. Tyramine was purchased from Nutritional Biochemical Corporation (Cleveland, OH).

Stock solutions of SP were made by dissolving SP in saline which contained 0.01 N acetic acid and were stored at – 60°C. The vehicle was saline with 0.01 N acetic acid and was used to dilute the SP stock. Reserpine solution was prepared according to the recipe given by Dr Peter Rice (personal communication): 50 mg reserpine plus 125 mg anhydrous citric acid were dissolved in 1 ml benzyl alcohol and 5 ml Tween 80; distilled water was added to a total volume of 50 ml. Other drugs were prepared daily.

Results

Effects of substance P on beating rate and force in guinea-pig isolated atria

Substance P caused negative changes in rate and force of isolated right atrium. Figure 1 shows an actual representative trace of heart rate and contractile force responses to SP in right atrium. Within 1 min after administration of SP, there was a fall in rate and a decrease in contractile force. Cardiac rate and force reductions occurred during the same period and lasted about 1 min. The inotropic and chronotropic changes produced by SP were concentration-related and were significantly different from those of the vehicle (Figure 2). There were no significant changes in basal rate or contrac-

tility in right atria over the experimental period. In atria in which tachyphylaxis was tested, the rate effects of SP were $-12.6 \pm 1.1\%$ for first administration and $-11.4 \pm 1.1\%$ for the second. The force changes for the first and the second applications of SP were $-10.8 \pm 0.6\%$ and $-9.7 \pm 0.7\%$, respectively. There were no significant differences in these responses.

In left atria ($n = 4$), which were electrically paced (180 beats min^{-1}), SP had no significant effect on contractile force at concentrations of up to 3×10^{-5} M (data not shown). But in electrically paced right atria ($n = 3$), P caused a negative inotropic effect (~70% of baseline) which was similar to that in spontaneously beating right atria.

The role of adrenergic neurones in the actions of SP was evaluated by both depletion of NA and blockade of adrenoceptors. Both adrenoceptor blockade and NA depletion reduced the baseline of contractile force and rate (Table 1). However, neither of the changes was significant. Nadolol and phentolamine at 10^{-6} M produced about a 250 fold blockade of the effects of exogenous isoprenaline on guinea-pig right atria (pD_2 values for control and treated atria were 6.8 ± 0.1 and 9.2 ± 0.2, respectively). Blockade of adrenoceptors by nadolol and phentolamine did not significantly change the rate or the force effects of SP in right atria (Figure 2). However, depletion of NA by reserpine pretreatment significantly potentiated the negative chronotropic and inotropic effects of SP in isolated right atria. With depletion of NA, the greatest rate fall by SP changed from $-11.8 \pm 1.0\%$ to $-21.0 \pm 3.1\%$ and the greatest force reduction changed from $-18.6 \pm 1.1\%$ to $-32.0 \pm 2.5\%$ (Figure 2).

The role of cholinergic nerves in the heart on the actions of SP was evaluated by both depletion of ACh and blockade of muscarinic receptors. Neither pretreatment affected the baseline level of heart rate and contractile force (Table 1). Atropine at 10^{-6} M produced about a 3,000 fold blockade of

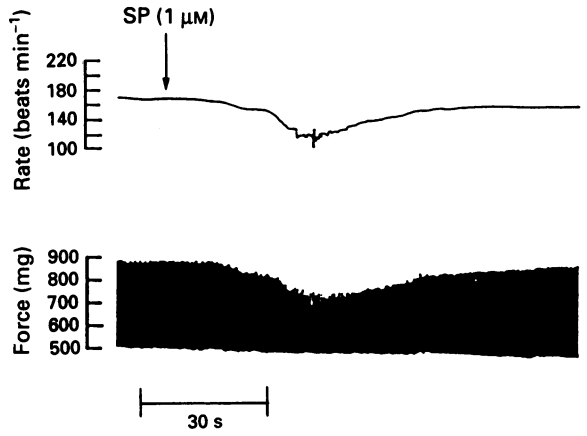


Figure 1 A representative experiment illustrating the time course of changes for contractile rate and force of right atria following administration of substance P (10^{-6} M).

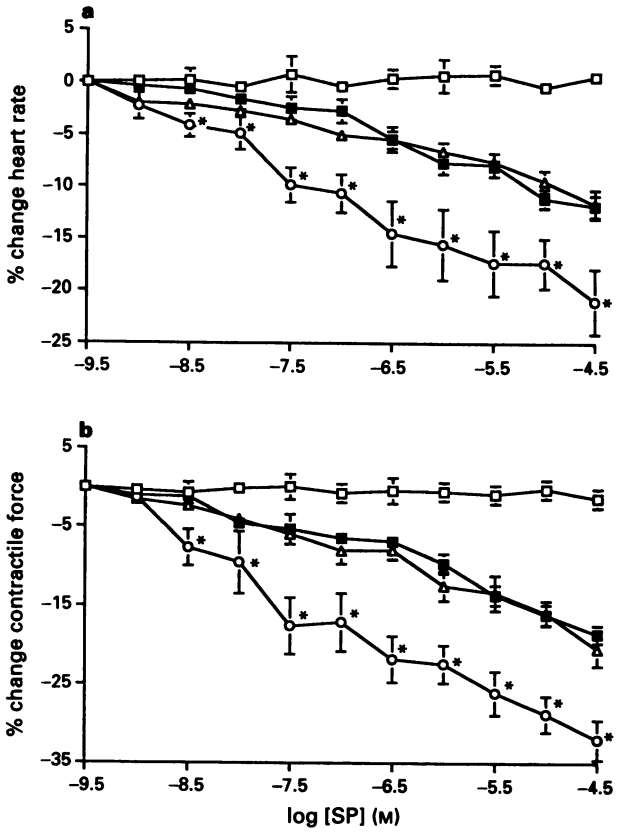


Figure 2 Effects of substance P (SP) on contractile rate (a) and force (b) in right atria without pretreatment (■; $n = 8$) and following pretreatment with either reserpine (1 mg kg^{-1}, i.p. one day before, ○; $n = 10$) or nadolol and phentolamine (10^{-6} M each in the buffer, △; $n = 8$); (□) represents vehicle application ($n = 7$). *Significant difference from SP alone ($P < 0.05$).

Table 1 Basal heart rate (B/M), contractile force and greatest changes in rate and force induced by substance P (SP) in different groups of right atria of guinea pigs

	Heart rate				*Contractile force*			
	Baseline (B/M)	*Greatest Effect (B/M)*	*Greatest change (B/M)*	*(%)*	*Baseline (mg)*	*Greatest Effect (mg)*	*Greatest change (mg)*	*(%)*
SP alone ($n = 8$)	149.1 ± 7.4[c]	131.5 ± 8.6	17.6 ± 2.6	−11.8 ± 1.0	867.5 ± 21.4	706.1 ± 19.9	161.4 ± 5.6	−18.6 ± 1.1
Atropine ($n = 9$)	151.4 ± 19.2	139.0 ± 19.6	12.4 ± 2.2	−8.2 ± 1.1	852.0 ± 19.1	782.2 ± 19.6	69.8 ± 2.2	−8.2 ± 0.7
HC-3[a] ($n = 8$)	155.3 ± 17.3	145.7 ± 13.0	9.6 ± 4.5	−6.1 ± 1.6	868.8 ± 13.3	828.8 ± 12.9	40 ± 2.0	−4.6 ± 0.6
N + P[b] ($n = 8$)	147.3 ± 13.0	130.2 ± 11.7	17.1 ± 2.6	−11.6 ± 1.4	817.5 ± 17.5	650.7 ± 14.1	166.8 ± 2.6	−20.4 ± 2.2
Reserpine ($n = 9$)	130.4 ± 9.1	103.0 ± 9.3	27.4 ± 7.4	−21.0 ± 3.1	817.2 ± 16.0	555.6 ± 13.0	261.6 ± 11.7	−32.0 ± 2.5
Reserpine + atropine ($n = 9$)	138.2 ± 9.6	125.2 ± 10.0	13.0 ± 2.4	−9.4 ± 1.1	832.2 ± 13.9	697.4 ± 13.5	134.8 ± 5.4	−16.2 ± 2.2
Reserpine + HC-3 ($n = 9$)	128.5 ± 9.1	114.4 ± 7.7	14.1 ± 2.3	−10.9 ± 1.2	822.2 ± 10.9	670.9 ± 6.4	151.3 ± 13.0	−18.4 ± 4.1

[a]Depletion of ACh by hemicholinium-3 (20 μM). [b]Adrenoceptor blockade by nadolol and phentolamine. [c]All values are means ± s.e.mean.

the effects of exogenous ACh on guinea-pig right atria (pD_2 values for control and treated atria were 6.6 ± 0.2 and 3.1 ± 0.1, respectively). In the presence of atropine, rate and force reductions to SP were significantly blocked in right atria (Figure 3). Depletion of ACh also significantly blocked the rate and force reductions by SP. The greatest rate fall changed from $-11.8 \pm 1.0\%$ to $-5.3 \pm 1.1\%$ (atropine pretreatment) or to $-6.0 \pm 1.7\%$ (ACh depletion). The greatest contractile force reduction changes from $-18.6 \pm 1.1\%$ to $-8.2 \pm 0.7\%$ (atropine pretreatment) or to $-4.6 \pm 0.6\%$ (ACh depletion).

Effects of depletion of ACh and muscarinic blockade were also evaluated in the atria which were also depleted of NA (Figure 4). SP produced much less negative rate and force effects in the group with both NA and ACh depletion than in atria with only NA depletion. In both no-pretreatment atria and NA depleted atria, muscarinic receptor blockade by atropine had similar effects on the actions of SP as those noted with depletion of ACh (Figures 3 and 4).

Reserpine pretreatment increased cardiac chronotropic sensitivity to ACh. The pD_2 values of heart rate for ACh in control and reserpine pretreated right atria were 6.6 ± 0.2 and 7.8 ± 0.1, respectively. Therefore, pretreatment with reserpine shifted the concentration-response curve for ACh by about 16 fold to the left.

Effects of substance P on heart rate and force in guinea-pig isolated hearts

In guinea-pig Langendorff heart preparations, SP caused negative changes in rate and force which were similar to those in right atrial preparations (Figure 1). These changes were concentration-related and were significantly different from those of the vehicle (Figure 5). The basal rate and contractility did not change significantly over the experimental period. There were no changes in perfusion pressure by SP application. In hearts in which tachyphylaxis were tested, there were no significant differences on rate and force effects of SP between the same two concentrations of SP.

Atropine at 10^{-6} M had no effect on baseline heart rate and contractile force but significantly blocked the negative inotropic and chronotropic effects of SP (Figure 5). Nadolol and phentolamine (10^{-6} M each) did not change the effects of SP on rate and force.

Discussion

The present data describe the effects of SP on contractile rate and force in guinea-pig heart and atria. SP elicited negative changes on contractile rate which are consistent with the earlier findings of Hoover & Hancock (1988). Our study also showed SP to have negative inotropic effects in left ventricle and right atria.

SP immunoreactivity has been found in atria, ventricles, coronary arteries and around intrinsic cardiac ganglion cells of guinea-pig heart (Weihe *et al.*, 1984; Papka & Urban, 1987). Based on observations in guinea-pig heart studies that specific binding of [^{125}I]-SP is associated with cardiac parasympathetic ganglia, substance P-induced negative inotropic and chronotropic effects may be due to stimulation of cholinergic neurones (Hoover & Hancock, 1988). We demonstrated that atropine antagonized the reduction of rate and force induced by SP which suggests that muscarinic receptors mediate the negative effects of SP. However, these results do not indicate whether or not ACh release is involved because

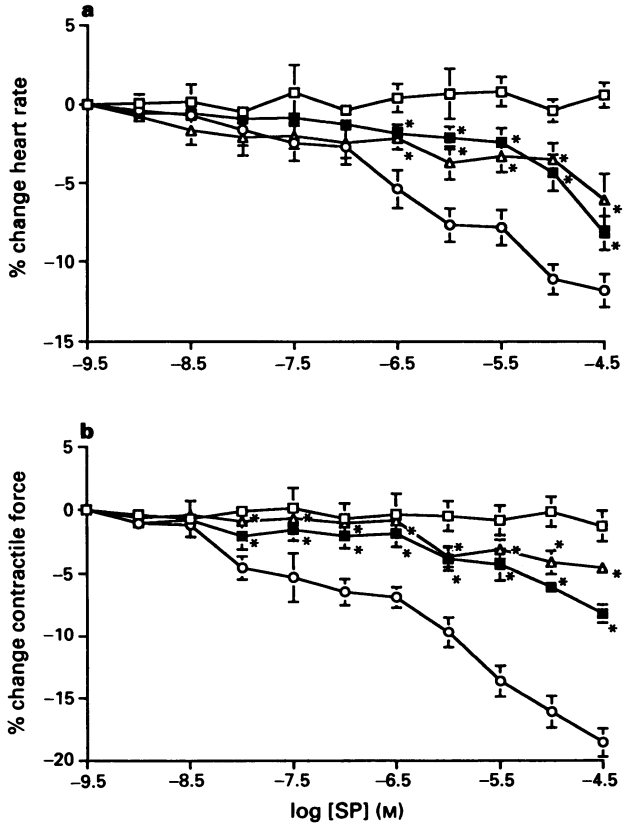


Figure 3 Effects of substance P (SP) on contractile rate (a) and force (b) in right atria without pretreatment (○; $n = 8$) and following pretreatment with either atropine (10^{-6} M, ■; $n = 9$) or ACh depletion (20 μM hemicholinium-3, △; $n = 9$); (□) represents vehicle application ($n = 7$). *Significant difference from SP alone ($P < 0.05$).

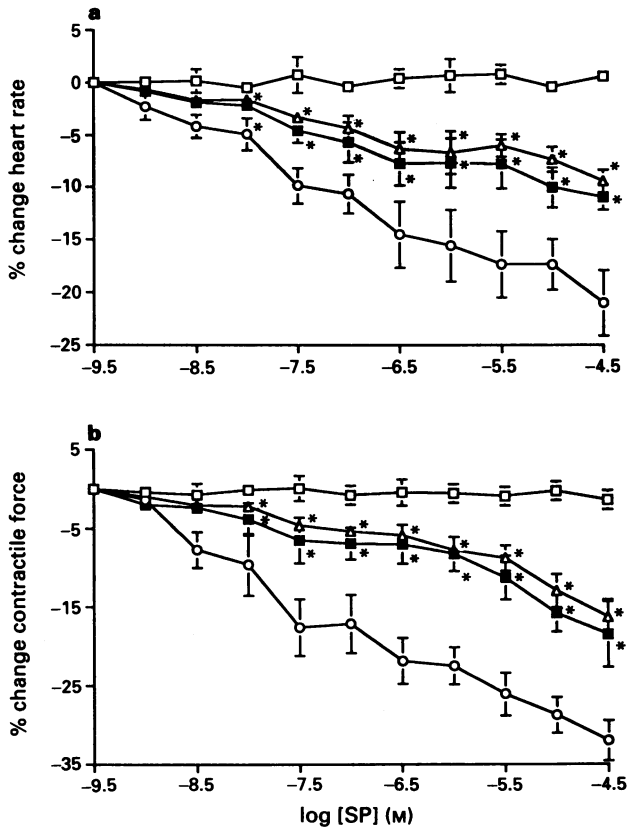


Figure 4 Effects of substance P (SP) on contractile rate (a) and force (b) in right atria following pretreatment with reserpine (1 mg kg^{-1}, i.p. on day before, ○; $n = 10$), following pretreatment with both reserpine and ACh depletion (20 μM hemicholinium-3, ■; $n = 9$), or following both reserpine pretreatment and atropine (10^{-6} M, △; $n = 9$); (□) represents vehicle application ($n = 7$). *Significant difference from reserpine control ($P < 0.05$).

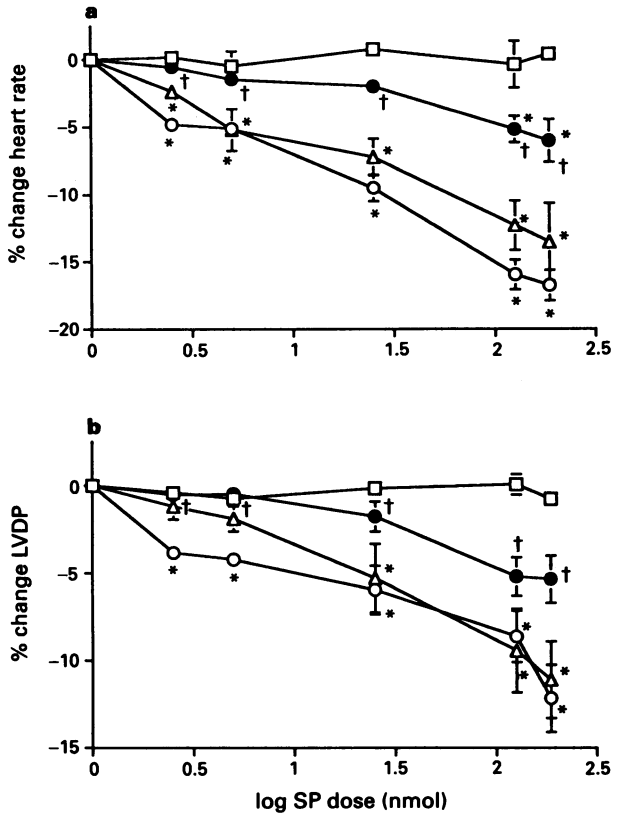


Figure 5 Comparison of the heart rate (a) and left ventricular developed pressure (LVDP, b) effects of substance P (SP, ○; $n = 11$) with those of vehicle (□; $n = 5$), atropine pretreatment (●; $n = 6$), nadolol and phentolamine pretreatment (△; $n = 6$) on isolated Langendorff heart preparations. *Significant difference from vehicle treatment group ($P < 0.05$). †Significant difference from SP alone ($P < 0.05$).

SP may elicit effects by (1) releasing ACh and/or changing the sensitivity of muscarinic receptors to ACh, (2) acting through muscarinic receptors, or (3) other mechanism(s).

To determine whether release of ACh in the heart mediates the effects of SP, we performed functional studies of SP in the right atria which were depleted of ACh. Depletion of ACh significantly attenuated both the negative rate and force effects of SP indicating that SP releases ACh from cholinergic nerve endings in the guinea-pig heart or right atria and that ACh mediates the rate and force effects of SP. The fact that the muscarinic blockade and the depletion of ACh antagonized the effects of SP to a similar degree suggests that SP elicits its effects mainly through release of ACh. However, substance P still produces cardiac effects after muscarinic receptor blockade or depletion of ACh which suggests that other mechanism(s) of action are also involved. SP may have a direct receptor effect on the sinoatrial node, cardiac conductive tissues, and cardiac muscle or other factors may mediate the effects of SP. Nitric oxide is now recognized not only to be synthesized and released in endocardium (Schulz *et al.*, 1991), cardiac myocytes (Schulz *et al.*, 1992; Brady *et al.*, 1993), and cardiac nerve fibres and neurones (Hassall *et al.*, 1992; Klimaschewski *et al.*, 1992), but also has negative effects on the contractile force of myocardium (Finkel *et al.*, 1992) and isolated myocytes (Brady *et al.*, 1993). Based on the fact that some effects of SP in other tissues are mediated by nitric oxide (Jin *et al.*, 1993; Ziche *et al.*, 1993), we hypothesize that nitric oxide may also mediate local cardiac effects of substance P. Future studies are necessary to investigate the relationship between actions of SP and nitric oxide in the heart.

In order to determine if adrenergic neurones in the heart mediate the effects of SP, NA was depleted from hearts prior to experiments. Depletion of NA by reserpine potentiates the rate and force reductions in right atria. However, α- and β-adrenoceptor blockade by phentolamine and nadolol (10^{-6} M) did not potentiate the rate or force reductions to SP as NA depletion did. We observed that 10^{-6} M nadolol and phentolamine can produce about a 250 fold blockade of effects of exogenous isoprenaline on guinea-pig right atria (data not shown). Additionally, the antagonistic potency, pA_2, of nadolol against effects of isoprenaline has been reported to be 9.78 ± 0.05 (Kuwahara *et al.*, 1987). Thus, this concentration of nadolol and phentolamine (10^{-6} M) should be high enough to antagonize adequately the effects of NA adrenoceptors. Our results suggest that the adrenergic nervous system does not mediate the effets of SP.

The effects of reserpine pretreatment may be explained by its supersensitizing effect on cardiac tissue. Reserpine has been reported to hypersensitize adrenoceptors to their agonists (Hawthorn & Broadley, 1982; Tenner *et al.*, 1984). However, up-regulation of β-adrenoceptors should oppose the effects of SP and it is also unlikely because up-regulation of β-adrenoceptors takes longer than 24 h (Rice *et al.*, 1987). The finding that reserpine pretreatment shifted the heart rate concentration-response curve of ACh to the left by 16 fold indicates that reserpine pretreatment enhances the sensitivity of the muscarinic receptor to ACh. Other studies have reported that supersensitivity can also be produced to a number of non-adrenergic agonists such as calcium and glucagon by reserpine pretreatment (Meghji *et al.*, 1978; Tenner & Carrier, 1978). Based on these observations, the effects of reserpine pretreatment on SP responses may be explained by its ability to produce nonspecific supersensitivity in cardiac tissues.

Substance P caused a negative inotropic effect in both spontaneously beating right atria and electrically paced right atria, but it did not significantly change the contractile force of paced left atria. This finding can be explained by the distribution of cholinergic neurones in the heart. There are more parasympathetic nerve endings in the right atria than in the left atria (Cabot & Cohen, 1980). Since most of the effects of SP are mediated by ACh release, it is not surprising that the effects of SP are higher in right atria than in left.

The cardiac effects of SP we observed are relatively low compared to the responses in Langendorff hearts with the same dose (25 nmol) in the studies of Hoover (1989). Those experiments employed a perfusate with albumin. We consider that our data probably underestimate the actions of endogenous SP released focally in the heart. The reasons for this is that many endopeptidases, especially membrane-bound enzymes, are capable of degrading SP (Lee *et al.*, 1981). Due to the difficulty of contractility measurement (foam formation in gassed solution), we did not use peptidase inhibitors in our experiments. Therefore, the relatively small changes in our preparations may be due to the degradative effects of endopeptidases in heart on SP.

In conclusion, SP is a neuropeptide which has negative inotropic and chronotropic effects in guinea-pig hearts and right atria. SP elicits its effects mainly through releasing ACh. However, SP still produces cardiac effects after muscarcinic receptor blockade or depletion of ACh which suggests that other mechanism(s) are also involved. SP itself may have direct effects on cardiac tissue. The presence and the local effects of SP in the heart suggest its importance in the local regulation of cardiac functions. The role of cardiac SP in pathological conditions needs to be examined.

The authors appreciate the comments and advice provided by Drs G.O. Carrier and G. Abou-Mohamed.

References

AIZAWA, H., MIYAZAKI, N., INOUE, H., IKEDA, T. & SHIGEMATSU, N. (1990). Effects of endogenous tachykinins on neuro-effector transmission of vagal nerve in guinea pig tracheal tissue. *Respiration*, **57**, 338–342.

BRADY, A., WARREN, J., POOLE-WILSON, P., WILLIAMS, T. & HARDING, S. (1993). Nitric oxide attenuates cardiac myocyte contraction. *Am. J. Physiol.*, **265**, H176–H182.

BROADLEY, K.J. (1979). The Langendorff heart preparation: reappraisal of its role as a research and teaching model for coronary vasoactive drugs. *J. Pharmacol. Methods*, **2**, 143–156.

BURCHER, E., ATTERHOG, J.-H., PERNOW, B. & ROSELL, S. (1977). Cardiovascular effects of substance P: Effects on the heart and regional blood flow. In *Substance P*, ed. von Euler U.S. & Pernow, B. pp. 261–268. New York: Raven Press.

CABOT, J.B. & COHEN, D.H. (1980). Neural control of the avian heart. In *Hearts and heart-like organs*. ed. Bourne, G.H. Vol. 1. pp. 199–258. New York: Academic Press.

FINKEL, M.S., ODDIS, C.V., JACOB, T.D., WATKINS, S.C., HATTLER, B.G. & SOMMONS, R.L. (1992). Negative inotropic effects of cytokines on the heart mediated by nitric oxide. *Science*, **257**, 387–389.

GEPPETTI, P., MAGGI, C.A., PERRETTI, F., FRILLI, S. & MANZINI, S. (1988). Simultaneous release by bradykinin of substance P and calcitonin gene-related peptide immunoreactivities from capsaicin-sensitive structures in guinea pig heart. *Br. J. Pharmacol.*, **94**, 288–290.

GLAVINOVIC, M.I. (1988). Effect of blockade of choline uptake by hemicholinium-3 on synaptic output. *Neuroscience*, **25**, 283–289.

HASSALL, C.J.S., SAFFREY, M.J., BELAI, A., HOYLE, C.H.V., MOULES, E.W., MOSS, J., SCHMIST, H.H.H.W., MURAD, F., FÖRSTERMANN, U. & BURNSTOCK, G. (1992). Nitric oxide synthase immunoreactivity and NADPH-diaphorase activity in a subpopulation of intrinsic neurons of the guinea pig heart. *Neurosci. Lett.*, **143**, 65–68.

HAWTHORN, M.H. & BROADLEY, K.J. (1982). β-Adrenoceptor ligand binding and supersensitivity to isoprenaline of ventricular muscle after chronic reserpine pretreatment. *Naunyn-Schmied Arch. Pharmacol.*, **320**, 240–245.

HÖKFELT, T., KELLERTH, J.O., NILSSON, G. & PERNOW, B. (1975). Experimental immunohistochemical studies on the localization and distribution of substance P in cat primary sensory neurons. *Brain Res.*, **100**, 235–252.

HOOVER, D.B. (1987). Effects of capsaicin on release of substance P-like immunoreactivity and physiological parameters in isolated perfused guinea pig heart. *Eur. J. Pharmacol.*, **141**, 489–492.

HOOVER, D.B. (1989). Effects of substance P on rate and perfusion pressure in the isolated guinea pig heart. *J. Pharmacol. Exp. Ther.*, **252**, 179–184.

HOOVER, D.B. & HANCOCK, J.C. (1988). Distribution of substance P binding sites in guinea pig heart and pharmacological effects of substance P. *J. Auton. Nerv. Syst.*, **23**, 189–197.

HOUGLAND, M.W. & HOOVER, D.B. (1983). Detection of substance P-like immunoreactivity in nerve fibers in the heart of guinea pigs but not rats. *J. Auton. Nerv. Syst.*, **8**, 295–301.

JIN, J.G., MISRA, S., GRIDER, J.R., MAKHLOUF, G.M. (1993). Functional difference between substance P and neurokinin A: relaxation of gastric muscle by substance P is mediated by vasoactive intestinal peptide and nitric oxide. *Am. J. Physiol.*, **264**, G678–G685.

KATZ, D.M. & KARTEN, H.J. (1980). Substance P in the vagal sensory ganglia: localization in cell bodies and pericullar arborizations. *J. Comp. Neurol.*, **193**, 549–564.

KAZUSHI, T. & YOSHIAKI, M. (1991). Effects of substance P on norepinephrine release from vascular adrenergic neurons in spontaneously hypertensive rats. *Am. J. Hypertens.*, **4**, 327–332.

KLIMASCHEWSKI, L., KUMMER, W., MAYER, B., COURAUD, J.Y., PREISSLER, U., PHILIPPIN, B. & HEYM, C. (1992). Nitric oxide synthase in cardiac nerve fibers and neurons of rat and guinea pig heart. *Circ. Res.*, **71**, 1533–1537.

KUWAHARA, M., AMANO, H., KUBO, T. & MISU, Y. (1987). A trial for kinetic evaluation of the antagonistic potency of several beta-antagonists on presynaptic beta-adrenoceptors. *Jpn. J. Pharmacol.*, **43**, 445–448.

LEE, C.M., SANDBERG, B.E.B., HANLEY, M.R. & IVERSEN, L.L. (1981). Purification and characterization of a membrane-bound substance P-degrading enzyme from human brain. *Eur. J. Biochem.*, **114**, 315–327.

LUNDBERG, J.M., HUA, Y.Y. & FREDHOLM, B.B. (1984). Capsaicin-induced stimulation of guinea-pig atrium: Involvement of a novel sensory transmitter or a direct action on myocytes? *Naunyn-Schmied. Arch. Pharmacol.*, **325**, 176–182.

MAGGI, C.A. & MELI, A. (1988). The sensory-efferent function of capsaicin-sensitive sensory neurone. *Gen. Pharmacol.*, **19**, 1–43.

MEGHJI, P., TENNER, T.E. Jr. & MCNEILL, J.H. (1978). Reserpine-induced supersensitivity to the inotropic and phosphorylase activating effects of glucagon in the perfused rat heart. *Eur. J. Pharmacol.*, **51**, 55–62.

PAPKA, R.E., FURNESS, J.B., DELLA, N.G. & COSTA, M. (1981). Depletion by capsaicin of substance P-immunoreactivity and acetylcholinesterase activity from nerve fibers in the guinea pig heart. *Neurosci. Lett.*, **27**, 47–53.

PAPKA, R.E. & URBAN, L. (1987). Distribution, origin and sensitivity to capsaicin of primary afferent substance P-immunoreactive nerves in the heart. *Acta Physiol. Hungarica*, **69**, 459–468.

REINECKE, M., WEIHE, E. & FORSSMANN, W.G. (1980). Substance P-immunoreactive nerve fibers in the heart. *Neurosci. Lett.*, **20**, 265–269.

RICE, P.J., TAYLOR, D.A., VALINSKI, W.A., HEAD, R.J. & FLEMING, W.W. (1987). Norepinephrine depletion and sensitivity changes in rat heart induced by pretreatment with reserpine. *J. Pharmacol. Exp. Ther.*, **240**, 764–771.

SCHULZ, R., NAVA, E. & MONCADA, S. (1992). Induction and potential biological relevance of a calcium-independent nitric oxide synthase in the myocardium. *Br. J. Pharmacol.*, **105**, 575–580.

SCHULZ, R., SMITH, J.A., LEWIS, M.J. & MONCADA, S. (1991). Nitric oxide synthase in cultured endocardial cells of the pig. *Br. J. Pharmacol.*, **104**, 21–24.

SHIRAKAWA, J., NAKANISHI, T., TANIYAMA, K., KAMADONO, S. & TANAKA, C. (1989). Regulation of the substance P-induced contraction via the release of acetylcholine and gamma-aminobutyric acid in the guinea pig urinary bladder. *Br. J. Pharmacol.*, **98**, 437–444.

STANOVNIK, L., LOGONDER-MLINSEK, M. & ERJAVEC, F. (1986). The effect of compound 48/80, substance P and pentagastrin on the isolated guinea pig atrium. *Agents Actions*, **18**, 197–200.

TENNER, T.E. Jr. & CARRIER, G.O. Jr. (1978). Reserpine-induced supersensitivity to the chronotropic and inotropic effects of calcium in rabbit atria. *J. Pharmacol. Exp. Ther.*, **295**, 183–192.

TENNER, T.E., WALTHALL, E.B. & RAMANADHAM, S. (1984). β-Adrenoceptor density changes and reserpine induced supersensitivity. *Proc. West. Pharmacol. Soc.*, **27**, 5–9.

WEIHE, E., REINECKE, M., OPHERK, D. & FORSSMANN, W.G. (1981). Peptidergic innovation (substance P) in the human heart. *J. Mol. Cell. Cardiol.*, **13**, 331–333.

WEIHE, E., REINECKE, M. & FORSSMANN, W.G. (1984). Distribution of vasoactive intestinal polypeptide-like immunoreactivity in the mammalian heart. Interrelation with neurotensin- and substance P-like immunoreactive nerves. *Cell Tissue Res.*, **236**, 527–540.

WHARTON, J., POLAK, J.M., MCGREGOR, G.P., BISHOP, A.E. & BLOOM, S.R. (1981). The distribution of substance P-like immunoreactive nerves in the guinea pig heart. *Neuroscience*, **6**, 2193–2204.

YAU, W.M. & YOUTHER, M.L. (1982). Direct evidence for a release of acetylcholine from the myenteric plexus of guinea pig small intestine by substance P. *Eur. J. Pharmacol.*, **81**, 665–668.

ZICHE, M., MORBIDELLI, L., PARENTI, A., AMERINI, S., GRANGER, H.J. & MAGGI, C.A. (1993). Substance P increases cyclic GMP levels on coronary postcapillary venular endothelial cells. *Life. Sci.*, **53**, PL229–PL234.

(Received June 21, 1994
Revised September 1, 1994
Accepted September 15, 1994)

British Journal of Pharmacology (1995) 114, 289-296 © 1995 Stockton Press All rights reserved 0007-1188/95 $9.00

Influence of nitric oxide synthase inhibition, nitric oxide and hydroperoxide on insulin release induced by various secretagogues

[1]Georgios Panagiotidis, Björn Åkesson, *Ewa L. Rydell & Ingmar Lundquist

Department of Pharmacology, University of Lund, Lund, Sweden and *Department of Pharmacology, University of Linköping, Linköping, Sweden

1 Recent studies have suggested that the generation of nitric oxide (NO) and hydrogen peroxide (H_2O_2) by islet NO synthase and monoamine oxidase, respectively, may have a regulatory influence on insulin secretory processes. We have investigated the pattern of insulin release from isolated islets of Langerhans in the presence of various pharmacological agents known to perturb the intracellular levels of NO and the oxidation state of SH-groups.

2 The NO synthase inhibitor, N^G-nitro-L-arginine methyl ester (L-NAME) dose-dependently increased L-arginine-induced insulin release. D-Arginine did not influence L-arginine-induced insulin secretion. However, D-NAME which reportedly has no inhibitory action on NO synthase, modestly increased L-arginine-induced insulin release, but was less effective than L-NAME. High concentrations (10 mM) of D-arginine as well as L-NAME and D-NAME could enhance basal insulin release.

3 The intracellular NO donor, hydroxylamine, dose-dependently inhibited insulin secretion induced by L-arginine and L-arginine + L-NAME.

4 Glucose-induced insulin release was increased by NO synthase inhibition (L-NAME) and inhibited by the intracellular NO donor, hydroxylamine. Sydnonimine-1 (SIN-1), an extracellular donor of NO and superoxide, induced a modest suppression of glucose-stimulated insulin release. SIN-1 did not influence insulin secretion induced by L-arginine or the adenylate cyclase activator, forskolin.

5 The intracellular 'hydroperoxide donor' *tert*-butylhydroperoxide in the concentration range of 0.03–3 mM inhibited insulin release stimulated by the nutrient secretagogues glucose and L-arginine. Low concentrations (0.03– 30 μM) of *tert*-butylhydroperoxide, however enhanced insulin secretion induced by the phosphodiesterase inhibitor isobutylmethylxanthine (IBMX).

6 Islet guanosine 3':5'-cyclic monophosphate (cyclic GMP) content was not influenced by 10 mM L-arginine or *tert*-butylhydroperoxide at 3 or 300 μM but was markedly increased (14 fold) by a high hydroxylamine concentration (300 μM). In contrast, islet adenosine 3':5'-cyclic monophosphate (cyclic AMP) content was increased (3 fold) by L-arginine (10 mM) and (2 fold) by *tert*-butylhydroperoxide (300 μM).

7 Our results strongly suggest that NO is a negative modulator of insulin release induced by the nutrient secretagogues L-arginine and glucose. This effect is probably not mediated to any major extent by the guanylate cyclase-cyclic GMP system but may rather be exerted by the S-nitrosylation of critical thiol groups involved in the secretory process. Similarly the inhibitory effect of *tert*-butylhydroperoxide is likely to be elicited through affecting critical thiol groups. The mechanism underlying the secretion-promoting action of *tert*-butylhydroperoxide on IBMX-induced insulin release is probably linked to intracellular Ca^{2+}-perturbations affecting exocytosis.

8 Taken together with previous data the present results suggest that islet production of low physiological levels of free radicals such as NO and H_2O_2 may serve as important modulators of insulin secretory processes.

Keywords: Isolated islets; insulin release; L-arginine; N^G-nitro-D-arginine methyl ester; N^G-nitro-L-arginine methyl ester; D-arginine; hydroxylamine; *tert*-butylhydroperoxide; glucose; cyclic GMP; cyclic AMP

Introduction

Synthesis of nitric oxide (NO) from L-arginine has been identified as an important mechanism implicated in the regulation of cellular function and communication (see Moncada *et al.*, 1991). Very recently, evidence has been obtained for the occurrence of NO synthase activity in both endocrine cells and nerves of the islets of Langerhans (Schmidt *et al.*, 1992; Vincent, 1992; Panagiotidis *et al.*, 1992; Corbett *et al.*, 1993). Previous data (Laychock *et al.*, 1991; Schmidt *et al.*, 1992) suggested that the islet NO-system had a promoting action on insulin secretion. In contrast, however, we recently presented *in vitro* results showing that the NO system in fact is a negative modulator of L-arginine-induced insulin release (Panagiotidis *et al.*, 1992). The insulinotropic action of L-arginine is complex and has partially been attributed to a direct depolarizing effect of the cationic amino acid. Since NO synthase inhibition increased L-arginine-induced insulin release (Panagiotidis *et al.*, 1992) we suggested that the stimulating effect of L-arginine was in part counteracted by the concomitant production of NO. In other tissues the L-arginine-derived NO is thought to act principally by stimulating guanylate cyclase, resulting in the elevation of guanosine 3':5'-cyclic monophosphate (cyclic GMP) (Moncada *et al.*, 1991). With regard to insulin secreting mechanisms we recently hypothetised (Panagiotidis *et al.*, 1992) that the inhibitory action of NO might be exerted

[1] Author for correspondence.

through an interaction of NO with thiol groups essential for the secretory process. In fact, it has been known for a long time that certain membrane thiols are involved in the stimulus-secretion coupling of glucose-induced release of insulin (see Hellman *et al.*, 1974; Ammon & Mark, 1985). Thus the formation of S-nitrosothiols may change the balance of critical intracellular and/or membrane thiols of the β-cells. Such a mechanism is in close agreement with our recent proposal that hydrogen peroxide (H_2O_2) generated by the activation of islet monoamine oxidase may inhibit certain insulin secreting processes by oxidizing critical thiol groups (Lundquist *et al.*, 1991; Panagiotidis *et al.*, 1993a,b,c).

The aim of the present investigation was to study in more detail the effect of NO and 'H_2O_2' (as mimicked by *tert*-butylhydroperoxide) on insulin secretion induced by various secretagogues. This was accomplished by means of the NO synthase inhibitor, N^G-nitro-L-arginine methylester (L-NAME), the intracellular NO donor hydroxylamine (De Master *et al.*, 1989), the extracellular donor of NO and superoxide sydnonimine-1 (SIN-1) (Hogg *et al.*, 1992) as well as the intracellular 'hydroperoxide donor' *tert*-butylhydroperoxide (Orrenius & Moldéus, 1984).

Methods

Animals

Female mice of the NMRI strain (B & K, Universal, Sollentuna, Sweden) weighing 25–30 g, were used throughout the experiments. A standard pellet diet (ASTRA-Ewos, Södertälje, Sweden) and tap water were available *ad libitum* before all experiments.

Drugs and chemicals

N^G-nitro-L-arginine methyl ester (L-NAME), D-NAME, L- and D-arginine, 3-isobutyl-1-methylxanthine (IBMX) and hydroxylamine were from Sigma Chemicals, St Louis, MO, U.S.A. *tert*-Butylhydroperoxide was purchased from Merck AG, Darmstadt, Germany. Collagenase (CLS-4) was obtained from Worthington Biochemical Corp., Freehold, NJ, U.S.A. Bovine serum albumin was from ICN Biomedicals Ltd., High Wycombe, Bucks, U.K. Sydnonimine-1 (SIN-1) was kindly supplied by GEA Ltd., Pharmaceutical Research Laboratories, DK-2650 Hvidovre, Denmark. The radioimmunoassay kits for insulin determination were obtained from NOVO Ltd., Bagsvaerd, Denmark. The antibodies for cyclic GMP and cyclic AMP determination were prepared in our laboratory. The preparation and characterization of the antiserum were made according to Steiner *et al.* (1972). [^{125}I]guanosine or [^{125}I]adenosine 3′:5′-cyclic phosphoric acid was from NEN Dupont, Dreiech, Germany. All other drugs and chemicals were from British Drug Houses Ltd., Poole, Dorset, U.K. or Merck AG., Darmstadt, Germany.

Experimental protocol

Preparation of isolated islets from the mice was performed by retrograde injection of a collagenase solution *via* the bile-pancreatic duct (Gotoh *et al.*, 1985). Freshly isolated islets were preincubated in a HEPES-supplemented KRB-buffer as previously described (Panagiotidis *et al.*, 1992). After preincubation the buffer was changed and the islets were incubated with the test agents for 60 min at 37°C in an incubation box (30 cycles min^{-1}) if not otherwise stated. The incubation vials contained 8 islets per 1.5 ml buffer except when islets were incubated for cyclic nucleotide determination where 75–80 islets per vial were needed. Immediately after incubation an aliquot of the medium was removed and frozen for subsequent assay of insulin. For analysis of islet cyclic GMP and cyclic AMP the incubation was stopped by the removal of buffer and addition of 0.5 ml ice-cold 10% trichloroacetic acid (TCA), followed by immediate freezing in a −70°C ethanol bath. When assayed, 0.5 ml H_2O was added and the samples were sonicated for 3 × 5 s in a Branson Sonifier Cell disrupter followed by centrifugation at 1.100 *g* for 15 min. The supernatants were collected and extracted with 4 × 2 ml of water-saturated diethyl ether. The aqueous phase was recovered and freeze dried, using a Lyovac GT 2 freeze dryer. The residue was then dissolved in 450 µl 50 mM Na-acetate buffer (pH 6.2). Both cyclic GMP and cyclic AMP were determined by radioimmunoassay according to Steiner *et al.* (1972). In order to improve sensitivity of the assays, the samples were acetylated with acetic acid anhydride as described by Harper & Brooker (1975).

Results

Effect of NO synthase inhibition on basal and stimulated insulin secretion

Figure 1a shows the effect of different concentrations of the NO synthase inhibitor L-NAME (an L-arginine analogue) on basal insulin secretion (7 mM glucose) from isolated islets. L-NAME-concentrations of 0.1–5.0 mM did not significantly influence basal insulin release. A high concentration of L-NAME (10 mM), however, induced a 3 fold increase in insulin secretion.

Figure 1b and 1c illustrate the influence of NO synthase inhibition on insulin release stimulated by L-arginine and glucose, respectively. Concentrations of L-NAME which did not affect basal insulin secretion (Figure 1a) dose-dependently potentiated L-arginine-induced insulin release (Figure 1b). Furthermore, NO synthase inhibition did also increase glucose-stimulated insulin secretion (Figure 1c).

Effect of D-arginine and D-NAME on basal and L-arginine-stimulated insulin secretion

Figure 2a compares the effects of L-arginine and D-arginine, the stereoisomer of L-arginine, on insulin release. Similar to 5 mM L-NAME (Figure 1a) 5 mM D-arginine had no insulin releasing effect (Figure 2a). However, unlike L-NAME, D-arginine did not influence L-arginine-induced insulin release. Figure 2b shows that D-NAME, which similar to D-arginine, reportedly is devoid of NO synthase inhibitory properties modestly increased L-arginine-induced insulin release but to a significantly lower level than did L-NAME. A high concentration of D-arginine (10 mM) (Figure 2a), however, induced a moderate insulin response which was approximately 4 times less than that of 10 mM L-arginine (Figure 2b). D-NAME (10 mM) could stimulate basal insulin release to the same extent as L-NAME (Figure 2b).

Effect of the intracellular NO donor, hydroxylamine, on the secretion of insulin induced by L-arginine and glucose

Figure 3 illustrates the effect of the intracellular NO donor hydroxylamine on insulin secretion induced by 10 mM L-arginine in the presence of 7 mM basal glucose (Figure 3a). Figure 3b shows the effect of hydroxylamine on insulin release stimulated by 16.7 mM glucose. The NO donor dose-dependently inhibited L-arginine stimulated insulin release which was almost totally suppressed at 3 mM hydroxylamine. Glucose-induced insulin release appeared less sensitive to the drug, although a total suppression was again achieved at 3 mM hydroxylamine. Hydroxylamine did not influence basal (7 mM glucose) insulin secretion (data not shown).

Effect of the extracellular NO and superoxide donor SIN-1 on insulin secretion induced by glucose, L-arginine and forskolin

The next series of experiments examined the effect of the NO and superoxide donor SIN-1, which is believed to release NO

and superoxide extracellularly. Figure 4a shows that SIN-1 significantly reduced insulin release stimulated by 16.7 mM glucose. This inhibition was modest and detectable already at 0.3 μM SIN-1 but was less pronounced than the inhibitory effect of hydroxylamine (Figure 3b). SIN-1 had no influence on insulin secretion induced by L-arginine (Figure 4b) or by the adenylate cyclase activator, forskolin (Figure 4c). Note that the SIN-1 experiments were run only for 35 min because of the reported rapid deterioration of this compound.

Effect of the intracellular 'hydroperoxide donor' tert-butylhydroperoxide on insulin secretion induced by L-arginine, glucose and isobutylmethylxanthine (IBMX)

In analogy with the experiments on intracellular delivery of NO by hydroxylamine we then examined the effect of intracellular hydroperoxide by employing *tert*-butylhydroperoxide. Data from previous *in vivo* experiments suggested that an intracellular generation of H_2O_2 by the activation of islet monoamine oxidase might impair glucose-induced but promote IBMX-induced insulin release (Lundquist *et al.*, 1991; Panagiotidis *et al.*, 1993b,c, 1994). Figure 5a and b illustrate the effect of *tert*-butylhydroperoxide on insulin secretion induced by 10 mM L-arginine and 16.7 mM glucose, respectively. The 'hydroperoxide donor' markedly suppressed both L-arginine- and glucose-induced insulin release. In contrast insulin secretion induced by IBMX, an activator of the cyclic AMP system, was enhanced by low levels of *tert*-butylhydroperoxide (0.03–30 μM) (Figure 5c). A very high concentration of *tert*-butylhydroperoxide (3 mM) suppressed IBMX-induced insulin release. *tert*-Butylhydroperoxide did not influence basal (4 mM glucose) insulin secretion (data not shown).

Comparative effects of hydroxylamine and tert-butylhydroperoxide on insulin secretion induced by L-arginine + L-NAME

In order to examine the effect of hydroxylamine and *tert*-butylhydroperoxide on L-arginine-induced insulin secretion in the absence of endogenous NO production, a series of experiments was performed with the NO synthase inhibitor L-NAME. Figure 6a shows that hydroxylamine dose-dependently suppressed L-arginine-induced insulin release in the presence of L-NAME with a total inhibition at 3 mM. Figure 6b shows that *tert*-butylhydroperoxide was less potent in this respect displaying an inhibitory action of approximately 50%

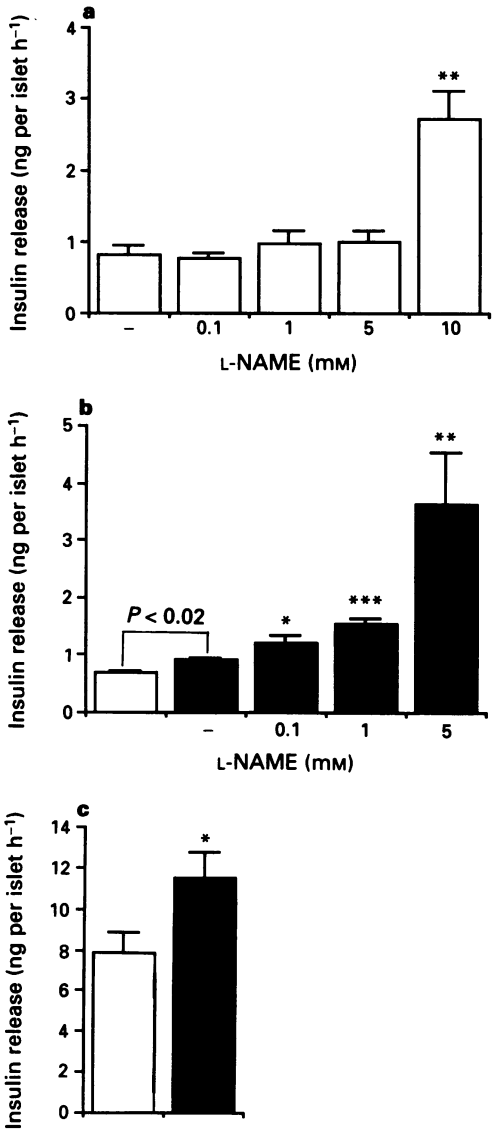


Figure 1 (a) Effect of different concentrations of N^G-nitro-L-arginine methyl ester (L-NAME) on basal insulin secretion (7 mM glucose) from isolated islets. Values are mean ± s.e.mean from 6–10 batches of islets $^{**}P<0.01$ *vs* basal control. (b) Influence of different concentrations of L-NAME on insulin release from isolated islets stimulated by L-arginine 5 mM in the presence of basal glucose 7 mM (solid columns). Glucose 7 mM basal control is denoted by an open column. Values are mean ± s.e.mean from 6–10 batches of islets, $^{*}P<0.05$, $^{**}P<0.01$, $^{***}P<0.001$ compared to 5 mM L-arginine without addition of L-NAME. (c) Glucose-induced (16.7 mM) insulin release from isolated islets in the absence (open column) or presence (solid column) of 5 mM L-NAME. Values are mean ± s.e.mean from 6–10 batches of islets, $^{*}P<0.05$.

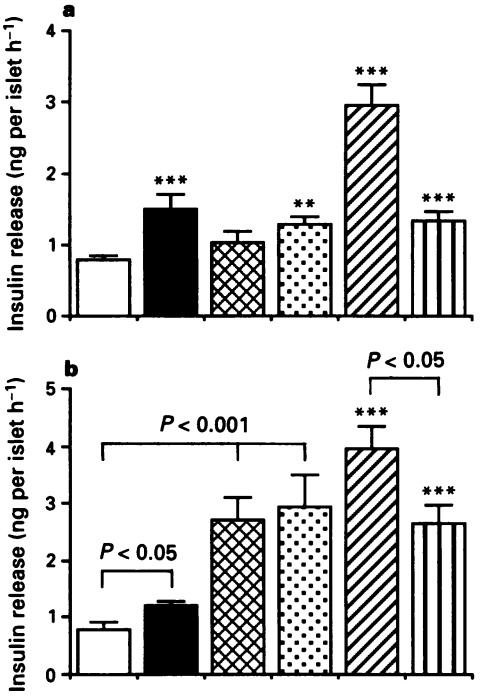


Figure 2 (a) Effect of L-arginine 5 mM (solid column), D-arginine 5 mM (cross-hatched column), L-arginine 5 mM + D-arginine 5 mM (stippled column), L-arginine 10 mM (hatched column) and D-arginine 10 mM (striped column) on insulin secretion from isolated islets in the presence of 7 mM glucose. Basal control (7 mM glucose) is denoted by an open column. Values are mean ± s.e.mean from 6–10 batches of islets, $^{**}P<0.01$, $^{***}P<0.001$ compared to basal control. (b) Effect of L-arginine 5 mM (solid column), L-NAME 10 mM (cross-hatched column), D-NAME 10 mM (stippled column), L-arginine 5 mM + L-NAME 5 mM (hatched column) and L-arginine 5 mM + D-NAME 5 mM (striped column) on insulin secretion from isolated islets in the presence of 7 mM glucose. Basal control (7 mM glucose) is denoted by an open column. Values are mean ± s.e.mean from 6–10 batches of islets, $^{***}P<0.001$, compared to L-arginine 5 mM.

of the L-arginine + L-NAME insulin response at 0.3 and 3 mM.

Effect of L-arginine, hydroxylamine and tert-butylhydroperoxide on islet cyclic GMP and cyclic AMP levels

Table 1 shows the effect of 10 mM L-arginine as well as concentrations of 3 and 300 μM hydroxylamine and *tert*-butylhydroperoxide on the levels of cyclic GMP and cyclic AMP in isolated mouse islets at 7 mM glucose. The glucose concentration in the control incubation medium was 7 mM. It is seen that only 300 μM hydroxylamine influenced the cyclic GMP levels. At this concentration the NO donor evoked a 14 fold increase in islet cyclic GMP compared to control levels. In contrast, the cyclic AMP levels were increased by L-arginine as well as by the 300 μM concentration of *tert*-butyl-hydroperoxide (Table 1).

Discussion

The present results show that the L-arginine-analogues L-NAME (an NO synthase inhibitor), and D-arginine (which does not generate NO), acted differently on insulin release when incubated together with L-arginine. Increasing concentrations of L-NAME (0.1–5.0 mM), which did not influence basal insulin release, induced a dose-related potentiation of the insulin response evoked by a submaximal concentration of L-arginine (5 mM). D-Arginine (5 mM), however, did not influence L-arginine-induced insulin release. On the other hand D-NAME (5 mM) which reportedly is devoid of NO synthase-inhibitory properties (Radomski *et al.*, 1990; Rees *et al.*, 1990) also increased the insulin release induced by L-arginine but was less effective than L-NAME. Moreover, a high concentration (10 mM) of L-NAME, D-NAME or D-arginine could *per se* induce insulin secretion, D-arginine being less efficient in this respect. The data suggest that the observed effects of the L-arginine analogue L-NAME, at least partially, could be ascribed to its cationic properties. However, the fact the D-NAME was less effective than L-NAME in increasing L-arginine-induced insulin release strongly suggests that part of the effect was due to NO synthase inhibi-

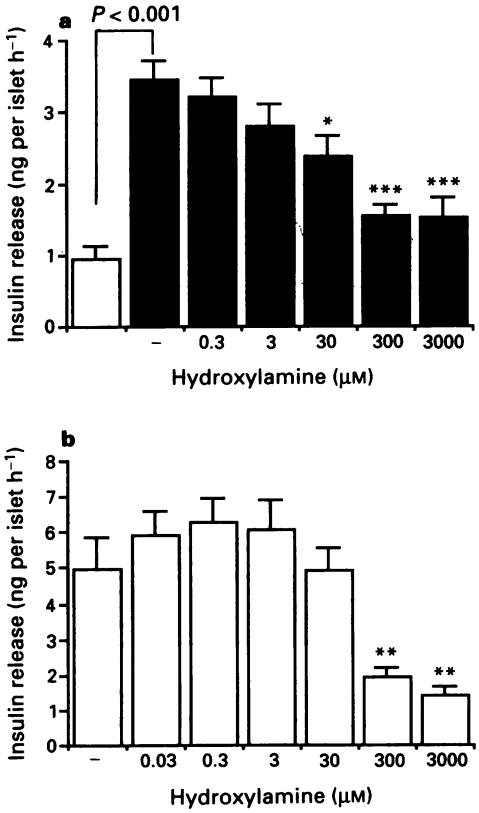


Figure 3 (a) Effect of different concentrations of hydroxylamine on insulin release from isolated islets stimulated by L-arginine 10 mM in the presence of basal glucose 7 mM (solid columns). Glucose 7 mM basal control is also shown (open column). Values are mean ± s.e.mean from 9 batches of islets, $*P<0.05$, $***P<0.001$ compared to 10 mM L-arginine without addition of hydroxylamine. (b) Effect of different concentrations of hydroxylamine on glucose-induced insulin secretion (16.7 mM glucose) from isolated islets. Values are mean ± s.e.mean from 9 batches of islets, $**P<0.01$.

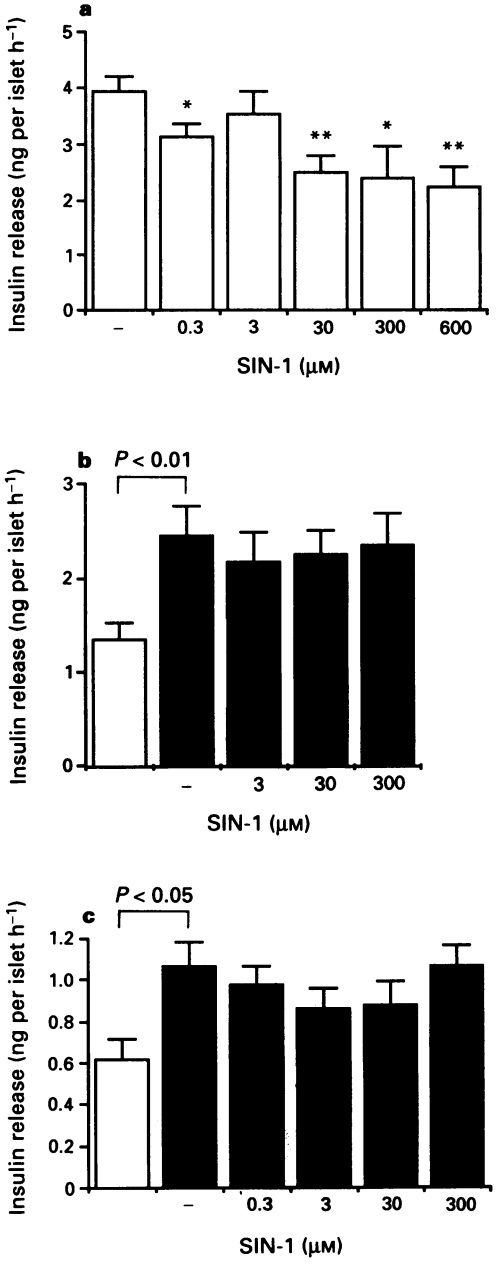


Figure 4 (a) Effect of different concentrations of sydnonimine-1 (SIN-1) on glucose induced insulin secretion (16.7 mM glucose) from isolated islets during a 35 min incubation period. Values are mean ± s.e.mean from 9 batches of islets, $*P<0.05$, $**P<0.01$ compared to 16.7 mM glucose without addition of SIN-1. (b) Effect of SIN-1 on L-arginine-stimulated (10 mM) insulin release in the presence of 7 mM glucose (solid columns). Glucose 7 mM basal control is also shown (open column). Values are mean ± s.e.mean from 7 batches of islets. (c) Effect of SIN-1 on insulin release from isolated islets stimulated by forskolin (20 μM) in the presence of 4 mM glucose (solid columns). Glucose 4 mM basal control is also shown (open column). Values are mean ± s.e.mean from 9 batches of islets.

tion. It should be noted, however, that the stereoisomer D-arginine, which carries the same cationic properties as L-arginine and does not generate NO, was a weaker insulin secretagogue than L-arginine even in the presence of L-NAME. This suggests that other unknown factors may contribute to the difference in the insulin releasing action of D- and L-arginine. One explanation might be the existence of different transport mechanisms across the plasma membrane as previously shown in endothelial cells (Bogle *et al.*, 1992). Thus, D-arginine might not be accumulated as rapid as or to the same extent as L-arginine and L- or D-NAME. However, taken together our data indicate that L-arginine has a dual

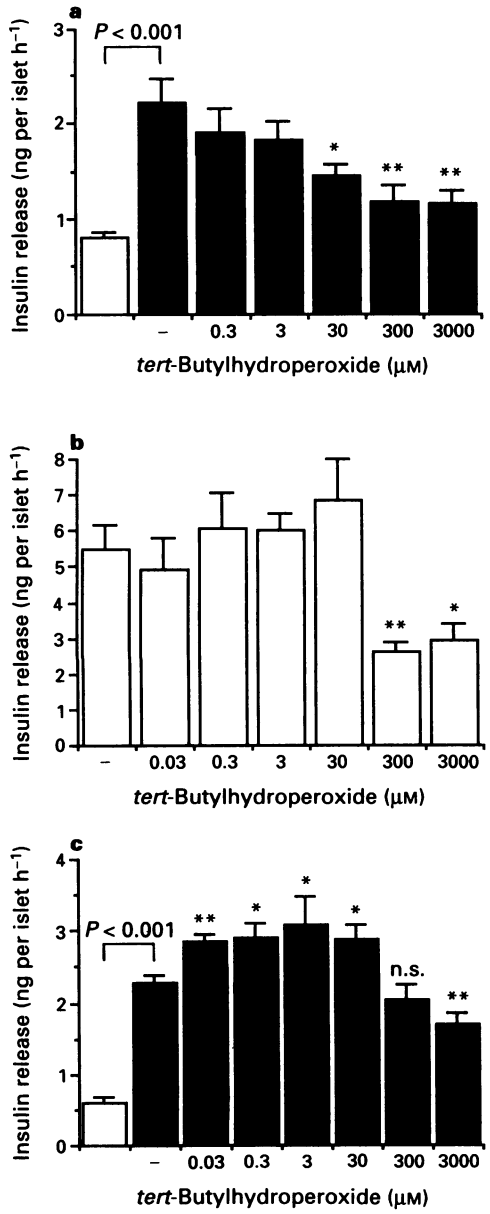


Figure 5 (a) Effect of different concentrations of *tert*-butylhydroperoxide on insulin release from isolated islets stimulated by L-arginine 10 mM in the presence of basal glucose 7 mM (solid columns). Glucose 7 mM basal control is also shown (open column). Values are mean ± s.e.mean from 6–9 batches of islets, $*P<0.05$, $**P<0.01$ compared to 10 mM L-arginine without addition of *tert*-butylhydroperoxide. (b) Effect of different concentrations of *tert*-butylhydroperoxide on glucose-induced insulin secretion (16.7 mM glucose) from isolated islets. Values are mean ± s.e.mean from 6 batches of islets, $*P<0.05$, $**P<0.01$ compared to 16.7 mM glucose without addition of *tert*-butylhydroperoxide. (c) Effect of different concentrations of *tert*-butylhydroperoxide on insulin release from isolated islets stimulated by isobutylmethylxanthine (IBMX) 1 mM in the presence of basal glucose 4 mM (solid columns). Glucose 4 mM basal control is also shown (open column). Values are mean ± s.e.mean from 9 batches of islets, $*P<0.05$, $**P<0.01$ compared to 1 mM IBMX without addition of *tert*-butylhydroperoxide.

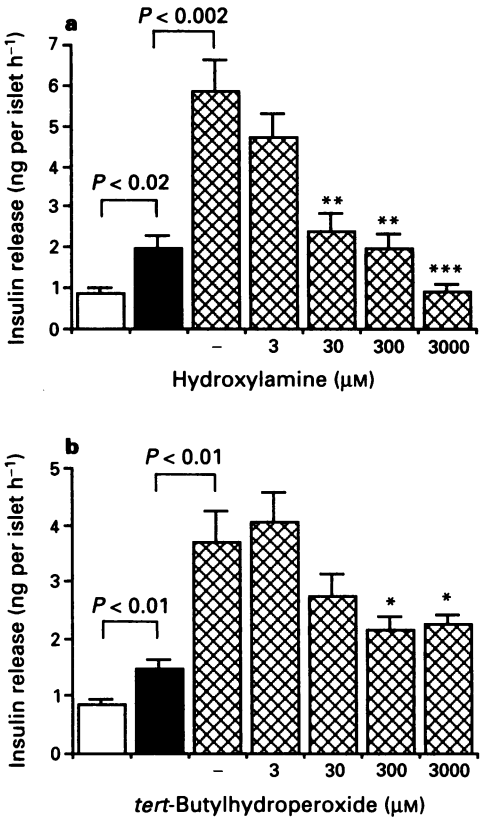


Figure 6 (a) Influence of different concentrations of hydroxylamine on insulin release from isolated islets stimulated by L-arginine 5 mM + N^G-nitro-L-arginine methyl ester (L-NAME) 5 mM in the presence of basal glucose 7 mM (cross-hatched columns). Effects of basal glucose (7 mM) (open column), and L-arginine 5 mM (solid column) are also shown. Values are mean ± s.e.mean from 6–9 batches of islets, $**P<0.01$, $***P<0.001$ compared to 5 mM L-arginine + L-NAME without addition of hydroxylamine. (b) Influence of different concentrations of *tert*-butylhydroperoxide on insulin release from isolated islets stimulated by L-arginine 5 mM + L-NAME 5 mM in the presence of basal glucose 7 mM (cross-hatched columns). Effects of basal glucose (7 mM) (open column), and L-arginine 5 mM (solid column) are also shown. Values are mean ± s.e.mean from 6–9 batches of islets, $*P<0.05$ compared to 5 mM L-arginine + L-NAME 5 mM without addition of *tert*-butylhydroperoxide.

Table 1 Accumulated levels of cyclic GMP and cyclic AMP in isolated islets after a 60 min incubation period in the presence of 10 mM L-arginine or different concentrations of hydroxylamine and *tert*-butylhydroperoxide

	Cyclic GMP (amol/islet)	*Cyclic AMP* (fmol/islet)
Control	333 ± 14	6.19 ± 1.27
L-Arginine 10 mM	358 ± 39	17.12 ± 3.12**
Hydroxylamine 3 μM	351 ± 19	9.66 ± 1.25
Hydroxylamine 300 μM	4675 ± 950***	7.88 ± 1.26
tert-Butylhydroperoxide 3 μM	481 ± 74	5.94 ± 0.62
tert-Butylhydroperoxide 300 μM	320 ± 41	11.20 ± 0.71*

Basal medium (control) contained 7 mM glucose + 0.2 mM IBMX.
Means ± s.e.mean from 5–7 batches of islets. Asterisks (*) denote significant difference *vs* control. $*P<0.02$; $**P<0.005$; $***P<0.001$.

action on insulin release as previously suggested (Panagiotidis *et al.*, 1992). Thus the cationic depolarizing action of L-arginine promotes insulin secretion, whereas the NO derived from L-arginine metabolism negatively modulates the secretory process.

The results from previous investigations with rat islets or cells from the clonal pancreatic β-cell line, HIT-T15, as well as RINm5F insulinoma cells using the NO synthase inhibitor N^G-monomethyl-L-arginine (L-NMMA) (Laychock *et al.*, 1991; Schmidt *et al.*, 1992) suggested that NO enhances L-arginine-stimulated insulin release. The reason for this discrepancy in results is presently unclear. However, the β-cell lines may have a different reaction pattern compared with normal islets. Further, we recently observed that during our incubation conditions L-arginine-induced insulin release also from rat islets was enhanced by NO synthase inhibition (data not shown). These results are also compatible with previous data on the effect of L-NMMA on insulin release from cultured rat islets (Jansson & Sandler, 1991). Moreover, in contrast to previous reports (Laychock *et al.*, 1991; Schmidt *et al.*, 1992; Jones *et al.*, 1992) our present results suggest that glucose-induced insulin secretion (16,7 mM glucose) is increased in the presence of NO synthase inhibition. This may suggest that L-NAME inhibited a basal 'tone' of NO generation within the isolated islets in the presence of high glucose and/or that L-NAME exerted a cationic potentiation of glucose-induced insulin secretion. The fact that 10 mM of either sterioisomeric form of NAME alone released the same amounts of insulin favours the latter assumption. Thus, to study in more detail the inhibition of NO synthase activity in islet β-cells, a new generation of NO synthase inhibitors has to be developed that hopefully does not share the cationic properties of the L-arginine analogues.

In accordance with our suggestion that NO in fact is a negative modulator of L-arginine-induced insulin secretion, the intracellular NO donor, hydroxylamine, displayed a dose-dependent inhibition of the insulin response to L-arginine alone and to the combined action of L-NAME + L-arginine. Moreover, glucose-induced insulin secretion was also markedly inhibited by intracellular NO generation induced by hydroxylamine.

Hydroxylamine is a known precursor of NO in biological systems and it has even been suggested that it may be an intermediate in the conversion of L-arginine to NO (DeMaster *et al.*, 1989). Further, previous data have suggested that hydroxylamine easily penetrates into cells where it is oxidized to NO and exerts its effects. Catalase is known to catalyze this reaction (DeMaster *et al.*, 1989).

With regard to SIN-1 the effect is probably in the interstitial environment as, from its chemical structure, this compound is not likely to gain access to the cell interior. Hence the 'mixed' free radicals, NO and superoxide, generated by SIN-1 (Hogg *et al.*, 1992) may act mainly extracellularly. It has previously been shown that direct oxidation of β-cell superficial thiols lead to Ca^{2+} uptake and subsequent increase of insulin secretion at low glucose (Ammon & Mark, 1985). However, oxidation of intracellular thiols inhibits glucose-induced insulin secretion (Ammon & Mark, 1985). Thus the action of SIN-1 is very complex, since this compound generates both superoxide and NO, which then can act both extra- and intracellularly. Apparently the intracellular effect of the evolved NO and superoxide dominates with regard to glucose-induced insulin release, whereas insulin release stimulated by L-arginine is unaffected (balance between extracellular and intracellular effects of free radicals?). Similarly forskolin-induced insulin release was unaffected by SIN-1 even at a very low glucose concentration (cyclic AMP is known to lower the threshold for glucose-induced insulin release) confirming earlier data showing that activation of the cyclic AMP system by (−)-isoprenaline is not affected by thiol oxidation (Ammon & Mark, 1985). Therefore, it should be noted that although the main effect of NO has been ascribed to the intracellular activation of guanylate cyclase, recent observations have suggested that NO might exert its action also through cyclic GMP-independent events (Stamler *et al.*, 1992). Thus S-nitrosylation of critical thiol groups on e.g. enzyme and receptor proteins has been suggested as a potential mechanism for modification of proteins with important regulatory functions (Stamler *et al.*, 1992).

The combined data on the effects of L-NAME on one hand and the intracellular NO donor hydroxylamine on the other thus strongly suggest that NO is a negative modulator of insulin secretion induced by L-arginine and glucose. However, it should be noted that up to date biochemical evidence for the presence of a constitutive NO synthase in islet tissue is restricted to the report of Schmidt *et al.* (1992) who used HIT T15 clonal pancreatic β-cells. Measurement of nitrite production as an indicator of NO synthase activity has been used by several authors (cf. Moncada *et al.*, 1991; Corbett *et al.*, 1993). However, this may be of limited value in short-term incubation of islet tissue, since according to our hypothesis much of the NO produced is 'trapped' by S-nitrosylation, (see also Stamler *et al.*, 1992). Moreover, comparatively high concentrations of NO synthase inhibitors (in the order of 10^{-4}–10^{-3} M) have been used to detect an inhibitory action on nitrite production from cultured islets (Welsh *et al.*, 1991; Corbett *et al.*, 1993). Therefore, a more detailed biochemical characterization of islet NO synthase(s) is needed. On the other hand, the immunohistochemical evidence for the occurrence of a constitutive NO synthase in islet β-cells seems to be very strong, since this has been demonstrated with three different antisera (Schmidt *et al.*, 1992; Corbett *et al.*, 1993). Moreover, islets cultured with 0.5 mM L-NMMA displayed a substantially reduced NADPH diaphorase staining (Corbett *et al.*, 1993). With regard to the inhibition of NO synthase it could be argued, however, that we used a comparatively high concentration of L-NAME (5 mM) (Moncada *et al.*, 1991; Förstermann *et al.*, 1991) in the L-arginine *vs.* L-NAME interaction experiments. Since the inhibiting action of L-NAME is competitive (Moncada *et al.*, 1991) and since concentrations of 5–10 mM L-arginine are needed to obtain a reliable insulin release (Gerich *et al.*, 1974) it was necessary to use the highest concentration of L-NAME that did not *per se* affect insulin release (cf. Figure 1a).

It has been known for a long time (see Hellman *et al.*, 1974; Ammon & Mark, 1985) that superficial thiols are of importance for certain insulin secretagogues, and that the reduced state of the intracellular GSH/GSSG system, which maintains the superficial thiols in the reduced state, is a prerequisite for glucose-stimulated Ca^{2+} uptake and insulin release. Hence it is not inconceivable that NO-induced S-nitrosylation may impair the function of critical thiol groups of importance for insulin secretion induced by glucose and L-arginine. This might be accomplished either directly or as a consequence of deranging the balance of the GSH/GSSG system. Our present finding that L-arginine-induced insulin release is more sensitive to NO-inhibition than insulin secretion stimulated by glucose is in good agreement with previous observations (Ammon & Mark, 1985) showing that glucose metabolism increases the GSH/GSSG ratio by generating NADPH from the pentose shunt.

Similar to the described effects of NO production, it has been proposed that the H_2O_2 evolution induced by the activation of islet monoamine oxidase activity negatively modulates glucose-induced insulin secretion by impairing the function of critical thiol groups (Lundquist *et al.*, 1991; Panagiotidis *et al.*, 1993a,b,c). The present results, which show that the intracellular 'hydroperoxide donor' *tert*-butylhydroperoxide inhibited insulin secretion induced by glucose and L-arginine strongly support such an assumption. In fact the pattern of insulin secretory suppression induced by *tert*-butylhydroperoxide ('H_2O_2') and hydroxylamine (NO) was remarkably similar, although on a molar basis NO appeared more potent in this respect. It should be emphasized, however, that although both hydroxylamine and *tert*-butylhydroperoxide

are believed to exert their effects intracellularly, the physiological activation of NO synthase (NO) and monoamine oxidase (H_2O_2) may induce a much more localized increase of these messengers, which makes precise comparisons difficult. Moreover, it is not finally established that *tert*-butylhydroperoxide has exclusively intracellular actions (Orrenius & Moldéus, 1984).

Recent *in vivo* studies have suggested that activation of islet monoamine oxidase by certain cyclic AMP-increasing agents such as the β_2-adrenoceptor agonist, terbutaline (Panagiotidis *et al.*, 1993b,c) and the phosphodiesterase inhibitor IBMX (Panagiotidis *et al.*, 1994) could facilitate the insulin releasing action of these agents by degrading inhibitory monoamines and producing small levels of exocytosis-promoting H_2O_2. In contrast to insulin release stimulated by nutrients such as glucose and L-arginine, the secretory process induced by cyclic AMP activating agents seem to operate largely independently of the GSH/GSSG balance as well as of extracellular Ca^{2+} (Ammon & Mark, 1985; Draznin, 1988; Salehi & Lundquist, 1993). The present *in vitro* results, which show that very small levels (0.03–30 μM) of the intracellular 'hydroperoxide donor' *tert*-butylhydroperoxide indeed enhanced IBMX-induced insulin release from isolated islets are in good agreement with our hypothesis. The detailed mechanism of action of this facilitation of IBMX-induced insulin release by hydroperoxide remains to be elucidated. However, it is known from other tissues that peroxides can promote granule fusion with membranes, and that H_2O_2 production can result in perturbation of intracellular Ca^{2+} homeostasis leading to an increase in cytosolic free Ca^{2+} concentration (Creutz, 1981; Orrenius & Moldeús, 1984).

Finally, a concentration of L-arginine (10 mM) which induced a large stimulation of insulin release in the presence of a physiological concentration of glucose (7 mM) did not affect islet cyclic GMP levels (Table 1). These results are in accordance with a recent study (Jones *et al.*, 1992) and do not suggest that L-arginine-derived NO initiates insulin secretion through increasing islet cyclic GMP content as previously proposed (Laychock *et al.*, 1991). In fact, the NO donor, hydroxylamine (at a concentration of 300 μM) induced a marked increase in islet cyclic GMP levels. This concentration of hydroxylamine almost totally *suppressed* insulin secretion induced by glucose or L-arginine. *tert*-Butylhydroperoxide on the other hand did not significantly influence the islet cyclic GMP content. Hence, most evidence thus far suggests that NO is a negative modulator of glucose- and L-arginine-induced insulin release and that cyclic GMP (at least at very high levels) may even contribute to this suppressive action (see also Vara & Tamarit-Rodriguez, 1991).

With regard to islet cyclic AMP we were able to show that 10 mM L-arginine brought about an increase of this nucleotide in islet tissue. This novel finding suggests that raised cyclic AMP levels may contribute to the insulin releasing action of L-arginine. However, it cannot be excluded that effects on cyclic AMP in the glucagon cells may be involved. Similarly, the stimulating effect of *tert*-butylhydroperoxide (300 μM) on islet cyclic AMP levels does not correlate to insulin release and thus may reflect either cyclic AMP changes in the glucagon cells or simply illustrate the notion that cyclic AMP itself is not an initiator of insulin release (Ammon & Mark, 1985).

In conclusion, suppression and enhancement of NO generation by the NO synthase inhibitor, L-NAME, on the one hand, and the intracellular NO donor hydroxylamine on the other, induced paralell changes in insulin release stimulated by L-arginine and glucose. These findings are compatible with NO being a negative modulator of the secretory events. The main effect of NO is probably not exerted through elevated cyclic GMP levels but rather through S-nitrosylation of certain thiol groups critical for the secretory process. Such an assumption is strengthened by the observation that the intracellular 'hydroperoxide donor' *tert*-butylhydroperoxide, a recognized thiol oxidant, induced almost similar changes in the insulin releasing pattern. Cyclic AMP activating secretagogues such as forskolin and IBMX appeared much less sensitive to the inhibitory action of NO and hydroperoxide. In contrast, small levels of hydroperoxide were found to enhance IBMX-induced insulin release. Thus the present data showing a differential *in vitro* effect of *tert*-butylhydroperoxide on insulin secretion induced by glucose and IBMX, respectively, are in good agreement with the results of previous *in vivo* experiments (Lundquist *et al.*, 1991; Panagiotidis *et al.*, 1993a,b,c) suggesting that the H_2O_2 generated by activation of islet monoamine oxidase activity inhibits glucose-induced insulin secretion and promotes insulin release stimulated by IBMX. Hence, taken together with previous data the present results suggest that islet production of low physiological levels of free radicals such as NO and H_2O_2 may serve as important modulators of insulin secretory processes.

This study was supported by the Swedish Medical Research Council (14X-4286), the Swedish Diabetes Association, the Crafoord Foundation, The Novo Nordisk Foundation and the Medical Faculty, University of Lund, Sweden. The technical assistance of Elsy Ling and Britt-Marie Nilsson is gratefully acknowledged.

References

AMMON, H.P.T. & MARK, M. (1985). Thiols and pancreatic β-cell function: a review. *Cell. Biochem. Funct.*, **3**, 157–171.

BOGLE, R.G., MONCADA, S., PEARSON, J.D. & MANN, G.E. (1992). Identification of inhibitors of nitric oxide synthase that do not interact with the endothelial cell L-arginine transporter. *Br. J. Pharmacol.*, **105**, 768–770.

CORBETT, J.A., WANG, J.L., MISKO, T.P., ZHAO, W., HICKEY, W.F. & MCDANIAL, M.L. (1993). Nitric oxide mediates IL-1β-Induced islet dysfunction and destruction: Prevention by dexamethasone. *Autoimmunity*, **15**, 145–153.

CREUTZ, C.E. (1981). cis-Unsaturated fatty acids induce the fusion of chromaffin granules aggregated by synexin. *J. Cell. Biol.*, **91**, 247–256.

DEMASTER, E.G., RAU, L., ARCHER, S.L. & WEIR, E.K. (1989). Hydroxylamine is a vasorelaxant and a possible intermediate in the oxidative conversion of L-arginine to nitric oxide. *Biochem. Biophys. Res. Commun.*, **163**, 527–533.

DRAZNIN, B. (1988). Intracellular calcium, insulin secretion, and action. *Am. J. Med.*, **85**, Suppl. 5A, 44–58.

FÖRSTERMANN, U., SCHMIDT, H.H.H.W., POLLOCK, J.S., SHENG, H., MITCHELL, J.A., WARNER, T.D., NAKANE, M. & MURAD, F. (1991). Isoforms of nitric oxide synthase. Characterization and purification from different cell types. *Biochem. Pharmacol.*, **42**, 1849–1857.

GERICH, J.E., CHARLES, M.A. & GRODSKY, G.M. (1974). Characterization of the effects of arginine and glucose on glucagon and insulin release from the perfused rat pancreas. *J. Clin. Invest.*, **54**, 833–841.

GOTOH, M., MAKI, T., KIYOIZUMI, T., SATOMI, S. & MONACO, A.P. (1985). An improved method for isolation of mouse pancreatic islets. *Transplantation*, **40**, 437–438.

HARPER, J.F. & BROOKER, G. (1975). Femtomole sensitive radioimmunoassay for cyclic AMP and cyclic GMP after 2'O-acetylation by acetic anhydride in aqueous solution. *J. Cycl. Nucl. Res.*, **1**, 207–218.

HELLMAN, B., IDAHL, L.-Å., LERNMARK, Å., SEHLIN, J. & TÄLJEDAL, I.-B. (1974). Membrane sulfhydryl groups and pancreatic beta cell recognition of insulin secretagogues. *Excerpt. Med. Int. Congr. Ser.*, **312**, 65–78.

HOGG, N., DARLEY-USMAR, V.M., WILSON, M.T. & MONCADA, S. (1992). Production of hydroxyl radicals from the simultaneous generation of superoxide and nitric oxide. *Biochem. J.*, **281**, 419–424.

JANSSON, L. & SANDLER, S. (1991). The nitric oxide synthase inhibitor II N^G-nitro L-arginine stimulates pancratic islet insulin release in vitro, but not in the perfused pancreas. *Endocrinology*, **128**, 3081–3085.

JONES, P.M., PERSAUD, S.J., BJAALAND, T., PEARSON, J.D. & HOWELL, S.L. (1992). Nitric oxide is not involved in the initiation of insulin secretion from rat islets of Langerhans. *Diabetologia*, **35**, 1020–1027.

LAYCHOCK, R.G., MODICA, M.E. & CAVANAUGH, C.T. (1991). L-Arginine stimulates cyclic guanosine 3',5'-monophosphate formation in rat islets of Langerhans and RIN m5F insulinoma cells: evidence for L-arginine: nitric oxide synthase. *Endocrinology*, **129**, 3043–3052.

LUNDQUIST, I., PANAGIOTIDIS, G. & STENSTRÖM, A. (1991). Effect of L-DOPA administration on islet monoamine oxidase activity and glucose-induced insulin release in the mouse. *Pancreas*, **6**, 522–527.

MONCADA, S., PALMER, R.M.J. & HIGGS, E.A. (1991). Nitric oxide: physiology, pathophysiology, and pharmacology. *Pharmacol. Rev.*, **43**, 109–142.

ORRENIUS, S. & MOLDÉUS, P. (1984). The multiple roles of glutathione in drug metabolism. *Trends. Pharmacol. Sci.*, **5**, 432–435.

PANAGIOTIDIS, G., ALM, P. & LUNDQUIST, I. (1992). Inhibition of islet nitric oxide synthase increases arginine-induced insulin release. *Eur. J. Pharmacol.*, **229**, 277–278.

PANAGIOTIDIS, G., LINDSTRÖM, P., STENSTRÖM, A. & LUNDQUIST, I. (1993a). Glucose modulation of islet monoamine oxidase activity in lean and obese hyperglycemic mice. *Metabolism*, **42**, 1398–1404.

PANAGIOTIDIS, G., STENSTRÖM, A. & LUNDQUIST, I. (1993b). Influence of β_2-Adrenoceptor stimulation and glucose on islet monoamine oxidase activity and insulin secretory response in the mouse. *Pancreas*, **8**, 368–374.

PANAGIOTIDIS, G., STENSTRÖM, A. & LUNDQUIST, I. (1993c). Effects of adrenergic and cholinergic stimulation on islet monoamine oxidase activity and insulin secretion in the mouse. *Eur. J. Pharmacol.*, **233**, 285–290.

PANAGIOTIDIS, G., STENSTRÖM, A. & LUNDQUIST, I. (1994). *In vivo* action of cyclic AMP modulating secretagogues on islet monoamine oxidase activity and insulin release. *Endocrine*, **2**, 571–576.

RADOMSKI, M.W., PALMER, R.M.J. & MONCADA, S. (1990). Characterization of the L-arginine:nitric oxide pathway in human platelets. *Br. J. Pharmacol.*, **101**, 325–328.

REES, D.D., PALMER, R.M.J., SHULZ, R., HODSON, H.F. & MONCADA, S. (1990). Characterization of three inhibitors of endothelial nitric oxide synthase *in vitro* and *in vivo*. *Br. J. Pharmacol.*, **101**, 746–752.

SALEHI, A. & LUNDQUIST, I. (1993). CA^{2+} deficiency, selective α-glucosidehydrolase inhibition, and insulin secretion. *Am. J. Physiol.*, **265**, E1–E9.

SCHMIDT, H.H.H.W., WARNER, T.D., ISHII, K., SHENG, H. & MURAD, F. (1992). Insulin secretion from pancreatic B cells caused by L-arginine-derived nitrogen oxides. *Science*, **255**, 721–723.

STAMLER, J.S., SIMON, D.I., OSBORNE, J.A., MULLINS, M.E., JARAKI, O., MICHEL, T., SINGEL, D.J. & LOSCALZO, J. (1992). S-Nitrosylation of proteins with nitric oxide: Synthesis and characterization of biologically active compounds. *Proc. Natl. Acad. Sci. U.S.A.*, **89**, 444–448.

STEINER, A.L., PARKER, C.W. & KIPNIS, D.M. (1972). Radioimmunoassay for cyclic nucleotides. *J. Biol. Chem.*, **247**, 1106–1120.

VARA, E. & TAMARIT-RODRIGUEZ, J. (1991). Does cyclic guanosine monophosphate mediate noradrenaline-induced inhibition of islet insulin secretion stimulated by glucose and palmitate? *Biochem. J.*, **278**, 243–248.

VINCENT, S.R. (1992). Nitric oxide and arginine-evoked insulin secretion. *Science*, **258**, 1376–1378.

WELSH, N., EIZIRIK, D.L., BENDTZEN, K. & SANDLER, S. (1991). Interleukin-1b-induced nitric oxide production in isolated rat pancreatic requires gene transcription and may lead to inhibition of the Krebs cycle enzyme aconitase. *Endocrinology*, **129**, 3167–3173.

(Received October 15, 1993
Revised June 22, 1994
Accepted September 15, 1994)

British Journal of Pharmacology (1995) 114, 297–302 © 1995 Stockton Press All rights reserved 0007–1188/95 $9.00

Selectivity of [^{125}I]-PD151242 for human, rat and porcine endothelin ET_A receptors in the heart

Markus G. Peter & [1]Anthony P. Davenport

Clinical Pharmacology Unit, University of Cambridge, Addenbrooke's Hospital, Cambridge CB2 2QQ

1 Endothelin-1 binds with high affinity to heart where it acts as a potent positive inotropic agent. Our aim was to characterize the labelled and unlabelled ET_A-selective antagonist PD151242 in heart tissues derived from man, rat and pigs by use of radioligand binding techniques.

2 Binding of [^{125}I]-PD151242 to sections of human left ventricle was time-dependent and reached equilibrium after 120 min at 23°C with an association rate constant of 0.0235 min^{-1} nM^{-1}. The binding was reversible at 23°C with a dissociation rate constant of 0.00144 min^{-1}.

3 Saturation binding assays with [^{125}I]-PD151242 revealed a single population of high affinity ET receptors in human left ventricle (K_D = 1.07 ± 0.08 nM; B_{max} = 29.8 ± 4.2 fmol mg^{-1} protein), porcine left ventricle (K_D = 1.92 ± 0.27 nM; B_{max} = 493 ± 248 fmol mg^{-1} protein), and rat heart (K_D = 0.64 ± 0.08 nM; B_{max} = 82.34.7 fmol mg^{-1} protein).

4 Unlabelled PD151242 competed with specific [^{125}I]-ET-1 binding to human left ventricle tissue in a biphasic manner with high affinity binding to the ET_A-site (K_D = 7.21 ± 2.83 nM) and lower affnity for the ET_B-subtype (K_D = 104 ± 23 μM), indicating a greater than 10000 fold selectivity to the high affinity site.

5 The ET_A-selective ligand FR139317 competed for [^{125}I]-PD151242 binding in human left ventricle with nanomolar affinity (K_D = 0.37 ± 0.10 nM), whereas the ET_B-selective compound, BQ3020, competed with only micromolar affinity (K_D = 1.5 ± 0.26 μM).

6 The novel ET_A-selective radioligand [^{125}I]-PD151242 binds with high affinity to human, rat and porcine heart. In human tissue, binding was shown to be reversible and highly selective for the ET_A-subtype making [^{125}I]-PD151242 a useful selective radioligand for further characterization of the ET_A-receptor in human tissue.

Keywords: PD151242; endothelin; FR139317; BQ3020; ET_A receptor; human left ventricle

Introduction

Endothelin-1 (ET-1) is a powerful constrictor of isolated cardiac vessels, such as the epicardial coronary arteries, interacting with vascular smooth muscle receptors (Davenport *et al.*, 1989). Like angiotensin II, ET-1 is a potent positive inotropic agent with nanomolar affinity for cardiac muscle receptors (Davenport *et al.*, 1989; Brodde *et al.*, 1992; Zerkowski *et al.*, 1992). The *in vitro* positive inotropic effect on human cardiac muscle strips was observed on both atrial and ventricular muscle (Schomisch Moravec *et al.*, 1989). The myocardial contractile actions of ET-1 have also been described in rat and rabbit papillary muscles (Li *et al.*, 1991), and the positive inotropic effect of ET-1 was characterized on rabbit, guinea-pig and rat isolated ventricular myocardium (Takanashi & Endoh, 1991).

Radiolabelled ET-1 binds with sub-nanomolar affinity to human (Hemsén *et al.*, 1990; Molenaar *et al.*, 1993), rat (Gu *et al.*, 1989; Bolger *et al.*, 1990) and porcine hearts (Takayanaki *et al.*, 1990). Quantitative autoradiography demonstrated that [^{125}I]-ET-1, [^{125}I]-ET-2 and [^{125}I]-ET-3 bound to human, porcine and rat ventricle when incubated in picomolar concentrations and binding to each label had a similar distribution (Davenport *et al.*, 1989; 1991; Wharton *et al.*, 1991; Takayanaki *et al.*, 1991; Bax *et al.*, 1993; Molenaar *et al.*, 1993). The presence of ET_B receptors in human atria and ventricle was confirmed with the iodinated sub-type selective ligands [^{125}I]-BQ3020 and [^{125}I]-[Ala^{1,3,11,15}]-ET-1 (Molenaar *et al.*, 1992). The ET_A-selective antagonist, BQ123, inhibited [^{125}I]-ET-1 binding in a biphasic manner identifying the presence of both ET_A and ET_B receptors in this tissue (Molenaar *et al.*, 1993). The ET_A-selective modified linear tripeptide FR139317 also inhibited [^{125}I]-ET-1 binding in a biphasic manner in rat and porcine hearts (Peter & Davenport, 1994a).

Whilst several radiolabelled ET_B selective compounds are available, we have recently developed and characterized the only radiolabelled ET_A-selective ligand, [^{125}I]-PD151242 (Figure 1) (Davenport *et al.*, 1994a,b). The highly selective ET_A-antagonists, BQ123 (Ihara *et al.*, 1992) and FR139317 (Sogabe *et al.*, 1993) do not have a tyrosine residue suitable for direct iodination. PD151242 was synthesized retaining the conserved L-Leu and D-Trp residues common to both BQ123 and FR139317. We have confirmed that this peptide retains antagonistic properties in human isolated vessels, as well as

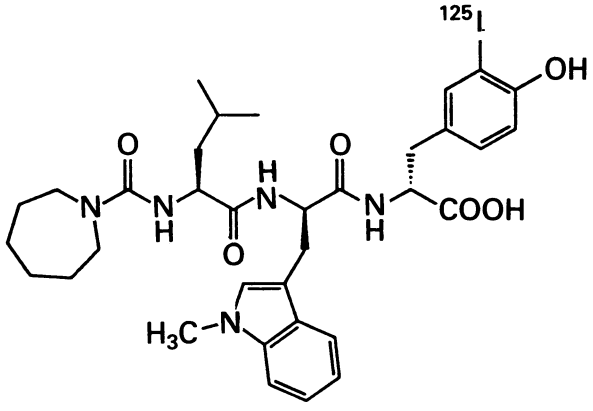


Figure 1 Structure of [^{125}I]-PD151242.

[1] Author for correspondence.

showing high selectivity for the ET_A receptor in human vasculature (Davenport *et al.*, 1994a). Our aim was to evaluate the radioligand in a model of the human heart which we have shown to express both receptor sub-types (Molenaar *et al.*, 1993). We have also compared the affinity of [^{125}I]-PD151242 for ET-receptors in human left ventricle to those in porcine and rat heart, as species differences in endothelin receptor-ligand binding interactions are known to exist (Nambi *et al.*, 1993). A preliminary account of this work has been presented to the British Pharmacological Society (Peter & Davenport, 1994b).

Methods

Heart tissue

Human left ventricular free walls were obtained from cardiac allograft recipients at Papworth Hospital, Cambridge, UK. Patients were all male (43–57 years of age) and drug therapy included calcium-antagonists, vasodilators, angiotensin-converting enzyme inhibitors, diuretics, digoxin and anticoagulants. The indications for transplantation were ischaemic heart disease and cardiomyopathy. Rat hearts were obtained from male Sprague-Dawley (200–250 g) rats, and porcine left ventricle from large white piglets from the same litter. Cardiac tissues were frozen in liquid nitrogen and stored at −70°C. Longitudinal cryostat tissue sections (10 μm) were cut for receptor autoradiography and protein determination, and mounted onto microscope slides coated with gelatine/chromic potassium sulphate (Fisons, UK/Sigma, Poole, UK). Slide mounted tissues were stored at −70°C until use (Davenport *et al.*, 1989).

Binding experiments

Association experiments were carried out with sections incubated for increasing time periods (0–240 min) with 0.7 nM [^{125}I]-PD151242. For dissociation experiments heart sections were incubated with [^{125}I]-PD151242 for 2 h at 23°C before incubating sections with an excess of HEPES buffer for increasing time periods (0–240 min and 24 h). For saturation and competition binding experiments slide mounted tissue sections were pre-incubated in HEPES buffer containing 50 mM HEPES, 5 mM $MgCl_2$, and 0.3% bovine serum albumin fraction V (Advanced Protein Products Ltd., Brierley Hill, UK) (pH 7.4) for 15 min at room temperature (23°C). For competition binding assays, sections were then transferred to HEPES buffer containing 0.1 nM [^{125}I]-ET-1 or 0.4 nM [^{125}I]-PD151242 in the absence or presence of potential ET-receptor agonists or antagonists for 120 min at room temperature (23°C). In saturation experiments sections were incubated with increasing concentrations (8 pM–8 nM) of [^{125}I]-PD151242 in incubation buffer for 120 min at 23°C. Non-specific binding was defined by the use 1 μM unlabelled ET-1 or PD151242, respectively. Sections were then rinsed in Tris buffer containing 50 mM Tris-HCl (pH 7.4) at 4°C three times for 5 min each and then scraped with filter paper and counted in a gamma counter (Gamma 5500, Beckmann).

Protein determination

Protein in sections (10 μm) of left ventricular free wall was determined after solubilization (0.5 M NaOH and 1% sodium dodecyl sulphate for 30 min at 80°C) using the Bio-rad DC 96-well microtiter plate system (Bio-rad Laboratories, Hertfordshire, UK) based on the Lowry-method. Microtiter plates were then analysed at 710 nm with an Titertek Multiskan PLUS/MKII (Labsystems, Finland).

Calculation of binding parameters

In association experiments for the calculation of k_{+1} the pseudo-first order method was used (Bylund & Yamamura, 1990). The data ($n = 3$) were plotted on a pseudo-first order association plot to give k_{obs} as its slope. Similarly, the dissociation data ($n = 3$) were analysed by a semilogarithmic plot of the dissociation data: the natural logarithm (ln) of B/B_0 is plotted as a function of time with the slope of this line being k_{-1}.

Saturation and competition binding data were analysed using EBDA and LIGAND (Munson & Rodbard, 1980; McPherson, 1983) to obtain the dissociation constant (K_D) and receptor density (B_{max}) values for the PD151242 were also determined from competitive binding experiments in which a single concentration of the radioligand (0.1 nM [^{125}I]-ET-1 or [^{125}I]-PD151242) and multiple concentrations of the same unlabelled ligand (ET-1 or PD151242, respectively) compete for binding to the receptor (DeBlasi *et al.*, 1989).

Data files of saturation and competition curves were run simultaneously with LIGAND to obtain final parameter estimates. In each case, the experimentally determined value for non-specific binding was used when estimating the binding parameters B_{max} and K_D. The presence of one, two or three sites was tested using the *F*-ratio test in LIGAND. The model adopted was that which provided the significantly best fit ($P < 0.05$) (Munson & Rodbard, 1980).

Ligands

BQ3020 ([Ala^{11,15}]Ac-ET-$1_{(6-21)}$); FR139317 ((N-[(hexahydro-1-azepinyl)carbonyl)L-Leu-(1-Me)D-Trp-3(2-pyridyl)-D-Ala) and PD151242, ((N-[(hexahydro-1-azepinyl)carbonyl)L-Leu-(1-Me)D-Trp-D-Tyr) were synthesized by solid phase t-Boc chemistry. BQ3020 was synthesized in house; FR139317 and PD151242 were synthesized by Dr A.M. Doherty, Parke-Davis Pharmaceutical Research Division, Ann Arbor, Michigan, U.S.A. Peptide concentration was determined by u.v.-spectrophotometry. [^{125}I]-PD151242 (2000 Ci mmol^{-1}) was synthesized (Amersham International plc., Amersham, Bucks, U.K.) from the unlabelled material by mild oxidation using an enzymatic method and purified to be carrier-free. [^{125}I]-ET-1 (2000 Ci mmol^{-1}) was obtained from Amersham and unlabelled ET-1 from Novabiochem (Nottingham, U.K.).

All other reagents were purchased from Sigma (Poole, U.K.).

Results

Kinetic experiments: association and dissociation

Binding of 0.7 nM [^{125}I]-PD151242 to sections of human left ventricle was time-dependent and reached equilibrium after 2 h with observed association rate constant $k_{obs} = 0.0172$ min^{-1}. After an incubation period of 2 h, the bound [^{125}I]-PD151242 dissociated from the binding sites with a $t_{\frac{1}{2}}$ values of approximately 300 min. The dissociation rate constant (k_{-1}) was determined to be 0.00144 min^{-1}. The association rate constant ($k_{+1} = [k_{obs} - k_{-1}]/F$) was estimated to be 0.0235 min^{-1} nM^{-1} (Figure 2).

Saturation experiments

Saturation experiments were used to compare the binding affinity fo [^{125}I]-PD151242 with heart tissue sections from different species. In each case a single class of high-affinity binding sites was identified with dissociation constants in the nM-range. For the human left ventricle a dissociation constant (K_D) of 1.07 ± 0.08 nM and a maximum binding capacity (B_{max}) of 29.8 ± 4.2 fmol mg^{-1} protein was determined. Binding affinity was highest in rat heart ($K_D = 0.64 \pm 0.08$ nM) and lowest in porcine left ventricle ($K_D = 1.92 \pm 0.27$ nM) ($n = 3$) (Table 1). Analysis of the saturation data indicated that the Hill coefficients were close to unity, and in each case a one-site fit was preferred to a two site model.

Competition experiments

In competition binding experiments, unlabelled ET-1 competed as expected in a monophasic manner with specific [^{125}I]-ET-1 binding (K_D = 0.74 ± 0.24 nM), unlike unlabelled PD151242 which competed biphasically, indicating the presence of two binding sites. Analysis of the binding data by LIGAND confirmed a two-site fit was preferred over a one- or three-site model for PD151242. The antagonist PD151242 had a 6 fold lower affinity for the high affinity site (K_D = 7.21 ± 2.83 nM) compared to the ET_A-selective antagonist, FR139317 (K_D = 1.20 ± 0.28 nM). However, PD151242 seemed

Table 1 Affinities, selectivities, and density of binding-sites for endothelin receptor radioligands in different tissues as derived from saturation binding analysis

Tissue	*Ligand*	n	K_D *[nM]*	B_{max} *(fmol mg^{-1})*	n_H
Human LV	[^{125}I]-PD151242	3	1.07 ± 0.08	29.7 ± 4.2	0.98 ± 0.04
Rat heart	[^{125}I]-PD151242	3	0.64 ± 0.08	82.0 ± 34.7	0.95 ± 0.04
Porcine LV	[^{125}I]-PD151242	3	1.92 ± 0.27	493 ± 248	0.99 ± 0.02
Porcine LV	[^{125}I]-ET-1	3	2.41 ± 0.51	1143 ± 204	0.98 ± 0.01
Human LV	[^{125}I]-ET-1*	5	0.35 ± 0.07	64.3 ± 9.8	0.97 ± 0.03

Hill coefficients (n_H), dissociation constants (K_D, nM) and maximal density of receptors (B_{max}, fmol mg^{-1} protein) for [^{125}I]-PD151242 in heart tissue sections from human, rat and pig and comparison with other endothelin receptor radioligands. Values represent the mean ± s.e.mean. (LV: left ventricule; from *Molenaar *et al.*, 1993).

Table 2 Competition binding experiments of ET_A-selective antagonists and the non-selective endogenous ligand ET-1 against [^{125}I]-ET-1 to human left ventricle tissue sections

Compound	n	K_D ET_A *[nM]*	K_D ET_B *[μM]*	B_{max} ET_A *(fmol mg^{-1})*	B_{max} ET_B *(fmol mg^{-1})*
FR139317	4	1.20 ± 0.28	287 ± 93	35.7 ± 2.3	21.9 ± 1.9
PD151242	5	7.21 ± 2.83	104 ± 23	26.5 ± 1.7	26.2 ± 1.6
ET-1	3		0.74 ± 0.24 nM		91.7 ± 3.2

Dissociation constant values (K_D $ET_{A/B}$; nM/μM) and maximal densities of receptors (B_{max} $ET_{A/B}$; fmol mg^{-1} protein) for subtype selective and non-selective ET-receptor ligands in human left ventricle free wall. Values are the mean ± s.e.mean.

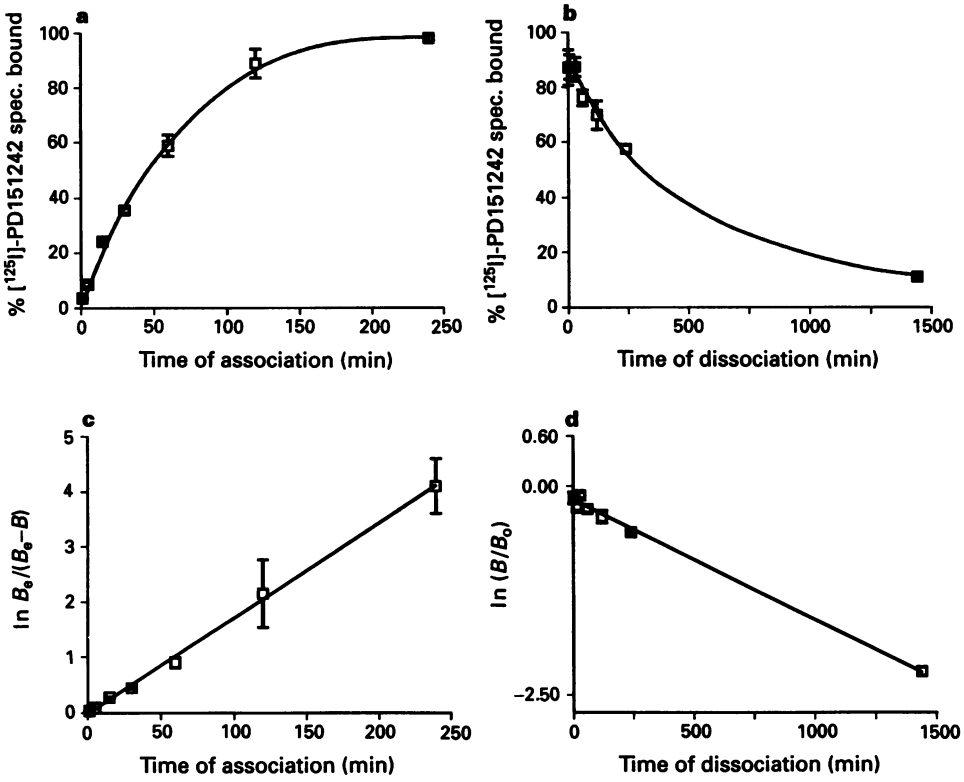


Figure 2 Association and dissociation of [^{125}I]-PD151242 bound to sections of human left ventricle tissue. (a) The time course of association of the specific binding with a fixed concentration of [^{125}I]-PD151242 and (b) the time course of dissociation of the specific binding after 2 h incubation with a fixed concentration of [^{125}I]-PD151242. Each experiment was carried out at 23°C (n = 3, mean ± s.e.mean). Semilogarithmic-plots of the association (c) and dissociation (d) of [^{125}I]-PD151242 were used to determine the association (k_{+1}) and dissociation (k_{-1}) rate constants. (c) Pseudo first-order association plot with the slope, which is k_{obs}, of 0.0172 min^{-1}. (d) The semilogarithmic plot of the dissociation data has a slope of 0.00144 min^{-1} (= k_{-1}). With $k_{+1} = (k_{obs} - k_{-1})/F$ = 0.236 min^{-1} × nM^{-1}, the dissociation constant K_D (= k_{-1}/k_{+1}) become 0.061 nM. B_e, B_0 and B correspond to the amounts of specific bound ligand at equilibrium, at t = 0 min, and at each time, respectively. F means the concentration of 'free' ligand added for the association experiment ([F] = 0.672 nM).

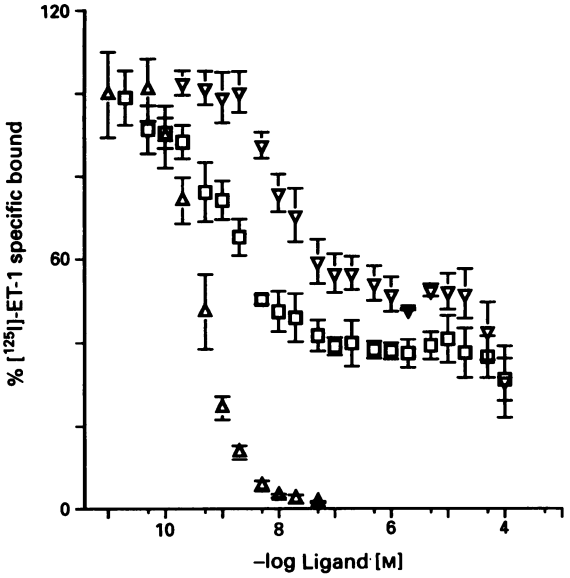


Figure 3 Inhibition of [^{125}I]-endothelin-1 ([^{125}I]-ET-1) specific binding to ET-receptors on human left ventricle tissue sections by the competitive inhibitor PD151242 (▽), the ET_A-selective antagonist, FR139317 (□) and the endogenous ligand ET-1 (△) for comparison. Both ET_A-selective antagonists competed in a biphasic manner consistent with binding for a high affinity ET_A and low affinity ET_B site. ET-1 competed in a monophasic way, which is characteristic for non-selective ligands.

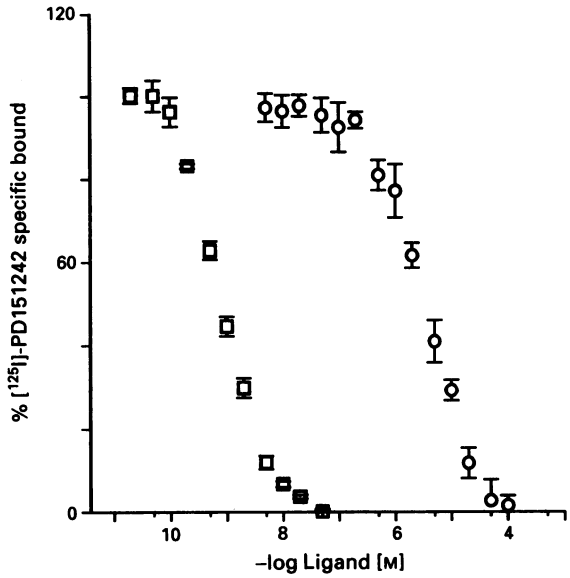


Figure 4 Competition binding for 0.4 nM [^{125}I]-PD151242 to tissue sections of human left ventricle by FR139317 (□) and BQ3020 (○). Results are expressed as percentages of the specific binding and data are the mean ± s.e.mean ($n = 3$).

Table 3 Dissociation constant values (K_D) and densities (B_{max}) of ET_A receptors for FR139317, BQ3020 and unlabelled PD151242 in human left ventricle derived from competition binding experiments with [^{125}I]-PD151242

Ligand	n	K_D	B_{max}
FR139317	3	0.37 ± 0.10 nM	49.0 ± 11.1
BQ3020	3	1.50 ± 0.26 μM	47.2 ± 6.1
PD151242	3	0.65 ± 0.46 nM	49.8 ± 15.7

Values are the mean ± s.e.mean as calculated by LIGAND; B_{max}: fmol mg^{-1} protein.

to compete for only 50% of [^{125}I]-ET-1 binding, whereas FR139317 competed with approximately 60% of the total specific [^{125}I]-ET-1 binding sites with high affinity (Table 2 and Figure 3). Both compounds only competed for the lower affinity binding-site at concentrations greater than 20 μM. FR139317 competed with the specific binding of [^{125}I]-PD151242 to tissue sections from human left ventricle with a K_D of 0.37 nM with a 4000 fold higher affinity than the ET_B-selective agonist, BQ3020 (Table 3 and Figure 4).

Discussion

In this study, we have shown that [^{125}I]-PD151242 bound with high affinity to tissue sections of human, rat and porcine hearts. In the human left ventricle, although the dissociation constant of [^{125}I]-PD151242 was 3 fold higher than the one calculated for [^{125}I]-ET-1 (Molenaar *et al.*, 1993) it was comparable to those of the available ET_B-selective ligands, [^{125}I]-BQ3020 and [^{125}I]-[Ala^{1,3,11,15}]ET-1 (Molenaar *et al.*, 1992). The affinity of [^{125}I]-PD151242 for ET_A-receptors calculated by saturation binding in human heart is within the range obtained in other human tissues including kidney (0.75 nM), aorta (0.76 nM), pulmonary (1.75 nM) and coronary arteries (0.51 nM) (Davenport *et al.*, 1994a,b). The K_D value for [^{125}I]-PD151242 calculated from saturation binding experiments was not significantly different from the K_D value calculated from competition assays where unlabelled PD151242 was used to displace the binding of [^{125}I]-PD151242. These results suggest that binding affinities are not altered by iodination of the ligand. Unlabelled PD151242 was slightly less effective in competing for the binding of [^{125}I]-ET-1 and the calculated K_D was seven fold higher. Although hearts from the same individual were used, this small discrepancy may arise from subtle variation in tissue from different individuals. The aim of the kinetic studies was to demonstrate that binding was saturable and reversible. The K_D value for [^{125}I]-PD151242 calculated from kinetic experiments (using a fixed concentration of ligand) was, however, lower than that calculated by saturation binding assays. The reason for this is unclear, but saturation assays measure specific binding over a wide concentration-range and are likely to yield more accurate estimates. A similar discrepancy was observed in human aorta (Davenport *et al.*, 1994a).

In saturation binding experiments, the Hill coefficient for [^{125}I]-PD151242 was close to unit for heart tissues derived from man, rat and pig, suggesting the presence of a single population of binding sites in each species. EBDA and LIGAND analysis of the saturation data indicated for all three species, that a 1-site fit was preferred to a 2- or 3-site model. However, one cannot exclude the possible existence of multiple binding sites with similar affinities. Densities of binding-sites were highest in porcine left ventricle which may be attributed to the fact that this tissue was derived from neonatal animals. The affinity of specific [^{125}I]-PD151242 binding to tissue sections of rat heart ($K_D \approx 0.6$ nM) is fairly similar to that obtained for specific [^{125}I]-ET-1 binding to crude membrane fractions prepared from rat heart ($K_D \approx 0.4$ nM; Gu *et al.*, 1989; Bolger *et al.*, 1990). Also, the dissociation constant of [^{125}I]-PD151242 in porcine left ventricle ($K_D \approx 1.9$ nM) is in concordance with that of [^{125}I]-ET-1 ($K_D \approx 2.4$ nM) to the same tissue.

Kinetic experiments indicated that [^{125}I]-PD151242 binding to human left ventricle was rapid and reversible, making it a useful radioligand for the ET_A receptor. These time course experiments confirm previous experimental data obtained in sections of human aorta with [^{125}I]-PD151242, where binding was also time-dependent and equilibrium was reached after 120 min. The association rate constant in human left ventricle (0.0234 nM^{-1} min^{-1}) is slower than in the vascular smooth muscle of human aorta (0.126 ± 0.017 nM^{-1} min^{-1}) but the dissociation rate constant was comparable: 0.00144 versus

$0.0025\ min^{-1}$, respectively (Davenport *et al.*, 1994a). [^{125}I]-PD151242 has also been used to show that ET_A receptors predominate in human renal artery and vein. Autoradiography on cross-sections of both vessels showed intense binding of the non-selective ligand [^{125}I]-ET-1 and the ET_A-selective [^{125}I]-PD151242 but only weak labelling of sites by the ET_B-selective ligand, [^{125}I]-BQ3020 (Maguire *et al.*, 1994).

The biphasic inhibition curve for [^{125}I]-PD151242 obtained when competing with the specific binding of [^{125}I]-ET-1 in human left ventricle indicated that the antagonist distinguished between a high- and low-affinity site present in this tissue. Because the ET_A-selective antagonist FR139317 competed against specifically bound [^{125}I]-PD151242 with a 4000 fold higher affinity than the ET_B-selective agonist BQ3020, it can be concluded that [^{125}I]-PD151242 labels the ET_A-subtype. This confirms data obtained from competition binding assays in human aorta with [^{125}I]-PD151242, where FR139317 competed with a dissociation constant of 0.55 nM and BQ3020 with only 2.36 μM (Davenport *et al.*, 1994a). Furthermore, the dissociation constant values for BQ3020 are similar when competing either against [^{125}I]-PD151242 ($K_D = 1.50 \pm 0.26$ μM) or [^{125}I]-ET-1 binding specifically to the ET_A-receptor subtype ($K_D ET_A = 2.04 \pm 0.21$ μM; Molenaar *et al.*, 1993) in human left ventricle. However, PD151242 competed only with 50% of the [^{125}I]-ET-1 binding sites compared to 62% by FR139317. As both these competition studies were carried out in tissues taken from the same hearts, this may suggest that PD151242 is identifying a subpopulation of those receptors recognised by FR139317 indicating further heterogeneity of ET_A-receptors in the human heart. Although cDNA for the ET_A and ET_B receptors has been cloned and both have been shown to be members of the G-protein-coupled receptor superfamily (Arai *et al.*, 1990; Sakamoto *et al.*, 1991), some evidence does exist for additional receptor sub-subtypes (Sokolovsky *et al.*, 1992), significant species differences (Kumar *et al.*, 1993), and an endothelin-3 specific receptor (ET_C) (Masaki *et al.*, 1991; Karne *et al.*, 1993).

Evidence suggests that the endothelins might be important modulators of both vascular tone and myocardial contractility following myocardial infarction (Yasuda *et al.*, 1990; Watanabe *et al.*, 1991; Matsuyama *et al.*, 1991; Tønnessen *et al.*, 1993). In addition, endothelins may be involved in the development of cardiac hypertrophy. For example, it has been shown that hypertrophy of rat cultured cardiomyocytes can be blocked by BQ123, an antagonist selective for the ET_A receptor. This implies a role for endogenous ET-1 in the pathogenesis of cardiac hypertrophy (Ito *et al.*, 1993; 1994). In concordance, Suzuki *et al.* (1993) demonstratd that cultured neonatal rat cardiomyocytes were able to synthesize and secrete ET-1. Thus, characterization of human myocardial ET receptors using subtype-selective ET radioligands, such as [^{125}I]-PD151242 which binds with a 10,000 fold selectivity for the ET_A compared to the ET_B receptor subtype, may be useful for delineating changes in ET receptors in cardiovascular diseases.

This work was supported by grants from the British Heart Foundation, SERC, Isaac Newton Trust, the Royal Society, and the Schering Research Foundation. We thank the consultant and theatre staff of Papworth Hospital (Cambridge, U.K.) for their permission to obtain cardiovascular tissue and Dr A.M. Doherty (Parke-Davis Pharmaceutical Research Division, Ann Arbor, Michigan, U.S.A.) for synthesizing FR139317 and PD151242.

References

ARAI, H., HORI, S., ARAMORI, I., OHKUBO, H. & NAKNISHI, S. (1990). Cloning and expression of cDNA encoding an endothelin receptor. *Nature*, **348**, 730–732.

BAX, W.A., BRUINVELS, A.T., VAN SUYLEN, R.-J., SAXENA, P.R. & HOYER, D. (1993). Endothelin receptors in the human coronary artery, ventricle and atrium. *Naunyn-Schmied. Arch. Pharmacol.*, **348**, 403–410.

BOLGER, G.T., LIARD, F., KROGSRUD, R., THIBEAULT, D. & JARAMILLO, J. (1990). Tissue specificity of endothelin binding sites. *J. Cardiovasc. Pharmacol.*, **16**, 367–375.

BRODDE, O.-E., BALS, S., BROEDE, A., KUNDE, K., SCHÄFER, E. & ZERKOWSKI, H.-R. (1992). Receptor systems mediating positive inotropic effect in isolated human right atrium. *Br. J. Pharmacol.*, **105**, 108P.

BYLUND, D.B. & YAMAMURA, H.I. (1990). Methods for receptor binding. In *Methods in Neurotransmitter Receptor Analysis*. ed. Yamamura, H.I., Enna, S.J. & Bylund, D.B. pp. 1–35. New York: Raven Press.

DAVENPORT, A.P., KUC, R.E., FITZGERALD, F., MAGUIRE, J.J., BERRYMAN, K. & DOHERTY, A.M. (1994a). [^{125}I]-PD151242: a selective radioligand for the human ET_A receptors. *Br. J. Pharmacol.*, **111**, 4–6.

DAVENPORT, A.P., KUC, R.E., HOSKINS, S.L., KARET, F.E. & FITZGERALD, F. (1994b). [^{125}I]-PD151242: a selective ligand for endothelin ET_A receptors in human kidney which localises to renal vasculature. *Br. J. Pharmacol.*, **113**, 1303–1310.

DAVENPORT, A.P., MORTON, A.J. & BROWN, M.J. (1991). Localization of endothelin-1 (ET-1), ET-2 and ET-3, mouse VIC, and sarafotoxin S6b binding sites in mammalian heart and kidney. *J. Cardiovasc. Pharmacol.*, **17** (Suppl. 7), S152–S155.

DAVENPORT, A.P., NUNEZ, D.J., HALL, J.A., KAUMANN, A.J. & BROWN, M.J. (1989). Autoradiographical localization of binding sites for porcine [^{125}I]endothelin-1 in humans, pigs and rats: functional relevance in humans. *J. Cardiovasc. Pharmacol.*, **13** (Suppl. 5), S166–S170.

DEBLASI, A., O'REILLY, K. & MOTULSKY, H.J. (1989). Calculating receptor number from binding experiments using same compound as radioligand and competitor. *Trends Pharmacol. Sci.*, **10**, 227–229.

GU, X.-H., CASLEY, D.J. & NAYLER, W.G. (1989). Characterization of [^{125}I]endothelin-1 binding sites in rat cardiac membrane fragments. *J. Cardiovasc. Pharmacol.*, **13** (Suppl. 5), S171–S173.

HÉMSEN, A., FRANCO-CERECEDA, A., MATRAN, R., RUDEHILL, A. & LUNDBERG, J.M. (1990). Occurrence, specific binding sites and functional effects of endothelin in human cardiopulmonary tissue. *Eur. J. Pharmacol.*, **191**, 319–328.

IHARA, M., NOGUCHI, K., SAEKI, T., FUKURODA, T., TSUCHIDA, S., KIMURA, S., FUKAMI, T., ISHIKAWA, K., NISHIKIBE, M. & YANO, M. (1992). Biological profiles of highly potent novel endothelin antagonists selective for the ET_A receptor. *Life Sci.*, **50**, 247–255.

ITO, H., HIRATA, Y., ADACHI, S., TANAKA, M., TSUJINO, M., KOIKE, A., NOGAMI, A., MARUMO, F. & HIROE, M. (1993). Endothelin-1 is an autocrine/paracrine factor in the mechanism of angiotensin II-induced hypertrophy in cultured rat cardiomyocytes. *J. Clin. Invest.*, **92**, 298–403.

ITO, H., HIROE, M., HIRATA, Y., FUJISAKI, H., ADACHI, S., AKIMOTO, H., OHTA, Y. & MARUMO, F. (1994). Endothelin ETA receptor antagonist blocks cardiac hypertrophy provoked by hemodynamic overload. *Circulation*, **89**, 2198–2203.

KARNE, S., JAYAWICKREME, C.K. & LERNER, M.R. (1993). Cloning and characterization of an ET-3 specific receptor (ET_c receptor) from *Xenopus laevis* dermal melanophores. *J. Biol. Chem.*, **268**, 19126–19133.

KUMAR, C.S., NUTHULAGANTI, P., PULLEN, M. & NAMBI, P. (1993). Novel endothelin receptors in the follicular membranes of *Xenopus laevis* oocytes mediate calcium responses by signal transduction through gap junctions. *Mol. Pharmacol.*, **44**, 153–157.

LI, K., STEWART, D.J. & ROULEAU, J.-L. (1990). Myocardial contractile actions of endothelin-1 in rat and rabbit papillary muscles. *Circ. Res.*, **69**, 301–312.

MAGUIRE, J.J., KUC, R.E., O'REILLY, G. & DAVENPORT, A.P. (1994). Vasoconstrictor endothelin receptors characterized in human renal artery and vein *in vitro*. *Br. J. Pharmacol.*, **113**, 49–54.

MASAKI, T. (1991). Tissue specificity of the endothelin-induced responses. *J. Cardiovasc. Pharmacol.*, **17** (Suppl. 7), S1–S4.

MATSUYAMA, K., YASUE, H., OKUMURA, K., SAITO, Y., NAKAO, K., SHIRAKAMI, G. & IMURA, H. (1991). Increased plasma level of endothelin-1-like immunoreactivity during coronary spasm in patients with coronary spastic angina. *Am. J. Cardiol.*, **68**, 991–995.

MCPHERSON, G.A. (1983). A practical computer based approach to the analysis of radioligand binding experiments. *Comp. Meth. Program. Biomed.*, **17**, 107–114.

MOLENAAR, P., KUC, R.E. & DAVENPORT, A.P. (1992). Characterization of two new ET_B-selective radioligands, [^{125}I]-BQ3020 and [^{125}I]-[Ala^{1,3,11,15}]ET-1 in human heart. *Br. J. Pharmacol.*, **107**, 637–639.

MOLENAAR, P., O'REILLY, G., SHARKEY, A., KUC, R.E., HARDING, D.P., PLUMPTON, C., GRESHAM, G.A. & DAVENPORT, A.P. (1993). Characterization and localization of endothelin receptor subtypes in the human atrioventricular conducting system and myocardium. *Circ. Res.*, **72**, 526–538.

MUNSON, P.J. & RODBARD, D. (1980). LIGAND: A versatile computerised approach for the characterisation of ligand binding systems. *Anal. Biochem.*, **107**, 220–239.

NAMBI, P., PULLEN, M. & SPIELMAN, W. (1994). Species differences in the binding characteristics of [^{125}I]IRL-1026, a potent agonist specific for endothelin-B receptors. *J. Pharmacol. Exp. Ther.*, **268**, 202–207.

PETER, M.G. & DAVENPORT, A.P. (1994a). Characterization of the ET_A antagonists BQ123 and FR139317 in human, rat and porcine heart, and the ET_B-selective antagonist IRL1038 in human tissue. *Br. J. Pharmacol.*, **112**, 122P.

PETER, M.G. & DAVENPORT, A.P. (1994b). [^{125}I]-PD151242 as an endothelin ET_A-selective radioligand in the human, rat and porcine heart. *Br. J. Pharmacol.*, **112**, 494P.

SAKAMOTO, A., YANAGISAWA, M., SAKURAI, T., TAKUWA, Y., YANAGISAWA, H. & MASAKI, T. (1991). Cloning and functional expression of human cDNA for the ET_B endothelin receptor. *Biochem. Biophys. Res. Commun.*, **178**, 656–663.

SCHOMISCH MORAVEC, C., REYNOLDS, E.E., STEWART, R.W. & BOND, M. (1989). Endothelin is a positive inotropic agent in human and rat heart *in vitro*. *Biochem. Biophys. Res. Commun.*, **159**, 14–18.

SOGABE, K., NIREI, H., SHOUBO, M., NOMOTO, A., AO, S., NOTSU, Y. & ONO, T. (1993). Pharmacological profile of FR139317, a novel, potent endothelin ET_A receptor antagonist. *J. Pharmacol. Exp. Ther.*, **264**, 1040–1046.

SOKOLOWSKY, M., AMBER, I. & GALRON, R. (1992). A novel subtype of endothelin receptors. *J. Biol. Chem.*, **267**, 20551–20554.

SUZUKI, T., KUMAZAKI, T. & MITSU, Y. (1993). Endothelin-1 is produced and secreted by neonatal rat cardiac myocytes *in vitro*. *Biochem. Biophys. Res. Commun.*, **191**, 823–830.

TAKANASHI, M. & ENDOH, M. (1991). Characterization of positive inotropic effect of endothelin on mammalian ventricular myocardium. *Am. J. Physiol.*, **261**, H611–H619.

TAKAYANAKI, R., HASHIGUCHI, T., OHASHI, M. & NAWATA, H. (1990). Regional distribution of endothelin receptor in porcine cardiovascular tissues. *Regul. Pept.*, **27**, 247–255.

TAKAYANAKI, R., OHNAKA, K., TAKASAKI, C., OHASHI, M. & NAWATA, H. (1991). Multiple subtypes of endothelin receptors in human and porcine tissues: characterisation by ligand binding, affinity labeling, and regional distribution. *J. Cardiovasc. Pharmacol.*, **17** (Suppl. 7), S127–S130.

TØNNESSEN, T., NAESS, P.A., KIRKEBØEN, K.A. & ? OTHERS (1993). Release of endothelin from the porcine heart after short term coronary artery occlusion. *Cardiovasc. Res.*, **27**, 1482–1485.

WATANABE, T., SUZUKI, N., SHIMAMOTO, N., FUJINO, M. & IMADA, A. (1991). Contribution of endogenous endothelin to the extension of myocardial infarct size in rats. *Circ. Res.*, **69**, 370–377.

WHARTON, J., RUTHERFORD, R.A.D., GORDON, L., MOSCOSO, G., SCHIEMBERG, I., GAER, J.A.R., TAYLOR, K.M. & POLAK, J.M. (1991). Localization of endothelin binding sites and endothelin-like immunoreactivity in human fetal heart. *J. Cardiovasc. Pharmacol.*, **17** (Suppl. 7), S378–384.

YASUDA, M., KOHNO, M., TAHARA, A., ITAGANE, H., TODA, I., AKIOKA, K., TERAGAKI, M., OKU, H., TAKEUCHI, K. & TAKEDA, T. (1990). Circulating immunoreactive endothelin in ischemic heart disease. *Am. Heart. J.*, **119**, 801–806.

ZERKOWSKI, H.-R., BROEDE, A., KUNDE, K., HILLEMANN, S., SCHÄFER, E., VOGELSANG, M., MICHEL, M.C. & BRODDE, O.-E. (1992). Comparison of the positive inotropic effects of serotonin, histamine, angiotensin II, endothelin and isoprenaline in the isolated human right atrium. *Naunyn-Schmied. Arch. Pharmacol.*, **347**, 347–352.

(Received July 18, 1994
Revised September 15, 1994
Accepted September 16, 1994)

British Journal of Pharmacology (1995) 114, 303–308 © 1995 Stockton Press All rights reserved 0007–1188/95 $9.00

S14080, a peripheral analgesic acting by release of an endogenous circulating opioid-like substance

[1]Sérgio H. Ferreira, Berenice B. Lorenzetti, *Michelle Devissaguet, †Daniel Lesieur & *Yannis Tsouderos

[1]Department of Pharmacology, Faculty of Medicine of Ribeirão Preto, Ribeirão Preto, S.P., 14049-900, Brazil; *Institut de Recherches Internationales Servier, Courbevoie, 92415, France and †Institut de Chimie Pharmaceutique, Lille, 59000, France

1 The oral administration of a benzothiazolinone derivative (benzoyl-6 dihydro-2,3 benzothiazole), S14080, caused dose-dependent antinociception in the rat paw pressure test, which represents a model of mechanical hyperalgesia. S14080 had no significant effect on the inflammatory oedema induced by carrageenin or on the tail flick test, nor did it possess a notable antipyretic effect.

2 Post-treatment with S14080 dose-dependently antagonized the hyperalgesia induced by prostaglandin E_2, bradykinin, dopamine and by the hyperalgesic cytokines reported to be released by carrageenin (tumour necrosis factor α, interleukin-1 and interleukin-8).

3 The blockade of prostaglandin E_2-induced paw hyperalgesia by oral pretreatment of the rats with S14080 was abolished by prior intraplantar administration of either naloxone or NorBNI which are non-specific and specific κ opioid antagonists, respectively.

4 Adrenalectomy abolished the oral antinociceptive effect of S14080.

5 Five consecutive daily injections of S14080 did not produce tolerance such as that seen with the central antinociceptive action of morphine.

6 As with peripherally acting opiates, the antinociceptive activity of S14080 was abolished by the intraplantar injection of agents which inhibit either arginine synthetase (N^G-monomethyl-L-arginine) or the activation of guanylate cyclase (methylene blue).

7 We conclude that S14080 is a new type of peripheral antinociceptive which, in rats, acts mainly by releasing an endogenous, opioid-like substance from the adrenal glands.

Keywords: Peripheral opioid antinociception; S14080 antinociception; adrenal glands antinociception; peripheral analgesia; endogenous opioid antinociception

Introduction

Hyperalgesia is a fundamental event in the manifestation of overt, inflammatory pain. Peripheral antinociceptives which interfere with inflammatory hyperalgesia can be divided into two broad groups: (a) those which prevent the sensitization of pain receptors (Ferreira, 1972; Ferreira *et al.*, 1973; Ferreira, 1980), e.g. cyclo-oxygenase inhibitors (non-steroidal anti-inflammatory drugs) and (b) those which directly abolish the ongoing sensitization of pain receptors, e.g. dipyrone and peripheral opioids (Ferreira & Nakamura, 1979; Lorenzetti & Ferreira, 1982; 1985; Ferreira *et al.*, 1984; Ferreira, 1990). There are, however, drugs in the second group which may act as antinociceptives, i.e., by blocking ongoing hyperalgesia, through the peripheral release of an endogenous, opioid-like substance. We have found that clonidine and St-91 (a clonidine analogue which does not cross the blood-brain barrier) cause peripheral antinociception which is abolished by the intraplantar administration of opioid antagonists (Nakamura & Ferreira, 1988). The clonidine antinociceptive activity was blocked by yohimbine, an α_2-adrenoceptor antagonist.

General screening of S14080, a benzothiazolinone (benzoyl-6 dihydro-2,3, benzothiazole (Follet-Houttemane *et al.*, 1991), revealed a marked antinociceptive effect on acetic acid-induced writhing in the mouse. In the present paper, we report investigations into the mechanism of this antinociceptive action of S14080. This substance was initially tested in the rat paw hyperalgesia assay (Ferreira *et al.*, 1978) employing carrageenin and mediators thought to be released by carregeenin such as prostaglandin E_2 dopamine, interleukin-1 (IL-1) and IL-8, as nociceptive stimuli. We have also compared the antinociceptive effect of S14080 with that of typical cyclo-oxygenase inhibitors (indomethacin) and of compounds which counteract ongoing hyperalgesia induced by prostaglandin E_2 (dipyrone). The antinociceptive profile of S14080 was not similar to that of indomethacin or dipyrone. Based on the abolition of its effect by adrenalectomy and opioid antagonists, S14080 appears to cause peripheral antinociception via the release of an endogenous opioid from the adrenal glands. In contrast to clonidine, this effect was not blocked by yohimbine.

The antinociceptive activity of S14080, like that of dipyrone and peripheral opioids, was abolished by methylene blue, an inhibitor of guanylate cyclase activation, and by N^G-monomethyl-L-arginine (L-NMMA), an inhibitor of the formulation of NO from L-arginine (Duarte *et al.*, 1991a,b; Ferreira *et al.*, 1991). The maximal effect of oral administration of S14080 was observed with 1 h of administration and no tolerance was observed following five days of repeated administration. These results suggest that S14080 constitutes a new type of peripheral antinociceptive whose mode of action involves the release of an endogenous opioid-like substance.

Methods

Animals

Male Wistar rats (130–180 g) with free access to food and water were used for the various experiments. When the drug was administered orally, the animals were deprived of food 12 h before testing although water was allowed *ad libitum*.

[1] Author for correspondence.

Nociceptive test

Hyperalgesia was measured by our modification (Ferreira *et al.*, 1978) of the Randall-Selitto (Randall & Selitto, 1957) test. In this test, a constant pressure of 20 mmHg is applied to the rat paw and discontinued (reaction time) when the animal exhibits a reaction characterized by the reduction of escape movements followed by an alteration in the respiratory frequency and the onset of a typical shivering reaction.

The intensity of hyperalgesia was quantified as the difference in reaction reduction time (Δ reaction time) obtained by subtracting the value measured 2 or 3 h after administration of the hyperalgesic substances from the control reaction time, measured prior to the administration of the hyperalgesic substance. Hyperalgesia was induced in the hind paws by the intraplantar (i.pl.) administration of 100 or 300 μg of carrageenin, 100 ng of prostaglandin E_2, 500 ng of bradykinin, 0.1 ng of IL-8, 10 μg of dopamine, 0.1 i.u. of IL-1β or 2.5 pg of tumour necrosis factor-α (TNF-α), injected in 100 μl of saline. These substances have been shown to produce quantitatively equivalent levels of hyperalgesia. The investigator was unaware of the order of drug treatments applied.

Oedema

The oedema induced by the i.pl. injection of carrageenin (100 and 300 μg) was measured plethysmographically (Ferreira, 1979). Oedema formation was defined as the difference in paw volume (μl) measured before and 2 or 3 h after i.pl. carrageenin administration.

Effect of S14080 on the hyperthermia induced by the intravenous injection of lipopolysaccharide (LPS)

Rectal temperature was measured by inserting a z thermistor probe (Y.S.I. nr. 401) 3 cm into the rectum. The animals were held gently during the temperature measurements. This procedure was performed at least twice, one day prior to the experiment in order to minimize possible stress-induced temperature changes. The experiments were conducted during a single, one-day period. Basal temperature was defined by recording four measurements taken at 30 min intervals, before the administration of the drugs. The experiments were conducted in the thermoneutral zone for rats (28 ± 1°C) (Gordon, 1990).

Presentation of the data and analysis

The dose, route and time of administration of each substance are indicated in the figure legends. The results are presented as the mean ± s.e.mean and the statistical analysis employed indicated. No statistical test was applied when the difference between means was greater than three s.e.mean. Standard errors smaller than the symbols used are not shown. A one-way analysis of variance (ANOVA) was used to compare the changes between different doses or treatments. When a significant effect was indicated, comparisons between individual means were subsequently tested using the Bonferroni procedure (Graph Pad in Stat, version 1.0). Differences were considered to be significant at $P \leq 0.05$. The ED_{50} and 95% confidence limits (c.l.) were calculated according to Litchfield & Wilcoxon (1949).

Drugs

Unless otherwise stated, the drugs were diluted in sterile saline. The following drugs were used: carrageenin (Viscarin Marine Colloids, U.S.A.), prostaglandin E_2 (Upjohn, U.S.A.), indomethacin (Merck, Sharp & Dohme, Brazil, dissolved in Tris-HCl buffer, pH 8.2), dipyrone and clonidine hydrochloride (Boehringer Ingelheim, Germany), methylene blue (Reagen, Brazil), N^G-monomethyl-L-arginine (L-NMMA, Wellcome, England), NorBNI (nor binaltorphimine dihydrochloride) (kindly provided by Dr K. Rice, NIH, U.S.A.), benzoyl-6 dihydro-2,3 benzothiazole (S14080, Institut de Rechereches Internationales Servier, France, dissolved in peanut oil from Sigma, U.S.A.), lipopolysaccharide (LPS) from *E. coli* 0111:B4, dopamine (3-hydroxytyramine hydrochloride) and bradykinin (Sigma, U.S.A.), yohimbine hydrochloride and morphine hydrochloride (Merck, Germany), IL-1β, IL-8 and TNFα (NIBSC preparations coded 86/680, 89/520 and 87/650 respectively), naloxone hydrochloride (Du Pont Pharmaceuticals, U.S.A.).

Results

The effect of oral administration of S14080 on hyperalgesia and oedema induced by two intraplantar injections (100 μg or 300 μg) of carrageenin

Oral pretreatment with S14080, 10–40 mg kg^{-1} resulted in dose-dependent antinociception for both low doses (ED_{50} = 17.5, c.l. 8.9–34.5 mg kg^{-1}) and high doses (ED_{50} = 41.0, c.l. 14.2–118.4 mg kg^{-1}) of carrageenin (Figure 1a,b; ANOVA, $P < 0.0001$).

In contrast to the antinociceptive effect on carrageenin-induced hyperalgesia, S14080 in doses up to 80 mg kg^{-1} had no antinociceptive action when assessed by the tail flick method (results not shown). This method detects the central effect of antinociceptive agents (Smith, 1965). There was no significant concomitant effect of S14080 on the accompanying oedema (Figure 1c,d; ANOVA, $P > 0.5$).

Antinociceptive action of S14080 on various hyperalgesic stimuli

In this series of experiments, S14080 was tested against hyperalgesic mediators reported to be released by carrageenin in the rat (Ferreira *et al.*, 1978; 1988; Nakamura & Ferreira, 1987; Cunha *et al.*, 1991; 1992). Figure 2 shows that the oral administration of S14080 produced dose-dependent antinociception after the application of prostaglandin E_2 (PGE_2), dopamine, bradykinin (BK), tumour necrosis factor α (TNF-α) or the recombinant interleukins-1β and 8 (IL-1β and IL-8). Control doses for the hyperalgesic substances were selected based on previous experiments in order to provide a qualitatively equivalent hyperalgesic response. The comparisons were made 3 h after the challenge when the hyperalgesia induced by the various substances reached a plateau.

Duration of antinociception following oral administration of S14080

S14080 (40 mg kg^{-1}) administered at different times before the measurement of hyperalgesia induced by PGE_2 caused a time-dependent antinociception. Hyperalgesia was induced by PGE_2 (100 ng/paw) and measurements were performed 3 h later. In this experiment, total inhibition of the hyperalgesia induced by PGE_2 alone was considered to be 100% (19.1 ± 0.5 s). Antinociception was maximal (92.7%; 1.4 ± 0.5 s) 1 h after oral S14080 administration and subsequently decreased with time, reaching less than 12% after 4 h (17.0 ± 1.0).

Intraplantar effect of NorBNI on the systemic action of indomethacin, dipyrone and S14080 upon PGE_2-induced hyperalgesia

Figure 3 shows the effect of NorBNI (5 μg/paw) on the systemic action of S14080 (10, 20 and 40 mg kg^{-1}), indomethacin (5 mg kg^{-1}) and dipyrone (20 mg kg^{-1}) upon PGE_2-induced hyperalgesia. Figure 3a shows that S14080 caused dose-dependent antinociception which was prevented

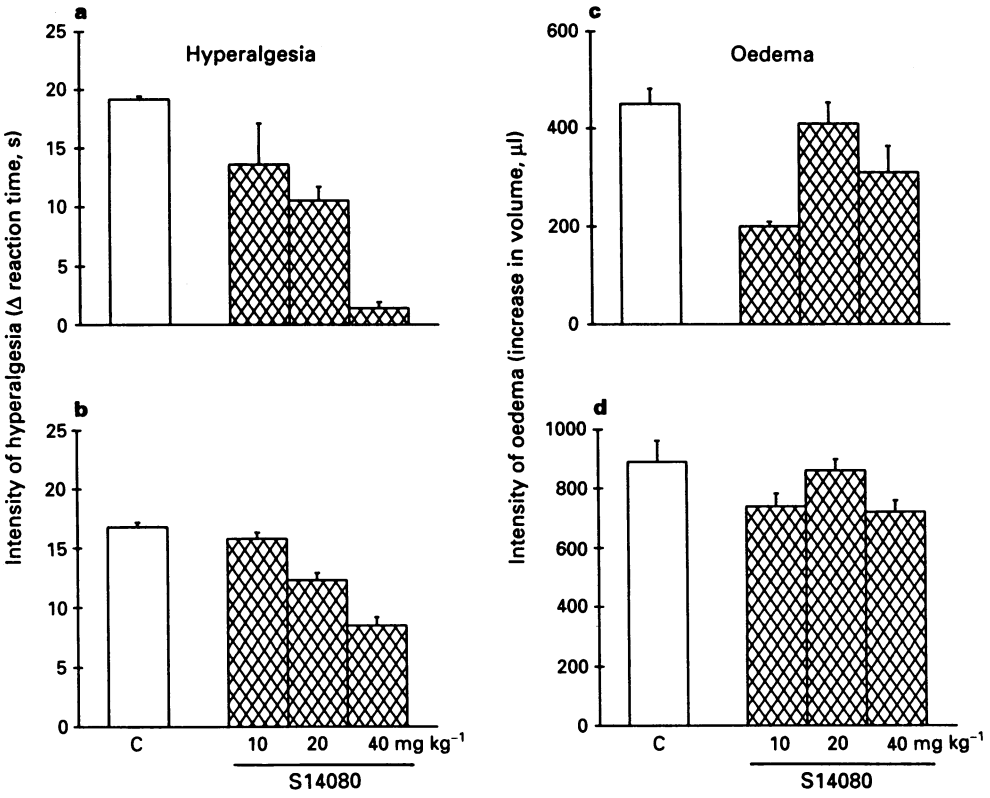


Figure 1 Analgesic and anti-oedematogenic effect of S14080 on the intraplantar injection of two doses of carrageenin (100 μg/paw in the a and c and 300 μg/paw in the b and d). S14080 was administered orally at the doses indicated 2 h after the carrageenin challenge. C represents the control hyperalgesia or oedema induced by carrageenin. Hyperalgesia and oedema were measured 3 h after carrageenin challenge. Data are the mean ± s.e.mean of five rats per group.

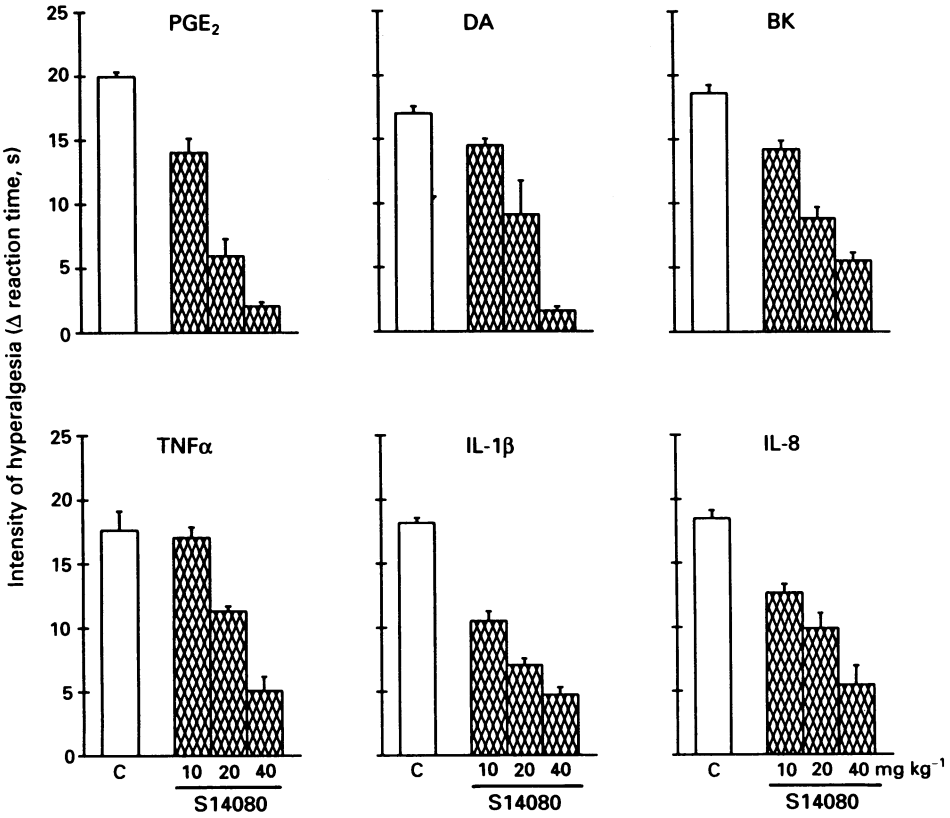


Figure 2 Analgesic effect of S14080 on the hyperalgesia induced by different stimuli. The control (C) doses of the hyperalgesic stimuli were: prostaglandin E_2 (PGE_2, 100 ng), dopamine (DA, 10 μg), bradykinin (BK, 500 ng), tumour necrosis factor (TNF-α, 2.5 pg), interleukin-1β (IL-1β, 0.1 UI) and interleukin 8 (IL-8, 0.1 ng). S14080 was administered 2 h after injection of the hyperalgesic stimulus. Data are the mean ± s.e.mean of five rats per group. The hyperalgesia was measured 3 h after injection of the stimuli.

by previous intraplantar injection of NorBNI; Figure 3b confirms earlier results (Lorenzetti & Ferreira, 1985) by showing that the administration of indomethacin or dipyrone resulted, respectively, in either the absence of antinociception or in intense antinociception on the hyperalgesic response to PGE_2 (open columns). The intraplantar injection of the opioid antagonist NorBNI did not affect either control prostaglandin hyperalgesia or the responses to the treatment with dipyrone or indomethacin (hatched columns). Naloxone (Nx, 1 μg/paw and 1 mg kg^{-1}) also abolished the action of S14080 (data not shown).

Yohimbine does not inhibit the antinociceptive action of S14080

As previously shown (Nakamura & Ferreira, 1988), the antinociceptive effect of clonidine (250 μg kg^{-1}, i.p.) against PGE_2-induced hyperalgesia (18.1 ± 0.6 s) was blocked (5.7 ± 0.4 s) by pretreatment with yohimbine, (1 mg kg^{-1}, i.p., 16.0 ± 0.6 s). The pretreatment of the animals with yohimbine, however, had no significant effect ($P > 0.05$ Bonferroni) on the antinociceptive action of S14080 (10, 20, 40 mg kg^{-1}, orally).

Adrenalectomy abolishes the oral antinociceptive potency of S14080

Sham operation did not alter the antinociceptive action of S14080 (40 mg kg^{-1}, p.o., 5.2 ± 0.5 s) or of dipyrone (40 mg kg^{-1}, p.o., 5.2 ± 0.4) on the hyperalgesia induced by prostaglandin E_2 (18.8 ± 0.5). Adrenalectomy, however, abolished the antinociception produced by S14080 (17.9 ± 0.7), without influencing the response to dipyrone (5.2 ± 0.7).

Response injections of S14080 do not induce tolerance

There was a significant difference compared to the effect of morphine after consecutive applications (ANOVA, $P < 0.05$). Antinociceptive tolerance to centrally acting opioids such as morphine occurred following five, consecutive daily treatments (8 mg kg^{-1}). After this period, there was no measurable difference between the control and treated hyperalgesic groups (ANOVA, $P < 0.05$, Figure 4). No variation in the antinociceptive effect was observed during the treatment with S14080 (40 mg kg^{-1}), (ANOVA, $P < 0.05$).

Methylene blue and L-NMMA inhibit S14080-induced antinociception

Figure 5 shows the effect of pretreatment with methylene blue (MB) or L-NMMA on the antinociceptive action of S14080 in hyperalgesic, PGE_2-treated paws. MB did not affect the hyperalgesia induced by PGE_2 but abolished the antinociceptive effect of S14080. A similar response was observed in paws pretreated with L-NMMA.

S14080 does not prevent the febrile response induced by LPS in rats

Oral pretreatment with S14080 (40 and 80 mg kg^{-1}) 30 min before the injection of LPS, unlike indomethacin (8 mg kg^{-1}),

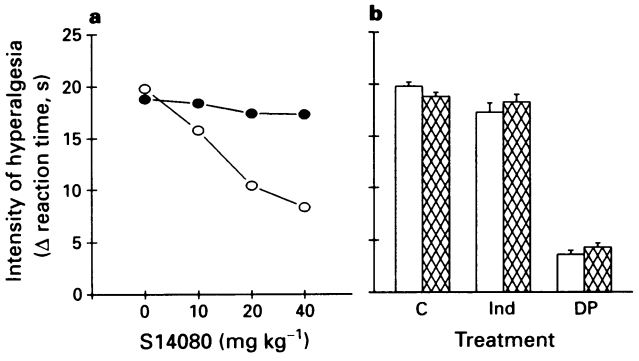


Figure 3 NorBNI, an opioid κ-antagonist, inhibits the analgesic action of S14080, but not that of indomethacin or dipyrone, in prostaglandin E_2 (PGE_2)-induced hyperalgesia. (a) Shows the analgesic effect of increasing doses of S14080 (○) on the hyperalgesia induced by PGE_2 (100 ng/paw). A single dose of NorBNI (5 μg/paw, ●) was sufficient to inhibit this action of S14080. (b) Shows that NorBNI (cross-hatched columns), in the same dose as for (a) had no influence on the responses to indomethacin (Ind, 5 mg kg^{-1}) or dipyrone (DP, 20 mg kg^{-1}) in PGE_2-induced (100 ng/paw) hyperalgesia. Note that NorBNI had no effect by itself on PGE_2-induced hyepralgesia (time 0 on (a) and open column C in (b)). In both (a) and (b), NorBNI and the analgesics were injected 90 min and 120 min, respectively, after PGE_2 application. Data are the mean ± s.e.mean of five animals per group. Hyperalgesia in all cases was measured 3 h after the intraplantar injection of PGE_2.

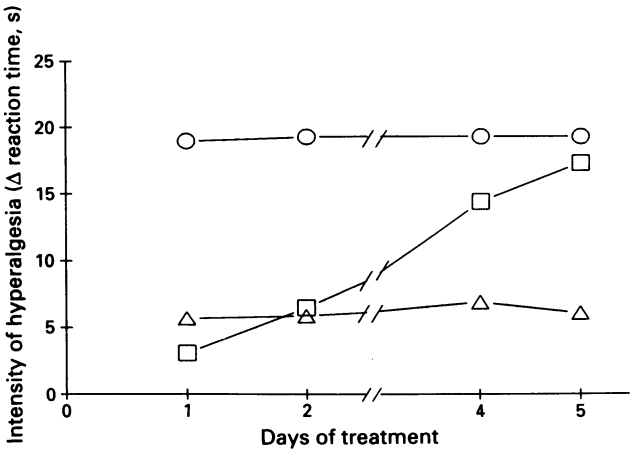


Figure 4 Lack of tolerance to S14080 as compared with morphine, a centrally acting opiate. S14080 (△, 40 mg kg^{-1}) and morphine (□, 8 mg kg^{-1}) were given orally, two times a day for five consecutive days. Prostaglandin (PGE_2) (○, 100 ng/paw) was injected in alternate paws 2 h before the first daily injection of the analgesics. Data are the mean ± s.e.mean of five animals per group. The intensity of hyperalgesia was measured 3 h after the PGE_2 challenge.

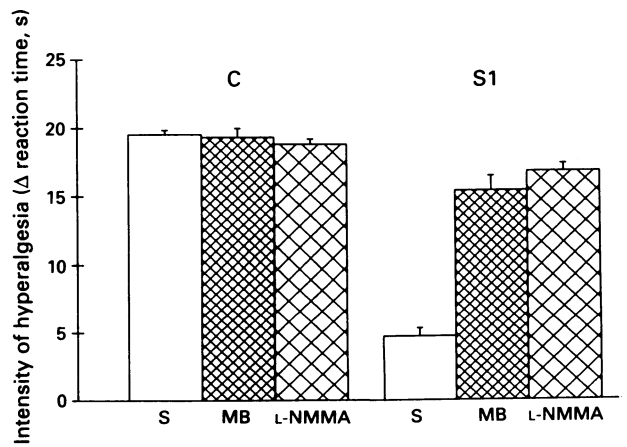


Figure 5 Methylene blue and N^G-monomethyl-L-argiine (L-NMMA) inhibit the analgesic action of S14080. Hyperalgesia was induced by the injection of prostaglandin E_2 (PGE_2, C, 100 ng/paw). Ninety minutes later, the animals were treated with methylene blue (MB, 500 μg/paw) or L-NMMA (50 μg/paw). S14080 (S1, 40 mg kg^{-1}) was administered orally 2 h after the prostaglandin challenge. The intensity of hyperalgesia was measured 3 h after the PGE_2 challenge. Data are the mean ± s.e.mean of five animals per group.

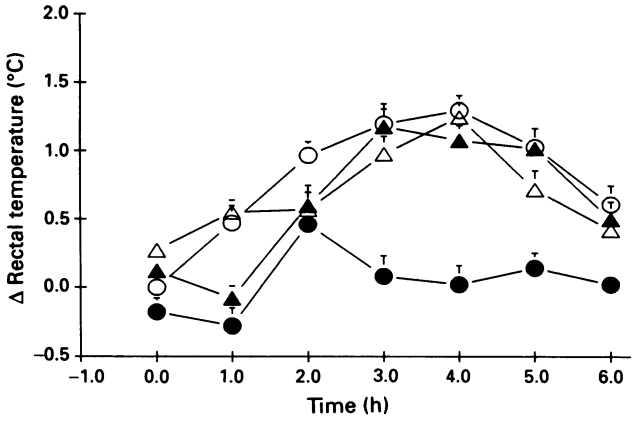


Figure 6 The effect of pretreatment with S14080 on the febrile response induced by lipopolysaccharide (LPS) in rats. Indomethacin (8 mg kg^{-1}) and S14080 (S14, 40 and 80 mg kg^{-1}) were administered orally 30 min before the intravenous administration of LPS (50 μg kg^{-1}). (○) Control; (●) indomethacin 8 mg kg^{-1}; S14080 (△) 40 mg kg^{-1}, (▲) 80 mg kg^{-1}. Rectal temperature was measured at 30 min intervals but only the hourly presented. Data are the mean ± s.e.mean of five to size animals per group.

had no significant antipyretic effect ($P>0.05$). There was, however, a transient blockade (1 h after LPS) of the febrile response with highest dose of S14080 (80 mg kg^{-1}, Figure 6).

Discussion

In the present study, we have demonstrated that S14080 produces dose-dependent antinociception but has an inconsistent effect on the inflammatory oedema induced in the rat paw by carrageenin. The antinociceptive effect of S14080 was maximal 1 h after oral administration and, unlike morphine, the animal did not show tolerance after five consecutive daily treatments.

Previous studies by our group have shown that several cytokines cause hyperalgesia in the rat paw via the local release of hyperalgesic mediators. IL-1 and IL-8-induced hyperalgesia is mediated by cyclo-oxygenase products or sympathetic mediators (Cunha *et al.*, 1991; Ferreira *et al.*, 1988). In carrageenin-induced hyperalgesia, the release of these cytokines is preceded by the liberation of TNF-α (Cunha *et al.*, 1992). Recently, we reported that the hyperalgesia induced by bradykinin in the rat paw was also mediated by the release of an array of these same hyperalgesic cytokines (Ferreira *et al.*, 1993a, 1993b). In the present study, S14080 displayed a dose-dependent, antinociceptive effect on hyperalgesia, not only against carrageenin, but also against mediators such as bradykinin, prostagland E_2, dopamine and hyperalgesic cytokines (IL-1, IL-8) which are thought to be released during the inflammatory reaction (Cunha *et al.*, 1991). Unlike indomethacin (a cyclo-oxygenase inhibitor), the general antinociceptive activity of S14080 against the various substances tested is typical of antinociceptives such as dipyrone and peripheral opiates which directly antagonize ongoing hyperalgesia (Lorenzetti & Ferreira, 1982; 1985; Ferreira *et al.*, 1984). However, although S14080 did act in a qualitatively similar manner to dipyrone (Lorenzetti & Ferreira, 1985), its antinociceptive effects were in fact antagonized by the intraplantar injection of either NorBNI or naloxone, which are κ and non-specific opioid antagonists, respectively. Thus, the mechanism of action of S14080 seems to be different from that of either indomethacin or dipyrone but has similarities to a peripheral, opioid effect. The absence of an antinociceptive role for S14080 in the tail flick test is in line with the suggestion that the site of action of S14080 is not central (Smith *et al.*, 1985).

The action of S14080 does not, however, seem to be via a direct antinociceptive effect on peripheral nociceptors since, in contrast with the action of dipyrone, S14080 antinociception was strongly inhibited by adrenalectomy. Overall, our results suggest that the major site of action of S14080 is the adrenal glands where it induces the release of an endogenous, opioid-like substance. Indeed, adrenal glands do contain a large quantity of endogenous opioids, particularly of enkephalin (North & Egan, 1983). We have already shown that clonidine causes peripheral antinociception through the release of an opioid-like substance (Nakamura & Ferreira, 1988). However, unlike clonidine, the antinociceptive effect of S14080 was not inhibited by yohimbine. Thus, S14080 appears to be independent of α_2-receptor activation which is associated with the hypotensive action of clonidine. We have suggested that clonidine-induced antinociception is not appropriate for clinical use since the antinociceptive action would probably be overshadowed by the hypotensive response, a phenomenon which would not be expected to occur with S14080. General screening of S14080 has shown no effect on rat blood pressure (unpublished results).

We have previously demonstrated that various antinociceptives block hyperalgesia by stimulation of the arginine/NO/cyclicGMP nociceptor pathway (Ferreira *et al.*, 1991; Duarte *et al.*, 1992). In line with this conclusion, we have shown here that S14080-mediated antinociception was also abolished by the intraplantar injection of agents which inhibit the arginine/nitric oxide/cyclicGMP pathway, namely L-NMMA, an inhibitor of NO synthetase, and methylene blue, an inhibitor of the activation of guanylate cyclase.

S14080 in doses which cause significant antinociception had an inconsistent effect on carrageenin-induced oedema, and a negligible antipyretic effect. In the rat, the antipyretic and anti-oedematogenic activities are the two major characteristics of non-steriodal anti-inflammatory drugs which inhibit cyclo-oxygenase. This suggests that the oral administration of S14080 has little or no effect on tissue cyclo-oxygenase. Alternatively, a poor distribution of S14080 within the central nervous system may explain the absence of an antipyretic effect. Whatever the mechanism of action maybe, a peripheral antinociceptive without an antipyretic effect is a clinically desirable characteristic in the follow up of patients in which the absence of fever is a sign of good prognosis.

In conclusion, S14080 appears to be a new type of antinociceptive which acts peripherally via the release of an endogenous, opioid-like substance.

The authors thank Ms I.R. Santos for technical assistance. This work was supported by FAPESP and CNPq (Brazil).

References

CUNHA, F.Q., LORENZETTI, B.B., POOLE, S. & FERREIRA, S.H. (1991). Interleukin 8 as a mediator of sympathetic pain. *Br. J. Pharmacol.*, **104**, 765–767.

CUNHA, F.Q., POOLE, S., LORENZETTI, B.B. & FERREIRA, S.H. (1992). The pivotal role of tumour necrosis factor alpha in the development of inflammatory hyperalgesia. *Br. J. Pharmacol.*, **107**, 660–664.

DUARTE, I.D.G., FACCIOLI, L.H. & FERREIRA, S.H. (1992). Blockade of the peripheral pain sensory system via the L-arginine: NO/cGMP pathway. In *The Biology of Nitric Oxide*, ed. Moncada, S., Marletta, M.A., Hibbs Jr., J.B. & Higgs, E.A. pp. 258–260. London and Chapel Hill: Portland Press Proceedings.

DUARTE, I.D.G., LORENZETTI, B.B. & FERREIRA, S.H. (1990a) Acetylcholine induces peripheral analgesia by release of nitric oxide. In *Nitric Oxide from L-Arginine: a Bioregulatory System.* ed. Moncada, S. & Higgs, E.A., pp. 165–170. Amsterdam: Elsevier Science Publishers.

DUARTE, I.D.G., LORENZETTI, B.B. & FERREIRA, S.H. (1990b). Peripheral analgesia and activation of the nitric oxide-cyclic GMP pathway. *Eur. J. Pharmacol.*, **186,** 289–293.

FERREIRA, S.H. (1972). Prostaglandins, aspirin-like drugs and analgesia. *Nature, New Biol.*, **240,** 200–203.

FERREIRA, S.H. (1979). A new method for measuring variations of rat paw volume. *J. Pharm. Pharmacol.*, **31,** 648.

FERREIRA, S.H. (1980). Peripheral analgesia: Mechanism of the analgesic action of aspirin like drugs and opiate-antagonists. *Br. J. Clin. Pharmacol.*, **10,** 237S–245S.

FERREIRA, S.H. (1990). A classification of peripheral analgesics based upon their mode of action. In *Migraine: Spectrum of Ideas.* ed. Sandler, M. & Collins, G.M. pp. 59–72. Oxford: University Press.

FERREIRA, S.H., DUARTE, I.D.G. & LORENZETTI, B.B. (1991). The molecular mechanism of action of peripheral morphine analgesia: stimulation of cGMP system via nitric oxide release. *Eur. J. Pharmacol.*, **201,** 121–122.

FERREIRA, S.H., LORENZETTI, B.B., BRISTOW, A.F. & POOLE, S. (1988). Interleukin-1β as a potent hyperalgesic agent antagonized by a tripeptide analogue. *Nature*, **334,** 698–700.

FERREIRA, S.H., LORENZETTI, B.B. & CORREA, F.M.A. (1978). Central and peripheral antialgesic action of aspirin-like drugs. *Eur. J. Pharmacol.*, **53,** 39–48.

FERREIRA, S.H., LORENZETTI, B.B., CUNHA, F.Q. & POOLE, S. (1993a). Bradykinin release of TNF-alpha plays a key role in the development of inflammatory hyperalgesia. *Agents Actions*, **38,** C7–C9.

FERREIRA, S.H., LORENZETTI, B.B. & POOLE, S. (1993b). Bradykinin initiates cytokine-mediated inflammatory hyperalgesia. *Br. J. Pharmacol.*, **110,** 1227–1231.

FERREIRA, S.H., LORENZETTI, B.B. & RAE, G.A. (1984). Is methylnalorphinium the prototype of an ideal peripheral analgesic? *Eur. J. Pharmacol.*, **99,** 23–29.

FERREIRA, S.H., MONCADA, S. & VANE, J.R. (1973). Prostaglandins and the mechanism of analgesic produced by aspirin-like drugs. *Br. J. Pharmacol.*, **49,** 86–97.

FERREIRA, S.H. & NAKAMURA, M. (1979). II – Prostaglandin hyperalgesia: the peripheral analgesia activity of morphine, enkephalins and opioid antagonists. *Prostaglandins*, **18,** 191–200.

FOLLET-HOUTTEMANE, C., BOIVIN, J.C., BONTE, J.P. & LESSIEUR, D. (1991). Structure de la benzol-6 dihydro-2,3 benzothiazole-1,3 One-2. *Acta Cryst.*, **C47,** 882–884.

GORDON, C.J. (1990). Thermal biology of the laboratory rat. *Physiol. Behav.*, **47,** 963–991.

LITCHFIELD, Jr, J.T. & WILCOXON, F. (1949). A simplified method of evaluating dose-effect experiments. *J. Pharmacol. Exp. Ther.*, **96,** 99.

LORENZETTI, B.B. & FERREIRA, S.H. (1982). The analgesic effect of quaternary analogues of morphine and nalorphine. *Braz. J. Med. Biol. Res.*, **15,** 285–290.

LORENZETTI, B.B. & FERREIRA, S.H. (1985). Mode of analgesic action of dipyrone: direct antagonism of inflammatory hyperalgesia. *Eur. J. Pharmacol.*, **114,** 375–381.

NAKAMURA, M. & FERREIRA, S.H. (1987). A peripheral sympathetic component in inflammatory hyperalgesia. *Eur. J. Pharmacol.*, **135,** 145–153.

NAKAMURA, M. & FERREIRA, S.H. (1988). Peripheral analgesic action of clonidine mediation by release of endogenous enkephalin like substance. *Eur. J. Pharmacol.*, **146,** 223–228.

NORTH, R.A. & EGAN, T.M. (1983). Actions and distributions of opioid peptides in peripheral tissues. *Br. Med. Bull.*, **39,** 71–75.

RANDALL, L.O. & SELITTO, J.J. (1957). A method for measurement of analgesic activity on inflammed tissue. *Arch. Int. Pharmacodyn. Ther.*, **111,** 409–419.

SMITH, T.W., FOLLENFANT, R.L. & FERREIRA, S.H. (1985). Antinociceptive models displaying peripheral opioid activity. *Int. J. Tissue React.*, **VII,** 61–67.

(Received May 31, 1994
Revised August 22, 1994
Accepted September 16, 1994)

British Journal of Pharmacology (1995) 114, 309-314 © 1995 Stockton Press All rights reserved 0007-1188/95 $9.00

Presence of vasoconstrictor 5HT$_1$-like receptors revealed by precontraction of rabbit isolated mesenteric artery

A. Choppin & [1]S.E. O'Connor

Synthélabo Recherche, Department of Preclinical Research, 31 Avenue Paul Vaillant-Couturier, 92225 Bagneux, France

1 A series of 5-hydroxytryptamine (5-HT) receptor agonists including 5-HT, 5-carboxamidotryptamine (5-CT) and sumatriptan produced little or no contraction of rabbit isolated mesenteric arteries under resting tone conditions, even at concentrations up to 10^{-4} M.

2 When the same agonists were retested in mesenteric artery preparations pre-contracted with the thromboxane-mimetic, U46619, each demonstrated concentration-related vasoconstrictor activity. 5-CT and 5-HT were especially potent and effective in this model giving EC_{50} values of 4.3×10^{-9} M and 1.6×10^{-8} M respectively and maximum effects equivalent to those of KCl 80 mM. In preparations precontracted by U46619 (conditions retained throughout the rest of the study) the order of agonist potency was 5-CT > 5-HT > RU 24969 = sumatriptan > 8-hydroxy-2-(di-n-propylamino)tetralin (8-OHDPAT) > cisapride.

3 The vasoconstrictor effects of 5-CT were competitively antagonized by methiothepin (pA_2 8.20) but resistant to antagonism by a range of other 5-HT receptor antagonists, i.e. pindolol (5-HT$_{1A}$/5-HT$_{1B}$), propranolol (5-HT$_{1B}$), spiperone (5-HT$_{2A}$), ondansetron (5-HT$_3$), ICS 205930 (5-HT$_3$/5-HT$_4$) and SDZ 205557 (5-HT$_4$). 5-CT responses were slightly antagonized by a high concentration of ritanserin (5-HT$_{2A}$/5-HT$_{2C}$). Responses to 5-HT and sumatriptan were also antagonized by methiothepin with similar affinity (pA_2/pK_B values $\simeq$ 8.0).

4 Metergoline and rauwolscine (10^{-7}-10^{-6} M) antagonized the effects of 5-CT in a non-competitive fashion giving pK_{Bapp} values of 7.13 (metergoline) and 6.86 (rauwolscine).

5 Vasoconstrictor responses to 5-HT were not modified in the presence of ritanserin (3×10^{-7} M) or spiperone (3×10^{-7} M) and only modestly antagonized by ketanserin (10^{-6} M) suggesting that 5-HT$_{2A}$ receptors do not make a significant contribution in this model.

6 Hence, precontraction of rabbit mesenteric arteries reveals potent vasoconstrictor effects of 5-HT and related agonists. Based on the agonist potency order and the antagonist studies performed, the receptor subtype responsible has the characteristics of a 5-HT$_1$-like (probably 5-HT$_{1D}$) receptor. This study therefore demonstrates a particularly striking example of vasoconstrictor synergy involving 5-HT$_1$-like receptors.

Keywords: 5-HT$_1$-like receptors; 5-HT$_{1D}$ receptors; vasoconstriction; rabbit isolated mesenteric arteries; 5-hydroxytryptamine (5-HT); 5-carboxamidotryptamine (5-CT); sumatriptan; vasoconstrictor synergy

Introduction

5-Hydroxytryptamine (5-HT) demonstrates potent vasoconstrictor effects *in vitro* or *in vivo*. Although in most vascular beds this effect is mediated by activation of the 5-HT$_{2A}$ subtype, an additional or exclusive role for 5-HT$_1$-like receptors has also been determined in certain vessels. These 5-HT$_1$-like receptors have been identified on the basis of their sensitivity to antagonism by methiothepin, relative insensitivity to ketanserin and potent agonist effects of 5-carboxamidotryptamine (5-CT) and, to a lesser extent, sumatriptan, according to criteria originally established by Bradley *et al.* (1986). 5-HT$_1$-like receptor-mediated vasoconstriction is most closely associated with specific types of blood vessel, notably cerebral arteries from a variety of species, including man (Parsons *et al.*, 1989; Connor *et al.*, 1989; Hamel & Bouchard, 1991), canine or human coronary arteries (Parsons *et al.*, 1992) and canine saphenous vein (Humphrey *et al.*, 1988).

However, recent *in vitro* observations suggest a wider presence of vasoconstrictor 5-HT$_1$-like receptors than would be indicated by the above analysis. Furthermore, in certain vascular tissues, the 5-HT$_1$-like receptor is virtually 'silent' and becomes functional only if the tissue is maintained at or above a threshold level of vasoconstriction. To date, such observations have been made in guinea-pig iliac artery (Sahin-Erdemli *et al.*, 1991), rabbit femoral artery (MacLennan & Martin, 1992), human coronary artery (Cocks *et al.*, 1993) and rabbit renal artery (Choppin & O'Connor, 1993). In the rabbit renal artery, we have demonstrated that agonists such as 5-HT, 5-CT and sumatriptan are virtually without activity under normal conditions of resting tone but show prominent methiothepin-sensitive spasmogenic effects in the presence of threshold vasoconstriction produced by histamine, U46619 (Choppin & O'Connor, 1993) or potassium chloride (Choppin & O'Connor, 1994).

In the present study, we have investigated the responsiveness of rabbit isolated mesenteric arteries to the vasoconstrictor effects of 5-HT and other 5-HT receptor agonists. We report that in this preparation, as in the examples cited above, 5-HT$_1$-like receptors (probably of the 5-HT$_{1D}$-subtype), mediate a vasoconstrictor effect which manifests itself only in pre-contracted vessels.

Methods

Male New Zealand white rabbits (2.0-2.2 kg) were killed by rapid exsanguination after being rendered unconscious by a blow to the neck. The main mesenteric arteries were cleared of adherent tissue or fat and place in Krebs solution (composition in mM: NaCl 118, KCl 4.7, $MgCl_2$ 1.2, KH_2PO_4 1.2, $CaCl_2$ 2.6, $NaHCO_3$ 25.0 and glucose 11.7) containing

[1] Author for correspondence.

prazosin 10^{-6} M and idazoxan 10^{-6} M to eliminate the possibility that 5-HT receptor agonists could directly or indirectly activate contractile α_1- and α_2-adrenoceptors (Black *et al.*, 1981; McGrath, 1977). The vascular endothelium was removed by passing a scored catheter through the arterial lumen. Ring segments (1.5–2 mm long) were suspended between two stainless steel wire hooks in 20 ml organ baths containing Krebs solution bubbled with 95% O_2:5% CO_2 at 37°C. Changes in isometric tension were recorded on a Grass polygraph model 7D.

Preparations were maintained at an initial resting tension of 1 g, repeatedly re-adjusted over a 2 h equilibration period during which the tissues were washed regularly. Following this, the tissues were first contracted by a maximal effective concentration of KCl (80 mM) with which all subsequent responses were compared. In a representative series of experiments the tension generated in response to 80 mM KCl was 3.23 ± 0.19 g ($n = 41$). A series of different 5-HT receptor agonists were tested for spasmogenic activity. A single cumulative agonist concentration-response curve was performed in each tissue, either in normal Krebs solution, or in the presence of a threshold vasoconstriction produced by the thromboxane-mimetic, U46619 (10^{-8} M). U46619 10^{-8} M caused a modest and sustained contraction (approximately 20–30% of the KCl maximum). With the exception of the preliminary studies which involved the comparison of resting tone conditions and pre-contracted tissues, all experiments were performed in tissues pre-contracted with U46619, 10^{-8} M. To evaluate the mechanism responsible for agonist-induced contraction, in certain experiments, receptor antagonists were added to the buffer solution 30 min before commencing the agonist concentration-response curve. Since a single agonist curve design was retained for the antagonist experiments, antagonist effects were analysed by comparing the antagonist-treated groups of tissues with the control group.

Contractions produced by agonists were measured as changes in tension from baseline (i.e. the tension immediately before agonist administration) and expressed as a percentage of KCl maximum as means ± s.e. Agonist potency and maximum response (E_{max}) were calculated by computer-assisted regression analysis of the full (sigmoid) curves ('ALLFIT'). Agonist potency was expressed as EC_{50} values, i.e. the molar concentration necessary to produce 50% of the maximum agonist response. EC_{50} values obtained in the presence of a receptor antagonist were compared with control EC_{50} values and the significance of the difference between the two means was determined by a Fisher's test. Differences with $P < 0.05$ were considered significant. n values refer to the number of tissue rings tested, with the number of animals used shown in parenthesis afterwards. The antagonist potency of methiothepin was evaluated by linear regression analysis according to the Schild equation using mean agonist EC_{50} values obtained in the presence and absence of antagonist to give a pA_2 value. Where full agonist concentration-response curves could only be achieved in the presence of a single antagonist concentration, a pK_B value was estimated with the following formula:

$$pK_B = -\log[\text{antagonist}] + \log\left(\frac{\text{mean } EC_{50} \text{ in the presence of antagonist}}{\text{mean } EC_{50} \text{ control}} - 1\right)$$

Where the effects of certain antagonists were insurmountable in nature, the apparent pK_B (pK_{Bapp}) was derived from a double-reciprocal regression as described by Kenakin (1993).

Drugs

Sources of compounds used were as follows: 5-HT creatinine sulphate, prazosin hydrochloride, (−)-propranolol hydrochloride, spiperone, U46619 (9,11,dideoxy-11α, 9α-epoxymethano-prostaglandin $F_{2\alpha}$) (Sigma); methiothepin maleate (Roche); rauwolscine hydrochloride (Research Biochemicals Inc.); 5-CT sulphate and maleate, 8-hydroxy-2-(di-n-propylamino)tetralin (8-OH-DPAT), 5-methoxy-3-(1,2,3,6-tetrahydro-4-pyridinyl)-1*H* indole succinate (RU 24969), sumatriptan succinate, cisapride, idazoxan, (3α-tropanyl)1H-indole-3-carboxylate hydrochloride (ICS 205-930), ondansetron hydrochloride, ketanserin tartrate, pindolol, cyanopindolol, metergoline, ritanserin and 2-methoxy-4-amino-5-chloro-benzoic acid 2-(diethylamino) ethyl ester (SDZ 205557) were all synthesized by the Department of Chemistry, Synthélabo Recherche.

Results

In mesenteric arteries bathed in normal Krebs solution under conditions of resting tone, the agonists used in this study exhibited little or no spasmogenic activity. Specifically, sumatriptan, RU 24969, 8-OH DPAT and cisapride were inactive at concentrations up to 10^{-4} M. 5-HT and 5-CT produced weak increases in tension at concentrations $> 10^{-7}$ M attaining 67 ± 13% and 31 ± 12% of the KCl maximum respectively at 10^{-4} M.

However, in tissues pre-contracted with U46619 (10^{-8} M), all the above agonists produced vasoconstrictor responses which were markedly more prominent than those observed in standard preparations. Figure 1 illustrates this comparison by showing concentration-response curves for 5-HT and sumatriptan in the presence and absence of U46619. In pre-

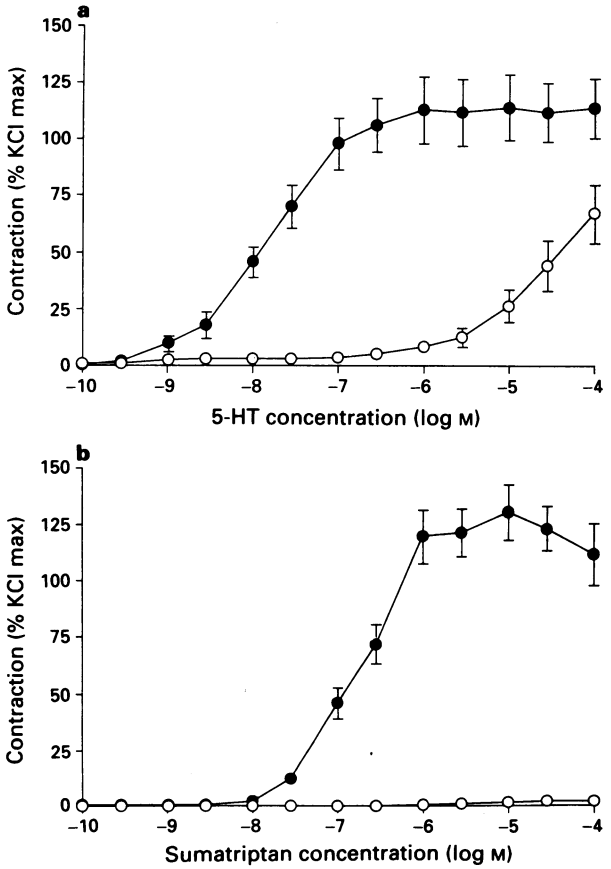


Figure 1 Comparison of the contractile efects of (a) 5-HT, (b) sumatriptan in rabbit mesenteric arteries either in normal Krebs buffer (○), or in Krebs buffer containing U46619 10^{-8} M (●) to cause a modest precontraction. All experiments were performed in the presence of prazosin 10^{-6} M and idazoxan 10^{-6} M. Contractile effects were expressed as percentages of the response to 80 mM KCl. Values shown are means ± s.e. $n = 6–7$ (3) (●) and $n = 5–7$ (2–3) (○). A single concentration-response curve was obtained in each tissue.

contracted tissues, the 5-HT concentration-response curve was displaced leftwards approximately 3000-fold giving a E_{max} of 114 ± 5% and a EC_{50} of 1.6 ± 0.4 × 10^{-8} M, $n = 6$ (3). The level of potentiation of 5-CT, sumatriptan and RU 24969 in the presence of U46619 was equally dramatic. The vasoconstrictor effects of each of the agonists in pre-contracted tissues is shown in Figure 2, $n = 6-9$ (3–5). 5-CT was the most potent compound tested with an EC_{50} of 4.3 ± 0.8 × 10^{-9} M and an E_{max} of 125 ± 6%, $n = 8$ (5). RU 24969 exhibited a complex concentration-response curve which reached a plateau between 10^{-6} and 3 × 10^{-5} M but then showed a further response at 10^{-4} M, probably representing a second component. For this compound, calculation of the EC_{50} was based on concentrations up to 3 × 10^{-5} M. The relative order of agonist potencies (mean EC_{50} values ± S.E.) was: 5-CT (4.3 ± 0.8 × 10^{-9} M) > 5-HT (1.6 ± 0.4 × 10^{-8} M) > RU 24969 (1.6 ± 0.5 × 10^{-7} M) = sumatriptan (1.9 ± 0.3 × 10^{-7} M) > 8-OH DPAT (8.0 ± 1.8 × 10^{-7} M) > cisapride (> 10^{-5} M).

The sensitivity of the three key agonists, 5-CT, 5-HT and sumatriptan to antagonism by methiothepin was evaluated using antagonist concentrations in the range 1 × 10^{-8}–3 × 10^{-7} M. Figure 3 shows the effects of methiothepin against 5-CT. Agonist-response curves were displaced rightwards in a concentration-related fashion. Schild analysis of these data gave a pA_2 value of 8.20 (95% confidence limits 7.92–8.48) with a slope of 0.98 which was not significantly different from 1, suggesting that the antagonism was competitive in nature. 5-HT and sumatriptan were similarly antagonized by methiothepin. In the case of 5-HT, the pA_2 value was 8.04 (95% confidence limits 7.66–8.42) (slope 1.17, not different from 1). The vasoconstrictor effects of sumatriptan were also antagonised concentration-dependently by methiothepin. Since sumatriptan is less potent than 5-CT and 5-HT, maximum agonist responses could not be clearly established after the higher concentrations of methiothepin. Therefore, antagonist affinity has been expressed as a pK_B estimate (8.20) calculated for the lowest dose of methiothepin (3 × 10^{-8} M) where a maximum response was achieved.

Metergoline and rauwolscine, over the concentration range 10^{-7}–10^{-6} M, also antagonized the vasoconstrictor responses to 5-CT and 5-HT (Figures 4 and 5). These antagonists generally demonstrated non-competitive characteristics, i.e. depression of agonist maximum response accompanied by rightwards displacement of the agonist concentration-response curve which sometimes showed a reduced slope. The pK_{Bapp} values calculated for metergoline 10^{-6} M were 7.13 against 5-CT and 7.86 against 5-HT. E_{max} values following 10^{-6} M metergoline were 80 ± 4% ($P < 0.01$) for 5-CT and 68 ± 4% ($P < 0.01$) for 5-HT. Rauwolscine antagonised 5-CT non-competitively ($pK_{Bapp} = 6.86$) with a E_{max} of 67 ± 2% ($P < 0.01$) in the presence of rauwolscine 10^{-6} M. However, rauwolscine (10^{-6} M) did not significantly reduce the maximum response to 5-HT. Therefore a pK_B value (6.87) was calculated for the highest antagonist concentration.

The effects of a range of other 5-HT receptor antagonists were tested against 5-CT-induced vasoconstriction and these results are summarised in Table 1. For antagonists that have potent 5-HT$_{2A}$ blocking properties (spiperone, ketanserin, ritanserin), these experiments were also performed with 5-HT as agonist (Table 1). With the exception of ketanserin 10^{-6} M (pK_B 6.43) and ritanserin 3 × 10^{-7} M which demonstrated a weak effect (pK_{Bapp} 6.08), none of these antagonists modified

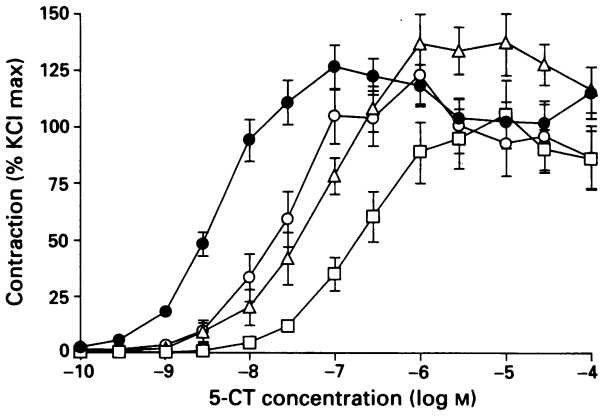


Figure 3 Antagonism by methiothepin of the vasoconstrictor effects of 5-carboxamidotryptamine (5-CT) in rabbit mesenteric arteries pre-contracted with U46619 (10^{-8} M). Cumulative concentration-response curves to the agonist were established under control conditions (●), or in the presence of 3 × 10^{-8} M (○), 10^{-7} M (△) or 3 × 10^{-7} M (□) methiothepin. The buffer also contained prazosin 10^{-6} M and idazoxan 10^{-6} M throughout. Contractile effects were expressed as a percentage of the response to 80 mM KCl. Values shown are means ± s.e. $n = 8$ (4–5). A single concentration-response curve was obtained in each tissue.

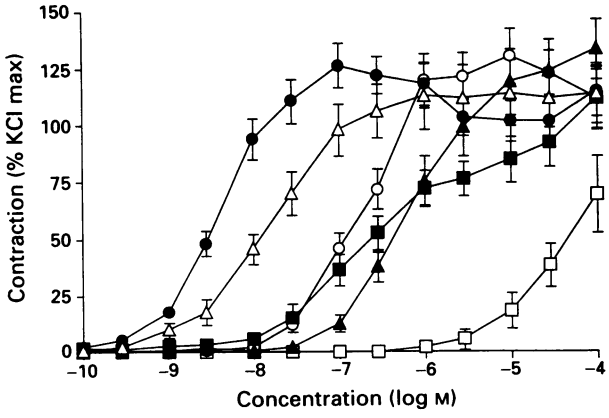


Figure 2 Comparison of the contractile effects of cumulative administration of various 5-hydroxytryptamine (5-HT) receptor agonists in rabbit mesenteric arteries pre-contracted with U46619 (10^{-8} M). Compounds shown at 5-CT (●), 5-HT (△), sumatriptan (○), RU 24969 (■), 8-OH-DPAT (▲) and cisapride (□). All experiments were performed in the presence of prazosin 10^{-6} M and idazoxan 10^{-6} M. Contractile effects were expressed as percentages of the response to 80 mM KCl. Values shown are means ± s.e. $n = 6-9$ (3–5). A single concentration-response curve was obtained in each tissue.

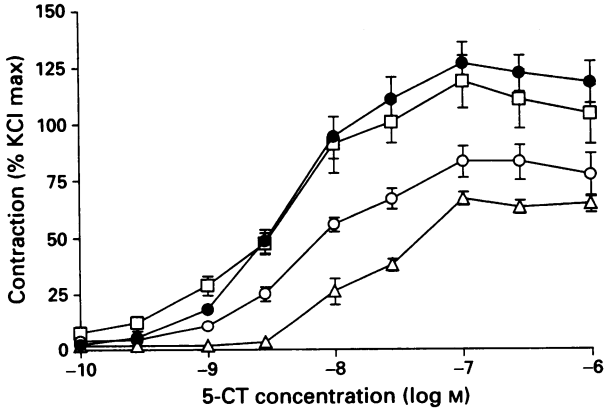


Figure 4 Antagonism by rauwolscine of the vasoconstrictor effects of 5-carboxamidotryptamine (5-CT) in rabbit mesenteric arteries pre-contracted with U46619 (10^{-8} M). Cumulative concentration-response curves to 5-CT were established under control conditions (●), or in the presence of 10^{-7} M (□), 3 × 10^{-7} M (○) or 10^{-6} M (△) rauwolscine. The buffer also contained prazosin 10^{-6} M and idazoxan 10^{-6} M throughout. Contractile effects were expressed as a percentage of the response to 80 mM KCl. Values shown are means ± s.e. $n = 6-7$ (4–5). A single concentration-response curve was obtained in each tissue.

the effects of 5-CT. 5-HT responses were also weakly antagonized by ketanserin ((pK_B = 6.45) but unaffected by spiperone 3×10^{-7} M or ritanserin 3×10^{-7} M. The 5-HT$_3$ antagonist ondansetron, the 5-HT$_4$ antagonist SDZ 205557 and the mixed 5-HT$_3$/5-HT$_4$ antagonist ICS 205930 had no effect on responses to 5-CT (Table 1).

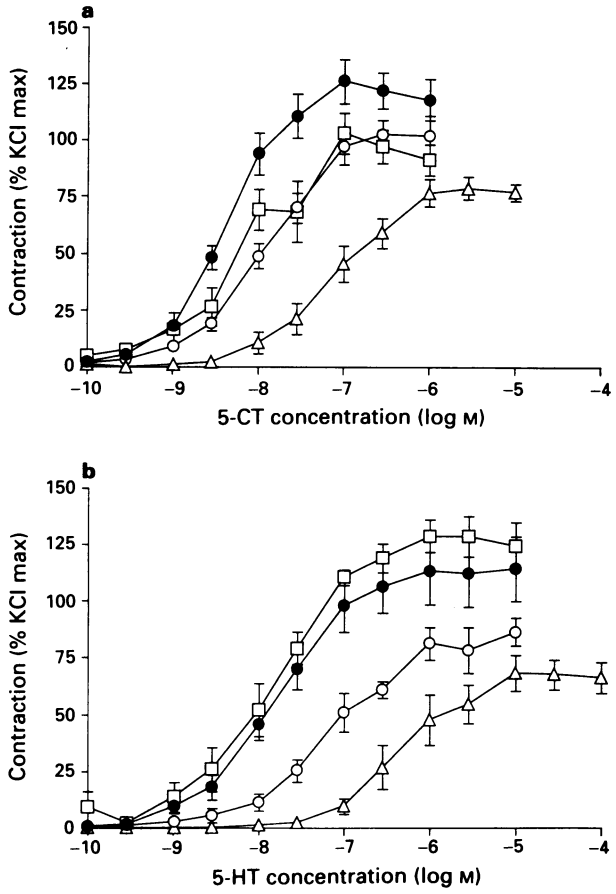


Figure 5 Antagonism by metergoline of the vasoconstrictor effects of (a) 5-carboxamidotryptamine (5-CT) and (b) 5-hydroxytryptamine (5-HT) in rabbit mesenteric arteries pre-contracted with U46619 (10^{-8} M). Cumulative concentration-response curves to each agonist were established under control conditions (●), or in the presence of 10^{-7} M (□), 3×10^{-7} M (○) or 10^{-6} M (△) metergoline. The buffer also contained prazosin 10^{-6} M and idazoxan 10^{-6} M throughout. Contractile effects were expressed as a percentage of the response to 80 mM KCl. Values shown are means ± s.e. $n = 5-8$ (2–5). A single concentration-response curve was obtained in each tissue.

Discussion

In this study, we report a striking amplification of the vasoconstrictor effects of a series of 5-HT receptor agonists in modestly pre-contracted (20–30% of KCl maximum) rabbit mesenteric arteries when compared with the same preparation under conditions of resting tone. For those agonists for which concentration-related responses could be detected using resting tone conditions (5-HT and 5-CT) their response curves were displaced righwards by 3–4 orders of magnitude. Similarly, sumatriptan and RU 24969 which were inactive up to 10^{-4} M in normal buffer showed vasoconstrictor activity at concentrations as low as 10^{-8} M in the presence of U46619. In precontracted tissues, 5-HT receptor agonists were capable of producing contractions of a magnitude at least equivalent to the response to 80 mM KCl. Therefore, this study provides an excellent example of synergy between vasoconstrictors acting by different mechanisms. The subsequent discussion will characterize the receptor involved in the contractile effects of 5-CT and the other agonists as the 5-HT$_1$-like subtype. Our study therefore extends the range of blood vessels in which vasoconstrictor 5-HT$_1$-like receptors have been identified to include the rabbit mesenteric artery, and emphasizes the importance of the choice of experimental conditions. The application of this practice to other vascular tissues could reveal additional examples of this receptor type. Conversely, evaluation of 5-HT-receptor agonists under conditions of resting tone only, may lead to erroneous conclusions regarding the possible existence of 5-HT$_1$-like receptors.

We have already observed an apparently similar phenomenon in rabbit renal arteries (Choppin & O'Connor, 1993; 1994). The level of agonist activity noted in the present study indicates that the mesenteric artery is more sensitive than the renal artery in this respect. 5-CT (EC_{50} 4×10^{-9} M in rabbit mesenteric artery, E_{max} 125%) was approximately 10 times less potent with a lower E_{max} in rabbit renal arteries precontracted with either 22 mM KCl, histamine or U46619. Indeed, the vasoconstrictor potency of 5-CT in precontracted mesenteric arteries equals or exceeds that reported in tissues which contain functionally active 5-HT$_1$-like receptors under resting tone conditions, e.g. human pial arterioles (Hamel & Bouchard, 1991), rabbit basilar arteries (Parsons & Whalley, 1989).

We have studied a range of receptor agonists and antagonists in U46619-precontracted preparations with the objective of identifying the 5-HT receptor subtype responsible for agonist-induced vasoconstriction. The potent agonist activity of 5-CT (> 5-HT) clearly implicates a 5-HT$_1$-receptor. A role of 5-HT$_3$ and 5-HT$_4$ receptors was not anticipated given their non-vascular locations and can be rapidly eliminated based on the relatively low affinity of

Table 1 The potencies of 5-carboxamidotryptamine (5-CT) and 5-hydroxytryptamine (5-HT) in rabbit mesenteric arteries in the absence and presence of various receptor antagonists

Antagonist		*EC_{50} 5-CT*	*EC_{50} 5-HT*
Control		$2.9 \pm 0.7 \times 10^{-9}$ M	$1.6 \pm 0.4 \times 10^{-8}$ M
SDZ 205557	3×10^{-6} M	$1.7 \pm 0.7 \times 10^{-9}$ M	–
Pindolol	3×10^{-6} M	$3.2 \pm 0.1 \times 10^{-9}$ M	–
Propranolol	10^{-7} M	$4.3 \pm 1.4 \times 10^{-9}$ M	–
Ondansetron	10^{-6} M	$2.6 \pm 0.6 \times 10^{-9}$ M	–
ICS 205930	3×10^{-6} M	$2.6 \pm 0.6 \times 10^{-9}$ M	–
Ritanserin	3×10^{-7} M	$1.1 \pm 0.5 \times 10^{-8}$ M*	$1.3 \pm 0.3 \times 10^{-8}$ M
Ketanserin	10^{-6} M	$9.3 \pm 0.7 \times 10^{-9}$ M**	$6.4 \pm 2.1 \times 10^{-8}$ M**
Spiperone	3×10^{-7} M	$5.2 \pm 2.8 \times 10^{-9}$ M	$1.3 \pm 0.3 \times 10^{-8}$ M
Methiothepin	3×10^{-7} M	$1.8 \pm 0.5 \times 10^{-7}$ M**	$2.1 \pm 0.8 \times 10^{-6}$ M**

All studies were performed in tissue pre-contracted by U46619 and in the presence of prasozin 10^{-6} M and idazoxan 10^{-6} M. Studies of ritanserin and ketanserin against 5-CT were performed in a separate series of experiments in which the control EC_{50} value for 5-CT was $4.3 \pm 0.8 \times 10^{-9}$ M. Data for each antagonist represents a separate group of tissues. *$P < 0.05$, **$P < 0.01$ versus control EC_{50} (Fisher's test). $n = 4-8$ (3–5).

5-CT for these subtypes (Eglen *et al.*, 1992), the inability of 5-HT$_3$ antagonists (ondansetron, ICS 205-930) and 5-HT$_4$-antagonists (SDZ 205557, ICS 205-930) to block 5-CT-induced vasoconstriction, and the weak spasmogenic effects of the 5-HT$_4$ agonist, cisapride. At least five 5-HT$_1$-subtypes have now been recognised on the basis of ligand binding studies and receptor cloning (Humphrey *et al.*, 1993), of which the recently-identified 5-HT$_{1E}$ subtype is unlikely to be involved because it shows low affinity for 5-CT (McAllister *et al.*, 1992). Considering the remaining 5-HT$_1$-subtypes characterized by radioligand binding techniques, the relative order of agonist potencies observed in the present study (5-CT > 5-HT > RU 24969 = sumatriptan > 8-OH-DPAT) most closely resembles the 5-HT$_{1D}$ recognition site (Hoyer, 1989; Hoyer & Schoeffter, 1991). Comparisons of relative agonist potencies obtained from a functional study (such as the present one) with relative binding site affinities ignore the possible dependence of the former on factors such as agonist efficacy and tissue receptor reserve. Nevertheless, the antagonist characterization performed also supports the involvement of a receptor similar to the 5-HT$_{1D}$ subtype. The ineffectiveness of the 5-HT$_{1A}$/5-HT$_{1B}$ antagonist pindolol and weak effects of the 5-HT$_{2A}$/5-HT$_{2C}$ antagonist, ritanserin, confirm the exclusion of 5-HT$_{1A}$, 5-HT$_{1B}$ and 5-HT$_{2C}$ subtypes. Furthermore, methiothepin, a potent but non-selective 5-HT$_1$-antagonist, blocked the vasoconstrictor effects of 5-CT, 5-HT and sumatriptan with similar affinity giving pA_2/pK_B values within the range 8.0–8.5. The antagonist effects of rauwolscine are also consistent with this hypothesis since this potent α_2-antagonist also shows significant affinity for 5-HT$_{1D}$ binding sites (Hoyer & Schoeffter, 1991).

The lack of antagonist properties of the potent 5-HT$_{2A}$ antagonists, spiperone and ritanserin and the weak inhibitory effects of ketanserin when tested against 5-HT induced contractions excludes a significant role for 5-HT$_{2A}$ receptors since these antagonists were tested at concentrations 200–1000 times greater than their published affinity for 5-HT$_{2A}$ receptors (Hoyer & Schoeffter, 1991). Hence, the vasoconstrictor properties of 5-HT receptor agonists in pre-contracted rabbit mesenteric arteries appear to be largely if not solely due to stimulation of a 5-HT$_1$-receptor with similarities to the 5-HT$_{1D}$ binding site. The ability to eliminate a contribution from 5-HT$_{2A}$ receptors is also important for the interpretation of the methiothepin data since, in addition to being a potent 5-HT$_1$-antagonist, methiothepin also blocks 5-HT$_{2A}$ receptors at low concentrations (Hoyer & Schoeffter, 1991). The lack of a significant 5-HT$_{2A}$ component distinguishes this tissue by comparison with rabbit femoral artery (MacLennan & Martin, 1992) and rabbit renal artery (Choppin & O'Connor, 1994), both of which demonstrate vasoconstriction mediated through dual 5-HT$_1$-like/5-HT$_{2A}$ receptor populations.

The 5-HT$_1$-receptor implicated in the present study fulfills the criteria established by Bradley *et al.* (1986) for a functional 5-HT$_1$-like receptor. Unfortunately, no direct radioligand binding site equivalent to these functional responses in vascular tissues has been identified and a recent revision of 5-HT receptor nomenclature concluded that such sites are still best described as 'vascular 5-HT$_1$ receptors' (Humphrey *et al.*, 1993). Analysis of agonist and antagonist characteristics indicates that the receptor present in the pre-contracted rabbit mesenteric artery is very similar to other 5-HT receptors mediating vasoconstriction. Notably, those in guinea-pig iliac artery (Schoeffter & Sahin-Erdemli, 1992), rabbit renal artery (Choppin & O'Connor, 1994) and human pial artery (Hamel & Bouchard, 1991) which have been variously classified as 5-HT$_1$-like, 5-HT$_{1D}$-like or 5-HT$_{1D}$ in nature. We have already underlined the similarity of the receptor found in the rabbit mesenteric artery to the 5-HT$_{1D}$ binding site, however, the relatively modest antagonist potency of metergoline in our study appears somewhat inconsistent with a 5-HT$_{1D}$ classification. The possibility that metergoline sensitivity could provide a means of differentiating between the functional 5-HT$_1$-like vascular receptor and the 5-HT$_{1D}$ recognition site has already been proposed (Parsons, 1991). Metergoline shows very high 5-HT$_{1D}$ binding affinity (pIC_{50} 9.1, Hoyer & Schoeffter, 1991), but is notably less active as an antagonist of 5-HT$_1$-like receptor-mediated vasoconstriction (Humphrey *et al.*, 1988; Hamel & Bouchard, 1991). Our own data tend to confirm this distinction; however, whether or not this difference alone is sufficient to disallow the 5-HT$_{1D}$ classification is debatable.

Ketanserin was a weak antagonist of both 5-CT and 5-HT induced responses in our study (p$K_B \simeq 6.4$). At these relatively high concentrations such antagonist activity is clearly unrelated to 5-HT$_{2A}$ receptors. These results are consistent with reports from other rabbit vascular preparations that ketanserin shows a low affinity for 5-HT$_1$-like receptors (Martin & MacLennan, 1990; Tadipatri *et al.*, 1991). In this context it is interesting to note that ketanserin is one of the few compounds capable of distinguishing between the cloned human 5-HT$_{1D\alpha}$- and 5-HT$_{1D\beta}$-subtypes, showing moderate affinity for the former (pK_D 7.0–7.5) while being inactive at the latter (pK_D < 5) (Kaumann *et al.*, 1993). Although this could suggest that rabbit vascular 5-HT$_1$-like receptors are similar to the cloned 5-HT$_{1D\alpha}$-subtype, the available data is insufficient allow a definitive conclusion. An additional factor which may complicate interpretation of low affinity antagonist properties of ketanserin in functional studies such as our own, is its weak calcium antagonist effects (Razzaque *et al.*, 1994).

In summary, this study demonstrates the existence in the rabbit mesenteric artery of 5-HT$_1$-like receptors mediating vasoconstriction. These receptors are functionally silent unless tissues are subjected to a modest pre-contraction, applied, in the case of this study, by the thromboxane-mimetic, U46619.

References

BLACK, J.L., FRENCH, R.J. & MYLECHARANE, E.J. (1981). Receptor mechanisms for 5-HT in rabbit arteries. *Br. J. Pharmacol.*, **74**, 619–626.

BRADLEY, P.B., ENGEL, G., FENIUK, W., FOZARD, J.R., HUMPHREY, P.P.A., MIDDLEMISS, D.N., MYLECHARANE, E.J., RICHARDSON, B.P. & SAXENA, P.R. (1986). Proposals for the classification and nomenclature of functional receptors for 5-HT. *Neuropharmacol.*, **25**, 563–576.

CHOPPIN, A. & O'CONNOR, S.E. (1993). Pre-contraction with histamine and U46619 unmasks a 5-HT$_1$-like receptor in rabbit renal artery. *Eur. J. Pharmacol.*, **231**, 469–472.

CHOPPIN, A. & O'CONNOR, S.E. (1994). 5-HT$_{1D}$-like receptors mediate contraction of partially-depolarised rabbit renal arteries. *J. Pharmacol. Exp. Ther.*, **270**, 650–655.

COCKS, T.M., KEMP, B.K., PRUNEAU, D. & ANGUS, J.A. (1993). Comparison of contractile responses to 5-hydroxytryptamine and sumatriptan in human isolated coronary artery: synergy with the thromboxane A$_2$-receptor agonist, U46619. *Br. J. Pharmacol.*, **110**, 360–368.

CONNOR, H.E., FENIUK, W. & HUMPHREY, P.P.A. (1989). Characterisation of 5-HT receptors mediating contraction of canine and primate basilar artery by using GR 43175, a selective 5-HT$_1$-like receptor agonist. *Br. J. Pharmacol.*, **96**, 379–387.

EGLEN, R.M., PERKINS, L.A., WALSH, L.K.M. & WHITING, R.L. (1992). Agonist action of indole derivatives at 5HT$_1$-like, 5-HT$_2$, 5HT$_3$ and 5-HT$_4$ receptors in vitro. *J. Auton. Pharmacol.*, **12**, 321–333.

HAMEL, E. & BOUCHARD, D. (1991). Contractile 5-HT$_1$ receptors in human isolated pial arterioles: correlation with 5-HT$_{1D}$ binding sites. *Br. J. Pharmacol.*, **102**, 227–233.

HOYER, D. (1989). 5-HT receptors and effector coupling mechanisms in peripheral tissues. In *Peripheral Actions of 5-Hydroxytryptamine*. ed. Fozard, J.R. pp. 72–88. Oxford University Press: New York.

HOYER, D. & SCHOEFFTER, P. (1991). 5-HT receptors: subtypes and second messengers. *J. Recept. Res.*, **11**, 197–214.

HUMPHREY, P.P.A., FENIUK, W., PERREN, M.J., CONNOR, H.E., OXFORD, A.W., COATES, I.H. & BUTINA, D. (1988). GR 43175, a selective agonist for the 5-HT$_1$-like receptor in dog isolated saphenous vein. *Br. J. Pharmacol.*, **94**, 1123–1132.

HUMPHREY, P.P.A., HARTIG, P. & HOYER, D. (1993). A proposed new nomenclature for 5-HT receptors. *Trends Pharmacol. Sci.*, **14**, 233–236.

KAUMANN, A.J., PARSONS, A.A. & BROWN, A.M. (1993). Human arterial constrictor serotonin receptors. *Cardiovasc. Res.*, **27**, 2094–2103.

KENAKIN, T.P. (1993). *Pharmacological Analysis of Drug-Receptor Interaction*, 2nd Edition, p. 334. Raven Press, New York.

MARTIN, G.R. & MACLENNAN, S.J. (1990). Analysis of the 5-HT receptor in rabbit saphenous vein exemplifies the problems of using exclusion criteria for receptor classification. *Naunyn-Schmied. Arch. Pharmacol.*, **342**, 111–119.

MACLENNAN, S.J. & MARTIN, G.R. (1992). Effect of the thromboxane A$_2$-mimetic U46619 on 5-HT$_1$-like and 5-HT$_2$ receptor-mediated contraction of the rabbit isolated femoral artery. *Br. J. Pharmacol.*, **107**, 418–421.

MCALLISTER, G., CHARLESWORTH, A., SNODIN, C., BEER, M.S., NOBLE, A.J., MIDDLEMISS, D.N., IVERSEN, L.L. & WHITING, P. (1992). Molecular cloning of a serotonin subtype from human brain (5HTIE): a fifth 5HT1-like subtype. *Proc. Natl. Acad. Sci. U.S.A.*, **89**, 5517–5521.

MCGRATH, M.A. (1977). 5-HT and neurotransmitter release in canine blood vessels. *Circ. Res.*, **41**, 428–435.

PARSONS, A.A. (1991). 5-HT receptors in human and animal cerebrovasculature. *Trends Pharmacol. Sci.*, **12**, 310–315.

PARSONS, A.A., STUTCHBURY, C., RAVAL, P. & KAUMANN, A.J. (1992). Sumatriptan contracts large coronary arteries of beagle dogs through 5-HT$_1$-like receptors. *Naunyn Schmied. Arch, Pharmacol.*, **346**, 592–596.

PARSONS, A.A. & WHALLEY, E.T. (1989). Evidence for the presence of 5-HT$_1$-like receptors in rabbit isolated basilar arteries. *Eur. J. Pharmacol.*, **174**, 189–196.

PARSONS, A.A., WHALLEY, E.T., FENIUK, W., CONNOR, H.E. & HUMPHREY, P.P.A. (1989). 5-HT$_1$-like receptors mediate 5-HT-induced contraction of human isolated basilar artery. *Br. J. Pharmacol.*, **96**, 434–449.

RAZZAQUE, Z., LONGMORE, J. & HILL, R.G. (1994). Differences in the effects of ketanserin on 5-HT-receptor mediated responses in rabbit saphenous vein and guinea pig jugular vein. *Br. J. Pharmacol.*, **112**, 474P.

SAHIN-ERDEMLI, I., HOYER, D., STOLL, A., SEILER, M.P. & SCHOEFFTER, P. (1991). 5-HT$_1$-like receptors mediate 5-HT-induced contraction of guinea-pig isolated iliac artery. *Br. J. Pharmacol.*, **102**, 386–390.

SCHOEFFTER, P. & SAHIN-ERDEMLI, I. (1992). Further characterisation of the 5-HT$_1$-like receptor mediating contraction of guinea pig iliac artery. *Eur. J. Pharmacol.*, **219**, 295–301.

TADIPATRI, S., VAN HEUVEN-NOLSEN, D., FENIUK, W. & SAXENA, P.R. (1991). Analysis of the 5-HT receptors mediating contractions in the rabbit isolated renal artery. *Br. J. Pharmacol.*, **104**, 887–894.

(Received May 23, 1994
Revised September 16, 1994
Accepted September 19, 1994)

British Journal of Pharmacology (1995) 114, 315–322 © 1995 Stockton Press All rights reserved 0007–1188/95 $9.00

Inhibition by dizocilpine (MK-801) of striatal dopamine release induced by MPTP and MPP^+: possible action at the dopamine transporter

[1]P.B.S. Clarke & M. Reuben

Department of Pharmacology and Therapeutics, McGill University, 3655 Drummond St, Montreal, Canada H3G 1Y6

1 The NMDA-type glutamate receptor antagonist, dizocilpine (MK-801) can protect against neurotoxicity associated with 1-methyl-4-phenyl-1,2,3,6-tetrahydropyridine (MPTP) and its principal metabolite, the 1-methyl-4-phenylpyridinium ion (MPP^+). It has been suggested that these neurotoxic effects may be mediated by release of excitatory amino acids, but possible alternative mechanisms have been little investigated.

2 MPTP and MPP^+ (0.1–1000 μM) were tested in superfused rat striatal synaptosomes preloaded with [^{3}H]-dopamine. Both MPTP (10 μM and higher) and MPP^+ (1 μM and higher) evoked an immediate and concentration-dependent release of [^{3}H]-dopamine. The maximal effect exceeded that achievable with nicotine. For subsequent experiments, submaximal concentrations of MPTP (50 μM) and MPP^+ (10 μM) were tested.

3 MK-801 (0.1–100 μM) inhibited responses to MPTP (50 μM) and MPP^+ (10 μM) in a concentration-dependent manner. However, further tests of NMDA-type glutamate receptor involvement proved negative. Responses to MPTP or MPP^+ were unaffected by the omission of Mg^{2+} or Ca^{2+} and were not reduced by the NMDA receptor antagonists, AP-7 (200 μM) and kynurenic acid (300 μM). In this assay, N-methyl-D-aspartate (even in the absence of Mg^{2+} and with added glycine and strychnine) did not evoke [^{3}H]-dopamine release.

4 In crude membrane preparations of rat cerebral cortex, MPTP and MPP^+ inhibited high-affinity [^{3}H]-nicotine binding to nicotinic cholinoceptors (IC_{50} 1.8 μM and 26 μM, respectively).

5 [^{3}H]-dopamine release evoked by nicotine (1 μM) was blocked by the nicotinic antagonists, mecamylamine and chlorisondamine, and by MK-801 (all at 100 μM); K^+-evoked release was not affected. Release evoked by MPTP and MPP^+ was significantly attenuated by MK-801 but not by mecamylamine or chlorisondamine.

6 At a high concentration (10 μM), the selective dopamine uptake inhibitor, nomifensine, completely blocked [^{3}H]-dopamine release evoked by amphetamine 0.3 μM and MPP^+ 10 μM, attenuated responses to MPTP 50 μM and did not affect responses to 12 mM K^+. MK-801 100 μM evinced a similar profile but was less effective.

7 MK-801 inhibited [^{3}H]-dopamine uptake in striatal synaptosomes with an IC_{50} of 115 μM.

8 It is concluded that high concentrations of MK-801 inhibit the acute dopamine release evoked by MPTP and MPP^+ in synaptosomes. This antagonism may occur, at least in part, through inhibition of the cell membrane dopamine transporter. MPTP and MPP^+ also appear to interact with brain nicotinic cholinoceptors but the functional consequences of this interaction are not yet clear.

Keywords: Dizocilpine; MK-801; MPTP; MPP^+; nicotinic receptors; striatum; dopamine; excitatory amino acid receptors; N-methyl-D-aspartate

Introduction

The mechanisms by which systemic administration of 1-methyl-4-phenyl-1,2,3,6-tetrahydropyridine (MPTP) results in destruction of nigrostriatal dopamine have been elucidated in some detail (Tipton & Singer, 1993). In briefest outline, MPTP is first converted to the 1-methyl-4-phenylpyridinium ion (MPP^+) (Markey *et al.*, 1984) which enters dopaminergic terminals via the dopamine transporter (Javitch *et al.*, 1985). Inside the terminal, MPP^+ inhibits mitochondrial respiration (Vyas *et al.*, 1986) with a consequent decline in ATP levels leading to a decline of energy-dependent processes (Scotcher *et al.*, 1990; Chan *et al.*, 1991).

An excitotoxic mechanism has also been proposed, based initially on the observation that intrastriatal administration of MPP^+ can lead to a massive rise in extracellular glutamate and aspartate (Carboni *et al.*, 1990). Subsequently, this notion was supported by a report describing protective effects of excitatory amino acid receptor antagonists in rats given an intranigral infusion of MPP^+ (Turski *et al.*, 1991). However, later work has yielded mixed results, with reports of full protection (Storey *et al.*, 1992; Srivastava *et al.*, 1993), partial protection (Santiago *et al.*, 1992; Trabatabaei *et al.*, 1992; Lange *et al.*, 1993; Chan *et al.*, 1993; Brouillet & Beal, 1993), or no protection afforded by the most commonly used antagonist, dizocilpine (MK-801) (Sonsalla *et al.*, 1989; Kupsch *et al.*, 1992; Sonsalla *et al.*, 1992; Finiels-Marlier *et al.*, 1993). In general, the source of these discrepancies is not clear. However, most positive reports using MK-801 have been associated with the administration of high systemic or intracerebral doses.

MPTP, MPP^+ and MK-801 all possess additional pharmacological or toxic actions. MPTP exerts actions in the brain that do not appear to depend on conversion to MPP^+ (Wilson *et al.*, 1990; Palombo *et al.*, 1991; Duchemin *et al.*, 1992). In addition, MPTP and/or MPP^+ can damage cells that are not known to express dopamine transporters (Namura *et al.*, 1987; Turski *et al.*, 1991; Tipton & Singer, 1993). Furthermore, MPTP and MPP^+ bear a structural

[1] Author for correspondence.

resemblance to the nicotinic receptor agonist, 1,1-dimethyl-4-phenylpiperazinium (DMPP), and MPTP binds quite potently to skeletal muscle nicotinic receptors (Hsu *et al.*, 1993). Nicotine administration can alter MPTP toxicity in mice (Janson *et al.*, 1992), but to date neither MPTP nor MPP^+ has been investigated for possible nicotinic actions in the CNS. In contrast, MK-801 has been shown to block CNS nicotinic receptors in addition to its better-known action at NMDA glutamate receptors (Ramoa *et al.*, 1990).

The aim of the present study was to identify pharmacological actions that might contribute to the neurotoxic effects of MPTP and MPP^+ or to the protective effects of MK-801. Initially, the investigation focussed on possible actions of MPTP or MPP^+ on NMDA-type glutamate or nicotinic receptors. Evidence was then obtained that high concentrations of MK-801 inhibit the cell membrane dopamine transporter. The possible implications of this action, which was reported some years ago (Snell *et al.*, 1988), has not previously been discussed in the context of MPTP toxicity.

Methods

Male Sprague-Dawley rats (Charles River, St. Constant, Quebec), weighing 200–250 g, were maintained on a 12 h/12 h light-dark cycle. Rats were housed four per cage, and food and water were available *ad libitum*. Rats were allowed to accommodate to the housing conditions for 4 days after arrival, and were drug-naive prior to testing.

Dopamine release from superfused synaptosomes

Methods for synaptosomal preparation and measurement of [^{3}H]-dopamine release were virtually identical to those described in detail elsewhere (Clarke *et al.*, 1994). In each assay, crude synaptosomal (P2) fraction was prepared from dissected striata from 4 rats and resuspended in superfusion buffer (SB) composed of the following, in mM concentrations: NaCl 128, KCl 2.4, $CaCl_2$ 3.2, KH_2PO_4 1.2, $MgSO_4$ 1.2, HEPES 25, D-glucose 10, L-ascorbic acid 1 and pargyline 0.1 at pH 7.5. The synaptosomal preparation was preloaded with [^{3}H]-dopamine.

The superfusion apparatus comprised 32 identical channels, each having a small polypropylene retention chamber, through which superfusate was pumped at 0.4 ml min^{-1}. Each experiment included two or more assays. At the start of each assay, 100 µl of the synaptosomal suspension was introduced to each superfusion chamber. During the next 30 min, synaptosomes were superfused with SB alone or with SB containing antagonist, as appropriate. Next, 13 samples per channel were collected in consecutive 1 min intervals: after a 5 min baseline collection period, a 1 min (0.4 ml) pulse of releasing drug or SB (prepared with or without antagonist as appropriate) was given. Finally, the filters holding the synaptosomes were removed in order to measure residual radioactivity (Wallac 1410 liquid scintillation counter, LKB, Sweden). In experiments using Ca^{2+}-free medium an equivalent molar concentration of Mg^{2+} and EGTA (2.25 mM) was substituted. For Mg^{2+}-free medium an equivalent molar concentration of Na^+ was added.

In each assay, data were collected simultaneously from all 32 channels. Each assay incorporated control (SB only) channels, and treatment conditions were counterbalanced across channels and assays. We refer to the tritium released as dopamine release, since it has been established that in similar synaptosomal preparations preloaded with [^{3}H]-dopamine, tritium released by nicotinic agonists or by depolarization largely corresponds to dopamine itself (Rapier *et al.*, 1988).

For each channel, the release occurring in each 1 min collection period was calculated as a percentage of basal release, determined from the first five samples collected. Drug-evoked release was taken as the peak value that occurred in the first 3 periods after a drug challenge. This measure of drug effect was used since it is less likely to be affected by receptor desensitization than the time-averaged drug effect ('area under the curve'). Basal release was 1710 ± 70 d.p.m. min^{-1} (mean ± s.e.mean, $n = 12$ series of assays), which corresponds to approximately 3 fmol mg^{-1} of original wet tissue. Across experiments, basal release (min^{-1}) ranged from 0.8 to 1.3% of residual radioactivity collected on the tissue filters (163,000 ± 11,000 d.p.m. per filter).

[^{3}H]-dopamine uptake by striatal synaptosomes

Striatal synaptosomes were prepared as for [^{3}H]-dopamine release (see above), with the following modifications. The P2 pellet was resuspended and incubated in SB alone at 37°C for 5 min (i.e. no [^{3}H]-dopamine present), followed by centrifugation at 12,000 *g* for 5 min and resuspension in SB (0.02 mg original tissue ml^{-1}). Synaptosomes were incubated (1 mg original tissue per well) in SB for 30 min at room temperature (RT), in uncoated polystyrene, U-bottom 96 multiwell plates (Dynatech Laboratories, Chantilly, VA, U.S.A.), with or without MK801 (1–1000 µM) or nomifensine (100 µM). Synaptosomes were then cooled to 4°C for 5 min before the addition of [^{3}H]-dopamine (0.12 µM). Incubation proceeded at RT for 10 min, followed immediately by filtration and washing in an Inotech cell harvester (Biosystems International Inc., Lansing, MI, U.S.A.) at 4°C, as previously described (El-Bizri & Clarke, 1994a). Radioactivity was measured in a liquid scintillation counter (Wallac 1410; Pharmacia LKB Biotech, Sweden).

[^{3}H]-nicotine binding to tissue homogenates

Animals were decapitated, and left and right cerebral cortices were dissected on ice, pooled, and immediately weighed before storage at − 40°C. The method of tissue homogenate preparation and radioligand binding has been described in detail elsewhere (El-Bizri & Clarke, 1994a). On the day of the assay, thawed tissue was resuspended, incubated at 37°C for 5 min, centrifuged at 15,000 *g* for 20 min then resuspended in an equal volume of fresh incubation buffer (concentrations in mM: NaCl 118, KCl 4.8, $CaCl_2$ 2.5, $MgSO_4$ (H_2O) 1.2, HEPES 20, NaOH 10). Tissue incubation was performed in uncoated polystyrene, U-bottom 96 multiwell plates (Dynatech Laboratories, Chantilly, VA, U.S.A.). The final volume of incubation in each well was 100 µl, containing the equivalent of 2 mg original wet tissue. Non-displaceable binding was determined in the presence of 10^{-5} M nicotine hydrogen tartrate. Tissue membranes were incubated with [^{3}H]-nicotine at 37°C for 20 min. Homogenates were filtered and washed, and the radioactivity counted, as previously described (El-Bizri & Clarke, 1994a).

As a check of radioligand purity (Romm *et al.*, 1990), saturation analysis of [^{3}H]-nicotine binding was performed with twenty-three concentrations of [^{3}H]-nicotine (0.1–19 nM). Inhibition binding experiments were performed under the same conditions with 1.0 nM [^{3}H]-nicotine; inhibiting drugs (MPTP, MPP^+) were added to the tissue suspension immediately before the radioligand.

Drugs

Chemicals and suppliers were as follows: [^{3}H]-dopamine ([8-^{3}H]-dopamine, specific activity 27.5 Ci $mmol^{-1}$) and [^{3}H]-nicotine (1-[N-methyl-^{3}H]-nicotine, specific activity 75.7 Ci $mmol^{-1}$) (New England Nuclear, Boston, MA, U.S.A.), l-nicotine hydrogen tartrate and N-methyl-D-aspartate (Sigma Chemical Corp., St. Louis, MO, U.S.A.), polyethyleneimine (ICN Biochemicals Canada, St. Laurent, Canada), nomifensine maleate, pargyline hydrochloride, kynurenic acid, MPTP hydrochloride and MPP^+ iodide (Research Biochemicals Inc., Natick, MA, U.S.A.), (±)-2-amino-7-phosphonoheptanoic acid (AP-7) (Cambridge Research Biochemicals, Cam-

bridge, U.K.). (+)-amphetamine sulphate (gift of SmithKline Beecham Pharma, Oakville, Canada), (+)-MK-801 HCl and mecamylamine HCl (gifts of Merck and Co., Rahway, NJ, U.S.A.), and chlorisondamine chloride (CHL) (gift of Ciba-Geigy, Summit, NJ, U.S.A.). Other chemicals and reagents were purchased from commercial sources. For superfusion, drugs were dissolved in buffer (SB).

Data analysis

Drug effects were examined by analysis of variance, using commercial software (Systat, Evanston, IL, U.S.A.). Multiple comparisons with a single control group were made with Dunnett's test (Dunnett, 1955) where variance appeared homogeneous; other multiple comparisons were made by Student's *t* test with Bonferroni's correction (Glantz, 1992). Probability values are 2-tailed. Radioligand binding data were analysed by nonlinear regression analysis (LIGAND, Elsevier Biosoft, Cambridge, U.K.).

Results

Experiment 1: Concentration-dependent effects of MPTP and MPP$^+$ on striatal [^{3}H]-dopamine release

MPTP and MPP$^+$ (0.1–100 μM) were tested separately, each in two assays. Both drugs evoked [^{3}H]-dopamine release in a concentration-dependent manner (Figure 1). Discernible effects were observed at concentrations as low as 10 μM and 1 μM, respectively. Evoked release was rapid in onset, with a latency comparable to that associated with nicotine. However, high concentrations of MPTP and MPP$^+$ produced much greater amounts of [^{3}H]-dopamine release than was obtained in parallel with nicotine which was applied at a concentration producing near maximal calcium-dependent release in this assay (El-Bizri & Clarke, 1994b).

Experiment 2: Concentration-dependent inhibition of responses to MPTP and MPP$^+$ by MK-801

Graded concentrations of MK-801 (0.01–100 μM) were tested against MPTP (50 μM) and MPP$^+$ (10 μM) in independent sets of assays (Figure 2). MK-801 reduced responses to both MPTP (MK-801 main effect: $F = 8.52$, d.f. 5,72, $P < 0.0001$) and MPP$^+$ ($F = 5.52$, d.f. 4,48, $P < 0.001$). In each case, significant effects were observed only at 10 and 100 μM. In the MPP$^+$ assays, MK-801 also affected basal release (main effect: $F = 7.38$, d.f. 5,56, $P < 0.0001$). However, the only significant change occurred at one concentration (10 μM: Dunnett's test $P < 0.0001$), and no such increase was observed in the MPTP assays (main effect: $F = 2.19$, d.f. 5,83, $P > 0.05$).

Experiment 3: Further tests of NMDA-type glutamate receptor involvement

Two other NMDA-type glutamate receptor antagonists (AP-7 200 μM and kynurenic acid 300 μM) were tested for their

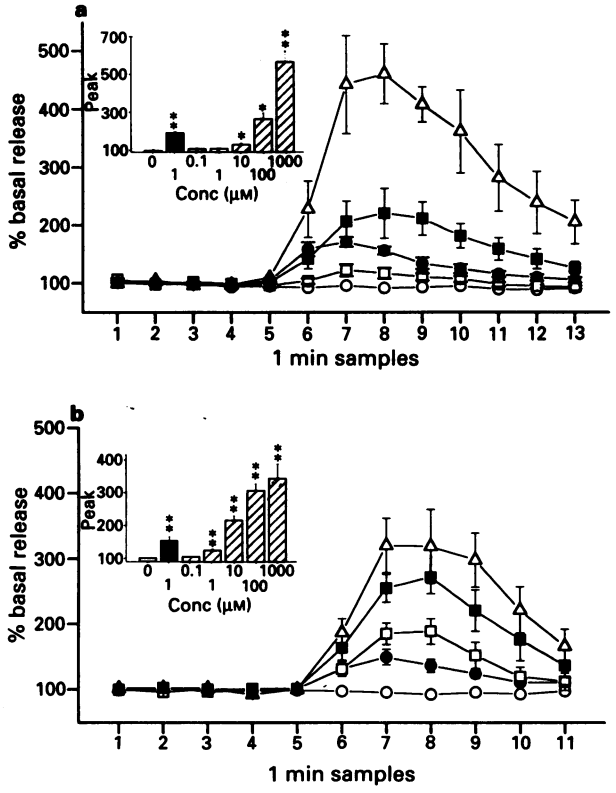


Figure 1 Effect of MPTP, MPP$^+$, and nicotine on [^{3}H]-dopamine release from striatal synaptosomes. Following superfusion with buffer for 30 min, basal release was measured for 5 min prior to the administration of a 1 min pulse of drug or buffer: nicotine 1 μM (●), buffer alone (○), and either MPTP (a) or MPP$^+$ (b) at 10 μM (□), 100 μM (■), or 1000 μM (△). The vertical axis represents the mean (± s.e.mean) release, calculated as a percentage of basal release ($n = 6$–15 channels). The inset shows the peak effect, expressed in the same way: buffer alone (open columns), nicotine (solid columns), and MPTP or MPP$^+$ (cross-hatched columns). $^*P < 0.05$, $^{**}P <$ 0.01–0.0001 vs. buffer alone (Student's *t* test with Bonferroni's correction).

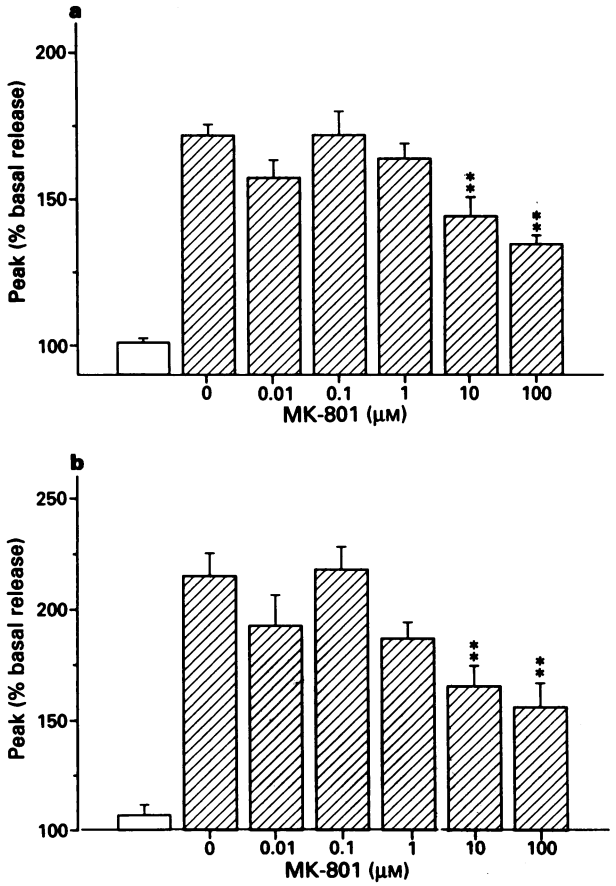


Figure 2 Effects of MK-801 (0.01–100 μM) on [^{3}H]-dopamine release evoked by a 1 min pulse of MPTP (a) or MPP$^+$ (b). Following 35 min of superfusion with MK-801 or buffer alone, synaptosomes were challenged with either MPTP 50 μM or MPP$^+$ 10 μM (cross-hatched) or with buffer alone (open columns). The vertical axis represents the mean (± s.e.mean) peak release, calculated as a percentage of basal release ($n = 10$–23 and 8–16, respectively). $^{**}P < 0.01$–0.0001 vs. MPTP or MPP$^+$ alone (Dunnett's test).

ability to reduce [^{3}H]-dopamine release evoked by MPTP 50 μM and MPP$^+$ 10 μM (Figure 3). Neither antagonist was effective. Tested in parallel, MK-801 (100 μM) significantly decreased [^{3}H]-dopamine release evoked by MPP$^+$; the apparent inhibition of MPTP-evoked release was not significant ($P > 0.1$).

Several attempts were made to demonstrate NMDA-evoked [^{3}H]-dopamine release under conditions where the other secretagogues were effective. However, NMDA gave uniformly negative results, even when Mg^{2+} was omitted from the superfusion buffer (data not shown). The following challenges were tested in different assays: (1) 1 min pulse of NMDA 500 μM + glycine 1 μM ± strychnine 1 μM; (2) 1 min pulse of NMDA 100 μM + glycine 10 μM; (3) 2 min pulse of NMDA 100 μM + glycine 10 μM ± strychnine 10 μM. In each assay, NMDA failed to release [^{3}H]-dopamine significantly, although parallel treatment with another agent (K$^+$ 12 mM, nicotine 1 μM, or MPP$^+$ 10 μM) was always effective.

Release of striatal [^{3}H]-dopamine resulting from NMDA receptor activation is reported to be calcium-dependent and enhanced by omission of Mg^{2+} (see Discussion). However, neither effect was observed with [^{3}H]-dopamine release evoked by MPTP 50 μM or MPP$^+$ 10 μM (Figure 4). The apparent increase in drug-evoked release resulting from the omission of external Ca^{2+} can be attributed to a 62% reduction in basal release seen in this condition.

Experiment 4: Inhibition of [^{3}H]-nicotine binding by MPTP and MPP$^+$

Nonlinear regression analysis revealed a single saturable component of [^{3}H]-nicotine binding to rat cortical membranes ($K_D = 1.02$ nM); the Scatchard plot was correspondingly linear ($r = 0.98$). Both MPTP and MPP$^+$ inhibited [^{3}H]-nicotine binding with IC_{50}s of 1.8 and 26 μM, respectively (Figure 5).

Experiment 5: Effects of the antagonists mecamylamine, chlorisondamine and MK-801 on MPTP- and MPP$^+$-evoked [^{3}H]-dopamine release

In one set of assays, K$^+$ 12 mM and MPTP 50 μM were examined in parallel; in another set, nicotine 1 μM and MPP$^+$ 10 μM were tested in parallel (Figure 6). Mecamylamine, chlorisondamine, and MK-801 all possess nicotinic antagonist activity (see Introduction), and applied at 100 μM, all three blocked responses to 1 μM nicotine (Figure 6b). Responses to K$^+$ were not significantly altered (Figure 6a). Dopamine release evoked by MPP$^+$ was significantly attenuated by MK-801 (Dunnett's test: $P < 0.01$) but not by mecamylamine or chlorisondamine ($P > 0.2$ for both) (Figure 6b). Similarly, only MK-801 significantly reduced MPTP-induced release ($P < 0.01$; Figure 6a). Basal release was not affected by antagonist administration in either set of assays (antagonist main effect: $F < 2.31$, d.f. 3, 88, $P > 0.08$).

Experiment 6: Inhibition of responses to MPTP, MPP$^+$ and (+)-amphetamine by nomifensine and MK-801

The dopamine uptake blocker, nomifensine, was tested for its ability to inhibit evoked [^{3}H]-dopamine release. Pilot studies showed that prolonged administration of nomifensine increased basal release. To avoid this, nomifensine was not administered prior to acute challenge (the standard procedure with other antagonists), but was instead co-administered with the agonist. Nomifensine (0.1–10 μM) was first tested against

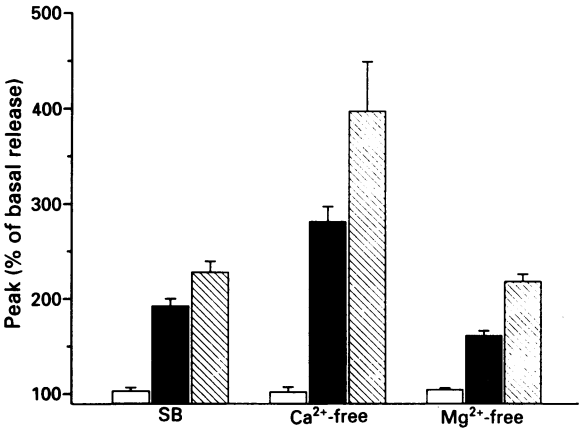


Figure 4 Effects of the omission of external calciuim or magnesium on [^{3}H]-dopamine release evoked by MPTP or MPP$^+$. Following 35 min of superfusion with superfusion buffer (SB) with or without Ca^{2+} or Mg^{2+}, synaptosomes were challenged with either SB alone (open columns), MPTP 50 μM (solid columns) or MPP$^+$ 10 μM (hatched columns). The vertical axis represents the mean (± s.e.mean) peak release, calculated as a percentage of basal release ($n = 6$–10).

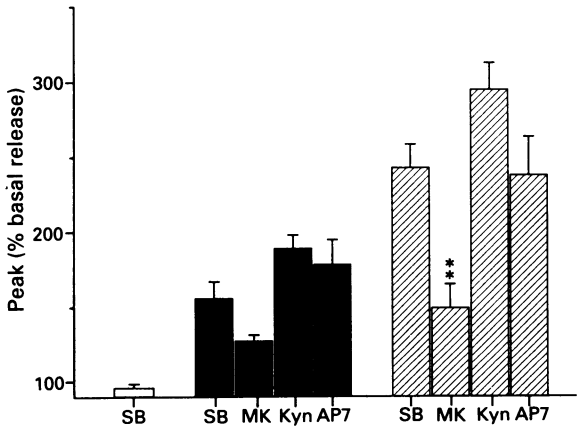


Figure 3 Effects of the glutamate receptor antagonists on [^{3}H]-dopamine release evoked by MPTP or MPP$^+$. Following 35 min of superfusion with antagonist (MK-801 100 μM, kynurenic acid (Kyn) 300 μM, or AP-7 200 μM) or with superfusion buffer alone (SB), synaptosomes were challenged with either MPTP 50 μM (solid columns) or MPP$^+$ 10 μM (hatched columns). Control channels (open columns) were superfused and challenged with SB only. The vertical axis represents the mean (± s.e.mean) peak release, calculated as a percentage of basal release ($n = 6$–10). **$P < 0.002$ vs. MPP$^+$ alone (Dunnett's test).

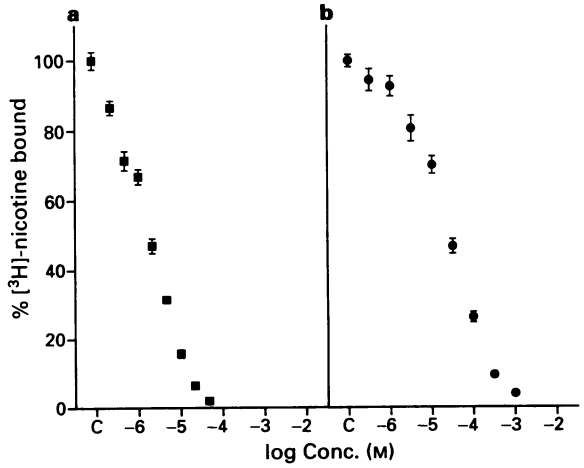


Figure 5 Effects of (a) MPTP and (b) MPP$^+$ on [^{3}H]-nicotine binding to rat cerebral cortex membranes. Displaceable binding was defined by the addition of excess non-radioactive (−)-nicotine. The vertical axis represents the mean (± s.e.mean) displaceable binding, calculated as a percentage of control (i.e. with no inhibitor present) ($n = 12$–16 wells).

K^+ 12 mM and (+)-amphetamine 0.3 μM (Table 1). The short test pulse of nomifensine did not increase [^{3}H]-dopamine release when administered alone and did not alter potassium-evoked release (nomifensine main effect: $F = 1.21$, d.f. 3, 24, $P > 0.3$). In contrast, amphetamine-induced release was attenuated in a concentration-dependent manner, with total block occurring at nomifensine 10 μM.

This concentration of nomifensine was then tested against MPTP 50 μM, MPP^+ 10 μM, (+)-amphetamine 0.3 μM, and K^+ 12 mM (Table 1). Nomifensine completely blocked MPP^+-induced release and attenuated the effect of MPTP. As before, the amphetamine effect was blocked and the K^+ effect was unchanged.

MK-801 (10 and 100 μM) was tested in parallel against (+)-amphetamine 0.3 μM, MPTP 50 μM and MPP^+ 10 μM. At 10 μM, MK-801 significantly reduced the response to MPP^+, but did not antagonize MPTP or (+)-amphetamine (Table 2). At 100 μM, MK-801 reduced responses to all three of these drugs (Table 2).

Experiment 7: Concentration-dependent inhibition of synaptosomal [^{3}H]-dopamine uptake by MK-801

In the absence of inhibitor, the mean uptake of [^{3}H]-dopamine by the synaptosomal preparation in the two assays was 52,000 d.p.m. mg^{-1} original tissue per well. Uptake was reduced by 97% by the addition of excess nomifensine (100 μM). Specific (i.e. nomifensine-sensitive) uptake was expressed as a percentage of the control condition (no inhibitor). Data normalized in this way were very similar between the two assays, and were therefore pooled. MK-801 (1–1000 μM) inhibited [^{3}H]-dopamine uptake in a concentration-dependent manner (Figure 7). A significant effect was first observed at 32 μM ($P < 0.01$), and the IC_{50} was 115 μM.

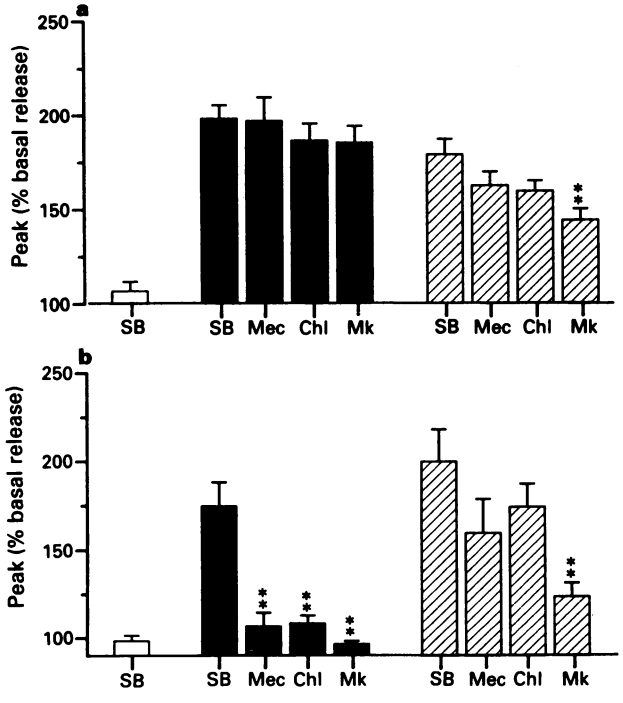


Figure 6 Effects of nicotinic antagonists on [^{3}H]-dopamine release evoked by MPTP or MPP^+. Following 35 min of superfusion with antagonist (100 μM mecamylamine (Mec), chlorisondamine (Chl), or MK-801 (MK)) or superfusion buffer alone (SB), synaptosomes were challenged with: (a) K^+ (solid columns) or MPTP 50 μM (hatched columns), or (b) nicotine 1 μM (solid columns) or MPP^+ 10 μM (hatched columns). Control channels (open columns) were superfused and challenged with SB only. The vertical axis represents the mean (± s.e.mean) peak release, calculated as a percentage of basal release ($n = 6$–15). $^{**}P < 0.01$–0.001 vs. agonist alone (MPTP or MPP^+; Dunnett's test).

Discussion

Acute administration of MPTP and MPP^+ induces striatal dopamine release both *in vivo* and from tissue slices *in vitro* (e.g. Markstein & Lahaye, 1984; Schmidt *et al.*, 1984; Pileblad *et al.*, 1984; Pileblad *et al.*, 1985; Snape *et al.*, 1988; Rollema *et al.*, 1988; Chan *et al.*, 1993). Previously, it was shown that MPTP-induced dopamine efflux from striatal slices was tetrodotoxin-insensitive (Schmidt *et al.*, 1984), but

Table 1 Drug-evoked [^{3}H]-dopamine release in the presence of the dopamine uptake blocker, nomifensine (Experiment 6)

	SB	*K^+*	*AMPH*	*MPTP*	*MPP^+*
Nomifensine					
0 μM	103 ± 2	160 ± 4	208 ± 4		
0.1 μM	103 ± 3	169 ± 10	197 ± 25		
1.0 μM	102 ± 2	151 ± 5	*158 ± 20		
10 μM	103 ± 4	161 ± 6	**109 ± 3		
0 μM	103 ± 3	148 ± 7	194 ± 4	151 ± 6	196 ± 8
10 μM	98 ± 1	160 ± 10	**103 ± 5	**118 ± 4	**105 ± 5

Drug challenge comprised a pulse of superfusion buffer (SB), K^+ 12 mM, (+)-amphetamine 0.3 μM, MPTP 50 μM, or MPP^+ 10 μM.
Evoked dopamine release is expressed as the peak effect, as a percentage of basal release. $^*P < 0.02$, $^{**}P < 0.005$ vs. drug challenge in absence of nomifensine ($n = 5$–10; Student's t test with Bonferroni's correction).

Table 2 Drug-evoked [^{3}H]-dopamine release in the presence of MK-801 (Experiment 6)

	SB	*AMPH*	*MPTP*	*MPP^+*
MK-801				
0 μM	99 ± 3	203 ± 14	164 ± 5	262 ± 6
10 μM		222 ± 12	163 ± 4	**205 ± 11
0 μM	101 ± 3	212 ± 11	155 ± 5	200 ± 9
100 μM		**159 ± 6	*132 ± 5	*158 ± 9

Drug challenge comprised a pulse of superfusion buffer (SB), (+)-amphetamine 0.3 μM, MPTP 50 μM, or MPP^+ 10 μM. Evoked dopamine release is expressed as the peak effect, as a percentage of basal release. $^*P < 0.05$, $^{**}P < 0.005$ vs. drug challenge in absence of MK-801 ($n = 7$–11; Student's t test with Bonferroni's correction).

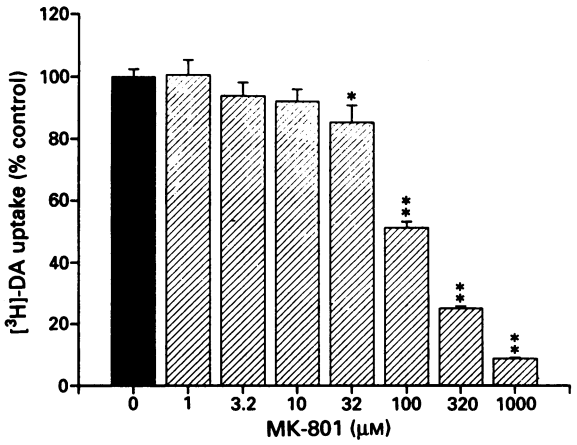


Figure 7 Inhibition of synaptosomal [^{3}H]-dopamine uptake by MK-801. Specific uptake of [^{3}H]-dopamine was defined by the addition of an excess of the selective dopamine uptake blocker, nomifensine (100 μM). The vertical axis represents the mean (± s.e.mean) specific uptake, calculated as a percentage of control (i.e. with no inhibitor present) ($n = 16$ wells). $^*P < 0.01$, $^{**}P < 0.0001$ vs. control (Dunnett's test).

such an approach cannot exclude indirect excitatory actions mediated trans-synaptically by diffusion of locally-released substances. The present study represents the first reported use of superfused synaptosomes to study this phenomenon, and provides perhaps the clearest indication to date that MPTP and MPP^+ can act directly on the dopaminergic terminals to promote dopamine release. Frequent sampling was employed, revealing a dopamine-releasing action that was very rapid, with a latency comparable to the dopamine-releasing actions of nicotine, high K^+, and amphetamine. Such a rapid action is unlikely to be due to the inhibition of mitochondrial respiration and depletion of intracellular ATP levels, a process which tends to occur more gradually after MPP^+ administration (Scotcher *et al.*, 1990; Chan *et al.*, 1991). In all of the present experiments, the monoamine oxidase inhibitor, pargyline, was included in the superfusion buffer, and thus the acute effect of MPTP did not depend on conversion to MPP^+. This observation serves to emphasize that the acute dopamine-releasing actions of MPTP and MPP^+ as studied here may not necessarily contribute to neurotoxicity.

Blockade of NMDA-type glutamate receptors

MK-801 inhibited the dopamine-releasing actions of both MPTP and MPP^+, but only at concentrations higher than those required to block NMDA receptors (Huettner & Bean, 1988; Willis *et al.*, 1991; Wamil & McLean, 1992). Additional tests of NMDA receptor involvement proved negative (Experiment 3). First, high concentrations of the potent NMDA receptor blockers AP-7 and kynurenic acid (Wong & Kemp, 1991) failed to inhibit responses to MPTP and MPP^+. Second, administration of NMDA, even at high concentrations and under conditions favouring NMDA receptor activation, did not release detectable amounts of [^{3}H]-dopamine. Third, MPTP- and MPP^+-induced [^{3}H]-dopamine release was not affected by removal of calcium or magnesium from the superfusion buffer; NMDA-induced dopamine release, where previously obtained from striatal synaptosomes, has been found to be calcium-dependent and greatly enhanced by omission of Mg^{2+} (Wang, 1991; Krebs *et al.*, 1991; Desce *et al.*, 1992).

Our inability to obtain NMDA-induced dopamine release accords with other negative reports in the literature (De Belleroche & Bradford, 1980; Carter *et al.*, 1988), but stands in contrast to the majority of published studies which are consistent with a direct releasing action of NMDA on striatal dopaminergic terminals (Snell & Johnson, 1986; Clow & Jhamandas, 1989; Wang, 1991; Krebs *et al.*, 1991; Johnson & Jeng, 1991; Desce *et al.*, 1992). Most of these positive reports were obtained with slowly-perfused synaptosomes (Krebs *et al.*, 1991; Desce *et al.*, 1992) or tissue slices treated with tetrodotoxin (Snell & Johnson, 1986; Clow & Jhamandas, 1989), in which dopamine release could conceivably be triggered indirectly via the release of some other mediator. However, this consideration does not apply to the studies of Wang (1991) and of Johnson & Jeng (1991), where NMDA-induced [^{3}H]-dopamine release was obtained from striatal synaptosomes with rapid perfusion.

Actions at nicotinic receptors

MK-801 antagonizes CNS nicotinic receptors in addition to NMDA receptors (Ramoa *et al.*, 1990; confirmed in Experiment 5). The possibility was therefore considered that MPTP and MPP^+ act at nicotinic receptors. In rat brain, a prominent population of nicotinic acetylcholine receptors is labelled with high affinity by [^{3}H]-nicotine (Clarke, 1987). Both MPTP and MPP^+ inhibited [^{3}H]-nicotine binding to rat brain membranes (Experiment 4), albeit considerably less potently than other known nicotinic agonists (Wonnacott, 1987). Nevertheless, the nicotinic receptor antagonists, mecamylamine and chlorisondamine, failed to reduce release evoked by MPTP and MPP^+ (Experiment 5), even when these antagonists were tested at concentrations more than sufficient to block nicotine-induced dopamine release (El-Bizri & Clarke, 1994b). Thus, although MPTP and MPP^+ appear to interact with brain nicotinic receptors, appreciable agonist activity was not detected at the concentrations tested.

Actions at the cell membrane dopamine transporter

Two principal mechanisms of drug-induced transmitter release have been proposed (Levi & Raiteri, 1993). The first, exemplified by depolarizing agents such as high K^+, is dependent upon external calcium but insensitive to uptake inhibitors (Raiteri *et al.*, 1979; also Experiment 6), and represents exocytotic secretion. The second mechanism, exemplified by (+)-amphetamine, has the reverse characteristics (Raiteri *et al.*, 1979; also Experiment 7), and reflects the efflux of cytosolic transmitter via its transporter. In this regard, dopamine release evoked by MPTP and MPP^+ bore at least a superficial resemblance to amphetamine: not only did the evoked release occur independently of external calcium (Experiment 3), but it was greatly reduced by nomifensine (Experiment 6) in a concentration that blocked [^{3}H]-dopamine uptake (Experiment 7). Similar results have been obtained previously in brain slices and whole animals, both in terms of calcium independence (Schmidt *et al.*, 1984; Sirinathsinghji *et al.*, 1988; Snape *et al.*, 1988; Sirinathsinghji *et al.*, 1988; Wilson *et al.*, 1991) and blockade by nomifensine (Markstein & Lahaye, 1984). However, since MPP^+ normally enters dopaminergic terminals via the dopamine transporter (Javitch *et al.*, 1985), the present observations imply either that MPP^+ acted intracellularly to release [^{3}H]-dopamine via a non-exocytotic mechanism, or that the drug acted extracellularly or intracellularly to release cytosolic dopamine. In contrast to MPP^+, MPTP-evoked dopamine release was not completely blocked by nomifensine (Experiment 6), indicating an additional, as yet unidentified mechanism of action.

The similar profile of action seen with nomifensine and MK-801 (Experiments 5 and 6) suggested that the latter might be acting at the cell membrane dopamine transporter to attenuate dopamine release evoked by MPTP and MPP^+. The results of the final experiment support this notion: MK-801 inhibited [^{3}H]-dopamine accumulation with an IC_{50} of 115 μM. As we subsequently discovered, a similar result has been reported previously but virtually ignored (Snell *et al.*, 1988). It is likely that this action of MK-801 reflects decreased dopamine influx, since in our experiments, the drug did not consistently increase basal [^{3}H]-dopamine release.

Can previous reports of protection by MK-801 be explained by block of the dopamine transporter?

Destruction of dopaminergic neurones following the administration of MPTP or MPP^+ can be completely prevented by the administration of dopamine uptake inhibitors (Ricaurte *et al.*, 1985). The finding that MK-801 inhibits the dopamine transporter therefore prompts a reconsideration of the literature on MPTP toxicity. Protection by MK-801, where obtained, has usually been associated with the administration of high doses. Thus, in the first such report (Turski *et al.*, 1991), MK-801 was co-infused with MPP^+ into the substantia nigra in a concentration of 0.25 M; transient protection also occurred after systemic administration of 3.4 mg kg^{-1}. Other studies have employed repeated systemic administration of MK-801 to rats, with mixed results. Thus, full protection against the dopamine depleting effects of intra-striatal or intra-nigral MPP^+ injection was reported after repeated administration of 5 mg kg^{-1} (6 or 12 q 4 h) (Storey *et al.*, 1992; Srivastava *et al.*, 1993), but somewhat lower doses (2.2 or 3.4 mg kg^{-1}) were ineffective (Sonsalla *et al.*, 1992; Santiago *et al.*, 1992).

Brain levels of MK-801 peak at around 10 μM and decline with a half-life of about 2 h in the rat, following a single injection of 5 mg kg^{-1}, i.p. (Vezzani *et al.*, 1989). Thus, protection against MPP^+ toxicity appears to require sustained brain concentrations of approximately 3–10 μM, a concentration-range at least one order of magnitude higher than that required to produce insurmountable, use-dependent blockade of NMDA receptors (Huettner & Bean, 1988; Willis *et al.*, 1991; Wamil & McLean, 1992). Such concentrations of MK-801 produced little inhibition of dopamine uptake (IC_{50} 115 μM) *in vitro*. Whether the drug is more potent *in vivo* or with sustained application is not known, but is a question that should not be ignored in studies where high doses of the drug are given.

If MK-801 should inhibit the cell membrane dopamine transporter *in vivo*, it would reduce MPP^+ uptake and also reduce release of cytosolic dopamine. The latter action could also be relevant to methamphetamine toxicity, which is inhibited by MK-801 by a mechanism that remains to be fully understood (Marshall *et al.*, 1993). Since it appears that the massive methamphetamine-induced release of cytosolic dopamine plays a causal role in the subsequent degeneration of dopaminergic nerve terminals (Weihmuller *et al.*, 1992; Marshall *et al.*, 1993), it will be of interest to examine the possibility that MK-801 inhibits the dopamine transporter *in vivo*.

We thank Dr Brian Collier for his valuable comments, and the following for donating drugs: SmithKline Beecham Pharma, Oakville, Canada ((+)-amphetamine), Merck and Co., Rahway, NJ, U.S.A. (MK-801, mecamylamine), Ciba-Geigy, Summit, NJ (chlorisondamine). This work was supported by the Medical Research Council of Canada. P.B.S.C. holds a Senior I Scholarship of the Fonds de la Recherche en Santé du Québec.

References

BROUILLET, E. & BEAL, M.F. (1993). NMDA antagonists partially protect against MPTP induced neurotoxicity in mice. *NeuroReport*, **4**, 387–390.

CARBONI, S., MELIS, F., PANI, L., HADJICONSTANTINOU, M. & ROSSETTI, Z.L. (1990). The non-competitive NMDA-receptor antagonist MK-801 prevents the massive release of glutamate and aspartate from rat striatum induced by 1-methyl-4-phenylpyridinium (MPP^+). *Neurosci. Lett.*, **117**, 129–133.

CARTER, C.J., L'HEUREUX, R.L. & SCATTON, B. (1988). Differential control of N-methyl-D-aspartate and kainate of striatal dopamine release in vivo: a trans-striatal dialysis study. *J. Neurochem.*, **51**, 462–468.

CHAN, P., DELANNEY, L.E., IRWIN, I., LANGSTON, J.W. & DI MONTE, D. (1991). Rapid ATP loss caused by 1-methyl-4-phenyl-1,2,3,6-tetrahydropyridine in mouse brain. *J. Neurochem.*, **57**, 348–351.

CHAN, P., LANGSTON, J.W. & DI MONTE, D.A. (1993). MK-801 temporarily prevents MPTP-induced acute dopamine depletion and MPP^+ elimination in the mouse striatum. *J. Pharmacol. Exp. Ther.*, **267**, 1515–1520.

CLARKE, P.B.S. (1987). Recent progress in identifying nicotinic cholinoceptors in mammalian brain. *Trends Pharmacol. Sci.*, **8**, 32–35.

CLARKE, P.B.S., REUBEN, M. & EL-BIZRI, H. (1994). Blockade of nicotinic responses by physostigmine, tacrine and other cholinesterase inhibitors in rat striatum. *Br. J. Pharmacol.*, **111**, 695–702.

CLOW, D.W. & JHAMANDAS, K. (1992). Characterization of L-glutamate action on the release of endogenous dopamine from the rat caudate-putamen. *J. Pharmacol. Exp. Ther.*, **248**, 722–728.

DE BELLEROCHE, J.S. & BRADFORD, H.F. (1980). Presynaptic control of the synthesis and release of dopamine from striatal synaptosomes: a comparison between the effects of 5-hydroxytryptamine, acetylcholine, and glutamate. *J. Neurochem.*, **35**, 1227–1234.

DESCE, J.M., GODEHEU, G., GALLI, T., ARTAUD, F., CHÉRAMY, A. & GLOWINSKI, J. (1992). L-glutamate-evoked release of dopamine from synaptosomes of the rat striatum: involvement of AMPA and N-methyl-D-aspartate receptors. *Neuroscience*, **47**, 333–339.

DUCHEMIN, A.M., GUDEHITHLU, K.P., NEFF, N.H. & HADJICONSTANTINOU, M. (1992). c-fos mRNA in mouse brain after MPTP treatment. *Neurochem. Int.*, **20**, 281–287.

DUNNETT, C.W. (1955). A multiple comparison procedure for comparing severeal treatments with a control. *J. Am. Statist. Assoc.*, **50**, 1096–1121.

EL-BIZRI, H. & CLARKE, P.B.S. (1994a). Regulation of nicotinic receptors in rat brain following quasi-irreversible nicotinic blockade by chlorisondamine and chronic treatment with nicotine. *Br. J. Pharmacol.*, **113**, 917–925.

EL-BIZRI, H. & CLARKE, P.B.S. (1994b). Blockade of nicotinic receptor-mediated release of dopamine from striatal synaptosomes by chlorisondamine and other nicotinic antagonists administered *in vitro*. *Br. J. Pharmacol.*, **111**, 406–413.

FINIELS-MARLIER, F., MARINI, A.M., WILLIAMS, P. & PAUL, S.M. (1993). The N-methyl-D-aspartate antagonist MK-801 fails to protect dopaminergic neurons from 1-methyl-4-phenylpyridinium toxicity in vitro. *J. Neurochem.*, **60**, 1968–1971.

GLANTZ, S.A. (1992). *Primer of Biostatistics*. New York: McGraw-Hill. 3rd edn.

HSU, K.S., FU, W.M. & LIN-SHIAU, S.Y. (1993). Studies on the neuromuscular blocking action of MPTP in the mouse phrenic nerve-diaphragm. *Neuropharmacology*, **32**, 597–603.

HUETTNER, J.E. & BEAN, B.P. (1988). Block of N-methyl-D-aspartate-activated current by the anticonvulsant MK-801: selective binding to open channels. *Proc. Natl. Acad. Sci. U.S.A.*, **85**, 1307–1311.

JANSON, A.M., FUXE, K. & GOLDSTEIN, M. (1992). Differential effects of acute and chronic nicotine treatment on MPTP-(1-methyl-4-phenyl-1,2,3,6-tetrahydropyridine) induced degeneration of nigrostriatal dopamine neurons in the black mouse. *Clin. Investigator*, **70**, 232–238.

JAVITCH, J.A., D'AMATO, R.J., STRITTMATTER, S.M. & SNYDER, S.H. (1985). Parkinsonism-inducing neurotoxin, N-methyl-4-phenyl-1,2,3,6-tetrahydropyridine: uptake of the metabolite N-methyl-4-phenylpyridine by dopamine neurons explains selective toxicity. *Proc. Natl. Acad. Sci. U.S.A.*, **82**, 2173–2177.

JOHNSON, K.M. & JENG, Y.-J. (1991). Pharmacological evidence for N-methyl-D-aspartate receptors on nigrostriatal dopaminergic nerve terminals. *Can. J. Physiol. Pharmacol.*, **69**, 1416–1421.

KREBS, M.O., DESCE, J.M., KEMEL, M.L., GAUCHY, C., GODEHEU, G., CHERAMY, A. & GLOWINSKI, J. (1991). Glutaminergic control of dopamine release in the rat striatum: evidence for presynaptic N-methyl-D-aspartate receptors on dopaminergic nerve terminals. *J. Neurochem.*, **56**, 81–85.

KUPSCH, A., LOSCHMANN, P.A., SAUER, H., ARNOLD, G., RENNER, P., PUFAL, D., BURG, M., WACHTEL, H. TEN BRUGGENCATE, G. & OERTEL, W.H. (1992). Do NMDA receptor antagonists protect against MPTP-toxicity? Biochemical and immunocytochemical analyses in black mice. *Brain Res.*, **592**, 74–83.

LANGE, K.W., LÖSCHMANN, P.-A., SOFIC, E., BURG, M., HOROWSKI, R., KALVERAM, K.T., WACHTEL, H. & RIEDERER, P. (1993). The competitive NMDA antagonist CPP protects substantia nigra neurons from MPTP-induced degeneration in primates. *Naunyn. Schmied. Arch. Pharmacol.*, **348**, 586–592.

LEVI, G. & RAITERI, M. (1993). Carrier-mediated rerlease of neurotransmitters. *Trends Neurosci.*, **16**, 415–419.

MARKEY, S.P., JOHANNESSEN, J.N., CHIUEH, C.C., BURNS, R.S. & HERKENHAM, M.A. (1984). Intraneuronal generation of a pyridinium metabolite may cause drug-induced parkinsonism. *Nature*, **311**, 464–467.

MARKSTEIN, R. & LAHAYE, D. (1984). Neurochemical investigations in vitro with 1-methyl-4-phenyl-1,2,3,6-tetrahydropyridine (MPTP) in preparations of rat brain. *Eur. J. Pharmacol.*, **106**, 301–311.

MARSHALL, J.F., O'DELL, S.J. & WEIHMULLER, F.B. (1993). Dopamine-glutamate interactions in methamphetamine-induced neurotoxicity. *J. Neural Transm.*, **91**, 241–254.

NAMURA, I., DOUILLET, P., SUN, C.J., PERT, A., COHEN, R.M. & CHIUEH, C.C. (1987). MPP+ (1-methyl-4-phenylpyridine) is a neurotoxin to dopamine-, norepinephrine- and serotonin-containing neurons. *Eur. J. Pharmacol.*, **136**, 31–37.

PALOMBO, E., PORRINO, L.J., CRANE, A.M., BANKIEWICZ, K.S., KOPIN, I.J. & SOKOLOFF, L. (1991). Cerebral metabolic effects of monoamine oxidase inhibition in normal and 1-methyl-4-phenyl-1,2,3,6-tetrahydropyridine acutely treated monkeys. *J. Neurochem.*, **56**, 1639–1646.

PILEBLAD, E., NISSBRANDT, H. & CARLSSON, A. (1984). Biochemical and functional evidence for a marked dopamine releasing action of N-methyl-4-phenyl-1,2,3,6-tetrahydropyridine (NMPTP) in mouse brain. *J. Neural Transm.*, **60**, 199–203.

PILEBLAD, E., FORNSTEDT, B., CLARK, D. & CARLSSON, A. (1985). Acute effect of 1-methyl-4-phenyl-1,2,3,6-tetrahydropyridine on dopamine metabolism in mouse and rat striatum. *J. Pharm. Pharmacol.*, **37**, 707–712.

RAITERI, M., CERRITO, F., CERVONI, A.M. & LEVI, G. (1979). Dopamine can be released by two mechanisms differentially affected by the dopamine transport inhibitor nomifensine. *J. Pharmacol. Exp. Ther.*, **208**, 195–202.

RAMOA, A.S., ALKONDON, M., ARACAVA, Y., IRONS, J., LUNT, G.G., DESHPANDE, S.S., WONNACOTT, S., ARONSTAM, R.S. & ALBUQUERQUE, E.X. (1990). The anticonvulsant MK-801 interacts with peripheral and central nicotinic acetylcholine receptor ion channels. *J. Pharmacol. Exp. Ther.*, **254**, 71–82.

RAPIER, C., LUNT, G.G. & WONNACOTT, S. (1988). Stereoselective nicotine-induced release of dopamine from striatal synaptosomes: concentration dependence and repetitive stimulation. *J. Neurochem.*, **50**, 1123–1130.

RICAURTE, G.A., LANGSTON, J.W., DELANNEY, L.E., IRWIN, I. & BROOKS, J.D. (1985). Dopamine uptake blockers protect against the dopamine depleting effect of 1-methyl-4-phenyl-1,2,3,6-tetrahydropyridine (MPTP) in the mouse striatum. *Neurosci. Lett.*, **59**, 259–264.

ROLLEMA, H., KUHR, W.G., KRANENBORG, G., DE VRIES, J. & VAN DEN BERG, C. (1988). MPP^+-induced efflux of dopamine and lactate from rat striatum have similar time courses as shown by in vivo brain dialysis. *J. Pharmacol. Exp. Ther.*, **245**, 858–866.

ROMM, E., LIPPIELLO, P.M., MARKS, M.J. & COLLINS, A.C. (1990). Purification of L-[^{3}H]nicotine eliminates low affinity binding. *Life Sci.*, **46**, 935–943.

SANTIAGO, M., VENERO, J.L., MACHADO, A. & CANO, J. (1992). In vivo protection of striatum from MPP^+ neurotoxicity by N-methyl-D-aspartate antagonists. *Brain Res.*, **586**, 203–207.

SCHMIDT, C.J., MATSUDA, L.A. & GIBB, J.W. (1984). In vitro release of tritiated monoamines from rat CNS tissue by the neurotoxic compound 1-methyl-phenyl-tetrahydropyridine. *Eur. J. Pharmacol.*, **103**, 255–260.

SCOTCHER, K.P., IRWIN, I., DELANNEY, L.E., LANGSTON, J.W. & DI MONTE, D., (1990). Effects of 1-methyl-4-phenyl-1,2,3,6-tetrahydropyridine and 1-methyl-4-phenylpyridinium ion on ATP levels of mouse brain synaptosomes. *J. Neurochem.*, **54**, 1295–1301.

SIRINATHSINGHJI, D.J., HEAVENS, R.P. & MCBRIDE, C.S. (1988). Dopamine-releasing action of 1-methyl-4-phenyl-1,2,3,6-tetrahydropyridine (MPTP) and 1-methyl-4-phenylpyridine (MPP+) in the neostriatum of the rat as demonstrated in vivo by the push-pull perfusion techniques: dependence on sodium but not calcium ions. *Brain Res.*, **443**, 101–116.

SNAPE, B.M., PILEBLAD, E., EKMAN, A., MAGNUSSON, T., CARLSSON, A. & ENGEL, J. (1988). The effects of 1-methyl-4-phenylpyridinium ion (MPP+) on the efflux and metabolism of endogenous dopamine in rat striatal slices. *J. Pharm. Pharmacol.*, **40**, 620–626.

SNELL, L.D. & JOHNSON, K.M. (1986). Characterization of the inhibition of excitatory amino-acid-induced neurotransmitter release in the rat striatum by phencyclidine-like drugs. *J. Pharmacol. Exp. Ther.*, **238**, 938–946.

SNELL, L.D., YI, S.-J. & JOHNSON, K.M. (1988). Compairson of the effects of MK-801 and phencyclidine on catecholamine uptake and NDMA-induced norepinephrine release. *Eur. J. Pharmacol.*, **145**, 223–226.

SONSALLA, P.K., NICKLAS, W.J. & HEIKKILA, R.E. (1989). Role for excitatory amino acids in methamphetamine-induced nigrostriatal dopaminergic toxicity. *Science*, **243**, 398–400.

SONSALLA, P.K., ZEEVALK, G.D., MANZINO, L., GIOVANNI, A. & NICKLAS, W.J. (1992). MK-801 fails to protect against the dopaminergic neuropathology produced by systemic 1-methyl-4-phenyl-1,2,3,6-tetrahydropyridine in mice or intranigral 1-methyl-4-phenylpyridinium in rats. *J. Neurochem.*, **58**, 1979–1982.

SRIVASTAVA, R., BROUILLET, E., BEAL, M.F., STOREY, E. & HYMAN, B.T. (1993). Blockade of 1-methyl-4-phenylpyridinium ion (MPP^+) nigral toxicity in the rat by prior decortication of MK-801 treatment: a stereological estimate of neuronal loss. *Neurobiol. Aging*, **14**, 295–301.

STOREY, E., HYMAN, B.T., JENKINS, B., BROUILLET, E., MILLER, J.M., ROSEN, B.R. & BEAL, M.F. (1992). 1-Methyl-4-phenylpyridinium produces excitotoxic lesions in rat striatum as a result of impairment of oxidative metabolism. *J. Neurochem.*, **58**, 1975–1978.

TABATABAEI, A., PERRY, T.L., HANSEN, S. & KRIEGER, C. (1992). Partial protective effect of MK-801 on MPTP-induced reduction of striatal dopamine in mice. *Neurosci. Lett.*, **141**, 192–194.

TIPTON, K.F. & SINGER, T.P. (1993). Advances in our understanding of the mechanisms of the neurotoxicity of MPTP and related compounds. *J. Neurochem.*, **61**, 1191–1206.

TURSKI, L., BRESSLER, K., RETTIG, K.J., LOSCHMANN, P.A. & WACHTEL, H. (1991). Protection of substantia nigra from MPP+ neurotoxicity by N-methyl-D-aspartate antagonists. *Nature*, **349**, 414–418.

VEZZANI, A., SERAFINI, R., STASI, M.A., CACCIA, S., CONTI, I., TRIDICO, R.V. & SAMANIN, R. (1989). Kinetics of Mk-801 and its effects on quinolinic acid-induced seizures and neurotoxicity in rats. *J. Pharmacol. Exp. Ther.*, **249**, 278–283.

VYAS, I., HEIKKILA, R.E. & NICKLAS, W.J. (1986). Studies on the neurotoxicity of 1-methyl-4-phenyl-1,2,3,6-tetrahydropyridine: inhibition of NADH-linked substrate oxidation by its metabolite 1-methyl-4-phenylpyridinium. *J. Neurochem.*, **46**, 1501–1507.

WAMIL, A.W. & MCLEAN, M.J. (1992). Use-, concentration-, and voltage-dependent limitiation by MK-801 of action potential firing frequency in mouse central neurons in cell culture. *J. Pharmacol. Exp. Ther.*, **260**, 376–383.

WANG, J.K.T. (1991). Presynaptic glutamate receptors modulate dopamine release from striatal synaptosomes. *J. Neurochem.*, **57**, 819–822.

WEIHMULLER, F.B., O'DELL, S.J. & MARSHALL, J.F. (1992). MK-801 protection against methamphetamine-induced striatal terminal injury is associated with attenuated DA overflow. *Synapse*, **11**, 155–163.

WILLIS, C.L., BRAZELL, C. & FOSTER, A.C. (1991). Plasma and CSF levels of dizocilpine (MK-801) required for neuroprotection in the quinolinate-injected rat striatum. *Eur. J. Pharmacol.*, **196**, 285–290.

WILSON, J.A., DOYLE, T.J. & LAU, Y.S. (1990). MPTP, MPDP+ and MPP+ cause decreases in dopamine content in mouse brain slices. *Neurosci. Lett.*, **108**, 213–218.

WILSON, J.A., LAU, Y.S., GLEESON, J.G. & WILSON, J.S. (1991). The action of MPTP on synaptic transmission is affected by changes in Ca2+ concentrations. *Brain Res.*, **541**, 342–346.

WONG, E.H.F. & KEMP, J.A. (1991). Sites for antagonism on the N-methyl-D-aspartate receptor channel complex. *Annu. Rev. Pharmacol. Toxicol.*, **31**, 401–425.

WONNACOTT, S. (1987). Brain nicotine binding sites. *Hum. Toxicol.*, **6**, 343–353.

(Received August 5, 1994
Revised September 16, 1994
Accepted September 20, 1994)

British Journal of Pharmacology (1995) 114, 323-328 © 1995 Stockton Press All rights reserved 0007-1188/95 $9.00

Modulation by nitric oxide of prostaglandin biosynthesis in the rat

Lidia Sautebin, Armando Ialenti, Angela Ianaro & [1]Massimo Di Rosa

Department of Experimental Pharmacology, University of Naples Federico II, Via Domenico Montesano, 49-80131 Naples, Italy

1 Modulation of prostaglandin biosynthesis *in vivo* by either exogenous or endogenous nitric oxide (NO) has been studied in the rat using arachidonic acid (AA)-induced paw oedema and measuring both the foot volume and the amount of 6-keto-prostaglandin $F_{1\alpha}$ (6-keto-$PGF_{1\alpha}$), the stable metabolite of prostacyclin (PGI_2), in the oedematous fluid recovered from inflamed paws.

2 Paw injections of 150 or 300 nmol of AA were virtually inactive whereas 600 nmol produced a moderate oedema which was greatly reduced by the NO synthase inhibitor L-N^G-nitro arginine methyl ester (L-NAME, 100 nmol/paw) and the NO scavenger haemoglobin (Hb, 30 μmol/paw), but unaffected by the inhibitor of the soluble guanylate cyclase, methylene blue (Mb, 3 μmol/paw) and L-arginine (15 μmol/paw).

3 The NO-donors (10 μmol/paw) 3-morpholino-sydnonimine-hydrochloride (SIN-1), S-nitroso-N-acetyl-D, L-penicillamine (SNAP) and sodium nitroprusside (SNP) significantly potentiated the paw oedema induced by AA (300 nmol/paw).

4 SIN-1 (2.5, 5 and 10 μmol/paw) produced a significant dose-dependent increase of the oedema induced by AA which was correlated with increased amounts of 6-keto-$PGF_{1\alpha}$ in the fluid recovered from inflamed paws.

5 Both oedema and prostaglandin biosynthesis induced by the combination AA + SIN-1 were greatly suppressed by either Hb (30 μmol/paw) or indomethacin (3 μmol/paw or 5 mg kg^{-1} s.c.) but unaffected by Mb (3 μmol/paw).

6 In LPS-treated rats (6 mg kg^{-1}, i.p.) doses of AA inactive in normal animals produced a remarkable oedema which was reduced by L-NAME or Hb, unaffected by Mb and increased by L-arginine.

7 These results demonstrate that NO increases prostaglandin biosynthesis *in vivo* through a guanosine 3':5'-cyclic monophosphate (cyclic GMP)-independent mechanism and suggest that the interaction between NO synthase and cyclo-oxygenase (COX) pathways may represent an important mechanism for the modulation of the inflammatory response.

Keywords: Arachidonic acid; endotoxin; nitric oxide; NO donors; oedema; prostaglandin biosynthesis

Introduction

Nitric oxide (NO) is generated from the terminal guanidino nitrogen atom(s) of the amino acid L-arginine by the enzyme NO synthase (NOS; for review see Moncada *et al.*, 1991). At least two types of NOS have been so far identified. One is constitutive (cNOS), Ca^{2+}/calmodulin-dependent and releases NO for short periods in response to receptor stimulation. The other enzyme is inducible (iNOS), Ca^{2+}-independent and, once expressed, generates NO for long periods. Both enzymes are inhibited by certain L-arginine analogues (Rees *et al.*, 1990), whereas glucocorticoids inhibit the induction of iNOS (Di Rosa *et al.*, 1990). The cNOS has been identified in vascular endothelium and brain, while iNOS is expressed after stimulation with bacterial lipopolysaccharide (LPS) or some cytokines in endothelial cells, smooth muscle cells, polymorphonuclear leucocytes and macrophages.

NO generated by cNOS is responsible for a variety of biological actions which include endothelium-dependent relaxation, inhibition of platelet aggregation and cell-to-cell communication in the central nervous system. These actions are a result of NO acting as the endogenous stimulator of soluble guanylate cyclase. NO produced in large quantities by iNOS plays an important role in host-defence response, in the pathogenesis of endotoxin shock and in autoimmune tissue destruction (Hibbs *et al.*, 1988; Kilbourn *et al.*, 1990; Kolb *et al.*, 1991).

We have shown that the L-arginine:NO pathway is involved in both acute and chronic inflammation since endogenous NO increases oedema formation and exacerbates adjuvant arthritis in the rat (Ialenti *et al.*, 1992; 1993). We have also shown that depending on the time course or on the type of inflammation, NO may be predominantly generated either by cNOS or by iNOS.

Prostaglandins play a major role as mediators of the inflammatory response. Prostaglandins are generated from arachidonic acid (AA) by the enzyme cyclo-oxygenase (COX). Like NOS, COX has been found in two forms, namely the constitutive, widely occurring enzyme (COX-1) and the inducible isoform (COX-2), which is expressed in endothelial cells and macrophages after stimulation with LPS or some cytokines (Maier *et al.*, 1990; Fu *et al.*, 1990; Masferrer *et al.*, 1990; 1992). Recently it has been reported that, in the mouse macrophage cell line RAW264.7, NO activates both COX-1 and COX-2 by a guanosine 3':5'cyclic monophosphate (cyclic GMP)-independent mechanism (Salvemini *et al.*, 1993). Furthermore we have shown that prostacyclin biosynthesis in the lung of LPS-treated rats is increased by L-arginine and decreased by NOS inhibitors suggesting that endogenous NO may modulate prostanoid production (Sautebin & Di Rosa, 1994).

The role of NO in inflammation may, therefore, depend not only on its own ability to increase vascular permeability and oedema formation, possibly by increasing local blood flow, but also on the concomitant enhancement of proinflammatory prostaglandin biosynthesis due to the activation of COX. In this study we have investigated *in vivo* the modulation of prostaglandin biosynthesis by either exogenous or

[1] Author for correspondence.

endogenous NO using the arachidonic acid (AA)-induced rat paw oedema and measuring both the foot volume and the amounts of 6-keto-$PGF_{1\alpha}$, the stable metabolite of prostacyclin (PGI_2), in the oedematous fluid recovered from inflamed paws.

Methods

Paw oedema was induced in male Wistar rats (140–160 g) by subplantar injection of 0.1 ml saline containing AA or other agents which were given alone or in combination. AA was dissolved in absolute ethanol before dilution in saline. Other agents injected into the rat paw were: the NO donors 3-morpholino-sydnonimine-hydrochloride (SIN-1), S-nitroso-N-acetyl-D, L-penicillamine (SNAP) and sodium nitroprusside (SNP), the NOS inhibitor L-N^G-nitro arginine methyl ester (L-NAME), the NO scavenger haemoglobin (Hb), the inhibitor of soluble guanylate cyclase methylene blue (Mb), L-arginine, D-arginine, linoleic acid and indomethacin. In some experiments indomethacin was also given s.c. 1 h before paw injections.

The volume of the paw was measured by a plethysmometer (Basile, Italy) immediately after the injection as previously described (Di Rosa and Willoughby, 1971). Subsequent readings of the volume of the same paw were carried out at 30 min intervals up to 120 min and compared to the initial readings. The increase in paw volume was taken as oedema volume. In some experiments rats were killed in an atmosphere of CO_2 immediately after the readings at 90 min. Each inflamed paw was cut at the level of the calcaneus using a guillotine and gently spun (250 *g* for 15 min) in order to recover a sample of the oedamatous fluid. The blood was removed by filtering the samples through a 10,000 Mr cut off filter (Centricon 10, Amicon). The amount of 6-keto-$PFG_{1\alpha}$ in the sample was measured by radioimmunoassay (McLouf, 1982).

The total amount (TA) of 6-keto-$PGF_{1\alpha}$ present in the entire oedematous fluid of each paw was calculated as follows:

$$TA = \frac{\text{6-keto-}PGF_{1\alpha}\text{ in the sample (pmol)} \times \text{paw oedema volume (ml)}}{\text{sample volume (ml)}}$$

and expressed as pmol of 6-keto-$PGF_{1\alpha}$ per paw.

In some experiments the oedema was induced in rats treated with bacterial Salmonella typhosa lipopolysaccharide (LPS, 6 mg kg^{-1}) given i.p. 6 h prior to the paw injections.

Some control or LPS-treated rats did not receive the paw injection as they were used for the assay of the iNOS in the lung. These animals were anaesthetized with urethane (1.3 g kg^{-1}, i.p.) 6 h after LPS injection and lungs removed and washed. The activity of iNOS in the soluble lung extracts was evaluated by a radioisotopic technique based on the conversion of L-[U-^{14}C]-arginine to [U-^{14}C]-citrulline (Salter *et al.*, 1991). Proteins were assayed according to the method of Bradford (1976).

SIN-1 was a gift from A.G. Casella (Frankfurt), SNAP was provided by Dr H. Hodson, Dept. of Medicinal Chemistry, Wellcome Research Labs. (Beckenham, U.K.). LPS was obtained from Difco, the anti-6 keto $PGF_{1\alpha}$ serum was a gift from Dr G. Folco (Milan), L-[U-^{14}C] arginine and 6-keto [5,8,9,11,12,14,15 (n) -^{3}H] $PGF_{1\alpha}$ were from Amersham. All other compounds were from Sigma.

Data are expressed as means ± s.e.mean. Comparisons were made by an unpaired Student's two-tailed *t* test. The level of statistically significant difference was defined as $P<0.05$.

Results

Exogenous NO increases AA-induced oedema

In preliminary experiments we established that injection into the rat paw of L-NAME (up to 100 nmol), Hb (up to 30 μmol), Mb (up to 3 μmol), L- or D-arginine (up to 15 μmol) did not produce any detectable oedema. Injection of SIN-1 produced a moderate dose-related oedema with a peak response occurring at 60 min. Thus at this time the oedema induced by 2.5, 5 and 10 μmol/paw was 0.15 ± 0.02 ml (n = 6), 0.24 ± 0.02 ml (n = 6) and 0.33 ± 0.01 ml (n = 6), respectively. When SIN-1 (10 μmol) was coinjected with 10 μmol Hb the oedema was greatly reduced (data not shown) while it was completely suppressed by 30 μmol Hb (Figure 1). Coinjection of Mb (3 μmol) greatly reduced the SIN-1 oedema at 30 and 60 min and virtually abolished it at 90 and 120 min whereas the oedema resulted unaffected by coinjection of L-NAME (100 nmol) or indomethacin (3 μmol). Injection of SNAP (10 μmol) or SNP (10 μmol) produced a slight oedema with a peak response also occurring at 60 min (0.18 ± 0.03 ml, n = 6 and 0.12 ± 0.02 ml, n = 5, respectively). At 90 min the oedemas induced by SNAP and SNP were 0.12 ± 0.01 ml (n = 6) and 0.07 ± 0.01 ml (n = 5), respectively. Both SNAP- and SNP-induced oedemas were suppressed by Hb and Mb and unaffected by L-NAME and indomethacin (not shown). These results suggest that the oedema induced by the NO donors SIN-1, SNAP and SNP was actually due to exogenous NO acting through a cyclic GMP-dependent mechanism.

Injection into the rat paw of 300 nmol AA produced a very slight oedema. However, when the same amount of AA was coinjected with 10 μmol SIN-1, the resulting oedema was enormously increased, with a peak response occurring at 90 min (Figure 2). The oedema induced by AA (300 nmol) at 90 min was also significantly potentiated when it was coinjected with 10 μmol SNAP (0.20 ± 0.02 ml, n = 6, $P<0.01$) or SNP (0.12 ± 0.01 ml, n = 5, $P<0.05$). Interestingly no interaction occurred between linoleic acid (300 nmol) and SIN-1 (10 μmol) since the resulting oedema was superimposable on the one produced by SIN-1 given alone (Figure 2).

The oedema induced by AA + SIN-1 was virtually abolished when these two agents were given together with 30 μmol Hb whereas it was unaffected when they were given with 3 μmol Mb or 100 nmol L-NAME (Figure 3). Since the SIN-1 mediated increase of AA-induced oedema was abolished by the NO scavenger, Hb and unaffected by the guanylate cyclase inhibitor, Mb it appears that NO was acting through a cyclic GMP-independent mechanism. Indomethacin (3 μmol) produced a marked inhibition of AA + SIN-1 oedema (Figure 3) and it was equally effective when given s.c. at 5 mg kg^{-1} 1 h prior the paw injection of AA + SIN-1, for it reduced the oedema by about 50% throughout the time course of the reaction, suggesting that PGs were actually generated into the inflamed paw.

When various dose-combinations of AA + SIN-1 were used, the resulting oedema greatly increased in a dose-related fashion (Figure 4).

We determined the amount of 6-keto-$PGF_{1\alpha}$, the stable metabolite of PGI_2, in the oedematous fluid recovered from the inflamed paw of rats (Table 1). The results of these experiments show that SIN-1 dose-dependently increased the amount of PGI_2 produced by the tissues of the inflamed paw. The SIN-1-mediated increase of PGI_2 was significantly reduced by Hb and indomethacin but was unaffected by Mb.

Endogenous NO increases AA-induced oedema

The oedema produced by paw injection of 150 or 300 nmol AA was virtually undetectable, while 600 nmol induced a measurable oedema with a peak response occurring at 90 min (Figure 5). The AA-induced oedema was greatly inhibited by

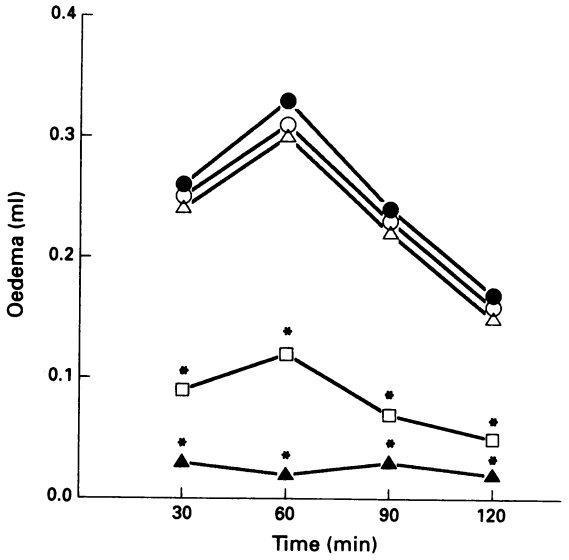


Figure 1 Effect of N^G-nitro-L-arginine methyl ester (L-NAME) 100 nmol (△), indomethacin 3 μmol (○), methylene blue 3 μmol (□) and haemoglobin 30 μmol (▲) on rat paw oedema induced by 3-morpholino-sydnonimine (SIN-1) 10 μmol. The oedema induced by 10 μmol SIN-1 given alone (control) is shown by (●). Data are expressed as means from 5–6 animals. Standard errors (not shown) were always less than 15% of the respective means. $*P<0.01$ *vs* control group.

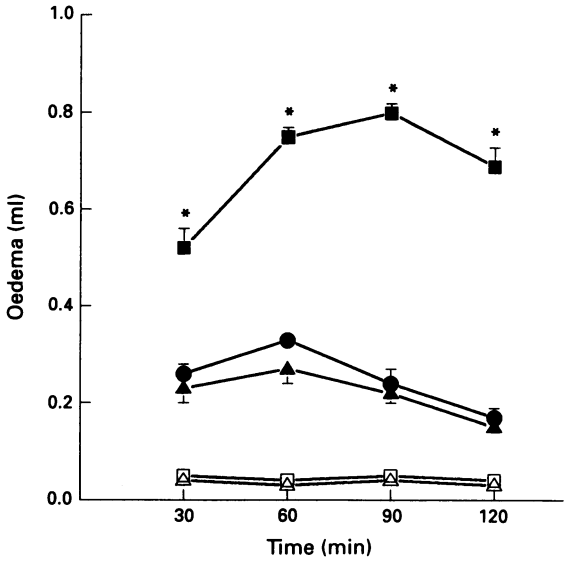


Figure 2 Rat paw oedema induced by 300 nmol arachidonic acid (AA) given alone (□) or in combination with 10 μmol 3-morpholino-sydnonimine (SIN-1) (■) and by 300 nmol linoleic acid given alone (△) or in combination with 10 μmol SIN-1 (▲). The oedema induced by 10 μmol SIN-1 alone (control) is shown by (●). Data are expressed as means ± s.e.mean from 5–6 animals. Standard errors less than 5% of the respective means are not shown because they are covered by the symbols. $*P<0.01$ *vs* control group.

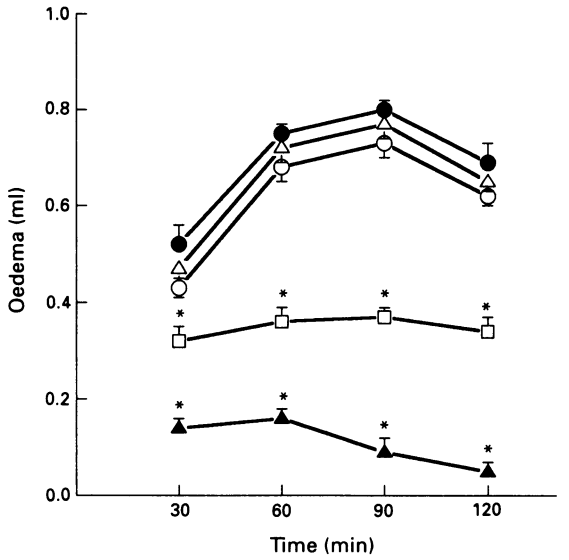


Figure 3 Effect of methylene blue (Mb) 3 μmol (△), N^G-nitro-L-arginine methyl ester (L-NAME) 100 nmol (○), indomethacin 3 μmol (□) and haemoglobin (Hb) 30 μmol (▲) on the oedema induced by the combination of arachidonic acid (AA) 300 nmol + 3-morpholino-syndnonimine (SIN-1) 10 μmol. The oedema induced by the combination AA + SIN-1 (control) is shown by (●). Data are expressed as means ± s.e.mean from 5–6 animals. $*P<0.01$ *vs* control group.

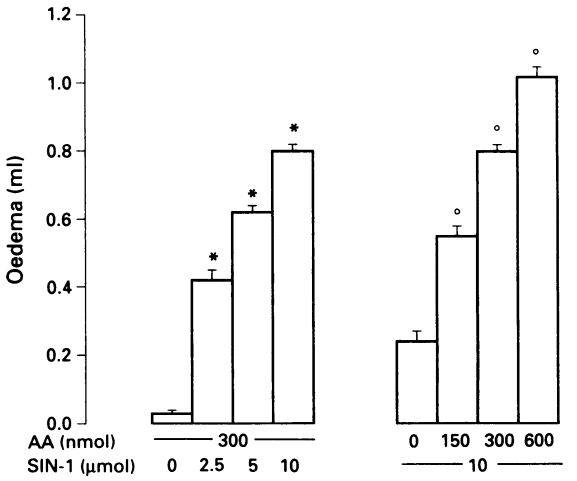


Figure 4 Rat paw oedema induced by various combinations of arachidonic acid (AA) and 3-morpholino-sydnonimine (SIN-1). Each column represents the mean value ± s.e.mean (bar) of the oedema occurring at 90 min. ($n=5-6$). $*P<0.01$ *vs* 300 nmol AA given alone; $°P<0.01$ *vs* 10 μmol SIN-1 given alone.

coinjection of indomethacin (3 μmol), showing that the response was due in part to COX activity. When AA (600 nmol) was coinjected with L-NAME (100 nmol) or Hb (30 μmol) the oedema was greatly reduced whereas it was not modified by Mb (3 μmol) showing that endogenous NO modulates AA-induced oedema by a cyclic GMP-independent mechanism. However when L-arginine (15 μmol) was coinjected with AA (600 nmol) no interaction occurred between these two agents for the resulting oedema was superimposable on the response of AA given alone (Figure 5). Since it is known that an excess of L-arginine does not increase the activity of the cNOS this result suggests that, in our conditions, it is the constitutive enzyme that generates the NO responsible of the enhanced formation of PGs from AA.

Therefore we decided to investigate the effect of L-arginine on AA-induced oedema in LPS-treated rats in which the iNOS is also expressed. The iNOS activity was measured in the lung since it has been shown that this tissue expresses

Table 1 Alterations in amounts of 6-keto-$PGF_{1\alpha}$ in rat paw oedema induced by arachidonic acid (AA, 300 nmol) given alone or coinjected with various agents

Group	*Agents* (μmol)	*6-keto-$PGF_{1\alpha}$* (pmol per paw)	n
1	AA	89 ± 12	5
2	SIN-1 10	104 ± 14	4
3	AA + SIN-1 2.5	189 ± 29†	4
4	AA + SIN-1 5	226 ± 15†	4
5	AA + SIN-1 10	288 ± 8†	7
6	AA + SIN-1 10 + Hb 30	92 ± 13*	4
7	AA + SIN-1 10 + Mb 3	254 ± 51	3
8	AA + SIN-1 10 + indomethacin 3	163 ± 25*	4
9	AA + SIN-1 10 + indomethacin 5 mg kg^{-1}	145 ± 12*	4

The amounts of 6-keto-$PGF_{1\alpha}$ were measured by radioimmunoassay in samples of the oedematous fluid recovered from the inflamed paws 90 min after the injections and expressed as total amount present in each paw. In group 9 indomethacin was given s.c. 1 h before paw injection. †$P<0.01$ *vs* group 1; *$P<0.01$ *vs* group 5. For abbreviations, see text.

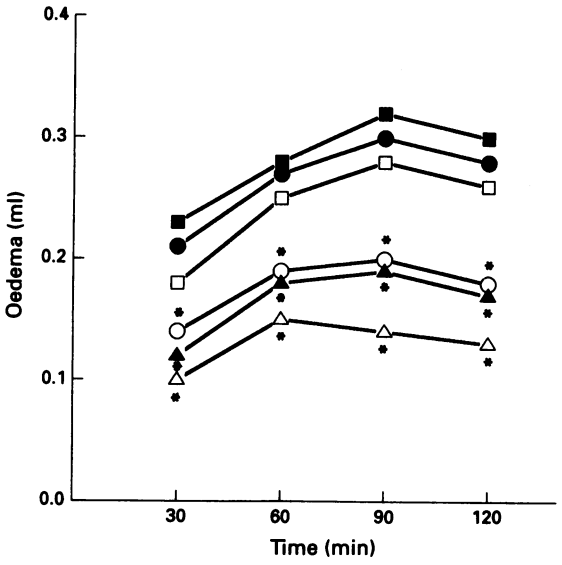


Figure 5 Effect of L-arginine 15 μmol (■), methylene blue 3 μmol (□), indomethacin 3 μmol (○), haemoglobin (Hb) 30 μmol (▲) and N^G-nitro-L-arginine methyl ester (L-NAME) 100 nmol (△) on rat paw oedema induced by 600 nmol arachidonic acid (AA). The oedema induced by 600 nmol AA given alone (control) is shown by (●). Data are expressed as means from 5–6 animals. Standard errors (not shown) were always less than 15% of the respective means. *$P<0.01$ *vs* control group.

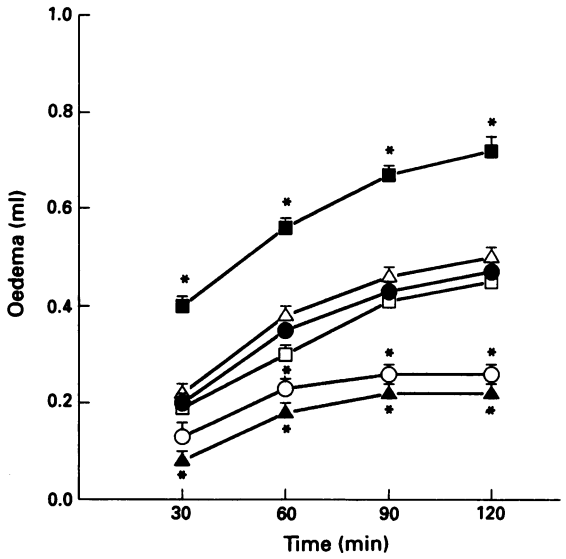


Figure 6 Effect of L-arginine 15 μmol (■), D-arginine 15 μmol (△), methylene blue 3 μmol (□), haemoglobin 30 μmol (○) and L-NAME 100 nmol (▲) on paw oedema induced by 300 nmol arachidonic acid (AA) in LPS-treated rats. The oedema induced by 300 nmol AA given alone (control) is shown by (●). Animals were treated with LPS (6 mg kg^{-1}, i.p.) 6 h before paw injection. Data are expressed as means ± s.e.mean from 5–6 animals. Standard errors less than 5% of the respective means are not shown because they are covered by the symbols. *$P<0.01$ *vs* control group.

Table 2 Alterations in amounts of 6-keto-$PGF_{1\alpha}$ in paw oedema induced in LPS-treated rats by arachidonic acid (AA, 300 nmol) given alone or coinjected with various agents

Group	*Agents* (μmol)	*6-keto-$PGF_{1\alpha}$* (pmol per paw)	n
1	AA (alone)	289 ± 21	7
2	AA + L-arginine 15	384 ± 54*	3
3	AA + D-arginine 15	286 ± 12	3
4	AA + L-NAME 0.1	102 ± 4**	4
5	AA + Hb 30	148 ± 8**	4
6	AA + Mb 3	278 ± 18	3

The amounts of 6-keto-$PGF_{1\alpha}$ were measured by radioimmunoassay in samples of the oedematous fluid recovered from the inflamed paws 90 min after the injections and expressed as the total amount present in each paw. Lipopolysaccharide (LPS, 6 mg kg^{-1}) was given i.p. 6 h before paw injection. *$P<0.05$, **$P<0.01$ *vs* group 1. For abbreviations, see text.

iNOS in LPS-challenged rats (Knowles *et al.*, 1990). The iNOS activity in the lung of control rats was undetectable whereas it was substantially induced in lungs removed 6 h after rats were treated with LPS (6 mg kg^{-1}, i.p.). Thus in our experimental conditions the conversion rate of L-arginine to L-citrulline was 14.2 ± 1.1 ($n = 5$) pmol min^{-1} per mg of lung proteins.

In LPS-treated rats, paw injection of 300 nmol AA induced a long lasting oedema (Figure 6) which was significantly greater when compared to the almost undetectable paw swelling produced by the same amount of AA given to normal rats (Figure 2). AA-induced oedema in LPS-treated rats was greatly reduced by coinjection of either L-NAME (100 nmol) or Hb (30 μmol) whereas it was unaffected by Mb (3 μmol). Interestingly, in LPS-treated rats, unlike normal rats (Figure 4), coinjection of L- but not of D-arginine (15 μmol) significantly enhanced AA-induced oedema. This enhancement probably depends on the increased amounts of NO generated by the iNOS, the enzyme isoform whose activity, unlike that of cNOS, is stimulated by an excess of substrate.

The amounts of 6-keto-$PGF_{1\alpha}$ found in the inflamed paws of LPS-treated rats correlated well with the severity of the oedema induced by AA alone or in combination with the various agents (Table 2).

These results suggest that the enhancement of AA-induced oedema in LPS-treated rats, although it may depend in part on the coexpression of COX-2 which increases the conversion of AA to prostaglandins is due to endogenous NO which regulates prostaglandin biosynthesis.

Discussion

In this study we have shown that both exogenous and endogenous NO greatly increase AA-stimulated biosynthesis of prostaglandins. The AA-induced rat paw oedema was significantly increased by the NO-donors SNAP, SNP and SIN-1, the active metabolite of molsidomine (Noack & Feelisch, 1989). SIN-1 produced a moderate oedema due to the release of exogenous NO acting through a cyclic GMP-dependent mechanism since it was suppressed by the NO scavenger, Hb and by the soluble guanylate cyclase inhibitor, Mb. This result is in agreement with our previous results showing that endogenous NO has a role in the regulation of increased vascular permeability and oedema formation, possibly by increasing local blood flow (Ialenti *et al.*, 1992).

Inactive doses of AA, but not of linoleic acid, when injected concomitantly with SIN-1, produced a marked paw oedema which was correlated with increased amounts of 6-keto-$PGF_{1\alpha}$, the stable metabolite of PGI_2, in the fluid recovered from inflamed paws.

Both oedema and PGI_2 biosynthesis induced by the combination AA + SIN-1 were greatly suppressed by either the NO scavenger Hb or the COX inhibitor indomethacin but remained unaffected by Mb, an inhibitor of the soluble guanylate cyclase. These results demonstrate that exogenous NO released by SIN-1 increases AA-stimulated prostaglandin biosynthesis by activating COX through a cyclic GMP-independent mechanism which, as has been suggested (Salvemini *et al.*, 1993), possibly depends on a direct interaction of NO with the iron-haeme centre of COX.

Our results suggest that endogenous NO, acting via the same cyclic GMP-independent mechanism, increases AA-stimulated prostaglandin biosynthesis in both normal rats, in which only cNOS and COX-1 are present, and in LPS-treated rats, in which the iNOS and COX-2 are also expressed.

In normal rats, the oedema induced by a high dose of AA was reduced by L-NAME, Hb or indomethacin, unaffected by Mb and, as expected, it was not modified by L-arginine since it is known that an excess of substrate does not increase the activity of cNOS. In LPS-treated rats, a low dose of AA, which was inactive in normal animals, induced a very marked oedema. This oedema correlated with increased prostaglandin biosynthesis which depended not only on the activity of COX-2 but also on the generation of large amounts of NO by the iNOS.

In LPS-treated animals, the AA-induced oedema was reduced by L-NAME, Hb and indomethacin, unaffected by Mb and, unlike in normal rats, was increased by L- but not by D-arginine. The LPS-induced iNOS can be stimulated by an excess of substrate, so that larger amounts of NO are generated which presumably in turn activated COX. These findings are also supported by our previous report showing that in the lung of LPS-treated rats PG generation was increased by L-arginine and decreased by NOS inhibitors (Sautebin & Di Rosa, 1994).

Our results demonstrate that NO increases AA-stimulated biosynthesis of prostaglandin *in vivo* by a cyclic GMP-independent mechanism and are in agreement with recent data showing that NO activates COX enzymes *in vitro* (Salvemini *et al.*, 1993).

The findings of this study may have physiological, pathological and therapeutic relevance. In normal rats, either inhibition of cNOS by L-NAME or inactivation of NO by Hb result in a reduced biosynthesis of prostaglandins suggesting that even in physiological conditions COX activity may be permanently stimulated by endogenous NO. Thus the synergistic inhibitory effects of NO and PGI_2 on vascular smooth muscle tone and platelets aggregation may depend not only on the concomitant elevation in target cells of the respective second messengers, cyclic GMP and cyclic AMP, but also on the increased biosynthesis of PGI_2 induced by NO interacting directly with COX through a cyclic GMP-independent mechanism.

In addition it is possible that the vasoconstriction and elevation of systemic blood pressure induced by NOS inhibitors (Gardiner *et al.*, 1990) could be due not only to the removal of endogenous NO but also to a consequent reduced production of vasodilator prostaglandins. This last mechanism might be of interest for a clearer understanding of the beneficial effects of NOS inhibitors observed in animals and man in the treatment of vascular dysfunctions occurring in cytokine-induced hypotension or LPS-induced shock (Kilbourn *et al.*, 1990; Thiemermann *et al.*, 1990; Petros & Vallance, 1993).

The interaction between the NO and COX pathways should also be relevant in acute and chronic inflammation which appear to be modulated by NO since in both types of process the degree of lesion was reduced by NOS inhibitors and exacerbated by L-arginine (Ialenti *et al.*, 1992; 1993). Thus in a pathological condition like inflammation in which the iNOS and COX-2 enzymes are coexpressed, there is an NO-mediated increase of proinflammatory prostaglandins that may amplify the inflammatory response.

We have shown that PGE_2 and iloprost (a stable analogue of PGI_2) both at nanomolar concentrations inhibited the LPS-stimulated induction of iNOS in the murine macrophage cell line J774 (Marotta *et al.*, 1992). Furthermore, PGE_2 and PGI_2 have been found to inhibit the release of TNF-α from activated mouse peritoneal macrophages (Marcinkiewicz, 1991), rat alveolar macrophages (Mohr *et al.*, 1992) and human peripheral blood mononuclear cells (Haynes *et al.*, 1992). Since it is known that this cytokine induces iNOS, these findings support the hypothesis that the NO-mediated overproduction of prostaglandins may also act as a negative feedback preventing excessive or prolonged induction of iNOS (Figure 7).

In conclusion we have demonstrated that NO modulates PG biosynthesis *in vivo*, in both physiological and pathological conditions, and suggest that not only does NO activate COX enzymes, as has been proposed by Salvemini *et al.* (1993), but also that in some pathological conditions, such as inflammation or sepsis, in which both iNOS and COX-2 are present, some products of COX may downregulate the expression of iNOS.

Finally it would be interesting to ascertain whether the therapeutic efficacy of nitrovasodilators, which is due to their release of exogenous NO, depends entirely on the activation of soluble guanylate cyclase or if it may be due, at least in part, to the stimulation of COX activity, via a cyclic GMP-independent mechanism, which in turn leads to increased production of vasodilator prostaglandins.

The authors wish to thank Annie Higgs for her assistance in the preparation of the manuscript.

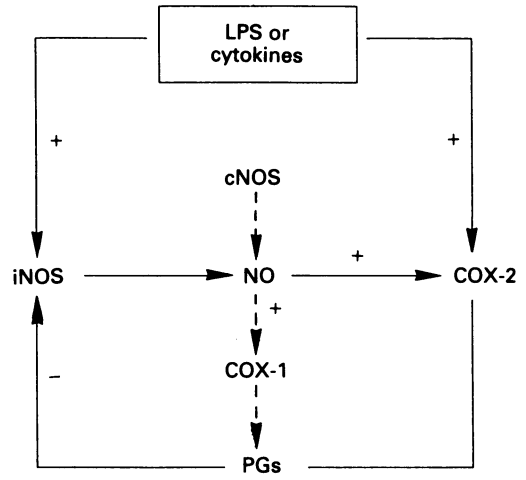


Figure 7 Model for the mutual interactions between NO synthase (NOS) and cyclo-oxygenase (COX) systems in physiological (dotted arrows) or pathological conditions (solid arrows). For details see Discussion.

References

BRADFORD, M.M. (1976). A rapid and sensitive method for the quantification of protein dye binding. *Anal. Biochem.*, **72**, 248–254.

DI ROSA, M., RADOMSKI, M., CARNUCCIO, R. & MONCADA, S. (1990). Glucocorticoids inhibit the induction of nitric oxide synthase in macrophages. *Biochem. Biophys. Res. Commun.*, **172**, 1246–1252.

DI ROSA, M. & WILLOUGHBY, D.A. (1971). Screens for anti-inflammatory drugs. *J. Pharm. Pharmacol.*, **23**, 297–298.

FU, J.Y., MASFERRER, J.L., SIEBERT K., RAZ, A. & NEEDLEMAN, P. (1990). The induction and suppression of prostaglandin H_2 synthase (cyclo-oxygenase) in human monocytes. *J. Biol. Chem.*, **265**, 16737–16740.

GARDINER, S.M., COMPTON, A.M., BENNETT, T., PALMER, R.M.J. & MONCADA, S. (1990). Regional haemodynamic changes during oral ingestion of N^G-nitro-L-arginine methyl ester in conscious Brattleboro rats. *Br. J. Pharmacol.*, **101**, 10–12.

HAYNES, D.R., WHITEHOUSE, M.W. & VERNON-ROBERTS, B. (1992). The prostaglandin E_1 analogue, misoprostol, regulates inflammatory cytokines and immune functions in vitro like the natural prostaglandins E_1, E_2 and E_3. *Immunology*, **76**, 251–257.

HIBBS, J.B., Jr., TAINTOR, R.R., VAVRIN, Z. & RACHLIN, E.M. (1988). Nitric oxide: a cytotoxic activated macrophage effector molecule. *Biochem. Biophys. Res. Commun.*, **157**, 87–94.

IALENTI, A., IANARO, A., MONCADA, S. & DI ROSA, M. (1992). Modulation of acute inflammation by endogenous nitric oxide. *Eur. J. Pharmacol.*, **211**, 177–182.

IALENTI, A., MONCADA, S. & DI ROSA, M. (1993). Modulation of adjuvant arthritis by endogenous nitric oxide. *Br. J. Pharmacol.*, **110**, 701–706.

KILBOURN, R.G., GROSS, S.S., JUBRAN, A., ADAMS, J., GRIFFITH, O.W., LEVI, R. & LODATO, R.F. (1990). N^G-methyl-L-arginine inhibits tumor necrosis factor-induced hypotension: implications for the involvement of nitric oxide. *Proc. Natl. Acad. Sci. U.S.A.*, **87**, 3629–3632.

KNOWLES, R.G., MERRETT, M., SALTER, M. & MONCADA, S. (1990). Differential induction of brain, lung and liver nitric oxide synthase by endotoxin in the rat. *Biochem. J.*, **270**, 833–836.

KOLB, H., KIESEL, U., KRÖNCKE, K.D. & KOLB-BACHOFEN V. (1991). Suppression of low dose streptozotocin induced diabetes in mice by administration of a nitric oxide synthase inhibitor. *Life Sci.*, **49**, PL-213–217.

MAIER, J.A.M., HLA, T. & MACIAG, T. (1990). Cyclo-oxygenase is an immediate early gene induced by interleukin-1 in human endothelial cells. *J. Biol. Chem.*, **265**, 10805–10808.

MARCINKIEWICZ, J. (1991). In vitro cytokine release by activated murine peritoneal macrophages: role of prostaglandins in the differential regulation of tumor necrosis factor alpha, interleukin-1 and interleukin-6. *Cytokine*, **3**, 327–332.

MAROTTA, P., SAUTEBIN, L. & DI ROSA, M. (1992). Modulation of induction of nitric oxide synthase by eicosanoids in the murine macrophage cell line J774. *Br. J. Pharmacol.*, **107**, 640–641.

MASFERRER, J.L., SEIBERT, K., ZWEIFEL, B & NEEDLEMAN, P. (1992). Endogenous glucocorticoids regulate an inducible cyclo-oxygenase enzyme. *Proc. Natl. Acad. Sci. U.S.A.*, **89**, 3917–3921.

MASFERRER, J.L., ZWEIFEL, B., SEIBERT, K. & NEEDLEMAN, P. (1990). Selective regulation of cellular cyclo-oxygenase by dexamethasone and endotoxin in mice. *J. Clin. Invest.*, **86**, 1375–1379.

MCLOUF, J. (1982). A radioimmunoassay for 6-keto-$PGF_{1\alpha}$. In *Methods in Enzymology; Prostaglandins and Arachidonic Acid Metabolism*, vol. **86**. ed. Lands, W.E.M. & Smith, W.L. p. 273. New York: Academic Press Inc.

MOHR, C., DAVIS, G.S., GRAEBNER, C., HEMENWAY, D.R. & GEMSA, D. (1992). Enhanced release of prostaglandin E_2 from macrophages of rats with silicosis. *Am. J. Respir. Cell. Mol. Biol.*, **6**, 390–396.

MONCADA, S., PALMER, R.M.J. & HIGGS, E.A. (1991). Nitric oxide: physiology, pathophysiology and pharmacology. *Pharmacol. Rev.*, **43**, 109–142.

NOACK, E. & FEELISCH, M. (1989). Molecular aspects underlying the vasodilator action of molsidomine. *J. Cardiovasc. Pharmacol.*, **14**, S1–S5.

PETROS, A. & VALLANCE, P. (1993). Nitric oxide synthase inhibitors in human septic shock. In *Nitric oxide: Brain and Immune System*. ed. Moncada, S., Nisticò, G. & Higgs, E.A., pp. 259–264. Portland Press Proceedings.

REES, D.D., PALMER, R.M.J., SCHULZ, R., HODSON, H.F. & MONCADA, S. (1990). Characterization of three inhibitors of endothelial nitric oxide synthase *in vitro* and *in vivo*. *Br. J. Pharmacol.*, **101**, 746–752.

SALTER, M., KNOWLES, R.G. & MONCADA, S. (1991). Widespread tissue distribution, species distribution and changes in activity of Ca^{2+}-independent nitric oxide synthase. *FEBS*, **291**, 145–149.

SALVEMINI, D., MISKO, T.P., MASFERRER, J.L., SEIBERT, K., CURRIE, M.G. & NEEDLEMAN, P. (1993). Nitric oxide activates cyclo-oxygenase enzymes. *Proc. Natl. Acad. Sci. U.S.A.*, **90**, 7240–7244.

SAUTEBIN, L. & DI ROSA, M. (1994). Nitric oxide modulates prostacyclin biosynthesis in the lung of endotoxin treated rats. *Eur. J. Pharmacol.*, (in press).

THIEMERMANN, C. & VANE, J. (1990). Inhibition of nitric oxide by bacterial lipopolysaccharides in the rat in vivo. *Eur. J. Pharmacol.*, **182**, 591–595.

(Received April 26, 1994
Revised August 4, 1994
Accepted September 20, 1994).

British Journal of Pharmacology (1995) 114, 329–338 © 1995 Stockton Press All rights reserved 0007–1188/95 $9.00

Cytosolic calcium concentration-force relation during contractions in the rabbit femoral artery: time-dependency and stimulus specificity

Yutaka Fukuizumi, Sei Kobayashi, Junji Nishimura & [1]Hideo Kanaide

Division of Molecular Cardiology, Research Institute of Angiocardiology, Faculty of Medicine, Kyushu University, 3-1-1 Maidashi, Higashi-ku, Fukuoka 812, Japan

1 By use of front-surface fluorometry with fura-2-loaded rabbit femoral arterial strips, both the cytosolic Ca^{2+} concentration ($[Ca^{2+}]_i$) and force were simultaneously monitored. By utilizing the $[Ca^{2+}]_i$-force curves, we were thus able to examine the temporal changes in the relationships between $[Ca^{2+}]_i$ and force ($[Ca^{2+}]_i$-force relationship) during contractions induced by a high external K^+ solution, noradrenaline (NA) and 5-hydroxytryptamine (5-HT).

2 The 'basic' $[Ca^{2+}]_i$-force relationship of the Ca^{2+}-induced contractions was obtained by the cumulative applications of extracellular Ca^{2+} (0–10 mM) during 118 mM K^+-depolarization (Ca^{2+}-contractions).

3 When each vascular strip was exposed to high external K^+ (30 mM K^+ –118 mM K^+) solutions, the $[Ca^{2+}]_i$ abruptly increased until it reached a peak, and then slightly decreased and eventually reached a steady-state level. The force also rapidly rose to reach a maximum plateau level. The changes in $[Ca^{2+}]_i$ were more rapid than those in the force. Thus, the $[Ca^{2+}]_i$-force curves observed during the contractions induced by high$^+$ (30 mM–118 mM) solutions showed a counter-clockwise rotation, over time. The entire curve shifted to the right, in a concentration-dependent manner, as compared with the line of the 'basic' $[Ca^{2+}]_i$-force relationship of the Ca^{2+}-contraction. However, the $[Ca^{2+}]_i$-force relationship of the steady-state of contractions induced by the single dose applications of high K^+ (30 mM–118 mM) overlapped with the line of the 'basic' $[Ca^{2+}]_i$-force relationship of Ca^{2+}-contractions.

4 As references, the levels of $[Ca^{2+}]_i$ and the force at rest (without stimulation) and at the steady-state of the contractions induced by a single dose application of 118 mM K^+ solution were designated as 0% and 100%, respectively. When the vascular strips were exposed to NA (10^{-5} M) and to 5-HT (10^{-4} M), the $[Ca^{2+}]_i$ abruptly rose, and reached a peak (107.1 ± 5.8% and 101.3 ± 2.8%, respectively) after 1 min and 2 min, respectively (the $[Ca^{2+}]_i$-rising phase), and thereafter declined with a similar time course (the $[Ca^{2+}]_i$-declining phase) until reaching a low steady level (the steady-state phase). The force induced by 10^{-5} M NA and 10^{-4} M 5-HT reached a peak at 4 min (129%) and at 2 min (115%), respectively, and thereafter gradually declined. In contrast to the similarity in the $[Ca^{2+}]_i$ transient between NA and 5-HT, the force induced by NA declined more slowly and reached higher steady levels than that seen with 5-HT. The level of force 20 min after the application of NA and 5-HT was 112% and 72%, respectively.

5 In the entire time course of the 5-HT-induced contraction, i.e., in $[Ca^{2+}]_i$-rising, $[Ca^{2+}]_i$-declining and the steady-state phases, the $[Ca^{2+}]_i$-force relation was almost the same as that of the Ca^{2+}-contractions. In the $[Ca^{2+}]_i$-rising phase of NA-induced contraction, the $[Ca^{2+}]_i$-force relation was similar to that of the Ca^{2+}-contractions. However, in the $[Ca^{2+}]_i$-declining and the steady-state phases, NA produced a greater force than that expected from a given change in the $[Ca^{2+}]_i$ of the Ca^{2+}-contractions, which resulted in a leftward shift of the $[Ca^{2+}]_i$-force relation. The extent of the leftward shift depended on the concentration of NA.

6 These results suggest that (1) changes in $[Ca^{2+}]_i$ precede changes in the force during the high K^+-induced contraction, (2) in the initial $[Ca^{2+}]_i$-rising phase of the contractions induced by NA or by 5-HT, the $[Ca^{2+}]_i$-force relation is similar to that of Ca^{2+}-contractions, and (3) in the subsequent $[Ca^{2+}]_i$-declining and the steady-state phases of the contractions, 5-HT demonstrated little enhancement in force for the given levels of $[Ca^{2+}]_i$, while NA induced a greater force for the given levels of $[Ca^{2+}]_i$, in the rabbit femoral artery. Based on the above findings we suggest the presence of a time-dependent and stimulus-specific modulation of the Ca^{2+} sensitivity in the contractile apparatus of arterial smooth muscles.

Keywords: Vascular smooth muscle; depolarization; 5-hydroxytryptamine; noradrenaline; cytosolic calcium

Introduction

Changes in the cytosolic concentrations of Ca^{2+} ($[Ca^{2+}]_i$) play a central role in the excitation-contraction coupling in vascular smooth muscle cells (Kuriyama *et al.*, 1982; Somlyo, 1985; Sommerville & Hartshorne, 1986, for review). The contraction of vascular smooth muscles is initiated by an increase in $[Ca^{2+}]_i$ and the subsequent phosphorylation of the myosin light chain by the complex of Ca^{2+}-calmodulin and the myosin light-chain kinase (Kamm & Stull, 1985). Several lines of evidence, obtained with the use of Ca^{2+} indicators and through studies of steady-state contractions, have suggested the presence of a greater force/Ca^{2+} ratio which was observed following stimulation with various kinds of agonists, as compared with that following the membrane depolarization with high K^+ (Morgan & Morgan, 1984; Himpens & Somlyo, 1988; Rembold & Murphy, 1988; Kodama *et al.*, 1989; Abe *et al.*, 1990; Hirano *et al.*, 1991). Using receptor-coupled permeabilized vascular smooth mus-

[1] Author for correspondence.

cle specimens with staphylococcal α-toxin (Nishimura *et al.*, 1988; Kitazawa *et al.*, 1989) and with β-escin (Kobayashi *et al.*, 1989), it was demonstrated that the enhancement of Ca^{2+} sensitivity is mediated by the receptor coupled activation of the G-protein. In addition to the steady-state relation between the Ca^{2+} and force, the Ca^{2+}-force relation may vary over time (the duration of contraction) because of the presence of a time-dependent activation and the inactivation of myosin light chain phosphatase (Kamm & Stull, 1985), an 'economic', low phosphorylation-high force state ('latch') (Murphy, 1989), and a cooperative reattachment of the unphosphorylated crossbridges (Somlyo & Somlyo, 1990), in vascular smooth muscles. However, temporal changes in the $[Ca^{2+}]_i$-force relation during vascular smooth muscle contractions has received relatively little attention, except for a few studies on pulmonary (Himpens *et al.*, 1990) and coronary arteries (Hirano *et al.*, 1991), in which the kinetics of the $[Ca^{2+}]_i$-force relation were not discussed in detail.

In the present study, we used three different types of stimuli: high external K^+-depolarization, 5-hydroxytryptamine (5-HT), and noradrenaline (NA). NA, which is released from sympathetic nerve endings, modulates vascular tone. 5-HT, which is released from aggregated platelets, causes vasospasm and hypertension. While these two agonists cause contractions mediated by specific receptor activation, it is generally accepted that depolarization with a high external K^+-solution induces contractions without stimulation of the receptor-coupled signal transduction. We used front-surface fluorometry of fura-2 to examine the temporal changes in the $[Ca^{2+}]_i$-force relation during contractions induced by high K^+-depolarization, 5-HT, and NA, and then compared them with the 'basic' $[Ca^{2+}]_i$-force relation of Ca^{2+}-induced contractions (Ca^{2+}-contractions), obtained by the cumulative applications of extracellular Ca^{2+} during 118 mM K^+-depolarization, in intact smooth muscle strips from the rabbit femoral artery. Based on our results we found that the $[Ca^{2+}]_i$-force relation is not constant during muscle contraction but varies, depending on the type of agonists as well as on the length of time after the application.

Methods

Tissue preparation

The study protocol was approved by the Animal Care and Committee of Research, Institute of Angiocardiology, Faculty of Medicine, Kyushu University. Japanese white rabbits (male, 16–20 weeks old, body weight 2.5–3.0 kg) were killed with sodium pentobarbitone (100 mg kg^{-1}, i.v.) and the femoral arteries were immediately excised. The adventitia and fat were removed by dissection, under a binocular microscope. The endothelial cells were then removed by rubbing the intraluminal surface with a cotton swab (Furchgott & Zawadzki, 1980). Medial preparations were cut into approximately 1 × 3 mm circular strips, 0.2 mm thick.

Fura-2 loading

The vascular strips thus obtained were loaded with the $[Ca^{2+}]_i$ indicator dye, fura-2 by incubation in the medium containing 50 μM fura-2/AM (an acetoxymethyl ester form of fura-2) and 2.5% foetal bovine serum for 4–5 h at 37°C. Subsequently, the strips were washed with physiological salt solution (PSS) containing 1.25 mM Ca^{2+} at 37°C to remove the dye from the extracellular space and were then equilibrated in normal PSS for at least 1 h before the initiation of measurements. The strips thus treated showed a specific peak of the fluorescence emission spectrum for fura-2 (500 nm) as well as a specific peak and valley of the fluorescence excitation spectrum for fura-2, 340 nm and 380 nm, respectively, which were determined by a fluorescence spectrophotometer (model 650-40, Hitachi, Tokyo, Japan). Loading the vascular strips with fura-2 did not alter the time course or the maximum levels of force development during the 118 mM K^+-induced depolarization (data not shown), which suggested that no tissue damage occurred due to any possible acidification of the cells as a result of formaldehyde release on AM-ester hydrolysis (Tsien *et al.*, 1982; Rink & Pozzan, 1985).

Measurement of force

The strips were mounted vertically in a quartz organ bath, and a force-transducer (strain gauge TB-612T, Nihon Kohden, Japan) was used. During a 1 h equilibration period, the strips were stimulated with 118 mM K^+ every 15 min, and the resting tension was increased, in a stepwise manner. After equilibration, the resting tension was adjusted to 350 mg. The force development was expressed as a percentage, assuming the values in normal (5.9 mM K^+) and 118 mM K^+ PSS to be 0% and 100%, respectively.

Measurement of $[Ca^{2+}]_i$

Changes in the fluorescence intensity of the fura-2-Ca^{2+} complex were simultaneously monitored during the measurement of the force, using front-surface fluorometry (Abe *et al.*, 1990; Hirano *et al.*, 1991; Ushio-Fukai *et al.*, 1993). The fluorescence intensity was measured by a fluorometer, which was specially designed for fura-2 fluorometry (CAM-OF-1), in collaboration with Japanese Spectroscopic Co, Tokyo, Japan. In brief, the strips were illuminated by guiding the alternating (400 Hz) 340 nm and 380 nm excitation light from a xenon light source through quartz optic fibres arranged in a concentric inner circle (diameter = 3 mm). The surface fluorescence of the strips was collected by glass optic fibres arranged in an outer circle (diameter = 7 mm) and introduced through a 500 nm band-pass filter (full width at half maximum transmission = 10 nm) into a photon-counting photomultiplier. The data of the ratio fluorescence (F340/F380; $[Ca^{2+}]_i$) and force, as well as F340 and F380, were presented on the recorder paper with a trace speed of 1 mm s^{-1} (for agonists stimulation) and 5 mm s^{-1} (for high K^+-depolarization) with a sampling rate of 400 Hz and/or were stored in a Macintosh computer using a data acquisition system (MacLab) with a sampling rate of 17 Hz. The ratio of the 500 nm fluorescence at 340 nm excitation to that at 380 nm excitation was expressed as a percentage, assuming the values in normal (5.9 mM K^+) and 118 mM K^+ PSS to be 0% and 100%, respectively. When the absolute values of $[Ca^{2+}]_i$ at 0% (at rest) and during 118 mM K^+-depolarization (100%) were determined in 8 separate and different measurements, using the equation described by Grynkiewicz *et al.* (1985) and K_d value of 224 nM (37°C), the 0% and 100% fluorescence ratios were 183 nM and 717 nM, respectively. These values are shown in the figures together with the % fluorescence ratio as the $[Ca^{2+}]_i$ levels for convenience.

Drugs and solutions

The physiological salt solution (PSS) consisted of the following composition (in mM): NaCl 123, KCl 4.7, $NaHCO_3$ 15.5, KH_2PO_4 1.2, $MgCl_2$ 1.2, $CaCl_2$ 1.25, and D-glucose 11.5. High K^+ PSS was identical with normal PSS, except for an equimolar substitution of KCl for NaCl. The Ca^{2+}-free solution was identical with normal PSS, except for a substitution of 2 mM ethyleneglycol-*bis*(β-aminoethylether)-*N*,*N*,*N*',*N*'-tetraacetic acid (EGTA) for 1.25 mM $CaCl_2$. All solutions were gassed with a mixture of 95% O_2 and 5% CO_2 (pH adjusted to 7.4 at 37°C). Noradrenaline hydrochloride (NA) and 5-hydroxytryptamine creatinine sulphate (5-HT) were purchased from Sigma (U.S.A.). Fura-1/AM was purchased from Dojindo Laboratories (Kumamoto, Japan).

Data analysis

The values are expressed as the mean ± the standard error (s.e.). Student's t test was used to determine the statistical significance. The statistical analysis of the shift of the $[Ca^{2+}]_i$-force curves was carried out by an analysis of covariance. $P<0.05$ was considered to be significant.

Results

Changes in $[Ca^{2+}]_i$ and the force development induced by the cumulative applications of extracellular Ca^{2+} during depolarization with 118 mM K^+ solution (Ca^{2+}-contraction)

Figure 1a shows representative recordings of the changes in the fluorescence ratio ($[Ca^{2+}]_i$) and the force development induced by depolarization with 118 mM K^+ in normal PSS (control contraction), followed by the cumulative applications of external Ca^{2+} (0–10 mM) during 118 mM K^+-depolarization. After recording the responses of the control contraction, the vascular strips were incubated in Ca^{2+}-free PSS containing 2 mM EGTA for 10 min, followed by a 5 min exposure to Ca^{2+}-free PSS without EGTA, and then the solution was changed to a Ca^{2+}-free-118 mM K^+ solution and the cumulative applications of extracellular Ca^{2+} (0–10 mM) were initiated during the 118 mM K^+-depolarization. Both $[Ca^{2+}]_i$ and the force increased stepwise with elevations of the extracellular Ca^{2+} concentration ($[Ca^{2+}]_o$). The data from 6 different measurements are summarized in Figure 1b and c. The relative value of fluorescence and force was expressed as a percentage, assuming the values in normal (5.9 mM K^+) and control 118 mM K^+ PSS to be 0% and 100%, respectively. The fluorescence increased from −24.4 ± 1.2% (at 0 mM $[Ca^{2+}]_o$) to 119.9 ± 4.5% (at 10 mM $[Ca^{2+}]_o$). The force increased from 0% to 120.4 ± 2.3%. We used the data in Figure 1b and c to determine the 'basic' $[Ca^{2+}]_i$-force relation of the Ca^{2+}-induced contractions (Ca^{2+}-contraction).

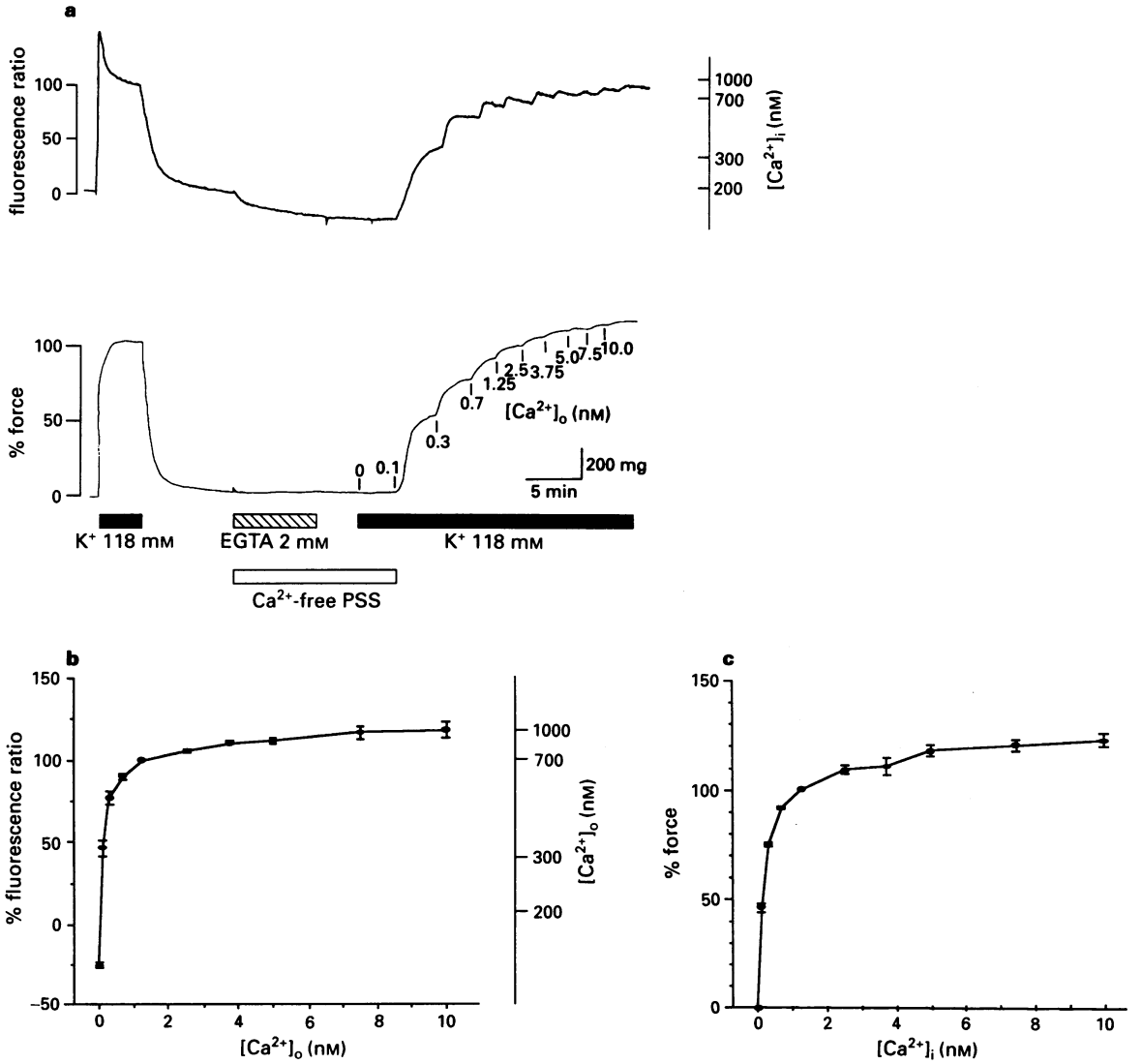


Figure 1 Changes in $[Ca^{2+}]_i$ and the force development induced by cumulative applications of various concentrations (0 mM–10 mM) of extracellular Ca^{2+} during 118 mM K^+-induced depolarization. (a) Representative recordings of changes in the fluorescence ratio ($[Ca^{2+}]_i$) (upper panel) and the force development (lower panel) induced by the cumulative applications of extracellular Ca^{2+} during 118 mM K^+-depolarization. The extracellular Ca^{2+} concentration ($[Ca^{2+}]_o$) is shown in the lower panel. Summaries of the data on changes in (b) the fluorescence ratio and (c) the force development in response to cumulative applications of extracellular Ca^{2+} (0–10 mM) in 118 mM K^+-depolarization. The data were obtained at the time of maximal force development at each application of extracellular Ca^{2+}. Each value is expressed as a % of fluorescence ratio and force, assuming the values obtained during the 118 mM K^+-depolarization in normal PSS to be 100%. The data represent the mean of 6 different measurements with s.e. shown in (b) and (c).

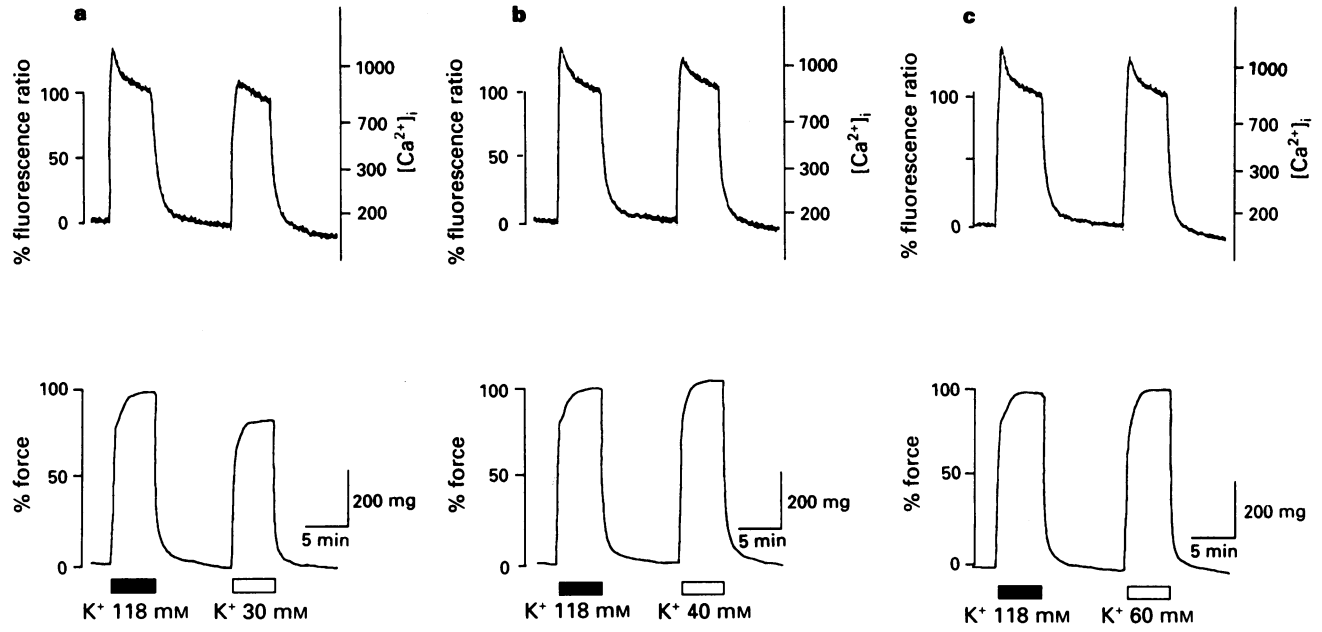


Figure 2 Representative recordings of changes in the fluorescence ratio ($[Ca^{2+}]_i$) (upper panel) and force development (lower panel) induced by (a) 30 mM K^+-, (b) 40 mM K^+-, (c) 60 mM K^+-depolarization. Prior to each measurement, the responses of $[Ca^{2+}]_i$ and force to 118 mM K^+-induced depolarization were determined as references.

Changes in $[Ca^{2+}]_i$, the force, and the $[Ca^{2+}]_i$-force relationship during the depolarization induced by various high external K^+ (30 mM–118 mM)-solutions

Figure 2 shows the representative recordings of changes in $[Ca^{2+}]_i$ and the force development induced by depolarization with immediate exchanging normal PSS with 60 mM K^+-, 40 mM K^+-, and 30 mM K^+-solutions after the control response to 118 mM K^+ solution. Figure 3a and b show the averaged time courses of these changes in $[Ca^{2+}]_i$ and force, obtained from 5 different measurements. When the vascular strips were exposed to 118 mM K^+ PSS, $[Ca^{2+}]_i$ rose abruptly to 137.8 ± 2.6% in the first 15 s, and then decreased to reach a lower steady level at 4 min; this level was assumed to be 100%. The force also rose rapidly and reached 77.9 ± 1.4% of the maximum in the first 15 s, and thereafter gradually increased to a maximum and steady level (100%) at 4 min. $[Ca^{2+}]_i$ and force remained at their steady levels as long as stimulus was maintained (at least for 30 min). The time course of changes in $[Ca^{2+}]_i$ and force, induced by depolarization with either a 30 mM K^+-, 40 mM K^+-, or 60 mM K^+-solution, was similar to those induced by depolarization with a 118 mM K^+ solution. Among the depolarizations induced by 40, 60, and 118 mM K^+, there was no significant difference in the peak $[Ca^{2+}]_i$, the steady state $[Ca^{2+}]_i$, or the maximum force, but these values were significantly higher than those of the depolarization induced by the 30 mM K^+-solution ($P<0.05$). $[Ca^{2+}]_i$ at 15 s after the stimulation with 118 mM K^+-, 60 mM K^+-, 40 mM K^+- and 30 mM K^+-solutions were 137.8 ± 2.6% (1650 nM), 110.4 ± 4.0% (866 nM), 94.4 ± 4.8% (653 nM) and 54.4 ± 5.3% (364 nM), respectively. Thus, the velocity of the elevation of $[Ca^{2+}]_i$ depended on the extracellular K^+ concentration ($[K^+]_o$) ($P<0.05$ by an analysis of variance). In contrast, the force at 15 s after application of 118 mM K^+, 60 mM K^+, 40 mM K^+ and 30 mM K^+-solutions was 77.9 ± 1.4%, 82.7 ± 1.8%, 80.6 ± 1.0% and 57.4 ± 3.7, respectively. These results indicate that there is no difference in the initial force development among the depolarization induced by 118 mM K^+-, 60 mM K^+- and 40 mM K^+-solutions, although they are greater than that induced by 30 mM K^+-solution ($P<0.05$ an analysis of covariance).

Figure 4 shows temporal changes in the $[Ca^{2+}]_i$-force relationship induced by depolarization with various concentrations of high K^+-solutions. The curves of $[Ca^{2+}]_i$-force relationship of contractions induced by a single application of 118 mM K^+-depolarization showed a counter-clockwise

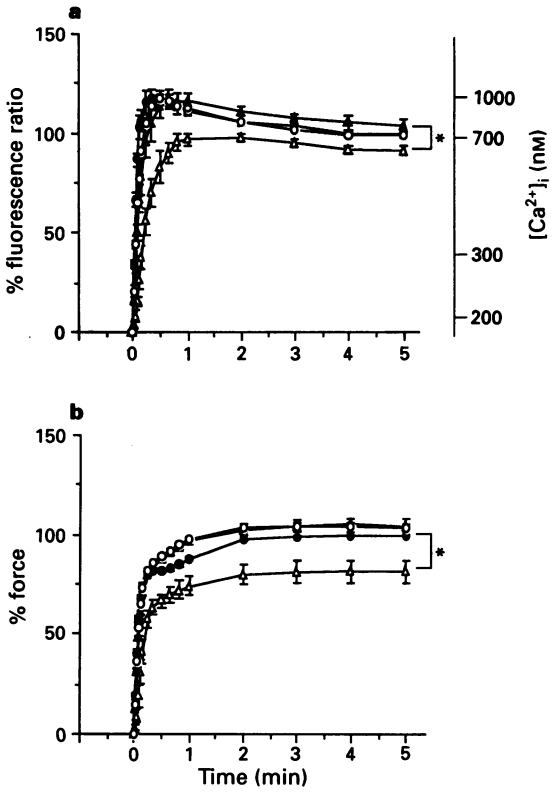


Figure 3 The time courses of changes in (a) the fluorescence ratio ($[Ca^{2+}]_i$) and (b) the force development of contractions induced by 30 mM (△), 40 mM (▲), 60 mM (○), and 118 mM (●) K^+-depolarization. The data represent the means of 5 different measurements with the s.e. The asterisks represent significant differences ($P<0.05$; vs. 118 mM K^+-induced depolarization at a 5 min application).

rotation over time, consisting of three components: (1) the initial disproportionately large elevation of $[Ca^{2+}]_i$ as compared to the elevation of force ($[Ca^{2+}]_i$-rising phase); (2) the subsequent increase in force, while $[Ca^{2+}]_i$ decreased until it reaches a lower steady level ($[Ca^{2+}]_i$-declining phase), and (3) a steady state, during continued stimulation (steady-state phase). In the $[Ca^{2+}]_i$-rising phase, the $[Ca^{2+}]_i$-force curve shifted to the right ($P<0.05$ by an analysis of covariance) from the line of the control $[Ca^{2+}]_i$-force relation of Ca^{2+}-contraction. The extent of the rightward shift of the $[Ca^{2+}]_i$-force curve in $[Ca^{2+}]_i$-rising phase depended on $[K^+]_o$. The higher the $[K^+]_o$, the more the curves shifted to the right. However, in the $[Ca^{2+}]_i$-declining phase, the $[Ca^{2+}]_i$-force curves, at any $[K^+]_o$, shifted toward the line of the $[Ca^{2+}]_i$-force relation of Ca^{2+}-contraction. The $[Ca^{2+}]_i$-force relation, in the steady-state phase of contractions induced by single dose applications of any high $[K^+]_o$, overlapped with the line of the $[Ca^{2+}]_i$-force relation of the Ca^{2+}-contraction.

In order to rule out the possibility of depolarization-induced neurotransmitter release, we examined the responses of $[Ca^{2+}]_i$ and of force to high K^+-depolarization in the strips denervated by incubation with 1 μM guanethidine, 0.3 μM tetrodotoxin, and 1 μM atropine, as described (Watanabe *et al.*, 1993). In the denervated strips, we obtained similar results to those in the non-denervated strips (data not shown).

Changes in the $[Ca^{2+}]_i$, force development and $[Ca^{2+}]_i$-force relationship during contractions induced by NA and by 5-HT

When each vascular strip was exposed to NA (10^{-5} M) and 5-HT (10^{-4} M) in PSS, $[Ca^{2+}]_i$ rose rapidly and reached a peak (the $[Ca^{2+}]_i$-rising phase) in 1 min and 2 min, respectively, and then slowly declined (the $[Ca^{2+}]_i$-declining phase) until reaching a steady state level (steady-state phase), with a similar time course (Figure 5). The peak levels of the $[Ca^{2+}]_i$ elevations induced by NA (10^{-5} M) and by 5-HT (10^{-4} M) were not significantly different ($P>0.05$): 107.1 ± 5.8% ($n=6$, 814 nM) and 101.3 ± 2.8% ($n=5$, 733 nM), respectively. The levels of $[Ca^{2+}]_i$ at 20 min (steady-state phase)

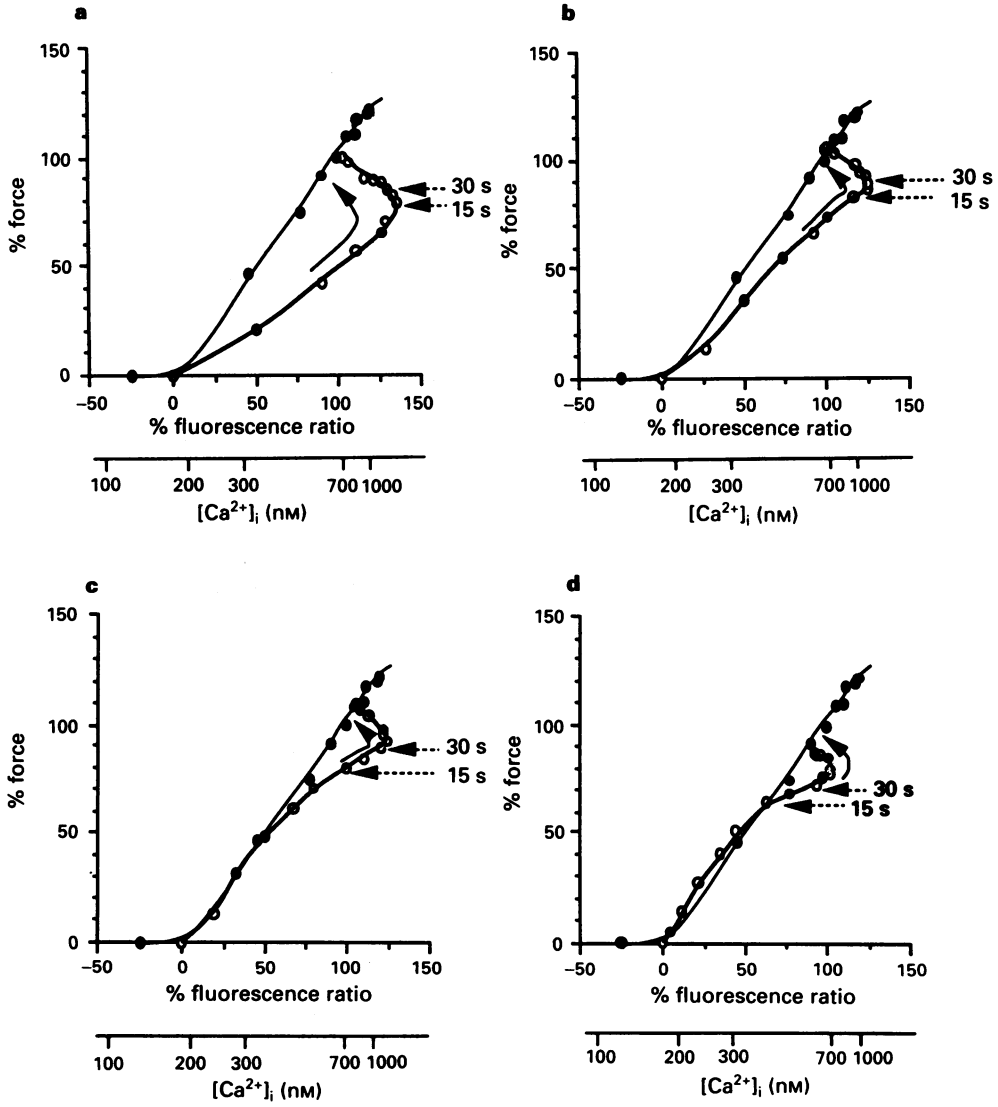


Figure 4 Temporal changes in the $[Ca^{2+}]_i$-force relation during contractions induced by membrane depolarization with (a) 118 mM K^+, (b) 60 mM K^+, (c) 40 mM K^+, and (d) 30 mM K^+ solutions. The individual points (○, the average of 5 experiments), are connected with thick solid lines, these figures represent the values at 2 s, 4 s, 6 s, 8 s, 10 s, 15 s, 20 s, 30 s, 1 min, 2 min, 3 min, 4 min and 5 min after the application of each stimulus. The s.e. bars were omitted for purposes of clarification, and the s.e. values were almost 8%. The curved arrows indicate the direction of time. (●) with a thin solid line indicates the $[Ca^{2+}]_i$-force relationship of contractions induced by the cumulative applications of Ca^{2+} during 118 mM K^+, which were based on the data in Figure 1b and c. The horizontal straight dashes with arrowheads indicate the points of time (15 s and 30 s) after the application of high K^+ solutions.

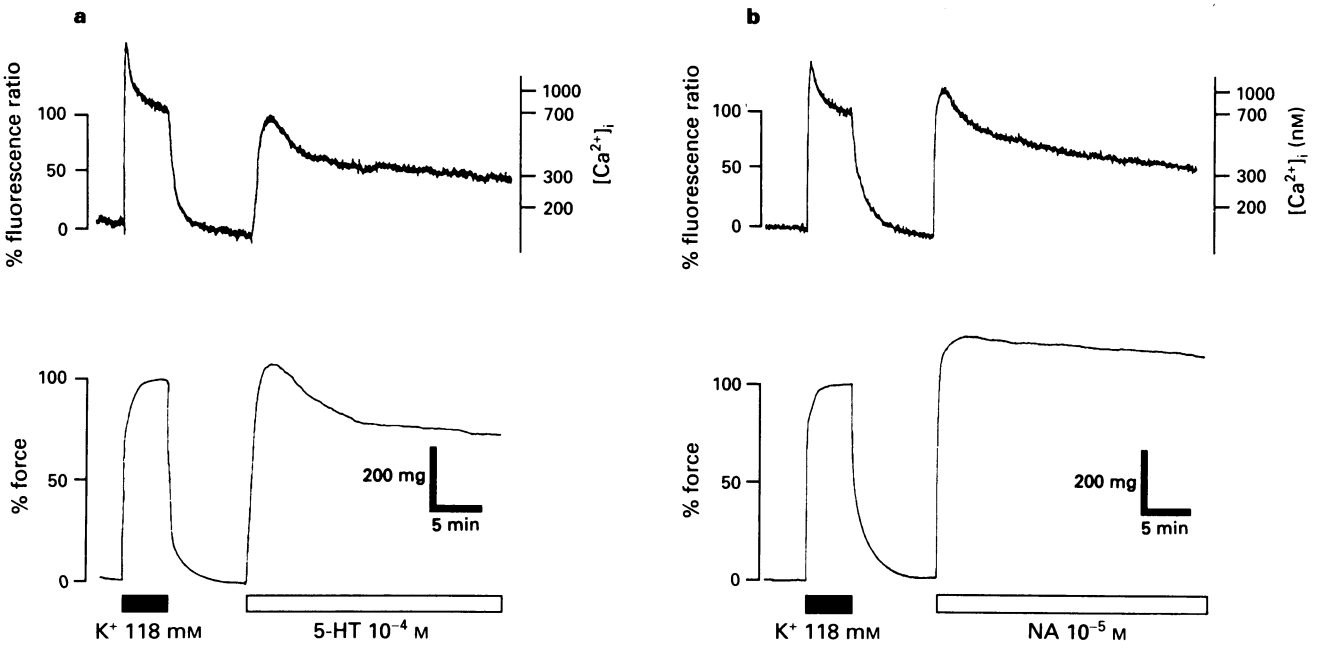


Figure 5 Representative recordings of changes in the fluorescence ratio ($[Ca^{2+}]_i$) (upper panel) and the force development (lower panel) of contractions induced by (a) 10^{-5} M noradrenaline (NA) and (b) 10^{-4} M 5-hydroxytryptamine (5-HT). Prior to the application, the reference responses of $[Ca^{2+}]_i$ and force to 118 mM K^+-induced depolarization were recorded.

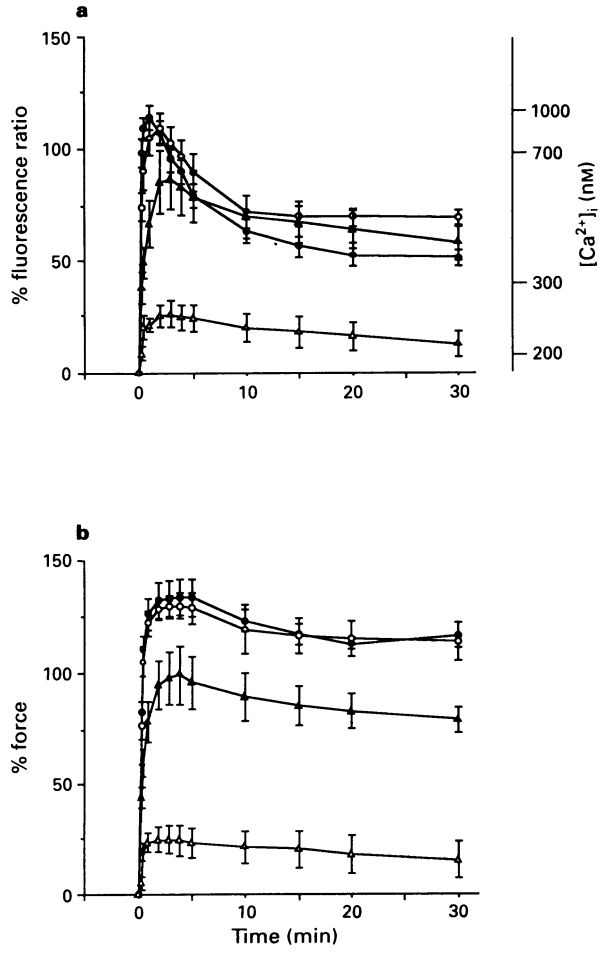


Figure 6 The time courses of the changes in (a) the fluorescence ratio ($[Ca^{2+}]_i$) and (b) the force development of contractions induced by 10^{-8} M (△), 10^{-7} M (▲), 10^{-6} M (○), 10^{-5} M (●) noradrenaline (NA). The data represent the mean of 5 or 6 different measurements with the s.e.

after the application of NA (10^{-5} M) and of 5-HT (10^{-4} M) were not significantly different ($P > 0.05$): 54.2 ± 3.8% ($n = 5$, 363 nM) and 62.2 ± 3.4% ($n = 5$, 405 nM), respectively. After the application of 10^{-4} M 5-HT, the force developed abruptly, reached a maximum at 2 min, and then slowly declined until reaching a steady state level. The extent of the force development at maximum and after 20 min (steady-state phase) was 115.0 ± 4.3% and 72.1 ± 5.0%, respectively. Thus, the time course of changes in the force development induced by 5-HT (10^{-4} M) was similar to that in $[Ca^{2+}]_i$. After the application of 10^{-5} M NA, the force developed abruptly, and reached a maximum of 4 min, and then gradually, but only slightly, declined. Although the $[Ca^{2+}]_i$ transients induced by NA (10^{-5} M) showed a similar time course to those induced by 5-HT (10^{-4} M), there was a marked difference in the time course of the force development between NA and 5-HT. During the $[Ca^{2+}]_i$-declining phase, the force induced by NA (10^{-5} M) was maintained at a much higher level than that expected from a similar level of $[Ca^{2+}]_i$ involved in the Ca^{2+}-contraction. The extent of force development at maximum and after 20 min was 128.8 ± 6.1% and 111.1 ± 2.0%, respectively.

Figure 6 shows the average time courses of the changes in $[Ca^{2+}]_i$ and the force development during contractions induced by various concentrations of NA, obtained from 5 or 6 different measurements. In the $[Ca^{2+}]_i$-rising phase, the effects of NA on both $[Ca^{2+}]_i$ and the force depended on the concentration of NA (10^{-8}–10^{-5} M). In either the $[Ca^{2+}]_i$-declining or steady-state phase, the concentration-dependent effects of NA on both $[Ca^{2+}]_i$ and the force were saturated at concentrations of 10^{-7} M and 10^{-6} M, respectively. Therefore, higher concentrations of NA ($> 10^{-7}$ M) induced a further increase in the force, but not in $[Ca^{2+}]_i$ (Figure 6), which resulted in a greater effectiveness of contraction for a given change in $[Ca^{2+}]_i$. As shown in Figure 7, the $[Ca^{2+}]_i$-force curves during contractions induced by various concentrations of NA showed a counter-clockwise rotation. In the $[Ca^{2+}]_i$-rising phase, the $[Ca^{2+}]_i$-force relation was not significantly different ($P > 0.05$ by an analysis of covariance) from that for Ca^{2+}-contractions. However, in the $[Ca^{2+}]_i$-declining and steady-state phases, NA ($> 10^{-7}$ M) produced a greater force

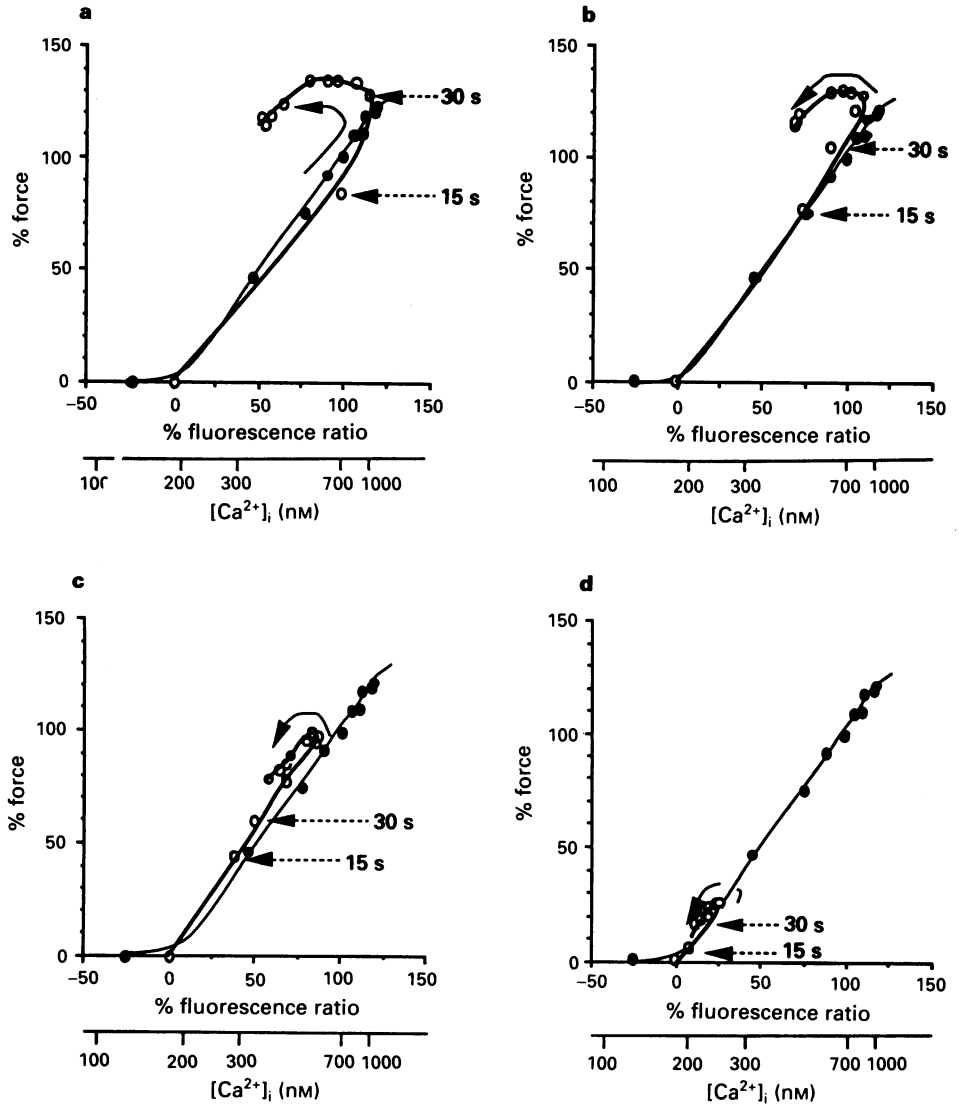


Figure 7 Temporal changes in the $[Ca^{2+}]_i$-force relation during contractions induced by (a) 10^{-5} M, (b) 10^{-6} M, (c) 10^{-7} M, and (d) 10^{-8} M noradrenaline (NA). The individual points (○, the average of 5 or 6 experiments), are connected with thick solid lines, these figures represent the values at 15 s, 30 s, 1 min, 2 min, 3 min, 4 min, 5 min, 10 min, 15 min, 20 min, and 30 min after the application of NA. The s.e. bars were omitted for the clarification of the figures, and the s.e. values were, at most, 10%. The curved arrows indicate the direction of time. (●) with a thin solid line indicates the $[Ca^{2+}]_i$-force relationship of contractions induced by cumulative applications of extracellular Ca^{2+} during 118 mM K^+-induced depolarization, which were based on the data in Figure 1b and c. The horizontal straight dashes with arrowheads indicate the points at the time (15 s and 30 s) after the application of NA.

than that expected from given changes in $[Ca^{2+}]_i$, and thus resulted in a leftward shift of the $[Ca^{2+}]_i$-force relation curve, as compared with the $[Ca^{2+}]_i$-force relation of the Ca^{2+}-contractions ($P<0.05$ by an analysis of covariance). The extent of the leftward shift of the $[Ca^{2+}]_i$-force curves in the $[Ca^{2+}]_i$-declining phase, as assessed by the width of the loop, depended on the concentration of NA.

Figure 8 shows the average time courses of the changes in $[Ca^{2+}]_i$ and the force development of contractions induced by various concentrations of 5-HT, obtained from 5 different measurements. In contrast to the effects of NA, the effects of 5-HT on $[Ca^{2+}]_i$ and on force depended on the concentration of 5-HT (10^{-7}–10^{-4} M), in any phase including $[Ca^{2+}]_i$-rising, $[Ca^{2+}]_i$-declining, or the steady-state. As shown in Figure 9, the $[Ca^{2+}]_i$-force curves during contractions induced by various concentrations of 5-HT showed a counter-clockwise rotation. In contrast to the stimulation with NA, in any phase, the $[Ca^{2+}]_i$-force relation was not significantly different ($P>0.05$ by an analysis of covariance) from that for Ca^{2+}-contractions. Only at 10^{-4} M, was 5-HT observed to shift the $[Ca^{2+}]_i$-force curve a little to the left, and this was seen only in $[Ca^{2+}]_i$-declining phase ($P<0.05$ by an analysis of covariance).

Discussion

We have characterized the temporal changes in the $[Ca^{2+}]_i$-force relation of contractions induced by high K^+, 5-HT and NA and compared them with the 'basic' $[Ca^{2+}]_i$-force relation of Ca^{2+}-contractions obtained by cumulative applications of extracellular Ca^{2+} in 118 mM K^+ in the rabbit femoral artery. We obtained evidence that these three types of stimuli induce different types of $[Ca^{2+}]_i$-force relations during contractions which vary with time after the application of stimuli.

It has been generally accepted that high K^+-induced depolarization of smooth muscles activates the voltage-operated Ca^{2+} channel and thus results in $[Ca^{2+}]_i$ elevation and consequent contractions through the Ca^{2+}-calmodulin

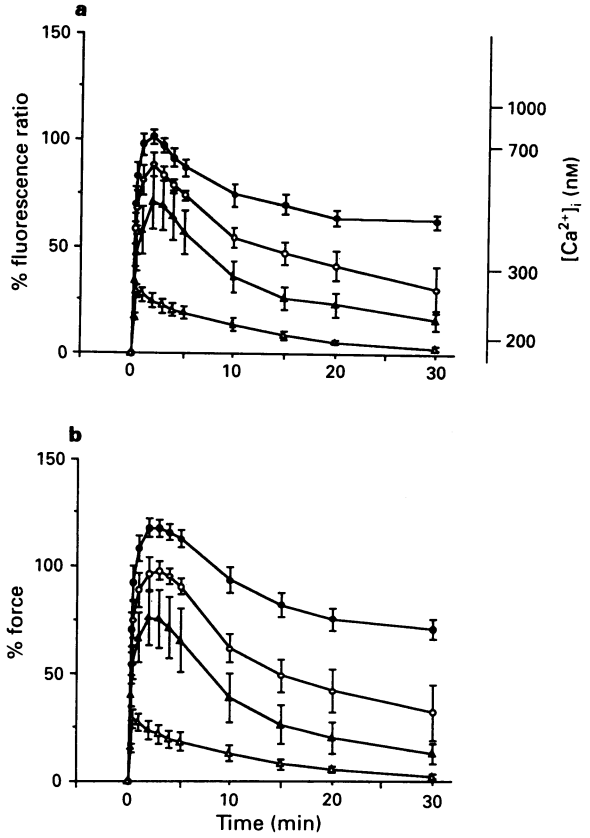


Figure 8 The time courses of changes in (a) the fluorescence ratio ($[Ca^{2+}]_i$) and (b) the force development of contractions induced by 10^{-7} M (Δ), 10^{-6} M (▲), 10^{-5} M (○) and 10^{-4} M (●) 5-hydroxytryptamine (5-HT). The data represent the mean of 5 different measurements with the s.e.

pathway (Sommerville & Hartshorne, 1986) without the stimulation of any other signal transduction systems. Although Ca^{2+} can be a potent stimulant of Ca^{2+}-dependent enzymes such as phospholipase C and certain isoforms of cyclic nucleotide phosphodiesterase, it is unlikely that a possible activation of such Ca^{2+}-dependent enzymes by $[Ca^{2+}]_i$ elevations during high K^+-depolarization would be sufficient to affect the 'basic' $[Ca^{2+}]_i$-force relationship, because of the following reasons: (1) we reported that the $[Ca^{2+}]_i$-force relationship of Ca^{2+}-contractions in intact smooth muscle of porcine coronary artery (Hirano *et al.*, 1991) is similar to that obtained with chemically skinned preparations (Itoh *et al.*, 1982), in which cytosolic proteins, such as phosphodiesterase, leak out of the cells. This similarity in the $[Ca^{2+}]_i$-force relationship was also observed in the present study on the rabbit femoral artery. Thus, the effects of the possible activation of phosphodiesterases on the 'basic' $[Ca^{2+}]_i$-force relationship would be minimal, if any, under our experimental conditions. (2) We reported that papaverine, a potent blocker of cyclic nucleotide phosphodiesterases, inhibits the Ca^{2+}-contractions during high K^+-depolarization with a similar potency (dose-dependency) at any $[Ca^{2+}]_o$ (Aoki *et al.*, 1994), which suggests that the activity of phosphodiesterases during the Ca^{2+}-contractions would be minimal. (3) It was shown that the two signal transduction pathways for phospholipase C and for modulation of $[Ca^{2+}]_i$-force relationship are dissociated at the level of G-protein/phospholipase C in smooth muscles (Kobayashi *et al.*, 1991). Therefore, it is unlikely that a possible activation of phospholipase C during high K^+-depolarization would modulate $[Ca^{2+}]_i$-force relationship.

In the present study, the $[Ca^{2+}]_i$-force relationship during contractions induced by single dose applications of high $[K^+]_o$ (30–118 mM) showed a counter-clockwise rotation with time (Figure 4), being compatible with the previous findings in other tonic smooth muscles, including the rabbit pulmonary artery (Himpens *et al.*, 1990) and the porcine coronary artery (Hirano *et al.*, 1991). The new findings are: (1) in the Ca^{2+}-rising phase, the $[Ca^{2+}]_i$-force relation shifted to the right, dependently on $[K^+]_o$, from the line of the 'basic' $[Ca^{2+}]_i$-force relation (Figure 4); and (2) in the steady-state phase, the $[Ca^{2+}]_i$-force relation overlapped the line of the 'basic' $[Ca^{2+}]_i$-force relation (Figure 4). Higher $[K^+]_o$ resulted in faster rate of rise of $[Ca^{2+}]_i$ and a greater right-side shift of the $[Ca^{2+}]_i$-force curve (Figure 4). Thus, it is likely that the rightward shift of the $[Ca^{2+}]_i$-force curve may be due to a delay in the mechanical response, as reflected by slow myosin light chain phosphorylation and the rapid rate of rise in $[Ca^{2+}]_i$ (Somlyo & Somlyo, 1990), especially in the initial Ca^{2+}-rising phase of the high K^+-induced contraction. In addition, a rightward shift of the $[Ca^{2+}]_i$-force relationship in the initial Ca^{2+}-rising phase was also observed in the lower concentration of K^+ (20 mM)-induced contractions and the extent of the shift was comparable to that obtained with the lowest concentrations of NA and 5-HT shown in Figures 7d and 9d (data not shown). This result also supports the notion that temporal changes in the $[Ca^{2+}]_i$-force relationship even in the initial Ca^{2+}-rising phase are regulated differently between stimulations with high K^+-depolarization and agonists.

One important and novel finding in this study is that NA enhanced the Ca^{2+} sensitivity of the contractile apparatus only in the late phase of the contraction; in the $[Ca^{2+}]_i$-declining and the steady-state phase and not in the early $[Ca^{2+}]_i$-rising phase (Figure 7). As for the $[Ca^{2+}]_i$-force relation curve, the time of onset for the increase in the Ca^{2+}-sensitivity of the contractile apparatus by agonists corresponds to the point on the curve that begins to shift to the left from the line of the 'basic' $[Ca^{2+}]_i$-force relation, thus making a counter-clockwise loop. At any concentration of NA, the enhancement of the Ca^{2+} sensitivity occurred immediately after the $[Ca^{2+}]_i$ reached a peak and started to decrease (Figure 7). The precise mechanisms which control the onset of the enhancement of the Ca^{2+} sensitivity of the contractile apparatus by agonists, are still unknown. The observed delay of onset cannot be explained by the presence of threshold $[Ca^{2+}]_i$ level for agonists to increase Ca^{2+} sensitivity, since it was reported that Ca^{2+} sensitivity can be potentiated either by agonists or by the activation of G-protein, even at the $[Ca^{2+}]_i$ level of a few hundred nM (Nishimura *et al.*, 1988; Kitazawa *et al.*, 1989; Kobayashi *et al.*, 1989), the level of which is close to the resting level of $[Ca^{2+}]_i$ of the rabbit femoral artery (= 183 nM, as described in Methods) and much lower than the $[Ca^{2+}]_i$ levels at the onset of the increase in Ca^{2+} sensitivity induced by NA (= 600–800 nM, as shown in Figure 7). The delay of potentiation in the Ca^{2+} sensitivity may be attributed to several, undetermined biological steps between the receptor stimulation and the increase in Ca^{2+} sensitivity. We previously reported that in the pig coronary artery, the Ca^{2+} sensitivity of the contractile apparatus is potentiated in the late, but not the initial, phase of histamine-induced contraction and is inhibited by a blocker of protein kinase C (PKC), H-7 (Hirano *et al.*, 1991), and that endothelin-induced potentiation of the Ca^{2+} sensitivity is also inhibited by H-7 (Kodama *et al.*, 1989). Nishimura *et al.* (1988) also reported that H-7 inhibited the NA-induced potentiation of the Ca^{2+} sensitivity in permeabilized preparations, and thus suggested the involvement of PKC. Several substrates for PKC may be regulatory proteins for muscle contraction and therefore could possibly modulate Ca^{2+} sensitivity of the contractile apparatus (Rasmussen *et al.*, 1987). In addition, the involvement of the inhibition of protein phosphatase in the modulation of Ca^{2+} sensitivity was also proposed (Somlyo & Somlyo, 1990). All these reports from various laboratories suggest that an increase in the Ca^{2+} sensitivity of the contrac-

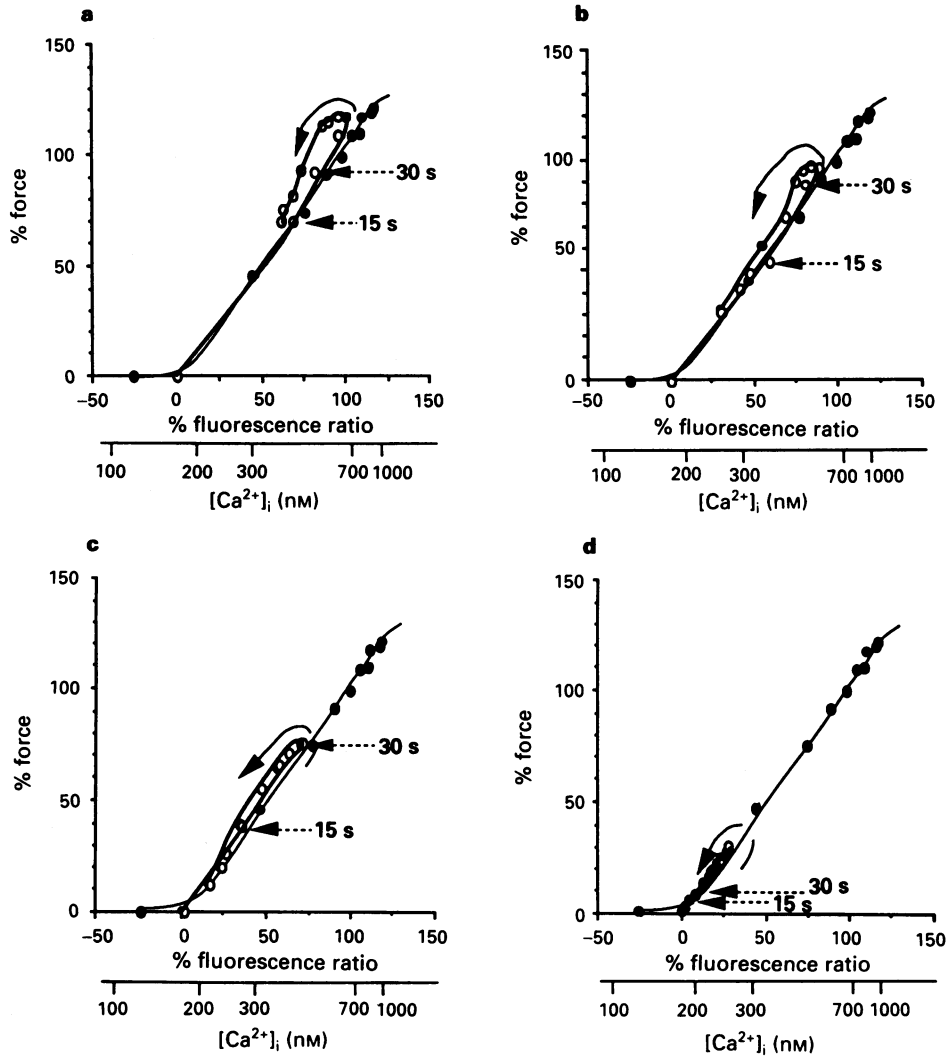


Figure 9 Temporal changes in the $[Ca^{2+}]_i$-force relation during contraction induced by (a) 10^{-4} M, (b) 10^{-5} M, (c) 10^{-6} M, and (d) 10^{-7} M 5-hydroxytryptamine (5-HT). The individual points (○, the average of 5 experiments), are connected with thick solid lines, in these figures represent the values at 15 s, 30 s, 1 min, 2 min, 3 min, 4 min, 5 min, 10 min, 15 min, 20 min, and 30 min after the application of 5-HT. The s.e. bars were omitted for clarification, while the s.e. values were found to be 14% at most. The curved arrows indicate the direction of time. (●) with thin solid line indicates the $[Ca^{2+}]_i$-force relationship of the contractions induced by the cumulative applications of extracellular Ca^{2+} during 118 mM K^+-induced depolarization, which were based on the data in Figure 1b and c. The horizontal straight dashes with arrowheads indicate the time (15 s and 30 s) after the application of 5-HT.

tile apparatus by agonists may be modulated by complicated and slow biological steps, presumably those including PKC, which is a time-consuming process.

Although the time course of changes in $[Ca^{2+}]_i$ induced by NA (10^{-5} M) and by 5-HT (10^{-4} M) were very similar, the time course of changes in the force in the late $[Ca^{2+}]_i$-declining phase differed between the NA- and 5-HT-induced contractions (Figure 5). In the $[Ca^{2+}]_i$-declining phase, the force development induced by 5-HT paralleled $[Ca^{2+}]_i$ (Figure 8); however, NA produced a greater force than that expected from the changes in the $[Ca^{2+}]_i$-force relation of the Ca^{2+}-contractions (Figure 6), thereby shifting the $[Ca^{2+}]_i$-force relation to the left and possibly increasing the Ca^{2+} sensitivity of the contractile apparatus. These results indicate that regarding NA and 5-HT, at concentrations which have similar efficacies in elevating $[Ca^{2+}]_i$, the former has a greater efficacy than the latter in increasing the Ca^{2+} sensitivity of the contractile apparatus. Although both Ca^{2+} mobilization and Ca^{2+}-sensitization are mediated by the activation of G-protein(s) coupled to a specific receptor, it is likely that the two processes (Ca^{2+} mobilization and Ca^{2+}-sensitization) may be dissociated in their intracellular signal transduction systems. This conclusion obtained from our present study on intact vascular smooth muscles thus also supports the observations in permeabilized (not intact) preparations that the two signal transduction pathways for Ca^{2+} release and Ca^{2+}-sensitization can be distinguished at the level of G-protein phospholipase C (Kobayashi *et al.*, 1991). The finding that 5-HT induced little potentiation of Ca^{2+} sensitivity, while NA enhanced Ca^{2+} sensitivity markedly (Figures 7 and 9), clearly indicates that the stimulus-specific activation of signal transduction systems (modulation of the Ca^{2+} sensitivity of contractile apparatus or intracellular Ca^{2+} mobilization) functions in intact vascular smooth muscles. However, it has to be noted that 5-HT has dual actions, vasoconstriction and dilatation, depending on the species, the vascular beds and the experimental conditions, mediated through 5-HT_2 and 5-HT_1 subtype receptors, respectively, and the latter became apparent when the former were inhibited (Kanaide *et al.*, 1987). It has been reported that the second messenger for 5-HT_1 receptor stimulation might be adenosine 3':5'-cyclic monophosphate (cyclic AMP) (Sumner *et al.*, 1989), which would thus decrease the Ca^{2+} sensitivity of the contractile apparatus (Ushio-Fukai *et al.*, 1993). Thus, 5-HT_1 subtype receptors may contribute to the slight enhancement of force for the increase in $[Ca^{2+}]_i$ in the case of the stimulation with 5-HT.

A significant shift of the $[Ca^{2+}]_i$-force relationships was

observed with only higher concentrations of NA ($>10^{-7}$ M). Since it is well known that α-receptors are localized in the postsynaptic area of adrenergic neuroterminals, it is likely that the concentration of neurotransmitters like NA could reach such high levels ($>10^{-7}$ M) in the very narrow space of the neuro-muscular junction. However, the exact concentrations of NA in such a narrow space have not yet been measured. Therefore, the physiological significance of agonists-induced modulation of $[Ca^{2+}]_i$-force relationships remains to be clarified.

In conclusion, the $[Ca^{2+}]_i$-force curve obtained with intact strips is considered to be a useful tool for analysing the temporal changes in the modulation of the Ca^{2+} sensitivity of the contractile apparatus in intact vascular smooth muscles. The present study indicates that: (1) changes in the force development of high K^+-induced contractions are delayed for the given changes in $[Ca^{2+}]_i$; (2) in the initial $[Ca^{2+}]_i$-rising phase of contraction induced by NA or by 5-HT, and the force development is determined mainly by $[Ca^{2+}]_i$, (3) in the late $[Ca^{2+}]_i$-declining phase of the contractions, 5-HT has little enhancement of force for a given change of $[Ca^{2+}]_i$ while NA has a greater effectiveness in contracting the rabbit femoral artery. A time-dependent and stimulus-specific modulation of the Ca^{2+} sensitivity of the contractile apparatus apparently functions in intact vascular smooth muscles and probably plays an important physiological role in regulating excitation-contraction coupling.

We thank B.T. Quinn for helpful comments. This study was supported in part by Grants-in-Aid for Developmental Scientific Research (No. 03557043), for General Scientific Research (No. 04454268, No. 05837015, and No. 05837016) from the Ministry of Education, Science and Culture, Japan, and Grants from the Japan Research Foundation for Clinical Pharmacology, from the Uehara Memorial Foundation, from Yokoyama Rinshouyakuri, from the Japan Heart Foundation, from the Japan Foundation of Cardiovascular Research, from the Ichiro Kanehara Foundation, from the Naito Foundation, from the Casio Science Promotion Foundation, from the Kaibara Morikazu Medical Science Promotion Foundation, from the Mochida Memorial Foundation, and from The Tokyo Biochemical Research Foundation.

References

AOKI, H., NISHIMURA, J., KOBAYASHI, S. & KANAIDE, H. (1994). Relationship between cytosolic calcium concentration and force in the papaverine-induced relaxation of medial strips of pig coronary artery. *Br. J. Pharmacol.*, **111**, 489–496.

ABE, S., KANAIDE, H. & NAKAMURA, M. (1990). Front-surface fluorometry with fura-2 and effects of nitroglycerin on cytosolic calcium concentrations and tension in the coronary artery of the pig. *Br. J. Pharmacol.*, **101**, 545–552.

FURCHGOTT, R.F. & ZAWADZKI, J.V. (1980). The obligatory role of endothelial cells in the relaxation of arterial smooth muscle by acetylcholine. *Nature*, **288**, 373–376.

GRYNKIEWICZ, G., POENIE, M. & TSIEN, Y. (1985). A new generation of Ca^{2+} indicators with greatly improved fluorescence properties. *J. Biol. Chem.*, **260**, 3440–3450.

HIMPENS, B. & SOMLYO, A.P. (1988). Free-calcium and force transients during depolarization and pharmacomechanical coupling in guinea-pig smooth muscle. *J. Physiol.*, **395**, 507–530.

HIMPENS, B., KITAZAWA, T. & SOMLYO, A.P. (1990). Agonist-dependent modulation of Ca^{2+} sensitivity in rabbit pulmonary artery smooth muscle. *Pflügers Arch.*, **417**, 21–28.

HIRANO, K., KANAIDE, H., ABE, S. & NAKAMURA, M. (1991). Temporal changes in the calcium-force relation during histamine-induced contractions of the strips of the coronary artery of the pig. *Br. J. Pharmacol.*, **102**, 27–34.

ITOH, T., KAJIWARA, M., KITAMURA, K. & KURIYAMA, H. (1982). Roles of stored calcium on the mechanical response evoked in smooth muscle cells of porcine coronary artery. *J. Physiol.*, **322**, 107–125.

KAMM, K.E. & STULL, J.T. (1985). The function of myosin and light chain kinase phosphorylation in smooth muscle. *Annu. Rev. Pharmacol. Toxicol.*, **25**, 593–620.

KANAIDE, H., HASEGAWA, M., KOBAYASHI, S. & NAKAMURA, M. (1987). Serotonin-induced cytosolic free calcium transients in cultured vascular smooth muscle cells. *Biochem. Biophys. Res. Commun.*, **143**, 532–538.

KITAZAWA, T., KOBAYASHI, S., HORIUTI, K., SOMLYO, A.V. & SOMLYO, A.V. (1989). Receptor-coupled, permeabilized smooth muscle – role of phosphatidylinositol cascade, G-proteins and modulation of contractile response to Ca^{2+}. *J. Biol. Chem.*, **264**, 5339–5342.

KOBAYASHI, S., GONG, M.C., SOMLYO, A.V. & SOMLYO, A.P. (1991). Ca^{2+} channel blockers distinguish between G protein-coupled pharmacomechanical Ca^{2+} release and Ca sensitization. *Am. J. Physiol.*, **260**, C364–C370.

KOBAYASHI, S., KITAZAWA, T., SOMLYO, A.V. & SOMLYO, A.P. (1989). Cytosolic heparin inhibits muscarinic and a-adrenergic Ca^{2+}-release in smooth muscle. *J. Biol. Chem.*, **264**, 17997–18004.

KODAMA, M., KANAIDE, H., ABE, S., HIRANO, K., KAI, H. & NAKAMURA, M. (1989). Endothelin-induced Ca-dependent contraction of the porcine coronary artery. *Biochem. Biophys. Res. Commun.*, **160**, 1302–1308.

KURIYAMA, H., ITO, Y., SUZUKI, H., KITAMURA, K. & ITOH, T. (1982). Factors modifying contraction-relaxation cycle in vascular smooth muscles. *Am. J. Physiol.*, **243**, H641–H662.

MORGAN, J.P. & MORGAN, K.G. (1984). Stimulus-specific patterns of intracellular calcium levels in smooth muscle of ferret portal vein. *J. Physiol.*, **351**, 155–167.

MURPHY, R.A. (1989). Special tonic contraction in smooth muscle. *Annu. Rev. Physiol.*, **357**, 539–551.

NISHIMURA, J., KOLBER, M. & VAN BREEMAN, D. (1988). Norepinephrine and GTP-r-s increase myofilament Ca^{2+}-sensitivity α-toxin permeabilized arterial smooth muscle. *Biochem. Biophys. Res. Commun.*, **157**, 677–685.

RASMUSSEN, H., TAKUWA, Y. & PARK, S. (1987). Protein kinase C in the regulation of smooth muscle contraction. *FASEB J.*, **1**, 177–185.

REMBOLD, C.W. & MURPHY, R.A. (1988). Myoplasmic $[Ca^{2+}]$ determines myosin phosphorylation in agonist-stimulated swine arterial smooth muscle. *Circ. Res.*, **63**, 593–603.

RINK, T.J. & POZZAN, T. (1985). Using quin-2 in cell suspensions. *Cell Calcium*, **6**, 133–145.

SOMLYO, A.P. (1985). Excitation-contraction coupling and the ultrastructure of smooth muscle. *Circ. Res.*, **57**, 497–507.

SOMLYO, A.P. & SOMLYO, A.V. (1990). Flash photolysis studies of excitation-contraction coupling, regulation, and contraction in smooth muscle. *Annu. Rev. Physiol.*, **52**, 857–874.

SOMMERVILLE, L.E. & HARTSHORNE, D.J. (1986). Intracellular calcium and smooth muscle. *Circ. Res.*, **57**, 497–507.

SUMNER, M.J., FENIUK, W. & HUMPHREY, P.P.A. (1989). Further characterization of the 5-HT receptor mediating vascular relaxation and elevation of cyclic AMP in porcine isolated vena cava. *Br. J. Pharmacol.*, **97**, 292–300.

TSIEN, R.Y., POZZAN, T. & RINK, T.J. (1982). Calcium homeostasis in intact lymphocytes: cytoplasmic free calcium monitored with a new, intracellular trapped fluorescent indicator. *J. Cell Biology*, **94**, 325–334.

USHIO-FUKAI, M., ABE, S., KOBAYASHI, S., NISHIMURA, J. & KANAIDE, H. (1993). Effects of isoprenaline on cytosolic calcium concentrations and on tension in the porcine coronary artery. *J. Physiol.*, **462**, 679–696.

WATANABE, C., YAMAMOTO, H., KOBAYASHI, S. & KANAIDE, H. (1993). Extracellular Ca^{2+}-dependent potentiation by cocaine of serotonin- and norepinephrine-induced contractions in rat vascular smooth muscle. *Circ. Res.*, **72**, 1191–1201.

(Received October 12, 1993
Revised July 25, 1994
Accepted September 20, 1994)

British Journal of Pharmacology (1995) 114, 339-348 © 1995 Stockton Press All rights reserved 0007-1188/95 $9.00

The use of receptor desensitization to analyse CCK_A and CCK_B/gastrin receptors coupled to contraction in guinea-pig stomach muscle

L.A. Bishop, V.P. Gerskowitch, R.A.D. Hull, [1]N.P. Shankley & J.W. Black

James Black Foundation, 68 Half Moon Lane, London SE24 9JE and Department of Analytical Pharmacology, Rayne Institute, King's College School of Medicine and Dentistry, 123 Coldharbour Lane, London SE5 9NU

1 The results of previous studies have been in conflict with respect to the involvement of specific cholecystokinin (CCK_A) and CCK_B/gastrin receptors in guinea-pig gastric muscle. Here, in an *in vitro*, guinea-pig gastric muscle assay, pentagastrin (PG) and tetragastrin (TG) behaved as high potency agonists and produced symmetrical concentration-effect curves. In contrast, cholecystokinin-octapeptide (CCK-8), while also behaving as a high potency agonist, produced flat asymmetrical curves. Unlike recent data reported using this tissue (Boyle *et al.*, 1993), the CCK_A receptor-selective antagonist, devazepide (3, 10, 30 nM) produced a rightward shift of the upper region of the CCK-8 curve rendering it biphasic. The lower phase was abolished by the CCK_B/gastrin receptor-selective antagonist, L-365260 (300 nM) indicating that the contractile effects of CCK-8 in this tissue are mediated by both receptor types.

2 L-365260 produced a concentration-dependent, parallel rightward displacement of PG concentration-effect curves. However, a flat Schild plot slope parameter (0.77 ± 0.06) was obtained. Therefore, an empirical pA_2 value of 8.64 ± 0.21 was estimated from the smallest dose ratio. This value is consistent with published values characteristic of an interaction at CCK_B/gastrin receptors.

3 TG (1 μM) was used to densensitize selectively the CCK_B/gastrin receptors in the gastric muscle assay and thereby expose a population of receptors capable of responding to subsequent stimulation by CCK-8 but not by PG. The selectivity of TG for CCK_B/gastrin- over CCK_A receptors was demonstrated by its low efficacy compared to CCK-8 in the guinea-pig gallbladder assay, a tissue shown previously to contain a homogeneous population of CCK_A receptors. In TG-desensitized gastric muscle, CCK-8 concentration-effect curves were symmetrical and could be displaced in a simple parallel fashion by devazepide at nanomolar concentrations consistent with an interaction at CCK_A receptors ($pK_B \sim 10$).

4 These results indicate that the guinea-pig gastric muscle contains both CCK_A- and CCK_B/gastrin receptors and the effects of CCK-8 are mediated via both of these receptors. Notwithstanding the complexity of the behaviour of L-365260, it was possible to obtain a reasonable description of the system using a simple 2-receptor model in which the effects of individual receptor activation were assumed to be additive. The absence of a simple competitive interaction of PG with L-365260 may indicate, for example, non-homogeneity of CCK_B/gastrin receptors or lack of concentration equilibrium between the bath and the receptor biophase.

Keywords: Cholecystokinin gastrin receptors; smooth muscle; stomach; gallbladder; pentagastrin; tetragastrin; devazepide; L-365260

Introduction

We have been investigating the pharmacology of gastrin receptors in isolated gastric acid secretion assays (Shankley *et al.*, 1992). Previously, we reported that histamine H_2- and muscarinic receptor antagonist affinity values can be significantly lower on these gastric secretory assays compared with non-secretory assays ostensibly expressing the same receptors (Shankley *et al.*, 1988; Welsh *et al.*, 1992). In order to quantify the extent of any CCK_B/gastrin receptor antagonist affinity underestimation, we needed to develop a comparative, non-secretory, assay for CCK_B/gastrin receptors. Selective agonists and antagonists are required for the pharmacological characterization of new assays. The native hormone, cholecystokinin (CCK) and its C-terminal octapeptide fragment, CCK-8, are non-selective agonists at CCK_A- and CCK_B/gastrin receptors while gastrin, pentagastrin (PG, tert-butyloxycarbonyl-β-Ala-Trp-Met-Asp-Phe-NH_2) and tetragastrin (TG, tert-butyloxycarbonyl-Trp-Leu-Asp-Phe-NH_2) behave as selective stimulants of CCK_B/gastrin receptors (see Watson & Girdlestone, 1994). Devazepide has been classified as a highly selective antagonist for CCK_A receptors (− log dissociation equilibrium constant, pK_B values: CCK_B/gastrin ~6.6; CCK_A ~10.0; Evans *et al.*, 1986) while L-365260 is selective for CCK_B/gastrin receptors (pK_B values: CCK_B/gastrin ~8.6; CCK_A ~6.6, Bock *et al.*, 1988).

Previously, the guinea-pig gastric muscle has been shown to contract in response to stimulation by both CCK and gastrin and the effects of the selective antagonists, devazepide and L-365260, have been examined (Bitar & Makhlouf, 1982; Huang *et al.*, 1989; Menozzi *et al.*, 1989; Grider & Makhlouf, 1990; Boyle *et al.*, 1992, 1993). The results of these studies are in conflict with respect to the involvement of specific CCK_A- or CCK_B/gastrin receptors in gastric smooth muscle contraction, in contrast to *in vitro* results in gastric acid secretory assays where CCK and gastrin only stimulate secretion by an action at CCK_B/gastrin receptors (Spraggs & Patel, 1989). For example, L-365260 was reported to be 50-fold more potent than devazepide as an inhibitor of gastrin-induced, guinea-pig gastric muscle contraction suggesting that the contraction was mediated by CCK_B/gastrin receptors (Huang *et al.*, 1989). In contrast, Grider & Makhlouf (1990) reported that devazepide (10 nM) abolished the contractile

[1] Author for correspondence.

responses of guinea-pig gastric muscle cells to CCK-8 and gastrin-17 indicating an interaction at CCK_A receptors. Boyle *et al.* (1992) reported that devazepide, at low nanomolar concentrations, inhibited CCK-8 with a pA_2 value of ~9.5 but did not inhibit PG-stimulated guinea-pig gastric muscle contraction. L-365260 inhibited PG-stimulated contractions (pA_2 value ~8.5) and hence it was concluded that both CCK_A- and CCK_B/gastrin receptors were coupled to contraction in guinea-pig gastric muscle.

In this paper, we describe our attempts to classify the receptors for CCK-8 and PG-induced contraction in guinea-pig stomach muscle. A preliminary account of this work was presented to the British Pharmacological Society (Bishop *et al.*, 1992a).

Methods

Guinea-pig stomach muscle strip assay

Following cervical dislocation, stomachs were removed from male guinea pigs (Dunkin Hartley, 300–500 g). Krebs-Henseleit solution, modified with a high K + concentration, (mM: Na^+ 143, K^+ 15.9, Ca^{2+} 2.5, Mg^{2+} 1.2, Cl^- 128, HPO_4^{2+} 1.2, D-glucose 10, HCO_3^- 25) was injected through a hypodermic needle placed under the serosal and muscle layers of the stomach in the middle region (corpus) between the greater and lessor curvature (avoiding pyloric tissue) to blister the muscle away from the sub-mucosa. Two preparations were obtained from each stomach. Thus, a strip of muscle approximately 2.5 cm by 1 cm was dissected from the dorsal and ventral surfaces of the stomach. The strips were tied with cotton thread to an isotonic transducer under an initial loading tension of 0.35 g. The preparations were incubated in 20 ml organ baths containing modified Krebs-Henseleit solution gassed with 95%O_2/5%CO_2 and maintained at 22°C. The higher concentration of K^+ and the lowering of temperature, from 37°C to 22°C, increased the size of agonist responses and improved the signal-to-noise ratio, respectively. Tissue length was continuously recorded with an isotronic transducer and responses are expressed as changes in mm chart record. The total amplification of the recording system was such that 200 mm of trace was equal to 1 mm of tissue length in all experiments.

Guinea-pig gallbladder muscle strip assay

The CCK_A-receptor gallbladder assay was performed as described by Bishop *et al.* (1992b). In brief, four longitudinal strips of smooth muscle were dissected from each gallbladder taken from male Dunkin-Hartley guinea pigs (250–500 g) and suspended in 20 ml organ baths maintained at 29°C in a Krebs-Henseleit solution with a low Ca^{2+} concentration (0.05 mM) and gassed with 95%O_2/5%CO_2. Following the application of a single 1 g load, the tissues were allowed to relax until a stable baseline was produced. Force was continuously recorded with an isometric transducer and responses are expressed as changes in mm chart record where 100 mm is equal to 1 g force in all experiments.

Experimental protocols

In all assays, eight preparations were used simultaneously. The preparations were allowed to stabilize for 60 min before experimental intervention during which time the bathing solutions were changed twice. Antagonists or vehicles were incubated for 60 min before single agonist concentration-effect curves were obtained by cumulative dosing at 0.5 or 1 log unit intervals. The total volume of all drugs added to the organ baths did not exceed 500 µl in a single experiment.

Protocols

Randomized block designs were used throughout for allocation of experimental treatments to each organ bath.

Data analysis

Concentration-effect curve data from individual preparations were fitted by means of an interactive least squares minimisation programme to a general logistic function to provide estimates of the midpoint location ($\log[A_{50}]$), midpoint slope parameter (p) and upper asymptote (α) of the curves as described previously (Black & Shankley, 1985). These parameters, expressed as mean ± s.e.mean, were used for subsequent analysis (Student's *t* test or one-way analysis of variance, as appropriate) and display of the data. When the programme was used to analyse the CCK-8 concentration-effect data obtained on the guinea-pig gastric muscle assay, the convergence criterion was not satisfied so that it was not possible to obtain parameter estimates. Therefore, in this case, the data points were expressed and plotted as means.

The effects of competitive antagonists were assessed using the method described by Trist & Leff (1985). In practice, when multiple antagonist concentrations were used, the data failed to meet the criteria for simple competition. Under these circumstances, a pA_2 value was estimated from the data with the lowest antagonist concentration. Where only a single antagonist concentration was examined, a competitive mechanism of antagonism was assumed provided there was a parallel shift of the agonist-concentration-effect curve with no significant change in the value of the upper asymptote; the K_B was thereupon calculated from the single dose-ratio following the approach used by Jenkinson (1992). These pA_2 and log K_B values were obtained by calculating the mean ± s.e.mean of the individual log(dose ratio-1) values. The dose-ratio values were calculated by subtraction of the individual log $[A_{50}]$ values obtained in the presence of the antagonist from the mean control log $[A_{50}]$ values.

Application of a two receptor model

Two-receptor model simulations of some of the experimental data obtained in the guinea-pig gastric muscle assay were obtained using the following model that is based on that described by Hough *et al.* (1980).

$$E = \frac{\alpha_1.[A]^{P_1}}{[A_{50}1]^{P_1} + [A]^{P_1}} + \frac{\alpha_2.[A]^{P_2}}{[A_{50}2]^{P_2} + [A]^{P_2}}$$

where α_1, P_1, $[A_{50}1]$ and α_2, P_2, $[A_{50}2]$ are the logistic curve parameters for the two receptor-mediated effects arising from CCK_B/gastrin and CCK_A-receptor-mediated stimulation, respectively.

Compounds

The sulphated C-terminal of CCK-8, obtained from Cambridge Research Biochemicals Ltd., was dissolved in 10% ethanol solution to a concentration of 2 mM. PG and TG, obtained from Sigma, were dissolved in dimethylformamide (DMF) to a concentration of 2 mM. 5-Methylfurmethide was a gift from Wellcome Research Laboratories and was dissolved in distilled water to a concentration of 2 mM. Devazepide and L-365260 (3R(+)-N-(2,3-dihydro-1-methyl-2-oxo-5-phenyl-1H-1,4-benzodiazepin-3-yl)-N'-(3-methylphenyl)urea), obtained from Merck Sharp and Dohme, were dissolved in DMF to concentrations of 20 mM. All subsequent dilutions were made in distilled water.

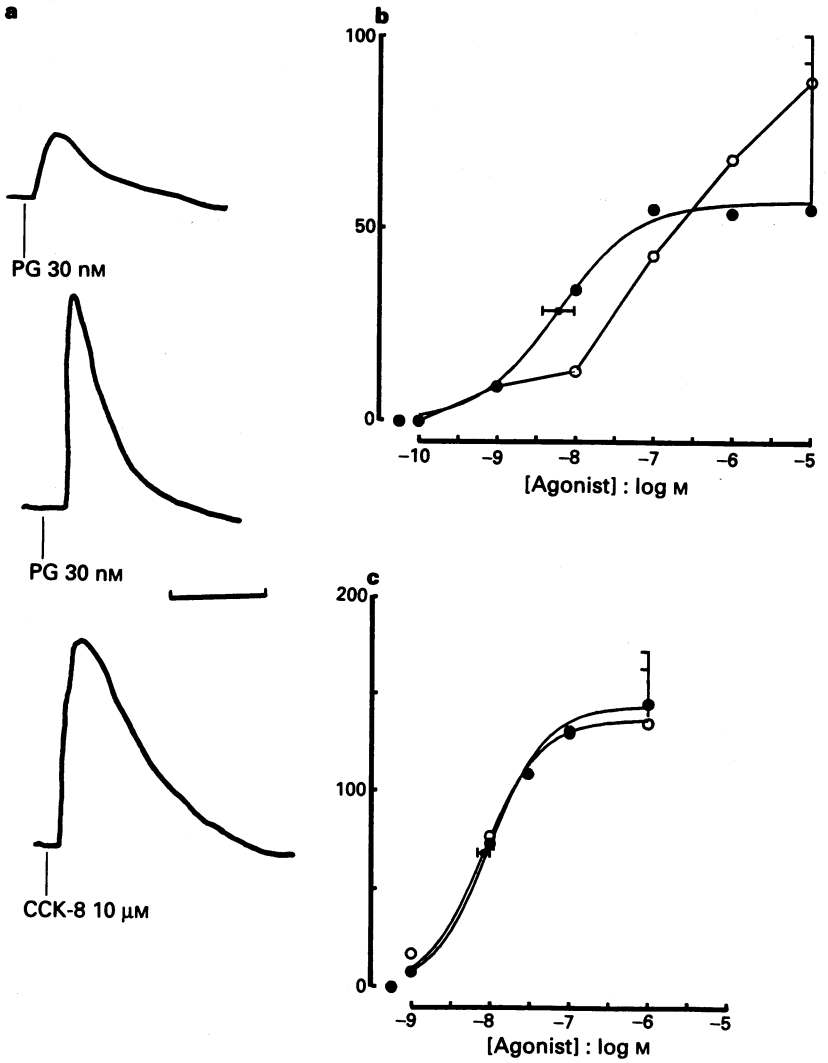


Figure 1 (a) Representative experimental trace, expressed as chart recorder displacement (mm) against time, of the individual contractions by pentagastrin (PG) and cholecystokinin octapeptide (CCK-8) obtained on the guinea-pig gastric muscle assay. (b) Concentration-effect curves to PG (●) and CCK-8 (○) ($n = 4/6$); (c) Concentration-effect curves to PG (●) and TG (○) ($n = 7$). Ordinate scales: contraction as mm chart record. Data shown are mean ± s.e.mean.

Results

Guinea-pig gastric muscle

Agonist concentration-effect data PG, TG and CCK-8 produced concentration-dependent contraction of guinea-pig gastric muscle (Figures 1a and 4a). Tetrodotoxin (0.5 μM) had no significant effect on the responses indicating that they were not neurally-mediated (data not shown). Each of the agonist responses faded, returning to baseline within 5–10 min; the rate of fade appeared to be dependent on the size of the peak contraction. However, by dosing at the peaks, it was possible to obtain fully-defined, cumulative, agonist concentration-effect curves over a period of approximately 30 min. In a preliminary experiment, PG control curves were obtained by cumulative dosing following brief (5 min) exposure to a near-maximally effective, sighting concentration of PG (0.1 μM). The response to the sighting administration (170 ± 23 mm trace, $n = 14$) was lower, but not significantly as tested, than the response to the same concentration obtained within a curve obtained by cumulative dosing (131 ± 20 mm trace). This suggests that there was no significant accumulation of the fade during the cumulative dosing.

During the development of the assay, the upper asymptote values of the agonist concentration-effect curves were found to be extremely variable both within and between experiments. We attempted to express the data obtained on each preparation as a percentage of the response to a sighting, near-maximally effective, concentration of KCl or the acetylcholine muscarinic receptor agonist, 5-methylfurmethide or PG or as a percentage of the wet weight of the tissue at the end of the experiment. However, we did not find a correlation between the size of the responses to the sighting agents or the wet weight and the upper asymptote of the curves obtained with the peptide agonists (data not shown). For example, we found that the value of the coefficient of variation associated with the upper asymptote values of the PG curves obtained following application of a sighting concentration of PG (10 μM) was slightly higher (15.7%) when the data were expressed as a percentage of the 'sighter response' than when expressed in terms of mm trace (14.8%). A paired-curve design was also precluded because the assay suffered a marked reduction in responsiveness following generation of the first curve. For example, in one experiment ($n = 8$), the upper asymptote values estimated for paired PG concentration-effect curves were 51 ± 7 and 30 ± 6 mm trace for the first and second curves, respectively. In addition, the variability was not reduced by pairing the preparations obtained from each stomach (data not shown). Therefore,

experiments were designed in which a single agonist concentration-effect curve was obtained on each preparation.

The activity of PG and TG were compared within a single experiment (Figure 1c). The concentration-effect curves obtained were symmetrical, equipotent, extended over approximately 2.5 log units and could be fitted to the logistic function (Table 1, Figure 1c). In contrast, CCK-8 concentration-effect curves obtained in a separate experiment with another set of PG curves, extended over approximately 5 log cycles, were asymmetrical about the midpoint location as judged-by-eye and could not be fitted by the logistic function (Figure 1b). Evidently, CCK-8 was behaving differently from PG and TG. Comparison of these two experimental data sets (Figure 1b and 1c) reveals the high variance of the maximum response obtained in the guinea-pig gastric muscle assay both between and within experiments. For example the mean values of the upper asymptotes of the two

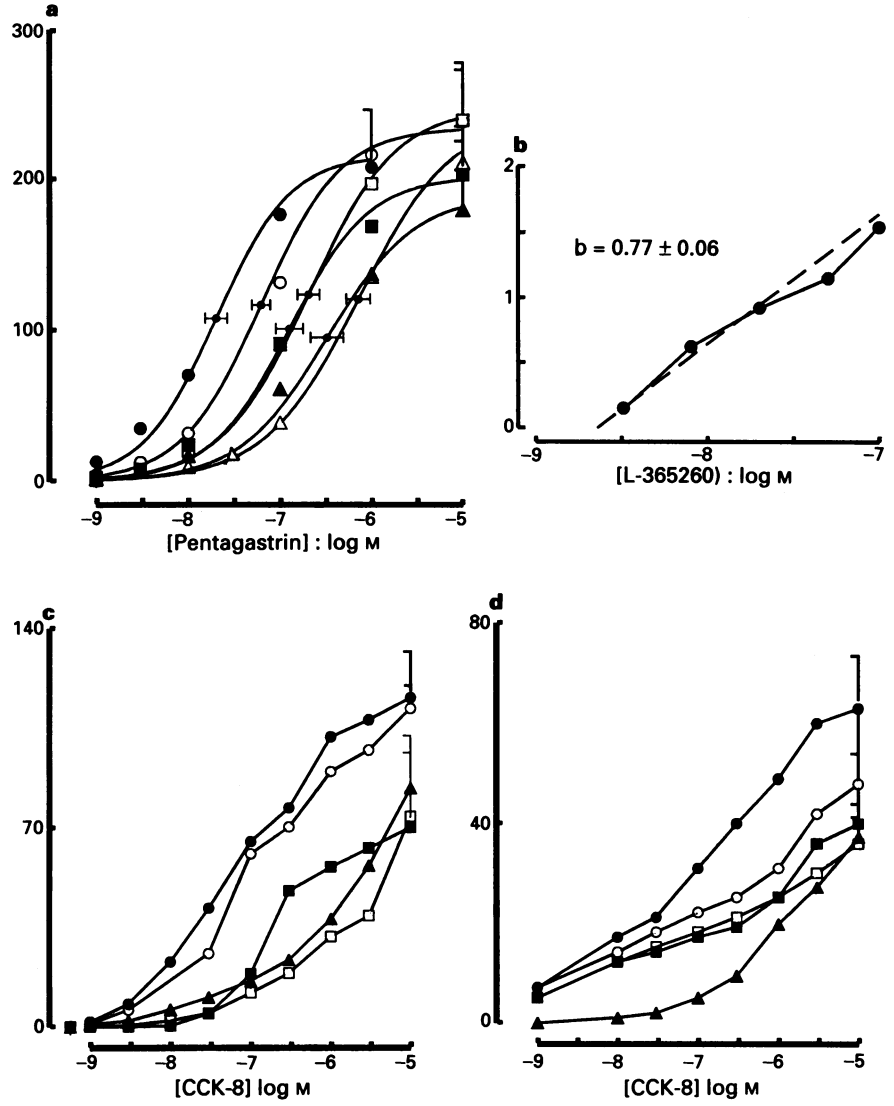


Figure 2 (a) Pentagastrin (PG) concentration-effect curves ($n = 7/8$) obtained on the guinea-pig gastric muscle assay in the absence (●) and presence of 3.2 nM (○), 8 nM (■), 20 nM (□), 50 nM (▲) and 100 nM (△) L-365260. Devazepide (10 nM) was present in the buffer solution to avoid potential confounding influences of CCK_A receptor activation. (b) Schild plot for the interaction between PG and L-365260: ordinate: log (r − 1) − where r is the dose ratio. The data points shown were derived by averaging the individual log (r − 1) values for each antagonist treatment, which in turn were calculated from the mean control log [A_{50}] value. The hatched line has unit slope and is located at the pA_2 value (8.64 ± 0.23) estimated in the analysis (see Results for details). (c) Cholecystokinin octapeptide (CCK-8) concentration-effect curves in the absence (● $n = 4$) and presence of 10 nM (○ $n = 2$), 30 nM (■ $n = 3$), 100 nM (□ $n = 5$) and 300 nM (▲ $n = 4$) L-365260. (d) CCK-8 concentration-effect curves ($n = 4/6$) in the absence (●) and presence of 3 nM (○), 10 nM (□), 30 nM devazepide (■) and, in combination, 30 nM devazepide and 300 nM L-365260 (▲). Ordinate scale for (a), (c) and (d): contraction as mm chart record. Data shown are mean ± s.e.mean.

Table 1 Logistic curve-fitting parameters for pentagastrin, tetragastrin and cholecystokinin-8 on guinea-pig gastric muscle and gallbladder assays

Assay	*Agonist*	n	*log[A_{50}]*	P	α *(mm)*
Guinea-pig gastric muscle	PG	7	−8.00 ± 0.05	1.22 ± 0.09	144 ± 18
	TG	6	−8.08 ± 0.08	1.21 ± 0.09	137 ± 37
	CCK-8(+TG 1 μM)	6	−7.00 ± 0.16	0.64 ± 0.06	161 ± 25
Guinea-pig gallbladder	CCK-8	4	−8.72 ± 0.25	0.69 ± 0.05	98 ± 3
	CCK-8(+TG 1 μM)	4	−8.82 ± 0.29	0.59 ± 0.12	99 ± 10

PG curves were 57 ± 38 and 144 ± 18 mm trace Figure 1b and 1c, respectively.

Analysis by antagonists The possibility that the CCK-8 response reflected simultaneous activation of both CCK_A- and CCK_B/gastrin receptors was initially investigated using the selective CCK_A- and CCK_B/gastrin receptor antagonists, devazepide and L-365260, respectively.

The CCK_B/gastrin receptor blocking activity of L-365260 was assessed with PG as agonist in the presence of 10 nM devazepide. This concentration of devazepide was considered selective because it was approximately 100 times more than and 40 times less than its reported K_B values at CCK_A and CCK_B/gastrin receptors, respectively. Thus, the selectivity of PG as a CCK_B/gastrin receptor agonist (see below) and the selectivity of devazepide as a CCK_A receptor antagonist, was used to reduce, as far as possible, the involvement of CCK_A receptors. Under these conditions, L-365260 produced a concentration-dependent, parallel, rightward displacement of PG concentration-effect curves (Figure 2a). However, the data did not fit the model of competitive antagonism because the Schild plot slope parameter was significantly different from unity (b = 0.77 ± 0.06) and so a valid pK_B value could not be estimated (Figure 2b). Notwithstanding this, a pA_2 value of 8.64 ± 0.21 was estimated from the dose ratio obtained with the lowest concentration of L-365260 (3.2 nM).

The effect of L-365260 on CCK-8 curves was complex (Figure 2c). Antagonism was observed at concentrations of 30 nM and above. It was not possible to fit the concentration-effect data to the logistic function and by inspection, it was apparent that a parallel, concentration-dependent, rightward shift was not obtained.

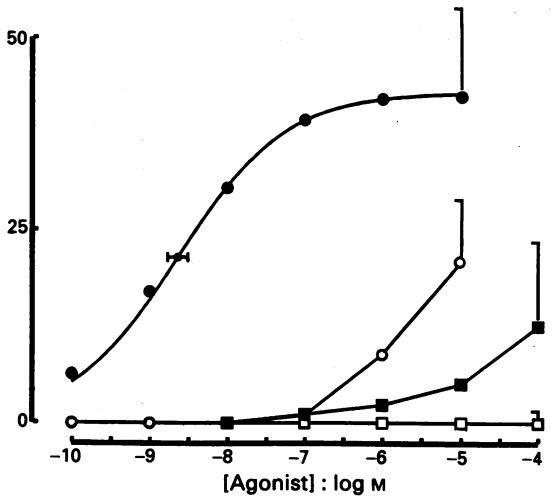


Figure 3 Agonist-concentration effect curves ($n = 4$) obtained in the guinea-pig gallbladder cholecystokinin octapeptide (CCK-8) (circles) and tetragastrin (TG) (squares) in the absence (●, ■) and presence (○, □) of 300 nM devazepide. Ordinate scale: contraction as mm chart record. Data shown are mean ± s.e.mean.

Devazepide (3, 10 and 30 nM) produced rightward shift of the upper region of the CCK-8 curve (Figure 2d). The lower, devazepide-resistant phase was abolished by concurrent pre-incubation with L-365260 (300 nM). Therefore, it appeared that the lower region of the curve (i.e. higher sensitivity to CCK-8) was mediated by CCK_B/gastrin receptors and the

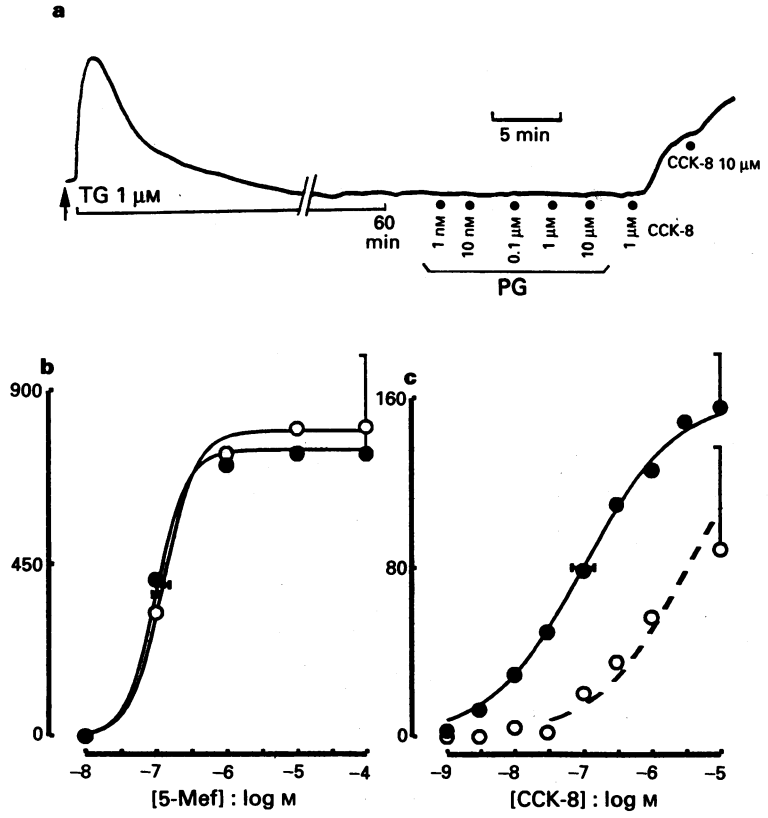


Figure 4 (a) Representative experimental trace, expressed as chart recorder displacement (mm) against time, showing the desensitization of CCK_B/gastrin, but not CCK_A receptors by 1 μM tetragastrin (TG) on the guinea-pig gastric muscle assay. (b) 5-Methylfurmethide (5-Mef) concentration-effect curves ($n = 4/6$) obtained on the guinea-pig gastric muscle assay in the absence (●) and presence of 1 μM TG (○). (c) CCK-8 concentration-effect curves ($n = 4/6$) obtained on the guinea-pig gastric muscle assay following pre-incubation with 1 μM TG in the absence (●) and presence (○) of 3 nM devazepide. The hatched line superimposed on the data obtained in the presence of devazepide was simulated using the control logistic curve-fitting parameters (Table 1) with the $[A_{50}]$ value increased by the factor $(1 + [B]/K_B)$, where $K_B = 0.1$ mM and [B] = 3 nM. Ordinate scale: contraction as mm chart record. Data shown are mean ± s.e.mean.

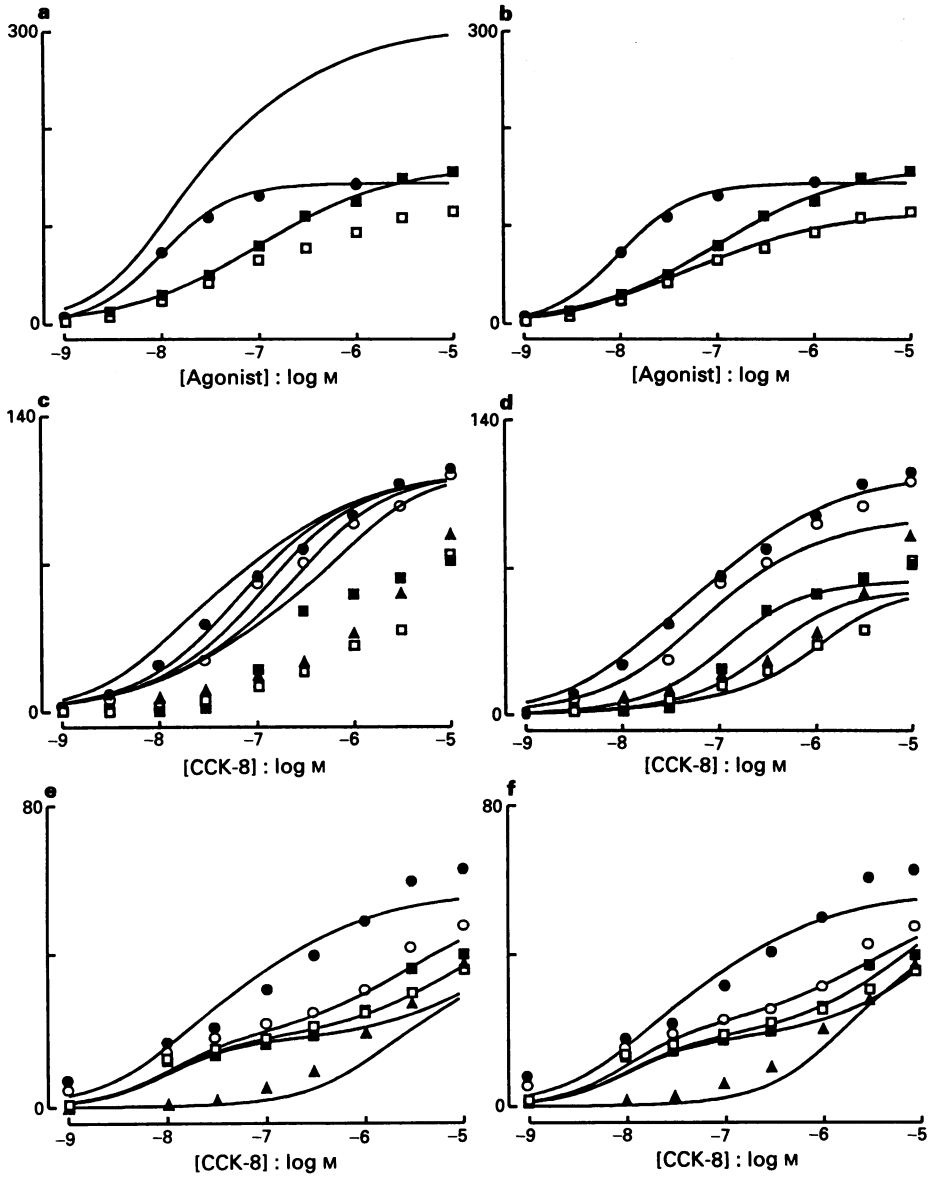


Figure 5 Two-receptor model simulations of the interaction between cholecystokinin octapeptide (CCK-8), pentagastrin (PG), devazepide and L-365260 in the guinea-pig gastric muscle assay. (a) Concentration-effect curve data obtained with PG (●), CCK-8 (□) and CCK-8 following desensitization with 1 μM tetragastrin (TG) (■), as shown previously in Figures 1c, 2c and 4c, respectively. The curves shown were simulated using the model shown in the methods and the parameter values given in Table 1 for PG and CCK-8 (+ TG 1 μM) which were assumed to be acting solely at the CCK_B/gastrin and CCK_A receptors, respectively. The parameter values for these curves were then used to obtain the simulation of the CCK-8 concentration-effect curve which it is assumed is due to the simultaneous activation of CCK_B/gastrin and CCK_A receptors. (b) Repeat of data and model simulations shown in (a) with the exception of reducing the values of α_1 (PG) and α_2 (CCK-8 + TG) (from 144 to 20 and 161 to 95, respectively) to account for the variance in maximum responses between experiments (see text for details and discussion). (c) CCK-8 concentration-effect curve data obtained in the absence (● $n = 4$) and presence of 10 nM (○ $n = 2$), 30 nM (■ $n = 3$), 100 nM (□ $n = 5$) and 300 nM (▲ $n = 4$) L-365260, as shown in Figure 2c. L-365260 was assumed to behave as a simple competitive antagonist of the CCK_B/gastrin receptors so that the value of $[A_{50}1]$ was increased by the factor $(1 + [B]/K_B)$, where [B] is the concentration of L-365260 and K_B was taken from the pA_2 value estimated from the interaction between L-365260 and PG (Figure 2b). The values of α_1 and α_2 were fixed at 25 and 80, respectively. (d) Repeat of data and model simulations shown in (c) with the exception of allowing the values of α_1 and α_2 to vary to account for the variance in maximum responses within the experiment. The values were (α_1) 20, 25, 45, 45, 45 and (α_2) 95, 70, 20, 15, 15 corresponding to the simulations of the data obtained in the presence of increasing concentrations of L-365260 as detailed in (c). (e) CCK-8 concentration-effect curve data ($n = 4/6$) obtained in the absence (●) and presence of 3 nM (○), 10 nM (□), 30 nM devazepide (■) and, in combination, 30 nM devazepide and 300 nM L-365260 (▲), as shown in Figure 2d. Devazepide and L-365260 were assumed to behave as simple competitive antagonists of CCK_A and CCK_B/gastrin receptors, respectively, so that the values of $[A_{50}1]$ and $[A_{50}2]$ were increased by the factor $(1 + [B]/K_B)$, where [B] is the concentration of antagonist and the K_B values (0.1 nM and 2.3 nM, respectively) were taken from the pA_2 values estimated from the analysis of the interactions between devazepide/CCK-8 (+ TG 1 μM) and L-365260/PG (Figures 4c and 2b, respectively). The values of α_1 and α_2 were fixed at 17 and 40, respectively. (f) Repeat of data and model simulations shown in (e) with the exception of allowing the values of α_1 and α_2 to vary to account for the variance in maximum responses within the experiment. The values used were (α_1) 17, 20, 17, 17, 17 and (α_2) 40, 37, 53, 60, 45 corresponding to the simulations of the data obtained in the absence and presence of increasing concentrations of devazepide and L-365260. Ordinate scale: mm chart record.

upper region (i.e. lower sensitivity to CCK-8) by CCK_A receptors. The complicated profiles of antagonism precluded the reliable measurement of dose ratios needed to estimate pK_B values for receptor classification. Therefore, as an alternative to selective competitive antagonism, CCK_B/gastrin receptor desensitization was tried as another method of simplifying the system and, in particular, exposing CCK_A receptors unadulterated by CCK_B/gastrin receptors.

Agonist activity in guinea-pig gallbladder

PG and TG are potent agonists at CCK_B/gastrin receptors but are less active at CCK_A-receptors (see Watson & Girdlestone, 1994). These compounds were thus considered potentially useful tools to desensitize CCK_B/gastrin receptors selectively in the stomach muscle. The choice of compound was aided by the use of the guinea-pig gallbladder assay. We previously showed in this tissue that the PG concentration-effect curve was located 3 log units to the right of the CCK-8 curve with a significantly lower maximum (Bishop *et al.*, 1992b). Because of this, and the fact that the effect was abolished by 100 nM devazepide, we argued that this effect was mediated exclusively by CCK_A receptors. TG contracted the gallbladder at a threshold concentration of 1 μM (Figure 3) and so appeared to be about 10 fold less potent than PG. For both agents fully-defined agonist concentration-effect curves could not be obtained because of limited solubility. Devazepide (300 nM), approximately 3000 fold its K_B value at CCK_A receptors, abolished the responses produced by TG, supporting the view that they were mediated by CCK_A receptors (Figure 3). The concentration of TG chosen (1 μM) for the desensitization of CCK_B/gastrin receptors in the guinea-pig gastric muscle assay was appoximately 100 fold higher than its $[A_{50}]$ value in that assay. In contrast, this was a threshold concentration in the gallbladder CCK_A receptor assay where it was shown to have no significant effect upon CCK-8 concentration-effect curves (Table 1).

CCK_B/gastrin receptor desensitization in guinea-pig gastric muscle

TG (1 μM) produced a rapid contraction of guinea-pig gastric muscle followed by a slower relaxation to the pre-stimulation baseline (Figure 4a). Subsequent addition of PG (1 nM–10 μM) had no effect (see Figure 4a). However, CCK-8 responses could still be obtained (Figure 4a) and the CCK-8 concentration-effect curve was now monotonic, symmetrical (Figure 4c, cf. Figure 1b) and could be fitted to the logistic function (see Table 1). This isolated CCK_A receptor curve, had the same maximum effect as the PG (the 'CCK_B/gastrin alone') curve but the midpoint slope was significantly flatter and the location was 1 log unit to the right of the PG curve and 1.5–2.0 log units to the right of the CCK-8 curve obtained on the guinea-pig gallbladder CCK_A receptor assay. The treatment with TG had no effect on concentration-effect curves to the ACh M-receptor agonist, 5-methylfurmethide, indicating that the desensitization was selective (Figure 4b). In addition, the desensitization was shown to last for at least 8 h (longer than any of the current experimental periods) as judged by the continuing absence of a response to 1 μM PG (data not shown).

Following desensitization with TG (1 μM), a single concentration of devazepide (3 nM), 30 fold its K_B at CCK_A receptors, was shown to produce a parallel, rightward, displacement of the CCK-8 concentration-effect curve (Figure 4c). Although the maximum of the shifted curve could not be fully-defined, the displacement of the curve by 1.5 log units was comparable with a pK_B value of ~ 10.

Discussion

Previous reports have been inconsistent with respect of the involvement of specific CCK_A- or CCK_B/gastrin receptors in the contractile effects of CCK-8 and PG in guinea-pig stomach muscle (Bitar & Makhlouf, 1982; Huang *et al.*, 1989; Menozzi *et al.*, 1989; Grider & Makhlouf, 1990; Boyle *et al.*, 1992; 1993). Boyle *et al.* (1993) have suggested that both were coupled to muscle contraction. Ideally, to simplify the bioassay, selective non-surmountable antagonists should be used to remove one of the other of the CCK_A- and CCK_B/gastrin receptor populations. However, no antagonist was available with sufficient selectivity. Therefore, we used selective CCK_B/gastrin receptor desensitization to separate the receptor populations, in addition to those compounds reported as agents for the discrimination and pharmacological characterization of CCK_A- or CCK_B/gastrin receptors (see Watson & Girdlestone, 1994).

PG and L-365260 have been previously classified as a selective agonist and competitive antagonist, respectively, at CCK_B/gastrin-receptors (see Watson & Girdlestone, 1994). As was expected from this classification, the PG concentration-effect curves were monophasic and displaced in parallel to the right in a concentration-dependent manner by L-365260 (Figure 2a). However, the corresponding Schild plot slope parameter value was significantly less than 1.00. It seems unlikely that the low slope was due to an action of pentagastrin at CCK_A-receptors because the experiment was performed in the presence of a concentration (10 nM) of the selective CCK_A receptor antagonist, devazepide, which was 100 fold greater than its reported K_B at CCK_A receptors (Bock *et al.*, 1988). Furthermore, the highest concentration of L-365260 used in the study (100 nM) is less than its reported K_B value at CCK_A receptors (Lotti & Chang, 1989). In addition to receptor heterogeneity, non-equilibrium conditions are also recognised as an explanation for low Schild plot slope parameters (see Kenakin, 1993). Boyle *et al.* (1992; 1993) also examined the interaction between pentagastrin and L-365260 in the same tissue, both in the absence and presence of devazepide (3 nM), but under isometric conditions at 37°C rather than isotonic conditions at 22°C. They obtained pA_2 values of 8.79 (95% c.l. 8.49–9.09) and 8.17 (95% c.l. 8.00–8.34) in the absence and presence of devazepide, respectively. It is interesting that, in agreement with the current data, the corresponding Schild plot slope parameter values were both less than 1 (0.75, 0.87, respectively), although in their study the 95% c.l. (0.39–1.10 and 0.58–1.19, respectively) included 1. However, these authors did recognise some irregularity in the behaviour of the system, when they found that the antagonism produced by the 'dipeptoid' CCK_B/gastrin receptor antagonist, CI988, which has also been classified as a competitive receptor antagonist (see Watson & Girdlestone, 1994), was not surmountable by PG in the presence of devazepide. The authors speculated that these results may be accounted for by 'allosteric interactions' between CCK_A- and CCK_B/gastrin receptors. Evidently, further studies using different CCK_B/gastrin receptor antagonists are needed to explore these possibilities.

In this study, the possibility that CCK-8 was interacting with a heterogeneous receptor population in gastric muscle was indicated by the finding that the CCK-8 concentration-effect data, in contrast to that obtained with PG, could not be fitted to the three-parameter logistic function and spanned a significantly wider concentration-range. Further evidence that receptor heterogeneity was responsible for the complex CCK-8 concentration-effect curve was provided by the non-parallel displacements obtained with the selective receptor antagonists. Although the inhibitory effect of L-365260 was complicated, the result indicated some involvement of CCK_B/gastrin receptors in the response to CCK-8. Devazepide, however, appeared to have little effect on responses to the lower concentrations of CCK-8 but shifted the upper region

of the curve implying that CCK_A receptors were also involved. This conclusion was supported by the finding that the devazepide-resistant, lower region of the CCK-8 concentration-effect curve was inhibited by L-365260. Collectively, these results suggest that both CCK_A- and CCK_B/gastrin receptors are coupled to muscle contraction in this tissue.

In agreement with earlier reports on the selectivity of gastrin peptide fragments for gastrin receptors (Morley *et al.*, 1965; Kaminski *et al.*, 1977; Holland *et al.*, 1982; Brand *et al.*, 1984), the shorter C-terminal fragment, TG, appeared to possess low affinity for the CCK_A receptor in the gallbladder assay as judged by the lack of effect of 1 μM on the CCK-8 concentration-effect curve. In this study, we apparently achieved selective operational elimination of the gastric muscle CCK_B/gastrin receptors using 1 μM TG (Table 1). Evidently, the desensitization was restricted to CCK_B/gastrin receptors because following pretreatment with TG, the muscarinic ACh receptor agonist, 5-methylfurmethide, concentration-effect curve was unaffected and it was still possible to obtain fully-defined CCK-8 concentration-effect curves. These curves were now symmetrical and could be fitted by the logistic function. The apparently different shape of the CCK-8 concentration-effect curve obtained following desensitization with TG further supports the view that CCK_B/gastrin receptors contribute to the complex CCK-8 concentration-effect curve obtained in untreated tissues. Interestingly, the slope of the CCK-8 curve obtained following pretreatment with TG ($P = 0.64 \pm 0.06$) was similar to that obtained in the guinea-pig gallbladder CCK_A receptor assay ($P = 0.69 \pm 0.05$). Desensitization produced a 'window' to permit the interaction between CCK-8 and devazepide (unconfounded by CCK_B/gastrin receptors) at CCK_A receptors as judged by the apparently parallel displacement of the agonist concentration-effect curve by devazepide. We were unable to study the effect of several concentrations of devazepide because the 'window' was limited both by the relatively low potency of CCK-8 and by its solubility. In fact, following desensitization with TG, the $[A_{50}]$ value of the CCK-8 concentration-effect curve was approximately 100 fold less than that obtained in the guinea-pig gallbladder CCK_A receptor assay (see Table 1). This suggests that the CCK_A receptors are present in lower concentrations and/or that the receptor coupling is less efficient in the gastric muscle than the gallbladder assay. Notwithstanding the low potency of CCK-8 following desensitization, the data obtained with the single concentration of devazepide were consistent with a competitive mechanism of action with a pK_B value of ~ 10 in accord with other reported affinity values (pK_B 9.98, Bishop *et al.*, 1992b; pA_2 9.89 and 9.93, Chang & Lotti, 1986; pA_2 9.6, Chang *et al.*, 1987; Louie *et al.*, 1988). The congruence of the values suggests that the relatively low operating temperature of the gastric muscle assay did not affect the affinity of the antagonist for the receptors.

In principle, there appears to be three parts to the analysis of systems that involve the concomitant activation of multiple receptors. The first is the characterization of the probe ligands, defining their selectivity and specificity. The second is the analysis of the system's response to activation of the individual receptors. The third is to find out, by modelling, how these analysed components need to combine to produce the system behaviour when it is operating under multiple stimulation. Several models of two receptor systems have been described. The simplest explanatory model to account for the simultaneous activation of two receptors that produce a single pharmacological effect is that first described by Hough *et al.* (1980). In the model, pharmacological effect is given by the algebraic sum of the effects produced by the selective stimulation of the individual receptors. Other, more complex, models have been considered in which the intracellular stimuli produced by activation of the two receptors are assumed to add algebraically and pharmacological effect is given as some specified function of the total stimuli obtained (e.g. Furchgott, 1981; Lemoine & Kaumann, 1983; Milnor, 1986). We started by considering the simplest model in which the CCK_B/gastrin and CCK_A-mediated responses were allowed to add algebraically such that neither the individual nor their combined effects could saturate the pharmacological effect machinery. The latter was consistent with the finding that, notwithstanding the high degree of variability between agonist concentration-effect curve asymptotes, we have consistently found that the maximum responses to CCK-8 and PG were generally only 10–20% of those to other contractile agents like KCl and 5-methylfurmethide that presumably share the same common effect machinery (for example, see Figure 4b).

Notwithstanding the complexity of the PG/L-365260 interaction, the data obtained suggest that CCK-8 (following TG pretreatment) and PG activate selectivity CCK_A and CCK_B/gastrin receptors, respectively. Assuming that PG and CCK-8 express the same potency at CCK_B/gastrin receptors, then the PG concentration-effect curve estimates the contribution of CCK_B/gastrin receptor activation to the control, composite, CCK-8 concentration-effect curve. Similarly, the CCK-8 concentration-effect curve obtained following TG pretreatment estimates the CCK_A receptor component if the assumption is made that TG did not desensitize the CCK_A receptors, as indicated from the gallbladder assay results. The simple model predicts that the composite CCK-8 control curve is given by the summation of the outputs of the two logistic equations that describe the PG and the CCK-8 (TG pretreated) concentration-effect curves (parameters as shown in Table 1). However, in practice, the summation produced a simulated curve that had nearly double the maximum of the experimental composite CCK-8 control curve (Figure 5a). Indeed, the upper asymptotes of the experimental CCK-8 control curve which, according to the simple addition of effects model, would represent the maximum response achievable by simultaneous activation of both CCK_B/gastrin and CCK_A receptors, is lower than the upper asymptotes generated by activation of the individual receptors. Similarly, the use of these 'control' curve parameters produced simulations that were not congruent with the data obtained in the experiments using the antagonists, devazepide and L-365260 (Figure 5c and e).

Before rejecting the simple two receptor model, we considered whether the apparent deviation from the model could be accounted for by the variability of the upper asymptotes of the agonist concentration-effect curves obtained on the gastric muscle assay. The variability was remarkably high both between and within assays and we were unable to reduce this variation by the use of 'sighting' responses, paired curve or paired tissue experimental designs. For example, the variability of the α values for PG, TG and CCK-8 (+TG 1 μM) in the stomach muscle assay (necessarily expressed as a coefficient of variation because of the differences between the measurement systems: i.e. % s.d./mean) was from 33–68% compared with 6–20% for the α values for CCK-8 in the gallbladder assay (calculated from Table 1). In contrast, the variability (s.d.) of the midpoint location ($[A_{50}]$) and slope (p) parameter estimates in the gastric muscle assay appeared to be no greater than those we have encountered in other pharmacological *in vitro* bioassays (e.g. from Table 1: s.d. of $\log[A_{50}]$ parameters: 0.13–0.39 for stomach muscle and 0.50–0.58 for the gallbladder; s.d. of mid-point slope parameters: 0.15 ± 0.24 for stomach muscle and 0.10–0.24 for the gallbladder). Therefore, model simulations were performed in which the values of $\log[A_{50}]$ and p, the robust parameters, were held constant throughout whereas the values of the upper asymptotes (α) were allowed to vary both between and within the experimental data sets. In this way we found model values of α which provided a reasonable simulation of the experimental data (see Figure 5). The simulations suggest that the asymmetry and flatness of the control CCK-8 curve was apparently due to the differences in the values of the midpoint slope and location of the CCK_B/

gastrin and CCK_A receptor-mediated component curves (Figure 5a,b). Moreover, the simulations support the assumption that the CCK_A receptors were not desensitized by the TG pretreatment and the conclusion that the CCK_A receptors are less well coupled and/or present in lower concentrations (100 fold) than in the guinea-pig gallbladder assay. The applicability of the simple two receptor model was demonstrated further by simulating the effect of devazepide and L-365260. By allowing the values of α to vary, it was possible to obtain a reasonable simulation of the families of CCK-8 concentration-effect curves obtained in the absence and presence of the antagonists (Figure 5d, f).

In conclusion, these studies support the hypothesis that both CCK_A and CCK_B/gastrin receptors are coupled to guinea-pig gastric muscle contraction. Moreover, although the ability to test the applicability of the model was severely weakened by the variability of the agonist asymptotes, the behaviour of the system is compatible with a simple, 'addition of effects', two-receptor model. Recently, it has been demonstrated that CCK-8 contracted another peripheral tissue assay, the guinea-pig isolated ileum longitudinal muscle myenteric plexus (LMMP), by activating both CCK_A- and CCK_B/gastrin receptors (Lucaites *et al.*, 1991; dal Forno *et al.*, 1992). The difference between the LMMP and the guinea-pig gastric muscle assay is that in the former, the two receptors were coupled by different mechanisms (the release of two different neurotransmitters, substance P and ACh). Apparently the combined activation could not be described by the existing explanatory models of two receptor systems, whereas in the latter, it appears that both receptor types are located directly on the smooth muscle cells and their simultaneous activation can be accounted for by a simple two-receptor model. Our initial aim was to develop a CCK_B/gastrin receptor assay that is unconfounded by CCK_A receptor activation. The results of the analysis suggest that this can be achieved using pentagastrin as agonist in the presence of a selective CCK_A receptor blocking concentration of devazepide.

References

BISHOP, L.A., GERSKOWITCH, V.P., HULL, R.A.D., SHANKLEY, N.P. & BLACK, J.W. (1992a). Characterization of the CCK_A and gastrin receptors coupled to muscle contraction in guinea-pig fundus using receptor desensitization. *Br. J. Pharmacol.*, **107**, 36P.

BISHOP, L.A., GERSKOWITCH, V.P., HULL, R.A.D., SHANKLEY, N.P. & BLACK, J.W. (1992b). Combined dose-ratio analysis of cholecystokinin receptor antagonists, devazepide, lorglumide and loxiglumide in the guinea-pig gall bladder. *Br. J. Pharmacol.*, **106**, 61–66.

BITAR, K.N. & MAKHLOUF, G.M. (1982). Receptors on smooth muscle cells: characterization by contraction and specific antagonists. *Am. J. Physiol.*, **242**, G400–G407.

BLACK, J.W. & SHANKLEY, N.P. (1985). The isolated stomach preparation of the mouse: a physiological unit for pharmacological analysis. *Br. J. Pharmacol.*, **86**, 571–579.

BOCK, M.G., DiPARDO, R.M., EVANS, B.E., RITTLE, K.E., FREIDINGER, R.M., CHANG, R.S. & LOTTI, V.J. (1988). Cholecystokinin antagonists. Synthesis and biological evaluation of 3-substituted 1,4-benzodiazepin-2-amines. *J. Med. Chem.*, **31**, 264–268.

BOYLE, S.J., TANG, K.W., McKNIGHT, A.T. & WOODRUFF, G.N. (1992). Characterization of CCK receptors in the circular muscle of the guinea-pig stomach corpus. *Br. J. Pharmacol.*, **106**, 9P.

BOYLE, S.J., TANG, K.W., WOODRUFF, G.N. & McKNIGHT, A.T. (1993). Characterization of CCK receptors in a novel smooth muscle preparation from the guinea-pig stomach by the use of the selective antagonists CI-988, L-365,260 and devazipide. *Br. J. Pharmacol.*, **109**, 913–917.

BRAND, S.J., ANDERSEN, B.N. & REHFELD, J.F. (1984). Complete tyrosine-O-sulphation of gastrin in neonatal rat pancreas. *Nature*, **309**, 456–458.

CHANG, R.S. & LOTTI, V.J. (1986). Biochemical and pharmacological characterization of an extremely potent and selective nonpeptide cholecystokinin antagonist. *Proc. Natl. Acad. Sci. U.S.A.*, **83**, 4923–4926.

CHANG, R.S.L., LOTTI, V.J. & CHEN, T.B. (1987). Characterization of [^{3}H]($\pm$)L-364,718 binding to solubilized cholecystokinin (CCK) receptors of rat pancreas. *Biochem. Pharmacol.*, **36**, 1709–1714.

EVANS, E., RITTLE, K.E., BOCK, M.G., DiPARDO, M., WHITTER, W.L., VEBER, D.F., ANDERSON, P.S. & FREIDINGER, R.M. (1986). Design of potent, orally effective nonpeptidal antagonists of the peptide hormone cholecystokinin. *Proc. Natl. Acad. Sci. U.S.A.*, **83**, 4918–4922.

DAL FORNO, G., URCIUOLI, P.M., VAN AMSTERDAM, F.T.M., TOSON, G., GAVIRAGHI, G. & TRIST, D. (1992). Evidence for two cholecystokinin receptors mediating the contraction of the guinea pig longitudinal muscle myenteric plexus. *J. Pharmacol. Exp. Ther.*, **261**, 1056–1063.

FURCHGOTT, R.F. (1981). Adrenergic and dopaminergic peripheral receptors. In *Proceedings of the 4th Meeting on Adrenergic Mechanisms*, pp. 10–29, Laboratorio de Farmacologia, Faculdade de Medicina, Porto, Portugal, 1981.

GRIDER, J.R. & MAKHLOUF, G.M. (1990). Distinct receptors for cholecystokinin and gastrin on muscle cells of stomach and gallbladder. *Am. J. Physiol.*, **259**, G184–G190.

HOLLAND, J., HIRST, B.H. & SHAW, B. (1982). Structure-activity studies with cholecystokinin on gastric secretion in the cat. *Peptides*, **3**, 891–895.

HOUGH, L., WEINSTEIN, H. & GREEN, J.P. (1980). One agonist and two receptors mediating the same effect: histamine receptors linked to adenylate cyclase in the brain. In *Receptors for Neurotransmitters and Peptide Hormones*. ed. Pepeu, G., Kuhar, M.S. & Enna, S.J. New York: Raven Press.

HUANG, S.C., ZHANG, L., CHIANG, H.C., WANK, S.A., MATON, P.N., GARDNER, J.D. & JENSEN, R.T. (1989). Benzodiazepine analogues L365,260 and L364,718 as gastrin and pancreatic CCK receptor antagonists. *Am. J. Physiol.*, **257**, G169–G174.

JENKINSON, D.H. (1992). How do we describe competitive antagonists: three questions of usage. *Trends Pharmacol. Sci.*, **12**, 53–54.

KAMINSKI, D.L., RUWART, M.J. & JELLINEK, M. (1977). Structure-function relationships of peptide fragments of gastrin and cholecystokinin. *Am. J. Physiol.*, **233**, 286–292.

KENAKIN, T.P. (1993). In *Pharmacologic Analysis of Drug-Receptor Interaction*. 2nd edition. New York: Raven Press. pp. 278–322.

LEMOINE, H. & KAUMANN, A.J. (1983). A model for the interaction of competitive antagonists with two receptor-subtypes characterized by a Schild plot with apparent slope unity. *Naunyn-Schmied. Arch. Pharmacol.*, **322**, 111–120.

LOTTI, V.J. & CHANG, R.S.L. (1989). A new potent and selective non-peptide gastrin antagonist and brain cholecystokinin receptor (CCK-B) ligand: L365260. *Eur. J. Pharmacol.*, **162**, 273–280.

LOUIE, D.S., LIANG, J.P. & OWYANG, C. (1988). Characterization of a new CCK antagonist, L364,718: in vitro and in vivo studies. *Am. J. Physiol.*, **255**, G261–G266.

LUCAITES, V.L., MENDELSOHN, L.G., MASON, N.R. & COHEN, M.L. (1991). CCK-8, CCK-4 and gastrin-induced contractions in guinea pig ileum: evidence for differential release of acetylcholine and substance P by CCK-A and CCK-B receptors. *J. Pharmacol. Exp. Ther.*, **256**, 695–703.

MENOZZI, D., GARDNER, J.D., JENSEN, R.T. & MATON, P.N. (1989). Properties of receptors for gastrin and CCK on gastric smooth muscle cells. *Am. J. Physiol.*, **257**, G73–G79.

MILNOR, W.R. (1986). Limitations of Schild plots in a two-receptor system: alpha adrenoceptors of vascular smooth muscle. *J. Pharmacol. Exp. Ther.*, **238**, 237–241.

MORLEY, J.S., TRACY, H.R. & GREGORY, R.A. (1965). Structure-function relationships in the active C-terminal tetrapeptide sequence of gastrin. *Nature*, **207**, 1356–1359.

SHANKLEY, N.P., BLACK, J.W., GANELLIN, C.R. & MITCHELL, R.C. (1988). Correlation between log P_{OCT/H_2O} and pK_B estimates for a series of muscarinic and histamine H_2-receptor antagonists. *Br. J. Pharmacol.*, **94**, 264–274.

SHANKLEY, N.P., WELSH, N.J. & BLACK, J.W. (1992). Histamine dependence of pentagastrin-stimulated gastric acid secretion in rats. *Yale J. Biol. Med.*, **65**, 613–619.

SPRAGGS, C.F. & PATEL, M. (1989). Comparison of the effects of gastrin/cholecystokinin-related peptides in rat gastric mucosa and guinea-pig ileum. *Br. J. Pharmacol.*, **98**, 661P.

TRIST, D.G. & LEFF, P. (1985). Quantification of H_2-agonism by clonidine and dimaprit in an adenylate cyclase assay. *Agents Actions*, **16**, 222–226.

WATSON, S.P. & GIRDLESTONE, D. (1994). In: *Receptors and Ion Channel Nomenclature*. Supplement. *Trends Pharmacol. Sci.*, Vol. 5.

WELSH, N.J., SHANKLEY, N.P. & BLACK, J.W. (1992). Comparison of antagonist pK_B estimates in lumen-perfused stomach assays from guinea-pig, rat and mouse. *Br. J. Pharmacol.*, **106**, 98P.

(Received April 29, 1994
Revised September 2, 1994
Accepted September 20, 1994)

British Journal of Pharmacology (1995) 114, 349-356 © 1995 Stockton Press All rights reserved 0007-1188/95 $9.00

Failure of nitric oxide donors to alter arrhythmias induced by acute myocardial ischaemia or reperfusion in anaesthetized rats

[1]Christopher S. Barnes & [2]Susan J. Coker

Department of Pharmacology and Therapeutics, University of Liverpool, P.O. Box 147, Liverpool L69 3BX

1 The aim of the present studies was to examine the effects of nitric oxide donors on arrhythmias induced by coronary artery occlusion and reperfusion, and on cardiac cyclic nucleotides. Experiments were performed in pentobarbitone-anaesthetized rats prepared for occlusion of the left coronary artery.

2 Sodium nitroprusside (0.1, 0.3 and 1 $\mu g\,kg^{-1}\,min^{-1}$) had no significant effects on the incidence of ventricular tachycardia, total ventricular fibrillation or the mortality resulting from 25 min of acute myocardial ischaemia when compared with values in controls. In addition, there was no alteration in the number of ventricular premature beats that occurred in survivors.

3 3-Morpholinosydnonimine-N-ethylcarbamide (SIN-1, 10, 20 and 40 $\mu g\,kg^{-1}\,min^{-1}$) caused marked hypotension but did not alter the incidence or severity of ischaemia-induced arrhythmias. In rats subject to abrupt reperfusion after 5 min of myocardial ischaemia, lower doses of SIN-1 (1, 3 and 10 $\mu g\,kg^{-1}\,min^{-1}$) still caused significant reductions in systolic and diastolic blood pressure but were devoid of antiarrhythmic activity.

4 In separate experiments in sham-operated rats, sodium nitroprusside (1 $\mu g\,kg^{-1}\,min^{-1}$), isosorbide dinitrate (30 and 60 $\mu g\,kg^{-1}\,min^{-1}$) and SIN-1 (20 and 40 $\mu g\,kg^{-1}\,min^{-1}$) had no significant effects on cardiac cyclic GMP content.

5 These results indicate that nitric oxide donors do not alter arrhythmias induced by acute coronary artery occlusion or reperfusion in anaesthetized rats. Although increases in total *cardiac* cyclic GMP could not be detected, the results suggest that, at least in the rat, cyclic GMP does not influence these arrhythmias.

Keywords: Nitric oxide; SIN-1; sodium nitroprusside; arrhythmias; myocardial ischaemia; coronary artery occlusion; reperfusion; cyclic AMP; cyclic GMP

Introduction

Nitric oxide has two effects which may be of particular importance in the setting of acute myocardial ischaemia. Firstly, it is a potent vasodilator, an activity that has been recognised since the discovery of endothelium-derived relaxing factor (Furchgott & Zawadzki, 1980) and its subsequent identification as nitric oxide (Palmer *et al.*, 1987). Secondly, nitric oxide prevents platelet adhesion and aggregation (Furlong *et al.*, 1987; Radomski *et al.*, 1987). Both antiplatelet actions and vasodilatation may reduce the severity of myocardial ischaemia and could therefore reduce the number or severity of arrhythmias associated with myocardial ischaemia. Prior to the recognition of the importance of endothelium-derived relaxing factor, there were reports that glyceryl trinitrate had antiarrhythmic activity in anaesthetized dogs subject to acute myocardial ischaemia (Borer *et al.*, 1974; Kent *et al.*, 1974; Stockman *et al.*, 1975). More recently, evidence has emerged which suggests that at least part of the antiarrhythmic benefit derived from ischaemic preconditioning is dependent on the release of endogenous nitric oxide (Vegh *et al.*, 1992). However, the studies with glyceryl trinitrate examined only single doses under particular experimental conditions. Little information is available about the effects of other nitric oxide donors or on dose-dependency in relation to effects on ischaemia-induced or reperfusion-induced arrhythmias.

Another reason for our interest in the possible effects of nitric oxide donors on arrhythmias associated with myocardial ischaemia is because these drugs increase guanosine 3':5'-cyclic monophosphate (cyclic GMP) (Kukovetz *et al.*, 1979). Previously, one conclusion that was drawn from studies with certain phosphodiesterase inhibitors was that increasing cardiac cyclic GMP may be antiarrhythmic (Holbrook & Coker, 1989). Although we have performed further studies with phosphodiesterase inhibitors, no firm conclusions about the possible influence of cyclic GMP on arrhythmias could be drawn from these experiments because we could not detect selective increases in cardiac cyclic GMP without concomitant increases in adenosine 3':5'-cyclic monophosphate (cyclic AMP) (Barnes, 1993). Thus, instead of using drugs to prevent the metabolism of cyclic GMP we decided to investigate the effects of alternative means of increasing cyclic GMP. One other pharmacological way to elevate cyclic GMP is to use nitrovasodilator drugs which release nitric oxide, which in turn stimulates soluble guanylyl cyclase to increase cyclic GMP production (Katsuki *et al.*, 1977). Thus, the aim of the present work was to examine the effects of nitric oxide donors on ischaemia-induced and reperfusion-induced arrhythmias and to measure the effects of nitric oxide donors on cardiac cyclic nucleotides. Studies on arrhythmias and cardiac cyclic nucleotides were performed with sodium nitroprusside and 3-morpholinosydnonimine-N-ethylcarbamide (SIN-1), a metabolite of molsidomine (Noack & Feelisch, 1989) and in addition the effects of isosorbide dinitrate on cyclic nucleotides were also determined. Some of these results have been published in abstract form after presentation to the British Pharmacological Society (Coker & Barnes, 1993).

Methods

Animal preparation

Experiments were performed on male Wistar rats (250 to 355 g) supplied by the departmental animal unit. These

[1] Present address: Xenova Ltd, 240 Bath Road, Slough, Berkshire SL1 4EF.
[2] Author for correspondence.

animals had been housed in small groups in a room maintained at 20°C on a 12 h light/dark cycle with food (Labsure CRM diet) and water available *ad libitum*. Rats were anaesthetized with sodium pentobarbitone, 60 mg kg^{-1}, i.p., and prepared for coronary artery occlusion by the methods of Clark *et al.* (1980) using equipment described in detail previously (Coker & Ellis, 1987).

The trachea, a carotid artery and a femoral vein were cannulated, to allow artificial respiration, measurement of arterial blood pressure and drug administration respectively. A left thoracotomy was performed as follows. An incision was made in the skin approximately 3 mm to the left of the midline, from the level of the xiphisternum up to the level of the clavicle. The underlying muscle layer (fibres running diagonally from the sternum up towards the foreleg) was cut along the same line as the skin incision, with any bleeding being controlled by gentle pressure with a gauze swab. The connective tissue between the next major muscle layer (fibres running longitudinally) and the ribs was cleared and the muscle layer eased back to reveal the ribs. An initial incision in the thoracic wall was made in the sixth intercostal space and extended along between the sixth and seventh ribs. Ribs six, five and four were then sectioned approximately 2 mm from the sternum, taking care to avoid the sternal arteries. These ribs were held back while the pericardium was incised and cleared from the heart. The heart was then exteriorised briefly while a fine silk ligature attached to a reverse cutting needle (Mersilk, W812; Ethicon) was placed around the left coronary artery close to its origin. Whilst the heart was exteriorised the left atrial appendage was allowed to fall back away from the ventricular surface. The needle was inserted into the ventricular wall at a point which normally lies just under the middle of the tip of the left atrial appendage. The needle was then manoeuvred so that it exited on the other side of the left coronary artery (which runs alongside the visible vein) level with the edge of the left atrial appendage alongside the pulmonary cone.

As soon as the initial incision in the thoracic wall was made, the rats were ventilated with room air at a rate of 54 strokes min^{-1}, a stroke volume of 1 to 1.5 ml 100 g^{-1} (adjusted to maintain an arterial Po_2 above 70 mmHg) and a positive end-expiratory pressure of 0.5 to 1 cmH_2O. Care was taken to ensure that the lungs were reinflated after the heart had been exteriorised briefly for placement of the ligature around the coronary artery. Rectal temperature was monitored with a thermometer and the anaesthetized rats were maintained at a temperature of 37 to 38°C by means of a heated table. A Lead I ECG was monitored along with arterial blood pressure, and drug or vehicle was infused at a rate of 0.05 ml min^{-1} (Harvard Apparatus Syringe Infusion Pump 22, Edenbridge, Kent) via the venous cannula.

Ischaemia-induced arrhythmias

After preparation and a 10 min stabilization period, drug or vehicle administration commenced and 10 min later the coronary artery was occluded to induce myocardial ischaemia. The arrhythmias that occurred during the first 25 min of myocardial ischaemia were identified in accordance with the definitions described in the Lambeth Conventions (Walker *et al.*, 1988). In survivors the total number of ventricular premature beats, including singles, bigeminy, salvos and ventricular tachycardia (defined as four or more consecutive ventricular premature beats) was counted. The incidence and duration of ventricular tachycardia and ventricular fibrillation were also recorded along with the mortality (due to sustained ventricular fibrillation, defined as continuous ventricular fibrillation persisting for at least 3 min).

Rats were excluded from the final analysis if any of the following occurred: arrhythmias prior to coronary artery occlusion; cardiac failure (defined as a profound reduction in arterial pressure, approaching zero within the first 5 min following coronary occlusion, usually accompanied by A–V block, which is probably due to the ligature being placed too deeply such that the septal branch of the left coronary artery is also occluded); no evidence of ischaemia after tying the ligature (changes in ST-segment or R wave amplitude, arrhythmias); mean blood pressure <60 mmHg prior to drug or vehicle administration. Any rats which were excluded were replaced immediately.

Reperfusion-induced arrhythmias

Reperfusion-induced arrhythmias were examined in separate groups of rats. Animals were prepared for coronary artery occlusion as described above. Instead of tying the ligature around the coronary artery permanently, both ends of the ligature were passed through a small plastic button and coronary artery occlusion was induced by applying tension to the ligature and clamping it with a small pair of rubber-sheathed Dieffenbach forceps. After 5 min of myocardial ischaemia the tension on the ligature was released to allow reperfusion. The resulting reperfusion-induced arrhythmias were monitored for 10 min. The exclusion criteria were the same as those defined above for the experiments on ischaemia-induced arrhythmias. In addition, rats were also excluded if severe arrhythmias (ventricular tachycardia or ventricular fibrillation) were occurring at the time (+ 10 s) when reperfusion should have occurred, or if there was no evidence that release of the ligature had resulted in reperfusion (i.e. no prevention or reversal of ischaemia-induced ST-segment changes).

Protocols for arrhythmia experiments

Two studies on ischaemia-induced arrhythmias and one on reperfusion-induced arrhythmias were performed. In each arrhythmia study there were 4 groups; three doses of drug and a contemporary vehicle control group. The first study on ischaemia-induced arrhythmias examined the effects of sodium nitroprusside (0.1, 0.3 and 1 $\mu g\,kg^{-1}\,min^{-1}$) and the second study looked at the effects of SIN-1 (10, 20 and 40 $\mu g\,kg^{-1}\,min^{-1}$). The effects of SIN-1 on reperfusion-induced arrhythmias were also investigated but in this study the doses of SIN-1 were 1, 3 and 10 $\mu g\,kg^{-1}\,min^{-1}$. Within each study, rats were allocated to individual drug or control groups in a random manner, with 12 rats in each group. Intravenous drug or vehicle infusion commenced 10 min before coronary artery occlusion and was maintained for the duration of the experiment.

Cyclic nucleotide experiments

Separate groups of sham-operated rats ($n = 5$ per group) were used to determine the effects of sodium nitroprusside (1 $\mu g\,kg^{-1}\,min^{-1}$), isosorbide dinitrate (30 and 60 $\mu g\,kg^{-1}\,min^{-1}$) and SIN-1 (20 and 40 $\mu g\,kg\,min^{-1}$) on cardiac cyclic nucleotide contents. These rats were prepared in exactly the same manner as those used for the arrhythmia experiments but the ligature placed around the coronary artery was not tied. At 15 min after starting drug or vehicle administration (equivalent to 5 min post-occlusion in the arrhythmia experiments, the time at which ectopic activity most often starts to occur) the heart was exteriorized, by pulling on the ligature around the coronary artery, and the heart was freeze-clamped in Wollenberger tongs (Biomedix, Pinner, Middlesex), which had been pre-cooled in liquid nitrogen. The frozen tissue was then stored at −80°C until assayed for cyclic nucleotides.

Frozen hearts were broken up under liquid nitrogen with a stainless steel PM3 pestle and mortar (Biomedix, Pinner, Middlesex) and pieces of ventricular tissue were weighed quickly. Two samples of approximately 100 mg each were taken for cyclic GMP determination and four samples, approximately 25 mg each, were taken for cyclic AMP determination. Each frozen sample was placed in a plastic vial containing 1 ml of ice-cold 6% w/v trichloroacetic acid

(TCA) and homogenized for 90 s (9 × 10 s bursts) in an Ultra Turrax homogenizer fitted with an 8N shaft. The homogenizer shaft was then rinsed with a further 0.5 ml TCA. The samples were centrifuged at 8000 *g* and 4°C for 15 min in an MSE 18 centrifuge after which the supernatant of each sample was removed and placed in a 10 ml glass test tube and capped. The TCA was extracted from each sample 4 times with 5 volumes of water-saturated diethyl ether. After the final extraction the samples were dried at 40 to 50°C for 5 min to evaporate any residual traces of ether and then stored at −20°C until assay.

Prior to assaying for cyclic nucleotides, the samples were concentrated by being freeze-dried overnight then reconstituted in 400 µl of assay buffer. Aliquots (100 µl for cyclic GMP and 50 µl for cyclic AMP) were assayed in duplicate with commercially available kits (TRK 500 and TRK 432 respectively, Amersham, UK). The detection limits, arbitrarily defined as the amount of unlabelled nucleotide necessary to reduce the binding of tritiated nucleotide by 15% compared with the zero standard were 0.16 pmol/tube for cyclic GMP and 0.24 pmol/tube for cyclic AMP. Taking into account the amount of tissue homogenized and the dilution factors, these values are equivalent to 6.4 and 76.8 pmol g^{-1} of heart for cyclic GMP and cyclic AMP respectively. For samples falling within the linear portions of the standard curves the intra-assay coefficient of variation for cyclic GMP was approximately 8% and that for cyclic AMP was <5%.

Drugs

SIN-1 (3-morpholinosydnonimine-N-ethylcarbamide) was a generous gift from Cassella AG, Frankfurt am Main, Germany, isosorbide dinitrate solution (Isoket 0.1%) was purchased from the Royal Liverpool University Hospital Pharmacy and sodium nitroprusside was purchased from Sigma, Poole. SIN-1 and sodium nitroprusside were made up as stock solutions of 1 mg ml^{-1} in normal saline, divided into aliquots and stored at −20°C until required. Further dilutions of all the nitric oxide donors were made in saline immediately prior to use and care was taken to ensure that all solutions of nitric oxide donors were protected from light. Diethyl ether and trichloroacetic acid (TCA) were obtained from FSA Laboratory Supplies, Loughborough, and sodium pentobarbitone from RMB Animal Health Ltd, Dagenham.

Statistics

Where appropriate, values have been expressed as the mean ± s.e.mean or the geometric mean (with 95% confidence limits) of *n* experiments. Haemodynamic data were subject to analysis of variance with significance levels determined by modified *t* tests with Bonferroni correction. Cyclic nucleotide data and the numbers of ventricular premature beats were compared with Mann-Whitney U tests and the incidence of arrhythmias subject to χ^2 analysis (Fisher's exact test). A probability value of $P<0.05$ was considered to be significant.

Results

Effects of sodium nitroprusside on ischaemia-induced arrhythmias

In control rats the induction of acute myocardial ischaemia by coronary artery occlusion caused arrhythmias which varied in severity from single ventricular premature beats to terminal ventricular fibrillation. The majority of the arrhythmias occurred between 5 and 15 min post-occlusion. Ventricular tachycardia occurred in all the rats in this study, except one which received the middle dose of sodium nitroprusside (this animal had a few ectopic beats then went straight into terminal ventricular fibrillation). All of the rats in the control group for this particular study had ventricular fibrillation but this was only sustained, resulting in death, in 6 of the 12 rats. At least 75% of the rats in each group receiving sodium nitroprusside (0.1, 0.3 or 1 µg $kg^{-1}min^{-1}$) also had ventricular fibrillation and in at least half the animals in each of these drug groups this ventricular fibrillation was sustained. Thus administration of these doses of sodium nitroprusside did not significantly alter the total incidence of ventricular fibrillation or the mortality (Figure 1). There was also no significant difference in the total number of ventricular premature beats (including those occurring as ventricular tachycardia) that occurred in rats which survived the 25 min period of ischaemia between any of the groups receiving sodium nitroprusside and the controls (Figure 2).

Heart rate was not altered by infusion of sodium nitroprusside. Before and during drug infusion there were no significant differences between the values in the control group and the values at corresponding time points in any of the groups receiving sodium nitroprusside (Figure 3). In contrast, sodium nitroprusside did cause some reduction in systolic and diastolic arterial blood pressure. The values measured 5 and 10 min after commencing infusion of the highest dose of sodium nitroprusside (1 µg kg^{-1} min^{-1}) were significantly lower than those measured at the same time points in the control group (Figure 3).

Effects of SIN-1 on ischaemia-induced arrhythmias

Similar experiments were performed with another nitric oxide donor, SIN-1. Infusion of 10, 20 or 40 µg kg^{-1} min^{-1} of SIN-1, commencing 10 min before coronary artery occlusion did not alter the incidence of ventricular tachycardia (100% in each group), ischaemia-induced ventricular fibrillation or the mortality (Figure 4). Similarly, the number of ventricular premature beats that occurred in survivors was not changed by administration of SIN-1 (Figure 5). Although SIN-1 had no significant effects on the number or severity of the ischaemia-induced arrhythmias the doses used here did have profound haemodynamic actions. Figure 6 illustrates clearly that SIN-1 caused marked reductions in systolic and diastolic arterial pressure. In addition a significant bradycardia was also observed with all three doses of SIN-1 (Figure 6).

The severity of ischaemia-induced arrhythmias did not seem to be related to the degree of hypotension resulting from infusion of SIN-1. The haemodynamic values, measured 10 min after starting drug infusion, in all the rats which

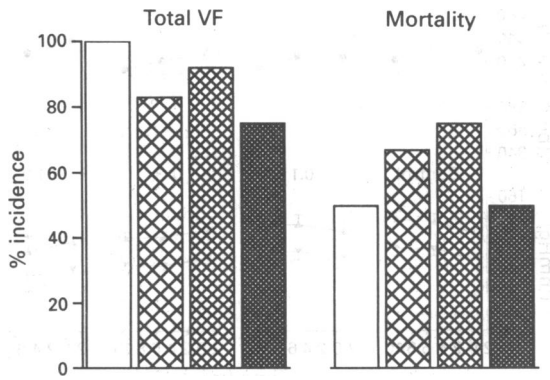


Figure 1 The effects of sodium nitroprusside 0.1 µg kg^{-1} min^{-1} (light cross-hatched columns), 0.3 µg kg^{-1} min^{-1} (medium cross-hatched columns) and 1 µg kg^{-1} min^{-1} (dense cross-hatched columns) compared with saline controls (open columns) on the total incidence of ventricular fibrillation (VF) and the mortality due to sustained VF that occurred during the first 25 min of acute myocardial ischaemia. $n = 12$ per group.

received SIN-1 were pooled and subdivided into survivors and non-survivors. Heart rate (370 ± 10 and 375 ± 11 beats min^{-1}), systolic blood pressure (65 ± 3 and 69 ± 3 mmHg) and diastolic blood pressure (43 ± 3 and 42 ± 2 mmHg) in survivors ($n = 23$) and non-survivors ($n = 13$) respectively, were not significantly different.

Effects of SIN-1 on reperfusion-induced arrhythmias

Further experiments were performed to investigate whether SIN-1 could alter the incidence or severity of reperfusion-induced arrhythmias. To avoid the profound hypotension observed previously, lower doses of SIN-1 were used in these studies. As anticipated, SIN-1 caused dose-dependent reductions in arterial blood pressure but of lesser magnitude than observed with the higher dose-range used in the study on ischaemia-induced arrhythmias. With the lowest dose of SIN-1 (1 $\mu g\ kg^{-1}\ min^{-1}$) the hypotension reached statistical significance only after 10 min of drug infusion. With the two higher doses the reductions in systolic and diastolic arterial blood pressure were significant 5 min after starting drug infusion (Figure 7). The effects on heart rate in this study are

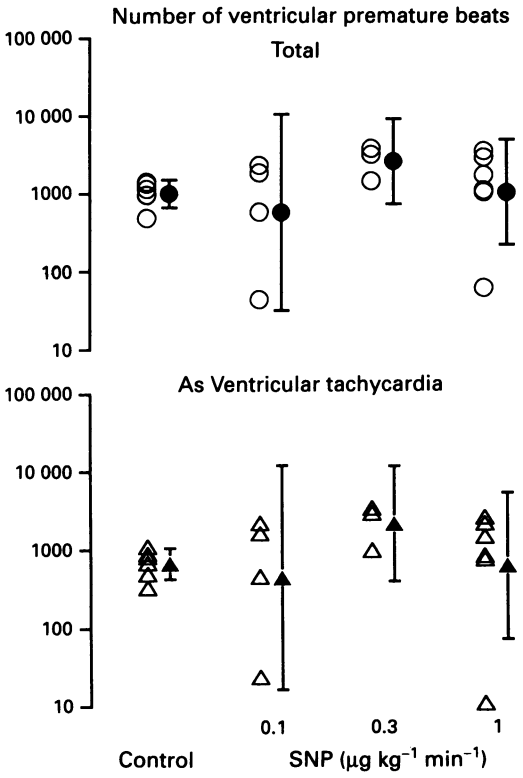


Figure 2 The effects of sodium nitroprusside 0.1, 0.3 and 1 $\mu g\ kg^{-1}\ min^{-1}$ on the number of ventricular premature beats that occurred in anaesthetized rats which survived the first 25 min of acute myocardial ischaemia (expressed as the total and as those occurring as ventricular tachycardia). Open symbols indicate values in individual animals; closed symbols indicate the geometric mean with the vertical bars indicating the 95% confidence limits.

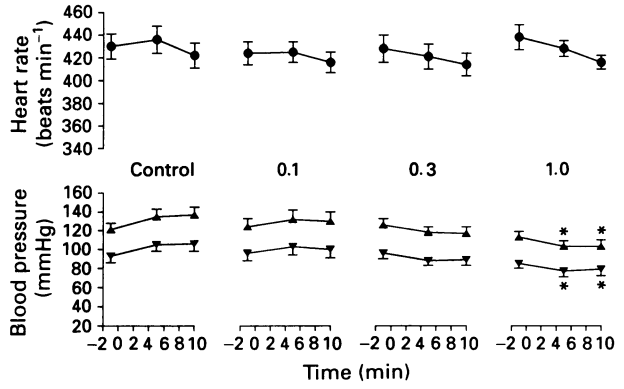


Figure 3 Heart rate, systolic (▲) and diastolic (▼) blood pressure measured 1 min before and 5 and 10 min after commencing infusion of saline or sodium nitroprusside at 0.1, 0.3 or 1 $\mu g\ kg^{-1}\ min^{-1}$ in the anaesthetized rats used to study ischaemia-induced arrhythmias. Each value is the mean ± s.e. mean, $n = 12$ per group. $^*P<0.01$ compared with the same time point in the control group, analysis of variance and modified t test (Bonferroni correction).

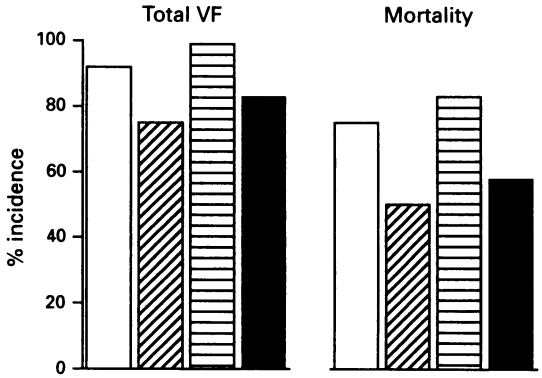


Figure 4 The effects of SIN-1, 10 $\mu g\ kg^{-1}\ min^{-1}$ (diagonally hatched columns), 20 $\mu g\ kg^{-1}\ min^{-1}$ (horizontally hatched columns) and 40 $\mu g\ kg^{-1}\ min^{-1}$ (solid columns) compared with saline controls (open columns) on the total incidence of ventricular fibrillation (VF) and the mortality due to sustained VF that occurred during the first 25 min of acute myocardial ischaemia. $n = 12$ per group.

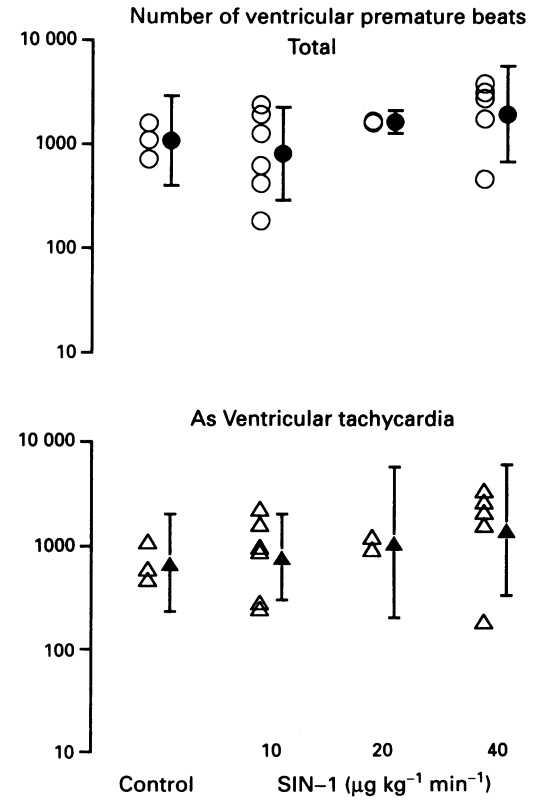


Figure 5 The effects of SIN-1, 10, 20 and 40 $\mu g\ kg^{-1}\ min^{-1}$ on the number of ventricular premature beats that occurred in anaesthetized rats which survived the first 25 min of acute myocardial ischaemia (expressed as the total and as those occurring as ventricular tachycardia). Open symbols indicate values in individual animals; the solid symbols indicate the geometric mean with the vertical bars indicating the 95% confidence limits.

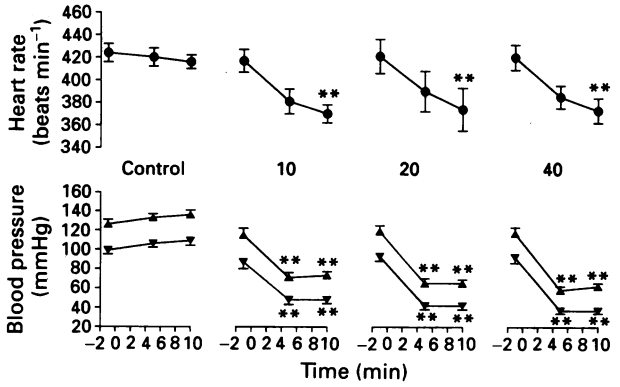


Figure 6 Heart rate, systolic (▲) and diastolic (▼) blood pressure measured 1 min before and 5 and 10 min after commencing infusion of saline or SIN-1 10, 20 or 40 $\mu g\,kg^{-1}\,min^{-1}$ in the anaesthetized rats used to study ischaemia-induced arrhythmias. Each value is the mean ± s.e. mean, $n = 12$ per group. $^{**}P<0.001$ compared with the same time point in the control group, analysis of variance and modified t test (Bonferroni correction).

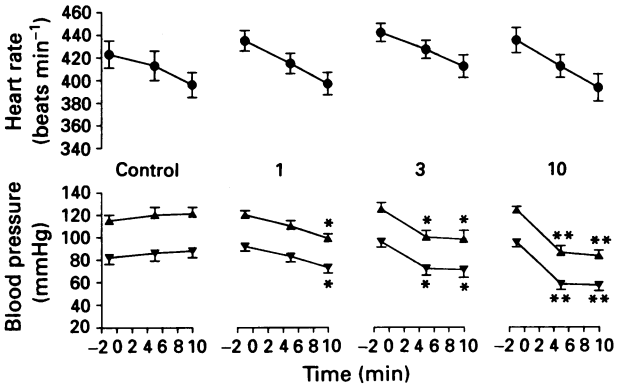


Figure 7 Heart rate, systolic (▲) and diastolic (▼) blood pressure measured 1 min before and 5 and 10 min after commencing infusion of saline or SIN-1 1, 3 or 10 $\mu g\,kg^{-1}\,min^{-1}$ in the anaesthetized rats used to study reperfusion-induced arrhythmias. Each value is the mean ± s.e. mean, $n = 12$ per group. $^{*}P<0.01$, $^{**}P<0.001$ compared with the same time point in the control group, analysis of variance and modified t test (Bonferroni correction).

more difficult to interpret. Figure 7 illustrates an apparent reduction in heart rate with SIN-1 but since heart rate also tended to decline in the control group no firm conclusion should be drawn from these data.

Abrupt reperfusion after 5 min of acute myocardial ischaemia usually causes severe arrhythmias which are rapid in onset but of brief duration compared to ischaemia-induced arrhythmias. In the control group for this particular study 8 out of 12 rats had reperfusion-induced ventricular fibrillation which was sustained resulting in death in all of these animals. None of the doses of SIN-1 significantly altered either the total incidence of reperfusion-induced ventricular fibrillation or the mortality (Figure 8). All of the rats had reperfusion-induced ventricular tachycardia. The arrhythmias started 7.3 ± 2.2 s after reperfusion in the controls and at 15.2 ± 3.7, 10.4 ± 2.9 and 7.6 ± 1.8 s in the rats which were receiving 1, 3 and 10 $\mu g\,kg^{-1}\,min^{-1}$ SIN-1 respectively. None of the latter values were significantly different from the value in the control group (Mann-Whitney U test). Similarly there were no significant differences in the duration of the reperfusion-induced arrhythmias in the survivors; the values were 179 ± 64, 152 ± 18, 190 ± 46 and 176 ± 42 s in the control, 1, 3 and 10 $\mu g\,kg^{-1}\,min^{-1}$ SIN-1 groups respectively. Thus, infusion of these doses of SIN-1 did not cause any significant

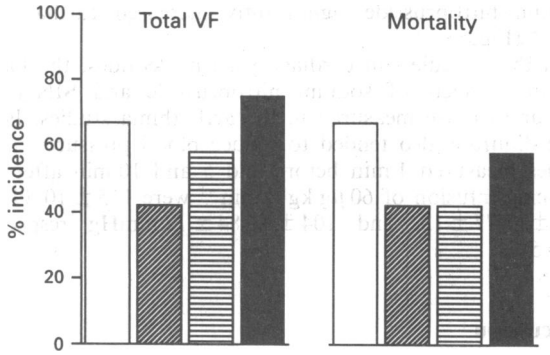


Figure 8 The effects of SIN-1, 1 $\mu g\,kg^{-1}\,min^{-1}$ (diagonally hatched columns), 3 $\mu g\,kg^{-1}\,min^{-1}$ (horizontally hatched columns) and 10 $\mu g\,kg^{-1}\,min^{-1}$ (solid columns) compared with saline controls (open columns) on the total incidence of ventricular fibrillation (VF) and the mortality due to sustained VF induced by reperfusion following 5 min of coronary artery occlusion. $n = 12$ per group.

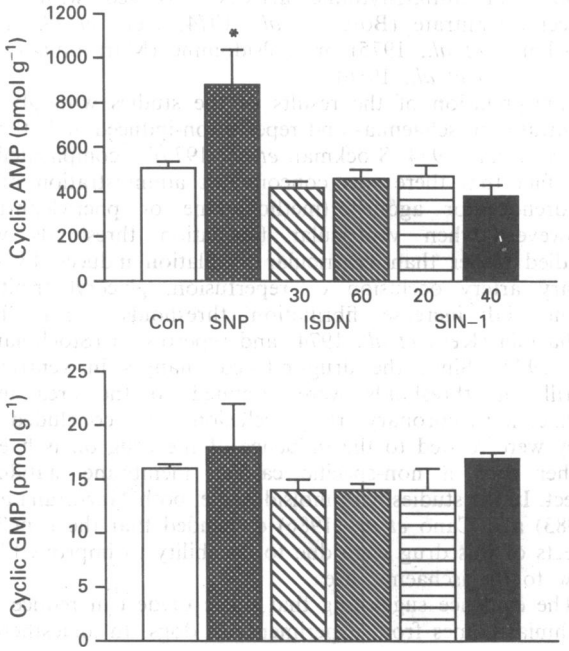


Figure 9 Cardiac cyclic nucleotide levels in anaesthetized rats which had received sodium nitroprusside (SNP), 1 $\mu g\,kg^{-1}\,min^{-1}$, isosorbide dinitrate (ISDN), 30 or 60 $\mu g\,kg^{-1}\,min^{-1}$, or SIN-1, 20 or 40 $\mu g\,kg^{-1}\,min^{-1}$ for 15 min prior to freeze-clamping of the heart. $n = 5$ per group. $^{*}P<0.05$ compared with control group, Mann-Whitney U test.

alterations in the incidence or severity of reperfusion-induced arrhythmias.

Effects of nitric oxide donors on cardiac cyclic nucleotides

Additional experiments were carried out to determine the effects of the nitric oxide donors, sodium nitroprusside, isosorbide dinitrate and SIN-1 on cardiac cyclic AMP and cyclic GMP contents. None of these nitric oxide donors caused any significant alteration in the value for cardiac cyclic GMP measured 15 min after starting drug infusion in anaesthetized rats prepared for coronary artery occlusion (Figure 9). The values for cardiac cyclic AMP in rats which had been receiving isosorbide dinitrate or SIN-1 were not different from the value in the control group. However,

sodium nitroprusside significantly increased cardiac cyclic AMP (Figure 9).

In these studies on cardiac cyclic nucleotides, the haemodynamic effects of sodium nitroprusside and SIN-1 were similar to those measured in the arrhythmia studies. Isosorbide dinitrate also tended to reduce blood pressure; e.g. the values measured 1 min before and 5 and 10 min after commencing infusion of 60 $\mu g\ kg^{-1}\ min^{-1}$ were $115 \pm 10/89 \pm 11$, $101 \pm 11/77 \pm 13$, and $104 \pm 11/84 \pm 12$ mmHg respectively ($n = 5$).

Discussion

The data presented above indicate clearly that in the anaesthetized rat, nitric oxide donors do not alter arrhythmias associated with acute myocardial ischaemia. Despite using two different nitric oxide donors and a wide range of doses giving haemodynamic responses varying from very mild to marked hypotension, there were no changes in the incidence or severity of either ischaemia-induced or reperfusion-induced arrhythmias. These results contradict previous reports of antiarrhythmic activity observed with either glyceryl trinitrate (Borer *et al.*, 1974; Kent *et al.*, 1974; Stockman *et al.*, 1975) or molsidomine (Martorana *et al.*, 1983; Cano *et al.*, 1986).

Interpretation of the results of the studies with glyceryl trinitrate on ischaemia- and reperfusion-induced arrhythmias (Borer *et al.*, 1974; Stockman *et al.*, 1979) is complicated by the fact that there was concomitant administration of an α-adrenoceptor agonist (methoxamine or phenylephrine). However, when ventricular fibrillation thresholds were studied rather than ventricular fibrillation induced by coronary artery occlusion or reperfusion, glyceryl trinitrate alone did increase fibrillation thresholds during both ischaemia (Kent *et al.*, 1974) and reperfusion (Stockman *et al.*, 1979). Since the drug-induced changes in ventricular fibrillation thresholds were confined to the area made ischaemic by coronary artery occlusion it was concluded that they were related to the influence of the drug on ischaemia rather than a non-specific cardiac membrane stabilizing effect. In the studies with molsidomine, both Martorana *et al.* (1983) and Cano *et al.* (1986) concluded that the beneficial effects of this drug were due to its ability to improve blood flow to the ischaemic area.

The evidence suggesting that nitric oxide can reduce arrhythmias comes from experiments in dogs. In anaesthetized rats, a single dose of glyceryl trinitrate (15 $\mu g\ kg^{-1}\ min^{-1}$) did not alter reperfusion-induced ventricular fibrillation or mortality (Kane *et al.*, 1984). Coronary collateral flow is relatively high in dogs but low in rats (Maxwell *et al.*, 1987). It is possible that nitric oxide may only be able to reduce arrhythmias in species where it can increase flow through collateral vessels to the ischaemic area, i.e. the antiarrhythmic effect is a consequence of a reduction in the severity of myocardial ischaemia. In contrast, however, it has been shown recently that pirsidomine reduced the number of ischaemia-induced ventricular premature beats in anaesthetized pigs (Wainwright & Martorana, 1993), a species with virtually no collateral flow (Maxwell *et al.*, 1987). Although ventricular premature beats were reduced in pigs, pirsidomine had no effect on the incidence of ventricular fibrillation (Wainwright & Martorana, 1993). Thus it seems that nitric oxide donors may reduce ventricular fibrillation only in species with good collateral flow.

A recent abstract provides further evidence which supports our present findings that nitric oxide donors do not influence ischaemia-induced arrhythmias in anaesthetized rats. In a similar model, C87-3754, an active metabolite of a novel sydnonimine (Bohn *et al.*, 1991), did not alter arrhythmias and the nitric oxide synthase inhibitor N^Gnitro-L-arginine methyl ester (L-NAME 100 mg kg^{-1}) also had no significant effects (Sun *et al.*, 1994). In addition, a recent study in our laboratory has also shown that administration of L-NAME (3, 10 or 30 mg kg^{-1}, i.v.), which caused significant dose-dependent increases in arterial blood pressure, had no effect on arrhythmias in anaesthetized rats subject to acute myocardial ischaemia (Aitchison & Coker, 1994). It is interesting to note that Sun *et al.* (1994) also found that L-NAME did not alter the marked antiarrhythmic effect of preconditioning in anaesthetized rats, whereas nitric oxide does appear to be involved in the antiarrhythmic effect of preconditioning in dogs (Vegh *et al.*, 1992). Thus it appears that neither endogenous nor exogenous nitric oxide influences arrhythmias associated with acute myocardial ischaemia in anaesthetized rats. Whether the failure of nitric oxide to have any antiarrhythmic activity in our experiments is related to the low collateral flow in the rat or some other feature unique to this particular species remains to be determined.

The results of the cyclic nucleotide assays indicate that administration of nitric oxide donors does not cause detectable increases in *cardiac* cyclic GMP. With the higher doses of SIN-1 marked reductions in arterial blood pressure were observed, which suggests that increases in vascular cyclic GMP did occur. The cardiac content of cyclic GMP is considerably lower than that of cyclic AMP. Our data indicate that there is approximately 25 fold less cardiac cyclic GMP than cyclic AMP and ratios indicating differences of up to 20 fold have been reported for rat heart by others (Kane *et al.*, 1985; Jones *et al.*, 1993). In vascular tissue there is much less difference between the levels of cyclic GMP and cyclic AMP. For example, in rat isolated aorta with endothelium, there is only 3 to 5 fold more cyclic AMP than cyclic GMP (Martin *et al.*, 1986). In addition, the amount of cyclic GMP in blood vessels is greater than in the whole heart. It is likely, therefore, that in the heart most of the cyclic GMP is in blood vessels (in endothelial cells, smooth muscle cells or platelets trapped in the coronary circulation as the heart was freeze-clamped) rather than in cardiac myocytes. Since the coronary vasculature represents a relatively small proportion of the heart, increases in coronary vascular cyclic GMP may have to be many times higher to be detected as increases in total *cardiac* cyclic GMP. We have confirmed that we could detect increases in cyclic GMP in rat isolated aortae incubated *in vitro* with sodium nitroprusside or SIN-1 (Barnes, 1993).

It is interesting to note that in the latter experiment, sodium nitroprusside increased both cyclic GMP and cyclic AMP (Barnes, 1993). Sodium nitroprusside was chosen for the first experiments on ischaemia-induced arrhythmias because it is inexpensive and readily available. At first we were puzzled by the results of the assays for cardiac cyclic nucleotides which showed that the highest dose of sodium nitroprusside used in the arrhythmia experiments did not alter cardiac cyclic GMP but did increase cyclic AMP significantly. However, it has been reported that there is a poor correlation between the vasodilator actions of sodium nitroprusside and its ability to increase vascular cyclic GMP and it has been suggested that sodium nitroprusside may have additional vasodilator activity (Feelisch, 1991). The elevation in cardiac cyclic AMP which we report here, supports the suggestion that sodium nitroprusside may indeed have additional actions. Whether these are a consequence of nitric oxide release from sodium nitroprusside or due to an independent mechanism cannot be determined from the present results. However, our data do suggest that sodium nitroprusside is not an ideal nitric oxide donor.

Having obtained the above results with sodium nitroprusside, we then decided to use an alternative nitric oxide donor and chose isosorbide dinitrate. The effects of this drug on cardiac cyclic nucleotides were examined first. Although this compound did not increase cyclic AMP it also failed to increase cardiac cyclic GMP and so was not used for arrhythmia experiments. Some recent reports contain evidence supporting our finding that isosorbide dinitrate did not increase cardiac cyclic GMP. No increases in plasma cyclic

GMP were detected in patients who had received isosorbide dinitrate orally, although significant reductions in blood pressure were observed (Shotan *et al.*, 1993). Similarly, neither oral nor i.v. administration of isosorbide dinitrate altered plasma cyclic GMP in rats (Kita *et al.*, 1994a,b).

We then examined the effects of SIN-1 since this compound does not need to interact with thiols to release nitric oxide (Feelisch, 1991). Again, and in this case, despite causing marked hypotension, cardiac cyclic GMP was not elevated. It was at this point that we reached the conclusion detailed above, that the drugs had not necessarily failed to increase cyclic GMP, but that any increase in vascular cyclic GMP which may have occurred could not be detected by measuring total *cardiac* cyclic GMP. SIN-1 was then used for the further arrhythmia studies.

The depressor responses to SIN-1 were greater than had been anticipated from preliminary pilot studies in closed chest rats. Comparison of the effects of SIN-1 on blood pressure in the ischaemia-induced and reperfusion-induced arrhythmia studies suggests that the responses obtained in the former experiments, although still dose-dependent were approaching maximum. It could be argued therefore that the degree of hypotension resulting from administration of these doses may have compromised myocardial perfusion. This could be expected to exacerbate arrhythmias, but SIN-1 also reduced heart rate, an effect which could be antiarrhythmic. There does not seem to be any obvious explanation for the bradycardia induced by SIN-1 in our experiments. In other species, SIN-1, or other sydnonimines, either caused tachycardia or had no effect on heart rate (Cano *et al.*, 1986; Groves *et al.*, 1993; Wainwright & Martorana, 1993). However, in the present study, the severity of arrhythmias did not appear to be related to the dose of SIN-1. In addition, subdivision of the rats into those which survived and those which died during the ischaemic period did not reveal any differences in blood pressure or heart rate. Thus it is unlikely that the haemodynamic effects of SIN-1 had a major influence on arrhythmias. Assuming that the hypotensive responses to SIN-1 indicate that elevations in cyclic GMP did occur in some areas (e.g. blood vessels), the lack of effect of SIN-1 on ischaemia-induced or reperfusion-induced arrhythmias suggests that cyclic GMP is not an important modulator of these events.

Thus to summarise, these studies have shown that nitric oxide donors do not alter arrhythmias induced by acute coronary artery occlusion or reperfusion in anaesthetized rats and suggest that, at least in the rat, cyclic GMP does not influence these arrhythmias. Further experiments are required to determine whether these results were obtained because of a particular feature found in the rat, such as low coronary collateral flow, or because nitric oxide is just not important in the rat coronary circulation.

This work was supported by a project grant from the British Heart Foundation. C.S.B. was in receipt of an MRC Studentship. We would like to thank Cassella AG for the gift of SIN-1.

References

AITCHISON, K.A. & COKER, S.J. (1994). Does endogenous nitric oxide influence ischaemia-induced arrhythmias? *J. Mol. Cell. Cardiol.*, **26**, (No. 6) LXVII.

BARNES, C.S. (1993). The potential influence of cyclic GMP on arrhythmias associated with myocardial ischaemia. *PhD Thesis, University of Liverpool.*

BOHN, H., BEYERLE, R., MARTORANA, P.A. & SCHONAFINGER, K. (1991). CAS 936, a novel sydnonimine with direct vasodilating and nitric oxide-donating properties: effects on isolated blood vessels. *J. Cardiovasc. Pharmacol.*, **19**, 522–527.

BORER, J.S., KENT, K.M., GOLDSTEIN, R.E. & EPSTEIN, S.E. (1974). Nitroglycerin-induced reduction in the incidence of spontaneous ventricular fibrillation during coronary artery occlusion in dogs. *Am. J. Cardiol.*, **33**, 517–520.

CANO, J-P., GUILLEN, J-C., JOUVE, R., LANGLET, F., PUDDU, P-E., ROLLAND, P-H. & SERRADIMIGNI, A. (1986). Molsidomine prevents post-ischaemic ventricular fibrillation in dogs. *Br. J. Pharmacol.*, **88**, 779–789.

CLARK, C., FOREMAN, M.I., KANE, K.A., McDONALD, F.M. & PARRATT, J.R. (1980). Coronary artery ligation in anesthetized rats as a method for the production of experimental dysrhythmias and for the determination of infarct size. *J. Pharmacol. Methods*, **3**, 357–368.

COKER, S.J. & BARNES, C.S. (1993). Effects of the nitric oxide donor SIN-1 on haemodynamics, ischaemia-induced arrhythmias and cardiac cyclic nucleotides. *Br. J. Pharmacol.*, **109**, 43P.

COKER, S.J. & ELLIS, A.M. (1987). Ketanserin and ritanserin can reduce reperfusion-induced but not ischaemia-induced arrhythmias in anaesthetised rats. *J. Cardiovasc. Pharmacol.*, **10**, 479–484.

FEELISCH, M. (1991). The biochemical pathways of nitric oxide formation from nitrovasodilators: appropriate choice of exogenous NO donors and aspects of preparation and handling of aqueous NO solutions. *J. Cardiovasc. Pharmacol.*, **17** (Suppl. 3), S25–S33.

FURCHGOTT, R.F. & ZAWADZKI, J.V. (1980). The obligatory role of endothelial cells in the relaxation of arterial smooth muscle by acetylcholine. *Nature*, **288**, 373–376.

FURLONG, B., HENDERSON, A.H., LEWIS, J.A. & SMITH, J.A. (1987). Endothelium-derived relaxing factor inhibits *in vitro* platelet aggregation. *Br. J. Pharmacol.*, **90**, 687–692.

GROVES, P.H., LEWIS, M.J., CHEADLE, H.A. & PENNY, W.J. (1993). SIN-1 reduces platelet adhesion and platelet thrombus formation in a porcine model of balloon angioplasty. *Circulation*, **87**, 590–597.

HOLBROOK, M. & COKER, S.J. (1989). Comparison of the effects of isobutylmethylxanthine and milrinone on ischaemia-induced arrhythmias and platelet aggregation in anaesthetized rabbits. *Br. J. Pharmacol.*, **98**, 318–324.

JONES, R.B., FRODSHAM, G., DICKENSON, K. & FOSTER, G.A. (1993). Effect of flosequinan on ischaemia-induced arrhythmias and on ventricular cyclic nucleotide content in the anaesthetized rat. *Br. J. Pharmacol.*, **108**, 1111–1116.

KANE, K.A., PARRATT, J.R. & WILLIAMS, F.M. (1984). An investigation into the characteristics of reperfusion-induced arrhythmias in the anaesthetized rat and their susceptibility to antiarrhythmic agents. *Br. J. Pharmacol.*, **82**, 349–357.

KANE, K.A., MORCILLO-SANCHEZ, E.J., PARRATT, J.R., RODGER, I.W. & SHAHID, M. (1985). The relationship between coronary artery occlusion-induced arrhythmias and myocardial cyclic nucleotide levels in the anaesthetized rat. *Br. J. Pharmacol.*, **84**, 139–145.

KATSUKI, S., ARNOLD, W., MITTAL, C. & MURAD, F. (1988). Stimulation of guanylate cyclase by sodium nitroprusside, nitroglycerin, and nitric oxide in various tissue preparations and comparison to the effects of sodium azide and hydroxylamine. *J. Cyclic Nucl. Res.*, **3**, 23–35.

KENT, K.M., SMITH, E.R., REDWOOD, D.R. & EPSTEIN, S.E. (1974). Beneficial electrophysiological effects of nitroglycerin during acute myocardial infarction. *Am. J. Cardiol.*, **33**, 516–517.

KITA, Y., HIRASAWA, Y., MAEDA, K., NISHIO, M. & YOSHIDA, K. (1994a). Spontaneous nitric oxide release accounts for the potent pharmacological actions of FK409. *Eur. J. Pharmacol.*, **257**, 123–130.

KITA, Y., SUGIMOTO, T., HIRASAWA, Y., YOSHIDA, K. & MAEDA, K. (1994b). Close correlation of the cardioprotective effect of FK409, a spontaneous NO releaser, with an increase in plasma cyclic GMP level. *Br. J. Pharmacol.*, **113**, 5–6.

KUKOVETZ, W.R., HOLZMANN, S., WURM, A. & POCH, G. (1979). Evidence for cyclic GMP-mediated relaxant effects of nitrocompounds in coronary smooth muscle. *Naunyn Schmied. Arch. Pharmacol.*, **310**, 129–138.

MARTIN, W., FURCHGOTT, R.F., VILLANI, G.M. & JOTHIANANDAN, D. (1986). Phosphodiesterase inhibitors induce endothelium-dependent relaxation of rat and rabbit aorta by potentiating the effects of spontaneously released endothelium-derived relaxing factor. *J. Pharmacol. Exp. Ther.*, **237**, 539–547.

MARTORANA, P.A., MOGILEV, A.M., KETTENBACH, B. & NITZ, R.-E. (1983). Effect of molsidomine on spontaneous ventricular fibrillation following myocardial ischemia and reperfusion in the dog. *Adv. Myocardiol.*, **4**, 605–613.

MAXWELL, M.P., HEARSE, D.J. & YELLON, D.M. (1987). Species variation in the coronary collateral circulation during regional myocardial ischaemia: a critical determinant of the rate of evolution and extent of myocardial infarction. *Cardiovasc. Res.*, **21**, 737–746.

NOACK, E. & FEELISCH, M. (1989). Molecular aspects underlying the vasodilator action of molsidomine. *J. Cardiovasc. Pharmacol.*, **14**, (Suppl. 11), S2–S5.

PALMER, R.M.J., FERRIGE, A.G. & MONCADA, S. (1987). Nitric oxide release accounts for the biological activity of endothelium-derived relaxing factor. *Nature*, **327**, 524–526.

RADOMSKI, M.W., PALMER, R.M.J. & MONCADA, S. (1987). Comparative pharmacology of endothelium-derived relaxing factor, nitric oxide and prostacyclin in platelets. *Br. J. Pharmacol.*, **92**, 181–187.

SHOTON, A., MEHRA, A., OSTRZEGA, E., HSUEH, W., DO, Y.S., FISHER, D.A., HURST, A., JOHNSON, J.V. & ELKAYAM, U. (1993). Plasma cyclic guanosine monophosphate in chronic heart failure: Hemodynamic and neurohumoral correlations and response to nitrate therapy. *Clin. Pharmacol. Ther.*, **54**, 638–644.

STOCKMAN, M.B., VERRIER, R.L. & LOWN, B. (1979). Effect of nitroglycerin on vulnerability to ventricular fibrillation during myocardial ischaemia and reperfusion. *Am. J. Cardiol.*, **43**, 233–238.

SUN, W., WAINWRIGHT, C.L. & PARRATT, J.R. (1994). The antiarrhythmic effect of ischaemic preconditioning is not prevented by inhibition of endothelium-derived nitric oxide in anaesthetized rats. *Br. J. Pharmacol.*, **112**, 380P.

VEGH, A., SZEKERES, L. & PARRATT, J.R. (1992). Preconditioning of the ischaemic myocardium; involvement of the L-arginine nitric oxide pathway. *Br. J. Pharmacol.*, **107**, 648–652.

WAINWRIGHT, C.L. & MARTORANA, P.A. (1993). Pirsidomine, a novel nitric oxide donor, suppresses ischemic arrhythmias in anaesthetized pigs. *J. Cardiovasc. Pharmacol.*, **22** (Suppl. 7) S44–S50.

WALKER, M.J.A., CURTIS, M.J., HEARSE, D.J., CAMPBELL, R.W.F., JANSE, M.J., YELLON, D.M., COBBE, S.M., COKER, S.J., HARNESS, J.B., HARRON, D.W.G., HIGGINS, A.J., JULIAN, D.J., LAB, M.J., MANNING, A.S., NORTHOVER, B.J., PARRATT, J.R., RIEMERSMA, R.A., RIVA, E., RUSSELL, D.C., SHERIDAN, D.J., WINSLOW, E. & WOODWARD, B. (1988). The Lambeth Conventions: Guidelines for the study of arrhythmias in ischaemia, infarction and reperfusion. *Cardiovasc Res.*, **22**, 447–455.

(Received June 7, 1994
Revised September 26, 1994
Accepted September 27, 1994)

British Journal of Pharmacology (1995) 114, 357-362 © 1995 Stockton Press All rights reserved 0007-1188/95 $9.00

Differential effect of sodium ions and guanine nucleotides on the binding of thioperamide and clobenpropit to histamine H_3-receptors in rat cerebral cortical membranes

E.A. Clark & [1]S.J. Hill

Department of Physiology & Pharmacology, Medical School, Queens' Medical Centre, Nottingham, NG7 2UH

1 Conflicting reports in the literature over heterogeneity (West *et al.*, 1990) or homogeneity (Arrang *et al.*, 1990) of histamine H_3-receptor binding sites may be attributed to the use of different incubation conditions. In the present study we have investigated the extent to which the binding of H_3-receptor ligands to rat cerebral cortical membranes can be modified by both sodium ions and guanine nucleotides.

2 The H_3-selective antagonist, thioperamide, discriminated between two specific binding sites for [^{3}H]-N$^\alpha$-methylhistamine ($IC_{50\,1}$ = 2.75 ± 0.87 nM, $IC_{50\,2}$ = 101.6 ± 12.0 nM, % site 1 = 24 ± 2%) in 50 mM Tris HCl buffer, but showed homogeneity of binding in 50 mM Na/K phosphate buffer.

3 Sodium ions markedly altered the binding characteristics of thioperamide (i.e. heterogeneity was lost and IC_{50} value shifted towards the high affinity site). The competition curves for a second H_3-antagonist, clobenpropit and the H_3-agonist N$^\alpha$-methylhistamine however, were unaltered in the presence of sodium ions.

4 Guanylnucleotides displaced only 60% of specific [^{3}H]-N$^\alpha$-methylhistamine binding and modulated thioperamide binding in the same way as sodium ions.

5 These data suggest that the H_3-receptor can exist in different conformations for which thioperamide, but not N$^\alpha$-methylhistamine and clobenpropit, show differential affinity.

6 The potential nature of these sites, and the implications of this apparent receptor heterogeneity for H_3-receptor antagonism by thioperamide, are discussed.

Keywords: Histamine H_3-receptors; [^{3}H]-N$^\alpha$-methylhistamine; sodium ions; guanylnucleotides

Introduction

Histamine receptors have been divided into three classes on the basis of pharmacological studies with receptor-selective agonists and antagonists (H_1, H_2 and H_3, Hill, 1990). Arrang *et al.* (1983; 1987b) have shown that histamine H_3-receptors can act presynaptically to inhibit the neuronal release and synthesis of histamine in rat cerebral cortical slices. In addition to their role in histaminergic neurotransmission (Arrang *et al.*, 1983; 1985; 1987b; Van der Werf *et al.*, 1987; Van der Vliet *et al.*, 1988), H_3-receptors have also been shown to interact with a variety of other neurotransmitter systems, e.g. cholinergic, peptidergic, 5-hydroxytryptaminergic and adrenergic (Schlicker *et al.*, 1988; 1989; Hew *et al.*, 1990; Clapham & Kilpatrick, 1992; Taylor & Kilpatrick, 1992).

Radioligand binding studies with the high affinity H_3-agonists [^{3}H]-R$^\alpha$-methylhistamine (Arrang *et al.*, 1990; Kilpatrick & Michel, 1991) and [^{3}H]-N$^\alpha$-methylhistamine (West *et al.*, 1990; Korte *et al.*, 1990) have successfully identified binding sites with the characteristics of H_3-receptors in both rat and guinea-pig tissues. The binding of ^{3}H-agonists to these sites has been shown to be regulated by guanine nucleotides (implying a G-protein linkage) and several cations (Arrang *et al.*, 1987a; 1990; Zweig *et al.*, 1992). Magnesium and sodium have been shown to inhibit [^{3}H]-R$^\alpha$-methylhistamine binding (Kilpatrick & Michel, 1991), and the presence of calcium ions was found to produce some heterogeneity of agonist binding (Arrang *et al.*, 1990).

Heterogeneity of H_3-receptor binding has also been reported by West *et al.* (1990) who identified two components in the binding of [^{3}H]-N$^\alpha$-methylhistamine to rat brain membranes in 50 mM Tris buffer that could be discriminated by the selective H_3-antagonist thioperamide. These data have been interpreted as evidence for multiple H_3-receptor subtypes (West *et al.*, 1990); however, an alternative possibility is that this heterogeneity of thioperamide binding reflects a differential affinity of this antagonist for different conformations of a single class of H_3-receptor. For example, in NG108-15 cells, heterogeneity of binding to opiate receptors has been observed for certain antagonists which display 'negative efficacy' i.e. they disrupt the spontaneous tendency of receptors to interact with G-proteins by having a higher affinity for 'uncoupled' receptors (Costa *et al.*, 1990;1992; Lefkowitz *et al.*, 1993). Furthermore, the binding of this type of antagonist, but not neutral antagonists (which have similar affinity for uncoupled and G-protein coupled receptors), can be markedly altered by sodium ions and guanine nucleotides (Costa *et al.*, 1990). Interestingly, Arrang *et al.* (1990) found no evidence for differential binding of thioperamide to H_3-receptors when ^{3}H-agonist binding to rat brain membranes was monitored in 50 mM Na/K phosphate buffer.

In this study we have directly compared the effect of sodium ions and guanine nucleotides on the binding characteristics of thioperamide, another H_3-selective antagonist, clobenpropit (Van der Goot *et al.*, 1992) and N$^\alpha$-methylhistamine in rat cerebral cortex.

Methods

Tissue preparation

Cerebral cortices were dissected from either male Hooded Lister rats (300-400g) or frozen male Hooded Lister rat brains and disrupted by hand with a ground glass homogenizer in 20 volumes of Tris HCl buffer (50 mM, pH 7.4), unless otherwise stated. Homogenates were centrifuged twice at 20,000*g* for 10 min. The final pellet was resuspended in 10 volumes of buffer and stored as aliquots at

[1] Author for correspondence.

−20°C. Samples were used within one month of preparation and protein concentration was determined by the method of Bradford (1976).

[^{3}H]-N$^\alpha$-methylhistamine binding assay

Homogenate (0.4–1.0 mg) was incubated with 1 nM [^{3}H]-N$^\alpha$-methylhistamine (84.1 Ci mmol^{-1}) in a total volume of 1 ml, 50 mM Tris HCl, pH 7.4, with or without competing ligands. Assays were performed in quadruplicate. Non-specific binding was defined in the presence of thioperamide 10 μM. Tubes were incubated for 60 min at 37°C then filtered through polyethylenimine (0.3%) pretreated Whatman GF/B filters (Burns *et al.*, 1983), using a Brandel cell harvester. Filters were washed twice with 4 ml ice-cold buffer and filter-bound radioactivity determined by liquid scintillation counting (45% efficiency).

Materials and chemicals

[^{3}H]-N$^\alpha$-methylhistamine (specific activity 84.1 Ci mmol^{-1}) was obtained from NEN DuPont. (Herts, England). Betahistine, histamine, mepyramine, guanosine 5'triphosphate (GTP), guanosine 5'-*o*-(3-thiotriphosphate) (GTPγS) and 5'-guanylimidodiphosphate (GppNHp) were purchased from Sigma Chemical Co. (Dorset, England). Burimamide, norburimamide, N$^\alpha$-methylhistamine, R$^\alpha$-methylhistamine, SKF 91486b (3-(imidazole-4-yl)-propylguanidine sulphate) and thioperamide were obtained from Smith-Kline French laboratories (Herts, England) and tiotidine from ICI Pharmaceutical (Macclesfield, England). Gifts of clobenpropit and phenylbutanoylhistamine from Glaxo Group Research (Herts, England) are gratefully acknowledged. Frozen male Hooded Lister rat brains were purchased from Charles River U.K. Ltd.

Data analysis

Curves for the specific binding of [^{3}H]-N$^\alpha$-methylhistamine at different concentrations of ^{3}H-ligand were fitted by the non-linear regression program Inplot4 (ISI). The equation fitted was:

$$\text{Specific binding} = \frac{B_{max} \times L}{(L^n + K_d^n)}$$

where B_{max} is the maximal specific binding site capacity, L is the concentration of [^{3}H]-N$^\alpha$-methylhistamine, K_d is the dissociation constant and n is the Hill coefficient.

Curves of inhibition of [^{3}H]-N$^\alpha$-methylhistamine were initially fitted to a logistic equation using Inplot4. The equation fitted was:

$$\%\ \text{inhibition of specific binding} = \frac{100 \times D^n}{D^n + (IC_{50})^n}$$

where D is the concentration of competing ligand, IC_{50} is the concentration of non-radioactive inhibitor producing 50% inhibition of the specific binding of 1 nM [^{3}H]-N$^\alpha$-methylhistamine and n is the Hill coefficient. Apparent dissociation constants (K_i) were determined using the expression derived from the Cheng & Prusoff equation (1973):

$$K_i = IC_{50}/(1 + L/K_d)$$

where L is the radioligand concentration and K_d is its dissociation constant.

To determine whether the inhibition curves for each inhibitor deviated significantly from those expected for binding to a single site, the analysis was repeated with the Hill coefficient constrained to a value of unity. Statistical analysis of the change in residual sums of squares obtained from the two fits was analysed using the *F*-variance ratio test i.e. $F = (R_2\text{-}R_1)\ (df_2\text{-}df_1)/R_1\text{-}df_1$, where R_2 and R_1 represent the residuals with and without the constraint on the Hill coefficient, and df_2 and df_1 are the respective degrees of freedom.

Data for inhibitors with a Hill coefficient significantly less than unity were also fitted to a two site model:

$$\%\ \text{inhibition of specific binding} = \frac{C}{(D + IC_{50}H)} + \frac{(100\text{-}C)}{(D + IC_{50}L)}$$

where C is the percentage of high affinity sites, D is the concentration of inhibitor and $IC_{50}H$ and $IC_{50}L$ are the respective IC_{50} values for the high and low affinity sites.

Data are expressed as mean ± s.e.mean and *n* represents the number of separate individual experiments performed.

Results

Characterization of [^{3}H]-N$^\alpha$-methylhistamine binding

[^{3}H]-N$^\alpha$-methylhistamine specific binding to rat cerebral cortical membranes in 50 mM Tris HCl buffer (pH 7.4), was rapid ($t_{1/2} < 5$ min), and saturable (i.e. equilibrium was reached within 20 min and binding remained stable for at least 1 h). Results were consistent with either fresh or frozen tissue. Scatchard analysis of saturation binding data (Figure 1) disclosed a single class of high affinity sites ($K_d = 2.06 \pm 0.17$ nM, $B_{max} = 65.6 \pm 9.8$ fmol mg^{-1} protein; $n = 6$). Results from competition studies, using Tris HCl (50 mM, pH 7.4) buffer showed that inhibition of [^{3}H]-N$^\alpha$-methylhistamine binding by a range of compounds (Figure 2)

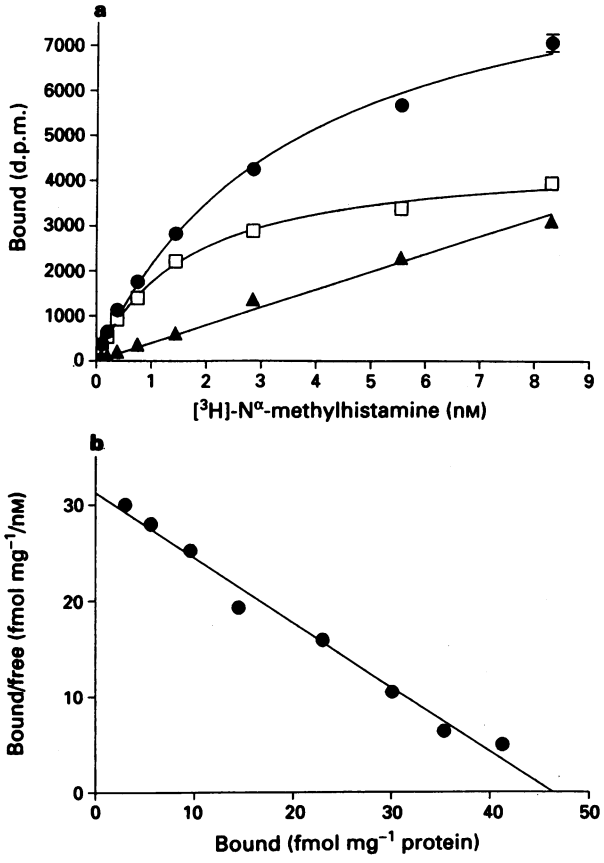


Figure 1 Saturation of [^{3}H]-N$^\alpha$-methylhistamine binding at equilibrium. (a) Binding isotherm, (□) specific binding; (●) total binding; (▲) non-specific binding. Non-specific binding was determined in the presence of thioperamide 10 μM. (b) Scatchard analysis of the specific binding data shown in (a). Data shown are representative of three separate experiments. Each point is the average of four determinations.

were characteristic of histamine H_3-receptor binding. Corresponding IC_{50} and K_i values are shown in Table 1. With the exception of thioperamide, all of the compounds inhibited [^{3}H]-N$^\alpha$-methylhistamine binding with Hill coefficients (n_H), not significantly different from unity. However, thioperamide gave a shallow slope ($n_H = -0.73 \pm 0.02$), and the data fitted significantly better to a two component competition model than with a sigmoidal competition curve ($P<0.05$). With this analysis, thioperamide discriminated between two binding sites, one of high affinity ($IC_{50\ 1} = 2.75 \pm 0.87$ nM) and one of low affinity ($IC_{50\ 2} = 101.6 \pm 12.0$ nM) in the ratio 24:76 ± 2% (high:low) ($n = 15$). This heterogeneity in binding shown by thioperamide was subsequently lost if the experiments were performed in 50 mM sodium/potassium phosphate buffer (Table 2).

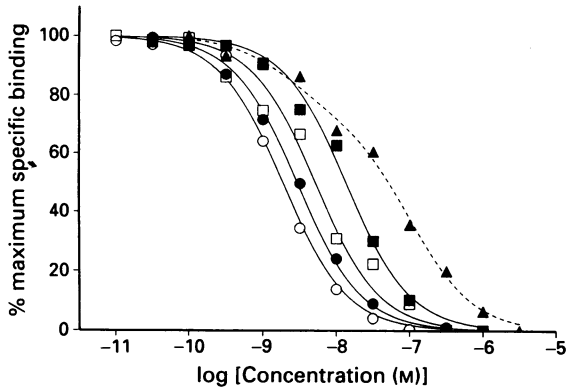


Figure 2 Competition binding with [^{3}H]-N$^\alpha$-methylhistamine in rat cerebral cortical membranes. Non-specific binding was determined in the presence of thioperamide 10 μM. Specific binding was defined as the difference between total and non-specific binding. Data are expressed as percentage maximum specific binding. Each curve represents the mean of three separate experiments and the s.e.mean was less than 5% in all cases: (○) clobenpropit; (●) N$^\alpha$-methylhistamine; (□) R$^\alpha$-methylhistamine; (■) SKF 91486b; (▲) thioperamide.

Table 1 Inhibition of [^{3}H]-N$^\alpha$-methylhistamine binding in rat cerebral cortex by various compounds acting at histamine receptors

	IC_{50} (nM)	K_i (nM)
Clobenpropit	1.6	1.1
N$^\alpha$-methylhistamine	4.8	3.2
R$^\alpha$-methylhistamine	7.6	5.1
SKF 91486 b	16	11
Histamine	20	14
Thioperamide*	65	48
Burimamide	340	230
Phenylbutanoylhistamine	750	500
Norburimamide	8,900	6,000
Betahistine	50,000	34,000
Mepyramine	42,000	28,000
Tiotidine	>100,000	>67,000

Each IC_{50} value is the average of between three and six separate experiments. K_i values were calculated using Cheng & Prussoff equation (1973). *$n_H = -0.73 \pm 0.02$, significantly different from unity ($P<0.05$).

Effects of sodium ions

Competition binding experiments were performed with three H_3-selective ligands, thioperamide, a second antagonist, clobenpropit and the agonist N$^\alpha$-methylhistamine, in the presence of 0, 50 and 100 mM NaCl. Specific binding of 1 nM [^{3}H]-N$^\alpha$-methylhistamine was decreased by 37.9 ± 4.4% and 47.9 ± 0.8% in the presence of 50 and 100 mM NaCl respectively ($n = 4$). Sodium ions had no effect on the binding characteristics of clobenpropit or N$^\alpha$-methylhistamine. However, with thioperamide (Figure 3), the inhibition curve was shifted to the left and the Hill coefficient was increased to unity i.e. towards the high affinity site. (Data are summarized in Table 2). In saturation studies, the presence of 100 mM NaCl produced a 31 ± 6% reduction in receptor density (i.e. B_{max} decreased from 86.0 ± 0.7 fmol mg^{-1} to 59.3 ± 4.8 fmol mg^{-1} protein) without significantly altering the apparent affinity for [^{3}H]-N$^\alpha$-methylhistamine ($K_d = 2.02 \pm 0.09$ nM and 2.15 ± 0.13 nM in the absence and presence of 100 mM NaCl respectively) ($n = 3$).

Effects of guanylnucleotides

We investigated the effects of guanosine triphosphate (GTP) and the two non-hydrolysable analogues guanosine 5′-*o*-(3-thiotriphosphate) (GTPγS) and 5′-guanylimidodiphosphate (GppNHp) on [^{3}H]-N$^\alpha$-methylhistamine binding. The order of potency for inhibition of binding was GTPγS IC_{50} = (0.2 ± 0.0 μM) > GppNHp (1.5 ± 0.1 μM) > GTP (39.2 ± 0.6 μM) ($n = 3$). All three compounds were able to displace only 58 ± 2% of specific binding (Figure 4). The presence of

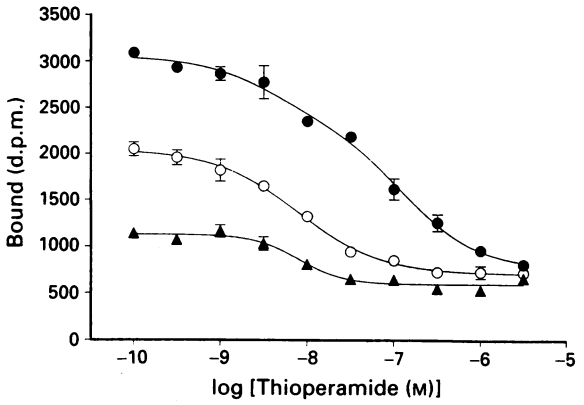


Figure 3 Competition binding curves for thioperamide were performed in the absence (●), and presence of 50 mM (○) and 100 mM (▲) NaCl. Non-specific binding was determined with thioperamide 10 μM. Values are the mean ± s.e.mean of three individual experiments.

Table 2 Comparison between the inhibition binding curves for thioperamide, clobenpropit and N$^\alpha$-methylhistamine in 50 mM Tris HCl ± sodium ions and 50 mM Na/K phosphate buffers

	Tris HCl (50 mM) + 0 mM *NaCl*	*Tris HCl* (50 mM) + 50 mM *NaCl*	*Tris HCl* (100 mM) + 100 mM *NaCl*	*Na/K phosphate* (50 mM)
N$^\alpha$-methylhistamine	6.2 ± 0.2	5.52 ± 0.02	7.7 ± 0.3	4.0 ± 0.6
Clobenpropit	1.3 ± 0.2	1.10 ± 0.10	1.5 ± 0.2	1.1 ± 0.2
Thioperamide	64.9 ± 4.5*	8.40 ± 0.70	7.1 ± 0.4	9.0 ± 0.4

IC_{50} values are expressed as mean ± s.e.mean of three individual experiments. *$n_H = -0.73 \pm 0.02$, significantly different from unity ($P<0.05$).

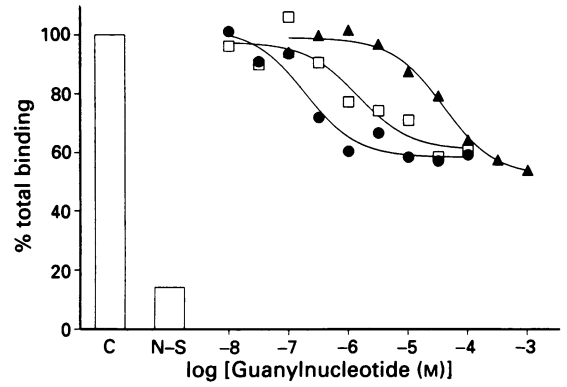


Figure 4 Inhibition of [^{3}H]-N$^\alpha$-methylhistamine binding by guanylnucleotides: (●) GTPγS; (□) GppNHp; (▲) GTP. Data are expressed as percentage total binding. Non-specific binding (15% total binding) was determined in the presence of thioperamide 10 μM. Values represent the mean of three separate experiments and s.e.mean was less than 5% in all cases.

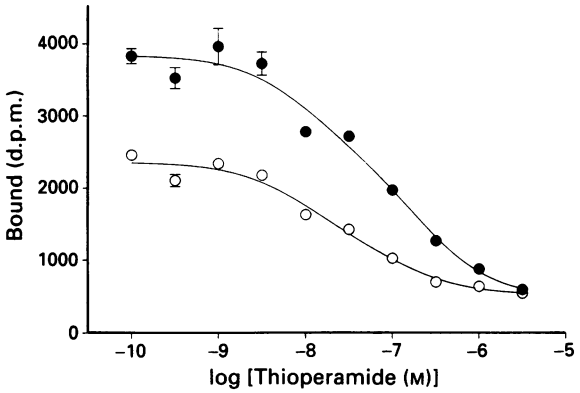


Figure 5 Inhibition of [^{3}H]-N$^\alpha$-methylhistamine binding by thioperamide in the absence (●) and presence (○) of GTPγS (3×10^{-5} M). Data shown are from a single experiment which is representative of three separate experiments. Data points are the mean ± s.e.mean of quadruplet determinations.

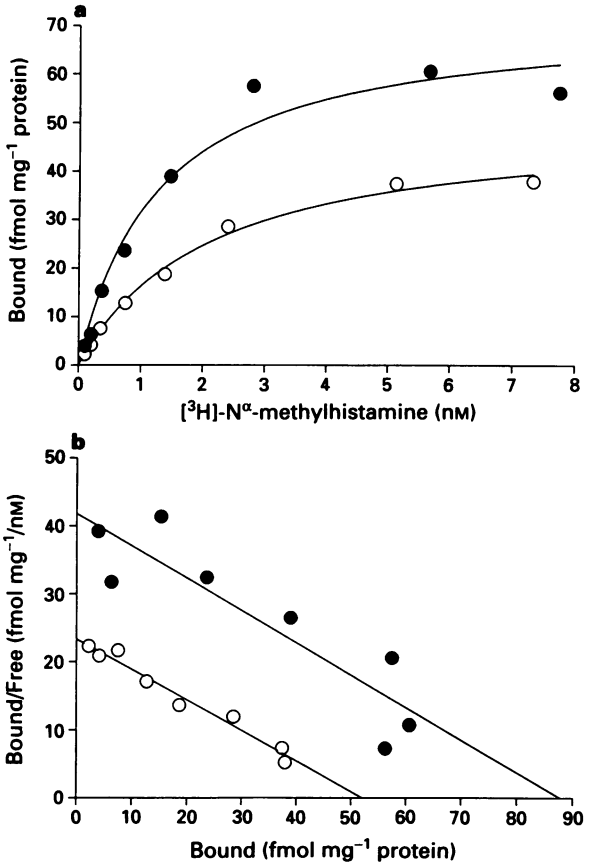


Figure 6 Saturation binding experiments in the absence (●) and presence (○) of GTPγS (3×10^{-5} M). (a) Specific binding, determined from the difference between total binding (in the absence of) and non-specific binding (in the presence of) thioperamide 10 μM. (b) Scatchard analysis of the specific binding shown in (a). Data shown represent one of two experiments.

GTPγS (3×10^{-5}M) produced a decrease in specific binding, an increase in Hill coefficient towards unity and a shift in IC_{50} towards the high affinity site of the thioperamide concentration-response curve (Figure 5), i.e. a single site with an $IC_{50} = 22.1 \pm 0.5$ nM was observed when GTPγS is present, compared with two sites ($IC_{50\ 1} = 1.98 \pm 0.68$ nM (25%); $IC_{50\ 2} = 104.7 \pm 35.5$ nM (75%) in the control ($n = 3$)). Also, saturation binding in the presence of GTPγS (3×10^{-5}M) produced a 44 ± 3% decrease in B_{max} with no change in K_d for [^{3}H]-N$^\alpha$-methylhistamine ($n = 3$), (Figure 6); these results imply that sodium ions and guanylnucleotides modulate thioperamide binding in the same way.

Discussion

High affinity specific binding of [^{3}H]-N$^\alpha$-methylhistamine to membranes of rat cerebral cortex was saturable and consistent with the labelling of a single class of histamine H_3-receptors. The apparent dissociation constants obtained for a range of non-radioactive H_3-receptor antagonists were consistent with those values obtained from antagonism of histamine H_3-receptor-mediated functional responses (Arrang *et al.*, 1983; 1985; 1987a,b; Van der Werf *et al.*, 1987; Van der Vliet *et al.*, 1988; Schlicker *et al.*, 1988; Hew *et al.*, 1990; Clapham & Kilpatrick, 1992; Taylor & Kilpatrick, 1992). With the exception of the H_3-antagonist thioperamide, the inhibition of [^{3}H]-N$^\alpha$-methylhistamine binding by all other compounds (both agonists and antagonists) was consistent with a simple mass action equilibrium with a single class of non-interacting H_3-receptor sites. In the case of thioperamide, however, the inhibition curve obtained had a Hill coefficient significantly less than unity and could be described by a two-component model comprising high affinity ($IC_{50} = 2.75$ nM) and low affinity ($IC_{50} = 101.6$ nM) sites in the ratio 24:76% (high:low). This heterogeneity in binding shown by thioperamide was subsequently lost if the experiments were performed in 50 mM sodium/potassium phosphate buffer. These observations are consistent with the observations of both West *et al.* (1990) and Arrang *et al.* (1990) who made measurements in either Tris buffer of sodium/potassium phosphate buffer respectively. These data suggest that the ionic composition of the incubation media may alter the conformation of the H_3-receptor.

In the present study we have evaluated the effect of sodium ions on the binding characteristics of thioperamide, the agonist N$^\alpha$-methylhistamine and a second high affinity H_3-antagonist, clobenpropit. Specific binding of 1nM [^{3}H]-N$^\alpha$-methylhistamine was decreased by 40–50% in Tris buffer containing 50 or 100 mM NaCl. Sodium ions had no effect on the binding characteristics of the clobenpropit or N$^\alpha$-methylhistamine. However, with thioperamide, the inhibition curve was shifted to the left and the Hill coefficient was increased to unity i.e. towards the high affinity site. The IC_{50} obtained for thioperamide in the presence of sodium ions was 8 nM. This would suggest that sodium ions can alter the conformation of the H_3-receptor in such a way that one binding site (for which thioperamide has lower affinity, but

which clobenpropit is unable to resolve because of its equal affinity for both conformations) is lost.

This selective effect of sodium ions on the binding of only certain antagonists has also been observed in studies of the binding of opioid ligands in NG108-15 cells (Costa *et al.*, 1992). In the NG108-15 cell line the binding of classical 'neutral' opiate receptor antagonists was not affected by sodium ions and was consistent with binding to a single population of high affinity sites (Costa *et al.*, 1992). In contrast, however, the binding of the putative 'negative' opiate receptor-antagonist, ICI 174864 (which via its proposed negative receptor efficacy is capable of reducing basal GTPase activity in the absence of any agonist occupancy of the receptor; Costa *et al.*, 1990), indicated the presence of two affinity states (Costa *et al.*, 1992). Furthermore, in the presence of sodium ions the proportion of low affinity sites was markedly reduced (Costa *et al.*, 1992). In the NG108-15 cell membranes, the most likely explanation for these effects is that there is spontaneous coupling of opiate receptors to G-proteins (leading to some degree of agonist-independent constitutive receptor activity) which can be prevented by the presence of sodium ions (Costa *et al.*, 1990; Lefkowitz *et al.*, 1993). If 'negative' antagonists such as ICI 174864 possess negative efficacy by virtue of a higher affinity for un-coupled relative to that for G-protein-coupled receptors, then the presence of sodium ions would tend to stabilize the binding of this type of antagonist into a single high affinity state. This is precisely what was observed with thioperamide at the H_3-receptor in the present study.

Evidence for the linkage of H_3-receptors to their effector systems via G-proteins has been provided by the observation in this and other studies (Arrang *et al.*, 1990; West *et al.*, 1990; Kilpatrick & Michel, 1991; Zweig *et al.*, 1992) that ^{3}H-agonist binding can be modulated by guanylnucleotides. West *et al.* (1990) reported a decrease in both B_{max} and K_d of [^{3}H]-N$^\alpha$-methylhistamine in the presence of GTPγS. In the present study we have observed that approximately 40% of [^{3}H]-N$^\alpha$-methylhistamine specific binding sites in rat cerebral cortical membranes were GTP-sensitive (seen by a reduction in B_{max} in the presence of GTPγS), suggesting that they are typically linked to a G-protein. In most G-protein-coupled receptor systems, the effect of added GTPγS is to shift the resting equilibrium between high affinity G-protein-coupled receptors and low affinity uncoupled receptors in favour of the low affinity sites. However, since we are monitoring high affinity ^{3}H-agonist binding over a fairly narrow concentration-range, this type of behaviour would be seen as a reduction in apparent B_{max} (i.e. the low affinity sites would no longer be detectable). It is clear in our study, however, that the remainder of the [^{3}H]-N$^\alpha$-methylhistamine binding sites were unaffected by GTP, yet still had high affinity for the ^{3}H-agonist ligand. Another feature of the studies performed in the presence of GTPγS is that the guanine nucleotide appeared to modulate the binding characteristics of thioperamide and [^{3}H]-N$^\alpha$-methylhistamine in a similar way to that produced by sodium ions. Thus, in the presence of GTPγS, the binding of thioperamide appeared to be to a homogeneous population of sites with an IC_{50} of 20 nM and the B_{max} for [^{3}H]-N$^\alpha$-methylhistamine was reduced by a similar amount to that produced by sodium ions.

The molecular nature of the high affinity GTP-insensitive ^{3}H-agonist H_3-receptor sites remains to be established, although some insight may be provided by the ternary complex model recently developed by Lefkowitz and colleagues (1993) to account for constitutive receptor activity. In this model, it is proposed that a receptor can exist (in terms of agonist affinity) in a low affinity state R or in a high affinity intermediate form R* which is the only form capable of interacting directly with the G-protein (and can do this even in an agonist-unoccupied state).

$$R \rightleftharpoons R^* \rightleftharpoons R^*G$$

Ligands with differential affinity for each conformation e.g. agonists, can then alter the proportions of each isomer at equilibrium. R* provides a possible explanation for high affinity H_3-agonist binding in the presence of guanine nucleotides if a significant proportion of the H_3-receptors present in rat cerebral cortex are able to isomerise spontaneously into the active conformation R*. This would lead to a higher affinity for H_3-agonists but a reduced signal to noise ratio owing to a higher inherent basal receptor activation (due to the potential for R* to couple to G-proteins to form R*G in the absence of agonist; Lefkowitz *et al.*, 1993). These properties are not, however, incompatible with those expected for an autoreceptor function. If this is the case, then a corollary of this putative mechanism is that sodium ions and guanine nucleotides prevent the formation of R*-G-protein complexes (R*G) and reduce the number of receptors in the R* conformation (i.e. convert a proportion of them to uncoupled low affinity R forms of the receptor). Furthermore, the data obtained with thioperamide would indicate that thioperamide has a higher affinity for the R* form compared to the G-protein-coupled R*G conformation which could convey a degree of 'negative' efficacy. It is assumed that any binding to R which has a low agonist affinity would not be detectable within the concentration range of [^{3}H]-N$^\alpha$-methylhistamine used in these studies.

There is no evidence available at the present time to indicate whether thioperamide is capable of expressing 'negative' efficacy or not. This would be largely dependent upon the extent to which H_3-receptors in different cells and tissues are constitutively active. Thioperamide has been observed to elicit a concentration-dependent increase in [^{3}H]-histamine release in rat cerebral cortical slices (Arrang *et al.*, 1983) but this could simply be due to antagonism of endogenously released histamine exerting a negative feedback effect on [^{3}H]-histamine release. Most information on constitutive activity and the evaluation of the potential for established receptor-antagonists (e.g. prazosin) to possess negative efficacy has come from mutagenesis studies of cloned receptors (Kjelsberg *et al.*, 1992; Lefkowitz *et al.*, 1993; Samama *et al.*, 1993a,b; Tian *et al.*, 1993; Chidiac *et al.*, 1993). Consequently, the resolution of this issue may have to await similar mutagenesis studies on the histamine H_3-receptor.

The authors would like to thank Glaxo Group Research and the Medical Research Council for their financial support.

References

ARRANG, J.M., GARBARG, M., LANCELOT, J.C., LECOMTE, J.M., POLLARD, H., ROBBA, M., SCHUNACK, W. & SCHWARTZ, J.-C. (1987a). Highly potent and selective ligands for histamine H_3-receptors. *Nature*, **327**, 117–123.

ARRANG, J.M., GARBARG, M. & SCHWARTZ, J.-C. (1983). Auto-inhibition of brain histamine release mediated by a novel class (H_3) of histamine receptor. *Nature*, **302**, 832–837.

ARRANG, J.M., GARBARG, M. & SCHWARTZ, J.-C. (1985). Autoregulation of histamine release in brain by presynaptic H_3-receptors. *Neuroscience*, **15**, 553–562.

ARRANG, J.M., GARBARG, M. & SCHWARTZ, J.-C. (1987b). Auto-inhibition of histamine synthesis mediated by presynaptic H_3-receptors. *Neuroscience*, **23**, 149–157.

ARRANG, J.M., ROY, J., MORGAT, J.L., SCHUNACK, W. & SCHWARTZ, J.-C. (1990). Histamine H_3-receptor binding in rat brain membranes : modulations by guanine nucleotides and divalent cations. *Eur. J. Pharmacol., (Mol. Pharmacol. section)*, **188**, 219–227.

BRADFORD, M.M. (1976). A rapid and sensitive method for the quantification of microgram quantities of protein utilizing the principle of protein-dye binding. *Anal. Biochem.*, **72**, 248–254.

BURNS, R.F., WENDLING, K.I. & PUGSLEY, T.A. (1983). A rapid filtration assay for soluble receptors using polyethylenimine-treated filters. *Anal. Biochem.*, **132**, 74–81.

CHENG, Y.C. & PRUSOFF, W.H. (1973). Relationship between the inhibition constant K_i and the concentration of inhibitor which causes 50% inhibition IC_{50} of an enzymic reaction. *Biochem. Pharmacol.*, **22**, 3099–3108.

CHIDIAC, P., HEBERT, T.E., VALIQIETTE, M., DENNIS, M. & BOUVIER, M. (1993). Inverse agonist activity of β-adrenergic antagonists. *Mol. Pharmacol.*, **45**, 490–499.

CLAPHAM, J., & KILPATRICK, G.J. (1992). Histamine H_3-receptors modulate the release of [^{3}H]-ACh from slices of rat endorinal cortex : Evidence for the possible existence of H_3-receptor subtypes. *Br. J. Pharmacol.*, **107**, 919–923.

COSTA, T., LANG, J., GLESS, C. & HERZ, A. (1990). Spontaneous association between opiod receptors and GTP-binding regulatory proteins in native membranes : Specific regulation by antagonists and sodium ions. *Mol. Pharmacol.*, **37**, 383–394.

COSTA, T., OGINO, Y., MUNSON, P.J., ONARAN, O. & RODBARD, D. (1992). Drug efficacy at guanine nucleotide-binding regulatory protein-linked receptors : Thermodynamic interpretation of negative antagonism and of receptor activity in the absence of ligand. *Mol. Pharmacol.*, **41**, 549–560.

HEW, R.W.S., HODGKINSON, C.R. & HILL, S.J. (1990). Characterization of histamine H_3-receptors in guinea-pig ileum with H_3 selective ligands. *Br. J. Pharmacol.*, **101**, 621–624.

HILL, S.J. (1990). Distribution, properties & functional characteristics of three classes of histamine receptor. *Pharmacol. Rev.*, **42**, 45–83.

KILPATRICK, G.J. & MICHEL, A.D. (1991). Characterisation of the binding of the histamine H_3-receptor agonist ^{3}H-R$^\alpha$-methylhistamine to homogenates of rat and guinea-pig cortex. *Agents Actions*, **33**, 69–75.

KJELSBERG, M.A., COTECCHIA, S., OSTROWSKI, J., CARON, M.G. & LEFKOWITZ, R.J. (1992). Constitutive activation of the α_1-adrenergic receptor by all amino-acid substitutions at a single site. *J. Biol. Chem.*, **267**, 1430–1433.

KORTE, A., MYERS, J., SHIH, N.Y., EGAN, R.W. & CLARK, M.A. (1990). Characterisation and tissue distribution of H_3-histamine receptors in guinea-pigs by N$^\alpha$-methylhistamine. *Biochem. Biophys. Res. Commun.*, **168**, 979–986.

LEFKOWITZ, R.J., COTECCHIA, S., SAMAMA, P. & COSTA, T. (1993). Constitutive activity of receptors coupled to guanine nucleotide regulatory proteins. *Trends Pharmacol. Sci.*, **14**, 303–307.

SAMAMA, P., COTECCHIA, S., COSTA, T. & LEFKOWITZ, R.J. (1993a). A mutation-induced activated state of the β_2-adrenergic receptor: extending the ternary complex model. *J. Biol. Chem.*, **268**, 4625–4636.

SAMAMA, P., PEI, G., COSTA, T., COTECCHIA, S. & LEFKOWITZ, R.J. (1993b). Negative antagonists promote an inactive conformation of the β_2-adrenergic receptor. *Mol. Pharmacol.*, **45**, 390–394.

SCHLICKER, E., BETZ, R. & GOTHERT, M. (1988). Histamine H_3-receptor mediated inhibition of serotonin release in the rat brain cortex. *Naunyn-Schmied. Arch. Pharmacol.*, **337**, 558–590.

SCHLICKER, E., FINK, K., HINTERHANER, M. & GOTHERT, M. (1989). Inhibition of noradrenaline release in the rat brain cortex via presynaptic H_3-receptors. *Naunyn-Schmied. Arch. Pharmacol.*, **340**, 633–638.

TAYLOR, S.J. & KILPATRICK, G.J. (1992). Characterization of histamine H_3-receptors controlling non-adrenergic, non-cholinergic contractions of the guinea-pig isolated ileum. *Br. J. Pharmacol.*, **105**, 667–674.

TIAN, W-N., DUZIC, E., LANIER, S. & DETH, R.C. (1993). Determinants of α_2-adrenergic receptor activation of G proteins: Evidence for a precoupled receptor/G protein state. *Mol. Pharmacol.*, **45**, 524–531.

VAN DER GOOT, H., SCHEPERS, M.J.P., STERK, G.J. & TIMMERMAN, H. (1992). Isothiourea analogues of histamine as potent agonists or antagonists of the histamine H_3-receptor. *Eur. J. Med. Chem.*, **27**, 511–518.

VAN DER VLIET, A., VAN DER WERF, J.F., BAST, A. & TIMMERMAN, H. (1988). Frequency-dependent autoinhibition of histamine release from rat cortical slices : a possible role for H_3-receptor reserve. *J. Pharm. Pharmacol.*, **40**, 577–579.

VAN DER WERF, J.F., BAST, A., BIJLOO, G.J., VAN DER VLIET, A. & TIMMERMAN, H. (1987). HA autoreceptor assay with superfused slices of rat brain cortex and electrical stimulation. *Eur. J. Pharmacol.*, **138**, 199–206.

WEST, R.E., ZWEIG, A., SHIH, N.Y., SIEGEL, M.I., EGAN, R.W. & CLARK, M.A. (1990). Identification of two H_3-receptor subtypes. *Mol. Pharmacol.*, **38**, 610–613.

ZWEIG, A., SIEGEL, M.I., EGAN, R.W., CLARK, M.A., SHORR, R.G.L. & WEST, R.E. Jr. (1992). Characterisation of a digitonin-solubilized bovine brain H_3-histamine receptor coupled to a guanine nucleotide binding protein. *J. Neurochem.*, **59**, 1661–1666.

(Received August 5, 1994
Accepted September 27, 1994)

British Journal of Pharmacology (1995) 114, 363-368 © 1995 Stockton Press All rights reserved 0007-1188/95 $9.00

Effects of nitric oxide synthase inhibition combined with nitric oxide inhalation in a porcine model of endotoxin shock

[1]Peter Klemm, *Christoph Thiemermann, Gisela Winklmaier, Piero A. Martorana & Rainer Henning

SBU Cardiovascular Agents, CASSELLA AG, Frankfurt am Main, Germany and *The William Harvey Research Institute, St Bartholomew's Hospital Medical College, London, U.K.

1 The present investigation compares the effects of intravenous infusion of the NO synthase inhibitor N^G-monomethyl-L-arginine (L-NMMA) with that of an inhalation with NO gas in a porcine model of endotoxin (lipopolysaccharide, LPS) shock. In addition, the effects of the combination of these two treatments were also investigated.

2 Male pigs were anaesthetized and instrumented for the measurement of haemodynamic parameters. Blood samples were withdrawn at different time intervals for determination of blood gases, pH, and plasma levels of nitrite/nitrate and tumour necrosis factor.

3 Endotoxin infusion (15 $\mu g\,kg^{-1}\,h^{-1}$ for 3 h) caused a progressive fall in mean arterial blood pressure (MABP) and cardiac output (CO) and a biphasic increase in mean pulmonary arterial pressure (MPAP) and pulmonary vascular resistence (PVR). A continuous infusion of L-NMMA (0.1 $mg\,kg^{-1}\,min^{-1}$) significantly attenuated the fall in MABP, but did not affect MPAP, CO and PVR. NO-inhalation (50 p.p.m.) did not affect MABP, but significantly blunted the biphasic increase in MPAP and PVR and significantly delayed the fall in CO. The combination of L-NMMA infusion (0.1 $mg\,kg^{-1}\,min^{-1}$) with NO-inhalation (50 p.p.m.) completely prevented the fall in MABP, significantly improved CO, and attenuated the biphasic increase in MPAP and PVR.

4 Endotoxin also caused a decline in PaO_2 and a rise of $PaCO_2$. Infusion of L-NMMA neither affected the fall in PaO_2 nor the increase in $PaCO_2$. In contrast, inhalation with NO gas alone as well as the combined administration of L-NMMA infusion and NO-inhalation completely prevented the fall in PaO_2 and significantly protected against the increase in $PaCO_2$.

5 Infusion of endotoxin for 180 min resulted in a mortality of 58%, which was not affected by L-NMMA (63%). In contrast, treatment of LPS-animals with either NO-inhalation alone or NO-inhalation plus L-NMMA completely prevented mortality.

6 This investigation demonstrates that treatment with NO-inhalation, in order to prevent the dramatic increase in MPAP, PVR and the alterations in peripheral blood gases combined with systemic L-NMMA to improve systemic MABP and thus organ perfusion, may be a new therapeutic regimen in the treatment of septic shock.

Keywords: Nitric oxide; nitric oxide inhalation; nitric oxide synthase; circulatory shock; sepsis; endotoxaemia

Introduction

Endotoxin is the initiator of the sepsis syndrome (Bone, 1991) which is characterized by hypotension, a diminished response to vasoconstrictors and myocardial dysfunction (Suffredini *et al.*, 1989; Parillo *et al.*, 1990). In contrast to the systemic vasodilatation, pulmonary hypertension often occurs in the acute phase of endotoxaemia. This may lead to right-sided heart failure, pulmonary oedema, hypoxia and death (Zapol *et al.*, 1977; Demling *et al.*, 1981).

Endotoxin leads to the induction of a calcium-independent nitric oxide (NO) synthase (NOS) (Szabo *et al.*, 1993; Julou-Schaeffer *et al.*, 1991) resulting in an overproduction of the vasodilator. This excessive formation of NO contributes importantly to the severe hypotension seen in endotoxin shock (Thiemermann & Vane, 1990; see Thiemermann, 1994 for review). NO synthase inhibition by N^G-monomethyl-L-arginine (L-NMMA) ameliorates the hypotension elicited by endotoxin in various animal models of circulatory shock (Rees *et al.*, 1989; Thiemermann & Vane, 1990; Cobb *et al.*, 1992) as well as in human septic shock (Petros *et al.*, 1991). However, the administration of NOS inhibitors, which are not selective for the inducible isoforms of NOS, also causes a concomittant inhibition of the constitutive NOS in the endothelium and may increase the incidence of organ ischaemia, microvascular thrombosis and mortality (Hutcheson *et al.*, 1990; Harbrecht *et al.*, 1992; Shultz & Raij, 1992; Wright *et al.*, 1992). Moreover, the non-selective NOS inhibitor N^G-nitro-L-arginine methyl ester (L-NAME) causes detrimental haemodynamic effects in pigs with septic shock (Robertson *et al.*, 1994).

Inhalation with NO gas, on the other hand, reduces the endotoxin-induced pulmonary hypertension without affecting systemic vascular resistence in pigs with septic shock (Weitzberg *et al.*, 1993).

Therefore, the present investigation compares the effects of an intravenous infusion with the NOS inhibitor N^G-monomethyl-L-arginine (L-NMMA) with that of an inhalation with NO gas in a porcine model of endotoxin shock. In addition, the effects of a combination of systemic administration of L-NMMA with inhalation of NO gas was also investigated.

Methods

Haemodynamic measurements

Thirtyone male pigs weighing 18.0 to 22.0 kg were used. The animals were fasted overnight, but had free access to water. The pigs were premedicated (ketaminchloride 25 $mg\,kg^{-1}$,

[1] Author for correspondence.

i.m.) and then anaesthetized with pentobarbitone sodium (20 mg kg^{-1}, i.v. bolus, followed by an i.v. infusion of 15 mg kg^{-1} h^{-1}). All animals were intubated, and connected to a respirator for positive pressure ventilation with a mixture of room air and 60% oxygen (tidal volume: 400–450 ml $breath^{-1}$; respiration rate: 10–15 breaths min^{-1}). Arterial blood gases were monitored at regular time intervals. The femoral artery, carotid artery and jugular vein were cannulated for the measurement of the haemodynamic parameters. Haemodynamic data were recorded continuously on a multichannel polygraph recorder. The mean arterial blood pressure (MABP) was measured with a catheter-tip manometer (Typ PC 350 Millar Instruments, Houston, Texas, U.S.A.) placed in the femoral artery. Left ventricular pressure (LVP) was recorded with a tip-catheter passed retrogradely from the carotid artery into the left ventricle. Heart rate (HR) was calculated from the LVP waveform and the left ventricular end-diastolic pressure (LVEDP) was measured on a high sensitivity scale. Myocardial contractility (dP/dt_{max}) was measured as the rate of rise of LVP. Mean pulmonary artery pressure (MPAP) was measured by means of a thermodilution catheter (Statham 5F, SP 5105) positioned in the pulmonary artery via the jugular vein. Cardiac output (CO) was determined by the thermodilution method and calculated as the mean of three subsequent measurements (CO computer, Statham SP 1435, Gould Statham Instruments, CA, U.S.A.). In addition, venous catheters were placed in the left and right external thoracic veins for administration of compounds and LPS. During the course of the experiment, 500 ml of Ringer solution was infused. The experiment started after a 1 h stabilization period.

Nitrite and nitrate determination

Nitrite (NO_2^-) was measured by means of the Griess reaction. The determination of nitrate (NO_3^-) was realized via reduction with a high-pressure cadmium column according to Green *et al.* (1982). The system allows quantitative reduction of NO_3^- and automatically eliminates interference from other compounds normally present in the plasma.

Determination of tumor necrosis factor

Plasma levels of tumour necrosis factor (TNFα) were determined by means of a TNFα-bioassay which is based on the porcine kidney cell line PK (15) as recently described by Bertoni *et al.* (1992). TNFα activity was determined by measuring the cytostatic effect of TNFα on the PK (15) cell line. A standard curve of cytostasis was obtained by using human recombinant TNFα (Biomar, Marburg) yielding progressive cytostasis ranging from 10–1000 u ml^{-1} of TNFα. The bioactivity of TNFα in the experimental samples was determined and compared against the standard curve.

Experimental protocol

Twentyfive animals received a continuous infusion of *Escherichia coli* lipopolysaccharide (LPS, 15 μg kg^{-1} min^{-1} for 180 min, Serotype 0111:B04, Sigma) and were randomly divided into four groups. A group of 7 pigs (LPS) received LPS only and served as endotoxin controls. In another group of 6 animals, L-NMMA was given as an infusion (0.1 mg kg^{-1} min^{-1}) starting 30 min prior to LPS and continued throughout the duration of the experiment. Another 6 animals were ventilated with a mixture of room air and oxygen (60%) containing NO gas (50 p.p.m.). Inhalation with NO gas was started 30 min prior to LPS infusion and continued until the end of the experiment. The concentration of the NO-gas (Messer Griesheim, Germany) was adjusted via a volumetrically calibrated flowmeter. In a further group of 6 animals, a combination of an intravenous infusion of L-NMMA (0.1 mg kg^{-1} min^{-1}) and NO-inhalation (50 p.p.m.) was administered. Another 6 animals received saline alone and served as sham-operated controls.

In all groups, haemodynamic parameters were measured and recorded continuously and samples of arterial blood were taken before and at 15, 30, 45, 60, 90, 120, 150 and 180 min after starting the infusion of LPS and used for the determination of NO_2^-, NO_3^- and TNFα, arterial oxygen tension (PaO_2), arterial carbon dioxide tension ($PaCO_2$), pH as well as leukocyte and platelet counts. At the end of the experiment, all animals were killed by an overdose of sodium pentobarbitone.

Materials

Lipopolysaccharide (*E. coli* serotype 0111:B04), N^G-monomethyl-L-arginine (L-NMMA) were obtained from Sigma Chemical Co. The NO-gas inhalation setup was supplied by Messer Griesheim (Hoechst, Wuppertal).

Statistical analysis

All results in figures and tables are expressed as mean ± s.e.mean of *n* determinations. Statistical analysis of the results was performed by one-way analysis of variance (ANOVA) followed, if appropriate, by a Bonferoni test for multiple comparisons.

Results

Cardiovascular response

Baseline values for MABP, MPAP, CO and PVR (Figure 1a–d) were not significantly different between any of the groups studied. In sham-operated controls, no change in either haemodynamics or blood gas parameters were detected during the 180 min experimental period. Endotoxin infusion (15 μg kg^{-1} min^{-1}) caused a progressive fall in MABP from 111 ± 3 mmHg (time 0) to 40 ± 2 mmHg (180 min) and in CO from 3800 ± 280 ml min^{-1} (time 0) to 1865 ± 180 ml min^{-1} (time 180 min). This severe hypotension in LPS-controls was associated with a rise in HR from 101 ± 6 beats min^{-1} (time 0) to 137 ± 11 beats min^{-1} (time 180 min) (data not shown). MPAP and PVR markedly increased within the first 60 min of endotoxin infusion, after which time the values slightly declined and then slowly rose again for the rest of the experiment (Figure 1b,d). Continuous infusion of L-NMMA partially and significantly attenuated the fall in MABP caused by LPS-infusion (Figure 1a), but had no effect on MPAP, CO and PVR (Figure 1b–d). Treatment of LPS-pigs with NO-inhalation alone significantly attenuated the acute rise in MPAP and PVR caused by infusion of LPS (Figure 1b,d) and completely abolished the secondary delayed increases in MPAP and PVR seen in LPS-controls between 90 and 180 min. NO-inhalation also significantly delayed the fall in CO (Figure 1c), but did not significantly affect the fall in MABP (Figure 1a). The combination of infusion with NO-inhalation completely prevented the LPS-induced fall in MABP, significantly improved CO, attenuated the initial rise in MPAP and PVR (0–60 min) and completely abolished the delayed increase (90–180 min) of both these parameters (Figure 1a–d).

Blood gases and pH

Basal values for PaO_2, $PaCO_2$ and pH were not different among any of the groups studied (Figure 2a,b). Infusion of endotoxin resulted in a decline in PaO_2 and a rise in $PaCO_2$ to 74.2 ± 16 and 62.5 ± 6.6 mmHg at 180 min, respectively (Figure 2a,b). Infusion of L-NMMA in LPS-treated animals neither affected the fall in PaO_2, nor the increase in $PaCO_2$ (Figure 2a,b). In contrast, both inhalation with NO gas alone and the combined administration of L-NMMA infusion and

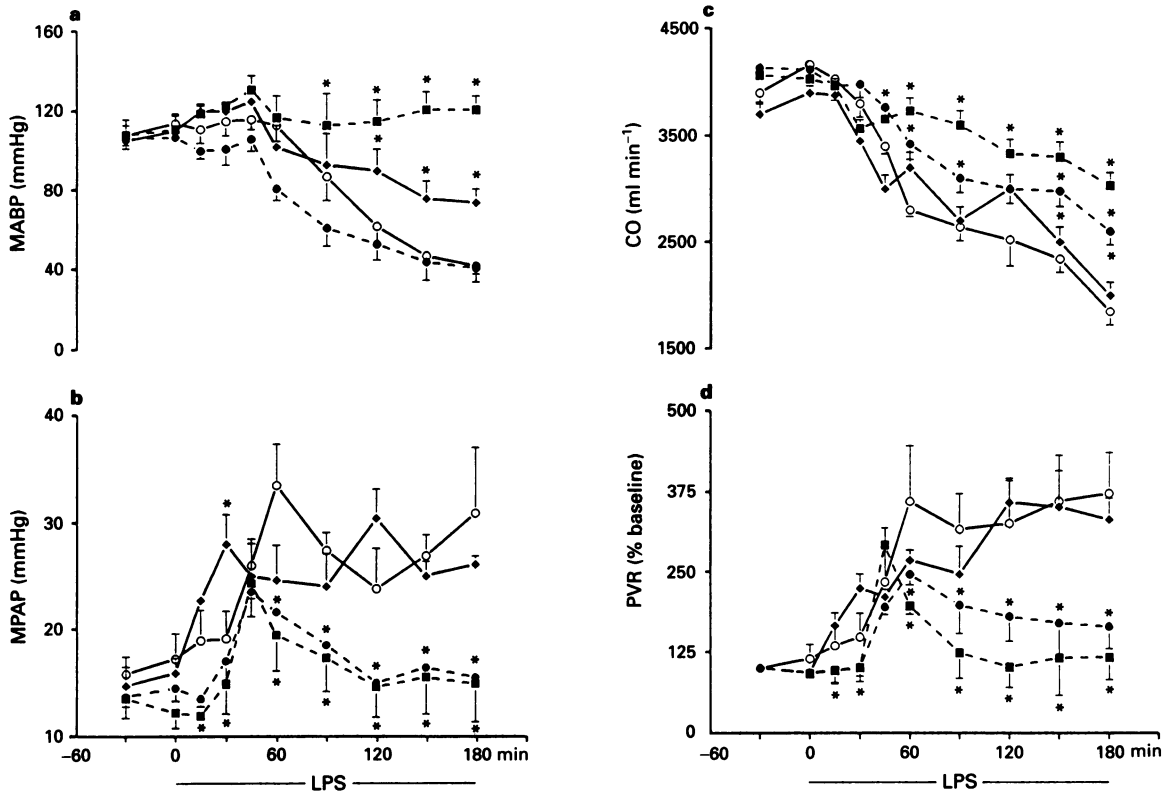


Figure 1 Mean arterial blood pressure (MABP; a), mean pulmonary artery pressure (MPAP; b), cardiac output (CO; c) and pulmonary vascular resistence (PVR; d) during endotoxin infusion in anaesthetized pigs. Groups of animals received either lipopolysaccharide (LPS) alone (O, 15 $\mu g\,kg^{-1}\,min^{-1}$, $n = 7$) or LPS and NO-inhalation (●, 50 p.p.m., $n = 6$), LPS and N^G-monomethyl-L-arginine (L-NMMA, ◆, 0.1 $mg\,kg^{-1}\,min^{-1}$, $n = 6$) or an infusion of L-NMMA combined with NO-inhalation (■, concentrations as above, $n = 6$). Data are expressed as means ± s.e.mean of n observations. $^*P<0.05$ represent significant differences when compared to LPS at the same timepoint.

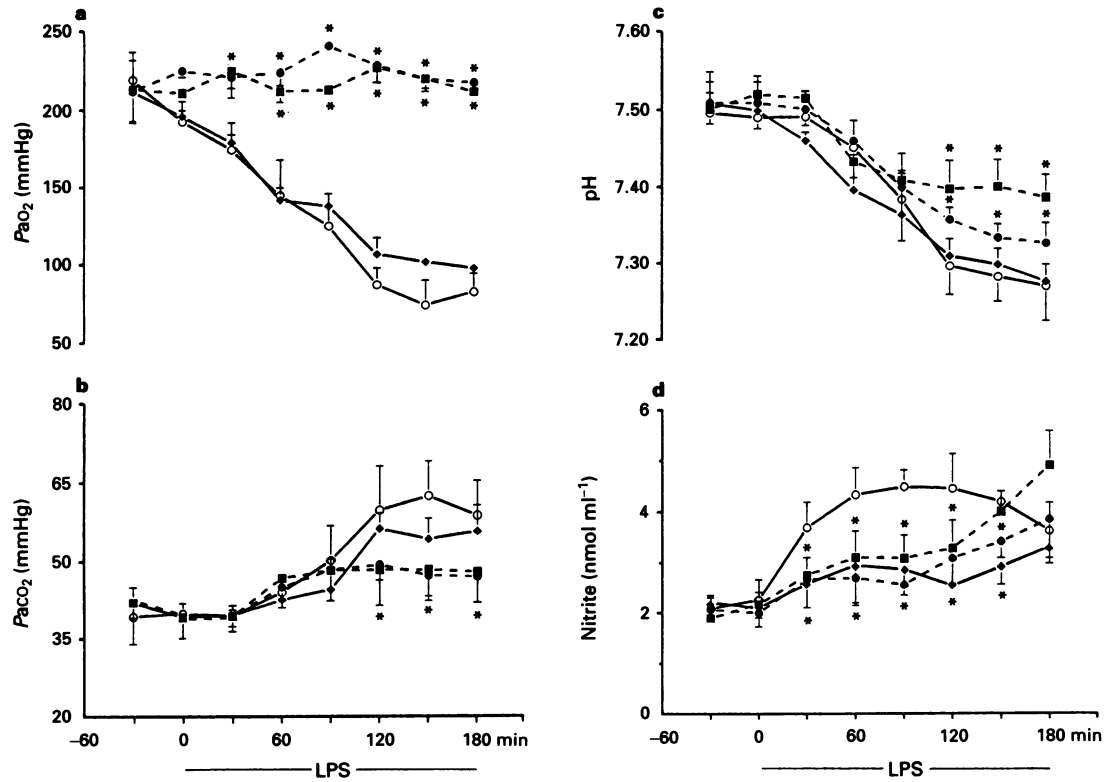


Figure 2 Arterial partial pressure of oxygen (Pa_{O_2}; a), arterial partial pressure of CO_2 (Pa_{CO_2}; b), arterial pH (pH; c) and plasma nitrite level (NO_2^-; d) during endotoxin infusion. Groups of animals received either lipopolysaccharide (LPS) alone (O, 15 $\mu g\,kg^{-1}\,min^{-1}$, $n = 7$) or LPS and NO-inhalation (●, 50 p.p.m., $n = 6$), LPS and N^G-monomethyl-L-arginine (L-NMMA, ◆, 0.1 $mg\,kg^{-1}\,min^{-1}$, $n = 6$) or an infusion of L-NMMA combined with NO-inhalation (■, concentrations as above, $n = 6$). Data are expressed as means ± s.e.mean of n observations. $^*P<0.05$ represent significant differences when compared to LPS at the same timepoint.

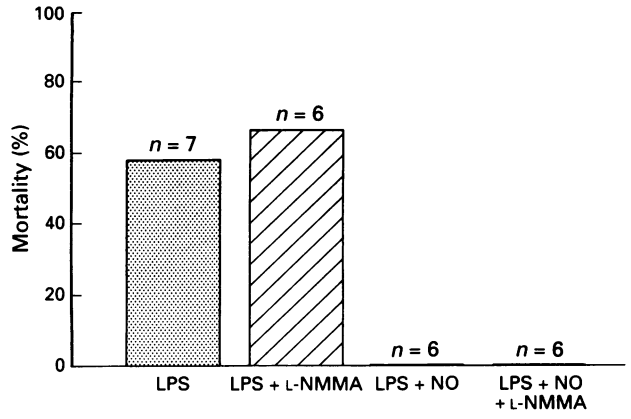


Figure 3 Effect of the different treatments on survival rate in anaesthetized pigs. Groups of animals received either only lipopolysaccharide (LPS, $n = 7$) or LPS and NO-inhalation (50 p.p.m., $n = 6$), LPS and L-NMMA, (0.1 mg kg^{-1} min^{-1}, $n = 6$) or an infusion of L-NMMA combined with NO-inhalation (concentrations as above, $n = 6$).

NO-inhalation completely prevented the fall in PaO_2 and partially, but significantly, protected against the increase in $PaCO_2$ (Figure 2a,b).

In pigs treated with LPS-infusion, the arterial pH fell from 7.5 ± 0.02 (time 0) to 7.27 ± 0.01 at 180 min (Figure 2c). Treatment with L-NMMA did not affect this acidosis, while both NO-inhalation and the combined treatment with L-NMMA infusion plus NO-inhalation partially prevented the fall in arterial pH (Figure 2c).

White blood cell and platelet counts

Infusion of LPS caused a significant fall in white blood cell and platelet counts from $13000 \pm 1000\ \mu l^{-1}$ and $638000 \pm 39000\ \mu l^{-1}$ (time 0) to $3000 \pm 320\ \mu l^{-1}$ and $238000 \pm 16000\ \mu l^{-1}$ (time 180 min), respectively. Neither the infusion of L-NMMA, nor the inhalation of NO or the combination treatment affected the neutrocytopenia or thrombocytopenia caused by LPS (data not shown).

Plasma levels of nitrite, nitrate and TNFα

In LPS-animals, baseline plasma levels of NO_2^- and NO_3^- were 2.0 ± 0.15 nmol ml^{-1} and 54.5 ± 7.3 nmol ml^{-1}, respectively. NO_2^- increased significantly in the first 30 min after LPS and reached a maximum between 60 and 120 min after commencing the LPS-infusion (Figure 2d). In contrast, infusion of LPS did not affect the plasma levels of NO_3^- (data not shown). L-NMMA infusion, NO-inhalation and the combination treatment significantly inhibited the LPS-induced increase in plasma NO_2^- levels (Figure 2d).

LPS infusion resulted in a transient increase in plasma TNFα levels with peak TNFα levels being detected at 90 min after starting the LPS-infusion. None of the different treatments caused a significant attenuation of the rise in plasma TNFα-levels afforded by LPS.

Mortality

The number of pigs in each group which died during the course of the experiment is presented in Figure 3. In control animals, endotoxaemia for 180 min was associated with a mortality of 58%. This high mortality associated with endotoxaemia was not affected by L-NMMA treatment. In contrast, none of the LPS-animals treated either with NO inhalation alone or with NO-inhalation plus L-NMMA died during the course of the experiment.

Discussion

Using a porcine model of septic shock, this study demonstrates that (i) neither the systemic administration of the NOS inhibitor L-NMMA, nor the inhalation of NO-gas alone prevented all of the haemodynamic changes caused by endotoxaemia, (ii) the combined treatment of NO-gas inhalation together with an intravenous infusion of L-NMMA abolished all of the haemodynamic alterations afforded by LPS; and (iii) the improved survival seen either with NO-gas inhalation alone or with the combined treatment is due to an attenuation of the severe increase in PVR afforded by endotoxin in this species.

Infusion of low-dose endotoxin in the anaesthetized pig resulted in a rapid and sustained fall in MABP, a fall in PaO_2, an increase in $PaCO_2$, acidosis as well as an increase in the plasma levels of TNFα. Endotoxaemia also resulted in a rapid and sustained increase in plasma NO_2^- (breakdown product of NO) levels, which were significantly higher than in sham-operated controls between 30 and 180 min after the start of the endotoxin infusion. This increase in plasma NO_2^- is due to an enhanced formation of NO arising from both activation of the constitutive NOS (early phase) as well as the induction of NOS (delayed phase) (Szabo *et al.*, 1993). The finding, however, that endotoxaemia was not associated with a significant rise in plasma nitrate levels is not entirely surprising, for NO_2^- is the predominant metabolite of NO (Ignarro *et al.*, 1993). This finding also suggests that plasma NO_2^- levels are a more sensitive indicator than nitrate levels for measuring the kinetics of NO formation *in vivo*. All of the above-mentioned haemodynamic and biochemical alterations also occur in patients with septic shock (Parillo *et al.*, 1990; Bone, 1991).

Interestingly, endotoxaemia in the anaesthetized pig was also associated with a significant fall in CO which, in man, is only seen in the late, hypodynamic phase of septic shock (Parillo *et al.*, 1990). It is well known that even brief periods of endotoxaemia in the pig are associated with a substantial, biphasic rise in MPAP and PVR (Weitzberg *et al.*, 1993), which in turn accounts for the observed fall in CO. This biphasic rise in MPAP and PVR is due to the formation of the vasoconstrictor thromboxane A_2 (first phase) (Hardie & Olson, 1987; Leeper-Woodford *et al.*, 1981; Weitzberg *et al.*, 1993), as well as the development of a pulmonary oedema (second phase) (Demling *et al.*, 1981). These pathophysiological alterations in MPAP and PVR during the acute phase of endotoxaemia are peculiar to this species and have not been described in man (Parillo *et al.*, 1990).

Intravenous administration of L-NMMA largely attenuated the rise in plasma NO_2^- and partially attenuated the severe hypotension afforded by endotoxaemia in the pig. Similar beneficial haemodynamic effects of L-NMMA have been observed in a variety of animal models of endotoxaemia (see Thiemermann, 1994 for review) as well as in patients with septic shock (Petros *et al.*, 1994). Systemic administration of L-NMMA, however, did not affect the rise in MPAP and PVR, the fall in CO, the rise in plasma TNFα or the changes in arterial blood gases brought about by endotoxaemia. In contrast, systemic administration of L-NMMA to patients with septic shock significantly enhanced MPAP and PVR, and also resulted in a fall in CO from elevated (hyperdynamic phase of septic shock) towards normal levels (Petros *et al.*, 1994). A fall in CO below normal levels has, however, been reported in septic dogs treated with the NOS inhibitor NO_2Arg (Kilbourn *et al.*, 1990; Klabunde & Ritger, 1991). In contrast to L-NMMA however, L-NAME is a more potent inhibitor of the constitutive NOS present in the vascular endothelium (Moore *et al.*, 1990) and, hence, causes a much more pronounced coronary vasoconstriction. The fact that L-NAME is a more potent inhibitor of endothelial NOS than L-NMMA may also account for the finding that L-NAME (Robertson *et al.*, 1994), but not L-NMMA (this study), caused a significant rise in MPAP and PVR in pigs with

septic shock. Inhibition of endothelial NOS by non-selective NOS inhibitors such as L-NMMA may result in excessive vasoconstriction and also enhanced adhesion of platelets and polymorphonuclear cells to the endothelium (see Thiemermann, 1994 for review). We demonstrate here, however, that infusion of L-NMMA, at doses which attenuated the fall in MABP caused by endotoxaemia in the pig, did not exacerbate the endotoxin-induced fall in platelet or polymorphonuclear cell counts. Similarly, in patients with septic shock, L-NMMA enhances the peripheral vascular resistence without exacerbating the thrombocytopenia or neutropenia associated with sepsis (Petros *et al.*, 1994).

Treatment of septic pigs with NO-gas inhalation alone attenuated the rise in MPAP and PVR afforded by endotoxin. Moreover, NO-gas inhalation also attenuated the LPS-induced fall in CO. This finding further supports our hypothesis that the fall in CO associated with endotoxaemia in the pig is secondary to a rise in MPAP and PVR and, hence, due to a reduction in left ventricular filling pressure. In addition, inhalation with NO-gas also attenuated the alterations in gas exchange (fall in Pa_{O_2} and rise in Pa_{CO_2}) as well as the resulting acidosis afforded by endotoxaemia in pigs. Inhalation with NO-gas leads to a selective vasodilatation of blood vessels adjacent to ventilated areas, for NO is rapidly inactivated by haemoglobin and, hence, has no systemic haemodynamic effects (Weitzberg *et al.*, 1993). This selective vasodilatation of ventilated areas leads to a shift in blood flow from non-ventilated to ventilated areas of the lung (positive steal phenomenon), which in turn causes an improved ventilation to perfusion matching (Sprague *et al.*, 1992; Weitzberg *et al.*, 1993). Thus, NO-inhalation therapy improves the efficacy of the Euler-Liljestrand reflex. A similar redistribution of blood flow from non-ventilated to ventilated areas of the lung was also observed in patients with ARDS receiving NO-inhalation therapy (Rossaint *et al.*, 1993). Whether the beneficial effects of NO-gas inhalation therapy on gas exchange are primarily due to the above-mentioned effects on pulmonary haemodynamics or, in part, due to inhibition of platelet aggregation (Radomski *et al.*, 1987) or neutrophil adhesion (Kubes, 1991) in the pulmonary circulation is unclear.

Surprisingly, our study demonstrates that inhalation of NO-gas also attenuated the rise in plasma NO_2^- afforded by LPS. Although the mechanism of this effect is unclear, it is conceivable that inhalation with NO-gas inhibits the formation of NO, and hence NO_2^-, by alveolar macrophages and polymorphonuclear leucocytes. The finding that NO inhalation alone did not prevent the rise in plasma NO_2^- between 120 and 180 min may well be due to the fact that inhalation with NO-gas for several hours may itself result in an accumulation of NO_2^- in the plasma (Forstell *et al.*, 1991).

NO-gas inhalation therapy, but not infusion of L-NMMA prevented the high mortality caused by endotoxaemia in the pig. This finding strongly suggests that the cause of death is related to the LPS-induced, pronounced rise in MPAP and PVR as well as severe alterations in gas exchange, but not due to the observed severe hypotension, for (i) NO-gas inhalation, but not L-NMMA, abolished these alterations in pulmonary haemodynamics and gas exchange; and (ii) L-NMMA, but not NO-gas inhalation, partially prevented the fall in MABP caused by LPS.

Interestingly, treatment of pigs with NO-gas inhalation together with infusion of L-NMMA abolished all of the LPS-induced alterations in gas exchange, haemodynamics and mortality. Most importantly, the combined treatment abolished the hypotension afforded by LPS, while L-NMMA alone only partially prevented this hypotension. Thus, the severe hypotension observed in this model of endotoxaemia in the pig is due to a fall in peripheral vascular resistence (which is prevented by L-NMMA) and a fall in CO which occurs secondary to pulmonary vasoconstriction (which is prevented by NO-gas inhalation).

Thus, this study demonstrates that the combined treatment with NO-gas inhalation and systemic administration of L-NMMA is superior to either treatment alone in preventing the LPS-induced alterations in gas exchange, haemodynamics and mortality in anaesthetized pigs. Whether this combined treatment is also superior to the use of non-selective NOS inhibitors alone in the treatment of patients with septic shock remains to be investigated. We speculate that NO-gas inhalation therapy will, at least, attenuate the rise in PVR afforded by non-selective NOS inhibitors, such as L-NMMA, in patients with septic shock (Petros *et al.*, 1994).

References

BERTONI, G., KUHNERT, P., PETERHANS, E. & PAULI, U. (1993). Improved bioassay for the detection of porcine tumor necrosis factor using a homologous cell line: PK(15). *J. Immunol. Methods*, **93**, 267–271.

BONE, R.C. (1991). Sepsis, the sepsis syndrome, multi-organ failure: a plea for comparable definitions. *Ann. Intern. Med.*, **114**, 332–333.

COBB, J.P., NATANSON, C. & KOEV, C.A. (1992). The haemodynamic effect of N^G-methyl-L-arginine in endotoxaemic compared to normal canines. *Crit. Care Med.*, **20**, S61–S65.

DEMLING, R.H., SMITH, M., GUNTHER, G., FLYNN, J.T. & GEE, M.H. (1981). Pulmonary injury and prostaglandin production during endotoxaemia in conscious sheep. *Am. J. Physiol.*, **240**, H383–386.

FORSTELL, C., FRATACCI, M.D., WAIN, J.C., JONES, R. & ZAPOL, W.M. (1991). Inhaled nitric oxide. A selective pulmonary vasodilator reversing hypoxic pulmonary vasoconstriction. *Circulation*, **83**, 2038–2047.

GREEN, L.C., WAGNER, D.A., GLOGOWSKI, J., SKIPPER, P.L., WISHNOK, J.S. & TANNENBAUM, S.R. (1982). Analysis of nitrate, nitrite and [15N] nitrate in biological fluids. *Anal. Biochem.*, **126**, 131–138.

HARBRECHT, B.G., BILLIAR, T.R., STADLER, J., DEMETRIS, A.J., OCHOA, J., CURREN, R.D. & SIMMONS, R.L. (1992). Inhibition of nitric oxide synthesis during endotoxaemia promotes intrahepatic thrombosis and an oxygen radical-mediated hepatic injury. *J. Leukocyte Biol.*, **52**, 390–394.

HARDIE, E.M. & OLSON, N.C. (1987). Prostaglandin and thromboxane levels during endotoxin-induced respiratory failure in pigs. *Prostaglandins Leukot. Med.*, **28**, 255–265.

HUTCHESON, I.R., WHITTLE, B.J.R. & BOUGHTON-SMITH, N.K. (1990). Role of nitric oxide in maintaining vascular integrety in endotoxin-induced acute intestinal damage in the rat. *Br. J. Pharmacol.*, **101**, 815–820.

IGNARRO, L.J., FUKUTO, J.M., GRISCAVAGNE, J.M., ROGERS, N.E. & BRYNS, R.E. (1993). Oxidation of nitric oxide in aqueous solution to nitrite but not nitrate: comparison with enzymatically formed nitric oxide from L-arginine. *Proc. Natl. Acad. Sci. U.S.A.*, **90**, 8103–8107.

JULOU-SCHAEFFER, G., GRAY, G.A., FLEMMING, G.I., SCHOTT, C.C., PARATT, J.R. & STOCLET, J.S. (1991). Activation of the L-arginine/nitric oxide pathway is involved in vascular hyporeactivity induced by endotoxin. *J. Cardiovasc. Pharmacol.*, **17**, S207–S212.

KILBOURN, R.G., JUBRAN, A., GROSS, S.S., GRIFFITH, O.W., LEVI, R., ADAMS, J. & LODATO, R.F. (1990). Reversal of endotoxin-mediated shock by N^G-methyl-L-arginine, an inhibitor of nitric oxide synthesis. *Biochem. Biophys. Res. Commun.*, **172**, 1132–1138.

KLABUNDE, R.E. & RITGER, R.C. (1991). NG-Monomethyl-L-arginine (NMA) restores arterial blood pressure but reduces cardiac output in a canine model of endotoxic shock. *Biochem. Res. Commun.*, **178**, 1135–1140.

KUBES, P., SUZUKI, M. & GRANGER, D.N. (1991). Nitric oxide: an endogenous modulator of leukocyte adhesion. *Proc. Natl. Acad. Sci. U.S.A.*, **88**, 4651–4655.

LEEPER-WOODFORD, S.K., CAREY, P.D., BYRNE, K., FISHER, B.J., BLOCHER, C., SUGERMAN, H.J. & FOWLER III, A.A. (1991). Ibuprofen attenuates plasma tumor necrosis factor activity during sepsis-induced acute lung injury. *J. Appl. Physiol.*, **71**, 915–923.

MOORE, P.K., AL-SWAYEH, O.A., CHONG, N.W., EVANS, R.A. & GIBSON, A. (1990). N^G-nitroarginine (L-NOARG), a novel L-arginine reversible inhibitor of endothelium-dependent vasodilation *in vitro*. *Br. J. Pharmacol.*, **99**, 408–412.

PARILLO, M.M., ASHTON, D.S., NATANSON, C., SUFFREDINI, A.F., DANNER, R.L., CUNNION, R.E. & OGNIBENE, F.P. (1990). Septic shock in humans: advances in the understanding of pathogenesis, cardiovascular dysfunction and therapy. *Ann. Intern. Med.*, **113**, 227–242.

PETROS, A., BENNETT, D. & VALLANCE, P. (1991). Effect of nitric oxide inhibitors on hypotension in patients with septic shock. *Lancet*, **338**, 1557–1558.

PETROS, A., LAMB, G., LEONE, A., MONCADA, S., BENNETT, D. & VALLANCE, P. (1994). Effects of a nitric oxide synthase inhibitor in humans with septic shock. *Cardiovasc. Res.*, **28**, 34–39.

RADOMSKI, M.W., PALMER, R.M.J. & MONCADA, S. (1987). The antiaggregating properties of vascular endothelium: interactions between prostacyclin and nitric oxide. *Br. J. Pharmacol.*, **92**, 639–646.

REES, D.D., PALMER, R.M.J. & MONCADA, S. (1989). Role of endothelium-derived nitric oxide in the regulation of blood pressure. *Proc. Natl. Acad. Sci. U.S.A.*, **86**, 3375–3378.

ROBERTSON, F.M., OFFNER, P.J., CICERI, D.P., BECKER, W.K. & PRUIT, B.A. (1994). Detrimental haemodynamic effects of nitric oxide synthase inhibition in septic shock. *Arch. Surg.*, **129**, 149–156.

ROSSAINT, R., PISON, U., GERLACH, H. & FALKE, K.J. (1993). Inhaled nitric oxide: its effects on pulmonary circulation and airway smooth muscle cells. *Eur. Heart Journal*, **14**, (Suppl. I), 133–140.

SHULTZ, P.J. & RAIJ, L. (1992). Endogenously synthetized nitric oxide prevents endotoxin-induced glomerular thrombosis. *J. Clin. Invest.*, **90**, 1718–1725.

SPRAGUE, R.S., THIEMERMANN, C. & VANE, J.R. (1992). Endogenous endothelium-derived relaxing factor opposes hypoxic pulmonary vasoconstriction and supports blood flow to hypoxic alveoli in anaesthetized rabbits. *Proc. Natl. Acad. Sci. U.S.A.*, **89**, 8711–8715.

SUFFREDINI, A.F., FROMM, R.E., PARKER, M.M., BRENNER, M., KOVACS, J.A., WELEY, R.A. & PARILLO, J.E. (1989). The cardiovascular response of normal humans to the administration of endotoxin. *New Engl. J. Med.*, **321**, 280–287.

SZABO, C., MITCHELL, J.A., THIEMERMANN, C. & VANE, J.R. (1993). Nitric oxide-induced hyporeactivity to noradrenaline precedes the induction of nitric oxide synthase in endotoxin shock. *Br. J. Pharmacol.*, **108**, 786–792.

THIEMERMANN, C. (1994). The role of the arginine:nitric oxide pathway in circulatory shock. *Adv. Pharmacol.*, **28**, 45–79.

THIEMERMANN, C. & VANE, J.R. (1990). Inhibition of nitric oxide synthesis reduces the hypotension induced by bacterial lipopolysaccharide in the rat *in vivo*. *Eur. J. Pharmacol.*, **182**, 591–595.

WEITZBERG, E. (1993). Circulatory responses to endothelin-1 and nitric oxide with special references to endotoxin shock and nitric oxide inhalation. *Acta Physiol. Scand.*, **148**, (Suppl. 611), 1–72.

WEITZBERG, E., RUDEHILL, A. & LUNDBERG, J.M. (1993). Nitric oxide inhalation attenuates pulmonary hypertension and improves gas exchange in endotoxin shock. *Eur. J. Pharmacol.*, **233**, 85–94.

WRIGHT, C.E., REES, D.D. & MONCADA, S. (1992). Protective and pathological roles of nitric oxide in endotoxin shock. *Cardiovasc. Res.*, **26**, 48–57.

ZAPOL, W.M. & SNIDER, M.T. (1977). Pulmonary hypertension in severe acute respiratory failure. *New Engl. J. Med.*, **296**, 476–480.

(Received June 29, 1994
Revised September 14, 1994
Accepted September 28, 1994)

British Journal of Pharmacology (1995) 114, 369-376 © 1995 Stockton Press All rights reserved 0007-1188/95 $9.00

Dotarizine versus flunarizine as calcium antagonists in chromaffin cells

Mercedes Villarroya, Luis Gandía, Baldomero Lara, Almudena Albillos, Manuela G. López & [1]Antonio G. García

Departamento de Farmacología, Facultad de Medicina Universidad Autónoma de Madrid, Arzobispo Morcillo, 4; 28029 Madrid, Spain

1 Dotarizine is a novel piperazine derivative structurally related to flunarizine that is currently being evaluated in clinical trials for its antimigraine and antivertigo effects. This clinical profile may be related to its Ca^{2+} antagonist properties. Therefore, the actions of both compounds as calcium antagonists were compared in bovine chromaffin cells.

2 Dotarizine and flunarizine blocked $^{45}Ca^{2+}$ uptake into K^+ depolarized chromaffin cells (70 mM K^+/0.5 mM Ca^{2+} for 60 s) in a concentration-dependent manner, with IC_{50}s of 4.8 and 6.7 μM, respectively.

3 Dotarizine and flunarizine also inhibited the whole-cell Ca^{2+} and Ba^{2+} currents (I_{Ca}, I_{Ba}) in voltage-clamped chromaffin cells, induced by depolarizing test pulses to 0 mV, during 50 ms, from a holding potential of −80 mV. Blockade exhibited IC_{50}s of 4 μM for dotarizine and 2.2 μM for flunarizine. Dotarizine increased the rate of inactivation of I_{Ca} and I_{Ba}; inhibition of whole-cell currents was use-dependent.

4 Transient increases of the cytosolic Ca^{2+} concentration, $[Ca^{2+}]_i$, produced by K^+ stimulation (70 mM K^+ for 5 s) of single fura-2-loaded chromaffin cells, were also inhibited by dotarizine and flunarizine with IC_{50}s of 1.2 and 0.6 μM, respectively. Upon washout of dotarizine, the $[Ca^{2+}]_i$ increases recovered fully after 5–10 min. In contrast, the responses remained largely inhibited 10 min after washing out flunarizine.

5 Catecholamine release induced by K^+ stimulation (10-s pulses of 70 mM) was inhibited by dotarizine with an IC_{50} of 2.6 μM and by flunarizine with an IC_{50} of 1.2 μM. The blocking effects of both compounds developed slowly, and was fully established after 20–30 min of superfusion. While blockade by dotarizine quickly reversed upon its washout, that of flunarizine lasted even 25 min after washing out.

6 Catecholamine release from electroporated chromaffin cells triggered by 10 μM Ca^{2+} was not affected by 10 μM dotarizine or flunarizine.

7 Overall, the results suggest that dotarizine behaves as a Ca^{2+} antagonist in bovine chromaffin cells. It exhibits a potency similar to flunarizine in blocking Ca^{2+} entry, Ca^{2+} channels, Ca_i^{2+} signals and secretion. The dotarizine effects are readily reversible suggesting that in contrast to flunarizine, it does not accumulate in cells. Dotarizine is devoid of intracellular effects on the secretory machinery. All its blocking effects on Ca^{2+} entry, $[Ca^{2+}]_i$ rise and secretion are probably due to blockade of various Ca^{2+} channel subtypes in chromaffin cells. This blockade is use-dependent and seems to be due to the increase by dotarizine of the rate of Ca^{2+} channel inactivation.

Keywords: Dotarizine; flunarizine; chromaffin cell; calcium antagonists, calcium channels

Introduction

Classifications of calcium antagonists (Fleckenstein, 1983; Godfraind, 1987) vary according to their chemical structure (1,4-dihydropyridines, arylalkylamines, benzothiazepines, piperazines), pharmacological and clinical profiles (cardioselective, vasculoselective) or type of voltage-dependent Ca^{2+} channels they block (L-type selective, 'wide-spectrum' Ca^{2+} channel blockers). Though selective L-type Ca^{2+} channel blockers have useful indications in cardiovascular diseases (i.e. hypertension, cardiac ischaemic disease), 'wide-spectrum' Ca^{2+} antagonists might provide additional tissue protective effects in ischaemic conditions. These may be useful in treating clinical conditions such as migraine, in which multiple oetiopathogenic factors coincide. In this condition, various vasoactive neurotransmitters including 5-hydroxytryptamine (5-HT) and catecholamines have been implicated.

Though several calcium antagonists have been useful in the treatment of migraine, the 'wide-spectrum' Ca^{2+} channel blockers, cinnarizine and flunarizine, are being widely used for this clinical condition (Todd & Benfield, 1989). Dotarizine, 1-(diphenylmethyl)-4-[3-(2-phenyl-1,3-dioxalan-2-1)-propyl]-piperazine, is a novel piperazine derivative structurally related to flunarizine (Figure 1). Like flunarizine, dotarizine exhibits slight histamine receptor and α-adrenoceptor blocking properties, but shows a higher anti-5-HT receptor activity, both *in vitro* and *in vivo* (Brasó *et al.*, 1989; 1994; Cartheuser *et al.*, 1994). Dotarizine is currently being investigated clinically as an antimigraine and antivertigo drug. Its therapeutic effects might be related to its anti-5-HT receptor blocking properties and/or Ca^{2+}-entry blocking properties. In fact, dotarizine inhibited $^{45}Ca^{2+}$ uptake and vessel contractility in rabbit basilar and aortic smooth muscle. The authors of this observation (Tejerina *et al.*, 1993) concluded that 'in rabbit, dotarizine inhibits Ca^{2+} entry through Ca^{2+} channels, being more selective for the basilar artery, probably by acting on multiple sites to decrease the availability of intracellular free Ca^{2+} required for activation'. In relation to this Ca^{2+} antagonist effect, more direct methodological approaches are required to ans-

[1] Author for correspondence.

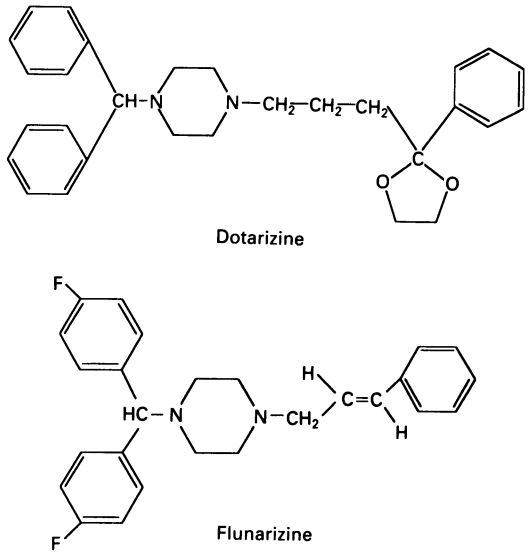


Figure 1 Chemical structures of dotarizine and flunarizine.

wer the following questions: (i) whether dotarizine acts only on vascular L-type Ca^{2+} channels, or also on other neuronal Ca^{2+} channels of the N-, P- or Q-types (Olivera *et al.*, 1994); (ii) if dotarizine can affect the changes in cytosolic Ca^{2+} concentrations (Ca_i^{2+}) evoked by the activation of those Ca^{2+} channel subtypes; (iii) whether dotarizine inhibits the release of neurotransmitters by blocking cytosolic Ca^{2+} signals; and (iv) whether dotarizine acts selectively on the cell plasmalemma or also has an intracellular site of action.

The chromaffin cell, maintained in primary cultures prepared from bovine adrenal glands, constitutes an excellent model to answer these questions. These cells express various Ca^{2+} channels of the neuronal subtype besides cardiovascular L-type channels (Gandia *et al.*, 1993; Albillos *et al.*, 1993). In addition, the chromaffin cell stores and secretes the catecholamines dopamine, noradrenaline and adrenaline when extracellular Ca^{2+} gains the cell interior through these diverse Ca^{2+} channels (Jiménez *et al.*, 1993; Michelena *et al.*, 1993). We present here the results of a study aimed at defining the effects of dotarizine on the following parameters in bovine chromaffin cells: (1) $^{45}Ca^{2+}$ uptake stimulated with K^+ depolarization; (2) whole-cell currents through Ca^{2+} channels using Ca^{2+} or Ba^{2+} as charge carriers; (3) increases of the $[Ca^{2+}]_i$ upon K^+-stimulation of single fura-2-loaded cells; (4) catecholamine release from intact chromaffin cells briefly depolarized with high-K^+ solutions; and (5) catecholamine release triggered by application of Ca^{2+}/EGTA [ethylenebis(oxonitrilo)tetracetate] buffers to electroporated chromaffin cells. Because of their similar chemical structure and clinical indications (migraine, vertigo), most studies presented here with dotarizine were run in parallel to flunarizine.

Methods

Preparation and culture of bovine chromaffin cells

Bovine adrenomedullary chromaffin cells were isolated following standard methods (Livett, 1984) with some modifications (Moro *et al.*, 1990). Cells were suspended in Dulbecco's modified Eagle's medium (DMEM) supplemented with 5% foetal calf serum, 10 μM cytosine arabinoside, 10 μM fluorodeoxiuridine, 50 iu ml^{-1} penicillin and 50 μg ml^{-1} streptomycin. Cells were plated at a density of 5×10^5 cells/well in 24-multiwell Costar plates for $^{45}Ca^{2+}$ uptake studies. For measurements of $[Ca^{2+}]_i$ and whole-cell currents, cells were plated on 1 cm diameter glass coverslips at a density of 5×10^4 cells per coverslip. For secretion experiments, 5×10^6 cells were plated in 5 cm diameter plastic Petri dishes. Cells were used 1–4 days after plating. Medium was replaced after 24 h and then after 2–3 days.

Measurements of $^{45}Ca^{2+}$ uptake

$^{45}Ca^{2+}$ uptake studies were carried out in cells after 2–3 days in culture. Before the experiment, cells were washed twice with 0.5 ml Krebs-HEPES (4-(2-hydroxyethyl)-1-piperazine-ethanesulphonic acid) solution of the following composition (mM): NaCl 140, KCl 5.9, $MgCl_2$ 1.2, $CaCl_2$ 0.5, glucose 11, HEPES 10, at pH 7.2 and 37°C. $^{45}Ca^{2+}$ uptake into chromaffin cells was studied by incubating the cells at 37°C with $^{45}CaCl_2$ at a final concentration of 4 μCi ml^{-1} in the presence of Krebs-HEPES (basal uptake) or high K^+ solution (Krebs-HEPES containing 70 mM KCl with isosmotic reduction of NaCl). This incubation was carried out for 1 min; at the end of this period, the test medium was rapidly aspirated and the uptake reaction was ended by adding 0.5 ml of a cold Ca^{2+}-free Krebs-HEPES containing 10 mM $LaCl_3$. Finally, cells were washed 5 times more with 0.5 ml of Ca^{2+}-free Krebs-HEPES containing 10 mM $LaCl_3$ and 2 mM EGTA, at 15 s intervals.

To measure radioactivity retained by chromaffin cells, the cells were scraped with a plastic pipette tip while adding 0.5 ml 10% trichloroacetic acid; 3.5 ml of scintillation fluid (Ready Micro, Beckman) was added and the samples counted in a Packard beta counter. Results are expressed as % of $^{45}Ca^{2+}$ taken up by control cells.

Measurements of whole-cell currents through Ca^{2+} channels

Membrane currents were measured with the whole-cell configuration of the patch-clamp technique (Hamill *et al.*, 1981). Coverslips containing the cells were placed in an experimental chamber mounted on the stage of a Nikon Diaphot inverted microscope. The chamber was continuously perfused with a control Krebs solution containing (in mM): NaCl 145, $MgCl_2$ 1, $CaCl_2$ 2, HEPES/NaOH 10, tetrodotoxin (TTX) 0.005, pH 7.4. For current recording, 10 mM Ba^{2+} or 10 mM Ca^{2+} (instead of 2 mM Ca^{2+}) was used as the charge carrier. Cells were dialyzed with an intracellular solution containing (in mM): NaCl 10, CsCl 100, TEA.Cl 20, Mg.ATP 5, EGTA 14, HEPES/CsOH 20, Na.GTP 0.3, pH 7.2.

Whole-cell recordings were made with fire-polished electrodes (resistance 2–5 MΩ) mounted on the headstage of a DAGAN 8900 patch-clamp amplifier, allowing cancellation of capacitance transient and compensation of series resistance. A Labmaster data acquisition and analysis board and a 386-based microcomputer with pCLAMP software (Axon Instruments, Inc., CA, U.S.A.) were used to acquire and analyse the data. Solutions were exchanged by use of multi-barrelled concentration-clamp device, the common outlet of which was placed with 100 μm of the cell to be patched.

Intracellular Ca^{2+} measurements

Cells attached to glass coverslips were loaded with fura-2/AM (2.5 μM for 60 min at 37°C, in the incubator). Then the cells were washed with Krebs-HEPES of the following composition (in mM): NaCl 140, KCl 5.9, $MgCl_2$ 1.2, $CaCl_2$ 2, glucose 11, HEPES 10 at pH 7.3. They were kept for 10 min at 37°C in an incubator before being placed on the stage of an inverted microscope, in a chamber allowing their continuous superfusion with Krebs-HEPES. High K^+ (70 mM in 2 mM Ca^{2+})- and dotarizine- or flunarizine (1, 3 and 10 μM)-containing solutions were applied to the cell under investigation using the fast superfusion device employed in the electrophysiological studies. Only one experimental protocol was run for each single coverslip. Single cell fluorescence

measurements were performed by exciting the fura-2-loaded cells with alternating 360 and 390 nm filtered light. The apparent $[Ca^{2+}]_i$ was calculated from the ratio of the fluorescent signals (short over long wavelengths) according to Grynkiewicz *et al.* (1985). Calibration constants were experimentally determined as described by Almers & Neher (1985). Experimental fluorescence data were sampled every 0.5 s by a computer which provided continuously the $[Ca^{2+}]_i$ values in μM.

On-line measurement of catecholamine release from intact chromaffin cells

Bovine chromaffin cells (5×10^6) were introduced in a microchamber for cell superfusion at room temperature (22 ± 2°C) with a Krebs-HEPES of the following composition (in mM): NaCl 144, KCl 5.9, $MgCl_2$ 1.2, glucose 11, $CaCl_2$ 2 and HEPES 10, at pH 7.4. The perfusion rate was 2 ml min^{-1}. The liquid flowing from the perfusion chamber reached an electrochemical detector model Metrohm AG CH-9100 Hersau that monitored 'on line' under the amperometric mode, the amount of catecholamines secreted (Borges *et al.*, 1986). The cells were stimulated for secretion with a Krebs-HEPES solution containing 70 mM K^+ (appropriate reduction of NaCl was made for iso-osmolarity), for 10 s at 5 min intervals by means of electrovalves.

Catecholamine release from electroporated cells

Cells were washed in Ca^{2+}-free Krebs-HEPES solution and resuspended (3×10^6 ml^{-1}) in an electroporation buffer of the following composition (in mM): potassium glutamate 140, $MgCl_2$ 3, EGTA 1, HEPES 20, pH 7, K-ATP 2 and 0.5% bovine serum albumin. Cells were rendered permeable by 10 discharges of 1,500 V at a capacitance of 3 μF using a Gene Pulser apparatus (Bio-Rad) with 10 s in between the discharges, in a cuvette (0.5 ml) with two electrodes 0.4 cm apart. Then, cells were placed in a microchamber and superfused at room temperature with the electroporation buffer at 1 ml min^{-1}. Catecholamine release was triggered by application of a Ca^{2+}/EGTA buffer containing 10 μM free Ca^{2+}. Catecholamine release was monitored on-line with electrochemical detection as described for intact cells.

Materials and solutions

The following materials were used: collagenase from *Clostridium histolyticum* (Boehringer-Mannheim); bovine serum albumin fraction V, cytosine arabinoside, fluorodeoxiuridine, tetrodotoxin (TTX) and EGTA (Sigma); foetal calf serum, penicillin and streptomycin (GIBCO); scintillation fluid Ready micro (Beckman); $^{45}Ca^{2+}$ (specific activity 10–40 mCi mg^{-1} calcium, Amersham). Fura-2 AM was obtained from Molecular Probes, Eugene, Oregon, U.S.A. Dotarizine was from Grupo Ferrer (Barcelona, Spain) and flunarizine from the Janssen Research Foundation, Beerse, Belgium. All other chemicals were reagent grade.

Dotarizine and flunarizine were dissolved in dimethylsulphoxide (DMSO, Merck) at 10^{-2} M and diluted in saline solutions to the desired concentrations. The highest concentrations of DMSO used (not more than 0.1%) had no effects on any of the parameters studied.

Statistical analysis

Data are expressed as means ± s.e.mean. IC_{50}s for each drug were estimated through non-linear regression analysis of ISI software, for a PC computer. Differences between non-paired groups were compared by Student's *t* test with the statistical programme Statworks TM; a value of *P* equal to or smaller than 0.05 was taken as the limit of statistical significance.

Results

Effects of dotarizine and flunarizine on $^{45}Ca^{2+}$ uptake

First we wished to compare the effects of dotarizine and flunarizine on $^{45}Ca^{2+}$ entry into K^+-depolarized chromaffin cells. Thus, cells were depolarized with 70 mM K^+ (with equimolar reduction of Na^+) for 60 s and $^{45}Ca^{2+}$ uptake was evaluated in the presence of different concentrations of both drugs. Before stimulation, cells were preincubated with each concentration of the drug for 10 min.

High K^+ stimulation for 1 min induced $^{45}Ca^{2+}$ uptake (in the presence of 0.5 mM $^{40}Ca^{2+}$) of 3,840 ± 345 c.p.m. per 5×10^5 cells (data from 59 individual wells from 10 different batches of cells). In basal conditions (1 min incubation in Krebs-HEPES solution containing 4 μCi ml^{-1} $^{45}Ca^{2+}$ plus 0.5 mM $^{40}Ca^{2+}$), cells retained 897 ± 151 c.p.m. (data from 32 individual wells from 10 different batches of cells). Thus, the mean ratio evoked/basal Ca^{2+} uptake was 4.3.

Both dotarizine and flunarizine inhibited K^+-evoked Ca^{2+} uptake into chromaffin cells in a concentration-dependent manner. The IC_{50} to inhibit the K^+ response was 4.8 μM for dotarizine and 6.7 μM for flunarizine. No significant difference was found between both IC_{50}s; however, considering the individual values at given concentrations, dotarizine was slightly more potent than flunarizine in blocking $^{45}Ca^{2+}$ entry (Figure 2).

Effects of dotarizine and flunarizine on whole-cell Ba^{2+} and Ca^{2+} currents

Dotarizine and flunarizine probably interrupted Ca^{2+} entry into K^+ depolarized chromaffin cells by blocking voltage-dependent Ca^{2+} channels. It was, therefore, desirable to test this possibility by directly measuring whole-cell Ba^{2+} or Ca^{2+} currents (I_{Ba} or I_{Ca}) in voltage-clamped chromaffin cells. The blocking effects of dotarizine and flunarizine on I_{Ba} or I_{Ca} were tested by superfusing bovine chromaffin cells with increasing concentrations (1–10 μM) of dotarizine or flunarizine during 10 min. Currents were elicited by 50 ms depolarizing pulses to 0 mV applied from a holding potential of −80 mV, at 15 s intervals. Figure 3a (left panel) shows the blocking effects of dotarizine on I_{Ba}. Currents records were obtained before (control) and 10 min after superfusion of the cell with each concentration of the drug. Dotarizine blocked

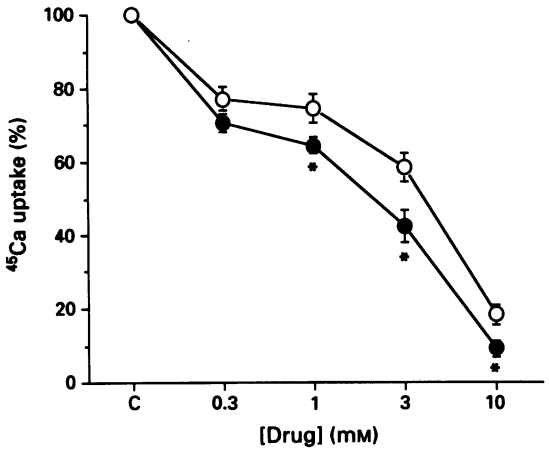


Figure 2 Effects of dotarizine (●) and flunarizine (○) on $^{45}Ca^{2+}$ uptake into chromaffin cells stimulated with 70 mM K^+ for 60 s. Before stimulation, cells were preincubated with each concentration of dotarizine or flunarizine for 10 min. In each individual experiment, $^{45}Ca^{2+}$ uptake (ordinate scale) was normalized to 100% ($^{45}Ca^{2+}$ taken up by cells in the absence of drugs). Data are means ± s.e.mean of at least 4 triplicate experiments from different batches of cells. *$P<0.05$, compared to flunarizine.

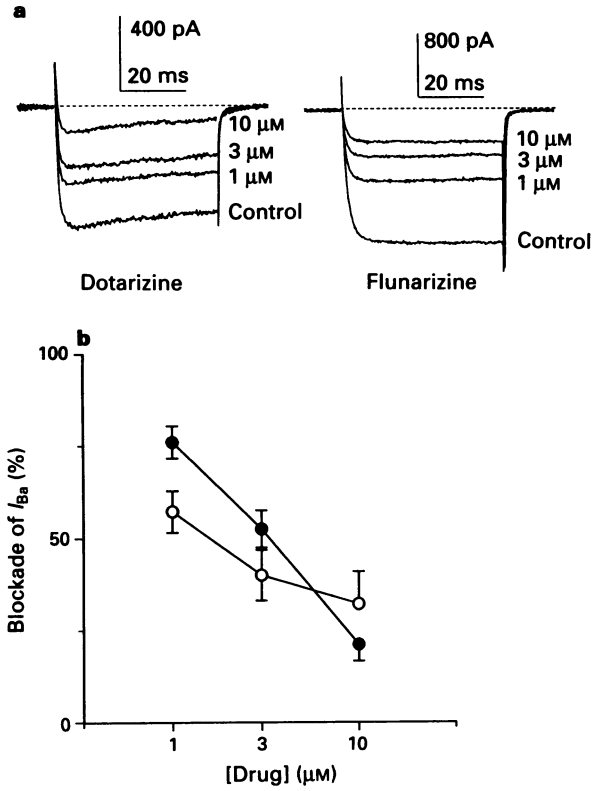


Figure 3 Effects of dotarizine and flunarizine on whole-cell Ba^{2+} currents through Ca^{2+} channels. (a) Original current records in two different cells were obtained either before (control) or after treatment of the cell with increasing concentrations of dotarizine (left panel) or flunarizine (right panel). Each concentration of drug was superfused for 10 min. Cells were held at −80 mV and 50 ms depolarizing pulses to 0 mV were applied at 15 s intervals. (b) Concentration-dependency of the blocking effects of dotarizine (●) and flunarizine (○) on whole-cell Ba^{2+} currents. Data are expressed as percentage of blockade of I_{Ba} and represent the mean ± s.e.mean of 6–9 different cells.

I_{Ba} by 24 ± 4% ($n = 9$ cells), 48 ± 5% ($n = 8$ cells) and 79 ± 4% ($n = 8$ cells) at 1, 3 and 10 μM, respectively. When the effects of flunarizine were tested (right panel in Figure 3a), blockade of I_{Ba} was characterized by a slow onset of action. Averaged results on the blockade of I_{Ba} by dotarizine and flunarizine are shown in Figure 3b. A clear concentration-dependency for the blocking effects of both compounds was seen. The apparent IC_{50}s were estimated to be 2.2 μM for flunarizine and 4 μM for dotarizine. These values are slightly lower than those obtained measuring $^{45}Ca^{2+}$ uptake.

At the highest concentration used (10 μM) dotarizine seemed to increase the rate of inactivation of the remaining current (see left panel in Figure 3a). It was, therefore, of interest to study further the mechanism of blockade of dotarizine. In the experiments shown in Figure 4, 5-s depolarizing test pulses were applied to cells superfused with external solutions containing 10 mM Ca^{2+} or 10 mM Ba^{2+} as charge carriers. It is interesting to note two characteristics of the dotarizine effects: (i) the blockade of peak I_{Ca} or peak I_{Ba} is time-dependent; (ii) the blockade of the late current is greater than the blockade of the initial peak current. The time-dependency of blockade is probably due to the lipophilicity of piperazine derivatives which accumulate progressively in lipid-rich membranes (see later when describing the secretion experiments). The greater blockade of the late current is better seen in Figure 4b and 4d where expanded records from panels (a) and (b) are shown. It apparently seems that dotarizine greatly accelerates the inactivation of I_{Ba} and I_{Ca} and that the drug drastically diminishes the area of the current traces. Upon wash out of dotarizine, the narrowed area quickly expanded, though the decreased peak current recovered little. The acceleration of inactivation was also seen even with much shorter pulses (15 ms instead of 5 s), as shown in the inset of Figure 5.

Another interesting point was the possibility that dotarizine inhibited I_{Ba} in a use-dependent manner. This was tested by monitoring the development of dotarizine blockade at two frequencies of stimulation (Figure 5). Short depolarizing test pulses (15 ms) were applied initially at 0.033 Hz.

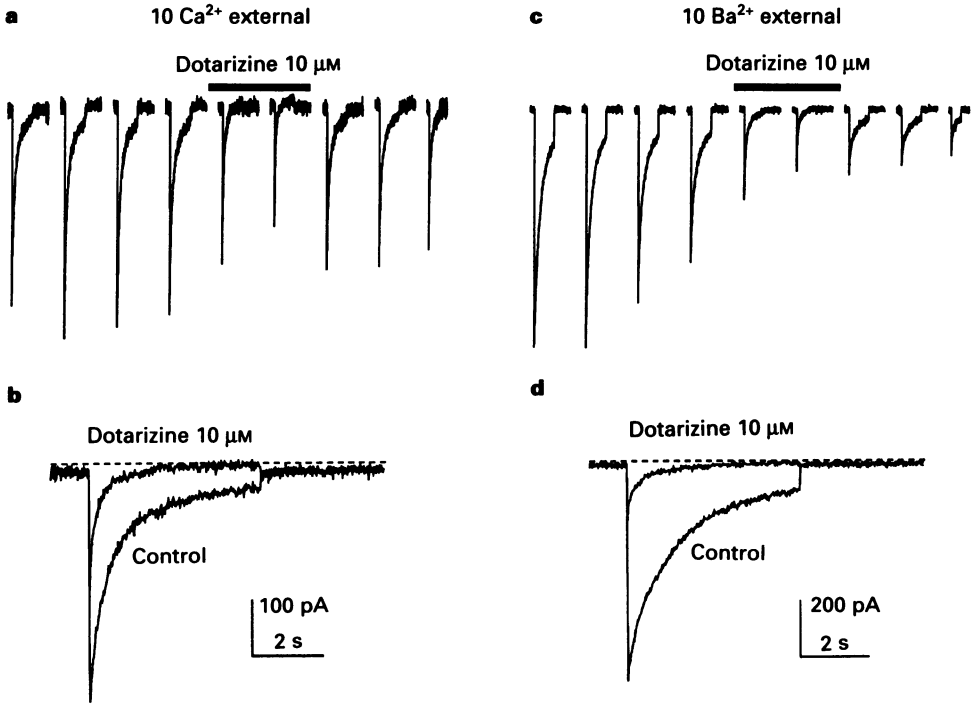


Figure 4 Effects of dotarizine (10 μM in all cases) on whole-cell currents through Ca^{2+} channels using 10 mM Ca^{2+} (a, b) or 10 mM Ba^{2+} (c, d) as charge carriers. Long depolarizing test pulses (5 s duration) to 0 mV were applied from a holding potential of −80 mV. Test pulses were sequentially applied to a voltage-clamped chromaffin cell at 30 s intervals. Dotarizine was present during the time shown by horizontal bars in (a) and (c). Panels (b) and (d) are records from (a) and (c) with an expanded time scale.

Upon addition of dotarizine the initial I_{Ba} (about 900 pA) started to slowly decline. After a 10-min stimulation period, the frequency of stimulation was increased to 0.2 Hz. The rate of blockade was accelerated, suggesting that dotarizine was blocking the Ca^{2+} channels in a use-dependent manner. Washout of dotarizine produced a partial and slowly developing recovery of I_{Ba}.

Effects of dotarizine and flunarizine on cytosolic Ca^{2+} transients

A single fura-2-loaded chromaffin cell was first perfused with Krebs-HEPES solution until a stable basal $[Ca^{2+}]_i$ was achieved (usually, around 100 nM). The compounds themselves did not increase the basal $[Ca^{2+}]_i$ at concentrations of 1–10 μM.

Application of 5-s pulses of 70 mM K^+ in 2 mM Ca^{2+} produced a rapid increase of $[Ca^{2+}]_i$ to a peak of 1.5 μM; the $[Ca^{2+}]_i$ quickly returned to basal levels. The peaks were very reproducible on sequential applications of K^+ at 5 min intervals. When the K^+ responses were stable, dotarizine or flunarizine were superfused for 5 min in Krebs-HEPES solution, and then the K^+ pulse was repeated in the presence of each drug (Figure 6). The percentage of blockade was measured at the peak of the third stimulus. As with I_{Ba} currents, blockade of the Ca_i^{2+} signals by dotarizine or flunarizine was time-dependent (see Figure 6a).

Dotarizine (1 μM) blocked the K^+-evoked increase of $[Ca^{2+}]_i$ by 37 ± 2% ($n = 4$ cells), while flunarizine blocked it by 68.3 ± 2.4% ($n = 6$ cells). When dotarizine 3 μM and 10 μM was superfused, the blockade was 84 ± 2.2% and 83 ± 2.8, respectively. At these concentrations, flunarizine blocked by 93 ± 2% and 100% the Ca_i^{2+} signals. The IC_{50} for dotarizine blockade was 1.2 μM and for flunarizine 0.6 μM (Figure 6c). These values were 4 fold and 10 fold lower than the values obtained for $^{45}Ca^{2+}$ uptake inhibition (see Table 1).

The reversibility of the blocking effects of both compounds differed considerably. For instance, only 5 min after washing out the highest concentration of dotarizine used (10 μM), the recovery of the K^+-evoked $[Ca^{2+}]_i$ increase was almost fully established (Figure 6a, right traces). In contrast, at 5 or 10 min after washout of flunarizine, the Ca_i^{2+} signal was still suppressed.

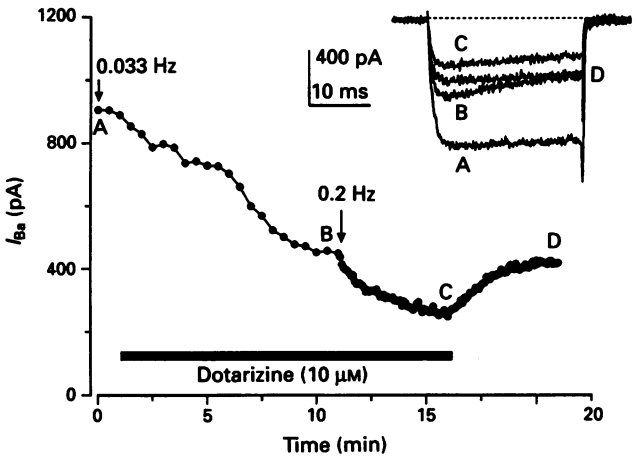


Figure 5 Use-dependent inhibitory effects of dotarizine on I_{Ba}. Short test pulses to 0 mV (15 ms duration) from a holding potential of −80 mV, were sequentially applied at the frequencies shown by the arrows. Dotarizine was present as shown by the horizontal bar. In (b) the stimulation frequency was increased from 0.033 Hz to 0.2 Hz. Inset: original traces taken at the points of the time-course curve, reflected by the letters. Observe the change in kinetics of the current (greater inactivation) of traces B and C (dotarizine present) with respect to traces A (control) and D (washout of dotarizine).

Effects of dotarizine and flunarizine on catecholamine secretion

Stimulation of bovine chromaffin cells for 10 s with 70 mM K^+ at 5 min intervals gave reproducible secretory peaks for over a 2 h perfusion period. The mean oxidation current observed with high K^+ stimulation was 300 ± 20 nA. Figure 7a shows the time-dependent blocking effects of dotarizine on K^+-evoked catecholamine secretion. The gradual blockade of secretion suggests gradual accumulation of dotarizine in the

Table 1 Summary of IC_{50}s of dotarizine and flunarizine to block the different parameters studied in bovine chromaffin cells (values in μM)

	Dotarizine	*Flunarizine*
$^{45}Ca^{2+}$ uptake	4.8	6.7
I_{Ba}	4	2.2
$[Ca^{2+}]_i$	1.2	0.6
Secretion	2.6	1.2

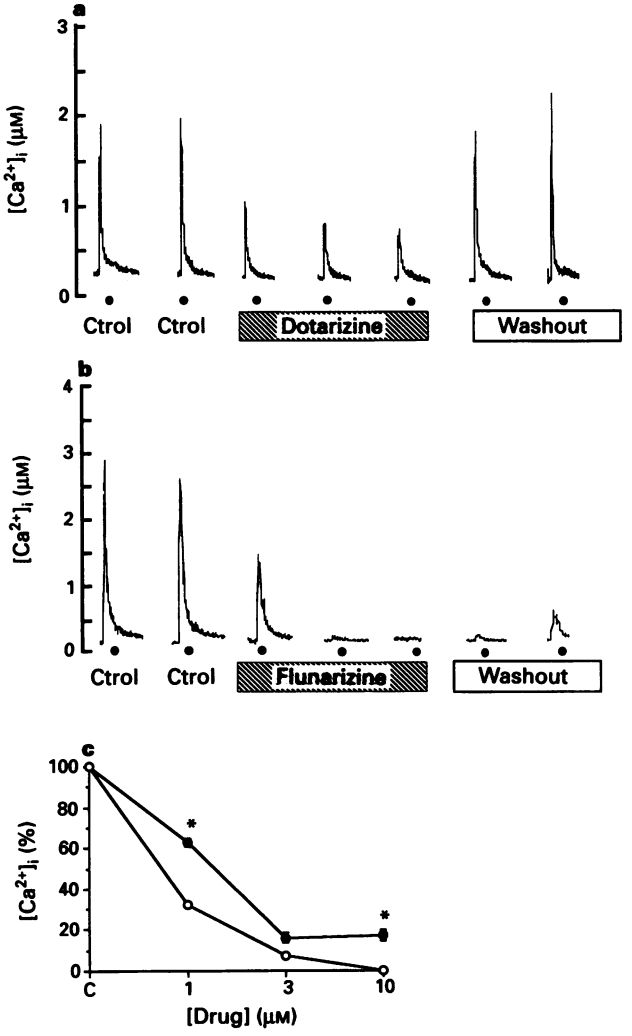


Figure 6 Effects of dotarizine and flunarizine on the changes in cytosolic Ca^{2+} concentrations induced by K^+. Short depolarizing pulses (5 s) of high K^+ (70 mM) were given to a fura-2-loaded single chromaffin cell at 5 min intervals (●). When the K^+ responses were stabilized, 10 μM dotarizine (a) or 10 μM flunarizine (b) were superfused for 5 min before giving the K^+ pulse. After the third stimulus in the presence of the drug, the recovery of the Ca_i^{2+} signal at 5 and 10 min was tested. (c) $[Ca^{2+}]_i$ values (ordinate scale) were normalized to 100% (K^+ responses in the absence of drug), and represented versus the concentration of dotarizine (●) and flunarizine (○). *$P < 0.05$, compared to flunarizine.

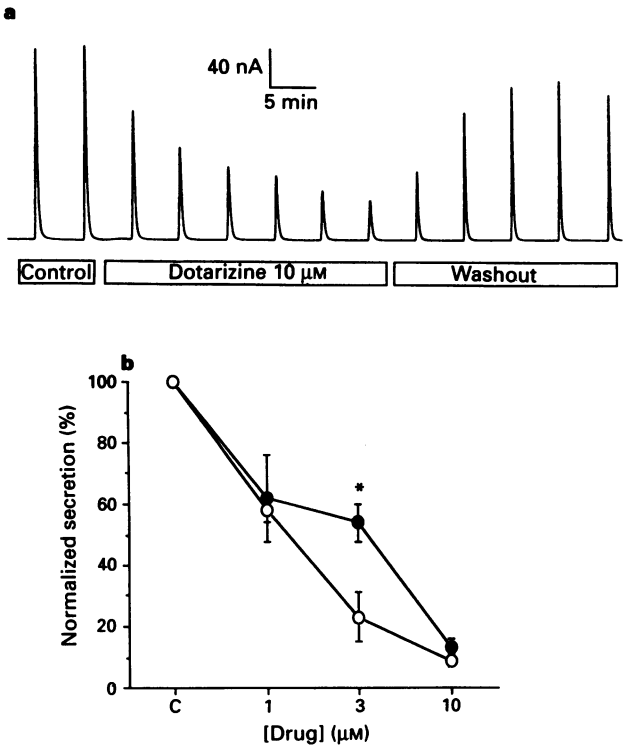


Figure 7 In (a), original traces of catecholamine secretory responses are shown. Cells were stimulated at 5-min intervals with 10-s pulses of a solution containing 70 mM K^+ and 2 mM Ca^{2+}. Dotarizine (10 μM) was present as shown by the horizontal bar at the bottom of the figure. (b) Shows concentration-response curves for dotarizine (●) and flunarizine (○) on such K^+-evoked secretory responses. Data are expressed as percentage with respect to control secretion in the absence of the drug (100%) and correspond to the mean ± s.e.mean of 4 to 8 individual experiments. The effect of dotarizine and flunarizine are represented as their effects after a 30-min superfusion period. A single concentration of each drug was assayed in individual batches of cells (protocol shown in a). *$P<0.01$ with respect to flunarizine.

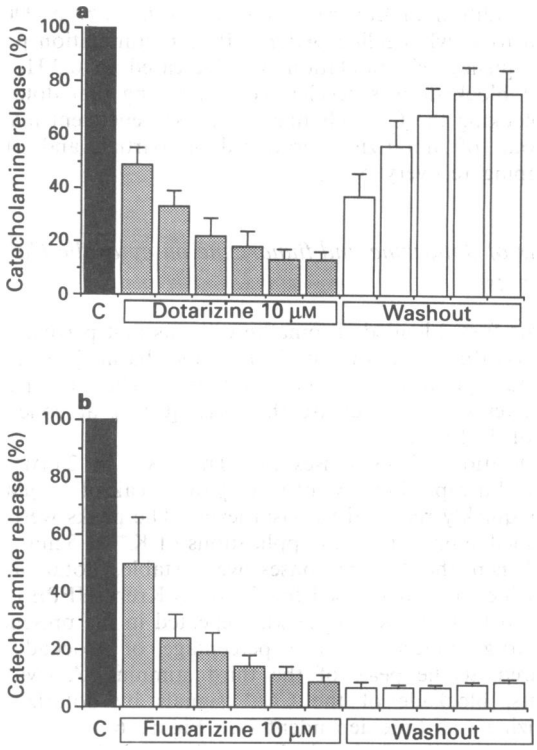


Figure 8 (a) Time-dependent inhibition by dotarizine of catecholamine secretion, and reversal of its blocking effects upon washout. Each column corresponds to secretion induced by a pulse of 70 mM K^+/2 mM Ca^{2+} for 10 s, applied at 5 min intervals to intact superfused chromaffin cells. The shaded columns represent the effect of dotarizine and the lighter ones the washout. (b) Time-dependent inhibition and washout of flunarizine on secretion induced by 70 mM K^+/2 mM Ca^{2+} for 10 s at 5 min intervals in bovine chromaffin cells. The shaded columns show the blocking effects of flunarizine at 5 min intervals and the open columns the washout of these blocking effects. Data are expressed as the mean percentage of control secretion (100%) ± s.e.mean of $n = 5$ in (a) and $n = 6$ in (b).

plasma membrane. The gradual recovery suggests a quick washout of the drug from such membrane. Concentration-response curves for dotarizine and flunarizine on secretion are represented in Figure 7b. Both drugs blocked secretion in a concentration-dependent manner with IC_{50} values of 1.22 μM for flunarizine and 2.6 μM for dotarizine. Statistical differences were observed only at the concentration of 3 μM ($P<0.01$).

Figure 8a shows the time-dependent effects of dotarizine on catecholamine secretion induced by K^+. As the cells were continuously superfused and secretion was monitored 'on line', it was possible to study the rate of instauration of the effects of the drug as well as its reversibility. Dotarizine gradually blocked secretion; a maximum effect of 87% inhibition was obtained after 25 to 30 min of perfusion with dotarizine. When washing out the drug, its blocking effects were quickly reversed. Figure 8b shows the results obtained with flunarizine. As with dotarizine, its blocking effects on secretion were established in a time- and concentration-dependent manner. After 30 min perfusion of the drug 42, 77 and 91% inhibition of secretion was obtained with 1, 3 and 10 μM flunarizine, respectively. The most outstanding difference between these two drugs was the washout of their blocking effects on secretion. Dotarizine was readily washed while flunarizine washed out only partially after a 25 min period (66% after 1 μM and 39% after 3 μM); with 10 μM, even further blockade of secretion was observed during the washout period.

Catecholamine release from electroporated chromaffin cells

The results on $^{45}Ca^{2+}$ uptake, I_{Ca}, I_{Ba} and on $[Ca^{2+}]_i$ increases suggested that the blocking effects of dotarizine and flunarizine on catecholamine release were due to restriction of the access of extracellular Ca^{2+} to the secretory machinery. However, a direct intracellular effect on exocytosis could not be discarded with the above mentioned experiments. It was, therefore, interesting to test the effects of the two compounds on exocytosis triggered by micromolar concentrations of Ca^{2+} from electroporated chromaffin cells (Knight & Baker, 1982).

Figure 9a shows the secretory profiles obtained upon Ca^{2+} application (10 μM for 3 min) to electroporated cells superfused with the electroporation solution (see Methods). Ca^{2+} was applied once the base-line for secretion stabilized. Secretion rose sharply to a peak, followed by a plateau that started to decline after 2 min. When returning to the 0 Ca^{2+} solution, the secretory rate quickly went to basal levels. When present, dotarizine or flunarizine (10 μM) were added during the electroporation procedure and were kept in contact with the electroporated cells throughout the rest of the experiment. The secretory profiles obtained in the presence of these drugs were similar to the control profile. Measurements of peak secretions from various experiments produced averaged values which were similar in control cells, and in cells treated with dotarizine or flunarizine (Figure 9b).

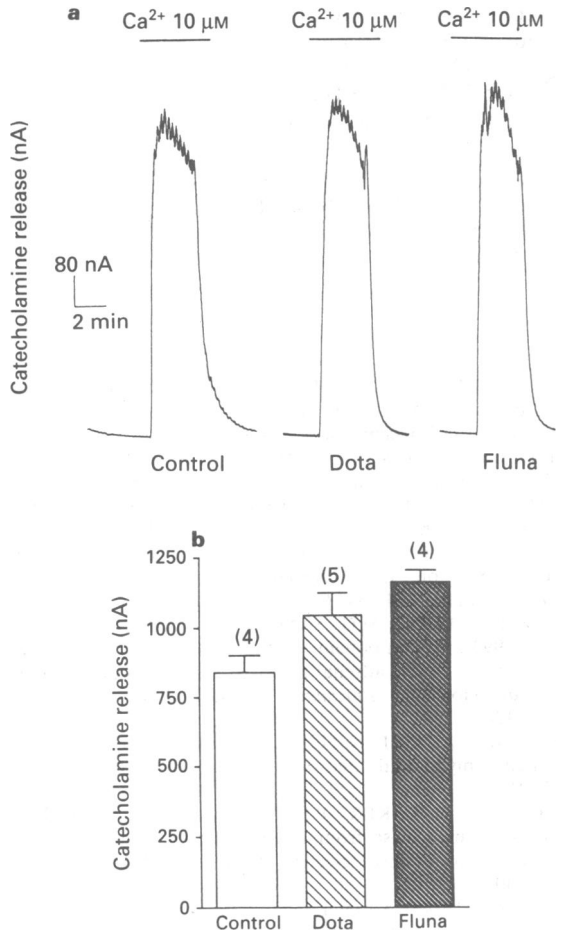


Figure 9 Effects of dotarizine and flunarizine on catecholamine release from electroporated chromaffin cells. Secretion was triggered by the application of a Ca^{2+}/EGTA solution containing 10 μM free Ca^{2+} (see Methods). Cells were stimulated to secrete only once. In (a) copies of original traces of three secretory responses from 3 cell pools from the same batch are shown. Dotarizine or flunarizine (10 μM) were present during the electroporation procedure and during the rest of the experiment. Catecholamine release is expressed as oxidation current in nA (see calibration bar). In (b) averaged results obtained from experiments using the protocol in (a) are plotted. Results are mean ± s.e.mean of the number of experiments shown in parentheses above each column.

Discussion

The experiments presented here demonstrate that dotarizine blocks Ca^{2+} entry, whole-cell currents through voltage-dependent Ca^{2+} channels, $[Ca^{2+}]_i$ increase and catecholamine secretion in chromaffin cells subjected to depolarizing stimuli. These effects are concentration- and time-dependent, and readily reversible upon washing out the drug. In general, the effects of dotarizine were visible at 1 μM concentration and near maximal at the 10 μM concentration. The graded effects of increasing concentrations speak in favour of a selective action at a specific target. In addition, the fact that 10 μM dotarizine did not itself increase the basal $[Ca^{2+}]_i$, the spontaneous release of catecholamines nor secretion from electroporated cells also supports its specificity. Finally, the reversibility of its effects on all parameters studied strengthen this view.

As far as their potencies are concerned, dotarizine and flunarizine were equally effective (see Table 1). Thus, to block $^{45}Ca^{2+}$ uptake, dotarizine exhibited an IC_{50} of 4.8 μM and flunarizine of 6.7 μM. The increases in $[Ca^{2+}]_i$ were blocked with IC_{50}s of 1.2 and 0.6 μM and catecholamine release had IC_{50}s of 2.6 and 1.2 μM, respectively for dotarizine and flunarizine. Slight differences between the various parameters studied might be due to unavoidable differences in protocols. For instance, $^{45}Ca^{2+}$ uptake was studied by exposing the cells for 60 s to a solution containing 70 mM K^+ and 0.5 mM Ca^{2+}. Each group of cells was stimulated only once. Increments in $[Ca^{2+}]_i$, however, were tested by applying repetitive 10 s pulses of a solution containing 70 mM K^+ and 2 mM Ca^{2+}. To study secretion, a similar protocol was used (repetitive 10-s pulses with a solution containing 70 mM K^+ and 2 mM Ca^{2+}). Finally, the effects on I_{Ba} were checked by applying short, 50 ms depolarizing pulses. Such differences can also be explained by the fact that the changes in $[Ca^{2+}]_i$ are not proportional to Ca^{2+} entry through Ca^{2+} channels. In this way, Ca^{2+} mobilization from intracellular stores present in bovine chromaffin cells (Burgoyne *et al.*, 1989) also contribute to the final $Ca^{2+}{}_i$ signal. This $Ca^{2+}{}_i$ mobilization could be particularly sensitive to dotarizine and flunarizine. Experiments now under way will clarify this issue.

An interesting and drastic difference between dotarizine and flunarizine relied on the different reversibility of their effects. Thus, after blocking the $[Ca^{2+}]_i$ increments and secretion, washout of flunarizine did not lead to a reversal of its blocking effects, at least for a 30-min period. This might be due to the high lipophilicity of flunarizine which favours its accumulation in lipid-reach membranes. For instance, the partitioning/transfer of flunarizine from an aqueous phase into phospholipid bilayers shows a binding/partitioning coefficient of 28,700 M^{-1}, supporting the notion that this drug is particularly membrane active (Thomas & Seelig, 1993). On the other hand, at 1 μM concentration, flunarizine can reach tissue/medium ratios as high as 682 in rat aorta and 784 in left atrium (Scheufler & Peters, 1990).

In contrast to flunarizine, the blocking effects of dotarizine were readily reversible upon washout of the drug. In fact, the Ca_i^{2+} signals and the secretory responses recovered after 5–10 min washout of dotarizine, suggesting that dotarizine does not accumulate in cells. It is likely that the extrapyramidal, Parkinson-like effects described for flunarizine are due to the accumulation of the drug in basal ganglia, leading to a strong blockade of dopamine release (Todd & Benfield, 1989). Because of its ready reversibility, it is unlikely that dotarizine might suffer a similar accumulation process in the brain. Therefore, dotarizine might be devoid of the adverse effects associated to flunarizine.

All the effects of dotarizine and flunarizine on $^{45}Ca^{2+}$ uptake, $[Ca^{2+}]_i$ and secretion can be explained through their ability to block voltage-dependent Ca^{2+} channels. As in neurones (Olivera *et al.*, 1994), multiple types of voltage-dependent Ca^{2+} channels have been discovered in bovine chromaffin cells. Thus, they contain ω-conotoxin GVIA-sensitive N-type Ca^{2+} channels (Hans *et al.*, 1990), ω-agatoxin IVA-sensitive P-type Ca^{2+} channels (Albillos *et al.*, 1993), and dihydropyridine-sensitive Ca^{2+} channels (Garcia *et al.*, 1984). Dihydropyridine Ca^{2+} antagonists block only partially the whole-cell current through Ca^{2+} channels (Gandía *et al.*, 1993; Albillos *et al.*, 1993) and catecholamine release from the intact bovine adrenal gland (Gandía *et al.*, 1990; Jiménez *et al.*, 1993) and from isolated chromaffin cells (Boarder *et al.*, 1987; but see Ceña *et al.*, 1983). In contrast, dotarizine and flunarizine inhibited almost completely whole-cell I_{Ba} and catecholamine release in bovine chromaffin cells (this study) and intact glands (Fuente *et al.*, 1992), suggesting that they have a wider-spectrum than most Ca^{2+} channel blockers known to date. They seem to act on a site different from the sites for dihydropyridines, ω-conotoxin GVIA and ω-agatoxin IVA which might be common to the various Ca^{2+} channel subtypes identified in neurones. Recently, Olivera *et al.* (1994) have suggested that Ca^{2+} channels might have a macrosite common to all of them, but with various microsites having different affinities for various toxins blocking specific channel subtypes. In this context, dotarizine and flunarizine might eventually become interesting probes to investigate molecular features related to those macrosites and microsites

on various Ca^{2+} channel subtypes. In fact, flunarizine has been shown to block low-threshold as well as high-threshold Ca^{2+} channels in neurones (Kaneda & Akaike, 1989; Takahashi & Akaike, 1991).

In conclusion, like flunarizine, dotarizine behaves as a wide-spectrum calcium antagonist in bovine chromaffin cells. However, dotarizine presents the advantage over flunarizine of the reversibility of its blocking effects. This may have clinical implications, since the accumulation of drugs in tissue cells is associated with a greater incidence of adverse reactions. In this context, dotarizine might prove clinically safer than flunarizine in treating patients suffering migraine or vertigo. Its Ca^{2+} antagonist effects (this paper) as well as those on 5-HT_1 and 5-HT_2 receptors (Brasó *et al.*, 1994) might contribute to this clinical profile.

This work was supported, in part, by Grupo Ferrer (Barcelona, Spain) and grants from DGICYT (No PM91-0022-C02-01 and PM92-0039) to A.G.G. and from Universidad de Córdoba to B.L. We thank Mrs Carmen Molinos for the typing of this manuscript.

References

ALBILLOS, A., GARCIA, A.G. & GANDIA, L. (1993). ω-Agatoxin-IVA-sensitive calcium channels in bovine chromaffin cells. *FEBS Lett.*, **336**, 259–262.

ALMERS, W. & NEHER, E. (1985). The Ca signal from fura-2 loaded mast cells depends strongly on the method of dye loading. *FEBS Lett.*, **192**, 13–18.

BOARDER, M.R., MARRIOTT, D. & ADAMS, M. (1987). Stimulus secretion coupling in cultured chromaffin cells. Dependency on external sodium and on dihydropyridine-sensitive calcium channels. *Biochem. Pharmacol.*, **36**, 163–167.

BORGES, R., SALA, F. & GARCIA, A.G. (1986). Continuous monitoring of catecholamine release from perfused cat adrenals. *J. Neurosci. Methods*, **16**, 389–400.

BRASO, A., AGUT, J., RUIZ, A., CARTHEUSER, C.F., SACRISTAN, A. & ORTIZ, J.A. (1994). Dotarizine effects on 5-HT_2 and 5-HT_1 receptors. *XIIth Int. Congr. Pharmacol.*, Montreal, Canada.

BRASO, A., CARTHEUSER, C., SACRISTAN, A. & ORTIZ, J.A. (1989). Dotarizine, a promising N-benhydrylpiperazine for migraine prophylaxis due to an additional antiserotoninergic effect. *4th Int. Symp. Calcium Antagonists, Pharmacol. Clin. Res.*, Florence, May 25–27, p. 261.

BURGOYNE, R.D., CHEEK, T.R., MORGAN, A., O'SULLIVAN, A.J., MORETON, R.B., BERRIDGE, M.J., MATA, A.M., COLYER, J., LEE, A.G. & EAST, J.M. (1989). Distribution of two distinct Ca^{2+}-ATPase like proteins and their relationship to the agonist-sensitive calcium store in adrenal chromaffin cells. *Nature*, **342**, 72–74.

CARTHEUSER, C.F., BRASO, A., SACRISTAN, A. & ORTIZ, J.A. (1994). Effects of dotarizine on peripheral and pulmonary circulation and cardiac dynamics in dogs. *Pharmacology*, **48**, 187–193.

CEÑA, V., NICOLAS, G.P., SANCHEZ-GARCIA, P., KIRPEKAR, S.M. & GARCIA, A.G. (1983). Pharmacological dissection of receptor associated and voltage sensitive ionic channels involved in catecholamine release. *Neuroscience*, **10**, 1455–1462.

FLECKENSTEIN, A. (1983). History of calcium antagonists. *Circ. Res.*, **52** (Suppl. I), 3–16.

FUENTE, M.-T., DE LA, GUANTES, J.M., VALLE, M. DEL & GARCIA, A.G. (1992). Mechanism of blockade by flunarizine of bovine adrenal catecholamine release. *Eur. J. Pharmacol.*, **229**, 189–196.

GANDIA, L., ALBILLOS, A. & GARCIA, A.G. (1993). Bovine chromaffin cells posses FTX-sensitive calcium channels. *Biochem. Biophys. Res. Commun.*, **194**, 671–676.

GANDIA, L., MICHELENA, P., DE PASCUAL, R., LOPEZ, M.G. & GARCIA, A.G. (1990). Different sensitivities to dihydropyridines of catecholamine release from cat and ox adrenals. *Neuroreport*, **1**, 119–122.

GARCIA, A.G., SALA, F., REIG, J.A., VINIEGRA, S., FRIAS, J., FONTERIZ, R.I. & GANDIA, L. (1984). Dihydropyridine Bay K 8644 activates chromaffin cell calcium channels. *Nature*, **309**, 69–71.

GODFRAIND, T. (1987). Classification of calcium antagonists. *Am. J. Cardiol.*, **59**, 11B–23B.

GRYNKIEWICZ, G., POENIE, M. & TSIEN, R.Y. (1985). A new generation of Ca^{2+} indicators with greatly improved fluorescence properties. *J. Biol. Chem.*, **260**, 3440–3450.

HAMILL, O.P., MARTY, A., NEHER, E., SACKMANN, B. & SIGWORTH, F.J. (1981). Improved patch-clamp techniques for high-resolution current recording from cells and cell-free membrane patches. *Pflügers Arch. Eur. J. Physiol.*, **391**, 85–100.

HANS, M., ILLES, P. & TAKEDA, K. (1990). The blocking effects of ω-conotoxin on Ca^{2+} current in bovine chromaffin cells. *Neurosci. Lett.*, **114**, 63–68.

JIMENEZ, R.R., LOPEZ, M.G., SANCHO, C., MAROTO, R. & GARCIA, A.G. (1993). A component of the catecholamine secretory response in the bovine adrenal gland is resistant to dihydropyridines and ω-conotoxin. *Biochem. Biophys. Res. Commun.*, **191**, 1278–1283.

KANEDA, M. & AKAIKE, N. (1989). The low-threshold Ca current in isolated amygdaloid neurons in the rat. *Brain Res.*, **497**, 187–190.

KNIGHT, D.E. & BAKER, P.F. (1982). Calcium-dependence of catecholamine release from bovine adrenal medullary cells after exposure to intense electric fields. *J. Membr. Biol.*, **68**, 107–140.

LIVETT, B.G. (1984). Adrenal medullary chromaffin cells in vitro. *Physiol. Rev.*, **64**, 1103–1161.

MICHELENA, P., GARCIA-PEREZ, L.E., ARTALEJO, A.R. & GARCIA, A.G. (1993). Dissociation between cytosolic calcium and secretion in chromaffin cells superfused with calcium ramps. *Proc. Natl. Acad. Sci. U.S.A.*, **90**, 3284–3288.

MORO, M.A., LOPEZ, M.G., GANDIA, L., MICHELENA, P. & GARCIA, A.G. (1990). Separation and culture of living adrenaline- and noradrenaline-containing cells from bovine adrenal medullae. *Anal. Biochem.*, **185**, 243–248.

OLIVERA, B.M., MILJANICH, G., RAMACHANDRAN, J. & ADAMS, M.E. (1994). Calcium channel diversity and neurotransmitter release: the ω-conotoxins and ω-agatoxins. *Annu. Rev. Biochem.*, **63**, 823–867.

SCHEUFLER, E. & PETERS, T. (1990). Phosphatidylserine monolayers as models for drug uptake into membranes and tissue. *Cell Biol. Int. Reports*, **14**, 381–388.

TAKAHASHI, K. & AKAIKE, N. (1991). Calcium antagonist effects on low-threshold (T-type) calcium current in rat isolated hippocampal CA1 pyramidal neurons. *J. Pharmacol. Exp. Ther.*, **256**, 169–175.

TEJERINA, T., CHULIA, T. & GONZALEZ, P. (1993). Effects of dotarizine on $^{45}Ca^{2+}$ movements and contractile responses in vascular smooth muscle. *Eur. J. Pharmacol.*, **239**, 75–81.

THOMAS, P.G. & SEELIG, J. (1993). Binding of the calcium antagonist flunarizine to phosphatidylcholine bilayers: charge effects and thermodynamics. *Biochem. J.*, **291**, 397–402.

TODD, P.A. & BENFIELD, P. (1989). Flunarizine. A reappraisal of its pharmacological properties and therapeutic use in neurological disorders. *Drugs*, **38**, 481–499.

(Received July 26, 1994
Revised September 16, 1994
Accepted September 29, 1994)

British Journal of Pharmacology (1995) 114, 377-382 © 1995 Stockton Press All rights reserved 0007-1188/95 $9.00

Tonic and use-dependent block of sodium currents in isolated cardiac myocytes by bisaramil

[1]Michael K. Pugsley & *David A. Saint

Department of Pharmacology & Therapeutics, Faculty of Medicine, University of British Columbia, 2176 Health Sciences Mall, Vancouver, B.C., Canada V6T 1Z3 and *Protein Dynamics Unit, Department of Chemistry, Australian National University, Canberra, A.C.T. 2601, Australia

1 The effects of bisaramil on sodium currents in rat isolated cardiac myocytes were examined by use of tight-seal, whole-cell patch clamp techniques. Bisaramil produced a concentration-dependent, readily reversible reduction in peak transient sodium current. When the sodium current was evoked at 3 s intervals the estimated ED_{50} for bisaramil was about 11 μM.

2 Bisaramil (16 μM) produced a shift in the inactivation curve to hyperpolarized potentials of about 10 mV, but produced no change in the voltage-dependence of activation.

3 The block of the sodium current by bisaramil showed a profound use-dependence. A concentration of 10 μM produced a considerable block of the current with repeated stimulation. The recovery from block was biphasic, showing fast and slow components which had time constants of about 40 ms and 5 s respectively.

5 Bisaramil produced little tonic block of the sodium current at concentrations of 100 μM; at 300 μM it produced tonic block of around 50%, with extreme use-dependence.

6 Bisaramil appeared not to interact primarily with the inactivated form of the channel, since lengthening the depolarizing pulses did not affect the degree of block produced.

Keywords: Cardiac; transient sodium current; Class I antiarrhythmic; use-dependence; YUTAC

Introduction

Bisaramil (3-methyl, 7-ethyl, 9-α-(4-chlorobenzoyloxy)-3,7-diazabicyclo[3.3.1]-nonane hydrochloride) is an anti-arrhythmic drug developed for the management of ventricular arrhythmias. It has been shown to be effective against both chemical and ischaemic models of arrhythmogenesis (Paroczai *et al.*, 1990; Haruno & Hashimoto, 1993). In isolated cardiac tissue, bisaramil produces an increase in ventricular fibrillation thresholds (Paroczai *et al.*, 1990). In addition it decreases V_{max}, action potential amplitude and overshoot potentials in guinea-pig papillary muscle (Sunami *et al.*, 1991; Paroczai *et al.*, 1992). Electrophysiological studies in multicellular preparations show that bisaramil (3 μM) produces a use-dependent block of the maximum rate of depolarization of the action potential (Sunami *et al.*, 1991). However, there are at present no detailed accounts of the effect of bisaramil on sodium currents in isolated cardiac myocytes.

This study describes the effect of bisaramil on the transient sodium current in rat isolated cardiac myocytes recorded by use of whole-cell clamp techniques. The results of these experiments show that bisaramil can be reasonably described as a drug having strong sodium channel inhibitory effects.

Methods

Isolation of cardiac myocytes

All experiments were performed according to guidelines established by the Animal Care Committee of the Australian National University.

Enzymatic isolation of myocytes was carried out according to the method used previously (Saint *et al.*, 1992). Briefly, male Wistar rats (300-350 g) were killed by cervical dislocation, the hearts removed and washed in ice-cold, calcium-free Tyrode solution for 5 min before Langendorff perfusion at 37°C. After 5 min, enzymatic dissociation was begun in 25 μM calcium Tyrode solution containing protease (0.1 mg ml^{-1}. Sigma Type XIV), collagenase (1 mg ml^{-1}, Worthington CLS II), and foetal calf serum (1 μg ml^{-1}).

After 35 min the ventricles were removed, cut into pieces in fresh 25 μM calcium-Tyrode solution and triturated to dissociate myocytes. Cell suspensions were centrifuged, washed in 200 μM calcium-Tyrode solution, resuspended in 1 mM calcium-Tyrode solution and plated onto glass coverslips. The glass coverslips were transferred to the recording chamber, which had a volume of about 0.5 ml and perfused with recording solution at a flow rate of 0.5 to 1 ml min^{-1}.

Solutions and drugs

All experiments were performed at room temperature (22-25°C) in a bath solution containing (mM): NaCl 70, TES 10, KCl 5.4, $MgCl_2$ 1.0, $CaCl_2$ 2, $CoCl_2$ 5, CsCl 5, glucose 10, choline Cl 60, pH adjusted to 7.4 with 1.0 M NaOH. The pipette solution contained (mM): CSF 140, TES 10, $MgCl_2$ 1, K-EGTA 10, $CaCl_2$ 2, ATP-disodium 10 and was adjusted to pH 7.4 with 1.0 M KOH. These solutions are designed to block all ionic currents other than sodium currents. The concentrations of sodium were chosen to reduce the sodium current amplitude, in order to reduce the severity of series resistance problems.

Data recording and analysis

Electrodes were prepared from borosilicate glass using a two-stage puller (Narishige Scientific Instruments, Tokyo, Japan) and resistances were typically between 1-5 MOhm when containing the pipette solution. Myocyte currents were recorded 5-10 min after achieving whole-cell patch clamp configuration (Hamill *et al.*, 1981). Current recording was performed with an Axopatch 200 amplifier (Axon Instruments), with at least 85% compensation of series resistance in all experiments. The amplifier also allowed for initial compensation of both capacitative transients and leak currents. Where necessary, final capacitance and leak compensation

[1] Author for correspondence.

was performed digitally at the time of analysis by subtraction of the current produced by a 20 mV hyperpolarizing pre-pulse which always preceded the test pulse.

Results

Under whole cell recording conditions, sodium currents were evoked at 3 s intervals by a voltage step to − 40 mV from a potential of − 150 mV. Bisaramil was added to the perfusing solution and sufficient time allowed for steady state block of the current to develop (usually 2 min). Examples of the currents obtained in one cell are shown in Figure 1a. A 50% block of the current was produced by between 8 and 16 μM bisaramil. The concentration-dependence of block is shown in Figure 1b, which shows data from similar experiments in four cells. The estimated ED_{50} from these cells was 11 μM. The block by bisaramil of the sodium current was readily reversible; Figure 1 also shows an experiment in which the magnitude of the current was monitored during a brief application of 30 μM bisaramil. At the stimulation rate used (6 s interval between pulses) onset of block appeared complete in about 1 min, and recovery took about 3 min.

The effects of 16 μM bisaramil on the voltage-dependence of inactivation and activation of the sodium current were also investigated: 16 μM bisaramil produced a shift in the inactivation curve of about 10 mV to hyperpolarized potentials (Figure 2a). This result was confirmed in 4 cells, the mean shift being 12 mV (range 8 to 15). In one cell, 30 μM bisaramil was added; it produced a shift of about 30 mV (data not shown). Bisaramil 16 μM did not produce any shift in the voltage-dependence of activaton of the sodium current, as shown in Figure 2b. This result was also confirmed in 4 cells.

These experiments to estimate the potency of bisaramil were complicated somewhat by the marked use-dependence of the block produced by the drug. Figure 3a shows sodium currents evoked by a train of depolarizations at a frequency of 40 Hz under control conditions and evoked by an identical train of stimuli after 3 min equilibration in 100 μM bisaramil (Figure 3b). No stimuli were given during this equilibration period. The first current of the train was reduced somewhat, by about 20%, indicating some tonic block, and subsequent currents showed a dramatic attenuation with successive stimuli, indicative of a substantial use-dependent block. The concentration-dependence of these effects was investigated by allowing the cell to equilibrate for 3 to 4 min in either 10 μM, 30 μM or 100 μM bisaramil before applying trains of stimuli at 40 Hz. The results are shown in Figure 3c. No frequency-dependent attenuation of the current was apparent in the absence of bisaramil under these conditions. Increasing concentrations of bisaramil produced increasing degrees of attenuation of the peak current amplitude with successive stimuli, although very little tonic block was produced, as

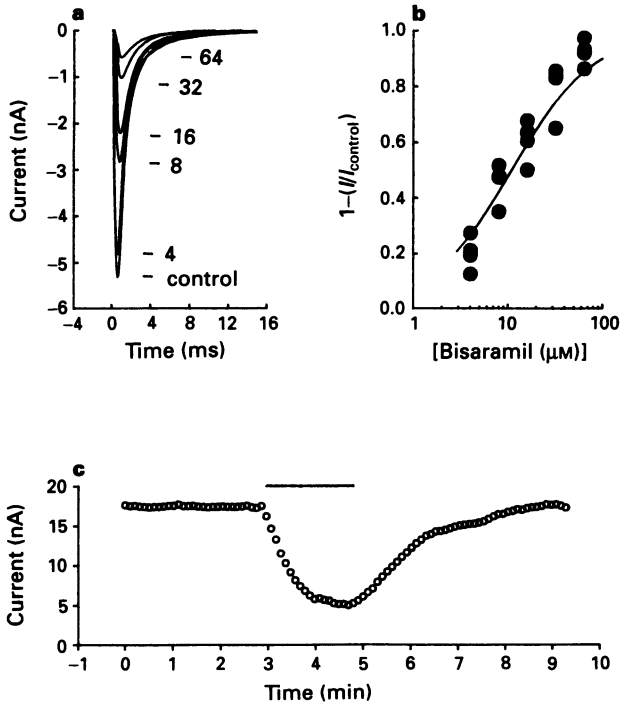


Figure 1 Concentration-dependent block of the transient sodium current by bisaramil. Currents were evoked at 3 s intervals by a voltage step to − 40 mV from a pre-pulse potential of − 150 mV. (a) Shows currents obtained under control conditions and with various concentrations of bisaramil (shown by markers, in μM); (b) shows the data from 4 cells plotted as normalized block of peak current amplitude against concentration of bisaramil; (c) shows the time course of onset and recovery from block induced by bisaramil. Sodium currents were evoked at 6 s intervals. At the time indicated by the bar, 30 μM bisaramil was added to the solution perfusing the cells. The maximum sodium current amplitude is shown plotted against time.

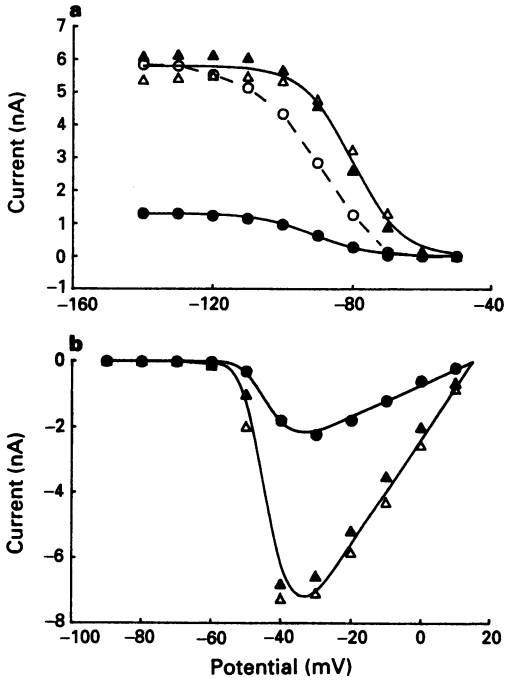


Figure 2 Effect of bisaramil on the voltage-dependence of the sodium current. (a) Shows the voltage-dependence of inactivation of the sodium current under control and recontrol conditions (▲ and △) and in the presence of 16 μM bisaramil (●). Sodium currents were evoked by voltage pulses to − 30 mV from various pre-pulse potentials. The data are plotted as the peak current amplitude against pre-pulse potential. The lines show the fits of the equation

$$I = I_{max}/1 + \exp((v\text{-}v')/k)$$

with values of I_{max} = 5.8 nA, v′ = − 80 mV and k = 8 for control/recontrol and I_{max} = 1.3 nA, v′ = − 91 mV and k = 7 for bisaramil. (○) Bisaramil data scaled to the same maximum current as the control/recontrol. (b) Shows the current-voltage relation for the sodium current in control/recontrol and with 16 μM bisaramil. Sodium currents were evoked by depolarizing pulses to various potentials from a fixed pre-pulse potential of − 140 mV. The data are plotted as peak current amplitude against pulse potential. The conventions for symbols are as in (a). The lines are the best fits of the equation

$$I = G_{max}/1 + \exp((v\text{-}v')/k)x(E_{rev}\text{-}v)$$

with values of E_{rev} = 15 mV, k = 3.5 and v′ = − 43 mV for both sets of data. G_{max} was 16 nS for control/recontrol and 4.8 nS for bisaramil.

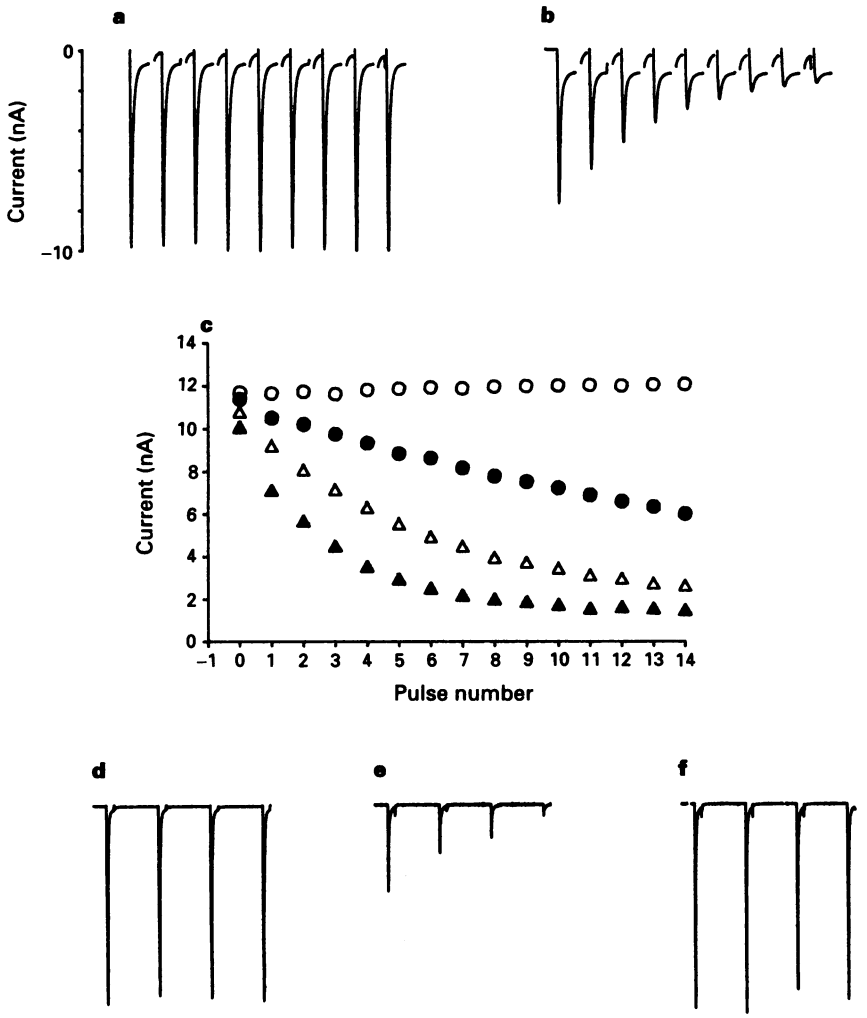


Figure 3 Use-dependent block and tonic block by bisaramil at different concentrations. (a) Shows sodium currents evoked by a train of pulses to − 40 mV from a potential of − 120 mV, delivered at 40 Hz. After equilibration for 3 min in solution containing 100 μM bisaramil, an identical train of stimuli evoked the currents shown in (b). Pronounced attenuation of the current was produced with successive stimuli. (c) Shows the effect of different concentrations of bisaramil upon the currents evoked by trains of stimuli at 40 Hz. The peak sodium current for each stimulus in the train is plotted against pulse number. The plots show control data (○), and data in the presence of 10 μM (●), 30 μM (△) and 100 μM (▲) bisaramil. The cell was equilibrated in each concentration of bisaramil for 3 min before the train of stimuli was delivered. (d) Shows the sodium currents evoked in a different cell by a train of four stimuli at 20 Hz in control solution. In (e) are shown currents evoked by an identical train given after the cell had been equilibrated for 8 min in solution containing 300 μM bisaramil. The currents evoked after 9 min in recontrol solution are shown in (f).

long as sufficient time was allowed for recovery between trains. In a few experiments 300 μM bisaramil was applied to the cells. A typical example of the results is shown in Figure 3d. After 8 min equilibration in 300 μM bisaramil in the absence of any stimulation, the peak current amplitude of the first current evoked was reduced by about 50% (Figure 3e). The use-dependence of the block by this concentration was very pronounced; after only four pulses at 20 Hz the current was essentially abolished. In one experiment 500 μM bisaramil was applied to the cell. Even after 10 min in this solution, a sodium current could be evoked. Frequency-dependent block was extreme at this concentration.

In these experiments it became apparent that recovery from block by bisaramil took some considerable time. This is illustrated by the result shown in Figure 4a, in which two trains of stimuli at 20 Hz were delivered with an interval between them of 4 s. The bathing solution contained 100 μM bisaramil. A rapid diminution of the current was seen during the first train, but at the beginning of the second train recovery from this block was minimal, despite the 4 s gap between trains. This result suggested that the frequency-dependence of block by bisaramil had a slow component. This slow phase of frequency-dependent block is illustrated in Figure 4b, which shows the attenuation of the current by trains of stimuli of a wide range of frequencies in the presence of 100 μM bisaramil. As expected, higher frequencies of stimulation produced a more rapid block of the sodium current (Figure 4c). However, it was apparent that even stimulation rates as low as pulses delivered at 10 s intervals produced a substantial block of the current.

In order to study this frequency-dependence further, experiments were performed in the presence of 30 μM bisaramil, which allowed analysis at higher stimulation rates.

Figure 5 shows the block of the current produced by successive stimuli for trains of stimuli with frequencies of between 0.5 and 80 Hz. At the slower stimulation rates, between 0.5 and 12 Hz, there was little difference discernible in the attenuation of the current with successive stimuli. This suggests that, at these stimulation rates, the interval between pulses is short compared to the rate of recovery from block. However, at higher rates of stimulation, i.e., 70 or 80 Hz, the attenuation of the current with successive pulses becomes

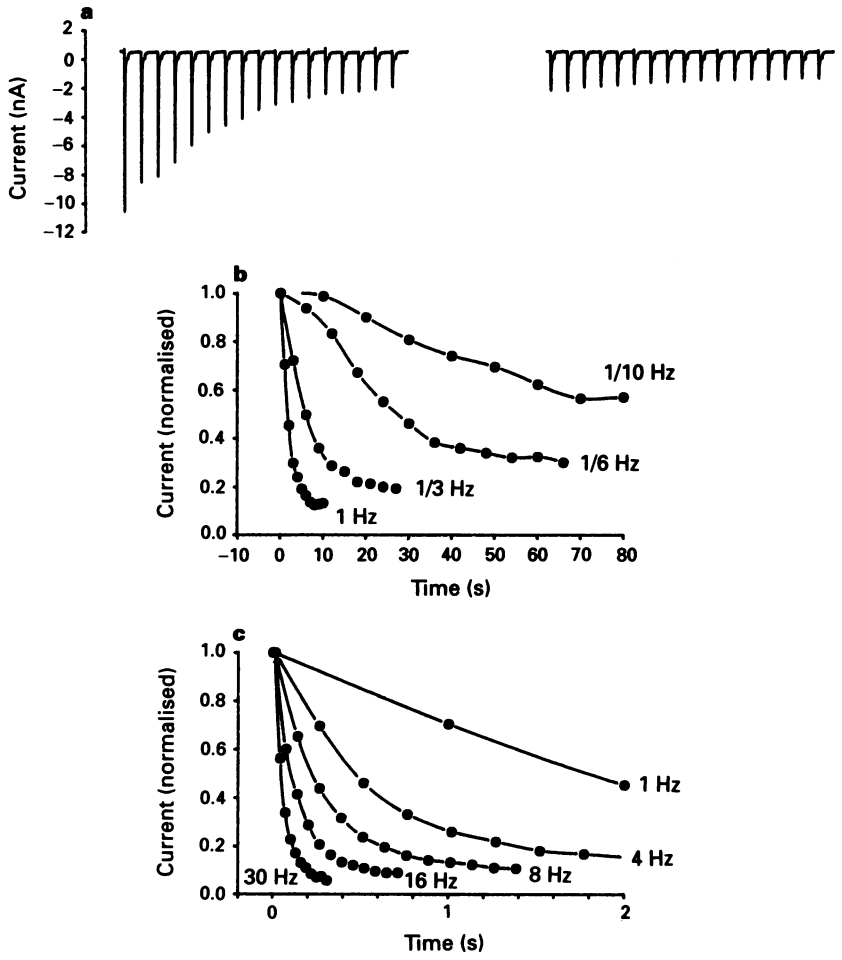


Figure 4 Use-dependent block by bisaramil over a wide range of frequencies. In (a) the sodium currents evoked by a train of depolarizing pulses from − 120 mV to − 40 mV delivered at 20 Hz in solution containing 100 μM bisaramil are shown. The train was repeated after a 4 s delay, yielding the currents shown after the break in the baseline. (b and c). Trains of pulses to − 40 from − 120 mV were delivered at various frequencies ranging between 1/10 Hz and 30 Hz. The data are plotted as the peak current amplitude (normalized to the first current size) against the time at which it was evoked. Trains of stimuli were delivered at 1/10 Hz, 1/6 Hz, 1/3 Hz, 1 Hz (shown in b) and 4 Hz, 8 Hz, 16 Hz and 30 Hz (shown in c on an expanded time scale).

more pronounced. This result could arise if there was a second kinetic component to the recovery from block with a shorter time constant.

The rate of recovery from block was therefore investigated more thoroughly with a double-pulse type methodology. Sodium currents were evoked by pairs of identical depolarizing pulses, the interval between the pulses being varied. The size of the current evoked by the second pulse was then plotted against the interval between the pulses, to give a measure of the rate of recovery from block. Such an experiment is illustrated in Figure 6. The rate of recovery from the block in these experiments could never be adequately fitted with a single exponential. However, the recovery could be well described by the equation

$$1-[\beta x(\alpha/e^{t/\tau_1}) + ((1-\alpha)/e^{t/\tau_2})]$$

which describes recovery from an incomplete block as the sum of two exponentials. For the data shown, a reasonable fit was obtained with $\beta = 0.65$, $\alpha = 0.6$, $\tau_1 = 40$ ms and $\tau_2 = 5$ s. A similar analysis in 3 more cells gave values for the time constants of recovery of between 20 and 50 ms for the fast recovery, and 3 and 8 s for the slow recovery. It should be noted, however, that this method of estimating recovery time constants is not accurate, since a unique solution to equation 1 cannot generally be found. Nevertheless, it was clear from the data that two exponential components having widely different time constants were always necessary to describe the recovery from block.

The use-dependence of block could arise because of an interaction of bisaramil with either the open channel, or the inactivated channel. This question was addressed by giving pairs of voltage pulses to evoke sodium currents and varying the duration of the first pulse, as shown in Figure 7. Prolonging the depolarization does not change the length of time for which the channels are open, but a prolonged depolarization holds the channels in the inactivated state for a longer period of time. If the drug interacts with the inactivated form of the channel, one would therefore expect an increased degree of block with prolonged depolarizations. As shown in Figure 7, this did not occur; prolonging the depolarization from 5 ms to almost 50 ms did not substantially affect the degree of block of the subsequent current.

Discussion

The data show that bisaramil produces a concentration-dependent, readily-reversible block of the transient sodium current in cardiac myocytes and shifts the inactivation curve for the sodium current to more hyperpolarized potentials, although no shift in the activation curve was apparent. This spectrum of actions is very similar to that seen with class I anti-arrhythmic agents, eg. lignocaine (Bean *et al.*, 1983) and quinidine (Snyders & Hondeghem, 1990).

These results corroborate earlier suggestions, from studies performed in intact animals and isolated cardiac tissues, that

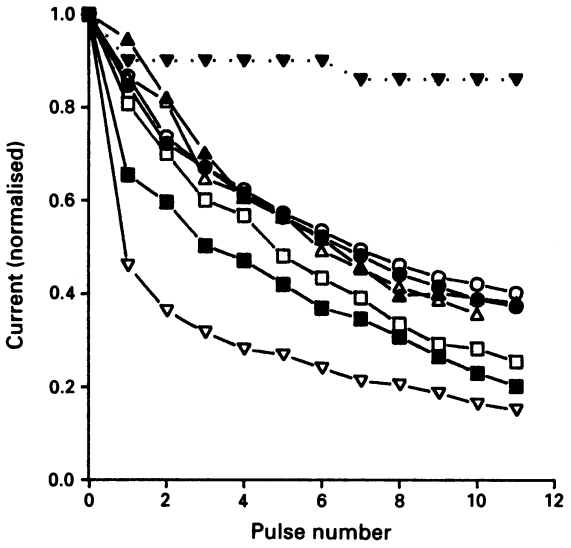


Figure 5 Use-dependence of block at higher frequencies. Trains of pulses to − 40 mV from − 120 mV were given in a solution containing 30 μM bisaramil. The magnitude of the current evoked by each pulse is plotted against the pulse number. The currents are plotted as a fraction of the first current in each train. The trains of pulses at frequencies of 0.5 Hz, 1 Hz, 5 Hz and 12 Hz (○, ●, △, ▲) produced use-dependent block which was indistinguishable. At a frequency of 21 Hz, however, a noticeably more pronounced block was produced (□), and this block was accentuated at frequencies of 70 Hz, (■) and 90 Hz (▽). In the same cell in the absence of bisaramil there was no attenuation of current amplitude at frequencies up to 90 Hz (▼).

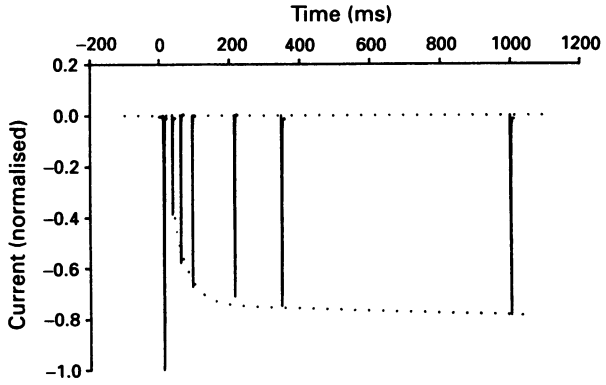


Figure 6 Biphasic recovery from block. Pairs of depolarizing pulses were delivered in a solution containing 100 μM bisaramil, with a variable delay between pulses. The currents evoked are shown plotted at the time that they were evoked, normalized to the size of the first current. The dotted line shows the fit of the equation

$$1-[\beta.(\alpha/e^{t/\tau_1}) + ((1-\alpha)/e^{t/\tau_2})]$$

to the peak current amplitude with $\beta = 0.65$, $\alpha = 0.6$, $\tau_1 = 40$ ms and $\tau_2 = 5$ s.

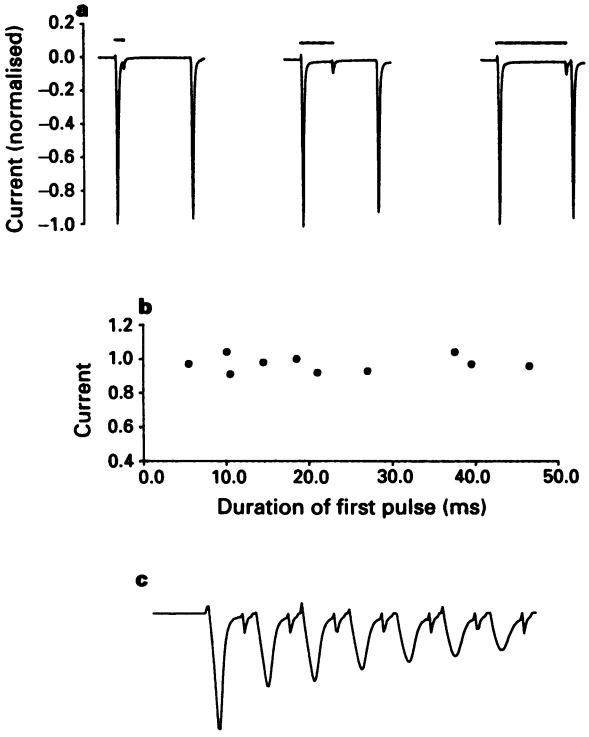


Figure 7 The effect of changing the duration of depolarization. Pairs of depolarizing pulses were given with a delay of 50 ms between the pulses. The duration of the first pulse was varied over the range 5 ms to 46 ms. The currents evoked are shown (a), with the first current magnitude normalized. The bar above the current trace shows the duration of the first depolarization. (b) The magnitude of the second pulse, as a fraction of the first, is plotted against the duration of the first pulse. There was no correlation of the second current size with duration of the first pulse. (c) In the same experiment, a train of stimuli at 40 Hz produced an obvious frequency-dependent block.

bisaramil probably produces its anti-arrhythmic actions via blockade of cardiac sodium channels (Paroczai *et al.*, 1990; 1992; Haruno & Hashimoto, 1993).

Use-dependence of the block by bisaramil has been reported by Sunami *et al.* (1991), in experiments in which action potentials were recorded from multicellular preparations. The data presented here in single myocytes confirm that bisaramil shows a marked frequency-dependent block, which can be dissected into a fast and a slow component. The two components of frequency-dependence appear to arise from a biphasic recovery from block, which occurs with a mixture of a fast recovery, having a time constant of the order of a few tens of milliseconds, and a slow recovery with a time constant of the order of seconds. In practice, the presence of the very slow component of recovery means that care must be exercised in the interpretation of results such as dose-response curves, since the presence of the slow component means that a substantial use-dependent block is present, even when the sodium current is evoked at 3 s intervals. Because of this very slow component of recovery from block, it was very difficult to obtain an estimate of the tonic block produced by bisaramil, since one would have to evoke the sodium current at such a slow rate that time-dependent changes, which are inevitable in patch clamp experiments, obscure the results. Nevertheless, the data suggest that the degree of tonic block produced by bisaramil is small, at least at concentrations encountered in animal experiments, since exposing the cell to 100 μM bisaramil for several minutes attenuated the magnitude of the first pulse in the train by only about 10%. Exposure of the cells to bisaramil 300 μM for several minutes attenuated the first current evoked by 50%. At this concentration of bisaramil the use-dependence of block was such that the current was completely blocked after only three depolarizing pulses were given.

On the basis of the data presented here we conclude that bisaramil produces its antiarrhythmic actions primarily by blocking the transient sodium current and hence can be classified as a class I agent. Use-dependence of block is a useful property for an anti-arrhythmic agent, since rapid firing of action potentials will be suppressed, but the normal firing of action potentials will not be greatly affected. The biphasic frequency-dependence of block by bisaramil may be advantageous in this respect.

We wish to thank The British Columbia Medical Services Foundation, The Heart and Stroke Foundation of BC and Yukon (M.K.P.) and the National Health and Medical Research Council of Australia (D.A.S.) for support of this project. Bisaramil was a gift to Prof. M.J.A. Walker and M.K.P. from Gedeon Richter Ltd, Budapest, Hungary. This work was completed while M.K.P. was a Visiting Fellow at the Dept. of Chemistry, A.N.U. from Prof. M.J.A. Walker's Laboratory at U.B.C.

References

BEAN, B.P., COHEN, C.J. & TSIEN, R.W. (1983). Lidocaine block of cardiac sodium channels. *J. Gen. Physiol.*, **81**, 613–642.

HAMILL, O.P., MARTY, A., NEHER, E., SAKMANN, B. & SIGWORTH, F.J. (1981). Improved patch-clamp techniques for high resolution current recording from cells and cell free membrane patches. *Pflügers Arch.*, **391**, 85–100.

HARUNO, A. & HASHIMOTO, K. (1993). Antiarrhythmic effects of bisaramil in canine models of ventricular arrhythmias. *Eur. J. Pharmacol.*, **233**, 1–6.

PAROCZAI, M., KARPATI, E. & SOLTI, F. (1990). The effects of bisaramil on experimental arrhythmias. *Pharmacol. Res.*, **22**, 463–480.

PAROCZAI, M., KARPATI, E., MARKO, R. & KECSKEMETI, V. (1992). Electrophysiological actions of a new antiarrhythmic drug, bisaramil, on isolated heart preparations. *Pharmacol. Res.*, **25**, 75–85.

SAINT, D.A., JU Y.-K. & GAGE, P.W. (1992). A persistent sodium current in cardiac myocytes. *J. Physiol.*, **453**, 219–231.

SNYDERS, D.J. & HONDEGHEM, L.M. (1990). Effects of quinidine on the sodium current of guinea pig ventricular myocytes. *Circ. Res.*, **66**, 565–579.

SUNAMI, S., SAWANOBORI, T., ADANIYA, H. & HIRAOKA, M. (1991). Electrophysiological properties of a new antiarrhythmic agent, bisaramil, on guinea-pig, rabbit and canine cardiac preparations. *Naunyn Schmeid. Arch. Pharmacol.*, **344**, 323–330.

(Received May 13, 1994
Revised September 9, 1994
Accepted September 30, 1994)

British Journal of Pharmacology (1995) 114, 383-390 © 1995 Stockton Press All rights reserved 0007-1188/95 $9.00

Regulation of histamine- and UTP-induced increases in Ins(1,4,5)P_3, Ins (1,3,4,5)P_4 and Ca^{2+} by cyclic AMP in DDT_1 MF-2 cells

[1]Henk Sipma, Marry Duin, [2]Ben Hoiting, Adriaan den Hertog & Adriaan Nelemans

Department of Pharmacology/Clinical Pharmacology, Groningen Institute for Drugs Studies, University of Groningen, Bloemsingel 1, 9713 BZ Groningen, The Netherlands

1 Stimulation of P_{2U}-purinoceptors with UTP or histamine H_1-receptors with histamine gave rise to the formation of inositol 1,4,5-trisphosphate (Ins(1,4,5)P_3) and inositol 1,3,4,5-tetrakisphosphate (Ins(1,3,4,5)P_4) in DDT_1 MF-2 smooth muscle cells.

2 Stimulation of P_{2U}-purinoceptors or histamine H_1-receptors caused an increase in cytoplasmic Ca^{2+}, consisting of an initial peak, representing the release of Ca^{2+} from internal stores and a sustained phase representing Ca^{2+} influx.

3 The P_{2U}-purinoceptor-mediated Ca^{2+}-entry mechanism was more sensitive to UTP than Ca^{2+}-mobilization (EC_{50}: 3.3 μM ± 0.4 μM vs 55.1 μM ± 9.2 μM), in contrast to these processes activated by histamine H_1-receptors (EC_{50}: 5.8 μM ± 0.6 μM vs 3.1 μM ± 0.5 μM).

4 Pre-stimulation of cells with several adenosine 3':5'-cyclic monophosphate (cyclic AMP) elevating agents, reduced the histamine H_1-receptor-mediated formation of Ins(1,4,5)P_3 and Ins(1,3,4,5)P_4. Forskolin completely inhibited Ins(1,4,5)P_3 formation (IC_{50}: 158 ± 24 nM) whereas Ins(1,3,4,5)P_4 formation was inhibited by only 45% (IC_{50}: 173 ± 16 nM). The P_{2U}-purinoceptor-mediated production of these inositol phosphates was not affected by cyclic AMP.

5 Forskolin and isoprenaline reduced the histamine-induced increase in cytoplasmic Ca^{2+}, as measured in Ca^{2+} containing medium and in nominally Ca^{2+}-free medium but did not change the UTP-induced increase in cytoplasmic Ca^{2+}.

6 These results clearly demonstrate that cyclic AMP differentially regulates components of the histamine induced phospholipase C signal transduction pathway. Furthermore, cyclic AMP does not affect the phospholipase C pathway activated by stimulation of P_{2U}-purinoceptors in DDT_1 MF-2 cells.

Keywords: Ins(1,4,5)P_3; Ins(1,3,4,5)P_4; Ca^{2+}; cyclic AMP; UTP; histamine; DDT_1 MF-2 cell

Introduction

Stimulation of mammalian cells with a wide variety of agonists, acting on cell surface receptors leads, via heterotrimeric regulatory G-proteins, to activation of phospholipase C resulting in the formation of the second messengers diacylglycerol, inositol 1,4,5-trisphosphate (Ins(1,4,5)P_3) and inositol 1,3,4,5-tetrakisphosphate (Ins(1,3,4,5)P_4). The role of Ins(1,4,5)P_3 in the release of Ca^{2+} from intracellular structures by binding to specific receptors is well established (Berridge & Irvine, 1989), whereas a role for Ins(1,3,4,5)P_4 in this process was proposed more recently (Elly *et al.*, 1990; Hoiting *et al.*, 1990; Gawler *et al.*, 1991; Molleman *et al.*, 1991).

In smooth muscle cells the receptor stimulated increase in the cytoplasmic Ca^{2+} concentration leads to an initial phase of contraction of the intact tissue mediated by Ca^{2+}/calmodulin-dependent myosin light chain kinases (Kamm & Stull, 1985). Stimulation of receptors activating adenylyl cyclase or direct activation of adenylyl cyclase by forskolin (Seamon & Daly, 1986) gives rise to the production of adenosine 3':5'-cyclic monophosphate (cyclic AMP), a concomitant activation of protein kinase A and relaxation of the smooth muscle cells (Abdel-Latif, 1991). Several pathways are suggested for protein kinase A to inhibit contraction of smooth muscle, including effects on Ca^{2+} metabolism: (1) inhibition of phosphoinositide hydrolysis and Ins(1,4,5)P_3 production (Hall *et al.*, 1989; Manolopoulos *et al.*, 1991); (2) phosphorylation of the Ins(1,4,5)P_3 receptors resulting in diminished Ca^{2+} release from intracellular stores (Xuan *et al.*, 1991; Tang *et al.*, 1992); (3) enhanced Ca^{2+} uptake into intracellular stores (Mueller & van Breemen, 1979); (4) stimulation of Ca^{2+} extrusion (Bülbring & den Hertog, 1980); (5) inhibition of Ca^{2+} influx into cells (Bülbring & Tomita, 1987; Chen & Rembold, 1992). Also, phosphorylation of myosin light chain kinase by protein kinase A reduces its affinity for the Ca^{2+}/calmodulin complex, thereby inhibiting myosin light chain phosphorylation and contraction (Adelstein *et al.*, 1978).

We have shown previously that stimulation of histamine H_1-receptors or P_2-purinoceptors on DDT_1 MF-2 smooth muscle cells, derived from a Syrian hamster vas deferens, leads to the formation of Ins(1,4,5)P_3 and Ins(1,3,4,5)P_4, release of Ca^{2+} from intracellular stores and influx of Ca^{2+} across the plasma membrane (Hoiting *et al.*, 1990; Molleman *et al.*, 1989; 1991). The P_2-purinoceptors were recently identified as P_{2U}-purinoceptors (Van der Zee *et al.*, 1992). Remarkably, stimulation of DDT_1 MF-2 cells with histamine or nucleotides results in Ca^{2+} release from partly different stores (Den Hertog *et al.*, 1992). Others observed a diminished accumulation of cytoplasmic Ca^{2+} after stimulation of histamine H_1-receptors (Dickenson *et al.*, 1993) or α_1-adrenoceptors in the presence of cyclic AMP (Schachter *et al.*, 1992) and a cyclic AMP-mediated reduced formation of inositol phosphates (Gerwins *et al.*, 1992; Dickenson *et al.*, 1993).

We show here that cyclic AMP differentially affects the histamine-mediated formation of Ins(1,4,5)P_3 and Ins(1,3,4,5)P_4 and that cyclic AMP regulates the activation of the phospholipase C pathway mediated by histamine H_1-receptors but not by P_{2U}-purinoceptors in DDT_1 MF-2 cells.

[1] Author for correspondence.
[2] Present address: University Centre for Pharmacy, A. Deusinglaan 2, 9713 AW, Groningen, The Netherlands.

Methods

Cell culture

DDT_1 MF-2 cells, derived from a Syrian hamster vas deferens (Norris *et al.*, 1974) were cultured in Dulbecco's modified essential medium supplemented with 7 mM $NaHCO_3$, 10 mM HEPES at pH 7.2 (DMEM) and 10% foetal calf serum at 37°C in 5% CO_2 (Molleman *et al.*, 1989).

Preparation of samples for cyclic AMP, Ins(1,4,5)P_3, and Ins(1,3,4,5)P_4 measurements

DDT_1 MF-2 cells were grown in monolayers in 9.6 cm^2 plastic wells as described earlier (Hoiting *et al.*, 1990). The medium was replaced by 2 ml DMEM at 20°C 30 min before starting the experiment by adding agonists. Before adding P_{2U}-purinoceptor- or histamine H_1-receptor agonists, some cell preparations were pre-exposed to forskolin (1 μM) for 10 min or to isoprenaline (10 μM, 10 min) and phentolamine (2 μM, 10 min) to avoid α-adrenoceptor specific events. Cimetidine (10 μM, 5 min in advance) was added to avoid histamine H_2-receptor-mediated events. After removing the medium, reactions were stopped with 400 μM 5% trichloroacetic acid (TCA) and placed on ice for at least 45 min.

Samples were washed 3 times with 800 μl water saturated diethylether and neutralised with KOH (25 μl, 0.2 M).

Measurements of cyclic AMP

A radioligand binding assay was used to determine cyclic AMP concentrations, using a standard curve of cyclic AMP in ether extracted TCA solution (Brown *et al.*, 1971). To reach equilibrium, 50 μl sample was incubated with a buffer composed of 50 mM Tris-HCl (pH 7.4), 4 mM EDTA, 20 μg cyclic AMP binding protein, 200 μg bovine serum albumin and 10 μl [^{3}H]-cyclic AMP (190 nM, 40 Ci $mmol^{-1}$) to a total volume of 160 μl at 4°C for at least 2 h. The reaction was terminated by adding 500 μl of a charcoal suspension (Norit A special, 3.5 g l^{-1}) followed by centrifugation to remove the excess [^{3}H]-cyclic AMP. Radioactivity in the supernatant was measured by scintillation counting.

Measurements of Ins(1,4,5)P_3

Mass measurements of Ins(1,4,5)P_3 were performed as described earlier, using a standard curve of Ins(1,4,5)P_3 in ether-extracted TCA solution (Molleman *et al.*, 1991). In brief, samples were assayed in 25 mM Tris/HCl (pH = 9.0), 1 mM EDTA, 1 mg bovine serum albumin, [^{3}H]-Ins(1,4,5)P_3 (3.3 Ci $mmol^{-1}$, 2000 c.p.m./assay) and about 1 mg binding protein for 15 min. The binding protein was isolated from fresh beef liver (Chilvers *et al.*, 1989). Bound and free radioactivity were separated by centrifugation. The radioactivity in the pellet was determined by scintillation counting.

Measurements of Ins(1,3,4,5)P_4

Binding protein for Ins(1,3,4,5)P_4 was prepared from pig cerebellum as described earlier by Donié & Reiser (1989). A standard curve of Ins(1,3,4,5)P_4 in ether-extracted TCA solution was used to determine Ins(1,3,4,5)P_4 contents. Samples were assayed for 20 min at 0°C in a mixture (total volume 80 μl) containing 1 mM EDTA, 25 mM sodium acetate

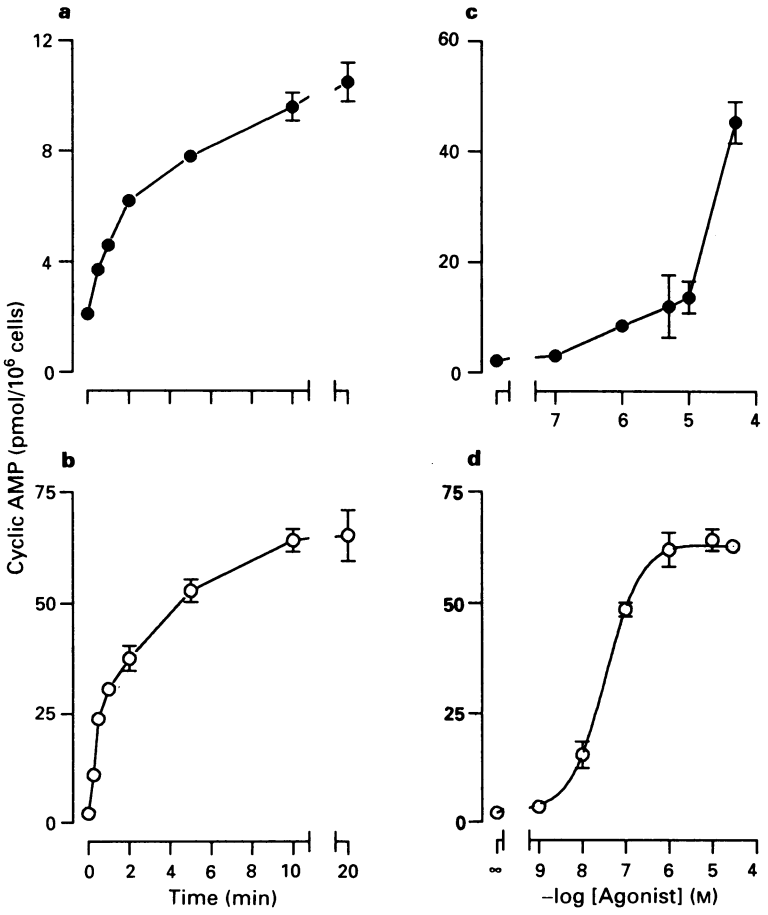


Figure 1 Forskolin and isoprenaline induced formation of cyclic AMP in DDT_1 MF-2 cells. The time-dependent increase in the intracellular cyclic AMP level elicited by (a) forskolin (1 μM) or (b) isoprenaline (10 μM). The concentration-dependent formation of cyclic AMP evoked by exposure of cells to (c) forskolin or (d) isoprenaline for 10 min. Each point represents the mean ± s.e.mean of 4 experiments.

(pH 5.0), 25 mM potassium phosphate, bovine serum albumin (2.5 mg ml^{-1}), Ins(1,3,4,5)P_4 binding protein (150 μg) and [3-^{32}P]-Ins(1,3,4,5)P_4 (5000 c.p.m./assay). Membrane bound ligand was separated from free-ligand by centrifugation (10.000 *g*, 2 min). Radioactivity in the pellet was determined by scintillation counting. [3-^{32}P]-Ins(1,3,4,5)P_4 was obtained after phosphorylation of Ins(1,4,5)P_3 with γ^{32}P-ATP of high specific activity (3000 Ci mmol^{-1}), using a recombinant rat brain Ins(1,4,5)P_3-kinase expressed in *Escherichia coli* as described previously (Takazawa *et al.*, 1990).

Measurements of intracellular calcium

Intracellular concentrations were measured as described earlier (Hoiting *et al.*, 1990). Cells (10^6 cells ml^{-1}) suspended in DMEM containing 10% foetal calf serum were loaded with Indo-1 AM (1.5 μM) for 45 min at 37°C. The cells were collected by centrifugation (5 min, 1000 *g*) and washed two times before the fluorescence measurement with a buffer solution containing (mM): NaCl 145, KCl 5, $MgSO_4$ 0.5, $CaCl_2$ 1, glucose 10, HEPES 10 (pH 7.4) (Hesketh *et al.*, 1983). Calcium-free solution contained Mg^{2+} (6.2 mM) to prevent membrane leakage and EGTA (0.4 mM) to remove extracellular Ca^{2+} (Den Hertog, 1981). Indo-1 fluorescence of the cells (excitation: 325 nm; emission 400 nm and 480 nm) was measured at 22°C. Forskolin or isoprenaline and phentolamine were added 10 min before stimulation of histamine H_1-receptors or nucleotide receptors of cells, mounted in the fluorescence spectrophotometer. The cell suspension was continuously magnetically stirred. The internal calcium concentration was calculated (Hesketh *et al.*, 1983) using 0.015% of Triton X-100 as permeabilizing agent.

Statistics

Data are represented as mean ± s.e.mean. Student's unpaired *t* test was used to determine whether data were significantly different from control values. A sigma plot logistic curve fit programme (Jandel Scientific, U.S.A.) was used to determine EC_{50} values and to analyse binding parameters obtained from the respective radioligand binding assays.

Chemicals

Adenosine 3':5'-cyclic monophosphate (cyclic AMP), adenosine 5'-O-(3-thiotrisphosphate) (ATPγS), inositiol 1,4,5-trisphosphate sodium salt, inositol 1,3,4,5-tetrakisphosphate sodium salt, 8'-bromo-cyclic AMP and hexokinase were obtained from Boehringer (Germany). Adenosine 5'-triphosphate (ATP) and uridine 5'-triphosphate (UTP) were obtained from Serva (Germany). Pertussis toxin (PTX), cimetidine, isoprenaline, forskolin and 3-isobutyl-1-methylxanthine were purchased from Sigma (U.S.A.). Histamine dihydrochloride was obtained from Fluka (Switzerland). Indo-1 AM was from Molecular probes (U.S.A.) and [2,8-^{3}H]-adenosine 3':5'-cyclic monophosphate, D-[2-^{3}H]-inositol 1,4,5-trisphosphate from Du Pont-New England Nuclear (U.S.A.).

Results

Activation of adenylyl cyclase

Stimulation of DDT$_1$ MF-2 cells with forskolin (1 μM) leads to a fourfold increase in the basal cellular cyclic AMP level

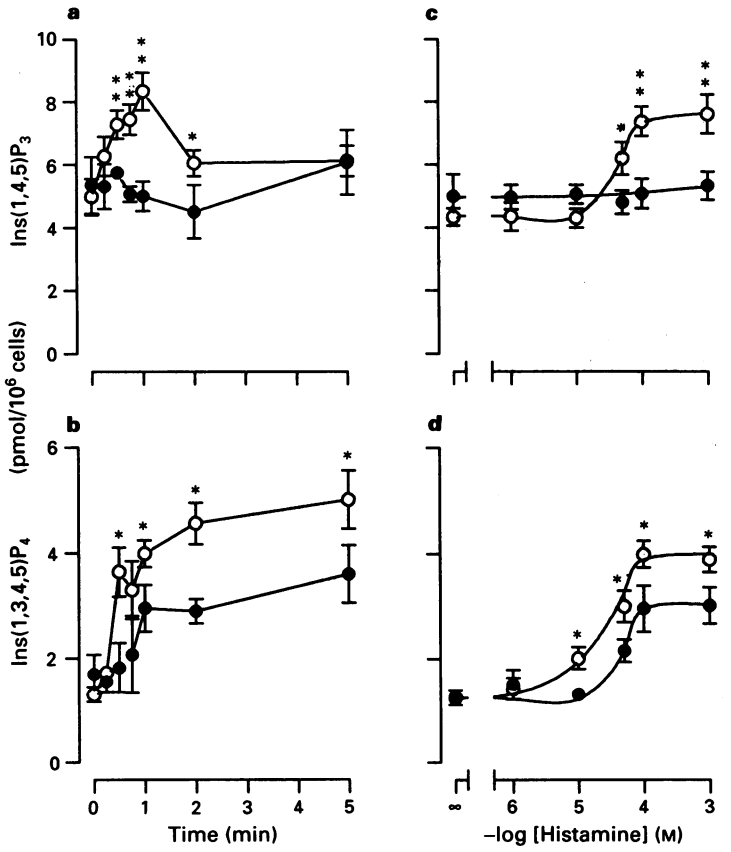


Figure 2 The effect of cyclic AMP on the histamine-induced formation of Ins(1,4,5)P_3 and Ins(1,3,4,5)P_4 in DDT$_1$ MF-2 cells. The time-dependent formation of (a) Ins(1,4,5)P_3 and (b) Ins(1,3,4,5)P_4 evoked on stimulation with histamine (100 μM) of non-pretreated cells (○) and forskolin (1 μM, 10 min) pretreated cells (●). The formation of (c) Ins(1,4,5)P_3 and (d) Ins(1,3,4,5)P_4 evoked by stimulation of non-pretreated cells (○) and forskolin (1 μM, 10 min) pretreated cells (●) with different concentrations of histamine for 1 min. Data are expressed as the means ± s.e.mean of 5 or more experiments. Pretreated significantly different from non-pretreated; $*P<0.05$; $**P<0.01$.

within 10 min (Figure 1a). Exposure of cells to isoprenaline (10 μM, 10 min) results in a much more pronounced increase in the cyclic AMP level (Figure 1b). Cellular cyclic AMP showed a constant rise at forskolin concentrations in the range of 0.1 μM–10 μM (Figure 1c). A sharp rise in cyclic AMP was observed at higher cyclic AMP concentrations, possibly caused by occupation of a low affinity site for forskolin (Cussac *et al.*, 1993). Intracellular cyclic AMP was maximally enhanced by isoprenaline at a concentration of 1 μM (EC_{50}: 34.6 nM ± 0.6; Figure 1d).

Cyclic AMP affects the histamine-induced phospholipase C pathway

The effect of pretreatment of DDT_1 MF-2 cells with forskolin (1 μM, 10 min) or isoprenaline (10 μM, 10 min) on the histamine H_1-receptor-induced phospholipase C pathway was investigated. Cimetidine (10 μM) was used to block histamine H_2-receptors. Specific radioligand binding assays were used to quantify Ins(1,4,5)P_3 and Ins(1,3,4,5)P_4 accumulation. The increase in Ins(1,4,5)P_3 was totally inhibited in forskolin pre-stimulated cells (Figure 2a,c). Ins(1,3,4,5)P_4 formation was completely blocked during the first 30 s of histamine stimulation and was only partly blocked after 1 min in forskolin pre-exposed cells (Figure 2c,d). Pre-exposure of cells to isoprenaline (1 μM, 10 min) or a phosphodiesterase inhibitor, 3-isobutyl-1-methyl-xanthine (200 μM, 10 min, 11.5 ± 1.9 pmol cyclic AMP per 10^6 cells) or a cyclic AMP analogue, 8'-bromo-cyclic AMP (1 mM, 30 min) likewise caused inhibition of histamine-induced formation of Ins(1,4,5)P_3 and Ins(1,3,4,5)P_4 (Table 1). The inhibitory effects of forskolin showed similar concentration-dependencies for Ins(1,4,5)P_3 (IC_{50}: 158 μM ± 24 μM) and Ins(1,3,4,5)P_4 (IC_{50}: 173 μM ± 16 μM) production (Figure 3). However, forskolin can totally abolish Ins(1,4,5)P_3 formation, while about 55% of histamine induced Ins(1,3,4,5)P_4 formation measured after 1 min is not sensitive to enhanced cyclic AMP.

It can be expected that the histamine H_1-receptor-mediated increase in cytoplasmic Ca^{2+} ($[Ca^{2+}]_i$) is also negatively regulated by intracellular cyclic AMP. Therefore, histamine-induced elevations of $[Ca^{2+}]_i$ were measured by Indo-1 fluorescence in Ca^{2+} containing medium and in nominally Ca^{2+}-free medium. The effects of pretreatment of cells with forskolin or isoprenaline on basal $[Ca^{2+}]_i$ and on $[Ca^{2+}]_i$ achieved after agonist stimulation are shown as representative tracings in Figure 4 and summarized in Table 2. Not only the peak increase in $[Ca^{2+}]_i$, but also the sustained increase measured 2 min after stimulation with histamine, caused exclusively by influx of Ca^{2+} from the extracellular environment (Molleman *et al.*, 1991), is reduced by pretreatment of cells with forskolin or isoprenaline (Figure 4, Table 2). In Ca^{2+}-free medium forskolin and isoprenaline likewise attenuated the histamine-induced maximal accumulation of $[Ca^{2+}]_i$ (Figure 4, Table 2). The effects of enhanced cyclic AMP on inositol phosphates and $[Ca^{2+}]_i$ accumulation were all dependent on the histamine concentration as summarized in Table 3. Neither forskolin, isoprenaline, phentolamine (2 μM), added to exclude α_1-adrenoceptor activation by

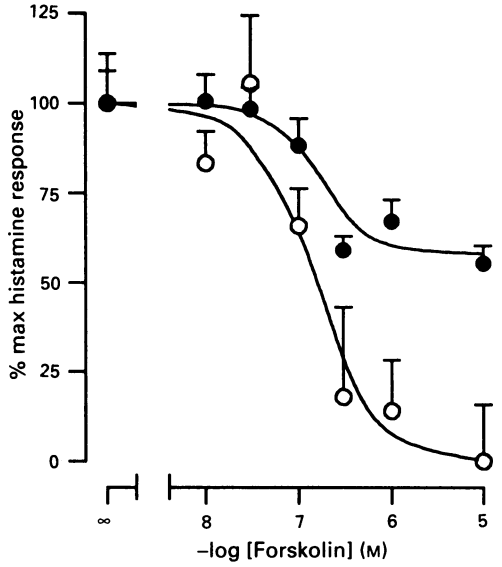


Figure 3 Forskolin differentially inhibits histamine-induced Ins(1,4,5)P_3 and Ins(1,3,4,5)P_4 formation. Cells were pre-exposed to different concentrations of forskolin for 10 min before stimulation with histamine (100 μM, 1 min). Data are represented as percentage of the histamine-induced stimulation in the absence of forskolin. Ins(1,4,5)P_3 (○), Ins(1,3,4,5)P_4 (●). Control basal and stimulated levels are presented in Table 1. Data are expressed as means ± s.e.mean of 6 experiments.

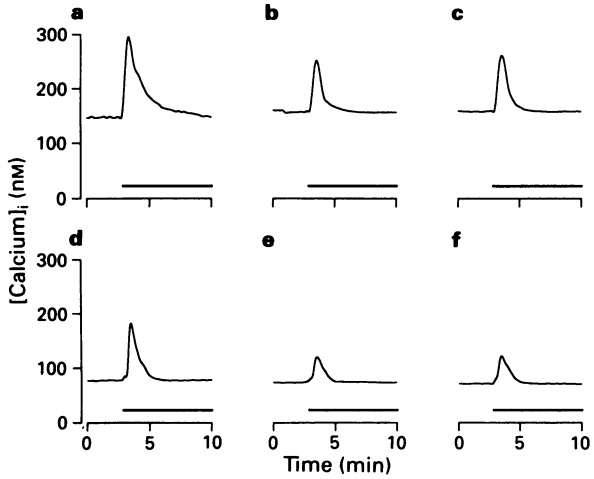


Figure 4 The effect of cyclic AMP on the histamine-induced increase in $[Ca^{2+}]_i$ in DDT_1 MF-2 cells. Before stimulation with histamine (100 μM) cells were either not pretreated (a,d) or pre-exposed to forskolin (1 μM, 10 min, b,e) or to isoprenaline (1 μM, 10 min, c,f). Tracings are representative of at least 4 experiments performed in the presence (a,b,c) or absence (d,e,f) of extracellular Ca^{2+}. Horizontal bars indicate the presence of histamine.

Table 1 The effect of several cyclic AMP elevating agents on basal and histamine-stimulated Ins(1,4,5)P_3 and Ins(1,3,4,5)P_4 in DDT_1 MF-2 cells

	Ins(1,4,5)P_3 (pmol/10^6 cells)		*Ins(1,3,4,5)P_4* (pmol/10^6 cells)	
Treatment	*Basal*	*Stimulated*	*Basal*	*Stimulated*
Histamine	4.2 ± 0.3	6.3 ± 0.3	1.3 ± 0.1	4.2 ± 0.3
Histamine + isoprenaline	4.1 ± 0.4	4.5 ± 0.5*	1.4 ± 0.2	2.8 ± 0.3*
Histamine + IBMX	3.6 ± 0.3	4.5 ± 0.8*	1.3 ± 0.2	2.9 ± 0.1*
Histamine + 8'-bromo cyclic AMP	4.7 ± 0.4	4.7 ± 0.4**	1.1 ± 0.1	2.4 ± 0.2**

Cells were pretreated with isoprenaline (1 μM, 10 min), 3-isobutyl-1-methyl-xanthine (200 μM, 10 min) or 8'-bromo cyclic AMP (1 mM, 30 min) before stimulation with histamine (100 μM, 1 min) and Ins(1,4,5)P_3 and Ins(1,3,4,5)P_4 were measured. Data are expressed as means ± s.e.means of 6 experiments. Significantly different from control stimulation *$P<0.05$; **$P<0.01$.

Table 2 The effect of adenylyl cyclase stimulation on histamine- and UTP-induced increases in $[Ca^{2+}]_i$ in DDT_1 MF-2 cells

	$[Ca^{2+}]_i$ (nM) *extracellular Ca^{2+} present*			$[Ca^{2+}]_i$ (nM) *no extracellular Ca^{2+} present*	
Treatment	*Basal*	*Peak increase*	*2 min*	*Basal*	*Peak increase*
Histamine	163 ± 5	170 ± 17	23 ± 2	79 ± 4	104 ± 14
Histamine + forskolin	160 ± 6	115 ± 20*	12 ± 2*	71 ± 3	46 ± 3*
Histamine + isoprenaline	165 ± 4	111 ± 14*	12 ± 2*	69 ± 4	53 ± 4*
UTP	169 ± 6	182 ± 11	63 ± 3	75 ± 3	115 ± 9
UTP + forskolin	161 ± 5	204 ± 13	64 ± 4	71 ± 3	117 ± 6
UTP + isoprenaline	173 ± 7	179 ± 7	64 ± 3	71 ± 3	110 ± 9

Cells were pretreated with forskolin (1 μM, 10 min) or isoprenaline (1 μM, 10 min). Stimulated Ca^{2+} levels are given at their peak value and 2 min after stimulation with histamine (100 μM) or UTP (1 mM). Data are expressed as means ± s.e.mean of 4 or more experiments. Significantly different from control stimulation. *$P<0.01$.

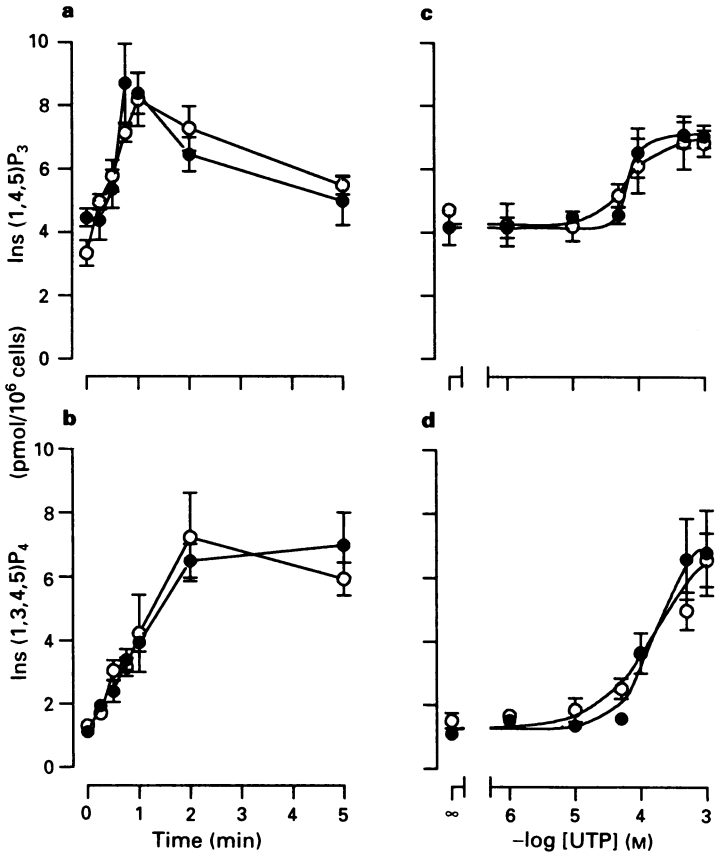


Figure 5 The effect of cyclic AMP on the UTP-induced formation of $Ins(1,4,5)P_3$ and $Ins(1,3,4,5)P_4$ in DDT_1 MF-2 cells. The time dependent formation of (a) $Ins(1,4,5)P_3$ and (b) $Ins(1,3,4,5)P_4$ evoked by stimulation with UTP (100 μM) of non-pretreated cells (○) and forskolin (1 μM, 10 min) pretreated cells (●). The formation of (c) $Ins(1,4,5)P_3$ and (d) $Ins(1,3,4,5)P_4$ evoked by stimulation of non-pretreated cells (○) and forskolin (1 μM, 10 min) pretreated cells (●) with different concentrations of UTP for 1 min. Data are expressed as the mean ± s.e.mean of 5 or more experiments.

isoprenaline, nor cimetidine gave rise to accumulation of $[Ca^{2+}]_i$ themselves (not shown).

Cyclic AMP and the P_{2U}-purinoceptor activated phospholipase C pathway

In order to investigate the effect of an enhanced cellular cyclic AMP level on the P_{2U}-purinoceptor-induced phospholipase C pathway, DDT_1 MF-2 cells were either pretreated with forskolin (1 μM, 10 min) or with isoprenaline (10 μM, 10 min) before exposure to agonists of the P_{2U}-purinoceptor. In this study, UTP was used as P_{2U}-purinoceptor agonist in order to avoid undesirable influences of breakdown products of ATP, in particular adenosine. Adenosine has been shown to act synergistically on ATP-induced phosphoinositide hydrolysis and enhancement of $[Ca^{2+}]_i$ in DDT_1 MF-2 cells (Gerwins *et al.*, 1992). Neither the time course nor the maximum value of $Ins(1,4,5)P_3$ and $Ins(1,3,4,5)P_4$ production upon stimulation with UTP (100 μM) were significantly altered by an enhanced cyclic AMP level (Figure 5a,b). Similar results were obtained when the non hydrolysable ligand, ATPγS (100 μM), was used as a P_{2U}-purinoceptor agonist (not shown). UTP-induced concentration-dependent accumulation of $Ins(1,4,5)P_3$ and $Ins(1,3,4,5)P_4$ was also not affected by pretreatment of cells with forskolin (Figure 5c,d, Table 3).

Similar negative results were obtained for the UTP-induced accumulation of $[Ca^{2+}]_i$. Both Ca^{2+} release and Ca^{2+} entry were unaffected by forskolin or isoprenaline pretreatment (Tables 2,3). Stimulation of DDT_1 MF-2 cells with ATP

Table 3 The effect of adenylyl cyclase stimulation on EC_{50} values of histamine- and UTP-induced inositol phosphate formation and Ca^{2+} metabolism in DDT_1 MF-2 cells

	Histamine (EC_{50} μM)			*UTP* (EC_{50} μM)		
	Control	*Forskolin*	*Isoprenaline*	*Control*	*Forskolin*	*Isoprenaline*
$Ins(1,4,5)P_3$	46.1 ± 0.9	>1000*	ND	74.3 ± 0.9	68.4 ± 3.0	ND
$Ins(1,3,4,5)P_4$	26.3 ± 2.7	48.5 ± 4.2*	ND	138 ± 7	141 ± 7	ND
Ca^{2+}-release	3.1 ± 0.5	6.2 ± 1.2*	ND	55.1 ± 9.2	92.7 ± 25.1	ND
Ca^{2+}-entry	5.8 ± 0.6	11.7 ± 1.5*	13.4 ± 0.9*	3.3 ± 0.4	3.9 ± 0.6	3.1 ± 0.2
Maximal $[Ca^{2+}]_i$	5.0 ± 0.2	14.0 ± 0.8*	15.9 ± 1.5*	6.6 ± 0.3	6.9 ± 1.0	5.8 ± 0.7

EC_{50} values are obtained after logistic curve fitting and presented as best fitted value ± s.e.mean. Cells were stimulated with histamine or UTP after pretreatment with forskolin (1 μM, 10 min) or isoprenaline (10 μM, 10 min). Ca^{2+}-release was measured in the absence of extracellular Ca^{2+}. Ca^{2+}-entry represents the increase in $[Ca^{2+}]_i$ obtained after 2 min of agonist stimulation in Ca^{2+}-containing medium. Maximal $[Ca^{2+}]_i$ represents the peak $[Ca^{2+}]_i$ obtained in the presence of extracellular Ca^{2+}. ND: not determined. Significantly different from control: $*P<0.01$.

resulted in a similar concentration-dependent elevation of $[Ca^{2+}]_i$ as stimulation with UTP. Pre-exposure of the cells with forskolin did not affect the ATP induced increase in $[Ca^{2+}]_i$ (not shown).

Discussion

In this study the effect of cellular cyclic AMP on histamine H_1-receptor and P_{2U}-purinoceptor-mediated formation of inositol phosphates and increase in $[Ca^{2+}]_i$ was investigated in DDT_1 MF-2 smooth muscle cells. In order to enhance cellular cyclic AMP levels, two different methods were used. Forskolin, which acts directly on the catalytic subunit of adenylyl cyclase (Seamon & Daly, 1986) gave rise to a four-fold increase in the basal cyclic AMP level, whereas the β-adrenoceptor agonist, isoprenaline, enhanced the cyclic AMP level to a much larger extent. Apparently isoprenaline is more effective than forskolin at the concentrations used in activating the formation of cyclic AMP as measured by cyclic AMP mass in contrast to the equipotent action of these agents found by determination of *the novo* synthesis of cyclic AMP in DDT_1 MF-2 cells (Dickenson *et al.*, 1993).

Exposure of DDT_1 MF-2 cells to histamine leads to the production of inositol phosphates, the release of Ca^{2+} from intracellular compartments and entry of Ca^{2+} from the external environment (Molleman *et al.*, 1991). These events are histamine H_1-receptor specific (Molleman *et al.*, 1991; White *et al.*, 1993). Enhanced cyclic AMP produced with forskolin or isoprenaline, as well as elevated cyclic AMP achieved by other means (by inhibiting cyclic AMP breakdown with the phosphodiesterase inhibitor, 3-isobutyl-1-methyl-xanthine and pre-exposure of cells to 8'-bromo cyclic AMP) was effective in blocking the histamine-induced production of $Ins(1,4,5)P_3$ and $Ins(1,3,4,5)P_4$. The formation of $Ins(1,4,5)P_3$ and the formation of $Ins(1,3,4,5)P_4$ during the first 30 s of stimulation were completely abolished in forskolin pretreated cells. However, while $Ins(1,4,5)P_3$ formation is completely blocked for at least 5 min, $Ins(1,3,4,5)P_4$ formation was inhibited by only 45% after 1 min of histamine stimulation. The forskolin concentration-dependency for inhibition was similar for $Ins(1,4,5)P_3$ and $Ins(1,3,4,5)P_4$ formation. These results suggest, that histamine induces cyclic AMP-sensitive formation of $Ins(1,4,5)P_3$ and $Ins(1,3,4,5)P_4$ and that histamine stimulates a slowly evolving, cyclic AMP insensitive and $Ins(1,4,5)P_3$-independent pathway of $Ins(1,3,4,5)P_4$ production. It is not clear from where this $Ins(1,3,4,5)P_4$ originates. It has been shown previously in permeabilized cells or in purified enzyme systems, that the $Ins(1,4,5)P_3$ 3-kinase exhibits a very high affinity and low capacity for $Ins(1,4,5)P_3$ and is activated by increased $[Ca^{2+}]_i$ (Biden *et al.*, 1988; Morris *et al.*, 1988). Thus, another possible explanation of our results is that $Ins(1,4,5)P_3$ is phosphorylated immediately and at a high rate in DDT_1 MF-2 cells, especially under those conditions when production of $Ins(1,4,5)P_3$ is reduced. A similar discrepancy between phorbol ester-induced inhibition of $Ins(1,4,5)P_3$ and $Ins(1,3,4,5)P_4$ production was observed in adrenal chromaffin cells, though $Ins(1,4,5)P_3$ production was not completely blocked in this case (Boarder *et al.*, 1992). In some studies a stimulatory action of cyclic AMP on partly purified $Ins(1,4,5)P_3$ 3-kinase has been established (Biden *et al.*, 1988; Sim *et al.*, 1990). We also observed a minor activation of $Ins(1,4,5)P_3$ 3-kinase in forskolin pretreated cells as measured in permeabilized DDT_1 MF-2 cells (unpublished observation). However, activation of $Ins(1,4,5)P_3$ 3-kinase by cyclic AMP seems not to be prominent in intact cells, since the ratio $Ins(1,4,5)P_3/Ins(1,3,4,5)P_4$ is not changed in forskolin pretreated cells after stimulation with UTP.

It should be noticed, that in pretreated cells, in parallel with $Ins(1,3,4,5)P_4$ formation, internal Ca^{2+} release and Ca^{2+}-entry is observed under conditions where no $Ins(1,4,5)P_3$ is formed, suggesting that under these circumstances $Ins(1,3,4,5)P_4$ formation plays an important role in the enhancement of intracellular Ca^{2+} in DDT_1 MF-2 cells.

Forskolin and isoprenaline were equally effective in diminishing the histamine H_1-receptor-induced release of Ca^{2+} from intracellular stores and the entry of Ca^{2+}, though isoprenaline increased the cellular cyclic AMP level to a much larger extent than forskolin. Apparently, a small increase in cellular cyclic AMP already elicits a full effect on the histamine-induced phospholipase C pathway. Similar results, describing the influence of cyclic AMP on total inositol phosphate formation and release of stored Ca^{2+} have been described (Dickenson *et al.*, 1993). An explanation for these results might be that cyclic AMP modulates the filling state of the histamine-sensitive Ca^{2+} store or the Ca^{2+}-pump activity in the plasma membrane, thereby modulating phospholipase C activity. However, it has been found that the production of inositol phosphates is not dependent on Ca^{2+}-release from internal stores (Den Hertog *et al.*, 1992) or on Ca^{2+}-entry from the extracellular space (Schachter *et al.*, 1992) in DDT_1 MF-2 cells. This means that the diminished production of inositol phosphates cannot be explained by this model. A more reliable explanation is that cyclic AMP-activated protein kinase A exerts its effect on the histamine-induced activation of phospholipase C or prior to this point at the G-protein and/or receptor level.

The EC_{50} values obtained for the histamine-induced formation of $Ins(1,4,5)P_3$ and $Ins(1,3,4,5)P_4$ are remarkably higher than those found for the histamine-evoked release of Ca^{2+} or Ca^{2+}-entry, suggesting that a small and local production of inositol phosphates is sufficient to elicit the emptying of histamine sensitive Ca^{2+}-pools.

Stimulation of DDT_1 MF-2 cells with ATP also gives rise to production of inositol phosphates and an increase in $[Ca^{2+}]_i$ (Molleman *et al.*, 1989; Hoiting *et al.*, 1990; Gerwins *et al.*, 1992). ATP and UTP share about the same potency for these P_2-purinoceptor-activated processes (Van der Zee *et al.*, 1992), thus classifying this receptor as a P_{2U}-purinoceptor

(Fredholm *et al.*, 1994). Forskolin did not affect the UTP or ATPγS-induced generation of Ins(1,4,5)P_3 and Ins(1,3,4,5)P_4. In accordance with this, the related increase in $[Ca^{2+}]_i$, originating from release of stored Ca^{2+} and from Ca^{2+}-entry was not affected by cyclic AMP. These results show that cyclic AMP does not interfere with P_{2U}-purinoceptor-mediated phospholipase C activation.

Surprisingly, it was found that the EC_{50} values of the UTP-induced accumulation of Ins(1,4,5)P_3 and Ins(1,3,4,5)P_4 and the EC_{50} value found for the release of Ca^{2+} were much higher than the values found for the Ca^{2+}-influx and the maximal rise in $[Ca^{2+}]_i$. These data suggest that some cellular component, not directly related to activation of phospholipase C, plays a role in the UTP activated Ca^{2+}-entry process.

Stimulation of nucleotide receptors results in a decline in the prestimulated cyclic AMP level (Sipma *et al.*, 1994). Simultaneous activation of phosphoinositide hydrolysis and inhibition of adenylyl cyclase activity upon stimulation of P_2-purinoceptors was observed in several tissues including rat hepatocytes (Okajima *et al.*, 1987) and mouse ventricular myocytes (Yamada *et al.*, 1992). The lack of effect of cyclic AMP on the nucleotide receptor-mediated phospholipase C pathway in DDT_1 MF-2 cells is not due to a compensatory decrease in cyclic AMP caused by nucleotide receptor stimulation because: (1) stimulation of cells with micromolar concentrations of UTP does not significantly reduce cyclic AMP, while at these concentrations UTP is able to raise $[Ca^{2+}]_i$, which is not affected by forskolin or isoprenaline pretreatment. (2) UTP decreases the isoprenaline-induced cyclic AMP content to about 2 times the level found with forskolin in the absence of UTP, while isoprenaline did not affect the UTP-induced increase in Ins(1,4,5)P_3, Ins(1,3,4,5)P_4 and $[Ca^{2+}]_i$. (3) Agonists of the nucleotide receptor decrease forskolin induced cyclic AMP to a level that is still sufficient to reduce the histamine-induced increase in Ins(1,4,5)P_3 and Ins(1,3,4,5)P_4.

These observations suggest that, in contrast to P_{2U}-purinoceptor stimulation, histamine H_1-receptor stimulation is modulated by cyclic AMP-activated protein kinase A, which phosphorylates some component in the signal transduction pathway leading to activation of phospholipase C. Previous experiments showed that the P_{2U}-receptor coupled G-protein that activates phospholipase C, is sensitive to pertussis toxin (Gerwins *et al.*, 1992; personal observation), in contrast to histamine H_1-receptor coupled G-protein (White *et al.*, 1993; personal observation). These different G-proteins may function as a target for cyclic AMP discrimination. The cloning of the bovine and rat histamine H_1-receptor (Fujimoto *et al.*, 1993; Yamashita *et al.*, 1991) has revealed the existence of phosphorylation sites in the third intracellular loop of the receptor, which is thought to interact with a putative G-protein. Such consensus sites for protein kinase A phosphorylation have not been found in the third intracellular loop of the recently cloned P_{2U}-purinoceptor (Lustig *et al.*, 1993), suggesting another site for cyclic AMP discrimination.

In summary, the results show that cyclic AMP differentially affects histamine-induced Ins(1,4,5)P_3 and Ins(1,3,4,5)P_4 formation and that cyclic AMP regulates histamine H_1 receptor but not P_{2U}-purinoceptor stimulation leading to the formation of inositol phosphates and a rise in $[Ca^{2+}]_i$.

Labelled Ins(1,3,4,5)P_4 was kindly provided by P. van Dijken and P. van Haastert, Dept. of Biochemistry, University of Groningen, The Netherlands and C. Erneux, School of Medicine, Free University of Brussels, Belgium.

References

ABDEL-LATIF, A.A. (1991). Biochemical and functional interactions between the inositol 1,4,5-trisphosphate-Ca^{2+} and cyclic AMP signalling systems in smooth muscle. *Cell. Signal.*, **3**, 371–385.

ADELSTEIN, R.S., CONTI, M.A., HATHAWAY, D.R. & KLEE, C.B. (1978). Phosphorylation of smooth muscle myosin light chain kinase by the catalytic subunit of adenosine 3',5'-monophosphate-dependent protein kinase. *J. Biol. Chem.*, **253**, 8347–8350.

BERRIDGE, M.J. & IRVINE, R.F. (1989). Inositol phosphates and cell signalling. *Nature*, **341**, 197–205.

BIDEN, T.J., VALLAR, L. & WOLLHEIM, C.B. (1988). Regulation of inositol 1,4,5-trisphosphate metabolism in insulin-secreting RINm5F cells. *Biochem. J.*, **251**, 435–440.

BOARDER, M.R. & CHALLISS, J. (1992). Role of protein kinase C in the regulation of histamine and bradykinin stimulated inositol polyphosphate turnover in adrenal chromaffin cells. *Br. J. Pharmacol.*, **107**, 1140–1145.

BROWN, B.L., ALBANO, J.D.M., EKINS, R.P., SGHERZI, A.M. & TAMPION, W. (1971). A simple and sensitive saturation assay method for the measurement of adenosine-3',5'-cyclic monophosphate. *Biochem. J.*, **121**, 561–562.

BÜLBRING, E. & DEN HERTOG, A. (1980). The action of isoprenaline on the smooth muscle of guinea-pig taenia coli. *J. Physiol.*, **304**, 277–296.

BÜLBRING, E. & TOMITA, T. (1987). Catecholamine action in smooth muscle. *Pharmacol. Rev.*, **39**, 49–96.

CHEN, X.L. & REMBOLD, C.M. (1992). Cyclic nucleotide-dependent regulation of Mn^{2+} influx, $[Ca^{2+}]_i$, and arterial smooth muscle relaxation. *Am. J. Physiol.*, **263**, C468–C473.

CHILVERS, E.R., CHALLIS, R.A., BARNES, P.J. & NAHORSKI, S.R. (1989). Mass changes of inositol 1,4,5-trisphosphate in trachealis muscle following agonist stimulation. *Eur. J. Pharmacol.*, **164**, 587–590.

CUSSAC, D., KORDON, C., ENJALBERT, A. & SALTARELLI, D. (1993). VIP-induced cross-talk between G-proteins in membranes from rat anterior pituitary cells. *Cell. Signal.*, **5**, 119–137.

DEN HERTOG, A. (1981). Calcium and -action of catecholamines of guinea-pig taenia caeci. *J. Physiol.*, **316**, 109–125.

DEN HERTOG, A., HOITING, B., MOLLEMAN, A., VAN DEN AKKER, J., DUIN, M. & NELEMANS, S.A. (1992). Calcium from separate receptor-specific intracellular stores induced by histamine and ATP in a hamster cell line. *J. Physiol.*, **454**, 591–607.

DICKENSON, J.M., WHITE, T. & HILL, S.J. (1993). The effects of elevated cyclic AMP levels on histamine-H_1-receptor-stimulated inositol phospholipid hydrolysis and calcium mobilization in the smooth-muscle cell line DDT_1 MF-2. *Biochem. J.*, **292**, 409–417.

DONIÉ, F. & REISER, G. (1989). A novel, specific binding protein assay for quantification of intracellular inositol 1,3,4,5-tetrakisphosphate ($InsP_4$) using a high affinity receptor from cerebellum. *FEBS Lett.*, **254**, 155–158.

ELLY, J.A., HUNYADY, L., BAUKAL, A.J. & CATT, K.J. (1990). Inositol 1,3,4,5-tetrakisphosphate stimulates calcium release from bovine adrenal microsomes by a mechanism independent of the inositol 1,4,5-trisphosphate receptor. *Biochem. J.*, **268**, 333–338.

FREDHOLM, B.B., ABBRACHIO, M.P., BURNSTOCK, G., DALY, G., HARDEN, T.K., JACOBSON, K.A., LEFF, P. & WILLIAMS, M. (1994). International Union of Pharmacology Nomenclature: classification of purinoceptors. *Pharmacol. Rev.*, **46**, 143–156.

FUJIMOTO, K., HORIO, Y., SUGAMA, K., ITO, S., LIU, Y.Q. & FUKUI, H. (1993). Genomic cloning of the rat histamine H_1 receptor. *Biochem. Biophys. Res. Commun.*, **190**, 294–301.

GAWLER, D.J., POTTER, B.V.L., GIGG, R. & NAHORSKI, S.R. (1991). Interactions between inositol tris- and tetrakis-phosphates. *Biochem. J.*, **276**, 163–167.

GERWINS, P. & FREDHOLM, B.B. (1992). ATP and its metabolite adenosine act synergistically to mobilize intracellular calcium via the formation of inositol 1,4,5-triphosphate in a smooth muscle cell line. *J. Biol. Chem.*, **267**, 16081–16087.

HALL, I.P., DONALDSON, J. & HILL, S.J. (1989). Inhibition of histamine-stimulated inositol-phospholipid hydrolysis by agents which increase cyclic AMP levels in bovine tracheal smooth muscle. *Br. J. Pharmacol.*, **97**, 603–613.

HESKETH, T.R., SMITH, G.A., MOORE, J.P., TAYLOR, M.V. & METCALFE, J.C. (1983). Free cytoplasmic calcium concentration and mitogenic stimulation of lymphocytes. *J. Biol. Chem.*, **258**, 4876–4882.

HOITING, B., MOLLEMAN, A., DUIN, M. & DEN HERTOG, A. (1990). The P_2-purinoceptor mediated inositol phosphate formation in relation to cytoplasmic calcium in DDT_1 MF-2 smooth muscle cells. *Eur. J. Pharmacol.*, **189**, 31–39.

KAMM, K.E. & STULL, J.T. (1985). The function of myosin and myosin light chain phosphorylation in smooth muscle. *Annu. Rev. Pharmacol. Toxicol.*, **25**, 593–620.

LUSTIG, K.D., SHIAU, A.K., BRAKE, A.J. & JULIUS, D. (1993). Expression cloning of an ATP receptor from mouse neuroblastoma cells. *Proc. Natl. Acad. Sci. U.S.A.*, **90**, 5113–5117.

MANOLOPOULOS, V.G., PIPILI-SYNETOS, E., DEN HERTOG, A. & NELEMANS, S.A. (1991). Inositol phosphates formed in rat aorta after α_1-adrenoceptor stimulation are inhibited by forskolin. *Eur. J. Pharmacol.*, **207**, 29–36.

MOLLEMAN, A., NELEMANS, A. & DEN HERTOG, A. (1989). P_2-mediated membrane currents in DDT_1 MF-2 smooth muscle cells. *Eur. J. Pharmacol.*, **169**, 167–174.

MOLLEMAN, A., HOITING, B., DIUN, M. VAN DEN AKKER, J., NELEMANS, A. & DEN HERTOG, A. (1991). Potassium channels regulated by inositol 1,3,4,5-tetrakisphosphate and internal calcium in DDT_1 MF-2 smooth muscle cells. *J. Biol. Chem.*, **266**, 5658–5663.

MORRIS, A.J., MURRAY, K.J., ENGLAND, P.J., DOWNES, P. & MICHELL, R.H. (1988). Partial purification and some properties of rat brain inositol-1,4,5-trisphosphate 3-kinase. *Biochem. J.*, **251**, 157–163.

MUELLER, E. & VAN BREEMEN, C. (1979). Role of intracellular Ca^{2+} sequestration in β-adrenergic relaxation of smooth muscle. *Nature*, **281**, 682–683.

NORRIS, J.S., GORSKI, J. & KOHLER, P.O. (1974). Androgen receptors in a syrian hamster ductus deferens tumor cell line. *Nature*, **248**, 422–424.

OKAJIMA, F., TOKUMITSU, Y., KONDO, Y. & UI, M. (1987). P_2-purinergic receptors are coupled to two signal transduction systems leading to inhibition of cAMP generation and to the production of inositol triphosphate in rat hepatocytes. *J. Biol. Chem.*, **262**, 13483–13490.

SCHACHTER, J.B., IVINS, J.K., PITTMAN, R.N. & WOLFE, B.B. (1992). Competitive regulation of phospholipase C responses by cAMP and calcium. *Mol. Pharmacol.*, **41**, 577–586.

SEAMON, K.B. & DALY, J.W. (1986). Forskolin: its biological and chemical properties. *Adv. Cyclic Nucl. Prot. Phosphoryl. Res.*, **20**, 1.

SIM, S.S., KIM, J.W. & RHEE, S.G. (1990). Regulation of D-Myo-inositol 1,4,5-trisphosphate 3-kinase by cAMP-dependent protein kinase and protein kinase C. *J. Biol. Chem.*, **265**, 10367–10372.

SIPMA, H., DEN HERTOG, A. & NELEMANS, A. (1994). The phospholipase C activating P_{2U}-purinoceptor also inhibits cyclic AMP formation in DDT_1 MF-2 smooth muscle cells. *Eur. J. Pharmacol. Mol. Pharmacol. Section*, **268**, 431–437.

TAKAZAWA, K., VANDEKERCKHOVE, M., DUMONT, J.E. & ERNEUX, C. (1990). Cloning and expression in Escherichia coli of rat brain cDNA encoding a Ca^{2+}/calmodulin-sensitive inositol 1,4,5-trisphosphate 3-kinase. *Biochem. J.*, **272**, 107–112.

TANG, D.C., STULL, J.T., KUBOTA, Y. & KAMM, K.E. (1992). Regulation of Ca^{2+} dependence of smooth muscle contraction. *J. Biol. Chem.*, **267**, 2232–2239.

VAN DER ZEE, L., NELEMANS, A. & DEN HERTOG, A. (1992). Nucleotide receptors on DDT_1 MF-2 vas deferens cells. *Eur. J. Pharmacol.*, **215**, 317–320.

WHITE, T., DICKENSON, J.M. & HILL, S.J. (1993). Histamine H_1-receptor-mediated inositol phospholipid hydrolysis in DDT_1 MF-2 cells: agonist and antagonist properties. *Br. J. Pharmacol.*, **108**, 196–203.

XUAN, Y.T., DAVID WATKINS, W. & WHORTON, R. (1991). Regulation of endothelin-mediated calcium mobilization in vascular smooth muscle cells by isoproterenol. *Am. J. Physiol.*, **260**, C492–C502.

YAMADA, M., HAMAMORI, Y., AKITA, H. & YOKOYAMA, M. (1992). P_2-purinoceptor activation stimulates phosphoinositide hydrolysis and inhibits accumulation of cAMP in cultured ventricular myocytes. *Circ. Res.*, **70**, 477–485.

YAMASHITA, M., FUKUI, H., SUGAMA, K., HORIO, Y., ITO, S., MIZUGUCHI, H. & WADA, H. (1991). Expression of cloning of a cDNA encoding the bovine histamine H_1 receptor. *Proc. Natl. Acad. Sci. U.S.A.*, **88**, 11515–11519.

(Received July 25, 1994
Accepted September 30, 1994)

British Journal of Pharmacology (1995) 114, 391-399 © 1995 Stockton Press All rights reserved 0007-1188/95 $9.00

Inhibition of delayed rectifier K^+-current by levcromakalim in single intestinal smooth muscle cells: effects of cations and dependence on K^+-flux

D. McHugh & [1]D.J. Beech

Department of Pharmacology, University of Leeds, Leeds LS2 9JT

1 Whole-cell voltage-clamp recordings were made from single smooth muscle cells isolated from the longitudinal layer of the guinea-pig small intestine.

2 Levcromakalim ((-)Ckm) inhibited delayed rectifier K-current ($I_{K(DR)}$) and induced a voltage-independent K-current ($I_{K(-Ckm)}$). Both effects were inhibited similarly by glibenclamide. In some cells, however, $I_{K(-Ckm)}$ could be induced without any effect on $I_{K(DR)}$.

3 Ba^{2+} caused a voltage-dependent block of $I_{K(-Ckm)}$. The IC_{50} was 0.2 mM at -40 mV (6 cells), but at 0 mV 2 mM Ba^{2+} caused only a $26 \pm 7\%$ inhibition ($n = 5$). Ba^{2+} had much less effect on $I_{K(DR)}$, 2 mM Ba^{2+} having no inhibitory effect on current elicited by depolarization to -30 mV ($n = 6$) or 0 mV ($n = 5$).

4 Low concentrations of Zn^{2+} blocked $I_{K(-Ckm)}$ while having little effect on $I_{K(DR)}$. Zn^{2+} (40 μM) caused a $77 \pm 1\%$ reduction of $I_{K(-Ckm)}$ at -30 mV ($n = 4$) but $I_{K(DR)}$ was inhibited by only $10 \pm 3\%$ at the same voltage ($n = 4$).

5 Inward current amplitudes were compared in 135 mM Rb^+ and 135 mM K^+ bath solutions. (-)Ckm-activated Rb^+-current was only 4% of the K^+-current, whereas delayed rectifier Rb^+-current was larger than K^+-current.

6 (-)Ckm did not inhibit $I_{K(DR)}$ if $I_{K(-Ckm)}$ was blocked. In the presence of 2 mM Ba^{2+} or 135 mM Rb^+, (-)Ckm did not induce current nor did it inhibit the delayed rectifier. When $[Rb^+]_o$ was 25 mM and $[K^+]_i$ was 130 mM, (-)Ckm elicited outward current and inhibited outward delayed rectifier current (at voltages positive of the reversal potential) but it did not elicit inward current or inhibit inward delayed rectifier current (at voltages negative of the reversal potential).

7 These experiments indicate that (-)Ckm-activated K channels are more sensitive to inhibition by Ba^{2+} and Zn^{2+} and pass inward Rb^+ current less well than delayed rectifier K channels. They also suggest that (-)Ckm does not modulate delayed rectifier K channels directly or via an intermediate protein but that the inhibitory effect of (-)Ckm on $I_{K(DR)}$ arises as a consequence of K^+-flux through (-)Ckm-activated K channels.

Keywords: Levcromakalim; smooth muscle; K channel

Introduction

Levcromakalim and other K channel opener drugs are potent activators of K channels in smooth muscle cells (Hamilton *et al.*, 1986; Beech & Bolton, 1989a; reviewed by Edwards & Weston, 1993a). The target channel has a small conductance and is related to the ATP-sensitive K channels of other cell types (Kajioka *et al.*, 1991). It is notable for its apparent requirement for intracellular nucleoside diphosphates in order to open and for it sensitivity to inhibition by nanomolar concentrations of glibenclamide (Kajioka *et al.*, 1991; Beech *et al.*, 1993a,b). An additional effect of levcromakalim, acting in the same concentration range, is *inhibition* of delayed rectifier K-current (Beech & Bolton, 1989a; Edwards *et al.*, 1993). The effect also occurs with other K channel opener drugs (Ibbotson *et al.*, 1993a) and has been observed in ventricular myocytes (Heath & Terrar, 1994) and in an insulinoma cell line (Edwards & Weston, 1993b). It is of importance for our understanding of the mechanism of action of levcromakalim because it is the foundation of the 'conversion hypothesis' which proposes that levcromakalim- and ATP-sensitive K channels are modulated states of a delayed rectifier K channel (Edwards *et al.*, 1993; Edwards & Weston, 1993b; Ibbotson *et al.*, 1993b); inhibition of delayed rectifier K-current occurring as delayed rectifier K channels are shifted into a voltage-independent gating mode. If conversion does not occur the implication would appear to be that K channel opener drugs activate a regulatory protein which activates ATP-sensitive K channels and inhibits delayed rectifier K channels.

If the 'conversion hypothesis' is true, it might be expected that levcromakalim-induced and delayed rectifier K-currents would be affected similarly by substances which block K channels and indeed this is true for 4-aminopyridine, quinidine and phencyclidine (Beech & Bolton, 1989a). In this study we have extended this approach, investigating the effects of Ba^{2+}, Zn^{2+} and Rb^+, cations which might be expected to interact in or near K channel pore regions (Armstrong *et al.*, 1982; Gilly & Armstrong, 1982; Kwok & Kass, 1993; see also Hille, 1992). As a result we have found marked differences in the properties of the levcromakalim-induced and delayed rectifier K-currents. We then used this information to investigate the mechanism underlying the effect of levcromakalim on the delayed rectifier and suggest an explanation where there is no direct action of levcromakalim (or a binding protein) on delayed rectifier K channels.

Methods

Male guinea-pigs (350-400 g) were killed by cervical dislocation followed by exsanguination. Longitudinal muscle was removed from the ileum and jejunum by peeling it off in 1 cm

[1] Author for correspondence.

lengths and placing it immediately in Hanks solution containing (mM): NaCl 137, NaH_2PO_4 0.34, KCl 5.4, K_2HPO_4 0.44, glucose 8, HEPES 5, $CaCl_2$ 0.01 and titrated to pH 7.4 with NaOH. Four pieces of muscle (length = 2–4 mm) were then transferred into Hanks solution at 37°C for 10 min before being resuspended in a mixture of collagenase (0.4 mg ml^{-1}) and pronase (0.24–0.4 mg ml^{-1}) in Hanks solution for 20 min at 37°C. At the end of this period, the tissues were cleaned of the enzyme mixture by washing in Hanks solution and single cells were isolated by gentle trituration. Cells were stored at 2°C and used within 10 h.

Recordings were made using the whole-cell configuration of the patch-clamp technique (Hamill *et al.*, 1981) at room temperature (20–25°C). Patch pipettes were made from borosilicate glass (Clark Electromedical Instruments: o.d. 1.5 mm, i.d. 0.86 mm) and had resistances of 1–4 MΩ after fire-polishing. The patch-clamp amplifier was either an Axopatch-ID or an Axopatch-200A (Axon Instruments, Inc.) and data were captured to a 386 or 486 PC after digitization by a CED 1401 or a 1401 plus (Cambridge Electronic Design Ltd.). Currents were filtered at 0.5–1 kHz using a Bessel filter. Voltage-clamp command paradigms and data analysis were performed using CED software and Origin 2.8 (MicroCal Inc, Northampton, MA, U.S.A.). Results are expressed as mean ± s.e.mean. Statistical comparisons were made using the Students *t* test.

Solutions (Table 1) were titrated to pH 7.4 using NaOH (bath solutions) or KOH (pipette solution). Na_2ATP (1 mM) was added to the pipette solution and the pH re-titrated to pH 7.4. It was then filtered (pore size 0.2 μm; Gelman Sciences) and frozen in aliquots at − 18°C. Salts were purchased from either BDH, Sigma or Aldrich. EGTA (ethylene glycol-*bis*(β-aminoethyl ether) *N,N,N',N'*-tetraacetic acid), HEPES (N-2-hydroxy-ethylpiperazine-*N'*-2-ethanesulphonic acid) and glibenclamide were purchased from Sigma. Glibenclamide and levcromakalim were prepared as 10 or 100 mM stocks in dimethylsulphoxide (DMSO). The final concentration of DMSO was ≤ 0.1% for all experiments. Levcromakalim ((-)Ckm) was a generous gift from Dr T.C. Hamilton (SKB). Junction potentials between bath and

Table 1 Composition of solutions (mM; A-E are bath solutions)

	NaCl	*KCl*	*RbCl*	*$CaCl_2$*	*$MgCl_2$*	*$CdCl_2$*	*Glucose*	*HEPES*	*EGTA*	*pH*
A	130	5	0	1.5	1.2	0.1	8	10	0	7.4
B	110	25	0	1.5	1.2	0.1	8	10	0	7.4
C	110	0	25	1.5	1.2	0.1	8	10	0	7.4
D	0	135	0	1.5	1.2	0.1	8	10	0	7.4
E	0	0	135	1.5	1.2	0.1	8	10	0	7.4
Pipette	0	130	0	0	2	0	0	10	10	7.4

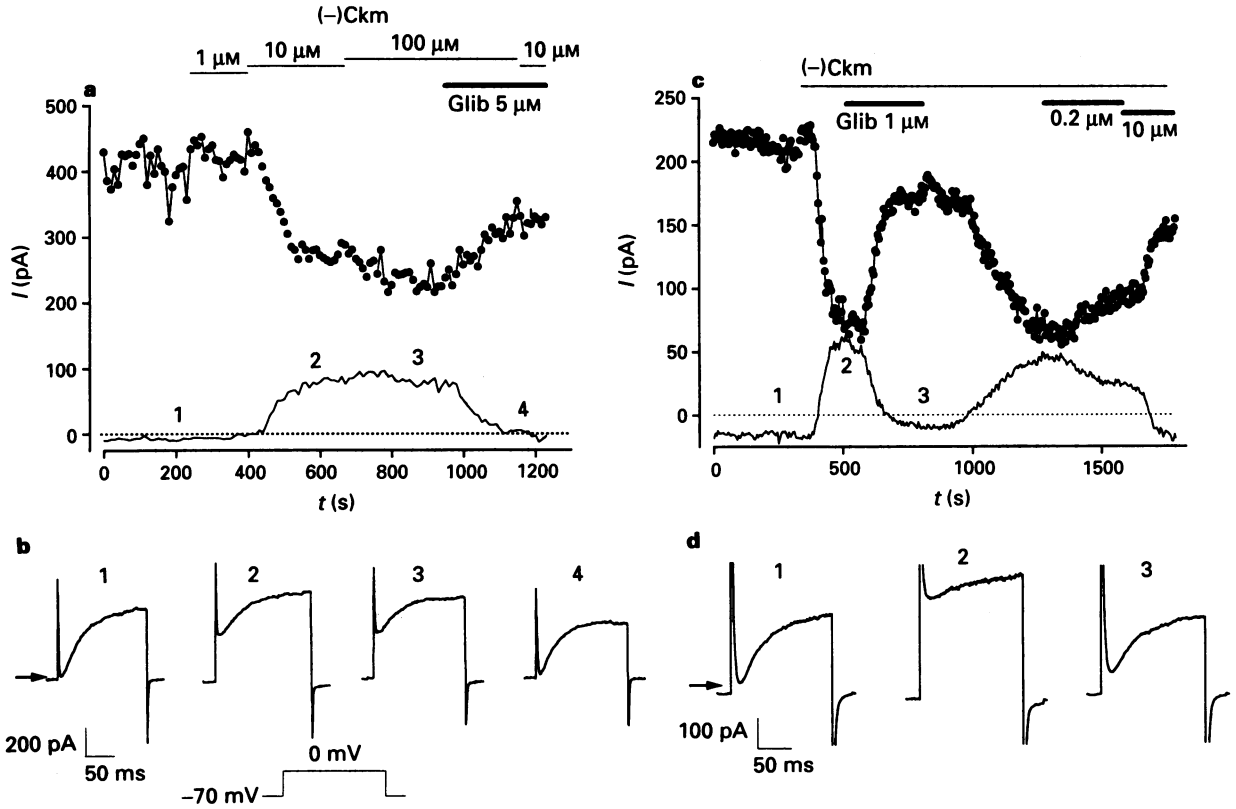


Figure 1 Induction of $I_{K(-Ckm)}$ and inhibition of $I_{K(DR)}$; whole-cell currents were recorded from cells bathed in solution A. (a) Plotted are the amplitudes of $I_{K(DR)}$ (●—●, upper record) and the absolute current value at − 40 mV (continuous record). Levcromakalim ((-)Ckm, 10 μM) induced $I_{K(-Ckm)}$ and inhibited $I_{K(DR)}$, and both effects were reduced by glibenclamide. $I_{K(DR)}$ was elicited by 150 ms depolarizing steps to 0 mV from a holding potential of − 70 mV every 10 s. $I_{K(-Ckm)}$ was the additional current occurring in response to (-)Ckm during 150 ms voltage steps to − 40 mV applied every 10 s. (b) Examples of actual currents (1–4). The arrow marks zero current. (c) Plotted are the amplitudes of $I_{K(DR)}$ (●—●, upper record) and the absolute current value at − 40 mV (continuous record) in the presence of (-)Ckm (10 μM) and various concentrations of glibenclamide (0.2–10 μM). Currents were measured as described in (a). (d) The single currents shown (1–3) are taken from the points marked in the plot. In this experiment 1 mM GDP was included in the pipette solution.

pipette solutions were measured using a 3 M KCl reference electrode and were $\leqslant 3$ mV; correction for these potentials was not made. Substances were applied using a bath-perfusion system. The bath volume was $\cong 150$ µl and the flow rate through it $\cong 4$ ml min^{-1}. The solutions in the bath were fully exchanged in <1 min.

Results

Inhibition of delayed rectifier K-current by (-)Ckm

In these experiments, delayed rectifier K-current ($I_{K(DR)}$) was defined as the time-dependent current that developed during a square depolarizing step from the holding potential (− 70 mV or − 80 mV) to − 30 mV or more positive. (-)-Ckm-induced K-current ($I_{K(-Ckm)}$) is not voltage-activated (Beech & Bolton, 1989a) and was measured (for example) during a step from − 70 mV to − 40 mV, or at a constant depolarized holding potential at which delayed rectifier K channels were inactivated (positive of − 20 mV). The bath solution contained Cd^{2+}, which abolished Ca^{2+}-influx through voltage-gated Ca channels (Beech, 1993), and the recording pipette solution included 10 mM EGTA to buffer $[Ca^{2+}]_i$ to a low and stable level.

When $I_{K(-Ckm)}$ and $I_{K(DR)}$ were measured simultaneously a pronounced inhibition of $I_{K(DR)}$ was often observed to occur concomitantly with the induction of $I_{K(-Ckm)}$. Two of the clearest examples are shown in Figure 1. In the first experiment, increasing concentrations of (-)Ckm were bath-applied (Figure 1a,b): 10 µM (-)Ckm induced a $I_{K(-Ckm)}$ of 100 pA and a simultaneous reduction in $I_{K(DR)}$; 100 µM (-)Ckm caused no further change in either current. Glibenclamide (5 µM) abolished $I_{K(-Ckm)}$, and $I_{K(DR)}$ returned towards pre-(-)Ckm levels. The ability of glibenclamide to reverse both effects of (-)Ckm is seen better in Figure 1c,d. (-)Ckm (10 µM) induced 60 pA of $I_{K(-Ckm)}$ and a 145 pA reduction of $I_{K(DR)}$. Glibenclamide (1 µM) almost abolished $I_{K(-Ckm)}$ and $I_{K(DR)}$ increased by 100 pA, and after wash-out of glibenclamide $I_{K(-Ckm)}$ returned and $I_{K(DR)}$ declined again. A lower concentration of glibenclamide (200 nM) partially inhibited $I_{K(-Ckm)}$ and caused a small increase in $I_{K(DR)}$. Scaling and superimposing the amplitudes of $I_{K(-Ckm)}$ and $I_{K(DR)}$ showed that the two K-currents changed with exactly the same time-course (not shown). It has been shown previously that glibenclamide ($\leqslant 10$ µM) has no effect on holding current at − 40 mV or on $I_{K(DR)}$ in the absence of (-)Ckm (Beech *et al.*, 1993a,b). It appears from Figure 1 that glibenclamide did not completely reverse the effect of (-)Ckm on $I_{K(DR)}$. We cannot, however, exclude the possibility that this small glibenclamide-insensitive effect was explained by run-down of $I_{K(DR)}$, which occurred gradually in several experiments.

In some recordings $I_{K(-Ckm)}$ was induced and yet there was no change in $I_{K(DR)}$ (e.g. Figure 2a,b). To express the variability of the effect of (-)Ckm and to look for a correlation between its two effects the amplitude of the reduction of $I_{K(DR)}$ was plotted against the amplitude of $I_{K(-Ckm)}$ for cells where the two currents were recorded simultaneously (Figure 2c). There was no correlation between the two effects and $I_{K(DR)}$ was never inhibited unless $I_{K(-Ckm)}$ occurred.

Effects of Ba^{2+}

Ba^{2+} inhibits (-)Ckm-induced $^{86}Rb^+$-flux with an IC_{50} of 30 µM (Quast, 1993). We compared the effects of bath-applied Ba^{2+} on $I_{K(-Ckm)}$ and $I_{K(DR)}$ (Figure 3). In Figure 3a the absolute amplitude of current at − 40 mV is plotted and $I_{K(-Ckm)}$ was about 70 pA. The addition of 0.02 mM Ba^{2+} had little effect but 0.2 mM Ba^{2+} caused about a 25 pA decline in outward current and 2 mM Ba^{2+} a further 35 pA reduction; 5 µM glibenclamide had only a slight additional effect. In control experiments Ba^{2+} was shown to have no effect on holding current in the absence of (-)Ckm (note also Figure 3c,d). The IC_{50} for the effect of Ba^{2+} on $I_{K(-Ckm)}$ at − 40 mV was 0.2 mM (Figure 3b). The effect of Ba^{2+} on $I_{K(-Ckm)}$ was voltage-dependent, as might be predicted from work on ATP-sensitive K channels in skeletal muscle (Quayle *et al.*, 1988). At a constant holding potential of 0 mV, 2 mM Ba^{2+} inhibited $I_{K(-Ckm)}$ by 26 ± 7% ($n = 5$). To allow a direct comparison with $I_{K(DR)}$ (which is elicited by depolarizations positive of − 40 mV) we also determined the sensitivity of $I_{K(-Ckm)}$ to block of 2 mM Ba^{2+} at − 30 mV and found 71 ± 6% inhibition ($n = 4$). Figure 3c,d shows examples of $I_{K(DR)}$ elicited by depolarizing to − 30 mV or 0 mV in the absence and presence of 2 mM Ba^{2+}. Ba^{2+} had little effect, slightly increasing the peak amplitude of $I_{K(DR)}$ elicited by depolarizing to − 30 mV (3 ± 3% increase, $n = 6$) or 0 mV (6 ± 3% increase, $n = 5$). In some of these cells, Ba^{2+} slowed the rate of activation of $I_{K(DR)}$ but the mean time constant of a single exponential fitted to the activation time-course at 0 mV was not significantly affected (37 ± 6 ms compared with 60 ± 15 ms, $P > 0.05$, $n = 6$). Thus, Ba^{2+} can strongly inhibit $I_{K(-Ckm)}$ while having little effect on $I_{K(DR)}$.

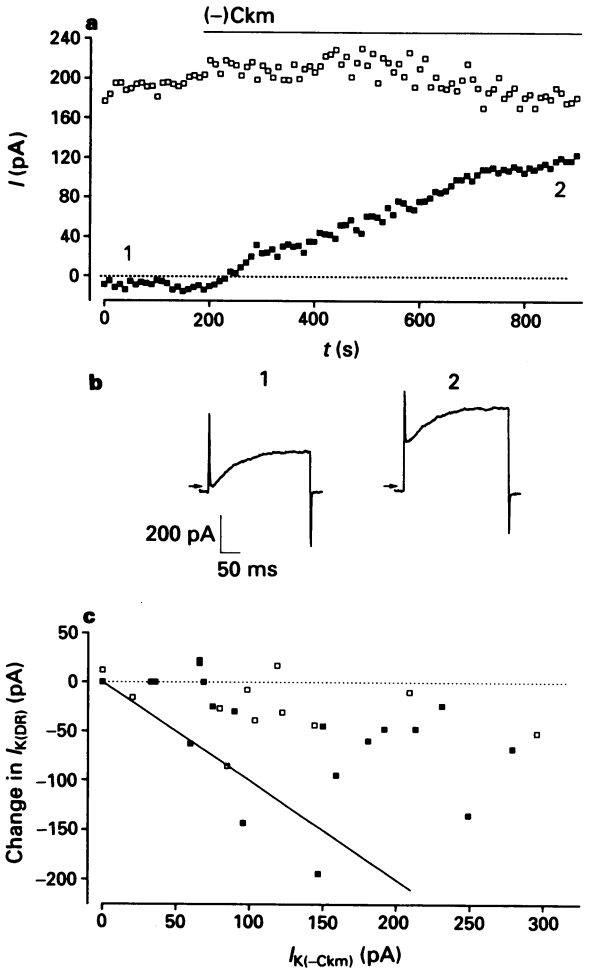


Figure 2 Relationship between the induction of $I_{K(-Ckm)}$ and the effects of levcromakalim ((-)Ckm) on $I_{K(DR)}$. Solution A was in the bath. (a) Example of a cell where $I_{K(-Ckm)}$ was induced by (-)Ckm (10 µM) but where there was no effect on $I_{K(DR)}$. $I_{K(DR)}$ was elicited by 250 ms depolarizing steps to 0 mV from a holding potential of − 70 mV every 10 s (□) and $I_{K(-Ckm)}$ (■) was assessed as in Figure 1(a). Actual currents are shown in (b). (c) Data points for 30 cells to which (-)Ckm (10 µM) was bath-applied. $I_{K(DR)}$ was elicited by 150 or 250 ms depolarizing steps applied every 10 s from a holding potential of − 70 mV to − 20 mV (□) or 0 mV (■). $I_{K(-Ckm)}$ was recorded at − 40 mV in all cases but the amplitude plotted has been multiplied by 3 for the 0 mV data or by 1.7 for the − 20 mV data (from Figure 2b in Beech & Bolton, 1989a). The line is the relationship if, for example, induction of 50 pA of $I_{K(-Ckm)}$ gave a 50 pA loss of $I_{K(DR)}$.

Effects of Zn^{2+}

Low concentrations of Zn^{2+} inhibit ATP-sensitive K-current but not delayed rectifier K-current in cardiac myocytes (Kwok & Kass, 1993). We have compared the effects of Zn^{2+} on $I_{K(-Ckm)}$ and $I_{K(DR)}$ (Figure 4). Kwok & Kass (1993) also showed that Cd^{2+} was a potent blocker of ATP-sensitive K channels in cardiac myocytes. However, we have found no effect of 100 μM Cd^{2+} on $I_{K(-Ckm)}$; in fact, all experiments were in the presence of 100 μM Cd^{2+} (Table 1). Zn^{2+} was a more potent blocker of $I_{K(-Ckm)}$ than Ba^{2+}, 40 μM Zn^{2+} caused an 85 ± 5% ($n = 4$) reduction of $I_{K(-Ckm)}$ at − 30 mV (e.g. Figure 4a). In contrast, 40 μM Zn^{2+} had only a small effect on $I_{K(DR)}$ elicited by depolarizing to − 30 mV (10 ± 3% reduction, $n = 4$) or 0 mV (5 ± 4% reduction, $n = 4$) (e.g. Figure 4b–d). Thus Zn^{2+}, like Ba^{2+}, has a more potent inhibitory effect on $I_{K(-Ckm)}$ than $I_{K(DR)}$.

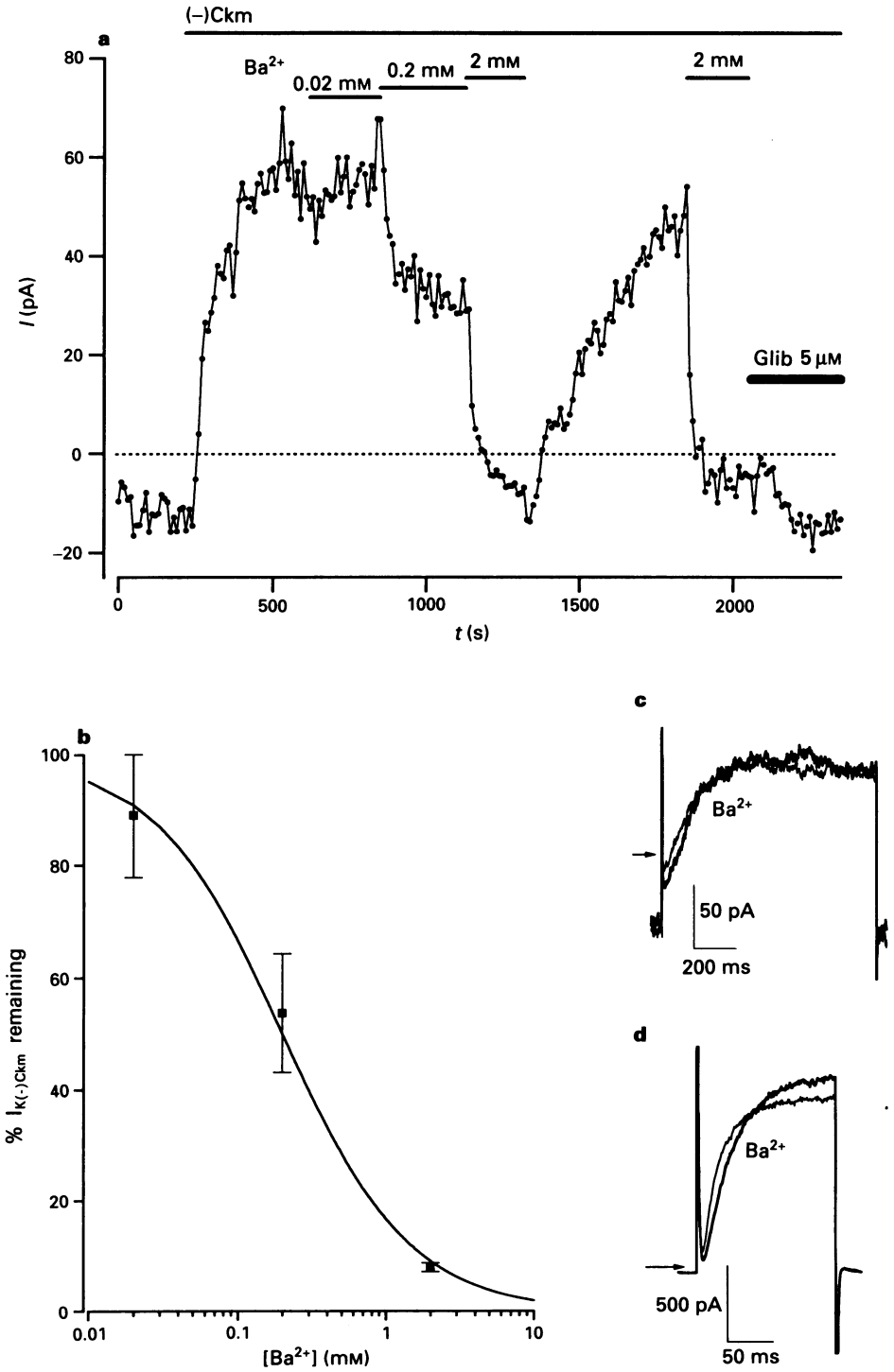


Figure 3 Effect of Ba^{2+}. Solution A was in the bath. (a) Plot of the amplitude of current at − 40 mV, showing the effect of several concentrations of Ba^{2+} on $I_{K(-Ckm)}$, which was induced by bath-applied levcromakalim ((-)Ckm, 10 μM). (b) Plotted is the mean percentage of $I_{K(-Ckm)}$ remaining in the presence of 0.02, 0.2 and 2 mM Ba^{2+} ($n = 4$–6). The curve is the Hill equation with a slope of 1, fitted by a least-squares method. The mid-point (IC_{50}) is at 0.2 mM. (c,d) The effect of Ba^{2+} on $I_{K(DR)}$. $I_{K(DR)}$ was elicited by: (c) 1 s steps to − 30 mV from a holding potential of − 80 mV; (d) 200 ms steps to 0 mV from − 70 mV. Example current records are shown for before and once 2 mM Ba^{2+} had been bath-applied.

Current carried by Rb^+

The amplitudes of inward K^+ currents were compared with inward Rb^+ currents through (-)Ckm-activated and delayed rectifier K channels. When the NaCl in the bath solution was replaced with KCl $I_{K(-Ckm)}$ was inward at voltages negative to 0 mV and averaged -298 ± 1 pA at -120 mV ($n = 3$). However, when K^+ was replaced by 135 mM Rb^+ in the same cells $I_{Rb(-Ckm)}$ averaged only -12 ± 1 pA ($n = 3$), giving $I_{Rb(-Ckm)}/I_{K(-Ckm)} \cong 0.04$ (e.g. Figure 5a). In contrast, delayed rectifier K channels allowed a large inward Rb^+-current (Figure 5b). Depolarizing from a holding potential of -70 mV to -20 mV in 135 mM K^+ gave an average $I_{K(DR)}$ of -212 ± 95 pA and changing to 135 mM Rb^+ gave an $I_{Rb(DR)}$ of -427 ± 129 pA ($n = 3$), leading to an $I_{Rb(DR)}/I_{K(DR)}$ of 2.0. In the same cells, depolarizing from a holding potential of -70 mV to -10 mV gave $I_{Rb(DR)}/I_{K(DR)}$ as 1.2. It also appeared that exchanging K^+ for Rb^+ may have caused the activation curve for delayed rectifier K channels to shift to more negative voltages (Figure 5b) but this phenomenon was not investigated further. From these experiments it was apparent that delayed rectifier K channels passed inward Rb^+-current much better than (-)Ckm-activated K channels.

No effect on $I_{K(DR)}$ when current through (-)Ckm-activated channels is blocked

As 2 mM Ba^{2+} almost abolished $I_{K(-Ckm)}$ and yet had little effect on $I_{K(DR)}$ we tried to investigate the effect of (-)Ckm on $I_{K(DR)}$ in the absence of contaminating $I_{K(-Ckm)}$ by working in the presence of 2 mM Ba^{2+}. However, under this condition a distinct effect of (-)Ckm (10 or 100 μM) on $I_{K(DR)}$ was never observed; a mean inhibition of $5 \pm 2\%$ was measured ($n = 7$). Similarly, if we measured inward delayed rectifier current in the presence of 135 mM extracellular Rb^+, (-)Ckm (10 or 100 μM) again had no distinct effect; a mean inhibition of $3 \pm 2\%$ was measured ($n = 4$). We, therefore, investigated if the effect of (-)Ckm on $I_{K(DR)}$ might occur simply because there was K^+-flux through (-)Ckm-activated K channels.

By experimenting with 25 mM RbCl extracellularly and 130 mM KCl in the pipette solution we were able to induce an outward current with (-)Ckm at voltages positive of -40 mV but little or no inward current at voltages negative of -40 mV. Outward and inward delayed rectifier currents were, however, observed. (We chose to record in the presence of 25 mM Rb^+ rather than 135 mM Rb^+ because the outward current induced by (-)Ckm was larger). Measurement of the amplitudes of outward and inward delayed rectifier currents before and during the response to (-)Ckm (Figure 6a,b) revealed that the outward delayed rectifier current (labelled 1 in Figure 6a) was reduced in 6 experiments by $19 \pm 5\%$ as outward (-)Ckm-induced current (labelled 2) occurred (96 ± 25 pA at -15 mV). In contrast, there was little effect on inward delayed rectifier current ($2.5 \pm 1\%$ reduction; labelled 4) and induced inward current was small (0 pA at -65 mV and -4 ± 2 pA at -80 mV, $n = 6$). When recording with 25 mM K^+ extracellularly, (-)Ckm (10 μM) inhibited inward delayed rectifier current ($34 \pm 9\%$ reduction; compare, for example, the current traces labelled 'control' and 'Ckm (DR only)' in Figure 6d) and induced inward current

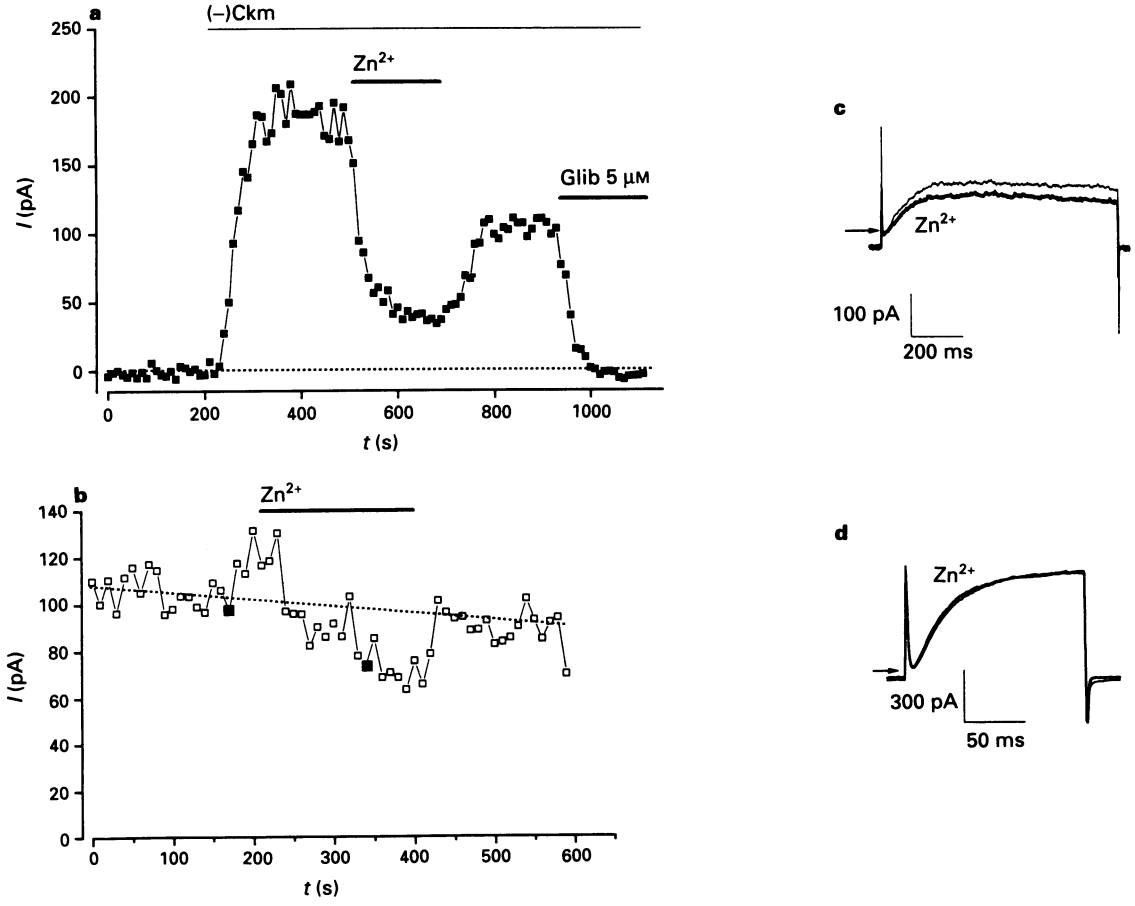


Figure 4 Effect of Zn^{2+}. Solution A was in the bath. (a) Plot of current sampled every 10 s at a holding potential of -30 mV showing inhibition by Zn^{2+} of $I_{K(-Ckm)}$. Levcromakalim ((-)Ckm) was bath-applied at 10 μM. (b) The effect of Zn^{2+} on $I_{K(DR)}$. Plotted is the amplitude of $I_{K(DR)}$ elicited by 1 s-steps to -30 mV from a holding potential of -80 mV in the absence and presence of Zn^{2+} (40 μM). The dotted line describes our estimate of the time-course of run-down of the delayed rectifier, and the filled symbols indicate the points at which sample traces were taken for (c). (d) In another cell, currents elicited by steps to 0 mV from a holding potential of -70 mV in the absence and presence of Zn^{2+} (40 μM).

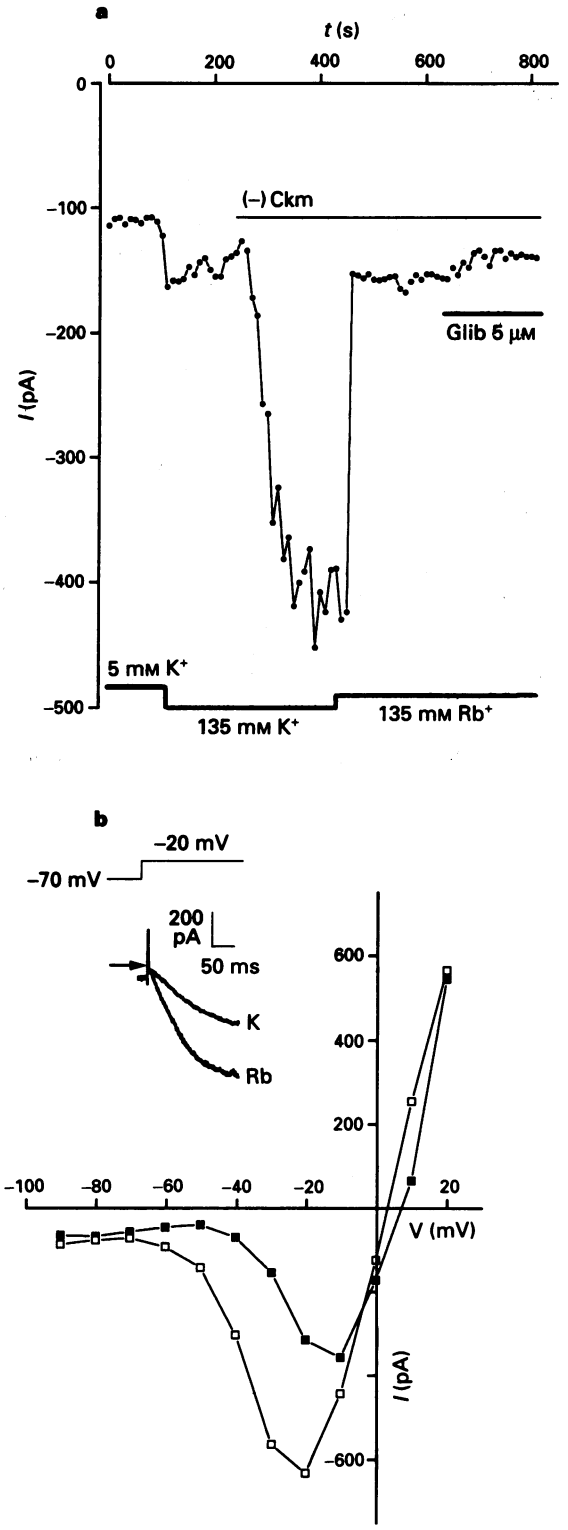


Figure 5 Inward K^+-current and Rb^+-current through levcromakalim ((-)Ckm)-activated K channels and delayed rectifier K channels. (a) Inward currents elicited by bath-applied (-)Ckm (10 μM) in the presence of 135 mM K^+ (solution D) or 135 mM Rb^+ (solution E). Ramp changes in potential from − 40 mV to − 120 mV (duration 400 ms) were applied every 10 s and the current amplitude at − 120 mV is plotted. (b) Plot of the amplitude of current at the end of a 200 ms test step from the holding potential of − 70 mV (without subtraction of leak current) in the presence of 135 mM K^+ (■) and then 135 mM Rb^+ (□). Actual currents are inset for the − 20 mV test potential (the arrow indicates zero current). The slightly positive reversal potential in (b) cannot be explained solely by a junction potential as all junction potentials were measured as ≤ 3 mV (see Methods). It is plausible, however, that a Donnan equilibrium potential could contribute to the effect.

(− 98 ± 16 pA at − 65 mV and − 140 ± 21 pA at − 80 mV, $n = 3$). An example is shown in Figure 6c,d. Thus, (-)Ckm inhibited delayed rectifier current only when (-)Ckm-induced current was flowing in the same direction.

Discussion

In these guinea-pig intestinal smooth muscle cells we have been able to demonstrate that, as in portal vein cells (Beech & Bolton, 1989a; Ibbotson *et al.*, 1993b), (-)Ckm does inhibit delayed rectifier K-current ($I_{K(DR)}$) via a glibenclamide-sensitive mechanism. A hypothesis which explains this effect is that (-)Ckm converts delayed rectifier K channels from a voltage-dependent to a voltage-independent gating mode. If this were true it might be expected that both $I_{K(-Ckm)}$ and $I_{K(DR)}$ would be similarly sensitive to inhibition by Ba^{2+} and Zn^{2+} and that both could be carried equally well by Rb^+ instead of K^+. However, in this study we have shown that $I_{K(-Ckm)}$ can be strongly inhibited by concentrations of Ba^{2+} or Zn^{2+} that have little or no effect on $I_{K(DR)}$, and although $I_{Rb(DR)}$ was larger than $I_{K(DR)}$, $I_{Rb(-Ckm)}$ was only 4% of $I_{K(-Ckm)}$. In addition, we have used these effects of cations to show that (-)Ckm inhibits $I_{K(DR)}$ only when there is K^+-flux through (-)Ckm-activated K channels and consequently suggest there is no direct effect of (-)Ckm or a (-)Ckm-binding protein on delayed rectifier K channels.

A number of observations indicate that (-)Ckm only inhibits $I_{K(DR)}$ when it can induce K^+-current. The strongest evidence for this was found when we observed outward and inward delayed rectifier currents but only outward (-)Ckm-induced current (Figure 6). (-)Ckm inhibited delayed rectifier current only when there was (-)Ckm-induced current in the same direction. Other observations are also consistent with the view that it was K^+-flux through (-)Ckm-activated K channels which caused the reduction in $I_{K(DR)}$. (-)Ckm had no effect on delayed rectifier current when (-)Ckm-induced current was prevented with Ba^{2+} or Rb^+, and $I_{K(DR)}$ was never inhibited unless $I_{K(-Ckm)}$ was induced. In an insulinoma cell line, margatoxin had no effect on $I_{K(DR)}$ but it did inhibit $I_{K(-Ckm)}$ and the ability of (-)Ckm to inhibit $I_{K(DR)}$ (Edwards & Weston, 1993b). When intracellular Mg^{2+} levels were very low, (-)Ckm did not induce K-current (Beech *et al.*, 1993b) or inhibit $I_{K(DR)}$ (Edwards *et al.*, 1993). Both $I_{K(DR)}$ and A-type K-current were inhibited by KCO drugs in rat portal vein smooth muscle cells (Ibbotson *et al.*, 1993a; Figure 1), suggesting activation of a non-specific mechanism. (-)Ckm 100 μM did not induce K^+-current or inhibit delayed rectifier K^+-current in defolliculated *Xenopus* oocytes expressing the delayed rectifier K channel protein *drk1* (D.J. Beech, unpublished observation). Lastly, the ability of glibenclamide to prevent the actions of (-)Ckm on $I_{K(DR)}$ also supports the hypothesis because it can be explained simply by closure of (-)Ckm-activated K channels.

A reasonable explanation for why K^+-flux through (-)Ckm-activated K channels reduced $I_{K(DR)}$ would seem to be that the flux caused the K^+ concentration in the vicinity of delayed rectifier K channels to deviate from that of the bulk solution so that the driving force on K^+ was reduced, and perhaps also so that the conductance of the channels was reduced. A rough estimate of what the change in local $[K^+]$ might have been can be gained from a mathematical reconstruction of $I_{K(DR)}$ and $I_{K(-Ckm)}$ (from Hodgkin & Huxley, 1952). By this approach we found that the (-)Ckm-induced reduction in outward delayed rectifier K-current at − 15 mV shown in Figure 6d could be described well if an effective K^+-equilibrium potential of − 25 mV was assumed, a value 18 mV depolarized of the calculated K^+-equilibrium potential for the bulk solutions. If local $[K^+]_o$ and $[K^+]_i$ changed equally then the effective $[K^+]_o/[K^+]_i$ would become 44.5 mM/120.5 mM, but if only $[K^+]_i$ was depleted (see below) then $[K^+]_o/[K^+]_i$ would become 25 mM/67 mM.

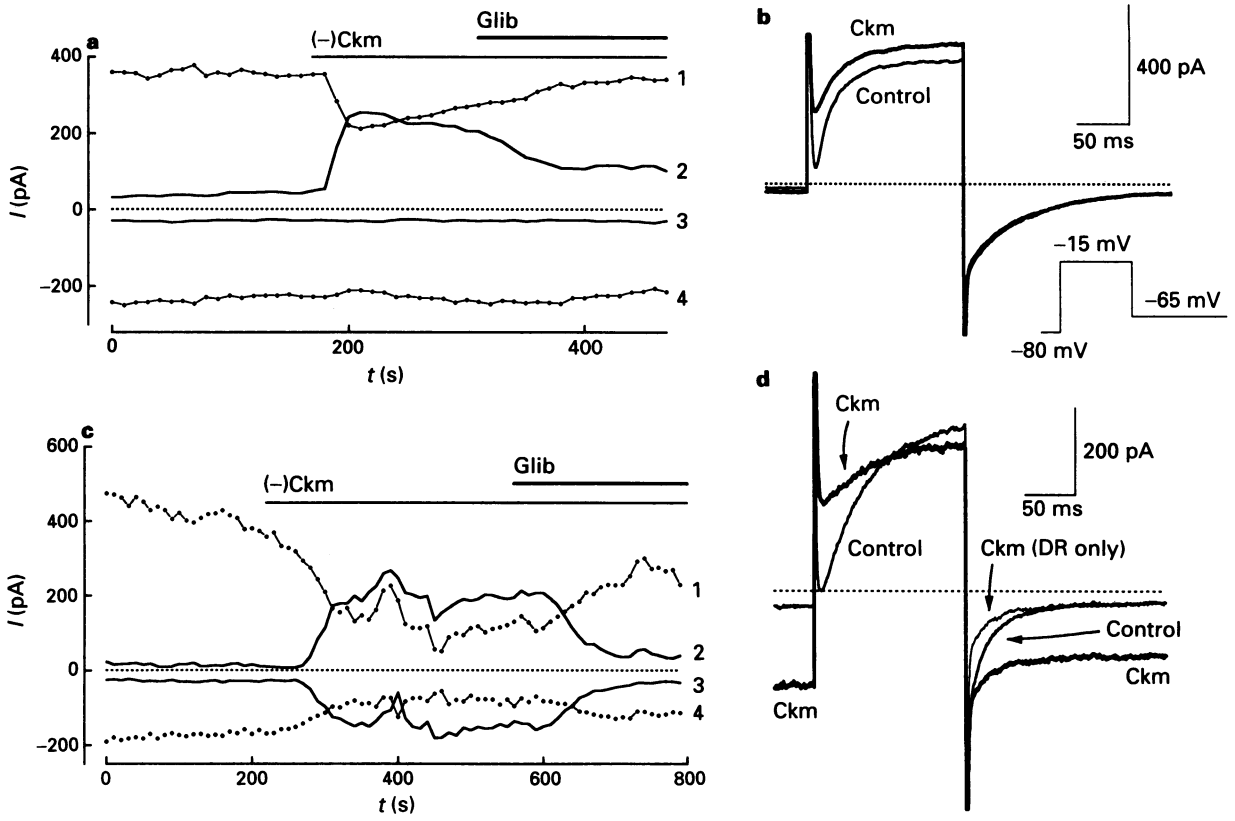


Figure 6 Dependence on K^+-flux. In the upper part (a, b) bath solution C (25 mM Rb^+) was used, and in the lower part (c, d) bath solution B (25 mM K^+) was used. In both (a) and (c) there are plots against time of the amplitude of delayed rectifier current at − 15 mV (outward current, 1) and − 65 mV (inward current, 4). Delayed rectifier current was defined as the difference between the current measured 10 ms after the start of the voltage step to − 15 mV (1) or − 65 mV (4) and that at the end of the voltage step. Also plotted is the amplitude of the quasi-instantaneous current on depolarization to − 15 mV (2), which was defined as the 'dip point' once the capacity current had decayed but before delayed rectifier current was appreciably activated (see b and d), and the steady-state current occurring on repolarization to − 65 mV (3). In all cases points were sampled every 10 s but for plots 2 and 3 the data points have been joined by lines so that a continuous record is apparent. Levcromakalim ((-)Ckm 10 μM) and glibenclamide (1 μM) were bath-applied to both cells as marked by the horizontal bars. (b) A diagram of the voltage protocol and examples of actual currents for the Rb^+ experiment shown in (a): before the application of (-)Ckm (thin line) and in the presence of (-)Ckm but not glibenclamide (thick line). (d) examples of actual currents for the K^+ experiment shown in (c): before the application of (-)Ckm (thin line) and in the presence of (-)Ckm but not glibenclamide (thick line). In (d) a modified version of the 'Ckm' current trace has been superimposed for the period at − 65 mV (but not − 80 mV and − 15 mV). This trace has been labelled 'Ckm (DR only)' because the steady-state current in the presence of (-)Ckm at − 65 mV has been subtracted, leaving only delayed rectifier (DR) current. Note especially from this figure that when the bath solution contained 25 mM Rb^+, (-)Ckm induced outward but not inward current (labelled 2 and 3 respectively in (a)) and inhibited outward but not inward delayed rectifier current (labelled 1 and 4 respectively in (a)). Both inward and outward currents were affected when the bath solution contained 25 mM K^+.

When considering a K^+ accumulation-depletion hypothesis it might be expected that a correlation should exist between the amplitude of $I_{K(\text{-Ckm})}$ and the amplitude of the inhibition of $I_{K(DR)}$. Although in an individual cell the inhibition of $I_{K(DR)}$ was proportional to the amplitude of $I_{K(\text{-Ckm})}$, comparing data from 30 different cells showed there was no correlation between the two effects (Figure 2c). If, however, the local $[K^+]$ change occurred because there was a structural feature in the cell that generated an 'unstirred layer' (see below) the volume and geometry of this layer could well vary between cells and so the degree of accumulation/depletion would vary. A second point to consider is that when the $[K^+]$ changes the reversal potential must also change. However, the change may not be readily detectable because any shift in reversal potential will be proportional to the amplitude of $I_{K(\text{-Ckm})}$ and as $I_{K(\text{-Ckm})}$ will be small in the region of the reversal potential little shift will occur. In addition, if the unstirred layers are small (see below), deviation from and re-equilibration with the bulk solution will be rapid as the amplitude of $I_{K(\text{-Ckm})}$ changes. We have not been able to detect a significant change in reversal potential as $I_{K(\text{-Ckm})}$ increases (unpublished observation; see also Beech *et al.*, 1993b), and the activation, deactivation and inactivation time-courses of $I_{K(DR)}$ are not altered when it is inhibited by (-)Ckm (Figures 1 and 6; analysis not shown; Beech & Bolton, 1989a).

Frankenhaeuser & Hodgkin (1956) considered the possibility that K^+ accumulated in an extracellular aqueous space between the membranes of the *Loligo* axon and the adjacent Schwann cells when repetitive action potentials were evoked. The accumulation and recovery rates were variable but they had time constants that ranged from 30–100 ms. It was predicted that the extracellular space had a thickness of 30 nm. A similar space may exist in single smooth muscle cells between the plasma and sarcoplasmic reticulum membranes. This intracellular space appears to have a thickness of 12–20 nm and it is fragmented (Somlyo & Franzini-Armstrong, 1985), in contrast to the continuous Frankenhaeuser-Hodgkin Space. The intracellular space in smooth muscle cells has previously been considered as a restriction to equilibration between ions in the bulk cytoplasm and those at the membrane by Chen *et al.* (1992) who have developed a 'superficial buffer barrier' hypothesis to explain intracellular Ca^{2+}-handling. If this intracellular space is also a barrier to K^+ movements the degree and rate at which accumulation occurs will depend on the complex geometry of the space and on the permeability of the sarcoplasmic reticulum membrane to K^+. Even without an intracellular space $[K^+]$ may change

sufficiently near an open (-)Ckm-activated K channel to affect current through a delayed rectifier K channel because ion channels can be very close to each other, within 8 nm (Gogol & Unwin, 1988). It has been proposed that this type of interaction occurs between voltage-gated Ca channels and Ca-activated K channels. Local changes in $[Ca^{2+}]$ are predicted to occur within 10–100 nm of open voltage-gated Ca channels and the changes develop and decline in the sub-millisecond time scale (Smith & Augustine, 1988; Roberts *et al.*, 1990). In smooth muscle cells, Ca^{2+}-activated K^+-current occurs in <20 ms when voltage-gated Ca channels open in response to a square depolarizing voltage step (Ohya *et al.*, 1987), and more detailed experiments on hair cells have shown that Ca^{2+}-influx through Ca channels can affect Ca-activated K channels within a millisecond (Roberts *et al.*, 1990).

The hypothesis that (-)Ckm acts by converting delayed rectifier K channels into a voltage-independent gating mode is based on several observations; (1) (-)Ckm simultaneously inhibits $I_{K(DR)}$ as it induces $I_{K(-Ckm)}$; (2) $I_{K(-Ckm)}$ and $I_{K(DR)}$ show similarities in their sensitivities to various K channel inhibitors, both are resistant to inhibition by charybdotoxin and apamin and both are inhibited by similar concentrations of 4-aminopyridine, quinidine, phencyclidine and nicardipine (Beech & Bolton, 1989a; S.G. Brown and D.J. Beech, unpublished observations); (3) (-)Ckm-activated channels and delayed rectifier channels have a similar unitary conductance, in the region of 5 to 20 pS with a near-physiological K^+-gradient (Beech & Bolton, 1989b; Boyle *et al.*, 1992; Volk & Shibata, 1993; Beech *et al.*, 1993b); (4) a protein kinase inhibitor and a dephosphorylating agent can induce K-current and inhibit $I_{K(DR)}$ (Edwards *et al.*, 1993). If our K^+-flux hypothesis is true, observations (1) and (4) can no longer be used to support the conversion hypothesis. Observation (2) is interesting but weakened by the findings that Ba^{2+}, Zn^{2+} and Rb^+ interact differently with (-)Ckm-activated K channels and delayed rectifier K channels. If the conversion hypothesis is not true the pharmacological similarities between $I_{K(-Ckm)}$ and $I_{K(DR)}$ may suggest structural similarities between the underlying channel proteins. If the conversion hypothesis is true (-)Ckm must not only modulate the gating of delayed rectifier channels but also increase their sensitivity to Ba^{2+} and Zn^{2+} and reduce their ability to pass Rb^+. The suggestion that the underlying channels have a similar unitary conductance (observation 3) requires further study because the conductances have not been compared under identical conditions. Finally, the conversion hypothesis is weakened by the data in Figure 2 because $I_{K(-Ckm)}$ can occur without loss of $I_{K(DR)}$ (see also Russell *et al.*, 1992). Thus, although initially attractive, the conversion hypothesis seems unlikely to be true.

(-)Ckm-like drugs act to open an ATP-sensitive K channel which, in smooth muscle cells, has been noted for its dependence on intracellular nucleotide diphosphates (Kajioka *et al.*, 1991; Beech *et al.*, 1993a,b; Kamouchi *et al.*, 1993; Zhang & Bolton, 1994). We suggest that this channel is distinct at a molecular level from K channels of the delayed rectifier type, and that (-)Ckm-like drugs (or a (-)Ckm-binding protein) do not interact directly with delayed rectifier K channels but instead, by inducing K^+-flux, cause the K^+ concentration in the vicinity of delayed rectifier K channels to deviate from that of the bulk solution in such a way that the driving force on K^+ ions is diminished. Primary sequence data for a rat heart K_{ATP} channel further establish a molecular distinction between delayed rectifier and K_{ATP} channels (Ashford *et al.*, 1994).

We are grateful for support from the Wellcome Trust and to Prof. D. Wray for the use of *Xenopus* oocyte recording equipment. We also thank Prof. B. Hille and Dr L. Wollmuth for advice, and Dr T. Hamilton (SKB) for the gift of levcromakalim.

References

ARMSTRONG, C.M., SWENSON, R.P. & TAYLOR, S.R. (1982). Block of squid axon K channels by internally and externally applied barium ions. *J. Gen. Physiol.*, **80**, 663–682.

ASHFORD, M.L.J., BOND, C.T., BLAIR, T.A. & ADELMAN, J.P. (1994). Cloning and functional expression of a rat heart K_{ATP} channel. *Nature*, **370**, 456–459.

BEECH, D.J. (1993). Inhibitory effects of histamine and bradykinin on calcium current in smooth muscle cells isolated from guinea-pig ileum. *J. Physiol.*, **463**, 565–583.

BEECH, D.J. & BOLTON, T.B. (1989a). Properties of the cromakalim-induced potassium conductance in smooth muscle cells isolated from the rabbit portal vein. *Br. J. Pharmacol.*, **98**, 851–864.

BEECH, D.J. & BOLTON, T.B. (1989b). Two components of potassium current activated by depolarization of single smooth muscle cells from the rabbit portal vein. *J. Physiol.*, **418**, 293–309.

BEECH, D.J., ZHANG, H.-L., NAKAO, K. & BOLTON, T.B. (1993a). K channel activation by nucleotide diphosphates and its inhibition by glibenclamide in vascular smooth muscle cells. *Br. J. Pharmacol.*, **110**, 573–582.

BEECH, D.J., ZHANG, H.-L., NAKAO, K. & BOLTON, T.B. (1993b). Single channel and whole-cell K-currents evoked by levcromakalim in smooth muscle cells from the rabbit portal vein. *Br. J. Pharmacol.*, **110**, 583–590.

BOYLE, J.P., TOMASIC, M. & KOTLIKOFF, M.I. (1992). Delayed rectifier potassium channels in canine and porcine airway smooth muscle cells. *J. Physiol.*, **447**, 329–350.

CHEN, Q., CANNELL, M. & VAN BREEMEN, C. (1992). The superficial buffer barrier in vascular smooth muscle. *Can. J. Physiol. Pharmacol.*, **70**, 509–514.

EDWARDS, G., IBBOTSON, T. & WESTON, A.H. (1993). Levcromakalim may induce a voltage-independent K-current by modifying the gating properties of the delayed rectifier. *Br. J. Pharmacol.*, **110**, 1037–1048.

EDWARDS, G. & WESTON, A.H. (1993a). The pharmacology of ATP-sensitive K-channels. *Annu. Rev. Pharmacol. Toxicol.*, **33**, 597–637.

EDWARDS, G. & WESTON, A.H. (1993b). Induction of a glibenclamide-sensitive K-current by modification of a delayed rectifier channel in rat portal vein and insulinoma cells. *Br. J. Pharmacol.*, **110**, 1280–1281.

FRANKENHAEUSER, B. & HODGKIN, A.L. (1956). The after-effects of impulses in the giant nerve fibres of *Loligo*. *J. Physiol.*, **131**, 341–376.

GILLY, W.F. & ARMSTRONG, C.M. (1982). Divalent cations and the activation kinetics of potassium channels in squid giant axon. *J. Gen. Physiol.*, **79**, 965–996.

GOGOL, E. & UNWIN, N. (1988). Organization of connexons in isolated rat liver gap junctions. *Biophys. J.*, **54**, 105–112.

HAMILL, O.P., MARTY, E., NEHER, B., SAKMANN, B. & SIGWORTH, F.J. (1981). Improved patch-clamp techniques for the high-resolution current recording from cells and cell-free membrane patches. *Pflügers Archiv.*, **391**, 85–100.

HAMILTON, T., WEIR, S. & WESTON, A.H. (1986). Comparison of the effects of BRL 34915 and verapamil on electrical and mechanical activity in rat portal vein. *Br. J. Pharmacol.*, **88**, 103–111.

HEATH, B.M. & TERRAR, D.A. (1994). Effect of glibenclamide, forskolin, and isoprenaline on the parallel activation of K_{ATP} and reduction of I_K by cromakalim in cardiac myocytes. *Cardiovasc. Res.*, **28**, 818–822.

HILLE, B. (1992). *Ionic Channels of Excitable Membranes*. Second Edition. U.S.A. Sinauer Assoc. Inc.

HODGKIN, A.L. & HUXLEY, A.F. (1952). A quantitative description of membrane current and its application to conduction and excitation in nerve. *J. Physiol.*, **117**, 500–544.

IBBOTSON, T., EDWARDS, G., NOACK, TH. & WESTON, A.H. (1993a). Effects of P1060 and aprikalim on whole-cell currents in rat portal vein; inhibition by glibenclamide and phentolamine. *Br. J. Pharmacol.*, **108**, 991–998.

IBBOTSON, T., EDWARDS, G., NOACK, TH. & WESTON, A.H. (1993b). Antagonism of levcromakalim by imidazoline- and guanidine-derivatives in rat portal vein: involvement of the delayed rectifier. *Br. J. Pharmacol.*, **110**, 1556–1564.

KAJIOKA, S., KITAMURA, K. & KURIYAMA, H. (1991). Guanosine diphosphate activates an adenosine 5'-triphosphate-sensitive K^+ channel in the rabbit portal vein. *J. Physiol.*, **444**, 397–418.

KAMOUCHI, M., KAJIOKA, S., SAKAI, T., KITAMURA, K. & KURIYAMA, H. (1993). A target channel for the LP-805-induced hyperpolarization in smooth muscle cells of the rabbit portal vein. *Naunyn-Schmied. Arch. Pharmacol.*, **347**, 329–335.

KWOK, W.-M. & KASS, R.S. (1993). Block of cardiac ATP-sensitive K^+ channels by external divalent cations is modulated by intracellular ATP. *J. Gen. Physiol.*, **102**, 693–712.

OHYA, Y., KITAMURA, K. & KURIYAMA, H. (1987). Cellular calcium regulates outward currents in rabbit intestinal smooth muscle cell. *Am. J. Physiol.*, **252**, C401–410.

QUAST, U. (1993). Do the K^+ channel openers relax smooth muscle by opening K channels? *Trends Pharmacol. Sci.*, **14**, 332–337.

QUAYLE, J.M., STANDEN, N.B. & STANFIELD, P.R. (1988). The voltage-dependent block of ATP-sensitive potassium channels of frog skeletal muscle by caesium and barium ions. *J. Physiol.*, **405**, 677–697.

ROBERTS, W.M., JACOBS, R.A. & HUDSPETH, A.J. (1990). Colocalisation of ion channels involved in frequency selectivity and synpatic transmission of presynaptic active zones of hair cells. *J. Neuroscience.* **10**, 3664–3684.

RUSSELL, S.N., SMIRNOV, S.V. & AARONSON, P.I. (1992). Effects of BRL 38227 on potassium currents in smooth muscle cells isolated from rabbit portal vein and human mesenteric artery. *Br. J. Pharmacol.*, **105**, 549–556.

SMITH, S.J. & AUGUSTINE, G.J. (1988). Calcium ions, active zones and synaptic transmitter release. *Trends Neurosci.*, **11**, 458–464.

SOMLYO, A.V. & FRANZINI-ARMSTRONG, C. (1985). New views of smooth muscle structure using freezing, deep-etching and rotary shadowing. *Experientia*, **41**, 841–856.

VOLK, K.A. & SHIBATA, E.F. (1993). Since delayed rectifier potassium channels from rabbit coronary artery myocytes. *Am. J. Physiol.*, **264**, H1146–1153.

ZHANG, H. & BOLTON, T.B. (1994). Intracellular GDP, metabolic inhibition and pinacidil activate glibenclamide-sensitive K-channels in smooth muscle of rat mesenteric artery. *Br. J. Pharmacol.*, **112**, 464P.

(Received June 15, 1994
Revised July 15, 1994
Accepted September 19, 1994)

British Journal of Pharmacology (1995) 114, 400–404 © 1995 Stockton Press All rights reserved 0007–1188/95 $9.00

Mediation by 5-hydroxytryptamine$_{2B}$ receptors of endothelium-dependent relaxation in rat jugular vein

Elizabeth S. Ellis, Clare Byrne, Olive E. Murphy, Nicholas S. Tilford & [1]Gordon S. Baxter

SmithKline Beecham Pharmaceuticals, New Frontiers Science Park, Third Avenue, Harlow, Essex CM19 5AD

1 An 'atypical' 5-HT$_2$ receptor which is located on the endothelium of rat jugular vein has been described. In the present study we have further defined the nature of the 5-HT$_2$ receptor subtype present in this preparation.

2 In experiments conducted in the presence of ketanserin to preclude involvement of 5-HT$_2$ receptors, the mixed 5-HT$_{2B/2C}$ antagonist, SB 200646, acted as an antagonist of 5-HT at the endothelial 5-HT receptor (pA$_2$ = 7.2). Yohimbine, which exhibits negligible affinity for rat 5-HT$_{2C}$ receptors but has high 5-HT$_{2B}$ receptor affinity, acted as a potent but non-surmountable antagonist (pA$_2 \geqslant 7.3$) in rat jugular vein. Neither yohimbine nor SB 200646 affected endothelium-dependent relaxations induced by carbachol.

3 Mianserin also acted as a surmountable antagonist (pA$_2$ = 7.3) and the 5-HT$_{2B}$ agonist, BW 723C86, acted as a potent partial agonist (pEC$_{50}$ [95% C L], intrinsic activity ± s.e.mean = 7.9 [7.6–8.3], 0.84 ± 0.04). Responses to BW 723C86 were antagonized by SB 200646 (0.3 μM) yielding an 'apparent' pA$_2$ [95% CL] of 7.03 [6.76–7.32].

4 These data are consistent with the presence of 5-HT$_{2B}$ receptors mediating endothelium-dependent relaxation of rat jugular vein.

Keywords: 5-HT$_{2B}$ receptors vascular endothelium SB 200646 BW 723C86

Introduction

Atypical 5-hydroxytryptamine (5-HT) receptors which mediate endothelium-dependent relaxation have been identified in a number of blood vessels. Whilst some have been classified as 5-HT$_1$-like (Schoeffter & Hoyer, 1990; Gupta, 1992), others may be tentatively classified as subtypes of the 5-HT$_2$ receptor family. Thus, endothelial 5-HT receptors mediating relaxation of rabbit jugular vein (Leff *et al.*, 1987), rat jugular vein (Bodelsson *et al.*, 1992), piglet vena cava (Sumner, 1991) and pig pulmonary artery (Glusa, 1992) share some pharmacological identity with both 5-HT$_{2B}$ (Wainscott *et al.*, 1993) and 5-HT$_{2C}$ (Hoyer *et al.*, 1989) receptors. It has been proposed that the endothelial 5-HT receptor in rat jugular vein and pig pulmonary artery represent the first examples of peripheral 5-HT$_{2C}$ receptors (Bodelsson *et al.*, 1992; Glusa, 1992). However, as 5-HT$_{2C}$ and 5-HT$_{2B}$ receptors possess close pharmacological similarity (see Baxter *et al.*, 1994) it is plausible that 5-HT$_{2B}$ receptors may be involved. In this regard, a close relationship between the 5-HT receptor in rat jugular vein and 5-HT$_{2B}$ receptors in rat stomach fundus was discounted only on the basis of a difference in the antagonist potency of mianserin (Bodelsson *et al.*, 1992).

We have recently demonstrated that a novel ligand, SB 200646 (N-1-methyl-5-indolyl)-*N'*-(3-pyridyl) urea HCl) exhibits moderate affinity for cloned rat 5-HT$_{2C}$ receptors and putative 5-HT$_{2B}$ receptors in rat stomach fundus, but little or no affinity for rat 5-HT$_{2A}$ and many other 5-HT receptors (Forbes *et al.*, 1993; Baxter *et al.*, 1994). In the present study we have used SB 200646 and a number of other ligands which may permit discrimination of 5-HT$_2$ receptor subtypes in the rat to characterize further 5-HT$_{2C}$-like receptors which mediate relaxation of the jugular vein in this species. A preliminary account of this work has been reported previously (Ellis *et al.*, 1994).

[1] Author for correspondence.

Methods

Rat jugular vein was set up as described by Bodelsson *et al.* (1992). Briefly, segments of the external sub-maxillary branch of the jugular vein were carefully removed from male Sprague Dawley rats (250–300 g) and placed in Krebs solution of the following composition (mM): NaCl 118, KCl 4.7, KH_2PO_4 1.2, $MgSO_4$ 1.2, glucose 11.1, $NaHCO_3$ 25, $CaCl_2$ 2.5 and indomethacin 0.003. Vessels were cleared of excess connective tissue and ring segments (5 mm long) were suspended, under a tension equivalent to 5 mN, between stainless steel wires (150 μm diameter) in oxygenated (95% O_2/5% CO_2) Krebs solution at 37°C. To expose relaxant responses to agonists, tone was induced in each preparation with the stable thromboxane-mimetic, U-46619 (0.1 μM). This concentration of U-46619 produced a contraction which was approximately 70% of the maximum response attainable with this agonist. In many preparations the responses to U-46619 were not well maintained and this interfered with the measurement of 5-HT-induced relaxation. For this reason, each preparation was challenged with U-46619 (0.1 μM) prior to construction of concentration-effect curves to determine their suitability. Any preparations which did not maintain a reasonably stable contractile response to U-46619, or upon which relaxant responses to 5-HT were ill defined, were not used. All experiments were conducted in the presence of ketanserin (0.1 μM) to prevent interactions of agonists at 5-HT$_{2A}$ receptors (Bodelsson *et al.*, 1992) and after exposure of tissues to pargyline (100 μM for 15 min followed by washout) to inhibit monoamine oxidase.

Agonist concentration-effect curves were fitted to the following equation using Kaleidagraph (Synergy Software) on an Apple Macintosh II Ci computer.

$$E = \frac{\alpha}{1 + (EC_{50}/[A])^n} \quad (1)$$

α, [A] and n represent the maximum response, agonist concentration and curve mid-point slope factor, respectively. The EC$_{50}$ is the concentration of agonist that produces 50% of the maximal response. On repetition, curves to 5-HT were

reproducible and EC_{50} location parameters differed by less than 2 fold. For this reason, correction factors were not routinely applied to account for changes in sensitivity between first and second concentration-effect curves.

Antagonist affinity

pA_2 values were calculated according to the method of Arunlakshana & Schild (1959). A single pA_2 value was obtained for each antagonist by plotting $-\log_{10}$ molar antagonist concentration against the $-\log_{10}$ of all of the concentration-ratios determined in individual experiments. Concentration-ratios were obtained by dividing the EC_{50} location parameter for the 2nd agonist concentration-effect curve by that for the 1st concentration-effect curve constructed in the presence and absence of antagonist respectively. Tissues were equilibrated with antagonists for 1 h before the construction of second concentration-effect curves.

Responses were recorded with Dynamometer UH1 isometric transducers coupled to a MACLAB/8 (AD instruments) recording system and Apple Macintosh II Ci computer.

Compounds used

5-Hydroxytryptamine (5-HT), carbachol HCl and yohimbine HCl were obtained from Sigma Chemical Company (Dorset). SB 200646 (N-1-methyl-5-indolyl-)*N'*-(3-pyridyl) urea HCl) and mianserin (racaemic) were synthesized at SmithKline Beecham Pharmaceuticals, Harlow, Essex. Sincere thanks to Dr Graeme Martin for supplying a sample of BW 72386 ([±]-1-[5-(2-thenyloxy)-1H-indol-3-yl]-propan-2-amine HCl).

Results

Mechanical removal of the endothelium, by rotating/sliding the vessel along a 200 μm o.d. stainless steel wire, abolished relaxant responses to both carbachol and 5-HT confirming the previously established endothelium-dependent nature of the relaxant response to both agonists in this preparation (Bodelsson *et al.*, 1992). In experiments where care was taken not to damage the endothelium, cumulative addition of 5-HT (0.1 nM–0.3 μM) caused concentration-dependent relaxations (Figure 1).

Whilst some inter-tissue variability was apparent, location parameters of 5-HT concentration-effect curves constructed in the same tissues were reproducible (pEC_{50} [95% CL] estimates of 8.6 [8.5–8.7], and 8.6 [8.4–8.7], $n = 22$ for control and repeat curves, respectively). SB 200646 (0.3–3.0 μM) and mianserin (0.1 and 0.3 μM) caused concentration-dependent rightward displacements of concentration-effect curves for 5-HT with no significant effect on maximum response (Figures 2 and 3). Schild regression analysis yielded pA_2 estimates of 7.2 for SB 200646 and 7.3 for mianserin (Figures 2 and 3). The slopes of the regression were 1.05 and 1.1, respectively, and were not significantly different from unity. In contrast, yohimbine acted as a non-surmountable antagonist, reducing the maximum response and causing a dextral displacement ± s.e.mean of concentration-effect curves for 5-HT by 1.6 ± 0.5, 14.9 ± 5 and 41.3 ± 13 fold at concentrations of 0.03, 0.1 and 0.3 μM respectively (Figure 4). The mean ± s.e.mean reduction is maximum response to 5-HT at these same concentrations were 11.8 ± 4.0, 22.6 ± 4.8 and 28.3 ± 8, respectively. These data are consistent with an apparent pA_2 for yohimbine of ≥ 7.3. Neither yohimbine (0.3 μM) nor SB 200646 (3 μM) antagonized responses to carbachol (Figure 5).

BW 723C86, which acts as a potent partial agonist at 5-HT$_{2B}$ receptors in rat stomach fundus and a weak agonist at 5-HT$_{2A}$ receptors in rat caudal artery (*see* Ellis *et al.*, 1994), also caused potent relaxation of rat jugular vein (Figure 6) and was a partial agonist relative to 5-HT (pEC_{50} [95% CL] = 7.9, [7.6–8.2], mean intrinsic activity ± s.e. mean = 0.84 ± 0.04, $n = 4$). Relaxations induced by BW 723C86 were antagonized by 1.0 μM SB 200646 yielding an *apparent* mean pA_2 [95% CL] of 7.03 [6.76–7.32], $n = 3$, indicating a common site of action.

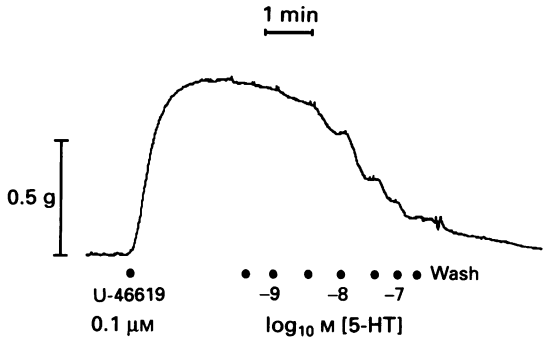


Figure 1 Typical trace of a cumulative (0.5 $\log_{10}$ increments) concentration-effect curve to 5-HT in rat jugular vein.

Discussion

In the present study we have confirmed the 5-HT$_2$-like status of the endothelial 5-HT receptor mediating relaxation of rat jugular vein (Bodelsson *et al.*, 1992) using selective pharmacological probes which allow discrimination of rat 5-HT$_2$ receptor subtypes *in vitro*. In the presence of the 5-HT$_{2A}$ antagonist, ketanserin (Van Neuten *et al.*, 1981), the mixed

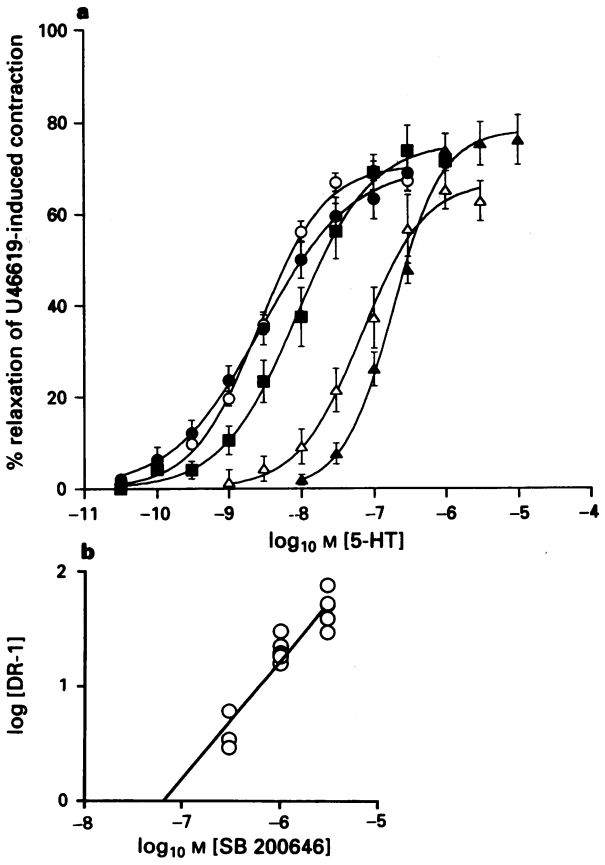


Figure 2 (a) Cumulative concentration-effect curve to 5-HT in the absence (○, first curve, ●, second curve) and presence of 0.3 (■), 1 (△) and 3 (▲) μM SB 200646 in rat jugular vein. Each point represents the arithmetic mean ± s.e.mean of $n \geq 4$ experimental determinations. (b) Schild regression analysis derived from agonist concentration-ratios determined at 0.3, 1 and 3 μM SB 200646.

5-HT$_{2C/2B}$ receptor ligand, SB 200646, acted as a potent and surmountable antagonist of 5-HT in rat jugular vein. The affinity for SB 200646 (pA$_2$ = 7.2) is of the same order as those determined at both rat stomach fundus 5-HT$_{2B}$ receptors (pA$_2$ = 7.5; Baxter *et al.*, 1994) and cloned rat 5-HT$_{2C}$ receptors (pK_i = 6.86; Forbes *et al.*, 1993). The finding that yohimbine also possessed antagonist activity in rat jugular vein at concentrations consistent with its pA$_2$ at 5-HT$_{2B}$ receptors permits further definition of the subtype involved. Yohimbine exhibits low affinity for rat 5-HT$_{2A}$ receptors (pA$_2$ = $<$6.3) and cloned rat 5-HT$_{2C}$ receptors (pK_i = $<$5.3, Martyn Wood personal communication) but high affinity for cloned rat 5-HT$_{2B}$ receptors and 5-HT$_{2B}$ receptors in rat stomach fundus (Clineschmidt *et al.*, 1985; Wainscott *et al.*, 1993). Unfortunately it was not possible to obtain a more robust estimate of the affinity for yohimbine versus 5-HT in the rat jugular vein as it was a non-surmountable antagonist in this preparation. Whilst yohimbine does act as a surmountable antagonist at 5-HT$_{2B}$ receptors in the smooth muscle of rat stomach fundus (Clineschmidt *et al.*, 1985; Baxter *et al.*, 1994), this preparation shows relatively stable, well maintained contractile responses to 5-HT. In contrast, activation of endothelial 5-HT$_{2B}$ receptors in rat jugular vein leads to production of a metabolically labile messenger, nitric oxide, which causes relaxant responses which are not

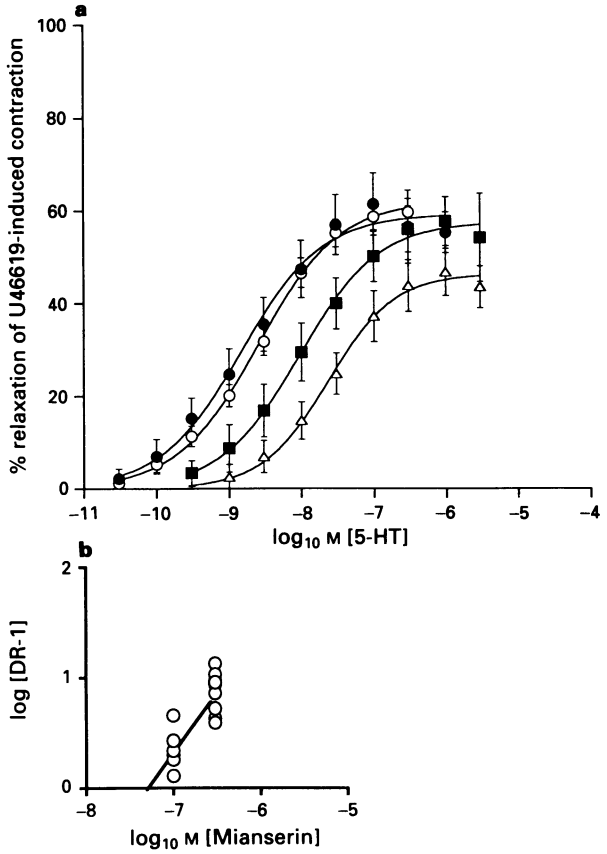


Figure 3 (a) Cumulative concentration-effect curve to 5-HT in the absence (○, first curve, ●, second curve) and presence of 0.1 (■) and 0.3 (△) μM mianserin in rat jugular vein. Each point represents the arithmetic mean ± s.e.mean of $n \geq 4$ experimental determinations. (b) Schild regression analysis derived from agonist concentration-ratios determined at 0.1 and 0.3 μM mianserin.

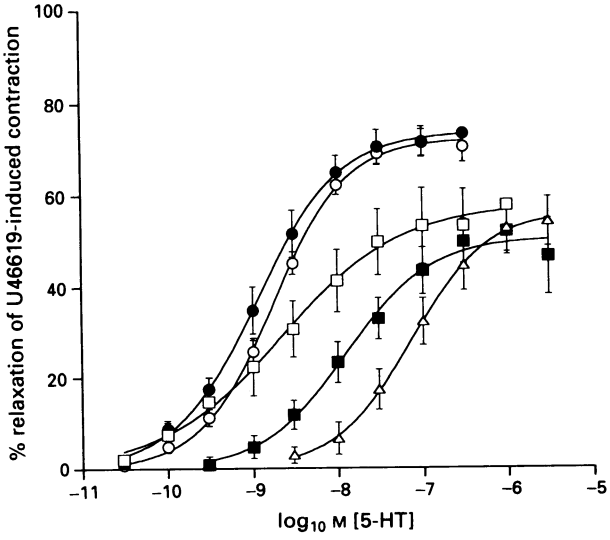


Figure 4 Cumulative concentration-effect curve to 5-HT in the absence (○, first curve, ●, second curve) and presence of 0.03 (□), 0.1 (■) and 0.3 (△) μM yohimbine in rat jugular vein. Each point represents the arithmetic mean ± s.e.mean of $n \geq 4$ experimental determinations.

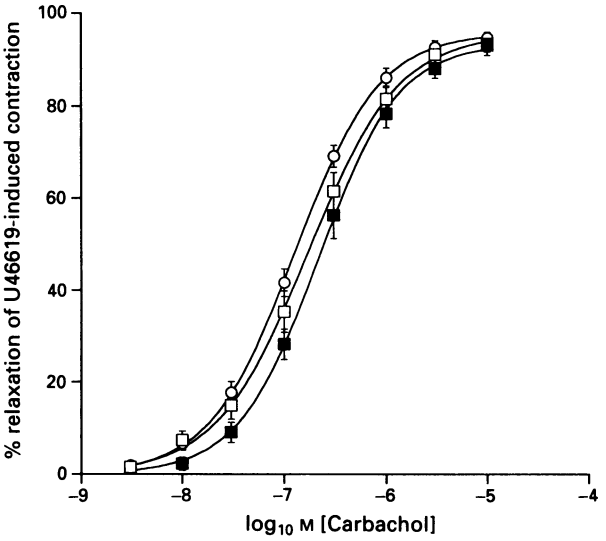


Figure 5 Cumulative concentration-effect curve to carbachol in the absence and presence of 3 μM SB 200646 (□) and 0.3 μM (■) yohimbine in rat jugular vein. Each point represents the arithmetic mean ± s.e.mean of $n \geq 4$ experimental determinations.

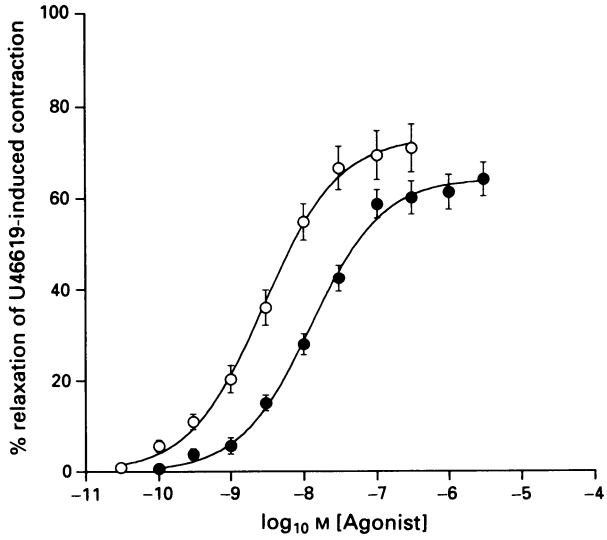


Figure 6 Cumulative concentration-effect curve to 5-HT (○) and BW 723C86 (●) in rat jugular vein. Each point represents the arithmetic mean ± s.e.mean of $n \geq 4$ experimental determinations.

generally as well maintained (*see* Bodelsson *et al.*, 1992). It is also likely that the jugular vein, like the rat stomach fundus, possesses a low 'effective receptor reserve' for 5-HT (Clineschmidt *et al.*, 1985; Baxter *et al.*, 1994). A combination of these factors may contribute to the exposure of non-surmountable antagonism with yohimbine in the present study. It is also worth pointing out that the depression of maximum response to 5-HT after exposure to yohimbine appeared to be concentration-independent. We can offer no satisfactory explanation for these observations at this time.

Other investigators have discounted a possible affiliation of the rat jugular vein 5-HT receptor with the rat stomach fundus receptor (5-HT$_{2B}$) on the basis of differences in sensitivity to antagonism by mianserin (Bodelsson *et al.*, 1992). In the present study the pA_2 estimated for mianserin agreed well with that reported for cloned 5-HT$_{2B}$ receptors ($pK_i = 7.3$; Wainscott *et al.*, 1992) and naturally expressed 5-HT$_{2B}$ receptors in rat stomach fundus longitudinal muscle ($pA_2 = 7.6$; Baxter *et al.*, 1994). The reason for the discrepancy between the present study and that conducted by Bodelsson *et al.* (1992) is not known; however, it is worth pointing out that mianserin possesses a complex profile of action in rat stomach fundus. In the studies of Clineschmidt *et al.* (1985) mianserin antagonized the effects of 5-HT in a concentration-independent manner and evoked methysergide-insensitive contractions in its own right. This contractile response to mianserin in the rat fundus preparation has also been observed by other investigators (Frankhuyzen & Bonta, 1974), however, in contrast to the findings of Clineschmidt *et al.* (1985), these investigators reported that mianserin failed to antagonize responses to 5-HT at concentrations up to 1 μM whilst still conferring protection versus the non-surmountable properties of phenoxybenzamine, methysergide and cyproheptadine. Such observations suggest that the use of mianserin for the characterization of 5-HT$_2$ receptors must be regarded with some caution, especially in view of its high affinity for other receptor subtypes.

The antagonist data obtained in this study present compelling evidence for the existence of 5-HT$_{2B}$ receptors mediating the endothelium-dependent relaxation of the jugular vein of the rat. We have extended this characterization by our finding that BW 723C86, which acts as a potent agonist at 5-HT$_{2B}$ receptors in rat stomach fundus, was also a potent agonist in rat jugular vein. This ligand shows some selectivity for a vascular endothelial receptor in rabbit jugular vein over a number of other 5-HT receptors and displays low potency at 5-HT$_{2A}$ receptors in rabbit aorta and low affinity for 5-HT$_{2C}$ binding sites in pig choroid plexus (Martin *et al.*, 1993 and personal communication). We have confirmed the low potency of BW 723C86 at 5-HT$_{2A}$ receptors in the caudal artery of the rat ($pEC_{50} \leqslant 5.3$, intrinsic activity $\geqslant 0.4$, Ellis *et al.*, 1994). The data suggest that BW723C86 may act as a reasonably selective 5-HT$_{2B}$ agonist, however, no data has been reported regarding 'functional' activity of BW 723C86 at rat 5-HT$_{2C}$ receptors. In this regard, whilst functional data at the rat homologue are not available, we have observed some agonist activity with BW 723C86 at human cloned 5-HT$_{2C}$ receptors expressed in SH-SY5Y cells ($pEC_{50} = 6.5$, intrinsic activity relative to 5-HT = 1, Martyn Elliot personal communication).

It is plausible that 5-HT$_{2B}$ receptors may mediate endothelium-dependent relaxation induced by 5-HT in other species. However, although the endothelial receptors which are present in blood vessels of pig and rabbit have a similar pharmacological profile to that observed in rat jugular vein (Leff *et al.*, 1987; Sumner, 1991; Glusa, 1992), the occurrence of robust operational differences confound explicit classification as 5-HT$_{2B}$. For example, mesulergine (1.0 μM) which is ineffective as an antagonist in piglet vena cava (Sumner, 1991), is a moderately potent antagonist in rabbit ($pA_2 \geqslant 7.3$, Martin *et al.*, 1993) and rat jugular vein ($pA_2 = 7.84$, Bodelsson *et al.*, 1992). Yohimbine also appears to discriminate between endothelial 5-HT receptors in rat and rabbit jugular vein preparations in that it possesses an approximately 50 fold higher affinity for the receptor in the former preparation (Bodelsson *et al.*, 1992; Martin *et al.*, 1993). It is notable that the mouse and rat cloned 5-HT$_{2B}$ receptor homologues show quite profound differences in pharmacology (Compare Loric *et al.*, 1992; Waiscott *et al.*, 1993). For example, the rat receptor possessed high affinity for 5-HT ($pK_i = 8.0$), whilst that displayed by the mouse homologue is much lower ($pK_i = 5.9$). Differences also exist with respect to antagonist binding. It is therefore possible that the pharmacological differences between members of the 'atypical' endothelial receptor family reflect only species variation in pharmacology of 5-HT$_{2B}$ receptors.

In conclusion, by using pharmacological probes that possess selectivity for rat 5-HT$_2$ receptor subtypes, we present compelling evidence that an 'atypical' receptor mediating relaxation of rat jugular vein is a 5-HT$_{2B}$ receptor. The use of ligands such as SB 200646 and BW 723C86 should aid definition of 5-HT$_2$ receptor subtypes in other species and permit a greater understanding of the physiological role of 5-HT receptors on vascular endothelium.

References

ARUNLAKSHANA, O. & SCHILD, H.O. (1959). Some quantitative uses of drug antagonism. *Br. J. Pharmacol. Chemother.*, **14**, 48–58.

BAXTER, G.S., MURPHY, O.E. & BLACKBURN, T.P. (1994). Further characterisation of 5-hydroxytryptamine receptors (putative 5-HT$_{2B}$) in rat stomach fundus longitudinal muscle. *Br. J. Pharmacol.*, **112**, 323–331.

BODELSSON, M., TÖRNEBRANDT, K. & ARNEKLO-NOBIN, B. (1992). Endothelial relaxing 5-hydroxytryptamine receptors in the rat jugular vein: similarity with the 5-hydroxytryptamine$_{1C}$ receptor. *J. Pharmacol. Exp. Ther.*, **264**, 709.

CLINESCHMIDT, B.V., REISS, D.R., PETTIBONE, D.J. & ROBINSON, J.L. (1985). Characterization of 5-hydroxytryptamine receptors in rat stomach fundus. *J. Pharmacol. Exp. Ther.*, **235**, 696–708.

ELLIS, E.S., BYRNE, C., MURPHY, O.E. & BAXTER, G.S. (1994). 5-HT$_{2B}$-like receptors mediate endothelium-dependent relaxation of rat jugular vein. *Br. J. Pharmacol.*, **112**, 477P.

FORBES, I.T., KENNETT, G.A., GADRE, A., HAM, P., HAYWARD, C.J., MARTIN, R.T., THOMPSON, M., WOOD, M.D., BAXTER, G.S., GLEN, A., MURPHY, O.E., STEWART, B.A. & BLACKBURN, T.P. (1993). N-(1-methyl-5-indolyl)-N'-(-3-pyridyl) urea hydrochloride: the first selective 5-HT$_{1C}$ receptor antagonist. *J. Med. Chem.*, **36**, 1104–1107.

FRANKHUYZEN, A.L. & BONTA, I.L. (1974). Effect of mianserin, a potent anti-serotonin agent on the isolated rat stomach fundus preparation. *Eur. J. Pharmacol.*, **25**, 40–50.

GLUSA, E. (1992). Evidence for 5-HT$_{1C}$ receptor-mediated, endothelium-dependent relaxation of porcine pulmonary arteries in vitro. In: *5-Hydroxytryptamine Mechanisms in Primary Headaches*. ed. Olesen, J. & Saxena, P.R. pp. 168–172. New York: Raven Press.

GUPTA, P. (1992). An endothelial 5-HT receptor that mediates relaxation in guinea-pig isolated jugular vein resembles the 5-HT$_{1D}$ subtype. *Br. J. Pharmacol.*, **106**, 703–709.

HOYER, D., WAEBER, C., SCHOEFFTER, P., PALACIOS, J.M. & DRAVID, A. (1989). 5-HT$_{1C}$ receptor-mediated stimulation of inositol phosphate production in pig choroid plexus. *Naunyn-Schmeid Arch. Pharmacol.*, **339**, 252–258.

LEFF, P., MARTIN, G.R. & MORSE, J.M. (1987). Differential classification of vascular smooth muscle and endothelial cell 5-HT receptors by use of tryptamine analogues. *Br. J. Pharmacol.*, **91**, 321–331.

LORIC, S., LAUNAY, J.M., COLAS, J.F. & MAROTEAUX, L. (1992). New mouse 5-HT$_2$-like receptor, expression in brain, heart and intestine. *Fed. Eur. Biochem. Soc.*, **312**, 203–207.

MARTIN, G.R., BROWNING, C. & GILES, H. (1993). Further characterisation of an atypical 5-HT receptor mediating endothelium-dependent vasorelaxation. *Br. J. Pharmacol.*, **110**, 137P.

SCHOEFFTER, P. & HOYER, D. (1990). 5-Hydroxytryptamine (5-HT)-induced endothelium-dependent relaxation of pig coronary arteries is mediated by 5-HT receptors similar to the 5-HT$_{1D}$ receptor subtype. *J. Pharmacol. Exp. Ther.*, **252**, 387–395.

SUMNER, M.J. (1991). Characterization of the 5-HT receptor mediating endothelium-dependent relaxation in porcine vena cava. *Br. J. Pharmacol.*, **102**, 938–942.

VAN NEUTEN, J.M., JANSSEN, P.A.J., VAN BEEK, J., XHONNEUX, R., VERBEUREN, T.J. & VANHOUTTE, P.M. (1981). Vascular effects of ketanserin (R 41 468), a novel antagonist of 5-HT$_2$ serotonergic receptors. *J. Pharmacol. Exp. Ther.*, **218**, 217–230.

WAINSCOTT, D.B., COHEN, M.L., SCHENCK, K.W., ADIA, J.E., NISSEN, J.S., BAEZ, M., KURSAR, J.D., LUCAITES, V.L. & NELSON, D.L. (1993). Pharmacological characteristics of the newly cloned 5-Hydroxytryptamine$_{2F}$ receptor. *Mol. Pharmacol.*, **43**, 419–426.

(Received June 8, 1994
Revised September 15, 1994
Accepted September 19, 1994)

British Journal of Pharmacology (1995) 114, 405-413 © 1995 Stockton Press All rights reserved 0007-1188/95 $9.00

In vivo pharmacological characterization of the non-peptide endothelin receptor antagonist SB 209670

[1]Stephen A. Douglas, *Richard M. Edwards, †John D. Elliott & Eliot H. Ohlstein

Departments of Cardiovascular and *Renal Pharmacology and †Medicinal Chemistry, SmithKline Beecham Pharmaceuticals, P.O. Box 1539, 709 Swedeland Road, King of Prussia, Pennsylvania 19406-0939, U.S.A.

1 The aim of the present study was to assess the ability of SB 209670, a high affinity non-peptide endothelin receptor antagonist (0.4 and 18 nM K_is at human cloned ET_A and ET_B receptors, respectively), to inhibit the haemodynamic actions of endothelin-1 *in vivo*.

2 Systemic administration of (±)-SB 209670, given either as a bolus i.v. injection or as a continuous i.v. infusion, did not alter basal haemodynamic parameters in the anaesthetized rat.

3 Infusion of (±)-SB 209670 ($10\ \mu g\ kg^{-1}\ min^{-1}$) selectively inhibited the depressor and carotid vasodilator response to exogenous endothelin-1: $100\ \mu g\ kg^{-1}\ min^{-1}$ was required to inhibit significantly the biphasic haemodynamic actions of endothelin-1. The haemodynamic actions of angiotensin II and calcitonin gene-related peptide were unaltered by $100\ \mu g\ kg^{-1}\ min^{-1}$ (±)-SB 209670.

4 Bolus i.v. administration of (±)-SB 209670 ($1\ mg\ kg^{-1}$) selectively inhibited the depressor and carotid vasodilator actions of endothelin-1: $10\ mg\ kg^{-1}$ (±)-SB 209670 was required to inhibit the secondary vasoconstrictor actions of endothelin-1.

5 (±)-SB 209670 ($10\ mg\ kg^{-1}$) was also effective at antagonizing the pressor actions of endothelin-1 in the conscious rat for up to 3 h after intraduodenal administration thereby demonstrating that the antagonist was bioavailable upon enteric administration. This dose of (±)-SB 209670 did not alter basal haemodynamic parameters in the conscious rat.

6 Thus, (±)-SB 209670 is an effective endothelin receptor antagonist *in vivo*. Using the doses defined in this study, SB 209670 may, therefore, serve as a useful tool for understanding the role of endogenous endothelin-1 in the control of cardiovascular function under both physiological and pathophysiological conditions.

Keywords: Endothelin receptor antagonist; endothelin-1; SB 209670; regional haemodynamics; ET_A-receptor subtype; ET_B-receptor subtype

Introduction

The identification of a novel non-peptide endothelin receptor antagonist, SB 209670, has recently been reported by Ohlstein *et al.* (1994b,c). This molecule, designed using a conformational model of endothelin-1 (Elliott *et al.*, 1994b), is a high affinity ligand at human cloned ET_A and ET_B receptors (0.4 and 18 nM K_is, respectively; Nambi *et al.*, 1994). *In vitro* studies have demonstrated that SB 209670 is a potent, competitive endothelin receptor antagonist, producing concentration-dependent, parallel rightward shifts in the endothelin-1 concentration-response curves in rat isolated aortae (endothelin-1-induced ET_A receptor-mediated vascular contraction; K_b of 0.4 nM) and rabbit pulmonary arteries (sarafotoxin S6c-induced ET_B receptor-mediated vascular contraction; K_b of 52 nM; Ohlstein *et al.*, 1994a,b,c). SB 209670 is 45, 180 and 775 fold more potent than BQ-123, Ro 47-0203 (bosentan) and PD142893, respectively, in inhibiting ET_A receptor-mediated vascular contraction (Ohlstein *et al.*, 1994a). *In vitro*, the functional antagonism produced by SB 209670 is specific for endothelin-1: 10 μM SB 209670 does not inhibit noradrenaline-, arginine vasopressin- or KCl-induced contraction in rat isolated aortae, or angiotensin II-induced contraction in rabbit isolated aortae (Ohlstein *et al.*, 1994a). SB 209670 is a chiral molecule with the (+)-antipode being at least three orders of magnitude more potent than the (−)-antipode: (±)-SB 209670 inhibits endothelin-1-mediated contraction in human isolated circumflex coronary arteries with a K_b of 7 ± 3 nM (Ohlstein *et al.*, 1994a). Since the development of efficacious endothelin receptor antagonists has the potential to define directly the precise role of endogenous endothelin-1 in the control of cardiovascular physiology and pathophysiology, the aim of the present study was to assess the ability of (±)-SB 209670 to inhibit selectively the haemodynamic actions of exogenously administered endothelin-1 in the rat. Furthermore, in order to demonstrate that the antagonist was bioavailable, studies were designed to assess the ability of (±)-SB 209670 to inhibit the vasopressor actions of endothelin-1 following intraduodenal administration of antagonist. A preliminary account of some of the work described in this study was presented to the Federation of American Societies for Experimental Biology and the XIIth International Congress of Pharmacology (Douglas *et al.*, 1994a,b; Ohlstein *et al.*, 1994b).

Methods

Surgical preparation of anaesthetized rats

Male Sprague-Dawley rats (Charles River) were prepared for haemodynamic evaluation as previously described (Douglas *et al.*, 1992). Briefly, rats were anaesthetized with sodium pentobarbitone ($65\ mg\ kg^{-1}$, i.p.) allowing cannulation of the left jugular vein and right femoral artery and vein (PE50 polyethylene tubing; Clay Adams) for bolus i.v. agonist administration, measurement of arterial blood pressure and continuous infusion of antagonist, respectively. Instantaneous arterial blood pressure was recorded with a miniature Gould P231D pressure transducer (Grass Instrument Co.) linked to a Model 79D Grass polygraph; this signal was used to derive mean arterial pressure and heart rate. Body temperature was maintained at 37 ± 1°C using a K-20-F water blanket

[1] Author for correspondence.

(American Hamilton). In addition, a PE240 tracheal cannula was inserted to allow the animal to be artificially respired with room air (54 cycles min^{-1}; 10 ml kg^{-1}; Harvard Apparatus).

Effect of continuous i.v. infusion of (±)-SB 209670 on the systemic haemodynamic actions of endothelin-1, angiotensin II and human calcitonin gene-related peptide in the anaesthetized rat

Once basal haemodynamic parameters had stabilized following completion of the initial surgical preparation, an infusion of either saline vehicle (150 µl min^{-1}) or (±)-SB 209670 (1–100 µg kg^{-1} min^{-1}) was initiated via the right femoral vein cannula. This infusion was maintained throughout the duration of the experiment. Following a 30 min equilibration period, the rats received a bolus i.v. injection of endothelin-1 (300 pmol kg^{-1} via the jugular vein). In order to demonstrate that (±)-SB 209670 selectively inhibited the vascular actions of endothelin-1, rats also received 300 pmol kg^{-1} doses of angiotensin II and human calcitonin gene-related peptide. Angiotensin II and human calcitonin gene-related peptide were studied because, like endothelin-1, they are potent vasoactive peptides producing pronounced pressor and depressor responses, respectively. The doses of the peptides employed were approximately equivalent to their ED_{50}s as vasoactive agonists in the anaesthetized rat (Douglas & Hiley, 1991; Douglas *et al.*, 1992). All agonists were washed through the venous cannula with 100 µl saline. Changes in mean arterial pressure and heart rate were monitored following agonist administration. Each animal was used to study the effects of a single dose of antagonist or vehicle only. Throughout the duration of these studies animals received supplemental i.v. doses of sodium pentobarbitone (approximately 3 mg kg^{-1} at appropriate time points) in order to maintain a satisfactory level of anaesthesia.

Effect of continuous i.v. infusion of (±)-SB 209670 on the carotid haemodynamic actions of endothelin-1 in the carotid bed of the anaesthetized rat

In a separate set of rats which had been prepared for blood pressure measurement, a pulsed Doppler flow probe, linked to the polygraph via a 545C-4 directional flowmeter (Bioengineering, The University of Iowa, U.S.A.), was placed around the right carotid artery for measurement of carotid blood flow and vascular resistance. This vascular bed was chosen since endothelin-1 is known to act as both a vasodilator and vasoconstrictor in this resistance bed (Gardiner *et al.*, 1989). Following a 30 min continuous i.v. infusion of either saline vehicle or (±)-SB 209670 (10–100 µg kg^{-1} min^{-1}), a dose-response curve was constructed to endothelin-1 (1–1000 pmol kg^{-1}). Thus, it was possible to establish whether or not the inhibitory effects of (±)-SB 209670 on the systemic haemodynamic actions of endothelin-1 were paralleled by similar inhibitory actions in a regional vascular bed.

Effect of (±)-SB 209670 administered as a bolus i.v. injection on the systemic and carotid haemodynamic actions of endothelin-1 in the anaesthetized rat

In a separate group of experiments, the effect of a bolus i.v. dose of (±)-SB 209670 on the systemic and carotid haemodynamic responses to endothelin-1 were studied. Once basal haemodynamic parameters had stabilized, changes in resting haemodynamic parameters were recorded over a 5 min period following the bolus i.v. administration of either (±)-SB 209670 (1–10 mg kg^{-1}) or saline vehicle (equal volume 1 ml kg^{-1}). Once this initial 5 min period was complete, the animals then received a bolus i.v. dose of endothelin-1 (300 pmol kg^{-1} via the jugular vein). Changes in mean arterial pressure, heart rate and carotid blood flow (and, therefore, vascular resistance) were monitored following agonist administration. Each animal was used to study the effects of a single dose of antagonist or vehicle only.

Effect of (±)-SB 209670 administered as a bolus intraduodenal injection on the systemic pressor actions of endothelin-1 in the conscious rat

Male Sprague-Dawley rats were prepared with chronic indwelling catheters following the protocol of Ohlstein *et al.* (1992). Briefly, rats were anaesthetized with sodium methohexitone (100 mg kg^{-1}, i.p.) allowing catheters to be placed in the abdominal aorta (to record systemic arterial blood pressure and heart rate) and vena cava (for i.v. bolus administration of endothelin-1, 200 pmol kg^{-1}) via the left femoral artery and vein. An additional length of Tygon tubing was sutured into the duodenum for bolus intraduodenal administration of saline vehicle or 3–10 mg kg^{-1} (±)-SB 209670 (this route of administration was chosen over gastric lavage since it was less stressful to the conscious rats and therefore, facilitated accurate repeated haemodynamic recordings). All tubing was tunneled under the skin and exited at the midscapular region. Tubing was filled with a dextrose:heparin solution (1 ml contained 0.5 g dextrose and 1000 units ml^{-1} heparin) to prevent obstructive thrombus formation. Following completion of the surgery, animals were housed in Plexiglass cages under a 12 h light-dark cycle with access to standard laboratory chow and drinking water *ad libitum*. Animals were allowed at least 3 days recovery from surgical intervention prior to undergoing experimentation, during which time they were trained to become accustomed to placement in a restraining cage.

Table 1 Continuous i.v. infusion of (±)-SB 209670 does not alter basal systemic haemodynamic parameters in the anaesthetized rat

		Dose of (±)-SB 209670		
	Saline (*n* = 7)	*1 µg kg^{-1} min^{-1}* (*n* = 4)	*10 µg kg^{-1} min^{-1}* (*n* = 8)	*100 µg kg^{-1} min^{-1}* (*n* = 8)
Body weight (g)	407 ± 21	435 ± 13	386 ± 10	402 ± 12
Prior to infusion				
Mean arterial pressure (mmHg)	98 ± 5	105 ± 12	104 ± 9	99 ± 5
Heart rate (min^{-1})	331 ± 28	322 ± 25	304 ± 17	304 ± 5
After 30 min infusion				
Mean arterial pressure (mmHg)	88 ± 8	91 ± 12	101 ± 6	91 ± 7
Heart rate (min^{-1})	306 ± 21	282 ± 24	283 ± 16	282 ± 15

Statistical comparisons between saline-treated rats and those which received (±)-SB 209670 (1–100 µg kg^{-1} min^{-1}) performed by analysis of variance (ANOVA; Fisher's protected least squares difference): no statistical differences were identified. Values shown are the mean ± s.e.mean; *n* represents the number of animals examined in each group.

On the day of experimentation animals were placed in a restraining cage following which they received a bolus i.v. dose of endothelin-1 (control response). Thirty minutes later, immediately prior to a repeat dose of endothelin-1, either saline vehicle or (±)-SB 209670 was administered as an intraduodenal bolus dose. Repeat doses of endothelin-1 were administered every 30 min over a 4 h period following administration of (±)-SB 209670 or saline.

Materials

All drugs and peptides were made freshly each day and stored on ice throughout the duration of the experiment in a light tight container. Endothelin-1 was purchased from American Peptide Co., Inc. (Santa Clara, CA, U.S.A.) and angiotensin II acetate and human calcitonin gene-related peptide were obtained from Sigma Chemical Co. (St. Louis, MO,

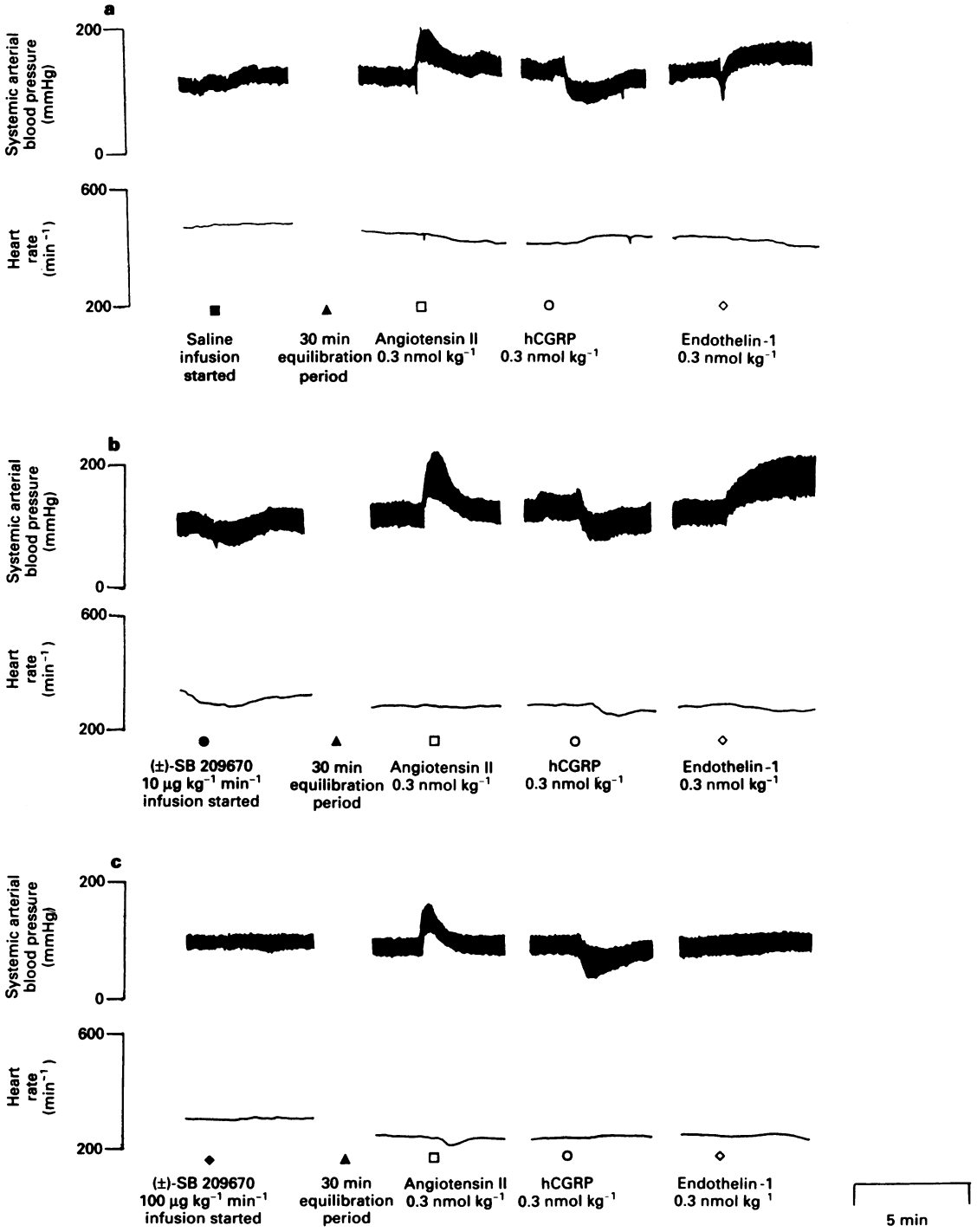


Figure 1 Representative experimental traces showing the effects of 0.3 nmol kg^{-1} angiotensin II (□), human calcitonin gene-related peptide (○) and endothelin-1 (◇) on systemic arterial pressure and heart rate in the anaesthetized rat during continuous i.v. of either (a) saline (■) or (b) 10 (●) or (c) 100 (◆) μg kg^{-1} min^{-1} (±)-SB 209670 infusion. After initiating the infusion of (±)-SB 209670, a 30 min equilibration period (▲) was allowed prior to administration of agonists. The figure (b) illustrates that the continuous infusion of 10 μg kg^{-1} min^{-1} (±)-SB 209670 selectively attenuates the initial hypotensive actions of bolus i.v. endothelin-1. The secondary hypertensive response to endothelin-1 is antagonized only by a higher dose of 100 μg kg^{-1} min^{-1} (±)-SB 209670 (c). Although 100 μg kg^{-1} min^{-1} (±)-SB 209670 inhibits the haemodynamic actions of endothelin-1, the responses to angiotensin II and calcitonin gene-related peptide remain unaltered following administration of antagonist demonstrating the selectivity of (±)-SB 209670 for endothelin-1.

U.S.A.). Stock solutions of peptides (40 μM) were dissolved in distilled water: all serial dilutions were made using saline as the diluent. (±)-SB 209670 ([(±)-(1S, 2R, 3S)-3-(2-carboxymethoxy-4-methoxyphenyl)-1-(3, 4-methylenedioxy-phenyl)-5-(prop-1-yloxy) indane 2-carboxylic acid]) was synthesized in the Department of Medicinal Chemistry, SmithKline Beecham Pharmaceuticals and was dissolved in saline vehicle (0.9% NaCl, w/v).

Statistical analysis

Values are expressed as the mean ± s.e.mean and *n* represents the number of animals used in a particular group. Statistical analysis was performed by analysis of variance (ANOVA; Fisher's protected least squares difference). Differences were considered to be significant where $P<0.05$.

All experiments were performed in specific accordance with the guidelines of the Animal Care and Use Committee, SmithKline Beecham Pharmaceuticals and the American Association for Laboratory Animal Care.

Results

Continuous i.v. infusion of (±)-SB 209670 selectively inhibits the systemic and carotid haemodynamic actions of endothelin-1 in the anaesthetized rat

Relative to saline-treated animals, a 30 min i.v. infusion of (±)-SB 209670 (1–100 μg kg^{-1} min^{-1}) had no effect on basal mean arterial blood pressure or heart rate (Table 1, Figure 1).

The lowest dose of antagonist studied (1 μg kg^{-1} min^{-1}) failed to produce a significant inhibition of either the systemic vasodepressor or vasopressor response to endothelin-1. However, infusion of a ten fold higher dose of (±)-SB 209670 (10 μg kg^{-1} min^{-1}) selectively inhibited the initial hypotensive response to bolus i.v. endothelin-1 administration (Figures 1b and 2a). This dose of antagonist did not alter the secondary hypertensive response to endothelin-1 (Figure 1b, 2b). Indeed, significant inhibition of the secondary increase in blood pressure to endothelin-1 was observed only during the infusion of 100 μg kg^{-1} min^{-1} (±)-SB 209670 (Figure 1c, 2b).

(±)-SB 209670, at 100 μg kg^{-1} min^{-1}, a dose which produced ~80% inhibition of both endothelin-1-induced initial systemic hypotension and secondary systemic hypertension, failed to antagonize the vasopressor response to angiotensin II or the depressor response to human calcitonin gene-related peptide (Figures 1c, 2c and 2d). Thus, the inhibitory action of (±)-SB 209670 was selective for endothelin-1 since no antagonism was observed with other unrelated vasoactive peptides.

In animals with similar basal mean arterial blood pressures, heart rates and carotid blood flow and vascular resistance (Table 2), the dose of (±)-SB 209670 (10 μg kg^{-1} min^{-1}) which selectively inhibited the systemic vasodepressor response to bolus i.v. administration of endothelin-1 was also found to inhibit selectively the vasodilatation observed following bolus i.v. endothelin-1 administration in the carotid vascular bed (Figure 3a). This dose of (±)-SB 209670 failed

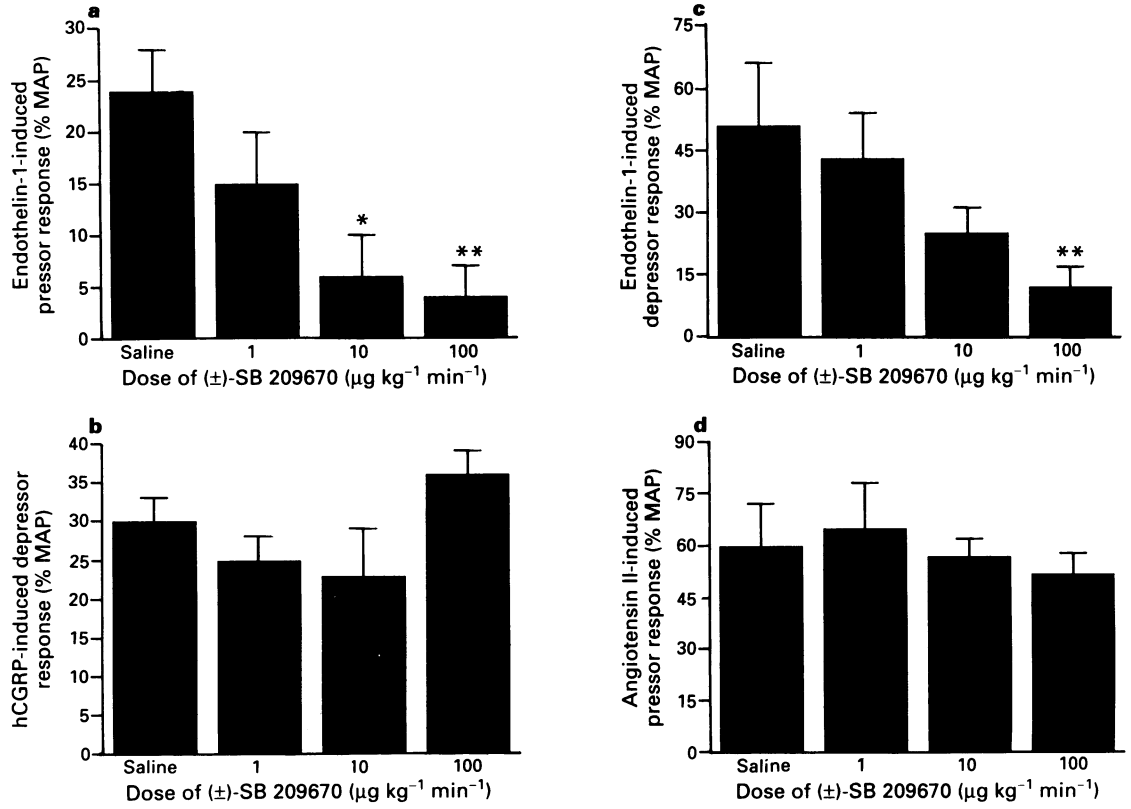


Figure 2 Effect of continuous i.v. infusion of 1 ($n=4$), 10 ($n=8$) or 100 ($n=8$) μg kg^{-1} min (±)-SB 209670 on the (a) initial vasodepressor and (b) secondary vasopressor actions of endothelin-1 (0.3 nmol kg^{-1}, i.v. bolus) compared to (c) the vasodepressor actions of human cacitonin gene-related peptide (hCGRP, 0.3 nmol kg^{-1}, i.v. bolus) and (d) the vasopressor actions of angiotensin II (0.3 nmol kg^{-1}; i.v. bolus). Low dose infusions of (±)-SB 209670 (10 μg kg^{-1} min^{-1}) selectively inhibit the initial vasodepressor actions of endothelin-1: significant inhibition of the secondary pressor actions of endothelin-1 is observed only with 100 μg kg^{-1} min^{-1}. (±)-SB 209670 did not alter the haemodynamic actions of the other vasoactive peptides examined. In addition, 30 min i.v. infusion of (±)-SB 209670 did not alter basal haemodynamic parameters. Statistical comparisons performed by analysis of variance (ANOVA: Fisher's protected least squares difference): $^{*}P<0.05$ and $^{**}P<0.01$ for animals which received (±)-SB 209670 compared to saline-treated control rats ($n=7$). Values are expressed as the mean ± s.e.mean; *n* is the range of the number of animals used at the different doses studied.

Table 2 Continuous i.v. infusion of (±)-SB 209670 does not alter basal regional haemodynamic parameters in the anaesthetized rat

	Dose of (±)-SB 209670		
	Saline (n = 6)	10 μg kg^{-1} min^{-1} (n = 5)	100 μg kg^{-1} min^{-1} (n = 6)
Body weight (g)	314 ± 5	329 ± 16	311 ± 5
Basal haemodynamic parameters			
Mean arterial pressure (mmHg)	97 ± 7	92 ± 5	93 ± 3
Heart rate (min^{-1})	340 ± 12	337 ± 8	346 ± 6
Carotid flow (kHz)	6.28 ± 1.23	8.72 ± 0.78	7.11 ± 0.54

Statistical comparisons between saline-treated rats and those which received (±)-SB 209670 (1–100 μg kg^{-1} min^{-1}) performed by analysis of variance (ANOVA; Fisher's protected least squares difference): no statistical differences were identified. Values shown are the mean ± s.e.mean; *n* represents the number of animals examined in each group.

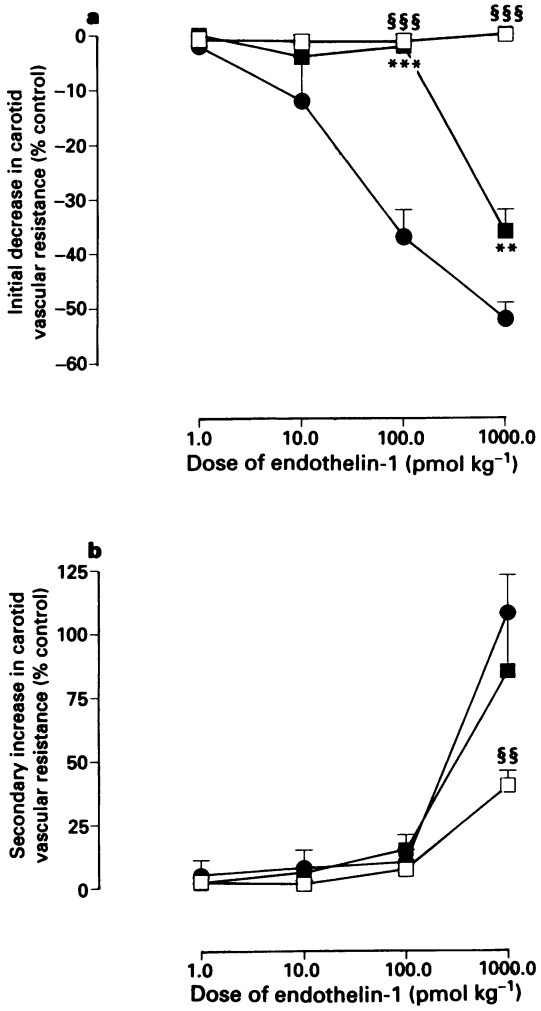


Figure 3 Dose-response curves for the (a) initial vasodilator and (b) secondary vasoconstrictor actions of endothelin-1 (1–1000 pmol kg^{-1}, i.v. bolus) in the carotid vascular bed of the anaesthetized rat during the continuous infusion of either 10 (■; *n* = 5) or 100 (□; *n* = 6) μg kg^{-1} min^{-1} (±)-SB 209670. Control responses (●; *n* = 6) were obtained during the continuous infusion of saline vehicle. Low dose infusions of (±)-SB 209670 (10 μg kg^{-1} min^{-1}) selectively inhibit the initial regional vasodilator actions of endothelin-1 in the carotid bed: significant inhibition of the endothelin-1-induced secondary vasoconstriction is observed only using 100 μg kg^{-1} min^{-1} reflecting the observations made on the endothelin-1-induced haemodynamic changes. Statistical comparisons performed by use of analysis of variance (ANOVA; Fisher's protected least squares difference): $^{**}P < 0.01$ and $^{***}P < 0.001$ and §§$P < 0.01$ and §§§$P < 0.001$ for animals which received 10 and 100 μg kg^{-1} min^{-1} (±)-SB 209670, respectively, compared to saline-treated control rats. Values are expressed as the mean ± s.e.mean; *n* is the range of the number of animals used at the different doses.

to inhibit the secondary vasoconstrictor actions of endothelin-1 (Figure 3b) and, as was the case in the systemic circulation, the carotid vasoconstrictor actions of endothelin-1 could be inhibited only by a ten fold higher dose of antagonist (100 μg kg^{-1} min^{-1}; Figures 3a and b).

Bolus i.v. injection of (±)-SB 209670 selectively inhibits the systemic and carotid haemodynamic actions of endothelin-1 in the anaesthetized rat

Relative to saline-treated animals, the bolus i.v. administration of (±)-SB 209670 (1–10 mg kg^{-1}) had no effect on basal mean arterial blood pressure, heart rate or carotid haemodynamics (Table 3 and Figure 4).

In a similar fashion to those observations made during the i.v. infusion of antagonist, (±)-SB 209670 (1 mg kg^{-1}) selectively inhibited the initial systemic vasodepressor response and associated decrease in carotid vascular resistance to endothelin-1 administration: it did not alter the secondary hypertensive response to endothelin-1 (Figure 5). Significant inhibition of the secondary increase in blood pressure and carotid vasoconstriction to endothelin-1 could be inhibited only using 10 mg kg^{-1} (±)-SB 209670 (Figures 4, 5).

Bolus intraduodenal administration of (±)-SB 209670 inhibits the systemic pressor actions of endothelin-1 in the conscious rat

Mean arterial pressure in rats was not altered 30 min after the bolus intraduodenal administration of (±)-SB 209670 (systemic blood pressure went from 104 ± 4 to 103 ± 5 mmHg following intraduodenal saline administration, from 104 ± 4 to 103 ± 7 mmHg following intraduodenal administration of 3 mg kg^{-1} (±)-SB 209670 and from 97 ± 2 to 99 ± 3 mmHg following intraduodenal administration of 10 mg kg^{-1} (±)-SB 209670; *n* = 5 in each group).

Intraduodenal administration of 10 mg kg^{-1} (±)-SB 209670 produced a significant inhibition of the hypertensive responses to repeated endothelin-1 injections (200 pmol kg^{-1}, i.v. bolus every 30 min). Significant inhibition was observed 60 min after the administration of (±)-SB 209670, an effect which persisted for the next 2 h (Figure 6). Significant inhibition could not be observed with a lower dose of 3 mg kg^{-1} (±)-SB 209670. Due to the susceptibility of the initial, transient endothelin-1-induced depressor response to desensitization (Le Monnier de Gouville *et al.*, 1990), similar comparisons could not be made for the vasodepressor actions of endothelin-1 using this repeat dosing procedure. Nevertheless, the data clearly indicated that (±)-SB 209670 was bioavailable following intraduodenal administration.

Discussion

SB 209670 is a high affinity, functional and competitive non-peptide endothelin receptor antagonist *in vitro* (K_is of 0.4

Table 3 Bolus i.v. administration of (±)-SB 209670 does not alter basal systemic haemodynamic parameters in the anaesthetized rat

	Saline ($n = 9$)	Dose of (±)-SB 209670 1 mg kg^{-1} ($n = 6$)	10 mg kg^{-1} ($n = 4$)
Body weight (g)	315 ± 14	329 ± 16	316 ± 5
Prior to bolus administration			
Mean arterial pressure (mmHg)	88 ± 6	88 ± 5	81 ± 9
Heart rate (min^{-1})	378 ± 7	361 ± 18	375 ± 15
Carotid flow (kHz)	4.16 ± 0.88	2.94 ± 0.28	3.60 ± 0.88
Carotid resistance (mmHg kHz^{-1})	28.6 ± 5.5	25.3 ± 5.4	32.3 ± 14.7
5 min after bolus administration			
Mean arterial pressure (mmHg)	89 ± 6	86 ± 6	80 ± 7
Heart rate (min^{-1})	380 ± 7	358 ± 17	369 ± 13
Carotid flow (kHz)	4.25 ± 0.88	3.13 ± 0.27	3.90 ± 1.04
Carotid resistance (mmHg kHz^{-1})	28.2 ± 5.5	29.0 ± 3.7	30.2 ± 1.4

Statistical comparisons between saline-treated rats and those which received (±)-SB 209670 (1–10 mg kg^{-1}) performed by analysis of variance (ANOVA; Fisher's protected least squares difference): no statistical differences were identified. Values shown are the mean ± s.e.mean; *n* represents the number of animals examined in each group.

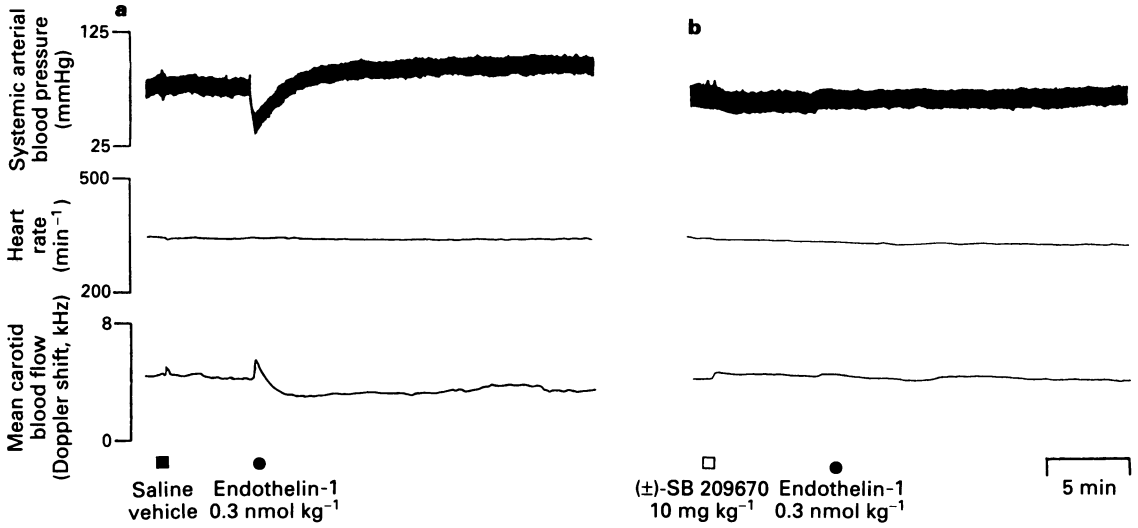


Figure 4 Representative experimental traces showing the effects of 0.3 nmol kg^{-1} endothelin-1 (●) on mean arterial pressure, heart rate and carotid artery blood flow in the anaesthetized rat following the bolus i.v. administration of either (a) saline (■) or (b) 10 mg kg^{-1} (±)-SB 209670 (□). The figure illustrates that bolus i.v. administration of 10 mg kg^{-1} (±)-SB 209670 inhibits both the vasodilator and vasoconstrictor actions of endothelin-1. In addition, (±)-SB 209670 did not alter basal haemodynamic parameters.

and 18 nM at human cloned ET_A and ET_B receptors, respectively; Ohlstein *et al.*, 1994b,c; Elliott *et al.*, 1994b, Nambi *et al.*, 1994). Relative to other endothelin receptor antagonists reported in the literature, SB 209670 is extremely potent being 45, 180 and 775 fold more potent than BQ-123, bosentan (Ro 47-0203) and PD142893 at inhibiting ET_A receptor-mediated vascular contraction, respectively (Ihara *et al.*, 1991; Cody *et al.*, 1992; Doherty *et al.*, 1993; Roux *et al.*, 1993; Ohlstein *et al.*, 1994a).

This study demonstrated that continuous i.v. infusion or bolus i.v. administration of (±)-SB 209670 was effective in antagonizing both the systemic haemodynamic changes and the alterations in carotid blood flow associated with the i.v. bolus administration of endothelin-1. Such findings are consistent with SB 209670 acting as a functional endothelin receptor antagonist *in vitro* (Ohlstein *et al.*, 1994a; Nambi *et al.*, 1994). *In vitro*, the functional antagonism produced by SB 209670 is specific for endothelin-1: 10 μM SB 209670 does not inhibit noradrenaline-, arginine vasopressin- or KCl-induced contraction in rat isolated aortae, or angiotensin II-induced contraction in rabbit isolated aortae. Similarly, a dose of (±)-SB 209670 which inhibited both the initial vasodepressor and secondary vasopressor actions of endothelin-1 did not alter the *in vivo* vasodilator and vasoconstrictor responses to human calcitonin gene-related peptide and angiotensin II, respectively. SB 209670 is a chiral molecule with the (+)-antipode being at least three orders of magnitude more potent than the (−)-antipode *in vitro* (Ohlstein *et al.*, 1994a). Therefore, the pharmacological antagonism of the endothelin-1 induced haemodynamic changes observed in this study is likely to reflect the affinity of the (+)-antipode (rather than the (−)-antipode) present in racemic SB 209670. Indeed, the antagonism observed *in vivo* with 10 mg kg^{-1} (±)-SB 209670 is indistinguishable from that observed with the same dose of (+)-SB 209670 (Ohlstein *et al.*, 1994c).

Systemic administration of (±)-SB 209670 (either bolus i.v. injection or continuous i.v. infusion), did not alter basal haemodynamic parameters in the anaesthetized rat. This is in accord with previous observations made with the ET_A-selective endothelin receptor antagonist, BQ-123, supporting the hypothesis that, at least acutely, endothelin plays a relatively insignificant role in the maintenance/control of basal haemodynamics in the normotensive Sprague-Dawley rat. This contrasts the haemodynamic role of endogenous

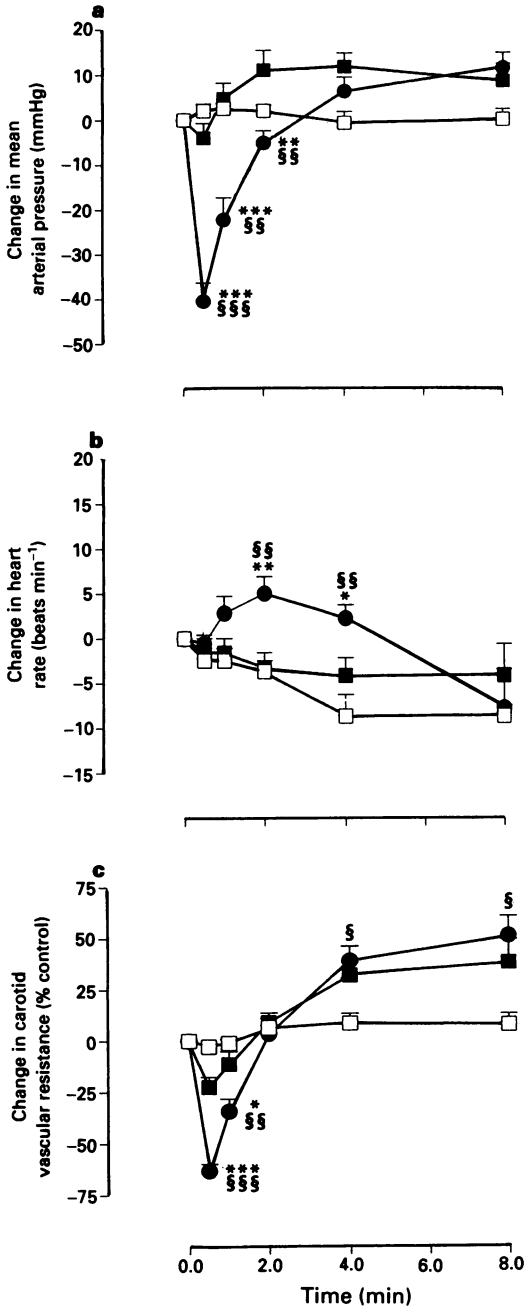


Figure 5 Effect of pretreatment with 1 (■; $n = 6$) or 10 (□; $n = 4$) mg kg^{-1} (±)-SB 209670 on the changes in (a) mean arterial pressure, (b) heart rate and (c) carotid vascular resistance observed in the anaesthetized rat following i.v. administration of 0.3 nmol kg^{-1} endothelin-1. (●; $n = 9$) represents the changes observed in control animals pretreated with an equal volume of saline vehicle. Low dose administration of (±)-SB 209670 (1 mg kg^{-1}) selectively inhibited the initial depressor actions of endothelin-1: significant inhibition of the endothelin-1-induced secondary pressor and regional vasoconstriction is observed only with 10 mg kg^{-1} (±)-SB 209670 reflecting the observations made during the continuous i.v. infusion of antagonist. Statistical comparisons performed by use of analysis of variance (ANOVA; Fisher's protected least squares difference): $^{*}P < 0.05$, $^{**}P < 0.01$ and $^{***}P < 0.001$ and §$P < 0.01$, §§$P < 0.01$ and §§§$P < 0.001$ for animals which received 1 and 10 mg kg^{-1} (±)-SB 209670, respectively, compared to saline-treated control rats. Values shown are the mean ± s.e.mean; n represents the number of animals examined in each group.

endothelin-1 in hypertensive strains of rat where this peptide may be involved in the abnormal elevation of total peripheral resistance (Douglas *et al.*, 1992; 1994c; 1995; Elliott *et al.*, 1994a).

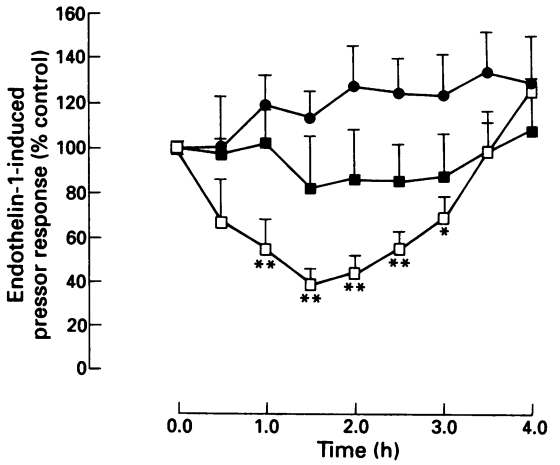


Figure 6 Effect of bolus intraduodenal administration of 3 (■; $n = 5$) or 10 (□; $n = 5$) mg kg^{-1} (±)-SB 209670 on the increases in mean arterial pressure observed in the conscious rat following repeated i.v. administration of 0.3 nmol kg^{-1} endothelin-1; (●; $n = 5$) represents the changes observed in control animals pretreated with an equal volume of saline vehicle. The figure demonstrates that (±)-SB 209670 is bioavailable following intraduodenal administration. Statistical comparisons performed by use of analysis of variance (ANOVA; Fisher's protected least squares difference): $^{*}P < 0.05$ and $^{**}P < 0.01$ for animals which received 10 mg kg^{-1} (±)-SB 209670 compared to saline-treated control rats. Values shown are the mean ± s.e. mean; n represents the number of animals examined in each group.

Infusion of 10 μg kg^{-1} min^{-1} (±)-SB 209670 selectively inhibited the depressor and carotid vasodilator responses to exogenous endothelin-1: a higher dose of 100 μg kg^{-1} min^{-1} was required to inhibit significantly both components of the biphasic haemodynamic response to endothelin-1. Similarly, bolus i.v. administration of (±)-SB 209670 (1 mg kg^{-1}) selectively inhibited the depressor and carotid vasodilator actions of endothelin-1: 10 mg kg^{-1} (±)-SB 209670 was required to inhibit the secondary vasoconstrictor actions of endothelin-1. Whilst (±)-SB 209670 selectively inhibited the vasodepressor and carotid vasodilator actions of endothelin-1, it is interesting to note that neither 10 μg kg^{-1} min^{-1} (i.v. infusion) nor 1 mg kg^{-1} (i.v. bolus) potentiated the secondary pressor actions of endothelin-1 significantly. However, although not significantly different from control responses, the peak increase in mean arterial pressure was observed sooner following i.v. bolus endothelin-1 administration in the presence of 1 mg kg^{-1} (±)-SB 209670 (at approximately 1–2 min after agonist administration) relative to vehicle-treated rats (at approximately 4–8 min after agonist administration). Thus, it is possible that at these doses, (±)-SB 209670 was having some antagonistic effect against the pressor/vasoconstrictor component of the haemodynamic response to endothelin-1. However, an i.v. infusion of a dose of (±)-SB 209670 greater than the 'no effect dose' of antagonist (1 μg kg^{-1} min^{-1}) and smaller than the 'minimum' dose required to inhibit the vasodilator actions of endothelin-1 (10 μg kg^{-1} min^{-1}) was not studied in order to validate such a hypothesis i.e. an i.v. infusion of 3 μg kg^{-1} min^{-1}. Similarly, a bolus i.v. dose of less than 1 mg kg^{-1} (±)-SB 209670 was not studied.

It has been suggested that the pressor actions of endothelin-1 are mediated by the ET_A receptor subtype since endothelin-1 is more potent than endothelin-3 as a pressor agonist (Spokes *et al.*, 1989; Douglas & Hiley, 1991; Ohlstein & Douglas, 1993). In contrast, the potencies of endothelin-1 and endothelin-3 as vasodepressor agonists are not significantly different, raising the possibility that this response is mediated by the ET_B receptor. This proposition is supported by the observation that the pressor actions of endothelin-1

are inhibited selectively by BQ-123 over a dose-range which does not attenuate the depressor actions of endothelin-1 (Douglas *et al.*, 1992). However, such a classification is now recognized as being an oversimplification. Several ET_B-selective agonists, including BQ-3020, sarafotoxin S6c and [$Ala^{1,3,11,15}$]endothelin-1, increase vascular tone *in vivo* e.g. BQ-3020 increases renal, hindquarter and mesenteric vascular resistances in the conscious rat via a mechanism which is insensitive to the ET_A-selective antagonist FR 139317 (Gardiner *et al.*, 1994b). Indeed, it is now appreciated that ET_B-receptors make a significant contribution to the contractile actions of endothelin-1 both *in vitro* (Harrison *et al.*, 1992; Moreland *et al.*, 1992; Panek *et al.*, 1992; Sumner *et al.*, 1992; Warner *et al.*, 1993) and *in vivo* (Hiley *et al.*, 1989; Douglas & Hiley, 1991; Bigaud & Pelton, 1992; Gardiner *et al.*, 1994b). Furthermore, although radioligand binding studies and functional assays demonstrate that SB 209670 exhibits approximately 30 fold selectively for the ET_A receptor subtype over the ET_B receptor subtype (Nambi *et al.*, 1994; Ohlstein *et al.*, 1994a), the observation that (±)-SB 209670 selectively inhibits the depressor and carotid vasodilator actions of endothelin-1 in the anaesthetized rat demonstrates that the haemodynamic actions of endothelin-1 are not simply the function of ET_B-mediated vasodilatation followed by ET_A-mediated vasoconstriction.

Similar observations to those reported here with SB 209670 have been made with a chemically distinct endothelin receptor antagonist: although less potent than SB 209670, the ET_A/ET_B receptor antagonist, Ro 46-2005 (10 mg kg^{-1}, i.v. bolus) selectively inhibits the vasodepressor actions of endothelin-1 (this dose of Ro 46-2005 did not inhibit the secondary pressor actions of endothelin-1; Clozel *et al.*, 1993a,b). Indeed, a dose of 30 mg kg^{-1} bosentan (Ro 47-0203) is only effective at blocking the secondary pressor actions of endothelin-1 if the dose of endothelin-1 is lowered from 500 to 50 pmol kg^{-1} (Gardiner *et al.*, 1994a). Similarly, bolus i.v. administration of either PD 145065 or PD 142893 selectively inhibits the depressor response to endothelin-1 in the anaesthetized rat (Doherty *et al.*, 1993). Clozel *et al.* (1993b) postulated that the selective inhibition of the dilator actions of endothelin-1 by Ro 46-2005 was the result of a pharmacokinetic phenomenon: since the dilator actions of endothelin-1 are mediated *via* an ET_B-receptor subtype linked to endothelium-derived nitric oxide release *in vitro* (De Nucci *et al.*, 1988; Hiley *et al.*, 1989; Douglas & Hiley, 1990), it was suggested that Ro 46-2005 gained preferential access to this endothelial receptor over the ET_A and ET_B receptor subtypes located on the smooth muscle deeper within the tunica media. The observations reported in this study, where i.v. bolus administration of (±)-SB 209670 selectively inhibits the depressor and carotid vasodilator actions of endothelin-1, would lend support to such a hypothesis. However, since several chemically diverse antagonists with different physico-chemical properties (PD 145065 and PD 142893, linear C-terminal hexapeptide analogues; SB 209670, an indane carboxylate; Ro 46-2005, a pyrimidyl sulphonamide) exhibit this phenomenon, a pharmacokinetic explanation is questionable. Furthermore, the present study demonstrated that this phenomenon was also observed during the sustained i.v. infusion of (±)-SB 209670, during which time the levels of antagonist at the tunica intima and media would have been expected to have approached some type of equilibrium. Several alternative pharmacodynamic explanations exist to explain the differences in sensitivity to endothelin receptor antagonism including differences in ET_A/ET_B spare receptor reserves, receptor-coupling mechanisms or binding kinetics. Finally, it is also possible that in the intact animal, vasodilatation may be mediated by an hitherto uncharacterized non-ET_A (possibly a subtype of the ET_B receptor) which is more sensitive than the ET_A/ET_B receptors mediating vasoconstriction to SB 209670, Ro 46-2005, PD 145065 and PD 142893 (Douglas *et al.*, 1992; Warner *et al.*, 1993).

In summary, (±)-SB 209670 is a bioavailable, efficacious selective endothelin receptor antagonist in the intact rat and may, therefore, serve as a useful pharmacological tool for understanding the pathophysiological role of endogenous endothelin-1 in the control of numerous disease processes including essential hypertension, cerebral vasospasms, vascular restenosis and arterial vasospasm following angioplasty and acute renal dysfunction (Brooks *et al.*, 1994; Douglas *et al.*, 1994d,e; 1995; Elliott *et al.*, 1994a; Ohlstein *et al.*, 1994c; Sulpizio *et al.*, 1994).

The authors wish to thank A. Lago, R. Cousins, A. Gao, J. Leber and E. Weidley, Departments of Renal Pharmacology and Medicinal Chemistry, SmithKline Beecham Pharmaceuticals for their expert technical assistance and for the synthesis of (±)-SB 209670.

References

BIGAUD, M. & PELTON, J.T. (1992). Discrimination between ET_A- and ET_B-receptor-mediated effects of endothelin-1 and [$Ala^{1,3,11,15}$] endothelin-1 by BQ-123 in the anaesthetized rat. *Br. J. Pharmacol.*, **107**, 912–918.

BROOKS, D.P., DEPALMA, P.D., GELLAI, M., NAMBI, P., OHLSTEIN, E.H., ELLIOTT, J.D., GLEASON, J. & RUFFOLO, R.R. (1994). Nonpeptide endothelin receptor antagonists. III: effect of SB 209670 and BQ-123 on acute renal failure in anesthetized dogs. *J. Pharmacol. Exp. Ther.* (in press).

CLOZEL, M., BREU, V., BURRI, K., CASSAL, K.M., FISCHLI, W., GRAY, G.A., HIRTH, G., LÖFFLER, B.M., MÜLLER, M., NEIDHART, W. & RAMUZ, H. (1993a). Pathophysiological role of endothelin revealed by the first orally active endothelin receptor antagonist. *Nature*, **365**, 759–761.

CLOZEL, M., BREU, V., GRAY, G.A. & LÖFFLER, B.M. (1993b). *In vivo* pharmacology of Ro 46-2005, the first synthetic nonpeptide endothelin receptor antagonist: implications for endothelin physiology. *J. Cardiovasc. Pharmacol.*, **22** (Suppl. 8), S377–S379.

CODY, W.L., DOHERTY, A.M., HE, J.-X., DEPUE, P.L., RAPUNDALO, S.T., HINGORANI, G.A., MAJOR, T.C., PANEK, R.L., DUDLEY, D.T., HALEEN, S.J., LADOUCEUR, D., HILL, K.E., FLYNN, M.A. & REYNOLDS, E.E. (1992). Design of a functional antagonist of endothelin. *J. Med. Chem.*, **35**, 3301–3303.

DE NUCCI, G., THOMAS, R., D'ORLEANS-JUSTE, P., ANTUNES, E., WALDER, C., WARNER, T.D. & VANE, J.R. (1988). Pressor effects of circulating endothelin are limited by its removal from the pulmonary circulation and by the release of prostacyclin and endothelium-derived relaxing factor. *Proc. Natl Acad. Sci. U.S.A.*, **85**, 9797–9800.

DOHERTY, A.M., CODY, W.L., HE, J.X., DEPUE, P.L., CHANG, X.M., WELCH, K.M., FLYNN, M.A., REYNOLDS, E.E., LADOUCEUR, D., DAVIS, L.S., KEISER, J.A. & HALEEN, S.J. (1993). *In vitro* and *in vivo* studies with a series of hexapeptide endothelin antagonists. *J. Cardiovasc. Pharmacol.*, **22** (Suppl. 8), S98–S102.

DOUGLAS, S.A., ELLIOTT, J.D. & OHLSTEIN, E.H. (1992). Regional vasodilation to endothelin-1 is mediated by a non-ET_A receptor subtype in the anaesthetized rat: effect of BQ-123 on systemic haemodynamic responses. *Eur. J. Pharmacol.*, **221**, 315–324.

DOUGLAS, S.A., ELLIOTT, J.D. & OHLSTEIN, E.H. (1994a). SB 209670 inhibits the hemodynamic effects of endothelin-1 (ET-1) in the anesthetized rat. *FASEB J.*, **8**, A42.

DOUGLAS, S.A., ELLIOTT, J.D. & OHLSTEIN, E.H. (1994b). Pharmacological characterization of the nonpeptide endothelin receptor antagonist SB 209670. *Can J. Physiol. Pharmacol.*, **72** (Suppl. 1), 110.

DOUGLAS, S.A., EZEKIEL, M., GELLAI, M. & OHLSTEIN, E.H. (1994c). BQ-123, a selective endothelin (ETA) receptor antagonist, lowers blood pressure in different rat models of hypertension. *J. Hypertension*, **12**, 561–567.

DOUGLAS, S.A., GELLAI, M., EZEKIEL, M., FEUERSTEIN, G.Z., ELLIOTT, J.D. & OHLSTEIN, E.H. (1995). Antihypertensive actions of the novel, non-peptide endothelin receptor antagonist SB 209670. *Hypertension*, (in press).

DOUGLAS, S.A. & HILEY, C.R. (1990). Endothelium-dependent vascular activities of endothelin-like isopeptides in the isolated superior mesenteric arterial bed of the rat. *Br. J. Pharmacol.*, **101**, 81–88.

DOUGLAS, S.A. & HILEY, C.R. (1991). Endothelium-dependent mesenteric vasorelaxant effects and systemic actions of endothelin (16-21) and other endothelin-related peptides in the rat. *Br. J. Pharmacol.*, **104**, 311–320.

DOUGLAS, S.A., LOUDEN, C., VICKERY-CLARK, L.M., STORER, B.L., HART, T., FEUERSTEIN, G.Z., ELLIOTT, J.D. & OHLSTEIN, E.H. (1994d). A role for endogenous endothelin-1 in neointima formation following rat carotid artery balloon angioplasty: protective effects of the novel nonpeptide endothelin receptor antagonist SB 209670. *Circ. Res.*, **75**, 190–197.

DOUGLAS, S.A., VICKERY-CLARK, L.M. & OHLSTEIN, E.H. (1994e). Functional evidence that balloon angioplasty results in transient nitric oxide synthase induction. *Eur. J. Pharmacol.*, **255**, 81–89.

ELLIOTT, J.D., EZEKIEL, M., GELLAI, M., DOUGLAS, S.A. & OHLSTEIN, E.H. (1994a). Antihypertensive effect of the endothelin receptor antagonist SB 209670 in conscious spontaneously hypertensive rats (SHR). *FASEB J.*, **8**, A7.

ELLIOTT, J.D., LAGO, A., COUSINS, R.D., GAO, A., LEBER, J.D., ERHARD, K., EGGLESTON, D., NAMBI, P., LEE, J.A., BROOKS, D.P., FEUERSTEIN, G., RUFFOLO, R.R., Jr, WEINSTOCK, J., GLEASON, J.G., PEISHOFF, C.E. & OHLSTEIN, E.H. (1994b). (1S, 2R, 2S)-3-(2-carboxymethoxy-4-methoxyphenyl)-1-(3,4-methylenedioxy phenyl)-5-(prop-1-yloxy)indane-2-carboxylic acid, a potent and selective non-peptide endothelin receptor antagonist. *J. Med. Chem.*, **37**, 1553–1557.

GARDINER, S.M., COMPTON, A.M. & BENNETT, T. (1989). Regional haemodynamic effects of endothelin-1 in conscious, unrestrained Wistar rats. *J. Cardiovasc. Pharmacol.*, **13** (Suppl. 5), S202–S204.

GARDINER, S.M., KEMP, P.A. & BENNETT, T. (1994a). Effects of bosentan (Ro 47-020), an ET_A-, ET_B-receptor antagonist, on regional haemodynamic responses to endothelins in conscious rats. *Br. J. Pharmacol.*, **112**, 823–830.

GARDINER, S.M., KEMP, P.A., MARCH, J.E., BENNETT, T., DAVENPORT, A.P. & EDVINSSON, L. (1994b). Effects of an ET_A-receptor antagonist, FR 139317, on regional haemodynamic responses to endothelin-1 and [$Ala^{11,15}$]Ac-endothelin-1 (6-21) in conscious rats. *Br. J. Pharmacol.*, **112**, 477–486.

HARRISON, V.J., RANDRIANTSOA, A. & SCHOEFFER, P. (1992). Heterogeneity of endothelin-sarafotoxin receptors mediating contraction of pig coronary artery. *Br. J. Pharmacol.*, **105**, 511–513.

HILEY, C.R., DOUGLAS, S.A. & RANDALL, M.D. (1989). Pressor effects of endothelin-1 and some analogs in the perfused superior mesenteric arterial bed of the rat. *J. Cardiovasc. Pharmacol.*, **13** (Suppl. 5), S197–S199.

IHARA, M., NOGUCHI, K., SAEKI, T., FUKURODA, S., TSUCHIDA, S., KIMURA, T., FUKAMI, K. & YANO, M. (1991). Biological profiles of highly potent novel endothelin antagonists selective for the ET_A receptor. *Life Sci.*, **50**, 247–255.

LE MONNIER DE GOUVILLE, A.-C., LIPPTON, H., COHEN, G., CAVERO, I. & HYMAN, A. (1990). Vasodilator activity of endothelin-1 and endothelin-3: rapid development of cross-tachyphylaxis and dependence on the rate of endothelin administration. *J. Pharmacol. Exp. Ther.*, **254**, 1024–1028.

MORELAND, S, MCMULLEN, D.M., DELANEY, C.L., LEE, V.G. & HUNT, J.T. (1992). Venous smooth muscle contains vasoconstrictor ET_B-like receptors. *Biochem. Biophys. Res. Commun.*, **184**, 100–106.

NAMBI, J., WU, H.L., PULLEN, M., ELSHOURBAGY, N., OHLSTEIN, E.H., BROOKS, D.P., ELLIOTT, J.D., GLEASON, J. & RUFFOLO, R.R. Jr. (1994). Non-peptide endothelin receptor antagonists. I: effects on binding and signal transduction in human ET_A and ET_B receptors. *J. Pharmacol. Exp. Ther.*, (in press).

OHLSTEIN, E.H., BECK, G., DOUGLAS, S.A., NAMBI, P., GLEASON, J.G., RUFFOLO, R.R., Jr, FEUERSTEIN, G.Z. & ELLIOTT, J.D. (1994a). Non-peptide endothelin receptor antagonists. II: pharmacological characterization of SB 209670. *J. Pharmacol. Exp. Ther.*, (in press).

OHLSTEIN, E.H. & DOUGLAS, S.A. (1993). Endothelin-1 modulates vascular smooth muscle structure and vasomotion: implications in cardiovascular pathology. *Drug Develop. Res.*, **29**, 108–128.

OHLSTEIN, E.H., GELLAI, M., BROOKS, D.P., VICKERY, L., JUGUS, J., SULPIZIO, A., RUFFOLO, R.R., Jr, WEINSTOCK, J. & EDWARDS, R.M. (1992). The antihypertensive effect of the angiotensin II receptor antagonist DuP 753 may not be due solely to angiotensin II receptor antagonism. *J. Pharmacol. Exp. Ther.*, **262**, 595–601.

OHLSTEIN, E.H., NAMBI, P., DOUGLAS, S.A., BECK, G., GLEASON, J., RUFFOLO, R.R., Jr, FEUERSTEIN, G. & ELLIOTT, J.D. (1994b). SB 209670, a rationally designed potent non-peptide endothelin receptor antagonist. *FASEB J.*, **8**, A803.

OHLSTEIN, E.H., NAMBI, P., DOUGLAS, S.A., EDWARDS, R.M., GELLAI, M., LAGO, A., LEBER, J.D., COUSINS, R.D., GAO, A., PEISHOFF, C.E., BEAN, J.W., EGGLESTON, D., ELSHOURBAGY, N., KUMAR, C., LEE, J.A., YUE, T.-L., LOUDEN, C., BROOKS, D.P., RUFFOLO, R.R. Jr, FEUERSTEIN, G., WEINSTOCK, J., GLEASON, J.G. & ELLIOTT, J.D. (1994c). SB 209670, a rationally designed nonpeptide endothelin receptor agonist. *Proc. Natl Acad. Sci U.S.A.*, **91**, 8052–8056.

PANEK, R.L., MAJOR, T.C., HINGORANI, G.P., DOHERTY, A.M., TAYLOR, D.G. & RAPUNDALO, S.T. (1992). Endothelin and structurally related analogs distinguish between endothelin receptor subtypes. *Biochem. Biophys. Res. Commun.*, **184**, 566–571.

ROUZ, S.P., CLOZEL, M., SPRECHER, Y., GRAY, G. & CLOZEL, J.-P. (1993). Ro 47-0203, a new endothelin receptor antagonist, reverses chronic vasospasm in experimental subarachnoid hemorrhage. *Circulation*, **88**, I–170.

SPOKES, R.A., GHATEI, M.A. & BLOOM, S.R. (1989). Studies with endothelin-3 and endothelin-1 on rat blood pressure and isolated tissues: evidence for multiple endothelin receptor subtypes. *J. Cardiovasc. Pharmacol.*, **13** (Suppl. 5), S191–S192.

SULPIZIO, A.C., HIEBLE, J.P., MITCHELL, M., SAUERMELCH, C. & WILLETTE, R.N. (1994). Nonpeptide endothelin receptor antagonists: cerebrovascular characterization and effects on delayed cerebral vasospasm. *Can. J. Physiol. Pharmacol.*, **72** (Suppl. 1), 169.

SUMNER, M.J., CANNON, T.R., MUNDIN, J.W., WHITE, D.G. & WATTS, I.S. (1992). Endothelin ETA and ETB receptors mediate vascular smooth muscle contraction. *Br. J. Pharmacol.*, **107**, 858–860.

WARNER, T.D., ALLCOCK, G.H., MICKLEY, E.J., CORDER, R. & VANE, J.R. (1993). Comparative studies with the endothelin receptor antagonist BQ-123 and PD 142893 indicate at least three endothelin receptors. *J. Cardiovasc. Pharmacol.*, **22** (Suppl. 8), S117–S120.

(Received August 8, 1994
Revised September 15, 1994
Accepted September 19, 1994)

British Journal of Pharmacology (1995) 114, 414-418 © 1995 Stockton Press All rights reserved 0007-1188/95 $9.00

Contribution of a cholinergic reflex mechanism to allergen-induced bronchial hyperreactivity in permanently instrumented, unrestrained guinea-pigs

[1]Ruud E. Santing, Yfke Pasman, Clemens G. Olymulder, Ad F. Roffel, Herman Meurs & Johan Zaagsma

Department of Medicinal Chemistry and Molecular Pharmacology, University Centre for Pharmacy, A. Deusinglaan 2, 9713 AW Groningen, The Netherlands

1 In conscious, permanently instrumented, unrestrained, ovalbumin-sensitized guinea-pigs the development of allergen-induced bronchial hyperreactivity to histamine- and methacholine-inhalation was investigated after the early as well as after the late asthmatic response.

2 The allergen-induced increase in bronchial reactivity to histamine was significantly higher than to methacholine.

3 The muscarinic receptor antagonist, ipratropium bromide (1.0 mM, 3 min inhalation), blocked methacholine-induced bronchoconstriction and caused a significant 1.7 fold inhibition of the histamine-induced bronchoconstriction of control animals.

4 A lower dose of ipratropium bromide (0.1 mM, 3 min inhalation) had no significant effect on histamine-induced bronchoconstriction in control animals, but significantly reduced the allergen-induced increase in bronchial reactivity to histamine between the early and late asthmatic response. At 1.0 mM ipratropium bromide, no further reduction was observed.

5 These results clearly indicate that an exaggerated cholinergic reflex mechanism contributes to allergen-induced bronchial hyperreactivity to histamine.

Keywords: Bronchial hyperreactivity; vagal reflex mechanism; allergic guinea-pigs; ipratropium bromide; histamine; methacholine

Introduction

Bronchial hyperreactivity (BHR) is a common feature of allergic asthma, characterized by an increased airway narrowing in response to various bronchoconstrictor stimuli, including pharmacological agents, such as histamine and methacholine, and chemical irritants such as SO_2. The increased bronchoconstriction to SO_2 can be reversed by administration of the muscarinic receptor antagonist, atropine (Simonsson *et al.* 1967; Alanko & Poppius, 1974), suggesting an increased cholinergic reflex activity in these patients. In man as well as in animals, histamine has been shown to induce bronchoconstriction by acting directly on airway smooth muscle, but also by stimulating afferent vagal sensory nerve endings just beneath the airway epithelium, leading to cholinergic reflex bronchoconstriction by the release of acetylcholine from efferent postganglionic vagal nerve endings that project on airway smooth muscle. Cholinoceptor agonists appear not to evoke this vagal reflex mechanism (Vidruk *et al.* 1977; Holtzman *et al.* 1980).

BHR in allergic asthmatic patients is invariably associated with an influx of inflammatory cells, predominantly eosinophils and neutrophils, into the airways (Chung, 1986; Wardlaw *et al.* 1988). Cytotoxic mediators derived from these inflammatory cells may damage the airway epithelium, therewith exposing sensory nerve endings beneath the airway epithelium (Frigas & Gleich, 1986). In addition, these mediators may inactivate presynaptically located, autoinhibitory muscarinic M_2-receptors, thus causing enhanced acetylcholine release from efferent vagal nerve terminals after stimulation of the reflex arc (Jacoby *et al.* 1993). Evidence for a reduced M_2-muscarinic receptor function contributing to enhanced cholinergic reflex bronchoconstriction in asthmatics was recently presented by Minette *et al.* (1989).

In animal studies, this M_2-receptor dysfunction has been observed *in vivo* after repeated allergen provocation (Fryer & Wills-Karp, 1991). In a recently developed guinea-pig model of allergic asthma, characterized by allergen-induced early (EAR) and late (LAR) phase asthmatic responses, bronchial hyperreactivity and airway inflammation (Santing *et al.* 1992; 1994), a similar M_2-receptor dysfunction was already present between the early and late asthmatic reaction after a single allergen provocation. Loss of M_2-receptor function was indicated by a strongly decreased potentiation by selective M_2-receptor antagonists of the cholinergic twitch contraction of tracheal smooth muscle induced by electrical field stimulation that causes neurotransmitter release from the vagal nerve terminals (Ten Berge *et al.*, 1992).

In the present study we investigated the severity of allergen-induced BHR towards histamine and methacholine and the contribution of a cholinergic reflex bronchoconstriction to the allergen-induced BHR towards histamine *in vivo*.

Methods

Animals

Specific pathogen-free guinea-pigs (Charles River SAVO, Kiszlegg, Germany), were used in this study. All animals were sensitized to ovalbumin at 4 weeks of age, weighing approximately 250 g. A shift to immunoglobulin E (IgE) class antibodies was obtained by using an allergen solution containing 100 μg ovalbumin and 100 mg $Al(OH)_3$ per ml saline (Andersson, 1980). The allergen solution was gently rotated for 60 min to obtain an alu-gel, and 0.5 ml was injected i.p., while another 0.5 ml was divided over seven s.c. injection sites in the proximity of lymphnodes in the paws, lumbar regions and neck (Van Amsterdam *et al.*, 1991). The animals were operated on 4 weeks after sensitization and used experimentally in weeks 5 to 7. The animals were

[1] Author for correspondence.

housed in individual cages in climate-controlled animal quarters and were given water and food *ad libitum*. All protocols described were approved by the University of Groningen Animal Health Committee, which is responsible for the care and proper use of experimental animals.

Measurement of airway function

Airway function was assessed by measurement of pleural pressure (P_{pl}) as described previously (Santing *et al.*, 1992). In brief, a small latex balloon, connected to a saline-filled cannula, was surgically implanted inside the thoracic cavity. The free end of the cannula was driven subcutaneously to the neck of the animal, where it was exposed and attached permanently. Via an external fluid-filled cannula the pleural balloon was connected to a pressure transducer (Gould P23ID, Gould Medical BV, Bilthoven, The Netherlands). P_{pl} (in cmH_2O) was continuously measured by feeding the signals into an A/D converter interfaced to an Atari 1040 ST computer. P_{pl} data were sampled for 10 s every minute. Breath by breath variation was normally less than 15%. Incidental large variations caused by sudden movements or deep sighs were rejected from the calculation.

Using a combination of flow, measured with a pneumotachograph implanted inside the trachea, and pleural pressure, measured with the latex balloon, we have previously shown that changes in P_{pl} are linearly related to changes in airway resistance and hence can be used as a sensitive index for both allergic and non-allergic bronchoconstriction (Santing *et al.*, 1992). Baseline P_{pl}-measurement remained stable for several weeks, and no signs of inflammation were observed at the sites of surgery for at least five weeks after the operation. Airway function can be registered repeatedly and continuously, for periods of at least 24 h, while the animals are unaware of the measurements being taken.

Provocation procedures

Ovalbumin, histamine and methacholine provocations were performed by inhalation of aerosolized solutions. These provocations were carried out in a specially designed animal cage with a volume of 9 l, in which the guinea-pigs could move freely (Santing *et al.*, 1992). A DeVilbiss nebulizer (type 646, DeVilbiss, Somerset, PA, U.S.A.) driven by an airflow of 8 l min^{-1}, provided the aerosol with an output of 0.43 ml min^{-1}. The animals were habituated to the experimental conditions and the provocation procedure on two sequential days at least one week after operation, when preoperative weight was restored. On the first day, the animals were placed inside the provocation cage unconnected to the transducers. Three consecutive inhalations with saline were performed, lasting 3 min each and separated by a 7 min interval. The next day, this protocol was repeated with the animals connected to the measurement system.

On the experimental days after the habituation protocol, allergen, histamine, methacholine, and saline provocations were performed as indicated below. All provocations were preceded by an adaptation period of at least 30 min, followed by two consecutive control inhalations with saline as described above. A baseline P_{pl}-value was calculated by averaging the P_{pl}-values from the last 20 min of the adaptation period. Histamine and methacholine provocations were performed starting with a 25 $\mu g\ ml^{-1}$ solution in saline, followed by increasing dosage steps of 25 $\mu g\ ml^{-1}$. Identical to the preceding saline inhalations, each provocation lasted 3 min and was separated from the previous provocation by a 7 min interval. Animals were challenged until the P_{pl} increased by more than 100% above baseline for at least three consecutive min. The concentration causing a 100% increase in P_{pl} (PC_{100}) was calculated by linear interpolation of the concentration-P_{pl} response curve. After the histamine and methacholine provocations, P_{pl} returned to baseline within 30 min.

Allergen provocations were performed by inhalation of increasing concentrations of 1.0, 3.0 and 5.0 mg ml^{-1} ovalbumin in saline for 3 min each, separated by 7 min intervals, until an increase in P_{pl} of more than 100% was observed. Under these conditions none of the animals developed anaphylactic shock after allergen provocation.

Experimental protocol

Allergen-induced BHR towards histamine and methacholine In a first group of animals, allergen provocations were performed 24 h after a PC_{100}-measurement with either histamine or methacholine. At 6 h (between the early and late asthmatic reaction) and at 24 h (after the late asthmatic reaction) after allergen provocation, the PC_{100}-values were established again to assess allergen-induced BHR for histamine or methacholine, respectively. On the allergen provocation day, airway function was continuously measured during the whole procedure for the quantitative assessment of early (usually between 0 and 5 h after allergen provocation (Santing *et al.*, 1994)) and late (usually between 8 and 24 h after allergen provocation (Santing *et al.*, 1994)) phase asthmatic responses. Between the measurements of histamine and methacholine PC_{100} values at 6 h and 24 h, the animals were placed in a larger cage, where they could move around freely and eat and drink *ad libitum*. During this transfer the animals remained connected to the measurement system.

Effect of ipratropium bromide on histamine- and methacholine-induced bronchoconstriction In another group of animals, the effects of three increasing concentrations of ipratropium bromide or saline on histamine- or methacholine-induced bronchoconstriction were tested. Thirty min after the assessment of histamine or methacholine PC_{100}, the first concentration of ipratropium (or saline) was inhaled for 3 min. Ten min afterwards the next PC_{100}-measurement was started by inhalation of histamine or methacholine at 2 concentration steps below the maximal concentration of the preceding PC_{100}-measurement. In this way, histamine- or methacholine-induced bronchoconstriction occurred approximately 30 min after ipratropium bromide inhalation. This procedure was repeated 2 times, using 10 fold higher concentrations of ipratropium bromide or saline. For histamine, a concentration range of 0.1, 1.0 and 10.0 mM ipratropium bromide was used, and for methacholine this range was 0.01, 0.1, and 1.0 mM ipratopium bromide.

Effect of ipratropium bromide on allergen-induced BHR towards histamine At least 7 days after testing the effects of ipratropium bromide on histamine- or methacholine-induced bronchoconstriction, the PC_{100} towards histamine was (re-) established. Allergen provation was performed 24 h thereafter. At 5 h after allergen provocation the PC_{100} towards histamine was measured again to assess allergen-induced BHR. Identical to the procedure described above, ipratropium bromide (0.1 or 1.0 mM) was inhaled for 3 min at 5.5 h after allergen provocation. Subsequently, histamine PC_{100}-values were determined at 6 h and 24 h after allergen provocation.

In addition, two control groups were used. A first control group received saline instead of allergen and 0.1 mM ipratropium bromide at 5.5 h after saline inhalation. The second control group received saline instead of ipratropium bromide at 5.5 h after allergen provocation. During the experimental period, airway function was continuously measured for the quantitative assessment of early and late phase asthmatic responses.

Data analysis

The magnitudes of the allergen-induced early and late asthmatic responses were expressed as the area under the P_{pl}

time-response curve (AUC) between 0 and 6 h after allergen provocation for the early response, and between 8 and 24 h after provocation for the late response. P_{pl} was expressed as percentage change from baseline and AUC was determined by trapezoid integration over discrete (5 min) time-periods. Based on AUC-values from saline control provocations, threshold values (mean + 2 × s.d.; 99% confidence interval) of 1185% 5 min for a positive early response and 2790% 5 min for a positive late response were defined (Santing *et al.*, 1994). Using these criteria, animals were characterized as single early responders and dual responders (i.e. animals expressing an early as well as late asthmatic response).

Changes in allergen-induced asthmatic reactions as well as in airway reactivity towards histamine or methacholine were analysed by Student's *t* test for paired or unpaired data as indicated. Differences were considered to be statistically significant when $P<0.05$. All data are presented as average ± s.e. mean.

Chemicals

Histamine hydrochloride, ovalbumin (grade III), and aluminium hydroxide were obtained from Sigma Chemical Co. (St. Louis, MO, U.S.A.), and methacholine chloride from Aldrich (Milwaukee, WI, U.S.A.). Ipratropium bromide was a gift from Boehringer Ingelheim GmbH (Ingelheim am Rhein, Germany).

Results

Allergen-induced BHR towards histamine or methacholine

Allergen-induced increases in bronchial reactivity towards histamine and methacholine inhalation are presented in Table 1. Only dual responding animals (16 out of 32) were used for this evaluation, because it was previously found that the bronchial reactivity to histamine at 6 h and 24 h after allergen provocation was significantly increased in dual responding animals only (Santing *et al.* 1994). The early asthmatic response averaged 4,839 ± 958% 5 min in the histamine challenged animals and 5,140 ± 1,458% 5 min in the methacholine challenged animals. For the late asthmatic response these values were 8,460 ± 1,593% 5 min and 7,945 ± 1,281% 5 min, respectively. No significant differences were observed between histamine and methacholine-challenged animals. Bronchial reactivity was significantly enhanced after the early asthmatic response (6 h after provocation) as well as after the late asthmatic response (24 h after provocation) (Table 1), while the former was significantly larger, when tested with histamine ($P<0.001$; $n=15$) as well as with methacholine ($P<0.05$; $n=11$). Comparison of the developed BHR towards histamine and methacholine showed that the BHR for histamine was significantly larger than for methacholine, at 6 h ($P<0.05$) as well as 24 h after allergen provocation ($P<0.001$; unpaired analysis) (Table 1).

Effect of ipratropium bromide on histamine- and methacholine-induced bronchoconstriction

Bronchial reactivity for histamine (Figure 1a) and methacholine (Figure 1b) was assessed four times per animal with an interval of approximately 1 h. In the control group, saline inhalations had no effect on the subsequent PC_{100}-values for histamine, while a small but significant decrease in PC_{100}-values for methacholine was observed between the first and second determination ($P<0.01$), which was unaltered during subsequent PC_{100}-measurements, Ipratropium bromide, in a concentration of 0.1 mM, reduced the sensitivity to methacholine 2.5 fold ($P<0.05$; Figure 1b), but had no significant effect on histamine-induced bronchoconstriction (Figure 1a). However, 1.0 mM ipratropium, a concentration that caused a 50 fold reduction in the response to methacholine inhalation ($P<0.001$; Figure 1b), decreased the sensitivity to histamine 1.7 fold ($P<0.05$; Figure 1a). Increasing the concentration of ipratropium to 10 mM caused a 2.0 fold decrease in histamine PC_{100} ($P<0.05$; Figure 1a). However, this value was not significantly different from that obtained in the presence of 1.0 mM ipratropium.

Table 1 Allergen-induced changes in bronchial reactivity to histamine and methacholine in dual responding guinea-pigs between the early and late asthmatic response (6 h) and after the late asthmatic response (24 h)

Compound applied	n	*Ratio PC_{100} (pre-post-allergen provocation)* 6 h *after allergen provocation*	24 h
Histamine	15	3.04 ± 0.32***	1.68 ± 0.10***
Methacholine	11	1.96 ± 0.31*/†	1.17 ± 0.05**/†††

Data represent mean values ± s.e.mean. Mean PC_{100} before allergen provocation for histamine: 137.7 ± 16.9 and for methacholine 96.7 ± 9.0. Statistical analysis: *$P<0.05$, **$P<0.01$, ***$P<0.001$, Student's paired *t* test compared to before allergen provocation; †$P<0.05$, †††$P<0.001$, Student's unpaired *t* test compared to BHR for histamine.

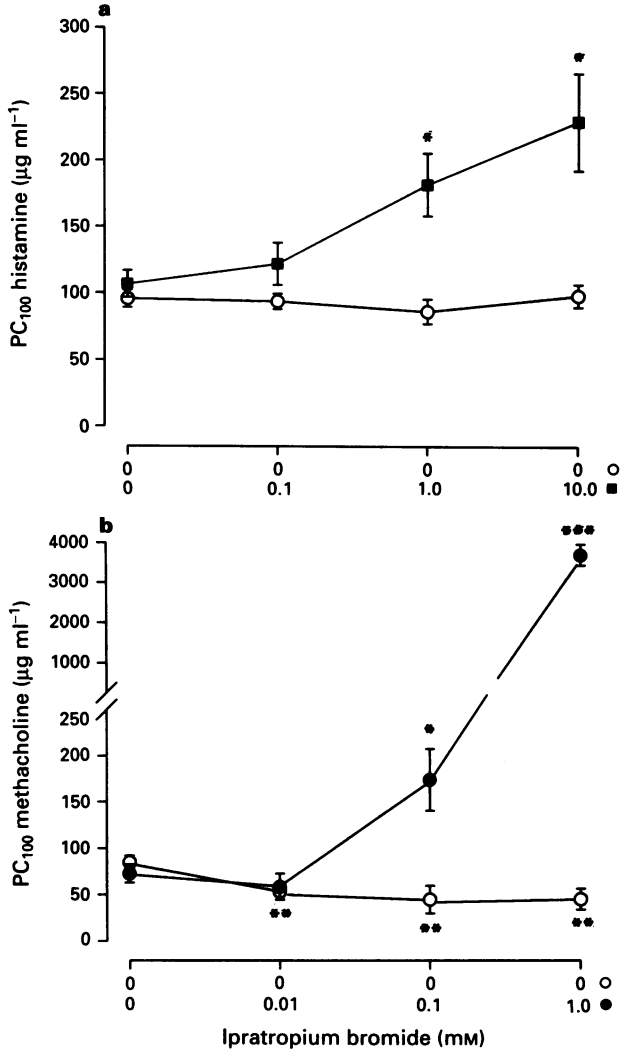


Figure 1 Effect of ipratropium bromide (●: 0.01 to 1.0 mM; ■: 0.1 to 10 mM) or saline inhalation (○) on histamine (a) and methacholine (b) PC_{100}. Subsequent PC_{100} measurements were performed with an interval of approximately 1 h, with ipratropium bromide or saline being administered 30 min after the preceding PC_{100} measurement. Data represent the average ± s.e. mean of 5–7 animals. Statistical analysis: *$P<0.05$, **$P<0.01$, ***$P<0.001$, Student's paired *t* test compared to first measurement.

Effect of ipratropium bromide on allergen-induced BHR towards histamine

Saline inhalation did not affect the reactivity of the airways to histamine-aerosol measured 5 h later. Moreover, 0.1 mM ipratropium, administered 5.5 h after saline inhalation, did not significantly affect the PC_{100}-value for histamine at 6 h and 24 h after saline inhalation (Figure 2). A second group of animals was treated with saline instead of ipratropium at 5.5 h after allergen provocation. In these animals the bronchial reactivity to histamine was significantly increased at 5 h ($P<0.01$) as well as at 6 h ($P<0.01$) and 24 h ($P<0.05$) after allergen provocation, compared to the PC_{100} before allergen provocation. No significant difference in the PC_{100} for histamine was measured between 5 h and 6 h after allergen provocation (Figure 2).

The PC_{100} for histamine at 5 h after allergen provocation was similarly decreased in all groups (Figure 2). Treatment with 0.1 mM ipratropium bromide at 5.5 h after allergen provocation significantly reduced the BHR to histamine at 6 h as compared to 5 h after the provocation ($P<0.01$; $n=5$; Figure 2). A 10 fold higher ipratropium concentration applied at 5.5 h after allergen provocation did not further increase the PC_{100} for histamine (Figure 2).

Bronchial reactivity to histamine at 24 h after allergen provocation was significantly increased compared to prechallenge values in all three allergen provocation groups ($P<0.05$, each). Moreover, ipratropium bromide inhalations (0.1 mM or 1.0 mM) applied at 5.5 h after allergen provocation did not significantly affect the histamine PC_{100} at 24 h after allergen provocation as measured in the absence of ipratropium bromide. No significant differences were observed in the severity of the early as well as the late asthmatic response between the different allergen-challenged groups (not shown).

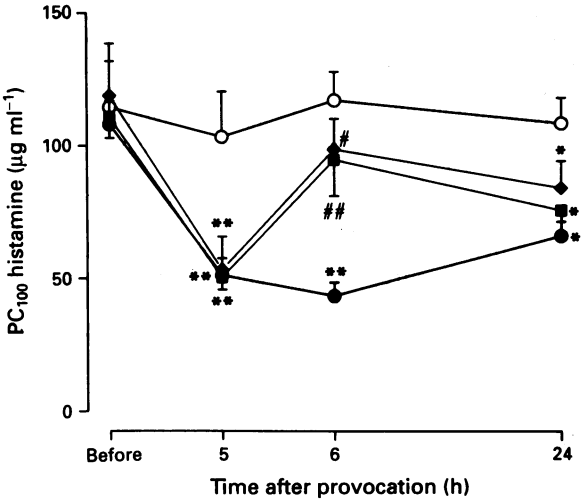


Figure 2 Effect of ipratropium inhalation on allergen-induced bronchial hyperreactivity to histamine. Saline (●), or ipratropium (■, 0.1 mM; ◆, 1 mM) inhalation was performed at 5.5 h after allergen provocation. Open symbols represent data from a control inhalation with saline instead of allergen. In these animals, 0.1 mM ipratropium was administered at 5.5 h after saline inhalation. Data represent the average ± s.e. mean of 5–6 animals. Statistical analysis: $*P<0.05$, $**P<0.01$, Student's paired t test compared to 24 h prechallenge (before): # $P<0.05$; ## $P<0.01$, Student's paired t test compared to 5 h value.

Discussion

In this study, allergen-induced BHR to histamine in permanently instrumented, unrestrained guinea-pigs was significantly higher than with methacholine. Acute methacholine-induced bronchoconstriction is thought to act primarily through direct stimulation of the airway smooth muscle (Vidruk *et al.*, 1977; Holtzman *et al.*, 1980). By contrast, part of the histamine-induced bronchoconstriction may also be mediated by afferent vagal nerve endings located beneath the airway epithelium (Vidruk *et al.*, 1977; Holtzman *et al.*, 1980).

The increased BHR towards histamine as compared to methacholine would suggest that this vagal reflex mechanism may contribute to the allergen-induced BHR towards histamine. In control animals, it was found that inhalation of 1 mM ipratropium bromide strongly inhibited the methacholine response and significantly reduced the histamine-induced bronchoconstriction. A 10 fold increase in ipratropium concentration did not further reduce the histamine PC_{100}-value. These results clearly demonstrate that acetylcholine released from the efferent vagus nerve endings indeed contributes to histamine-induced bronchoconstriction in this guinea-pig model. This mechanism presumably involves stimulation of histamine H_1-receptors on myelinated afferent nerve endings beneath the airway epithelium (Vidruk *et al.*, 1977).

To determine the vagal contribution to allergen-induced BHR towards histamine between the early and late asthmatic reaction, BHR was measured at 5 h and 6 h after allergen provocation, with ipratropium bromide applied in between. While saline did not significantly affect the severity of BHR, ipratropium bromide markedly inhibited the allergen-induced increase in bronchial reactivity towards histamine.

The clear inhibition of histamine-hyperreactivity after allergen provocation by an ipratropium concentration as low as 0.1 mM, which had virtually no effect on non-allergen provoked animals, clearly indicates that histamine-induced vagal reflex bronchoconstriction is increased after allergen provocation. A 10 fold increase of the ipratropium concentration did not further reduce the hyperreactivity for histamine, indicating that in addition to the cholinergic component, other mechanisms are also involved. This is also illustrated by the hyperreactivity observed with methacholine as the agonist, which does not involve a vagal reflex mechanism.

Both concentrations of ipratropium bromide did not affect the magnitude of the late asthmatic reaction as well as the BHR to histamine after this reaction. This finding may, however, be due to the washout of ipratropium bromide during the late reaction. Several mechanisms may account for the enhanced bronchial reactivity after allergen provocation. Firstly, disruption of the airway epithelium by cytotoxic mediators released from inflammatory cells (Frigas & Gleich, 1986) or opening of tight junctions between the airway epithelial cells by endogenous histamine released after allergen provocation (Braude *et al.*, 1984), may facilitate the access of various bronchoconstrictor compounds to the airway smooth muscle.

Secondly, a dysfunction of autoinhibitory muscarinic M_2-receptors, located presynaptically on airway smooth muscle, has recently been postulated in asthmatic patients (Minette *et al.*, 1989) as well as in allergic guinea-pigs (Fryer & Wills-Karp, 1991). In our guinea-pig model, a similar M_2-dysfunction has been observed *in vitro*, 6 h after allergen provocation (Ten Berge *et al.*, 1992). The pathological mechanisms causing this M_2-dysfunction presumably involve cationic proteins, released from activated eosinophils, including major basic protein (MBP), eosinophilic cationic protein (ECP) and eosinophil peroxidase (EPO) (Fryer & Jacoby, 1992). Very recently, Jacoby and coworkers (1993) observed that MBP and EPO, but not ECP displaces [^{3}H]-N-methylscopolamine from M_2-receptors in heart membranes via allosteric antagonism. It is therefore possible that allergen-induced eosinophilic infiltration of the airways leads to M_2-receptor dysfunction, thereby eliminating the negative feedback control on acetylcholine release. This may potentiate vagally mediated bronchoconstriction, as indicated by the enhanced BHR for histamine in the present study.

Thirdly, increased mucus secretion and oedema formation, resulting in a reduced airway calibre, may amplify airway narrowing due to smooth muscle contraction. However, in the present study this is unlikely because airway function (P_{pl}) assessed between the early and late asthmatic response, as well as after the late response, had returned to baseline value.

In conclusion, we have shown that in this new guinea-pig model of asthma, the allergen-induced increase in bronchial hyperreactivity to histamine was significantly higher than to methacholine. Ipratropium bromide inhalation in a concentration (0.1 mM), which had no significant effect on histamine-induced bronchoconstriction in control animals, significantly reduced histamine-induced bronchoconstriction at 6 h after allergen provocation, indicating that the cholinergic reflex bronchoconstriction which contributes to histamine-induced bronchoconstriction is increased after allergen provocation. This allergen-induced exaggerated cholinergic contribution to histamine-induced bronchoconstriction may at least partly explain the markedly enhanced bronchial reactivity to histamine after allergen exposure.

This study was financially supported by the Netherlands Asthma Foundation. Ipratropium bromide was a kind gift from Boehringer Ingelheim GmbH (Ingelheim am Rhein, Germany).

References

ALANKO, K. & POPPIUS, H. (1974). Anticholinergic blocking of prostaglandin-induced bronchoconstriction. *Br. Med. J.*, **1**, 294.

ANDERSSON, P. (1980). Antigen-induced bronchial anaphylaxis in actively sensitized guinea pigs. *Allergy*, **35**, 65–71.

BRAUDE, S., ROYSTON, D., COE, C. & BARNES, P.J. (1984). Histamine increased lung permeability by an H_2-receptor antagonism. *Lancet*, **ii**, 372–374.

CHUNG, K.F. (1986). Role of inflammation in the hyperreactivity of the airways in asthma. *Thorax*, **41**, 657–662.

FRIGAS, E. & GLEICH, G.J. (1986). The eosinophil and the pathophysiology of asthma. *J. Allergy Clin. Immunol.*, **77**, 527–537.

FRYER, A.D. & JACOBY, D.B. (1992). Function of pulmonary M_2 muscarinic receptors in antigen-challenged guinea pigs is restored by heparin and poly-l-glutamate. *J. Clin. Invest.*, **90**, 2292–2298.

FRYER, A.D. & WILLS-KARP, M. (1991). Dysfunction of M_2-muscarinic receptors in pulmonary parasympathetic nerves after antigen challenge. *J. Appl. Physiol.*, **71**, 2255–2261.

HOLTZMAN, M.J., SHELLER, J.R., DIMEO, M., NADEL, J.A. & BOUSHEY, H.A. (1980). Effect of ganglionic blockade on bronchial reactivity in atopic subjects. *Am. Rev. Respir. Dis.*, **122**, 17–25.1

JACOBY, D.B., GLEICH, G.J. & FRYER, A.D. (1993). Human eosinophil major basic protein is an endogenous allosteric antagonist at the inhibitor muscarinic M_2 receptor. *J. Clin. Invest.*, **91**, 1314–1318.

MINETTE, P.A.H., LAMMERS, J-W.J., DIXON, C.M.S., MCCUSCKER, M.T. & BARNES, P.J. (1989). A muscarinic agonist inhibits reflex bronchoconstriction in normal but not in asthmatic subjects. *J. Appl. Physiol.*, **67**, 2461–2465.

SANTING, R.E., MEURS, H., VAN DER MARK, TH.W., REMIE, R., OOSTEROM, W.C., BROUWER, F. & ZAAGSMA, J. (1992). A novel method to assess airway function parameters in chronically instrumented, unrestrained guinea pigs. *Pulm. Pharmacol.*, **5**, 265–272.

SANTING, R.E., OLYMULDER, C.G., ZAAGSMA, J. & MEURS, H. (1994). Relationships between allergen-induced early and late phase airway obstructions, bronchial hyperreactivity and inflammation in conscious, unrestrained guinea pigs. *J. Allergy Clin. Immunol.*, **93**, 1021–1030.

SIMONSSON, B.G., JACOBS, F.M. & NADEL, J.A. (1967). Role of the autonomic nervous system and the cough reflex in the increased responsiveness of airways in patients with obstructive airway disease. *J. Clin. Invest.*, **46**, 1812–1818.

TEN BERGE, R.E.J., ROFFEL, A.F., VAN DER ZANDE, J., SANTING, R.E. & ZAAGSMA, J. (1992). Dysfunction of prejunctional M_2-muscarinic receptors in tracheal preparations of IgE-sensitized guinea pigs after the early allergic reaction. *Am. Rev. Respir. Dis.*, **145**, A437.

VAN AMSTERDAM, R.G.M., SANTING, R.E., DE BOER, J., BROUWER, F. & ZAAGSMA, J. (1991). IgG- and IgE-mediated histamine release from superfused guinea-pig airway tissues. *J. Pharm. Pharmacol.*, **10**, 694–698.

VIDRUK, E.H., HAHN, H.L., NADEL, J.A. & SAMPSON, S.R. (1977). Mechanisms by which histamine stimulates rapidly adapting receptors in dog lungs. *J. Appl. Physiol.*, **43**, 397–402.

WARDLAW, A.J., DUNETTE, S., GLEICH, G.J., COLLINS, J.V. & KAY, A.B. (1988). Eosinophils and mast cells in bronchoalveolar lavage in subjects with mild asthma: relationship to bronchial hyperreactivity. *Am. Rev. Respir. Dis.*, **137**, 62–69.

(Received July 22, 1994
Revised September 22, 1994
Accepted September 28, 1994)

British Journal of Pharmacology (1995) 114, 419–427 © 1995 Stockton Press All rights reserved 0007–1188/95 $9.00

Mechanism of activation of nonselective cation channels by putative M_4 muscarinic receptor in guinea-pig chromaffin cells

[1]Masumi Inoue & Itsusei Imanaga

Department of Physiology, School of Medicine, Fukuoka University, Fukuoka 814-01, Japan

1 Mechanisms involved in the generation of nonselective cation currents (I_{NS}) by muscarinic agonists in the chromaffin cell were investigated by the perforated patch method.

2 Bath application of muscarine (0.1–30 μM) produced an inward I_{NS} with or without a transient outward current at −40 mV, whereas oxotremorine (0.06–60 μM) induced I_{NS} alone. Rectangular hyperbolas with EC_{50}s of 2.01 and 0.21 μM were fitted to muscarine- and oxotremorine-induced I_{NS}s, respectively, and the maximal amplitude of the former was about 3.4 times larger than that of the latter.

3 In 36% of the cells exposed to Ca^{2+}-free solution, muscarine I_{NS} was suppressed, being 53% of control 20 min after the perfusion, and in four cells that were incubated with Ca^{2+}-free solution for 2 h or more, the I_{NS} averaged 44% of that induced subsequently in normal solution. In contrast, muscarine I_{NS} was enhanced by about 30% when A-23187 was added to normal solution.

4 W-7 and W-5, calmodulin-related agents, were almost equally potent in inhibiting muscarine I_{NS}, whereas compound 5, a potent inhibitor of calmodulin-dependent kinase II (CaM kinase II), produced no evident inhibition.

5 HA1004, a weak kinase C inhibitor, induced a reversible suppression of muscarine I_{NS} with an IC_{50} of 163 μM, whereas H-8, another kinase inhibitor, produced an even small degree of inhibition. Administration of phorbol 12, 13-dibutyrate did not mimic muscarinic stimulation of NS channels; rather, it led to a progressive inhibition of I_{NS} and this inhibition was almost complete within 20 min. An inactive phorbol ester had no such effect.

6 The muscarinic antagonists, pirenzepine and AF-DX 116, shifted the dose-response curve for the muscarine I_{NS} to the right in a parallel manner. The K_Ds for pirenzepine and AF-DX 116 were estimated to be 13 nM (95% confidence interval, 11–16 nM) and 365 nM (283–470 nM), respectively.

7 These results suggest that muscarine efficiently produces I_{NS}, probably through binding to the M_4 subtype, that intracellular Ca^{2+} has a facilitating, but not an essential role in the generation of I_{NS}, and that neither CaM kinase II nor protein kinase C is involved.

Keywords: M_4 muscarinic receptor; nonselective cation current; muscarine; oxotremorine; PI turnover; intracellular Ca^{2+}; calmodulin-dependent kinase II; protein kinase C

Introduction

Stimulation of muscarinic receptors with muscarine or oxotremorine induces activation of nonselective cation (NS) channels through a GTP-binding protein in the guinea-pig chromaffin cell (Inoue & Kuriyama, 1991; Inoue & Yoshii, 1992). This channel has a substantial permeability to Ca^{2+} and the current-voltage relationship exhibits a negative slope below −20 to −30 mV. NS channels with similar properties have also been found in smooth muscle cells in the rabbit jejunum (Benham *et al.*, 1985) and in the guinea-pig ileum (Inoue & Isenberg, 1990a,b). In a previous study (Inoue & Imanaga, 1993), we obtained evidence that phosphorylation may be responsible for activation of the channel. The general kinase inhibitor, H-7 (Hidaka *et al.*, 1984) reversibly suppressed the muscarine-induced nonselective cation current (I_{NS}), as did the calmodulin antagonists, trifluoperazine (Levin & Weiss, 1977) and calmidazolium (Belle, 1981). Muscarine, but not oxotremorine, markedly enhanced phosphatidyl inositol (PI) turnover in bovine adrenal chromaffin cells as well as in nerve ending preparations from the rat and guinea-pig cerebral cortex (Fisher *et al.*, 1983). This enhancement of PI turnover may result in generation of the second messengers inositol trisphosphate (IP_3) and diacylglycerol (DG) (Nishizuka, 1992). Thus, IP_3 might mediate the production of I_{NS} through mobilizing intracellular Ca^{2+} (Berridge, 1993) and subsequently stimulating calmodulin-dependent kinase II (CaM kinase II) (Shenolikar, 1988). Alternatively, DG might generate I_{NS} through activating protein kinase C (PKC) (Nishizuka, 1992). The primary objective of our experiment was to address the question of whether CaM kinase II or PKC is responsible for the generation of I_{NS}. For this purpose, we compared the efficacy of muscarine and oxotremorine in inducing I_{NS} and examined effects of calmodulin- and PKC-related agents. We also attempted to elucidate the muscarinic receptor subtype involved in activation of NS channels. mRNA extracted from the bovine adrenal medulla exclusively hybridized with a M_4 cDNA probe, suggesting the presence of M_4 receptors in adrenal chromaffin cells. Consistent with this notion, (Fernando *et al.*, 1991) molecular biological techniques have shown that the muscarinic receptor subtype in the rat adrenal phaeochromocytoma cell line, PC 12, were M_4 (Ashkenazi *et al.*, 1988). Our previous study with muscarinic antagonists and pertussis toxin treatment (Inoue & Kuriyama, 1991) also suggest a possible involvement of the M_4 receptor in the generation of I_{NS}. However, the estimated K_Ds for antagonists were not completely compatible with this notion. Thus, this issue was re-examined, using the perforated patch method. With this technique, stable I_{NS} was elicited repetitively by muscarinic stimulation, and reliable K_Ds were obtained.

Methods

Preparation

Female guinea-pigs (240–350 g) were killed by a blow to the neck and the adrenal glands were immediately put into ice-

[1] Author for correspondence.

cooled Ca^{2+}-free balanced salt solution. Adrenal medullae were dissected from the adrenal cortex under a dissecting microscope, then were cut into three to six pieces and incubated for 30 min with 0.25% collagenase dissolved in a nominally Ca^{2+}-free solution. During the initial 10 min of this enzyme treatment, the preparation was gently agitated by bubbling with 99.9% O_2 to facilitate digestion. After the incubation, the tissues were washed three or four times in Ca^{2+}-free solution and gently dissociated with a fire-polished Pasteur pipette. The isolated cells were kept in Ca^{2+}-free solution at room temperature (24 ± 1°C) for 3–10 h.

Current recording

The whole-cell current was recorded using the perforated patch method (Horn & Marty, 1988). Dispersed chromaffin cells were left in the bath for a few minutes to facilitate attachment to the bottom of the bath, before perfusion with a external solution at a rate of about 1 ml min^{-1}. Currents were recorded with an EPC-7 (List, Germany) patch clamp amplifier. Currents were fed into a pen recorder after filtering at 3 or 5 Hz and into a video cassette recorder after digitizing with an analog-to-digital converter. Series resistance in whole-cell recording was 26.7 ± 5.8 MΩ (mean ± s.e.mean, $n = 6$).

Solutions

The normal external solution contained (in mM): NaCl 137, KCl 5.4, $CaCl_2$ 1.8, $MgCl_2$ 0.5, NaH_2PO_4 0.53, D-glucose 5, HEPES 5 and NaOH 4. The pH was adjusted to 7.4. In Ca^{2+}-free experiments, Ca^{2+} was replaced with 3.6 mM Mg^{2+}. The internal (pipette) solution contained (in mM): K isethionate 120, KCl 20, NaCl 10, HEPES 10 and KOH 2.6. The pH was 7.2. On the day of the experiment, fresh nystatin was dissolved in dimethyl sulfoxide and was added to the internal solution, at a final concentration of 100 μg ml^{-1}. This nystatin solution was subjected to vortex-mixing for 5 min. The liquid junction potential between the external solution and nystatin solution was about 3 mV and was not corrected for membrane potential measurements. All the experiments were done at a holding potential of −40 mV and at 24 ± 1°C. Chemicals were added to the perfusate. The results are expressed as means ± s.e.mean and Student's t test was used to determine statistical significance.

Analysis of dose-response curves

The sigmoid curve $I = I_{max}\ [A]^n/([A]^n + K_A^n)$ was fitted by computer using a non-linear least-squares method to the peak current (I) induced by the agonist (A): I_{max} is a maximum value of I, [A] is the concentration of agonist, K_A is a constant equal to the EC_{50} or IC_{50} and n is a Hill coefficient. The antagonists, pirenzepine and AF-DX 116, were assumed to act competitively; their K_Ds were estimated by Schild analyses (Arunlakshana & Schild, 1959).

Chemicals

Sources of chemicals were as follows: (±)-muscarine chloride, oxotremorine sesquifumarate, phorbol 12, 13-dibutyrate, 4α-phorbol 12, 13-didecanoate, A-23187, and nystatin (Sigma, U.S.A.); HA1004 [N-(2-guanidinoethyl)-5-isoquinolinesulfonamide hydrochloride] and H-8[N-(2-(methylamino)ethyl)-5-isoquinolinesulfonamide dihydrochloride] (Seikagaku, Japan); pirenzepine dihydrochloride and AF-DX 116 (11-[[2-[(diethylamino)methyl]-1-piperidinyl]acetyl]-5,11-dihydro-6H-pyrido[2,3-b)][1,4]benzodiazepine-6-one) (Boehringer Ingelheim, Germany); W-7[N-(6-aminohexyl)-5-chloro-1-naphthalenesulfonamide hydrochloride] (Biomol Research, U.S.A.); W-5 [N-(6-aminohexyl)-1-naphthalenesulfonamide hydrochloride] (Molecular Probes, U.S.A.); compound 5 [N-(2′, 5′-dihydroxybenzyl)-3-amino-salicyclic acid] (LC services, U.S.A.); collagenase (Yakult, Japan). The phorbol esters were dissolved in dimethyl sulfoxide in such a way that the final concentration of the solvent was always less than 0.1%.

Results

Differences in response to muscarine and oxotremorine

Figure 1 shows current responses to muscarine and oxotremorine at a holding potential of −40 mV in the same chromaffin cell. The addition of muscarine at concentrations equal to, or greater than 3 μM to the perfusate induced a transient outward current (I_O) with concomitant generation of I_{NS}. The presence of oxotremorine at concentrations up to 60 μM never produced I_O but did produce I_{NS} consistently ($n = 9$). In one series of experiments, transient I_O was produced in zero, 50, and 83% of six cells by 1, 3, and 10 μM muscarine, respectively and the amplitude of I_O increased according to the concentration. In a previous study (Inoue & Kuriyama, 1990), we suggested that this transient I_O is due to Ca^{2+} mobilized from intracellular stores.

Consistent with this notion, a second application of muscarine in a nominally Ca^{2+}-free solution failed to induce I_O and prior exposure to 5 mM caffeine under Ca^{2+}-free conditions led to a marked reduction of I_O in response to muscarine (not shown). Thus, it is likely that muscarine, but not oxotremorine, can facilitate PI turnover with the subsequent generation of I_O.

The putative difference between muscarine and oxotre-

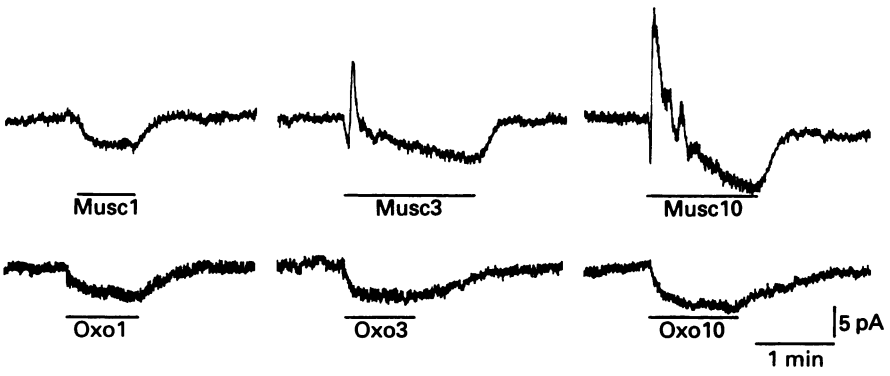


Figure 1 Differences in current response of a guinea-pig chromaffin cell to muscarine and oxotremorine. Muscarine (Musc) and oxotremorine (Oxo) each at 1, 3 and 10 μM were added to the perfusate during the periods indicated by horizontal lines. Drug application was interrupted for 2 to 3 min between records. Holding potential, −40 mV. Upper and lower panels, from the same cell.

morine in inducing PI hydrolysis might relate to that in generating I_{NS}. As the concentration of muscarine was increased from 1 μM, the generation of I_{NS} was markedly enhanced with the concomitant production of I_O; in contrast 3 μM oxotremorine produced a maximal activation of I_{NS} (Figure 1). Thus, we investigated quantitatively the potency and efficacy of muscarine and oxotremorine in the cells where high concentrations of muscarine induced no apparent I_O (potency and efficacy are used differently here: the former refers to dose-dependent properties and the latter refers to magnitudes of response e.g., Hoyer & Boddeke, 1993). For a comparison among different cells, amplitudes of I_{NS} were expressed relative to that produced by 1 μM muscarine. Figure 2a illustrates I_{NS} in response to various concentrations of muscarine and 1 μM oxotremorine. The amplitude of 1 μM oxotremorine-induced I_{NS} was about 70% (71 ± 4%, $n = 6$) of that seen with 1 μM muscarine. Oxotremorine-induced I_{NS}s (▽ in Figure 2b) were well fitted by a rectangular hyperbola with a K_A of 0.21 μM and an I_{max} of 0.88. These values of the parameters are in fairly good accord with those obtained previously using a conventional patch clamp technique. The muscarine-induced currents were fitted by a rectangular hyperbola with a K_A of 2.01 μM and an I_{max} of 3.00 (○ in Figure 2b).

Effect of Ca^{2+} removal on I_{NS}

In the ileal smooth muscle, ACh failed to produce a depolarization due to I_{NS} in the absence of Ca^{2+} (Inoue & Isenberg, 1990b), whereas in the chromaffin cell, oxotremorine induced the current in a nominally Ca^{2+}-free solution (Inoue & Kuriyama, 1991). To investigate whether the difference of I_{NS} between the chromaffin cell and the smooth muscle cell can be ascribed to genuine properties of NC channels in the former, chromaffin cells were exposed for 20 min to Ca^{2+}-free solution in the presence or absence of 0.5 mM EGTA. When perfused with a nominally Ca^{2+}-free solution, amplitudes of I_{NS} in response to 1 or 3 μM muscarine decreased successively in two of eight cells tested. Figure 3a illustrates such a decrease in I_{NS} in one of these two cells. The amplitude of the current was reduced by 37% and 57% 2 min and 10 min after start of the perfusion. This decrease of I_{NS} was completely reversed at 4 min, but not at 1 min, after switching back to normal solution. The addition of 0.5 mM EGTA to Ca^{2+}-free solution produced a successive decrease of the muscarinic I_{NS} in three of six cells tested. Figure 3b summarizes time courses of I_{NS} in the five cells where reduction was observed in the presence or absence of EGTA (●) and in the nine cells (▲) where noticeable decreases did not occur. This suppression of I_{NS} by Ca^{2+} removal was not influenced by concentrations of muscarine. Figure 4a shows I_{NS}s induced by various concentrations of muscarine before and after perfusion with Ca^{2+}-free solution in the same cell. I_{NS} in response to 3 μM muscarine, in this cell, was reduced to 50% of control 10 min after perfusion with a nominally Ca^{2+}-free solution and remained at this level for the following 12 min. Muscarine-induced I_{NS}s elicited in the absence of external Ca^{2+} still fell approximately on the dose-response curve for the control I_{NS}, obtained in Ca^{2+}-containing medium (Figure 4b).

The finding that I_{NS} decreased successively under Ca^{2+}-free conditions in 5/14 of the cells tested suggests the presence of two groups of I_{NS} in the chromaffin cell, only one of which is partially dependent on extracellular Ca^{2+}. Alternatively, the difference might be accounted for by the rate of decrease in intracellular $[Ca^{2+}]$ after Ca^{2+} removal. To explore this possibility, we investigated effects of a long incubation of cells in Ca^{2+}-free solution. After over 2 h incubation in a nominally Ca^{2+}-free solution, cells were exposed to 3 μM muscarine; then, the response to the same concentration of muscarine was determined in the presence of Ca^{2+}. The amplitude of I_{NS} in the absence of external Ca^{2+} was 44 ± 6% ($n = 4$) of the

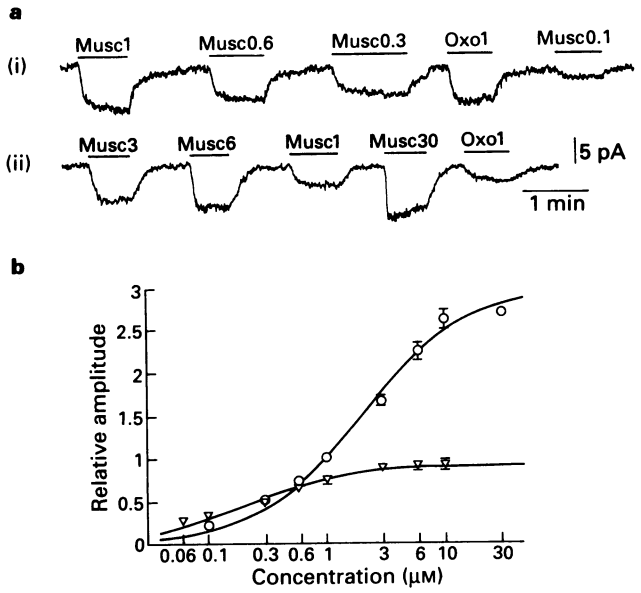


Figure 2 Dose-response relationship for muscarine and oxotremorine-induced nonselective cation currents. (a) Nonselective cation currents (I_{NS}) in response to muscarine and oxotremorine: (i) I_{NS} induced by 0.1, 0.3, 0.6, and 1 μM muscarine (Musc) and 1 μM oxotremorine (Oxo); (ii) I_{NS}s induced by 1, 3, 6, and 30 μM muscarine and 1 μM oxotremorine; (i) and (ii) from different cells. (b) Muscarine (○)- and oxotremorine (▽)-induced I_{NS}s were plotted against their concentrations. Amplitudes of both I_{NS}s were expressed relative to that of 1 μM muscarine-induced I_{NS} measured in the same cells. Data represent mean ± s.e.mean of 3 to 26 and 2 to 8 observations at each concentration of muscarine and oxotremorine, respectively. Rectangular hyperbolas (lines) with K_A of 2.01 μM and I_{max} of 3.00 (r, 0.963) and with K_A of 0.21 μM and I_{max} of 0.88 (r, 0.952) were fitted to muscarine- and oxotremorine-induced I_{NS}s.

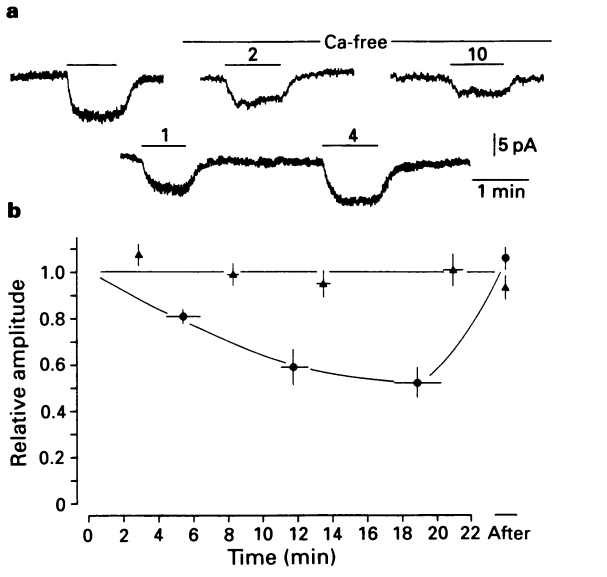


Figure 3 Effects of Ca^{2+} removal on muscarine-induced I_{NS}. (a) Muscarine-induced I_{NS} in the presence and absence of external Ca^{2+}: 3 μM muscarine was added to normal or nominally Ca^{2+}-free solution during the periods indicated by horizontal lines. The numbers above lines represent approximate times after perfusion with Ca^{2+}-free or normal solution. (b) Summary of 1 or 3 μM muscarine-induced I_{NS} which was successively decreased (●) or was maintained (▲) in Ca^{2+}-free solution. Amplitudes of I_{NS} elicited in Ca^{2+}-free and after switching back to normal (After) were expressed relative to that before perfusion with Ca^{2+}-free in the same cell and plotted against the time of perfusion; (●) and (▲) represent mean ± s.e. mean of 5 and 9 cells (see text). Straight line and curve were drawn through (●) and (▲) by eye.

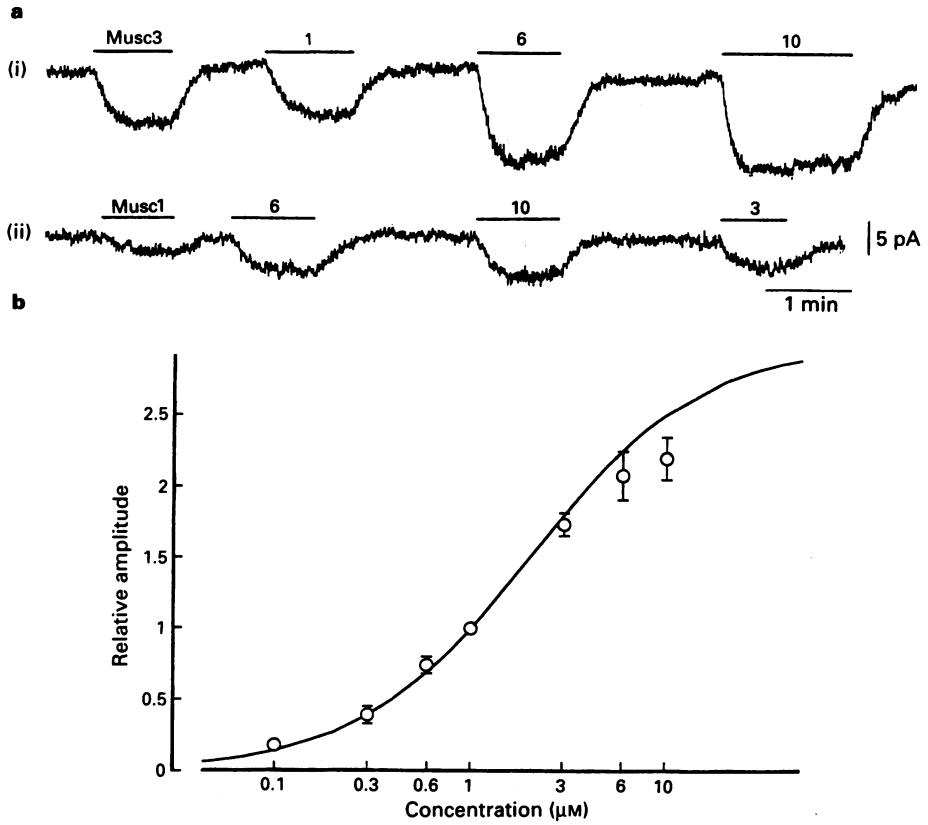


Figure 4 Reduction of muscarine-induced I_{NS} by Ca^{2+} removal did not depend on the concentration. (a) I_{NS}s in response to muscarine (Musc) before (i) and after (ii) removal of external Ca^{2+}: 1 to 10 μM muscarine was added to normal (i) and to Ca^{2+}-free solution (ii) during the indicated period. About 10 min after start of perfusion with Ca^{2+}-free solution, I_{NS} in response to 3 μM was reduced to 50% of I_{NS} elicited in normal solution. (b) I_{NS} obtained after reduction was plotted against concentrations of muscarine. Data represent mean ± s.e.mean of 2 to 11 observations at each concentration. The curve was the same as that for muscarine-induced I_{NS} in normal Ca^{2+} medium shown in Figure 2.

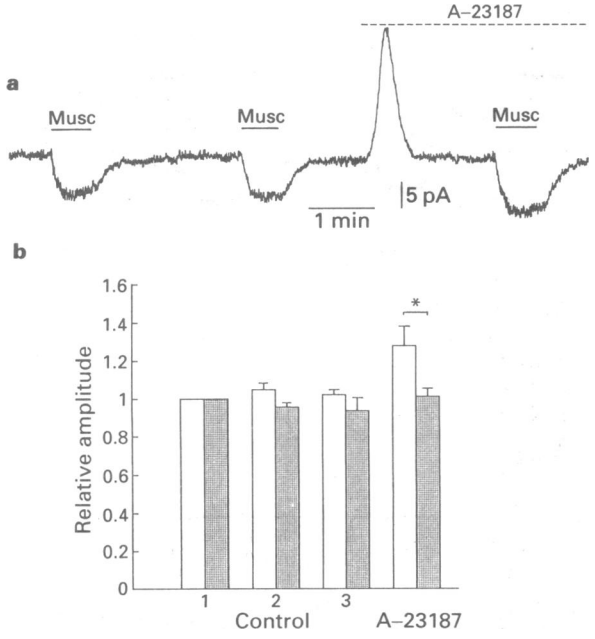


Figure 5 Potentiation of muscarine-induced I_{NS} by A-23187. (a) Muscarine-induced I_{NS} in the presence and absence of 0.5 μM A-23187: 3 μM muscarine (Musc) was added to normal solution during the periods indicated by horizontal lines in the presence (interrupted line) or absence of A-23187. (b) Summary of muscarine-induced I_{NS} in the presence or absence of A-23187 under normal (open column, $n = 6$) or Ca^{2+}-free conditions (stippled column, $n = 4$). Amplitudes of I_{NS} were expressed relative to that of I_{NS} induced by the first application of muscarine. Before administration of 0.5 or 1 μM A-23187, I_{NS} was generated consecutively three times by application of muscarine. Data are mean ± s.e.mean. There is no significant change among these three I_{NS}s. *Statistical significance ($P < 0.05$).

response in the presence of normal external Ca^{2+}. This value of I_{NS} did not differ from the 53 ± 6% ($n = 5$) seen about 20 min after perfusion with Ca^{2+}-free solution. Thus, we conclude that the apparent heterogeneity of I_{NS} with respect to Ca^{2+} removal is due to a difference in the rate of decrease in intracellular $[Ca^{2+}]$.

Effects of A-23187 on I_{NS}

The foregoing results suggest that the activity of NS channels in the chromaffin cell also depends partially on intracellular Ca^{2+}. To elucidate further this putative Ca^{2+}-dependent property, the effects of A-23187, a Ca^{2+} ionophore, were examined. When 0.5 or 1 μM A-23187 was added to normal solution, outward currents were transiently generated in three of six cells (Figure 5a). After decay of this outward current, the level of holding current reverted to control, with no noticeable generation of an inward current. Subsequently, the application of 3 μM muscarine produced a larger I_{NS} (30% increase). This enhancement of the muscarine-induced I_{NS} was not due to a spontaneous variation of current since I_{NS} of a constant amplitude was generated three consecutive times before the addition of the Ca^{2+} ionophore and the enhancement did not occur in the absence of external Ca^{2+} (Figure 5b). Thus, the enhancing effect of A-23187 is likely to be due to an increase in intracellular $[Ca^{2+}]$.

Effects of calmodulin-related agents

The results obtained with Ca^{2+} removal and A-23187 indicate that Ca^{2+} mobilization is not a prerequisite for the generation of I_{NS}; however, this observation does not exclude the involvement of CaM kinase II. We then investigated the possible involvement of this kinase using the inhibitors W-5 and W-7. If calmodulin was present in the signal pathway,

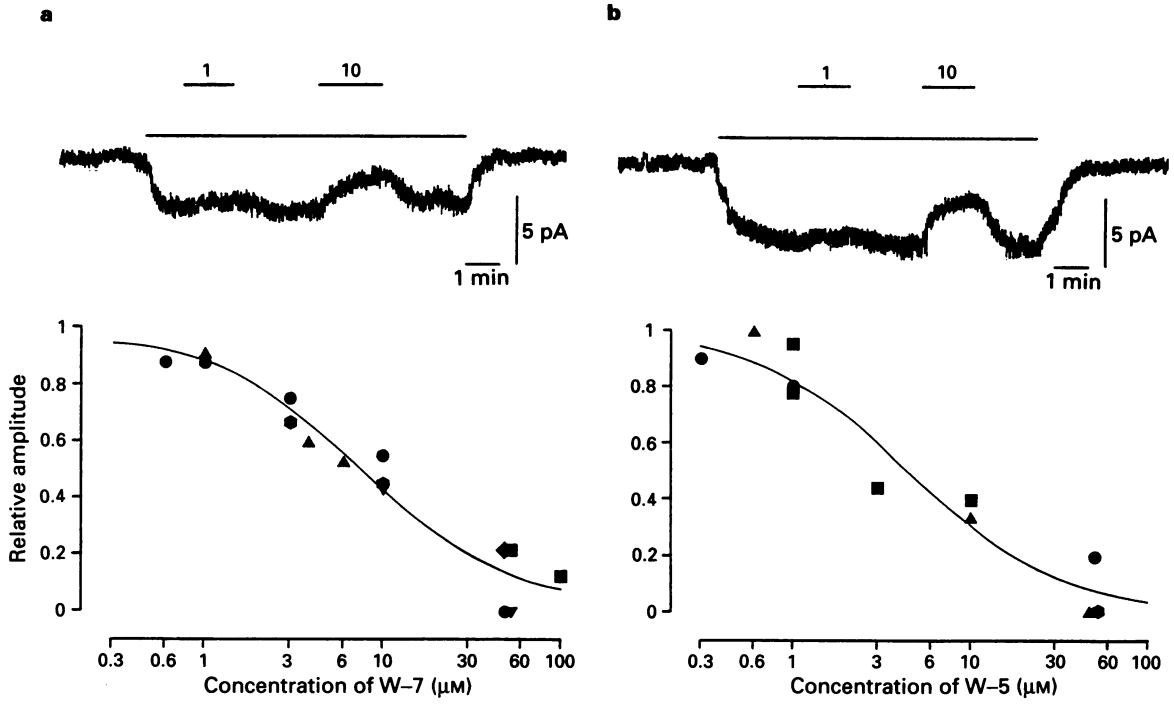


Figure 6 Dose-response curves for W-7 and W-5-induced inhibition of I_{NS}. (a) and (b) Dose-dependent inhibition by W-7 and W-5, respectively. Upper, actual traces of 1 μM muscarine-induced I_{NS} in the presence and absence of W-7 or W-5. Muscarine was added to normal solution during the period indicated by a horizontal line, and 1 and 10 μM W-7 or W-5 were further added to muscarine-containing perfusate during the indicated period. Lower, amplitudes of I_{NS} in the presence of W-7 or W-5 were expressed relative to that in the absence. Rectangular hyperbolas with IC_{50}s of 7.6 ($r = 0.970$) and 4.6 μM ($r = 0.964$) were fitted to the inhibitions by W-7 and W-5, respectively. The same symbols in each figure represent the same cells.

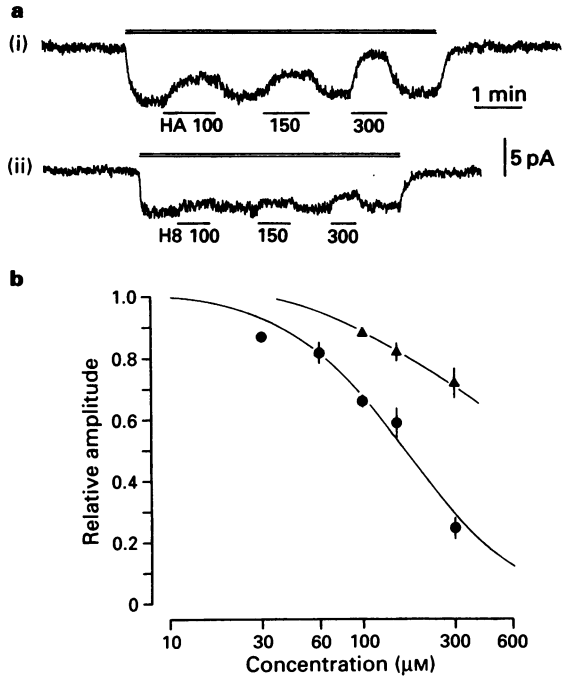


Figure 7 Effects of HA1004 and H-8 on muscarine-induced I_{NS}. (a) HA1004 (i) or H-8 (ii) induced reversible inhibition of 3 μM muscarine-induced I_{NS} in a dose-dependent manner; 100, 150, or 300 μM HA1004 or H-8 was added to muscarine-containing solution (double line) during the indicated period. (b) Relative amplitudes of muscarine I_{NS} in the presence of HA1004 (●) or H-8 (▲) were plotted against concentrations. I_{NS} in the presence of inhibitor was expressed relative to that in the absence. Sigmoid curve with I_{max} of 1, K_A of 163 μM, and Hill coefficient of −1.5 (r, 0.945) was fitted to data for HA1004 inhibition (see Methods). The curve for H-8 inhibition was drawn by eye. Data for HA1004 and H-8 represent mean ± s.e.mean of 3 to 7 observations at each concentration and of 5 to 6, respectively.

W-7 should induce a more potent inhibition than W-5 (Hidaka *et al.*, 1981). When W-5 or W-7 was added to normal solution, the holding current level at −40 mV was not significantly altered. On the other hand, the addition of either agent to 1 μM muscarine-containing perfusate led to the inhibition of I_{NS} in a dose-dependent manner (upper part of Figure 6). This inhibition did not require pretreatment, and withdrawal of W-5 or W-7 readily restored I_{NS} to the control level. The lower panels of Figure 6 represent summaries of the dose-dependent inhibition. Rectangular hyperbolas with IC_{50}s of 4.6 and 7.6 μM fit well to data points for W-5 and W-7, respectively. Next, we investigated effects of compound 5 since this agent has been reported to be a potent inhibitor ($IC_{50} = 0.2$ μM) of CaM kinase II (O'Dell *et al.*, 1991). Simultaneous application of 10 μM compound 5 and 1 μM muscarine for at least 10 min induced no change in I_{NS}. The amplitude of muscarine-induced I_{NS} was 102.3 ± 2.7% ($n = 3$) of I_{NS} prior to the application.

Effects of protein kinase C-related agents

Another possible mediator of the muscarinic signal is PKC. The reversible suppression of I_{NS} by H-7, a general kinase inhibitor, is compatible with the involvement of this kinase, although the IC_{50} for the inhibition was about 50 times larger than a K_i against PKC (Inoue & Imanaga, 1993). Thus we investigated effects of HA1004 and H-8 on 3 μM muscarine-induced I_{NS} since these agents are 6.7 and 2.5 times less potent than H-7, respectively (Hidaka *et al.*, 1984). When HA1004 or H-8 was added to normal solution, the holding current level of −40 mV was not significantly altered. On the other hand, the addition of either agent to the 3 μM muscarine-containing perfusate resulted in the dose-dependent inhibition of I_{NS}. Figure 7a shows that suppression by the inhibitors did not require pretreatment and termination of the application readily restored the current to the control level. With the addition of 300 μM HA1004 or H-8, I_{NS} was

reduced to 25 ± 3% ($n = 8$) or 72 ± 5% ($n = 5$) of control, values smaller or larger than that (46 ± 3%) in the presence of H-7, respectively. Figure 7b summarizes the dose-dependent inhibitions. Data points for HA1004 fell on a sigmoid curve with a Hill coefficient of −1.5 and an IC_{50} of 163 μM. This value of IC_{50} was smaller than that (254 μM) for the H-7 inhibition. These results suggest that PKC may not be involved in production of the current.

The effects of phorbol esters on muscarine I_{NS} were then examined (Figure 8). When 1 μM phorbol 12, 13-dibutyrate was added to the perfusate, the holding current level was not noticeably altered. On the contrary, I_{NS} in response to 3 μM muscarine was successively diminished during the application (●). About 5 min after start of the treatment, I_{NS} induced by muscarine (added to normal solution without the phorbol ester) was suppressed by 67 ± 14% ($n = 4$) and 20 min later the response disappeared almost completely. On the other hand, 4α-phorbol 12, 13-didecanoate, inactive in stimulating PKC (Castagna *et al.*, 1982), was without effect (▲). When one cell was subjected to treatment with the inactive phorbol ester and then with the active phorbol ester for 20 min each, I_{NS} was completely suppressed. Thus, the inhibition by phorbol 12, 13-dibutyrate is probably linked to the activation of PKC.

Properties of the receptor responsible for muscarine I_{NS}

Previous K_Ds for pirenzepine and AF-DX 116 found in oxotremorine-induced I_{NS} may have been distorted by run-down of the current under conditions of conventional whole-cell recording, even though care had been taken to lessen the distortion. In the present experiment, most of this kind of error could be avoided by use of the nystatin method. Figure 9a shows I_{NS}s induced by various concentrations of muscarine in the presence and absence of 60 nM pirenzepine. As the full development of inhibition required at least 5 min of pretreatment, the effect of pirenzepine was investigated five min after application. This inhibition was reversed readily by washout of the antagonist. It is evident that the pirenzepine shifts the dose-response curve for muscarine-induced I_{NS} to the right by sixfold (Figure 9b). A similar comparison of the dose-response curve in presence and absence of 10, 30, 60, or 100 nM pirenzepine was done in the same cells, and the shift of dose-response curve was measured with respect to the amplitude of control I_{NS} induced by 1 μM muscarine. Schild analysis of these shifts gave an apparent K_D of 13 nM (95% confidence interval, 11 to 16 nM) for pirenzepine (Figure 9c).

In contrast to pirenzepine, the inhibition by AF-DX 116 developed fully with pretreatment for 2 min. This inhibition was also readily reversed after washout. Figure 10a shows I_{NS}s induced by various concentrations of muscarine in the presence and absence of 3 μM AF-DX 116. This inhibitor at 3 μM shifted the dose-response curve to the right by 8.8fold (Figure 10b). Schild analysis of the shifts in the presence of 0.3, 1, and 3 μM AF-DX 116 gave an apparent K_D of 365 nM (95% confidence interval, 283 to 470 nM) for AF-DX 116 (Figure 10c).

Discussion

Bath application of muscarine, but not oxotremorine, induced a transient I_O, probably due to activation of Ca^{2+}-dependent K^+ channels (Inoue & Kuriyama, 1990). This current was not induced by a second application of muscarine and was markedly diminished by prior exposure to caffeine under Ca^{2+}-free conditions. These results suggest that transient I_O is due to Ca^{2+} mobilized from intracellular store sites, which are at least in part caffeine-sensitive. Thus, muscarine is probably capable of stimulating PI hydrolysis in some chromaffin cells. This notion is consistent with the biochemical results that muscarine, but not oxotremorine, conspicuously enhanced PI hydrolysis in nerve ending preparations of the rat and guinea-pig cerebral cortex and in bovine chromaffin cells (Fisher *et al.*, 1983). However, the stimulation of PI turnover by muscarine may not account for its high efficiency in generating I_{NS} since neither the IP_3-Ca^{2+}-CaM Kinase II nor the DG-PKC pathway was involved in muscarinic stimulation of NS channels. The reasons for this conclusion are given below.

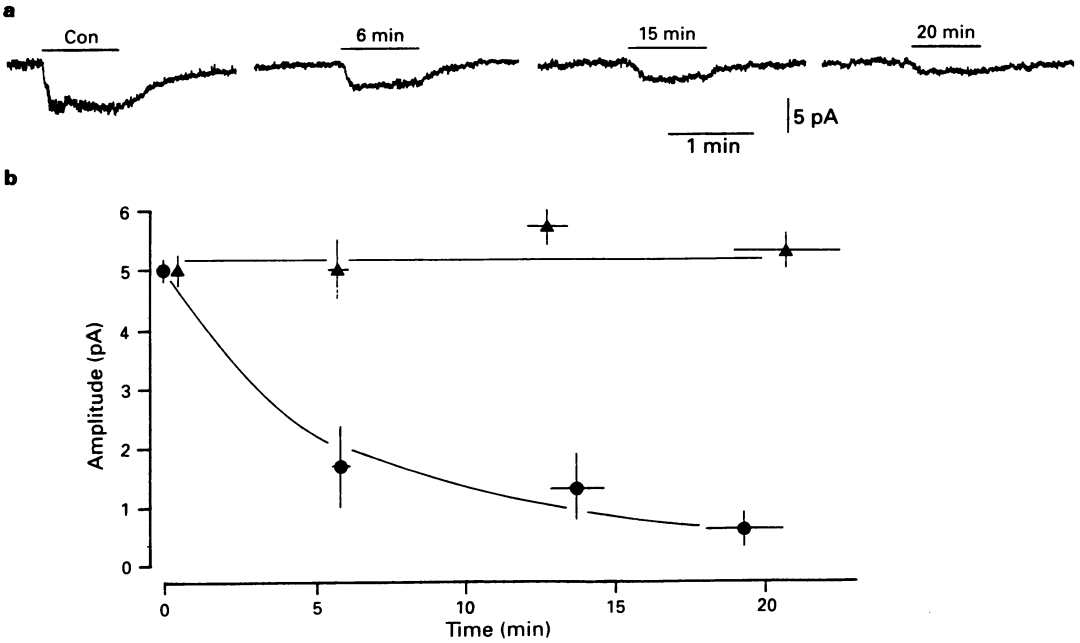


Figure 8 Inhibition of muscarine-induced I_{NS} by phorbol 12, 13-dibutyrate. (a) 3 μM muscarine induced I_{NS} before (Con) and 6, 15, and 20 min after application of 1 μM phorbol 12, 13-dibutyrate. Muscarine was added to normal solution, without the phorbol ester, for the indicated period. (b) Summary of 3 μM muscarine induced I_{NS} before and after application of 1 μM phorbol 12, 13-dibutyrate (●) or 1 μM 4α-phorbol 12, 13-didecanoate (▲). Data are mean ± s.e.mean of 4 and 3 cells for the former and the latter, respectively.

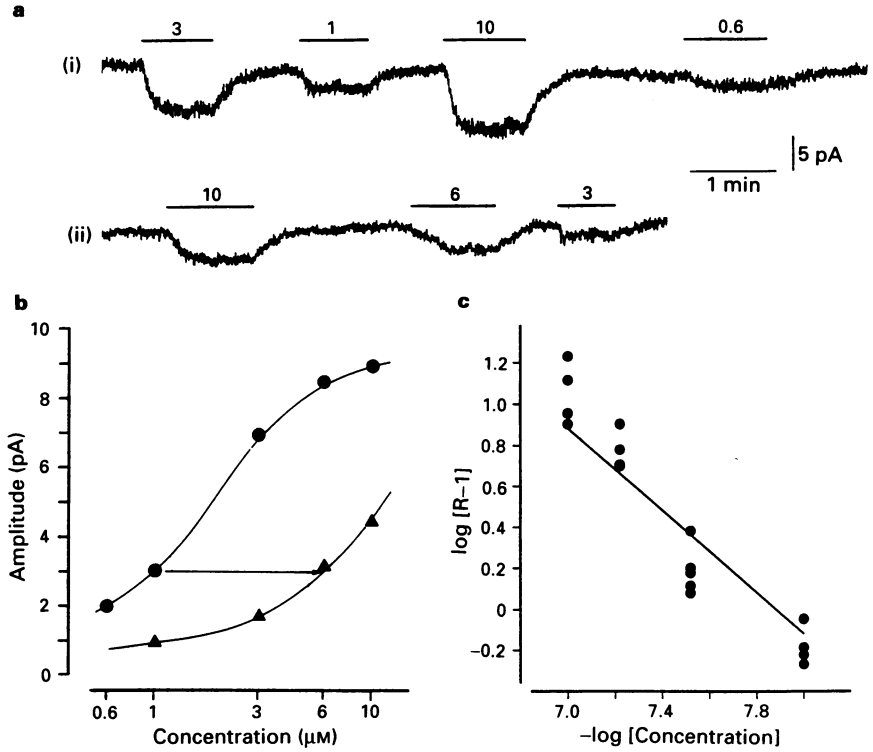


Figure 9 Antagonism of muscarine-induced I_{NS} with pirenzepine. (a) Muscarine-induced I_{NS} in the absence (i) and presence (ii) of 60 nM pirenzepine. In (i) 0.6, 1, 3, or 10 μM muscarine was added to normal solution during the indicated period; in (ii) 3, 6, or 10 μM was applied with pirenzepine, 5 min after pretreatment (see text). (b) Dose-response curves for muscarine I_{NS} in the absence (●) and presence (▲) of 60 nM pirenzepine. The amplitude of I_{NS} was plotted against concentrations of muscarine, and curves were drawn through data points by eye. Arrow indicates 6-fold shift of the dose-response curve. (a) and (b) the same cell. (c) Schild plot. Concentrations of muscarine responsible for the amplitude of 1 μM muscarine-induced I_{NS} were measured in the presence of 10, 30, 60, and 100 nM, as shown in (b). The ratios of these concentrations to 1 μM (control) were represented by R. Logarithms of R − 1 were plotted against − logarithms of pirenzepine concentrations. $y = 7.88\text{-}x$ was fitted to data points with a least-squares method (r, 0.935). K_D for pirenzepine is obtained with $y = 0$ and is 13 nM (95% confidence interval, 11 to 16 nM).

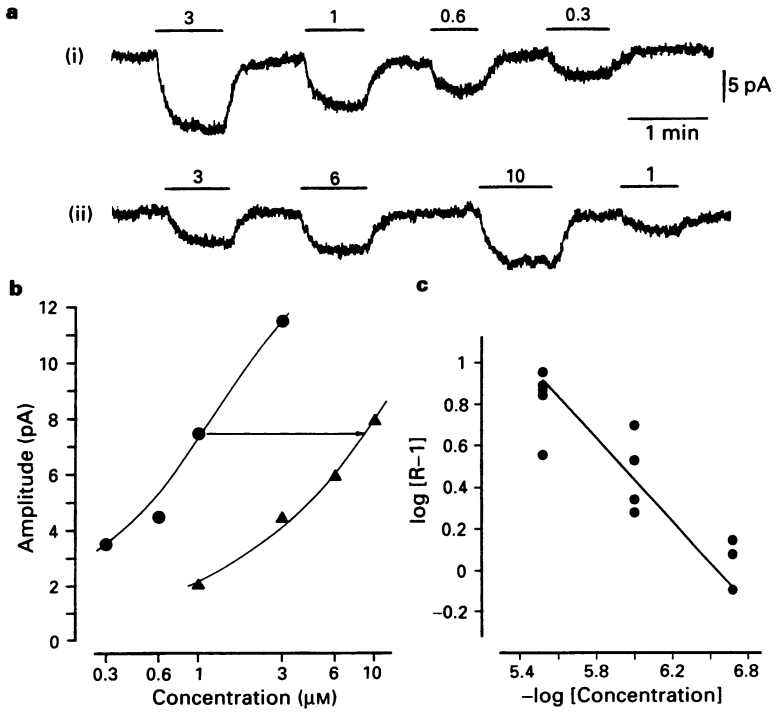


Figure 10 Antagonism of muscarine-induced I_{NS} with AF-DX 116. (a) Muscarine-induced I_{NS} in the absence (i) and presence (ii) of 3 μM AF-DX 116. In (i) 0.3, 0.6, 1 or 3 μM muscarine was added to normal solution during the indicated period; in (ii) 1, 3, 6, or 10 μM was applied with the antagonist, 2 min after pretreatment (see text). (b) Dose-response curves for muscarine I_{NS} in the absence (●) and presence (▲) of 3 μM AF-DX 116. The amplitude of I_{NS} was plotted against muscarine concentrations. Arrow indicates 8.8-fold shift of the dose-response curve. (c) Schild plot. Concentrations of muscarine responsible for the amplitude of 1 μM muscarine-induced I_{NS} were measured in the presence of 0.3, 1 and 3 μM AF-DX 116. R has the same meaning as for Figure 9. Logarithms of R − 1 were plotted against − logarithms of AF-DX 116 concentrations. $y = 6.44\text{-}x$ was fitted to data points with a least-squares method (r, 0.873). K_D for AF-DX 116 is obtained with $y = 0$ and is 365 nM (95% confidence interval, 283 to 470 nM).

An increase in intracellular [Ca^{2+}] was not a prerequisite for the generation of I_{NS}. Under Ca^{2+}-free conditions, a second application of muscarine always failed to evoke a transient I_O, probably due to the depletion of intracellular Ca^{2+}. In contrast, I_{NS} was suppressed only in about one third of cells exposed to Ca^{2+}-free solution. Thus, this successive decrease in I_{NS} in some cells may not be attributed to a diminished mobilization of intracellular Ca^{2+}, but rather to a slow decrease in the resting [Ca^{2+}]. In support of this notion, the amplitude of the I_{NS}s measured in the cells incubated in Ca^{2+}-free solution for more than 2 h was 44% of the current elicited subsequently in normal solution. Furthermore, the muscarine-induced I_{NS} was enhanced by application of the Ca^{2+} ionophore A-23187, but only in the presence of external Ca^{2+}. Thus, intracellular Ca^{2+} apparently plays a facilitating but not an essential role in generating I_{NS} and CaM kinase II probably does not activate NS channels. This idea was further supported by failure of the CaM kinase II inhibitors KN-62 (Inoue & Imanaga, 1993) and compound 5 to suppress the muscarine-induced I_{NS}. In addition, W-5 and W-7 were found to be equally potent as inhibitors of the response. If calmodulin is involved in the transduction process, W-7 should be more potent than W-5. Other calmodulin-dependent processes may not be involved.

The Ca^{2+} dependent PKCs, which are classified as classical PKCs (cPKC) (Nishizuka, 1992), are also unlikely to mediate the generation of I_{NS}. The rank order of isoquinolinesulfonamides in inhibiting I_{NS} was HA1004>H-7>H-8, being different from that (H-7>H-8>HA1004) in suppressing cPKCs (Hidaka *et al.*, 1984). Furthermore, bath application of phorbol 12, 13-dibutyrate did not mimic muscarinic stimulation of the current, rather it resulted in a successive suppression of I_{NS}. The time course of this suppression was roughly compatible with that of internalization of muscarinic receptors induced by phorbol ester in NIE-115 neuroblastoma cells (Liles *et al.*, 1986), where the predominant subtype is of the M_4 (Ashkenazi *et al.*, 1989). In addition, the failure of phorbol ester to produce I_{NS} excludes a possible involvement of another group of PKCs termed new PKC, which is insensitive to Ca^{2+} but is activated by phosphatidylserine and DG or phorbol esters. Whether the other group of PKCs termed atypical PKC is responsible for generation of I_{NS} remains an open question. So-called calmodulin antagonists, such as calmidazolium or W-5, were potent in inhibiting the muscarinic I_{NS}. These antagonists are known to inhibit not only calmodulin, but also PKCs, probably through binding a hydrophobic site of the enzymes (Hidaka & Hagiwara, 1987).

The dose-response curves for muscarine- and oxotremorine-induced I_{NS}s (Figure 2) show that muscarine is more efficient but less potent than oxotremorine. This difference between the two might be accounted for by the muscarinic subtypes involved. The results with pirenzepine and AF-DX 116, however, suggest that the same subtype is responsible for both currents. The K_D value of the muscarine-stimulated receptor for pirenzepine was estimated to be 13 nM, being about one fourth of that (50 nM) in case of oxotremorine stimulation (Inoue & Kuriyama, 1991). In light of the present findings, this difference may relate to an insufficient development of inhibition in the previous experiment, where cells were pretreated with the antagonist for only 2 min. On the contrary, the K_D value for AF-DX 116 was 365 nM, being 5.2 times larger than that (70 nM) found for the oxotremorine-stimulated receptor. This previous value is extremely small and indeed is smaller than that for the M_2 expressed in mammalian cell lines (Bonner *et al.*, 1988; Buckley *et al.*, 1989) or oocytes (Fukuda *et al.*, 1987), the subtype which has the highest affinity for the antagonist among the five subtypes (Bonner, 1989). Thus, the previous value might have been erroneously estimated, possibly because of run-down of I_{NS} under conventional whole-cell conditions. The K_Ds of muscarine-stimulated receptors for pirenzepine and AF-DX 116 agree with those of the M_4 endogenously present in NG 108-15 cells (Michel *et al.*, 1989) and that expressed in Chinese hamster ovary cells (CHO-K1) (Buckley *et al.*, 1989; Dörje *et al.*, 1991). Although these K_Ds alone would not exclude a possible involvement of M_1, the presence of only m4 transcript in the bovine adrenal medulla (Fernando *et al.*, 1991) and the rat phaeochromocytoma PC 12 cell line (Ashkenazi *et al.*, 1988) suggests that the M_4 receptor is involved in the generation of I_{NS} induced by muscarine and probably by oxotremorine.

We propose that muscarine efficiently stimulates the M_4 muscarinic receptor subtype to produce I_{NS} and that the second messengers resulting from PI hydrolysis, Ca^{2+} and PKC, do not transduce this response.

The study was supported in part by a Grant-in-Aid from the Ministry of Education, Science and Culture of Japan and by a grant from Uehara Memorial Foundation. Pirenzepine and AF-DX 116 are kind gifts from Boehringer Ingelheim (Germany).

References

ARUNLAKSHANA, O. & SCHILD, H.O. (1959). Some quantitative uses of drug antagonists. *Br. J. Pharmacol.*, **14**, 48–58.

ASHKENAZI, A., PERALTA, E.G., WINSLOW, J.W., RAMACHANDRAN, J. & CAPON, D.J. (1988). Functional role of muscarinic acetylcholine receptor subtype diversity. *Cold Spring Harbor Symp. Quant. Biol.*, **53**, 263–272.

ASHKENAZI, A., RAMACHANDRAN, J. & CAPON, D.J. (1989). Acetylcholine analogue stimulates DNA synthesis in brain-derived cells via specific muscarinic receptor subtypes. *Nature*, **340**, 146–150.

BELLE, H.V. (1981). R 24 571: a potent inhibitor of calmodulin-activated enzymes. *Cell Calcium*, **2**, 483–494.

BENHAM, C.D., BOLTON, T.B. & LANG, R.J. (1985). Acetylcholine activates an inward current in single mammalian smooth muscle cells. *Nature*, **316**, 345–347.

BERRIDGE, M.J. (1993). Inositol trisphosphate and calcium signalling. *Nature*, **361**, 315–325.

BONNER, T.I. (1989). New subtypes of muscarinic acetylcholine receptors. *Trends Pharmacol. Sci. Suppl.*, 11–15.

BONNER, T.I., YOUNG, A.C., BRANN, M.R. & BUCKLEY, N.J. (1988). Cloning and expression of the human and rat m5 muscarinic acetylcholine receptor genes. *Neuron*, **1**, 403–410.

BUCKLEY, N.J., BONNER, T.I., BUCKLEY, C.M. & BRANN, M.R. (1989). Antagonist binding properties of five cloned muscarinic receptors expressed in CHO-K1 cells. *Mol. Pharmacol.*, **35**, 469–476.

CASTAGNA, M., TAKAI, Y., KAIBUCHI, K., SANO, K., KIKKAWA, U. & NISHIZUKA, K. (1982). Direct activation of calcium-activated, phospholipid-dependent protein kinase by tumor-promoting phorbol esters. *J. Biol. Chem.*, **257**, 7847–7851.

DÖRJE, F., WESS, J., LAMBRECHT, G., TACKE, R., MUTSCHLER, E. & BRANN, M.R. (1991). Antagonist binding profiles of five cloned human muscarinic receptor subtypes. *J. Pharmacol. Exp. Ther.*, **256**, 727–733.

FERNANDO, J.C.R., ABDALLAH, E.-S.A.M., EVINGER, M., FORRAY, C. & EL-FAKAHANY, E.E. (1991). The presence of an M_4 subtype muscarinic receptor in the bovine adrenal medulla revealed by mRNA and receptor binding analyses. *Eur. J. Pharmacol.*, **207**, 297–303.

FISHER, S.K., KLINGER, P.D. & AGRANOFF, B.W. (1983). Muscarinic agonist binding and phospholipid turnover in brain. *J. Biol. Chem.*, **258**, 7358–7368.

FUKUDA, K., KUBO, T., AKIBA, I., MAEDA, A., MISHINA, M. & NUMA, S. (1987). Molecular distinction between muscarinic acetylcholine receptor subtypes. *Nature*, **327**, 623–625.

HIDAKA, H. & HAGIWARA, M. (1987). Pharmacology of the isoquinoline sulfonamide protein kinase C inhibitors. *Trends Pharmacol. Sci.*, **8**, 162–164.

HIDAKA, H., INAGAKI, M., KAWAMOTO, S. & SASAKI, Y. (1984). Isoquinolinesulfonamides, novel and potent inhibitors of cyclic nucleotide dependent protein kinase and protein kinase C. *Biochemistry*, **23**, 5036–5041.

HIDAKA, H., SASAKI, Y., TANAKA, T., ENDO, T., OHNO, S., FUJII, Y. & NAGATA, T. (1981). N-(6-aminohexyl)-5-chloro-1-naphthalene-sulfonamide, a calmodulin antagonist, inhibits cell proliferation. *Proc. Natl. Acad. Sci. U.S.A.*, **78**, 4354–4357.

HORN, R. & MARTY, A. (1988). Muscarinic activation of ionic currents measured by a new whole-cell recording method. *J. Gen. Physiol.*, **92**, 145–159.

HOYER, D. & BODDEKE, H.W.G.M. (1993). Partial agonists, full agonists, antagonists: dilemmas of definition. *Trends Pharmacol. Sci.*, **14**, 270–275.

INOUE, R. & ISENBERG, G. (1990a). Effect of membrane potential on acetylcholine-induced inward current in guinea-pig ileum. *J. Physiol.*, **424**, 57–71.

INOUE, R. & ISENBERG, G. (1990b). Intracellular calcium ions modulate acetylcholine-induced inward current guinea-pig ileum. *J. Physiol.*, **424**, 73–92.

INOUE, M. & IMANAGA, I. (1993). Phosphorylation-dependent regulation of nonselective cation channels in guinea pig chromaffin cells. *Am. J. Physiol.*, **34**, C343–C348.

INOUE, M. & KURIYAMA, H. (1990). Muscarine induces two distinct current responses in adrenal chromaffin cells of the guinea-pig. *Jpn. J. Physiol.*, **40**, 679–691.

INOUE, M. & KURIYAMA, H. (1991). Muscarinic receptor is coupled with a cation channel through a GTP-binding protein in guinea-pig chromaffin cells. *J. Physiol.*, **436**, 511–529.

INOUE, M. & YOSHII, M. (1992). Modulation of ion channels by somatostatin and acetylcholine. *Prog. Neurobiol.*, **38**, 203–230.

LEVIN, R. & WEISS, B. (1977). Binding of trifluoperazine to the calcium-dependent activator of cyclic nucleotide phosphodiesterase. *Mol. Pharmacol.*, **13**, 690–697.

LILES, W.C., HUNTER, D., MEIER, K.E. & NATHANSON, N.M. (1986). Activation of protein kinase C induces rapid internalization and subsequent degradation of muscarinic acetylcholine receptors in neuroblastoma cells. *J. Biol. Chem.*, **261**, 5307–5313.

MICHEL, A.D., DELMENDO, R., STEFANICH, E. & WHITING, R.L. (1989). Binding characteristics of the muscarinic receptor subtype of the NG 108–15 cell line. *Naunyn-Schmied. Arch. Pharmacol.*, **340**, 62–67.

NISHIZUKA, Y. (1992). Intracellular signalling by hydrolysis of phospholipids and activation of protein kinase C. *Science*, **258**, 607–614.

O'DELL, T.J., KANDEL, E.R. & GRANT, S.G.N. (1991). Long-term potentiation in the hippocampus is blocked by tyrosine kinase inhibitors. *Nature*, **353**, 558–560.

SHENOLIKAR, S. (1988). Protein phosphorylation: hormones, drugs, and bioregulation. *FASEB J.*, **2**, 2753–2764.

Received June 14, 1994
Revised August 10, 1994
Accepted September 22, 1994)

British Journal of Pharmacology (1995) 114, 428–432 © 1995 Stockton Press All rights reserved 0007–1188/95 $9.00

Pharmacological evidence that nitric oxide may be a retrograde messenger in the enteric nervous system

[1]S.Y. Yuan, [2,*]J.C. Bornstein & J.B. Furness

Departments of Physiology and *Anatomy and Cell Biology, University of Melbourne, Parkville, Vic. 3052, Australia

1 The effects of inhibition of nitric oxide synthase on neuro-neuronal and neuromuscular transmission during motility reflexes in the small intestine of the guinea-pig were examined.

2 Isolated segments of intestine were secured in a three chambered organ bath so that different parts of the reflex pathways could be independently exposed to drug-containing solutions. Reflexes were evoked by distension or compression of the mucosa in two adjacent chambers and reflex responses were recorded from the circular muscle with intracellular microelectrodes in the third chamber. Thus, the actions of drugs at connections between sensory neurones and interneurones, between interneurones and other interneurones and at motor neurones could be distinguished.

3 N^G-monomethyl-L-arginine (L-NMMA; 100 μM), an inhibitor of nitric oxide synthase, did not affect the ascending excitatory reflex when added to either the central stimulation chamber or the recording chamber.

4 In contrast, L-NMMA (100 μM) enhanced the descending inhibitory reflex when added to the chamber in which stimuli were applied. This effect was prevented by prior exposure to L-arginine (100 μM), which had no effect by itself. Conduction of reflexes between the stimulus chamber and the recording chamber was unaffected by the presence of L-NMMA in an intervening chamber.

5 L-NMMA (100 μM) added to the recording chamber depressed the descending inhibitory reflex, an effect that was prevented by previous exposure to L-arginine.

6 The nitric oxide donor, sodium nitroprusside (100 μM), added to the stimulus chamber, depressed both ascending excitatory and descending inhibitory reflexes. When added to the middle chamber, sodium nitroprusside had no effect on conduction of reflexes through this chamber.

7 It is deduced that nitric oxide, released from the cell bodies of descending interneurones, suppresses transmission from synaptic connections made with them by enteric sensory neurones.

Keywords: Nitric oxide; intestinal motility; neurotransmitters; enteric nervous system; peristaltic reflex

Introduction

Over the last few years it has become clear that nitric oxide (NO) is almost certainly a transmitter of inhibitory motor neurones in the gastrointestinal tract (Stark & Szurszewski, 1992; Sanders & Ward, 1992). However, nitric oxide synthase (NOS) is not confined to neurones innervating muscle. It is found in many axons that terminate on the cell bodies and/or dendrites of neurones (Vincent & Kimura, 1992), although roles of NO in neuro-neuronal communication are not well defined by present experimental data.

In the guinea-pig gastrointestinal tract, immunohistochemical studies have shown that NOS is in inhibitory motor neurones innervating circular muscle, and in interneurones that run anally along the intestine and provide terminals to other myenteric ganglia (Costa *et al.*, 1992b; McConalogue & Furness, 1993). However, NOS-immunoreactivity is not found within neurones that have been identified electrophysiologically as sensory neurones, the circumferentially projecting AH/Dogiel type II neurones (unpublished observation). The NOS-containing interneurones are a subset of descending interneurones found within the guinea-pig small intestine and are also immunoreactive for several other bioactive substances, including vasoactive intestinal peptide, gastrin releasing peptide and dynorphin (Costa *et al.*, 1992a).

Mechanical stimulation of the intestinal wall evokes stereotyped reflexes consisting of excitation oral to the point of stimulation (ascending excitation) and relaxation anal to the point of stimulation (descending inhibition) (Bayliss & Starling, 1899; Smith *et al.*, 1990; Yuan *et al.*, 1991). The neuronal pathways responsible for these reflexes include mechanosensitive enteric sensory neurones which excite either ascending or descending interneurones. The respective interneurones then excite either excitatory motor neurones or inhibitory motor neurones (Bornstein *et al.*, 1991a).

In this study, we have examined whether the descending interneurones that contain NOS, and presumably release NO, modulate neurotransmission in the reflex pathways that control intestinal motility. To distinguish the sites of action of NO, a three chambered organ bath was used. Each chamber was separately perfused and reflexes were evoked with mechanical stimuli (distension or compression of the mucosal villi (Yuan *et al.*, 1991; 1994)) in the central chamber and in one end chamber. The reflex responses were recorded intracellularly from the circular muscle in the chamber at the other end of the preparation. This arrangement allowed drugs to be applied selectively to the region of the active sensory neurones, to a region in which the only active synapses would be those of interneurones and to a region containing the motor neurones supplying the circular muscle (Yuan *et al.*, 1994).

Methods

In all experiments isolated segments of small intestine from adult guinea-pigs of 200–300 g, were used that were killed by a blow to the head and cutting the carotid arteries.

The dissection, superfusing solutions, recording procedures and methods for stimulation by distension or compression of

[1] Present address: Department of Physiology, Flinders University School of Medicine, Bedford Park, S.A. 5042, Australia
[2] Author for correspondence.

the mucosa are described elsewhere (Yuan *et al.*, 1991; 1994). Opened segments were pinned, mucosa uppermost, in a three chambered organ bath in which it was possible to superfuse separately different regions of the intestine (Yuan *et al.*, 1994). The partitions in this bath were separated by 10 mm and each partition was 1 mm thick, the central chamber had a volume of 1 ml and the outer chambers volumes of 3 ml. Set into the base of the bath were 2 distending balloons (11 mm apart): one in the central chamber and the other at an end. Mechanical stimuli, distension and/or compression of the mucosal villi (Yuan *et al.*, 1991), were applied to the intestinal wall in two of the chambers, while intracellular recordings were made from the circular muscle in the third with the distance between the centre of the nearer stimulation balloon and the recording site being 11 mm (Figure 1). The sensory neurones typically project less than 1 mm along the intestine (Bornstein *et al.*, 1991b), so stimuli applied in one chamber would excite only sensory neurones in that chamber and conduction of reflex activity between chambers would be via interneurones. Intracellular recordings were made from either the oral end or the anal end of the intestinal segment, so that both the ascending excitatory and the descending inhibitory pathway were studied (Yuan *et al.*, 1991). Each chamber was perfused separately. Nicardipine (3 μM) was present throughout each experiment to reduce spontaneous and neurogenic contractions which might dislodge the intracellular recording electrodes (Smith *et al.*, 1990).

Drugs were made up fresh each day in physiological saline and added to either the central stimulation chamber or the recording chamber by altering the perfusate reservoir. Thus, drugs were applied to specific points within each reflex pathway. In a previous study using this organ bath arrangement, it was found that the responses to reflex stimulation (distensions and mucosal compressions each lasting 9 s) remained reproducible over at least 30 min following the first stimulus (Yuan *et al.*, 1994). Accordingly, drugs were added to the relevant chamber immediately following the initial control responses and their effects were tested 15 min later. The drugs were then washed out, and responses were again recorded after another 15 min. In all experiments, the durations of the stimuli were 9 s.

Data were analysed by measuring the maximum amplitudes of the excitatory junction potentials (i.j.ps) and inhibitory junction potentials (i.j.ps). Data are expressed as mean ± standard error from at least 4 preparations. The significance of any differences was determined by a paired *t* test comparing the initial control with the response in the presence of a drug; differences were taken to be significant when $P<0.05$. Washout results were used to determine whether effects were reversible.

Results

Compound e.j.ps were recorded in the circular muscle oral to the stimulus when the mucosa was distorted by compression or the intestine was distended. Compound i.j.ps were evoked anal to these stimuli. The different stimuli were delivered 2 min apart, so that any interactions between the reflexes were prevented (Yuan *et al.*, 1992).

Inhibition of NOS had markedly different effects on the ascending and descending reflex pathways. The NOS inhibitor L-NMMA (100 μM) (Moncada *et al.*, 1991) added to the chamber from which responses were evoked, to the chamber through which responses were conducted or to the chamber in which recordings were made, had no significant effect on compound e.j.ps recorded from the circular muscle oral to either stimulus (Figure 2). In contrast, L-NMMA altered the responses to activation of the descending inhibitory pathway, with its effect depending on the site of application.

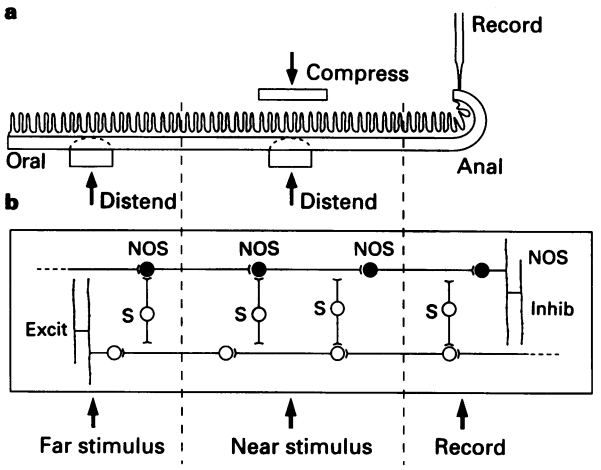


Figure 1 (a) Schematic diagram of the organ bath used in this study. Divisions between chambers are shown by dashed lines. (b) The neuronal circuit hypothesized to mediate motility reflexes in guinea-pig ileum (Bernstein *et al.*, 1991a). Chains of interneurones run orally (ascending interneurones) or anally (descending interneurones). At each level, interneurones receive input from local sensory neurones (S) and provide output to excitatory (ascending pathway) or inhibitory motor neurones supplying the circular muscle (descending pathway). Some descending interneurones and inhibitory motor neurones (filled cell bodies) contain NO synthase (NOS) (Costa *et al.*, 1992b). Drugs in the central chamber act on sensory neurones and interneurones in this chamber, but only on interneurones in pathways excited from the distant stimulation chamber. Drugs in the recording chamber act on transmission to motor neurones and on their transmission to the muscle.

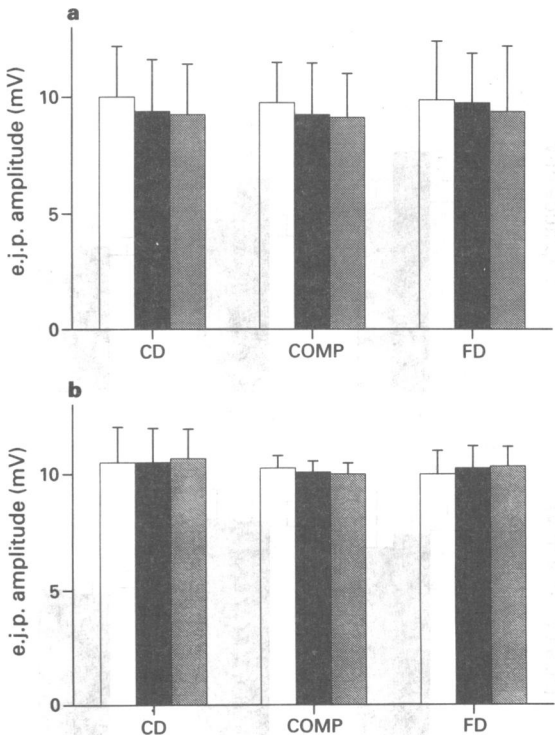


Figure 2 The NO synthase (NOS) inhibitor, N^G-monomethyl-L-arginine (L-NMMA; 100 μM) did not affect the ascending pathway when applied in the central (a) or the recording chamber (b). CD, distension in the central stimulation chamber; COMP, mucosal compression in the central chamber; FD, distension in the far chamber, Stimuli applied in the far chamber evoke reflexes which must propagate through the central chamber to be recorded, thus drugs in the central chamber would act on interneurones in the pathways excited from the far chamber. Open columns, controls; solid columns, responses in L-NMMA; and cross-hatched columns responses after washout.

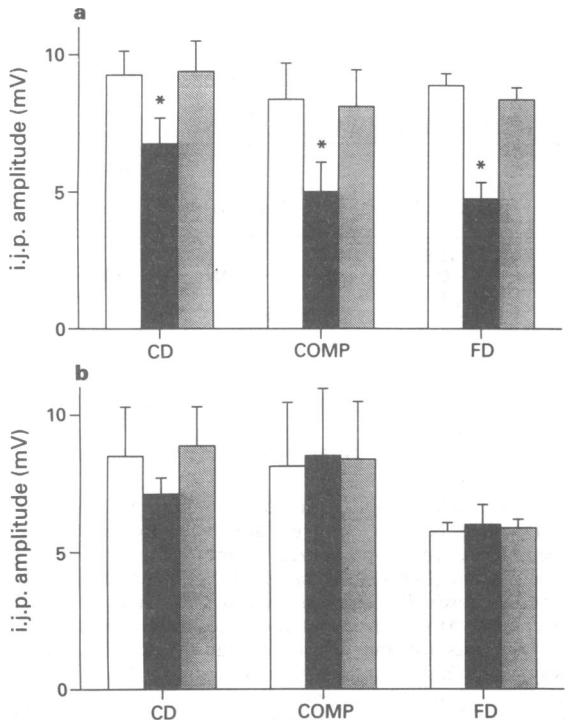


Figure 3 The effects of N^G-monomethyl-L-arginine (L-NMMA 100 μM) in the recording chamber on descending inhibitory reflexes in control solutions (a) and when L-arginine (100 μM) was present throughout the experiment (b). CD, distension in the central stimulation chamber; COMP mucosal compression in the central chamber; and FD distension in the far chamber. Open columns, controls; solid columns, responses in L-NMMA and cross-hatched columns, responses after washout. *Significantly different from control ($P<0.05$; paired t test).

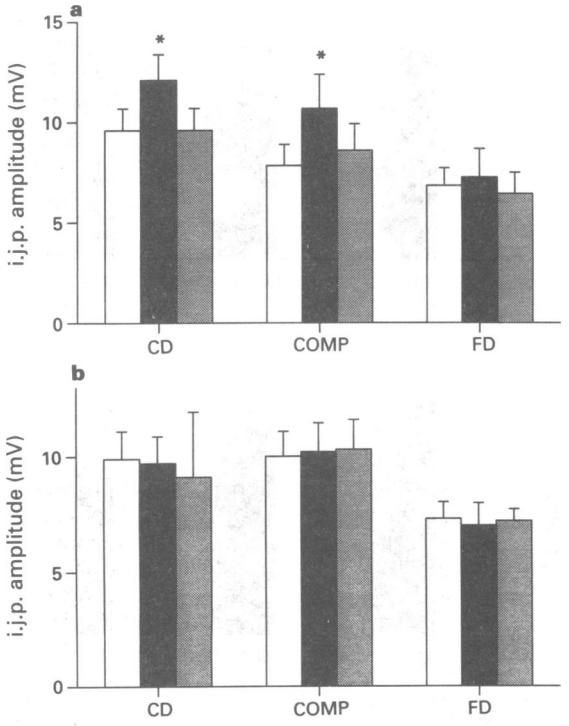


Figure 4 The effects of N^G-monomethyl-L-arginine (L-NMMA 100 μM) in the central stimulation chamber on descending inhibitory reflexes in control solutions (a) and when L-arginine (100 μM) was present throughout the experiment (b). CD, distension in the central stimulation chamber; COMP mucosal compression in the central chamber; and FD distension in the far chamber. Open columns, controls; solid columns, responses in L-NMMA and cross-hatched columns, responses after washout. *Significantly different from control ($P<0.05$; paired t test).

When added to the recording chamber, L-NMMA (100 μM) *depressed* compound i.j.ps evoked by either distension or compression of the mucosal villi (Figure 3a). When L-arginine (100 μM), the normal substrate for NOS, was added to this chamber it produced no change in the reflex (not illustrated). The depression produced by L-NMMA, however, was completely abolished when L-arginine, which opposes the effect of synthase inhibition (Moncada *et al.*, 1991), was present throughout the experiments (Figure 3b).

Addition of L-NMMA (100 μM) to the central chamber *enhanced* descending reflexes evoked by stimuli applied in this chamber (Figure 4a). L-Arginine (100 μM) had no effect by itself, but prevented the enhancement produced by L-NMMA (Figure 4b).

Conduction of reflexes through the central chamber was unaffected by L-NMMA (Figure 4a). In these experiments, reflexes were initiated from the oral end chamber, recordings were made in the anal end chamber and the L-NMMA was placed in the central chamber.

While the effects of inhibition of endogenous NO synthesis were confined to the descending pathway, the effects of the NO donor sodium nitroprusside (SNP) were not (Figure 5). When reflexes were elicited from the central chamber and recordings were made in the adjacent chamber, SNP (100 μM) added to the central chamber depressed both ascending and descending reflexes evoked by mucosal compression or by distension (Figure 5). There was no effect of SNP on conduction of either ascending or descending reflexes along the intestine in experiments in which the end chambers were used for stimuli and recording and SNP was added to the chamber in between (Figure 5).

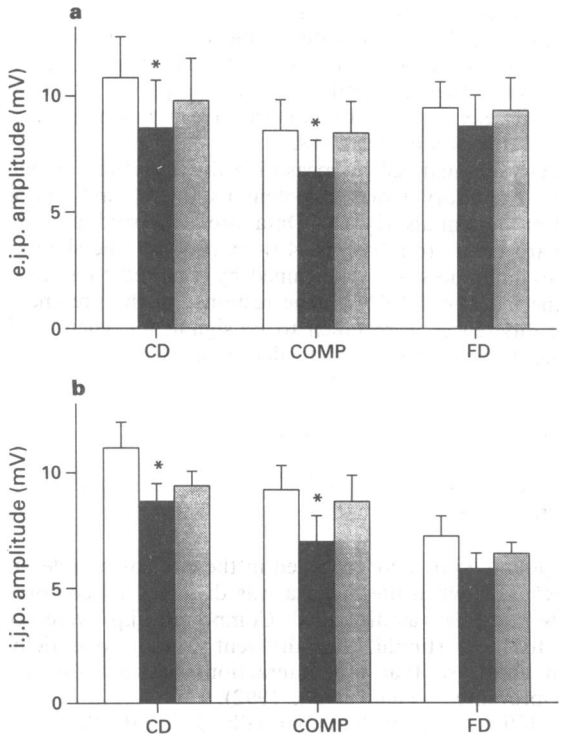


Figure 5 The effect of a NO donor, sodium nitroprusside (100 μM), added to the central stimulation chamber on (a) the ascending reflex ($n = 5$) and (b) the descending reflex ($n = 6$). CD, distension in the central stimulation chamber; COMP mucosal compression in the central chamber; and FD distension in the far chamber. Open columns, controls; solid columns, responses in L-NMMA; and cross-hatched columns, responses after washout. In each case, the NO donor depressed reflexes evoked from the central chamber, but had no significant effect on transmission of reflexes through this chamber. *Significantly different from control ($P<0.05$; paired t test).

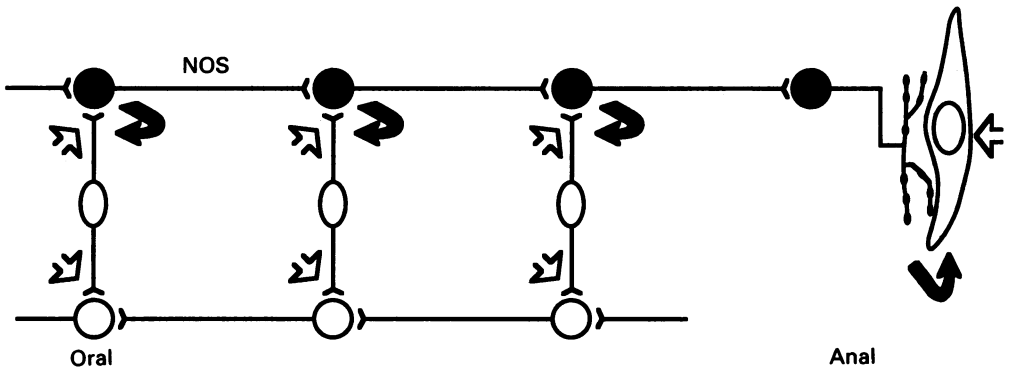


Figure 6 Potential sites of action of endogenous (solid arrow) and exogenous (open arrow) NO in the reflex pathways. Neurones that contain NOS have filled cell bodies, those lacking NOS have open cell bodies. Blockade of the synthesis of NO appears to *depress* inhibitory transmission from inhibitory motor neurones to the circular muscle, but has no effect on excitatory transmission. It also appears to *enhance* transmission from sensory neurones to interneurones in the reflex pathways. NO supplied by the donor, SNP, depressed transmission from sensory neurones to both ascending and descending pathways. However, the only neuronal sources of endogenous NO that could alter sensory to interneurone transmission are the cell bodies of NOs-containing descending interneurones.

Discussion

The present observations indicate that NO can modulate intestinal reflexes via an action on neurones, in addition to its role in inhibitory neuromuscular transmission (Figure 6). Immunohistochemical studies indicate that NOS is found within descending interneurones and inhibitory motor neurones, but not in enteric sensory neurones (Costa *et al.*, 1992b). The failure, however, of either L-NMMA or SNP to alter transmission of the reflexes along the intestine suggests that, despite the presence of this enzyme in descending interneurones, NO is not involved in orthograde transmission from such neurones during descending inhibitory reflexes. Nevertheless, the enhancement of descending, but not ascending, reflexes by L-NMMA suggests that NO released from the descending interneurones inhibits transmission at some point in the descending reflex pathway. As this effect is observed when L-NMMA is in the stimulation chamber, the most likely sites of action are the synapses between sensory neurones and interneurones. If NO acts at these synapses, it would be as a retrograde transmitter, released by the interneurone cell body, or dendrites, and acting back on the synaptic endings of the sensory neurone to inhibit transmission (Figure 6). Interestingly, NO from the donor, SNP, inhibits both ascending and descending reflexes, when added to the stimulation chamber. This suggests that responsiveness to exogenous NO occurs at sensory neurone to interneurone synapses, but not interneurone to interneurone synapses of both ascending and descending reflexes.

The conclusion that SNP acts at sensory to interneurone connections is consistent with the results of Kunze *et al.* (1993). They found that transmission from sensory neurones to descending interneurones is largely via slow excitatory synaptic potentials (e.p.s.ps), and it has been reported that NO (from SNP) selectively depresses non-cholinergic slow e.p.s.ps in myenteric neurones (Tamura *et al.*, 1993). Neither the present results nor those of Tamura *et al.* (1993) can exclude the possibility that the effect of NO is on the intracellular mechanism responsible for generation of the slow e.p.s.ps within the NOS-immunoreactive interneurones, rather than being on the release of neurotransmitter from sensory neurones. Such an intracellular site of action would account for the specificity of the NOS inhibitor for the descending pathway.

The reduction of the amplitudes of the compound i.j.ps seen when L-NMMA was added to the recording chamber provides further evidence that NO plays a significant role in transmission from inhibitory motor neurones to the circular muscle. The simplest explanation for this observation is that L-NMMA interferes with the synthesis and release of NO from the inhibitory motor neurones, thereby reducing its effects on the circular muscle. This is consistent with the results of a variety of other workers who have come to similar conclusions as a result of experiments employing electrical stimulation to excite the inhibitory motor neurones (for reviews see Sanders & Ward, 1992; Stark & Szurszewski, 1992). However, this interpretation conflicts with the observations of Smith and colleagues, who found that the compound i.j.ps evoked in descending reflexes in the guinea-pig small intestine were abolished by apamin (Smith & Furness, 1988; Smith *et al.*, 1990). Electrically evoked i.j.ps in this preparation have two components: an initial fast component, which is blocked by apamin and a later, slower component, which is insensitive to apamin, but is blocked by inhibitors of NOS (Niel *et al.*, 1983; Lyster *et al.*, 1992). The apamin-sensitive component is, if anything, enhanced by inhibition of NOS (Lyster *et al.*, 1992). The compound i.j.ps evoked by distension reach their peak amplitude within 0.5 s of the beginning of the response (Smith *et al.*, 1990); accordingly, the amplitudes measured in the present experiments almost certainly correspond to the fast component of the electrically evoked i.j.ps. Thus, there is a discrepancy between the effects of inhibition of NOS on the electrically evoked fast i.j.ps and reflexly evoked i.j.ps, which might suggest that, although NO does not play a role in transmission between interneurones, it may play a role in transmission between interneurones and the inhibitory motor neurones.

The difficulty of interpreting the results of NOS inhibition in the recording chamber highlights a general problem when drugs which may act at several sites to have opposing effects are applied to all classes of neurones simultaneously. A knowledge of effects of NOS inhibitors at specific sites does not allow the final outcome for behaviour of the whole organ to be readily predicted when inhibition of NOS facilitates one arm of the reflex arc, and depresses, but does not abolish, the other. Nor does application of a NOS inhibitor to the whole organ allow the sites of action to be clearly deduced. The final outcome in each case will depend on the relative roles of the different interacting parts of the system.

This work was supported by a grant from SmithKline Beecham Australia and a grant from the National Health and Medical Research Council of Australia. We thank Mr Jim Pringle for his help in constructing the organ bath and Dr Tom Cocks for helpful comments on the manuscript.

References

BAYLISS, W.M. & STARLING, E.H. (1899). The movements and innervation of the small intestine. *J. Physiol.*, **24**, 99–143.

BORNSTEIN, J.C., FURNESS, J.B., SMITH, T.K. & TRUSSELL, D.C. (1991a). Synaptic responses evoked by mechanical stimulation of the mucosa in morphologically characterized myenteric neurones of the guinea pig ileum. *J. Neurosci.*, **11**, 505–518.

BORNSTEIN, J.C., HENDRIKS, R., FURNESS, J.B. & TRUSSELL, D.C. (1991b). Ramifications of the axons of AH-neurones injected with the intracellular marker biocytin in the myenteric plexus of the guinea pig small intestine. *J. Comp. Neurol.*, **314**, 437–451.

COSTA, M., BROOKES, S.J.H., WATERMAN, S.A. & MAYO, R. (1992a). Enteric neuronal circuitry and transmitters controlling intestinal motor function. *In Advances in the Innervation of the Gastrointestinal Tract* ed. Holle, G.E. & Wood, J.D. pp. 115–121 Exerpta Medica, Amsterdam, London, New York, Tokyo: Elsevier Scientific Publishers B.V.

COSTA, M., FURNESS, J.B., POMPOLO, S., BROOKES, S.J.H., BORNSTEIN, J.C., BREDT, D.S. & SNYDER, S.H. (1992b). Projections and chemical coding of neurones with immunoreactivity for nitric oxide synthase in the guinea pig small intestine. *Neurosci. Lett.*, **148**, 121–125.

KUNZE, W.A.A., FURNESS, J.B. & BORNSTEIN, J.C. (1993). Simultaneous intracellular recordings from enteric neurones reveals that myenteric AH neurones transmit via slow excitatory postsynaptic potentials. *Neuroscience*, **55**, 685–694.

LYSTER, D.J., BYWATER, R.A.R., TAYLOR, G.S. & WATSON, M.J. (1992). Effects of a nitric oxide synthase inhibitor on noncholinergic junction potentials in the circular muscle of the guinea-pig ileum. *J. Auton. Nerv. Syst.*, **41**, 187–196.

MCCONALOGUE, K. & FURNESS, J.B. (1993). Projections of nitric oxide synthesizing neurones in the guinea-pig colon. *Cell Tiss. Res.*, **271**, 545–553.

MONCADA, S., PALMER, R.M.J. & HIGGS, E.A. (1991). Nitric oxide: physiology, pathophysiology, and pharmacology. *Pharmacol. Rev.*, **43**, 109–142.

NIEL, J.P., BYWATER, R.A.R. & TAYLOR, G.S. (1983). Apamin-resistant post-stimulus hyperpolarization in the circular muscle of the guinea-pig ileum. *J. Auton. Nerv. Syst.*, **9**, 565–569.

SANDERS, K.M. & WARD, S.M. (1992). Nitric oxide as a mediator of nonadrenergic noncholinergic neurotransmission. *Am. J. Physiol.*, **262**, G379–G392.

SMITH, T.K., BORNSTEIN, J.C. & FURNESS, J.B. (1990). Distension-evoked ascending and descending reflexes in the circular muscle of guinea-pig ileum: an intracellular study. *J. Auton. Nerv. Syst.*, **29**, 203–213.

SMITH, T.K. & FURNESS, J.B. (1988). Reflex changes in circular muscle activity elicited by stroking the mucosa: An electrophysiological analysis in the isolated guinea-pig. *J. Auton. Nerv. Syst.*, **25**, 205–218.

STARK, M.E. & SZURSZEWSKI, J.H. (1992). Role of nitric oxide in gastrointestinal and hepatic function and disease. *Gastroenterology*, **103**, 1928–1949.

TAMURA, K., SCHEMANN, M. & WOOD, J.D. (1993). Actions of nitric oxide-generating sodium nitroprusside in myenteric plexus of guinea pig small intestine. *Am. J. Physiol.*, **265**, G887–G893.

VINCENT, S.R. & KIMURA, H. (1992). Histochemical mapping of nitric oxide synthase in the rat brain. *Neuroscience*, **46**, 755–784.

YUAN, S.Y., BORNSTEIN, J.C. & FURNESS, J.B. (1994). Investigation of the role of 5-HT_3 and 5-HT_4 receptors in ascending and descending reflexes to the circular muscle of guinea-pig small intestine. *Br. J. Pharmacol.*, **112**, 1095–1100.

YUAN, S.Y., FURNESS, J.B. & BORNSTEIN, J.C. (1992). Post-stimulus depression of reflex changes in circular muscle activity in the guinea-pig small intestine. *J. Auton. Nerv. Syst.*, **40**, 171–180.

YUAN, S.Y., FURNESS, J.B., BORNSTEIN, J.C. & SMITH, T.K. (1991). Mucosal compression elicits polarized reflexes and enhances responses of the circular muscle to distension in the small intestine. *J. Auton. Nerv. Syst.*, **35**, 219–226.

(Received June 28, 1994
Revised September 5, 1994
Accepted September 28, 1994).

British Journal of Pharmacology (1995) 114, 433-441 © 1995 Stockton Press All rights reserved 0007-1188/95 $9.00

Necessity of protein kinase C activity for maintenance of acetylcholine receptor function at snake twitch fibre endplates

Jean C. Hardwick & [1]Rodney L. Parsons

Department of Anatomy and Neurobiology, College of Medicine, University of Vermont, Burlington, VT 05405, U.S.A.

1 The extent of recovery of endplate sensitivity following a 5 or 10 min exposure to carbachol was determined from measurements of miniature endplate current (m.e.p.c.) amplitudes in voltage-clamped snake twitch fibre endplates. M.e.p.c. amplitude recovery was dependent on the carbachol concentration (0.27–5.4 mM) and duration of application. Staurosporine pretreatment (0.5 μM for ~15 min) further decreased the extent of m.e.p.c. amplitude recovery.

2 The decrease in m.e.p.c. amplitude at control endplates exposed to high concentrations of agonist (5.4 mM carbachol for 10 min) was due to an apparent decrease in postsynaptic receptor density, not to a change in the conductance of the acetylcholine (ACh)-activated channels.

3 Pretreatment with either 1 μM lavendustin A or 50 μM KN-62 had no effect on m.e.p.c. amplitude recovery, whereas pretreatment with either 0.5 μM staurosporine, 50 μM sphingosine, or 0.5 μM calphostin C significantly reduced m.e.p.c. amplitude recovery following carbachol exposure.

4 Sphingosine and staurosporine produced a concentration-dependent decrease in the extent of m.e.p.c. amplitude recovery, but had no effect on m.e.p.c. characteristics in the absence of carbachol. In addition, this decrease in m.e.p.c. amplitude was not due to the presence of a subpopulation of small amplitude m.e.p.cs.

5 Prolonged treatment (18–20 h) of muscles with 200 nM phorbol 12-myristate 13-acetate (PMA), to down regulate protein kinase C, resulted in a significant reduction in m.e.p.c. amplitudes following exposure to carbachol. Conversely, treatment wtih 200 nM 4αPMA, an inactive analogue, had no effect on m.e.p.c. amplitude recovery.

6 Only large amplitude ACh-activated channels (~50 pS) were recorded from fibres either in the presence of 50 μM sphingosine or from fibres chronically exposed to PMA. However, following recovery from a 10 min exposure to 540 μM carbachol, both small conductance (~25 pS) and large conductance ACh-activated channels were recorded in both sphingosine- and phorbol-treated preparations. The conductance of these two populations of channels was virtually identical to those seen in staurosporine-treated fibres following carbachol exposure.

7 We conclude that protein kinase C is required for full recovery of AChR sensitivity following carbachol-induced receptor inactivation. Exposure to high concentrations of agonist for prolonged periods appears to result in the inactivation of a subpopulation of receptors. These receptors must be replaced or reactivated by a process involving protein kinase C. When this phosphorylation step is inhibited, the AChRs remain in an activatable form, but with a reduced conductance.

Keywords: Single channels; staurosporine; m.e.p.cs; snake twitch fibre endplates; acetylcholine receptors

Introduction

Muscle acetylcholine receptors (AChRs) are activated transiently by rapid onset, brief exposures of a nicotinic agonist such as carbachol. However, as the duration of exposure increases, some AChRs become refractory to further agonist stimulation and are said to be 'desensitized' (Katz & Thesleff, 1957). Recovery from desensitization induced by relatively short exposures to agonist is rapid and virtually complete with the desensitized receptors reverting back to an activatible state (Feltz & Trautman, 1982; Dilger & Liu, 1992). However, as the duration of exposure or concentration of agonist is increased, recovery can become incomplete. We found previously that prolonged exposure of snake twitch fibres to the nicotinic agonist, carbachol, produced incomplete recovery of miniature endplate current (m.e.p.c.) amplitudes and that this recovery was further reduced by pretreatment with a protein kinase inhibitor, staurosporine (Hardwick & Parsons, 1993a). The decrease in endplate sensitivity following carbachol exposure with staurosporine treatment was associated with the appearance of a population of small conductance (~25 pS) ACh-activated channels in addition to the normal (~50 pS) channels observed in control endplates both prior to and following agonist exposure (Hardwick & Parsons, 1993a). We proposed that the reduced m.e.p.c. amplitude at staurosporine-treated endplates following carbachol exposure resulted because neurally released quanta of acetylcholine activated a mixture of large and small conductance ACh-activated channels (Hardwick & Parsons, 1993a).

Staurosporine is a commonly used pharmacological tool in studies investigating the role of protein phosphorylation in cellular functions. Because of this well documented action, we suggested that phosphorylation of the AChR or a closely related protein, by a staurosporine-sensitive kinase is required to convert a population of receptor channel complexes with a small conductance state to those with a large conductance state (Hardwick & Parsons, 1993a). However, since staurosporine is a potent inhibitor of several protein kinases (Tamaoki *et al.*, 1986), we were not able to determine which protein kinase(s) might be required to convert the small conductance AChRs to the large conductance level. Furthermore, because inhibition of kinase activity was not measured directly, we could not rule out the possibility that the decrease in m.e.p.c. recovery by staurosporine was due to a pharmacological action of staurosporine pretreatment unrelated to kinase inhibition (Lo & Breitwieser, 1994). Consequently, the present studies were undertaken to examine the effects of several structurally different protein kinase

[1] Author for correspondence.

inhibitors on m.e.p.c. amplitude recovery and single channel properties before and after carbachol exposure. Our results demonstrate that several unrelated protein kinase C (PKC) inhibitors decrease the extent of m.e.p.c. amplitude recovery by the same amount. Furthermore, our results suggest that phosphorylation of the AChR or a closely related protein, by PKC is required for the conversion of the conductance of some channels from the small to the large value.

Methods

General methods

All of the experiments were done at room temperature on twitch fibre endplates of costocutaneous muscles isolated from garter snakes (*Thamnophis*) as described previously (Connor *et al.*, 1984; Hardwick *et al.*, 1991; Hardwick & Parsons, 1993a,b). Snakes were killed by rapid decapitation and the costocutaneous muscles, with portions of the rib and skin, were pinned out on sylgard-coated petri dishes in a control physiological solution containing in mM: NaCl 159, KCl 2.5, $MgCl_2$ 4.2, $CaCl_2$ 1.0, HEPES 1.0, pH 7.3 (Dionne & Parsons, 1981). For electrophysiological experiments, the muscles were switched to either a sodium propionate solution consisting of (in mM): Na propionate 159, K propionate 2.5, $MgSO_4$ 4.2, Ca propionate 1.0, HEPES 1.0, pH 7.3, or an isotonic potassium propionate solution for 20–30 min, containing in mM: K propionate 161, $MgCl_2$ 4.2, $CaCl_2$ 1.0, CsCl 5.0, HEPES 1.0, pH 7.3. The isotonic potassium solution was used in most experiments for several reasons. First, in this solution the frequency of miniature endplate currents (m.e.p.cs) is increased (generally about 10–20 events s^{-1} after approximately 20 min in the potassium propionate solution) which allows many m.e.p.cs to be recorded in a brief time period. Second, the membrane potential remained constant (approximately 0 mV) during agonist-induced activation and recovery. Third, in depolarized muscles, agonist-induced contracture of the fibres is minimized and the endplate can be clamped to several different voltages with only one monovalent cation, K^+, contributing to the recorded currents. The preparations could be maintained in the isotonic potassium solution for up to 90 min with no change in m.e.p.c. characteristics or frequency of release (Hardwick *et al.*, 1991).

Carbachol, staurosporine (Calbiochem, La Jolla, CA, U.S.A.), lavendustin A (Gibco BRL, Grand Island, NY, U.S.A.), (+)-erythro-sphingosine, calphostin C, KN-62, phorbol 12-myristate 13-acetate (PMA), and 4α-phorbol 12-myristate 13-acetate (4αPMA, LC Laboratories, MA, U.S.A.) were added directly to the solution bathing the muscles. Concentrated stocks of staurosporine, lavendustin A, calphostin C, KN-62 (1-[N,O-Bis(5-isoquinoline sulfonyl)-N-methyl-L-tyrosyl-4-phenylpiperizine), PMA, and 4αPMA were made up in dimethylsulphoxide (DMSO) and then diluted just prior to use (0.05% DMSO final). Stock solutions of sphingosine were made up in acidified ethanol and diluted just prior to use (0.1% EtOH final). We found no effect of either 0.05% DMSO or 0.1% EtOH alone on m.e.p.c. characteristics (data not shown).

For chronic exposure to phorbol esters, muscles were maintained in the normal sodium solution at room temperature for 18–20 h. Muscles were kept in either control solution alone, solution containing 200 nM PMA, or 200 nM 4αPMA. For single channel recordings, the muscles were treated for 18 h with PMA or 4αPMA and the phorbol concentrations were maintained during enzymatic cleaning of the muscles (an additional 3 h, Hardwick & Parsons, 1993a).

M.e.p.cs were recorded from individual endplates prior to carbachol exposure. The preparation was then incubated in solution containing 270 μM to 5.4 mM carbachol for times ranging from 5 to 10 min. The preparation was then washed with agonist-free solution and m.e.p.cs recorded again at times ranging from 5–15 min following the start of the wash.

Electrophysiological methods

For standard voltage clamp experiments, the endplate region of an individual endplate was voltage clamped by a two microelectrode system similar to that employed in previous studies (Dionne & Parsons, 1981; Connor *et al.*, 1984; Hardwick *et al.*, 1991; Hardwick & Parsons, 1993a,b). M.e.p.cs were recorded from fibres voltage clamped to −100 mV with a cutoff filter of 2 kHz and stored on PCM recorder (A.R. Vetter Co.) for later analysis. Mean m.e.p.c. amplitude and decay time constants were determined from an average of 50–100 m.e.p.cs using the programme SCAN, generously provided by Dr John Dempster (University of Strathclyde). The detection limit for m.e.p.c. amplitude measurements was usually approximately 1.2–2 nA. For measurement of endplate currents (e.p.cs), endplates voltage clamped to −100 mV were locally perfused with 20 μM carbachol as previously described (Connor *et al.*, 1984; Hardwick *et al.*, 1991). M.e.p.c. amplitude distributions were constructed from 500–1000 m.e.p.cs collected from a single endplate.

Single channel recordings were made on enzymatically cleaned endplates using the cell attached patch technique as previously described (Hamill *et al.*, 1981; Hardwick & Parsons, 1993a). Muscles were bathed in the isotonic potassium solution. The patch pipette also contained the isotonic potassium solution with the $MgCl_2$ concentration raised to 8.2 mM to facilitate seal formation and 1 μM ACh to activate the channels. Single channel activity was recorded with an Axopatch-1C amplifier with the output signal low-pass filtered at 5 kHz (4-pole Bessel) and stored on a PCM recorder for later analysis using the programme pClamp (Axon Instruments) with a sampling rate of 33 kHz.

Statistical analysis

All results are expressed as the mean ± s.e.mean obtained from '*n*' fibres as indicated. In additon, for the majority of experiments, data were obtained from at least three different animals, unless otherwise indicated. Statistical significance was determined by Student's two-tailed *t*-test or analysis of variance (ANOV) with $P<0.05$ considered significant.

Results

AChR inactivation increases as a function of agonist concentration and duration of exposure

To quantitate the dependence of m.e.p.c. amplitude recovery on carbachol concentration and time of exposure, we measured the extent of m.e.p.c. amplitude recovery in control and 0.5 μM staurosporine-treated muscle preparations following either a 5 min or 10 min exposure to carbachol using concentrations which ranged from 270 μM to 5.4 mM. In control fibres, voltage clamped to −100 mV, m.e.p.c. amplitude recovery following a 5 min exposure to low concentrations of carbachol was 90–100% (Figure 1). However, as the duration of carbachol exposure or concentration was increased, the extent of recovery was progressively decreased. In preparations pretreated wtih 0.5 μM staurosporine, the extent of recovery was consistently less than that seen in control endplates (see also Table 2).

We have proposed that the incomplete recovery of m.e.p.c. amplitude following prolonged carbachol exposure occurred because some AChRs were inactivated (Hardwick & Parsons, 1993b). However, it might be suggested that following a 10 min exposure to high carbachol concentrations, there was an alteration in presynaptic function causing a reduction in the ACh content of individual vesicles. This would also produce a decrease in m.e.p.c. amplitude. Therefore, to demonstrate that the decrease in m.e.p.c. amplitude was indeed due to a decrease in postsynaptic sensitivity, we measured the endplate current (e.p.c.) produced by local perfusion of

20 μM carbachol prior to, and after exposure to 5.4 mM carbachol. The results indicated that both the m.e.p.c. amplitude and the e.p.c. amplitude decreased following carbachol exposure (Table 1). The extent of recovery of m.e.p.c. amplitude was greater than that of the e.p.c. due to the acceleration of the rate of desensitization following carbachol exposure. Because of this acceleration, the amplitude of the carbachol-induced e.p.c. is attenuated to a greater extent than that of the m.e.p.c. (Hardwick *et al.*, 1991).

The decrease in postsynaptic sensitivity seen after a 10 min exposure to 5.4 mM carbachol could have resulted from either a decrease in the number of functional receptors or a decrease in the single channel conductance of individual AChRs. We have not attempted to measure AChR number, but we have tested whether there was a decrease in the single channel conductance. Previously, we found no change in the single channel conductance at control fibres following a 5 min exposure to 540 μM carbachol (Hardwick & Parsons, 1993a). In the present studies, we recorded single channel currents from control endplates exposed to 5.4 mM carbachol for 10 min (Table 1). In 6 patches on control fibres from three different animals, a single population of ACh-activated channels was consistently observed which had an estimated slope conductance of 48 pS.

We also tested whether, following staurosporine pretreatment, the conductance of the small channels was altered following exposure to high concentrations of carbachol. Four patches from endplates in two different animals were made on staurosporine-treated endplates following a 10 min exposure to 5.4 mM carbachol (Table 1). Small conductance channels were observed in all 4 patches and large conductance channels were observed in 2 of the 4 patches.

The values of the single channel conductances obtained for both control and staurosporine-treated fibres following a 10 min exposure to 5.4 mM carbachol were not different from the values reported previously following a 5 min exposure to 540 μM carbachol (Hardwick & Parsons, 1993a).

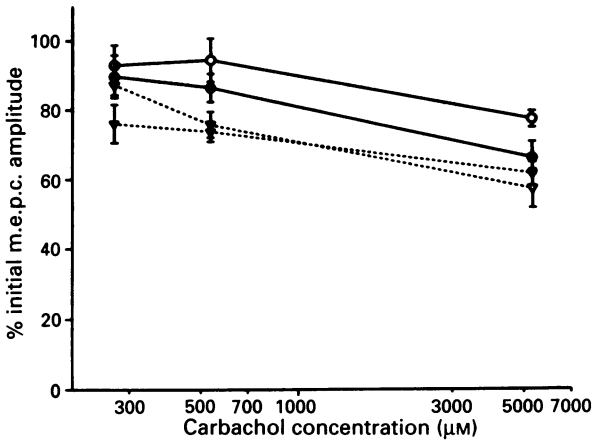


Figure 1 Concentration- and time-dependent inhibition of m.e.p.c. amplitude recovery in control and staurosporine-treated fibres: amplitudes in potassium-depolarized endplates voltage clamped to −100 mV were recorded prior to and following exposure to carbachol for either 5 (open symbols) or 10 min (closed symbols) in control (○, ●) and 0.5 μM staurosporine-treated (△, ▲) fibres. Values shown are the m.e.p.c. amplitude following carbachol exposure as a percentage of the average amplitude prior to treatment. The extent of m.e.p.c. amplitude recovery decreased with increasing concentration of carbachol and increasing time of exposure. Staurosporine treatment resulted in a further decrease in the extent of m.e.p.c. amplitude recovery which was also concentration- and time-dependent.

Table 1 Effects of high concentrations of carbachol (CCh) on control and staurosporine-treated fibres

	m.e.p.c. amplitude (nA)	*e.p.c.$_{CCh}$* (nA)	*Slope conductance* (pS)
Prior to agonist exposure	−5.77 ± 0.19 (n = 18)	35 ± 3 (n = 12)	49 ± 2
After carbachol exposure:			
Control fibres	−3.59 ± 0.26* (n = 6)	16 ± 4* (n = 7)	48 ± 4
Staurosporine-treated	−3.25 ± 0.24* (n = 8)	11 ± 2* (n = 4)	44 ± 4 25 ± 2

*P < 0.05 vs values prior to agonist exposure.

M.e.p.c. amplitudes at endplates voltage-clamped to −100 mV were determined in preparations maintained in the isotonic potassium solution. These endplates were also perfused with 20 μM carbachol to test the postsynaptic sensitivity (e.p.c.$_{CCh}$). Some preparations were then treated for 15 min with 0.5 μM staurosporine and then all preparations were incubated with 5.4 mM carbachol for 10 min, washed and the same parameters were determined again at different endplates. In separate preparations, the ACh-induced single channel conductance was determined at control and staurosporine-treated endplates following a 10 min exposure to 5.4 mM carbachol as indicated in the Methods. The estimated slope conductance determined by linear regression of the current-voltage relationship is shown here. In the staurosporine-treated endplates only, a second population of small conductance channels was observed.

Inhibition of protein phosphorylation appears to be responsible for the staurosporine-induced decrease in the extent of m.e.p.c. amplitude recovery

The results of our earlier studies using staurosporine and a similar protein kinase inhibitor, K252A, only suggested kinase inhibition as the mode of action and did not indicate which kinase might be affected (Hardwick *et al.*, 1991). Consequently, in the present study, we compared the effectiveness of several protein kinase inhibitors on m.e.p.c. amplitude recovery to (a) further support our suggestion that the effect of staurosporine is due to protein kinase inhibition and (b) to identify which protein kinase might be involved. The concentration of each inhibitor employed was at least 10–100 times its known K_i to insure that an effective concentration was achieved. All of the inhibitors were added to the potassium solution bathing the fibres for 10–15 min before exposure to carbachol. Control fibres were kept in the potassium solution for similar periods of time. M.e.p.cs were recorded from 2–3 endplates voltage clamped to −100 mV prior to treatment with the inhibitor, and again following a 5–10 min application of 540 μM carbachol. The extent of m.e.p.c. amplitude recovery was determined by comparing the amplitudes after carbachol exposure to those prior to pretreatment with inhibitor. In addition to staurosporine, which inhibits protein kinase C (PKC), cyclic AMP-dependent protein kinase (PKA), tyrosine protein kinase (TyrK), and Ca^{2+}-calmodulin-dependent protein kinase (CaMK) (Tamaoki *et al.*, 1986; Nakano *et al.*, 1987; Ruegg & Burgess, 1989; Yanagihara *et al.*, 1991), we pretreated fibres with 1 μM lavendustin A, a specific inhibitor of TyrK (Onoda *et al.*, 1989), 50 μM sphingosine, an inhibitor of PKC and CaMK (Hannun *et al.*, 1986; Jefferson & Schulman, 1988), 0.5 μM calphostin C, an inhibitor of PKC (Kobayashi *et al.*, 1989), and 50 μM KN-62, a specific inhibitor of CaMK-II (Tokumitsu *et al.*, 1990). Prior to exposure to carbachol, m.e.p.cs were measured in fibres pretreated with the inhibitors listed. There was no change in either m.e.p.c. amplitudes (Table 2) or decay time constants (data not shown) in the presence of the various inhibitors. Following a 10 min exposure to 540 μM carbachol, only fibres pretreated with staurosporine, sphingosine, and calphostin C showed a significant decrease in the extent of m.e.p.c. amplitude recovery (Table 2). Examples of average m.e.p.cs from control, staurosporine, and sphingosine-treated fibres before and after carbachol exposure are shown in Figure 2.

Table 2 Effects of protein kinase inhibitors on the recovery of m.e.p.c. amplitudes following exposure to 540 μM carbachol (CCh)

	Before CCh m.e.p.c. amplitude (nA)	*After CCh m.e.p.c. amplitude* (nA)	*% recovery*	n	*Kinases inhibited*	*Ref.*
Control	−6.07 ± 0.26	−5.39 ± 0.19	89	14	–	–
Lavendustin A 1 μM	−5.92 ± 0.19^{NS}	−5.46 ± 0.08	84	6	TyrK	1
KN-62 50 μM	−5.61 ± 0.14^{NS}	−5.59 ± 0.15	99	6	CaMK-II	2
Staurosporine 0.5 μM	−6.40 ± 0.18^{NS}	−4.28 ± 0.27*	64	13	PKC, PKA, CaMK, TyrK	3,4,5
Sphingosine 50 μM	−5.80 ± 0.18^{NS}	−3.88 ± 0.19*	67	15	PKC, CaMK	6,7
Calphostin C 0.5 μM	−5.84 ± 0.22^{NS}	−4.07 ± 0.24*	71	18	PKC	8

*$P<0.05$ versus control recovery by ANOVA, NS, not significantly different from controls.
References: (1) Onoda *et al.* (1989); (2) Tokumitsu *et al.* (1990); (3) Tomaoki *et al.* (1986); (4) Nakano *et al.* (1987); (5) Yanagihara *et al.* (1991); (6) Hannun *et al.* (1986); (7) Jefferson & Schulman (1988); (8) Kobayashi *et al.* (1989).
Amplitudes of m.e.p.cs were determined in preparations prior to, and then following a 10 min exposure to 540 μM carbachol. Preparations were treated with the concentration of inhibitor indicated for 15 min prior to recording m.e.p.cs. None of the inhibitors tested altered m.e.p.c. amplitudes prior to agonist exposure. Lavendustin A and KN-62 pretreatment produced no significant change in the recovery of m.e.p.c. amplitude following carbachol exposure. Staurosporine, sphingosine, and calphostin C pretreatment significantly reduced the extent of recovery of m.e.p.c. amplitude following carbachol exposure as compared to control endplates. Values shown are the mean ± s.e.mean of *n* endplates from 3 or more different animals. The percent recovery was determined from the m.e.p.c. amplitude following carbachol exposure versus the m.e.p.c. amplitude prior to agonist.

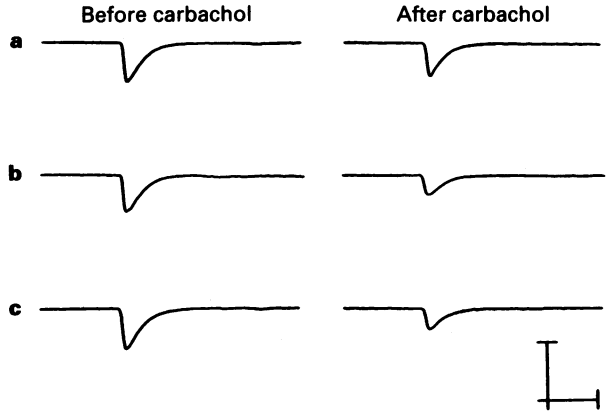


Figure 2 Average m.e.p.cs prior to, and following carbachol exposure in control, staurosporine, and sphingosine-treated preparations: m.e.p.cs were recorded from endplates voltage-clamped to −100 mV prior to, and then following a 10 min exposure to 540 μM carbachol in (a) control, (b) 0.5 μM staurosporine-treated, and (c) 50 μM sphingosine-treated preparations. The current traces are the average of 50–100 individual m.e.p.cs from a single endplate. Prior to agonist exposure, there is no difference in the amplitude or decay of the m.e.p.cs. Following carbachol exposure, the amplitude of the m.e.p.cs at staurosporine- and sphingosine-treated endplates is significantly reduced with no apparent change in the decay rate. Calibration bars: X axis = 5 ms, Y axis = 10 nA.

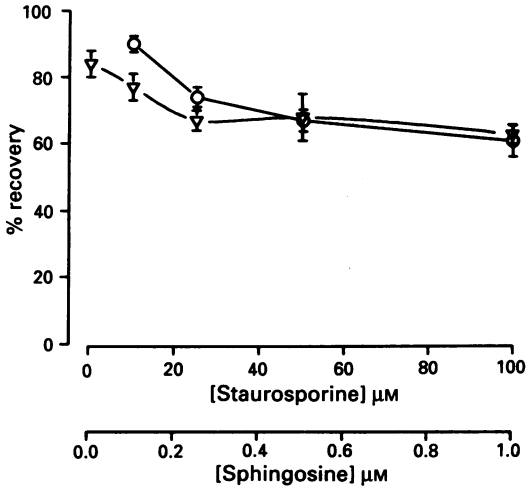


Figure 3 Concentration-dependence of the inhibition of m.e.p.c. amplitude recovery by staurosporine and sphingosine. Preparations were pretreated with concentrations of sphingosine ranging from 10–100 μM (○) or staurosporine ranging from 0.1–1.0 μM (△) for 15 min: m.e.p.c. amplitudes were determined at endplates voltage-clamped at −100 mV prior to, and then following a 10 min exposure to 540 μM carbachol. The results are expressed as the percentage recovery of the initial m.e.p.c. amplitude from 4 or more preparations.

We compared the concentration-dependence of the inhibition of m.e.p.c. amplitude recovery by staurosporine and sphingosine to determine if the degree of inhibition of m.e.p.c. amplitude was similar between the different inhibitors. Staurosporine and sphingosine produced a concentration-dependent reduction in m.e.p.c. amplitude recovery with the maximum effect for both being approximately 60% of the initial amplitude (Figure 3).

The decrease in m.e.p.c. amplitude recovery at staurosporine- or sphingosine-treated endplates is not due to the presence of a subpopulation of small m.e.p.cs or a shift in the reversal potential

A difference in mean m.e.p.c. amplitude following recovery from the carbachol application could have occurred if the m.e.p.c. amplitude distribution was changed from a unimodal distribution to a bimodal distribution with a small amplitude peak along with the normal peak. Consequently, we determined the m.e.p.c. amplitude distribution from endplates in the presence of 50 μM sphingosine or 0.5 μM staurosporine, and then again following a 10 min exposure to 540 μM carbachol.

Typical examples of the m.e.p.c. amplitude distributions are given in Figure 4. The results show that both before and after carbachol exposure, the m.e.p.c. amplitude distributions are unimodal, although the modal value of the m.e.p.c. amplitude is significantly less after recovery at the inhibitor-treated endplates. Therefore, the decrease in mean m.e.p.c. amplitude following carbachol exposure is not due to the presence of a second small population of m.e.p.cs along with the control sized m.e.p.cs, but rather to a shift in the whole distribution to smaller values.

Previously, we showed at staurosporine-treated fibres that the decrease in m.e.p.c. amplitude following recovery from carbachol exposure occurred over a wide voltage-range and was not due to a shift in the reversal potential (Hardwick & Parsons, 1993a). We also determined the peak m.e.p.c. cur-

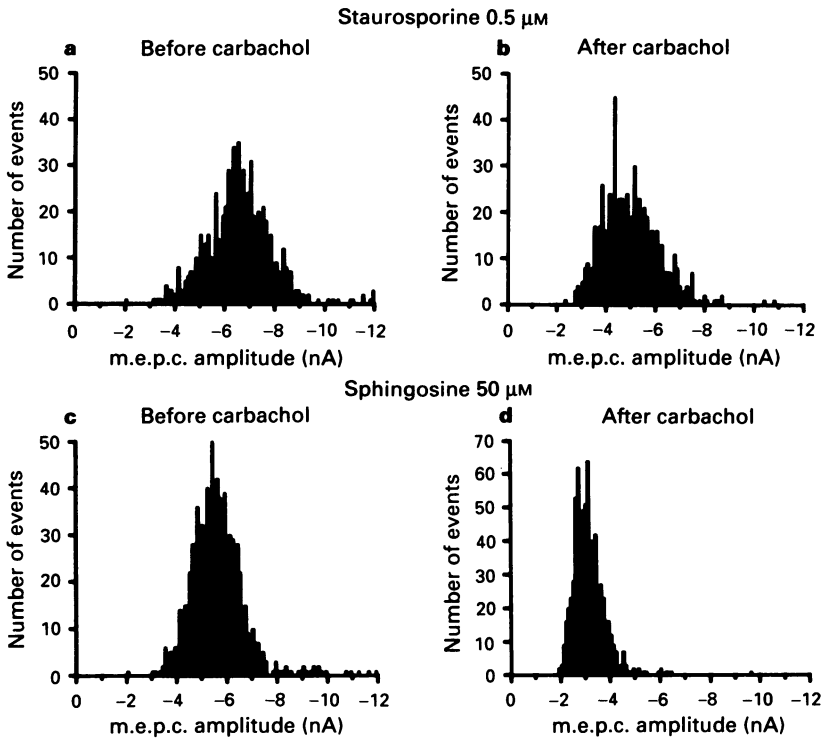


Figure 4 Amplitude distribution of m.e.p.cs before and after carbachol exposure in staurosporine- and sphingosine-treated preparations. Preparations were pretreated with either 0.5 μM staurosporine (a) or 50 μM sphingosine (b) for 15 min: m.e.p.cs were recorded at endplates voltage-clamped to −100 mV prior to, and then following a 10 min exposure to 540 μM carbachol. The histograms represent the distribution obtained from a single endplate under each condition: m.e.p.c. amplitudes were unimodally distributed under all conditions examined. However, following exposure to carbachol (CCh), the m.e.p.c. distribution was shifted toward smaller amplitudes with both inhibitors. The mean and modal values for the histograms shown are as follows: staurosporine before CCh, mean = −6.58 nA, mode = −6.55 nA; staurosporine after CCh, mean = −5.02 nA, mode = −4.37 nA; sphingosine before CCh, mean = −5.23 nA, mode = −5.45 nA; sphingosine after CCh, mean = −3.17 nA, mode = −3.15 nA.

rent amplitude-voltage relationship in preparations pretreated with 50 μM sphingosine, prior to, and then following a 10 min exposure to 540 μM carbachol. There was no difference in either the shape or slope of the current-voltage relationship with sphingosine treatment prior to carbachol exposure as compared to control endplates (V_{Rev} approximately 0 mV). Following exposure to carbachol, there was a decrease in m.e.p.c. amplitude at all voltages in the sphingosine-treated preparations with no significant shift in the reversal potential (V_{Rev} = − 3.9 mV ± 4.3).

Chronic treatment with phorbol esters to down regulate PKC also reduces the extent of m.e.p.c. amplitude recovery following carbachol exposure

The results with the protein kinase inhibitors suggested that inhibition of PKC might be the common mechanism of action for the reduction in m.e.p.c. amplitude following carbachol exposure. Therefore, we wanted to test whether chronic exposure to phorbol esters, which reduces PKC activity by down regulation of the enzyme (Rodriquez-Pena & Rosengurt, 1984), would also inhibit m.e.p.c. amplitude recovery. For these experiments, muscles were maintained in normal sodium solution alone, sodium solution containing 200 nM PMA, or solution containing the inactive analogue of PMA, 4αPMA (200 nM), for 18–20 h at room temperature. Initially, we attempted to measure m.e.p.cs following a 20–30 min incubation in the isotonic potassium solution. However, we found that PMA-treated preparations maintained in isotonic potassium demonstrated a marked increase in the frequency of m.e.p.cs, making the determination of individual m.e.p.c. amplitudes impossible. Therefore, this series of experiments was done with muscles maintained in a sodium propionate solution containing 0.3 μM tetrodotoxin (TTX), to prevent action potentials. Propionate was substituted for chloride in the solution to prevent the accumulation of chloride in the muscle with agonist-induced depolarization (Nastuk & Parsons, 1970; Jenkinson & Terrar, 1973; Feltz & Jaoul, 1974). Although m.e.p.c. frequency was much less in the sodium solution, it was still possible to collect sufficient events to determine an average m.e.p.c. amplitude prior to, and then following a 10 min exposure to 540 μM carbachol. We also determined the effects of 0.5 μM staurosporine on m.e.p.c. amplitude recovery in the sodium propionate solution. Staurosporine treatment reduced the extent of m.e.p.c. amplitude recovery, following carbachol exposure, to approximately 68%, whereas recovery was approximately 88% in control fibres in the sodium propionate solution. Chronic exposure to PMA decreased the extent of m.e.p.c. amplitude recovery (Table 3) to a similar extent. In contrast, chronic exposure to the inactive phorbol had no effect on m.e.p.c. recovery following carbachol exposure.

Small conductance ACh-activated channels are present following exposure to carbachol at sphingosine- and PMA-treated endplates

The decrease in m.e.p.c. amplitude in staurosporine-pretreated endplates following carbachol exposure was accompanied by the appearance of a population of small conductance ACh-activated channels (Hardwick & Parsons, 1993a). We therefore initiated patch clamp studies to (a) establish whether small conductance channels were also present following carbachol exposure at endplates from muscle preparations acutely treated with 50 μM sphingosine or chronically treated with 200 nM PMA and (b) to determine

Table 3 Effect of chronic exposure to 200 nM phorbol 12-myristate 13-acetate (PMA) and 200 nM 4α-phorbol 12-myristate 13-acetate (4αPMA) on m.e.p.c. amplitudes and time constants before and after exposure to carbachol

	Before carbachol		*After carbachol*		
	m.e.p.c. amplitude (nA)	*Decay time constant* (ms)	*m.e.p.c. amplitude* (nA)	*% recovery*	*Decay time constant* (ms)
Chronic control	−3.56 ± 0.17 (7)	2.80 ± 0.09 (7)	−2.97 ± 0.10 (12)	83	2.66 ± 0.09 (12)
4αPMA 200 nM	−3.37 ± 0.14 (12)	2.89 ± 0.08 (12)	−2.79 ± 0.06 (14)	83	2.39 ± 0.10 (13)
PMA 200 nM	−3.46 ± 0.15 (14)	3.01 ± 0.17 (14)	−2.51 ± 0.08* (19)	73	2.56 ± 0.08 (16)

*$P < 0.05$ versus control endplates.
Muscles were maintained in sodium propionate solution containing 0.3 μM tetrodotoxin. Preparations were treated for 18–20 h with normal sodium solution (chronic control), or control solution containing 200 nM PMA or 200 nM 4αPMA. M.e.p.cs were recorded from endplates voltage clamped to −100 mV prior to, and then following a 10 min exposure to 540 μM carbachol in sodium propionate. Chronic exposure to 4αPMA had no effect on m.e.p.c. amplitude recovery whereas chronic exposure to PMA resulted in a significant reduction in m.e.p.c. amplitude following carbachol exposure. Values shown are the mean ± s.e.mean of *n* fibres, shown in parentheses.

Table 4 Characteristics of acetylcholine (ACh)-activated single channel currents

	Before carbachol exposure				*After carbachol exposure*			
	Amplitude (pA)	*Open time* (ms)	*Conductance* (pS)	n	*Amplitude* (pA)	*Open time* (ms)	*Conductance* (pS)	n
Control	−4.84 ± 0.29[1]	1.65 ± 0.19	49 ± 8[1]	9	−4.66 ± 0.39[1]	2.45 ± 0.49	49 ± 6[1]	7
EtOH 0.1%	−4.73 ± 0.29	1.36 ± 0.08	45 ± 3	7	−5.18 ± 0.42	1.38 ± 0.11	50 ± 4	5
4αPMA	−5.09 ± 0.10	2.39 ± 0.40	49 ± 1	7	−5.13 ± 0.22	2.31 ± 0.40	48 ± 2	5
Staurosporine	−5.26 ± 0.26[1]	1.88 ± 0.20	47 ± 7[1]	5	−5.23 ± 0.11[1]	2.49 ± 0.40	53 ± 2[1]	8
					−2.38 ± 0.29[1]	1.20 ± 0.27	23 ± 1[1]	7
Sphingosine	−5.21 ± 0.26	2.02 ± 0.33	52 ± 3	6	−5.11 ± 0.24	3.08 ± 0.97	52 ± 1	6
					−2.91 ± 0.25	1.44 ± 0.44	28 ± 1	6
PMA	−4.89 ± 0.15	2.04 ± 0.15	46 ± 4	5	−5.15 ± 0.16	1.82 ± 0.14	47 ± 3	8
					−2.20 ± 0.24	1.83 ± 0.06	22 ± 2	4

[1]Hardwick & Parsons (1993a).
ACh-activated single channel currents were measured in preparations acutely treated (15–30 min) with 0.1% EtOH or 50 μM sphingosine, or in preparations chronically treated (18–20 h) with either 200 nM 4αPMA or 200 nM PMA, both prior to and then following a 10 min exposure to 540 μM carbachol. The mean channel amplitude at −100 mV, arithmetic mean open time and the estimated slope conductances were unchanged by exposure to either 0.1% EtOH or 4αPMA before and after carbachol. In the sphingosine- and PMA-treated preparations prior to carbachol exposure, the channels also were predominantly of the large conductance type. Following exposure to carbachol, two populations of channels were consistently observed in both the sphingosine-treated and the PMA-treated preparations. These small conductance channels were similar in amplitude, open time, and slope conductance to those observed in staurosporine-treated preparations following carbachol exposure. The values shown are the mean amplitude and open times at −100 mV ± s.e.mean with the number of endplates in parentheses. All recordings were obtained from 2–3 different animals under each condition. The slope conductance was determined from regression analysis of the current-voltage relationship under each condition.

whether the conductance of these channels was similar to those seen at staurosporine-treated endplates following recovery. We also recorded from preparations maintained in 0.1% EtOH as a vehicle control for the sphingosine preparations and fibres chronically treated with 200 nM 4αPMA.

ACh-activated (1 μM) currents were recorded from cell attached patches on enzymatically-cleaned endplates of fibres before and after a 10 min exposure to 540 μM carbachol. Recordings were initially made with the patch held at −100 mV. Thereafter, whenever possible, recordings were also made at several other voltages to estimate the slope conductance. Because the rate of desensitization is accelerated following carbachol exposure (Hardwick *et al.*, 1991; Hardwick & Parsons, 1993a) we were often unable to obtain recordings at several voltages from a single patch.

Recordings of ACh-activated channels from preparations treated with 0.1% EtOH, sphingosine, PMA and 4αPMA alone consisted of predominately one population of channels with amplitudes at −100 mV, mean open times and slope conductances (47–52 pS) similar to that seen at control endplates (Table 4). As in previous studies (Hardwick *et al.*, 1993a), treatment with the protein kinase inhibitors alone produced no significant change in channel conductance. However, in one patch from a sphingosine-treated endplate a small conductance channel was observed along with the normal, large conductance channels. The amplitude and slope conductance of this channel was similar to that seen at staurosporine-treated endplates following exposure to carbachol (data not shown).

Following a 10 min exposure to carbachol, only large conductance ACh-activated channels were observed at 0.1% EtOH and 4αPMA treated endplates (Figure 5). Conversely a mixture of small and large conductance channels were observed at sphingosine- and PMA-treated endplates (Figure 5). The characteristics of the small conductance channels under both conditions were identical to those seen previously in staurosporine-treated preparations following carbachol exposure (Table 4). Arithmetic mean open times were also determined for the different channel populations. There were no significant differences in the mean open times of the large conductance channels following carbachol exposure as compared to those recorded from control, untreated endplates. In addition, there was no difference in the single channel characteristics of the small conductance channels in staurosporine-treated endplates versus sphingosine- and PMA-treated endplates. The mean open time of these small channels was similar to, or even slightly less, than that of the large conductance channels.

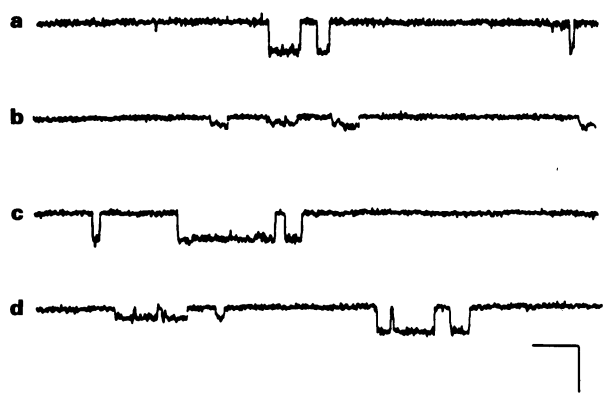


Figure 5 Acetylcholine (ACh)-activated single channel currents following carbachol exposure. ACh (1 μM)-activated currents were recorded from endplates following a 10 min exposure to 540 μM carbachol. The traces shown were all recorded at a holding potential of −100 mV. Channels were recorded from endplates treated with (a) 0.1% EtOH, (b) 50 μM sphingosine, (c) 200 nM 4α-phorbol 12-myristate 13-acetate (4αPMA) and (d) 200 nM PMA. Similar small conductance channels were observed in preparations treated with staurosporine, sphingosine, or PMA following carbachol exposure. Calibration bars: X axis = 5 ms, Y axis = 10 pA.

Discussion

Nicotinic AChRs at the motor endplate are desensitized by a sustained application of agonist (Katz & Thesleff, 1957). AChR recovery from desensitization is virtually complete with rapid perfusion techniques of agonist application for a few hundred milliseconds or less (Dilger & Liu, 1992), but with repeated applications or longer durations, the peak response often fades (Dilger & Brett, 1990; Naranjo & Brehm, 1993). Thus it appears that there is a decrease in the number of functional AChRs as either agonist concentration or duration of exposure increases. We suggest that the progressive decrease in extent of m.e.p.c. amplitude recovery as a function of carbachol concentration and length of exposure observed at control fibres in the present study is most easily explained as a decrease in the number of functional AChRs. The fact that both m.e.p.c. amplitude and e.p.c. amplitude decreased in parallel indicates a decrease in postsynaptic sensitivity rather than a decrease in the amount of ACh per vesicle was responsible for the decrease in m.e.p.c. amplitude. This decrease in the amount of functional receptors could represent an irreversible inactivation of a subpopulation of receptors, which we previously proposed (Hardwick & Parsons, 1993a) or could also be due to a decrease in the probability of opening of receptors.

Previously, we proposed that the decrease in m.e.p.c. amplitude recovery at staurosporine-treated preparations resulted from an inhibition of protein kinase activity (Hardwick *et al.*, 1991; Hardwick & Parsons, 1993a,b). In the present study, we tested the effects of several different protein kinase inhibitors on the extent of m.e.p.c. amplitude recovery. Inhibition of TyrK, CaMK, and PKA did not appear to alter m.e.p.c. recovery. Instead, inhibition of PKC appeared to be the common mechanism of the reduced m.e.p.c. recovery and appearance of small conductance ACh-activated single channels. This conclusion received additional support from the observation that chronic treatment with the phorbol ester PMA, which leads to the down regulation of PKC (Rodriquez-Pena & Rozengurt, 1984), also inhibited the recovery of m.e.p.c. amplitudes following carbachol exposure. Thus, we conclude that inhibition of PKC is the mechanism responsible for the decreased m.e.p.c. recovery and presence of small conductance ACh-activated channels.

We have suggested that m.e.p.c. amplitude is reduced during recovery from carbachol exposure in staurosporine-treated preparations, at least in part, because neurally released ACh activates a mixture of small and large conductance channels (Hardwick & Parsons, 1993a). Identical small conductance channels were found in the present study following carbachol exposure at PMA- and sphingosine-treated endplates. Consequently, we suggest that the reduced m.e.p.c. amplitude after recovery observed at these endplates also resulted from the activation of a mixture of small and large conductance channels.

We have tried to approximate the percentage of channels which have small conductance values, required to reduce the m.e.p.c. amplitude to the extent seen at the inhibitor-treated endplates. At normal twitch fibre endplates both before, and after carbachol exposure, and at kinase-inhibited endplates prior to carbachol, the m.e.p.c. amplitude can be approximated by the relationship:

$$I_{m.e.p.c.} = N\gamma_L\ (E_M - E_{ACh})$$

where N equals the number of activatable channels, γ_L equals the large conductance value and $(E_M - E_{ACh})$ equals the driving force for the ACh-induced current. We suggest that at control endplates the reduction in m.e.p.c. amplitude seen following recovery from a prolonged exposure to carbachol occurs because of a reduction in N, the number of functional receptors, because γ_L is not changed by agonist exposure. Therefore, as the concentration and duration of agonist exposure increases, the number of activatable receptors decreases.

At the inhibitor-treated preparations, following recovery from carbachol exposure, the m.e.p.c. amplitude is due to the activation of two channel types so that the m.e.p.c. amplitude should be approximated by the relationship:

$$I_{m.e.p.c.} = N_L\gamma_L\ (E_M - E_{ACh}) + N_S\gamma_S\ (E_M - E_{ACh})$$

where γ_S equals the conductance value of the second channel population. Given that the conductance value of γ_L is approximately twice that of γ_S and assuming the total number of channels $(N_L + N_S)$ is not decreased below N of control preparations also exposed to carbachol, we estimate that the reduced m.e.p.c. amplitude after recovery from a 10 min exposure to 540 μM carbachol occurred because at least 40% of the functioning AChRs were of the small conductance type and the remainder were the large conductance type. Such an estimate is not inconsistent with the relative proportion of large and small conductance channels observed in our patch recordings.

Slow type channels observed at tonic endplates also have a small conductance value similar to that observed here with a longer mean open time than fast type channels seen at twitch endplates (Dionne, 1988; Ruff & Spiegel, 1990). However, it does not appear that the small conductance channels present at kinase-inhibited twitch endplates following recovery from carbachol are slow type channels. Determination of the mean open times of these small conductance channels demonstrate that they have a similar, or slightly shorter open time, than that of the large conductance channels. In addition, because the endplates at tonic fibres contain a mixture of fast and slow type channels, the m.e.p.cs display a much slower rate of decay than twitch fibre m.e.p.cs. The voltage-dependence of this decay rate is also markedly different in twitch and tonic fibres. Measurements of m.e.p.c. decay rates under all conditions tested in the present study demonstrated no change in the decay rate at −100 mV and no change in the voltage-dependence of the time constant (between −50 and −150 mV, data not shown). Therefore, we propose that the small conductance channel observed in the kinase-inhibited fibres represents a reduced conductance class of the fast type twitch AChRs. We also suggest that, in control preparations, conversion of this small conductance channel to the normal, large conductance channel is the result of phosphorylation of either the AChR itself, or a closely related protein, by PKC. This process is probably very rapid since no conversion of small to large channels was observed in our recordings.

However, it should be noted that the earliest measurements of single channel activity were not made until at least 3 min following the removal of the carbachol solution.

Although we cannot establish at this time whether the substrate for protein phosphorylation is the AChR itself (Huganir, 1988) or an accessory protein, indirect evidence suggesting the latter was derived from the results of studies examining the effects of colchicine treatment described in the following report. We found that m.e.p.c. amplitude recovery is also decreased in muscle preparations treated with colchicine (Hardwick & Parsons, 1995). In the absence of carbachol exposure, m.e.p.c. amplitude and decay rates are uneffected by colchicine treatment. Following carbachol exposure, however, there is a decrease in m.e.p.c. amplitude and a small conductance ACh-activated channel was observed similar to that seen in kinase-inhibited fibres. Therefore, we speculate that alteration of a subsynaptic protein, perhaps one required for anchoring of the AChR, occurs with prolonged agonist exposure. Several of the proteins known to be found in close conjunction with the AChRs have also been shown to be substrates for PKC (Hall & Sanes, 1993; Wagner *et al.*, 1993). In addition, studies examining the effects of down regulation of PKC in cells expressing muscle-type nicotinic AChRs demonstrated a profound alteration in cytoskeletal organization with chronic phorbol treatment (Bencherif & Lukas, 1993). Consequently, we suggest that if the dephosphorylated form of an anchoring protein is not functional then some AChRs might not be adequately stabilized in the membrane. Further, we propose that it may be these poorly stabilized AChRs which exhibit the low conductance state. Previously, we proposed that during a prolonged exposure to carbachol, some AChRs are irreversibly inactivated and must be replaced in order to maintain the high density of receptors present at the endplate (Hardwick & Parsons, 1993b). We suggested that some replacement AChRs may be recruited from a presynthesized, but not previously activated, pool of receptors. The small conductance channels seen following carbachol exposure at staurosporine-treated endplates could be the recently recruited AChR which would normally be converted to the large conductance state by a PKC-dependent pathway. However, results from other investigators using standard labelling techniques give no evidence of a pool of spare AChRs of this magnitude in skeletal muscle. An alternative hypothesis is that, during prolonged exposure to carbachol, either a subpopulation of AChRs or a closely-associated protein become dephosphorylated. Full recovery then occurs only after rephosphorylation of the affected proteins by PKC. The role of dephosphorylation in recovery is currently under investigation in our laboratory. Preliminary results from preparations pretreated with an inhibitor of the calcium-calmodulin-dependent protein phosphatase (calcineurin) in combination with staurosporine demonstrated no observable decrease in the amplitude of m.e.p.c. recovery following carbachol exposure (unpublished observations).

In conclusion, the results presented here establish that the decrease in the extent of endplate recovery in kinase-inhibited preparations is due to the inhibition of protein phosphorylation and that PKC is probably the kinase affected. The results also indicate that the small conductance channel seen at kinase-inhibited endplates is not a slow type ACh-activated channel, but rather a form of the fast-type channel with a reduced single channel conductance.

We would like to thank Drs Cynthia Forehand and Carson Cornbrooks for critical review of the manuscript. We would also like to thank Mr Dean Melen for excellent technical assistance and Dr John Dempster for the generous gift of the programme SCAN. This work was supported by NIH grants NS 08580 to J.C.H. and NS 23978 to R.L.P.

References

BENCHERIF, M & LUKAS, R.J. (1993). Cytochalasin modulation of nicotinic cholinergic receptor expression and muscarinic receptor function in human TE671/RD cells: a possible functional role of the cytoskeleton. *J. Neurochem.*, **61**, 852–864.

CONNOR, E.A., FIEKERS, J.F., NEEL, D.S., PARSON, R.L. & SCHNITZLER, R.M. (1984). Comparison of cholinergic activation and desensitization at snake twitch and slow muscle fibre endplates. *J. Physiol.*, **351**, 657–674.

DILGER, J.P. & BRETT, R.S. (1990). Direct measurement of the concentration- and time-dependent open probability of the nicotinic acetylcholine receptor channel. *Biophys. J.*, **57**, 723–731.

DILGER, J.P. & LIU, Y. (1992). Desensitization of acetylcholine receptors in BC3H-1 cells. *Pflügers Arch.*, **420**, 479–485.

DIONNE, V.E. (1988). Two types of nicotinic acetylcholine receptor channels at slow fibre end-plates of the garter snake. *J. Physiol.*, **409**, 313–331.

DIONNE, V.E. & PARSONS, R.L. (1981). Characteristics of the acetylcholine-operated channel at twitch and slow fibre neuromuscular junctions of the garter snake. *J. Physiol.*, **310**, 145–158.

FELTZ, A. & JAOUL, A. (1974). Direct estimates of chloride activity in muscle fibres depolarized by carbachol. *Br. J. Pharmacol.*, **51**, 304–306.

FELTZ, A. & TRAUTMANN, A. (1982). Desensitization at the frog neuromuscular junction: a biphasic process. *J. Physiol.*, **322**, 257–272.

HALL, Z.W. & SANES, J.R. (1993). Synaptic structure and development: the neuromuscular junction. *Neuron*, **10**, 99–121.

HAMILL, O.P., MARTY, A., NEHER, E., SAKMANN, B. & SIGWORTH, F. (1981). Improved patch-clamp techniques for high resolution current recording from cells and cell free membrane patches. *Pflügers Arch.*, **391**, 85–100.

HANNUN, Y.A., LOOMIS, C.R., MERRILL, A.H. & BELL, R.M. (1986). Sphingosine inhibition of protein kinase C activity and of phorbol dibutyrate binding in vitro and in human platelets. *J. Biol. Chem.*, **261**, 12604–12609.

HARDWICK, J.C., CONIGLIO, L.M. & PARSONS, R.L. (1991). Staurosporine inhibits the extent of acetylcholine receptor recovery from carbachol-induced desensitization in snake twitch fibres. *Br. J. Pharmacol.*, **104**, 879–886.

HARDWICK, J.C. & PARSONS, R.L. (1993a). Mechanism of staurosporine-induced decrease in acetylcholine receptor recovery from desensitization. *Br. J. Pharmacol.*, **108**, 741–748.

HARDWICK, J.C. & PARSONS, R.L. (1993b). Necessity of divalent cations for recovery from carbachol-induced nicotinic acetylcholine receptor inactivation at snake twitch fibre endplates. *Br. J. Pharmacol.*, **110**, 889–895.

HARDWICK, J.C. & PARSONS, R.L. (1995). Requirement of a colchicine-sensitive component of the cytoskeleton for acetylcholine receptor recovery. *Br. J. Pharmacol.*, **114**, 442–446.

HUGANIR, R.L. (1988). Regulation of the nicotinic acetylcholine receptor channel by a protein phosphorylation. *Curr. Top. Membr. Transp.*, **33**, 147–163.

JEFFERSON, A.B. & SCHULMAN, H. (1988). Sphingosine inhibits calmodulin-dependent enzymes. *J. Biol. Chem.*, **263**, 15241–15244.

JENKINSON, D.H. & TERRAR, D.A. (1973). Influence of chloride ions on changes in membrane potential during prolonged application of carbachol to frog skeletal muscle. *Br. J. Pharmacol.*, **47**, 363–376.

KATZ, B. & THESLEFF, S. (1957). A study of the 'desensitization' produced by acetylcholine at the motor end-plate. *J. Physiol.*, **138**, 63–80.

KOBAYASHI, E., NAKANO, H., MORIMOTO, M. & TAMAOKI, T. (1989). Calphostin C (UCN-1028C), a novel microbial compound, is a highly potent and specific inhibitor of protein kinase C. *Biochem. Biophys. Res. Commun.*, **159**, 584–553.

LO, C.F. & BREITWIESER, G.E. (1994). Protein kinase-independent inhibition of muscarinic K^+ channels by staurosporine. *Am. J. Physiol.*, **266**, C1128–C1132.

NAKANO, H., KOBAYASHI, E., TAKAHASHI, I., TAMAOKI, T., KUZUU, Y. & IBA, H. (1987). Staurosporine inhibits tyrosine-specific protein kinase activity of rous sarcoma virus transforming protein p60. *J. Antibiot.*, **40**, 706–708.

NARANJO, D. & BREHM, P. (1993). Modal shifts in acetylcholine receptor channel gating confer subunit-dependent desensitization. *Science*, **250**, 1811–1814.

NASTUK, W.L. & PARSONS, R.L. (1990). Factors in the inactivation of postjunctional membrane receptors of frog skeletal muscle. *J. Gen. Physiol.*, **56**, 218–249.

ONODA, T., IINUMA, H., SASAKI, Y., HAMADA, M., ISSHIKI, K., NAGANAWA, H. & TAKEUCMI, T. (1989). Isolation of a novel tyrosine kinase inhibitor, lavendustin A, from Streptomyces griseolavendus. *J. Nat. Prod.*, **52**, 1252–1257.

RODRIQUEZ-PENA, A. & ROZENGURT, E. (1984). Disappearance of Ca^{2+} sensitive, phospholipid dependent protein kinase activity in phorbol ester-treated 3T3 cells. *Biochem. Biophys. Res. Commun.*, **120**, 1053–1059.

RUEGG, U.T. & BURGESS, G.M. (1989). Staurosporine, K-252, and UCN-01: potent by nonspecific inhibitors of protein kinases. *Trends Pharmacol. Sci.*, **10**, 218–220.

RUFF, R.L. & SPIEGEL, P. (1990). Ca sensitivity and acetylcholine receptor currents of twitch and tonic snake muscle fibres. *Am. J. Physiol.*, **259**, C911–C919.

TAMAOKI, T., NOMOTO, H., TAKAHASHI, I., KATO, Y., MORIMOTO, M. & TOMITA, F. (1986). Staurosporine, a potent inhibitor of phospholipid/Ca^{++} dependent protein kinase. *Biochem. Biophys. Res. Commun.*, **135**, 397–402.

TOKUMITSU, H., CHIJIWA, T., HAGIWARA, M., MIZUTANI, A., TERASAWA, M. & HIDAKA, H. (1990). KN-62, 1-[N,O-bis(5-isoquinolinesulfonyl)-N-methyl-L-tyrosyl]-4-phenylpiperazine, a specific inhibitor of Ca2 + /calmodulin-dependent protein kinase II. *J. Biol. Chem.*, **265**, 4315–4320.

WAGNER, K.R., COHEN, J.B. & HUGANIR, R.L. (1993). The 87K postsynaptic membrane protein from Torpedo is a protein-tyrosine kinase substrate homologous to dystrophin. *Neuron*, **10**, 511–522.

YANAGIHARA, N., TACHIKAWA, E., IZUMI, F., YASUGAWA, S., YAMAMOTO, H. & MIYAMOTO, E. (1991). Staurosporine: an effective inhibitor for Ca^{2+}/calmodulin-dependent protein kinase II. *J. Neurochem.*, **56**, 294–298.

(Received June 27, 1994
Revised September 12, 1994
Accepted September 28, 1994)

British Journal of Pharmacology (1995) 114, 442-446 © 1995 Stockton Press All rights reserved 0007-1188/95 $9.00

Requirement of a colchicine-sensitive component of the cytoskeleton for acetylcholine receptor recovery

Jean C. Hardwick & [1]Rodney L. Parsons

Department of Anatomy and Neurobiology, College of Medicine, University of Vermont, Burlington, VT 05405, U.S.A.

1 The effect of colchicine treatment on acetylcholine receptor function was examined in potassium depolarized, voltage-clamped snake twitch fibre endplates. Receptor function was assessed by analysis of miniature endplate currents (m.e.p.c.) as well as acetylcholine (ACh)-induced single channel currents.

2 Pretreatment of snake muscle fibres with colchicine (10 μM to 100 μM) for 16–18 h had no effect on m.e.p.c. amplitude or decay rates. At higher concentrations (1 mM), there was a slight decrease in the average m.e.p.c. amplitude.

3 Colchicine produced a concentration-dependent decrease in the extent of m.e.p.c. amplitude recovery following a 10 min exposure to 540 μM carbachol. Exposure of 100 μM colchicine-treated preparations to 0.5 μM staurosporine further reduced the extent of m.e.p.c. amplitude recovery following carbachol exposure.

4 The decrease in m.e.p.c. amplitude following carbachol exposure was not due to a shift in the m.e.p.c. reversal potential. In addition, the distribution of m.e.p.c. amplitudes remained unimodal in both control and colchicine (100 μM)-treated preparations following carbachol exposure.

5 In addition to the normal, large conductance (~48 pS) ACh-activated channels, a population of small conductance (~29 pS) channels was observed in colchicine-treated preparations following exposure to carbachol. In preparations treated with both colchicine and staurosporine and then exposed to carbachol, the conductance of these small channels was identical to that of colchicine or staurosporine alone.

6 We suggest that prolonged exposure of snake twitch fibre endplates to agonist results in the activation and desensitization of ACh receptors. Furthermore, we propose that for a subpopulation of the inactivated receptors, restoration of function requires both the integrity of a subsynaptic cytoskeletal component and phosphorylation by a staurosporine-sensitive protein kinase. One plausible mechanism is that some receptors become destabilized in the membrane and phosphorylation of a cytoskeletal component, whose distribution may depend on an intact microtubular system, is required to re-anchor these receptors. If this anchoring process is inhibited either by disruption of the cytoskeleton with colchicine, or inhibition of the kinase by staurosporine, these receptors remain activatable, but have a reduced conductance.

Keywords: Staurosporine; m.e.p.cs; single channels; colchicine; ACh receptors; snake twitch fibre endplates; cytoskeleton

Introduction

The neuromuscular junction consists of a highly specialized region of postsynaptic membrane in close conjunction with a complicated, multicomponent cytoskeleton (Hall & Sanes, 1993). This cytoskeleton appears to play a vital role in the aggregation and stabilization of acetylcholine receptors during development (Froehner, 1991; Hall & Sanes, 1993). Treatment of cultured myotubes with agents which disrupt cytoskeletal organization inhibits the formation of acetylcholine receptor (AChR) clusters (Bloch, 1983; Connolly, 1984; Wallace, 1988). In addition, agents which disrupt the microtubular network appear to inhibit the lateral movement of AChRs in the membrane (Bloch, 1983; Connolly, 1984). Recent studies have also suggested that tyrosine phosphorylation of the AChR itself is an important step in the clustering process (Wallace *et al.*, 1991; Wallace, 1994). Calcium (Bloch, 1983; Peng, 1984), calmodulin (Peng, 1984), and protein kinase C (Wallace, 1988; Ross *et al.*, 1988) have also been suggested to play a role in the formation of synapses. Although many aspects of synapse formation during development have been described, relatively little is known about the maintenance of AChRs in adult muscle.

Our previous studies demonstrated that, following a prolonged exposure of snake twitch fibres to the nicotinic agonist carbachol, endplate sensitivity did not recover fully (Hardwick & Parsons, 1993a,b). This recovery was further reduced by the addition of agents which inhibit protein kinase C (Hardwick & Parsons, 1995). Since both the AChR itself and several of the subsynaptic proteins associated with the receptor can be substrates for PKC (Huganir 1988; Hall & Sanes, 1993; Wagner *et al.*, 1993), we wanted to examine the effects of an agent known to alter the subsynaptic cytoskeleton on the recovery of AChR function following agonist-induced activation and desensitization. If a population of AChRs become destabilized with agonist exposure and must be re-anchored to restore complete function, then disruption of the underlying cytoskeleton might reduce recovery.

We demonstrate here that pretreatment of snake twitch fibres with colchicine reduces the extent of m.e.p.c. amplitude recovery following carbachol application. Further, the decrease in m.e.p.c. amplitude results from the activation of large and small conductance channels similar to those seen in staurosporine-treated endplates, suggesting that these two agents may be inhibiting different aspects of the same process.

Methods

General methods

All experiments were done at room temperature on potassium-depolarized twitch fibre endplates of cos-

[1] Author for correspondence.

tocutaneous muscles isolated from garter snakes (*Thamnophis*) as described previously (Conor *et al.*, 1984; Hardwick *et al.*, 1991; Hardwick & Parsons, 1993a,b) and in the preceding manuscript (Hardwick & Parsons, 1995).

Colchicine (Sigma) was added to the control physiological solution (10 μM to 1 mM) and the muscle preparations were incubated at room temperature for 16–18 h. Control preparations were maintained in the physiological sodium solution without colchicine for identical time periods. At the end of the incubation time, the preparations were washed and then incubated in the isotonic potassium solution for recording.

Electrophysiological methods

Recordings of m.e.p.c. amplitudes and ACh-activated single channel currents were obtained by the same methods as described in the preceding manuscript (Hardwick & Parsons, 1995).

Statistical analyses

All results are expressed as the mean ± s.e.mean obtained from *n* fibres as indicated. In addition, fibres for each series of experiments were obtained from at least three different animals. Statistical significance was determined by Students two-tailed *t* test or analysis of variance (ANOVA) with $P<0.05$ considered significant.

Results

Colchicine pretreatment decreases m.e.p.c. amplitude recovery

In the first series of experiments, we tested whether colchicine, an inhibitor of microtubule polymerization, affected the extent of m.e.p.c. amplitude recovery. For these experiments, muscle preparations were incubated at room temperature for 16–18 h in the control, sodium-containing physiological solution with concentrations of colchicine ranging from 10 μM to 1 mM. Control preparations were kept for an identical time period at room temperature in the control solution alone. All the preparations were then washed with colchicine-free solution and incubated in an isotonic potassium propionate solution for 15–20 min before starting m.e.p.c recordings. M.e.p.cs were recorded from 2–3 endplates voltage-clamped to −100 mV in control and colchicine-treated preparations prior to, and then following a 10 min exposure to 540 μM carbachol.

Treatment with colchicine concentrations of 10–100 μM alone did not alter either mean m.e.p.c. amplitude or decay time constant (Table 1). However, with 1 mM colchicine, m.e.p.c. amplitude (but not the decay time constant) was decreased by 10–15%. Following exposure to carbachol, mean m.e.p.c. amplitude was significantly less in preparations treated with colchicine concentrations of 50 μM or higher, than m.e.p.c. amplitudes at control endplates (Figure 1). Further, the concentration-dependence of the decrease in extent of m.e.p.c. amplitude recovery was quite steep so that a maximal effect (~30% decrease) was seen with 50 μM colchicine pretreatment and no greater change occurred at the higher concentrations.

The m.e.p.c. amplitude distribution remains unimodal after carbachol exposure

Previously, we showed that in the potassium propionate solution, m.e.p.c. amplitudes at control twitch fibres were normally distributed (Hardwick *et al.*, 1991). We also determined the m.e.p.c. amplitude distribution for control and colchicine-treated fibres, in the absence of and following a 10 min exposure to 540 μM carbachol. Typical examples of the m.e.p.c. amplitude distributions obtained are given in Figure 2. The results indicated that with all conditions the m.e.p.c. amplitudes were primarily unimodal although both the mean and modal value of the m.e.p.c. amplitude were significantly less after recovery in the colchicine-pretreated fibres than in the other three examples. Therefore, the decrease in mean m.e.p.c. amplitude was not due to the presence of a second small population of m.e.p.cs along with control sized m.e.p.cs but rather due to a shift in the whole distribution to smaller amplitudes.

We also determined the current-voltage relationship for m.e.p.cs in colchicine-treated preparations and found no change in the reversal potential either prior to, or following carbachol exposure, as compared to control preparations (data not shown).

Staurosporine produces a further decrease in m.e.p.c. amplitude in colchicine-treated preparations

In preparations pretreated with staurosporine, the extent of m.e.p.c. amplitude recovery following carbochol exposure is

Table 1 Effects of colchicine concentration on m.e.p.c. amplitude and decay rates

		m.e.p.c. amplitude (nA)	*Decay time constant (ms)*	n
Control		−6.11 ± 0.21	1.46 ± 0.11	13
Colchicine	10 μM	−6.03 ± 0.24	1.27 ± 0.10	8
	50 μM	−5.97 ± 0.29	1.67 ± 0.07	8
	100 μM	−6.39 ± 0.18	1.57 ± 0.07	15
	1 mM	−5.34 ± 0.13*	1.67 ± 0.17	7

*$P<0.02$ versus control

M.e.p.c. amplitudes and decay rates were determined in endplates voltage-clamped to −100 mV in the isotonic potassium solution from preparations previously incubated for 16–18 h at room temperature in the control sodium solution alone or in sodium solution containing the indicated concentration of colchicine. Colchicine treatment had no significant effect on m.e.p.c. amplitude except at the highest concentration (1 mM). There was no significant change in decay rates at any concentration. Values represent the mean ± s.e.mean from *n* endplates.

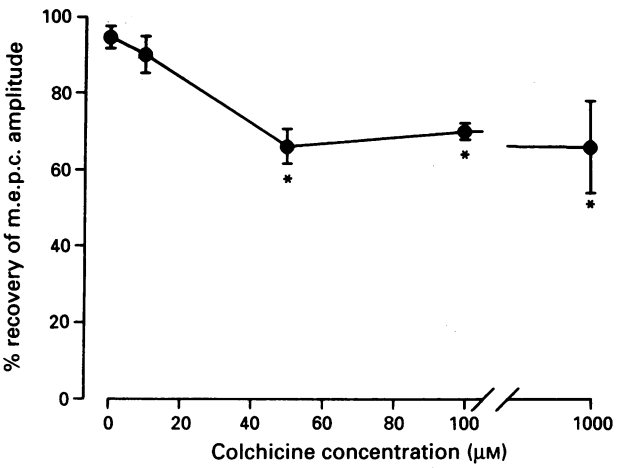


Figure 1 Concentration-dependent inhibition of m.e.p.c. amplitude by colchicine following exposure to carbachol. M.e.p.c. amplitudes at −100 mV were measured prior to, and following a 10 min exposure to 540 μM carbachol in preparations pretreated with concentrations of colchicine ranging from 10 μM to 1 mM. The results are expressed as the percentage of the initial m.e.p.c. amplitude (mean ± s.e.mean from 7 or more endplates). As the colchicine concentration was increased to 50 μM or above, there was a significant decrease ($P<0.05$) in the extent of m.e.p.c. amplitude recovery following carbachol exposure as compared to the control preparations.

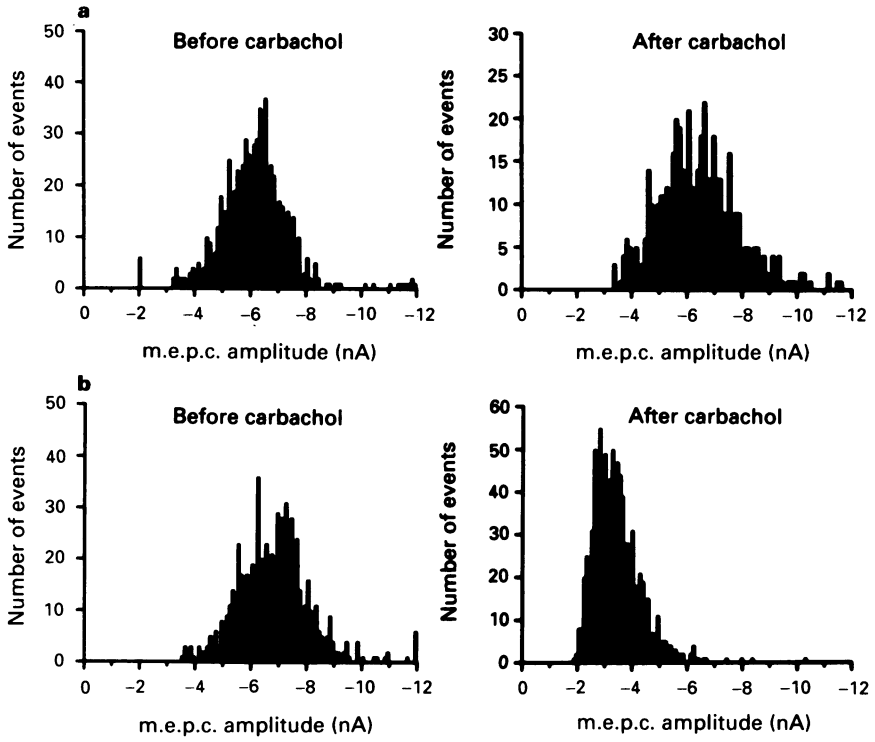


Figure 2 M.e.p.c. amplitude distributions in control and 100 μM colchicine-treated preparations before and after carbachol exposure. M.e.p.c. amplitude distributions were obtained from endplates voltage-clamped to −100 mV in preparations maintained in control sodium solution alone for 16–18 h at room temperature (control, panel a) or with 100 μM colchicine (b). Following a 10 min exposure to 540 μM carbachol (CCh), the distributions remained unimodal for both control and colchicine-treated endplates, however both the mean and mode were shifted to a smaller value in the colchicine-treated endplate. The mean and modal values for each distribution shown are as follows: Control before CCh; mean = −6.16 nA, mode = −6.55 nA, control after CCh; mean = −6.38 nA, mode = −6.65 nA, colchicine before CCh; mean = −6.82 nA, mode = −6.25 nA, colchicine after CCh; mean = −3.44 nA, mode = −2.81 nA.

significantly decreased (Hardwick *et al.*, 1991; Hardwick & Parsons, 1993a). In the present study, we tested whether pretreatment with colchicine would alter the ability of staurosporine to decrease m.e.p.c. amplitude recovery. For these experiments, muscle preparations were incubated for 16–18 h in the control sodium solution containing 100 μM colchicine, washed, and then incubated with 0.5 μM staurosporine in potassium propionate solution for 15 min before exposure to carbachol for 10 min. In the colchicine-pretreated preparations, staurosporine significantly reduced the extent of m.e.p.c. amplitude recovery below that produced by colchicine treatment alone (Table 2). Treatment with colchicine alone produced a maximal inhibition to ~70% of control amplitudes, whereas the combination of colchicine and staurosporine produced a maximal inhibition to ~60%, a value similar to that produced by staurosporine alone.

Small conductance ACh-activated channels are present at colchicine-treated endplates

We observed in previous studies that the decrease in m.e.p.c. amplitude in staurosporine-treated endplates following carbachol exposure was associated with the appearance of a population of small conductance ACh-activated channels (Hardwick & Parsons, 1993a). We therefore initiated patch clamp studies to determine whether an alteration in the conductance of ACh-activated channels also contributed to the decrease in m.e.p.c. amplitude following recovery at colchicine-treated endplates. ACh-activated (1 μM) currents were recorded from cell attached patches on enzymatically-cleaned endplates of fibres from colchicine-treated preparations (100 μM, 16–18 h) prior to, and following a 10 min exposure to 540 μM carbachol. Recordings were initially made with the patch held at −100 mV. Thereafter, whenever possible, recordings were also made at several other voltages to estimate the slope conductance (Figure 3). Because the rate of desensitization is accelerated following carbachol exposure (Hardwick *et al.*, 1991; Hardwick & Parsons, 1993a), it was often impossible to obtain recordings at several voltages from a single patch.

Recordings were obtained from 10 patches on colchicine-treated fibres prior to carbachol exposure and from 9 patches on colchicine-treated fibres following carbachol exposure. In

Table 2 Effects of 100 μM colchicine treatment on m.e.p.c. amplitude and decay rates following carbachol exposure

	m.e.p.c. amplitude (nA)	*% recovery*	*Decay time constant (ms)*	n
Control	−5.35 ± 0.15	88%	1.51 ± 0.09	21
Colchicine	−4.82 ± 0.15*	78%	1.62 ± 0.06	31
Colchicine + staurosporine	−4.13 ± 0.15†	67%	1.68 ± 0.12	13

*$P<0.05$ versus control recovery; †$P<0.05$ versus colchicine recovery.

M.e.p.c. amplitudes and decay time constants were determined in voltage-clamped endplates from control fibres and fibres treated with 100 μM colchicine for 16–18 h both prior to (see Table 1), and following a 10 min exposure to 540 μM carbachol. Following carbachol exposure, there was a significant decrease in m.e.p.c. amplitude in colchicine-treated fibres with no significant change in decay rates. Pretreatment of colchicine-treated preparations with 0.5 μM staurosporine resulted in a significant decrease in m.e.p.c. amplitude as compared to colchicine treatment alone.

Table 3 Characteristics of acetylcholine (ACh)-activated single channel currents

	Amplitude at −100 mV (pA)	*Mean open time (ms)*	*Slope conductance (pS)*	n
Before carbachol treatment:				
Colchicine-treated	−4.50 ± 0.25	1.99 ± 0.27	44 ± 3	11
	−2.58	1.67	22 ± 2	1
After 10 min 540 μM carbachol:				
Colchicine	−4.94 ± 0.19	2.83 ± 0.41	48 ± 2	8
recovery	−2.95 ± 0.15	1.52 ± 0.24	29 ± 1	7
Colchicine/	−4.91 ± 0.23	2.17 ± 0.24	47 ± 2	5
staurosporine	−2.52 ± 0.08	1.18 ± 0.57	27 ± 4	3
recovery				

ACh (1 μM)-induced single channel currents were measured from cell attached patches at colchicine-treated fibres prior to and following a 10 min exposure to 540 μM carbachol. In colchicine-treated fibres not exposed to carbachol, only one population of channels was normally seen. Following carbachol exposure, two populations of channels were consistently observed. Some colchicine-treated preparations were also pretreated with 0.5 μM staurosporine prior to carbachol exposure. Two populations of channels were observed at these endplates as well. Slope conductances (mean ± s.e.mean) were determined from linear regression analysis of the current-voltage relationship for each treatment. Values shown are the mean ± s.e.mean of *n* endplates for the current amplitudes and arithmetic open times.

9 of the 10 patches made on colchicine-treated endplates not exposed to carbachol, a single population of large conductance ACh-activated channels was seen. The amplitude, open time, and slope conductance values for these channels were similar to those determined previously in untreated control fibres (Table 3, Hardwick & Parsons, 1995). In 1 patch from a colchicine-treated fibre, two channel populations were observed, a typical large conductance channel and a second small conductance channel. The current amplitude at −100 mV and the estimated slope conductance was similar to that of the small conductance channel observed previously in staurosporine-treated endplates following carbachol exposure (Table 3).

ACh-activated channels were also recorded from cholchicine-treated endplates following a 10 min exposure to carbachol. A mixture of large and small amplitude channels were observed under these conditions. The amplitude, open times and slope conductances of the large channels were similar to those seen in the colchicine-treated fibres not exposed to carbachol (Table 3). In addition, the small conductance channels had a similar amplitude, open time and conductance to those seen in staurosporine-treated fibres following carbachol exposure (Table 3, Hardwick & Parsons, 1995).

We also recorded single channel currents from colchicine-treated preparations which were then incubated with 0.5 μM staurosporine before exposure to 540 μM carbachol for 10 min. Recordings were made from 4 separate patches and of those, 3 had both large and small channels and 1 had only large channels. Both the amplitudes at −100 mV and the estimated slope conductances were essentially the same, following carbachol exposure, as preparations treated with colchicine alone (Table 3).

Discussion

A variety of studies have demonstrated the importance of the cytoskeleton in AChR cluster formation (Bloch, 1983; Connolly, 1984; Wallace, 1988; Froehner, 1991). An extensive network of microtubules is associated with the postsynaptic membrane (Jasmin *et al.*, 1990; 1991) and several cytoplasmic proteins have been suggested as potential factors in the



Figure 3 Acetylcholine (ACh)-activated single channel currents following carbachol exposure in colchicine-treated preparations. ACh (1 μM)-activated currents were recorded from endplates treated initially with 100 μM colchicine for 18–20 h and then exposed to 540 μM carbachol for 10 min (a). Some preparations were also pretreated with 0.5 μM staurosporine prior to carbachol exposure (b). A mixture of small and large conductance channels were observed under both conditions. Calibration bars: X axis = 5 ms, Y axis = 10 pA.

clustering and anchoring of AChRs including the 43K protein (Froehner *et al.*, 1990), the 58K protein (Froehner *et al.*, 1987; Butler *et al.*, 1992), and an 87K protein (Carr *et al.*, 1989; Butler *et al.*, 1992; Wagner *et al.*, 1993). Studies by Bloch, (1983) and Connolly (1984) suggest that depolymerization of microtubules results in an inhibition of lateral movement of the AChRs in the membrane. Bloch (1983) also observed a significant change in vinculin organization around cultured myotube AChR clusters following colchicine treatments. Cytoskeletal elements have been shown to play an active role in the regulation of several different ion channels including the N-methyl-D-aspartate receptor-channel (Rosenmund & Westbrook, 1993), Ca^{2+}-channels (Johnson & Byerly, 1993), and epithelial Na^{+}-channels (Cantiello *et al.*, 1991). Regulation of these channels by cytoskeletal elements was also demonstrated to be ATP-dependent, suggesting the possible involvement of protein kinases (Rosenmund & Westbrook, 1993; Johnson & Byerly, 1993). Work in our laboratory demonstrated the requirement for PKC activity in the restoration of normal AChR function at the neuromuscular junction following prolonged agonist exposure (Hardwick & Parsons, 1995). Consequently, we have examined the potential role of cytoskeletal elements in this process by testing the effects of colchicine on endplate resensitization.

Pretreatment with 10–100 μM colchicine alone had no effect on m.e.p.c. amplitude or decay time constant. Also, in the majority of single channel recordings from preparations treated with 100 μM colchicine, only large conductance channels were seen. These observations indicated that treatment with these concentrations of colchicine had no remarkable effect on existing, activatable receptors.

Following carbachol exposure, the extent of m.e.p.c. amplitude recovery was decreased at colchicine-treated endplates. Similar to the results found in the preceding study (Hardwick & Parsons, 1995), this decrease in m.e.p.c. amplitude was not associated with either a change in the m.e.p.c. reversal potential or change in the shape of the m.e.p.c amplitude distribution.

The decrease in m.e.p.c. amplitude recovery in colchicine-treated fibres was accompanied by the appearance of a population of small conductance AChRs, just as was seen previously with PKC inhibition (Hardwick & Parsons, 1993a,b; Hardwick & Parsons, 1995). In colchicine-treated fibres not exposed to carbachol, a 44–50 pS channel was the major class of channels observed. Following carbachol exposure, a mixture of small (29 pS) and large (48 pS) conductance channels were observed at colchicine-treated endplate. In addition, there was no apparent difference in the mean open times of the large and small conductance channels, as was also observed in the previous study (Hardwick & Parsons, 1995).

We found that the combination of pretreatment with colchicine and staurosporine resulted in a further reduction of

m.e.p.c. amplitude. However, the maximum inhibition of m.e.p.c. amplitude recovery of colchicine and staurosporine combined never exceeded that of staurosporine alone (Hardwick & Parsons, 1995). Since both colchicine treatment and staurosporine treatment result in the appearance of a similar population of small conductance channels, it seems likely that the two agents may be inhibiting different aspects of the same process.

The results presented here do not identify the mechanism underlying the effect of colchicine treatment on AChR recovery. However, the following scheme is presented as one possible explanation. First, exposure to high concentration of agonist for a prolonged time activates and desensitizes virtually all functional AChRs (Hardwick *et al.*, 1991). We propose that a subpopulation of these receptors become destabilized in the membrane, perhaps due to an activation-dependent dephosphorylation of either an anchoring protein or the AChR itself. It is these destabilized receptors which have a reduced conductance. In order to restore normal function, these destabilized AChRs must be re-anchored in the membrane, a process which we suggest requires an intact subsynaptic microtubular network and phosphorylation by PKC. Although hypothetical at this point, this scheme is consistent with the results of others which demonstrate that (a) AChR mobility is affected by cytoskeletal disruption (Bloch, 1983; Connolly, 1984; Wallace, 1988; Froehner, 1991) and that (b) the AChR, as well as several other proteins known to be involved in AChR anchoring contain sites for phosphorylation (Huganir, 1988; Hall & Sanes, 1993; Wagner *et al.*, 1993).

In conclusion, the results presented indicate that full recovery of endplate sensitivity following prolonged exposure to carbachol requires an intact subsynaptic cytoskeleton as well as phosphorylation of the AChR or an associated protein by PKC. Furthermore, it is evident that interference with elements of the cytoskeleton by colchicine treatment or the inhibition of PKC results in the appearance of the same population of small conductance AChRs and that the decrease in m.e.p.c. amplitude observed with both treatments following recovery results from the activation of a mixture of large and small conductance channels.

We would like to thank Drs Cynthia Forehand and Carson Cornbrooks for critical review of early versions of this manuscript. We would also like to thank Mr Dean Melen for excellent technical assistance and Dr John Dempster for the generous gift of the programme SCAN. This work was supported by NIH grants NS 08580 to J.C.H. and NS 23978 to R.L.P.

References

BLOCH, R.J. (1983). Acetylcholine receptor clustering rat myotubes: Requirements for Ca^{2+} and effects of drugs which depolymerize microtubules. *J. Neurosci.*, **3**, 670–2680.

BUTLER, M.H., DOUVILLE, K., MURNANAE, A.A., KRAMARDY, N.R., COHEN, J.B., SEALOCK, R. & FROEHNER, S.C. (1992). Association of the M_r 58,000 postsynaptic protein of electric tissue with *Torpedo* dystrophin and the M_r 87 000 postsynaptic protein. *J. Biol. Chem.*, **267**, 6213–6218.

CANTIELLO, H.F., STOW, J.L., PRAT, A.G. & AUSIELLO, D.A. (1991). Actin filaments regulate epithelial Na^+ channel activity. *Am. J. Physiol.*, **261**, C882–C886.

CARR, C., FISCHBACH, G.D. & COHEN, J.B. (1989). A novel M_r 87 000 protein associated with acetylcholine receptors in *Torpedo* electric organ and vertebrate skeletal muscle. *J. Cell Biol.*, **109**, 1753–1764.

CONNOLLY, J.A. (1984). Role of the cytoskeleton in the formation, stabilization, and removal of acetylcholine receptor cluster in cultured muscle cells. *J. Cell Biol.*, **99**, 148–154.

CONNOR, E.A., FIEKERS, J.F., NEEL, D.S., PARSONS, R.L., & SCHNITZLER, R.M. (1984). Comparison of cholinergic activation and desensitization at snake twitch and slow muscle fibre endplates. *J. Physiol.*, **351**, 657–674.

FROEHNER, S.C. (1991). The submembrane machinery for nicotinic acetylcholine receptor clustering. *J. Cell Biol.*, **114**, 1–7.

FROEHNER, S.C., LUETJE, C.W., SCOTLAND, P.B. & PATRICK, J. (1990). The postsynaptic 43K protein clusters muscle nicotinic acetylcholine receptors in *Xenopus* oocytes. *Neuron*, **5**, 403–410.

FROEHNER, S.C., MURNANE, A.A., TOBLER, M., PENG, H.B. & SEALOCK, R. (1987). A postsynaptic M_r 58 000 (58K) protein concentrated at acetylcholine receptor-rich sites in the Torpedo electroplaques and skeletal muscle. *J. Cell Biol.*, **104**, 1633–1646.

HALL, Z.W. & SANES, J.R. (1993). Synaptic structure and development: The neuromuscular junction. *Neuron*, **10**, 99–121.

HARDWICK, J.C., CONIGLIO, L.M. & PARSONS, R.L. (1991). Staurosporine inhibits the extent of acetylcholine receptor recovery from carbachol-induced desensitization in snake twitch fibres. *Br. J. Pharmacol.*, **104**, 879–886.

HARDWICK, J.C. & PARSONS, R.L. (1993a). Mechanism of staurosporine-induced decrease in acetylcholine receptor recovery from desensitization. *Br. J. Pharmacol.*, **108**, 741–748.

HARDWICK, J.C. & PARSONS, R.L. (1993b). Necessity of divalent cations for recovery from carbachol-induced acetylcholine receptor inactivation. *Br. J. Pharmacol.*, **110**, 889–895.

HARDWICK, J.C. & PARSONS, R.L. (1993b). Necessity of divalent cations for recovery from carbachol-induced acetylcholine receptor inactivation. *Br. J. Pharmacol.*, **110**, 889–895.

HARDWICK, J.C. & PARSONS, R.L. (1995). Necessity of protein kinase C activity for maintenance of acetylcholine receptor functions at snake twitch fibre endplates. *Br. J. Pharmacol.*, **114**, 433–441.

HUGANIR, R.L. (1988). Regulation of the nicotinic acetylcholine receptor channel by a protein phosphorylation. *Curr. Top. Memb. Transp.*, **33**, 147–163.

JASMIN, B.J., CHANGEUX, J-P. & CARTAUD, J. (1990). Compartmentalization of cold-stable and acetylated microtubules in the subsynaptic domain of chick skeletal muscle fibre. *Nature*, **344**, 673–675.

JASMIN, B.J., CHANGEUX, J-P. & CARTAUD, J. (1991). Organization and dynamics of microtubules in *Torpedo marmorata* electrocyte: Selective association with specialized domains of the postsynaptic membrane. *Neurosci.*, **43**, 151–162.

JOHNSON, B.D. & BYERLY, L. (1993). A cytoskeletal mechanism for Ca^{2+}. *Neuron*, **10**, 797–804.

PENG, H.B. (1984). Participation of calcium and calmodulin in the formation of acetylcholine receptor clusters. *J. Cell Biol.*, **98**, 550–557.

ROSENMUND, C. & WESTBROOK, G.L. (1993). Calcium-induced actin depolymerization reduces NMDA channel activity. *Neuron*, **10**, 805–814.

ROSS, A., RAPUANO, M. & PRIVES, J. (1988). Induction of phosphorylation and cell surface redistribution of acetylcholine receptors by phorbol ester and carbamylcholine in cultured chick muscle cells. *J. Cell Biol.*, **107**, 1139–1145.

WAGNER, K.R., COHEN, J.B. & HUGANIR, R.L. (1993). The 87K postsynaptic membrane protein from Torpedo is a protein-tyrosine kinase substrate homologous to dystrophin. *Neuron*, **10**, 511–522.

WALLACE, B.G. (1988). Regulation of agrin-induced acetylcholine receptor aggregation by Ca^{++} and phorbol ester. *J. Cell Biol.*, **107**, 267–278.

WALLACE, B.G. (1994). Staurosporine inhibits agrin-induced acetylcholine receptor phosphorylation and aggregation. *J. Cell Biol.*, **125**, 661–668.

WALLACE, B.G., QU, Z. & HUGANIR, R.L. (1991). Agrin induces phosphorylation of the nicotinic acetylcholine receptor. *Neuron*, **6**, 869–878.

(Received June 27, 1994
Revised September 12, 1994
Accepted September 28, 1994).

British Journal of Pharmacology (1995) 114, 447-453 © 1995 Stockton Press All rights reserved 0007-1188/95 $9.00

Species-related differences in inotropic effects of angiotensin II in mammalian ventricular muscle: receptors, subtypes and phosphoinositide hydrolysis

Akira Ishihata & [1]Masao Endoh

Department of Pharmacology, Yamagata University School of Medicine, Yamagata 990-23, Japan

1 Experiments were carried out to clarify the mechanisms responsible for variations in the positive inotropic effect (PIE) of angiotensin II (AII) on ventricular muscles from various mammals. We examined the density of AII receptors, the relative proportions of receptor subtypes and the acceleration of the hydrolysis of phosphoinositide that was induced by AII, as well as the PIE of AII in ventricular muscles from the rabbit, dog, rat and ferret.

2 In the rabbit, AII (1 μM) in the presence of bupranolol (0.3 μM) and prazosin (0.1 μM) elicited a concentration-dependent PIE, which was antagonized by a selective AT_1 subtype antagonist, losartan, but not by an AT_2 antagonist, PD123319. AII did not have any inotropic effects in ventricular muscles from the dog, rat and ferret.

3 Specific high-affinity binding of [^{125}I]-AII, with a similar K_d value in each case (1–2 nM), was observed with membrane fractions derived from ventricular muscle of all four species tested.

4 In the rabbit, losartan and PD123319 each displaced approximately 50% of [^{125}I]-AII specific binding having high affinity for the receptors, and indicating that AT_1 and AT_2 subtypes were present in equal numbers. In the other species the AT_1 subtype of receptors was predominant.

5 In all four species AII caused a concentration-dependent acceleration of the hydrolysis of phosphoinositide in ventricular slices that had been prelabelled with *myo*-[^{3}H]-inositol.

6 The results indicate that the signal-transduction process distal to acceleration of the hydrolysis of phosphoinositide may be responsible for the wide range of species variations in the inotropic action of AII on mammalian ventricular myocardium.

Keywords: Angiotensin II; AT_1 receptor; AT_2 receptor; positive inotropic effect; species difference; hydrolysis of phosphoinositide; binding of [^{125}I]-angiotensin II; losartan; PD123319

Introduction

Angiotensin II (AII) elicits a positive inotropic effect (PIE) in the cardiac muscles of certain mammalian species that include man (Moravec *et al.*, 1990) and the rabbit (Dempsey *et al.*, 1971; Freer *et al.*, 1976; Ishihata & Endoh, 1993). Direct activation of specific receptors by AII is considered to trigger a signal-transduction process that results in the PIE (Dempsey *et al.*, 1971; Freer *et al.*, 1976; Kobayashi *et al.*, 1978; Moravec *et al.*, 1990). However, the AII-induced PIE varies widely among different mammalian species. In addition to AII receptor density differences between species, the presence of two subtypes of AII receptors, AT_1 and AT_2, may contribute to these species-dependent variations.

AT_1 receptors consist of 359 amino acid residues with seven putative membrane-spanning domains and they belong to the family of G protein-coupled receptors (Sasaki *et al.*, 1991; Iwai *et al.*, 1991). AT_2 receptors, on the other hand, appear not to interact with G proteins (Bottari *et al.*, 1991). Nevertheless, the receptors can be distinguished using the nonpeptide AT_1-selective antagonist losartan and the AT_2-selective antagonist PD123319 (Whitebread *et al.*, 1989; Dudley *et al.*, 1990). It has been shown that both subtypes are present in rabbit ventricular myocardium (Rogg *et al.*, 1990).

Activation of AII receptors in cardiac muscle is coupled to various signal-transduction processes, which include activation of the slow Ca^{2+} channel (Freer *et al.*, 1976) and acceleration of the hydrolysis of phosphoinositide (Leung *et al.*, 1986; Baker & Singer, 1988; Baker *et al.*, 1989; Baker & Aceto, 1989). We recently demonstrated that, in the rabbit ventricular muscle, the PIE of AII is elicited via activation of AT_1 receptors in association with acceleration of the hydrolysis of phosphoinositide (Ishihata & Endoh, 1993). In the present study, the density of AII receptors, the relative proportion of AT_1 and AT_2 receptor subtypes and the acceleration of the hydrolysis of phosphoinositide induced by AII have each been determined in the ventricular muscles of the rabbit, dog, rat and ferret. The results are discussed in terms of the mechanisms responsible for the wide range of species-dependent variations in the AII-induced PIE on mammalian cardiac muscle.

Methods

Isolation of ventricular muscles and experimental procedures

Male albino rabbits weighing 1.5–2.2 kg, male Wistar rats weighing 250–350 g, mongrel dogs weighing 5–10 kg and male ferrets weighing 1.5–2.0 kg were used for the experiments. The rabbits were anaesthetized by intravenous administration of sodium pentobarbitone (35 mg kg^{-1}) into a marginal ear vein; 1000 u kg^{-1} heparin sodium was administered simultaneously. The heart was removed immediately, and two or three papillary muscles were excised from the right ventricle. Rats and ferrets were lightly anaesthetized with ether and heparinized (1500 u kg^{-1}, i.p.), and right ventricular papillary muscles were isolated. Dogs were anaesthetized with sodium pentobarbitone (35 mg kg^{-1}, i.v.) and right ventricular trabeculae were excised. Muscles were mounted in 20 ml organ baths that contained Krebs-

[1] Author for correspondence.

Henseleit solution (plus 0.057 mM ascorbic acid and 0.027 mM disodium EDTA to prevent the autoxidation of compounds examined). The solution was bubbled with 95% O_2 and 5% CO_2 at 37°C and the pH of the solution was 7.4 when bubbled with the gas mixture. Concentrations of the various constituents of the solution were as follows (mM): Na^+ 142.9, K^+ 5.9, Mg^{2+} 1.2, Ca^{2+} 2.5, $H_2PO_4^-$ 1.2, HCO_3^- 24.9, SO_4^{2-} 1.2, Cl^- 127.8 and glucose 11.1. In the case of rat papillary muscles, the extracellular concentration of Ca^{2+} ions was reduced to 1.25 mM. Ventricular muscles were electrically stimulated by square-wave pulses of 5 ms duration and a voltage that was approximately 20% greater than the threshold. Pulses were applied at a frequency of 1 Hz for rabbits, rats and ferrets and 0.5 Hz for dogs. The developed tension was recorded on a thermal pen-writing oscillograph (Recti-Horiz-8K; NEC-San-ei Instrument, Tokyo, Japan) via strain-gauge transducers (Shinkoh UL 10 GR; Minebea, Tokyo, Japan). During the 60 min equilibration period, papillary muscles were stretched to a length that gave 90% of the maximal contractile force. (±)-Bupranolol (0.3 μM) and prazosin (0.1 μM) were allowed to act for 20 min before the administration of AII and were both present in the solution in the organ bath throughout the experiments to avoid any interference by α- and β-adrenoceptor stimulation as a result of the release of catecholamines (Dempsey *et al.*, 1971). At the end of each experiment, the maximal contractile force was determined in each muscle by administration of isoprenaline (1–10 μM) after washing out of other drugs for at least 1 h and the basal force of contraction had returned to the control level. The concentration was elevated in a stepwise manner until the maximal response was achieved.

Radioligand-binding assay

Details of the experimental procedures used to prepare the membrane fraction and of the binding assay were essentially the same as those described previously by Takanashi & Endoh (1991). In brief, pieces of ventricular muscle, including free walls and septum (rabbits, rats or ferrets) or right ventricular free wall (dogs), were excised and homogenized in 10 volumes of ice-cold buffer (0.25 M sucrose containing 5 mM tris(hydroxymethyl)aminomethane (Tris)-HCl and 1 mM $MgCl_2$, pH 7.4) in a Polytron PT-10 (Kinematica, Lucerne, Switzerland) with three bouts of 15 s each at a setting of 7. The homogenate was centrifuged at 500 *g* for 15 min at 4°C. The supernatant was filtered through a single layer of cheesecloth and centrifuged at 50,000 *g* for 20 min at 4°C. The resultant pellet was washed twice with ice-cold incubation buffer (50 mM Tris-HCl, 10 mM $MgCl_2$, pH 7.5) by repeated resuspension and recentrifugation. The final pellet was resuspended in ice-cold incubation buffer that contained 2 mg ml^{-1} bovine serum albumin and 0.2 mg ml^{-1} bacitracin.

[^{125}I]-angiotensin II binding to membrane fractions was carried out as follows. The incubation mixture contained 150 μl of a suspension of membranes (approximately 150–300 μg of protein), 50 μl of a solution of [^{125}I]-angiotensin II at various concentrations (specific activity, ca. 2,000 Ci $mmol^{-1}$) and 50 μl of incubation buffer (for total binding) or unlabelled AII (1 μM; for nonspecific binding). In the experiments to examine displacement of [^{125}I]-AII, the incubation mixture contained 150 μl of the membrane fraction, 50 μl of [^{125}I]-AII (0.25 nM) and 50 μl of a solution of unlabelled competitor at various concentrations. The incubation, started by the addition of the membrane fraction, was carried out for 60 min at 25°C and terminated by addition of 2 ml of ice-cold incubation buffer. Reaction mixtures were subjected to rapid filtration under reduced pressure through glass-fibre Whatman GF/C filters (presoaked in incubation buffer that contained 2 mg ml^{-1} bovine serum albumin), using a Brandel 24R cell-harvester (Brandel, Gaithersburg, MD, U.S.A.). The filters were immediately washed three times with 4 ml of ice-cold incubation buffer. After drying of filters (1 h at 90°C) the radioactivity trapped on to the filters was quantitated with an automatic gamma counter (1470 WIZARD; Wallac Oy, Turku, Finland) at an efficiency of more than 78%.

Nonspecific binding of [^{125}I]-AII was defined as the radioactivity that bound to membrane fractions that was not displaced by a high concentration of unlabelled AII (1 μM). Specific binding of [^{125}I]-AII was defined in terms of total radioactivity minus radioactivity due to nonspecific binding. Each binding assay was carried out in duplicate. Protein was quantitated by the method of Lowry *et al.* (1951).

Quantitation of [^{3}H]-inositol phosphates

Hearts were quickly removed from rabbits, rats, dogs and ferrets, and placed in Krebs-Henseleit solution that was bubbled with 95% O_2:5% CO_2 at 4°C. The experimental procedure was the same as that described previously (Ishihata & Endoh, 1993). In brief, ventricular slices (0.5 mm thick) were prepared with a tissue slicer (Thomas, Philadelphia, PA, U.S.A.) and were equilibrated in Krebs-Henseleit solution for 30 min. Each experiment was carried out in duplicate. Each tube contained one slice of ventricle that had been cut and trimmed to an appropriate size (ca. 40 mg and 0.5 mm in thickness). The slice in each tube was preincubated with 24 μCi *myo*-[^{3}H]-inositol in 4 ml Krebs-Henseleit solution for 120 min. Then the solution was changed to fresh solution that contained 5 mM *myo*-inositol and 10 mM LiCl, and all the experiments were performed in the presence of this Li^+-containing solution. (±)-Bupranolol (0.3 μM) and prazosin (0.1 μM) were added to the solution 20 min before administration of an agonist to avoid any interference by activation of adrenoceptors. At the end of the incubation, the slices were quickly blotted, frozen in liquid nitrogen and weighed. Then the slices were put into 1.0 ml of a mixture of chloroform, methanol and 12 N HCl (100:200:1, v/v). After the addition of 0.2 ml of 5 mM EDTA, the tissue was homogenized with a homogenizer (Polytron PT-10). The tip of the homogenizer was rinsed with 0.5 ml of a mixture of chloroform, methanol, 12 N HCl and 5 mM EDTA (100:200:1:80, v/v), and the rinsing fluid was added to the original solution. Chloroform (0.4 ml) and 5 mM EDTA (0.5 ml) were added sequentially and the samples were centrifuged at 1,400 *g* for 20 min to separate the aqueous and organic phases. An aliquot of the aqueous layer was removed, neutralized with 1 M KOH and applied to column that contained a 50% slurry of AG1-X8 (anion-exchange resin, 100–200 mesh, formate form; Bio-Rad, Richmond, CA, U.S.A.). Each column was washed first with 20 ml distilled water, and the resulting glycerophosphoryl esters were eluted with 8 ml 5 mM sodium tetraborate-60 mM sodium formate as described previously (Berridge *et al.*, 1983; Takanashi & Endoh, 1991). Then [^{3}H]-inositol phosphates were eluted by 0.2 M ammonium formate in 0.1 M formate as described by Berridge *et al.* (1983). Aliquots of the eluate were monitored for radioactivity, after addition to a scintillation mixture (ACS-II; Amersham, Arlington Heights, IL, U.S.A.) in a scintillation counter (Tri-Carb 1500; Packard, Downers Grove, IL, U.S.A.) with an efficiency of 66%. Since it had been determined in a preliminary experiment that the radioactivity of [^{3}H]-inositol trisphosphate (IP_3) and of [^{3}H]-inositol bisphosphate was low, probably because of their rapid metabolism to [^{3}H]inositol monophosphate (IP_1), IP_1 was used as an indicator of the hydrolysis of phosphoinositide (Ishihata & Endoh, 1993).

Drugs

The drugs used were obtained from the sources listed in parentheses: prazosin hydrochloride (Pfizer Taito, Tokyo, Japan); (±)-bupranolol HCl (Kaken Pharmaceutical, Tokyo, Japan); AII (Peptide Institute, Osaka, Japan); saralasin ([Sar^1, Val^5, Ala^8]angiotensin II; Sigma Chemical,

St. Louis, MO, U.S.A.); losartan (2-n-butyl-4-chloro-5-hydroxymethyl-1-[(2'-(1H-tetrazole-5-yl)biphenyl-4-yl)methyl] imidazole, potassium salt; Du Pont, Wilmington, DE, U.S.A.); (−)-isoprenaline hydrochloride, *myo*-inositol and lithium chloride (Sigma Chemical, St. Louis, MO, U.S.A.); *myo*-[^{3}H]inositol (specific activity 115.5 Ci.mmol^{-1}; Amersham, Buckinghamshire, UK); PD123319-121b ((S)-1-[[4-dimethylamino)-3-methylphenyl]methyl]-5-(diphenylacetyl)-4,5,6,7-tetrahydro-1H-imidazo[4,5-c]pyridine-6-carboxylic acid, ditrifluoroacetate, dihydrate; Warner-Lambert, Ann Arbor, MI, U.S.A.). The stock solution of isoprenaline was prepared in 1% w/v ascorbic acid, further diluted with 0.9% w/v NaCl solution and kept ice-cold.

Analysis of data and statistics

In the radioligand-binding assay, the maximum number of binding sites (B_{max}) and the equilibrium dissociation constant (K_d) were determined from a Scatchard plot. Analysis of the curve for the displacement of [^{125}I]-AII by nonlinear curve-fitting was performed by use of the LIGAND programme. The inhibition constant (K_i) was calculated from the following formula: $K_i = IC_{50}(1 + L^*.K_d^{-1})^{-1}$, where L^* is the concentration of radioactive ligand used and K_d is the dissociation constant. Experimental values are presented as means ± s.e.mean. Statistical analysis was performed by one-way analysis of variance, and when the F ratio indicated a significant difference, differing pairs were compared by Tukey's test. A P value of less than 0.05 was considered to indicate a significant difference.

Results

Inotropic effects of angiotensin II on ventricular muscles from different mammalian species

Figure 1 shows the effects of AII on the force of contraction in the presence of bupranolol (0.3 μM) and prazosin (0.1 μM) on ventricular muscles isolated from the rat, dog and ferret. AII (1 μM) did not have any inotropic effect in rat and ferret papillary muscles, or in dog ventricular trabeculae. However isoprenaline, administered after washing out of the drugs for 1 h elicited a concentration-dependent PIE in these preparations. By contrast, in the rabbit ventricular papillary muscle, AII elicited a concentration-dependent PIE (Figure 2). The PIE was inhibited by the selective AT_1-receptor antagonist, losartan (at 1 and 10 μM, Figure 2a), but not by PD123319 (Figure 2b).

Characteristics of binding of [^{125}I]-angiotensin II to ventricular muscles from different mammalian species

Figure 3a shows results of a representative experiment, namely analysis of the saturation binding of [^{125}I]-AII to a membrane fraction derived from rabbit ventricular muscle, indicating that specific high-affinity binding was saturable. Analysis of the data as a Scatchard plot indicated the presence of an apparently unique class of binding sites (Figure 3b) with a mean K_d value of 0.97 nM and a B_{max} of 37.3 fmol mg^{-1} protein (Table 1). Specifically bound [^{125}I]-AII (0.25 nM) was displaced by saralasin and AII in a monophasic manner, which suggested the presence of a single class of binding sites with high affinity for [^{125}I]-AII (Figure 4). These results are in agreement with previous findings in the rabbit (Mukherjee *et al.*, 1982; Baker *et al.*, 1984; Rogg *et al.*, 1990). By contrast, losartan and PD123319 displaced specifically bound [^{125}I]-AII in a biphasic manner, an indication of the presence of two subtypes of AII receptor in the rabbit myocardium (Figure 4). In the presence of PD123319 (10 μM), losartan displaced [^{125}I]-AII from the remaining binding sites and these sites had a high affinity for losartan ($pK_i = 7.89 \pm 0.11$, $n = 3$), as shown in Figure 5a. By contrast, in the presence of 1 μM of losartan, PD123319 displaced the remaining bound [^{125}I]-AII in a monophasic manner and bound to receptors with high affinity ($pK_i = 7.13 \pm 0.17$, $n = 4$) (Figure 5b). From the results of the displacement experiments using these selective antagonists, we estimated that the AT_1 and AT_2 subtypes accounted for 46% and 54% of the total population of AII

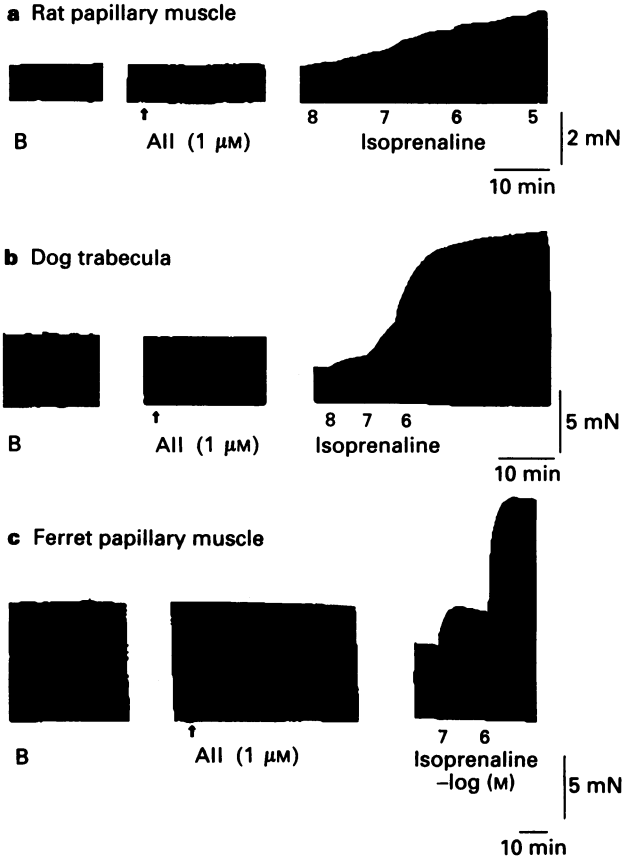


Figure 1 Influence of angiotensin II (AII, 1 μM) on the force of contraction in isolated right ventricular muscles from (a) the rat, (b) dog and (c) ferret in the presence of 0.3 μM bupranolol and 0.1 μM prazosin. The effects of isoprenaline after washing out of the drugs are shown in the right panel for comparison. B, Basal force of contraction.

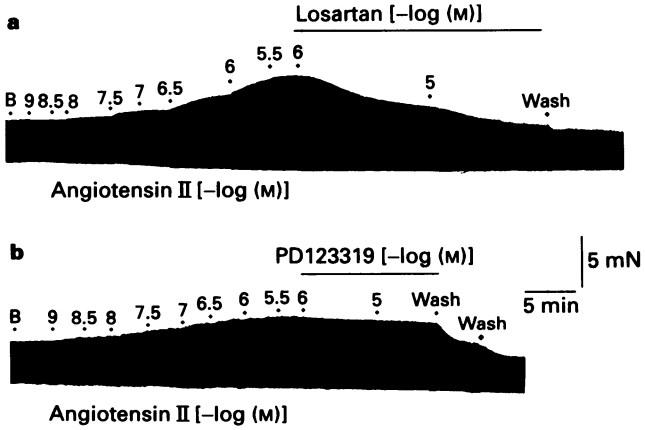


Figure 2 The concentration-dependent effects of angiotensin II (AII 1 μM) on the force of contraction in the presence of 0.3 μM bupranolol and 0.1 μM prazosin and the influence of losartan and PD123319 on the positive inotropic effect of AII in isolated right ventricular papillary muscles from the rabbit. (a) Losartan (1 and 10 μM) was applied when the tension developed by exposure to AII had reached a maximum. (b) PD123319 (1 and 10 μM) was applied when the AII-induced PIE had reached a maximum. B, Basal force of contraction.

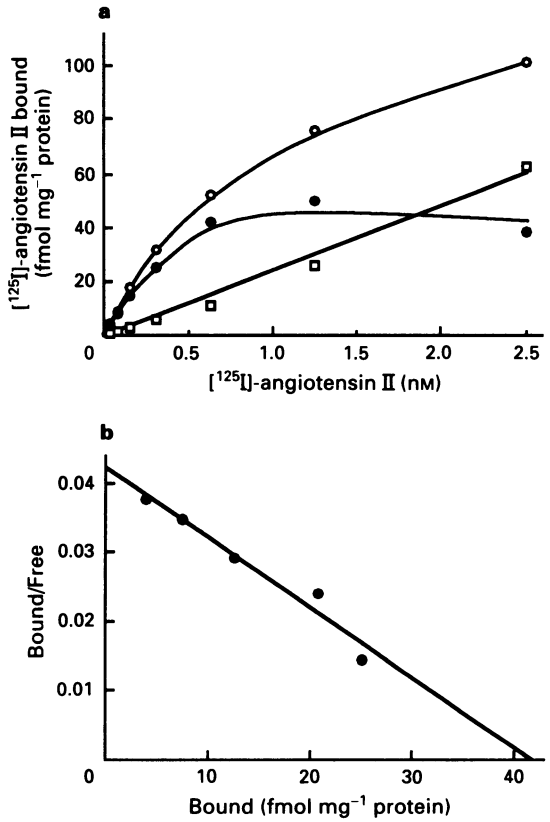


Figure 3 (a) Curves for the saturation binding of [^{125}I]-angiotensin II ([^{125}I]-AII) to the membrane fraction derived from the right ventricular myocardium of the rabbit. Specific binding (●) was defined as total binding (○) minus nonspecific binding (□). (b) Scatchard plot of data calculated from the values in (a). The slope of the regression line was determined by the least-squares methods. Values presented are means of duplicate determinations in a representative experiment.

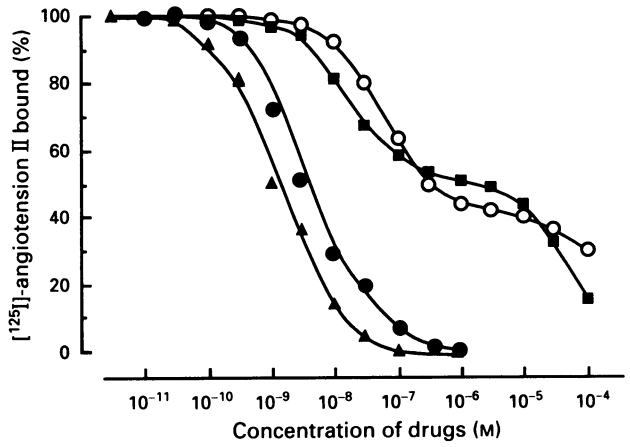


Figure 4 Competition for binding to rabbit ventricular membranes between [^{125}I]-angiotensin II ([^{125}I]-AII, 0.25 nM) and unlabelled AII and non selective and selective antagonists of AII. (●) AII; (▲) saralasin; (■) losartan; (○) PD123319.

receptors in the rabbit ventricular muscle, respectively (Table 2).

Binding experiments with a similar protocol were carried out with membrane fractions from ventricular muscles of the rat, dog and ferret. Saturable high-affinity binding sites for [^{125}I]-AII were found in all of these species. Scatchard analysis of the data indicated the presence of a single class of binding sites in each case. The B_{max} and K_d values for [^{125}I]-AII with membrane fractions from the various species are listed in Table 1. B_{max} values for AII receptors in ventricular muscles from the rabbit, rat and ferret were similar, but the B_{max} value for the dog was significantly higher than the value for the rat (Table 1). The K_d values for [^{125}I]-AII with membrane fractions derived from ventricular muscles of these species were not significantly different from each other when evaluated by ANOVA.

The relative proportions of the subtypes of the AII receptor in the membrane fractions from these species were analysed in terms of displacement of [^{125}I]-AII (0.25 nM) by losartan and PD123319 (Figure 6). In the membrane frac-

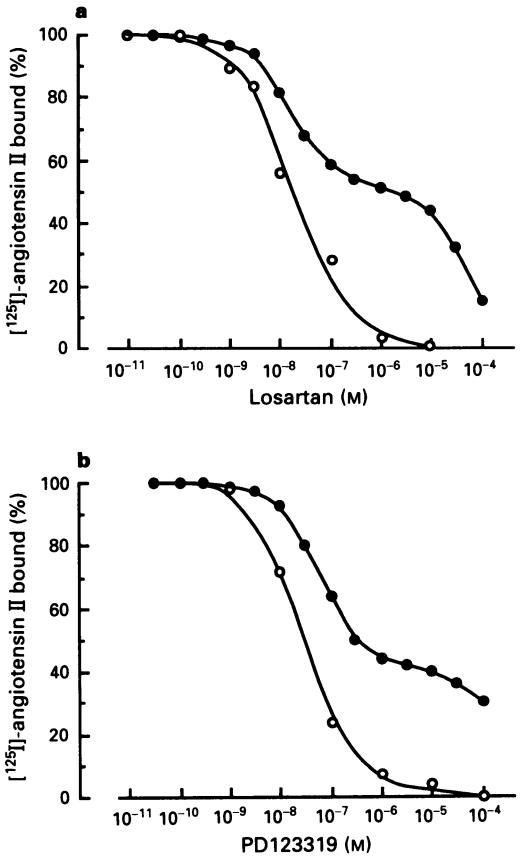


Figure 5 (a) Displacement of [^{125}I]-angiotensin II ([^{125}I]-AII, 0.25 nM) from rabbit ventricular membranes by losartan in the absence (●) and in the presence (○) of PD123319 (10 μM). Binding of [^{125}I]-AII was decreased by PD123319 to 53% of the value in its absence. (b) Displacement of [^{125}I]-AII (0.25 nM) from rabbit ventricular membranes by PD123319 in the absence (●) and in the presence (○) of losartan (1 μM). Binding of [^{125}I]-AII was decreased by losartan to 45% of the value in its absence.

Table 1 Dissociation constants (K_d) and the maximum numbers of binding sites (B_{max}) for [^{125}I]-angiotensin II in membrane fractions derived from the ventricular myocardium of the rabbit, dog, rat and ferret

	Rabbit	*Dog*	*Rat*	*Ferret*
n	4	4	3	4
K_d (nM)	0.97 ± 0.12	1.90 ± 0.20	1.46 ± 0.21	1.51 ± 0.11
B_{max} (fmol mg^{-1} protein)	37.3 ± 5.03	76.1 ± 13.9*	20.7 ± 2.31	37.0 ± 4.55

All values represent means ± s.e.mean in duplicate determinations; *n*, numbers of experiments. *$P < 0.05$ *vs.* the corresponding value in the rat.

Table 2 The binding affinity of losartan and of PD123319 and the relative proportions of the two subtypes of angiotensin II receptor in membrane fractions derived from the ventricular myocardium of the rabbit, dog, rat and ferret

		Losartan-sensitive sites		*PD123319-sensitive sites*		
Species	*PIE*	*pKi*	%	pKi	%	*n*
Rabbit	+	7.89 ± 0.11	46.2 ± 4.67	7.13 ± 0.17	54.2 ± 1.56	4
Dog	–	6.91 ± 0.04	>90	ND	ND	4
Rat	–	7.74 ± 0.46	>90	ND	ND	3
Ferret	–	6.90 ± 0.05	>90	ND	ND	4

All values represent means ± s.e.mean in duplicate determinations; *n*, numbers of experiments; PIE, positive inotropic effect of angiotensin II; ND, not detectable.

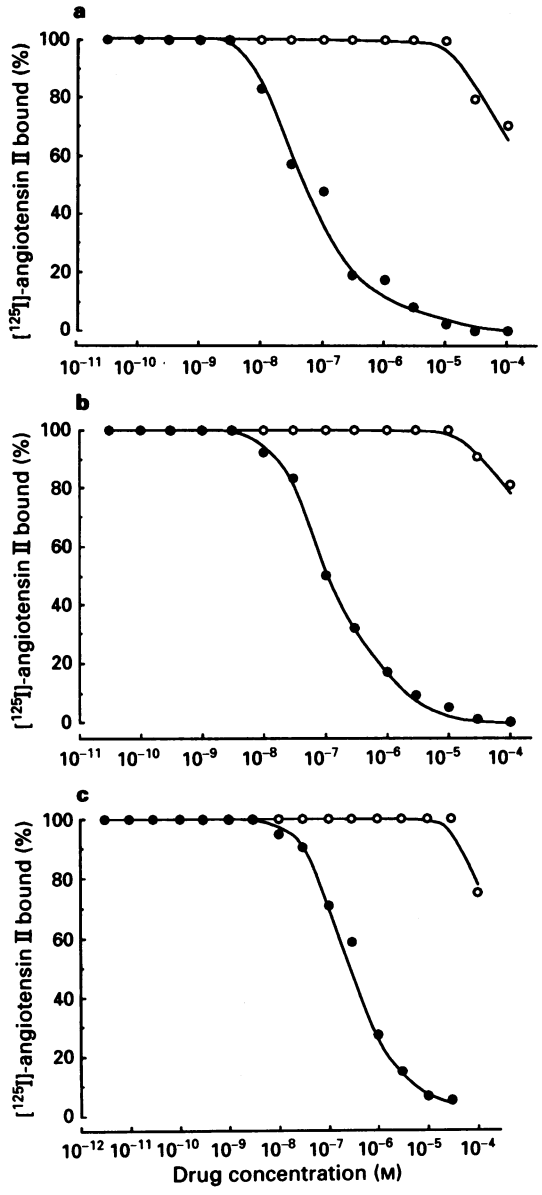


Figure 6 Displacement of [^{125}I]-angiotensin II ([^{125}I]-AII 0.25 nM) from ventricular membrane fractions from (a) the dog, (b) rat and (c) ferret by selective antagonists of AII, PD123319 (○) and losartan (●).

tions derived from ventricular muscles of the rat, dog and ferret, losartan displaced specifically bound [^{125}I]-AII monophasically in a concentration-dependent manner and with high affinity, whereas PD123319 did not displace the binding with high affinity (up to 10 μM) in these species (Figure 6 and Table 2).

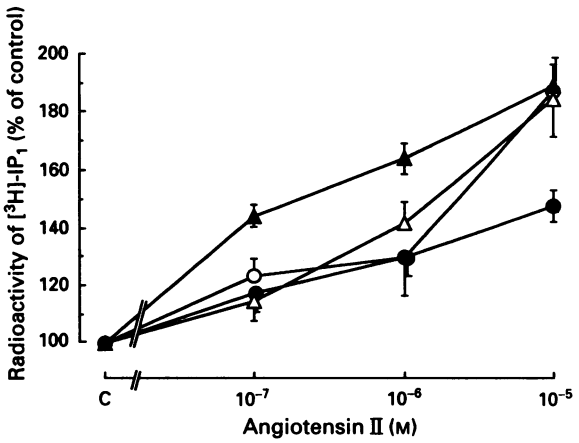


Figure 7 The angiotensin II (AII)-induced accumulation of [^{3}H]-IP$_1$ in ventricular slices from the rabbit (▲), rat (●), dog (○) and ferret (△) that had been prelabelled with *myo*-[^{3}H]-inositol. Concentration-response curves for the accumulation of [^{3}H]-IP$_1$ were generated from data observed 30 min after the addition of AII in the presence of 10 mM LiCl, 0.3 μM bupranolol and 0.1 μM prazosin. Each value indicates the mean ± s.e.mean of results from four or five experiments. C, Control.

Effects of angiotensin II on the hydrolysis of phosphoinositide in ventricular muscles from different mammalian species

Concentration-response curves for the effects of AII on the accumulation of [^{3}H]-IP$_1$ were generated in slices of ventricular muscles from the dog, rat, ferret and rabbit, and the results are presented in Figure 7. Concentration-dependent increases in the accumulation of [^{3}H]-IP$_1$ were induced by AII (0.1–10 μM) in muscle slices isolated from each species. The maximal response to AII in terms of accumulation of [^{3}H]-IP$_1$ in rat ventricles (148.1 ± 5.4%; $n = 5$) was significantly smaller than that in the rabbit. At concentrations of 0.1 and 1 μM, the increase in the accumulation of [^{3}H]-IP$_1$ in response to AII in the rabbit was significantly higher than the increase in other species. However, at 10 μM AII, the increases in the accumulation of [^{3}H]-IP$_1$ were identical in the rabbit, dog and ferret (Figure 7).

Discussion

A wide range of species-dependent variations is apparent in the inotropic effect of AII in mammalian cardiac muscle (Dempsey *et al.*, 1971; Moravec *et al.*, 1990; Ishihata & Endoh, 1993). The PIE of AII was observed only in rabbit ventricular muscle among the mammalian species that we examined in this study. While the reasons for the species-dependent differences in the AII-induced inotropic effect have not been determined, various aspects of the signal-transduction process, including the density of receptors, the

relative proportions of subtypes, second messengers and the subsequent steps that lead to the functional modulation, may be involved. Receptors for AII have been demonstrated in the cardiac muscles of various animals, including the rabbit, chicken, cat and man (Wright *et al.*, 1983; Baker *et al.*, 1984; Rogers, 1984; Rogers *et al.*, 1985, Aceto & Baker, 1990; Moravec *et al.*, 1990). Consistent with these previous findings, saturable high-affinity binding sites for [^{125}I]-AII comparable to those in the rabbit ventricle were found in membrane fractions of rat, dog and ferret ventricular muscles, but AII did not have a PIE in these species. These results indicate that the absence of AII receptors is not the reason for the inability of AII to exert an inotropic effect in these species.

In the rabbit ventricular myocardium, the PIE of AII was inhibited by losartan but was unaffected by PD123319 (Scott *et al.*, 1992; Ishihata & Endoh, 1993). The pK_i value for losartan for displacement of the specific binding of [^{125}I]-AII to the membrane fraction of rabbit ventricle was 7.89, which coincided with the pA_2 value (8.00) for losartan when it antagonizes the PIE of AII. This result provides a further indication that activation of the AT_1 subtype of receptor plays a crucial role in the induction of the PIE of AII in the rabbit. The AT_1 subtype of receptor accounts for 50% of the entire population of AII receptors in the rabbit ventricular myocardium and the other 50% are of the AT_2 subtype that can bind PD123319 with high affinity (Whitebread *et al.*, 1989; Rogg *et al.*, 1990). The latter subtype does not appear to be involved in regulation of myocardial contractility in the rabbit heart (Scott *et al.*, 1992; Ishihata & Endoh, 1993).

It appears crucial to determine whether the AII receptors in the ventricular muscles of the other species in which AII did not produce a PIE are of the AT_1 or the AT_2 subtype. By contrast to the findings in rabbit ventricular myocardium, losartan but not PD123319 displaced specifically bound [^{125}I]-AII with high affinity for the membrane fractions derived from rat, dog and ferret (Table 2 and Figure 6), indicating that the AII receptors in these species are mostly of the AT_1 subtype. These findings imply that neither the AII receptor density nor the distribution of its subtypes accounts for the species-dependent variation of the AII-induced PIE.

Activation of AT_1 receptors is coupled with acceleration of the hydrolysis of phosphoinositide in guinea-pig and rabbit cardiac muscle (Baker & Singer, 1988; Ishihata & Endoh, 1993). We examined, therefore, the effect of AII on the hydrolysis of phosphoinositide in ventricular myocardium of other species in which AII did not elicit a PIE. We found that AII accelerated the hydrolysis of phosphoinositide with comparable potency and efficacy in all of the tested species (Figure 7). Hence, the acceleration of the hydrolysis of phosphoinositide induced by AII is dissociated from the PIE. These findings are in strong contrast to the previous observations, in the rabbit ventricular myocardium, of a close correlation between the hydrolysis of phosphoinositide and the PIE induced via receptors for endothelin, AII and α_1-adrenoceptors (Takanashi *et al.*, 1991; Takanashi & Endoh, 1991; 1992; Ishihata & Endoh, 1993).

Therefore, while the present findings revealed that the dissociation of the acceleration of the hydrolysis of phosphoinositide from PIE might be responsible for the species-dependent variations in the mammalian ventricular myocardium, the reason for dissociation of the PIE from the AII-induced acceleration of the hydrolysis of phosphoinositide in the rat, dog and ferret ventricular myocardium remains to be determined. Although the functional relevance of the acceleration of the hydrolysis of phosphoinositide in mediating the PIE of AII, as well as that of α_1-agonists and endothelin, has not yet been established, evidence has currently been accumulating to indicate that the process that includes activation of protein kinase C by diacylglycerol, as well as inositol 1,4,5-trisphosphate (IP_3), the product of phosphoinositide hydrolysis, may lead to modulation of Ca^{2+} signalling in both the facilitatory and the inhibitory direction. Since the coupling of receptors to these divergent transduction processes, which include Ca^{2+} channels, different types of K^+ channel, the Na^+/H^+ exchanger, Na^+, K^+- ATPase and contractile proteins, appears to vary markedly depending on the species (Endoh, 1991), we postulate that the difference in the extent of the coupling with facilitatory and inhibitory pathways that are triggered by activation of AII receptors may be crucial for determination of the final inotropic response to AII of individual species.

Dissociation of PIE from acceleration of the hydrolysis of phosphoinositide has been reported previously. While AII accelerated the hydrolysis of phosphoinositide in both atrial and ventricular muscle, it produced a PIE via AT_1 receptors only in atrial (Feolde *et al.*, 1993) and not ventricular muscle (Baker *et al.*, 1992). It has also been shown that AII activates phospholipase D as well as phospholipase C (Sadoshima & Izumo, 1993). In rat smooth muscle, AII has been shown to activate Na^+/H^+ exchange in association with the acceleration of the hydrolysis of phosphoinositide via activation of AT_1 receptors (Berk *et al.*, 1987; Ko *et al.*, 1992), but such results from cardiac muscle are still lacking at present. The physiological relevance of the AT_2 subtype of receptor in regulation of cardiac function is unknown, but various functional roles for this subtype have been proposed in other cellular systems. For example, AT_2 receptors may be involved in handling of water in the kidney (Keiser *et al.*, 1992), synthesis of prostaglandin in human astrocytes (Jaiswal *et al.*, 1991), as well as in increases in transient K^+ and delayed-rectifier K^+ currents (Kang *et al.*, 1993) and in decreases in levels of cyclic GMP (Summers *et al.*, 1991) in rat cultured neurones. Although the AT_2-receptor antagonist PD123319 displaced AII from its binding sites, it affected neither the basal force nor the AII-induced PIE. Since pretreatment with PD123319 and with another AT_2 antagonist, PD121981 (Scott *et al.*, 1992), did not affect the inhibition by losartan of the AII-induced PIE, there may be no functionally relevant mutual or allosteric interaction between AT_1 and AT_2 receptors in the regulation of cardiac contractility. Therefore, it is not considered likely that the sparse distribution of AT_2 receptors in the rat, dog and ferret ventricular myocardium is responsible for the absence of a PIE of AII in these species.

In summary, the AT_1 subtype of receptor for AII is present in ventricular muscles of the rat, dog and ferret, in which AII does not elicit a PIE. Since AII stimulates the hydrolysis of phosphoinositide in these species, we postulate that the dissociation of the production of IP_3 and diacylglycerol from the PIE may be responsible for the species-dependent variations in the AII-induced inotropic actions on mammalian ventricular myocardium.

This study was supported in part by a Grant-in-Aid (no. 05770058) for the Encouragement of Young Scientists (A) and by a Grant-in-Aid (no. 03253102) for the Scientific Research on Priority Areas from the Ministry of Education, Science and Culture, Japan. The authors are grateful to Du Pont, Pharmaceuticals & Biotechnology R & D Delaware, U.S.A. for a generous supply of the selective AT_1-receptor antagonist losartan; to Dr Joan A. Keiser, Warner-Lambert Co., Ann Arbor, MI, U.S.A, for a generous supply of the selective AT_2-receptor antagonist PD123319; to Pfizer Taito, Tokyo, for prazosin; and to Kaken Pharmaceutical Co., Tokyo, for (±)-bupranolol.

References

ACETO, J.F. & BAKER, K.M. (1990). [Sar[1]]angiotensin II receptor-mediated stimulation of protein synthesis in chick heart cells. *Am. J. Physiol.*, **258**, H806–H813.

BAKER, K.M. & ACETO, J.F. (1989). Characterization of avian angiotensin II cardiac receptors: coupling to mechanical activity and phosphoinositide metabolism. *J. Mol. Cell. Cardiol.*, **21**, 375–382.

BAKER, K.M., BOOZ, G.W. & DOSTAL, D.E. (1992). Cardiac actions of angiotensin II: role of an intracardiac renin-angiotensin system. *Annu. Rev. Physiol.*, **54**, 227–235.

BAKER, K.M., CAMPANILE, C.P., TRACHTE, G.J. & PEACH, M.J. (1984). Identification and characterization of the rabbit angiotensin II myocardial receptor. *Circ. Res.*, **54**, 286–293.

BAKER, K.M. & SINGER, A. (1988). Identification and characterization of guinea pig angiotensin II ventricular and atrial receptors: coupling to inositol phosphate production. *Circ. Res.*, **62**, 896–904.

BAKER, K.M., SINGER, H.A. & ACETO, J.F. (1989). Angiotensin II receptor mediated stimulation of cytosolic free calcium and inositol phosphates in chick myocytes. *J. Pharmacol. Exp. Ther.*, **251**, 578–585.

BERK, B.C., BROCK, T.A., GIMBRONE, Jr., M.A., CRAGOE, Jr., E. & ALEXANDER, W.R. (1987). Early agonist-mediated ionic events in cultured vascular smooth muscle cells. *J. Biol. Chem.*, **262**, 5065–5072.

BERRIDGE, M.J., DAWSON, R.M.C., DOWNNES, C.P., HESLOP, J.P. & IRVINE, R.F. (1983). Changes in the levels of inositol phosphate after agonist-dependent hydrolysis of membrane phosphoinositides. *Biochem. J.*, **212**, 473–482.

BOTTARI, S.P., TAYLOR, V., KING, I.N., BOGDAL, Y., WHITEBREAD, S. & DE GASPARO, M. (1991). Angiotensin II AT_2 receptors do not interact with guanine nucleotide binding proteins. *Eur. J. Pharmacol. Mol. Pharmacol.*, **207**, 157–163.

DEMPSEY, P., MCCALLUM, Z., KENT, K. & COOPER, T. (1971). Direct myocardial effects of angiotensin II. *Am. J. Physiol.*, **220**, 477–481.

DUDLEY, D.T., PANEK, R.L., MAJOR, T.C., LU, G.H., BRUNS, R.F., KLINKEFUS, B.A., HODGES, J.C. & WEISHAAR, R.E. (1990). Subclasses of angiotensin II binding sites and their functional significance. *Mol. Pharmacol.*, **38**, 370–377.

ENDOH, M. (1991). Signal transduction of myocardial α_1-adrenoceptors: regulation of ion channels, intracellular calcium, and force of contraction–a review. *J. Appl. Cardiol.*, **6**, 379–399.

FEOLDE, E., VIGNE, P. & FRELIN, C. (1993). Angiotensin AT_1 receptors mediate a positive inotropic effect of angiotensin II in guinea pig atria. *Eur. J. Pharmacol.*, **245**, 63–66.

FREER, R.J., PAPPANO, A.J., PEACH, M.J., BING, K.T., MCLEAN, M.J., VOGEL, S. & SPERELAKIS, N. (1976). Mechanism for the positive inotropic effect of angiotensin II on isolated cardiac muscle. *Circ. Res.*, **39**, 178–183.

ISHIHATA, A. & ENDOH, M. (1993). Pharmacological characteristics of the positive inotropic effect of angiotensin II in the rabbit ventricular myocardium. *Br. J. Pharmacol.*, **108**, 999–1005.

IWAI, N., YAMANO, Y., CHAKI, S., KONISHI, F., BARDHAN, S., TIBBETTS, C., SASAKI, K., HASEGAWA, M., MATSUDA, Y. & INAGAMI, T. (1991). Rat angiotensin II receptor: cDNA sequence and regulation of the gene expression. *Biochem. Biophys. Res. Commun.*, **177**, 299–304.

JAISWAL, N., TALLANT, E.A., DIZ, D.I., KHOSLA, M.C. & FERRARIO, C.M. (1991). Subtype 2 angiotensin receptors mediate prostaglandin synthesis in human astrocytes. *Hypertension*, **17**, 1115–1120.

KANG, J., SUMNERS, C. & POSNER, P. (1993). Angiotensin II type 2 receptor-modulated changes in potassium currents in cultured neurons. *Am. J. Physiol.*, **265**, C607–C616.

KEISER, J.A., BJORK, F.A., HODGES, J.C. & TAYLOR, Jr D.G. (1992). Renal hemodynamic and excretory responses to PD 123319 and losartan, nonpeptide AT_1 and AT_2 subtype-specific angiotensin II ligands. *J. Pharmacol. Exp. Ther.*, **262**, 1154–1160.

KO, Y., GORG, A., APPENHEIMER, M., WIECZOREK, A.J., DUSING, R., VETTER, H. & SACHINIDIS, A. (1992). Losartan inhibits the angiotensin II-induced stimulation of the phosphoinositide signaling system in vascular smooth muscle cells. *Eur. J. Pharmacol. Mol. Pharmacol.*, **227**, 215–219.

KOBAYASHI, M., FURUKAWA, Y. & CHIBA, S. (1978). Positive chronotropic and inotropic effects of angiotensin II in the dog heart. *Eur. J. Pharmacol.*, **50**, 17–25.

LEUNG, E., JOHNSTON, C.I. & WOODCOCK, E.A. (1986). Stimulation of phosphatidylinositol metabolism in arterial and ventricular myocytes. *Life Sci.*, **39**, 2215–2220.

LOWRY, O.H., ROSEBROUGH, N.J., FARR, A.L. & RANDALL, R.J. (1951). Protein measurement with the Folin phenol reagent. *J. Biol. Chem.*, **193**, 265–275.

MORAVEC, S.C., SCHLUCHTER, M.D., PARANANDI, L., CZERSKA, B., STEWART, R.W., ROSENKRANZ, E. & BOND, M. (1990). Inotropic effects of angiotensin II on human cardiac muscle in vitro. *Circulation*, **82**, 1973–1984.

MUKHERJEE, A., KULKARNI, P.V., HAGHANI, Z. & SUTKO, J.L. (1982). Identification and characterization of angiotensin II receptors in cardiac sarcolemma. *Biochem. Biophys. Res. Commun.*, **105**, 575–581.

ROGERS, T.B. (1984). High affinity angiotensin II receptors in myocardial sarcolemmal membranes. *J. Biol. Chem.*, **259**, 8106–8114.

ROGERS, T.B., GAA, S.T. & ALLEN, I.S. (1985). Identification and characterization of functional angiotensin II receptors on cultured heart myocytes. *J. Pharmacol. Exp. Ther.*, **236**, 438–444.

ROGG, H., SCHMID, A. & DE GASPARO, M. (1990). Identification and characterization of angiotensin II receptor subtypes in rabbit ventricular myocardium. *Biochem. Biophys. Res. Commun.*, **173**, 416–422.

SADOSHIMA, J. & IZUMO, S. (1993). Signal transduction pathways of angiotensin II-induced c-*fos* gene expression in cardiac myocytes in vitro. *Circ. Res.*, **73**, 424–438.

SASAKI, K., YAMANO, Y., BARDHAN, S., IWAI, N., MURRAY, J.J., HASEGAWA, M., MATSUDA, Y. & INAGAMI, T. (1991). Cloning and expression of a complementary DNA encoding a bovine adrenal angiotensin II type-1 receptor. *Nature*, **351**, 233–236.

SCOTT, A.L., CHANG, R.S.L., LOTTI, V.J. & SIEGL, P.K.S. (1992). Cardiac angiotensin receptors: effects of selective angiotensin II receptor antagonists, DUP753 and PD121981, in rabbit heart. *J. Pharmacol. Exp. Ther.*, **261**, 931–935.

SUMNERS, C., TANG, W., ZELEZNA, B., GAULT, T. & RAIZADA, M.K. (1991). Functional AII receptor subtypes in neuronal and astrocyte glial cultures from one-day-old rat brain. *FASEB J.*, **5**, A871 (Abstr.).

TAKANASHI, M. & ENDOH, M. (1991). Characterization of positive inotropic effect of endothelin on mammalian ventricular myocardium. *Am. J. Physiol.*, **261**, H611–H619.

TAKANASHI, M. & ENDOH, M. (1992). Concentration- and time-dependence of phosphoinositide hydrolysis induced by endothelin-1 in relation to the positive inotropic effect in the rabbit ventricular myocardium. *J. Pharmacol. Exp. Ther.*, **262**, 1189–1194.

TAKANASHI, M., NOROTA, I. & ENDOH, M. (1991). Potent inhibitory action of chlorethylclonidine on the positive inotropic effect and phosphoinositide hydrolysis mediated via myocardial *alpha*$_1$-adrenoceptors in the rabbit ventricular myocardium. *Naunyn-Schmied. Arch. Pharmacol.*, **343**, 669–673.

WHITEBREAD, S., MELE, M., KAMBER, B. & DE GASPARO, M. (1989). Preliminary biochemical characterization of two angiotensin II receptor subtypes. *Biochem. Biophys. Res. Commun.*, **163**, 284–291.

WRIGHT, G.B., ALEXANDER, R.W., EKSTEIN, L.S. & GIMBRONE, M. A. Jr. (1983). Characterization of the rabbit ventricular myocardial receptor for angiotensin II. *Mol. Pharmacol.*, **24**, 213–221.

(Received June 23, 1994
Accepted September 6, 1994)

British Journal of Pharmacology (1995) 114, 454-460 © 1995 Stockton Press All rights reserved 0007-1188/95 $9.00

Desensitization of the nicotine-induced mesolimbic dopamine responses during constant infusion with nicotine

Maureen E.M. Benwell, David J.K. Balfour & Claire E. Birrell

Department of Pharmacology and Clinical Pharmacology, University of Dundee Medical School, Ninewells Hospital, Dundee DD1 9SY

1 The effects of constant nicotine infusions (0.25, 1.0 and 4.0 mg kg^{-1} day^{-1}) on extracellular dopamine levels in the nucleus accumbens (NAc) and on locomotor activity have been compared with the changes evoked by repeated daily injections (0.4 mg kg^{-1} day^{-1} for 5 days) of the drug.

2 The extracellular dopamine concentration in the NAc was significantly increased ($P<0.05$) following a challenge dose of nicotine (0.4 mg kg^{-1}, s.c.) in animals which had been pretreated with daily injections of the drug. This effect was accompanied by an enhanced locomotor response to nicotine.

3 The stimulant effects of nicotine on mesolimbic dopamine secretion and on locomotor activity were significantly inhibited ($P<0.01$) by the prior administration of mecamylamine (2.0 mg kg^{-1}, s.c.) but not by hexamethonium (2.0 mg kg^{-1}, s.c.).

4 The constant infusion of nicotine at a rate of 1 and 4 but not 0.25 mg kg^{-1} day^{-1} abolished the sensitized dopamine response in the NAc to an injection of nicotine in animals pretreated with the drug. The locomotor responses to nicotine in the nicotine-pretreated rats were significantly attenuated by the infusion of nicotine at all 3 doses, although the nicotine induced locomotor activity, in the rats infused with 0.25 mg kg^{-1} day^{-1} was also significantly ($P<0.05$) higher than that observed in the rats treated acutely with nicotine.

5 Significantly ($P<0.01$) enhanced mesolimbic dopamine responses, to a challenge injection of nicotine (0.4 mg kg^{-1}, s.c.), were observed 2 and 7 days after termination of the infusion of nicotine (4 mg kg^{-1} day^{-1} for 14 days); locomotor responses were enhanced ($P<0.01$) 1, 2 and 7 days after termination of the infusion.

6 The results suggest that sensitized mesolimbic dopamine responses to nicotine occur as a result of stimulation of centrally located nicotinic receptors but that these receptors may be desensitized during periods of chronic exposure to nicotine at doses which may be relevant to smoking.

Keywords: Nicotine; repeated injection; constant infusion; mesolimbic dopamine; locomotor activity; sensitization; desensitization

Introduction

A considerable body of evidence indicates that the mesolimbic dopamine system is involved in mediating the reinforcing properties of many pyschostimulant drugs of abuse (Wise & Bozarth, 1987). It is now clear that this system is also stimulated by injections of nicotine (Clarke *et al.*, 1988; Di Chiara & Imperato, 1988; Damsma *et al.*, 1989; Benwell & Balfour, 1992) and that the rewarding (Singer *et al.*, 1982; Corrigall *et al.*, 1992) and locomotor stimulant (Clarke *et al.*, 1988; Reavill & Stolerman, 1990; Benwell & Balfour, 1992) effects of this drug may be dependent upon its ability to stimulate mesolimbic dopamine secretion. Moreover, repetitive daily injections of the drug appear to sensitize the mesolimbic system to a subsequent challenge with the drug (Benwell & Balfour, 1992). Intermittent exposure to tobacco smoke also increases the turnover of dopamine in the mesolimbic dopamine system, an effect which has been shown to be due to the nicotine content of the tobacco (Fuxe *et al.*, 1987). Therefore, it is thought that activation of mesolimbic dopamine systems may be responsible for the 'pleasurable' effects of smoking (Balfour, 1990). However, in all of these studies, the effects of nicotine were tested at a time when the plasma concentration of the alkaloid was either very low or negligible. In contrast, the profile of plasma nicotine in smokers often results in significant trough levels being maintained between cigarettes for much of the day (Russell, 1990; Benowitz *et al.*, 1990).

In one of the few studies to date which have considered the effect of constant exposure to nicotine on brain dopamine systems, the results have indicated that chronic nicotine may decrease dopamine turnover in the brain, suggesting that desensitization of the stimulant responses to nicotine may occur (Kirch *et al.*, 1987). It has long been recognised that peripheral nicotinic cholinoceptors, especially those present on autonomic ganglia, are susceptible to depolarization block following prolonged exposure to nicotine (Rang & Dale, 1992). This phenomenon is thought to be responsible for the acute tolerance which develops to some of the effects of nicotine, such as nicotine-induced increases in heart rate, during periods of continuous exposure (Russell & Feyerabend, 1978; West & Russell, 1987). The up-regulation of central nicotinic receptors which occurs with smoking (Benwell *et al.*, 1988) or prolonged exposure to nicotine (Marks *et al.*, 1985; Schwartz & Kellar, 1985) suggests that central nicotinic receptors may also desensitize. It is presumed that the nicotinic receptors which mediate the stimulatory effects of nicotine on mesolimbic dopamine systems are those reported to be located on the dopaminergic neurones themselves (Clarke *et al.*, 1988). However, little attention has been paid to the possibility that the effects of nicotine on mesolimbic dopamine activity can be desensitized when the drug is present in concentrations which are regularly maintained in the plasma of habitual smokers for much of the day. The purpose of this study was to investigate this possibility by comparing the effects of constant nicotine infusions on mesolimbic dopamine activity and nicotine-

[1] Author for correspondence.

induced locomotor stimulation with the responses to nicotine administered as an injection. In addition, the study has also investigated the extent to which the constant infusion of nicotine, at doses which achieve plasma levels comparable to those found in smokers, influences the responses to nicotine when administered as an acute injection both during and at various intervals following cessation of nicotine infusions.

Methods

Animals and drug pretreatments

Male Sprague–Dawley rats, bred in the Biomedical Services Unit, Ninewells Hospital and Medical School, from stock purchased from Interforna Ltd and weighing 250–350g at the start of the experiments were used throughout. The animals had free access to food and water and were housed in pairs prior to and singly following surgery. In the experiments where the influence of mecamylamine and hexamethonium on nicotine-induced responses were investigated, all animals were pretreated for 5 days with daily subcutaneous injections of (−)-nicotine hydrogen tartrate (0.4 mg kg^{-1}, free base dissolved in isotonic saline and adjusted to pH 7.0 by the addition of a small quantity of NaOH). In the experiments involving the constant infusion of nicotine, all animals were implanted subcutaneously, while anaesthetized with halothane (3%), with Alzet minipumps (2ml2) containing either saline or (−)-nicotine hydrogen tartrate dissolved in saline and delivering 0.25, 1.0 or 4.0 mg kg^{-1} day^{-1} of (−)-nicotine free base concentration for 14 days. On days, 9–13, half of the saline and half of each of the nicotine-infused groups also received daily subcutaneous (s.c.) injections of saline while the remainder of the animals received daily injections of nicotine (0.4 mg kg^{-1}, s.c.). In the experiments in which the effects of nicotine were investigated following removal of the infusion pumps, rats were infused with either saline or nicotine (4 mg kg^{-1} day^{-1}) and received daily injections of saline on days 9–13 as described and the pumps were removed, under halothane anaesthesia, on day 14. Measurements were then made on days 15, 16 or 21.

Stability of nicotine in the Alzet minipumps and plasma nicotine estimation

These parameters were assessed by adding [^{3}H]-(−)-nicotine hydrogen tartrate to the nicotine in the osmotic minipumps. In the experiments designed to measure the concentration of nicotine in the plasma, the final specific activity of the [^{3}H]-(−)-nicotine was 1.305, 0.326 and 0.081 mCi $mmol^{-1}$ for the doses of 0.25, 1.0 and 4.0 mg kg^{-1} day^{-1}, respectively. The rats were killed on day 14 of the infusion and blood collected by cardiac puncture, centrifuged to obtain the plasma and stored at −70°C until assayed. The radioactivity was extracted into chloroform from plasma made alkaline with the addition of NaOH and samples of the chloroform extract spotted onto alkylated silica gel thin layer chromatography (t.l.c.) plates and run in a system of methanol:ammonia (100:1.5). The plasma concentration of nicotine was estimated by counting the radioactivity which co-chromatographed with unlabelled nicotine carrier followed by back calculation. The stability of the (−)-nicotine in the pumps was assessed by spotting samples of the solutions remaining in the pumps at day 14 on alkylated silica gel t.l.c. plates and run in the system described above.

Implantation of microdialysis probe

This procedure was carried out at least 3 h after the last of the pretreatments, i.e., on day 5 in the mecamylamine/hexamethonium experiments and on day 13 in the infusion experiments. In the case of the withdrawal experiments, the probes were implanted on days 14, 15 and 20 to investigate the effects of nicotine 1, 2 and 7 days following pump removal respectively. The dialysis probe and its implantation into the nucleus accumbens were carried out as described previously (Benwell & Balfour, 1992). The position of the probes was routinely determined histologically from sections prepared at postmortem from tissue fixed in formalin.

Microdialysis and estimation of locomotor activity

Eighteen to 24 h following implantation of the dialysis probe, the animals were placed individually in a black perspex activity box (40 cm square × 25 cm high) where the locomotor activity is assessed by 4 photocells located on adjacent sides of the box as described by Vale & Balfour (1989). At this time, the dialysis loop was connected, via a liquid swivel, to a syringe pump containing Ringer solution composition mM (NaCl 147 KCl 4.0 and $CaCl_2$ 1.25) which was perfused at a constant rate of 1.7 µl min^{-1}. Following a 40–60 min equilibration period, dialysate samples were removed at 20 min intervals for 60 min to establish a stable baseline level of dopamine and its metabolites, dihydroxyphenylacetic acid (DOPAC) and homovanillic acid (HVA). At this time, in the experiments investigating the effects of mecamylamine and hexamethonium, a third of the animals received injections of saline (s.c.), a third received mecamylamine (2.0 mg kg^{-1} s.c.) and the remainder received hexamethonium (2.0 mg kg^{-1}, s.c.) and another 3 × 20 min samples were taken. At this time, the rats were challenged with nicotine (0.4 mg kg^{-1} s.c.) and at least 5 more 20 min samples were taken. In the experiments investigating the effects of nicotine infusions, the response of all animals to a

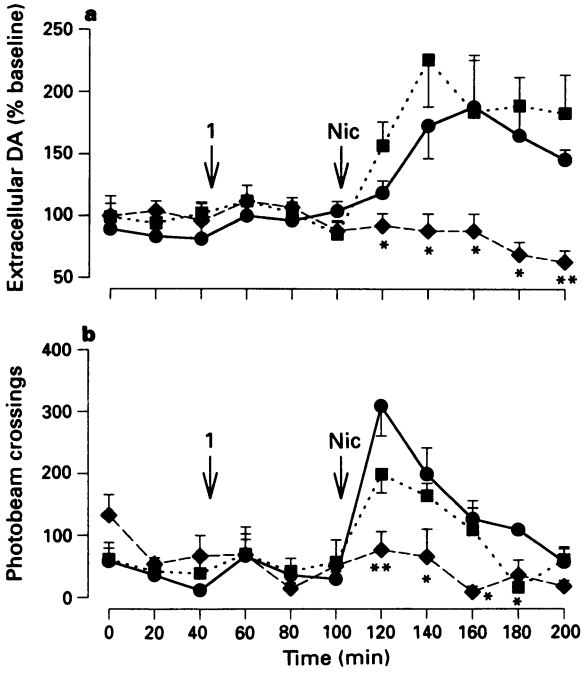


Figure 1 The effect of mecamylamine and hexamethonium on nicotine-induced changes in NAc dopamine and locomotion. All rats were pretreated with daily injections of nicotine (0.4 mg kg^{-1} s.c.) for 5 days. On day 6, the rats received either saline (●, $n = 4$), mecamylamine (◆, 2.0 mg kg^{-1} s.c., $n = 5$) or hexamethonium (■, 2.0 mg kg^{-1} s.c., $n = 4$) at the time indicated by the first arrow (1). All animals received an injection of nicotine (0.4 mg kg^{-1}, s.c.) at the time indicated by the second arrow (Nic). The results in (a) are the extracellular dopamine (DA) levels in the NAc expressed as percentages of the means ± s.e.mean of the 3 samples removed before the nicotine injection. The results in (b) are the means ± s.e.mean of the locomotor activity in these animals. $^*P<0.05$, $^{**}P<0.01$; significantly different when compared to the saline-injected group.

saline injection (s.c.) was tested once a stable baseline had been obtained and a further 3 × 20 min samples taken before all animals received a challenge dose of nicotine (0.4 mg kg^{-1} s.c.) and at least 5 more 20 min samples taken. The concentrations of dopamine, DOPAC and HVA in the dialysates were assayed by injecting the samples directly onto a high performance liquid chromatography (h.p.l.c.) system as described elsewhere (Benwell & Balfour, 1992).

Data analysis

In each experiment, the mean concentrations of dopamine and its metabolites, for the 3 samples collected after the saline, mecamylamine or hexamethonium injection and before the administration of nicotine, were estimated and defined as 100%. The concentration of dopamine and its metabolites in each sample collected during the experimental day were then expressed as percentages of these mean values. Statistical analysis of the locomotor activity and the dialysis data was performed by analysis of variance for repeated measures with infusion and pre-injection as independent factors in the infusion experiments and pretreatment with saline, mecamylamine and hexamethonium as independent factors in the mecamylamine/hexamethonium experiments. *Post hoc* analyses were performed, where appropriate, using Duncan's test or a paired *t* test.

Drugs

(−)-Nicotine hydrogen tartrate, mecamylamine hydrochloride and hexamethonium bromide were obtained commercially from Sigma Chemical Company; [^{3}H]-(−)-nicotine from New England Nuclear; EDTA from Fisons PLC; h.p.l.c. grade methanol from Rathburn Chemical Ltd and all other h.p.l.c. grade reagents from British Drug Houses.

Results

Stability of nicotine in the Alzet minipump and plasma concentrations

Fourteen days after implantation, 93 ± 3% of the tritium labelling remaining in the pumps co-chromatographed with authentic nicotine. The concentrations of nicotine achieved in the plasma, at this time, were 9 ± 4, 24 ± 5 and 87 ± 12 ng ml^{-1} during the infusion of nicotine at rates of 0.25, 1.00 and 4.00 mg kg^{-1} day^{-1} respectively. There was a significant correlation ($r = 0.92$, $n = 4$/concentration) between the doses of nicotine administered and the plasma nicotine concentration achieved.

Pretreatments and basal dopamine and metabolite levels

The basal levels of dopamine, DOPAC and HVA in the dialysates obtained from the nucleus accumbens of the saline-infused/saline-injected rats were 0.142 ± 0.032, 12.23 ± 3.00 and 5.72 ± 1.12 pmol 20 µl^{-1} respectively. Although there was a tendency for the basal dopamine levels to be lower (0.081 ± 0.012) in the nicotine-infused rats and higher (0.201 ± 0.053) in those pretreated with saline infusions and daily injections of nicotine, these did not prove significantly different in comparison with those obtained from the saline-infused/saline-injected control rats.

The effect of mecamylamine and hexamethonium on nicotine-induced stimulation of mesolimbic dopamine secretion and locomotion

Injection of saline, mecamylamine or hexamethonium had no significant effect on the extracellular concentration of dopamine in the NAc (Figure 1a) or on locomotor activity (Figure 1b) during the 60 min following these treatments. However, the injection of nicotine was associated with a significant (F time (7,21) = 3.05, $P<0.05$) increase in the extracellular level of dopamine in the NAc of the saline-injected animals, an effect which was completely abolished (F mecamylamine × time (7,49) = 4.26, $P<0.01$) when the rats had received mecamylamine 60 min before being challenged with nicotine. The nicotine-induced locomotor response (F time (7,21) = 8.42, $P<0.01$) was also completely inhibited (F mecamylamine × time (7,49) = 5.72, $P<0.01$) in these animals. There were no significant changes in the nicotine-induced effects on NAc dopamine secretion and locomotor activity which could be attributed to the prior administration of hexamethonium.

The influence of nicotine infusions on mesolimbic dopamine and locomotor responses to nicotine boli-dopamine

There was no significant effect on the extracellular levels of dopamine in the NAc which could be attributed to the infusion of nicotine nor the prior exposure to nicotine as daily injections when the rats were injected with saline on the test day. With respect to the responses to a challenge injection of nicotine, administered on the test day, statistical analysis of the overall data revealed a significant interaction (F infusion × pre-injection × time (21,231) = 1.61, $P<0.05$) between the infusion of nicotine, the pre-injections and the injection of nicotine on the test day. In rats which had been pre-injected daily with saline, the increase in the extracellular level of dopamine in the NAc, evoked by a test injection of nicotine to saline-infused rats, did not reach statistical significance (Figure 2a). However, a test injection of nicotine did produce an increase in this parameter in the animals

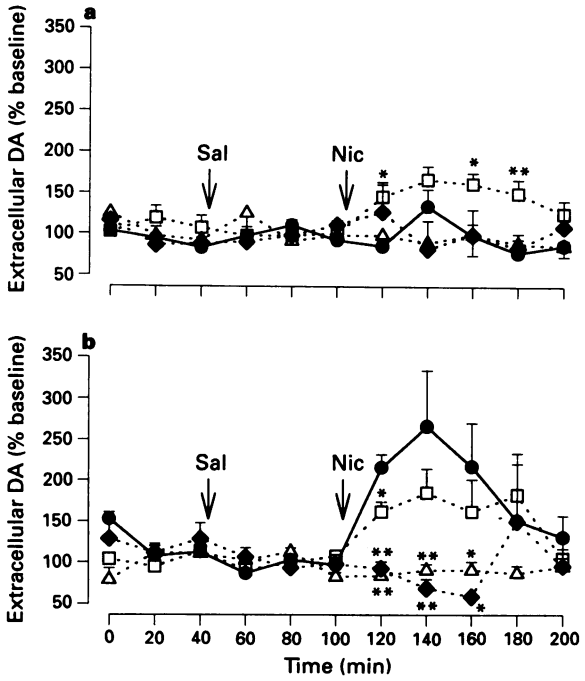


Figure 2 The influence of nicotine on extracellular dopamine in the NAc. The rats were implanted with osmotic minipumps delivering either saline (●) or nicotine at rates of 0.25 (□), 1.0 (Δ) and 4.0 (◆) mg kg^{-1} day^{-1} for 14 days. On days 9–13, the animals also received daily injections of saline (a) or nicotine (0.4 mg kg^{-1}, s.c., b). On day 14, the responses of all animals to test injections of saline (Sal) and nicotine (Nic, 0.4 mg kg^{-1} s.c.) were tested. The results are the extracellular dopamine (DA) levels in the NAc expressed as percentages of the means ± s.e.mean of the 3 samples removed before the nicotine injection. There are 4–8 observations in each group. *$P<0.05$, **$P<0.01$; significantly different when compared to the saline-infused group.

receiving a constant infusion of the lowest dose of nicotine (0.25 mg kg^{-1} day^{-1}) which was significant (F (7,63) = 2.92, $P<0.01$) in comparison with the saline-infused/saline pre-injected controls. No significant changes were observed when nicotine was injected during the infusion of nicotine at rates of 1 or 4 mg kg^{-1} day^{-1}. In agreement with results of previous studies (Benwell & Balfour, 1992), the administration of nicotine, to saline-infused rats pre-injected with daily injections of the drug, was associated with a significant enhancement (F pre-injection × time (7,63) = 2.71, $P<0.05$) of the increase in extracellular dopamine in the NAc seen in the saline pre-injected animals (Figure 2b). In these nicotine pre-injected animals, this enhanced response was completely abolished ($P<0.01$) in the animals receiving constant infusions of nicotine at rates of 1 and 4 mg kg^{-1} day^{-1}. Although there appeared to be an attenuation of the mesolimbic dopamine response to a bolus dose of nicotine, during the constant infusion of the lowest dose used in this study (0.25 mg kg^{-1} day^{-1}), this did not attain statistical significance. In fact, the NAc dopamine levels were significantly increased (F (7,21) = 2.65, $P<0.05$) following a bolus injection of nicotine in these rats receiving this low dose infusion.

The injection of saline had no influence on the extracellular levels of DOPAC or HVA in any of the treatment groups studied. The injection of nicotine, on the test day, was associated with a significant increase in the extracellular concentration of DOPAC (F (7,70) = 6.95, $P<0.01$) and HVA (F (7,70) = 5.44, $P<0.01$) in the NAc of the saline-infused animals, an effect which was not influenced by pre-injection with nicotine. However, the infusions did affect the nicotine-induced increases in DOPAC (F infusion × time (21,231) = 2.79, $P<0.01$) and HVA (F infusion × time (21,231) = 2.4, $P<0.01$).

The levels of DOPAC were reduced from a peak level of 155 ± 12% of the pre-nicotine injection levels between 60 and 80 min post-nicotine injection, in the saline-infused rats, to 119 ± 4, 113 ± 15 and 114 ± 8% during the infusion of 0.25, 1.0 and 4.0 mg kg^{-1} day^{-1} respectively. The level of HVA in the extracellular fluid at this time was significantly ($P<0.05$) reduced from 128 ± 10% in the saline-infused rats to 97 ± 6% during the constant infusion of the highest dose of nicotine only. The reductions during the constant infusions of 0.25 and 1.0 mg kg^{-1} day^{-1} to 121 ± 7 and 108 ± 7% respectively, did not attain significance.

The injection of saline had no significant effects on locomotion in any of the treatment groups. However, the injection of nicotine on the test day stimulated (F (7,231) = 72.43, $P<0.001$) locomotor activity in all groups of animals and statistical analysis of the overall data revealed a significant interaction (F infusion × pre-injection × time (21,231) = 1.94, $P<0.01$) between the infusion of nicotine, the pre-injections and the stimulant response evoked by an injection of nicotine on the test day. In rats which had been pre-injected daily with saline, the increase in the locomotor activity, evoked by a test injection of nicotine to the animals being constantly infused with the lowest dose of nicotine (0.25 mg kg^{-1} day^{-1}), was significantly greater (F (7,70) = 3.96, $P<0.01$) than the behavioural response in the saline-infused controls (Figure 3a). However, the locomotor responses elicited during the infusion of 1 and 4 mg kg^{-1} day^{-1} were not significantly different from the saline-infused controls. The administration of nicotine to saline-infused rats pre-injected with daily injections of the drug, was associated with a significant enhancement (F pre-injection × time (7,63) = 7.73, $P<0.001$) of the increase in the locomotor activity seen in the animals pre-injected with saline. In the

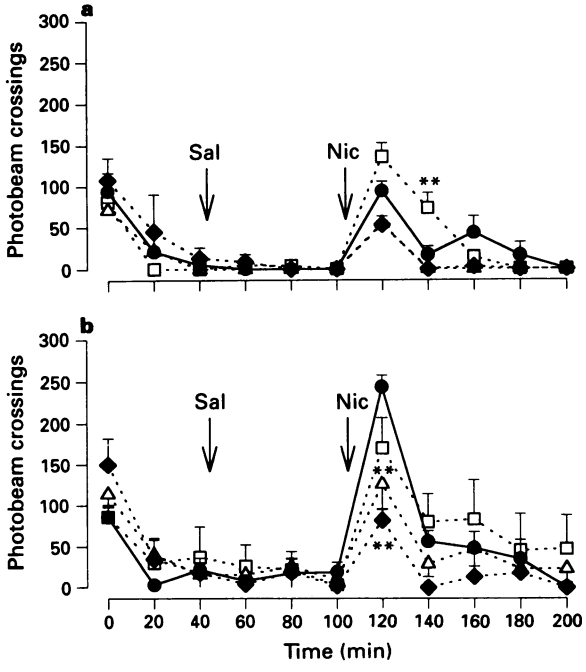


Figure 3 The influence of nicotine on locomotor activity. The rats were implanted with osmotic minipumps delivering either saline (●) or nicotine at rates of 0.25 (□), 1.0 (Δ) and 4.0 (◆) mg kg^{-1} day^{-1} for 14 days. On days 9–13, the animals also received daily injections of saline (a) or nicotine (0.4 mg kg^{-1} s.c., b). On day 14, the responses of all animals to test injections of saline (Sal) and nicotine (Nic, 0.4 mg kg^{-1} s.c.) were tested. The results are the means ± s.e.mean of 4–8 observations in each group. *$P<0.05$, **$P<0.01$; significantly different when compared to the saline-infused group.

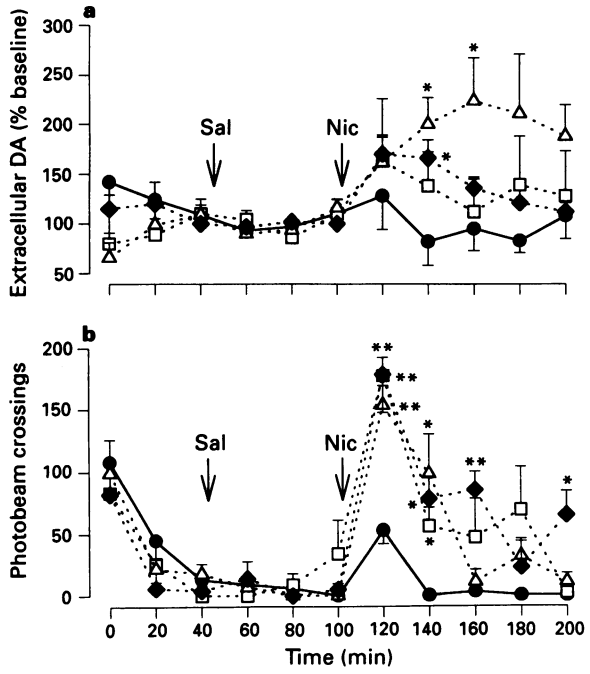


Figure 4 The influence of nicotine on extracellular dopamine in the NAc and locomotor activity following cessation of the nicotine infusions. The rats were implanted with osmotic minipumps delivering nicotine at a rate of 4.0 mg kg^{-1} day^{-1} for 14 days. The effects of a bolus injection of saline (Sal) and nicotine (Nic, 0.4 mg kg^{-1} s.c.) were tested during the infusion (●, $n=4$) and at 1 (□, $n=6$), 2(Δ, $n=4$) and 7 (◆, $n=6$) days after removal of the infusion pumps. The results in (a) are the extracellular dopamine (DA) levels in the NAc expressed as percentages of the means ± s.e.mean of the 3 samples removed before the nicotine injection. The results in (b) show the locomotor activity. The results are the means ± s.e.mean of 4–6 observations in each group. *$P<0.05$, **$P<0.01$; significantly different when compared to the response obtained during the infusion of nicotine.

nicotine pre-injected animals (Figure 3b), the enhanced behavioural effect was significantly (F infusion × pre-injection × time $(7,63) = 2.76$, $P<0.05$) attenuated by the constant infusion of nicotine at a rate of 0.25 mg kg^{-1} day^{-1} (Figure 3b) and was completely abolished in the animals receiving constant infusions of nicotine at rates of 1 (F $(7,70) = 4.58$, $P<0.01$) and 4 (F $(7,63) = 8.12$, $P<0.01$) mg kg^{-1} day^{-1}.

The effects of nicotine boli following termination of the constant infusion of nicotine

As shown in Figure 4a, there were no significant changes in the extracellular dopamine levels in the NAc which could be attributed to the acute injection of saline during or at 1, 2 or 7 days after termination of the infusion of nicotine (4.0 mg kg^{-1} day^{-1} for 14 days). The extracellular dopamine levels in the NAc of rats, receiving a constant infusion of nicotine at a rate of 4 mg kg^{-1} day^{-1}, remained unchanged following an acute challenge with nicotine. However, within 24 h of cessation of this infusion, the extracellular dopamine levels were increased by an acute nicotine injection, an effect which achieved significance 2 (F infusion × time $(7,49) = 2.27$, $P<0.05$) and 7 (F infusion × time $(7,49) = 3.03$, $P<0.01$) days after removal of the osmotic minipumps. Figure 4b shows the locomotor responses in these animals. The stimulation (F $(7,91) = 32.27$, $P<0.001$) of locomotor activity, induced by acute nicotine, was significantly enhanced at 1 (F infusion × time $(7,42) = 4.39$, $P<0.01$), 2 (F infusion × time $(7,49) = 7.01$, $P<0.01$) and 7 (F infusion × time $(7,49) = 5.24$, $P<0.01$) days after cessation of the nicotine infusion when compared with the responses obtained when nicotine was administered during the infusion.

Discussion

This study has established that over 90% of the nicotine in the osmotic minipumps remained as nicotine over the 14 day period and allows the conclusion that any effects observed are likely to be due to the nicotine released from the pumps. Moreover, the plasma concentrations of nicotine which were achieved are consistent with those reported by Jansson *et al.* (1989) and Neil Grunberg (personal communication). They also fall within the range which has been reported to occur in smokers in that the lowest dose (0.25 mg kg^{-1} day^{-1}) gave a plasma level (~9ng ml^{-1}) which lies at the lower end of the range and also a level which is often found following overnight abstinence and the 1 mg kg^{-1} day^{-1} dose resulted in levels (~24 ng ml^{-1}) commonly reported in smokers (Russell, 1990; Benowitz *et al.*, 1990; Henningfield *et al.*, 1993). The highest dose (4.0 mg kg^{-1} day^{-1}) resulted in nicotine levels (~87 ng ml^{-1}) similar to those found in arterial blood following the inhalation of smoke from cigarettes (Henningfield *et al.*, 1993).

It has previously been reported that the stimulant effects of acute nicotine administration on mesolimbic dopamine secretion is centrally mediated since it is blocked by the nicotinic antagonist, mecamylamine, but not by hexamethonium, which does not readily cross the blood brain barrier (Imperato *et al.*, 1986). The present study has demonstrated that the sensitized stimulant effects of nicotine on NAc dopamine secretion, seen in animals which have received prior intermittent treatment with the drug, is also completely inhibited by mecamylamine, but not by hexamethonium. Furthermore, the locomotor stimulant effects of nicotine, in these animals, were completely abolished by mecamylamine but not hexamethonium. Therefore, it would appear that the stimulant effects exerted by nicotine on both mesolimbic dopamine activity and locomotion, in animals with prior experience of the drug, are mediated by central nicotinic receptors.

As reported previously (Benwell & Balfour, 1992), the acute injection of nicotine to drug naive animals appeared to cause a modest increase in the extracellular level of dopamine in the NAc which was close to significance. However, nicotine evoked a mesolimbic dopamine response in saline pre-injected animals receiving a constant infusion of the lowest dose of nicotine tested (0.25 mg kg^{-1} day^{-1}) which was significantly greater than that seen in the saline-infused controls. Therefore prolonged exposure to this low level of nicotine is, itself, capable of priming the mesolimbic dopamine system to be more responsive to a bolus dose of nicotine. This did not, however, occur when saline pre-injected rats were challenged with an acute injection of the drug during the infusion of 1 or 4 mg kg^{-1} day^{-1}. In agreement with previous studies (Benwell & Balfour, 1992), there was an enhanced mesolimbic dopamine response, seen when nicotine was injected into rats which had been previously exposed to the drug with daily pre-injections of nicotine (0.4 mg kg^{-1}, s.c.). One of the principal findings of the present study is that this enhanced response was attenuated or abolished when nicotine was maintained in the plasma at concentrations which are commonly found in habitual smokers. For instance, when nicotine is infused at a rate of 1.0 mg kg^{-1} day^{-1}, which produces a plasma concentration of approximately 24 ng ml^{-1}, there is complete inhibition of the increase in extracellular dopamine and attenuation of the elevation of DOPAC within the NAc, which are evoked by an injection of nicotine. The HVA response is also reduced when the infusion dose is increased to 4.0 mg kg^{-1} day^{-1}. In addition, the infusions of nicotine at doses of 1 mg kg^{-1} day^{-1} or greater abolished the enhanced locomotor stimulant response to nicotine in these rats, data which support the conclusion that the enhanced behavioural response to the drug may be related to its effects on mesolimbic dopamine (Benwell & Balfour, 1992). The nature of this reduced sensitivity to nicotine remains to be established. However, exhaustion of the dopamine stores available for release is unlikely since the constant infusion of nicotine has been reported to evoke, if anything, an increase in the tissue levels of dopamine in the NAc and enhance amphetamine-induced release of [^{3}H]-dopamine from slices prepared from the NAc (Fung, 1989). Previous studies have indicated that smoking may be associated with an increase in the density of nicotinic receptors in the human brain (Benwell *et al.*, 1988) which is very likely to be attributable to the nicotine content of tobacco since this up-regulation is also observed in experimental animals following chronic treatment with nicotine (Marks *et al.*, 1985; Schwartz & Kellar, 1985). These changes have been interpreted as evidence that desensitization of central nicotinic receptors occurs. Indeed, it has been proposed that the apparent neuroprotective effect of smoking in Parkinson's disease may be due to desensitization of the nicotinic receptors located on nigrostriatal dopamine systems which results in reduced firing rates of these neurones and thus reduced energy demands (Jansson *et al.*, 1986; 1988; 1989). Therefore, the most likely explanation for the reduced sensitivity of the mesolimbic dopamine system to nicotine injections, observed when the plasma nicotine levels are maintained at 24 ng ml^{-1} and above, is that the receptors which mediate the effects of nicotine on mesolimbic dopamine secretion are desensitized with prolonged exposure to nicotine at this level. Clarke & Pert (1985) demonstrated the presence of nicotinic receptors on the membranes of both the nerve terminal and somatodendritic regions of this neural pathway. Recent results (Benwell *et al.*, 1993; Nisell *et al.*, 1994; Reavill & Stolerman, 1990) suggest that the postsynaptic, somatodendritic receptors in the Ventral Tegmental area are the best candidates for mediating the effects of nicotine on mesolimbic dopamine secretion and the enhanced locomotor responses, at least at the dose of nicotine (0.4 mg kg^{-1}, s.c.) which was used in the present study. Therefore, it seems reasonable to suggest that these receptors are desensitized during the constant infusion of nicotine.

Previous studies have suggested that the locomotor stimulant effects of nicotine are related to its ability to stimulate mesolimbic dopaminergic neurones (Clarke *et al.*, 1988; Balfour *et al.*, 1990). The present study suggests that there is a clear dose-relationship between the ability of the infusions to attenuate both the nicotine-induced increases in the concentration of dopamine in the extracellular space of the NAc and locomotor stimulation. However, the temporal correlation between these two parameters is not particularly close since the peak extracellular level of dopamine in the NAc appears to lag behind the peak locomotor effect and to be of longer duration. Although the nicotine-induced locomotor stimulation was completely inhibited by mecamylamine, this parameter was only attenuated and not abolished during the infusion of nicotine at a rate of $1\ mg\ kg^{-1}\ day^{-1}$ and this was despite the apparent total inhibition of the dopamine overflow in the NAc in these animals. It is unlikely that this was due simply to a submaximal desensitizing dose since a locomotor stimulant effect, of similar magnitude, was still evident when the infusion dose was increased four fold. The explanation for this remains unclear although it is consistent with the possibility that the locomotor responses to the drug may be mediated by heterogeneous nicotinic receptors and that the same subtype is responsible for the enhanced locomotor effect and activation of mesolimbic dopaminergic neurones. Activation of a different subtype may mediate the residual locomotor stimulation and this may be less susceptible to desensitization but equally sensitive to mecamylamine.

The desensitization of the central nicotinic receptors, associated with the mesolimbic dopamine system, is clearly a reversible phenomenon since enhanced mesolimbic and locomotor responses are evoked, in response to a bolus dose of nicotine, 24 h after abstinence from nicotine. This sensitization to nicotine was still apparent 7 days after cessation of the nicotine infusion. Therefore, prolonged desensitization also leads to sensitized responses to nicotine administered as a bolus during period of abstinence. However, it remains to be established whether the mechanisms involved in the development of sensitization, induced by low level chronic exposure to nicotine, and the sensitization seen during periods of abstinence from desensitizing doses of the drug are the same as those involved in the increased responsiveness seen following intermittent exposure to nicotine.

There is a widely held view that stimulation of mesolimbic dopaminergic neurones plays a central role in the rewarding and addictive properties of psychostimulant drugs, including nicotine (Wise & Bozarth, 1987; Corrigall *et al.*, 1992; Singer *et al.*, 1982). The data described here are of relevance in this regard. The results imply that plasma nicotine levels of $10\ ng\ ml^{-1}$ and above may attenuate the mesolimbic dopamine response to a nicotine bolus. Therefore, if increased dopamine secretion in the mesolimbic system is the principal mediator of the rewarding properties of nicotine, the results suggest that this will be attenuated or abolished in people who smoke or use nicotine preparations in a way which maintains levels significantly above $10\ ng\ ml^{-1}$. Acute tolerance to many of the effects of nicotine develops with repeated exposure during a single day (Russell & Feyerabend, 1978; West & Russell, 1987; Perkins *et al.*, 1993), observations which when taken in conjunction with the increased density of nicotinic receptors in human brain tissue taken from habitual smokers (Benwell *et al.*, 1988) provides evidence that repetitive or prolonged periods of receptor desensitization may, indeed, occur with smoking. Therefore, it seems reasonable to speculate that, although stimulation of mesolimbic dopamine systems may be an important factor in the development of nicotine addiction, for heavy smokers who smoke in a way which maintains their nicotinic receptors in a desensitized state for much of the day, other neural mechanisms may also be important in contributing to the reinforcing effects of the drug. It is also possible that people who smoke most heavily and consequently are likely to maintain the highest plasma levels of nicotine and be most addicted to the drug, are actually smoking to maintain nicotinic receptors in a desensitized state. If this is the case, it is possible that re-sensitization of the central nicotinic receptors following periods of desensitization is aversive to the heavy smoker. It is particularly interesting that both sensitization and desensitization of responses to nicotine appear to be achieved over the plasma nicotine ranges which smokers could be expected to experience. It has been suggested that smokers can vary their pattern of nicotine intake to help them stay alert and concentrate or to relax depending upon the situation (Warburton, 1990). Therefore, it is tempting to speculate that smokers learn to titrate their nicotine intake to achieve either sensitization or desensitization depending on whether they wish to be alert or to relax.

In conclusion, the data presented here suggest that the nicotinic receptors, responsible for the stimulant effects of nicotine on NAc dopamine secretion and enhanced locomotor responses, may be susceptible to desensitization when nicotine is administered at a rate which maintains the plasma concentration at levels commonly found in smokers. The results clearly support the hypothesis that the up-regulation of nicotinic receptors, observed in brain tissue taken at post mortem from habitual smokers, is caused by prolonged periods of receptor desensitization. In addition, the data also cast doubt on hypotheses for nicotine dependence which assumes that the administration of the compound invariably causes stimulation of mesolimbic dopamine secreting neurones.

These studies were performed with financial support from VERUM Foundation and the Wellcome Trust.

References

BALFOUR, D.J.K. (1990). Nicotine as the basis of the smoking habit. In *Psychotropic Drugs of Abuse*. ed. Balfour, D.J.K. pp. 453–481. Oxford, New York: Pergamon Press.

BALFOUR, D.J.K., BENWELL, M.E.M. & VALE, A.L. (1990). Studies on the role of mesolimbic dopamine in behavioural responses to chronic nicotine. In *Effects of Nicotine on Biological Systems*. ed. Adlkofer, F. & Thurau, K. pp. 406–416. Basel: Birkhäuser.

BENOWITZ, N.L., PORCHET, H. & JACOB, P. III (1990). Pharmacokinetics, metabolism and pharmacodynamics of nicotine. In *Nicotine Psychopharmacology; Molecular, Cellular and Behavioural Aspects*. ed. Wonnacott, S., Russell, M.A.H. & Stolerman, I.P. pp. 112–157. Oxford: Univ. Press.

BENWELL, M.E.M. & BALFOUR, D.J.K. (1992). The effects of acute and repeated nicotine treatment on nucleus accumbens dopamine and locomotor activity. *Br. J. Pharmacol.*, **105**, 849–856.

BENWELL, M.E.M., BALFOUR, D.J.K. & ANDERSON, J.M. (1988). Evidence that smoking increases the density of nicotine binding sites in human brain. *J. Neurochem.*, **50**, 243–247.

BENWELL, M.E.M., BALFOUR, D.J.K. & LUCCHI, H.M. (1993). Influence of tetrodotoxin and calcium on changes in extracellular dopamine levels evoked by systemic nicotine. *Psychopharmacology*, **112**, 467–474.

CLARKE, P.B.S. & PERT, A. (1985). Autoradiographic evidence for nicotinic receptors on nigrostriatal and mesolimbic dopamine neurones. *Brain Res.*, **348**, 355–358.

CLARKE, P.B.S., FU, D.S., JAKUBOVIC, A. & FIBIGER, H.C. (1988). Evidence that mesolimbic activation underlies the locomotor stimulant action of nicotine in rats. *J. Pharmacol. Exp. Ther.*, **246**, 701–708.

CORRIGALL, W.A., FRANKLIN, K.B.J., COEN, K.M. & CLARKE, P.B.S. (1992). The mesolimbic dopaminergic system is implicated in the reinforcing effects of nicotine. *Psychopharmacology*, **107**, 285–289.

DAMSMA, G., DAY, J. & FIBIGER, H.C. (1989). Lack of tolerance to nicotine-induced dopamine release in the nucleus accumbens. *Europ. J. Pharmacol.*, **168**, 363–368.

DI CHIARA, G. & IMPERATO, A. (1988). Drugs abused by humans preferentially increase synaptic dopamine concentrations in the mesolimbic system of freely moving rats. *Proc. Natl. Acad. Sci. U.S.A.*, **85**, 5274–5278.

FUNG, Y.K. (1989). Effects of chronic nicotine pretreatment on (+)-amphetamine and nicotine-induced synthesis and release of [^{3}H]-DA from [^{3}H]-tyrosine in rat nucleus accumbens. *J. Pharm. Pharmacol.*, **41**, 66–68.

FUXE, K., ANDERSSON, K., HARFSTRAND, A. & AGNATI, L.F. (1986). Increases in dopamine utilisation in certain limbic dopamine terminal populations after a short period of intermittent exposure of male rats to cigarette smoke. *J. Neural. Transm.*, **67**, 15–29.

HENNINGFIELD, J.E., STAPLETON, J.M., BENOWITZ, N.L., GRAYSON, R.F. & LONDON, E.D. (1993). Higher levels of nicotine in arterial rather than venous blood after cigarette smoking. *Drug Alcohol Depend.*, **33**, 23–29.

IMPERATO, A., MULAS, A. & DI CHIARA, G. (1986). Nicotine preferentially stimulated dopamine release in the limbic system of freely moving rats. *Eur. J. Pharmacol.*, **132**, 337–338.

JANSSON, A.M., FUXE, K., AGNATI, L.F., JANSSON, A., BJELKE, B., SUNDSTROM, E., ANDERSSON, K., HARFSTRAND, A., GOLDSTEIN, M. & OWMAN, C. (1989). Protective effects of chronic nicotine treatment on lesioned nigrostriatal dopamine neurons in the male rat. *Prog. Brain Res.*, **79**, 257–265.

JANSSON, A.M., FUXE, K., AGNATI, L.F., KITAYAMA, I., HARFSTRAND, A., ANDERSSON, K. & GOLDSTEIN, M. (1988). Chronic nicotine treatment counteracts the disappearance of tyrosine hydroxylase immunoreactive nerve cell bodies, dendrites and terminals in the mesostriatal dopamine system of the male rat after partial hemi-transection. *Brain Res.*, **455**, 332–345.

JANSSON, A.M., FUXE, K., KITAYAMA, I., HARFSTRAND, A. & AGNATI, L.F. (1986). Morphometric studies on the protective action of nicotine on the substantia nigra dopamine nerve cells after partial hemi-transection in the male rat. *Neurosci. Lett.*, **26**, S88.

KIRCH, D.G., GERHARDT, G.A., SHELTON, R.C., FREEDMAN, R. & WYATT, R.J. (1987). Effect of chronic nicotine administration on monoamine and monoamine metabolite concentration in rat brain. *Clin. Neuropharmacol.*, **10**, 376–383.

MARKS, M.J., STITZEL, J.A. & COLLINS, A.C. (1985). Time course of the effects of chronic nicotine infusion on drug responses and brain receptors. *J. Pharmacol. Exp. Ther.*, **235**, 619–628.

NISELL, M., NOMIKOS, G.G. & SWENSSON, T.H. (1994). Systemic nicotine-induced dopamine release in the rat nucleus accumbens is regulated by nicotinic receptors in the ventral tegmental area. *Synapse*, **16**, 36–44.

PERKINS, K.A., GROBE, J.E., EPSTEIN, L.H., CAGGUILA, A., STILLER, R.L. & JACOB, R.J. (1993). Chronic and acute tolerance to subjective effects of nicotine. *Pharmacol. Biochem. Behav.*, **45**, 375–381.

RANG, H. & DALE, M.M. (1992). In *Pharmacology (2nd edition)* pp. 142–181. Edinburgh, London: Churchill Livingston.

REAVILL, C. & STOLERMAN, I.P. (1990). Locomotor activity in rats after administration of nicotinic agonists intracerebrally. *Br. J. Pharmacol.*, **99**, 273–278.

RUSSELL, M.A.H. (1990). Nicotine intake and its control over smoking. In *Nicotine Psychopharmacology; Molecular, Cellular and Behavioural Aspects.* ed. Wonnacott, S., Russell, M.A.H. & Stolerman, I.P. pp. 374–418. Oxford: Univ. Press.

RUSSELL, M.A.H. & FEYERABEND, C. (1978). Cigarette smoking: a dependence on high nicotine boli. *Drug Metab. Rev.*, **8**, 29–57.

SINGER, G., WALLACE, M. & HALL, R. (1982). The effects of dopaminergic nucleus accumbens lesions on the aquisition of schedule-induced self-injection of nicotine in the rat. *Pharmacol. Biochem. Behav.*, **17**, 579–581.

SCHWARTZ, R.D. & KELLAR, K.J. (1985). In vivo regulation of [^{3}H]-acetylcholine recognition sites in brain by nicotinic cholinergic drugs. *J. Neurochem.*, **45**, 427–433.

VALE, A.L. & BALFOUR, D.J.K. (1989). Aversive environmental stimuli as a factor in the psychostimulant response to nicotine. *Pharmacol. Biochem. Behav.*, **32**, 857–860.

WARBURTON, D.M. (1990). The pleasures of nicotine. In *Effects of Nicotine on Biological Systems/Advances in Pharmacological Sciences.* ed Adlkofer, F. & Thurau, K. pp. 473–483. Basel: Birkhäuser Verlag.

WEST, R.J. & RUSSELL, M.A.H. (1987). Cardiovascular and subjective effects of smoking before and after 24 abstinence from cigarettes. *Psychopharmacology*, **92**, 118–121.

WISE, R.A. & BOZARTH, M.A. (1987). A psychomotor stimulant theory of addiction. *Psychol. Rev.*, **94**, 469–492.

(Received April 25, 1994
Revised September 8, 1994
Accepted September 14, 1994)

British Journal of Pharmacology (1995) 114, 461-467 © 1995 Stockton Press All rights reserved 0007-1188/95 $9.00

Postsynaptic nicotinic receptor desensitized by non-contractile Ca^{2+} mobilization via protein kinase-C activation at the mouse neuromuscular junction

[1]Ikuko Kimura, Katsuya Dezaki, Hiroshi Tsuneki & Masayasu Kimura

Department of Chemical Pharmacology, Faculty of Pharmaceutical Sciences, Toyama Medical and Pharmaceutical University, 2630 Sugitani, Toyama 930-01, Japan

1 Non-contractile Ca^{2+} mobilization (unaccompanied by muscle contraction) was initiated by nerve stimulation in the presence of neostigmine (more than 0.03 μM) at the endplate region of mouse diaphragm muscles. In the process of nicotinic receptor desensitization, the depressant effect of non-contractile Ca^{2+} on contractile Ca^{2+} mobilization was investigated by measurement of Ca^{2+}-aequorin luminescence.

2 When the phrenic nerve was stimulated with paired pulses having intervals of 150, 300, 600, 1000 and 2000 ms, contractile Ca^{2+} transients were elicited during the generation of non-contractile Ca^{2+} mobilization. The amplitude of the contractile Ca^{2+} transients elicited by the second pulse (S_2) was depressed at the shorter pulse intervals, but recovered to the initial contractile response (S_1) at longer pulse intervals.

3 The extent of depression of S_2 was enhanced by increasing the concentration of neostigmine (0.03 to 0.3 μM). When a low concentration (0.05 μM) of pancuronium, a competitive nicotinic antagonist, completely blocked non-contractile Ca^{2+} mobilization, the depression of S_2 was diminished.

4 The depression of S_2 was enhanced when the peak amplitude of non-contractile Ca^{2+} mobilization was raised by increasing the external Ca^{2+} concentration from 1.3 to 5 mM.

5 Staurosporine (10 nM), a protein kinase-C inhibitor, diminished the depression of S_2 despite large amounts of non-contractile Ca^{2+} mobilization. The diminishing effect of staurosporine was counteracted by TPA (0.1 μM), a protein kinase-C activator.

6 These findings suggest that non-contractile Ca^{2+} mobilization may enhance the desensitization of the postsynaptic nicotinic receptor via activation of protein kinase-C at the neuromuscular junction.

Keywords: Nicotinic acetylcholine receptor; non-contractile calcium; protein kinase-C; desensitization; neuromuscular postsynapse

Introduction

We previously reported that contractile and non-contractile Ca^{2+} mobilization is generated simultaneously at the neuromuscular junction by nerve stimulation in the presence of anticholinesterase agents (Kimura *et al.*, 1989). The mechanism of non-contractile Ca^{2+} mobilization is completely different from that of contractile Ca^{2+} mobilization, because (1) non-contractile Ca^{2+} mobilization requires the prolonged activation of nicotinic acetylcholine receptors (AChRs) as a result of accumulating acetylcholine (ACh) in the synaptic cleft and is specifically blocked by competitive nicotinic antagonists such as (+)-tubocurarine and pancuronium at low concentrations that have no effect on contractile Ca^{2+} transients (Kimura *et al.*, 1989); (2) a higher concentration (5 mM) of external Ca^{2+} increases non-contractile Ca^{2+} mobilization, but decreases contractile Ca^{2+} transients (Kimura *et al.*, 1989); (3) non-contractile Ca^{2+} mobilization is not due to Ca^{2+} release from sarcoplasmic reticulum (SR) (Kimura *et al.*, 1991a,b) and (4) activation of protein kinase-A within muscle cells is essential to mobilize non-contractile Ca^{2+} (Kimura *et al.*, 1993).

Non-contractile Ca^{2+} is not linked to muscle contraction despite the fact that much larger amounts of Ca^{2+} are mobilized than during contractile Ca^{2+} mobilization. Non-contractile Ca^{2+} is mobilized under desensitizing conditions, since desensitization to nerve stimulation readily occurs after inhibiting cholinesterase (Magleby & Pallotta, 1981). The increase in intracellular Ca^{2+} accelerates the rate of nicotinic AChR desensitization in skeletal muscles (Manthey, 1970; Nastuk & Parsons, 1970; Miledi, 1980). We therefore suspect that non-contractile Ca^{2+} may prevent the nicotinic AChR from responding to excessive stimulation by accumulated ACh. The functional role of non-contractile Ca^{2+}, however, has not been established. In the present study, we investigated the depressant effect of non-contractile Ca^{2+} on contractile Ca^{2+} mobilization using paired-pulse stimulation to elucidate the functional role of non-contractile Ca^{2+} mobilization in the process of nicotinic AChR desensitization.

[1] Author for correspondence.

Methods

Muscle preparations

Male ddY mice (7-9 weeks old, 28-42 g) were killed by decapitation. The right phrenic nerve-diaphragm muscle with the tendon was isolated, and cut into a strip 10 mm wide. The corner of a muscle strip was fixed with pins on rubber plates in a chamber. Modified Krebs' solution (mM: NaCl 122, KCl 5.9, $CaCl_2$ 2.5, $MgCl_2$ 1.2, $NaHCO_3$ 15.5 and glucose 11.5) was perfused through the chamber at a rate of 1.5 ml min^{-1}. The tendon was tied with silk thread and connected to an isometric transducer (Nihon Kohden, Tokyo, Japan), and the resting tension was adjusted to 200 mg. The bath solution was maintained at 36°C by a heated copper plate under the chamber regulated by a thermomodule (Komatsu Electronics, Kanagawa, Japan). The solution was equilibrated with 95% O_2 and 5% CO_2.

Measurement of intracellular Ca^{2+} transients

We adopted the same procedures for measuring Ca^{2+}-aequorin luminescence (Ca^{2+} transients) as in the previous paper (Kimura *et al.*, 1990). The aequorin solution (1 mg ml^{-1}) was expelled from the micropipette into the end-plate region of 40 to 50 muscle fibres by 2 s nitrogen gas pressure pulses of 5–6 kg cm^{-2} delivered by a pressure system having two pressure valves (J262D23, Asco, Toyama, Japan) operated electromagnetically. Ca^{2+} transients emitted from the aequorin-injected area were amplified with a photomultiplier tube (Hamamatsu Photonics, Shizuoka, Japan) and measured with a photon counter (Hamamatsu Photonics). The open gate time of the photon counter was set at 10 ms and the closed gate time at 20 μs. To decrease photon loss, one end of an acrylic optical fibre (Ryo-mi Plastics, Toyama, Japan) was placed near the injected area, 0.5 mm away from the surface of the muscle, and the other end attached to the photomultiplier tube. When the phrenic nerve was stimulated supramaximally (0.4–0.8 V) at 0.1 Hz with a 0.1 ms duration square pulse via a pair of platinum electrodes placed 1 mm apart, Ca^{2+} transients and twitch tension were recorded simultaneously. The signals were averaged with a signal processor (San-ei, Tokyo, Japan) to improve the signal-to-noise ratio. The records for 30 Ca^{2+} transient signals obtained 5 to 10 min after the generation of non-contractile Ca^{2+} mobilization were analysed. The normalization procedures were as follows. The peak amplitude of both non-contractile and contractile Ca^{2+} transients was expressed as a percentage of contractile Ca^{2+} transients obtained during the 5 to 0 min before neostigmine was applied. The duration of non-contractile Ca^{2+} mobilization was determined at e^{-1} amplitude of the signal.

Analysis of paired-pulse stimulation data

The phrenic nerve was stimulated with paired-pulses having intervals of 150, 300, 600, 1000 and 2000 ms, 5 min after the generation of non-contractile Ca^{2+} mobilization by application of neostigmine. The ratio (S_2/S_1) of the peak amplitude of contractile Ca^{2+} transients elicited by the second pulse (S_2) to that by the first pulse (S_1) was used to normalize the changes in S_2. S_2 was calculated as the difference between the amplitude of non-contractile Ca^{2+} mobilization and the actually measured peak amplitude of contractile Ca^{2+} transients. A decrease in the S_2/S_1 value indicates the increased depression of S_2.

Drugs and solutions

Aequorin (1-(5-isoquinolinesulfonyl)-2-methylpiperazine dihydrochoride, Wako Pure Chemical, Osaka, Japan) was dissolved in Ca^{2+}-free distilled water containing EDTA (5 μM). Caffeine (Nacalai Tesque, Tokyo, Japan), H-7 (Seikagaku, Tokyo, Japan), neostigmine methylsulphate (Sigma Chemical, MO, U.S.A.), 12-O-tetradecanoylphorbol 13-acetate (TPA, 0.01% N,N-dimethylformamide solution; Sigma), pancuronium bromide (Sankyo, Tokyo, Japan) and staurosporine (0.003–0.01% N,N-dimethylformamide solution; Kyowa Medix, Tokyo, Japan) were bath-applied.

Statistical analysis

Data are expressed as means ± s.e. One-way analysis of variance (ANOVA) with the Scheffe multiple-comparison test was used to determine statistical significances at P levels of 0.05 or 0.01.

Results

Neostigmine concentration-dependently increases contractile and non-contractile Ca^{2+} transients

To investigate the relationship between the amounts of ACh accumulated in the synaptic cleft and non-contractile Ca^{2+} mobilization, the muscle preparations were exposed to various concentrations of an anticholinesterase agent, neostigmine. Non-contractile Ca^{2+} mobilization was initiated by nerve stimulation in the presence of neostigmine (more than 0.03 μM) (Figure 1a). The peak amplitude of non-contractile

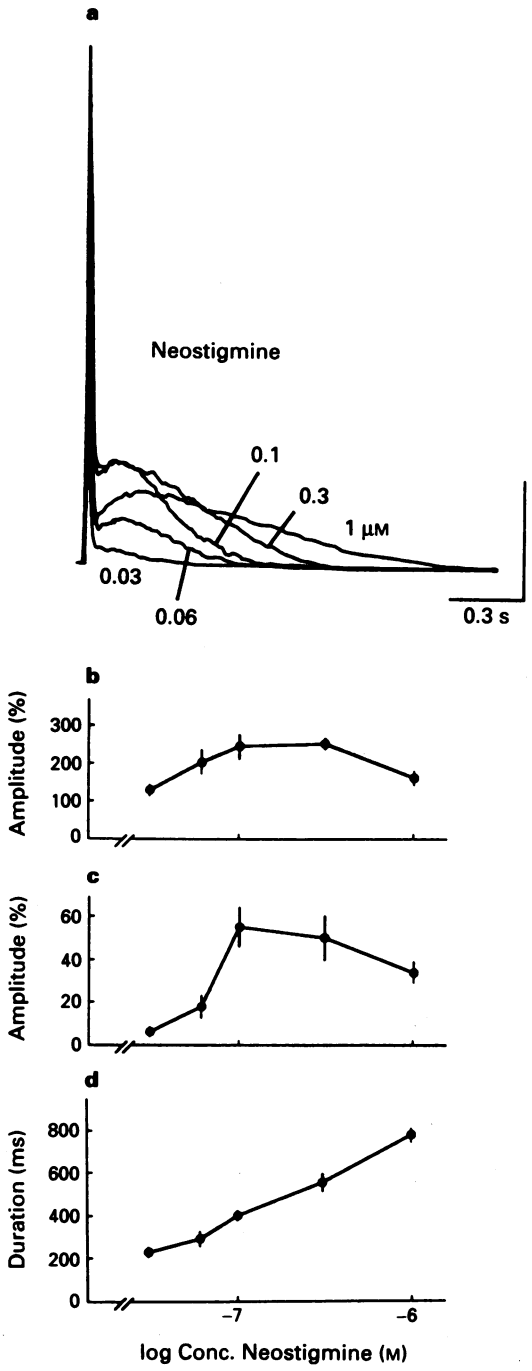


Figure 1 Changes in contractile and non-contractile Ca^{2+} transients in diaphragm muscles of mice in response to increasing neostigmine concentrations. (a) Typical traces of averaged records for 30 signals of Ca^{2+} transients during the 5 to 10 min after generation of non-contractile Ca^{2+} transients by application of neostigmine (0.03–1 μM). The large, rapid increase in Ca^{2+} represents the contractile transients, and the slower prolonged increase represents the non-contractile transients. Data obtained from separate experiments have been normalized and superimposed. The ordinate calibration bar represents 50% of the amplitude of contractile Ca^{2+} transients obtained 5 to 0 min before the application of neostigmine. Log concentration-response curves for the effect of neostigmine on the peak amplitude of contractile Ca^{2+} transients (b), and on the peak amplitude (c) and duration (d) of non-contractile Ca^{2+} transients are shown. Data are means ± s.e. of 5 to 10 separate experiments.

Ca^{2+} mobilization yielded a maximum response at 0.1–0.3 μM (Figure 1c). The duration of non-contractile Ca^{2+} mobilization was concentration-dependently prolonged by neostigmine (0.03–0.3 μM) (Figure 1d). At a higher neostigmine concentration (1 μM), the peak amplitude of non-contractile Ca^{2+} mobilization was slightly decreased, but its duration was even more prolonged. The total amount of non-contractile Ca^{2+} mobilization was the same at both the 0.3 μM and 1 μM concentrations (data not shown).

The peak amplitude of contractile Ca^{2+} transients was increased by application of neostigmine (0.03–0.3 μM) (Figure 1b). This augmenting effect of neostigmine on the peak amplitude tended to decrease at 1 μM. No changes in the duration of contractile Ca^{2+} transients was observed (data not shown).

Non-contractile Ca^{2+} depresses contractile Ca^{2+} transients elicited by the second pulse

To elucidate the effect of non-contractile Ca^{2+} on contractile Ca^{2+} mobilization, the phrenic nerve was stimulated with paired pulses with intervals of 150, 300, 600, 1000 and 2000 ms in the presence of neostigmine (0.03 μM). The amplitudes of the contractile Ca^{2+} transients elicited by the second pulse were depressed at shorter pulse intervals as non-contractile Ca^{2+} mobilization increased, but were restored to the initial contractile response at longer pulse intervals as non-contractile Ca^{2+} mobilization decreased (Figure 2a). Twitch tension was depressed in the same manner as the change in contractile Ca^{2+} transients. The amplitude of the first twitch tension was 118 ± 2% ($n = 29$) for the response before application of neostigmine, and those of the second twitch tension were 96 ± 3% ($n = 7$), 102 ± 4% ($n = 7$), 103 ± 3% ($n = 9$) and 112 ± 4% ($n = 6$) at pulse intervals of 150, 300, 600 and 1000 ms respectively. When the concentration of neostigmine was increased to 0.1 μM, contractile Ca^{2+} transients elicited by the second pulse were more depressed (Figure 2a), whereas non-contractile Ca^{2+} mobilization was larger as stated above. The blocking action of neostigmine on nicotinic AChR-channels may be ruled out, since low concentrations of neostigmine used in this study have no effect on mouse endplate channels (Chang *et al.*, 1987). Thus, the depression of contractile transients may depend on the amount of ACh accumulated in the synpatic cleft, suggesting that these contractile response phenomena may be caused by nicotinic AChR desensitization.

To evaluate the extent of depression of contractile Ca^{2+} transients quantitatively, the ratio (S_2/S_1) of the peak amplitude of the contractile response elicited by the second pulse (S_2) to that by the first pulse (S_1) was calculated. The S_2/S_1 values were decreased both by shortening the pulse intervals and by increasing the concentrations of neostigmine (Figure 2b). These findings suggest that the decrease in S_2/S_1 may be correlated with the increase in peak amplitude of non-contractile Ca^{2+} mobilization.

In the absence of neostigmine, when no non-contractile Ca^{2+} mobilization was generated, all of the contractile Ca^{2+} transients elicited by paired-pulse stimulation were almost constant, demonstrating that the contractile response was unaffected by paired pulses with these intervals (Figure 3a). Caffeine (5 mM), a promoter of Ca^{2+} release from the SR, increased contractile Ca^{2+} transients to the same extent as neostigmine; however, the second paired-pulse contractile Ca^{2+} transients were hardly depressed at all (Figure 3b). These findings indicate that there is little interaction between two successive contractile Ca^{2+} transients.

To determine whether non-contractile Ca^{2+} depresses contractile Ca^{2+} transients, the effect of blocking non-contractile Ca^{2+} mobilization on S_2/S_1 values was investigated. After pretreatment for 30 min with pancuronium (0.05 μM), a competitive nicotinic antagonist, neostigmine (0.3 μM) was applied in combination with pancuronium, and the preparation was then stimulated with paired pulses. Non-contractile Ca^{2+} mobilization was blocked by pancuronium at the low concentration with no effect on contractile Ca^{2+} mobilization elicited by the first pulse, as previously reported (Kimura *et al.*, 1989). All of the S_2/S_1 values of contractile transients examined at 150, 300, 600 and 1000 ms intervals were significantly increased by pancuronium (Figure 4), indicating that blockade of non-contractile Ca^{2+} mobilization caused

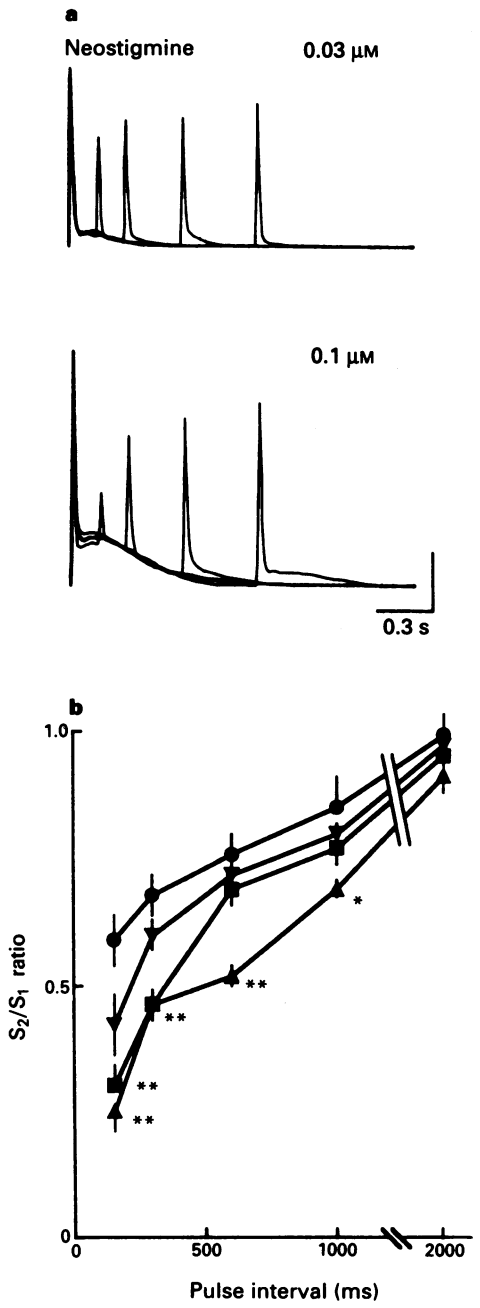


Figure 2 Neostigmine concentration-dependent depression of contractile Ca^{2+} transients elicited during generation of non-contractile Ca^{2+} transients in mouse diaphragm muscles. (a) Typical traces of averaged records for 30 Ca^{2+} transient signals elicited by paired-pulse nerve stimulation with intervals of 150, 300, 600 and 1000 ms during the 8 to 13 min after application of 0.03 μM (above) and 0.1 μM neostigmine (below). Data obtained from separate experiments have been normalized and superimposed. The ordinate calibration bar represents 50% of the amplitude of contractile Ca^{2+} transients before the application of neostigmine. (b) Effects of neostigmine (●: 0.03 μM, ▼: 0.06 μM, ■: 0.1 μM, ▲: 0.3 μM) on the time course of the ratio of contractile Ca^{2+} transients elicited by the second pulse (S_2) to those elicited by the first pulse (S_1). The data shown are means ± s.e. of 5 to 9 separate experiments. $^*P < 0.05$, $^{**}P < 0.01$; significantly different from the response to neostigmine (0.03 μM) at each pulse interval based on one-way ANOVA.

the decrease in S_2/S_1 to diminish. Very little decrease in S_2/S_1 was observed in the presence of pancuronium without neostigmine ($S_2/S_1 = 0.95 \pm 0.03$ at a pulse interval of 150 ms, $n = 5$). Thus, non-contractile Ca^{2+} may depress contractile Ca^{2+} mobilization.

The depression of contractile Ca^{2+} transients by non-contractile Ca^{2+} is dependent on the external Ca^{2+} concentration

The relationship between the extent of changes in S_2/S_1 and the amounts of non-contractile Ca^{2+} mobilized was further investigated. Simultaneously with exposure of the preparation to neostigmine (0.3 μM), the $[Ca^{2+}]_o$ was changed either to 1.3 mM or to 5 mM. The peak amplitude of non-contractile Ca^{2+} mobilization depends on the external Ca^{2+} concentration (1.3–5 mM), as shown previously (Kimura *et al.*, 1989). When non-contractile Ca^{2+} mobilization was reduced by decreasing $[Ca^{2+}]_o$ from 2.5 to 1.3 mM, S_2 was higher than under the normal conditions (2.5 mM $[Ca^{2+}]_o$), despite using the same pulse intervals (Figure 5a). In contrast, increasing non-contractile Ca^{2+} mobilization by raising $[Ca^{2+}]_o$ to 5 mM caused a decrease in the S_2 of the contractile transients. The time course of S_2/S_1 revealed different patterns at various concentrations of $[Ca^{2+}]_o$ (Figure 5b). The largest increase in the difference between the peak amplitudes of non-contractile Ca^{2+} mobilization at each $[Ca^{2+}]_o$ was observed at a pulse interval of 300 ms, where the peak amplitudes were 7 ± 3%, 32 ± 8% and 63 ± 8% for contractile Ca^{2+} transients before application of neostigmine at 1.3 mM, 2.5 mM and 5 mM $[Ca^{2+}]_o$, respectively. The S_2/S_1 value decreased from 0.79 to 0.24 when the $[Ca^{2+}]_o$ was raised from 1.3 to 5 mM (Figure 5c). Thus, the decrease in the S_2/S_1 value of contractile Ca^{2+} transicents was dependent on the peak amplitude of non-contractile Ca^{2+} mobilization, which was regulated by $[Ca^{2+}]_o$.

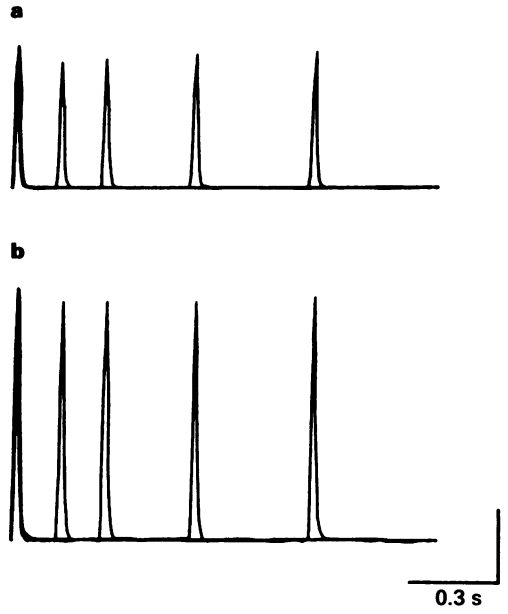


Figure 3 Negligible interaction between two successive contractile Ca^{2+} transients elicited by paired-pulse nerve stimulation with (b) and without 5 mM caffeine (a). Typical traces of averaged records for 30 contractile Ca^{2+} transient signals elicited by paired-pulse stimulation with intervals of 150, 300, 600 and 1000 ms in the absence of neostigmine, showing no influence of the increase in the first contractile Ca^{2+} transients (S_1) on the second contractile transients (S_2). Data obtained from separate experiments have been normalized and superimposed. The ordinate calibration bar represents 50% of the amplitude of the contractile Ca^{2+} transients before the application of caffeine.

Non-contractile Ca^{2+} may depress contractile Ca^{2+} transients via activation of protein kinase-C

To investigate the involvement of protein kinase-C in non-contractile Ca^{2+}-induced depression of contractile Ca^{2+} mobilization, staurosporine (10 nM), a protein kinase-C inhibitor, was added 30 min before the addition of neostig-

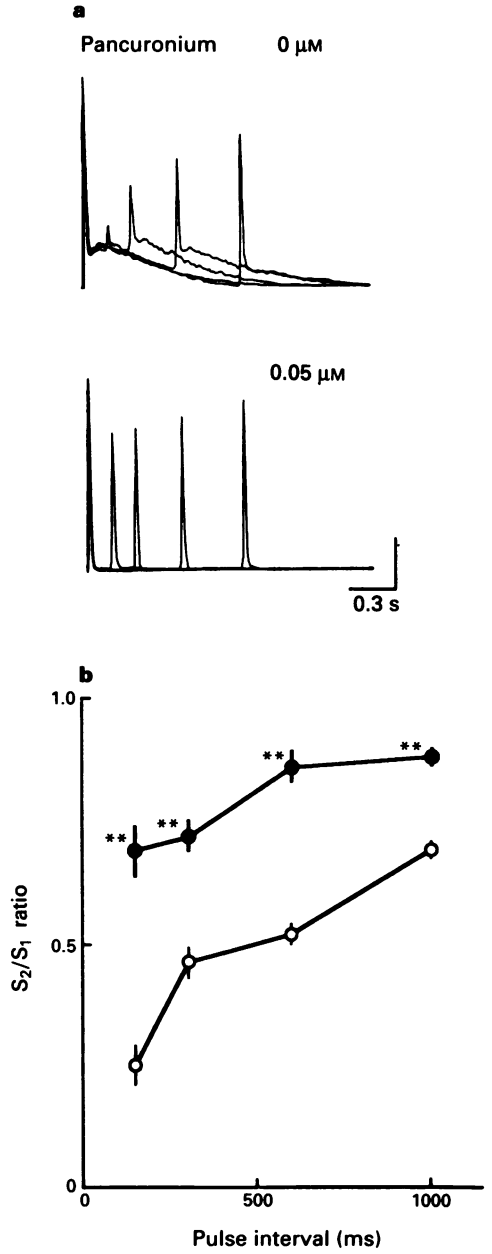


Figure 4 Influence of pancuronium-induced blockade of non-contractile Ca^{2+} transients on contractile Ca^{2+} transients elicited by the second pulse: evidence for the depressant effect of non-contractile Ca^{2+}. Pancuronium (0.05 μM) was added 30 min before neostigmine (0.3 μM). (a) Typical traces of averaged records for 30 Ca^{2+} transient signals in response to paired-pulse nerve stimulation with intervals of 150, 300, 600 and 1000 ms during the 8 to 13 min after application of neostigmine in the absence (above) and presence of pancuronium (below). Data obtained from separate experiments have been normalized and superimposed. The ordinate calibration bar represents 50% of the amplitude of the contractile Ca^{2+} transients before the application of neostigmine. (b) Effects of pancuronium (●: 0.05 μM) on the time course of the ratio of the second contractile Ca^{2+} transients (S_2) to the first contractile transients (S_1) in the presence of neostigmine (0.3 μM). Data shown are means ± s.e. of 4 to 5 separate experiments. $^{**}P < 0.01$; significantly different from the control response with neostigmine alone (○) at each pulse interval based on one-way ANOVA.

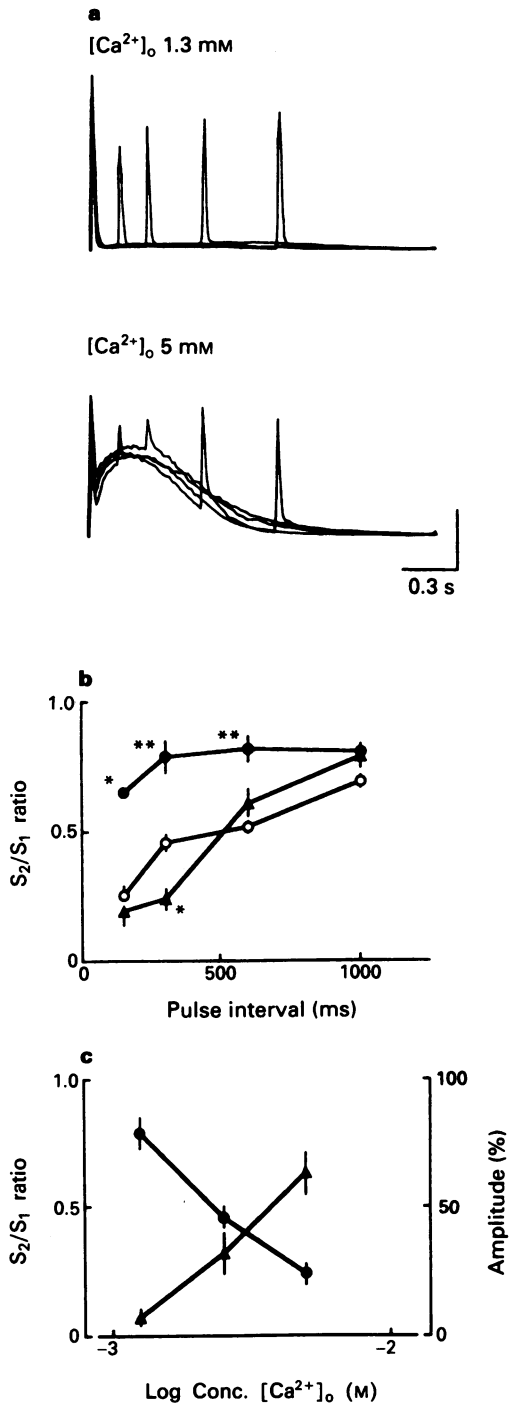


Figure 5 External Ca^{2+} concentration ($[Ca^{2+}]_o$)-dependency of the depressant effect of non-contractile Ca^{2+} on contractile Ca^{2+} transients elicited by the second pulse. (a) Typical traces of averaged records for 30 Ca^{2+} transient signals in response to paired-pulse stimulation with intervals of 150, 300, 600 and 1000 ms during the 8 to 13 min after application of 0.3 μM neostigmine at low (1.3 mM, above) and high $[Ca^{2+}]_o$ (5 mM, below). Data obtained from separate experiments have been normalized and superimposed. The ordinate calibration bar represents 50% of the amplitude of the contractile Ca^{2+} transients obtained before the application of neostigmine. Typical traces at normal $[Ca^{2+}]_o$ (2.5 mM) are shown in Figure 4a (above). (b) Influence of $[Ca^{2+}]_o$ (●: 1.3 mM, ○: 2.5 mM, ▲: 5 mM) on the time course of the ratio of the second contractile Ca^{2+} transients (S_2) to the first contractile transients (S_1) in the presence of neostigmine (0.3 μM). Data shown are means ± s.e. of 5 to 7 separate experiments. $*P<0.05$, $**P<0.01$; significantly different from the responses with neostigmine at normal $[Ca^{2+}]_o$ (2.5 mM) at each pulse interval based on one-way ANOVA. (c) Log concentration-response curves of $[Ca^{2+}]_o$ on the S_2/S_1 ratio obtained at a pulse interval of 300 ms (●) and on the peak amplitude of the non-contractile Ca^{2+} transients elicited by the first pulse (▲).

mine (0.3 μM). Staurosporine (10 nM) diminished the depression of the contractile Ca^{2+} transients elicited by the second pulse, despite having no effect on non-contractile Ca^{2+} mobilization (Figure 6a). The S_2/S_1 values at 150, 600 and 1000 ms intervals were significantly higher in the presence of staurosporine than those in its absence (Figure 6b). H-7 (10 μM), a protein kinase-C inhibitor, also increased S_2/S_1 at 150, 600 and 1000 ms intervals, despite large amounts of non-contractile Ca^{2+} mobilization (data not shown). Blocking actions on activated nicotinic channels may be ruled out, since H-7 has no effect on endplate channels at this concentration (Reuhl *et al.*, 1992). Moreover, TPA, a specific activator of protein kinase-C, inhibited the diminishing effect of staurosporine on the depression of contractile transients (Figure 6b) at the lower concentration (0.1 μM), but did not affect either type of Ca^{2+} transients alone. These findings indicate that non-contractile Ca^{2+} may depress contractile Ca^{2+} mobilization via activation of protein kinase-C.

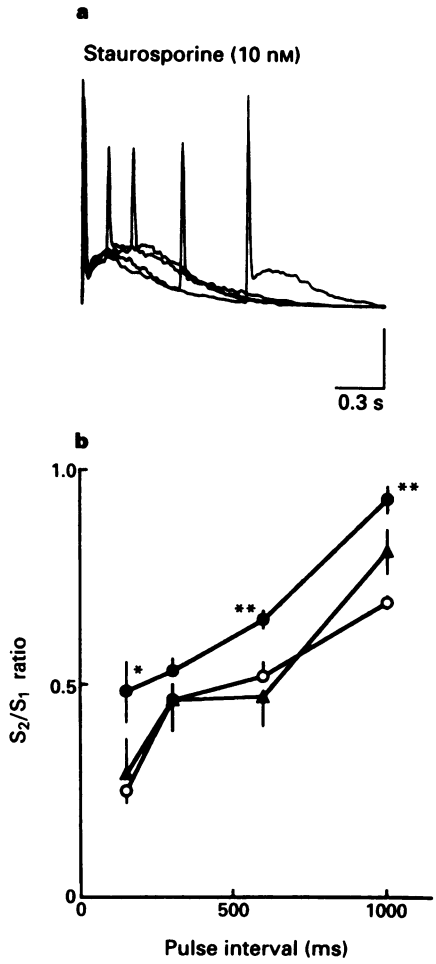


Figure 6 Involvement of protein kinase-C in non-contractile Ca^{2+}-induced depression of contractile Ca^{2+} transients. Staurosporine (10 nM) was added 30 min before neostigmine (0.3 μM). TPA (0.1 μM) was added 10 min before the addition of staurosporine. (a) Typical traces of averaged records for 30 Ca^{2+} transient signals in response to paired-pulse stimulation with intervals of 150, 300, 600 and 1000 ms during the 8 to 13 min after application of neostigmine in the presence of staurosporine. Data obtained from separate experiments have been normalized and superimposed. The ordinate calibration bar represents 50% of the amplitude of the contractile Ca^{2+} transients before the application of neostigmine. Typical traces of control responses in the presence of neostigmine alone are shown in Figure 4a (above). (b) Effects of staurosporine (●: 10 nM) alone and in the presence of TPA (▲: 0.1 μM) on the time course of the ratio of S_2 to S_1 in the presence of neostigmine. Data shown are means ± s.e. of 3 to 7 separate experiments. $*P<0.05$, $**P<0.01$; significantly different from the control response with neostigmine alone (○) at each pulse interval based on one-way ANOVA.

Discussion

Nicotinic AChR desensitization readily develops as a result of the accumulation of nerve-released ACh at the neuromuscular junction after cholinesterase inhibition. Non-contractile Ca^{2+} mobilization occurs via the nicotinic AChR only under such desensitizing conditions and depends on the amount of ACh accumulated in the synaptic cleft (Kimura *et al.*, 1989; 1993). These findings led us to examine the relationship between non-contractile Ca^{2+} mobilization and the desensitization using paired-pulse stimulation of a motor nerve.

There is no direct causal relationship between contractile and non-contractile Ca^{2+} mobilization, since geographutoxin II, a skeletal muscle Na^+ channel blocker (Cruz *et al.*, 1985; Ohizumi *et al.*, 1986), selectively blocked contractile Ca^{2+} transients without affecting non-contractile Ca^{2+} mobilization (Kimura *et al.*, 1991b), and caffeine (5 mM) increased contractile Ca^{2+} transients but decreased non-contractile Ca^{2+} mobilization (Kimura *et al.*, 1991a). Nevertheless, the contractile Ca^{2+} transients elicited by the second pulse (S_2) during the generation of non-contractile Ca^{2+} mobilization were depressed at shorter pulse intervals, but were restored to the initial contractile response (S_1) at longer pulse intervals. The rapid depression of contractile Ca^{2+} transients followed by gradual recovery to initial values is a phenomenon quite similar to the time course of the nicotinic AChR desensitization, measured by paired pulses of ACh using the patch clamp technique (Franke *et al.*, 1992; Bufler *et al.*, 1993). Moreover, the extent of the depression of S_2, indicated by the decrease in S_2/S_1, was enhanced by increasing concentrations of neostigmine. S_2/S_1 did not decrease in the absence of neostigmine. These changes in contractile transients were also considered to be consistent with concentration-dependent agonist enhancement of both the rate and extent of the nicotinic AChR desensitization (Adams, 1975; Chesnut, 1983; Dilger & Liu, 1992). Thus, the decrease in S_2/S_1 observed in this study appears to reflect nicotinic AChR desensitization.

The extent of depression of contractile Ca^{2+} transients was dependent on the peak amplitude of non-contractile Ca^{2+} mobilization regulated by $[Ca^{2+}]_o$. The development of nicotinic AChR desensitization is enhanced by increasing $[Ca^{2+}]_o$ (Manthey, 1966; 1970; Nastuk & Parsons, 1970; Nojima *et al.*, 1992), a consequence of accumulation of Ca^{2+} at the inner surface of the sarcolemmal membrane due to Ca^{2+} influx via the nicotinic AChR (Miledi, 1980; Chesnut, 1983). Intracellular Ca^{2+} release from the SR, however, is unrelated to desensitization of nicotinic AChR since caffeine does not affect the rate of desensitization (Magazanik & Vyskočil, 1970). Non-contractile Ca^{2+} may stabilize nicotinic AChR in refractory states and protect it against overexcitation at the motor endplate, depressing contractile Ca^{2+} mobilization.

The depolarization of postsynaptic membranes is prolonged by the persistent action of ACh accumulated after cholinesterase inhibition. However, the depression of contractile Ca^{2+} transients observed in this study is not involved in the depolarizing blockade of nicotinic AChR (Burns & Paton, 1951), since the recovery time from the depression of contractile Ca^{2+} transients based on the second pulse is 10–20 fold longer than the duration of the prolonged endplate potential in the presence of anticholinesterase agents.

S_2 was hardly depressed at all when S_1 was increased by caffeine in the absence of neostigmine, although complete recovery of Ca^{2+} content in the SR has been reported to require a few seconds (Somlyo *et al.*, 1985). Therefore, the depression of the second contractile Ca^{2+} transients by paired-pulse stimulation may not be due to the inactivation or depletion caused by the first Ca^{2+} release from the SR (Schneider & Simon, 1988).

When non-contractile Ca^{2+} mobilization was depressed either by 1.3 mM $[Ca^{2+}]_o$ or by 0.05 μM pancuronium in the presence of neostigmine, the decrease in S_2/S_1 was greatly reduced (Figures 4b and 5b). However, part of the decrease still remained. This remaining part may reflect the direct desensitizing effect of ACh accumulated after the cholinesterase inhibition, since the nicotinic agonist can directly cause nicotinic AChR desensitization even in the absence of external Ca^{2+} (Nelson *et al.*, 1980).

We have previously reported that TPA (0.3–1 μM), a protein kinase-C activator, depresses contractile Ca^{2+} transients elicited by single-pulse nerve stimulation in mouse diaphragm muscle (Kimura *et al.*, 1993). After pretreatment with protein kinase-C inhibitors, even large amounts of non-contractile Ca^{2+} failed to depress the second contractile Ca^{2+} transients elicited by paired-pulse stimulation. Protein kinase-C is translocated from the cytosol to plasma membranes in a Ca^{2+}-dependent manner (Kraft & Anderson, 1983; Melloni *et al.*, 1985). Activation of nicotinic AChR causes translocation of protein kinase-C to postsynaptic membranes, thereby activating the protein kinase in skeletal muscle (Eusebi *et al.*, 1987). The agonist-induced phosphorylation of nicotinic AChR in rat myotubes is dependent on external Ca^{2+} and is abolished by nicotinic AChR-channel blockers, suggesting that Ca^{2+} influx via the nicotinic AChR-channel is crucial to the activation of protein kinase-C (Miles *et al.*, 1994). The protein kinase-C which is activated via the nicotinic AChR has been shown to enhance the receptor desensitization (Eusebi *et al.*, 1987). The results of the present study suggest that nicotinic AChR-operated non-contractile Ca^{2+} may desensitize the receptor via activation of protein kinase-C within skeletal muscle cells. The depressant effect of protein kinase-C on the second contractile Ca^{2+} transients elicited by paired-pulse stimulation may not be due to a decrease in ACh release from motor nerve terminals, since the activator of protein kinase-C instead increases ACh release (Eusebi *et al.*, 1986; Caratsch *et al.*, 1988). In addition, the skeletal muscle dihydropyridine-sensitive Ca^{2+} channels in the transverse-tubule membranes are activated by protein kinase-C phosphorylation (Chang *et al.*, 1991). Thus, we may also exclude any possible interaction between protein kinase-C and the muscular processes, such as modulation of Ca^{2+} release from SR.

In conclusion, the non-contractile Ca^{2+} may enhance the desensitization of postsynaptic nicotinic AChRs via activation of protein kinase-C, depressing the contractile Ca^{2+} mobilization at the neuromuscular junction.

This work was supported in part by Grant-in-Aid for JSPS Fellows (No. 061200) from the Ministry of Education, Science and Culture, Japan, and by Scientific Research Grant (1994) from Suzuken Memorial Foundation, Japan. H.T. is a J.S.P.S. Research Fellow.

References

ADAMS, P.R. (1975). A study of desensitization using voltage clamp. *Pflügers Arch.*, **360**, 135–144.

BUFLER, J., FRANKE, C., WITZEMANN, V., RUPPERSBERG, J.P., MERLITZE, S. & DUDEL, J. (1993). Desensitization of embryonic nicotinic acetylcholine receptors expressed in *Xenopus* oocytes. *Neurosci. Lett.*, **152**, 77–80.

BURNS, B.D. & PATON, W.D.M. (1951). Depolarization of the motor end-plate by decamethonium and acetylcholine. *J. Physiol.*, **115**, 41–73.

CARATSCH, C.G., SCHUMACHER, S., GRASSI, F. & EUSEBI, F. (1988). Influence of protein kinase C-stimulation by a phorbol ester on neurotransmitter release at frog end-plates. *Naunyn-Schmied. Arch. Pharmacol.*, **337**, 9–12.

CHANG, C.C., CHEN, S.M. & HONG, S.J. (1987). Concentration dependence of the effects of neostigmine on the endplate potential and neuromuscular transmission in a mammalian muscle. *Asia Pacif. J. Pharmacol.*, **2**, 87–92.

CHANG, C.F., GUTIERREZ, L.M., MUNDINA-WEILENMANN, C. & HOSEY, M.M (1991). Dihydropyridine-sensitive calcium channels from skeletal muscle. II. Functional effects of differential phosphorylation of channel subunits. *J. Biol. Chem.*, **266**, 16395–16400.

CHESNUT, T.J. (1983). Two-component desensitization at the neuromuscular junction of the frog. *J. Physiol.*, **336**, 229–241.

CRUZ, L.J., GRAY, W.R., OLIVERA, B.M., ZEIKUS, R.D., KERR, L., YOSHIKAMI, D. & MOCZYDLOWSKI, E. (1985). *Conus geographus* toxins that discriminate between neuronal and muscle sodium channels. *J. Biol. Chem.*, **260**, 9280–9288.

DILGER, J.P. & LIU, Y. (1992). Desensitization of acetylcholine receptors in BC3H-1 cells. *Pflügers Arch.*, **420**, 479–485.

EUSEBI, F., GRASSI, F., NERVI, C., CAPORALE, C., ADAMO, S., ZANI, B.M. & MOLINARO, M. (1987). Acetylcholine may regulate its own nicotinic receptor-channel through the C-kinase system. *Proc. R. Soc. Lond. B*, **230**, 355–365.

EUSEBI, F., MOLINARO, M. & CARATSCH, C.G. (1986). Effects of phorbol ester on spontaneous transmitter release at frog neuromuscular junction. *Pflügers Arch.*, **406**, 181–183.

FRANKE, C., HATT, H., PARNAS, H. & DUDEL, J. (1992). Recovery from the rapid desensitization of nicotinic acetylcholine receptor channels on mouse muscle. *Neurosci. Lett.*, **140**, 169–172.

KIMURA, I., KONDOH, T. & KIMURA, M. (1989). Postsynaptic nicotinic ACh receptor-operated Ca^{2+} transients with neostigmine in phrenic nerve-diaphragm muscles of mice. *Brain Res.*, **507**, 309–311.

KIMURA, I., KONDOH, T. & KIMURA, M. (1990). Changes in intracellular Ca^{2+} produced in the mouse diaphragm by neuromuscular blocking drugs. *J. Pharm. Pharmacol.*, **42**, 626–631.

KIMURA, I., KONDOH, T., TSUNEKI, H. & KIMURA, M. (1991a). Reversed effect of caffeine on non-contractile and contractile Ca^{2+} mobilization operated by acetylcholine receptor in mouse diaphragm muscle. *Neurosci. Lett.*, **127**, 28–30.

KIMURA, I., TSUNEKI, H., DEZAKI, K. & KIMURA, M. (1993). Enhancement by calcitonin gene-related peptide of nicotinic receptor-operated noncontractile Ca^{2+} mobilization at the mouse neuromuscular junction. *Br. J. Pharmacol.*, **110**, 639–644.

KIMURA, M., KIMURA, I., KONDOH, T. & TSUNEKI, H. (1991b). Noncontractile acetylcholine receptor-operated Ca^{++} mobilization: suppression of activation by open channel blockers and acceleration of desensitization by closed channel blockers in mouse diaphragm muscle. *J. Pharmacol. Exp. Ther.*, **256**, 18–23.

KRAFT, A.S. & ANDERSON, W.B. (1983). Phorbol esters increase the amount of Ca^{2+}, phospholipid-dependent protein kinase associated with plasma membrane. *Nature*, **301**, 621–623.

MAGAZANIK, L.G. & VYSKOČIL, F. (1970). Dependence of acetylcholine desensitization on the membrane potential of frog muscle fibre and on the ionic changes in the medium. *J. Physiol.*, **210**, 507–518.

MAGLEBY, K.L. & PALLOTTA, B.S. (1981). A study of desensitization of acetylcholine receptors using nerve-released transmitter in the frog. *J. Physiol.*, **316**, 225–250.

MANTHEY, A.A. (1966). The effect of calcium on the desensitization of membrane receptors at the neuromuscular junction. *J. Gen. Physiol.*, **49**, 963–976.

MANTHEY, A.A. (1970). Further studies of the effect of calcium on the time course of action of carbamylcholine at the neuromuscular junction. *J. Gen. Physiol.*, **56**, 407–419.

MELLONI, E., PONTREMOLI, S., MICHETTI, M., SACCO, O., SPARATORE, B., SALAMINO, F. & HORECKER, B.L. (1985). Binding of protein kinase C to neutrophil membranes in the presence of Ca^{2+} and its activation by a Ca^{2+}-requiring proteinase. *Proc. Natl. Acad. Sci. U.S.A.*, **82**, 6435–6439.

MILEDI, R. (1980). Intracellular calcium and desensitization of acetylcholine receptors. *Proc. R. Soc. Lond. B.*, **209**, 447–452.

MILES, K., AUDIGIER, S.S.M., GREENGARD, P. & HUGANIR, R.L. (1994). Autoregulation of phosphorylation of the nicotinic acetylcholine receptor. *J. Neurosci.*, **14**, 3271–3279.

NASTUK, W.L. & PARSONS, R.L. (1970). Factors in the inactivation of postjunctional membrane receptors of frog skeletal muscle. *J. Gen. Physiol.*, **56**, 218–249.

NELSON, N., ANHOLT, R., LINDSTROM, J. & MONTAL, M. (1980). Reconstitution of purified acetylcholine receptors with functional ion channels in planar lipid bilayers. *Proc. Natl. Acad. Sci. U.S.A.*, **77**, 3057–3061.

NOJIMA, H., MUROI, M., KIMURA, I. & KIMURA, M. (1992). Indirect inhibitory effect of succinylcholine on acetylcholine-activated channel activities and its modulation by external Ca^{2+} in mouse skeletal muscles. *Br. J. Pharmacol.*, **105**, 23–26.

OHIZUMI, Y., MINOSHIMA, S., TAKAHASHI, M., KAJIWARA, A., NAKAMURA, H. & KOBAYASHI, J. (1986). Geographutoxin II, a novel peptide inhibitor of Na channels of skeletal muscles and autonomic nerves. *J. Pharmacol. Exp. Ther.*, **239**, 243–248.

REUHL, T.O.K., AMADOR, M., MOORMAN, J.R., PINKHAM, J. & DANI, J.A. (1992). Nicotinic acetycholine receptors are directly affected by agents used to study protein phosphorylation. *J. Neurophysiol.*, **68**, 407–416.

SCHNEIDER, M.F. & SIMON, B.J. (1988). Inactivation of calcium release from the sarcoplasmic reticulum in frog skeletal muscle. *J. Physiol.*, **405**, 727–745.

SOMLYO, A.V., McCLELLAN, G., GONZALEZ-SERRATOS, H. & SOMLYO, A.P. (1985). Electron probe X-ray microanalysis of post tetanic Ca^{2+} and Mg^{2+} movement across the sarcoplasmic reticulum in situ. *J. Biol. Chem.*, **260**, 6801–6807.

(Received May 23, 1994
Revised September 13, 1994
Accepted September 19, 1994)

British Journal of Pharmacology (1995) 114, 468–474 © 1995 Stockton Press All rights reserved 0007–1188/95 $9.00

Inhibitory action of SR33557 on L-type calcium current in single ventricular myocytes of rat

Kenji Yasui & [1]Philip Palade

Department of Physiology and Biophysics, The University of Texas Medical Branch, Galveston, TX 77555-0641, U.S.A.

1 The effect of SR33557 on L-type Ca^{2+} currents in rat ventricular myocytes was investigated by use of the whole-cell patch-clamp technique.

2 SR33557 inhibited Ca^{2+} current (I_{Ca}) in a concentration-dependent manner without change in the current-voltage relationship.

3 The inhibitory effect of SR33557 on I_{Ca} was dependent on the holding potential (V_h). The IC_{50} values were estimated to be 2.2×10^{-8} M at $V_h = -50$ mV and 9.0×10^{-6} M at $V_h = -80$ mV. SR33557 (10^{-7} M) shifted the steady state inactivation curve of I_{Ca} toward more negative potentials. Thus, the affinity of the drug for inactivated channels was considerably higher than for resting channels.

4 Blockade of I_{Ca} by SR33557 was both tonic and use-dependent.

5 The time constant of onset of block was 36.4 s at -50 mV and 41.9 ± 11.1 s at -40 mV.

6 The time course of unblock was voltage-dependent. The time constant declined from 400.7 ± 68.1 s at -50 mV to 5.2 ± 1.2 s at -80 mV.

7 The rate of block of I_{Ca} was related to the number of openings per unit time and to the amount of time spent depolarized. The affinity of drug for open channels was considered to be similar to that for inactivated channels.

8 These results suggest that SR33557 inhibits L-type Ca^{2+} current through binding to both open and inactivated channels in rat ventricular myocytes.

Keywords: SR33557; calcium current; patch-clamp; ventricular myocytes

Introduction

Voltage-gated L-type Ca^{2+} channels are the major entry pathway for Ca^{2+} and play an important role in excitation-contraction coupling (EC coupling) in excitable cells. The L-type Ca^{2+} channel can be blocked by a variety of structurally heterogeneous organic compounds collectively referred to as Ca^{2+} channel antagonists. On the basis of electrophysiological and binding studies (Lee & Tsien, 1983; Uehara & Hume, 1985; Glossmann *et al.*, 1985), at least three distinct classes of Ca^{2+} channel antagonist have been identified as follows: (1) the phenylalkylamines such as verapamil and D600; (2) the benzothiazepines such as diltiazem and (3) the 1,4-dihydropyridines (DHP) such as nifedipine and PN200-110. Many of these classical Ca^{2+} channel antagonists are widely used in the therapy of a number of cardiovascular diseases. In electrophysiological studies (Lee & Tsien, 1983; Uehara & Hume, 1985), the phenylalkylamines exhibit a strong use-dependent blockade of Ca^{2+} currents and the 1,4-dihydropyridines exert a predominantly tonic blockade. The benzothiazepines have an intermediate character.

SR33557 is a novel indolizinsulphone calcium antagonist, which is chemically unrelated to any of the three classes of Ca^{2+} antagonists. This compound possesses high affinity for a site in skeletal muscle (Schmid *et al.*, 1989; Sol-Rolland *et al.*, 1991), heart (Nokin *et al.*, 1990; Chatelain *et al.*, 1991) and brain membranes (Nokin *et al.*, 1989; Kenny *et al.*, 1993). SR33557 is a potent antagonist of both K^+- and noradrenaline-induced contraction in rat aorta (Nokin *et al.*, 1989) and inhibits L-type Ca^{2+} current in the rat aortic cell line A7r5 (Schmid *et al.*, 1989). Furthermore, Bois *et al.* (1991) reported that in skeletal muscle, SR33557 completely blocks the EC-coupling associated with the voltage-sensor activity of the DHP-sensitive Ca channel at very low concentrations (the 10 nM range), at which concentration a large component of L-type Ca^{2+} channel activity is preserved.

However, detailed studies of the inhibitory action of SR33557 on L-type Ca^{2+} current have not yet been performed. In the present study, we investigated the Ca^{2+} channel blocking effect of SR33557 from the standpoint of drug binding to different channel states in single rat ventricular myocytes.

Methods

Cell preparation

Single ventricular myocytes were obtained from the hearts of adult Sprague-Dawley rats (200–350 g) by enzymatic dissociation as described by Yazawa *et al.* (1990). The normal Tyrode solution used for cell isolation contained (mM): NaCl 140, KCl 5.4, $MgCl_2$ 0.5, $CaCl_2$ 1, HEPES 10, NaH_2PO_4 0.25, glucose 5.6 (pH = 7.3). Cells were stored in a KB-like solution containing (mM): KCH_3SO_3 108, K-phosphate 8, KCl 4, $MgSO_4$ 2.5, glucose 25, taurine 25, creatine 6, pyruvic acid 6 (pH = 7.3) at 4°C (Isenberg & Klockner, 1982). The single myocytes were Ca^{2+} tolerant in that they did not supercontract in the presence of 1 mM Ca^{2+}.

Electrophysiological measurement

Ca^{2+} currents were recorded by the whole-cell patch-clamp technique (Hamill *et al.*, 1981), and a Dagan 3900 amplifier (Dagan, Mineapolis, MN, U.S.A.). Cells were bathed in external solution containing (mM): NaCl 140, CsCl 3, $MgCl_2$ 0.5, $CaCl_2$ 1, HEPES 10, NaH_2PO_4 0.25, glucose 5.6, tetrodotoxin (TTX) 0.01 (pH = 7.3). Pipettes had resistances of 3 – 5 MΩ when filled with internal solution containing (mM): Cs-aspartate 120, CsCl 20, Na_2ATP 3, Na_2phosphocreatine 3, $MgCl_2$ 3.5, EGTA 10, $CaCl_2$ 0.65, HEPES 5 (pH = 7.3). TTX was used to block Na^+ current and intra-

[1] Author for correspondence.

and extracellular K^+ was replaced with Cs^+ to block K^+ currents. All electrophysiological experiments were performed at room temperature (21–23°C). Current signals were filtered at 2 kHz and sampled at 4 kHz. Data were analysed using an IBM-AT clone and pCLAMP software (Axon Instruments, Foster City, CA, U.S.A.). Amplitude of Ca^{2+} current was measured as the difference between the holding current and peak Ca^{2+} current. Under our experimental conditions, the holding current was minimal. All data were obtained from 36 cells. Cell capacitance and peak amplitude of Ca^{2+} current evoked by the pulse from − 50 mV to 0 mV under control conditions were 186.2 ± 4.1 pF and 935.3 ± 35.5 pA, respectively.

Statistics

Results are expressed as mean ± s.e.mean. In the recovery time constant experiment, time constants were computed for each cell at each potential. Data were analysed by the Friedman test to assess the significance of time constant differences at different potentials. In the first frequency-dependence experiment (Figure 7), data were analyzed in a manner analogous to the randomized complete block design. The blocking factor was cell. Treatment arrangement was a two-factor factorial design. The two factors were frequency (0.1, 0.33 and 1 Hz) and pulse number (2-15). Fisher's least significant difference was used for multiple comparison with Bonferroni adjustment for number of comparisons. In the second frequency-dependence experiment (Figure 8), the same analysis method was used. The two factors were pulse duration (30, 75 and 150 ms) and cumulative time of depolarization (150, 300 and 450 ms). All tests were assessed at the 0.05 level of significance.

Drugs

SR33557, ((2-isopropyl-1-((4-(3-(N-methyl-*N*-(3,4-dimethoxy-β-phenethyl)-amino)propyloxy) benzenesulphonyl))-indolizine was a generous gift from Sanofi-Pharma, Brussels, Belgium.

Results

Blocking of I_{Ca} by SR33557

Figure 1 shows the time course of the inhibitory action of the calcium current by SR33557 (10^{-7} M). Depolarizing pulses of 150 ms duration to 0 mV from the holding potential of − 50 mV were applied every 30 s. The application of SR33557 induced a substantial decrease in I_{Ca} and its effect reached a steady state after 6–7 min. At this point, the drug was washed out. However, the recovery of I_{Ca} was very small at this holding potential.

Figure 2 illustrates the current-voltage relationship (I–V curve) for I_{Ca} before and 7 min after application of 10^{-7} M SR33557. Cells were depolarized for 150 ms from the holding potential of − 50 mV to various potentials ranging from − 40 mV to + 50 mV every 10 s. Before this protocol was applied to the cell, it was depolarized from − 50 mV to 0 mV every 30 s. SR33557 did not affect the shape of the I–V curve; i.e., the threshold potential and the potential at which I_{Ca} was maximum remained unchanged.

Dose-response curves for the inhibitory action of SR33557 on I_{Ca} were obtained with two different holding potentials (V_h = − 50 and − 80 mV). I_{Ca} was elicited by depolarizing pulses of 150 ms to 0 mV every 30 s. As shown in Figure 3, at holding potentials of − 50 mV and − 80 mV, SR33557 reduced the peak I_{Ca} in a concentration-dependent manner. The IC_{50} value at $V_h = -50$ mV was estimated at 2.2×10^{-8} M. However, at $V_h = -80$ mV, 50% inhibition of the peak I_{Ca} could not be obtained even with 10^{-6} M drug. By extrapolating the line with the same regression function as at $V_h = -50$ mV, an IC_{50} value at − 80 mV was estimated at 9.0×10^{-6} M. These data suggest that SR33557 interacts with an inactivated state of the channel in preference to the rested state.

Effects on steady state availability of I_{Ca}

To clarify the voltage-dependent inhibitory action of SR33557, steady state inactivation curves of I_{Ca} were

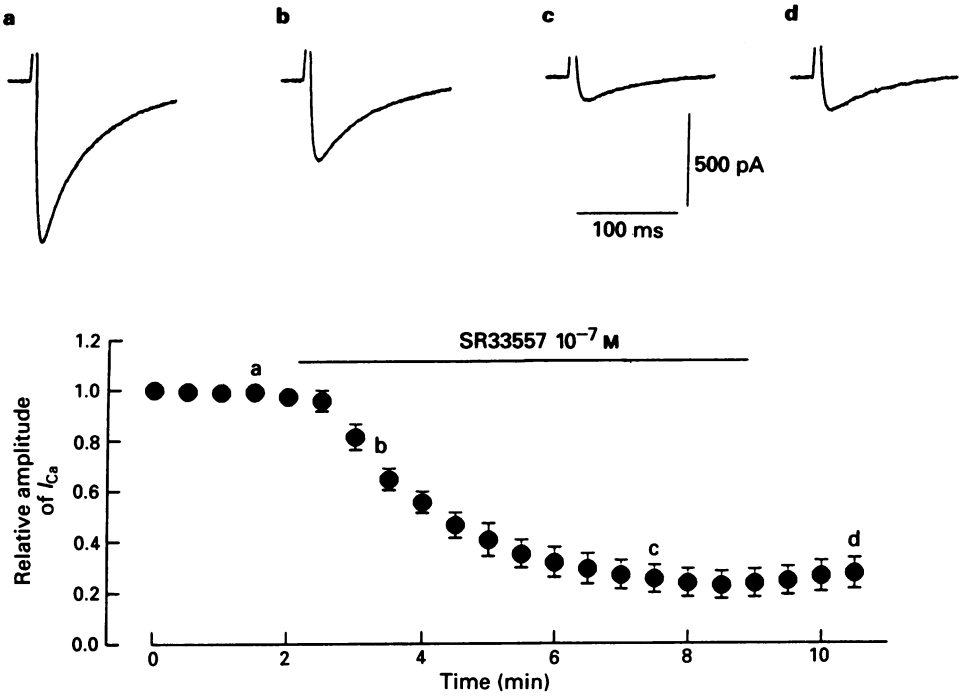


Figure 1 Time course of I_{Ca} inhibition by SR33557 (10^{-7} M). Cells were depolarized to 0 mV from the holding potential of − 50 mV for 150 s every 30 s. SR33557 was applied to the cell for 7 min and was washed out. At the top of the figure, current traces of I_{Ca} corresponding to the letters in the graph are shown (the myocyte had a capacitance of 183 pF, control peak I_{Ca} at 0 mV = 849 pA). Capacity compensation was not employed. Peak I_{Ca} in response to the first pulse in the control was taken as 1.0. The symbols and vertical bars indicate the mean and s.e.mean of four experiments, respectively.

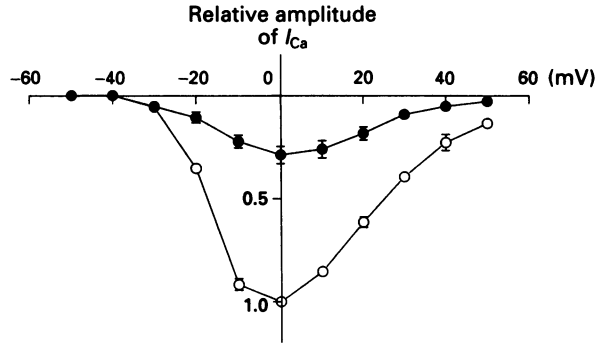


Figure 2 $I-V$ relationships of I_{Ca} before and after the application of SR33557. Pulses of 150 ms were applied from − 50 mV to various potentials ranging from − 40 mV to + 50 mV every 10 s. Before this protocol, the cells were depolarized from − 50 mV to 0 mV every 30 s; (○) control; (●) obtained 7 min after the application of 10^{-7} M SR33557. Peak amplitudes of I_{Ca} evoked by the pulse from − 50 mV to 0 mV in the control were normalized as 1.0. The symbols indicate the mean (with s.e.mean) of five experiments, respectively.

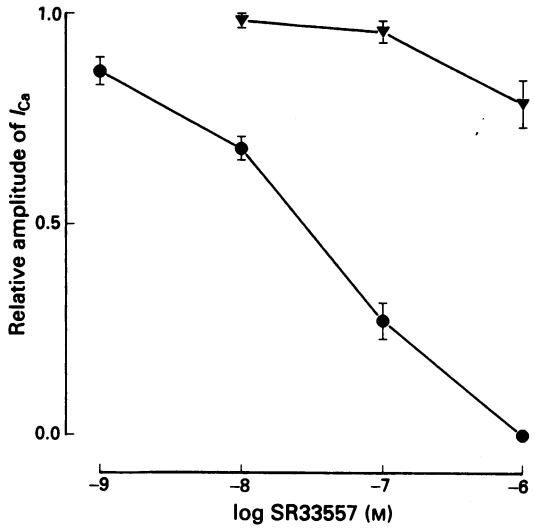


Figure 3 Relationships between the concentration of SR33557 and the relative amplitude of I_{Ca} activated from two different holding potentials (− 50 mV, ●; − 80 mV, ▲). I_{Ca} was elicited by a depolarizing pulse from the holding potential to 0 mV for 150 ms. The amplitude of I_{Ca} before the application of drug was normalized as 1.0. Each point indicates the mean ± s.e.mean of 5–6 experiments.

obtained before and after application of SR33557 using a two-pulse protocol (Figure 4a). A test pulse of 150 ms to 0 mV was preceded by a prepulse of either 5 s or 120 s duration to various potentials. The holding potential was set at − 80 mV. SR33557 (10^{-7} M) was used in the experiments, and at the holding potential of − 80 mV this concentration of SR33557 did not induce a significant inhibition of I_{Ca} without a prepulse (Figure 3). As shown in Figure 4b, SR33557 produced hyperpolarizing shifts in steady state inactivation curves. The mid points of the curves shifted by 3.4 mV (circles) and 10.0 mV (triangles), with 5 s and 120 s prepulses, respectively. Datyner & Cohen (1993) have reported slow inactivation of L-type Ca^{2+} current in Purkinje myocytes. In the absence of drug here, the steady state inactivation curve with 120 s prepulses was shifted (1.1 mV) to more negative potentials than seen with 5 s prepulses (Figure 4b); this may reflect a manifestation of slow inactivation of I_{Ca} in rat ventricular cells. A bigger shift of the curve by SR33557 with 120 s prepulses might be due to additional binding of SR33557 to inactivated channels produced by the slow inactivation mechanism. Another explanation for this phenomenon could be a slow binding rate of SR33557 to Ca^{2+} channels (see later). In either case, these findings further suggest that SR33557 possesses a high affinity for the inactivated state of the calcium channel.

Existence of tonic and use-dependent block

As shown in Figure 3, at a concentration of 10^{-7} M, SR33557 blocked I_{Ca} by about 75% when stimulated regularly (from − 50 mV to 0 mV every 30 s). However, in the absence of such regular stimulation a long (120 s) prepulse to − 50 mV induced only about 20% block of I_{Ca} with 10^{-7} M SR33557 (Figure 4). This difference suggested the existence of two components of the inhibitory action of SR33557 on I_{Ca}, one component (tonic) dependent on the holding potential and the other (use-dependent) manifest only with regular stimulation.

To examine tonic and use-dependent blockade of I_{Ca} by SR33557, depolarizing pulses of 150 ms from − 50 mV to 0 mV were applied every 30 s. Pulse application was interrupted and 10^{-7} M SR33557 was applied. Three minutes after drug application, pulses were restarted for 2 min to evoke the first series of I_{Ca} in the presence of drug, interrupted for 3 min, and restarted again to evoke the second series of I_{Ca}. As shown in Figure 5, the current amplitude was reduced (tonic block) to 88.0 ± 7.1% of control during the early 3 min exposure to SR33557 and inhibition increased progressively on repetition of the pulse, reaching 66.8 ± 8.3% for the

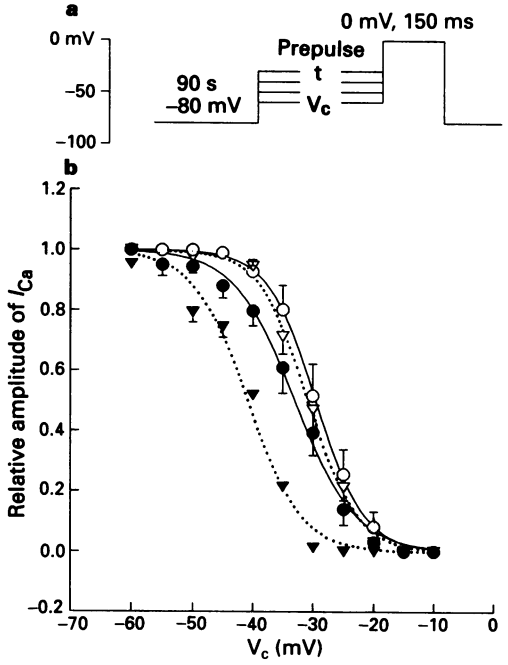


Figure 4 Effects of SR33557 on steady state inactivation curves of I_{Ca}. (a) Protocol: prepulses of 5 s or 120 s to various potentials (V_c) were followed by a 150 ms test pulse to 0 mV. Before each trial, the cell was clamped at − 80 mV for 90 s for unblocking. (b) Graph shows normalized plot of I_{Ca} in the absence (open symbols) and presence (filled symbols) of 10^{-7} M SR33557. The peak amplitudes of I_{Ca} evoked by the step pulse from − 80 mV to 0 mV in the control were normalized as 1.0. Each point indicates the mean ± s.e.mean of 3–5 cells. The mean data were fitted using the equation $y = 1/(1 + \exp(V_c - V_{0.5})/K)$ where V_c is the prepulse potential, $V_{0.5}$ is the mid point of steady state inactivation curve and K is the slope factor of the curve. In the 5 s prepulse experiments (circles), $V_{0.5} = -29.6$ mV, $K = 4.0$ for control; $V_{0.5} = -33.0$ mV, $K = 5.0$ for SR33557. In the 120 s prepulse experiment (triangles), $V_{0.5} = -30.7$ mV, $K = 4.0$ for control; $V_{0.5} = 40.7$ mV, $K = 4.5$ for SR33557. Experiments with 120 s prepulses were performed on different cells than those used for 5 s prepulses. Control values were always determined prior to drug application.

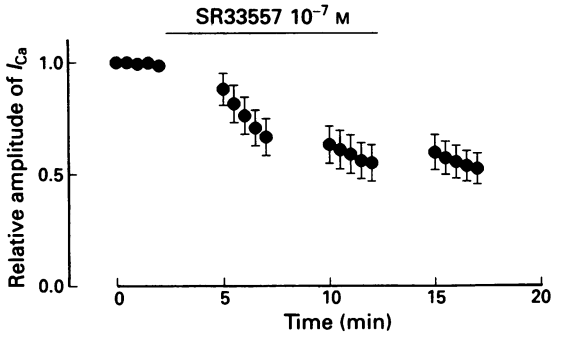


Figure 5 Existence of tonic and use-dependent block. A 150 ms pulse to 0 mV from the holding potential of − 50 mV was applied at 30 s intervals for 2 min and then 10^{-7} M SR33557 was added without application of pulses. Three min later, a train of pulses was applied twice with a 3 min quiescent period in between. Three min after wash-out of the drug, a train of pulses was applied again. The amplitude of I_{Ca} evoked by the pulse before application of the drug was normalized as 1.0. Each point indicates the mean ± s.e.mean from four experiments.

fifth I_{Ca} point. The current reduction in the second series of I_{Ca} during exposure to SR33557 developed to a greater extent, but in a similar manner to that in the first series of I_{Ca} (63.3 ± 8.4% to 55.0 ± 8.1%). These findings show that SR33557 blocks I_{Ca} in both a tonic and use-dependent fashion.

The time- and voltage-dependence of tonic block

We next studied the time- and voltage-dependence of tonic block. The holding potential was set to − 80 mV, changed to − 50 mV or − 40 mV for various durations (0.1, 0.3, 1, 3, 10, 30 and 100 s), and depolarized to 0 mV for 150 ms. SR33557, 10^{-7} M was used in the experiments. When cells were clamped at − 80 mV for 90 s before each protocol, I_{Ca} recovered almost completely from blockade. Control measurements showed no significant change in I_{Ca} when these procedures were followed in the absence of drug. The blockade of I_{Ca} by SR33557 increased as the duration of − 50 mV or − 40 mV holding potential was prolonged. The mean values of four experiments were fitted by the equation $y = 1\text{-}A \times (1\text{-}\exp(-t/\tau))$. τ and A indicate the time constant of tonic block and the final extent of block, respectively. At − 40 mV, τ and A were calculated as 41.9 ± 11.1 s and 0.68 ± 0.20, respectively. Since at − 50 mV the cells showed a much smaller decrease in I_{Ca}, too imprecise for data fitting of individual experiments, we used the mean values at each prepulse duration for fitting, which precluded statistical analysis. At − 50 mV, τ and A were 36.4 s and 0.16, respectively. Thus, at these potentials, the binding rates of SR33557 to Ca^{2+} channels were similar. The slow binding rate of SR33557 could explain why the shift of the mid point of steady-state inactivation curves with 5 s prepulses seen in Figure 4 was quite small.

The time- and voltage-dependence of unblock

The experimental protocol in Figure 6a was used to examine the dependence of recovery from conditioned block on time and membrane potential. Conditioned block was achieved by 15 depolarizing pulses (depolarization of 150 ms from − 50 mV to 0 mV at 0.33 Hz) leading to I_{Ca} (c15), in the presence of 10^{-7} M SR33557. Clamping at − 80 mV for 90 s before each protocol allowed almost complete recovery of I_{Ca} from blockade. The amplitude of I_{Ca} restored by the test unblocking pulse, I_{Ca} (test)-I_{Ca} (c15), was compared with the reference I_{Ca} restored by a 90 s, − 80 mV prepulse, i.e. I_{Ca} (ref)-I_{Ca} (c15). The fraction of I_{Ca} restored by unblock is

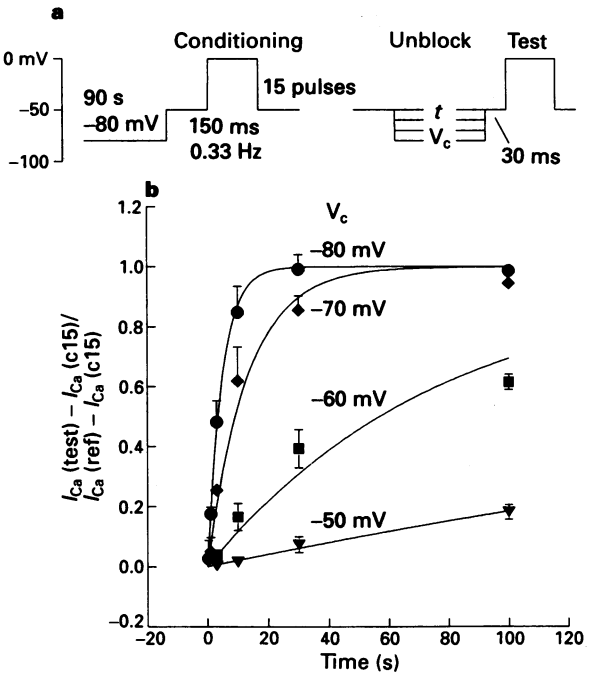


Figure 6 Dependence of the recovery from I_{Ca} block by SR33557 on time and membrane potential. (a) Protocol: Cells were pretreated with 10^{-7} M SR33557. Before each trial, membrane potential was held at − 80 mV for 90 s to restore I_{Ca}. Block was then induced by 15 pulses (150 ms pulses from − 50 mV to 0 mV at 0.33 Hz). After 3 s at − 50 mV, a subsequent unblocking pulse (to potential V_c for duration t) was applied and followed after 30 ms at − 50 mV by a 150 ms test pulse to 0 mV. (b) I_{Ca} restored by an unblocking pulse, I_{Ca} (test), was normalized with respect to I_{Ca} restored by the reference unblock (at − 80 mV for 90 s), I_{Ca} (ref), which was the first of the fifteen conditioning pulses. The fraction of I_{Ca} restored by an unblocking pulse, $[I_{Ca}\text{ (test)} - I_{Ca}\text{ (c15)}]/[I_{Ca}\text{ (ref)} - I_{Ca}\text{ (c15)}]$ was plotted as a function of the duration of an unblocking pulse, where I_{Ca} (c15) was the 15th of the conditioning pulses. V_c: (●) − 80 mV; (◆) − 70 mV; (■) − 60 mV; (▼) − 50 mV. This protocol was performed in three cells and the data of all unblocking pulses (at − 80, − 70, − 60 and − 50 mV) were obtained from each cell. The symbols show the mean and s.e.mean. Curves are drawn according to $A \times (1 - \exp(-t/\tau))$; at $V_c = -80$ mV, $\tau = 5.2 \pm 1.2$ s, A = 1.0; at $V_c = -70$ mV, $\tau = 13.2 \pm 4.1$ s, A = 1.0; at $V_c = -60$ mV, $\tau = 76.7 \pm 13.3$ s, A = 0.95; at $V_c = -50$ mV, $\tau = 400.8 \pm 68.2$ s, A = 0.8. The mean values of τ were used for curve fitting.

plotted against the duration of the unblocking pulse in Figure 6b. There was complete recovery at potentials more negative than − 60 mV, the rate of recovery being faster the more negative the unblocking voltage. Fitting with a single time constant, that time constant of recovery was 5.2 ± 1.2 s and 13.2 ± 4.1 s, at − 80 mV and − 70 mV, respectively ($n = 3$). Assuming that the recovery was 95% and 80% at the unblocking voltage of − 60 mV and − 50 mV (steady state in Figure 4), the time constant increased further to 76.7 ± 13.3 s at − 60 mV and 400.8 ± 68.2 s at − 50 mV ($n = 3$). The time constants at all potentials are significantly different from each other. This finding shows that the time course of recovery from block is faster at more negative potentials.

Frequency-dependence of block

Use-dependent block can be due to exposure of drug to open states of the channel, or to inactivated states of the channel, or both. Previous data (Figures 3 and 4) suggested drug interaction with inactivated states. To determine the association of drug with open channels, we varied the number of openings per unit time and the duration of each depolarization.

We first varied the number of openings per unit time. Cells were clamped at − 80 mV for 90 s to unblock the channels before each trial. In each trial, fifteen 150 ms pulses from − 50 mV to 0 mV were applied at various frequencies (0.1, 0.33 and 1 Hz). Since the time allowed for tonic block was short, the first pulse did not show any apparent block I_{Ca} at 10^{-7} M SR33557. As shown in Figure 7a, the amplitude of I_{Ca} decreased progressively with repeated depolarization in the presence of drug (filled symbols). At 1 Hz, a decrease of I_{Ca} also appeared in the control (open squares). To assess the frequency-dependence of blockade of I_{Ca} precisely, the amplitude of I_{Ca} at each frequency was compared in the presence and absence of drug, and the relative values obtained from three experiments were plotted as a function of pulse number (Figure 7b). At the three frequencies blockade of I_{Ca} did not display statistically significant differences. The rate-dependence instead comes from a direct relation between channel block and number of openings.

The next experiment was designed to investigate whether block is related to the duration of the conditioning pulse. Before each trial, cells were clamped at − 80 mV for 90 s to restore I_{Ca}. Sixteen depolarizing pulses from − 50 mV to 0 mV were applied for 30, 75 or 150 ms, at 1, 0.4 or 0.2 Hz, respectively. Under these conditions the total amount of time spent depolarized was the same with each protocol, and so was the total amount of time spent at the holding potential. Data obtained from one cell in the presence and absence of 10^{-7} M SR33557 are shown in Figure 8a. The dependence of [I_{Ca} (drug)/I_{Ca} (cont)] on the number of pulses is plotted in Figure 8b. These data were obtained from four cells. Block

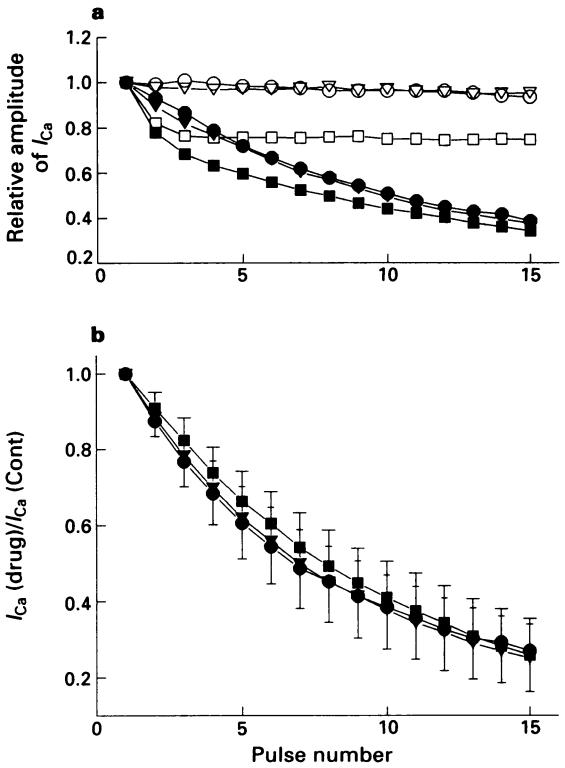


Figure 7 Dependence of I_{Ca} block by SR33557 on the rate of stimulation. Fifteen 150 ms pulses from − 50 mV to 0 mV were delivered at 0.1 (circles), 0.33 (triangles) and 1 Hz (squares) before (open symbols) and after application of 10^{-7} M SR33557 (filled symbols). The cell was clamped at − 80 mV for 90 s to restore I_{Ca} from block before each trial. (a) I_{Ca} decrease, during stimulation. The amplitude of the first I_{Ca} elicited by a train of pulses in the control was normalized as 1.0. Data shown were obtained from one cell (153 pF, control I_{Ca} = 820 pA). (b) The relative value of I_{Ca} in the presence of drug normalized against I_{Ca} in the control for each pulse number was plotted as a function of pulse number. Each point indicates the mean ± s.e.mean obtained from three experiments.

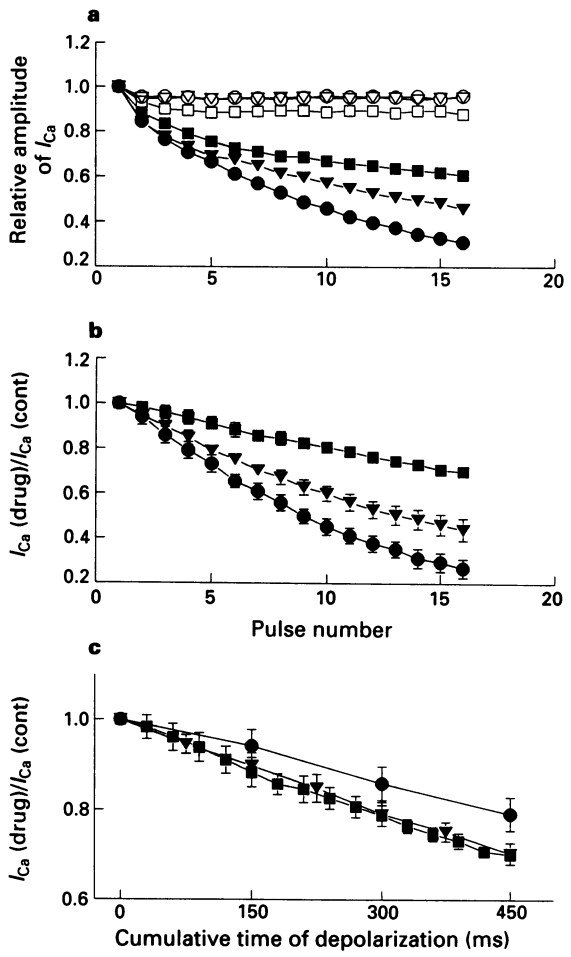


Figure 8 Dependence of I_{Ca} block by SR33557 on the duration of the conditioning pulse. Sixteen pulses from − 50 mV to 0 mV were applied for 30 ms at 1 Hz (squares), for 75 ms at 0.4 Hz (triangles) and for 150 ms at 0.2 Hz (circles) in the absence (open symbols) and the presence of 10^{-7} M SR33557 (filled symbols). Each trial was followed by an unblocking pulse (for 90 s at − 80 mV). (a) I_{Ca} decrease during stimulation. The amplitude of the first I_{Ca} of a train of pulses in control was normalized as 1.0. Data shown were obtained from one cell (189 pF, control I_{Ca} = 830 pA). (b) The relative value of I_{Ca} in the presence of drug normalized against I_{Ca} in the control for each pulse number was plotted as a function of pulse number. (c) The decay of I_{Ca} as a function of cumulative time of test pulse depolarization. Each point indicate the mean ± s.e.mean obtained from four experiments (b,c).

was pulse dependent at each pulse duration but the blocking effectiveness of pulses increased with pulse duration. In Figure 8c, I_{Ca} (drug)/I_{Ca} (cont) was plotted against cumulative time of test pulse depolarization. Although there is no statistical difference between pulse duration (30, 75 and 150 ms) and cumulative time of depolarization (150, 300 and 450 ms), the two shorter pulses tend to block I_{Ca} more effectively than 150 ms pulses. For example, at cumulative time of 450 ms, I_{Ca} evoked by 30, 75 and 150 pulse duration trains was 70.0 ± 1.3, 70.4 ± 2.4 and 79.1 ± 3.7% (vs control), respectively. With short pulses, channels reside proportionately longer in open states, with longer pulses progressively longer in inactivated states. These results suggest that SR33557 binds not only to inactivated channels (Figures 3 and 4) but also to open channels with similar high affinity and relatively slow kinetics.

Discussion

It has been reported that in rat heart sarcolemmal membrane, SR33557 binds with high affinity to a novel binding site

associated with the L-type calcium channel and has a strong negative allosteric interaction with the binding site for 1,4-dihydropyridines (PN200-110), phenylalkylamines (D888) and benzothiazepines (diltiazem) (Nokin *et al.*, 1990; Chatelain *et al.*, 1991). These findings are in agreement with data from studies in guinea-pig cerebal membrane (Nokin *et al.*, 1989) and in rabbit skeletal muscle (Schmid *et al.*, 1989).

The present study demonstrates that SR33557 inhibits Ca^{2+} current in rat single ventricular cells. SR33557 exerted voltage- and frequency-dependent blockade of I_{Ca}. The inhibitory effects of various Ca antagonists on myocardial Ca^{2+} channels may be explained according to the modulated receptor hypothesis (Hondeghem & Katzung, 1977; Hille, 1977a,b) which postulates that drug affinity for the Ca^{2+} channel is modulated by channel state (rested, open, inactivated state). In these experiments, SR33557 produced tonic block (Figures 4 and 5, holding potential of -50 mV), i.e. block of Ca^{2+} channels in the absence of stimulation. However, 10^{-7} M SR33557 induced tonic block at -50 mV, but did not reduce I_{Ca} elicited by 150 ms depolarizing pulses from a holding potential of -80 mV to 0 mV at 30 s intervals. These phenomena can be explained by the faster unbinding rates of SR33557 from channels at more negative potentials (-80 mV, 5.2 ± 1.2 s; -70 mV, 13.2 ± 4.1 s; -60 mV, 76.8 ± 13.3 s; -50 mV, 400.8 ± 68.2 s; Figure 6) and the binding rates of SR33557 (-50 mV, 36.4 s). These findings also suggest that SR33557 binds to inactivated channels more than to resting channels. The shift of the steady state inactivation curve in the negative direction also shows that SR33557 binds to the inactivated state. According to Bean *et al.* (1983) and Sanguinetti & Kass (1984), the dissociation constant for SR33557 binding to the inactivated channels (K_i) can be calculated from the equation:

$$\Delta V_{0.5} = K \times \ln(1 + [D]/K_i)/(1 + [D]/K_r),$$

where $\Delta V_{0.5}$ and K are the shift in the midpoint of the steady state inactivation curve and the slope factor of the curve, respectively, [D] is the concentration of SR33557, and K_r is the dissociation constant for SR33557 binding to the rested state channels. K_r was estimated at 9.0×10^{-6} M (Figure 3). In Figure 4, $\Delta V_{0.5}$ and K were 10.0 mV and 4.25 (mean value of curves), respectively, with 10^{-7} M SR33557 in the 120 s prepulse experiment. K_i is calculated to be 1.04×10^{-8} M, suggesting that binding to inactivated channels is about 865 times tighter than to resting channels.

The blockade of I_{Ca} by SR33557 was also frequency-dependent. The rate of blocking depended on the number of pulses applied. However, blocking rate was likely to be proportional to the cumulative time of depolarization. If inactivated state binding is more dominant than open state binding in drug-channel interaction, short pulse trains delivered at high frequency would be less effective than long pulse trains delivered at lower frequency. Although the effect was not statistically significant, short pulse trains (30 and 75 ms) were slightly more effective than a 150 ms long pulse train (Figure 8). Therefore, these findings suggest that SR33557 interacts with the open state as well as the inactivated state (c.f. McDonald *et al.*, 1984, Figure 9).

In the modulated receptor theory, neutral and 'lipid-soluble drug forms are thought to come and go from the receptor via a hydrophobic region of the membrane, while charged and less lipid-soluble forms pass via a hydrophilic region. The hydrophilic pathway is open only when the gates of the channel are open' (Hille, 1977b). As the pK_a value of SR33557 is 8.7 (Chatelain *et al.*, 1992) and the drug is predominantly charged at pH 7.3 in the external solution, use-dependent block of I_{Ca} is produced by SR33557. SR33557 also exhibits tonic block of I_{Ca}. The inhibitory action of I_{Ca} by SR33557 was more similar to that of diltiazem rather than D-600, which shows use-dependent block but no tonic block (Lee & Tsien, 1983; McDonald *et al.*, 1984; Uehara & Hume, 1985). Tonic block by SR33557 might be induced by the relatively high lipid solubility of SR33557 itself (Chatelain *et al.*, 1992). Even after washing it out at $V_h = -80$ mV, subsequent application of pulses from $V_h = -50$ mV revealed the presence of significant residual drug (result not shown).

We thank Tatsuo Uchida (Biostatistician, Office of Biostatistics, UTMB) for analysing the experimental data statistically. This work was supported by HL42527 (P.P) and a grant-in-aid from the American Heart Association to Dr Sandor Györke, whose generous support and comments on the manuscript are gratefully acknowledged. K.Y. was supported by an international fellowship of the Japanese Heart Foundation.

References

BEAN, B.P., COHEN, C.J. & TSIEN, R.W. (1983). Lidocaine block of cardiac sodium channels. *J. Gen. Physiol.*, **81**, 613–642.

BOIS, P., ROMEY, G. & LAZDUNSKI, M. (1991). Indolizinsulphones. A class of blockers with dual discriminative effects on L-type Ca^{2+} channel activity and excitation-contraction coupling in skeletal muscle. *Pflügers Arch.*, **419**, 651–656.

CHATELAIN, P., BEAUFORT, P., MEYSMANS, L. & CLINET, M. (1991). Characterization of the slow calcium channel binding sites for [^{3}H] SR33557 in rat sarcolemmal membranes. *Mol. Pharmacol.*, **39**, 64–71.

CHATELAIN, P., MATTEAZZI, J.R. & LARUEL, R. (1992). Fluorescent studies on the interaction between a novel Ca^{2+} antagonist, SR33557, and membrane lipids. *Biochem. Pharmacol.*, **43**, 1513–1520.

DATYNER, N.B. & COHEN, I.S. (1993). Slow inactivation of L-type calcium current distorts the measurement of L- and T-type calcium current in Purkinje myocytes. *J. Gen. Physiol.*, **102**, 859–869.

GLOSSMANN, H., FERRY, D.R., GOLL, A., STRIESSNIG, J. & ZERNIG, G. (1985). Calcium channels and calcium channel drugs: recent biochemical and biophysical findings. *Arzneim. Forsch./Drug Res.*, **35**, 1917–1935.

HAMILL, O.P., MARTY, A., NEHER, E., SAKMANN, B. & SIGWORTH, F.J. (1981). Improved patch-clamp techniques for high-resolution current recording from cells and cell-free membrane patches. *Pflügers Arch.*, **391**, 85–100.

HILLE, B. (1977a). The pH-dependent rate of action of local anesthetics on the node of ranvier. *J. Gen. Physiol.*, **69**, 475–496.

HILLE, B. (1977b). Local anesthetics: hydrophilic and hydrophobic pathways for the drug receptor reaction. *J. Gen. Physiol.*, **69**, 497–515.

HONDEGHEM, L.M. & KATZUNG, B.G. (1977). Time- and voltage-dependent interactions of antiarrhythmic drugs with cardiac sodium channels. *Biochim. Biophys. Acta*, **472**, 373–398.

ISENBERG, G. & KLOCKNER, U. (1982). Calcium tolerant ventricular myocytes prepared by preincubation in a 'KB medium'. *Pflügers Arch.*, **395**, 6–18.

KENNY, B.A., FRASER, S. & SPEDDING, M. (1993). Identification of a novel calcium antagonist binding site in rat brain by SR33557. *Br. J. Pharmacol.*, **108**, 93–99.

LEE, K.S. & TSIEN, R.W. (1983). Mechanism of calcium channel blockade by verapamil, D-600, diltiazem and nitrendipine in single dialyzed heart cells. *Nature*, **302**, 790–794.

MCDONALD, T.F., PELZER, D. & TRAUTWEIN, W. (1984). Cat ventricular muscle treated with D600: Characteristics of calcium channel block and unblock. *J. Physiol.*, **352**, 217–241.

NOKIN, P., CLINET, M., POLSTER, P., BEAUFORT, P., MEYSMANS, L., GOUGAT, J. & CHATELAIN, P. (1989). SR33557, a novel calcium-antagonist: interaction with [^{3}H]-(±)-nitrendipine and [^{3}H]-(−)-desmethoxy-verapamil binding sites in cerebral membranes. *Naunyn-Schmied. Arch. Pharmacol.*, **339**, 31–36.

NOKIN, P., CLINET, M., BEAUFORT, P., MEYSMANS, L., LARUEL, R. & CHATELAIN, P. (1990). SR33557, a novel calcium blocker. II. Interaction with 1,4-dihydropyridine, phenylalkylamine and benzothiazepine binding sites in rat heart sarcolemmal membrane. *J. Pharmacol. Exp. Ther.*, **255**, 600–607.

SANGUINETTI, M.C. & KASS, R.S. (1984). Voltage-dependent block of calcium channel current in the calf cardiac Purkinje fiber by dihydropyridine calcium channel antagonists. *Circ. Res.*, **55**, 336–348.

SCHMID, A., ROMEY, G., BARHANIN, J. & LAZDUNSKI, M. (1989). SR33557, an indolizinsulfone blocker of Ca^{2+} channels: identification of receptor sites and analysis of its mode of action. *Mol. Pharmacol.*, **35**, 766–773.

SOL-ROLLAND, J., JOSEPH, M. & RINALDI-CARMONA, M. (1991). Interaction of SR33557 with skeletal muscle calcium channel blocker receptors in the baboon: Characterization of its binding sites. *J. Pharmacol. Exp. Ther.*, **257**, 595–602.

UEHARA, A. & HUME, J.R. (1985). Interactions of organic calcium channel antagonists with calcium channels in single frog atrial cells. *J. Gen. Physiol.*, **85**, 621–647.

YAZAWA, K., KAIBARA, M., OHARA, M. & KAMEYAMA, M. (1990). An improved method for isolating cardiac myocytes useful for patch-clamp studies. *Jpn. J. Physiol.*, **40**, 157–163.

(Received March 31, 1994
Revised July 20, 1994
Accepted September 20, 1994)

British Journal of Pharmacology (1995) 114, 475–481 © 1995 Stockton Press All rights reserved 0007–1188/95 $9.00

Pharmacological and biochemical analysis of FPL 67156, a novel, selective inhibitor of ecto-ATPase

B.E. Crack, C.E. Pollard, †M.W. Beukers, S.M. Roberts, *S.F. Hunt, *A.H. Ingall, K.C.W. McKechnie, †A.P. IJzerman & [1]P. Leff

Department of Pharmacology, Fisons R&D Labs, Bakewell Road, Loughborough, Leicestershire LE11 0RH; *Department of Medicinal Chemistry, Fisons R&D Labs, Bakewell Road, Loughborough, Leicestershire LE11 0RH and †Division of Medicinal Chemistry, LACDR, Leiden, The Netherlands

1 FPL 67156 (6-N,N-diethyl-β,γ-dibromomethylene-D-ATP), is a newly synthesized analogue of ATP.

2 In a rabbit isolated tracheal epithelium preparation, measuring P_{2U}-purinoceptor-dependent chloride secretion, FPL 67156 was discovered to potentiate the responses to UTP but not those to ATP-γ-S. UTP agonist-concentration effect (E/[A]) curves were shifted to the left by 5-fold in the presence of 100 μM FPL 67156. The differential effect of FPL 67156 on UTP and ATP-γ-S was hypothesized to be due to the greater susceptibility of UTP to enzymatic dephosphorylation and the ability of FPL 67156 to inhibit this process.

3 FPL 67156 was tested as an ecto-ATPase inhibitor in a human blood cell assay, measuring [γ^{32}P]-ATP dephosphorylation. The compound inhibited [γ^{32}P]-ATP degradation with a pIC_{50} of 4.6.

4 FPL 67156 was then tested for its effects on ATP and α,β-methylene-ATP responses at P_{2X}-purinoceptors in the rabbit isolated ear artery. In the concentration range 30 μM–1 mM, the compound potentiated the contractile effects of ATP but not those of α,β-methylene-ATP. At 1 mM, FPL 67156 produced a 34-fold leftward shift of ATP E/[A] curves.

5 The effects of FPL 67156 on ATP E/[A] curves in the rabbit ear artery were analysed using a theoretical model (Furchgott, 1972) describing the action of an enzyme inhibitor on the effects of a metabolically unstable agonist. This analysis provided an estimate of the pK_I for FPL 67156 as an ecto-ATPase inhibitor of 5.2.

6 Using appropriate assays, FPL 67156 was shown to have weak antagonist effects at P_{2X}- and P_{2T}-purinoceptors ($pA_2 \approx 3.3$ and 3.5 respectively), and weak agonist effects at P_{2U}-purinoceptors ($p[A_{50}] \approx 3.5$).

7 The degree of potentiation of ATP and UTP effects elicited by FPL 67156 confirms previous results concerning the influence that ecto-ATPase has on the position of E/[A] curves for metabolically unstable agonists. The magnitude of this influence is predicted to have a major effect on the agonist potency orders currently used to designate purinoceptors.

8 This study indicates FPL 67156 to be a potentially valuable probe in studies on the action of nucleotides and in the classification of purinoceptors.

Keywords: FPL 67156; P_{2X}-purinoceptors; P_{2U}-purinoceptors; ATP; ecto-ATPase; enzyme inhibition; agonist potency orders; receptor classification

Introduction

A well-recognised problem in the pharmacological classification of receptors is the susceptibility of natural agonists and synthetic analogues to enzymatic degradation by the assay tissues used. Of particular concern is the effect that metabolic processes have on the measured potency of agonists. In quantitative terms, this can be a substantial influence. For example, the potency of acetylcholine in chick smooth muscle is reduced by some 1000-fold due to acetylcholinesterase activity (Green *et al.*, 1978). Uptake and metabolism of noradrenaline by the guinea-pig trachea decreases the potency of this agonist by 30-fold (Foster, 1967). In the same tissue, the potency of adenosine is reduced by 350-fold due to the presence of adenosine deaminase (Satchell, 1984). Clearly, such displacement of agonist-concentration effect (E/[A]) curves from their 'true' positions is of major concern when considering agonist potency orders. For example, in the guinea-pig trachea, under conditions when enzymatic degradation operates, salbutamol is some 20 fold more potent than noradrenaline whereas, when degradation is blocked, the two agonists have indistinguishable potency (Kenakin, 1980).

In the case of nucleotide agonists, mechanisms for their enzymatic dephosphorylation have been well-demonstrated and characterized (Welford *et al.*, 1986; 1987), although evidence for the influence of these on the pharmacological potency of agonists has been limited (Welford *et al.*, 1987). However, a recent study conducted in our laboratory (Crack *et al.*, 1994) indicated that the measured potency of ATP at P_{2X}-purinoceptors in the rabbit isolated ear artery is reduced by some 400-fold by the operation of ecto-ATPase in that tissue. Moreover, when the potency of ATP is adjusted to reflect its true value, its position, relative to metabolically stable agonists such as α,β-methylene-ATP, changes dramatically. This result led us to suggest that the agonist potency order currently accepted to define P_{2X}-purinoceptors may need to be reconsidered. Importantly, that study was conducted without the benefit of a selective ecto-ATPase inhibitor. This is unlike those quoted above in relation to other receptor systems where substances like physostigmine, cocaine and dipyridamole were available to block the metabolic or transport processes concerned and quantify the associated changes in potency.

In the present paper we describe the discovery of FPL 67156, a novel ATP analogue synthesized at Fisons. Biochemical and pharmacological analyses of this compound

[1] Author for correspondence.

are described which indicate it to be a selective inhibitor of ecto-ATPase suitable for use in resolving the kinds of agonist potency and receptor classification issues described above. The results of this study extend and confirm our previous paper (Crack *et al.*, 1994) as regards the influence of ecto-ATPase on agonist potency and, in turn, on purinoceptor classification.

Methods

Rabbit ear artery

Male New Zealand White rabbits weighing 2–3.5 kg were killed with an overdose of pentobarbitone sodium (Euthatal) into the marginal ear vein. The ears were removed and the central ear artery located at the base of the ears. A small section of the artery was cleared of connective tissue and an incision was made to allow the insertion of a nylon cannula (external diameter 0.75 mm). The cannula was lightly scored with a scalpel blade prior to insertion into the vessel, to remove the vessel endothelium. The artery, mounted on the cannular, was then dissected from the ear, cleared of connective tissue and cut into 5 mm rings. These were mounted horizontally over tungsten wire hooks (0.25 mm diameter) in 10 ml organ baths. The lower hook was attached to a stationary support in the organ bath and the upper hook was connected to an Ormed transducer for recording changes in isometric force. Tissues were bathed in Krebs buffer (pH 7.4) of the following composition (mM): NaCl 117.6, NaH_2PO_4 0.9, $NaHCO_3$ 25.0, $MgSO_4$ 1.2, glucose 11.1, KCl 5.4 and $CaCl_2$ 2.6. The tissues were maintained at 37°C and gassed continuously with 95% O_2/5% CO_2. The Krebs solution also contained indomethacin (2.8 μM) to prevent the formation of cyclo-oxygenase products and 8-sulphophenyltheophylline (8-SPT) (300 μM) to exclude the possible influence of P_1-purinoceptor activation.

The tissues were subjected to an initial force of 1.0 g then allowed to equilibrate for a minimum of 1 h, during which time the force was adjusted to achieve a final value of 0.5–1.0 g. The tissues were then washed by exchange of the bath solution. Tissue viability was assessed by treatment with KCl (80 mM). Only those tissues producing an increase in force of 0.5 g or more were included in the study. The functional state of the endothelium was tested by subsequent addition of acetylcholine (1 μM). In these studies, the vasorelaxation response to acetylcholine was invariably less than 17% of the KCl-induced contraction. Tissues were then washed and allowed to re-equilibrate for 45 min.

Experimental protocols A paired curve design was adopted in which all tissues were initially treated with cumulative additions of ATP or α,β-methylene-ATP at 0.5 $\log_{10}$ unit intervals. Following washout and re-equilibration, FPL 67156 was applied for 45 min, then a second cumulative agonist-concentration effect (E/[A]) curve was constructed. Contractile effects were expressed as percentages of the first curve maximum.

Rabbit isolated epithelium

Male New Zealand White rabbits (2.5–4.0 kg) were killed with an overdose of pentobarbitone sodium (Euthatal) into the marginal ear vein. The thorax was opened and the trachea removed and placed in gassed Krebs solution of the following composition (mM): NaCl 117.6, KCl 5.4, $CaCl_2$ 2.6, $MgSO_4$ 1.2, $NaHCO_3$ 24.9, NaH_2PO_4 1.2 and glucose 11.1. Dissections were carried out at room temperature. The trachea was divided transversely into two segments. Each segment was opened along the posterior membrane, pinned flat, and bathed in gassed Krebs during the dissection. The epithelial sheet was dissected away from the underlying cartilaginous tissue and mounted in a Ussing chamber with an aperture of 0.64 cm^2. Both surfaces of the epithelial sheet were bathed with 10 ml of Krebs buffer warmed to 37°C and gassed with 95% O_2/5% CO_2 (pH 7.4) which also served to circulate the buffer using a gas-lift system.

Electrophysiological recordings The Ussing chamber was connected to a voltage clamp unit (DVC1000, World Precision Instruments Inc., Connecticut, U.S.A.) via 3 M KCl-4% agar bridges connected to silver-silver chloride electrodes. The trans-epithelial potential difference (V_t) was measured by electrodes sited close to the tissue surface and held at a value of 0 mV by passing current (the so called 'short circuit current' (I_{sc})) through the tissue via current electrodes. Under these conditions, where there is no concentration or electrical gradient for passive ion movement, only active ion transport will be measured. The contribution of fluid resistance to I_{sc} was corrected automatically.

Isolation of chloride transport pathway Preliminary experiments showed that the two major active transport processes in rabbit tracheal epithelium are sodium absorption and chloride secretion. In order to isolate the chloride secretion pathway, the Krebs bathing the apical surface of the tissue always contained amiloride (100 μM). To confirm that the residual I_{sc} was due largely to chloride secretion, bumetanide (100 μM) was added to the basolateral surface of the tissue to inhibit the cotransport process which accumulates chloride ions within the epithelial cells. This decreased I_{sc} from 48.5 ± 2.7 to 6.5 ± 2.4 μA cm^{-2} (s.e., $n = 3$). Furthermore, when low chloride Krebs (Na isethionate substituting for NaCl) rather than normal Krebs was used to bathe both sides of amiloride treated tissues, I_{sc} fell from 52.7 ± 5.6 to 9.6 ± 2.7 μA cm^{-2} (s.e., $n = 6$).

Experimental protocols When the baseline I_{sc} of each tissue was stable, ATP (30 μM) was added to the apical side of the tissue to establish viability. Once this response had reached a plateau, both the apical and basolateral sides of the system were drained and each side washed with 10 ml of Krebs. The basolateral side was then refilled with 10 ml of Krebs and the apical side with 10 ml of Krebs containing amiloride (100 μM). This washing and refilling procedure was used after each of the subsequent E/[A] curves which were time matched and constructed by cumulative addition of agonist in 0.5 $\log_{10}$ unit increments. Two consecutive E/[A] curves to ATP were obtained in each tissue. Then, following 5 min exposure of FPL 67156 (100 μM) or vehicle to the apical side, an E/[A] curve to UTP or ATP-γ-S was constructed. Preliminary experiments had shown that consecutive curves to UTP were not sufficiently reproducible to permit a paired curve design, so treatment and control E/[A] curves were obtained in different tissues in this preparation.

Ecto-ATPase assay

Human blood was obtained by venepuncture from healthy volunteers, heparinized then centrifuged (2000 *g*, 10 min). Plasma was removed, care being taken not to disturb the buffy coat. The remaining cells were washed twice with buffer of composition (mM) Tris 20, glucose 5, NaCl 140, KCl 5, adjusted with HCl to pH 7.4, 20°C. The cell suspensions were then diluted 7 fold with buffer.

[γ^{32}P]-ATP assays were carried out at 37°C in a shaking water bath. The total incubation volume was 200 μl, of which the added volume of cells was 75 μl. The incubation medium contained, in addition to buffer, NaN_3 (5.0 mM) and $CaCl_2$ (0.5 mM). The substrate concentration of ATP was 10 μM containing 80,000–90,000 d.p.m. [γ^{32}P]-ATP. This concentration was near the K_M determined in previous studies (Beukers *et al.*, 1993). FPL 67156 was added to achieve final concentrations in the range 0.1–1000 μM. Inhibitory effects were measured as percentages of degradation of 10 μM ATP in the absence of drugs, over a period of 30 min.

Incubations were terminated by addition of activated charcoal (400 µl of 40 mg ml^{-1} charcoal in 0.1 N HCl), then centrifugation (6500 *g*, 2 min). Supernatant samples of 350 µl were homogenized with 4 ml emulsifier (Emulsifier Safe, Packard) and radioactivity was counted in an LKB-Wallace 1214 Rackbeta Excel Spectrometer. Controls, without cells, were processed identically.

Drugs and materials

Acetylcholine bromide, adenosine 5'-triphosphate [disodium salt] (ATP), uridine 5'-triphosphate [disodium salt] (UTP), α,β-methylene ATP [dithidium salt], amiloride hydrochloride, bumetanide, dimethyl sulphoxide (DMSO) were obtained from the Sigma Chemical Co., Poole, U.K.; FPL 67156 (tetrasodium salt) was synthesized in the Medicinal Chemistry Department, Fisons by S.F. Hunt; 8(*p*-sulphophenyl)-theophylline (8-SPT), 2-methylthio-ATP [tetrasodium salt] were supplied by Research Biochemicals Inc., St. Albans, U.K.; adenosine-5'-O-(3-thiophosphate) (ATP-γ-S) [tetrasodium salt] was obtained from Boehringer Mannheim, Lewes, U.K.; activated charcoal, particle size 4–7 µm was supplied by Serva, Heidelberg, Germany; ATP (for ecto-ATPase studies) was obtained from Aldrich Chemie, Steinheim, Germany; [γ^{32}P]-ATP was from Amersham, U.K.

For rabbit ear artery experiments, ATP, FPL 67156 and 8-SPT were dissolved in distilled water. Indomethacin was prepared as a 28 mM solution in Na_2CO_3 (0.35 M) and subsequently diluted in Krebs solution.

For experiments in the rabbit epithelium, nucleotides were made up as stock solutions in normal Krebs solution. Amiloride hydrochloride was prepared as a 100 mM stock in DMSO and diluted in Krebs to give a final concentration of 100 µM. Bumetanide was prepared as a 100 mM stock in DMSO and 10 µl was added to the basolateral side of the chamber to give a final concentration of 100 µM.

Analysis of E/[A] curve data

Agonist concentration effect (E/[A]) data were fitted to the logistic function:

$$E = \frac{\alpha[A]^m}{[A_{50}]^m + [A]^m} \quad (i)$$

in which α, $[A_{50}]$ and m are respectively the asymptote, location and slope parameters. $[A_{50}]$ values were assumed to be log-normally distributed and are presented as their negative logarithms, $p[A_{50}]$.

Paired E/[A] curves obtained in the ear artery were fitted and the effects of FPL 67156 were tested by analysing paired changes in the three parameters i.e. $\Delta\alpha$, $\Delta p[A_{50}]$ and Δm. Preliminary analysis showed that variances of Δ values were not consistent amongst treatment groups. Therefore, non-parametric tests were adopted: the Kruskal-Wallis test for analysing group differences; Mann-Whitney U-test for individual comparisons. Data obtained in the epithelium were not paired, and the effects of FPL 67156 on parameter estimates were analysed by Student's *t* test.

In experiments in the rabbit epithelium, FPL 67156 demonstrated a degree of agonism and it was necessary to take this into account when analysing its effects on the positions of E/[A] curves. To do this, the method of Pöch & Holzmann (1980) was employed. Briefly, this method involves the comparison of experimental E/[A] curves with those predicted to apply when two agonists interact in the same system. This allows detection and quantification of any potentiating or antagonistic properties that the ligand may have over and above their agonist properties. In practice it works by plotting the theoretical E/[A] curve for one agonist in the presence of the other assuming that the two agonists are purely additive in their interaction. Deviation of the experimental curve from this theoretical line indicates potentiation (if the deviation is leftward) or antagonism (if the deviation is rightward).

Analysis of ecto-ATPase inhibition

Data for the inhibitory effects of FPL 67156 on ATP degradation were fitted to equation (i). The concentrations which produced 50% inhibition of degradation (IC_{50}) were read from the fitted lines and quoted as negative logarithms (pIC_{50}). Since the concentration of ATP used was near its K_M (Beukers *et al.*, 1993), IC_{50} values were assumed to approximate to K_i values for the purposes of theoretical modelling.

Theoretical analysis of ecto-ATPase inhibition

A theoretical model proposed by Furchgott was employed (Furchgott, 1972). In this model, agonist is applied to the organ bath at concentration $[A_o]$. The access of the agonist to biophase containing the receptors is considered to be diffusion rate-limited. The concentration of agonist within the biophase is defined as $[A_i]$, and its rate of entry is described by:

$$d[A_i]/dt = k_1([A_o] - [A_i]) \quad (ii)$$

in which k_1 is the diffusion constant for the agonist.

The degradation of agonist is assumed to be the consequence of enzyme activity within the biophase and to follow Michaelis-Menten kinetics:

$$d[A_i]/dt = V_{max}[A_i]/(K_M + [A_i]) \quad (iii)$$

At steady-state rates of agonist entry and degradation are balanced. Under this condition, the right-hand sides of equations (ii) and (iii) can be equated, and the following relationship can be derived:

$$k_1[A_i]^2 + (V_{max} + k_1K_M - k_1[A_o])[A_i] - k_1K_M[A_o] = 0 \quad (iv)$$

This is a quadratic equation in $[A_i]$. In theoretical simulations, values of k_1, V_{max} and K_M are chosen, then $[A_i]$, the active, biophase agonist concentration can be calculated in terms of $[A_o]$, the applied concentration, by numerical solution of equation (iv).

To generate theoretical E/[A] curves, values of $[A_i]$ were substituted into a simple hyperbolic function, equivalent to equation (i) with m set to unity, thereby producing curves plotted against the applied agonist concentration, $[A_o]$. To simulate the effect of enzyme inhibition, K_M was multiplied by the factor $(1 + [X]/K_I)$, in which X is a competitive inhibitor with a dissociation constant K_I. Since the enzyme inhibitor used, FPL 67156, also showed some receptor antagonism at high concentrations, it was necessary to simulate this component. This was done by multiplying the $[A_{50}]$ by the factor $(1 + [X]/K_B)$, in which K_B is the receptor dissociation constant of X.

Results

Figure 1 shows the effect of FPL 67156 (100 µM) on E/[A] curves to UTP (Figure 1a) and ATP-γ-S (Figure 1b) in the rabbit epithelium. In the presence of FPL 67156, UTP E/[A] curves were displaced to the left: control $p[A_{50}] = 6.01 \pm 0.17$ (s.e., $n = 5$); treatment $p[A_{50}] = 6.69 \pm 0.15$ (s.e., $n = 5$). This difference was significant ($P < 0.02$, unpaired *t* test). In contrast, FPL 67156 did not potentiate ATP-γ-S, indeed the E/[A] curve was displaced to the right: control $p[A_{50}] = 6.13 \pm 0.15$ (s.e., $n = 5$); treatment $p[A_{50}] = 5.75 \pm 0.08$ (s.e., $n = 5$). FPL 67156 alone produced a change in I_{sc} indicated by the raised base lines of the curves in its presence. It was not possible to construct a complete E/[A] curve for FPL 67156 so its potency as an agonist could only be estimated ($p[A_{50}] \leqslant 3.5$). Thus, FPL 67156 is considerably weaker than UTP and ATP-γ-S, and also ATP which has a $p[A_{50}]$ of 5.36 in this tissue (data not shown). The influence of this agonist

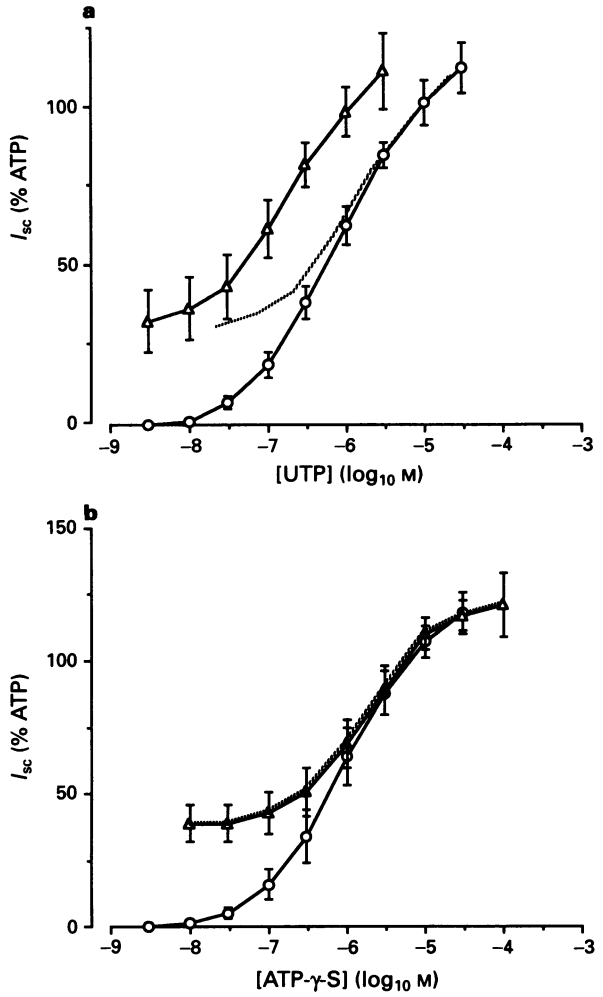


Figure 1 Effects of FPL 67156 on UTP and ATP-γ-S E/[A] curves in the rabbit tracheal epithelium preparation. The figure shows average data ($n = 5$) for the effects of UTP (a) and ATP-γ-S (b) on short-circuit current (I_{sc}) obtained in the absence (○) and presence (△) of FPL 67156 (100 μM). The dotted line depicts the theoretical dose-additive curve indicating the effects on UTP and ATP-γ-S E/[A] curves of FPL 67156 acting simply as an agonist. The leftward displacement of the experimental curve for UTP from the dose-additive line indicates synergy. The correspondence between the experimental curve for ATP-γ-S and the theoretical line indicates dose additivity.

effect on the location of the E/[A] curves to UTP and ATP-γ-S was analysed by the method of Pöch & Holzmann (1980). Thus, it was assumed that the agonist effects of FPL 67156, UTP and ATP-γ-S were subserved by the same receptor system and, therefore, that they were dose-additive. Theoretical lines were calculated indicating the position that the UTP and ATP-γ-S E/[A] curves should occupy in the presence of the experimentally found level of agonism produced by FPL 67156. These are depicted in Figure 1 as the dotted lines. Comparison of the experimental E/[A] curve for UTP in the presence of FPL 67156 with the theoretical additive curve indicated a clear leftward displacement (see Figure 1a). The p[A_{50}] of the theoretical curve was 5.8, some 8-fold to the right of the value of 6.69 for the experimental curve. In contrast, a similar analysis of the effects of FPL 67156 on the effects of ATP-γ-S showed no deviation between the position of the experimental E/[A] curve and the theoretical additive curve (see Figure 1b). Since it was known that UTP is more susceptible to enzymatic hydrolysis than ATP-γ-S (Welford *et al.*, 1987) we considered that the differential effect of FPL 67156 on the E/[A] curves for the two agonists may have been due to its ability to inhibit the breakdown of UTP and, therefore, to potentiate its effects.

FPL 67156 was tested as an inhibitor of ecto-ATPase in the human blood cell assay. The compound inhibited degradation of [γ^{32}P]-ATP with a pIC_{50} of 4.62 ± 0.03 (s.e., $n = 3$). Average data are shown in Figure 2.

Figure 3a shows the effects of FPL 67156 (30–1000 μM) on ATP E/[A] curves in the rabbit ear artery. Although a paired curve protocol was used, second curve data only are shown for clarity. Statistical analysis of the curve changes is given in Table 1. FPL 67156 produced substantial and highly significant leftward displacements of the ATP E/[A] curve. There were no significant effects on asymptote but there was a small (≈0.3 units compared with control) but significant decrease in slope in the presence of FPL 67156.

Assuming that FPL 67156 was behaving as an ecto-ATPase inhibitor in the rabbit ear artery, its effects were analysed using the model of Furchgott (1972) (see Methods). Figure 3b shows the resulting theoretical simulation. The values of the model parameters used to generate the simulation are recorded in Table 2. Figure 3 indicates a broad correspondence between the theoretical and experimental lines although there are some apparent inconsistencies. However, it is to be emphasised that Figure 3 shows second curve data for display purposes. Statistical analysis of the left-shifts of paired ATP E/[A] curves (Table 3) showed that the shifts predicted by modelling were consistent with the experimental values.

Of particular note are the following parameter estimates. The value of pK_I, the ecto-ATPase inhibitory potency, which needed to be chosen for FPL 67156 was higher than that obtained in the biochemical assay. The value was 5.2. Attempts to simulate the data with the lower values failed, in that the observed leftward shifts could not be generated at the concentrations of FPL 67156 used experimentally. Also, a p[A_{50}] value of 6.0 was used in the simulations. This value represents the location of the ATP E/[A] curve that would be obtained in the absence of ecto-ATPase activity (or following complete inhibition of the enzyme). Again, this value was necessarily chosen in order to allow the magnitude of leftward shifts observed in the experimental data. In the absence of FPL 67156, the average experimental p[A_{50}] value for ATP was 3.34 ± 0.19 (s.e., $n = 5$).

FPL 67156 (30–1000 μM) was tested against α,β-methylene-ATP in the rabbit ear artery. The results are shown in Figure 4. Again, second curves only are illustrated. FPL 67156 had no significant effects on the slope or asymptote of

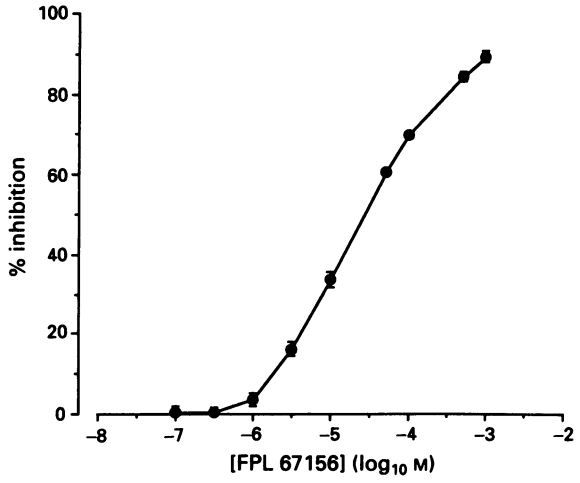


Figure 2 Effect of FPL 67156 on ATP dephosphorylation in human blood cells. The figure shows average data for the effect of FPL 67156 on [γ^{32}P]-ATP degradation. The estimated pIC_{50} was 4.62 ± 0.03 (s.e., $n = 3$).

Table 1 Statistical analysis of the effects of FPL 67156 on ATP E/[A] curves in the rabbit ear artery

	$\Delta\alpha$			Δm			$\Delta p[A_{50}]$		
[FPL 67156]	mean	s.e.	*n*	mean	s.e.	*n*	mean	s.e.	*n*
0 μM	5.6	3.2	5	0.09	0.08	5	0.19	0.15	5
30 μM	10.4	6.3	4	− 0.34*	0.13	4	− 0.48*	0.13	4
100 μM	21.2	4.5	5	− 0.30*	0.08	5	− 0.47	0.25	5
400 μM	23.8	6.0	5	− 0.33*	0.10	5	− 1.02*	0.13	5
1000 μM	12.9	7.0	5	− 0.19*	0.09	5	− 1.53*	0.16	5
Kruskal-Wallis test P-values:		0.13			0.034			0.001	

A paired curve design was adopted in which two ATP curves were constructed in each piece of tissue before and after exposures to FPL 67156 at the concentrations shown. Curve shape data are presented as mean paired differences in asymptote (α), slope (*m*) and location ($p[A_{50}]$) of curves, and *n* is the number of curve pairs for a particular treatment.
Mann-Whitney U-test: *indicates significant difference between treatment group and control.

α,β-methylene-ATP E/[A] curves. The paired control α,β-methylene-ATP E/[A] curves were virtually superimposable ($\Delta p[A_{50}] = -0.07 \pm 0.03$ (s.e., $n = 4$)) and the lower concentrations of FPL 67156 produced no measurable curve displacement. At the higher concentrations (300 μM and 1 mM) the compound caused small but significant rightward shifts. From the displacement of the α,β-methylene-ATP E/[A] curve at 1 mM an estimate of the pA_2 for FPL 67156 at P_{2X}-purinoceptors was made of 3.31 ± 0.06 (s.e., $n = 7$). This estimate was employed in the theoretical simulations of the

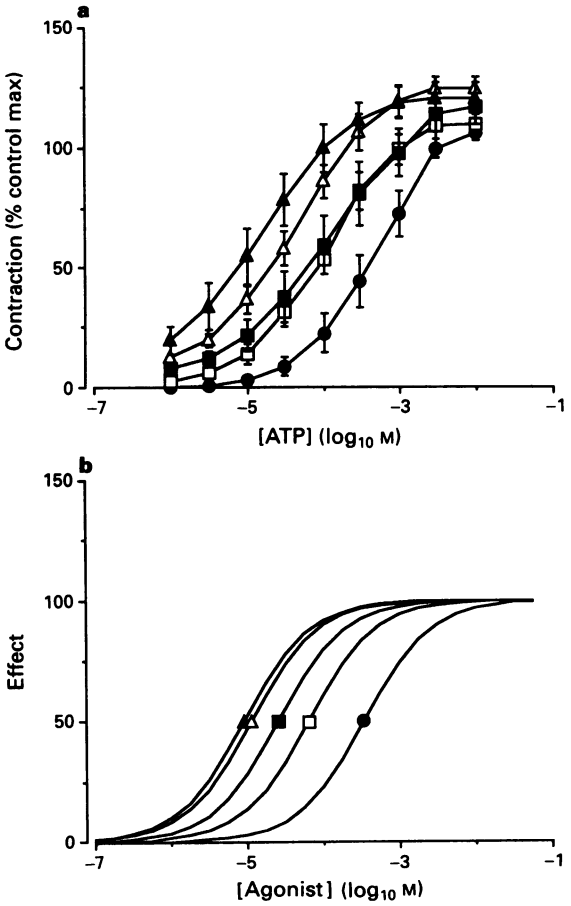


Figure 3 Effect of FPL 67156 on ATP E/[A] curves in the rabbit ear artery preparation: (a) shows average second-curve data ($n = 4,5$) obtained in the absence of FPL 67156 (●) and in its presence at the following concentrations (μM): 30 (□); 100 (■); 400 (△); 1000 (▲). (b) Shows theoretical simulations of the data using the model of Furchgott (1972). A pK_I value of 5.2 for FPL 67156 as an ecto-ATPase inhibitor was required to fit the data. Also required was an estimate of 6.0 for the $p[A_{50}]$ of ATP in the absence of ecto-ATPase activity. The other parameter values used in the simulation are recorded in Table 2.

Table 2 Model parameter values used in theoretical simulations

Parameter	*Value*
Diffusion constant for ATP; k_1	0.1 (min^{-1})
Ecto-ATPase; K_M	3×10^{-3} (M)
Ecto-ATPase; V_{max}	0.1 (M min^{-1})
Location of ATP E/[A] curve; $p[A_{50}]$	6.0 (− log M)
Dissociation constant for ecto-ATPase inhibition by FPL 67156; pK_I	5.2 (− log M)
Dissociation constant for P_{2X}-purinoceptor antagonism by FPL 67156; pK_B	3.3 (− log M)

Table 3 Comparison of experimental and theoretical E/[A] curve shifts analysing paired changes in $p[A_{50}]$ at each concentration of FPL 67156

	$\Delta p[A_{50}]$		
[FPL 67156] (μM)	*Experimental*	*Theoretical*	t *test*
30	0.67 ± 0.20	0.73	$P > 0.7$ (7 d.f.)
100	0.66 ± 0.29	1.13	$P > 0.1$ (8 d.f.)
400	1.21 ± 0.20	1.48	$P > 0.2$ (8 d.f.)
1000	1.72 ± 0.22	1.58	$P > 0.5$ (8 d.f.)

Experimental $\Delta p[A_{50}]$ values (and s.e.) were estimated from Table 1, and adjusted by 0.19 to account for the shift between the control ATP E/[A] curves. This analysis showed that there were no significant differences between the data and the predicted shifts.

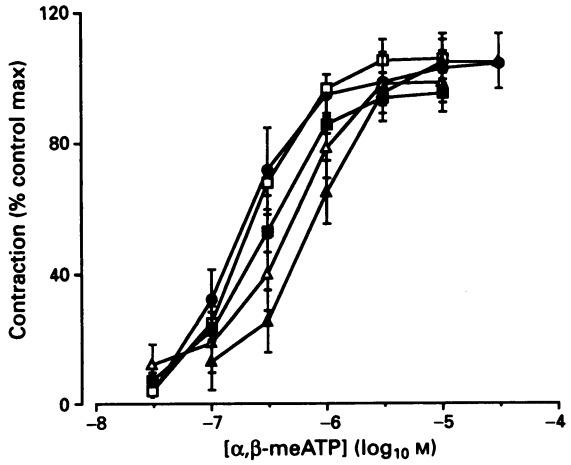


Figure 4 Effect of FPL 67156 on α,β-methylene ATP E/[A] curves in the rabbit ear artery preparation. The figure shows second curve data obtained in the absence of FPL 67156 (●) and in its presence at the following concentrations (μM): 30 (□); 100 (■); 400 (△); 1000 (▲) ($n = 3-7$). Paired analysis of $\Delta p[A_{50}]$ changes indicated significant rightward displacement (≈3-fold) at 1000 μM, from which a pA_2 estimate of 3.31 ± 0.06 (s.e., $n = 7$) was made.

effect of FPL 67156 on ATP. FPL 67156 alone produced some weak agonist responses at the higher concentrations ($\approx$15% at 1 mM).

FPL 67156 was tested for activity at P_{2T}-purinoceptors using an established assay (Humphries *et al.*, 1994). The compound behaved as a low affinity antagonist ($pA_2 \approx 3.5$, $n = 4$).

Discussion

The first indication that FPL 67156 may be an ecto-ATPase inhibitor was obtained in the rabbit tracheal epithelium preparation where it potentiated the effects of UTP, but not those of ATP-γ-S. Important in the analysis of these data was the ability to eliminate, as a complicating factor, the agonist effect of FPL 67156 itself. This was possible by use of the method of Pöch & Holzmann (1980). By plotting theoretical dose-additive curves it was possible to define the effect that FPL 67156 would have had, acting solely as an agonist, on the position of UTP and ATP-γ-S E/[A] curves. The clear separation of the experimental curve for UTP obtained in the presence of FPL 67156 from the theoretical additive curve indicated that FPL 67156 had acted synergistically with UTP. This was unlike the interaction between FPL 67156 and ATP-γ-S, which was shown to be simply additive. Although this analysis did not prove the involvement of ecto-ATPase inhibition, this was suggested by the fact that UTP had previously been found to be more susceptible than ATP-γ-S to enzymic dephosphorylation by tissues (Welford *et al.*, 1987). This encouraged us to seek direct evidence for ecto-ATPase inhibition by FPL 67156. Such evidence was obtained using the human blood cell assay where the compound inhibited [γ^{32}P]-ATP degradation in concentration-dependent manner with a pIC_{50} of 4.62.

Accepting that FPL 67156 could be classified as an ecto-ATPase inhibitor, its pharmacological effects were then studied using the rabbit ear artery preparation. This system has previously been shown to permit quantitative evaluation of the effects of agonists and antagonists acting at P_{2X}-purinoceptors (O'Connor *et al.*, 1990; Leff *et al.*, 1990; 1993). Recently, we used this preparation to analyse the ecto-ATPase inhibitory properties of ligands which also act as receptor antagonists (Crack *et al.*, 1994). We considered this system to be appropriate for providing a pharmacological estimate of the potency of FPL 67156 as an ecto-ATPase inhibitor.

As shown in Figure 3, FPL 67156 elicited substantial leftward shifts of ATP E/[A] curves whereas, in the concentration range 30–100 μM, FPL 67156 had no effect on the location of E/[A] curves to α,β-methylene-ATP, a metabolically stable agonist (Welford *et al.*, 1986). At the highest concentration used (1 mM), FPL 67156 potentiated ATP responses by 34-fold. In fact, at that concentration and at 400 μM, the compound also showed some P_{2X}-purinoceptor antagonism against the effects of α,β-methylene ATP, corresponding respectively to rightward shifts of 3-fold and 1.5-fold. This property would have opposed the leftward shift of ATP E/[A] curves produced by ecto-ATPase inhibition. So the degree to which ATP responses can be potentiated, considerable as it stands, may have been underestimated. This is an important consideration when quantifying the impact of ecto-ATPase on the position of the ATP E/[A] curve in this preparation.

In principle, the potentiating effect of FPL 67156 could have come about in two general ways, both related to ecto-ATPase inhibition. Desphosphorylation of the applied agonist may have produced other chemical species which oppose its pharmacological effects. Alternatively, as assumed here, the effects of metabolism may simply be to reduce the concentration of the agonist in the vicinity of the receptors. Inhibition of enzymatic degradation in both cases could lead to potentiation of the agonist responses. The former explanation was rejected in the present study for the following reasons. In the rabbit ear artery experiments the issue would have been the possible conversion of ATP to ADP, AMP and adenosine. In particular, accumulation of adenosine may have resulted in the activation of P_1-purinoceptors mediating a vasorelaxation response which would have opposed the P_{2X}-purinoceptor-mediated contractile effects of ATP. Inhibition of adenosine formation could then have led to potentiation of ATP effects. This explanation could be ruled out in this study because 8-SPT was present in all experiments at a concentration 30–100 fold higher than its dissociation constant for P_1-purinoceptors. Similarly, the possible complicating effects of metabolites active at P_{2Y}-purinoceptors could be excluded since these receptors are absent in this preparation (O'Connor *et al.*, 1990). Therefore, it was assumed that the potentiating effects of FPL 67156 could be attributed simply to the enhancement of the active concentration of ATP.

The model of Furchgott (1972) provides a formal way of analysing such data and it was used here to make a pharmacological estimate of the affinity of FPL 67156 as an ecto-ATPase inhibitor in the rabbit ear artery preparation. Evidently from Figure 3, it was possible to represent the experimental data quite accurately by the model. The parameters used to produce the simulations predicted parallel leftward displacements. In fact, there was some evidence for a flattening of the ATP E/[A] curves in the presence of FPL 67156. According to Furchgott's model, such shape changes can occur. However, the magnitude of the change in slope observed in the present data was only $\approx$0.3 units and we did not consider it necessary to accomodate such a small change during the modelling process. The important requirement of the theoretical analysis was to account for the magnitude of the leftward displacements observed and, as explained in the Results section, the choice of parameter values required to do this was not arbitrary. In particular, the estimates pK_I and $p[A_{50}]$ merit some attention.

The pK_I estimate of 5.2 was needed in order to simulate potentiation of ATP effects in the appropriate range of FPL 67156 concentrations. This pharmacological pK_I estimate is higher than the one made in the human blood cell assay (4.6). Why this is so is not known, but similar discrepancies were found in the preceding analysis of ecto-ATPase inhibition (Crack *et al.*, 1994). In that study, suramin and FPL 66301, an analogue of ATP, were tested in the same two preparations and the pK_I estimates were, respectively, 8-fold and 4-fold higher in the rabbit ear artery than in human blood cells. From the pharmacological point of view, we consider the estimate made in the rabbit ear artery to have the greater relevance because this is the value which indicates the operational concentration-range for the potentiating effects of FPL 67156.

A criticism of this interpretation could be that the difference in pK_I estimates arose from uncharacterized properties of FPL 67156 expressed in the pharmacological preparation but not in the biochemical assay. Such properties may have led to potentiation of the effects of ATP by mechanisms other than ecto-ATPase inhibition, resulting in an overestimation of the potency of FPL 67156 as an enzyme inhibitor. We consider this unlikely because potentiating mechanisms other than inhibition of agonist metabolism would have to operate at the receptor or post-receptor level and affect metabolically stable agonists as well as unstable ones. The fact that α,β-methylene-ATP E/[A] curves were completely unaffected by FPL 67156 at concentrations which produced substantial potentiation of those to ATP argues against the expression of additional potentiating properties.

An alternative explanation for the difference in the pK_I estimates made in the two systems is, of course, that two different assay tissues were involved. Ideally, the pharmacological and biochemical analyses would have been conducted in the same tissue and in this regard the ear artery would have been the system of choice. However, to our

knowledge, no assay of nucleotide metabolism has been published for this tissue and we felt it necessary to employ an established and available method, as exemplified by the blood cell assay (Beukers *et al.*, 1993). This leaves open the criticism that FPL 67156 was inhibiting two quite distinct enzymes in the two systems. Against this is the correlation between the pharmacological and biochemical pK_I estimates for FPL 67156, suramin and FPL 66301, namely 5.2, 5.2, 3.9 and 4.6, 4.3, 3.3 respectively (present study and Crack *et al.*, 1994). The similarity of the relative values suggests that the same enzyme is involved, and the systematic difference between the two sets of numbers (5-fold on average) would not be unexpected for the same enzyme operating under different conditions.

The $p[A_{50}]$ value of 6.0 used in the model corresponds to the potency of ATP in the absence of ecto-ATPase, or under conditions of complete block of the enzyme. In other words, it represents an estimate of the 'true' potency of ATP in the tissue. This value was necessary in the simulations to allow for the magnitude and concentration-dependence of the potentiations produced experimentally by FPL 67156. Evidently this estimate of ATP's potency is considerably higher than the experimental $p[A_{50}]$ obtained in the absence of FPL 67156, which was 3.34. A difference of this magnitude (approximately 400-fold) was concluded to apply in our previous study (Crack *et al.*, 1994). In those experiments, the effects of suramin and FPL 66301 on ATP responses in the rabbit ear artery preparation were analysed. In order to explain the magnitude of leftward shifts of E/[A] curves produced by each of these compounds an estimate of 6.0 for the 'true' $p[A_{50}]$ of ATP was again necessary.

In our previous paper (Crack *et al.*, 1994) we drew attention to the impact of ecto-ATPase on the experimental potency of ATP and, by implication, other metabolically unstable agonists. In the present study, the use of FPL 67156 has confirmed the degree to which the potency of ATP, at least, is underestimated in the rabbit ear artery preparation. It also emphasises our previous arguments regarding the need to re-evaluate the agonist potency order currently held to designate P_{2X}-purinoceptors (Burnstock & Kennedy, 1985). If the results of these analyses are accepted, then dramatic changes will occur in the positions that ATP and, by implication, other metabolically susceptible agonists such as 2-MeSATP, occupy in the potency order. According to such calculations, the potency order used to designate P_{2X}-purinoceptors would read: α,β-methylene-ATP = 2-MeSATP > ATP > β,γ-methylene-L-ATP > β,γ-methylene-D-ATP. This is in marked contrast with the reported order (O'Connor *et al.*, 1990): α,β-methylene-ATP > β,γ-methylene-L-ATP > β,γ-methylene-D-ATP > 2-MeSATP > ATP.

Similar arguments apply to the potency of UTP in the rabbit tracheal epithelium. Unfortunately, the agonist effects of FPL 67156 limited the concentration-range over which it could be used in that preparation. However, at 100 μM it produced a degree of potentiation of UTP that was very similar to its effects on the action of ATP in the rabbit ear artery, and the potency of UTP, relative to ATP-γ-S, clearly changed. We presume that the receptors in the rabbit tracheal epithelium belong to the P_{2U}-class. However, further experiments, conducted in the presence of FPL 67156, are required before a meaningful agonist potency order can be reported for this system.

Regarding the utility of FPL 67156 in purinoceptor classification, its relatively modest potency as an ecto-ATPase inhibitor is recognised. However, the compound was only weakly active at P_{2X}-, P_{2U}-, and P_{2T}-purinoceptors, demonstrating pA_2 or $p[A_{50}]$ values of 3.5 or less. Accepting the theoretical pK_I estimate (5.2), this means FPL 67156 has some 50-fold selectivity as an ecto-ATPase inhibitor. As such, it is hoped that this compound should have sufficient selectivity to approach the kinds of problems in pharmacological analysis described here and in our previous paper (Crack *et al.*, 1994).

References

BEUKERS, M.W., PIROVANO, I.M., VAN WEERT, A., KERKHOF, C.J.M, IJZERMAN, A.P. & SOUDIJN, W. (1993). Characterization of ecto-ATPase on human blood cells. *Biochem. Pharmacol.*, **46**, 1959–1966.

BURNSTOCK, G. & KENNEDY, C. (1985). Is there a basis for distinguishing two types of P_2-purinoceptor? *Gen. Pharmacol.*, **16**, 433–440.

CRACK, B.E., BEUKERS, M.W., MCKECHNIE, K.C.W., IJZERMAN, A.P. & LEFF, P. (1994). Pharmacological analysis of ecto-ATPase inhibition: evidence for combined enzyme inhibition and receptor antagonism in P_{2X}-purinoceptor ligands. *Br. J. Pharmacol.*, (in press).

FOSTER, R.W. (1967). The potentiation of the responses to noradrenaline and isoprenaline of the guinea-pig isolated tracheal chain preparation by desipramine, cocaine, phentolamine, phenoxybenzamine, guanethidine, metanephrine and cooling. *Br. J. Pharmacol.*, **31**, 466–482.

FURCHGOTT, R.F. (1972). The classification of adrenoceptors (adrenergic receptors). An evaluation from the standpoint of receptor theory. In *Handbook of Experimental Pharmacology*. Vol. 33, ed. Blaschko, H. & Muscholl, E., pp. 283–335. New York: Springer-Verlag.

GREEN, A.L., LORD, J.A.H. & MARSHALL, I.G. (1978). The relationship between cholinesterase inhibition in the chick biventer cervicis muscle and its sensitivity to exogenous acetylcholine. *J. Pharmac. Pharmacol.*, **30**, 426–431.

HUMPHRIES, R.G., TOMLINSON, W., INGALL, A.H., CAGE, P.A. & LEFF, P. (1994). FPL 66096: a novel, highly potent and selective antagonist at human platelet P_{2T}-purinoceptors. *Br. J. Pharmacol.*, **113**, 1057–1063.

KENAKIN, T.P. (1980). Errors in the measurement of agonist potency-ratios produced by uptake processes: a general model applied to β-adrenoceptor agonists. *Br. J. Pharmacol.*, **71**, 407–417.

LEFF, P., WOOD, B.E. & O'CONNOR, S.E. (1990). Suramin is a slowly-equilibrating but competitive antagonist at P_{2X}-receptors in the rabbit isolated ear artery. *Br. J. Pharmacol.*, **101**, 645–649.

LEFF, P., WOOD, B.E., O'CONNOR, S.E. & MCKECHNIE, K.C.W. (1993). Quantitative analysis of the agonist and antagonist actions of some ATP analogues at P_{2X}-purinoceptors in the rabbit ear artery. *Br. J. Pharmacol.*, **108**, 490–496.

O'CONNOR, S.E., WOOD, B.E. & LEFF, P. (1990). Characterization of P_{2X}-purinoceptors in rabbit isolated ear artery. *Br. J. Pharmacol.*, **101**, 640–644.

PÖCH, G. & HOLZMANN, S. (1980). Quantitative estimation of overadditive and underadditive drug effects by means of theoretical, additive dose-response curves. *J. Pharmacol. Meth.*, **4**, 179–188.

SATCHELL, D. (1984). Purine receptors in the trachea: studies with adenosine deaminase and dipyridamole. *Eur. J. Pharmacol.*, **102**, 545–548.

WELFORD, L.A., CUSACK, N.J. & HOURANI, S.M.O. (1986). ATP analogues and the guinea-pig taenia coli: a comparison of the structure-activity relationships of ectonucleotidases with those of the P_2-purinoceptor. *Eur. J. Pharmacol.*, **129**, 217–224.

WELFORD, L.A., CUSACK, N.J. & HOURANI, S.M.O. (1987). The structure-activity relationships of ectonucleotidases and of excitatory P_2-purinoceptors: evidence that dephosphorylation of ATP analogues reduces pharmacological potency. *Eur. J. Pharmacol.*, **141**, 123–130.

(Received May 31, 1994
Revised August 25, 1994
Accepted September 20, 1994)

British Journal of Pharmacology (1995) 114, 482–488 © 1995 Stockton Press All rights reserved 0007–1188/95 $9.00

Protein kinase C and tyrosine kinase pathways regulate lipopolysaccharide-induced nitric oxide synthase activity in RAW 264.7 murine macrophages

Andrew Paul, Robert H Pendreigh & [1]Robin Plevin

Department of Physiology and Pharmacology, University of Strathclyde, Royal College, 204 George Street, Glasgow, G1 1XW

1 In RAW 264.7 macrophages, lipopolysaccharide (LPS) and γ-interferon (IFNγ) alone or in combination stimulated the induction of nitric oxide synthase (iNOS) activity and increased the expression of the 130 kDa isoform of NOS.

2 LPS-induced NOS activity was reduced by incubation with CD14 neutralising antibodies and abolished in macrophages deprived of serum.

3 LPS stimulated a small increase in protein kinase C (PKC) activity in RAW 264.7 macrophages which was dependent on the presence of serum. However, IFNγ did not potentiate LPS-stimulated PKC activity.

4 The protein kinase C inhibitor, Ro-318220, abolished both LPS- and IFNγ-stimulated protein kinase C activity and the induction of NOS activity.

5 LPS- and IFNγ-induced NOS activity was reduced by the tyrosine kinase inhibitor genestein. Genestein also reduced LPS-stimulated protein kinase C activity but did not affect the response to the protein kinase C activator, tetradecanoylphorbol acetate (TPA).

6 Nicotinamide, an inhibitor of poly-ADP ribosylation, abolished LPS- and IFNγ-induced NOS activity.

7 Brefeldin A, an inhibitor of a factor which stimulates nucleotide exchange activity on the 21 kDa ADP-ribosylation factor, ARF, reduced LPS- and IFNγ-induced NOS activity by approximately 80%.

8 These results suggest the involvement of protein kinase C, tyrosine kinase and ploy-ADP ribosylation pathways in the regulation of the induction of nitric oxide synthase in RAW 264.7 macrophages by LPS and IFNγ.

Keywords: Nitric oxide synthase; lipopolysaccharide; interferon γ; protein kinase C; tyrosine phosphorylation; ADP-ribosylation

Introduction

The formation of nitric oxide (NO) is regulated by a family of enzymes known collectively as nitric oxide synthase (NOS). In endothelial cells, rapid NO production is regulated by a calcium-dependent, constitutively active isoform of the enzyme (Pollock *et al.*, 1991), whilst in macrophages an inducible calcium-independent isoform, which is not modified post-translationally, regulates NO synthesis over a period of several hours following cell stimulation with cytokines or the active component of endotoxin, lipopolysaccharide (LPS) (Lyons *et al.*,1992). Several isoforms of NOS with distinct cellular locations have been identified in other tissues including brain, liver and vascular smooth muscle cells (Marletta, 1993).

In macrophages, LPS alone or in combination with cytokins such as γ-interferon (IFNγ), has been shown to induce an increase in NOS activity through an increase in the transcription of the iNOS gene (Mitchell *et al.*, 1992; Lorsbach *et al.*, 1993). However, the intracellular signalling pathways by which LPS causes NOS induction are largely unresolved. A number of pathways have recently been implicated including the activation of protein kinase C (PKC) (Severn *et al.*, 1992), tyrosine phosphorylation (Weinstein *et al.*, 1992) and changes in cytoskeletal structure (Marczin *et al.*, 1993b). An additional pathway by which toxins may regulate cell responsiveness involves the activation of enzymes which regulate ADP-ribosylation of target proteins thereby modifying their activity (Moss and Vaughan, 1993). This includes the 21 kDa protein ADP ribosylation factor designated as ARF (Kahn *et al.*, 1993).

In this study we have assessed the effects of inhibitors of PKC, tyrosine phosphorylation and poly-ADP ribosylation on LPS-induced NOS activity in RAW 264.7 macrophages. We show that the activation of PKC is obligatory for the induction of NOS activity stimulated by LPS and IFNγ. The activation of PKC by LPS is regulated by a tyrosine phosphorylation event. LPS induction of NOS activity may also involve the activation of endogenous ADP ribosylation factors which are downstream of PKC activation.

Methods

Cell culture

RAW 264.7 murine macrophages, obtained from the European Cell Culture Collection, were cultured in Dulbecco's Modified Eagle's Medium containing 10% foetal calf serum (FCS), 2 mM glutamine, 250 iuml^{-1} penicillin and 250 μg ml^{-1} streptomycin.

Assessment of NOS activity

NOS activity was estimated by a modification of the method described by Mitchell *et al.* (1992). Cells were harvested from six well plates and centrifuged for 2 min at 1000 g. The supernatant was removed and the pellet resuspended in 25 mM HEPES buffer pH 7.5, containing 25 mM β-mercapto-

[1] Author for correspondence.

ethanol, 10 μM pepstatin, 10 μM leupeptin, 1% v/v Triton X-100 and incubated on ice for 30 min. The cell extracts were incubated in 10 mM HEPES buffer pH 7.4 containing 1 mM NADPH, 10 μM biopterin, 10 μM FAD, 10 μM FMN, and 10 mM L-arginine/[^{3}H]L-arginine (specific activity = 37 MBq ml^{-1}, 0.1 μCi per tube) for 15 min at 37°C. [^{3}H]L-citrulline was separated by Dowex cation-exchange chromatography and measured by liquid scintillation counting. The assay was characterized for linearity with time and cell number, NADPH-dependence and Ca^{2+}-independence (results not shown). IC_{50} values for N^G nitro-L-arginine methylester (L-NAME) and L-canavanine inhibition of LPS-induced NOS activity were (mean ± s.e.mean.) 53.2 ± 12.0 and 3.50 ± 2.6 μM, ($n = 3$). Constitutive NOS activity from rat cerebellar homogenates was shown to be NADPH- and calcium/calmodulin-dependent and was inhibited by L-NAME. Pretreatments with the compounds in the study were not effective against NOS activity assayed *in vitro* following induction with LPS.

Western blotting

For the detection of NOS protein levels, cells were washed twice in ice-cold PBS, then solubilized in hot (70°C) SDS–PAGE sample buffer. The samples were dispersed by repeated passage through a 21G needle and then transferred to eppendorf tubes. The samples were boiled for 10 min and then stored at −80°C until analysis. Aliquots (15–20 μg protein) were subjected to SDS–PAGE on 7% polyacrylamide slab gels and then blotted onto nitrocellulose. The nitrocellulose membranes were incubated for 3 h in 150 mM NaCl, 20 mM Tris, 0.02% Tween pH 7.4 (NaTT), containing 3% BSA then incubated overnight in NaTT containing 0.2% BSA and 1 μg ml^{-1} of anti-NOS antibody. Following six washes in NaTT, the membranes were incubated with anti-mouse Ig-HRP for 90 min and then washed a further 8 times in NaTT. The immunoblots were developed by the ECL detection system (Amersham).

PKC activity

For the assay of agonist-stimulated PKC activity a modified version of the method used by Alexander *et al.* (1990), was employed. Cells grown to confluency on 6 cm^2 plates were incubated with agonists for the time outlined. The cells were washed twice in a buffer containing mM: KCl 150, $MgCl_2$ 5.16, PIPES 12.5, EGTA 12.5 and $CaCl_2$ 8.17, pH 7.4 and permeabilised in the same buffer containing 0.5 units ml^{-1} of streptolysin-O, 200 μM ATP [γ-^{32}P]-ATP (300–450 c.p.m. pmol^{-1}) and 200 μM of the PKC peptide pseudosubstrate GS-peptide. Following a 10 min incubation period, the reaction was terminated by the addition of 100 μl of 25% (w/v) trichloroacetic acid in 2 M acetic acid. After 10 min on ice the cells were scraped and the extracts transferred to microfuge tubes and centrifuged at 14 000 *g* for 5 min at 4°C. Aliquots of the supernatants were spotted onto 3cm squares of P81 Whatman ion-exchange chromatography paper. The squares were washed (×3) in 30% acetic acid containing 1% phosphoric acid (10 min each wash) and then once in ethanol. The squares were dried and activity measured by scintillation counting. Non-specific phosphorylation (3–5% of total phosphorylation) in the absence of peptide was measured in each assay and subtracted from all samples. The linearity of phosphorylation over time (0–20 min) was confirmed in preliminary experiments (results not shown).

Materials

Mouse monoclonal antibodies to the 130 kDa macrophage and 140 kDa endothelial cell isoforms of NOS were gifts from Affiniti Research Products Ltd, Nottingham. The PKC pseudosubstrate peptide (GS-peptide) Pro-Leu-Ser-Arg-Thr-Leu-Ser-Val-Ala-Ala-Lys-Lys-COOH was synthesized by Dr E.G. Rowan (Department of Physiology and Pharmacology, University of Strathclyde, Glasgow) and by Epitope Peptides (Newcastle University, Newcastle). Anti-CD14 antibodies were purchased from Zymed Immunochemicals (San Francisco, U.S.A). [^{3}H]-L-arginine (specific activity 1.3 TBq mmol^{-1}) was purchased from N.E.N. (Stevenage, Herts.) [γ-^{32}P]-ATP (specific activity 110 GBq mmol^{-1}) was purchased from Amersham International (Amersham, Bucks.). All other chemicals were of the highest commercial grade available.

Statistics

Statistical analysis of the data was performed using an unpaired *t* test. Dose-response analysis was using an iterative curve fitting procedure (De Lean *et al.*, 1980).

Results

Induction of NOS activity by LPS

LPS (1 μg ml^{-1}) stimulated an increase in NOS activity in RAW 264.7 macrophages which was maximal 8–12 h following LPS addition (Figure 1a). IFNγ (10–100 iuml^{-1}) stimulated a small increase in NOS activity (results not shown);

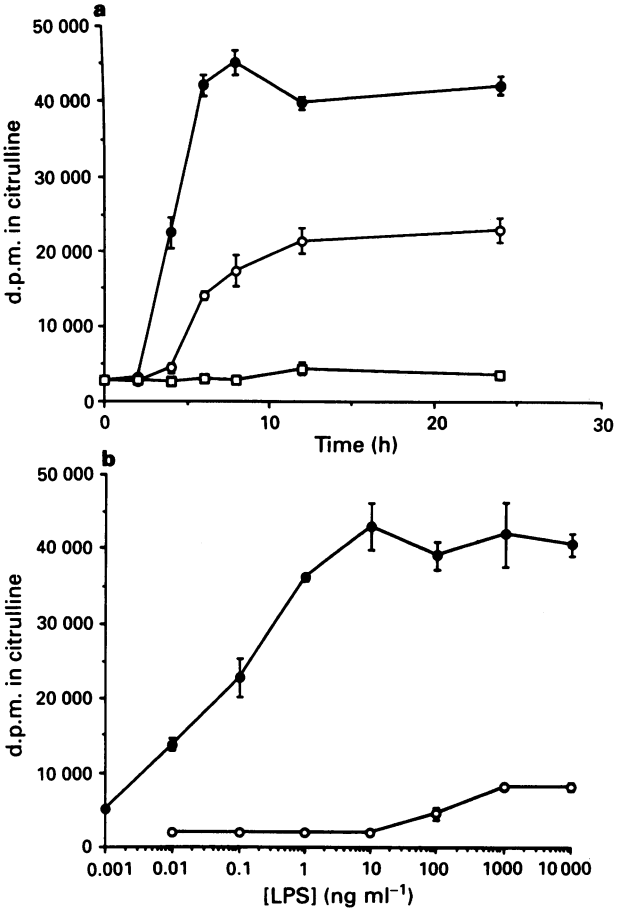


Figure 1 Time- and concentration-dependent induction of NOS activity in lipopolysaccharide (LPS) and interferonγ (IFNγ) treated RAW 264.7 macrophages. In (a) cells were incubated with vehicle (□), 1 μg ml^{-1} LPS (○) or 1 μg ml^{-1} LPS + 10 iuml^{-1} IFNγ (■) for the times indicated and then assayed for NOS activity as outlined in the Methods section. In (b) cells were incubated with increasing concentrations of LPS in the absence (○) or presence (●) of 10 iuml^{-1} of IFNγ for 8 h before the assay of NOS activity. Each point represents the mean ± s.e.mean. from a single experiment performed in triplicate and representative of four.

however, submaximal concentrations of IFNγ potentiated the response to LPS and increased the potency of the LPS response. The EC_{50} values for the LPS-induced NOS activity in the absence and presence of 10 iuml^{-1} IFNγ were 68.7 ± 23 ng ml^{-1} and 33.2 ± 14.5 pg ml^{-1} respectively ($n = 4$). (Figure 1b). A submaximal concentration of LPS also potentiated the response to IFNγ (results not shown).

The increase in NOS activity was also reflected in an increase in the levels of a protein which corresponds immunologically to the 130 kDa inducible isoform of NOS (Figure 2). However, in these cells there was no evidence of the presence of a protein corresponding to the 140 kDa isoforms of NOS found in endothelial cells (results not shown).

Characterization of LPS response

Addition of anti-CD14 antibodies (2.5 μg ml^{-1}) which cause activation of CD14, the receptor for the LPS/LBP complex (Wright *et al.*, 1990), stimulated a small insignificant increase in NOS activity in RAW 264.7 macrophages (Table 1). Anti-CD14 antibodies also potentiated the response to IFNγ, but did not potentiate the response to LPS and IFNγ in combination. Neutralising antibodies to CD14 (2.5 μg ml^{-1}) significantly reduced the response to LPS alone (% inhibition = 13, $n = 3$) or in combination with IFNγ (39.6 ± 7, $n = 3$) but were without effect upon the response to IFNγ alone.

The response to LPS was also dependent upon the presence of serum (Table 2). In the cells incubated for 12 h in serum-free media and then stimulated in serum-free conditions, LPS-induced NOS activity was abolished. This was in contrast to IFNγ-induced NOS activity, which showed a significant increase. In cells preincubated in normal serum conditions and then stimulated in the absence of serum the response to LPS was reduced by approximately 90% (90.3 ± 7, $n + 4$). Under these conditions IFNγ-induced NOS activity was not affected.

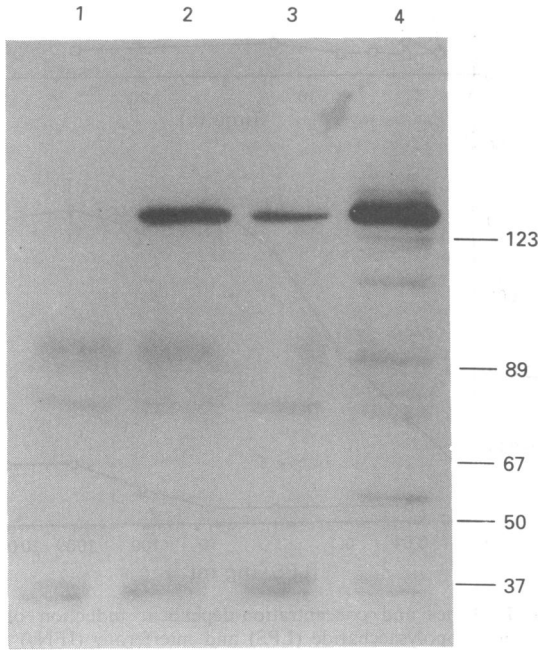


Figure 2 Increases in the expression of induced nitric oxide synthase (iNOS) in lipopolysaccharide (LPS) and interferon γ (IFNγ) treated RAW 264.7 macrophages. Cells were pretreated with vehicle (1), 1 μg ml^{-1} LPS (2), 30 iuml^{-1} IFNγ (3) or 1 ng ml^{-1} LPS + 10 iuml^{-1} IFNγ (4) for 12 h and then immunoblotted for inducible NOS levels as outlined in the Methods section. Each experiment is representative of two others.

Activation of PKC by LPS

In the presence of serum, LPS also stimulated a time-dependent increase in PKC activity (Figure 3a). The response was slow in onset, reaching a peak at 10 min following LPS stimulation at approximately 160–180% of basal values (185 ± 18%, $n = 6$). The PKC activator, TPA, also stimulated PKC activity to much greater extent, approximately 3–4 fold (3.26 ± 1.3, $n = 6$), and the maximum stimulation was obtained between 5 and 10 min. In serum-free conditions LPS, over a concentration range of 1 ng ml^{-1} to 3 μg ml^{-1}, failed to elicit a PKC response (Figure 3b). Only at supra-maximal concentrations (10 μg ml^{-1}) was PKC activity enhanced. In the presence of serum the potency of LPS was increased and an EC_{50} value in the range observed for the induction of NOS was recorded. Serum alone also stimulated a small increase in PKC activity (% basal values = 168 ± 14, $n = 4$) (Figure 3b). IFNγ also stimulated a small increase in

Table 1 The effect of CD14 antibodies on lipopolysaccharide (LPS)- and interferon γ (IFN-γ)-induced nitric oxide synthase (NOS) activity in RAW 264.7 macrophages

A	*Control*	*CD14 (activating)*
Basal	3141 ± 230	3850 ± 123^{NS}
LPS	7764 ± 485	12843 ± 943*
IFNγ	5598 ± 460	13621 ± 1561*
LPS + IFNγ	35473 ± 2762	40363 ± 2762*
B	*Control*	*CD14 (neutralising)*
Basal	4019 ± 200	3982 ± 470^{NS}
LPS	15892 ± 1348	8156 ± 414*
IFNγ	8402 ± 783	8606 ± 1172^{NS}
LPS + IFNγ	22870 ± 2645	15285 ± 1481*

In (**A**) Cells were incubated with 2.5 μg ml^{-1} of activating CD14 antibodies in the absebce or presence of 1 μg ml^{-1} of LPS, 30 iuml^{-1} IFNγ or 1 ng ml^{-1} LPS + 10 iuml^{-1} IFNγ for 8 h and assayed for NOS activity. In (**B**) cells were incubated with 2.5 μg ml^{-1} of a neutralising antibody under the same conditions. Each value represents the mean ± s.e.mean of three experiments performed in triplicate (d.p.m.) (NS – not significant; *Significantly different from control stimulation, $P < 0.05$).

Table 2 The effect of serum on lipopolysaccharide (LPS)- and interferon γ (IFN-γ)-induced nitric oxide synthase (NOS) activity in RAW 264.7 macrophages

A	*Serum*	*Serum-free (12 h)*
Control	3100 ± 40	3368 ± 237^{NS}
LPS	30003 ± 4824	3961 ± 372*
IFNγ	9423 ± 666	14567 ± 180*
LPS + IFNγ	38371 ± 3179	12006 ± 530*
B	*Serum*	*Serum-free*
Control	3295 ± 681	3332 ± 530^{NS}
LPS	30837 ± 2495	6012 ± 1092*
IFNγ	5699 ± 1435	5465 ± 1354^{NS}
LPS + IFNγ	36418 ± 5190	14992 ± 1555*

In (**A**) cells were incubated with 12 h in the absence or presence of 10% FCS before stimulation with 1 μg ml^{-1} of LPS, 30 iuml^{-1} IFNγ or 1 ng ml^{-1} LPS + 10 iuml^{-1} IFNγ for 8 h and assayed for NOS activity. In (**B**) cells were incubated with 12 h in the presence of 10% FCS before stimulation in the presence or absence of 10% serum. Each value (d.p.m.) represents the mean ± s.e.mean of at least three experiments performed in triplicate (NS – not significant; *Significantly different from control stimulation, $P < 0.05$).

PKC activity (% basal value = 137.0 ± 11, $n = 7$); however, this response was not potentiated by LPS and the PKC responses to each agent were less than additive (Table 3). Pretreatment of the cells with Ro-318220 (10 μM) also abolished LPS- and IFNγ-stimulated PKC activity in RAW 264.7 cells (Table 3).

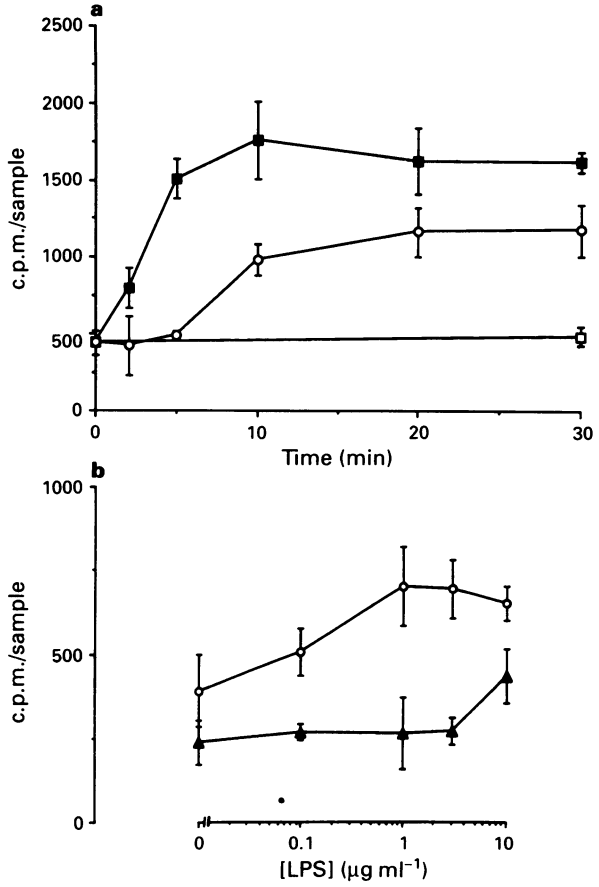


Figure 3 Serum-dependent lipopolysaccharide (LPS)-stimulated protein kinase C activity in RAW 264.7 macrophages. In (a) cells were incubated with vehicle (□), 100 nM TPA (■), or 1 μg ml^{-1} LPS (○) in the presence of 10% serum for the times indicated. In (b) cells were incubated with increasing concentrations of LPS in the presence (○) and absence (▲) of 10% serum for 15 min before assay. Protein kinase C activity was assayed as outlined in the Methods section. Each value represents the mean ± s.e.mean. from each single experiment where $n = 4$.

Table 3 The effect of Ro-318220 on tetradecanoyl phorbol acetate (TPA)-, lipopolysacharride (LPS)- and interferon γ (IFNγ)-stimulated protein kinase C activity in RAW 264.7 macrophages

	DMSO	*Ro-318220*
Basal	751 ± 128	729 ± 241^{NS}
TPA	2655 ± 416	755 ± 166*
LPS	1478 ± 360	723 ± 160*
IFNγ	1005 ± 119	618 ± 87^{NS}
LPS + IFNγ	1628 ± 321	614 ± 89*

Cells were pretreated with vehicle or 10 μM Ro-318220 for 30-min and then stimulated with either 100 nM TPA, 1 μg ml^{-1} of LPS, 30 iuml^{-1} IFNγ or 1 ng ml^{-1} LPS + 10 iuml^{-1} IFNγ for a further 15 min. Each value (c.p.m.) represents the mean ± s.e.mean of three experiments performed in duplicate (NS – not significant; *significantly different from dimethylsulphoxide (DMSO) controls, $P < 0.05$).

Involvement of PKC activation in NOS induction

Figure 4 shows the effect of the PKC inhibitor Ro-318220 (Davis *et al.*, 1989) on LPS and IFNγ induction on NOS activity. At a concentration of 10 μM, Ro-318220 abolished the response to LPS alone or in combination with IFNγ. The IC_{50} values for the effect of Ro-318220 on each of the induced responses were comparable (IC_{50} value for Ro-318220 (μM): LPS = 1.35 ± 0.6, LPS + IFNγ = 0.95 ± 0.3, $n = 4$). At a concentration of 10 μM, Ro-318220 also abolished NOS induction in response to IFNγ alone (results not shown, $n = 2$).

Involvement of tyrosine kinase activity in NOS induction

Pretreatment of the cells with the tyrosine kinase inhibitor, genestein, also significantly inhibited induced NOS activity in response to LPS or IFNγ alone or in combination (Figure 5).

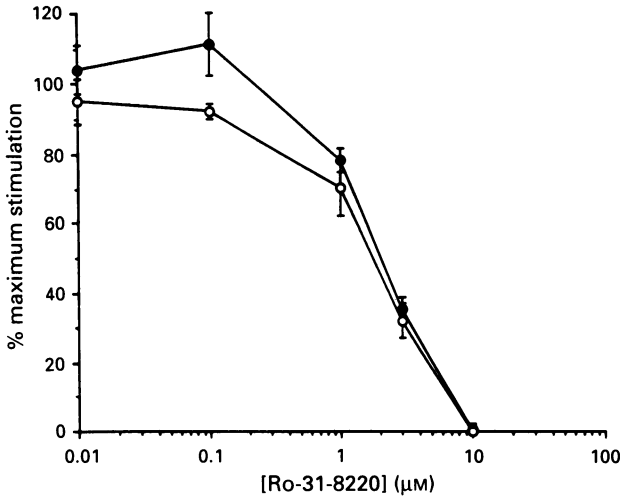


Figure 4 The effect of Ro-318220 on lipopolysaccharide (LPS)- and interferon γ (IFNγ)-induced nitric oxide synthase (NOS) activity in RAW 264.7 macrophages. Cells were incubated for 30 min with increasing concentrations of Ro-318220 before incubation with 1 μg ml^{-1} LPS (○), or 1 ng ml^{-1} LPS + 10 iuml^{-1} IFNγ (●) for 8 h. NOS activity was assayed as outlined in the Methods section. Each point represents the mean ± s.e.mean. of a single experiment performed in triplicate and representative of 4 others.

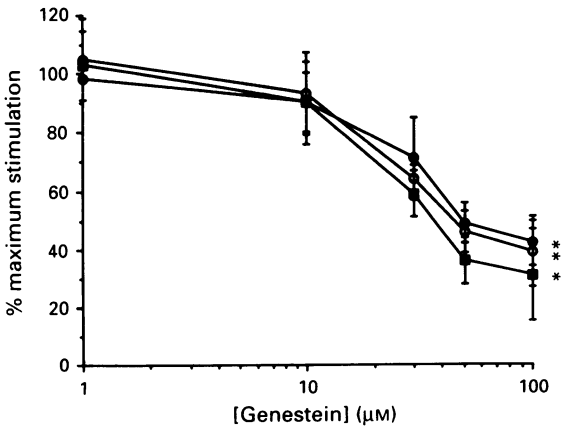


Figure 5 The effect of genestein on lipopolysaccharide (LPS)- and interferon γ (IFNγ)-induced nitric oxide synthase (NOS) activity in RAW 264.7 macrophages. Cells were preincubated with increasing concentrations of genestein for 1 h before incubation with 1 μg ml^{-1} LPS (○), 30 iuml^{-1} IFNγ (■) or 1 ng ml^{-1} LPS + 10 iuml^{-1} IFNγ (●) for 8 h. NOS activity was assayed as outlined in the Methods section. Each point represents the mean ± s.e.mean. where $n = 4$ (*Significantly different from control, $P < 0.05$).

However, inhibition was not complete even at the highest concentration of inhibitor used (100 μM), with approximately 40% of maximum activity remaining at this concentration. Genestein (100 μM) also reduced both LPS-stimulated PKC activity by approximately 40% in RAW 264.7 macrophages alone or in combination with IFNγ (Table 4). The small increase in PKC activity observed with IFNγ was not significantly reduced by genestein. Genestein was also without effect upon TPA-stimulated PKC activity (Table 4).

Involvement of poly-ADP ribosylation pathways in NOS induction

Preincubation of cells for 6 h with increasing concentrations of nicotinamide inhibited both LPS- and IFNγ-induced NOS activity in RAW 264.7 macrophages (Figure 6). At concentrations above 20 mM, the response was abolished although the steep slope of the inhibition did not allow an accurate determination of the IC_{50} value. Also at higher concentrations (50 mM) a loss in cell viability and protein was observed. However, nicotinamide at a concentration of 20 mM, which reduced induced NOS activity in response to LPS by 60–70%, did not significantly affect LPS-stimulated PKC activity (LPS-stimulated activity % basal values; control = 183 ± 12, nicotinamide (20 mM) = 194 ± 16, $n = 2$).

Table 4 The effect of genestein on tetradecanoyl phorbol acetate (TPA)-, lipopolysacharride (LPS)- and interferon γ (IFNγ)-stimulated protein kinase C activity in RAW 264.7 macrophages

	DMSO	*Genestein*
Basal	308 ± 66	335 ± 56^{NS}
TPA	1014 ± 33	1088 ± 97^{NS}
LPS	797 ± 128	522 ± 78*
IFNγ	545 ± 138	398 ± 86^{NS}
LPS + IFNγ	833 ± 74	504 ± 83*

Cells were pretreated with vehicle or 100 μM genestine for 60 min and then stimulated with either 100 nM TPA, 1 μg ml^{-1} of LPS, 30 iuml^{-1} IFNγ or 1 ng ml^{-1} LPS + 10 iuml^{-1} IFNγ for a further 15 min. Each value (d.p.m.) represents the mean ± s.e.mean of five experiments performed in duplicate (NS – not significant; *significantly different from dimethylsulphoxide (DMSO) controls, $P<0.05$).

Involvement of Golgi protein transport processes in NOS induction

In cells pretreated for 60 min with brefeldin A, an inhibitor of Golgi protein transport, LPS-stimulated NOS activity was reduced by approximately 80% (Figure 7). The effect was maximal between 1–3 μg ml^{-1}, increasing the concentration of brefeldin A up to 50 μg ml^{-1} did not further reduce the LPS response (data not shown). Brefeldin A also inhibited the response to IFNγ alone or in combination with IFNγ with LPS but to a lesser degree. Increasing the concentration of brefeldin A did not further reduce NOS activity in response to LPS and IFNγ in combination.

Discussion

LPS induced NOS activity in RAW 264.7 macrophages in a time- and concentration-dependent manner. This response was potentiated by the presence of IFNγ. This effect coincided with an increase in the levels of a protein which was identified immunologically as the 130 kDa isoform of iNOS expressed in macrophages. The increased level of iNOS observed following LPS and IFNγ pretreatment is believed to be the result of increased rate of NOS transcription (Lorsbach *et al.*, 1993).

In RAW 264.7 macrophages the response to LPS was also dependent on the presence of serum in the culture medium and was inhibited by neutralising antibodies to CD14. This is consistent with the initial binding of LPS to a specific serum binding protein (Schumann *et al.*, 1990; Martin *et al.*, 1992; Schumann, 1992) which allows functional interaction with the putative LPS receptor CD14 (Wright *et al.*, 1990). It has been suggested that LPS may activate macrophages through interaction with other LPS receptor subtypes without the involvement of a serum binding protein (Lei *et al.*, 1988). However, a negligible increase in NOS activity was observed in response to LPS alone in the absence of serum. Replacement of the serum in cells deprived of serum for 12 h allowed a full response to LPS to be obtained, suggesting no down-

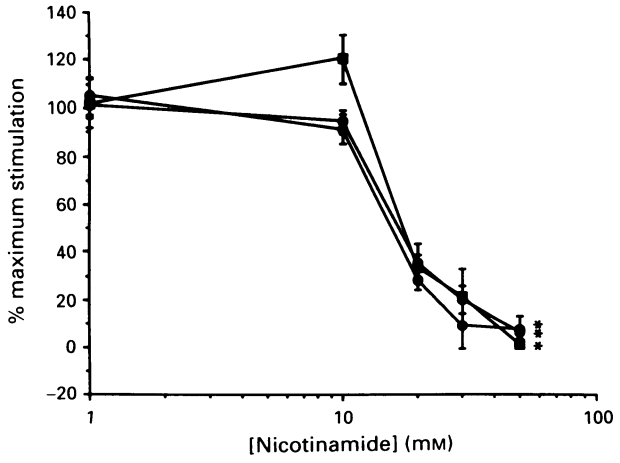


Figure 6 The effect of nicotinamide on lipopolysaccharide (LPS)- and interferon γ (IFNγ)-induced nitric oxide synthase (NOS) activity in RAW 264.7 macrophages. Cells were incubated for 6 h with increasing concentrations of nicotinamide before incubation with 1 μg ml^{-1} LPS (○), 30 iuml^{-1} IFNγ (■) or 1 ng ml^{-1} LPS + 10 iuml^{-1} IFNγ (●) for 8 h. Each value represents the mean ± s.e.mean. from 4 experiments performed in triplicate (*Significantly different from control, $P<0.05$).

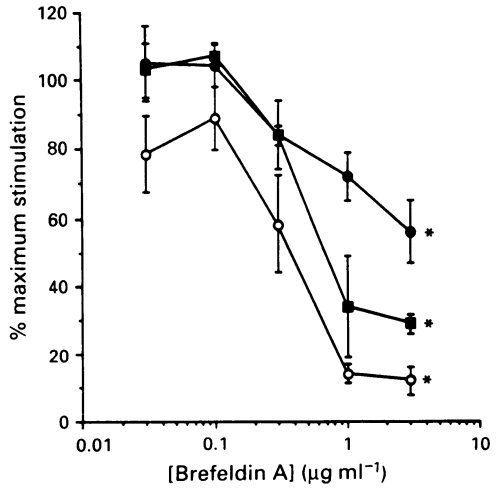


Figure 7 The effect of brefeldin A on lipopolysaccharide (LPS)- and interferon γ (IFNγ)-induced nitric oxide synthase (NOS) activity in RAW 264.7 macrophages. Cells were incubated with increasing concentrations of brefeldin A for 60 min before incubation with 1 μg ml^{-1} LPS (○), 30 iuml^{-1} IFNγ (■) or 1 ng ml^{-1} LPS + 10 iuml^{-1} IFNγ (●) for 8 h. Each value represents the mean ± s.e.mean. of 4 independent experiments performed in triplicate (*Significantly different from control, $P< 0.05$).

regulation of CD14 during the period of deprivation. In contrast, NOS induction in response to IFNγ was significantly potentiated by long term serum deprivation, suggesting possible up-regulation of the IFNγ receptor or cell signalling pathways activated by this cytokine.

However, we also found that the presence of serum was required for LPS to elicit a PKC response over the concentration-range observed for NOS induction; in serum-free conditions LPS stimulated a PKC response only at supramaximal concentrations. Although this suggests the requirement for a LPS binding protein as outlined above, we also found that serum alone stimulated PKC activity in RAW 264.7 macrophages. Thus, it is still unclear if LPS stimulates PKC *per se*, or as suggested previously by Rosen *et al.* (1989), facilitates the activation of PKC by other agents including serum.

In addition we found that LPS and IFNγ did not act in synergy with regards to PKC activation; the response to both agents in combination was additive. Although we cannot rule out activation of PKC isoforms such as PKCζ, which may not utilise the GS-peptide as an appropriate pseudosubstrate, these results suggest that the synergy observed between LPS and IFNγ at the level of NOS induction is likely to be due to the activation of another pathway. However, pretreatment with Ro-318220 abolished both LPS- and IFNγ-stimulated PKC and NOS activity, suggesting that the activation of PKC is an obligatory event in the regulation of NOS induction by both agents. A similar finding has been obtained with LPS-stimulated J774.2 macrophages (Severn *et al.*, 1992). Further, Sodhi and Kumar (1994) reported significant inhibition of NO production using LPS-stimulated murine peritoneal macrophages pretreated with the PKC inhibitors H-7 and chelerythrine chloride.

Activation of tyrosine kinase pathways is also involved in the regulation of NOS induction since genestein reduced the response to both LPS and IFNγ. This finding is in agreement with recent reports which show that in hepatocytes and aortic smooth muscle cells inhibitors of tyrosine phosphorylation also reduce LPS- or cytokine-induced NOS activity (Corbett *et al.*, 1993; Marczin *et al.*, 1993a). Pretreatment of the cells with the tyrosine phosphatase inhibitor sodium orthovanadate, did not affect either basal or cytokine-induced NOS activity suggesting that the inhibition of a tyrosine phosphatase is not involved in the induction process (results not shown). We also found that genestein reduced PKC activity in response to LPS alone or in combination with IFNγ. Genestein also marginally reduced IFNγ-stimulated PKC activity, although over several experiments this inhibition did not reach significance. However, genestein did not affect TPA-stimulation PKC activity suggesting that the activation of PKC by LPS is dependent on an initial tyrosine phosphorylation event. The absence of LPS-stimulated [^{3}H]-inositol phosphate accumulation or tyrosine phosphorylation of PLCγ in RAW 264.7 macrophages (unpublished results) implicates another phospholipid as the source of PKC activator and the involvement of another lipase such as phospholipase D or a phosphatidylcholine-specific phospholipase C.

Our results also implicate the involvement of a poly-ADP ribosylation pathway in the induction of NOS activity. We found that an inhibitor of endogenous poly-ADP ribosylations, nicotinamide, also inhibited LPS- and IFNγ-induced NOS activity. Similar findings have been observed in macrophages and fibroblasts (Haushildt *et al.*, 1991, 1992), suggesting an action of LPS on endogenous ADP ribosylation. In support of this hypothesis it has very recently been shown that LPS can stimulate the ADP-ribosylation of a number of proteins in macrophages (Pellat-Deceunynck *et al.*, 1994).

In addition we found that brefeldin A inhibited LPS- and IFNγ-induced NOS activity. Brefeldin A inhibits a nucleotide exchange factor present in Golgi membranes which stimulates GTP/GDP exchange on ADP ribosylation factor, a 21 kDa guanine nucleotide binding protein (Donaldson *et al.*, 1993; Helms and Rothman, 1993). ADP ribosylation factor (ARF) is known to catalyse the cholera toxin-mediated ADP ribosylation of the G-protein G_s and is involved in the action of enterotoxins (Moss and Vaughan, 1993). ARF has also been shown to be involved in the regulation of other signalling enzymes such as phospholipase D (Brown *et al.*, 1993). However, since brefeldin A may have actions upon protein trafficking which are not related to the inhibition of ARF activity, it remains to be determined if ARF or indeed a related ribosylation factor plays a role on the ADP-ribosylation observed in response to LPS.

In RAW 264.7 macrophages we found that brefeldin A or nicotinamide did not affect LPS-stimulated PKC activity, suggesting that PKC is acting upstream of, or parallel to, the ADP-ribosylation event. Recently, it has been shown that PKC is involved in the regulation of ARF binding to the Golgi complex (Antionetti De Matteis *et al.*, 1993). Thus, PKC may play a key role in the actions of LPS and IFNγ by regulating the activity of endogenous ADP ribosylation factors. It is possible that a tyrosine kinase pathway, in addition to regulating PKC, may be directly involved in the regulation of endogenous ADP-ribosylation factors.

In conclusion we have shown that multiple intracellular signalling events may be involved in the regulation of LPS- and INFγ-mediated induction of NOS in RAW 264.7 mouse macrophages. These include PKC, tyrosine kinase pathways and also the activation of an endogenous poly-ADP ribosylations factors.

We wish to thank Dr Anne Graham for critical reading of the manuscript. We wish to thank Dr I Varndell (Affiniti Research Products Ltd., Nottingham, England) for the kind gift of antibodies against NOS used in this study. We also wish to thank Dr G Lawton (Roche Products Ltd., Welwyn Garden City) for the kind gift of Ro-318220. This work was supported by grants from the Wellcome Trust. R.H.P. was a Wellcome Trust vacation scholarship student (1993).

References

ALEXANDER, D.R., GRAVES, J.D., LUCAS, S.C. & CANTRELL, D.A. (1990). A method for measuring protein kinase C activity in permeabilized lymphocytes by using peptide substrates. *Biochem. J.*, **268**, 303–308.

ANTONIETTA DE MATTEIS M., SANTINI G., KAHN, R.A., DI TOLLIO, G. & LUINI, A. (1993). Receptor and protein and kinase C regulation of ARF binding to the golgi complex. *Nature*, **364**, 818–821.

BROWN, A.H., GUTOWSKI, S., MOMAW, C.R., SLAUGHTER, C & STERNWEISS, P.C. (1993). ADP-ribosylation factor, a small GTP-dependent regulatory protein, stimulates phospholipase D activity. *Cell*, **75**, 1137–1144.

CORBETT, J.A., SWEETLAND, M.A., LANCASTER J.R. & MCDANIEL, M.L. (1993). A 1-hour pulse with IL-1β induces formation of nitric oxide and inhibits insulin secretion by rat islets of langerhans: evidence for a tyrosine kinase signalling mechanism. *FASEB. J.*, **7**, 369–374.

DAVIS, P., HILL, C.H., KEECH, E., LAWSON, G., NIXON, T.S., SEDGEWICK, A.D., WADSWORTH, S.E., WESTMACOTT, D. & WILKINSON, S.E. (1989). Potent selective inhibitors of protein kinase C. *FEBS Letts.*, **259**, 61–63.

DE LEAN, A., MUNSON, P.J. & RODBARD, D. (1980). Simultaneous analysis of a family of sigmoidal curves: application to bioassay and physiological dose response curves. *Am. J. Physiol.*, **235**, E97–E102.

DONALDSON, J.G., FINAZZI, D. & KLAUSNER, R.D. (1992). Brefeldin A inhibits golgi membrane-catalysed exchange of guanine nucleotide onto ARF protein. *Nature*, **360**, 350–352.

HAUSCHILDT, S., SCHEIPERS, P. & BESSLER, W.G. (1991). Inhibitors of (polyADP) polymerase suppress lipopolysaccharide-induced nitrite formation in macrophages. *Biochem. Biophys. Res. Commun.*, **179**, 865–871.

HAUSCHILDT, S., SCHEIPERS, P., BESSLER, W.G. & MULSCH, A. (1992). Induction of nitric oxide synthase in L929 cells by tumour necrosis factor α is prevented by inhibitors of poly(ADP-ribose) polymerase. *Biochem. J.*, **288**, 255–260.

HELMS, B.J. & ROTHMAN, J.E. (1992). Inhibition by brefeldin A of a Golgi membrane enzyme that catalyses exchange of guanine nucleotide bound to ARF. *Nature*, **360**, 352–354.

KAHN, R.A., YUCEL, J.K. & MALHOTRA, V. (1993). ARF signalling: A potential role for phospholipase D in membrane traffic. *Cell*, **75**, 1045–1048.

LEI, M.G. & MORISSON, D.C. (1988). Specific endotoxic lipopolysaccharide binding proteins on murine splenocytes. *J. Immunol.*, **141**, 996–1003.

LORSBACH, R.B., MURPHY, W.J., LOWENSTEIN, C.J., SNYDER, S.H. & RUSSELL, S.W. (1993). Expression of the nitric oxide synthase gene in mouse macrophages activated for tumor cell killing. *J. Biol. Chem.*, **268**, 1908–1913.

LYONS, R.C., ORLOFF, G.J. & CUNNINGHAM, J.M. (1992). Molecular cloning and functional expression of an inducible nitric oxide synthase from a murine macrophage cell line. *J. Biol. Chem.*, **267**, 6370–6374.

MARCZIN, N., PAPAPETROPOULOS, A. & CATRAVAS, J.D. (1993a). Tyrosine kinase inhibitors suppress endotoxin- and IL-1β-induced NO synthase in aortic smooth muscle cells. *Am. J. Physiol.*, **265**, H1014–1018.

MARCZIN, N., PAPAPETROPOULOS, A., JILLING, T. & CATRAVAS, J.D. (1993b). Prevention of nitric oxide synthase induction in vascular smooth muscle cells by microtubule depolymerising agents. *Br. J. Pharmacol.*, **109**, 603–605.

MARLETTA, M.A. (1993). Nitric oxide synthase-structure and mechanism. *J. Biol. Chem.*, **268**, 12331–12234.

MARTIN, T.R., MATHISON, J.C., TOBIAS, P.S., LETURCQ, D.J., MORIARTY, A.M., MAUNDER, R.J. & ULEVITCH, R.J. (1992). Lipopolysaccharide binding protein enhances the responsiveness for alveolar macrophages to bacterial lipopolysaccharide. *J. Clin. Invest.*, **90**, 2209–2219.

MITCHELL, J.A., KOLHAAS, K.L., MATSUMOTO, T., POLLOCK, J.S., FORSTERMANN, U., WARNER, T.D., SCHMIDT, H.H.W. & MURAD, F. (1992). Induction of NADPH-dependent diaphorase and nitric oxide synthase activity in aortic smooth muscle and cultured macrophages. *Mol. Pharmacol.*, **41**, 1163–1168.

MOSS, J. & VAUGHAN, M. (1993). ADP-ribosylation factors, 20 000 Mr guanine nucleotide-binding protein activators of cholera toxin and components of intracellular vesicular transport systems. *Cell Signalling*, **5**, 367–379.

PELLAT-DECEUNYNCK, C., WIETZERBIN, J. & DRAPIER, J-C. (1994). Nicotinamide inhibits nitric oxide mRNA induction in activated macrophages. *Biochem. J.*, **297**, 53–58.

POLLOCK, J.S., FORSTERMANN, U., MITCHELL, J.A., WARNER, T.D., SCHMIDT, H.H.H.W., NAKANE, M. & MURAD, F. (1991). Purification and characterisation of particulate endothelium-derived relaxing factor synthase from cultured and native bovine aortic endothelial cells. *Proc. Natl. Acad. Sci. USA*, **88**, 10480–10484.

ROSEN, A., NAIRN, A.C., GREENGARD, P., COHN, Z.A. & ADEREM, A. (1989). Bacterial lipopolysaccharide regulates the phosphorylation of the 68 kDa protein substrate in macrophages. *J. Biol. Chem.*, **264**, 9118–9121.

SCHUMANN, R.R. (1992). Function of Lipopolysaccharide (LPS)-binding protein (LBP) and CD14, the receptor for LPS/LBP complexes: a short review. *Res. Immunol.*, **143**, 11–15.

SCHUMANN, R.R., LEONG, S.R., FLAGGS, G.W., GRAY, P.W., WRIGHT, S.D., MATHISON, J.C., TOBIAS, P.S. & ULEVITCH, R.J. (1990). Structure and function of lipopolysaccharide binding protein. *Science*, **249**, 1429–1431.

SEVERN, A., WAKELAM, M.J.O. & LIEW, F.Y. (1992). The role of protein kinase C in the induction of nitric oxide synthase by murine macrophages. *Biochem. Biophys. Res. Commun.*, **188**, 997–1002.

SODHI, A. & KUMAR, R. (1994). Production of nitric oxide and its regulation in murine peritoneal macrophages treated with cis-platin and lipopolysaccharide. *Int. J. Immunopathol. Pharmacol.*, **7**, 65–77.

WEINSTEIN, S.L., SANGHERA, J.S., LEMKE, K., DEFRANCO, A.L. & PELECH, S.L. (1992). Bacterial lipopolysaccharide induces tyrosine phosphorylation and activation of mitogen-activated protein kinases in macrophages. *J. Biol. Chem.*, **267**, 14955–14963.

WRIGHT, S.D., RAMOS, R.A., TOBIAS, P.S., ULEVITCH, R.J. & MATHISON, J.C. (1990). CD14, a receptor for complexes of lipopolysaccharide (LPS) and LPS binding protein. *Science*, **249**, 1431–1433.

(Received April 7, 1994
Revised September 19, 1994
Accepted September 21, 1994)

British Journal of Pharmacology (1995) 114, 489–495 © 1995 Stockton Press All rights reserved 0007–1188/95 $9.00

Inhibition by wortmannin of M-current in bullfrog sympathetic neurones

[1]Takayuki Tokimasa, *Masaaki Ito, ††Mark A. Simmons, ††Carla R. Schneider, †Toshio Tanaka, *Takeshi Nakano & Takashi Akasu

Department of Physiology, Kurume University School of Medicine, Kurume 830, Japan, *Department of Internal Medicine, †Department of Cellular and Molecular Pharmacology, Mie University School of Medicine, Tsu 514, Japan and ††The Neuropharmacology Laboratory, Department of Pharmacology, Marshall University School of Medicine, Huntington, West Virginia 25755-9310, U.S.A.

1 The actions of wortmannin, an inhibitor of myosin light chain kinase (MLCK), on M-type potassium current of dissociated bullfrog sympathetic neurones have been examined.

2 The amplitude of M-current was measured by whole cell recordings from cells pretreated with wortmannin (0.01–10 μM) or the wortmannin vehicle, dimethylsulphoxide (0.0001–0.1 vol%), for 30 min. Internal (recording pipette) solutions having three different pCa values (6, 7 and 8) were used for the measurements.

3 Irrespective of the pCa, M-current was not detectable when the cells were pretreated with 10 μM wortmannin. Wortmannin, 3 μM, produced 85–95% inhibition of the M-current. Pretreatment with 10–30 nM wortmannin was without effect on M-current.

4 The M-current inhibition by wortmannin at concentrations of 0.1–1 μM depended on the pCa of the internal solution. Inhibition occurred only when the calcium-rich (pCa = 6) internal solution was used.

5 Pre-treatment of the cells with wortmannin (10 μM) did not affect rapidly-inactivating A-type or delayed rectifier-type potassium currents nor did it alter inwardly rectifying sodium-potassium current (I_H).

6 These observations show that M-current inhibition by wortmannin has two pharmacological profiles. One is calcium-dependent and occurs at lower concentrations (0.1–1 μM), and is attributed to inhibition of MLCK by wortmannin. At higher concentrations (3–10 μM), wortmannin has an additional, calcium-independent action, inhibiting the M-current by an unknown mechanism.

Keywords: Wortmannin; myosin light chain kinase; calmodulin; potassium current; autonomic neurones

Introduction

The M-current is a potassium current originally described in bullfrog sympathetic ganglion cells (Brown & Adams, 1980). The current is a non-inactivating outward current at potentials less negative than − 65 mV. Acetylcholine released from presynaptic nerve terminals inhibits M-current via muscarinic receptors, thereby increasing the excitability of the cell membrane. We have recently provided evidence suggesting that phosphorylation of myosin catalyzed by myosin light chain kinase (MLCK) acts to increase the amplitude of the M-current (Tokimasa & Akasu, 1991; Akasu *et al.*, 1993).

The goal of the present study was to obtain further evidence for the MLCK-dependence of the M-current by use of a microbial product, wortmannin, recently identified as an inhibitor of MLCK (Nakanishi *et al.*, 1992; Yano *et al.*, 1993). During the course of our experiments, wortmannin was reported to have the additional effect of inhibiting phosphatidylinositol 3-kinase with an IC_{50} value approximately 100 times lower than that for MLCK (Yano *et al.*, 1993). Hence, we have also examined whether the observed actions of wortmannin on M-current could result from its ability to inhibit phosphatidylinositol 3-kinase.

Three main approaches were adopted. First, cells were pretreated with wortmannin (0.1–10 μM) for 30 min and then subjected to whole-cell recordings of M-current. Second, internal (pipette) solutions having three different concentrations of free calcium ions were used for measuring the M-current amplitude. A calcium-rich (free calcium, 1 μM) solution was used to activate the calmodulin/MLCK-complex fully (Olwin *et al.*, 1984; Yazawa *et al.*, 1987). A calcium-deficient (free calcium, 10 nM) solution was used to test whether wortmannin has actions unrelated to calcium/calmodulin/MLCK-dependent processes. Another internal solution (free calcium, 100 nM) was used to compare the results in the present study with those reported for the actions of a peptide inhibitor, MLCK(783-804), on the M-current (Akasu *et al.*, 1993). For the third approach, wortmannin was applied directly to single cells while recording the M-current so that the acute actions of the drug could be observed.

These experiments have revealed two distinct effects of wortmannin on M-type potassium current. Some of our observations are consistent with our working hypothesis that wortmannin can inhibit the M-current by inhibiting MLCK. However, we will also provide evidence suggesting that wortmannin has a second, though quite selective inhibitory effect on the M-current, perhaps by exerting a direct blocking action at the M-channel.

Methods

Tissue culture

Dissociated bullfrog sympathetic neurones were incubated in a culture medium for 2–7 days as described previously (Tokimasa & Akasu, 1990a,b). The cells were resuspended in Ringer solution 2 h before electrophysiological experiments. This solution had the following composition (mM): NaCl 128,

[1] Author for correspondence at present address: Glaxo Institute for Molecular Biology, 14, chemin des Aulx-Case postale 674, 1228 Plan-les-Ouates, Geneva, Switzerland.

KCl 2.4, $CaCl_2$ 1.8, $MgCl_2$ 1.8 and HEPES 10 (pH adjusted with NaOH to 7.4).

Pretreatment of the cells with wortmannin

For pretreatment with wortmannin, the cells were resuspended in Ringer solution for 1.5 h then transferred to a Ringer solution containing wortmannin (0.01–10 μM) for 30 min. For the 24 h pretreatment, wortmannin (10 μM) was added to the culture medium 22 h before the cells were resuspended in Ringer solution. The cells were then resuspended for 2 h in a Ringer solution which contained wortmannin (10 μM). Following either of the above pretreatments, the cells were pipetted into the recording chamber then continuously superfused with Ringer solution containing no added wortmannin and 10–90 min later, electrophysiological experiments started. The superfusate always contained tetrodotoxin (3 μM) to block the inward sodium current.

Whole-cell recordings

Membrane currents were recorded in the whole-cell configuration with methods described previously (Simmons *et al.*, 1990; Tokimasa & Akasu, 1990a,b,c). The tip resistance of glass pipettes was 0.8–1.2 MΩ when filled with the pipette (internal) solution. A sample-and-hold/voltage-clamp amplifier (Axoclamp 2A, Axon Instruments) was used in most experiments (sampling rate, 9–11 kHz). Another amplifier (Axopatch 1C, Axon Instruments) was also used in a limited number of experiments. In either case liquid junction potentials between internal and external solutions have been corrected. Axodata 1.14 (Axon Instruments) and an ITC-16 interface (Instrutech) were used for data acquisition. Axograph 2.0 (Axon Instruments) and Sigmaplot 4.14 (Jandel) were used for analyzing the data. A single-cell superfusion system was used for direct applications of wortmannin during whole cell recordings. Wortmannin was applied intracellularly by inclusion in the pipette solution as described previously (Simmons *et al.*, 1990; Akasu *et al.*, 1993).

Internal solutions

Five different pipette (internal) solutions were used for measuring the amplitude of M-current. A 'normal calcium, plus calmodulin' solution had the following composition (mM): KCl 120, $MgCl_2$ 2.5, $CaCl_2$ 0.32, BAPTA 1, Na_2ATP 1.15, Na_2GTP 1.5, HEPES 10 and calmodulin 0.001 (Akasu *et al.*, 1993). The pCa was estimated as 7.0 (Godt & Lindley, 1982). The concentration of $CaCl_2$ was increased to 0.826 mM (pCa = 6.0) for preparing a 'calcium-rich, plus calmodulin' solution. The activity of the calcium/calmodulin/MLCK-complex should be maximal with this internal solution (Olwin *et al.*, 1984; Yazawa *et al.*, 1987). A 'normal calcium' solution was the same as the 'normal calcium, plus calmodulin' solution, but with calmodulin omitted. A 'calcium-deficient' solution was the same as the 'normal calcium' solution, but with concentration of $CaCl_2$ reduced from 0.32 mM to 0.045 mM, giving a calculated pCa of 8.0. An 'ATP-free' solution contained 5'-adenylylimidodiphophate (ANP-PNP) in place of 1.15 mM ATP, but no added $CaCl_2$ or calmodulin. The pH of the internal solutions was adjusted with KOH to 6.8.

M-current

M-type relaxations on the current trace were detected by use of two different protocols (see Akasu *et al.*, 1993). First, the M-current was continuously deactivated by setting a holding potential at − 65 mV. The cells were subjected to 5 different step commands starting from − 35 mV with − 10 mV increments every 4 s. Total duration of the steps was 0.5 s. The peak amplitude of the deactivating tails was measured upon stepping back to − 65 mV. Second, M-current was continuously activated at a holding potential of − 35 mV then briefly (0.5 s) deactivated during 6 different step commands starting from − 45 mV with − 15 mV increments every 5–6 s. The peak amplitude of the deactivating M-current tail was measured upon steps to − 60 mV.

A-current

The amplitude of the A-current was measured using conventional digital subtraction techniques as described previously (Tokimasa *et al.*, 1991; Akasu *et al.*, 1993). A- and M-currents were activated upon steps from − 100 mV to − 30 mV and M-current alone was activated upon steps from − 45 mV to − 30 mV.

Delayed rectifier potassium current

This potassium current was recorded by superfusing the cells with a modified Ringer solution of the following composition (mM): choline chloride 124, KCl 2.4, $BaCl_2$ 1.8, $MgCl_2$ 1.8, $CdCl_2$ 0.1, CsCl 2, 4-aminopyridine 3, scopolamine 0.0001 and HEPES 10 (pH adjusted with CsOH to 7.4) (Tokimasa *et al.*, 1993). Scopolamine was used to prevent muscarinic receptors from being activated by choline. The peak amplitude of the delayed rectifier was measured upon steps from − 120 mV to + 50 mV (Akasu *et al.*, 1993; Tokimasa *et al.*, 1993).

H-current

The cells were superfused with a potassium-rich (22.4 mM) Ringer solution to increase the amplitude of this inwardly rectifying sodium-potassium current (H-current or I_H: Tokimasa & Akasu, 1990a; Tokimasa *et al.*, 1990). I_H was activated during hyperpolarizing step commands (15–60 mV, 3 s) from the holding potential of − 50 mV. The amplitude of I_H was measured at the end of 3 s-pulses to − 110 mV. In cells which had not been pretreated with wortmannin (10 μM) for 24 h, the superfusate contained $BaCl_2$ (1.8 mM) to eliminate M-current since otherwise both I_H activation and M-current deactivation occur simultaneously upon steps from − 50 mV (Tokimasa & Akasu, 1990a).

MLCK activity

MLCK from chicken gizzard and calmodulin from bovine brain were purified as described previously (Walsh *et al.*, 1983; Ikebe *et al.*, 1987). The 20 kD light chain of myosin (LC20) was purified by the method of Hathaway & Haeberle (1983). The activity of MLCK was monitored using LC20 at 0.4 mg ml^{-1} in 30 mM Tris/HCl (pH 7.5) which contained 0.1 mM [γ-^{32}P]-ATP (DuPont-New England Nuclear), 1 mM $MgCl_2$, 30 mM KCl, 0.1 mM $CaCl_2$, 1 μg ml^{-1} calmodulin and 0.5 μg ml^{-1} MLCK (Walsh *et al.*, 1983). The specific activity of MLCK was measured at least three different times between 0.5 and 1.5 min after the start of the reaction.

Drugs

Drugs used were the disodium salt of adenosine 5'-triphosphate (Sigma), 4-aminopyridine (Sigma), lithium salt of 5'-adenylylimidodiphophate (Sigma), calmodulin obtained from bovine testes (Biomedical Technologies), guanosine 5'-triphosphate sodium salt (Sigma), scopolamine hydrochloride (Sigma), tetrodotoxin (Wako Pure Chemicals) and wortmannin isolated from the fungal strain *Penicillium fumiculosum* (Sigma). Wortmannin was dissolved in dimethylsulphoxide (Sigma) then stored at − 35°C. This stock solution (10 mM) was diluted first with Ringer solution by a factor of 10 then diluted further with Ringer solution to achieve the final concentration of the drug in the superfusate between 0.01 and 3 μM. The stock solution (10 mM) was diluted directly

with normal or modified Ringer solution for solutions containing wortmannin (10 μM).

Experiments were carried out at room temperature (22–24°C) under ordinary fluorescent lighting. Statistics are expressed as mean ± s.e.mean for the cells tested.

Results

Effects of wortmannin on MLCK activity

Wortmannin used in the present study has been isolated from the fungal strain *Penicillium fumiculosum* (see Methods). The drug (0.01–10 μM) was incubated with a reaction mixture lacking ATP for 3, 10 or 30 min. The phosphorylation reaction was initiated by adding [γ-^{32}P]-ATP. As shown in Figure 1, wortmannin is an effective inhibitor of MLCK. The ability of wortmannin to inhibit MLCK activity depended on both concentrations of the drug (0.1–10 μM) and the pre-incubation time (3–30 min). The IC_{50} for the wortmannin effect on MLCK was 0.09 μM with a 30 min pre-incubation. Higher IC_{50} values were obtained for the 10 min pre-incubation (0.2 μM) and the 3 min pre-incubation (0.9 μM). The presence of a higher concentration of calmodulin (50 μg ml^{-1}) in the reaction mixture did not significantly alter the actions of wortmannin on MLCK activity (data not shown). These results are consistent with recent observations with wortmannin obtained from *Talaromyces wortmannin* (Nakanishi *et al.*, 1992).

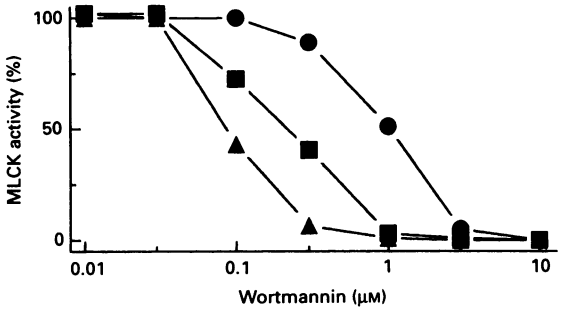


Figure 1 Dose-response curves for the actions of wortmannin on myosin light chain kinase (MLCK)-activity. Ordinate scale denotes the specific activity of MLCK with respect to its control value measured in the absence of wortmannin. Pre-incubation times were 3 min (●); 10 min (■) and 30 min (▲).

The effects of Ca^{2+} and calmodulin on M-current

M-current was recorded from cells which had not been pre-treated with wortmannin. Recordings were made first with the 'normal calcium, plus calmodulin' internal solution (pCa = 7, 1.15 μM ATP and 1 μM calmodulin present). Figure 2a shows an example of recordings obtained from one of 35 cells tested. As has been demonstrated previously (Adams *et al.*, 1982; Akasu *et al.*, 1993), the relaxation during the voltage step command, and that occurring after the termination of the command represent the activating ('on') M-current at − 35 mV followed by its deactivating tail current at − 65 mV, respectively. Consistent with previous observations that the M-current is not activated at potentials

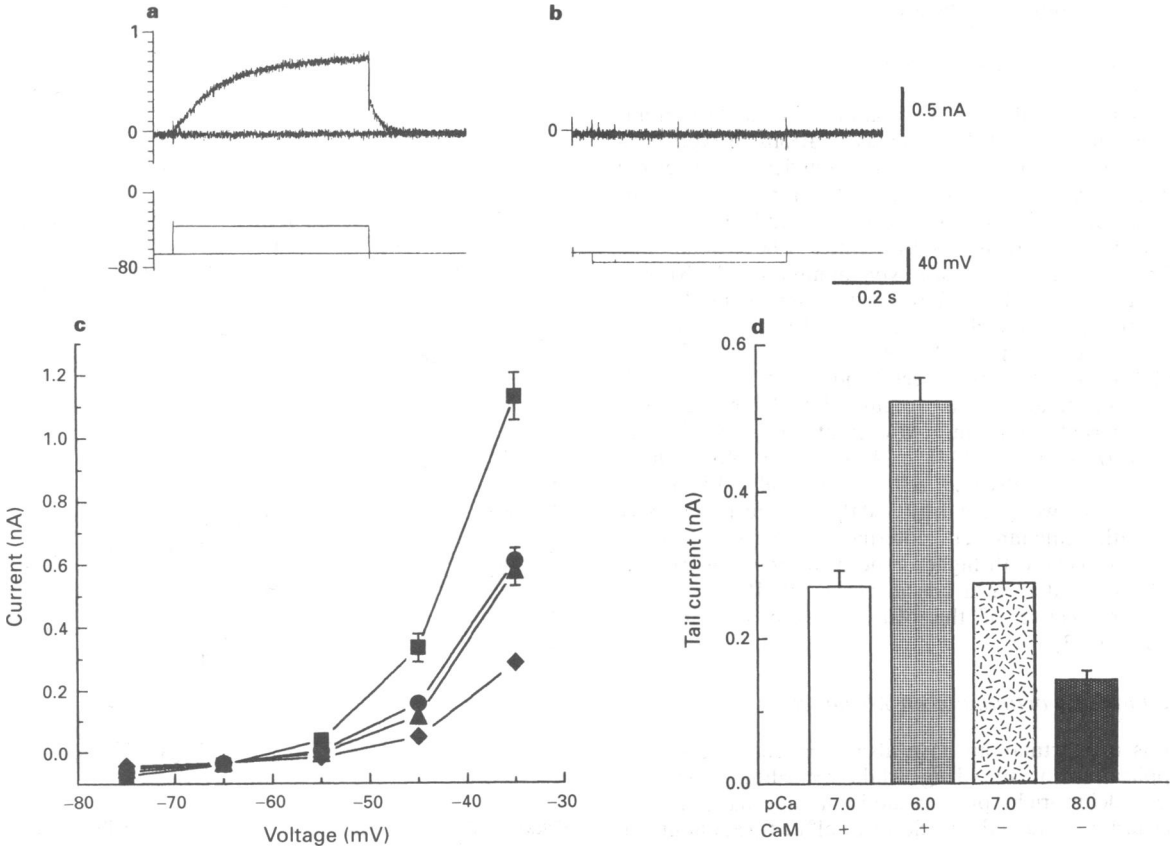


Figure 2 M-current in control cells. (a) Two superimposed current traces (top) are holding current at − 65 mV and M-type relaxations in response to a depolarizing step command (30 mV, 0.5 s) from the holding potential of − 65 mV. Ohmic current in response to a hyperpolarizing step command (10 mV, 0.5 s) is superimposed on the holding current in (b). (c)-(d) Results are based on pooled data. Four *I–V* curves in (c) were obtained using internal solutions termed the 'normal calcium (pCa = 7), plus calmodulin' solution (●, $n = 35$), the 'calcium-rich (pCa = 6), plus calmodulin' solution (■, $n = 21$), the 'normal calcium (pCa = 7)' solution (▲, $n = 8$) and the 'calcium-deficient (pCa = 8)' solution (◆, $n = 22$). (d) Amplitude histogram for the M-current tail upon stepping back from − 35 to − 65 mV. From left to right are the results with these four different internal solutions. CaM + on the abscissa scale denotes plus calmodulin in the internal solution.

negative to − 65 mV (Adams *et al.*, 1982), the current response during the hyperpolarizing step was essentially ohmic and of very small amplitude (Figure 2b). Depolarizing step commands to − 55 mV as well as to − 45 mV (pulse duration was 0.5 s for both commands) were also used to observe M-type relaxations. The amplitude of the 'on' current was measured at the end of step commands (between − 35 mV and − 75 mV in 10 mV-increments) then plotted as a function of the membrane potential at which it was measured, which gave current-voltage ($I-V$) curve between − 75 and − 35 mV. Results obtained from 35 cells are summarized in Figure 2c. The averaged peak amplitude of the tail current was 271 ± 22 pA ($n = 35$) upon stepping back from − 35 mV to the holding potential of − 65 mV (Figure 2d). In all cells, whole-cell recordings started about 3 min after the patch break and results were obtained during the next 2–5 min.

Essentially the same experiments as with the 'normal calcium, plus calmodulin' internal solution were repeated on 55 other cells using four other internal solutions (see Methods). Results are summarized in Figure 2c for the $I-V$ curve and Figure 2d for the tail current amplitude. The averaged peak amplitude of the tail current was 523 ± 32 pA ($n = 21$) with the 'calcium-rich, plus calmodulin' solution, 275 ± 24 pA ($n = 8$) with the 'normal calcium' solution and 143 ± 12 pA ($n = 22$) with 'calcium-deficient' solution upon stepping back from − 35 mV to the holding potential of − 65 mV. An unpaired t test shows that these values are significantly different from each other at the 5% level. In all 4 cells tested, the peak amplitude of the tail current was almost zero pA when measured with the 'ATP-free' internal solution, consistent with previous observations that M-current undergoes a rapid run-down when the internal solution does not contain a hydrolyzable form of ATP (Pfaffinger, 1988; Tokimasa & Akasu, 1991c; Simmons & Schneider, 1993).

M-current in cells pretreated with wortmannin

Figure 3 shows the effect of wortmannin on the M-current. Pretreatment of cells with lower concentrations of wortmannin (0.01–0.03 μM) for 30 min did not significantly affect the amplitude of the M-current. In 'calcium-rich, plus calmodulin' internal solution, the peak amplitude of the tail current in cells pretreated with vehicle (0.03 vol%) was 285 ± 35 pA ($n = 12$) and with wortmannin (0.03 μM) was 596 ± 53 pA ($n = 23$); this difference was significant. Vehicle alone had no significant effect. In 'normal calcium' internal solution the peak amplitude of the tail current was 226 ± 25 pA ($n = 5$) for vehicle cells and 202 ± 33 pA ($n = 8$) for wortmannin-treated cells (Figure 3c). With 'calcium-deficient' internal solution, M-current amplitude were 147 ± 19 pA ($n = 10$) and 146 ± 24 pA ($n = 6$) for vehicle cells and wortmannin-treated cells, respectively (Figure 3). Thus, the effect of wortmannin (0.3 μM) on M-current is only manifest with calcium-rich internal solutions. Finally, pretreatment of cells with higher concentrations of wortmannin (3–10 μM) resulted in a considerable (90–100%) loss of M-current irrespective of the pCa values of the internal solution (Figure 3).

Acute actions of wortmannin on M-current

The actions of wortmannin have also been observed during direct application of the drug while recording M-current using the 'calcium-rich, plus calmodulin' internal solution. The superfusate contained vehicle (0.1 vol%) throughout the experiments. Wortmannin was added to the superfusate approximately 180 s after the patch break and continued for another 600 s. Results obtained from these experiments are summarized in Figure 4 in which the currents were normalized to the maximum M-current for that particular cell. The average amplitude of the tail current at − 60 mV was 450 ± 60 pA when measured 2 min after the patch break ($n = 33$). In the absence of wortmannin, the M-current exhibited a slight run down with time. The run-down of M-current was much more rapid in the presence of wortmannin. When cells were superfused with 10 μM wortmannin, the M-current gradually disappeared over a 16 min recording period. At a concentration of 0.3 μM, wortmannin inhibited the M-current by an average of 60% over 16 min (Figure 4).

Wortmannin was also applied directly to the cell interior using the intracellular dialysis technique, via the patch pipette. (See Methods). Somewhat surprisingly, wortmannin (10 μM) which eliminates the M-current when applied extracellularly had no effect on M-current when applied intracellularly (Figure 4). Two-way analysis of variance showed that

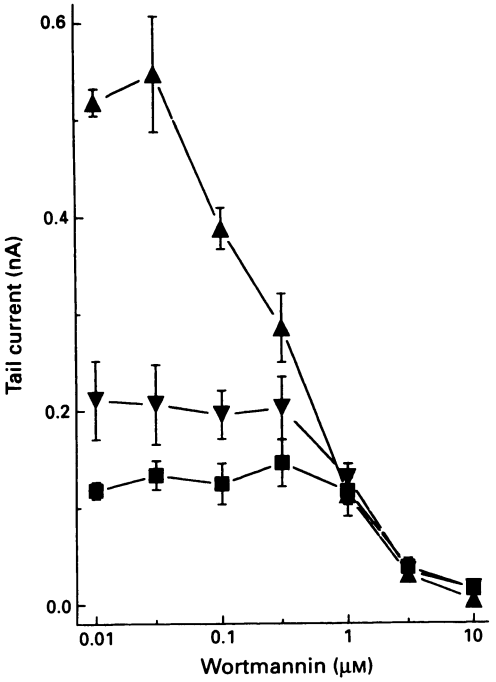


Figure 3 M-current inhibition by wortmannin. Results are based on pooled data ($n = 4–16$ cells at each concentration) obtained from cells pretreated with wortmannin (0.01–10 μM) for 30 min. Dose-response curves for the actions of wortmannin on the M-current tail at − 65 mV in 'calcium-rich, plus calmodulin' internal solution (▲), 'normal calcium' internal solution (▼) and 'calcium-deficient' internal solution (■).

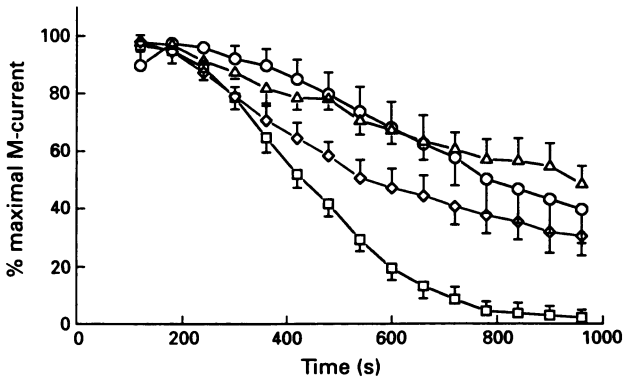


Figure 4 Effects of acute extracellular or intracellular application of wortmannin on M-current. The amplitude of the tail current (at − 60 mV, see Methods) were normalized so that the current recorded 120 s after patch break (abscissae) was set to 100%. Wortmannin was added to either the superfusate or the internal solution approximately 180 s after the patch break. The application was discontinued after another 600 s. Control cells (○, $n = 6$); 10 μM wortmannin in the internal solution (△, $n = 11$); 0.3 μM wortmannin added to the superfusate (◆, $n = 9$) and 10 μM wortmannin added to the superfusate (□, $n = 7$). Symbols show mean ± s.e.mean.

there is a statistically significant effect of both time ($P<0.001$) and wortmannin concentration ($P<0.003$). The effect of 10 μM wortmannin applied extracellularly was significantly different from the effect of either zero or 10 μM wortmannin applied intracellularly.

A-current and delayed rectifier current

The amplitude of A-type and delayed rectifier-type potassium currents was measured from cells pretreated with wortmannin (10 μM) or vehicle (0.1 vol%) alone, for 30 min (see Methods). The 'calcium-rich, plus calmodulin' internal solution was used.

The peak amplitude of A-current at −30 mV was 713 ± 81 pA ($n = 11$) and 617 ± 63 pA ($n = 6$), for control and wortmannin-treated cells, respectively (Figure 5a–c). The peak amplitude of delayed rectifier at +50 mV was 13.9 ± 2.2 nA ($n = 9$) and 15.9 ± 2.6 nA ($n = 7$) for the control and the wortmannin-treated cells, respectively (Figure 5d and 5e). Thus, wortmannin (10 μM) was without effects on these potassium currents, even when calcium-rich internal solutions are used.

Cyclic AMP-dependent H-current

Bullfrog sympathetic neurones also possess a cyclic AMP-dependent cationic inward rectifier current termed I_H

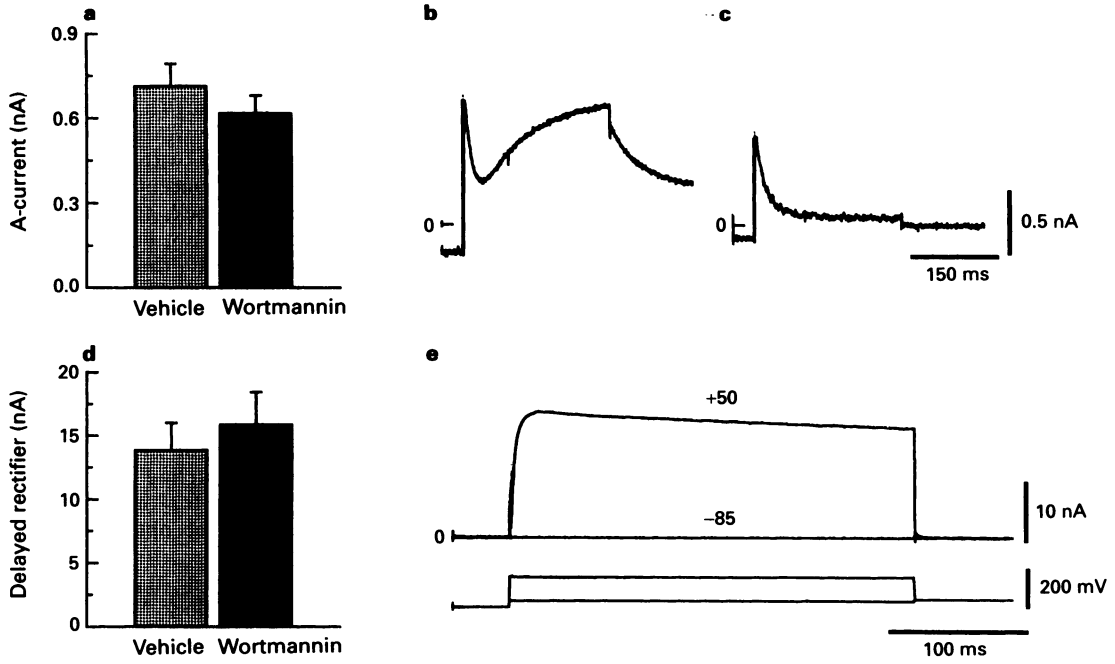


Figure 5 Lack of effect of wortmannin on A-current and delayed rectifier current. Pooled results are shown in (a) and (d). (a) The amplitude of A-current at −30 mV. Sample recordings are shown in (b) for a vehicle-treated cell and in (c) for a wortmannin-treated cell. Note the absence of M-current in the wortmannin-treated cell. (d) The peak amplitude of delayed recitifier at +50 mV. A sample recording for a wortmannin-treated cell is shown in (e). Ohmic current at −85 mV is also shown in this record. Above: current; below: voltage.

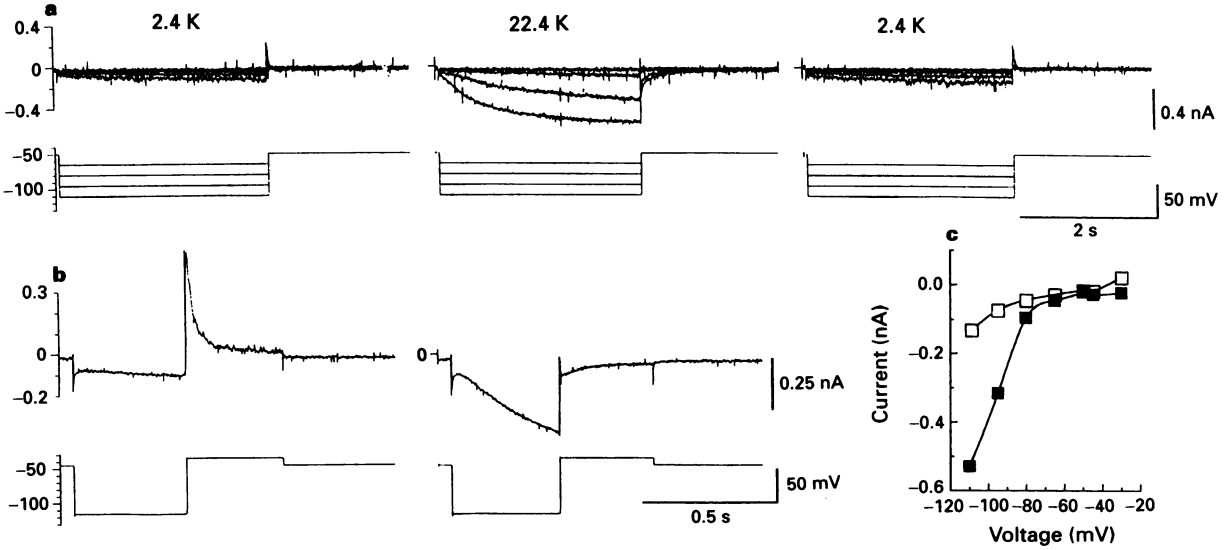


Figure 6 H-current of a cell pretreated with wortmannin (10 μM) for 24 h. (a) From left to right are: H-current with the concentration of KCl in the superfusate at 2.4, 22.4 and 2.4 mM. Above: current; below: voltage. Holding potential was −50 mV. (b) A mixture of A-current and H-current. Left: 2.4 mM KCl; right: 22.4 mM KCl. Above: current; below: voltage. (c) Current-voltage curves in 2.4 mM KCl (□) and 22.4 mM KCl (■). The amplitude of membrane current was measured at the end of 3 s-step pulses such as that shown in (a).

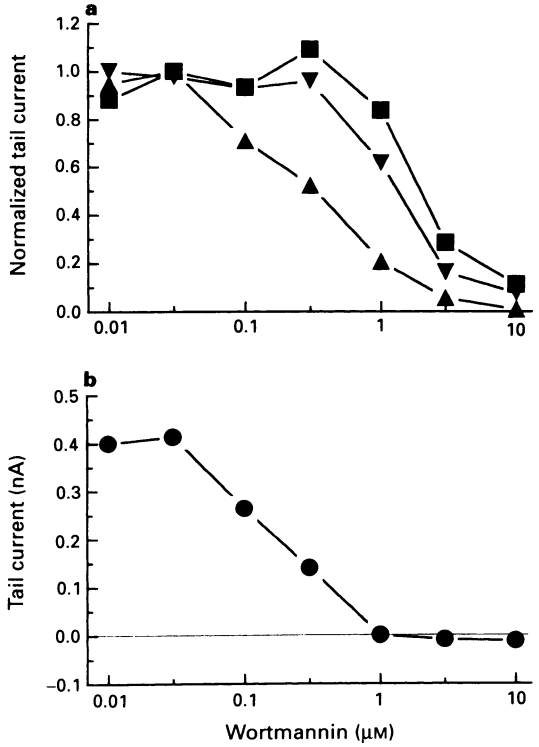


Figure 7 Plot of wortmannin effects with different intracellular calcium concentrations. Data points are based on those in Figure 3. (a) The dose-response curves for the three different internal solutions shown in Figure 3a have been normalised according to the maximum current amplitude: (▲) 'calcium-rich, plus calmodulin' solution; (▼) 'normal calcium' solution and (■) 'calcium-deficient' solution. (b) The amplitudes of the tail current measured with the 'calcium-deficient' internal solution (■ in Figure 3) was subtracted from that measured with the 'calcium-rich, plus calmodulin' internal solution (▲ in Figure 3).

(Tokimasa & Akasu, 1990a,c; Tokimasa *et al.*, 1990). In order to test any potential effects of wortmannin on cyclic AMP-dependent protein kinase, I_H was measured from cells pretreated with wortmannin (10 μM) ($n = 9$) or vehicle (0.1 vol%) ($n = 6$) for 24 h. The 'calcium-rich, plus calmodulin' internal solution was used. I_H averaged 574 ± 49 pA ($n = 9$) when measured at the end of 3 s-pulses to − 110 mV, in cells pretreated with wortmannin (Figure 6a). This was not significantly different ($P < 0.05$, unpaired t test) from I_H in cells pretreated with vehicle alone (510 ± 78 pA, $n = 6$) (see Tokimasa & Akasu, 1990a). Figure 6b also shows that A-current can be recorded even after the 24 h pretreatment of the cells with wortmannin (see Figure 5c).

Discussion

We have demonstrated that the M-current is larger when measured with a calcium-rich (free calcium at 1 μM) internal solution, than when measured with solutions containing free calcium ions between 10 and 100 nM. We have also demonstrated that wortmannin (0.1–1 μM) inhibits this calcium-activated portion of the M-current. These observations can be interpreted as further supporting our argument that a calcium-dependent process positively modulates M-current (Akasu *et al.*, 1993) and that this modulation is inhibited by relatively lower concentrations of wortmannin, presumably as a result of MLCK inhibition.

At higher concentrations (3–10 μM), however, wortmannin inhibits M-current irrespective of the pCa values for the internal solutions (Figure 3). We have considered two possibilities for the calcium-independent effect. First, calcium may modulate the sensitivity of MLCK to wortmannin in such a manner that MLCK is more sensitive to wortmannin when tested with calcium-rich internal solutions than when tested with calcium-deficient solutions. If this were the case, we would expect the wortmannin dose-response curve shown in Figure 3a to shift to the right as the intracellular concentration of calcium ions is decreased. To compare the wortmannin dose-response curves for three different concentrations of free calcium ions, the data points in Figure 3a have been re-plotted in Figure 7a so that the ordinate scale now represents the relative amplitude of the M-current. The estimated IC_{50} values of wortmannin are 0.33 μM, 1.1 μM and 2.8 μM for concentrations of free calcium in the internal solution at 1 μM, 100 nM, 100 nM and 10 nM, respectively. The main problem with this interpretation is that the slope of the curve with 1 μM of free calcium ions differs from that for 10 and 100 nM. This difference suggests that different mechanisms may be involved in mediating the actions of wortmannin at different free calcium concentrations.

The other possibility is that wortmannin has a direct M-channel blocking activity at the higher concentrations. In this case we would conclude that the wortmannin-induced inhibition of the M-current detected with the internal solution containing lower (10–100 nM) concentrations of free calcium ions is due to direct channel block, and that wortmannin at concentrations below 1 μM does not have this channel blocking activity. This implies that the dose-response curve indicated by the upward triangles (free calcium at 1 μM) in Figure 3a is a sum of two dose-response curves, one for calcium-dependent and the other for calcium-independent actions of wortmannin. The calcium-independent actions of wortmannin should be represented by the dose-response curve indicated by the square symbols in Figure 3a. By taking the dose-response curve for the concentration of free calcium ions at 1 μM and subtracting the calcium-dependent actions, a dose-response curve for the calcium-independent actions of wortmannin should be obtained. This subtracted curve is plotted in Figure 7b.

Possible mechanisms underlying the inability of intracellularly applied wortmannin to block M-current remain to be clarified. For example there is no evidence suggesting that MLCK has transmembrane structure, such as that occurring for adenylate cyclase (see Hartzell & Fischmeister, 1987; Hartzell & Budnitz, 1992).

Nonomura and his co-workers have reported that, in addition to affecting MLCK, wortmannin (10–30 nM) inhibits phosphatidylinositol 3-kinase (PI3-kinase) to less than 20% of its control activity, while leaving MLCK activity almost unaffected (Nakanishi *et al.*, 1992; Yano *et al.*, 1993). We have shown that M-current is insensitive to these concentrations of wortmannin (Figure 4a).

With regard to the actions of wortmannin on protein kinases other than MLCK and PI3-kinase, Nakanishi *et al.* (1992) have reported that wortmannin inhibits calcium-activated, phospholipid-dependent protein kinase (C-kinase; Nishizuka, 1984) only slightly without significantly affecting cyclic AMP-dependent protein kinase, cyclic GMP-dependent protein kinase and calmodulin-dependent protein kinase II. It is unlikely that wortmannin inhibited M-current by inhibiting C-kinase in the present study since activators of C-kinase have been shown to decrease the amplitude of M-current (Brown & Adams, 1987). The inability of wortmannin to inhibit cyclic AMP-dependent protein kinase agrees well with our observations that wortmannin does not alter the cyclic AMP-dependent cationic inward rectifier or I_H (Figure 6).

In summary, the data are consistent with inhibition of MLCK by wortmannin, thereby resulting in the removal of a tonic effect of MLCK on the M-current when the intracellular concentrations of calcium ions is very high.

The present study was supported by a Grant-In-Aid for Scientific Research (B-04454141 and C-03670066) from the Ministry of Education, Science and Culture of Japan. M.A.S. was supported by NS-(5999 from the National Institutes of Health.

References

ADAMS, P.R., BROWN, D.A. & CONSTANTI, A. (1982). M-currents and other potassium currents in bullfrog sympathetic neurones. *J. Physiol.*, **330**, 537–572.

AKASU, T., ITO, M., NAKANO, T., SCHNEIDER, C.R., SIMMONS, M.A., TANAKA, T., TOKIMASA, T. & YOSHIDA, M. (1993). Myosin light chain kinase occurs in bullfrog sympathetic neurons and may modulate voltage-dependent potassium currents. *Neuron*, **11**, 1133–1145.

BROWN, D.A. & ADAMS, P.R. (1980). Muscarinic suppression of a novel voltage-sensitive K^+ current in a vertebrate neurone. *Nature*, **283**, 673–676.

BROWN, D.A. & ADAMS, P.R. (1987). Effects of phorbol dibutyrate on M currents and M current inhibition in bullfrog sympathetic neurons. *Cell. Mol. Neurobiol.*, **7**, 255–269.

GODT, R.E. & LINDLEY, B.D. (1982). Influence of temperature upon contractile activation and isometric force production in mechanically skinned muscle fibers of the frog. *J. Gen. Physiol.*, **80**, 279–297.

HARTZELL, H.C. & BUDNITZ, D. (1992). Differences in effects of forskolin and an analog on calcium currents in cardiac myocytes suggest intra- and extracellular sites of action. *Mol. Pharmacol.*, **41**, 880–888.

HARTZELL, H.C. & FISCHMEISTER, R. (1987). Effect of forskolin and acetylcholine on calcium current in single isolated cardiac myocytes. *Mol. Pharmacol.*, **32**, 639–645.

HATHAWAY, D.R. & HAEBERLE, J.R. (1983). Selective purification of the 20,000-Da light chains of smooth muscle myosin. *Anal. Biochem.*, **135**, 37–43.

IKEBE, M., STEPINSKA, M., KEMP, B.E., MEANS, A.R. & HARTSHORNE, D.J. (1987). Proteolysis of smooth muscle myosin light chain kinase -Formation of inactive and calmodulin-independent fragments. *J. Biol. Chem.*, **262**, 13828–13834.

NAKANISHI, S., KAKITA, S., TAKAHASHI, I., KAWAHARA, K., TSUKUDA, E., SANO, T., YAMADA, K., YOSHIDA, M., KASE, H., MATSUDA, Y., HASHIMOTO, Y. & NONOMURA, Y. (1992). Wortmannin, a microbial product inhibitor of myosin light chain kinase. *J. Biol. Chem.*, **267**, 2157–2163.

NISHIZUKA, Y. (1994). The role of protein kinase C in cell surface signal transduction and tumour promotion. *Nature*, **308**, 693–698.

OLWIN, B.B., EDELMAN, A.M., KREBS, E.G. & STORM, D.R. (1984). Quantitation of energy coupling between Ca^{2+}, calmodulin, skeletal muscle myosin light chain kinase, and kinase substrates. *J. Biol. Chem.*, **259**, 10949–10955.

PFAFFINGER, P. (1988). Muscarinic and t-LHRH suppress M-current by activating an IAP-insensitive G-protein. *J. Neurosci.*, **8**, 3343–3353.

SIMMONS, M.A., BECKER, J.B. & MATHER, R.J. (1990). Desensitization of the inhibition of the M-current in sympathetic neurons: effects of ATP analogs, polyanions, and multiple agonist applications. *Neuron*, **4**, 557–562.

SIMMONS, M.A. & SCHNEIDER, C.R. (1993). Regulation of neuronal potassium current by intracellular nucleotide triphosphates. *Biophys. J.*, **64**, A312.

TOKIMASA, T. & AKASU, T. (1990a). Cyclic AMP regulates an inward rectifying sodium-potassium current in dissociated bullfrog sympathetic neurones. *J. Physiol.*, **420**, 409–429.

TOKIMASA, T. & AKASU, T. (1990b). Extracellular calcium ions are required for muscarine-sensitive potassium current in bullfrog sympathetic neurons. *J. Auton. Nerv. Syst.*, **29**, 163–174.

TOKIMASA, T. & AKASU, T. (1990c). ATP regulates muscarine-sensitive potassium current is dissociated bull-frog primary afferent neurones. *J. Physiol.*, **426**, 241–264.

TOKIMASA, T. & AKASU, T. (1991). M-channels may require calmodulin-dependent phosphorylation in bullfrog sympathetic and sensory neurons. *Neurosci. Res.*, Suppl. **14**, 161.

TOKIMASA, T., SUGIYAMA, K., AKASU, T. & MUTEKI, T. (1990). Volatile anaesthetics inhibit a cyclic AMP-dependent sodium-potassium current in cultured sensory neurones of bullfrog. *Br. J. Pharmacol.*, **101**, 190–192.

TOKIMASA, T., TSURUSAKI, M. & AKASU, T. (1991). Slowly inactivating potassium current in cultured bull-frog primary afferent and sympathetic neurones. *J. Physiol.*, **435**, 585–604.

TOKIMASA, T., TSURUSAKI, M., ISHIMATSU, M. & AKASU, T. (1993). Intracellular ATP changes the voltage-dependence of delayed rectifier potassium current in bullfrog primary afferent neurons. *Neurosci. Lett.*, **163**, 138–140.

WALSH, M.P., HINKINS, S., DABROWSKA, R. & HARTSHORNE, D.J. (1983). Smooth muscle myosin light chain kinase. *Methods Enzymol.*, **99**, 279–288.

YANO, H., NAKANISHI, S., KIMURA, K., HANAI, N., SAITOH, Y., FUKUI, Y., NONOMURA, Y. & MATSUDA, Y. (1993). Inhibition of histamine secretion by wortmannin through the blockade of phosphatidylinositol 3-kinase in RBL-2H3 cells. *J. Biol. Chem.*, **268**, 25846–25856.

YAZAWA, M., IKURA, M., HIKICHI, K., YING, L. & YAGI, K. (1987). Communication between two globular domains of calmodulin in the presence of mastoparan or caldesmon fragment. *J. Biol. Chem.*, **262**, 10951–10954.

(Received July 1, 1994
Revised September 8, 1994
Accepted September 22, 1994)

British Journal of Pharmacology (1995) 114, 496–502 © 1995 Stockton Press All rights reserved 0007–1188/95 $9.00

Comparisons of the effects of nicorandil, pinacidil, nicardipine and nitroglycerin on coronary vessels in the conscious dog: role of the endothelium

Bijan Ghaleh, *Jean-Luc Dubois-Randé, *Luc Hittinger, [1]Jean-François Giudicelli & *Alain Berdeaux

[1]Département de Pharmacologie, Faculté de Médecine Paris-Sud, 63 rue Gabriel Péri, 94276 - Le Kremlin Bicêtre Cédex, France and *Service de Cardiologie et Institut National de la Santé et de la Recherche Médicale, U400, Hôpital Henri Mondor, Créteil, France

1 The vasodilator properties of nicorandil on large and small coronary arteries were compared to those of nicardipine, pinacidil, nitroglycerin and acetylcholine in six conscious dogs.

2 Intravenous bolus injections of acetylcholine (0.1 $\mu g\,kg^{-1}$), nitroglycerin (0.3–3 $\mu g\,kg^{-1}$), pinacidil (10–100 $\mu g\,kg^{-1}$), nicardipine (3–30 $\mu g\,kg^{-1}$) and nicorandil (10–100 $\mu g\,kg^{-1}$) dose-dependently increased circumflex coronary artery diameter and decreased coronary vascular resistance, indicating vasodilator effects on both conduit and resistance coronary arteries.

3 Three days after removal of the endothelium of the circumflex coronary artery (balloon angioplasty), pinacidil- and nicardipine-induced dilatation of large coronary arteries was greatly reduced (both −76%, $P<0.01$) whereas that produced by nitroglycerin and nicorandil was decreased only slightly and to a similar extent for both drugs (−19%, $P<0.01$ and −28%, $P<0.05$, respectively).

4 Thus in conscious dogs, nicardipine- and pinacidil-induced dilatation of large coronary arteries is endothelium-dependent. In contrast, the vasodilator effects of nitroglycerin and nicorandil on conduit vessels are endothelium-independent.

5 Finally, our results demonstrate that nicorandil dilates the large coronary arteries through its nitrate-like action and that the ATP-potassium channel opening properties of the drug are not involved in this effect in the conscious dog.

Keywords: Nicorandil; potassium channel opener; calcium antagonist; nitroglycerin; coronary arteries; endothelium; conscious dogs

Introduction

It is now well established from both experimental and clinical studies that the endothelium modulates the responses of large and small coronary arteries to vasodilator and vasoconstrictor agents (Young & Vatner, 1986). However, among coronary vasodilators, only nitrate-like derivatives and NO donors clearly exert their vascular relaxant effect, at least at the level of large coronary arteries, through an endothelium-independent mechanism whether this effect has been investigated *in vitro* and *in vivo* (Drieu La Rochelle *et al.*, 1993). In contrast, for non-nitrate coronary vasodilators, there are discrepancies in the literature about the endothelium-dependency or -independency of their coronary effects, especially between the *in vivo* and *in vitro* data. The major factor responsible for these discrepancies may be that *in vivo* an endothelium-dependent dilatation of large coronary arteries develops secondary to the primary arteriolar dilatation and to the subsequent increase in coronary blood flow, a phenomenon that is not observed *in vitro* (Holtz *et al.*, 1983; Hintze & Vatner, 1984; Drieu La Rochelle *et al.*, 1992b). Although the flow-dependent component of the coronary vasodilator effect of a drug is suppressed when coronary flow is kept constant by means of an occluding device, a direct endothelium-dependent component, if present, does persist. The only way to solve the problem is to perform experiments in vessels without endothelium. Recently, we developed an experimental model in which the direct dilator effect of a drug can be investigated at the level of an epicardial coronary artery in the presence of a functional vascular endothelium and after its subsequent removal by balloon angioplasty (Drieu La Rochelle *et al.*, 1992a; Berdeaux *et al.*, 1994). This model was developed in conscious, chronically instrumented dogs to avoid the deleterious effects of general anaesthesia and acute surgery on coronary dynamics.

Among coronary vasodilators, nicorandil, an anti-anginal drug in currrent use, is of special interest because this drug has at least two mechanisms of action. On the one hand, because of its chemical structure, nicorandil can increase guanosine 3′:5′-cyclic monophosphate (cyclic GMP) in vascular smooth muscle cells (Meisheri *et al.*, 1991) through a nitrate-like effect (Sakai *et al.*, 1989). On the other hand, nicorandil can enhance membrane potassium conductance by opening ATP-sensitive potassium (K_{ATP}) channels (Weir & Weston, 1986; Meisheri *et al.*, 1991). However, even though nicorandil has these two mechanisms of action *in vitro*, controversies still exist about how the drug acts *in vivo*, especially regarding the role of the vascular endothelium in the coronary effects of the drug.

Thus, the goal of the present study was to investigate this problem by comparing the coronary vasodilator profile of nicorandil in the presence and in the absence of a functional endothelium at the level of a large epicardial coronary artery in six conscious dogs. The effects of nicorandil were compared in the same six animals to those of other coronary vasodilator drugs acting through different pharmacological mechanisms, i.e., nitroglycerin, pinacidil, nicardipine and acetylcholine.

Methods

Animal preparation

Six adult mongrel dogs weighing 20 to 31 kg, were anaesthetized with sodium pentobarbitone (30 $mg\,kg^{-1}$, i.v.),

[1] Author for correspondence.

intubated and ventilated with a respirator. Under sterile surgical conditions, a left thoracotomy through the fifth intercostal space was performed, and the heart was suspended in a pericardial cradle. Catheters were implanted in the descending thoracic aorta and in the pulmonary artery. A pair of ultrasonic dimension transducers, 5 MHz piezoelectric crystals (VD 5S, Triton Technology, San Diego, CA, U.S.A.), was attached to a Dacron backing and sutured using ethicon 5-0 suture (Ethicon, Inc., Sommersville, NJ, U.S.A.) to opposing surfaces of the left circumflex coronary artery 2 to 4 cm from its origin. Care was taken when positioning the transducers to limit dissection of, and damage to, any visible nerves; proper alignment of the crystals was confirmed during surgery by monitoring the ultrasonic signal with an oscilloscope. In addition, a 10 MHz Doppler flow probe (Crystal Biotech, Hopkinton, MA, U.S.A.) and, downstream of this, a hydraulic occluder (Jones Instruments, Silver Springs, MD, U.S.A.), were implanted distal to the dimension transducers. The pericardium was left partially closed and all wires and catheters were passed subcutaneously to the back of the dog and brought through the skin between the scapulae. The pneumothorax was evacuated through a chest tube inserted in the 6th intercostal space. Cefazolin (1 g) and gentamicin (80 mg) were administered 30 min before incision and at the end of surgery. The animal instrumentation and the ensuing experiments were performed in accordance with the official regulations of the French Ministry of Agriculture.

Measurement of haemodynamic parameters in conscious dogs

Aortic pressure was measured with a Statham P23ID pressure transducer (Statham Instruments, Oxnard, CA, U.S.A.). Left circumflex coronary artery external diameter was measured instantaneously by means of an ultrasonic transit-time dimension gauge with a resolution of ± 0.04 mm (Triton Technology Inc., System 6 model 200, San Diego, CA, U.S.A.). Left circumflex coronary blood flow was measured with a Doppler flowmeter (Triton Technology Inc., System 6 model 200, San Diego, CA, U.S.A.). Left circumflex coronary vascular resistance, which reflects coronary arteriolar tone, was calculated as the ratio of mean arterial pressure to mean coronary blood flow. Data were recorded continuously on a multichannel electrostatic recorder (ES 2000, Gould Instruments Inc., Cleveland, OH, U.S.A.).

Experimental protocol

All experiments were conducted at least 2–3 weeks after the initial surgery, when the dogs were healthy, apyretic and had been trained to lie quietly on their right side on the experimental table. After recording baseline haemodynamic parameters in the conscious state, the dogs received in randomized order and on separate days increasing doses of acetylcholine ($0.1-1\ \mu g\ kg^{-1}$), nitroglycerin ($0.3-3\ \mu g\ kg^{-1}$), nicardipine ($3-30\ \mu g\ kg^{-1}$), pinacidil ($10-100\ \mu g\ kg^{-1}$) and nicorandil ($30-300\ \mu g\ kg^{-1}$) as i.v. bolus injections through the pulmonary artery catheter. In addition, recordings were made of vasodilatation of the circumflex coronary artery during reactive hyperaemia evoked by the release of a 20 s coronary occlusion (Hintze & Vatner, 1984; Hayashi *et al.*, 1990).

As previously described (Drieu La Rochelle *et al.*, 1992a), three days after the last drug administration the dogs were lightly re-anaesthetized with propofol (200 mg, i.v.) and 0.5% halothane. Under aseptic conditions, an incision was made to expose the right carotid artery. An 8 French left coronary guiding catheter (Schneider Climo, Lyon, France) was inserted through the right carotid artery and positioned in the left coronary ostium under fluoroscopic guidance. A balloon angioplasty catheter (Thruflex, Medtronic, Fourmies, France) was inserted through the guiding catheter into the left circumflex coronary artery into the area of the piezoelectric crystals. The balloon was inflated with air and the catheter was moved backwards and forwards 3 times over the entire region between the proximal circumflex coronary artery and the area of the crystals. This procedure causes removal of the endothelium on each side of the crystals as previously demonstrated by histological and pharmacological studies (Berdeaux *et al.*, 1994), leaving the distal circumflex, the left anterior descending and the septal arteries intact. The balloon was then deflated and the catheter withdrawn. Two to three days after endothelium removal, i.e., before any significant endothelial regeneration occurred in this preparation (Hayashi *et al.*, 1988; Berdeaux *et al.*, 1994), the following experiments were performed. Dilatations of left circumflex coronary artery in response to nitroglycerin ($1\ \mu g\ kg^{-1}$), acetylcholine ($0.3\ \mu g\ kg^{-1}$), reactive hyperaemia (20 s), nicorandil ($100\ \mu g\ kg^{-1}$), nicardipine ($30\ \mu g\ kg^{-1}$) and pinacidil ($30\ \mu g\ kg^{-1}$) were assessed again. Because of the long-lasting effects of these drugs, only one dose of each was administered in the described order. The doses of nicardipine, pinacidil and nicorandil were selected as inducing similar non-maximal large coronary artery dilatations. Each drug was administered only when the effects of the previous one had completely disappeared, i.e., when all parameters had returned to their corresponding control values.

Drugs

The drugs used were nicardipine (Laboratoires Sandoz, Rueil-Malmaison, France), pinacidil (Laboratoires Léo, Montigny-le-Bretonneux, France), nitroglycerin (Laboratoires Besins-Iscovesco, Paris, France), acetylcholine hydrochloride (Sigma Chimie, la Verpillère, France) and nicorandil (Laboratoires Bellon, Neuilly sur Seine, France).

Data analysis

Data shown are mean values $\pm$ s.e. All haemodynamic parameters except coronary artery diameter were measured at baseline and at the time of the peak increase in coronary blood flow. Coronary artery diameter was measured before and at the time of its peak increase to a given stimulus. Results are expressed either as absolute or percentage changes from baseline values. Sequential changes of mean values among periods were evaluated by a two-way analysis of variance for repeated measures. When overall differences were detected, individual comparisons were made with a paired t test with Bonferroni's correction. Comparisons between the effects of a treatment before *vs.* after removal of the endothelium were performed on the absolute variations of the investigated parameter using a paired t test. Because of a slight but significant depression of the response to nitroglycerin after removal of the endothelium with a balloon (Hayashi *et al.*, 1988; Drieu La Rochelle *et al.*, 1992a), we calculated an index of large coronary artery dilatation as the ratio of the absolute change in mean coronary artery diameter induced by a given drug to its corresponding absolute change induced by nitroglycerin ($1\ \mu g\ kg^{-1}$). The effect of the procedure for removing the endothelium on the responses of the left circumflex coronary artery to a given drug was then assessed by comparing the ratios calculated before and after endothelium removal by using a paired t test.

These statistical analyses were performed on a PC compatible using BMDP statistical software (BMDP, Los Angeles, U.S.A.). A P value <0.05 was considered as significant.

Results

Coronary vascular responses with intact endothelium

As shown in Table 1 there was no significant difference between the baseline values of the different investigated

Table 1 Values of coronary and systemic haemodynamic parameters at baseline and at the time of peak increase in mean coronary blood flow (CBF) or mean coronary artery diameter (CAD) after acetylcholine, nitroglycerin, pinacidil, nicardipine and nicorandil administrations in the conscious dog with endothelium intact (E+) and after removal of endothelium (E−)

Drug		Heart rate		Mean arterial pressure		Mean coronary blood flow		Mean coronary artery diameter		Mean coronary vascular resistance	
		Baseline	Peak CBF	Baseline	Peak CBF	Baseline	Peak CBF	Baseline	Peak CAD	Baseline	Peak CBF
(μg kg^{-1})		(beats min^{-1})		(mmHg)		(cm s^{-1})		(μm)		(mmHg s cm^{-1})	
Acetylcholine											
0.1	E+	80 ± 5	95 ± 4**	88 ± 3	76 ± 2**	11.2 ± 2.4	19.2 ± 4.2**	2967 ± 248	3048 ± 243**	10.4 ± 3.0	5.0 ± 1.2**
0.3	E+	81 ± 6	104 ± 4**	87 ± 3	76 ± 2**	11.2 ± 2.4	22.7 ± 5.9**	2971 ± 246	3083 ± 249**	10.3 ± 3.0	4.5 ± 1.2**
1.0	E+	80 ± 5	109 ± 6**	86 ± 2	70 ± 2**	11.0 ± 2.4	27.3 ± 6.8**	2968 ± 246	3118 ± 246**	10.3 ± 2.8	3.5 ± 0.9**
0.3	E−	77 ± 5	99 ± 5**	96 ± 3^b	79 ± 2**^{b}	9.8 ± 1.9	22.7 ± 5.3**	3258 ± 286^b	3279 ± 287**^{b}	12.6 ± 3.4	4.4 ± 0.9**
Nitroglycerin											
0.3	E+	75 ± 6	80 ± 7*	88 ± 2	86 ± 2	11.3 ± 2.4	12.5 ± 2.5	2972 ± 246	3145 ± 244**	10.2 ± 2.9	9.4 ± 3.0
1.0	E+	76 ± 7	90 ± 7**	88 ± 2	84 ± 3**	11.3 ± 2.4	15.0 ± 2.4**	2978 ± 245	3179 ± 244**	10.3 ± 2.8	7.0 ± 2.0**
3.0	E+	75 ± 6	103 ± 4**	89 ± 3	80 ± 2**	11.3 ± 2.4	20.2 ± 3.5**	2973 ± 245	3205 ± 246**	10.5 ± 3.0	5.2 ± 1.6**
1.0	E−	79 ± 5	86 ± 6**	95 ± 2^a	89 ± 1**	10.7 ± 2.1	12.5 ± 1.9**^{b}	3243 ± 285^b	3403 ± 287**^{b}	11.7 ± 3.1	8.1 ± 1.3*
Pinacidil											
10	E+	85 ± 3	94 ± 5*	88 ± 3	84 ± 4**	11.0 ± 2.3	16.7 ± 3.5*	2948 ± 255	3013 ± 254**	10.5 ± 2.7	7.2 ± 2.3**
30	E+	84 ± 4	116 ± 9**	89 ± 4	81 ± 4**	11.0 ± 2.2	33.3 ± 6.8**	2949 ± 256	3149 ± 244**	10.3 ± 2.6	3.2 ± 0.9**
100	E+	84 ± 3	139 ± 9**	90 ± 4	74 ± 3**	11.7 ± 2.0	45.8 ± 7.3**	2952 ± 252	3225 ± 232**	9.8 ± 2.8	2.0 ± 0.5**
30	E−	85 ± 5	113 ± 5**	100 ± 6	95 ± 6**	10.8 ± 1.9	24.7 ± 3.3**^{b}	3301 ± 295^b	3345 ± 296*^{b}	11.1 ± 2.4	4.2 ± 0.6**
Nicardipine											
3	E+	82 ± 3	91 ± 5**	91 ± 6	86 ± 3**	11.7 ± 2.2	13.8 ± 2.1	2971 ± 248	3005 ± 250*	9.9 ± 2.9	7.2 ± 1.5**
10	E+	83 ± 4	113 ± 6**	91 ± 5	84 ± 3**	12.3 ± 2.0	19.3 ± 2.8**	2977 ± 249	3077 ± 246**	9.0 ± 2.2	5.0 ± 1.0**
30	E+	82 ± 3	135 ± 4**	96 ± 7	82 ± 4**	11.7 ± 2.3	25.8 ± 5.0**	2968 ± 258	3128 ± 254**	10.8 ± 3.2	4.0 ± 1.0**
30	E−	78 ± 5	129 ± 9**	97 ± 6	83 ± 4**	10.3 ± 1.8	22.5 ± 4.6**	3284 ± 298^b	3323 ± 302*^{b}	11.2 ± 2.5	4.7 ± 1.0**
Nicorandil											
30	E+	75 ± 5	84 ± 3*	89 ± 3	87 ± 4	11.0 ± 2.1	15.2 ± 2.7	2962 ± 245	3058 ± 241**	10.5 ± 3.0	6.9 ± 1.6**
100	E+	72 ± 5	105 ± 7**	94 ± 2	83 ± 4**	11.2 ± 2.3	32.3 ± 5.9**	2982 ± 245	3196 ± 236**	10.9 ± 2.9	3.7 ± 1.4**
300	E+	76 ± 4	133 ± 4**	92 ± 2	80 ± 1**	11.3 ± 2.6	47.7 ± 10.2**	2966 ± 249	3254 ± 240**	10.7 ± 2.9	2.2 ± 0.6**
100	E−	73 ± 5	109 ± 10**	97 ± 3^a	88 ± 3**	9.7 ± 2.0	30.5 ± 7.8**	3268 ± 289^b	3418 ± 291**^{b}	12.9 ± 3.1	4.3 ± 1.3**

Significant ($^aP<0.05$; $^bP<0.01$) vs. corresponding value before removal of endothelium. Significant ($*P<0.05$; $**P<0.01$) vs. baseline.
Values are mean ± s.e.mean.

parameters, measured or calculated before administration of any dose of any of the coronary vasodilators.

All drugs induced dose-dependent decreases in mean arterial pressure and coronary vascular resistance and dose-dependent increases in heart rate, coronary blood flow and coronary artery diameter, except the lowest doses of nitroglycerin (0.3 μg kg^{-1}) and nicorandil (30 μg kg^{-1}) for which the decrease in mean arterial pressure was not significant at the time of the peak increase in coronary blood flow. Furthermore, it must be noted that the tachycardia induced by nicardipine, pinacidil and nicorandil was more marked and of longer duration than that induced by acetylcholine and nitroglycerin, regardless of the dose administered (data not shown).

As shown in Table 1 and Figure 1, all vasodilators induced a dose-dependent decrease in coronary vascular resistance and dose-dependent increases in coronary blood flow and coronary artery diameter, except for nitroglycerin which at the lowest dose (0.3 μg kg^{-1}) selectively increased coronary artery diameter but had no effect on coronary vascular resistance. As shown in Table 2 and illustrated in Figures 2 and 3, the peak decrease in coronary vascular resistance induced by all vasodilator drugs always occurred earlier than the corresponding peak increase in coronary artery diameter. The effects on coronary vascular resistance observed after administration of nitroglycerin and acetylcholine were transient as coronary vascular resistance had returned to its baseline value when the maximal increase in coronary artery diameter occurred. In contrast, the decrease in coronary vascular resistance induced by nicardipine, pinacidil and nicorandil was still present when the peak effects of these drugs on coronary artery diameter occurred.

Coronary vascular responses after endothelium removal

As shown in Table 1, removal of the endothelium *per se* did not significantly affect the baseline values of mean coronary blood flow, mean coronary vascular resistance or heart rate. In contrast, coronary artery diameter was significantly increased by approximately 10%. Baseline values of mean arterial pressure before administration of acetylcholine, nitroglycerin and nicorandil were also slightly increased after endothelium removal. Because the occluder malfunctioned in one dog, responses during reactive hyperaemia were examined in only five dogs. Before endothelium removal, release of a 20 s coronary artery occlusion was associated with a 327 ± 35% increase in coronary blood flow and a delayed increase in coronary artery diameter of 178 ± 25 μm from a control value of 3064 ± 285 μm. After removal of the endothelium, and despite a similar increase in coronary blood flow (361 ± 28%), the increase in coronary artery diameter (14 ± 5 μm from a control value of 3397 ± 348 μm) was reduced by 91% ($P<0.01$) compared with the corresponding value before endothelium removal.

As shown in Figure 4, the increases in circumflex coronary artery diameter evoked by acetylcholine (− 82%, $P<0.001$), nicardipine (− 76%, $P<0.01$) and pinacidil (− 76%, $P<0.01$) were strongly reduced after endothelium removal. In contrast, nitroglycerin and nicorandil were still able to strongly dilate the coronary artery segment without endothelium although the response was significantly reduced relative to that evoked with intact endothelium (− 19%, $P<0.01$ and − 28%, $P<0.05$, respectively). In order to take into account this reduction in nitroglycerin responsiveness after endothelium removal which reflects a partial decrease in the

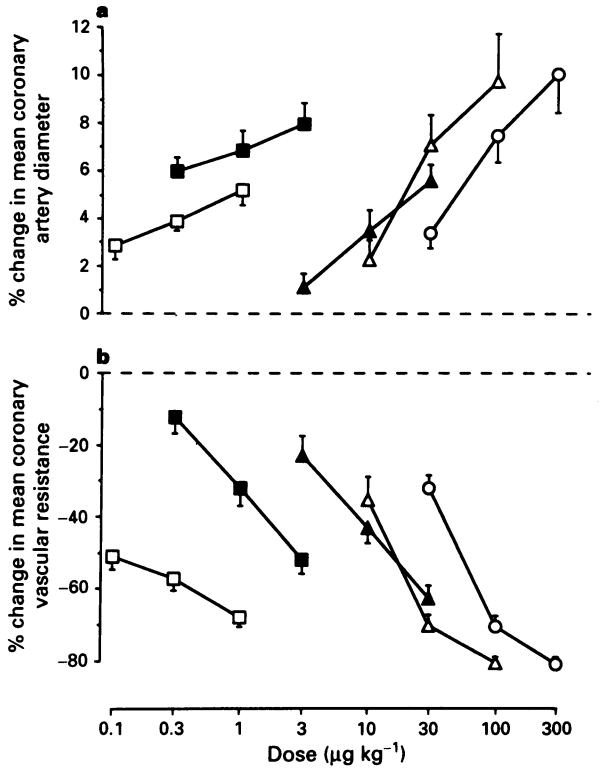


Figure 1 Dose-response curves for the maximal increase in mean coronary artery diameter (a, upper panel) and for the maximal decrease in mean coronary vascular resistance (b, lower panel) induced by increasing doses of acetylcholine (□), nitroglycerin (■), nicardipine (▲), pinacidil (△) and nicorandil (○) in conscious dogs with intact endothelium. Results are expressed as percent changes from the corresponding baseline values.

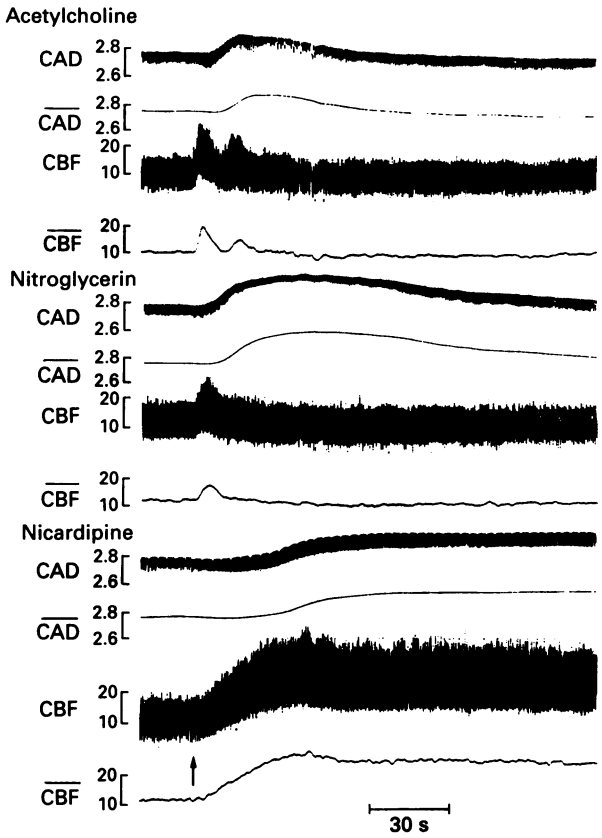


Figure 2 Representative tracings of the effects of the i.v. administration of acetylcholine (0.3 μg kg^{-1}), nitroglycerin (1 μg kg^{-1}) and nicardipine (30 μg kg^{-1}) on phasic and mean coronary artery diameter (CAD and $\overline{CAD}$, mm, respectively) and on phasic and mean coronary blood flow (CBF and $\overline{CBF}$, cm s^{-1}, respectively) in a conscious dog. The drugs were administered as a bolus at the time indicated by the arrow at the bottom of the figure.

reactivity of coronary smooth muscle cells (Drieu La Rochelle *et al.*, 1992a; Berdeaux *et al.*, 1994), we calculated the ratio of the absolute change in coronary artery diameter induced by each vasodilator drug to the corresponding absolute change induced by nitroglycerin (see Methods). Thus, as compared to nitroglycerin, large epicardial coronary artery responses to acetylcholine, nicardipine and pinacidil were still significantly reduced after endothelium removal (Table 3). In contrast, lack of endothelium did not affect the dilator response of the large epicardial coronary artery to nicorandil ($P = 0.29$). Furthermore, both nitroglycerin (1 μg kg^{-1}) and nicorandil (100 μg kg^{-1}) induced similar and non-significantly different increases in coronary artery diameter before (214 ± 29 μm and 201 ± 21 μm, respectively) and after endothelium removal (161 ± 17 μm and 150 ± 25 μm, respectively).

Discussion

The present study conducted in conscious dogs (a) compares the effects on large and small coronary arteries of nicorandil to those of acetylcholine, nitroglycerin, nicardipine and pinacidil, and (b) investigates the role of coronary endothelium in the vasodilator effects of these drugs at the level of the large epicardial coronary arteries.

It appears from our data that all drugs, at the doses investigated, induced a dose-dependent decrease in mean arterial pressure and an increase in heart rate. These results are in agreement with those of Cox *et al.* (1983) with acetylcholine and of Zhang *et al.* (1993) with nitroglycerin who showed that these drugs induce a transient tachycardia and a fall in mean arterial pressure. The positive chronotropic effects observed following administration of both potassium

Table 2 Values of the times (s) to peak decrease in coronary vascular resistance and increase in coronary artery diameter following administration of acetylcholine, nitroglycerin, pinacidil, nicardipine or nicorandil in the conscious dog with intact coronary endothelium

Drug (μg kg^{-1})	*Time (s) to peak* *Coronary vascular resistance*	*Coronary artery diameter*
Acetylcholine		
0.1	12 ± 1	30 ± 1
0.3	13 ± 1	32 ± 1
1	14 ± 1	40 ± 3
Nitroglycerin		
0.3	11 ± 2	48 ± 2
1	11 ± 2	54 ± 4
3	12 ± 2	65 ± 4
Pinacidil		
10	43 ± 2	73 ± 5
30	45 ± 4	108 ± 9
100	90 ± 15	267 ± 35
Nicardipine		
3	26 ± 4	53 ± 8
10	39 ± 3	83 ± 5
30	44 ± 6	175 ± 17
Nicorandil		
30	29 ± 2	64 ± 8
100	32 ± 3	117 ± 9
300	56 ± 8	265 ± 22

Values are mean ± s.e.mean.

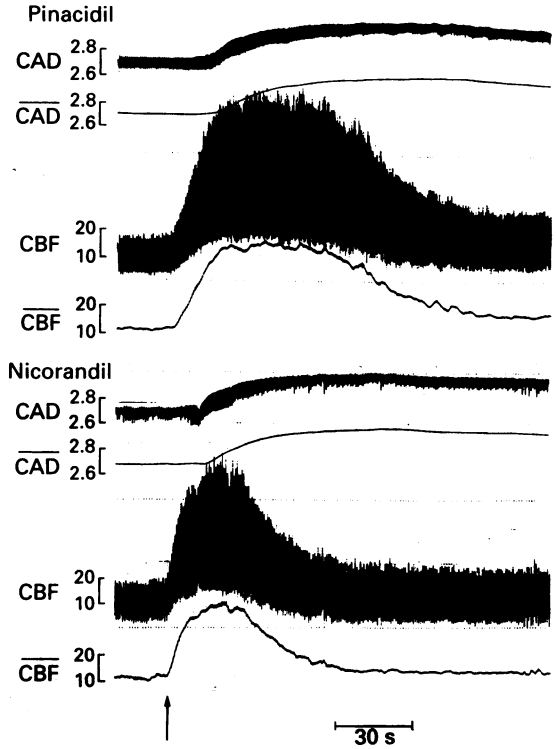


Figure 3 Representative tracings of the effects of the i.v. administration of pinacidil (30 $\mu g\,kg^{-1}$) and nicorandil (100 $\mu g\,kg^{-1}$) on phasic and mean coronary artery diameter (CAD and $\overline{CAD}$, mm, respectively) and on phasic and mean coronary blood flow (CBF and $\overline{CBF}$, $cm\,s^{-1}$, respectively) in a conscious dog. The drugs were administered as a bolus at the time indicated by the arrow at the bottom of the figure.

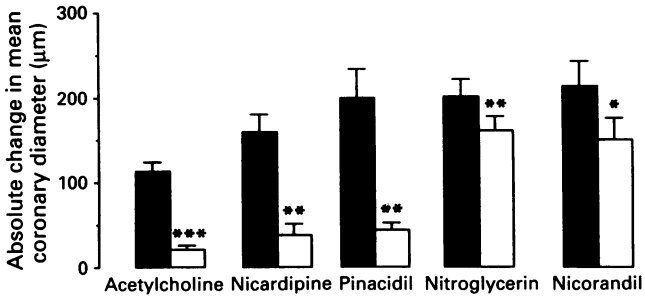


Figure 4 Peak increases in mean coronary artery diameter after acetylcholine (0.3 $\mu g\,kg^{-1}$), nicardipine (30 $\mu g\,kg^{-1}$), pinacidil (30 $\mu g\,kg^{-1}$), nitroglycerin (1 $\mu g\,kg^{-1}$) and nicorandil (100 $\mu g\,kg^{-1}$) administrations in conscious dogs before (solid bars) and after (open bars) endothelium removal. *, **, ***: significant ($P<0.05$; $P<0.01$; $P<0.001$) *vs.* before endothelium removal.

Table 3 Values of the ratios of absolute change in mean coronary artery diameter induced by reactive hyperaemia or a drug to the corresponding change induced by nitroglycerin (see Methods) calculated before and after coronary endothelium removal following reactive hyperaemia and administration of acetylcholine, pinacidil, nicardipine and nicorandil in the conscious dog

	With endothelium	*Without endothelium*
Reactive hyperaemia	0.82 ± 0.02	0.09 ± 0.04[a]
Acetylcholine 0.3 $\mu g\,kg^{-1}$	0.58 ± 0.07	0.14 ± 0.04[b]
Pinacidil 30 $\mu g\,kg^{-1}$	0.97 ± 0.09	0.27 ± 0.04[b]
Nicardipine 30 $\mu g\,kg^{-1}$	0.80 ± 0.09	0.25 ± 0.05[a]
Nicorandil 100 $\mu g\,kg^{-1}$	1.06 ± 0.09	0.92 ± 0.09

Value are mean ± s.e.mean.
Significant ([a]$P<0.01$; [b]$P<0.001$) vs. before removal of endothelium.

channel openers and calcium antagonists (McLeay *et al.*, 1983; Kawashima & Liang, 1985; Buckingham *et al.*, 1986) and observed here with nicardipine and pinacidil are reflexly mediated through unloading of the baroreceptors. Nicorandil also decreased blood pressure and increased heart rate. This tachycardia also most probably results from a compensatory increase in sympathetic tone elicited by hypotension since it is not observed in patients with congestive heart failure (Galié *et al.*, 1990), in whom the baroreceptor reflex is desensitized.

Our study confirms that nicorandil and the other investigated vasodilators dose-dependently dilate the large, as well as the small, coronary arteries (Vatner *et al.*, 1980; Hintze & Vatner, 1983; Cox *et al.*, 1983; Preuss *et al.*, 1985; Giudicelli *et al.*, 1990). However, although all these drugs act on the coronary vasculature, there are clearly some differences in the kinetics of their coronary effects. Thus, the peak decrease in coronary vascular resistance induced by nicardipine, pinacidil and nicorandil occurred later than that induced by acetylcholine and nitroglycerin. At the level of small coronary arteries, the effects on coronary blood flow following administration of both acetylcholine and nitroglycerin were transient and were no longer present at the time of peak increase in coronary artery diameter. In contrast, nicardipine, as well as both pinacidil and nicardipine, elicited a substantial and prolonged increase in coronary blood flow which was still present at the time of the peak increase in coronary artery diameter. It is not likely that the prolonged effect of nicorandil on small coronary arteries was due to a slow release of NO. Shen & Vatner (1993) have demonstrated that both the time to peak coronary vasodilatation as well as the duration of vasodilatation induced by lemakalim, a K_{ATP} channel opener, are significantly longer than those induced by nifedipine, acetylcholine and nitroglycerin. By using glibenclamide, Miwa *et al.* (1993) showed that the K_{ATP} channel opening properties of nicorandil are of major importance in the small endocardial vessels. Furthermore, glibenclamide has been reported to block the changes in coronary blood flow and coronary vascular resistance induced by nicorandil in anaesthetized dogs (Ogawa *et al.*, 1992). Thus, it is extremely likely that the dilatation of the small coronary arteries which nicorandil induced in our study was related to the drug's K_{ATP} channel opening properties.

Because an increase in coronary blood flow can trigger dilatation of large coronary arteries through an endothelium-dependent mechanism (Holtz *et al.*, 1983), we compared the responses of the large coronary arteries to the five investigated coronary dilators before and after endothelium removal by using a balloon angioplasty technique. As we showed previously (Berdeaux *et al.*, 1994), this procedure results in a local endothelium removal in the circumflex coronary artery at the site of attachment of the crystals. This is supported by the fact that coronary dilatation induced by reactive hyperaemia (flow-dependent dilatation) and acetylcholine (endothelium-dependent dilatation) were almost abolished, confirming the absence of functional coronary endothelium, in agreement with previous studies performed under similar experimental conditions (Inoue *et al.*, 1988; Hayashi *et al.*, 1988; Weidinger *et al.*, 1990). Our post-endothelium removal experiments were performed 2–3 days after angioplasty, when no functional regeneration of the endothelium has occurred; recovery of normal responses to removal of vascular occlusion, acetylcholine (Hayashi *et al.*, 1988) and treadmill exercise (Berdeaux *et al.*, 1994) requires about 9 days after endothelium removal. The observation that endothelium removal induced a significant increase in basal coronary artery diameter can be accounted for, as previously described, by a passive distension of the blood vessel during balloon inflation, rather than by the lack of endothelium *per se* (Berdeaux *et al.*, 1994).

Our experiments clearly showed that endothelium removal strongly reduced the dilatation of large coronary arteries induced by pinacidil, confirming our previous data which

indicated that potassium channel openers dilate large coronary arteries mainly through an endothelium-dependent mechanism (Drieu La Rochelle *et al.*, 1992a). More precisely, their mechanism of action seems to be mainly flow-dependent as increases in circumflex coronary diameter were no longer observed when coronary blood flow was maintained constant using a cuff occluder (Giudicelli *et al.*, 1990). Similarly, the nicardipine-induced increase in coronary artery diameter was almost completely abolished after endothelium removal. This result is in agreement with previous studies performed at constant coronary blood flow which showed that the dilatations of large coronary arteries induced by other calcium entry blockers such as nifedipine, verapamil and diltiazem are partly flow-dependent (Holtz *et al.*, 1983; Drieu La Rochelle *et al.*, 1992b). Thus it seems reasonable to conclude that the potassium channel opener, pinacidil, and the calcium antagonist, nicardipine, preferentially dilate coronary arterioles and secondarily dilate large coronary arteries through an indirect endothelium-dependent mechanism, which is most likely flow-dependent.

In contrast, the dilatation of large coronary arteries induced by nitroglycerin and nicorandil was only slightly decreased after endothelium removal, an effect previously described with nitroglycerin (Hayashi *et al.*, 1988; Drieu La Rochelle *et al.*, 1992a; Berdeaux *et al.*, 1994). As the response to organic nitrates is a widely accepted index of smooth muscle integrity after *in vivo* endothelium removal (Chu & Cobb, 1987; Hayashi *et al.*, 1988; Inoue *et al.*, 1988), the slight reduction in the nitroglycerin-induced responses probably reflects a small angioplasty-induced alteration of smooth muscle cells. Taking into account this alteration by calculation of a dilatation index (see Methods), our data show that the nicorandil-induced vasodilatation of large coronary arteries is endothelium-independent (Table 3). As potassium channel openers have been shown to dilate these vessels through an endothelium-dependent mechanism (see above), it seems likely that the nicorandil-induced dilatation of the large epicardial coronary arteries occurs through the drug's nitrate-like properties and that its K_{ATP} channel opening activity is not involved in this effect. This result is in agreement with a previous study reporting that the spasmolytic effect of nicorandil (Imagawa *et al.*, 1992) is not modified by administration of the K_{ATP} channel antagonist, glibenclamide. Miwa *et al.* (1993) have also reported that nicorandil-induced relaxation of epi-myocardial coronary arteries is not affected by glibenclamide, but is inhibited by oxyhaemoglobin.

In conclusion, the present study demonstrates that nicorandil dilates the large coronary arteries in conscious dogs through an endothelium-independent mechanism, by a nitrate-like action. It also shows that the drug's action on K_{ATP} channels is predominantly at the level of the small coronary arteries. Thus it seems that nicorandil contrasts with pinacidil and nicardipine which dilate large coronary arteries through an indirect endothelium-dependent mechanism.

The authors are greatly indebted to Alain Bizé for his excellent technical assistance. This work was supported by grant 930403 from Institut National de la Santé et de la Recherche Médicale.

References

BERDEAUX, A., GHALEH, B., DUBOIS-RANDE, J.L., VIGUE, B., DRIEU LA ROCHELLE, C., HITTINGER, L. & GIUDICELLI, J.F. (1994). Role of vascular endothelium in exercise-induced dilation of large epicardial coronary arteries in conscious dogs. *Circulation*, **89**, 2799–2808.

BUCKINGHAM, R.E., CLAPHAM, J.C., HAMILTON, T.C., LONGMAN, S.D., NORTON, J. & POYSER, R.H. (1986). BRL 34915, a novel antihypertensive agent: comparison of effects on blood pressure and other haemodynamic parameters with those of nifedipine in animal models. *J. Cardiovasc. Pharmacol.*, **8**, 798–804.

CHU, A. & COBB, F.R. (1987). Vasoactive effects of serotonin on proximal coronary arteries in awake dogs. *Circ. Res.*, **61** (Suppl II), 1181–1187.

COX, D.A., HINTZE, T.H. & VATNER, S.F. (1983). Effects of acetylcholine on large and small coronary arteries in conscious dogs. *J. Pharmacol. Exp. Ther.*, **225**, 764–769.

DRIEU LA ROCHELLE, C., DUBOIS-RANDE, J.L., RICHARD, V., HITTINGER, L., GIUDICELLI, J.F. & BERDEAUX, A. (1993). The role of NO release in the control of large and small coronary arteries in conscious dogs. *J. Cardiovasc. Pharmacol.*, **22** (Suppl 7), S17–S21.

DRIEU LA ROCHELLE, C., RICHARD, V., DUBOIS-RANDE, J.L., ROUPIE, E., GIUDICELLI, J.F., HITTINGER, L. & BERDEAUX, A. (1992a). Potassium channel openers dilate large epicardial coronary arteries in conscious dogs by an indirect, endothelium-dependent mechanism. *J. Pharmacol. Exp. Ther.*, **263**, 1091–1096.

DRIEU LA ROCHELLE, C., ROUPIE, E., RICHARD, V., GIUDICELLI, J.F. & BERDEAUX, A. (1992b). Action différentielle des dérivés nitrés et des vasodilatateurs artériels au niveau de la circulation coronaire. Approche expérimentale et conséquences thérapeutiques. *Arch. Mal. Coeur*, **85**, 67–71.

GALIE, N., VARANI, E., MAIELLO, L., BORIANI, G., BOSCHI, S., BINETTI, G. & MAGNANI, B. (1990). Usefulness of nicorandil in congestive heart failure. *Am. J. Cardiol.*, **65**, 343–348.

GIUDICELLI, J.F., DRIEU LA ROCHELLE, C. & BERDEAUX, A. (1990). Effects of cromakalim and pinacidil on large epicardial and small coronary arteries in conscious dogs. *J. Pharmacol. Exp. Ther.*, **255**, 836–842.

HAYASHI, Y., TOMOIKE, H., NAGASAWA, K., YAMADA, A., NISHIJIMA, H., ADACHI, H. & NAKAMURA, M. (1988). Functional and anatomical recovery of endothelium after deendothelialization of coronary artery. *Am. J. Physiol.*, **254**, H1081–H1090.

HINTZE, T.H. & VATNER, S.F (1983). Comparison of nifedipine and nitroglycerin on large and small coronary arteries and cardiac function in conscious dogs. *Circ. Res.*, **53** (Suppl I), 139–146.

HINTZE, T.H. & VATNER, S.F. (1984). Reactive dilation of large coronary arteries in conscious dogs. *Circ. Res.*, **54**, 50–57.

HOLTZ, J., GIESLER, M. & BASSENGE, E. (1983). Two dilatory mechanisms of antianginal drugs on epicardial coronary arteries *in vivo*: indirect, flow-dependent, endothelium-mediated dilation and direct smooth muscle relaxation. *Z. Kardiol.*, **72** (Suppl. 3), 98–106.

IMAGAWA, J., AKIMA, M., NABATA, H. & TAIRA, N. (1992). Spasmolytic action of nicorandil in canine conductive coronary arteries in vivo is not modified by glibenclamide. *J. Cardiovasc. Pharmacol.*, **19**, 108–114.

INOUE, T., TOMOIKE, H., HISANO, K. & NAKAMURA, M. (1988). Endothelium determines flow-dependent dilation of the epicardial coronary artery in dogs. *J. Am. Coll. Cardiol.*, **88**, 187–191.

KAWASHIMA, S. & LIANG, C.S. (1984). Systemic and coronary hemodynamic effects of pinacidil, a new antihypertensive agent, in awake dogs: comparison with hydralazine. *J. Pharmacol. Exp. Ther.*, **232**, 369–375.

MCLEAY, R.A.B., TERENCE, J.S., WATSON, R.D.S. & LITTLER, W.A. (1983). The effect of nifedipine on arterial pressure and reflex cardiac control. *Circulation*, **67**, 1084–1090.

MEISHERI, K.D., CIPKUS-DUBRAY, L.A., HOSNER, J.M. & KHAN, S.A. (1991). Nicorandil-induced vasorelation: functional evidence for K^+ channel-dependent and cyclic GMP-dependent components in a single vascular preparation. *J. Cardiovasc. Pharmacol.*, **17**, 903–912.

MIWA, A., KANETA, S., MOTOKI, K., JINNO, Y., KASAI, H., OKADA, Y., FUKUSHIMA, H. & OGAWA, N. (1993). Vasorelaxant mechanism of KRN2391 and nicorandil in porcine coronary arteries of different sizes. *Br. J. Pharmacol.*, **109**, 632–636.

OGAWA, N., FUKATA, Y., KANETA, S., JINNO, Y., FUKUSHIMA, H. & NISHIKORI, K. (1992). Comparison of KRN2391 with nicorandil and nifedipine on canine coronary blood flow: antagonism by glibenclamide. *J. Cardiovasc. Pharmacol.*, **20**, 11–17.

PREUSS, K.C., GROSS, G.J., BROOKS, H.L. & WARLTIER, D.C. (1985). Hemodynamic actions of nicorandil, a new antianginal agent, in the conscious dog. *J. Cardiovasc. Pharmacol.*, **7**, 709–714.

SAKAI, K. (1989). Nicorandil: animal pharmacology. *Am. J. Cardiol.*, **63**, 2J–10J.

SHEN, Y. & VATNER, S.F. (1993). Effects of a K + ATP channel opener, lemakalim, on systemic, coronary and regional vascular dynamics in conscious dogs: comparison with nifedipine, adenosine, nitroglycerin and acetylcholine. *J. Pharmacol. Exp. Ther.*, **256**, 1026–1037.

VATNER, S.F., PAGANI, M., MANDERS, W.T. & PASIPOULARIDES, A.D. (1980). Alpha adrenergic vasoconstriction and nitroglycerin vasodilation of large coronary arteries in conscious dogs. *J. Clin. Invest.*, **65**, 5–14.

WEIDINGER, F.F., MCLENACHAN, J.M., CYBULSKY, M.I., GORDON, J.B., RENNKE, H.G., HOLLENBERG, N.K., FALLON, J.T., GANZ, P. & COOKE, J.P. (1990). Persistent dysfunction of regenerated endothelium after balloon angioplasty of rabbit iliac artery. *Circulation*, **81**, 1667–1679.

WEIR, S.W. & WESTON, A.H. (1986). The effects of BRL 34915 and nicorandil on electrical and mechanical activity and on ^{86}Rb efflux in rat blood vessels. *Br. J. Pharmacol.*, **88**, 121–128.

YOUNG, M.A. & VATNER, S.F. (1986). Regulation of large coronary arteries. *Circ. Res.*, **59**, 579–596.

ZHANG, J., SOMERS, M. & COBB, F.R. (1993). Heterogenous effects of nitroglycerin on the conductance and resistance coronary arterial vasculature. *Am. J. Physiol.*, **264**, H1960–H1968.

(Received June 13, 1994
Revised August 30, 1994
Accepted September 23, 1994)

British Journal of Pharmacology (1995) 114, 503-509 © 1995 Stockton Press All rights reserved 0007-1188/95 $9.00

Electrophysiological effects of SD-3212, a new antiarrhythmic agent with vasodilator action, on guinea-pig ventricular cells

[1]Itsuo Kodama, Ryoko Suzuki, Kazuyasu Maruyama & Junji Toyama

Departments of Circulation and Humoral Regulation, Research Institute of Environmental Medicine, Nagoya University, Nagoya 464-01, Japan

1 The effects of SD-3212 on transmembrane action potentials were examined in right ventricular papillary muscles and in single ventricular myocytes isolated from guinea-pig hearts.

2 In papillary muscles, SD-3212 $\geq 3\,\mu M$ caused a significant decrease in the maximum upstroke velocity ($\dot{V}_{max}$) of action potential without affecting resting membrane potential. The inhibition of $\dot{V}_{max}$ was enhanced at higher stimulation frequencies.

3 In the presence of SD-3212, trains of stimuli at rates ≥ 0.5 Hz led to a use-dependent inhibition of $\dot{V}_{max}$. The time constant for the recovery of $\dot{V}_{max}$ from the use-dependent block was 1.3 s.

4 Voltage-dependence of $\dot{V}_{max}$ inhibition by SD-3212 was investigated in single myocytes. The curves relating membrane potential and $\dot{V}_{max}$ were shifted by SD-3212 ($10\,\mu M$) in a hyperpolarizing direction by 6.2 mV.

5 In myocytes treated with SD-3212 ($10\,\mu M$), the $\dot{V}_{max}$ of test action potentials preceded by conditioning clamp to 0 mV was decreased progressively as the clamp pulse duration was prolonged. $\dot{V}_{max}$ of test action potentials following a long (1 s) 0 mV clamp recovered at a time constant ranging from 1.01 to 1.22 s, being shorter at the more negative potential within a range from -70 to -90 mV.

6 These findings suggest that the primary electrophysiological effect of SD-3212 is a use- and voltage-dependent inhibition of sodium channels. From the onset and offset kinetics of the use-dependent block, SD-3212 is located between fast and intermediate kinetic Class-I drugs. From the state-dependence of sodium channel block, SD-3212 belongs to inactivated channel blockers.

Keywords: SD-3212; ventricular cell; action potential; $\dot{V}_{max}$; use-dependent block

Introduction

SD-3212 ((−)-(s)-2-[5-methoxy-2-[3-[methyl [2-[3,4 (methylenedioxy) phenoxy] ethyl] amino] phenyl]-4-methyl-2H-1,4-benzothiazin-3(4H)-one hydrogen fumarate) is a newly synthesized antiarrhythmic agent with vasodilator action (Miyawaki *et al.*, 1991; Nagashima *et al.*, 1992; Hirasawa *et al.*, 1992). This compound is a stereoisomer of semotiadil fumarate (SD-3211), a recently developed non-dihydropyridine type calcium antagonist (Miyawaki *et al.*, 1990; Fukuchi *et al.*, 1990; Teramoto, 1993). *In vitro* and *in vivo* experiments on rats, guinea-pigs, and dogs, showed that SD-3212 had a potent and long lasting inhibitory or protective action against ventricular tachyarrhythmias induced by chloroform, ouabain, adrenaline, coronary occlusion and reperfusion (Fukuchi *et al.*, 1990; Miyawaki *et al.*, 1991; Nagashima *et al.*, 1992). The antiarrhythmic potency of SD-3212 in these animal models is appreciably higher than that of SD-3211.

As to underlying mechanisms for the antiarrythmic activity of SD-3212, only limited information is available, and much remains to be clarified. The calcium antagonistic action of SD-3212 in vascular smooth muscle was shown to be less potent (approximately one tenth) than that of SD-3211 (Nakayama *et al.*, 1992). In experiments on cardiac muscle, SD-3212 ($1-10\,\mu M$), unlike SD-3211, decreased the maximum upstroke velocity ($\dot{V}_{max}$) of the action potential in a concentration-dependent manner (Miyawaki *et al.*, 1991). In Langendorff-perfused rabbit hearts, SD-3212 caused an inhibition of atrio-ventricular conduction with comparable prolongation of atrio His bundle (AH) and His bundle-ventricular (HV) intervals (unpublished data). *In vivo* experiments in dogs revealed that SD-3212 prolonged the intraventricular conduction time when the coupling interval of stimulation was relatively short, whereas the parameter was unaffected by SD-3211 (Nagashima *et al.*, 1992). These findings suggest that SD-3212 possesses an inhibitory effect on cardiac sodium channels, and this Class-I action could be responsible for its potent antiarrhythmic activity.

In the present study, we investigated the effects of SD-3212 on the transmembrane action potential in right ventricular papillary muscles as well as in single ventricular myocytes isolated from guinea-pig hearts. The modulation of drug-induced $\dot{V}_{max}$ inhibition by stimulation frequencies or by membrane potential level was studied extensively, in order to compare the characteristics of the sodium channel blocking actions of SD-3212 with other Class-I antiarrhythmic drugs.

Methods

Papillary muscle

Guinea-pigs of either sex weighing 200 to 250 g were killed by cervical dislocation under ether anaesthesia and hearts were quickly removed. Papillary muscles, 2 to 3 mm in length and 0.3 to 0.4 mm in diameter were dissected from the right ventricle. The preparation was mounted in a tissue bath and superfused continuously with Krebs-Ringer solution kept at 33°C and gassed with 95% O_2 and 5% CO_2. The composition of the solution was as follows (in mM): NaCl 120.3, KCl 4.0, $CaCl_2$ 1.2, $MgSO_4$ 1.3, $NaHCO_3$ 25.2 and glucose 5.5 (pH 7.4). The preparations were stimulated by a pair of 1.0 mm platinum wire electrodes placed 1.0 mm apart of either side of the muscles. Pulses used for stimulation were 0.5–1.0 ms in duration and 20% higher than the diastolic threshold in intensity unless otherwise specified. Equipment for recording transmembrane potential was the same as described pre-

[1] Author for correspondence.

viously (Kodama *et al.*, 1985; Toyama *et al.*, 1987). To study the use-dependent effect of SD-3212 on the maximum upstroke velocity ($\dot{V}_{max}$) of action potentials, the preparation was stimulated repetitively at varying rates ranging from 0.1 to 2.0 Hz. Resting periods of 30 s, which were sufficient to ensure full recovery from the rate-dependent decrease in $\dot{V}_{max}$, were interposed between the trains of stimuli. The experimental protocol is able to detect the existence of two types of drug-induced $\dot{V}_{max}$ inhibition, tonic and use-dependent block. The former is defined by the decrease of $\dot{V}_{max}$ of the first action potential preceded by the rest period, and the latter is the decrease of $\dot{V}_{max}$ during the trains (from the value of first action potential to the new steady-state level). The recovery of $\dot{V}_{max}$ from the use-dependent block was studied by applying a single test stimulus at various coupling intervals following a stimulation for 60 s at 1.0 Hz. The intensity of the test stimulus was adjusted to obtain a constant latency from the stimulus artifact to the initiation of action potential upstroke.

Single ventricular myocytes

Single ventricular myocytes were isolated enzymatically from guinea-pig hearts by the same procedure as described in our previous paper (Kodama *et al.*, 1990). A few drops of cell suspension were placed in a recording chamber attached to an inverted microscope. The chamber was perfused at a rate of 2 ml min^{-1} with normal Tyrode solution of the following composition (mM): NaCl 136.9, KCl 5.4, $CaCl_2$ 1.8, $MgCl_2$ 0.5, $NaHPO_4$ 0.33, HEPES 5.0 and glucose 5.0; pH was adjusted to 7.4 by adding NaOH, and the solution was equilibrated by 100% O_2. The temperature was maintained at 35°C. Following the increase in calcium concentration of the medium to 1.8 mM (normal Tyrode solution), 30 to 40% of myocytes deteriorated into round-shaped cells due to irreversible contracture. The remaining cells were tolerant to calcium; their intact rod-shape was maintained without spontaneous beating, and the experiments were carried out on these myocytes.

For $\dot{V}_{max}$ measurement, the whole-cell clamp technique was used with a patch pipette (2–3 Mohm) containing a solution of (mM): KCl 120.0, NaH_2PO_4 10.0, EGTA 1.0, MgATP 5.0 and HEPES 10.0; the pH was adjusted to 7.2 by adding KOH. Single cells were voltage-clamped by Axoclamp-2A (Axon Instruments, Burlingame, California, U.S.A.) in a single-electrode discontinuous mode (sampling frequency: 8–11 kHz). To elicit action potential, the voltage-clamp was switched to the current-clamp mode by computer-operated TTL signals, during which a square pulse (2 ms) for stimulation was applied. The upstroke velocity ($\dot{V}_{max}$) was sampled at 70 kHz by an on-line analysis system (Anno & Hondeghem, 1990). Details of the clamp pulse protocols are given in the results section.

Drug and data analysis

SD-3212 (Santen Pharmaceutical Co., Osaka, Japan) was dissolved in dimethyl sulphoxide (DMSO) to prepare stock solution at 10 mM, and it was diluted further with Krebs Ringer or Tyrode solution to obtain the final concentration required. Final DMSO concentrations did not exceed 0.3%, and did not significantly affect the results. Values are presented as means ± s.e. or means unless otherwise stated. Data were analysed by *t* test, analysis of variance, Dunnett's test and regression analysis. Differences were considered significant at $P<0.05$.

Results

Action potentials of papillary muscle

Effects of SD-3212 (1 μM to 10 μM) on the action potential configuration were examined in six papillary muscles constantly stimulated at 0.2 Hz or 1.0 Hz (Figure 1, Table 1).

After exposure to 1 μM SD-3212 for 40 min, action potential duration (APD) at late repolarization (APD_{80}) was slightly prolonged at both 0.2 Hz and 1.0 Hz stimulation. At higher concentrations of SD-3212, APD especially at early repolarization (APD_{30}) tended to be shortened, in a concentration-dependent manner. The latter change was, however, statistically insignificant because of variability among the preparations. $\dot{V}_{max}$ was decreased significantly by SD-3212 $\geq$ 3 μM only at the higher stimulation frequency

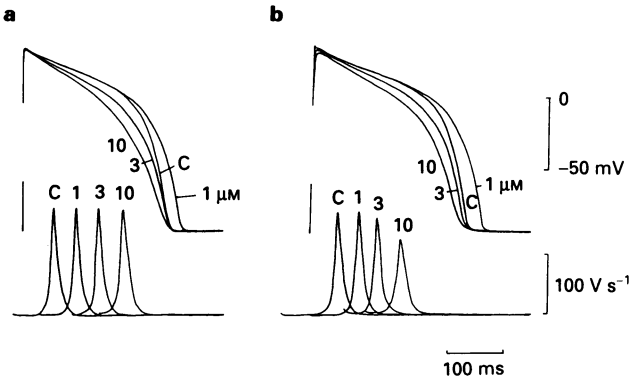


Figure 1 Effects of SD-3212 on transmembrane action potentials of papillary muscles. Upper traces are membrane action potentials, and lower traces are their differentiated upstroke spikes ($\dot{V}_{max}$). $\dot{V}_{max}$ was recorded at a faster sweep velocity. The preparation was constantly stimulated at 0.2 Hz (a) or at 1.0 Hz (b). The records were obtained before (control C) and 30–40 min after application of SD-3212 at 1, 3 and 10 μM.

Table I Effects of SD-3212 on action potential characteristics

		RP (mV)	*AMP* (mV)	APD_{30} (ms)	APD_{80} (ms)	$\dot{V}_{max}$ (Vs^{-1})
1.0 Hz	Control ($n=5$)	−91.4 ± 0.6	125.8 ± 2.0	223 ± 15	289 ± 11	174 ± 13
	SD-3212					
	1 μM	−91.8 ± 0.7	125.5 ± 2.2	239 ± 10	320 ± 8*	176 ± 10
	3 μM	−92.6 ± 0.1	124.8 ± 2.1	225 ± 13	301 ± 15	164 ± 15*
	10 μM	−90.6 ± 1.2	124.4 ± 2.6	208 ± 17	295 ± 16	143 ± 10*
0.2 Hz	Control ($n=5$)	−92.3 ± 0.6	126.3 ± 1.9	220 ± 13	292 ± 13	178 ± 12
	SDS-3212					
	1 μM	−92.7 ± 0.3	127.5 ± 1.3	237 ± 12*	314 ± 14*	184 ± 8
	3 μM	−92.4 ± 0.4	128.8 ± 1.1	218 ± 13	304 ± 14	183 ± 7
	10 μM	−92.7 ± 0.3	128.3 ± 1.2	199 ± 15	297 ± 17	176 ± 7

Values are means ± s.e.mean of five experiments. The preparations were constantly stimulated at 1.0 Hz or 0.2 Hz. Data were obtained before (control) and 40 min after application of SD-3212 at a given concentration. RP: resting membrane potential; AMP: amplitude of action potential; $\dot{V}_{max}$: maximum upstroke velocity of action potential; APD_{30} and APD_{80}: action potential duration from the upstroke to 30% and 80% repolarization. *Significantly different from control at $P<0.05$.

(1.0 Hz). Resting potential (RP) was unaffected even at 10 μM. IC_{20} of $\dot{V}_{max}$ inhibition induced by SD-3212 at 1.0 Hz, which was obtained by interpolation on a graph of log molar drug concentration versus response was 9.4 μM.

Use-dependent effects of $\dot{V}_{max}$

The effects of SD-3212 on $\dot{V}_{max}$ were examined with stimulation trains at different rates separated from each other by 30 s rest period. In control preparations, the value of $\dot{V}_{max}$ was almost unchanged with stimulation trains at rates from 0.1 to 2.0 Hz. After treatment with SD-3212, $\dot{V}_{max}$ of the first action potential in each train was slightly decreased, indicating a negligible or minimal tonic block (2.6 ± 1.0% at 3 μM and 4.4 ± 0.9% at 10 μM, $n = 5$). Further decline of $\dot{V}_{max}$ during the repetitive activity (use-dependent block) was observed at rates ≥ 0.5 Hz; the higher the stimulation frequency, the greater the block (Figure 2).

Figure 3 summarizes the percentage decrease of $\dot{V}_{max}$ from the first action potential to the new steady-state level, which was attained at around the 5th to 12th action potential. The use-dependent block of $\dot{V}_{max}$ by SD-3212 was greater at higher stimulation frequencies and at higher drug concentrations.

The beat-to-beat decline of $\dot{V}_{max}$ during stimulation trains at ≥ 0.5 Hz fitted a single exponential curve well (Figure 2), so that the onset rate per action potential (AP^{-1}) at which $\dot{V}_{max}$ fell to the new steady-state level could be calculated in each experiment (Table 2). The onset rate of the use-dependent block by SD-3212 was larger at the higher drug concentration and at the lower stimulation frequency (Table 2).

The recovery of $\dot{V}_{max}$ from the use-dependent block was studied by applying a single test stimulus at various coupling interval following a stimulation train for 60 s at 1.0 Hz. Before the application of the drug, the $\dot{V}_{max}$ of the test action potential recovered almost completely within 100 ms of the diastolic interval (the interval from the end of the last action potential to the beginning of the test action potential). The recovery process was approximated by a single exponential function with a mean time constant of 19 ± 2 ms ($n = 5$). After treatment with SD-3212 (10 μM), much slower $\dot{V}_{max}$ recovery was observed. Representative results are shown in Figure 4, where $\dot{V}_{max}$ of the test action potentials were plotted against the diastolic interval. In the presence of SD-3212, the recovery time course of longer than 100 ms was approximated by a single exponential function. The average time constant (τ_R) was 1.3 ± 0.2 s ($n = 5$).

V_{max} of single ventricular myocytes

In single ventricular myocytes, voltage-dependence of $\dot{V}_{max}$ inhibition by SD-3212 was investigated by using three clamp protocols. The baseline characteristics of action potential elicited in the cell at a long interstimulus interval (60 s) were as follows: RP, −80.6 ± 0.3 mV; $\dot{V}_{max}$, 568 ± 17 Vs^{-1}; APD_{80}, 178 ± 20 ms ($n = 8$).

First, the relationship between $\dot{V}_{max}$ and resting membrane potential from which the action potential originates were examined. Following a rest period of 60 s at a holding potential of −80 mV, which is long enough to eliminate the use-dependent depression of $\dot{V}_{max}$ by the drug, the membrane potential was clamped for 10 s to various levels (from −110 mV to −55 mV). At the end of the conditioning clamp, the voltage clamp was released and a stimulus was applied to elicit a test action potential. The decrease of $\dot{V}_{max}$

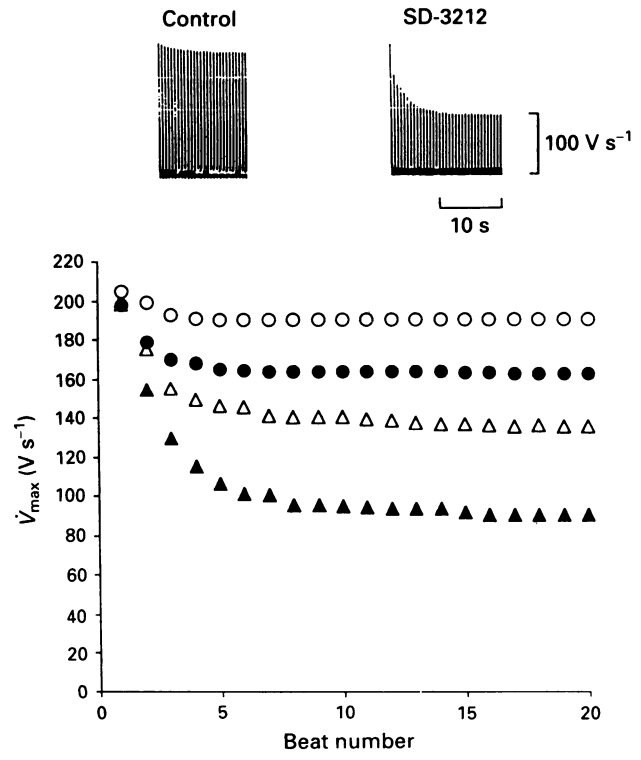


Figure 2 Use-dependent decrease of the maximum upstroke velocity ($\dot{V}_{max}$) of action potential in papillary muscles. Upper panels: differentiated upstroke spikes of action potentials during stimulation trains at 2.0 Hz after 30 s rest. The records were obtained before and 40 min after application of SD-3212 (10 μM). Lower graph: beat-to-beat change in $\dot{V}_{max}$ at the onset of stimulation trains in the presence of SD-3212 (10 μM) Ordinate scale: $\dot{V}_{max}$ Abscissa scale: number of beats (action potentials) from the initiation of stimulation train. Frequencies of stimulation were 0.2 Hz (○), 0.5 Hz (●), 1.0 Hz (△) and 2.0 Hz (▲).

Table 2 Tonic and use-dependent block of $\dot{V}_{max}$ by SD-3212

	n	*Tonic block* (%)	*Onset of use-dependent block* 1.0 Hz (AP^{-1})	2.0 Hz (AP^{-1})
SD-3212				
3 μM	(5)	2.6 ± 1.0	0.18 ± 0.03	0.14 ± 0.02
10 μM	(5)	4.4 ± 0.9	0.22 ± 0.05	0.20 ± 0.05

Values are means ± s.e.mean. n = number of preparations. AP^{-1}: per action potential.

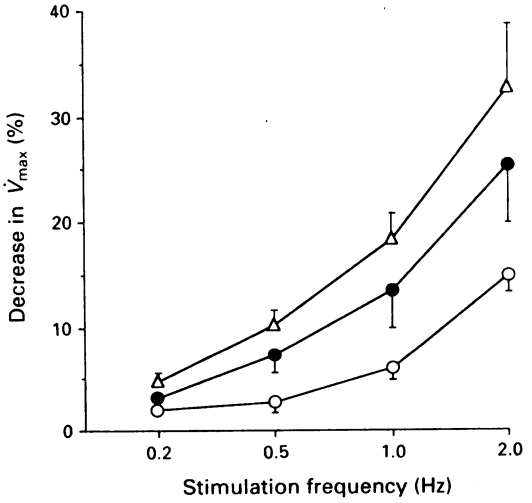


Figure 3 Relation between stimulation frequency and intensity of the use-dependent block. Ordinate scale: % decrease of maximum upstroke velocity ($\dot{V}_{max}$) of action potential from first action potential of stimulation trains to new steady-state level. Abscissa scale: stimulation frequency. Data were obtained 40-60 min after application of SD-3212 at 1 μM (○), 3 μM (●) and at 10 μM (△). Values are presented as means with s.e.means of five preparations.

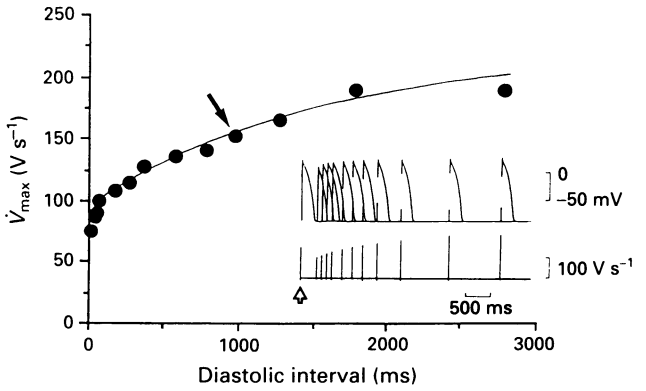


Figure 4 Recovery of $\dot{V}_{max}$ from the use-dependent block by SD-3212. Inset shows superimposed records of action potentials (upper trace) and their differentiated upstroke spikes (lower trace) after application of SD-3212 (10 μM). Following 1.0 Hz stimulation for 60 s, a single test stimulus was applied with various coupling intervals (an open arrow indicates the last conditioning stimulus). The graph shows $\dot{V}_{max}$ recovery in the presence of SD-3212 (10 μM). Ordinate scale: $\dot{V}_{max}$. Abscissa scale: diastolic interval (an interval from the end of the last conditioning action potential to the upstroke of the test action potential). The $\dot{V}_{max}$ recovery after SD-3212 was approximated by a single exponential function at a time constant of 1.0 s (solid arrow) for the data with diastolic intervals of over 100 ms.

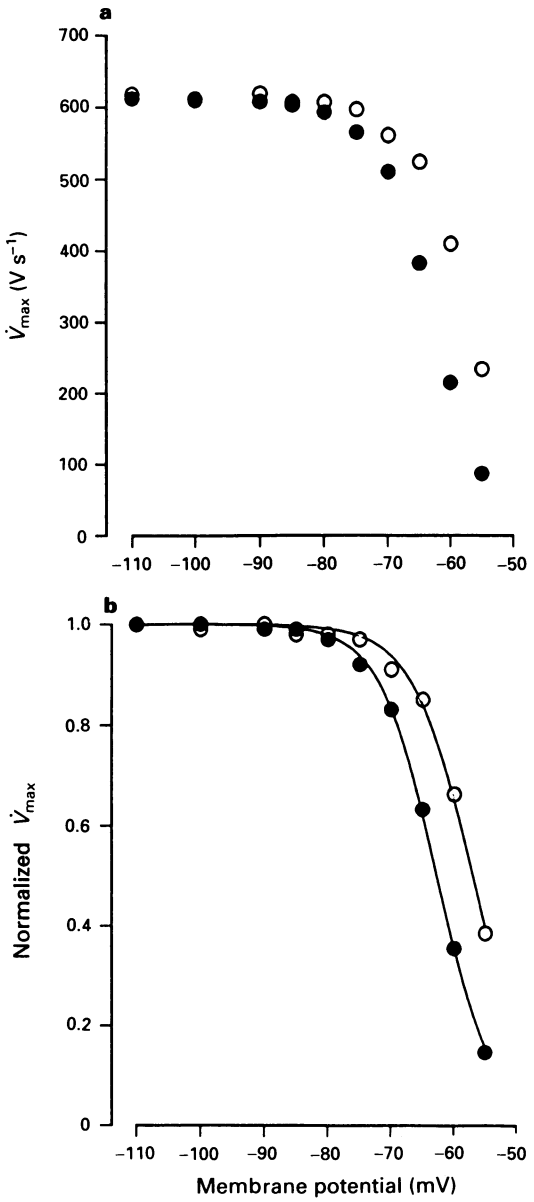


Figure 5 Voltage-dependence of $\dot{V}_{max}$ inhibition by SD-3212 in single ventricular myocytes. Ordinate scale: $\dot{V}_{max}$ of test action potential (a) and its fraction normalized by the value at the conditioning membrane potential of −110 mV (b). Abscissa scales: conditioning membrane potential from which a test action potential was elicited. Following a rest period of 60 s at a holding potential of −80 mV, the membrane potential was clamped for 10 s to various conditioning level (from −110 mV to −55 mV). At the end of the conditioning clamp, the voltage-clamp was released, and a test action potential was elicited to measure $\dot{V}_{max}$. Data were obtained before (○) and 20 min after application of SD-3212 at 10 μM (●).

by SD-3212 (10 μM) was more pronounced at less negative conditioning membrane potential (Figure 5a). A fraction of $\dot{V}_{max}$ was calculated in each experiment by normalizing the data with the value at −110 mV. The data points fitted the Bolzman equation;

$$y = (1 + \exp(Vm - Vh)k)^{-1} \quad (1)$$

where Vm is the conditioning clamp potential, Vh is the membrane potential showing a half maximal $\dot{V}_{max}$. Vh was changed from −55.2 ± 1.8 mV in control to −61.4 ± 2.1 mV after SD-3212, indicating a hyperpolarizing shift by 6.2 ± 1.1 mV ($n = 4$). The k value was almost identical (0.213 before, and 0.220 after SD-3212).

The second protocol was designed to determine whether the use-dependent $\dot{V}_{max}$ inhibition by SD-3212 is due to the blockade of an activated or inactivated sodium channel (Figure 6). Following a rest period of 60 s, the membrane potential was clamped up from the resting level (holding potential at −80 mV) to 0 mV for 10 to 2,000 ms. At the end of the conditioning depolarization, the membrane potential was clamped back to the holding voltage for 100 ms, which is long enough for a drug-free channel to reactivate fully (Carmeliet & Vereecke, 1979; Ebihara & Johnson, 1980), but short enough so that only partial dissociation of the drug from the blocked channel occurs (Grant *et al.*, 1984). The voltage-clamp was then released, and a stimulus was applied to elicit a test action potential. In untreated control myocytes, such a clamp pulse with a duration of less than 500 ms had no significant effect on the $\dot{V}_{max}$ of the test action potential. However, further prolongation of the clamp pulse duration resulted in a slight but significant $\dot{V}_{max}$ reduction probably due to slow inactivation of sodium channels (Saikawa & Carmeliet, 1982; Clarkson *et al.*, 1984). A clamp pulse of 2,000 ms in duration decreased $\dot{V}_{max}$ by 16.6 ± 1.6% ($n = 4$) from the value of action potential without the conditioning clamp (reference level). Treatment of the myocytes with SD-3212 (10 μM) for 10 to 20 min did not affect RP and $\dot{V}_{max}$ of the reference action potential. In such myocytes, a 0 mV conditioning clamp pulse caused a progressive decrease in $\dot{V}_{max}$ of the test action potential as the clamp pulse duration was prolonged (Figure 6). The decrease in $\dot{V}_{max}$ from the reference value was significant when the clamp pulse duration was longer that 50 ms, and reached 81.2 ± 2.8% ($n = 4$) at 2,000 ms. The change in $\dot{V}_{max}$ with each experiment was well fitted by single exponential function with a time constant of 332 ± 4 ms ($n = 4$). We also tested the effects of very short (2–5 ms) conditioning 0 mV prepulses in the presence of 10 μM SD-3212. They caused no significant decrease in $\dot{V}_{max}$ of test action potentials.

In the third protocol, the recovery process of $\dot{V}_{max}$ following a long (1 s) conditioning clamp to 0 mV was examined by introducing a test action potential with various coupling intervals during which the membrane potential was clamped back to −70 to −90 mV.

A representative experiment is shown in Figure 7. Under drug-free control conditions, the $\dot{V}_{max}$ of the test action

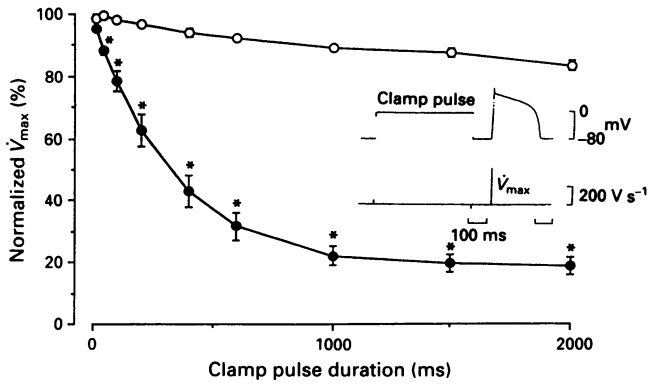


Figure 6 Effects of single 0 mV conditioning clamp pulse on the $\dot{V}_{max}$ inhibition induced by SD-3212. Ordinate scale: $\dot{V}_{max}$ of test action potential normalized by the value of action potential without clamp pulse (referenced at the tonic block subtracted value). Abscissa scale: duration of the conditioning 0 mV clamp. Values are presented as means ± s.e.mean of four cells. Data were obtained before (control, ○) and 20 min after application of SD-3212 at 10 μM (●). *Significantly different from control at $P<0.05$.

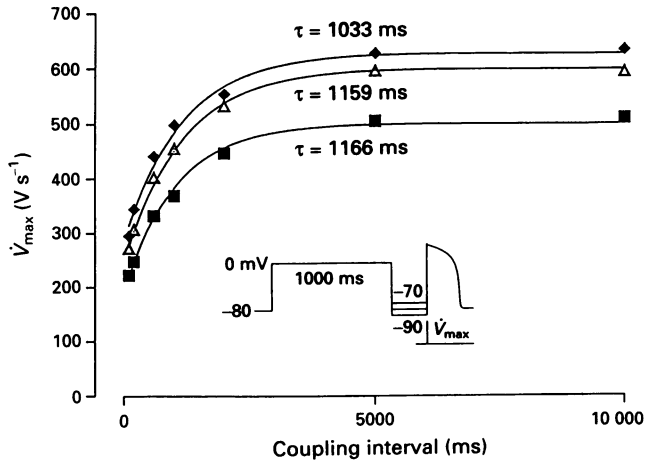


Figure 7 Recovery of $\dot{V}_{max}$ in a single ventricular myocyte treated with SD-3212 (10 μM). Following a long (1 s) conditioning clamp to 0 mV, the membrane potential was clamped back to −70 (■), −80 (△) or −90 (◆) mV, and a test action potential was elicited with various coupling intervals. Ordinate scale; $\dot{V}_{max}$ of test action potential. Abscissa scale: coupling interval from the end of 0 mV clamp to the upstroke of test action potentials. The time course of $\dot{V}_{max}$ recovery of test action potentials with a coupling intervals > 100 ms was approximated by a single exponential function with a time constant ranging from 1033 ms to 1166 ms.

potential recovered almost completely (95%) within 100 ms. The recovery process was approximated by a single exponential function with a mean time constant of 29 ± 3 ms at −70 mV, 25 ± 2 ms at −80 mV, and 22 ± 2 ms at −90 mV ($n = 4$). In the presence of SD-3212 (10 μM), the recovery time course of $\dot{V}_{max}$ with a coupling interval longer than 100 ms was approximated by a single exponential function with a time constant (τ_R) ranging from 1.03 s to 1.16 s. The average τ_R in four experiments showed a modest voltage-dependence; being shorter at the more negative potential: 1.14 ± 0.04 s at −70 mV, 1.22 ± 0.04 s at −80 mV and 1.01 ± 0.05 s at −90 mV.

Discussion

The present experiments on guinea-pig papillary muscles have revealed that SD-3212 ≥ 1 μM has a biphasic action on the repolarization of the action potential; low concentrations caused a moderate prolongation of APD, whereas this effect was reversed as the concentration was increased. At concentrations ≥ 3 μM, SD-3212 also caused a significant decrease in the maximum upstroke velocity ($\dot{V}_{max}$) of the action potential without affecting the resting membrane potential (RP). The effect on APD showing 'reverse dose-dependence' like quinidine or disopyramide (Wyse *et al.*, 1993) was not affected by stimulation frequencies, whereas the inhibition of $\dot{V}_{max}$ was observed only at higher stimulation frequencies (≥ 0.5 Hz). The biphasic effect on APD is probably due to a balance of the drug action on the outward potassium currents responsible for repolarization and that on the inward sodium and/or calcium currents flowing during the plateau phase of the action potential. Extensive voltage-clamp studies to measure individual ionic current will be required to clarify the mechanism, but this is out of the scope of the present study.

The decrease in $\dot{V}_{max}$ by SD-3212 without any change in RP reflects an inhibitory effect of the drug on the fast sodium inward current (I_{Na}), since the entire papillary muscle was excited simultaneously and there was no conduction within the preparation. Furthermore, a similar $\dot{V}_{max}$ inhibition was observed in single ventricular myocytes. The probable convex-shaped non-linear relationship between $\dot{V}_{max}$ and peak sodium inward current (I_{Na}) in cardiac cells (Cohen *et al.*, 1984; Sheets *et al.*, 1988) might introduce variable errors in estimating the precise amount of sodium channel block. Nevertheless, such a limitation does not invalidate $\dot{V}_{max}$ as a qualitative index, because voltage-clamp techniques currently available for I_{Na} measurement require more artificial experimental conditions (low temperature and low extracellular sodium concentrations) than those for $\dot{V}_{max}$ measurement.

The inhibition of $\dot{V}_{max}$ by SD-3212 was enhanced at the higher stimulation frequency. Thus, in normally polarized papillary muscles, SD-3212 at concentrations ranging from 1 to 10 μM caused negligible or minimal tonic $\dot{V}_{max}$ inhibition despite their marked use-dependent $\dot{V}_{max}$ inhibition. Such frequency-dependent $\dot{V}_{max}$ inhibition can be interpreted within the framework of the 'modulated receptor' hypothesis (Hondeghem & Katzung, 1977) or 'guarded receptor' hypothesis (Starmer *et al.*, 1984) to explain the interaction between local anaesthetic-type (Class-I) antiarrhythmic drugs and cardiac sodium channels. According to these hypotheses, the reduction of I_{Na} is due to the accumulation of drug-associated non-conducting channels (blocked channels). SD-3212, like most other Class-I antiarrhythmic drugs, may bind to the sodium channel receptor mainly during activated and/or inactivated states. This characteristic would lead to an accumulation of blocked channels during stimulation trains above certain rates.

The use-dependent block of $\dot{V}_{max}$ by SD-3212 was observed during stimulation trains at rates ≥ 0.5 Hz. The onset kinetics of use-dependent block was rapid (0.20 AP^{-1} at 10 μM, 2.0 Hz), and approximately 80 to 90% of the use-dependent block was attained within ten beats. The offset kinetics of use-dependent block by SD-3212 was also rapid; the average time constant of $\dot{V}_{max}$ recovery (τ_R) was 1.34 s. The τ_R value is longer than those described for fast kinetic Class-I drug such as lignocaine, mexiletine and tocainide (200–500 ms) (Campbell 1980; 1983 a,b), but still shorter than those for intermediate kinetic Class-I drugs such as quinidine, procainamide and aprindine (2.3–6.8 s) (Campbell 1980; 1983a,b; Kodama *et al.*, 1990). These observations may suggest that binding and dissociation kinetics of SD-3212 molecules to the cardiac sodium channels are quite rapid.

The relationship between $\dot{V}_{max}$ and membrane potential was examined in single ventricular cells following a rest period of 60 s (Figure 5). Under such experimental conditions, a decrease in $\dot{V}_{max}$ may reflect only the tonic block of sodium channels. The present data showed that the decrease in $\dot{V}_{max}$ by SD-3212 was more pronounced at less negative membrane potentials. This effect could be due to a high affinity of this drug for inactivated sodium channels.

It has been shown in our previous studies (Kodama *et al.*, 1987; 1990) that Class-I antiarrhythmic drugs can be subdivided into two groups in terms of their sodium channel blocking phase during the conditioning clamp pulse to 0 mV; one 'transient' and one 'maintained'. The former group of drugs (quinidine and disopyramide) may block the sodium channel mainly during its activated state, corresponding to the upstroke phase of the action potential, while the latter group (lignocaine, mexiletine, tocainide and aprindine) may do so predominantly during the inactivated state which correspond to the plateau phase of the action potential. In the present single cell experiments with SD-3212, we tested such a 'state-dependence' of sodium channel block by using a similar conditioning 0 mV clamp protocol. In the presence of SD-3212 (10 μM), the $\dot{V}_{max}$ of the test action potential, which was elicited 100 ms after the termination of 0 mV clamp, decreased progressively as the preceding clamp pulse duration was prolonged. The decay of $\dot{V}_{max}$ was well fitted to a single exponential function with a time constant of 332 ms. These findings may indicate that SD-3212 blocks the sodium channel primarily when it is in the inactivated state. Time constants for the onset of the inactivated channel block by SD-3212 are comparable to those for aprindine, but appreciably longer than lignocaine and mexiletine (Kodama *et al.*, 1990). Nevertheless, we cannot rule out a possibility that SD-3212 at higher concentrations blocks the sodium channel not only during the inactivated state but also during the activated state.

In the myocytes treated with SD-3212 (10 μM), the $\dot{V}_{max}$ recovery of test action potential following a long (1 s) 0 mV clamp was expressed by a single exponential function for the data points with coupling intervals $>$ 100 ms. This slow component of recovery may reflect the dissociation of the drug molecules (unbinding) from the sodium channels. Time constants of the $\dot{V}_{max}$ recovery in single myocytes, which are comparable to those of $\dot{V}_{max}$ recovery from the use-dependent block in papillary muscles (Figure 4), showed an appreciable voltage-dependence, being shorter at the more negative potential within the range from -70 to -90 mV. This voltage-dependence can be interpreted by its higher affinity for the inactivated state of sodium channels than the resting one. Under such conditions, hyperpolarization would enhance drug dissociation from channel receptors by increasing the resting fraction of drug-associated channels at the expense of their inactivated fraction (Hondeghem & Katzung, 1984; Grant *et al.*, 1984).

The *in vitro* concentration of SD-3212 used in the present study to decrease $\dot{V}_{max}$ is in a range of effective i.v. dose in dog experiments of arrhythmias (Nagashima *et al.*, 1992; Hirasawa *et al.*, 1992). Accordingly, it seems reasonable to conclude that the primary electrophysiological effect of this compound is a use- and voltage-dependent inhibition of fast sodium channels (Class-I action). From the onset and offset kinetics of the use-dependent $\dot{V}_{max}$ inhibition, SD-3212 is located between the fast and intermediate kinetic drugs. From the state-dependence of sodium channel block, SD-3212 belongs to inactivated channel blockers.

References

ANNO, T. & HONDEGHEM, L.M. (1990). Interactions of flecainide with guinea pig cardiac sodium channels. Importance of activation unblocking to the voltage dependence of recovery. *Circ. Res.*, **66**, 789–803.

CAMPBELL, T.J. (1980). Resting and rate-dependent depression of maximum rate of depolarization (Vmax) in guinea pig ventricular action potentials by mexiletine, and encainide. *J. Cardiovasc. Pharmacol.*, **12**, 1273–1286.

CAMPBELL, T.J. (1983a). Kinetics of onset of rate-dependent effects of Class-I antiarrhythmic drugs are important in determining their effects on refractoriness in guinea pig ventricle, and provide a theoretical basis for their subclassification. *Cardiovasc. Res.*, **17**, 344–352.

CAMPBELL, T.J. (1983b). Importance of physico-chemical properties in determining the kinetics of the effects of Class-I antiarrhythmic drugs on maximum rate of depolarization in guinea-pig ventricle. *Br. J. Pharmacol.*, **80**, 33–40.

CARMELIET, E. & VEREECKE, J. (1979). Electrogenesis of the action potential and automaticity. In *Handbook of Physiology. The Cardiovascular System*, I. ed. Berne, R.M. & Geiger, S.R. pp. 269–334. Bethesda, Maryland: American Physiological Society.

CLARKSON, C.W., MATSUBARA, T. & HONDEGHEM, L.M. (1984). Slow inactivation of Vmax in guinea pig ventricular myocardium. *Am. J. Physiol.*, **247**, H645–H654.

COHEN, C.J., BEAN, B.P. & TSIEN, R.W. (1984). Maximal upstroke velocity as an index of available sodium conductance. Comparison of maximal upstroke velocity and voltage clamp measurements of sodium current in rabbit Purkinje fibers. *Circ. Res.*, **54**, 635–651.

EBIHARA, L. & JOHNSON, E.A. (1980). Fast sodium current in cardiac muscle. A quantitative description. *Biophys. J.*, **32**, 779–790.

FUKUCHI, M., UEMATSU, T., NAGASHIMA, S., NAKASHIMA, M. (1990). Antiarrhythmic effects of benzothiazepine derivative (SD-3211) and its stereoisomer (SA-3212) in anesthetized rats and isolated perfused rat hearts compared with bepridil. *Naunyn-Schmied. Arch. Pharmacol.*, **341**, 557–564.

GRANT, A.O., STARMER, C.F. & STRAUSS, H.C. (1984). Antiarrhythmic drug action. Blockade of the inward sodium current. *Circ. Res.*, **55**, 427–439.

HIRASAWA, A., HARUNO, A., MATSUZAKI, T. & HASHIMOTO, K. (1992). Effects of a new antiarrhythmic drug, SD-3212, on canine ventricular arrhythmia models. *Jpn. Heart J.*, **33**, 851–861.

HONDEGHEM, L.M. & KATZUNG, B.G. (1977). Time and voltage-dependent interaction of antiarrhythmic drugs with cardiac sodium channels. *Biochem. Biophys. Acta*, **472**, 373–398.

HONDEGHEM, L.M. & KATZUNG, B.G. (1984). Antiarrhythmic agents: The modulated receptor mechanism of action of sodium and calcium channel-blocking drug. *Annu. Rev. Pharmacol. Toxicol.*, **24**, 387–423.

KODAMA, I., TOYAMA, J., TAKANAKA, C. & YAMADA, K. (1987). Block of activated and inactivated sodium channels by Class-I antiarrhythmic drugs studied by using the maximum upstroke velocity ($\dot{V}$max) of action potential in guinea-pig cardiac muscles. *J. Mol. Cell. Cardiol.*, **19**, 367–377.

KODAMA, I., HONJO, H., KAMIYA, K. & TOYAMA, J. (1990). Two types of sodium channel block by Class-I antiarrhythmic drugs studied by using $\dot{V}$max of action potential in single ventricular myocytes. *J. Mol. Cell. Cardiol.*, **22**, 1–12.

KODAMA, I., KONDO, N., SHIBATA, S. & YAMADA, K. (1985). Effects of dimethylpropranolol (UM-272) on the electrophysiological properties of guinea-pig ventricular muscles. *J. Pharmacol. Exp. Ther.*, **234**, 507–514.

MIYAWAKI, N., FURUTA, T., SHIGEI, T., YAMAUCHI, H. & ISO, T. (1990). Electrophysiological properties of SD-3211, a novel putative Ca^{2+} antagonist, in isolated guinea pig and rabbit hearts. *J. Cardiovasc. Pharmacol.*, **16**, 769–775.

MIYAWAKI, N., YAMAZAKI, F., FURUTA, T., SHIGEI, T. & YAMAUCHI, H. (1991). Antiarrhythmic effects of a novel Na^+ and Ca^{++} channel blocker, SD-3212: a comparison with its enantiomer (SD-3211). *Drug Dev. Res.*, **22**, 293–298.

NAGASHIMA, S., UEMATSU, T., ARAKI, T., MATSUZAKI, M., FUKUCHI, H. & NAKASHIMA, M. (1992). Antiarrhythmic and electrophysiological effects of SD-3212, a novel Na^+ and Ca^{++} channel blocker, in anesthetized dogs with myocardial infarction in comparison with its stereoisomer (SD-3211) and bepridil. *Naunyn-Schmied. Arch. Pharmacol.*, **345**, 688–695.

NAKAYAMA, K., MORIMOTO, K., NAZAWA, Y. & TANAKA, Y. (1992). Calcium antagonistic and binding properties of semotiadil (SD-3211), a benzothiazine derivative assessed in cerebral and coronary arteries. *J. Cardiovasc. Pharmacol.*, **20**, 380–391.

SAIKAWA, T. & CARMELIET, E. (1982). Slow recovery of the maximum rate of rise (Vmax) of the action potential in sheep cardiac Purkinje fibers. *Pflügers Arch.*, **394**, 90–93.

SHEETS, M.F., HANK, D.A. & FOZZARD, H.A. (1988). Nonlinear relation between Vmax and I_{NA} in canine cardiac Purkinje cells. *Circ. Res.*, **63**, 386–398.

STARMER, C.F., GRANT, A.O. & STRAUSS, H.C. (1984). Mechanism of use-dependent block of sodium channels in excitable membranes by local anesthetics. *Biophys. J.*, **46**, 15–27.

TERAMOTO, N. (1993). Mechanisms of the inhibitory action of semotiadil fumarate, a novel Ca antagonist, on the voltage-dependent Ca Current in smooth muscle cells of the rabbit portal vein. *Jpn. J. Pharmacol.*, **61**, 183–195.

TOYAMA, J., KAMIYA, K., KODAMA, I. & YAMADA, K. (1987). Frequency- and voltage-dependent effects of aprindine on the upstroke velocity of action potential in guinea pig ventricular muscles. *J. Cardiovasc. Pharmacol.*, **9**, 165–172.

WYSE, R.K., YE, V., & CAMPBELL, J.T. (1993). Action potential prolongation exhibits simple dose-dependence for sotalol, but reverse dose-dependence for quinidine and disopyramide: implications for proarrhythmia due to triggered activity. *J. Cardiovasc. Pharmacol.*, **21**, 316–322.

(Received April 25, 1994
Revised September 20, 1994
Accepted September 23, 1994)

British Journal of Pharmacology (1995) 114, 510–516 © 1995 Stockton Press All rights reserved 0007–1188/95 $9.00

Isothioureas: potent inhibitors of nitric oxide synthases with variable isoform selectivity

Garry J. Southan, Csaba Szabó & [1]Christoph Thiemermann

The William Harvey Research Institute, St. Bartholomew's Hospital Medical College, Charterhouse Square, London EC1M 6BQ

1 The induction of a calcium-independent isoform of nitric oxide (NO) synthase (iNOS) and a subsequent enhanced formation of NO has been implicated in the pathophysiology of a variety of diseases including inflammation and circulatory shock. Here we demonstrate that the S-substituted isothioureas, S-methylisothiourea (SMT), S-(2-aminoethyl)isothiourea (aminoethyl-TU), S-ethylisothiourea (ethyl-TU) and S-isopropylisothiourea (isopropyl-TU) potently inhibit iNOS activity in J774.2 macrophages activated with bacterial endotoxin with EC_{50} values 8–24 times lower than that of N^G-methyl-L-arginine (MeArg) and 200-times lower than that of N^G-nitro-L-arginine (L-NO_2Arg).

2 The inhibition of iNOS activity by these S-substituted isothioureas is dose-dependently prevented by excess of L-arginine suggesting that these isothioureas are competitive inhibitors of iNOS at the L-arginine binding site.

3 Ethyl-TU and isopropyl-TU are 4–6 times more potent than MeArg in inhibiting the constitutive NOS activity in homogenates of bovine aortic endothelial cells (eNOS) and are more potent pressor agents than MeArg in the anaesthetized rat. SMT is equipotent with MeArg, whereas aminoethyl-TU is 6-times less potent in inhibiting eNOS activity *in vitro*. Both SMT and aminoethyl-TU, however, elicit only weak pressor responses (approximately 15 mmHg at 10 mg kg^{-1}, i.v.) *in vivo*.

4 A comparison of the potencies of ethyl-, iso-propyl-, n-propyl-, t-butyl- and n-butyl-isothioureas on iNOS activity shows that the inhibitory activity of S-substituted isothioureas declines sharply if the side chain exceeds 2 carbon atoms in length. Similarly, substitution of the ethylene side chain of ethyl-TU also results in a diminished potency. Substitution of either one or both nitrogens of SMT with either amino or alkyl groups also substantially reduces its NOS inhibitory potency.

5 In conclusion, isothioureas represent a new class of NOS inhibitors which includes the most potent inhibitors of iNOS activity reported to date. Some members of this class (ethyl-TU and isopropyl-TU) are potent inhibitors of eNOS and iNOS with little selectivity towards either isoform, while others (SMT and aminoethyl-TU) are relatively selective inhibitors of iNOS activity. These latter agents may become useful tools for studying the role of iNOS in various disease models and may be useful in the therapy of diseases that are associated with an enhanced formation of NO due to iNOS induction, such as inflammation, circulatory shock or cancer.

Keywords: Nitric oxide; constitutive nitric oxide synthase; inducible nitric oxide synthase; blood pressure; circulatory shock; inflammation; endotoxin

Introduction

The induction of a distinct isoform of nitric oxide synthase (inducible NOS, iNOS) in various cells by agents such as bacterial lipopolysaccharide (LPS), interleukin-1, tumour necrosis factor and γ-interferon (IFN), leads to an enhanced formation of nitric oxide (NO) from its precursor, L-arginine. The NO produced may have physiological roles, for instance in the antimicrobial activity of activated macrophages (Moncada *et al.*, 1991; Nathan, 1992), but the sustained production of large quantities of NO following the induction of iNOS has been implicated in the pathogenesis of circulatory shock (Thiemermann & Vane, 1990; Meyer *et al.*, 1992; Nava *et al.*, 1992; Szabó *et al.*, 1993a; Thiemermann *et al.*, 1993; Szabó & Thiemermann, 1994; Thiemermann, 1994), diabetes (Corbett *et al.*, 1992), chronic inflammation (McCartney-Francis *et al.*, 1993; Stefanovic-Racic *et al.*, 1993; Miller *et al.*, 1993; Koprowski *et al.*, 1993; Vane *et al.*, 1994), transplant rejection (Langrehr *et al.*, 1993) and cancer (Piper *et al.*, 1993). Inhibition of iNOS activity may, therefore, be of significant therapeutic benefit in these conditions. However, the L-arginine based inhibitors of NOS currently used in experimental models and proposed for therapeutic intervention also inhibit the constitutive isoforms of NOS present in the brain (nNOS) or in endothelial cells (eNOS).

[1] Author for correspondence.

NO from endothelial NOS (eNOS) is involved in the regulation of blood pressure and organ blood flow distribution and inhibits the adhesion of platelets and polymorphonuclear granulocytes to the endothelial surface (Moncada *et al.*, 1991; Nathan, 1992; Dinerman *et al.*, 1993; Calver *et al.*, 1993; Vane, 1994; Lowenstein *et al.*, 1994). Dysfunction of NO formation by the vascular endothelium has been shown in a number of vascular and non-vascular diseases (Fujiwara *et al.*, 1986; Bucala *et al.*, 1991; Szabó *et al.*, 1992; Parker & Adams, 1993). In view of the physiological roles of eNOS and the pathophysiological implications of enhanced formation of NO by iNOS, pharmacological agents that selectively inhibit iNOS may well have a therapeutic advantage over those currently available. The L-arginine analogues N^G-cyclopropyl-L-arginine, N^G-methyl-L-arginine (MeArg), N^G-nitro-L-arginine (L-NOArg) and its methyl ester (after hydrolysis) are more potent inhibitors of eNOS than of iNOS, while MeArg, N^G-aminohomo-L-arginine and N^G-amino-L-arginine are equipotent inhibitors of both eNOS and iNOS (Gross *et al.*, 1990; 1991; Lambert *et al.*, 1991; 1992). Aminoguanidine and some related guanidines, however, are weaker inhibitors of eNOS than iNOS, and, hence, exhibit selectivity as inhibitors of iNOS (Corbett *et al.*, 1992; Misko *et al.*, 1993; Hasan *et al.*, 1993). Here we describe a novel class of potent NOS inhibitors, some of which show relative selectivity towards iNOS.

Methods

Cell culture

The mouse macrophage cell line J774.2 was cultured in Dulbecco's modified Eagle's medium (DMEM) with L-glutamine (4×10^{-3} M) and 10% foetal calf serum (FCS) as described (Szabó *et al.*, 1993b; 1994b). Cells were cultured in 96-well plates with culture medium (200 µl/well) until they reached confluence. To induce iNOS, fresh culture medium containing *E.coli* lipopolysaccharide (LPS, 1 µg ml^{-1}) was added. Nitrite accumulation in the cell culture medium was measured after 24 h. To assess the effects of various agents on the production of nitrite, they were added to the medium 6 h after induction of iNOS with LPS. At this time there is no detectable increase in the concentration of nitrite, and agents such as glucocorticoids, that inhibit the induction but not the activity of iNOS, have no effect on subsequent nitrite production (Szabó *et al.*, 1993b, 1994b). In some experiments, agents were applied together with excess L-arginine (in total 1.4, 10 or 30 mM in the culture medium, as opposed to 0.4 mM in normal DMEM).

Nitrite measurement

Nitrite production, an indicator of NO synthesis, was measured in the supernatant of J774.2 macrophages as previously described (Szabó *et al.*, 1993b; 1994b). Nitrite was measured by adding 100 µl of Griess reagent (1% sulphanilamide and 0.1% naphthylethylenediamine in 5% phosphoric acid) to 100 µl samples of cell culture medium. The optical density at 550 nm (OD_{550}) was measured with an Anthos 1.2.1 microplate reader (Anthos Labtechnik, Salzburg, Austria). Nitrite concentrations were calculated by comparison with OD_{550} of standard solutions of sodium nitrite (5–100 µM) prepared in culture medium.

Cell viability and respiration

Mitochondrial respiration, an indicator of cell viability, was assessed by the mitochondrial-dependent reduction of 3-(4,5-dimethylthiazol-2-yl)-2,5-diphenyltetrazolium bromide (MTT) to formazan (Szabó *et al.*, 1993b, 1994b). Cells in 96-well plates were incubated (37°C) with MTT (0.2 mg ml^{-1}) for 60 min. Culture medium was removed and the cells solubilized in DMSO (100 µl). The extent of reduction of MTT to formazan within cells was quantitated by measurement of OD_{550} with the Anthos microplate reader. Formazan production was expressed as a percentage of the values obtained from untreated cells. Inhibition of nitrite production by the drugs tested is only reported where there is no significant decrease in cell viability.

The hydrolysis of substituted isothioureas to thiols and urea

The rate of hydrolysis of S-substituted isothioureas at the pH of the experiments was estimated by measuring the release of free thiols (R_1-SH, see Figure 1). Isothioureas (0.5–5 mM) were incubated in 96-well plates at pH 7.4 or 12 in the presence of 2,2'-dithiodipyridine (Aldrithiol-2, 1 mM, at 37°C). Reduction of Aldrithiol-1 by the released thiol was measured by increased absorbance at 340 nm using the Anthos microplate reader. In addition, urea from the hydrolysis of S-methylisothiourea (SMT) (incubated at 37°C for 17 h at pH 7.4 or 12) was determined by heating for 10 min at 100°C with 2,3-butanedione monoxime under strongly acidic conditions and measuring spectrophotometrically at 405 nm.

Nitric oxide synthase assay

The intimal surfaces of fresh bovine aortae were scraped in the presence of buffer composed of (mM): Tris·HCl 50, EDTA 0.1, EGTA 0.1, 2-mercaptoethanol 12 and phenylmethylsulphonyl fluoride 1 (pH 7.4). Cell suspensions were then homogenized in the buffer (composition as above) on ice in an Ultra-Turrax T25 homogenizer (Janke & Kunkel, IKA Labortechnik, Staufen i. Br., Germany). Conversion of [^{3}H]-L-arginine to [^{3}H]-L-citrulline was measured in the homogenates as described (Szabó *et al.*, 1993a; Thiemermann *et al.*, 1993). Briefly, cell homogenate (50 µl) was incubated in the presence of [^{3}H]-L-arginine (10 µM, 5 kBq/tube), NADPH (1 mM), calmodulin (30 nM), tetrahydrobiopterin (5 µM) and calcium (2 mM) for 20 min at 37°C in HEPES (20 mM) buffer (pH 7.5). Reactions were stopped by dilution with 1 ml of ice cold HEPES (20 mM) buffer (pH 5.5) containing EGTA (2 mM) and EDTA (2 mM). Reaction mixtures were applied to Dowex 50W (Na^+ form) columns and the eluted [^{3}H]-L-citrulline activity was measured by scintillation counting (Beckman, LS3801; Fullerton, CA, U.S.A.).

Haemodynamic measurements

Male Wistar rats (260–320 g; Glaxo Laboratories Ltd., Greenford, Middx.) were anaesthetized with thiopentone sodium (Trapanal, 3% solution; 120 mg kg^{-1}, i.p.). The trachea was cannulated to facilitate respiration and rectal temperature was maintained at 37°C with a homeothermic blanket (BioSciences, Sheerness, Kent, U.K.). The right carotid artery was cannulated and connected to a pressure transducer (P23XL, Spectramed, Stratham, U.S.A.) for the measurement of phasic and mean arterial blood pressure (MAP) and heart rate which were displayed on a Grass model 7D polygraph recorder (Grass Instruments, Quincy, Mass, U.S.A.) (Thiemermann & Vane, 1990; Szabó *et al.*, 1993a). Left and right femoral veins were cannulated for the administration of drugs. Upon completion of the surgical procedure, cardiovascular parameters were allowed to stabilize for 10 min. After recording baseline haemodynamic parameters, animals received NOS inhibitors in a cumulative manner (0.001–10 mg kg^{-1}, i.v. bolus injections) with 5 min between injections.

Materials

Aminoguanidine, bacterial lipopolysaccharide (*E. coli*, serotype No. 0127:B8), calmodulin, DMEM, L-glutamine, MTT, NADPH, N^G-nitro-L-arginine, N^G-nitro-L-arginine methyl ester, sodium nitrite and Dowex 50W anion exchange resin were obtained from Sigma Chemical Co. (Poole, Dorset, U.K.). N^G-methyl-L-arginine monoacetate (MeArg) was obtained from Calbiochem (Nottingham, U.K.). Tetrahydrobiopterin was from Dr B. Schirks Laboratories, Jona, Switzerland. Foetal calf serum was obtained from Advanced Protein Products (West Midlands, U.K.). L-[2,3,4,5-^{3}H]-arginine hydrochloride was obtained from Amersham (Buckinghamshire, U.K.). N^G-amino-L-arginine was synthesized by Dr O.W. Griffith (Medical College of Wisconsin, Milwaukee U.S.A.). Methanethiol sodium salt, methyl-methanethiolsulphonate and methane disulphide were obtained Fluka (Gillingham, Dorset, U.K.). 2,3 Butanedione monoxime and 2,2'-dithiodipyridine (Aldrithiol), were obtained from Aldrich (Gillingham, Dorset, U.K.).

Drugs for both *in vitro* and *in vivo* experiments were dissolved in sterile, saline. Picrate salts (see Table 1) for use with cultured macrophages were first dissolved in dimethylsulphoxide (Sigma) and then diluted with 9 parts water. Neither the mode of dissolution nor the type of salt used (bromide, picrate etc.) had any influence on the inhibitory activity of a particular isothiourea.

Isothioureas

Compounds No. **6–8**, **19**, **25**, **29**, **30–34**, **43** and **44** in Table 1 were purchased from Aldrich. The other S-substituted isothioureas were generally prepared as salts from the appro-

priate thioureas or thiosemicarbazides (Aldrich) by reaction with alkyl or substituted alkyl halides by variations on established methods. In some cases, alkylation was achieved using alkyl *p*-toluenesulphonates. Typically, thiourea or the appropriate N-substituted thiourea was dissolved in boiling alcohol (isopropanol or ethanol) and refluxed for several hours with a slight excess of the appropriate alkyl halide or alkyl *p*-toluenesulphonate. Solutions were allowed to cool. Solvent and volumes were chosen to encourage crystallization of the product at this stage. Otherwise, the solvent was removed and the residues worked up into solid and recrystallized. For those compounds that did not crystallize as the hydro-halide salts, their picrate salts were precipitated from aqueous solution. For detailed synthetic procedures the reader is referred to the following reviews (and references therein); Schroeder, 1955; Reid, 1963 and to Olin & Dains, 1930. Elemental

Table 1 Inhibitory effect of substituted isothioureas and reference compounds on nitrite production by activated macrophages

	Reference compound		$^{a}EC_{50}$ (μM)
1	N^{G}-methyl-L-arginine (MeArg)		48
2	N^{G}-nitro-L-arginine (L-NOArg)		400
3	N^{G}-nitro-L-arginine methyl ester (L-NAME)		>1000 (^{b}32%)
4	N^{G}-amino-L-arginine		90
5	Aminoguanidine		130
	Compound		
	$*R_2 = R_3 = R_4 = H$)	$*R_1$	EC_{50} (μM)
6	Thiourea	–	>1000 (^{b}26%)
7	SMT	CH_3-	6
8	Ethyl-TU	CH_3-CH_2-	2
9	iso-Propyl-TU	CH_3-(CH_3-)CH_2-	2
10	n-Propyl-TU	CH_3-$(CH_2)_2$-	78
11	t-butyl-TU	$(CH_3)_3C$-	80
12	n-Butyl-TU	CH_3-$(CH_2)_3$-	280
13	sec-butyl-TU	CH_3-CH_2-(CH_3-)CH-	65
14	n-Pentyl-TU	CH_3-$(CH_2)_4$-	>1000 (^{b}46%)
15	Cyclopentyl-TU	cyclopentyl-	242
16	Isoamyl-TU	CH_3-(CH_3-)$(CH_2)_3$-	900
17	Lauryl-TU	CH_3-$(CH_2)_{11}$-	>10^{c}
18	Cetyl-TU	CH_3-$(CH_2)_{15}$-	>1000 (^{b}29%)
19	Benzyl-TU	$C_6H_5CH_2$-	100
20	4-Chlorobenzyl-TU	4-Cl-$C_6H_4CH_2$-	65
21	Chloroethyl-TU	Cl-CH_2-CH_2-	28
22	Cyanomethyl-TU	NC-CH_2-	>1000
23	Acetimido-TU	NH_2-CO-CH_2-	>1000 (^{b}6%)
24	Carboxy-methyl-TU	CO_2H-CH_2-	>1000 (^{b}21%)
25	Aminoethyl-TU	NH_2-CH_2-CH_2-	3
26	Methoxy-ethyl-TU	CH_3-O-CH_2-CH_2-	68
27	Ethoxy-ethyl-TU	CH_3-CH_2-O-CH_2-CH_2-	170
28	Phenoxy-propyl-TU	C_6H_5-O-CH_2-CH_2-CH_2-	200
29	Amidine-thiopropane-sulphonic acid	SO_3H-CH_2-CH_2-CH_2-	>1000 (^{b}29%)
30	3-Indolyl-TU	Indolyl	>10^{c}
	$R_2 = R_3 = H$	R_1 R_4	EC_{50} (μM)
31	2-Aminothiazoline	-CH_2-CH_2-^{d}	38
32	2-Aminothiazole	-CH_2 = CH_2-	470
33	2-Amino-1,3,4-thiadiazol	-CH_2-NH-	>1000
34	Pseudothiohydantoin	-CH_2-CO-	>1000
	R_1 = CH3, R_3 = H	R_2 R_4	EC_{50} (μM)
35	N-methyl-SMT	CH_3-, H	350
36	N,N'-dimethyl-SMT	CH_3-, CH_3	>1000 (^{b}43%)
37	N,N'-diethyl-SMT	CH_3-CH_2-, CH_3-CH_2-	>1000 (^{b}29%)
38	N-phenyl-SMT	C_6H_5-, H-	330
39	N-(4-nitrophenyl)SMT	4-NO_2-C_6H_4-, H-	310
40	N-amino-SMT	NH_2-, H-	630
41	N-amino-N'-methyl-SMT	NH_2- CH_3-	220
42	N-amino-N'-phenyl-SMT	NH_2- C_6H_5-	550
43	2-(Methylthio)imidazoline	-CH_2-CH_2-^{e}	860
44	N-cyano-N'-methyl-SMT	NC- CH_3-	>1000
	R_1 = CH3; R_4 = H	R_2 R_3	EC_{50} (μM)
45	N-amino-N-methyl-SMT	NH_2- CH_3	150

$*R_{1-4}$ refer to Figure 1. $^{a}EC_{50}$s calculated from 5 point dose-response curves (100 nM–1 mM). ^{b}Inhibition did not exceed 50% at 1 mM; percentage inhibition is given at 1 mM. ^{c}Lauryl-TU and 3-indolyl-TU are cytotoxic over 10 μM. ^{d}Cyclic compound: R_1 (^{e} or R_2) and R_4 are replaced by chain indicated to give a 5-membered ring. The compounds were used as the following salts: acetate (.CH_3CO_2H): **1**, **4**; chloride (.HCl): **5**, **19**, **20**; bromide (.HBr): **8**, **9**, **14–18**, **21–25**, **27**, **28**; iodide (.HI): **12**, **30**, **35**, **36**, **38**; *p*-toluene sulphonate (.HSO_3-C_6H_4-CH_3): **37**, **41**, **42**, **45**; sulphate (.1/2 H_2SO_4): 7; and picrate: **10**, **11**, **13**, **26**.

(C H N) compositions were all within 5% of theoretical. Melting points were found to be the same as available literature values.

Note that the nomenclature does not necessarily follow IUPAC conventions: names are intended to emphasize the group attached to the sulphur atom (R_1, Figure 1). N-substituted compounds are treated as derivatives of the parent compound, SMT, and are prefixed by N-. S-substituted-isothioureas may also be described as 2-substituted-thiopseudoureas.

Statistical evaluation

All values in the figures and text are expressed as mean ± s.e.mean of n observations. For each drug, at least 9 wells from 3 independent experiments were studied. Student's unpaired t test was used to compare means between groups. A P-value less than 0.05 was considered to be statistically significant.

Results

Many of the S-substituted isothioureas tested cause a dose-dependent inhibition of nitrite production by stimulated J744.2 macrophages, with a wide range of potencies (Table 1). They appear to do so by inhibiting the activity of iNOS, rather than its induction, for they inhibit nitrite accumulation when added to the medium at a time point when induction of iNOS has already occurred (i.e. 6 h after addition of LPS). The most potent isothioureas are those with only short alkyl chains on the sulphur atom ($R_1 = C_1$ or C_2, where R refers to Figure 1) and no substituents on the nitrogens ($R_2 = R_3 = R_4 = H$). Some of these have potencies of up to 24 times that of MeArg. A comparison of dose-response curves (Figure 2) shows the following order of potency for these compounds as inhibitors of iNOS (emboldened numbers refer to Table 1): S-ethyl-isothiourea (ethyl-TU, **8**) = S-isopropyl-isothiourea (isopropyl-TU, **9**) > S-(2-aminoethyl)isothiourea (aminoethyl-TU, **25**) > SMT (**7**) >> N^G-methyl-L-arginine (MeArg,**1**) >> N^G-nitro-L-arginine (L-NOArg, **2**). Increasing the length of R_1 (see Figure 1) or incorporating polar groups into R_1 results in diminished potencies of the isothioureas, with the notable exception of aminoethyl-TU (**25**). However, several compounds, e.g. chloroethyl-TU (**21**), methoxyethyl-TU (**26**) and 2-aminothiazoline (**31**) are of similar potency to MeArg (**1**) as inhibitors of iNOS activity (Table 1).

Increasing concentrations of L-arginine (1–30 mM) in the medium of macrophages treated with isothioureas caused a dose-dependent increase in the EC_{50} values of MeArg and selected isothiourea derivatives (Table 2).

To investigate the possible liberation of thiols (R_1-SH) deriving from the hydrolysis of isothioureas and their potential effects on iNOS activity, compounds that release methanethiol (a product of the hydrolysis of SMT) were tested for their inhibition of nitrite production in activated macrophages. At 0.1 mM, sodium methanethiolate and methyl-methanethiolsulphonate inhibited nitrite accumulation by 35 ± 3% and 45 ± 2%, respectively. At 1 mM, sodium methanethiolate and methane disulphide caused a 41 ± 9% and 32 ± 2% inhibition, respectively, and methyl-methanethiolsulphonate became cytotoxic ($n = 4–6$). Thus, these agents appear to be approximately 100 fold weaker than SMT as inhibitors of iNOS activity, and, hence, release of methanethiol is unlikely to account for the inhibitory effects of SMT. In addition, the amount of thiol released from SMT over 17 h at pH 7.4 (37°C) is equivalent to the hydrolysis of less than 0.2% of the SMT present ($n = 6$). A similar value (4 ± 6%) was obtained for the hydrolysis of SMT to urea at pH 7.4. At alkaline pH, however, 45 ± 3% of SMT was converted to urea in 17 h ($n = 6$).

S-substituted isothioureas also caused dose-dependent inhibition of eNOS activity in homogenates of bovine aortic endothelial cells (Figure 3). The most potent inhibitors of iNOS activity were often also found to be the most potent inhibitors of eNOS activity. However, the order of potency was different: isopropyl-TU (**9**) > ethyl-TU (**8**) > L-NOArg (**2**) > MeArg (**1**) = SMT (**7**) > aminoethyl-TU (**25**). The potencies of ethyl-TU (**8**) and isopropyl-TU (**9**) on eNOS were reflected in their pressor effects in the anaesthetized rat. These compounds were approximately equipotent, and caused significant increases in the MAP at doses as low as 1 μg kg^{-1} (Figure 4). At the intermediate dose of 0.1 mg kg^{-1}, SMT (**7**) and aminoethyl-TU (**25**) caused pressor responses similar to those of MeArg (**1**). At higher doses (1 and 10 mg kg^{-1}), however, the pressor effects of aminoethyl-TU

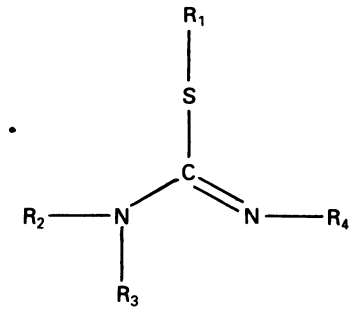


Figure 1 Generic structure of S-substituted isothioureas.

Table 2 Effect of NOS inhibitors (100 nM–1 mM) on the production of nitrite by stimulated J774.2 macrophages with increasing concentration of L-arginine (L-Arg) in the culture medium

	EC_{50} (μM)			
L-Arg (mM)	0.4*	1.4	10	30
MeArg	48	160	>1000	>>1000
SMT	6	23	160	230
Ethyl-TU	2	28	100	204
Isopropyl-TU	2	25	66	131
Aminoethyl-TU	3	35	90	270

*Normal DMEM.

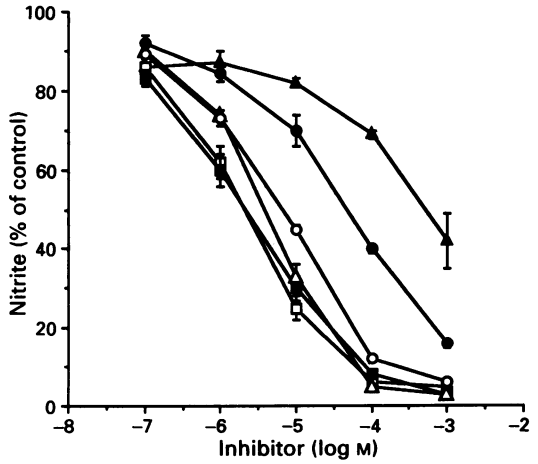


Figure 2 Effect of MeArg (●), L-NOArg (▲), SMT (○), ethyl-TU (□), aminoethyl-TU (△), and isopropyl-TU (■) when applied 6 h after lipopolysaccharide (LPS), on nitrite accumulation in the supernatant of culture J774.2 macrophages activated with LPS (1 μg ml^{-1}) for 24 h. Data (nitrite as % of control) are expressed as means ± s.e.mean of 9–12 wells from 3–4 independent experiments. Nitrite concentration in the culture medium at 24 h after LPS was 36 ± 1 μM. For abbreviations, see text.

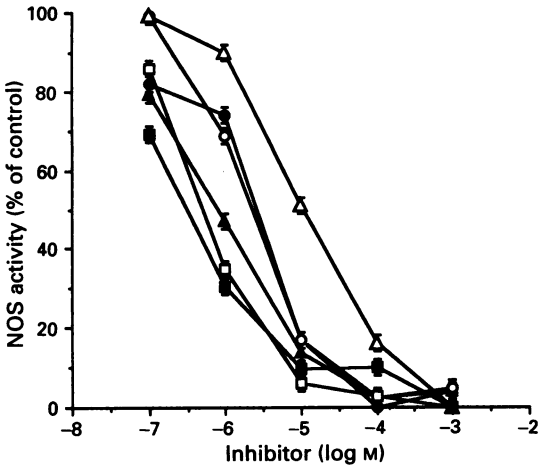


Figure 3 Effect of MeArg (●, EC_{50} = 6 μM), L-NOArg (▲, 1 μM), SMT (○, 5 μM), ethyl-TU (□, 7 μM), aminoethyl-TU (△, 12 μM), and isopropyl-TU (■, 0.5 μM) on eNOS activity, measured as formation of L-citrulline from L-arginine in homogenates of bovine endothelial cells in the presence of various co-factors and calcium (see Methods for details). Data (% of control activity, 4.12 ± 0.6 pmol mg^{-1} protein min^{-1}) are expressed as means ± s.e.mean of 5–6 experiments. For abbreviations, see text.

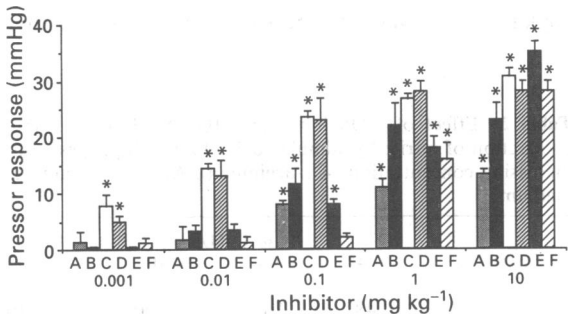


Figure 4 Changes in mean arterial blood pressure (MAP) in anaesthetized rats in response to intravenous injections of aminoethyl-TU (column A), SMT (column B), ethyl-TU (column C), isopropyl-TU (column D), MeArg (column E) and L-NOArg (column F) (0.001–10 mg kg^{-1}, i.v.). Baseline MAP prior to drug administration (128 ± 2 mmHg, n = 32) was not significantly affected by cumulative injection of vehicle (saline, n = 5). Data are expressed as means ± s.e.mean of n = 5–6 rats for each group, except SMT where n = 13. *Significant difference ($P < 0.05$) from baseline. For abbreviations, see text.

(**25**) were less than those seen with the other NOS inhibitors. Even at 10 mg kg^{-1}, the increase in the MAP seen with aminoethyl-TU (**25**) was only approximately 14 mmHg. Interestingly, L-NOArg (**2**), up to 0.1 mg kg^{-1}, failed to elicit any significant pressor response, but at higher doses it caused a pronounced pressor effect, which was similar to that caused by MeArg (**1**) (Figure 4).

Discussion

We demonstrate here that S-substituted isothioureas represent a novel class of NOS inhibitors. The EC_{50} values of some of these compounds (compounds **7**, **8**, **9** and **25**, Table 1) on iNOS activity in LPS-activated macrophages are significantly lower than those of previously reported NOS inhibitors. In addition, SMT (compound **7**, Table 1) and aminoethyl-TU (**25**) are more selective than MeArg (**1**) as inhibitors of iNOS, for they are more potent inhibitors of iNOS activity than MeArg, but less potent or equipotent to MeArg as inhibitors of eNOS activity.

Comparison of isothioureas with previously studied reference compounds, such as analogues of L-arginine, is probably the most informative estimate of their potencies. The rank orders of potency for these reference compounds on iNOS (**1**>**4**≫**2**) and eNOS (**2**>**1**>**5**) are similar to other studies. While EC_{50} values (Table 1) are somewhat higher than those reported for iNOS by some workers (Gross *et al.*, 1990; Hasan *et al.*, 1993), they are similar to those reported for cultured J774 or RAW 267.7 macrophages (Misko *et al.*, 1993; MacAllister *et al.*, 1994).

Of the compounds examined, there is a small subgroup of isothioureas that are more potent than MeArg (**1**) as inhibitors of iNOS activity in cultured macrophages: ethyl-TU (**8**) and isopropyl-TU (**9**) are approximately 24 times more potent and SMT (**7**) 6-times more potent than MeArg. These compounds have only short alkyl chains on the sulphur atom (R_1, Figure 1) and no substituents on either nitrogen. Comparison of the potencies of ethyl-, propyl-, butyl- and n-pentyl-isothioureas (**7-14**, Table 1) shows that their potencies as inhibitors of iNOS activity decline sharply if the R_1-chain extends beyond 2 carbon atoms from the sulphur. Substitution of the side chain of ethyl-TU (**8**) or SMT (**7**) (with a group X to give R_1 = $-CH_2-CH_2-X$ or R_1 = $-CH_2-X$, respectively) also results in a diminished inhibitory activity on iNOS (with the exception of aminoethyl-TU, which is 16 times more potent than MeArg). This is especially true when the substituent (X) is unsaturated (e.g. carbonyl, cyano. See compounds **22-24** in Table 1) and suggests that inductive, as well as steric, effects may influence the inhibitory activity of isothioureas on iNOS. Alkyl, amino or phenyl substituents on either one or both nitrogens of SMT substantially reduce its activity as an inhibitor of iNOS (compounds **35-45**, Table 1). Indeed, the only N-substituted compound which has a marked inhibitory effect on iNOS activity is the cyclic 2-aminothiazoline (**31**), where the imino nitrogen is linked to the sulphur. The unsaturated analogue, 2-aminothiazole (**32**), is over 10 fold weaker.

The inhibition of iNOS activity afforded by isothioureas is reduced by excess L-arginine (Table 2), demonstrating a competitive nature of the inhibition and suggesting that SMT and related compounds may occupy the L-arginine binding site of the active site of NOS.

Hydrolysis of S-substituted isothioureas can give rise to the corresponding thiols (R_1-SH) and (*inter alia*) ureas (R_2R_3N-CO-NHR_4). Ureas *per se* have no effect on iNOS activity, but some thiols do (unpublished observations). However, hydrolysis of isothioureas to the corresponding thiols is unlikely to be related to their mode of action, for (i) methanethiol (CH_3-SH, from SMT) is a weak inhibitor of nitrite accumulation, (ii) the rate of hydrolysis of some of these isothioureas to thiols is slow at pH 7.4 and (iii) there is no correlation between the inhibitory potencies of isothioureas and their ability to release the corresponding thiols (unpublished data). Although other metabolic transformation of isothioureas may occur in the cells or plasma, the rapid onset of the *in vivo* effects of isothioureas and the short incubation times used in the assay of eNOS strongly suggest that isothioureas themselves and not their metabolites are responsible for the observed inhibition of iNOS activity.

Isothioureas inhibit eNOS activity with an order of potency that is different from that seen on iNOS activity (Figure 3). The most potent inhibitors of iNOS, ethyl-TU (**8**) and isopropyl-TU (**9**), were also the most potent inhibitors of eNOS, with EC_{50} values 3–5 times lower than that of MeArg (**1**). SMT (**7**) and aminoethyl-TU (**25**), both considerably more potent than MeArg on iNOS, are only as potent as (**7**), or 6-times less potent than (**25**) MeArg on eNOS activity. Thus, when compared to MeArg, these compounds show a relative selectivity towards iNOS. In contrast, L-NOArg (**2**) preferentially inhibits eNOS activity when compared to MeArg (**1**) *in vitro* (see also: Gross *et al.*, 1990; 1991; Lambert *et al.*, 1991).

Recently, an arginine analogue, S-methylthiocitrulline, con-

taining the methylthiourea group (CH_3S-C(= NH)NH-) has been described as a potent inhibitor of NOS activity, with no apparent selectivity towards either eNOS or iNOS (Naravanan *et al.*, 1994). NOS inhibitors which are not L-arginine analogues (such as isothiourea, aminoguanidine or their derivatives) may represent a more promising approach than L-arginine analogues for the development of compounds that preferentially inhibit the activity of iNOS.

The increase in blood pressure afforded by known NOS inhibitors such as MeArg or L-NOArg is due to inhibition of eNOS activity. Thus, the pressor effects of such compounds are relevant measures of their potencies as inhibitors of eNOS *in vivo* (Gross *et al.*, 1990; Moncada *et al.*, 1991; Misko *et al.*, 1993; Hasan *et al.*, 1993). We have demonstrated that isothioureas have variable pressor effects in the anaesthetized rat (Figure 4). Ethyl-TU (**8**) and isopropyl-TU (**9**) elicit potent pressor responses (starting at doses as low as 1 $\mu g\,kg^{-1}$), whereas aminoethyl-TU (**25**) causes only modest increases in blood pressure even at doses as high as 10 $mg\,kg^{-1}$. SMT (**7**) and MeArg elicit comparable pressor responses in accord with their equivalent potencies as inhibitors of eNOS activity *in vitro*. We found that the pressor responses to L-NOArg (**2**), *in vivo*, are no greater than those to MeArg (**1**), despite L-NOArg being the more potent inhibitor of eNOS *in vitro*. This difference between the *in vivo* and *in vitro* potencies of L-NOArg vs. MeArg has also been described previously (Gross *et al.*, 1990). Such differences in the potencies of NOS inhibitors may be influenced *in vivo* by cellular uptake, distribution, metabolism, different co-factor availability etc. It is noteworthy in this respect that 7-nitro-indazole, a recently identified NOS inhibitor with selectivity towards the brain NOS isoform, is a weak pressor agent *in vivo*, but is a potent inhibitor of eNOS activity in endothelial cell homogenates with an EC_{50} similar to L-NOArg (Moore *et al.*, 1993; Babbedge *et al.*, 1993).

In the dose range of 0.01–0.1 $mg\,kg^{-1}$, MeArg (**1**), aminoethyl-TU (**25**) and SMT (**7**) elicited similar pressor effects, whereas L-NOArg (**2**) did not significantly increase blood pressure. As L-NOArg is the weakest inhibitor of iNOS activity among the compounds tested *in vivo*, a potential explanation for this phenomenon may be that a basal release of NO from iNOS may, to a small extent, contribute to the maintenance of normal blood pressure. In 'normal' animals, iNOS may be present in macrophages or in other cells and tissues (Umeda *et al.*, 1993; Morrissy *et al.*, 1994).

In conclusion, isothioureas represent a new class of NOS inhibitors. Some members of this class (ethyl-TU (**8**) and isopropyl-TU (**9**)) are potent NOS inhibitors with little isoform selectivity, whereas others (SMT (**7**) and aminoethyl-TU (**25**)) are relatively selective inhibitors of iNOS activity when compared to N^G-substituted L-arginine analogues. We have recently demonstrated that SMT has beneficial effects on haemodynamic parameters, survival rate and parameters of organ damage in rodent models of circulatory shock (Szabó *et al.*, 1994b). Thus, isothioureas may be potential tools for studying the role of NOS isoenzymes and iNOS in various pathophysiological conditions, such as circulatory shock, inflammation and cancer. In view of the accumulating evidence that supports the pathophysiological importance of iNOS in these diseases, such inhibitors may also be useful in the therapy of a variety of diseases associated with the induction of iNOS.

This work was partially supported by a grant from Glaxo Group Research Ltd. C.S. is a fellow of Lloyd's of London Tercentenary Foundation.

References

BABBEDGE, R.C., BLAND-WARD, P.A., HART, S.L. & MOORE, P.K. (1993). Inhibition of rat cerebellar nitric oxide synthase by 7-nitroindazole and related substituted indazoles. *Br. J. Pharmacol.*, **110**, 225–228.

BUCALA, R., TRACEY, K.J. & CERAMI, A. (1991). Advanced glycosylation products quench nitric oxide and mediate defective endothelium-dependent vasodilatation in experimental diabetes. *J. Clin. Invest.*, **87**, 432–438.

CALVER, A., COLLIER, J. & VALLANCE, P. (1993). Nitric oxide and cardiovascular control. *Exp. Physiol.*, **78**, 303–326.

CORBETT, J.A., TILTON, R.G., CHANG, K., HASAN, K.S., IDO, Y., WANG, J.L., SWEETLAND, M.A., LANCASTER, J.R., WILLIAMSON, J.R. & MCDANIEL, M.L. (1992). Aminoguanidine, a novel inhibitor of nitric oxide formation prevents diabetic vascular dysfunction. *Diabetes*, **41**, 552–556.

DINERMAN, J.L., LOWENSTEIN, C.J. & SNYDER, S.H. (1993). Molecular mechanisms of nitric oxide production. Potential relevance to cardiovascular disease. *Circ. Res.*, **73**, 217–222.

FUJIWARA, S., KASSELL, N.F., SASAKI, T., NAKAGOMI, T. & LEHMAN, L.M. (1986). Selective hemoglobin inhibition of endothelium-dependent vasodilatation of rabbit basilar artery. *J. Neurosurg.*, **64**, 445–452.

GROSS, S.S., JAFFE, E.A., LEVI, R. & GRIFFITH, O.W. (1991). Cytokine-activated endothelial cells express an isotype of nitric oxide synthase which is tetrahydrobiopterin-dependent, calmodulin-independent and inhibited by arginine analogs with a rank-order of potency characteristic of activated macrophages. *Biochem. Biophys. Res. Commun.*, **178**, 823–829.

GROSS, S.S., STUEHR, D.J., AISAKA, K., JAFFE, E.A., LEVI, R. & GRIFFIFTH, O.W. (1990). Macrophages end endothelial cell nitric oxide synthesis: cell-type selective inhibition by N^G-amino-arginine, N^G-nitroarginine and N^G-methylarginine. *Biochem. Biophys. Res. Commun.*, **170**, 96–103.

HASAN, K., HEESEN, B.J., CORBETT, J.A., MCDANIEL, M.L., CHANG, K., ALLISON, W., WOLFFENBUTTEL, B.H.R., WILLIAMSON, J.R. & TILTON, R.G. (1993). Inhibition of nitric oxide formation by guanidines. *Eur. J. Pharmacol.*, **249**, 101–106.

KOPROWSKI, H., ZHENG, Y.M., HEBER-KATZ, E., FRASER, N., RORKE, L., FU, Z.F., HANLON, C. & DIETZSCHOLD, B. (1993). In vivo expression of inducible nitric oxide synthase in experimentally induced neurologic diseases. *Proc. Natl. Acad. Sci. U.S.A.*, **90**, 3024–3027.

LAMBERT, L.E., FRENCH, J.F., WHITTEN, J.P., BARON, B.M. & MCDONALD, I.A. (1992). Characterization of cell selectivity of two novel inhibitors of nitric oxide synthesis. *Eur. J. Pharmacol.*, **216**, 131–134.

LAMBERT, L.E., WHITTEN, J.P., BARON, B.M., CHENG, H.C., DOHERTY, N.S. & MCDONALD, I.A. (1991). Nitric oxide synthesis in the CNS, endothelium and macrophages differs in its sensitivity to inhibition by arginine analogues. *Life Sci.*, **48**, 69–75.

LANGREHR, J.M., HOFFMAN, R.A., LANCASTER, J.R. & SIMMONS, R.L. (1993). Nitric oxide – a new endogeneous immunomodulator. *Transplantation*, **55**, 1205–1212.

LOWENSTEIN, C.J., DINERMAN, J.L. & SNYDER, S.H. (1994). Nitric oxide: a physologic messenger. *Ann. Intern. Med.*, **120**, 227–237.

MACALISTER, R.J., WHITLEY, G.S.J. & VALLANCE, P. (1994). Effects of guanidino and uremic compounds on nitric oxide pathways. *Kid. Int.*, **45**, 737–742.

MCCARTNEY-FRANCIS, N., ALLEN, J.B., MIZEL, D.E., ALBINA, J.E., XIE, Q.W., NATHAN, C.F. & WAHL, S.M. (1993). Suppression of arthritis by an inhibitor of nitric oxide synthase. *J. Exp. Med.*, **178**, 749–754.

MEYER, J., TRABER, L.D., NELSON, S., LENTZ, C.W., NAKAZAWA, H., HERNDON, D.N., NODA, H. & TRABER, D.L. (1992). Reversal of hyperdynamic response to continuous endotoxin administration by inhibition of NO synthase. *J. Appl. Physiol.*, **73**, 324–328.

MILLER, M.J.S., SADOWSKA-KROWICKA, H., CHOTINAREUMOL, S., KAKKIS, J.L. & CLARK, D.A. (1993). Inhibition of chronic ileitis by nitric oxide synthase inhibition. *J. Pharmacol. Exp. Ther.*, **264**, 11–16.

MISKO, T.P., MOORE, W.M., KASTEN, T.P., NICKOLS, D.A., CORBETT, J.A., TILTON, R.G., McDANIEL, M.L., WILLIAMSON, J.R. & CURRIE, M.G. (1993). Selective inhibition of the inducible nitric oxide synthase by aminoguanidine. *Eur. J. Pharmacol.*, **233,** 119–125.

MONCADA, S., PALMER, R.M.J. & HIGGS, E.A. (1991). Nitric oxide: physiology, pathophysiology and pharmacology. *Pharmacol. Rev.*, **43,** 109–141.

MOORE, P.K., WALLACE, P., GAFFEN, Z., HART, S.L. & BABBEDGE, R.C. (1993). Characterisation of the novel nitric oxide synthase inhibitor 7-nitroindazole and related indazoles: antinociceptive and cardiovascular effects. *Br. J. Pharmacol.*, **110,** 219–224.

MORRISSEY, J.J., McCRACKEN, R., KANETO, H., VEHASKARI, M., MONTANI, D. & KLAHR, S. (1994). Location of an iNOS mRNA in the normal kidney. *Kidney Int.*, **45,** 998–1005.

NARAVANAN, K., SPACK, L., HAYWARD, M. & GRIFFITH, O.W. (1994). S-methyl-L-thiocitrulline: a potent inhibitor of nitric oxide synthase with strong pressor activity in vivo. *FASEB J.*, **8,** A360.

NATHAN, C. (1992). Nitric oxide as a secretory product of mammalian cells. *FASEB J.*, **6,** 3051–3064.

NAVA, E., PALMER, R.M.J. & MONCADA, S. (1992). The role of nitric oxide in endotoxic shock: effects of N^G-monomethyl-L-arginine. *J. Cardiovasc. Pharmacol.*, **20,** (Suppl. 12), 132–134.

OLIN, J.F. & DAINS, F.B. (1930). The action of halogen hydrins and of ethylene oxide on the thioureas. *J. Am. Chem. Soc.*, **53,** 3322–3327.

PARKER, J.L. & ADAMS, H.R. (1993). Selective inhibition of endothelium-dependent vasodilator capacity by E. coli endotoxaemia. *Circ. Res.*, **72,** 539–551.

PIPER, P.J., FREEMANTLE, C., MAHADEVAN, V., RIVEROS-MORENO, V., BUTTERFLY, L.D.K., SPRINGALL, D.R. & POLAK, J.M. (1993). Effect of dexamethasone on inducible nitric oxide synthase expression and blood flow in murine tumours. *Endothelium.*, **1,** S51.

REID, E.E. (1963). Organic Chemistry of Bivalent Sulphur. New York: Chemical Publishing Co., Inc.

SCHROEDER, D.C. (1955). Thioureas. *Chem. Rev.*, **55,** 181–228.

STEFANOVIC-RACIC, M., STADLER, J. & EVANS, C.H. (1993). Nitric oxide and arthritis. *Arthritis Rheumat.*, **36,** 1036–1044.

SZABÓ, C., FARAGÓ, M., HORVÁTH, I., LOHINAI, Z. & KOVÁCH, A.G.B. (1992). Hemorrhagic hypotension impairs endothelium-dependent relaxations in the renal artery of the cat. *Cir. Shock*, **36,** 238–241.

SZABÓ, C., MITCHELL, J.A., THIEMERMANN, C. & VANE, J.R. (1993a). Nitric oxide-mediated hyporeactivity to noradrenaline precedes nitric oxide synthase induction in endotoxin shock. *Br. J. Pharmacol.*, **108,** 786–792.

SZABÓ, C., SOUTHAN, G.J. & THIEMERMANN, C. (1994a). Beneficial effects and improved survival in rodent models of septic shock with S-methyl-isothiourea sulphate, a novel, potent and selective inhibitor of inducible nitric oxide synthase. *Proc. Natl. Acad. Sci. U.S.A.*, (in press).

SZABÓ, C., SOUTHAN, G.J., WOOD, E., THIEMERMANN, C. & VANE, J.R. (1994b). Spermine inhibits the production of nitric oxide in immuno-stimulated J774.2 macrophages: requirement of a serum factor. *Br. J. Pharmacol.*, **112,** 355–356.

SZABÓ, C. & THIEMERMANN, C. (1994). Invited opinion: role of nitric oxide in hemorrhagic, traumatic and anaphylactic shock and in thermal injury. *Shock*, **2,** 1–11.

SZABÓ, C., THIEMERMANN, C. & VANE, J.R. (1993b). Dihydropyridine modulators of calcium channels inhibit the induction of nitric oxide synthase by endotoxin in cultured J774.2 cells. *Biochem. Biophys. Res. Commun.*, **196,** 825–830.

THIEMERMANN, C. (1994). Role of the L-arginine-nitric oxide pathway in circulatory shock. *Adv. Pharmacol.*, **28,** 45–79.

THIEMERMANN, C., SZABÓ, C., MITCHELL, J.A. & VANE, J.R. (1993). Vascular hyporeactivity to vasoconstrictor agents and haemodynamic decompensation in haemorrhagic shock is mediated by nitric oxide. *Proc. Natl. Acad. Sci. U.S.A.*, **90,** 267–271.

THIEMERMANN, C. & VANE, J.R. (1990). Inhibition of nitric oxide synthesis reduces the hypotension induced by bacterial lipopolysaccharide in the rat in vivo. *Eur. J. Pharmacol.*, **182,** 591–595.

UMEDA, T., GROSS, S.S., CUDD, A., POLAK, J.N., MACINTYRE, I. (1993). Osteoclasts contain both inducible and constitutive NOS isoforms: a key role in bone resorption? *Endothelium.*, **1,** S47.

VANE, J.R. (1994). The Cronian lecture, 1993: The endothelium: maestro of the blood circulation. *Proc. R. Soc. B.*, **343,** 225–246.

VANE, J.R., MITCHELL, J.A., APPLETON, I., TOMLINSON, A., BISHOP-BAILEY, D., CROXTALL, J. & WILLOUGHBY, D.A. (1994). Inducible isoforms of cyclooxygenase and nitric oxide synthase in inflammation. *Proc. Natl. Acad. Sci. U.S.A.*, **91,** 2046–2050.

(Received August 11, 1994
Revised September 22, 1994
Accepted September 23, 1994)

British Journal of Pharmacology (1995) 114, 517-523 © 1995 Stockton Press All rights reserved 0007-1188/95 $9.00

A reassessment of the modulatory role of cyclic AMP in catecholamine secretion by chromaffin cells

M. Parramón, M.P. González & [1]M.J. Oset-Gasque

Instituto de Bioquímica, Facultad de Farmacia, Universidad Complutense, 28040 Madrid, Spain

1 The role of adenosine 3':5'-cyclic monophosphate (cyclic AMP) in the regulation of catecholamine (CA) secretion in chromaffin cells remains equivocal from previous studies.

2 In the present study the effect of this cyclic nucleotide on basal CA secretion, as well as on intracellular calcium and membrane potential has been examined.

3 Forskolin and the permeable cyclic AMP analogue, 8-(4-chlorphenylthio)-adenosine-3'-5' monophosphate cyclic (pClpcAMP), increased basal CA secretion in a dose-dependent manner. The EC_{50}s were $0.43 \pm 0.10\,\mu M$ for forskolin and $39 \pm 9\,\mu M$ for pClpcAMP. Other agonists with adenylate cyclase activity such as stimulants of adenosine receptors, β-adrenoceptors, $GABA_B$ receptors and intestinal vasoactive peptide (VIP), also increased basal CA secretion in a highly significant manner. However, when they were added together with forskolin, CA secretion was not affected although an additive increase in cyclic AMP levels was produced.

4 Statistical analysis of the correlation between cyclic AMP levels and CA secretion evoked by these cyclic AMP increasing compounds showed that a significant direct correlation between both parameters existed only when low levels of cyclic AMP were produced by secretagogue stimulation. When the increase in intracellular cyclic AMP concentrations exceeded approximately 8 times the basal cyclic AMP levels the correlation was not significant. These results indicate a dual dose-dependent effect of cyclic AMP on basal CA secretion.

5 The stimulatory effect of low cyclic AMP on basal CA secretion was accompanied by an increase in membrane potential and in intracellular calcium concentrations ($[Ca^{2+}]_i$), the latter mainly being due to an increase in intracellular Ca^{2+} entry through L-type voltage-dependent Ca^{2+} channels.

6 The possible mechanisms involved in these cyclic AMP effects are discussed.

Keywords: Cyclic AMP; catecholamine secretion, chromaffin cells; cyclic AMP increasing compounds; calcium; nicotinic receptors; GABA receptors

Introduction

The coupling of stimulus to secretion is fundamental for cellular activity of secretory cells. The underlying signal which stimulates exocytotic secretion is, in general, an increase in intracellular Ca^{2+} ions which, in the case of catecholamine (CA) secretion by adrenal chromaffin cells, is mainly due to a calcium entry from the extracellular medium (Douglas & Ruben, 1963; Knight & Baker, 1982; Burgoyne, 1991, for a review). Moreover, other intracellular messengers may also be important in the regulation of catecholamine exocytosis, in particular the G-protein family (Bader *et al.*, 1989), inositol 1,4,5 tris-phosphate (IP_3) (Eberhard & Holz, 1987; Cheek & Thastrup, 1989) and adenosine 3:5-cyclic monophosphate (cyclic AMP) (Morita *et al.*, 1987).

Several studies on the role of cyclic AMP in the regulation of basal and evoked CA secretion, however have yielded apparently contradictory results. In digitonin and electropermeabilized chromaffin cells, some authors found that treatment of cells with forskolin or cyclic AMP analogues seemed to have a stimulatory effect on Ca^{2+}-dependent and Ca^{2+}-independent CA secretion (Peach, 1972; Gutman & Boonjaviroy, 1979; Knight & Baker, 1982; Bittner *et al.*, 1986) while others showed that cyclic AMP had no effect on basal CA secretion (Hochman & Perlman, 1976; Kumakura *et al.*, 1979; Morita *et al.*, 1987).

Results concerning cyclic AMP effects on evoked CA secretion are also contradictory. Some groups reported that an increase in cyclic AMP levels following forskolin treatment or use of 8-Br-cyclic AMP or cholera toxin (CTX), inhibited nicotine- but not high K^+-induced secretion (Baker *et al.*, 1985; Cheek & Burgoyne, 1987; Marriott *et al.*, 1988; Negishi *et al.*, 1989). In contrast, other groups have reported that an elevation of cyclic AMP with low doses of forskolin potentiates high K^+-induced secretion and the release elicited by suboptimal doses of acetylcholine (ACh) (Morita *et al.*, 1987; Higgins & Berg, 1988).

In a previous study we demonstrated that stimulation of $GABA_B$ receptors increases basal CA secretion by a mechanism involving cyclic AMP formation (Oset-Gasque *et al.*, 1993). These results agree with those of other groups showing that agonists which raise cyclic AMP levels in chromaffin cells, including vasoactive intestinal peptide (VIP) (Wilson, 1988), adenosine (Chern *et al.*, 1988) and dopamine D_1 agonists (Artalejo *et al.*, 1990), stimulate basal CA secretion. However, other cyclic AMP-increasing compounds, such as histamine H_2 agonists seem to increase CA secretion by a mechanism which differs from cyclic AMP synthesis (Choi *et al.*, 1993).

In order to clarify some of the conflicting results in the literature about the role of cyclic AMP in adrenal medulla function, the effect of cyclic AMP on basal CA secretion by chromaffin cells has been re-examined.

Our results indicate that all of the studied cyclic AMP-increasing agents are able to increase Ca^{2+}-dependent CA secretion by themselves. These effects were accompanied by changes in $[Ca^{2+}]_i$ and in membrane potential. Our results shed a new light on the role of cyclic AMP in chromaffin cells.

[1] Author for correspondence.

Methods

Cell isolation and culture

Bovine chromaffin cells were isolated from adrenal glands and cultured as described by Bader *et al.* (1981) with minor modifications. Cell viability was checked with trypan blue and chromaffin cells purity was assessed by specific dying with 3 mg ml^{-1} neutral red, which stains only the cells which contain CAs. Viability and purity were always higher than 90%. Cells were suspended in DMEM containing 10% FCS, antibiotics (100 u ml^{-1} penicillin, 100 $\mu g\ ml^{-1}$ streptomycin and 40 $\mu g\ ml^{-1}$ gentamicin), and cytostatics (10 μM fluorodeoxyuridine and 10 μM cytosine arabinoside), plated in 24 well Costar cluster dishes at a density of 0.5×10^6 cells/well and used 3–7 days after plating. For calcium and membrane potential measurements, cells were maintained in suspension at 4°C at a density of 10^6 cells ml^{-1} and used in the following 2–3 days.

Measurement of catecholamine secretion

Chromaffin cells were washed twice, at 10 min intervals, with 1 ml of a Krebs HEPES solution (Locke medium) containing (mM): NaCl 140, KCl 4.7, KH_2PO_4 1.2, $CaCl_2$ 2.5, $MgSO_4$ 1.2, glucose 11, ascorbic acid 0.5 and HEPES 15, pH = 7.5, at 37°C. This medium was removed and cells were stimulated for 10 min periods at 37°C with 0.5 ml of a fresh Locke medium containing the different secretagogues as indicated for each type of experiment. At the end of the incubation period the medium was removed and cells lysed with 0.1 M $HClO_4$ and then scraped off the plates. Incubation medium and cell lysates were used for the determination of CA secretion and total CA content, respectively. The CA determination, in both sample types, adequately diluted and neutralized (see below), was performed with an electrochemical detector (Metrohm 641 VA-detector) adjusted to + 580 mV and registered on an LKB recorder model 2210, a standard noradrenaline curve being used for calibration. Results were expressed as percentage of CA released in the incubation medium with respect to the total CA content (incubation medium + pellet).

Measurement of intracellular levels of cyclic AMP

Chromaffin cells, prepared as indicated above, were stimulated during a 10 min period with the secretagogues indicated. Incubations were performed in the presence of 0.5 mM IBMX in order to prevent cyclic AMP degradation. The medium was removed, cells lysed with 200 μl of 0.1 M $HClO_4$ and scraped off the plates. These cell lysates were neutralized with 1 M KOH, centrifuged in an Eppendorf centrifuge and supernatants were used for the assay of cyclic AMP. Intracellular cyclic AMP measurements were made with the cyclic AMP Radioimmunoassay Kit from Amersham, as described in the manufacturer's instructions.

Measurement of cytosolic [Ca^{2+}]

Changes in intracellular calcium concentration ($[Ca^{2+}]_i$) were monitored by measuring Fura-2 AM fluorescence. Cells were washed twice with Locke medium and incubated with 5 μM Fura-2 AM for 45 min at 37°C. Excess dye was removed by washing the cells twice with fresh Locke medium and the cells suspended in this medium at 10^6 cells ml^{-1}. Fluorescence (excitation wavelength = 380 nm, emission = 510 nm, slits, 5 nm exc. 10 nm em.) was monitored at 37°C in a well-stirred cuvette containing 1 ml of cell suspension with a Perkin-Elmer LS-50 spectrofluorimeter. At the end of each experiment 0.5% Triton X-100 was added to permeabilize the cells, allowing the dye to gain access to the extracellular calcium ($[Ca^{2+}]_e$). This $[Ca^{2+}]_e$ saturated the dye and provided a measure of the maximum fluorescence signal (F_{max}). To determine the intensity of the minimum fluorescence signals (F_{min}) 20 mM Tris base was added to raise the pH above 8.2, followed by 10 mM EGTA, which reduced the $[Ca^{2+}]$ to less than 1 nM. The $[Ca^{2+}]_i$ was calculated using the equation:

$$[Ca^{2+}]_i = K_D\ (F-F_{min})/(F_{max}-F)$$

The equilibrium dissociation constant (K_D) for $[Ca^{2+}]$-Fura being 224 nM.

Measurement of membrane potential

Changes in membrane potential of chromaffin cells were monitored with the fluorescent bisoxonol probe $DiBAC_4(3)$. This is a lipophylic anion whose distribution across the membrane is dependent upon the membrane potential. Thus, an increase in bisoxonol fluorescence indicates that the cell membrane has been depolarized, allowing more of this negatively charged dye to enter the cells (Waggoner, 1979). Cells at a density of 10^6 cells ml^{-1} were washed as for $[Ca^{2+}]_i$ measurements and suspended in Locke medium to which 0.2 μM bisoxonol was then added. Fluorescence was measured at wavelengths of 540 nm exc. and 565 nm em. at 37°C in a well stirred cuvette in a Perkin-Elmer spectrofluorimeter. Effectors were added at the concentrations indicated. Controls were obtained by using Locke medium instead of the effector. Fluorescence intensity is reported in arbitrary units.

Materials

Dulbecco's Modified Eagle's Medium (DMEM) was from ICN Biomedicals Ltd, Irvine, Scotland. Foetal calf serum (FCS) was from Sera-Lab, Sussex, England. Collagenase (E.C.3.4.4.19), 8-(4-chlorphenylthio)-adenosine-3′-5′ monophosphate cyclic (pClpcAMP), adenosine, vasoactive intestinal peptide (VIP) and (+)-N-(S-phenyl-isopropyl)-adenosine (PIA) were obtained from Boehringer Mannheim S.A. (Barcelona, Spain). Forskolin, 3-isobutyl-1-methyl xanthine (IBMX) and nifedipine were supplied by Sigma Chemical Co (St. Louis, MO, U.S.A.). (**R**)-(−)-isoprenaline was purchased from Aldrich Chem. Co (Madrid, Spain). Kits for cyclic AMP estimation were from Amersham Iberica (Madrid, Spain) and Fura-2 AM and bis-(1,3-dibutylbarbituric acid) trimethine oxonol ($DiBAC_4(3)$) were purchased from Molecular Probes (Eugene, U.S.A.). (−)-Baclofen and 3-aminopropyl phosphinic acid (3-APPA) were a gift from Ciba-Geigy (Basel, Switzerland). All other chemicals were reactive grade products from Merck (Darmstadt, Germany).

Statistics

The data shown are means ± s.e.mean of at least three experiments each one performed in duplicate. Statistical significance was estimated with Student's *t* test for unpaired observations. A *P* value of less than 0.05 was considered significant. Linear regressions were made by the method of minimum squares and fittings of concentration-response curves for estimation of EC_{50} or IC_{50} values by a weighted non-linear regression of minimum squares, using logistic curves.

Results

Effects of forskolin and cyclic AMP on basal CA secretion

Stimulation of chromaffin cells with forskolin or the non-hydrolyzable analogue of cyclic AMP, pClpcAMP, increased basal CA secretion in a concentration-dependent manner (Figure 1). Half maximal effects (EC_{50}) were obtained at 0.43 ± 0.10 μM of forskolin and 39 ± 9 μM of pClpcAMP. Maximal responses were evoked at doses of 1–2.5 μM of

forskolin and 1–10 mM of cyclic AMP and were of 2.3 ± 0.29 and 1.72 ± 0.14 times the basal levels of CA secretion for forskolin and cyclic AMP, respectively. Stimulation of cells with higher concentrations of both compounds produced a lower effect on CA secretion (data not shown).

Effects of adenylate cyclase stimulatory agonists on cyclic AMP levels and catecholamine secretion

In order to establish a possible correlation between cyclic AMP levels and CA secretion, we examined the ability of different agonists which are known to activate adenylate cyclase (AC) to increase both cyclic AMP levels and CA secretion.

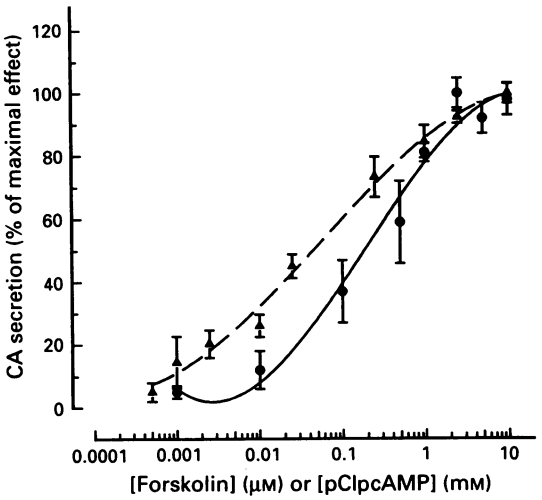


Figure 1 Dose-response curves of the effect of forskolin (●) and pClpcAMP (▲) basal catecholamine (CA) release by chromaffin cells. Cells were incubated with the indicated doses of forskolin and pClpcAMP at 37°C. CA release over a 10 min period is expressed as a percentage of maximal response over basal. Basal CA release was 3.2 ± 0.55% of total cellular CA content. Release data are means ± s.e.mean of three independent determinations each performed in duplicate. EC_{50}s: forskolin 0.43 ± 0.10 μM and pClpcAMP 39 ± 9 μM.

Table 1 Effect of some adenylate cyclase activators on intracellular cyclic AMP levels and on catecholamine secretion

Drug	*Intracellular cyclic AMP* (pmol/10^6 cells)	*CA secretion* (% over total c.c.)
Control	4.28 ± 0.31	2.72 ± 0.06
Baclofen 100 μM	6.30 ± 0.33***	4.30 ± 0.57***
3-APPA 100 μM	7.5 ± 1.05***	4.70 ± 0.61**
Adenosine 10 μM	8.20 ± 0.78***	5.50 ± 0.89***
PIA 10 μM	8.83 ± 0.33***	3.40 ± 0.16***
Baclofen 500 μM	8.73 ± 0.90***	6.28 ± 0.71**
Isoprenaline 30 μM	9.30 ± 0.87***	4.17 ± 0.78**
Isoprenaline 50 μM	12.00 ± 0.98***	8.37 ± 1.21***
3-APPA 500 μM	12.60 ± 1.27***	7.23 ± 1.06**
PIA 50 μM	18.70 ± 2.05***	3.53 ± 0.20***
VIP 20 μM	21.04 ± 2.45***	5.37 ± 0.46***
Forskolin 1 μM	32.00 ± 6.53***	7.10 ± 0.91***
Forskolin 1 μM + Adenosine 10 μM	37.70 ± 5.70***	2.60 ± 0.48***
+ Baclofen 500 μM	39.10 ± 7.80***	2.70 ± 0.61***
+ APPA 500 μM	41.50 ± 4.03***	2.60 ± 0.53***
+ PIA 50 μM	51.70 ± 6.30***	2.43 ± 0.45***
+ Isoprenaline 50 μM	52.55 ± 8.34***	2.27 ± 0.29***
+ VIP 20 μM	53.77 ± 5.58***	2.33 ± 0.41***

Cells were incubated with indicated agonists at 37°C for 10 min. Results are means ± s.e.mean of three duplicate experiments. Significantly different from the corresponding control at $*P<0.1-0.05$; $**P<0.01-0.025$ and $***P<0.005-0.001$.

Table 1 show that all tested agonists, of adenosine receptors (adenosine and PIA), β-adrenoceptors (isoprenaline), $GABA_B$ receptors (baclofen and 3-APPA) and VIP produce a significant increase in cyclic AMP levels accompanied by a stimulatory effect on basal CA secretion.

Additionally, the ability of forskolin to modify the effects of AC stimulatory agonists on both cyclic AMP levels and CA secretion was examined. As shown in Table 1, 1 μM forskolin produced an additive enhancement of cyclic AMP levels caused by these agonists. However, in contrast it was found to inhibit CA secretion evoked by the same agonists.

Correlation between CA secretion and intracellular cyclic AMP levels evoked by various compounds

In the preliminary analysis of results presented in Table 1, the correlation between both parameters, cyclic AMP levels and CA secretion (cyclic AMP/CA), produced by all cyclic AMP increasing compounds was not statistically significant.

In a second approximation, the analysis of correlation was performed by assembling the data in three different pools according to the increase in cyclic AMP levels produced by each (Figure 2).

In this figure the following correlations have been plotted: (a) Correlation cyclic AMP/CA for agonists increasing cyclic AMP levels up to 3–3.5 times basal values: (b) Correlation cyclic AMP/CA for agonists which increase cyclic AMP levels between 3.5 to 7.5 times the basal levels; (c) Correla-

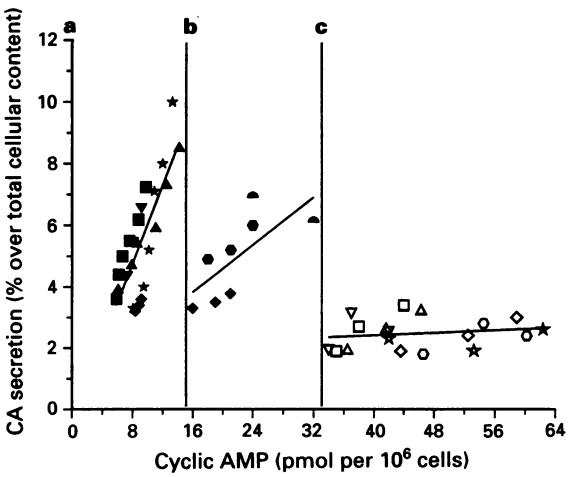


Figure 2 Correlation between CA secretion and cyclic AMP levels induced by different adenylate cyclase activators. Chromaffin cells were treated with different compounds in the absence or presence of 1 μM forskolin for 10 min and then CA secretion and cyclic AMP content were measured. CA secretion (% over total cellular content; ordinates) are plotted against cyclic AMP levels (pmol/10^6 cells; abcissae). Points represent means of duplicate determinations in each experiment. Statistical analysis of correlation were performed by assembling the data obtained by different compounds in three different pools according to the increase in cyclic AMP levels produced by them. (a) Up to 3–3.5 times basal values; (b) between 3.5 to 7.5 times basal values and (c) above 7.5 times basal values. Correlation coefficients (r) are 0.78, 0.71 and 0.18 for data from (a), (b) and (c) respectively. Number of data (n) are 24, 8 and 18 for data from (a), (b) and (c), respectively. Student's t test for the degrees of freedom number (t(n-2)) are 5.95, 2.48 and 0.74 for data from (a), (b) and (c) respectively. Statistical significance are $P<0.001$, $P<0.05$ and NS for data from (a), (b) and (c) respectively. Symbols represent: (a) (■) Bac 100–500 μM; (▲) APPA 100–500 μM; (▼) adenosine 10 μM; (◆) PIA 10 μM; (★) Isopren 30–50 μM: (b) (◆) PIA 50 μM; (●) VIP 20 μM; (◓) forskolin 1 μM. (c) (▽) forskolin + adenosine 10 μM; (□) forskolin + bac 0.5 mM; (△) forskolin + APPA 0.5 mM; (◇) forskolin + PIA 10 μM; (○) forskolin + isopren 50 μM; (☆) forskolin + VIP 20 μM; in each case forskolin = 0.1 μM. For abbreviations, see text.

tion cyclic AMP/CA for mixtures of agonists with forskolin, which increase cyclic AMP levels above 7.5 times basal values.

In this second approximation we observed that a significant direct correlation between intracellular cyclic AMP levels and CA secretion exist in the case of low levels of cyclic AMP to about 3–4 times the basal values (Figure 2a). At higher cyclic AMP levels of between 3.5 or 7.5 times the basal values (Figure 2b), a significant positive correlation also exists, but in this case the slope of the curve is less steep than in (a). The correlation for mixtures of agonists with forskolin giving higher values of cyclic AMP (approximately above 8 times the basal levels) was not statistically significant (Figure 2c).

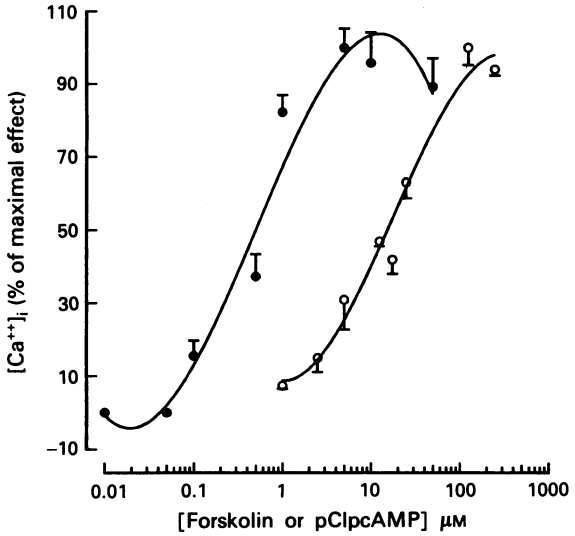


Figure 3 Concentration-dependence of cyclic AMP-induced increase in $[Ca^{2+}]_i$ in bovine cultured adrenal chromaffin cells. Cytosolic calcium was measured as indicated in Methods after stimulation of cells with indicated doses of forskolin (●) or pClpcAMP (○). $[Ca^{2+}]_i$ is expressed as a percentage of maximal effect (see text) from which basal $[Ca^{2+}]_i$ (145 ± 30 nM) was subtracted. Points are means ± s.e.mean of three different experiments each one performed in duplicate. EC_{50}s: forskolin 0.7 ± 0.2 μM and pClpcAMP 24 ± 9 μM.

Effect of bacterial toxins on cyclic AMP levels and CA secretion

In order to obtain additional evidence concerning the effects and mechanisms of action of cyclic AMP in CA secretion, cells were pre-treated for 4 h with bacterial toxins, CTX and pertussis toxin (PTX). PTX is known to block the ability of G_i proteins to interact with ligand-receptor complex and CTX produces a permanent activation of G_s proteins by inhibition of GTPase activity of its α subunits.

In basal conditions, PTX did not induce any modification of cyclic AMP levels but caused a significant increase in CA secretion (about 60% the basal levels). CTX induced a significant increase of 10 times the basal cyclic AMP levels and also increased CA secretion in a significant manner, although this effect was very small compared with the observed enhancement of cyclic AMP levels (between 30–40% the basal levels).

Effect of cyclic AMP and forskolin on $[Ca^{2+}]_i$

In order to test if the increase in CA secretion induced by cyclic AMP was mediated by an increase in $[Ca^{2+}]_i$, the ability of forskolin and pClpcAMP to increase $[Ca^{2+}]_i$ was examined.

As shown in Figure 3 both compounds increased $[Ca^{2+}]_i$ in a dose-dependent manner with EC_{50}s of 0.7 ± 0.2 μM for forskolin and 24 ± 9 μM for pClpcAMP. Maximal effects were obtained at doses of 1–5 μM of forskolin and 125 μM of pClpcAMP and represent a rise in $[Ca^{2+}]_i$ of 201 ± 26 and 229 ± 38 nM for forskolin and pClpcAMP, respectively. The rise in $[Ca^{2+}]_i$ was highly dependent on extracellular Ca^{2+} since this was significantly reduced by chelation of extracellular Ca^{2+} with EGTA (82 ± 17 nM and 90 ± 26 nM for forskolin and pClpcAMP, respectively) (Figure 4a and b) or by

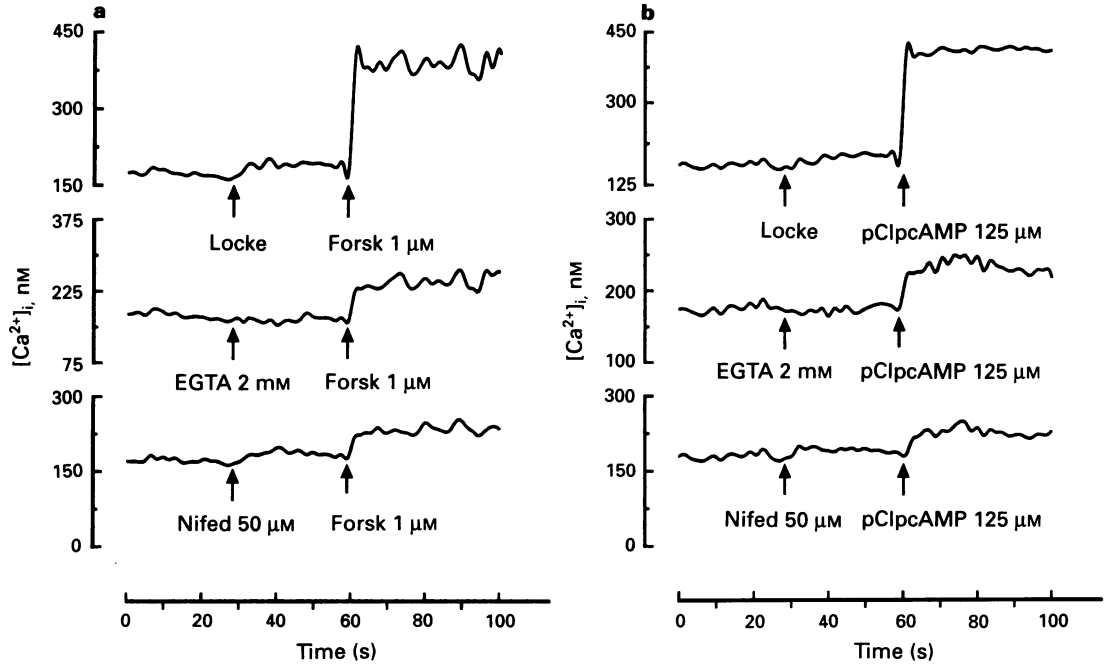


Figure 4 Effect of cyclic AMP-elevating compounds on $[Ca^{2+}]_i$ in different conditions. Cytosolic Ca^{2+} transients elicited by stimulation of chromaffin cells with (a) 1 μM forskolin and (b) 125 μM pClpcAMP. Superimposed records from different cell samples are traced. Drugs were added at times indicated by the arrows. Forsk, 1 μM forskolin; Nifed, 50 μM nifedipine. Similar records were obtained from different samples in 5 cell batches.

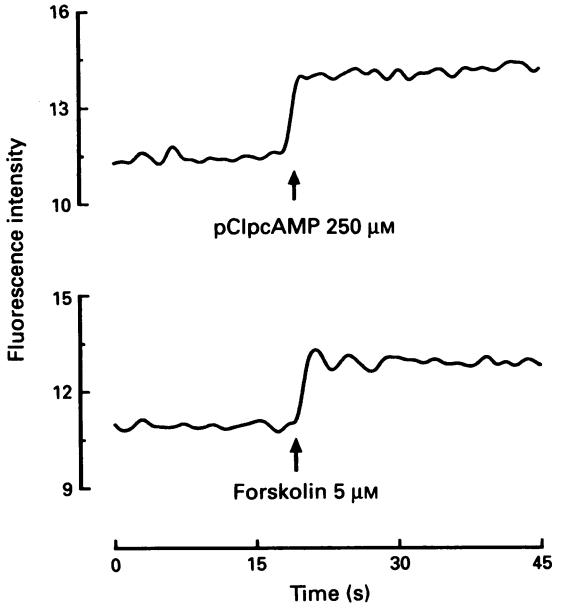


Figure 5 Effects of forskolin and pClpcAMP on resting membrane potential. Membrane potential was measured as indicated in Methods. Drugs were added as indicated by the arrows and membrane potential expressed in arbitrary fluorescence units. Similar records were obtained from 3–4 different samples in 3 different cell batches.

lowering $[Ca^{2+}]_e$ to 200 nM (data not shown). Moreover increase in $[Ca^{2+}]_i$ was strongly blocked by 50 μM nifedipine (60 ± 15 nM for forskolin and 65 ± 21 nM for pClpcAMP) (Figures 4a and b), thus indicating the involvement of L-type voltage-dependent Ca^{2+} channels as a gate for calcium entry from extracellular medium.

Effect of cyclic AMP and forskolin on membrane potential

Forskolin and pClpcAMP added to cell suspensions at concentrations of 5 and 250 μM, respectively, increase membrane potential as measured by the fluorescent bisoxonol probe $DiBAC_4(3)$ (Figure 5). The mean increase was of 3.5 ± 1 and 2.9 ± 0.2 units of fluorescence intensity for forskolin and pClpcAMP, respectively. These values are lower than those produced by 50 μM nicotine (4.5 ± 0.3) or muscimol (4.6 ± 0.4) in arbitrary fluorescence units.

Discussion

The role of intracellular messengers, including cyclic AMP, in the regulation of CA secretion by chromaffin cells is not well understood at present.

In a previous study dealing with the role of $GABA_B$ receptors in the modulation of chromaffin cell secretion we found that these agonists modulate CA secretion by a mechanism involving cyclic AMP synthesis (Oset-Gasque *et al.*, 1993). These results are in agreement with the reports showing that cyclic AMP increases basal and inhibits nicotine-evoked CA secretion (Peach, 1972; Gutman & Boonjaviroy, 1979; Knight & Baker, 1982; Baker *et al.*, 1985; Bittner *et al.*, 1986; Cheek & Burgoyne, 1987) although others indicate opposite results (Kumakura *et al.*, 1979; Morita *et al.*, 1987). In view of these discrepancies, the present work was undertaken in order to re-examine the role of cyclic AMP in these cells and further support our previous results. This study was carried out by analysing the effect of cyclic AMP on basal CA secretion, $[Ca^{2+}]_i$ and membrane potential in chromaffin cells.

Our results demonstrate that, in general, cyclic AMP has a stimulatory effect on basal CA secretion. This conclusion is supported by the fact that both agents, forskolin (an unspecific direct activator of AC) and a permeable non-hydrolizable cyclic AMP analogue (pClpcAMP) induced a significant increase of basal CA secretion (Figure 1). Moreover these agents were able to increase the membrane potential of chromaffin cells. These results indicate that cyclic AMP by itself depolarizes the cells and as a consequence is able to stimulate CA exocytosis.

The cyclic AMP-stimulated CA secretion is a Ca^{2+}-dependent event. This result is supported by the finding that forskolin and pClpcAMP increase $[Ca^{2+}]_i$ in a dose-dependent manner (Figure 3). This increase is mainly due to extracellular Ca^{2+} entry through voltage-dependent Ca^{2+}-channels since the treatment of cells with cyclic AMP in the absence of extracellular Ca^{2+} reduced the response on $[Ca^{2+}]_i$ more than 50%. A stronger inhibition was also observed by blocking Ca^{2+} entry through L-type voltage-dependent Ca^{2+} channels with nifedipine (Figure 4a and b). However, the fact that the response could not be completely blocked by these treatments could indicate that an additional mobilization of intracellular Ca^{2+} is able to take place. Nevertheless, the possible intracellular Ca^{2+} mobilization seems not to be able to evoke CA secretion, since our recent results indicate that secretory response of forskolin and cyclic AMP, as well as that of $GABA_B$ agonists or cyclic AMP increasing agents, is absolutely dependent on extracellular Ca^{2+} (Parramón *et al.*, 1994).

The mechanism by which cyclic AMP might open voltage-dependent Ca^{2+}-channels is unknown although it is probably by PKA phosphorylation of voltage-dependent Ca^{2+} channels (Artalejo *et al.*, 1990). In a first approximation it is logical to expect that direct phosphorylation alone of these channels by PKA would not be enough to open them since they are physiologically activated by voltage changes, and an additional depolarization prior to the opening of these channels must take place. There are different possible explanations of how this pre-depolarization is produced. One of them could be the blocking of Na^+-K^+-ATPase by PKA phosphorylation, thus inducing increases in $[Na^+]_i$ which is the main activatory mechanism of Na^+-Ca^{2+}-exchanger. This Na^+ entry pre-depolarizes cells and triggers the opening of voltage-dependent Ca^{2+} channels. This possibility has been examined by Morita *et al.* (1991a,b) to explain cyclic AMP facilitation of CA secretion evoked by nicotine. These authors show that cyclic AMP elevates $[Na^+]_i$ by inhibiting Na^+-K^+-ATPase activity, promoting Ca^{2+} uptake in exchange for internal Na^+. However these authors failed to observe an effect on basal secretion of cyclic AMP by itself, which should be observed if such a mechanism is operating in chromaffin cells.

The stimulatory effect of cyclic AMP on exocytosis of other hormones has been shown in other tissues such as bovine lactotrophs, where cyclic AMP directly facilitates Ca^{2+}-induced exocytosis of prolactin (Sikdar *et al.*, 1990) or in pancreatic β-cells where cyclic AMP promotes insulin release by a direct interaction with the secretory machinery, which accounts for as much as 80% of its effect (Ämmälä *et al.*, 1993).

Some of the previous studies on the effect of cyclic AMP on CA secretion in adrenal medulla have failed to demonstrate any significant effect on basal secretion (Morita *et al.*, 1987; Chern *et al.*, 1988; Marriot *et al.*, 1988; Morita *et al.*, 1991a), although others have demonstrated a significant increase in basal CA secretion by 1 μM forskolin (Bader *et al.*, 1989; Sontag *et al.*, 1991), cyclic AMP (Bittner *et al.*, 1986; Morgan *et al.*, 1993) or by cyclic AMP-elevating agonists such as VIP (Wilson, 1988), adenylate cyclase activating polypeptide (PACAP) (Isobe *et al.*, 1993) or adenosine (Castro *et al.*, 1990).

In order to assess our results further we tested the ability to increase basal CA secretion of some agonists which are

known to cause an elevation in cyclic AMP levels, such as adenosine and PIA, isoprenaline, VIP and $GABA_B$ agonists. All these agonists were able to induce a dose-dependent increase in basal CA secretion. This was found to occur in all cases along with an increase in intracellular cyclic AMP levels ($[cAMP]_i$). However, this parallelism between $[cAMP]_i$ and CA secretion did not always occur. This result seemed to be due to the very different levels of cyclic AMP produced by the different cyclic AMP-elevating compounds tested. We performed a correlation analysis of these data by assembling them into different pools according to the values of cyclic AMP and observed that a highly statistically significant correlation between $[cAMP]_i$ and cellular response existed only when $[cAMP]_i$ were below 3–3.5 times the basal values, which is a relatively moderate increase in cyclic AMP (Figure 2a). Higher levels of cyclic AMP (between about 3.5–7.5 times the basal levels) produced a lower increase in CA secretion than in the previous case and even failed to produce a significant increase in CA secretion when cyclic AMP levels were higher than 8 times the basal values (Figure 2b and c). Taken together these results indicate that this second messenger could influence the exocytotic machinery of CA secretion directly only when low increases in $[cAMP]_i$ by secretagogue stimulation are produced in the cell. These results are in close agreement with very recent results by Morgan *et al.* (1993) showing that cyclic AMP has a biphasic effect on Ca^{2+}-dependent CA secretion, peaking at around 1 μM and returning to control levels at 1 mM. Moreover the fall in the stimulatory effect of cyclic AMP at high levels seems to explain our finding of a low increase in basal CA secretion evoked by CTX in chromaffin cells (of only about a 30% the basal levels) in spite of the fact that this toxin produces a very strong increase in cyclic AMP of about 10 times the basal levels.

This is not the case of PTX-induced CA secretion. Although this toxin was able to induce an increase in cyclic AMP levels evoked by forskolin and $GABA_B$ agonists and also CA secretion (Oset-Gasque *et al.*, 1993) it did not increase cyclic AMP levels in basal conditions. These results suggest that PTX enhancement of basal CA secretion is not mediated by its effect as a blocker of inhibitory adenylate cyclase G proteins (G_i), a conclusion which is in agreement with results of Sontag *et al.* (1991). The effect of this toxin could be due to a direct increase in activation of voltage-dependent L-type Ca^{2+} channels or to an opening of voltage-independent G-type Ca^{2+} channels (Ceña *et al.*, 1991) or to an inactivation of other G-proteins of G_i type mediating tonic inhibition of secretion which prevents activation of phospholipase C (Wilson, 1992).

In conclusion, the data discussed above seem to suggest that cyclic AMP by itself has a regulatory role on basal CA secretion which is closely dependent on its intracellular level and is a stimulant only when a small increase in its levels is produced by secretagogue stimulation of chromaffin cells.

This work was supported by Research Grants CAM C168/91 from Comunidad Autónoma of Madrid and FISS 92/0241 from National Institute of Health of Madrid (Spain). M.P. is recipient of a CAM Fellowship. The authors thank D.A. Gilson for manuscript corrections.

References

ÄMMÄLÄ, C., ASHCROFT, M. & RORSMAN, P. (1993). Calcium-independent potentiation of insulin release by cyclic AMP in single β-cells. *Nature*, **363**, 356–358.

ARTALEJO, C.R., ARIANO, M.A., PERLMAN, R.L. & FOX, A.P. (1990). Activation of facilitation calcium channels in chromaffin cells by D_1 dopamine receptors through a cAMP/protein kinase A-dependent mechanism. *Nature*, **348**, 239–242.

BADER, M.F., CIESIELSKI-TRESKA, J., THIERSE, D., HESKETCH, J.E. & AUNIS, D. (1981). Immunocytochemical study of microtubules in chromaffin cells in culture and evidence that tubulin is not an integral protein of the chromaffin granule membrane. *J. Neurochem.*, **37**, 917–933.

BADER, M.F., SONTAG, J.M., THIERSE, D. & AUNIS, D. (1989). A reassessment of guanine nucleotide effects on catecholamine secretion from permeabilized adrenal chromaffin cells. *J. Biol. Chem.*, **264/28**, 16426–16434.

BAKER, E.M., CHEECK, T.R. & BURGOYNE, R.D. (1985). Cyclic AMP inhibits secretion from bovine chromaffin cells evoked by carbamylcholine but not by high K^+. *Biochim. Biophys. Acta*, **846**, 388–393.

BITTNER, M.A., HOLZ, R.W. & NEUBIG, R.R. (1986). Guanine nucleotide effects on catecholamine secretion from digitonin-permeabilized adrenal chromaffin cells. *J. Biol. Chem.*, **261**, 10182–10188.

BURGOYNE, R.D. (1991). Control of exocytosis in adrenal chromaffin cells. *Biochim. Biophys. Acta*, **1071**, 174–202.

CASTRO, E., TORRES, M., MIRAS-PORTUGAL, M.T. & GONZÁLEZ, M.P. (1990). Effect of diadenosine polyphosphates on catecholamine secretion from isolated chromaffin cells. *Br. J. Pharmacol.*, **100**, 360–364.

CEÑA, V., BROCKLEHURST, K.W., POLLARD, H.B. & ROJAS, E. (1991). Pertussis toxin stimulation of catecholamine release from adrenal medullary chromaffin cells: mechanism may be by a direct activation of L-type and G-type calcium channels. *J. Membrane Biol.*, **122**, 23–31.

CHEEK, T.R. & BURGOYNE, R.D. (1987). Cyclic AMP inhibits both nicotine-induced actin disassembly and catecholamine secretion from bovine adrenal chromaffin cells. *J. Biol. Chem.*, **262**, 11663–11666.

CHEEK, T.R. & THASTRUP, O. (1989). Internal Ca^{++} mobilization and secretion in bovine adrenal chromaffin cells. *Cell Calcium*, **10**, 231–221.

CHERN, Y.J., KIM, K.T., STARLEY, L.L. & WESTHEAD, E.W. (1988). Adenosine receptors activate adenylate cyclase and enhance secretion from bovine adrenal chromaffin cells in the presence of forskolin. *J. Neurochem.*, **50**, 1484–1493.

CHOI, A.Y., CAHILL, A.L., PERRY, B.D. & PERLMAN, R.L. (1993). Histamine evokes greater increases in phosphatidylinositol metabolism and catecholamine secretion in epinephrine-containing than in norepinephrine containing chromaffin cells. *J. Neurochem.*, **61**, 541–549.

DOUGLAS, W.W. & RUBEN, R.P. (1963). The mechanism of catecholamine release from the adrenal medulla and the role of calcium in stimulus-secretion coupling. *J. Physiol.*, **167**, 288.

EBERHARD, D.A. & HOLZ, R.W. (1987). Cholinergic stimulation of inositol phosphate formation in bovine adrenal chromaffin cells: distinct nicotinic and muscarinic mechanisms. *J. Neurochem.*, **49**, 1634–1643.

GUTMAN, Y. & BOONJAVIROY, P. (1979). Activation of adrenal medulla adenylate cyclase and catecholamine secretion. *Naunyn-Schmied. Arch. Pharmacol.*, **307**, 39–44.

HIGGINS, L.S. & BERG, D.K. (1988). Cyclic AMP-dependent mechanism regulates acetylcholine receptor function on bovine adrenal chromaffin cells and discriminates between new and old receptors. *J. Cell. Biol.*, **107**, 1157–1165.

HOCHMAN, J. & PERLMAN, R.L. (1976). Catecholamine secretion by isolated adrenal cells. *Biochim. Biophys. Acta*, **421**, 168–175.

ISOBE, K., NAKAI, T. & TAKUWA, Y. (1993). Ca^{2+}-dependent stimulatory effect of pituitary adenylate cyclase-activating polypeptide on catecholamine secretion from cultured porcine 19 adrenal medullary chromaffin cells. *Endocrinology*, **132/4**, 1757–1765.

KNIGHT, D.E. & BAKER, P.R. (1982). Calcium dependence of catecholamine release from bovine adrenal medullary cells after exposure to intense electric fields. *J. Membr. Biol.*, **68**, 107–140.

KUMAKURA, K., GUIDOTTI, A. & COSTA, E. (1979). Primary cultures of chromaffin cells: molecular mechanisms for the induction of tyrosine hydroxylase mediated by 8-Br-cyclic AMP. *Mol. Pharmacol.*, **16**, 865–876.

MARRIOTT, D., ADAMS, M. & BOARDER, M.R. (1988). Effect of forskolin and prostaglandin E_1 on stimulus secretion coupling in cultured bovine adrenal chromaffin cells. *J. Neurochem.*, **50**, 616–623.

MORGAN, A., WILKINSON, M. & BURGOYNE, R.D. (1993). Identification of Exo2 as the catalytic subunit of protein kinase A reveals a role for cyclic AMP in Ca^{2+}-dependent exocytosis in chromaffin cells. *EMBO J.*, **12/10,** 3747–3752.

MORITA, K., DOHI, T., KITAYAMA, S., KOYAMA, Y. & TSUJIMOTO, A. (1987). Enhancement of stimulation-evoked catecholamine release from cultured bovine adrenal chromaffin cells by forskolin. *J. Neurochem.*, **48,** 243–247.

MORITA, K., DOHI, T., KITAYAMA, S. & TSUJIMOTO, A. (1991a). Mechanism of cyclic AMP facilitation of stimulation-evoked catecholamine release in adrenal chromaffin cells. I. Evidence for enhancement of evoked increase in cytosolic free Na^+ concentration by cyclic AMP elevation. *Neurochem. Int.*, **19,** 1/2, 71–79.

MORITA, K., DOHI, T., KITAYAMA, S. & TSUJIMOTO, A. (1991b). Mechanism of cyclic AMP facilitation of stimulation-evoked catecholamine release in adrenal chromaffin cells. II. Inhibition of Na^+-K^+-ATPase by cyclic AMP. *Neurochem. Int.*, **19,** 1/2, 81–85.

NEGISHI, M., ITO, S. & HAYAISHI, O. (1989). Prostaglandin E_2 receptors in bovine adrenal medulla are coupled to adenylate cyclase via G_i and to phosphoinositide metabolism in a pertussis toxin-insensitive manner. *J. Biol. Chem.*, **264,** 3916–3922.

OSET-GASQUE, M.J., PARRAMÓN, M. & GONZÁLEZ, M.P. (1993). $GABA_B$ receptors modulate catecholamine secretion in chromaffin cells by a mechanism involving cyclic AMP formation. *Br. J. Pharmacol.*, **110,** 1586–1592.

PARRAMÓN, P., HERRERO, M.T., GONZÁLEZ, M.P. & OSET-GASQUE, M.J. (1994). $GABA_B$ receptors increase intracellular calcium concentrations in chromaffin cells through two different pathways. Their role in catecholamine secretion. *J. Neurosci. Res.* (in press).

PEACH, M.J. (1972). Stimulation of release of adrenal catecholamine by adenosine 3′-5′-cyclic monophosphate and theophylline in the absence of extracellular Ca^{++}. *Proc. Natl. Acad. Sci. U.S.A.*, **69,** 834–836.

SIKDAR, S.K., ZOREC, R. & MASON, W.T. (1990). cAMP directly facilitates Ca^{2+}-induced exocytosis in bovine lactotrophs. *FEBS Lett.*, **273,** 1/2, 150–154.

SONTAG, J.M., THIERSE, D., ROUOT, B., AUNIS, D. & BADER, M.F. (1991). A pertussis-toxin-sensitive protein controls exocytosis in chromaffin cells at a step distal to the generation of second messengers. *Biochem. J.*, **274,** 339–347.

WAGGONER, A.S. (1979). Dye indicators of membrane potential. *Annu. Rev. Biophys. Bioenerg.*, **8,** 47–68.

WILSON, S.P. (1988). Vasoactive intestinal peptide elevates cAMP levels and potentiates secretion in bovine adrenal chromaffin cells. *Neuropeptides*, **11,** 17–21.

WILSON, S.P. (1992). Vasoactive intestinal peptide is a secretagogue in bovine chromaffin cells pretreated with pertussis toxin. *Neuropeptides*, **23,** 187–192.

(Received April 29, 1994
Revised September 21, 1994
Accepted September 26, 1994)

British Journal of Pharmacology (1995) 114, 524-530 © 1995 Stockton Press All rights reserved 0007-1188/95 $9.00

Different effects of endothelin-3 on the Ca^{2+} discharge induced by agonists and Ca^{2+}-ATPase inhibitors in human platelets

[1]Catherine Astarie-Dequeker, Irina Korichneva & Marie-Aude Devynck

Pharmacology, CNRS URA 1482 Necker Medical School, 156, rue de Vaugirard, 75015 Paris, France

1 The present study demonstrates that endothelin-3 (ET-3), previously shown to attenuate thrombin-evoked aggregation of human platelets, delayed the dose-dependent aggregatory response to thapsigargin (Tg). As this Ca^{2+}-ATPase inhibitor induces platelet activation in part through the depletion of internal Ca^{2+}-stores, we examined the influence of ET-3 on Ca^{2+} discharge from internal pools.

2 Cytosolic Ca^{2+} concentration was evaluated with Fura-2 in the absence of Ca^{2+} influx. Platelet preincubation for 15 min with 5×10^{-7} M ET-3 decreased the Ca^{2+} release evoked by thrombin and U46619, a thromboxane-mimetic. However, ET-3 did not affect Ca^{2+} movements induced by 1 μM ADP. Addition of Tg (0.5 to 5 μM) to resting platelets induced a cytosolic [Ca^{2+}] rise with concentration-dependent increase of the initial rate and decrease of the time to reach the peak. ET-3 slowed down these dose-dependent effects with a more marked influence on the responses induced by low concentrations of Tg.

3 ET-3 did not modify the Ca^{2+} response to another Ca^{2+}-ATPase inhibitor, 2,5-di-(tert-butyl)-1,4-benzohydroquinone(tBuBHQ). The thromboxane A_2 receptor antagonist, SQ 29548, reduced by 53% the calcium signal evoked by 1 μM Tg, which became similar to that induced by 15 μM tBuBHQ. Under these conditions, the ET-3 effects were suppressed. A subsequent addition of thrombin induced a substantial further Ca^{2+} increase which was again sensitive to ET-3.

4 ET-3 attenuates Ca^{2+} mobilization from an internal pool dependent on the stimulation of thrombin and thromboxane A_2 receptors and insensitive to the direct effect of Ca^{2+}-ATPase inhibitors. The small but significant inhibitory effect of ET-3 leads us to propose that endothelin-3 acts as a modulator of platelet activation.

Keywords: Human platelets; Ca^{2+}; platelet aggregation; endothelin-3; thapsigargin; tBuBHQ

Introduction

The synergistic action of endothelium-derived relaxing factor (EDRF) and prostacyclin at the luminal surface of endothelial cells contributes to the antiaggregatory properties of the normal intima. In addition to these well-known vasorelaxant factors, the vascular endothelium releases potent vasoconstrictor peptides called endothelins (ETs). Data point to the role of endothelins in physiological functions, including platelet aggregation. ET-1 inhibits *ex vivo* and *in vivo* platelet aggregation in the rabbit (Thiemermann *et al.*, 1988; 1989; 1990; Lidbury *et al.*, 1990) and the dog (Herman *et al.*, 1989; Filep *et al.*, 1991). Evidence suggests that the release of cyclo-oxygenase products into the circulation mediates in part this inhibitory effect of endothelins. Indomethacin and aspirin indeed block the antiaggregatory action of ET-1 (Thiermermann *et al.*, 1988; Herman *et al.*, 1989; Filep *et al.*, 1991). More recently, we demonstrated a direct inhibitory effect of ET-1 and ET-3 on the aggregating response of human platelets to thrombin (Astarie-Dequeker *et al.*, 1992), recently confirmed by Touyz & Schiffrin (1993). This agrees with the recent work of Pietraszek *et al.* (1992), who reported that platelet preincubation with ETs inhibited platelet aggregation evoked by 5-hydroxytryptamine (5-HT).

The mechanism of endothelin-induced inhibition of aggregation still remains unknown. Preliminary data obtained in our laboratory suggested that ET-1 and ET-3 decrease Ca^{2+} transients induced by thrombin, probably by reducing the Ca^{2+} release from internal stores (Astarie-Dequeker *et al.*, 1992). Pietraszek *et al.* (1992) reached the same conclusion in platelets stimulated by 5-HT. Many platelet agonists elevate cytosolic calcium by an inositol 1,4,5-trisphosphate (IP_3)-dependent release of sequestered calcium (Pollock & Rink, 1986; Siess, 1989; Rink & Sage, 1990). However, IP_3 formation is not the only pathway for discharge of internal Ca^{2+} stores. For instance, ADP is effective in generating Ca^{2+} release from internal stores without significant hydrolysis of phosphatidylinositol biphosphate (PIP_2) (Fisher *et al.*, 1985; Dean & Adunyah, 1986). In addition, there are at least two types of calcium store in platelets (Brüne & Ullrich, 1991b; Authi *et al.*, 1993). Two structurally unrelated compounds, the sesquiterpene lactone tumour promoter, thapsigargin (Tg) and 2,5-di-(ter-butyl)-1-,4-benzohydroquinone (tBuBHQ) have proved to be useful in the investigation of cellular Ca^{2+} homeostasis. Independently of surface receptor occupancy, these two drugs inhibit the endoplasmic reticulum Ca^{2+}-ATPase and increase cytosolic Ca^{2+} levels by preventing Ca^{2+} reuptake (Thastrup, 1987; Thastrup *et al.*, 1987; 1990; Kass *et al.*, 1989). In platelets, Tg effects are mediated in part by the formation of eicosanoid endoperoxides/thromboxane (Brüne & Ullrich, 1991a). However, part of the platelet response occurs independently of eicosanoid formation (Brüne & Ullrich, 1991b). In contrast, tBuBHQ exerts an inherent cyclo-oxygenase inhibition (Brüne & Ullrich, 1991a). Tg and tBuBHQ can thus be used as pharmacological probes to reveal differences between receptor-dependent and -independent processes involved in the regulation of cytosolic Ca^{2+}.

In an attempt to elucidate the mechanism by which ET-3 affects Ca^{2+} homeostasis in human platelets, we investigated its influence on Ca^{2+} discharge from stores sensitive and insensitive to receptor stimulation. To this end, we have compared its effects on Ca^{2+} mobilization induced by receptor-dependent and receptor-independent stimuli, such as platelet agonists and Ca^{2+}-ATPase inhibitors, respectively.

[1] Author for correspondence.

Methods

Platelet preparation

Blood was collected from healthy volunteers who had taken no medications with known platelet-inhibiting properties for at least 10 days; 20 ml of blood was drawn by venipuncture and mixed with one-tenth volume of acid/citrate dextrose anticoagulant (2.73% citric acid, 4.48% trisodium citrate, and 2% glucose, (w/v)). Platelet-rich plasma (PRP) was then prepared by centrifugation at 530 g_{max} for 5 min at 20°C. All experiments were performed within 5 h of blood sampling, on platelets kept at room temperature until the beginning of experiments.

Platelet aggregation study

Platelet aggregation was carried out on washed platelets as previously described (Astarie-Dequeker *et al.*, 1992). Briefly, PRP was centrifuged at 270 *g* for 15 min at 20°C and the platelet pellet was resuspended in a standard medium containing, mM: NaCl 145, KCl 5, $MgCl_2$ 0.5, glucose 5 and HEPES 10, pH 7.4 at 37°C (buffer A). The platelet count was adjusted to $8-9 \times 10^7$ cells ml^{-1}. The aggregatory responses of washed platelets were evaluated 5 min after the addition of 1 mM $Ca(NO_3)_2$ by a turbidometric device (double-channel aggregometer, Coultronics). The changes in light transmission were characterized by the lag period after the addition of the agonist (s), the initial slope of the curve (%/min) and the maximal extent of aggregation (%). The responses to Tg in the presence and absence of ET-3 were alternatively repeated throughout the experiment.

Measurement of $[Ca^{2+}]_i$

Calcium measurements in intact platelets were performed with the fluorescent indicator Fura-2, as described previously (Astarie *et al.*, 1989). Briefly, PRP was incubated at 37°C with 2 μM Fura-2AM for 40 min. Platelets were then washed by centrifugation and resuspended in buffer A to give a final concentration of $8-9 \times 10^7$ cells ml^{-1}. Platelets were resuspended in buffer A containing 30 nM free Ca^{2+} adjusted with the required Ca-EGTA buffer. Experiments were carried out at 37°C on a Spex Fluorolog CM111 (Instruments S.A., Paris, France) equipped with a 450 W xenon lamp, two excitation monochromators and a dual-mirror chopping mechanism that allows a rapid alternating of excitation from 335 to 385 nm wavelengths with a fixed emission wavelength of 510 nm. Each fluorescence recording was systematically corrected for the autofluorescence of the cell suspension. None of the drugs tested modified either the intrinsic signal of platelets or the fluorescence properties of Fura-2. Free Ca^{2+} concentration was calculated from the experimental ratio of excitation fluorescence intensities ($R = I_{335}/I_{385}$) (Grinkiewicz *et al.*, 1985; Poenie *et al.*, 1985). Under these conditions, $[Ca^{2+}]_i$ was measured with inter- and intra-assay reproducibilities of $94.0 \pm 4.6\%$ ($n = 5$) and $95.7 \pm 4.4\%$ ($n = 10$), respectively. The response to agonists was repeatedly checked as control value during the evaluation of the ET-3 effect. The agonist-evoked $[Ca^{2+}]_i$ response was evaluated as the amplitude of $[Ca^{2+}]_i$ peak and the steady state $[Ca^{2+}]_i$ value at 3 min. The Tg effect was also analysed as the initial rate of the $[Ca^{2+}]_i$ rise and the time to reach the maximal value. Based on our previous observations (Astarie-Dequeker *et al.*, 1992), ET-3 was systematically added to the cell suspension 10 min before platelet activation.

Materials

Fura-2 acetoxymethyl ester (Fura-2AM) was obtained from Molecular probes (Eugene, OR, U.S.A.). tBuBHQ was from Calbiochem (Frankfurt, Germany) and SQ29548 [1S-[1,2(5Z), 3,4]]-7-[3-[[2-[(phenylamino)-carbonyl]-hydrazino]methyl-7-oxabicyclo[2.2.1]hept-2-yl]-5-heptenoic acid) was from Cayman Chemical Company (Ann Arbor, MI, U.S.A.). All other chemicals were purchased from Sigma Chemical Co (St Louis, MO, U.S.A.).

Statistics

Data are expressed as the mean values ± s.e.mean of *n* individual experiments from different donors. Statistical comparisons were based on non parametric Mann-Witney or Wilcoxon tests. Multiple comparisons were carried out by one or two-way analysis of variance and degree of freedom (df). Probability values lower than 5% were considered as significant.

Results

Effect of ET-3 on platelet aggregation induced by thapsigargin

In a previous study, we have demonstrated an inhibitory effect of ET-3 on platelet aggregation evoked by thrombin, associated with a decrease in Ca^{2+} discharge from the internal pool (Astarie-Dequeker *et al.*, 1992). Besides the conventional Ca^{2+} releasing agonists, Tg depletes internal calcium pools and causes human platelets to aggregate. We thus investigated the effect of ET-3 on the aggregatory response to Tg. At concentrations ranging from 0.1 to 5 μM, Tg produced an irreversible aggregation of washed platelets preceded by a lag phase that decreased in a concentration-dependent manner ($P < 0.001$, d.f.(6, 25)). The rate and extent of aggregation were maximal at 0.1 μM Tg. As presented on Figure 1, 5×10^{-7} M ET-3 delayed the onset of aggregation induced by 0.5 and 1 μM Tg, respectively (from 68 ± 8 to 82 ± 11 and 53 ± 6 to 62 ± 8 s, respectively, $n = 7$ and $P = 0.03$ for each). ET-3 had no effect on the initial rate and the extent of aggregation.

To evaluate the contribution of internal Ca^{2+}-pools in the anti-aggregatory effect of ET-3, we then tested its influence on the Ca^{2+} store discharge induced by platelet agonists (thrombin, a thromboxane-mimetic, U46619 and ADP) and Ca^{2+}-ATPase inhibitors (thapsigargin and tBuBHQ). In order to abolish the Ca^{2+} influx, the Ca^{2+} measurements were performed in a buffer containing 30 nM free Ca^{2+}.

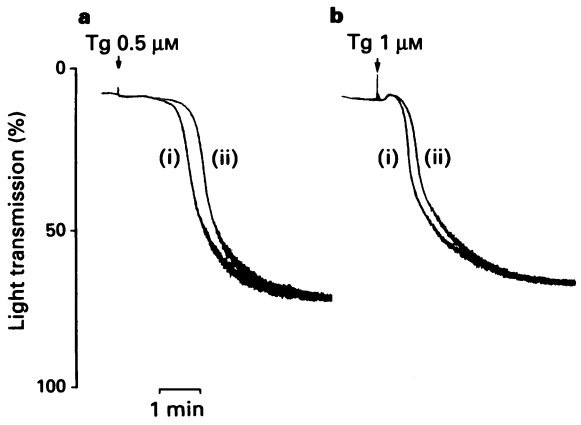


Figure 1 Effect of endothelin-3 (ET-3) on aggregatory response induced by thapsigargin (Tg). Washed platelets resuspended in buffer containing 1 mM Ca^{2+} were preincubated with (i) vehicle or (ii) 5×10^{-7} M ET-3 for 10 min before addition of (a) 0.5 or (b) 1 μM Tg, as indicated. These traces are representative of 7 independent experiments.

Effect of ET-3 on Ca^{2+} store discharge induced by thrombin, U46619 and ADP

We confirmed that, in the absence of Ca^{2+} influx, 5×10^{-7} M ET-3 decreased by $17 \pm 4\%$ the amplitude of the transient $[Ca^{2+}]$ peak evoked by 0.05 u ml^{-1} thrombin (from 116 ± 14 to 98 ± 13 nM, $n = 12$, $P = 0.03$). Similarly, it also diminished the Ca^{2+} discharge evoked by 0.1 and 1 μM (15S)-hydroxy-11,9-(epoxymethano) prosta-5Z,13E-dienoicacid (U46619), a thromboxane-mimetic (from 68 ± 8 to 55 ± 6 and 98 ± 12 to 74 ± 11 nM, $n = 9$ and 7, $P = 0.01$ and 0.02, respectively). However, the response to ADP (0.25-1 μM) which also transiently discharged internal Ca^{2+} stores was insensitive to a pretreatment with ET-3 (48 ± 8 in its presence compared to 40 ± 10 nM in its absence, $n = 5$, for 1 μM ADP).

Effect of ET-3 on Ca^{2+} store discharge induced by thapsigargin

Under conditions in which external calcium concentration was buffered to 30 nM, Tg transiently increased $[Ca^{2+}]_i$, which then stabilized at a new steady state level higher than the initial one (Figure 2). Tg at concentrations ranging from 0.1 to 5 μM increased in a concentration-dependent manner the initial rate of $[Ca^{2+}]_i$ rise and the magnitude of the $[Ca^{2+}]_i$ peak achieved ($P < 0.001$ and $P = 0.04$, d.f.(3, 51) for each). Simultaneously, it decreased the time to reach the peak ($P < 0.003$, d.f.(3, 51)). When platelets were pretreated with ET-3, the concentration-dependent effects of Tg were maintained but the responses to Tg were slowed down (Figure 3). Only for 0.1 μM Tg, ET-3 also diminished the amplitude of the maximal calcium response (from 97 ± 14 to 65 ± 14 nM, $P = 0.04$, $n = 7$). No ET-3 effect was detected on the basal steady state $[Ca^{2+}]_i$ value (Figure 3). As depicted in Figure 4, 5×10^{-7} M ET-3 decreased the initial rate of Ca^{2+} rise and thereby increased the time to reach the $[Ca^{2+}]_i$ peak. Such inhibitory effects decreased with increasing thapsigargin concentration ($P = 0.01$ and $P = 0.02$, d.f.(1,27), Figure 4a and b, respectively).

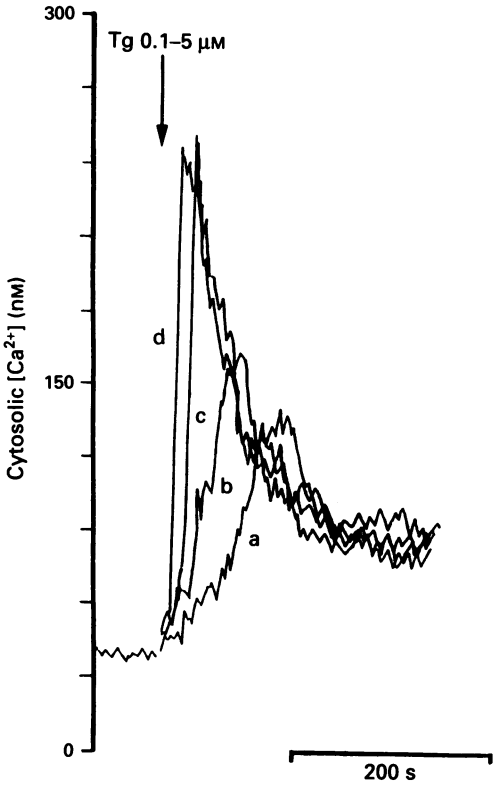


Figure 2 Dose-dependent effect of thapsigargin (Tg) on the mobilization of Ca^{2+} stores. Washed platelets loaded with Fura-2 were resuspended in buffer containing 30 nM Ca^{2+}. Representative tracings of the elevation of cytosolic $[Ca^{2+}]_i$ induced by (a) 0.1 (b), 0.5 (c), 1 (d) and 5 μM Tg, as indicated. Each trace is representative of 9–17 independent experiments.

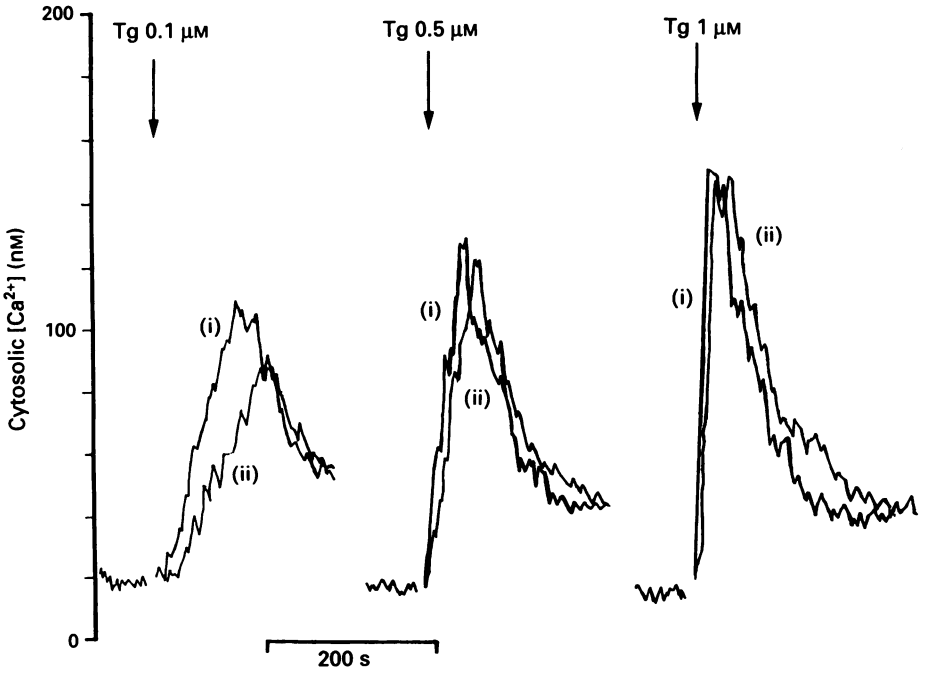


Figure 3 Tracings of the endothelin-3 (ET-3) effects on the Ca^{2+} release induced by thapsigargin (Tg). Fura-2-loaded platelets were incubated at 37°C with (i) vehicle or (ii) 5×10^{-7} M ET-3 for 10 min in a buffer containing 30 nM Ca^{2+} and stimulated by various concentrations of Tg. Each trace is representative of 6–8 independent experiments.

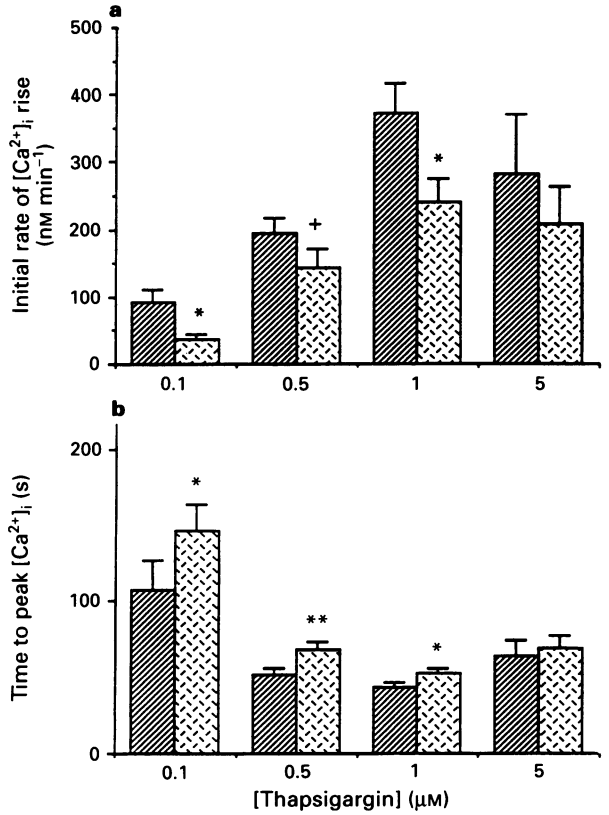


Figure 4 Effect of endothelin-3 (ET-3) on the initial rate and the time required to reach the $[Ca^{2+}]_i$ peak evoked by thapsigargin (Tg). Experiments performed as described in Figure 3 were analysed as (a) the initial rate and (b) the time to reach the $[Ca^{2+}]_i$ peak evoked by Tg in the presence (stippled columns) and the absence (hatched columns) of 5×10^{-7} M ET-3. Data are expressed as means ± s.e.mean of 6–8 experiments. Effects of ET-3 were evaluated by two-way analysis of variance and significance was assessed by Wilcoxon-test. $P = 0.01$ (a) and $P = 0.02$ (b) with d.f.(1,3) for each. $^*P<0.05$, $^+P<0.02$, $^*P<0.01$ and $^{**}P<0.005$ when compared to their respective controls.

To investigate which internal Ca^{2+} compartments were affected by ET-3, we first conducted experiments to determine, under our experimental conditions, the nature of these Ca^{2+} stores in human platelets. It is generally accepted that thrombin causes a rapid increase in cytosolic free Ca^{2+} due partially to IP_3-induced Ca^{2+} release from the dense tubular system. In a buffer containing 30 nM free Ca^{2+}, 0.05 u ml^{-1} thrombin mobilized sequestered Ca^{2+} to a similar extent to that induced by 1 μM Tg (+ 116 ± 14 and + 124 ± 14 nM, $n = 12$ and 17, respectively) but the time to reach the peak was shorter (12 ± 6 versus 57 ± 5 s, $n = 12$ and $n = 17$, respectively) (Figure 5a). Pretreatment with 1 μM Tg for 3 min decreased dramatically the amplitude of thrombin-evoked Ca^{2+} release (+ 24 ± 3 versus + 160 ± 21 nM, $n = 3$) (Figure 5b), suggesting that Tg had almost totally depleted agonist-sensitive Ca^{2+}-stores. Conversely, when thrombin signal returned back to the initial level, the subsequent addition of Tg induced a further Ca^{2+} release, comparable to the one observed with Tg alone (154 ± 34 versus 146 ± 40 nM, $n = 5$). Tg was thus able to discharge Ca^{2+} from a pool either insensitive to thrombin or replenished following thrombin stimulation, thereby becoming sensitive to Tg.

Effect of ET-3 on Ca^{2+} store discharge induced by the inhibition of reticulum Ca^{2+}-ATPase

It was proposed that in platelets Tg exerted its effects on $[Ca^{2+}]_i$ in part by a subsequent synthesis of thromboxane (Brüne & Ullrich, 1991a). We found that blockade of the self amplification mechanism of platelet activation with the thromboxane-receptor antagonist, SQ 29548 (3 μM) increased the time required to reach the $[Ca^{2+}]_i$ peak (from 59 ± 6 to 95 ± 16 s, $n = 6$, $P = 0.03$) and decreased by 53% the extent of Ca^{2+} released by 1 μM Tg (from 154 ± 20 to 71 ± 8 nM, $n = 6$, $P = 0.03$) (Figure 5b). Therefore, in the presence of SQ 29548, the Tg response was smaller than that obtained with thrombin alone (Figure 5a and b). Combined addition of SQ 29548 and Tg mimicked the calcium response evoked by another reticulum Ca^{2+}-ATPase inhibitor, tBuBHQ (Figure 6). SQ 29548 preincubation did not affect the responses to tBuBHQ, but significantly decreased the Ca^{2+} rise evoked by thrombin (from 121 ± 14 to 102 ± 18 nM, $n = 4$). However, the response to thrombin remained sensitive to ET-3 (from 138 ± 4 to 111 ± 5 nM, $n = 4$, in the absence and presence of ET-3, respectively). As shown in Figure 6, thrombin addition 3 min after 1 μM Tg or 15 μM tBuBHQ treatment still evoked a substantial further Ca^{2+} release. These increases were transient and returned to the initial level. Experiments were then carried out to test the effect of ET-3 under conditions which discriminate between a compartment sensitive to Ca^{2+}-ATPase inhibitors and an additional compartment which requires thrombin-activation (Figure 6). In the presence of 3 μM SQ 29548, ET-3 no longer influenced the initial rate and the time to reach the Ca^{2+} peak induced by 1 μM Tg (310 ± 60 to 300 ± 70 nM min^{-1} and 82 ± 15 to 86 ± 16 s, $n = 6$, in the absence and presence of ET-3 respectively). Qualitatively the same situation emerged when platelets were stimulated by tBuBHQ. However, applying thrombin afterwards revealed once more an inhibitory effect of ET-3 (Figure 6). ET-3 decreased by 34 and 36% the amplitude of the Ca^{2+} mobilization evoked by thrombin added subsequently to Tg in the presence of SQ 29548 or to tBuBHQ, respectively (from 62 ± 19 to 41 ± 17 nM and 100 ± 27 to 64 ± 11 nM, $n = 3$, respectively).

Discussion

This study suggests that ET-3 attenuates Ca^{2+} mobilization evoked by both thrombin and thromboxane receptor stimulation. The preferential target of ET-3 appears to be a receptor-dependent Ca^{2+} store, distinct from that sensitive to Ca^{2+}-ATPase inhibitors.

Up to now, little information has been available concerning the direct antiplatelet properties of ETs. They appear to depend on the agonists tested and experimental conditions used. Briefly, ETs were reported not to affect the aggregatory response to collagen, PAF, adrenaline and ADP (Battistini *et al.*, 1990; Ohlstein *et al.*, 1990; Joseph *et al.*, 1991) though the latter have also been described as facilitated by ET-3 (Matsumoto *et al.*, 1990). In contrast, we and some other authors have described an inhibitory effect of ETs on platelet aggregation evoked by either thrombin, adrenaline or 5-HT (Astarie-Dequeker *et al.*, 1992; Dockrell *et al.*, 1992; Pietraszek *et al.*, 1992; Touyz *et al.*, 1993). ETs have also been proposed to inhibit or potentiate 5-HT-induced platelet aggregation according to whether or not preincubation occurred (Pietraszek *et al.*, 1992). We demonstrate here that ET-3 also directly inhibits aggregation induced by a Ca^{2+}-ATPase inhibitor, Tg. ET-3 delayed the aggregatory response to Tg, but did not affect the slope and extent of aggregation, in contrast to its effect on thrombin-evoked aggregation (Astarie-Dequeker *et al.*, 1992). This suggested that ET-3 modulated preferentially the mechanism involved in the time required to initiate the Tg-induced aggregation but was unable to affect the response once initiated.

In vivo, endothelins exert anti-aggregatory effects, mediated in part by prostacyclin release (Thiemermann *et al.*, 1988; Herman *et al.*, 1989; Filep *et al.*, 1991) and by unknown mechanism(s) neither blocked by indomethacin nor associated with enhanced adenosine 3':5'-cyclic monophos-

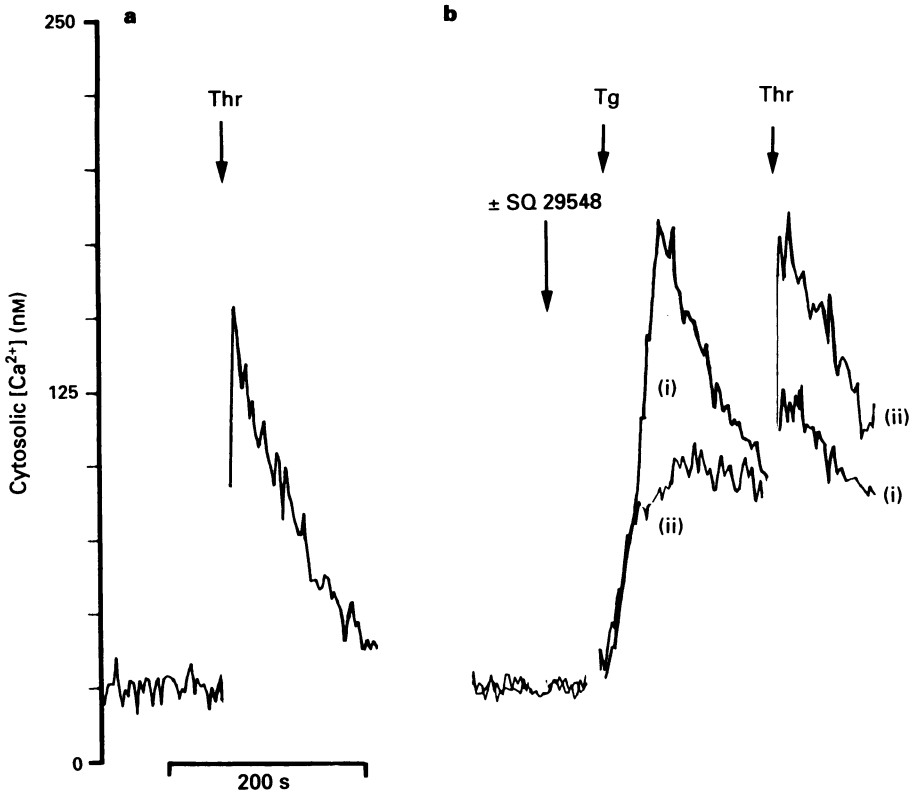


Figure 5 Tracing of Ca^{2+} mobilization induced by thrombin in platelets pretreated or not with thapsigargin (Tg) and SQ 29548. Fura-2-loaded platelets were resuspended in buffer containing 30 nM Ca^{2+} and activated by (a) 0.05 u ml^{-1} thrombin alone or (b) 0.05 u ml^{-1} thrombin added subsequently to 1 μM Tg in the presence (ii) or the absence (i) of 3 μM SQ 29548, as indicated. Each trace is representative of 6–12 independent experiments.

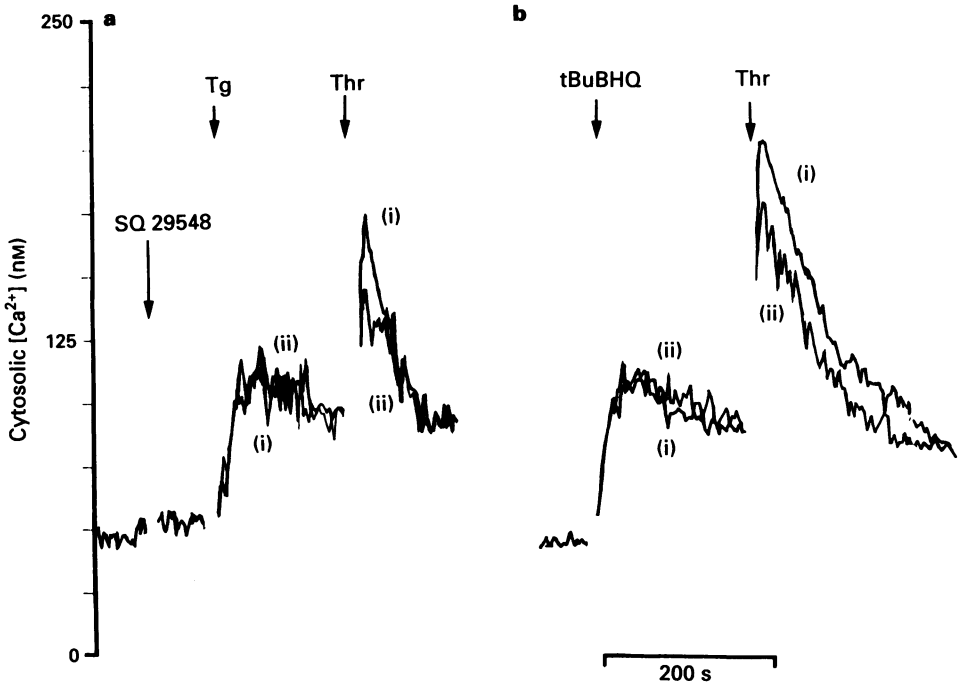


Figure 6 Tracing of endothelin-3 (ET-3) effect on Ca^{2+} mobilization evoked by Ca^{2+}-ATPase inhibitors and subsequent thrombin stimulation. Fura-2-loaded platelets were resuspended in buffer containing 30 nM Ca and preincubated at 37°C with (i) the vehicle or (ii) 5×10^{-7} M ET-3 for 10 min. Platelets were then activated either by (a) 1 μM thapsigargin in the presence of 3 μM SQ 29548 or by (b) 15 μM tBuBHQ and subsequently by 0.05 u ml^{-1} thrombin, as indicated. Each trace is representative of 3–6 independent experiments.

phate (cyclic AMP) or cyclic GMP levels (Thiemermann *et al.* 1989). We previously showed and confirmed here that ET-3 directly affects platelet aggregation induced by thrombin and Tg (Astarie-Dequeker *et al.* 1992). To elucidate the mechanisms involved, we have examined effects of ET-3 on a major modulator of platelet activation, cytosolic calcium and more precisely its influence on Ca^{2+} discharge from internal stores. Indeed, preliminary data led us to propose that ET-3 probably diminished the thrombin-induced Ca^{2+} release from internal stores. In addition, Tg induces platelet activation in part through the depletion of internal Ca^{2+}-stores. We now demonstrate that ET-3 pretreatment diminished the Ca^{2+} store discharge induced by both thrombin and a thromboxane-mimetic, but it did not affect the Ca^{2+} transients evoked by ADP. Thrombin, thromboxane A_2 and ADP induced platelet activation through receptor stimulation but via different and independent ways (Sage & Rink, 1986). Indeed, thrombin and thromboxane A_2 induce Ca^{2+} release and protein kinase C activation through inositol triphosphate and diacylglycerol production whereas the response to ADP is thought to have little or no dependence on stimulation-response coupling through the activation of phospholipase C (Siess, 1989; Packham *et al.*, 1993). ET-3, which essentially diminished the Ca^{2+} release evoked by thrombin and U46619, should thus affect a process resulting from thrombin- and thromboxane-receptor occupancy. These conclusions are in good agreement with the inability of ET-3 to modulate directly ADP-evoked aggregation (Battistini *et al.*, 1990; Ohlstein *et al.*, 1990).

To examine this last proposition, we investigated the effect of ET-3 on Ca^{2+} release from the different types of intracellular pools. To this end, we used Tg which is able under appropriate conditions to distinguish receptor-dependent processes from direct effects on Ca^{2+}-ATPase (Brüne & Ullrich, 1991a). In the absence of Ca^{2+} influx, Tg induced a dose-dependent Ca^{2+} discharge that was slowed down by pretreatment with ET-3. Its amplitude was also reduced, but only in the presence of low Tg concentrations. Tg increased Ca^{2+} to the same extent as thrombin but twice as much as another Ca^{2+}-ATPase inhibitor, tBuBHQ. Blockade of the thromboxane A_2 receptors attenuated Tg-induced Ca^{2+} transients. With such pretreatment, the $[Ca^{2+}]_i$ rise reached only 50% of that induced by thrombin and hence was similar to that evoked by tBuBHQ. Qualitatively the same situation occurred when the cyclo-oxygenase activity was inhibited (Brüne & Ullrich, 1991b). These data are consistent with a Tg-induced formation of stimulatory eicosanoids and with the participation of thromboxane A_2 in the Ca^{2+} response to Tg. We found that ET-3 did not influence the Ca^{2+} response evoked either by Tg in the presence of SQ 29548 or by tBuBHQ, indicating that the inhibitory effects of ET-3 on Tg response depended on thromboxane activity. This is in good agreement with the inhibitory effect of ET-3 on the Ca^{2+} response to a thromboxane-mimetic. ET-3 may for example prevent the liberation of thromboxane A_2 and endoperoxides, which interestingly also have a positive feedback function on the action of U46619 and thrombin. However, we demonstrated that ET-3 decreased the response to thrombin in the presence of a thromboxane receptor antagonist. In addition, ET-3 altered both the initiation of Ca^{2+} response and the maximal $[Ca^{2+}]_i$ value induced by low Tg concentrations only and hence under conditions of moderate thromboxane A_2 synthesis (Malcolm & Fitzpatrick, 1992). Though we cannot rule out an effect of ET-3 on thromboxane A_2 synthesis, it is evident that ET-3 also influenced the calcium signal independently of a self amplification process.

In platelets pretreated with Tg, thrombin induced a slight transient calcium signal. In contrast, blocking the thromboxane receptor dramatically decreased the Tg response without affecting the calcium mobilization induced by a subsequent addition of thrombin (Figure 6). Since thromboxane A_2 is known not to desensitize the thrombin receptor (Murray *et al.*, 1990), thrombin and thromboxane A_2 should mobilize Ca^{2+} from the same pool. In the absence of a self amplification mechanism, ET-3 did not modify the response to Ca^{2+}-ATPase inhibitors. Since Ca^{2+}-ATPase inhibitors induced a platelet response without a receptor stimulation process, we suggested that ET-3 affected the signal transduction generated as a consequence of surface receptor occupancy by agonists like thrombin and thromboxane A_2. This is consistent with the recent work of Pietraszek *et al.* (1992), who suggested that ETs stimulate protein kinase C. According to these authors, in platelets pretreated with ET-3, as in our study, the protein kinase C should be activated before addition of the second stimulus. Consequently, the coupling between receptor and phospholipase C should be inhibited by negative feedback. However, the mechanisms by which ETs activate protein kinase C are still obscure.

The addition of thrombin to platelets treated with Tg in the presence of SQ 29548 or with tBuBHQ induced a further transient Ca^{2+} rise, in conformity with the previous findings of Brüne & Ullrich (1991b). These authors proposed the presence of two Ca^{2+} pools in platelets: a compartment which requires receptor activation and an additional compartment sensitive to Ca^{2+}-ATPase inhibition, both compartments reflecting the classical IP_3-sensitive pool. Brüne & Ullrich (1991b) also showed that Tg added after pretreatment with thrombin in the presence of BW755C, as an inhibitor of cyclo-oxygenase and lipoxygenase, released sequestered Ca^{2+}. This led them to suggest that the Ca^{2+} reuptake following receptor stimulation occurs into the Tg-sensitive compartment. This is consistent with the maintained ability of thapsigargin to discharge Ca^{2+} when added subsequently to thrombin. ET-3 diminished the Ca^{2+}-discharge evoked by thrombin used as a second agonist after platelets were exposed to tBuBHQ or Tg in the presence of SQ 29548. This led us to consider that ET-3 influenced preferentially the Ca^{2+} release from an IP_3-sensitive pool dependent on receptor stimulation. However, the nature of Ca^{2+} stores remains unclear, as recent experiments conducted in saponin-permeabilized platelets demonstrated that Ca^{2+}-ATPase inhibitors discharged totally the IP_3-sensitive compartment whereas thrombin is able to mobilize both the Ins(1,4,5)P_3-sensitive and -insensitive pools (Authi *et al.*, 1993).

In conclusion, ET-3 modulated the Ca^{2+} mobilization from a compartment sensitive to thrombin and thromboxane A_2 receptor stimulation but insensitive to the direct effect of Ca^{2+}-ATPase inhibitors. Such inhibitory effects of ET-3 could participate in its anti-aggregatory effects that we previously described in response to thrombin (Astarie-Dequeker *et al.*, 1992). The modest influence of endothelin may bring into question its physiological relevance. However, we previously demonstrated that endothelin potentiates the platelet response to sodium nitroprusside. This led us to suggest that ET-3 acts as a modulator of platelet activation. In combination with prostacyclin or EDRF, it could thereby regulate the interaction between platelets and vessel wall and limit thrombus formation.

The authors thank Dr M. David-Dufilho for helpful comments.

References

ASTARIE, C., LEVENSON, J., SIMON, A., MEYER, P. & DEVYNCK, M.A. (1989). Platelet cytosolic proton and free calcium concentrations in essential hypertension. *J. Hypertens.*, **7**, 485–491.

ASTARIE-DEQUEKER, C., IOUZALEN, L., DAVID-DUFILHO, M. & DEVYNCK, M.A. (1992). In vitro inhibition by endothelins of thrombin-induced aggregation and Ca^{2+} mobilization in human platelets. *Br. J. Pharmacol.*, **106**, 966–971.

AUTHI, K.S., BOKKALA, S., PATEL, Y., KAKKAR, V.V. & MUNKONGE, F. (1993). Ca^{2+} release from platelet intracellular stores by thapsigargin and 2,5-di-(t-butyl)-1,4-benzohydroquinone: relationship to Ca^{2+} pools and relevance in platelet activation. *Biochem. J.*, **294**, 119–126.

BATTISTINI, B., FILEP, J.G., HERMAN, F. & SIROIS, P. (1990). Endothelin-1 does not affect human platelet aggregation in whole blood and platelet rich plasma. *Thromb. Res.*, **60**, 105–108.

BRÜNE, B. & ULLRICH, V. (1991a). Calcium mobilization in human platelets by receptor agonists and calcium-ATPase inhibitors. *FEBS Lett.*, **284**, 1–4.

BRÜNE, B. & ULLRICH, V. (1991b). Different calcium pools in human platelets and their role in thromboxane A_2 formation. *J. Biol. Chem.*, **266**, 19232–19237.

DEAN, W.C. & ADUNYAH, S.E. (1986). Effects of sulfhydryl reagents and other inhibitors on Ca^{2+} transport and inositol triphosphate-induced Ca^{2+} release from human platelets membranes. *J. Biol. Chem.*, **261**, 13071–13075.

DOCKRELL, M.E.C., WAUGH, C.J., HAYNES, W.G., WEBB, D.J. & WILLIAMS, B.C. (1992). Effect of endothelin-1 on adrenaline stimulated aggregation of human platelets: Evidence in support of a biphasic action (Abstract). *J. Vascular Res.*, **29**, 104.

FILEP, J., HERMAN, F., BATTISTINI, B., CHABRIER, P.E., BRAQUET, P. & SIROIS, P. (1991). Antiaggregatory and hypotensive effects of endothelin-1 in Beagle dogs: Role of prostacyclin. *J. Cardiovasc. Res.*, **17**, S216–S218.

FISCHER, G.J., BAKSHIAN, S. & BALDASSARE, J.J. (1985). Activation of human platelets by ADP causes a rapid rise in cytosolic free calcium without hydrolysis of phosphatidylinositol-4, 5 biphosphate. *Biochem. Biophys. Res. Commun.*, **129**, 958–964.

GRINKIEWICZ, G., POENIE, M. & TSIEN, R.Y. (1985). A new generation of calcium indicators with greatly improved fluorescence properties. *J. Biol. Chem.*, **260**, 3440–3450.

HERMAN, F., MAGJYAR, K., CHABRIER, P.E., BRAQUET, P. & FILEP. J. (1989). Prostacyclin mediates the antiaggregatory and hypotensive action of endothelin in anaesthetized beagle dogs. *Br. J. Pharmacol.*, **98**, 38–40.

JOSEPH, R., SCICLI, A.G., HAN, E., GRUNFELD, S., CARRETERO, O.A. & WELCH, K.M.A. (1991). Endothelin-1 and human platelet activity. *Thromb. Res.*, **61**, 529–536.

KASS, G.E.N., DUDDY, S.K., MOORE, G.A. & ORRENIUS, S. (1989). 2,5-Di(ter-butyl)1-,4-benzohydroquinone rapidly elevates cytosolic Ca^{2+} concentration by mobilizing the inositol 1,4,5-triphosphate-sensitive Ca^{2+}-pool. *J. Biol. Chem.*, **264**, 15192–15198.

LIDBURY, P.S., THIEMERMANN, C., KORBUT, R. & VANE, J.R. (1990). Endothelins release tissue plaminogen activator and prostanoids. *Eur. J. Pharmacol.*, **186**, 205–212.

MALCOLM, K.C. & FITZPATRICK, F.A. (1992). Indirect action of thapsigargin on human platelets: activation of eicosanoid biosynthesis and cellular signalling pathways. *J. Pharmacol. Exp. Ther.*, **260**, 1244–1249.

MATSUMOTO, Y., OZAKI, Y., KARIYA, T. & KUME, S. (1990). Potentiating effects of endothelin on platelet activation induced by epinephrine and ADP. *Biochem. Pharmacol.*, **40**, 909–911.

MURRAY, R., SHIPP, E.S. & FITZGERALD, G.A. (1990). Prostaglandin endoperoxide/thromboxane A_2 receptor desensitization. *J. Biol. Chem.*, **265**, 21670–21675.

OHLSTEIN, E.H., STORER, B., NAMBI, P., GIVEN, M. & LIPPTON, H. (1990). Endothelin and platelet function. *Thromb. Res.*, **57**, 967–974.

PACKHAM, M.A., LIVNE, A.A., RUBEN, D.H. & RAND, M.L. (1993). Activation of phospholipase C and protein kinase C has little involvement in ADP-induced primary aggregation of human platelets: effects of diacylglycerols, the diacylglycerol inhibitor R59022, staurosporine and okadaic acid. *Biochem. J.*, **290**, 849–856.

PIETRASZEK, M.H., TAKADA, Y. & TAKADA, A. (1992). Endothelins inhibit serotonin-induced platelet aggregation via a mechanism involving protein kinase C. *Eur. J. Pharmacol.*, **219**, 289–293.

POENIE, M., ALDERTON, J., TSIEN, R.Y. & STEINHARDT, R.A. (1985). Changes of free calcium levels with stages of the cell division cycle. *Nature*, **315**, 147–149.

POLLOCK, W.K. & RINK, T.J. (1986). Thrombin and ionomycin can raise platelet cytosolic Ca^{2+} to micromolar levels by discharge of internal Ca^{2+} stores: studies using Fura-2. *Biochem. Biophys. Res. Commun.*, **139**, 308–314.

RINK, T.J. & SAGE, S.O. (1990). Calcium signalling in human platelets. *Annu. Rev. Physiol.*, **52**, 431–449.

SAGE, S.O. & RINK, T.J. (1986). Kinetic differences between thrombin-induced and ADP-induced calcium influx and release from internal stores in Fura-2-loaded human platelets. *Biochem. Biophys. Res. Commun.*, **136**, 1124–1129.

SIESS, W. (1989). Molecular mechanisms of platelet activation. *Physiol. Rev.*, **69**, 58–141.

THASTRUP, O. (1987a). The calcium mobilizing and tumor promoting agent, thapsigargin elevates the platelet cytoplasmic free calcium concentration to a higher steady state level. A possible mechanism of action for the tumor promotion. *Biochem. Biophys. Res. Commun.*, **142**, 654–660.

THASTRUP, O., LINNEBJERG, H., BJERRUM, P.J., KNUDSEN, J.B. & BROGGER CHRISTENSEN, S. (1987b). The inflammatory and tumor promoting sesquiterpene lactone, thapsigargin, activates platelets by selective mobilization of calcium as shown by protein phosphorylations. *Biochim. Biophys. Acta*, **927**, 65–73.

THASTRUP, O., CULLEN, P.J., BJORD, K., HANLEY, M.R. & DAWSON, A.P. (1990). Thapsigargin, a tumor promoter, discharges intracellular Ca^{2+} stores by specific inhibition of the endoplasmic reticulum Ca^{2+}-ATPase. *Proc. Natl. Acad. Sci. U.S.A.*, **87**, 2466–2470.

THIEMERMANN, C., LIDBURY, P.S., THOMAS, G.R. & VANE, J.R. (1988). Endothelin inhibits *ex vivo* platelet aggregation in the rabbit. *Eur. J. Pharmacol.*, **158**, 181–182.

THIEMERMANN, C., LIDBURY, P.S., THOMAS, G.R. & VANE, J.R. (1989). Endothelin-1 releases prostacyclin and inhibits ex vivo platelet aggregation in the anesthetized rabbit. *J. Cardiovasc. Pharmacol.*, **13**, S138–S141.

THIEMERMANN, C., MAY, G.R., PAGE, C.P. & VANE, J.R. (1990). Endothelin-1 inhibits platelet aggregation in vivo: a study with ^{111}Indium-labelled platelets. *Br. J. Pharmacol.*, **99**, 303–308.

TOUYZ, R.M. & SCHIFFRIN, E.L. (1993). Effects of angiotensin II and endothelin-1 on platelet aggregation and cytosolic pH and free Ca^{2+} concentrations in essential hypertension. *Hypertension*, **22**, 853–862.

(Received June 21, 1994
Revised September 16, 1994
Accepted September 29, 1994)

British Journal of Pharmacology (1995) 114, 531-536 © 1995 Stockton Press All rights reserved 0007-1188/95 $9.00

Characterization of α_1-adrenoceptors mediating vasoconstriction to noradrenaline and nerve stimulation in the isolated perfused mesentery of rat

[1]T.J. Williams & D.E. Clarke

Mechanistic Studies, R2-101 Syntex Research, 3401 Hillview Ave., Palo Alto, CA 94303, U.S.A.

1 The objective of this study was to investigate the α_1-adrenoceptor subtype(s) mediating vasoconstrictor responses to perfused and neuronally-released noradrenaline (NA) in the isolated perfused mesentery preparation of rat.

2 Isolated mesenteric preparations (with gut attached) from male Sprague Dawley rats (250–300g) were perfused via the superior mesenteric artery with oxygenated Krebs solution at approximately 6 ml min^{-1}. The effects of antagonists on vasoconstrictor responses to either perfused (±)-NA or periarterial nerve stimulation (70 V, 2 ms pulse width, 10 s train) were determined.

3 Vasoconstrictor responses to perfused NA were antagonized by prazosin ($pA_2 = 9.3 \pm 0.1$), WB4101 ($pA_2 = 9.6 \pm 0.1$), 5-methyl urapidil (5-MU: $pA_2 = 9.0 \pm 0.1$), (+)-niguldipine (insurmountable) and spiperone ($pA_2 = 7.7 \pm 0.1$). The insurmountable nature of the antagonism by (+)-niguldipine (0.1 nM) was greatly reduced by co-perfusion with prazosin (10 nM). Chloroethylclonidine (CEC: 100 μM for 20 min, followed by 40 min washout) caused an approximate twofold increase in the EC_{50} for (±)-NA and reduced the maximum response by approximately 25%. Pre-treatment of tissues with CEC (100 μM as above) did not significantly alter affinity estimates for prazosin ($pA_2 = 9.2 \pm 0.1$), WB4101 ($pA_2 = 9.3 \pm 0.1$) or 5-MU ($pA_2 = 8.7 \pm 0.2$). Vasoconstrictor responses to periarterial nerve stimulation were antagonized by WB4101 > 5-MU > prazosin >> spiperone. CEC (100 μM as above) reduced nerve-stimulated responses by approximately 50%.

4 The affinity estimates for the various antagonists studied suggest that vasoconstrictor responses to both exogenous and neuronally-released NA are mediated via the same α_1-adrenoceptor subtype. The pharmacological profile most resembles the 'classical' α_{1A}-adrenoceptor, which, in turn, appears to be a rat homologue of the cloned bovine α_{1C}-adrenoceptor.

Keywords: Vasoconstriction; α_{1A}-adrenoceptors; α_{1C}-adrenoceptors; isolated perfused mesentery; prazosin; 5-methylurapidil; WB4101; (+)-niguldipine; (±)-noradrenaline

Introduction

The original sub-division of α_1-adrenoceptors, using operational and radioligand binding techniques, was into two subtypes: α_{1A}-adrenoceptors and α_{1B}-adrenoceptors. WB4101, 5-methylurapidil (5-MU) and (+)-niguldipine exhibit approximately 10, 70 and 100 fold selectivity for the α_{1A}-adrenoceptor subtype versus the α_{1B}-adrenoceptor subtype (Morrow & Creese, 1986; Gross *et al.*, 1988; Boer *et al.*, 1989). Compounds selective for the α_{1B}-adrenoceptor include spiperone (Michel *et al.*, 1989), risperidone (Sleight *et al.*, 1993) and the irreversible antagonist, chloroethylclonidine (CEC; Han *et al.*, 1987).

More recently, molecular biological studies have led to the cloning and expression of α_{1B}-, α_{1C}- and α_{1D}-adrenoceptor subtypes (Coteccia *et al.*, 1988; Schwinn *et al.*, 1990; Lomasney *et al.*, 1991; Perez *et al.*, 1991). However, the relationship between these cloned receptors and the pharmacological classification outlined above has been the subject of debate. To date, the cloned hamster α_{1B}-adrenoceptor appears to match closely the pharmacologically defined α_{1B}-adrenoceptor. The cloned bovine α_{1C}-adrenoceptor appears to correspond to the α_{1A}-adrenoceptor in rat (high affinity for WB4101, (+)-niguldipine and 5-MU). In this regard, mRNA for the α_{1C}-adrenoceptor has recently been reported in several rat tissues (Rokosh *et al.*, 1994). The pharmacological equivalent of the cloned α_{1D}-adrenoceptor remains to be determined. However, the cloned α_{1D}-adrenoceptor may equate with binding sites exhibiting high affinity for WB4101 but low affinity for 5-MU and (+)-niguldipine (see Ford *et al.*, 1994).

The key role of α_1-adrenoceptors in the control of vascular resistance is well-established, and the subdivision of α_1-adrenoceptors described above has led to the pharmacological characterization of NA-mediated responses in a number of vascular preparations from a variety of species (Tian *et al.*, 1990; Oriowo & Ruffolo, 1992). However, a large component of vascular resistance lies at the level of the arterioles and relatively few studies have characterized α_1-adrenoceptor-mediated responses in these specific vessels (but see Kong *et al.*, 1994). The aim of the present study was to characterize pharmacologically the α_1-adrenoceptor subtype(s) mediating NA-induced vasoconstrictor responses in the isolated perfused arterial mesenteric bed of rat. A preliminary account of these studies has been presented previously (Williams & Clarke, 1994).

Methods

Rat perfused isolated mesentery preparation

Fasted male Sprague Dawley rats (300–350g) were anaesthetized (sodium pentobarbitone, 60 mg kg^{-1}, i.p.) and the abdominal cavity opened. Heparin (6 mg in 0.25 ml saline) was administered via the femoral vein. After freeing the superior mesenteric artery from surrounding connective tissue the vessel was cannulated with a PE-90 polyethylene (Intramedic) cannula, which was secured with cotton ties. The

[1] Author for correspondence.

mesenteric artery was immediately perfused with Krebs solution to clear blood from the mesenteric vascular bed. Following surgical removal of the blood vessels and intestine from the rat, the contents of the intestine were removed by flushing with Krebs solution at room-temperature.

Preparations were placed on a gauze pad in a water-jacketed petri dish, and perfused with warm (37°C) oxygenated Krebs solution at a rate of approximately 6.0–6.5 ml min^{-1}. Perfusion pressure was measured with a pressure transducer and recorded on a Graphtec chart recorder. Perfusate was removed from the dish with a vacuum line.

The perfusate contained the following (mM):- Na^+ 143.5, K^+ 6.0, Mg^{2+} 1.2, Ca^{2+} 2.5, Cl^- 128.3, HCO_3^- 25, SO_4^{2-} 1.2, $H_2PO_4^-$ 1.2, glucose 11.0.

Ascorbate 100 μM (to minimize oxidation of NA), cocaine 30 μM. corticosterone 30 μM (to block neuronal and extraneuronal uptake of NA respectively), indomethacin 10 μM (to inhibit prostanoid production), propranolol 1 μM (to block β-adrenoceptors) and idazoxan 300 nM (to block α_2-adrenoceptors) were also included except where indicated in Results. pH (7.4) was maintained by gassing with 95% O_2, 5% CO_2.

Vasoconstrictor responses to perfused NA

Non-cumulative concentration-response curves (CRCs) were obtained to NA by perfusing preparations with Krebs solution containing agonist until a peak vasoconstrictor response (measured as an increase in perfusion pressure) was obtained; at this point the perfusing solution was switched to one free of agonist. The perfusion pressure was allowed to return to baseline before addition of the next ascending concentration of agonist.

Studies with antagonists were performed by adding antagonist to the perfusate following construction of the first CRC. Preparations were perfused with antagonist for 1 h prior to, and then during construction of a second CRC. In experiments where the effect of CEC was studied, CEC was perfused for 20 min, followed by a 40 min washout. Preparations receiving only vehicle for the antagonist were used to control for time-dependent shifts in the CRCs to agonist.

Estimates of antagonist affinity (pA_2) from single concentration studies were made from the fold increase in the EC_{50} values to NA (concentration-ratio, CR) as follows: $pA_2 = -\log\{[\text{antagonist}]/(CR-1)\}$. In experiments in which more than one concentration of antagonist was studied, resultant data were subjected to Schild analysis (Arunlakshana & Schild, 1959): Schild slopes not significantly different from 1 were constrained to 1 for the estimation of pA_2 values.

Vasoconstrictor responses to periarterial nerve stimulation

Vasoconstrictor responses were elicited by electrical stimulation of mesenteric nerves with a bipolar stimulating electrode placed around the mesenteric artery. Frequency-response curves (FRCs) were constructed by applying 10 s trains of 0.3 to 100 Hz (in threefold steps) at 70 V, 2 ms pulse duration. Trains were applied at 6 min intervals and peak vasoconstrictor responses measured. The perfusion fluid was identical to that described above, except that cocaine and corticosterone were omitted. This step was taken to maintain the physiological characteristics of the neuroeffector junctions. Blockade of NA reuptake could conceivably lead to 'spill-over' and perhaps to neuromuscular transmission via 'extra-synaptic' receptors.

In order to minimize the possible involvement of a purinergic component in the response to electrical stimulation purinoceptors were desensitized with 1 μM α,β-methylene ATP, a purinoceptor agonist (Kasakov & Burnstock, 1983). α,β-Methylene ATP was perfused 15 min prior to, and during the construction of each frequency-response curve. α,β-Methylene ATP produced a transient vasoconstrictor response, with perfusion pressure returning to baseline values after approximately 5 min. Under these conditions, initial studies showed that the vasoconstrictor response to nerve stimulation was inhibited completely by the adrenergic neurone blocking drug, guanethidine (1 μM), and by a high concentration of prazosin (1 μM) (data not shown).

The effects of antagonists on the frequency-response relationship were determined by perfusing the preparation with antagonist for 1 h prior to construction of a second frequency-response curve. The effects of CEC on the response to nerve stimulation were determined by perfusing the antagonist for 20 min or 40 min following the first FRC, followed by a 40 min washout and construction of a second FRC.

Chemicals

Drugs were obtained from the following sources: cocaine, idazoxan, 5-MU, (+)-niguldipine, spiperone, WB4101 (2-(2,6-dimethoxyphenoxyethyl)-aminoethyl-1,4-benzodioxane), and chloroethylclonidine (Research Biochemicals Inc., Natick, MA, U.S.A.), (±)-NA, corticosterone, prazosin and α,β-methylene ATP (Sigma Chemical Co., St. Louis, MO, U.S.A.). Solutions were prepared in deionised water or dimethylsulphoxide (5-MU, (+)-niguldipine, spiperone, prazosin and corticosterone).

Results

Vasoconstrictor responses to perfused NA

Perfused (±)-NA caused a concentration-dependent increase in perfusion pressure, with a maximum response typically in the range 80–120 mmHg, and an EC_{50} of approximately 5–10 μM NA. In time control experiments the second CRC to NA typically showed a small (approximately twofold) leftward shift, with little change in maximum response. The α_1-adrenoceptor antagonists, prazosin (Figure 1), WB4101, 5-MU and spiperone produced concentration-dependent rightward shifts in the concentration-response curve to NA. pA_2 estimates obtained by Schild analysis are shown in Table 1 (Schild slopes did not differ significantly from 1). The selective α_{1A}-adrenoceptor antagonist, (+)-niguldipine (Boer *et al.*, 1989), at subnanomolar concentrations, potently and insurmountably antagonized NA responses (Figure 2). At a concentration of 0.3 nM, (+)-niguldipine reduced the maximum response to NA to approximately 10% of control values. When perfused together with prazosin (10 nM), the ability of niguldipine (0.1 nM) to suppress the maximum response to NA was greatly diminished (Figure 3). The L-type calcium channel antagonist, nitrendipine (1 μM), was without effect on the CRC to NA (data not shown).

CEC at 1 μM was without effect on the CRC to NA: higher concentrations of CEC, (10 μM and 100 μM), produced a small rightward shift (approximately twofold after correction for the temporal shift) accompanied by a one-third reduction at 100 μM CEC in the maximum response to NA (Figure 4). Exposure of tissues to 100 μM CEC for 20 min (plus 40 min washout) prior to the first CRC did not significantly affect affinity estimates for prazosin (30 nM), WB4101 (10 nM) or 5-MU (10 nM) (Table 1).

Vasoconstrictor responses to periarterial nerve stimulation

Figure 5 shows the effect of increasing concentrations of prazosin on the frequency-response curve to peri-arterial nerve stimulation. In order to quantify and compare the inhibitory effects of antagonists, the area under the second frequency-response curve (in the presence of antagonist) was

expressed as a percentage of the area under the first frequency-response curve in the absence of antagonist. These data are represented in Figure 6, which shows that WB4101, 5-MU, prazosin and spiperone (respective order of potency) concentration-dependently inhibited the neuronal stimulation-induced vasoconstrictor response. As with prazosin, all drugs tested caused a reduction in the maximal response to stimulation, suggesting that increased stimulation frequencies liberate concentrations of endogenous agonist below those required to surmount the antagonism.

Figure 7 shows the effect of exposure to increasing concentrations of CEC (1 μM–100 μM) on the vasoconstrictor response to nerve stimulation. Employing a 20 min exposure time to CEC, 1 μM of the alkylating agent did not affect the frequency-response curve; higher concentrations of 10 μM and 100 μM CEC reduced the response to nerve stimulation to 79 ± 7% and 46 ± 5% of the first curve respectively (mean ± s.e.mean, $n = 7-12$ separate experiments). Although increasing the time of exposure of CEC to 40 min did not further reduce responses to nerve stimulation at a CEC concentration of 10 μM (64 ± 8% of area under first curve), further inhibition was observed with 100 μM CEC (19 ± 1% of area under first curve).

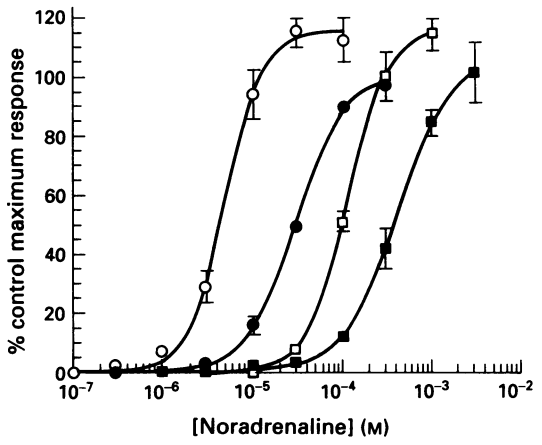


Figure 1 Antagonism by prazosin of vasoconstrictor responses to perfused noradrenaline (NA) in the isolated perfused mesentery preparation of rat. Prazosin (or vehicle) was perfused for 1 h prior to construction of the second concentration-response curve: (○) vehicle (●) prazosin 3 nM; (□) prazosin 10 nM; (■) prazosin 30 nM. Data shown are second concentration-response curves and give mean ± s.e.mean from 4 separate experiments.

Table 1 Antagonist affinity estimates versus (±)-noradrenaline-mediated vasoconstrictor responses in the isolated perfused mesentery of rat

Antagonist	pA_2	*Schild slope* (95% CL)	pA_2 (CEC-treated)
Prazosin	9.3 ± 0.1	0.96 (0.67–1.25)	9.2 ± 0.1
WB4101	9.6 ± 0.1	1.29 (0.75–1.83)	9.3 ± 0.1
5 MU	9.0 ± 0.1	1.24 (0.66–1.76)	8.7 ± 0.2
Niguldipine	US (0.03–0.3 nM)		ND
Spiperone	7.7 ± 0.1	1.13 (0.83–1.25)	ND

Antagonist affinities in preparations treated previously with CEC (100 μM, 20 min) are calculated from shifts using single antagonist concentrations (see text for concentrations used). US = insurmountable. ND = not determined. CEC, chloroethylclonidine; 5-MU, 5-methyl urapidil. Data are mean ± s.e.mean from 3–6 separate experiments.

Discussion

In addition to perfused NA, the present study has used endogenous, neuronally-released NA in an attempt to further characterize the α_1-adrenoceptor subtype(s) mediating vasoconstrictor responses in the isolated perfused mesenteric arterial bed of rat. Characterization of responses to nerve stimulation is of importance for two reasons. First, differential location of α_1-adrenoceptor subtypes, synaptic versus extrasynaptic, might lead to responses having distinctly different pharmacological profiles. Secondly, characterization of nerve-mediated responses may provide some insight into the role of α_1-adrenoceptor subtypes in the physiological maintenance and control of blood pressure. This is especially so as peripheral resistance, particularly in the mesenteric circulation, is a major determinant of systemic blood pressure.

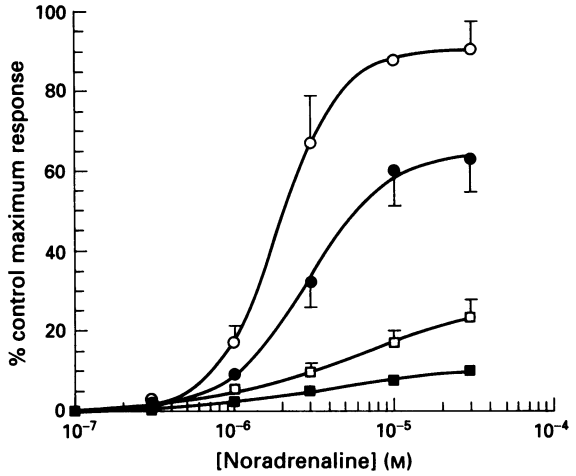


Figure 2 Antagonism by (+)-niguldipine of vasoconstrictor responses to perfused noradrenaline in the isolated perfused mesentery preparation of rat. (+)-Niguldipine (or vehicle) was perfused for 1 h prior to construction of the second concentration response curve: (○) vehicle; (●) niguldipine 0.03 nM; (□) niguldipine 0.1 nM; (■) niguldipine 0.3 nM. Data shown are second concentration-response curves and give mean ± s.e.mean from 4 separate experiments.

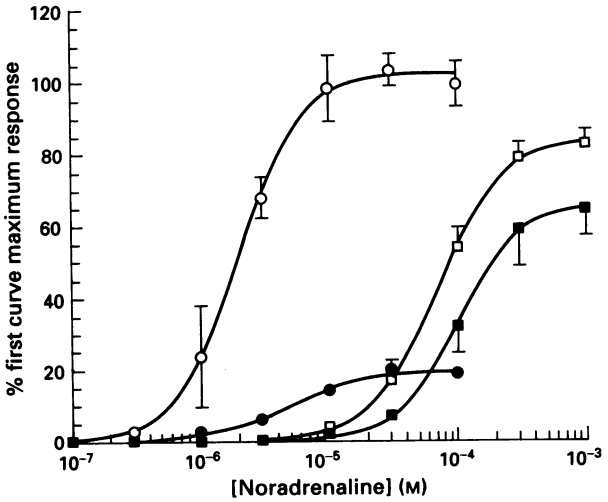


Figure 3 Effect of (+)-niguldipine (0.1 nM) or vehicle, perfused for 1 h in the presence or absence of prazosin (10 nM), on vasoconstrictor responses to perfused noradrenaline in the isolated perfused mesentery preparation of rat: (○) vehicle; (●) niguldipine 0.1 nM; (□) prazosin 10 nM; (■) prazosin 10 nM + niguldipine 0.1 nM. Data shown are second concentration-response curves and give mean ± s.e.mean from 4 separate experiments.

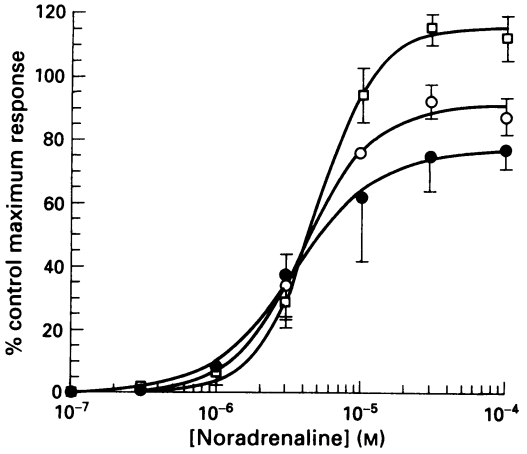


Figure 4 Effect of exposure to chloroethylclonidine (CEC) on vasoconstrictor responses to perfused noradrenaline (NA) in the isolated perfused mesentery preparation of rat. CEC (or vehicle) was perfused for 20 min (with 40 min washout) following construction of the first concentration-effect curve to NA: (□) vehicle; (○) CEC 10 μM (●) CEC 100 μM. Data shown are second concentration-response curves and give mean ± s.e.mean from 3-4 separate experiments.

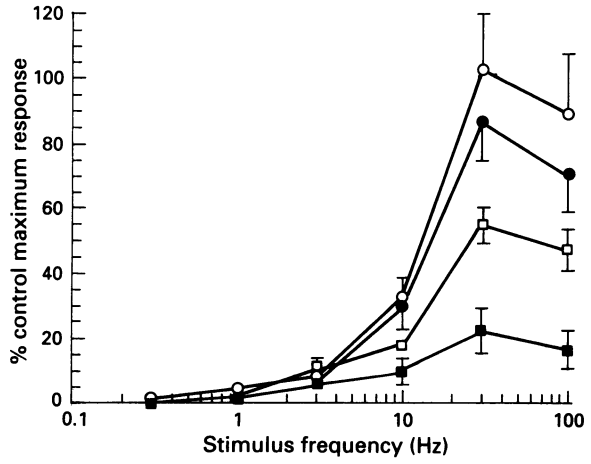


Figure 5 Effect of prazosin on vasoconstrictor responses to periarterial nerve stimulation in the isolated perfused mesentery preparation of rat (see text for stimulation parameters): (○) vehicle; (●) prazosin 0.3 nM; (□) prazosin 1.0 nM; (■) prazosin 3.0 nM. Data shown are second frequency-response curves and give mean ± s.e.mean from 4 separate experiments.

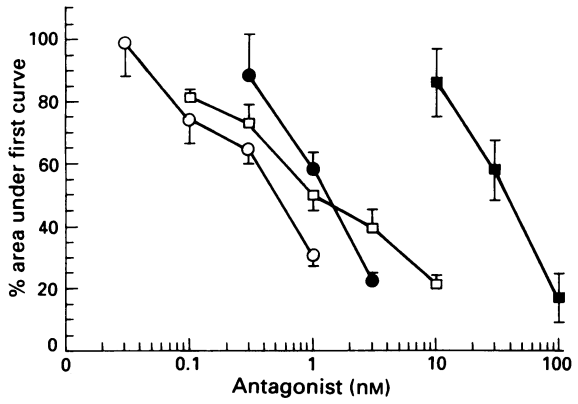


Figure 6 Inhibition by WB4101 5-methyl urapidil (5-MU), prazosin and spiperone of vasoconstrictor responses to periarterial nerve stimulation in the isolated perfused mesentery preparation of rat (see text for stimulation parameters): (○) WB4101; (●) prazosin; (□) 5-MU; (■) spiperone. Data shown are mean ± s.e.mean from 3–5 separate determinations.

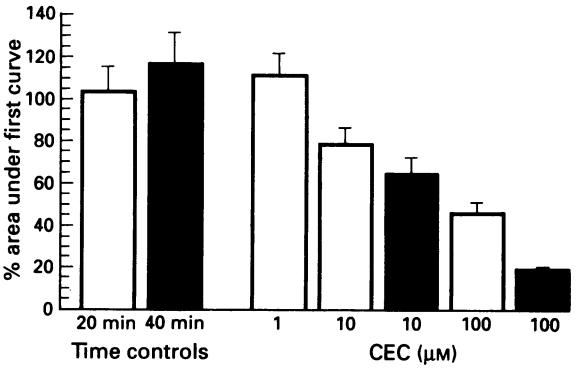


Figure 7 Effect of exposure to chloroethylclonidine (CEC) on vasoconstrictor responses to periarterial nerve stimulation in the isolated perfused mesentery preparation of rat (see text for stimulation parameters). CEC was perfused for 20 min (open columns) or 40 min (solid columns) following construction of the first frequency-response curve. A 40 min washout period was allowed before construction of a second frequency-response curve. Data shown are mean ± s.e.mean, from 4–12 separate experiments.

In the present study the vasoconstrictor response to perfused NA was antagonized with high affinity ($pA_2 = 9.3$) by the non-subtype-selective α_1-adrenoceptor antagonist, prazosin and also by the α_{1A}-adrenoceptor-selective antagonists WB4101, 5-MU and (+)-niguldipine (Morrow & Creese, 1986; Gross *et al.*, 1988; Hanft & Gross, 1989; Boer *et al.*, 1989). The affinity estimates obtained with WB4101 and 5-MU (9.6 and 8.9 respectively), plus the apparently high affinity for (+)-niguldipine, suggest strongly that the vasoconstrictor response to perfused NA is mediated via α_{1A}-adrenoceptors (Han *et al.*, 1990). This contention is supported by the observation that the pA_2 value for spiperone (7.7), which is approximately 10 fold selective for the α_{1B}-adrenoceptor subtype (Michel *et al.*, 1989), was closest to its affinity at α_{1A}-adrenoceptors as determined in ligand binding studies (pK_i s at α_{1A} and α_{1B}-adrenoceptors of 8.14 and 9.25 respectively; Michel *et al.*, 1989).

Although (+)-niguldipine also has high affinity for L-type calcium channels (Boer *et al.*, 1989), the protective effect of co-perfusion with prazosin (10 nM), together with the lack of effect of nitrendipine (1 μM) towards NA, serve to suggest that the insurmountable antagonism by (+)-niguldipine is related to an action at α_{1A}-adrenoceptors and not to blockade of L-type channels. Insurmountable antagonism towards responses to NA may result from lack of equilibrium between a high affinity antagonist and NA, as described by Clarke *et al.* (1991) in an isolated perfused kidney preparation of rat.

A number of studies have shown that CEC, despite having similar affinity at both α_{1A}- and α_{1B}-adrenoceptors, appears to alkylate preferentially the latter subtype (Han *et al.*, 1987; Minneman *et al.*, 1988). The modest effect of even large concentrations of CEC against perfused NA in the present study and the fact that CEC (100 μM) did not alter the apparent affinity estimate for prazosin, WB4101 or 5-MU, rules out the involvement of α_{1B}-adrenoceptors.

The interpretation of results from experiments in which nerve stimulation was used to elicit vasoconstrictor responses is complicated by a number of factors, including possible drug effects on NA release (see below) and the inability to calculate absolute antagonist affinities (as synaptic concentrations of NA are not known, and parallel shifts of frequency-

response curves were not obtained). However, the pharmacological characteristics of the stimulation-induced responses in the present study are similar to the results obtained with exogenously-perfused NA, and suggest that the two types of responses are mediated by similar receptors. Thus, stimulation-induced responses were antagonized with high affinity by prazosin and by the α_{1A}-selective antagonists, WB4101 and 5-MU. Similarly, spiperone was effective only at concentrations consistent with its binding affinity for α_{1A}-adrenoceptors.

At first sight, CEC appears to antagonize nerve-induced responses to a greater extent that those to perfused NA. However, it must be noted that for the competitive antagonists studied, a 50% reduction in response to electrical stimulation was obtained with concentrations of antagonist which approximated those producing a twofold shift in the CRC to exogenously-perfused NA. Taking this into account, the antagonism by CEC of neuronally-mediated vasoconstrictor responses is similar to its ability to antagonize responses to exogenously-perfused NA. Consideration of Figure 7 also shows a time-dependency for inhibition (alkylation) by CEC. This slow rate of alkylation, together with the lack of complete inhibition, is consistent with the reported action of CEC on the cloned α_{1C}- and α_{1D}-adrenoceptors, rather than on α_{1B}-adrenoceptors (Schwinn *et al.*, 1990; Perez *et al.*, 1991). This deduction does not imply a different adrenoceptor for nerve-induced vasoconstriction versus that elicited by exogenously-perfused noradrenaline, as we argue below that the cloned α_{1C}-adrenoceptor may equate with the functionally-defined 'classical' α_{1A}-adrenoceptor.

As a note of caution it must be pointed out that a recent publication by Bültmann & Starke (1993) concluded that CEC, acting as an 'irreversible' pre-junctional α_2-adrenoceptor agonist, significantly reduced field-stimulated [^{3}H]-NA release in an isolated vas deferens preparation from rat. The authors proposed that this action 'limits the suitability of CEC for the characterization of post-junctional α_1-adrenoceptors mediating responses to sympathetic nerve stimulation'. Although in the present study the α_2-adrenoceptor antagonist, idazoxan (300 nM) was included in the perfusion fluid, such a pre-junctional action of CEC on electrically-stimulated NA release cannot be excluded entirely.

In summary, the present study suggests that α_1-adrenoceptors mediating vasoconstrictor responses to both perfused and neuronally-released NA exhibit a pharmacological profile which is similar to that of the 'classical' α_{1A}-adrenoceptor. This study confirms and extends observations published recently by Kong *et al.* (1994) who, using the same preparation from rat, also concluded that NA-induced vasoconstriction appeared to be mediated largely via α_{1A}-adrenoceptors. This conclusion was based on a high affinity estimate for 5-MU (pA_2 value of 9.24 versus bolus doses of perfused NA) and a relatively small effect of CEC (10 μM for 1 h).

The question as to which of the currently cloned α_1-adrenoceptors most closely resembles the receptor characterized in the present study is the subject of debate, and has been addressed in a recent article from our laboratory (Ford *et al.*, 1994). Briefly, the cloned bovine α_{1C}-adrenoceptor appears to provide the closest match to the 'classical' α_{1A}-adrenoceptor, based on such criteria as high affinity for WB4101, 5-MU and (+)-niguldipine. Although expression of α_{1C}-adrenoceptor RNA in rat tissues was not detected by Schwinn *et al.* (1991), the same study also failed to detect the mRNA for the α_{1C}-adrenoceptor in bovine cortex, the tissue from which the α_{1C}-adrenoceptor was originally cloned. In a more recent report, Rokosh *et al.* (1994) have cloned a fragment of the α_{1C}-adrenoceptor from cardiac myocytes of rat, and have used an RNase protection assay to demonstrate abundant levels of mRNA for the α_{1C}-adrenoceptor in a number of rat tissues. These tissues include submaxillary gland, a tissue characterized previously in radioligand binding studies as containing only the 'classical' α_{1A}-adrenoceptor (Michel *et al.*, 1989). In addition, Forray and colleagues (1994) have reported the cloning and expression of a rat homologue of the α_{1C}-adrenoceptor which, while sharing many pharmacological characteristics of the bovine α_{1C}-adrenoceptor, is relatively insensitive to alkylation by CEC (only 19% loss of binding sites following 100 μM CEC, compared with 45% inactivation of the bovine α_{1C}-adrenoceptor). Cloning and expression of an α_{1C}-adrenoceptor from rat has also been reported by Perez *et al.* (1994): the authors concluded that the pharmacology of this receptor most resembled that of the α_{1A}-adrenoceptor.

The observations considered above suggest strongly that the α_{1A}-adrenoceptor characterized in the present study represents the rat homologue of the cloned bovine α_{1C}-adrenoceptor. Such an alignment is fully consistent with the pharmacological profile reported here. Whether the receptor should be called an α_{1A}- or α_{1C}-adrenoceptor awaits the decision of the adrenoceptor Nomenclature Committee.

References

ARUNLAKSHANA, O. & SCHILD, H.O. (1959). Some quantitative uses of drug antagonists. *Br. J. Pharmacol. Chemother.*, **14**, 48–54.

BOER, R., GRASSEGGER, A., SCHUDT, C. & GLOSSMANN, H. (1989). (+)- Niguldipine binds with very high affinity to Ca2+ channels and to a subtype of α_1-adrenoceptors. *Eur. J. Pharmacol.*, **172**, 131–145.

BÜLTMANN, R. & STARKE, K. (1993). Chloroethylclonidine: an irreversible agonist at prejunctional α_2-adrenoceptors in rat vas deferens. *Br. J. Pharmacol.*, **108**, 336–341.

CLARKE, D.E., WHITING, R.L., PFISTER, J. & BLUE, D.R. (1991). Antagonism of a1-adrenoceptor subtypes by niguldipine and 5-methyl-urapidil in rat kidney. *Br. J. Pharmacol.*, **102**, 196P.

COTECCHIA, S., SCHWINN, D.A., RANDALL, R.R., LEFKOWITZ, R.J., CARON, M.G. & KOBILKA, B.K. (1988). Molecular cloning and expression of the cDNA for the hamster α_1-adrenergic receptor. *Proc. Natl. Acad. Sci. U.S.A.*, **85**, 7159–7163.

FORD, A.P.D.W., WILLIAMS, T.J., BLUE, D.R. & CLARKE, D.E. (1994). α_1-Adrenoceptor classification: sharpening Occam's razor. *Trends Pharmacol. Sci.*, **15**,(6), 167–170.

FORRAY, C., BARD, J.A., LAZ, T.M., SMITH, K.E., VAVSSE, P.J.-J., WEINSHANK, R.L., GLUCHOWSKI, C. & BRANCHEK, T.A. (1994). Comparison of the pharmacological properties of the cloned bovine, human and rat α_{1C}-adrenergic receptors. *FASEB J.*, **8**, A353.

GROSS, G., HANFT, G. & RUGEVICS, C. (1988). 5-Methyl-urapidil discriminates between subtypes of the α_1-adrenoceptor. *Eur. J. Pharmacol.*, **151**, 333–335.

HAN, C., ABEL, P.W. & MINNEMAN, K.P. (1987). Heterogeneity of α_1-adrenergic receptors revealed by chloroethylclonidine. *Mol. Pharmacol.*, **32**, 505–510.

HAN, C., LI, J. & MINNEMAN, K.P. (1990). Subtypes of α_1-adrenoceptors in rat blood vessels. *Eur. J. Pharmacol.*, **190**, 97–104.

HANFT, G. & GROSS, G. (1989). Subclassification of α_1-adrenoceptor recognition sites by urapidil derivatives and other selective antagonists. *Br. J. Pharmacol.*, **97**, 691–700.

KASAKOV, L. & BURNSTOCK, G. (1983). The use of the slowly degradable analog, alpha, beta-methylene ATP to produce desensitisation of the P_2-purinoceptor: effect on non-adrenergic, non-cholinergic responses of the guinea-pig urinary bladder. *Eur. J. Pharmacol.*, **86**, 291–294.

KONG, J.-Q., TAYLOR, D.A. & FLEMING, W.W. (1994). Functional distribution of alpha-1 adrenoceptor subtypes in the mesenteric vasculature of the rat. *J. Pharmacol. Exp. Ther.*, **268**, 1153–1159.

LOMASNEY, J.W., COTECCHIA, S., LORENZ, W., LEUNG, W.-Y., SCHWINN, D.A., YANG-FENG, T.L., BROWNSTEIN, M., LEFKOWITZ, R.J. & CARON, M.G. (1991). Molecular cloning and expression of the cDNA for the α_{1A}-adrenergic receptor. *J. Biol. Chem.*, **266**, 6365–6369.

MICHEL, A.D., LOURY, D.N. & WHITING, R.L. (1989). Identification of a single α_1-adrenoceptor corresponding to the α_{1A}-subtype in rat submaxillary gland. *Br. J. Pharmacol.*, **98**, 883–889.

MINNEMAN, K.P., HAN, C. & ABEL, P.W. (1988). Comparison of α_1-adrenoceptor subtypes distinguished by chloroethylclonidine and WB4101. *Mol. Pharmacol.*, **33**, 509–514.

MORROW, A.L. & CREESE, I. (1986). Characterization of α_1-adrenergic receptor subtypes in rat brain: a reevaluation of [^{3}H]WB 4101 and [^{3}H]prazosin binding. *Mol. Pharmacol.*, **29**, 321–330.

ORIOWO, M.A. & RUFFOLO, R.R. (1992). Heterogeneity of postjunctional alpha 1-adrenoceptors in mammalian aortae: subclassification based on chloroethylclonidine, WB4101 and nifedipine. *J. Vasc. Res.*, **29**, 33–40.

PEREZ, D.M., CHEN, J.-L. & GRAHAM, R.M. (1994). Is the α_{1C}-adrenergic receptor the α_{1A}-subtype? *FASEB J.*, **8**, A353.

PEREZ, D.M., PIASCIK, M.T. & GRAHAM, R.M. (1991). Solution-phase library screening for the identification of rare clones: isolation of an α_{1D}-adrenergic receptor cDNA. *Mol. Pharmacol.*, **40**, 876–883.

ROKOSH, D.G., BAILEY, B.A., STEWART, A.F.R., KARNS, L.R., LONG, C.S. & SIMPSON, P.C. (1994). Distribution of α_{1C}-adrenergic receptor mRNA in adult rat tissues by RNase protection assay and comparison with $_{1B}$ and $_{1D}$. *Biochem. Biophys. Res. Commun.*, **200**, 1177–1184.

SCHWINN, D.A., LOMASNEY, J.W., LORENZ, W., SZKLUT, P.J., FREMEAU, R.T., YANG-FENG, T.L., CARON, M.G., LEFKOWITZ, R.J. & COTECCHIA, S. (1990). Molecular cloning and expression of the cDNA for a novel α_1-adrenergic receptor subtype. *J. Biol. Chem.*, **265**, 8183–8189.

SCHWINN, D.A., PAGE, S.O., MIDDLETON, J.P., LORENZ, W., LIGETT, S.B., YAMAMOTO, K., LAPETINA, E.G., CARON, M.G., LEFKOWITZ, R.J. & COTECCHIA, S. (1991). The α_{1C}-adrenergic receptor: Characterization of signal transduction pathways and mammalian tissue heterogeneity. *Mol. Pharmacol.*, **40**, 619–626.

SLEIGHT, A.J., KOEK, W. & BIGG, D.C.H. (1993). Binding of antipsychotic drugs at α_{1A}- and α_{1B}-adrenoceptors: risperidone is selective for the α_{1B}-adrenoceptors. *Eur. J. Pharmacol.*, **238**, 407–410.

TIAN, W.N., GUPTA, S. & DETH, R.C. (1990). Species differences in chloroethylclonidine antagonism at vascular alpha-1 adrenergic receptors. *J. Pharmacol. Exp. Ther.*, **253**, 877–883.

WILLIAMS, T.J. & CLARKE, D.E. (1994). Characterisation of the α_1-adrenoceptor mediating vasoconstrictor responses to noradrenaline and nerve stimulation in the rat isolated perfused mesentery. *Br. J. Pharmacol.*, **112**, 207P.

(Received May 20, 1994
Revised August 30, 1994
Accepted September 2, 1994).

British Journal of Pharmacology (1995) 114, 537-543 © 1995 Stockton Press All rights reserved 0007-1188/95 $9.00

Further characterization of [^{3}H]-CGS 21680 binding sites in the rat striatum and cortex

Ian P. Kirk & [1]Peter J. Richardson

University of Cambridge, Department of Pharmacology, Tennis Court Road, Cambridge CB2 1QJ

1 The putative high affinity binding site for the adenosine A_{2A} receptor agonist 2-*p*-(2-carboxyethyl)phenethyl-amino-5'-N- ethylcarboxamidoadenosine (CGS 21680) in the rat cerebral cortex was characterized by use of a number of selective A_1 and A_2 adenosine receptor ligands, and compared to the characteristics of the more abundant striatal A_{2A} receptor.

2 The binding of [^{3}H]-CGS 21680 to cortical membranes was performed at pH 5.5, in order to increase the amount of specific binding.

3 Reduction of the pH from 7.4 to 5.5 increased the apparent affinity of the striatal binding side for both agonists and antagonists. The relative order of potencies of both groups of ligands were the same at both pH values, and were consistent with binding to the A_{2A} receptor. There was no observable change in the B_{max}, the values being 415 and 446 fmol mg^{-1} protein at pH 5.5 and 7.4 respectively.

4 The cortical binding site yielded a B_{max} value of 117 fmol mg^{-1} protein. The relative order of potencies of the adenosine receptor ligands observed at this binding site were not the same as those observed in the striatum, exhibiting a profile with both A_1 and A_2 characteristics.

5 Further characterization of this cortical binding site in the presence of the A_1 selective antagonist 1,3-dipropyl-8-cyclopentylxanthine (DPCPX) revealed a more typical A_{2A} profile. This indicated that under the conditions used there were two components of [^{3}H]-CGS 21680 binding, approximately 20% of the A_1 receptor and 80% to the A_{2A} receptor.

6 It is concluded that in the cerebral cortex there is a CGS 21680 binding site showing the characteristic properties of the striatal A_{2A} receptor, and no evidence was obtained for the existence of a novel A_{2A}-like binding site.

Keywords: CGS 21680; A_{2A} receptor; rat striatum; rat cortex

Introduction

Adenosine has a number of effects within the CNS, where it is known to modulate neuronal function via a variety of mechanisms (Fredholm & Dunwiddie, 1988). Classification of adenosine receptors into A_1 and A_2 receptors was initially based on their effects on adenylate cyclase activity (Van Calker *et al.*, 1979); however, such criteria have since proven unsatisfactory and consequently receptor classification is now based on the relative potencies of a number of selective ligands. These criteria, together with advances in molecular cloning, have led to the currently accepted classification of adenosine receptors into A_1, A_{2A}, A_{2B} and A_3 subtypes (Abbrachio *et al.*, 1993).

At adenosine A_1 receptors the order of potency for the following agonists is **R**-phenylisopropyladenosine (**R**-PIA) > 5'-N-ethylcarboxamidoadenosine (NECA) > CGS 21680. There are also a number of selective antagonists including DPCPX and 8-cyclopentyl theophylline (CPT) (Bruns *et al.*, 1986). However, A_2 receptor selective ligands have only recently become available, CGS 21680 being the most widely used A_{2A} receptor radioligand. It is 185 fold selective for the A_2 over the A_1 receptor (Jarvis *et al.*, 1989; Jarvis & Williams, 1989) and does not bind to either A_{2B} or A_3 receptors (Yakel *et al.*, 1993; Zhou *et al.*, 1992). The relative order of potency for agonists at A_{2A} receptors is NECA > CGS 21680 > **R**-PIA > S-PIA, although selective antagonists are restricted to 4-amino-1-phenyl-[1,2,4] triazolo [4,3-a] quinoxaline (CP66,713) and 9-chloro-2-(2-furanyl)-5,6-dihydro-1,2,4-triazolo[1,5-c] quinazoline-5-imine (CGS 15943), which are only 16 and 5 fold (respectively) selective for the A_{2A} receptor over the A_1 (Sarges *et al.*, 1990; Williams *et al.*, 1987). More recently Shimada *et al.* (1992) reported that (E)-8-(3,4-dimethoxystyryl)-1,3-dipropyl-7-methylxanthine (KF17837) is a 50 fold A_{2A} selective antagonist, although it is not yet commercially available.

By use of [^{3}H]-CGS 21680, adenosine A_{2A} receptors have been shown to be restricted to the caudate putamen, nucleus accumbens, olfactory tubercle and parts of the globus pallidus (Jarvis & Williams, 1989). Furthermore, *in situ* hybridization has demonstrated an almost exclusive localization of the mRNA coding for this receptor to γ-aminobutyric acid (GABA)/Met-enkephalin containing neurones within the striatum (Schiffman *et al.*, 1991a,b). We and others have recently demonstrated that CGS 21680 modulates GABA release from striatal nerve terminals and slices (Mayfield *et al.*, 1993; Kirk & Richardson 1994), consistent with its localization within these neurones. However, the A_{2A} receptor has also been reported to be present on cholinergic interneurones where it stimulates acetylcholine release (Brown *et al.*, 1990; Kirkpatrick & Richardson, 1993; Kirk & Richardson, 1994). This is despite the absence of detectable A_{2A} receptor mRNA in striatal cholinergic neurones. It is therefore conceivable that sub-types of the adenosine A_{2A} receptor may exist within the striatum. Indeed, in post mortem human brain it has been demonstrated that there are two [^{3}H]-CGS 21680 binding sites, the least abundant of which was also present in the cortex (James *et al.*, 1992).

Furthermore, a number of functional studies have detected A_{2A} receptor-like effects in non-striatal brain areas. For example, O'Regan *et al.* (1992) reported that CGS 21680 was able to inhibit ischaemia-evoked GABA release from the rat cortex, and Sebastiao *et al.* (1994) have shown that the same agonist increased hippocampal neuronal excitability. In view of these reports and our reported A_{2A} mediated inhibition of GABA release from the rat striatum, it was of interest to see whether two CGS 21680 binding sites could be identified. We therefore set out to determine whether the previously des-

[1] Author for correspondence.

cribed, but uncharacterized CGS 21680 binding site in the rat cerebral cortex (Jarvis *et al.*, 1989; Wan *et al.*, 1990) was different from the well characterized striatal site.

Methods

Membrane preparation

Briefly, the cortex and striatum were dissected from whole rat brains into 5 ml ice cold 50 mM Tris-HCl buffer pH 7.4, and disrupted for 30 s with a polytron PT10-35 homogenizer at setting 8. The resultant suspension was centrifuged in a Sorvall RC5B centrifuge at 48,000 *g* for 20 min at 4°C. The pellet was frozen at − 20°C until used. On thawing the pellet was resuspended in 10% (w/v) Tris-HCl buffer containing adenosine deaminase at a concentration of 0.1 u ml^{-1} and incubated for 60 min at 4°C. The suspension was recentrifuged at 48,000 *g* for 20 min at 4°C and the pellet resuspended in 50 mM Tris-HCl buffer containing 50 mM $MgCl_2$ and 5 u ml^{-1} adenosine deaminase for use in binding assays.

Binding assays

Displacement studies were carried in 0.5 ml of buffer of the following composition: 50 mM Tris-HCl (pH 7.4), 10 mM $MgCl_2$ and 1 u ml^{-1} adenosine deaminase and 0.2 μCi of [^{3}H]-CGS 21680 (final concentration, 7 nM) containing 4.4 ± 0.4 and 1.0 ± 0.05 mg of protein for cortical and striatal membranes respectively. All incubations were performed in triplicate. Reactions were terminated after incubation for 90 min at 25°C by vacuum filtration through Whatman GF/B glass fibre filters, which were washed three times with 4 ml of ice cold Tris-HCl buffer. The filters were placed in scintillation vials with 8 ml of Emulsifier-Safe scintillation fluid (Packard) and left overnight before liquid scintillation counting. Non-specific binding was determined by the addition of N-ethylcarboxamido-adenosine (NECA) at a final concentration of 0.1 mM. When drugs were used dissolved in solvents such as dimethylsulphoxide (DMSO) or ethanol appropriate controls were run in parallel.

Binding studies performed at pH values other than 7.4 were as described above with the exception of the 90 min with radioligand. This step was carried out in 50 mM Tris-MES at the desired pH i.e. 5.5, all other steps were performed in Tris-HCl (pH 7.4). Protein concentrations were determined with the Folin-Ciocalteau reagent as described by Lowry *et al.* (1951), with bovine serum albumin used as standard.

Data analysis

Binding studies were analysed using the non-linear regression curve fitting programme Graph PAD in Plot, version 3.0 (Motulsky, 1989). The equations used were:

$$Y = A + \frac{B\text{-}A}{1 + (10^x/10^c)}$$

where Y is specific binding of radioligand, x is log concentration of the displacing ligand, A is the Y value at the bottom of the curve and C is the X value at the middle of the curve (the log IC_{50}). This equation describes the competition of a ligand for binding to one type of receptor. Alternatively the following was used:

$$Y = A + \frac{B\text{-}A}{100} \cdot \left[\frac{C}{1 + 10^{D/X}} + \frac{100\text{-}C}{1 + 10^{E/X}} \right]$$

A and B are the Y values at the bottom and top of the curve, C is the percentage of high affinity receptors and D and E are the log (IC_{50}) values for the high and low affinity receptors receptively. This equation describes a competition binding curve when the competing ligand has different affinities for two types of receptor for which the radioligand has identical affinities.

Receptor number (B_{max}) and dissociation constants (K_D) were determined according to De Blasi *et al.* (1989).

Statistical analysis

All results are given as mean ± s.e.mean with n = representing the number of experiments performed. Statistical significance was evaluated with a Student's two-tailed t test. A probability of $P<0.05$ was accepted as denoting a significant difference. Goodness of fit was assessed by the sum of the square of the distance of each point from the curve, i.e. the data points were not weighted. A partial F-test ($P<0.05$) was used to determine whether the binding was best described by the one-site or two-site binding model.

Drugs and chemicals

[^{3}H]-CGS 21680 (2-*p*-(-2-carboxyethyl)phenethylamino 5'-N-ethylcarboxamido-adenosine), (48.6 Ci $mmol^{-1}$) and [^{3}H]-DPCPX (8 cyclopentyl-1,3-dipropylxanthine), (88.2 Ci $mmol^{-1}$) were from DuPont-NEN. CGS 21680, DPCPX and CPT (8-cyclopentyl-theophylline) were from Research Biochemicals Incorporated, CGS15943 (9-chloro-2-(2-furanyl)-5,6-dihydro-1,2,4-triazolo[1,5-c]quinazoline-5-imine) was a gift from Ciba-Geigy, Summit, New Jersey, U.S.A. and CP66,713 (4-amino-1-phenyl[1,2,4]-triazolo[4,3a]quinoxaline) was a gift from Pfizer, Groton, CT, U.S.A. NECA (5'N-ethylcarboxamino adenosine), **R** and **S**-PIA (**R**/**S**-phenylisopropyladenosine) and adenosine deaminase (Type VIII) were from Sigma Chemicals. All other chemicals were of standard laboratory grade and were obtained from BDH Chemicals Ltd.

Results

In order to compare the striatal and cortical CGS 21680 binding sites, the ability of a number of selective A_1 and A_2 adenosine receptor ligands to displace [^{3}H]-CGS 21680 binding from membranes derived from both the rat cortex and striatum were examined.

[^{3}H]-CGS 21680 binding to striatal membranes at pH 7.4

An apparent K_D value of 10.5 ± 2.1 nM with a B_{max} value of 415 ± 37 fmol mg^{-1} protein was determined from competitive binding experiments using 7 nM [^{3}H]-CGS 21680 and varying concentrations of unlabelled CGS 21680 (Figure 1a). In order to characterize the striatal binding site further the ability of a number of ligands to displace [^{3}H]-CGS 21680 binding were investigated. Figure 1a also shows the displacement of [^{3}H]-CGS 21680 by the agonists NECA, **R**-PIA and **S**-PIA, while Figure 1b shows the displacement of binding by the antagonists CP66,713, CGS15943, CPT and DPCPX. Both agonists and antagonists exhibited a typical adenosine A_{2A} pharmacological profile i.e. NECA > CGS 21680 > **R**-PIA > S-PIA and CGS15943 > CP66,713 > CPT = DPCPX. The derived K_i values for both agonists and antagonists are shown in Table 1. All displacement curves were best described by a one site binding equation.

Since the binding of [^{3}H]-CGS 21680 to the cortical membranes was low, attempts were made to increase the amount of specific binding by reducing the pH to 5.5. It has recently been reported that optimum binding of CGS 21680 to the A_{2A} receptor occurs at this pH (Askalan & Richardson, 1994). Indeed lowering the pH increased the specific binding from 2127 ± 305 at pH 7.4 to 3080 ± 198 d.p.m. mg^{-1} protein at pH 5.5. In order to interpret fully binding to cortical mem-

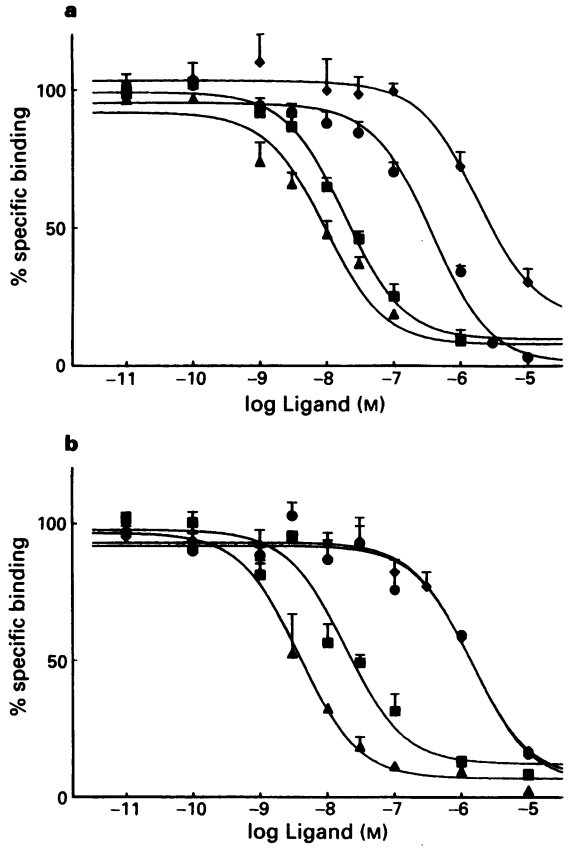


Figure 1 Displacement of 7 nM [^{3}H]-CGS 21680 from striatal membranes at pH 7.4 by adenosine receptor ligands was carried out as described in Methods. The data points represent the mean ± s.e.mean except when s.e.mean was less than the size of the symbol used. The number of determinations are shown in parentheses. The agonists are shown in (a): NECA (▲, 8); CGS 21680 (■, 8); R-PIA (●, 8); S-PIA (◆, 4), and the antagonists in (b): CGS 15943 (▲, 7); CP66,713 (■, 8); DPCPX (●,4); CPT (◆, 5). For abbreviations, see text.

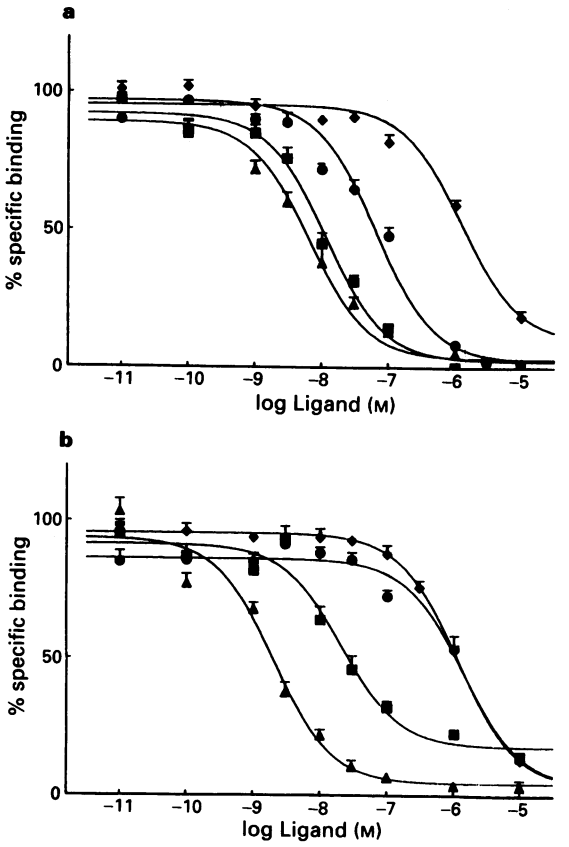


Figure 2 Displacement of 7 nM [^{3}H]-CGS 21680 from striatal membranes at pH 5.5 by adenosine receptor ligands was carried out as described in Methods. The data points represent the mean ± s.e.mean, except when s.e.mean was less than the size of the symbol used. The number of determinations are shown in parentheses. The agonists are shown in (a): NECA (▲, 4); CGS 21680 (■, 8); R-PIA (●, 7); S-PIA (◆, 3), and the antagonists in (b): CGS15943 (▲, 7); CP66,713 (■, 5); DPCPX (●, 5); CPT (◆, 5). For abbreviations, see text.

Table 1 Inhibition of [^{3}H]-CGS 21680 binding to rat striatal membranes at pH 7.4

Ligand	K_i *(nM)*
CGS 21680	10.5 ± 2.1 (8)
NECA	3.5 ± 0.9 (8)
R-PIA	172 ± 21 (8)
S-PIA	1712 ± 423 (4)
CGS15943	2.5 ± 0.5 (7)
CP66,713	11 ± 4.1 (8)
CPT	578 ± 127 (5)
DPCPX	529 ± 116 (4)

K_i values represent the mean ± s.e.mean with the number of determinations shown in parentheses. For abbreviations, see text.

Table 2 Inhibition of [^{3}H]-CGS 21680 binding to rat striatal membranes at pH 5.5

Ligand	K_i *(nM)*	*-fold increase in affinity* (K_D *pH 7.4/5.5)*
CGS 21680	2.8 ± 1.0 (8)	3.7
NECA	1.1 ± 0.2 (4)	3.2
R-PIA	20.8 ± 1.4 (7)	8.3
S-PIA	271 ± 49 (5)	6.3
CGS15943	0.5 ± 0.04 (7)	5.0
CP66,713	4.4 ± 1.5 (5)	2.5
CPT	264 ± 38 (5)	2.2
DPCPX	158 ± 35 (5)	3.3

K_i values represent the mean ± s.e.mean with the number of determinations shown in parentheses. For abbreviations, see text.

branes at pH 5.5, the effect of lowering the pH on the binding to striatal membranes was first evaluated.

[^{3}H]-CGS 21680 binding to striatal membranes at pH 5.5

A K_D value of 2.8 ± 1.8 nM for CGS 21680 was determined from competitive binding experiments at pH 5.5 with 7 nM [^{3}H]-CGS 21680. This can be compared with a value of 10.5 ± 2.1 nM observed at pH 7.4 (Table 1). There was no significant difference between the apparent receptor densities observed at the two pH values, the B_{max} value at pH 5.5 being 446 ± 16 fmol mg^{-1} protein. Further characterization of the striatal binding site by the agonists CGS 21680, NECA, R-PIA and S-PIA and antagonists CP66,713, CGS15943, CPT and DPCPX is shown in Figure 2. As for binding at pH 7.4, a typical A_{2A} receptor profile was observed, although an increase in affinity was seen for all

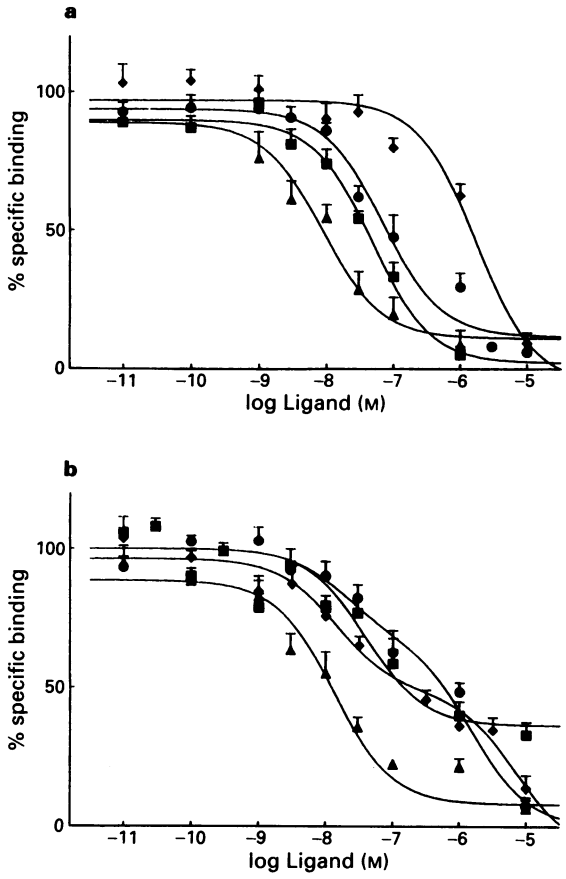


Figure 3 Displacement of 10 nM [^{3}H]-CGS 21680 from cortical membranes at pH 5.5 by adenosine receptor ligands was carried out as described in Methods. The data points represent the mean ± s.e.mean, except when s.e.mean was less than the size of the symbol used. The number of determinations are shown in parentheses: The agonists are shown in (a): NECA (▲, 4); CGS 21680 (■, 6); R-PIA (●, 6); S-PIA (◆, 7), and the antagonists in (b): CGS15943 (▲, 5); CP66,713 (■, 7); DPCPX (●, 8); CPT (◆, 5). For abbreviations, see text.

Table 3 Inhibition of [^{3}H]-CGS 21680 binding to rat cortical membranes at pH 5.5

Ligand	K_i *(nM)*	
CGS 21680	17.6 ± 5.8 (6)	
NECA	3.4 ± 0.8 (4)	
R-PIA	27 ± 3.6 (6)	
S-PIA	523 ± 81 (7)	
CGS15943	3.4 ± 1.3 (5)	
	Site 1	*Site 2*
CP66,713	23 ± 7 (7)	Insensitive
CPT	720 ± 127 (4)	2.9 ± 0.4 (4)
DPCPX	710 ± 204 (4)	0.7 ± 0.01 (4)

K_i values represent the mean ± s.e.mean with the number of determinations shown in parentheses. Site 1 represents the most abundant binding site. For abbreviations, see text.

compounds at the lower pH. The increases in affinity and the derived K_i values for both agonists and antagonists are also shown in Table 2, along with their Hill co-efficients. All displacement curves were, as for binding at pH 7.4, best described by a one site binding equation.

[^{3}H]-CGS 21680 binding to cortical membranes at pH 5.5

Binding to rat cortical membranes was evaluated at pH 5.5 with 10 nM [^{3}H]-CGS 21680 to further enhance specific binding. A K_D value of 17.6 ± 5.8 nM for CGS 21680 with a B_{max} value of 117 ± 22 fmol mg^{-1} protein as determined from competitive binding experiments. Further characterization of the cortical binding site by both the agonists CGS 21680, NECA, R-PIA and S-PIA and the antagonists CP66,713, CGS15943, CPT and DPCPX is shown in Figure 3, with their resultant Ki values shown in Table 3. The pharmacological profile of the agonists was similar to that observed in the striatum at pH 5.5, although the K_i values in the cortex were different having intermediate A_1/A_2 values. Furthermore, the profile for antagonists in the cortex was less clear, as CP66,713 showed a wide variability in its ability to displace [^{3}H]-CGS 21680 binding with an apparent 20–40% of the bound radiolabel being resistant to 10 μM CP66,713, and both CPT and DPCPX could be best fitted to a two site binding model yielding an abundant site of low affinity (presumptive A_{2A} receptor) and a less abundant site of higher affinity (possibly the A_1 receptor). This would therefore give an A_{2A}-like profile for the most abundant site (around 80%) of CGS15943 > CP66,713 > CPT = DPCPX, and an A_1-like profile for the remaining site (around 20%) of DPCPX- = CPT > CP66,713. The inability to resolve successfully CGS15943 binding into two sites may reflect its low selectivity for A_2 over A_1 receptors (Williams *et al.*, 1987).

In order to elucidate the nature of the less abundant second site (i.e. CP66,713 insensitive) the possibility of [^{3}H]-CGS 21680 binding to A_1 receptors was investigated. Displacement of 1 nM [^{3}H]-DPCPX from adenosine A_1 receptors in cortical membranes with unlabelled DPCPX gave B_{max} value for the A_1 receptor of 1164 ± 78 (6) and 983 ± 79 (6) fmol mg^{-1} protein, with K_d values of 2.2 ± 0.4 nM (6) and 1.9 ± 0.4 nM (6) at pH 7.4 and 5.5 respectively. No significant difference in the binding at the two pH values was observed. In addition, the K_i of CGS 21680 at the A_1 receptor was determined by displacement of 1 nM [^{3}H]-DPCPX with unlabelled CGS 21680, yielding K_i values of 879 ± 71 nM (6) and 738 ± 34 nM (7) at pH 7.4 and 5.5 respectively. From these data it was possible to calculate the fractional occupancy of the cortical membrane A_1 receptor by CGS 21680 under the conditions used in the assay.

In the cortical membrane binding assay, at pH 5.5 using 10 nM [^{3}H]-CGS 21680, the fractional occupancy of the A_1 receptor would have been 1.3%, corresponding to binding of 13 fmol mg^{-1} protein, since the B_{max} of the A_1 receptor was approximately 1000 fmol mg^{-1} protein. If it is assumed that the intermediate character of the cortical binding site was due to binding to both A_1 and (striatum-like) A_{2A} receptors, then the true A_{2A} receptor abundance would be significantly less than 117 fmol mg^{-1} protein. Under the conditions used, approximately 80% of this A_{2A} receptor would have been occupied by the radiolabel. Therefore of the label bound, more than 14% would have been due to A_1 receptor binding, close to the 20% of the label which bound to the low abundance site.

To confirm these findings further, the ability of both agonists and antagonists to displace [^{3}H]-CGS 21680 binding from cortical membranes (at pH 5.5) was repeated in the presence of 20 nM DPCPX to prevent binding to A_1 receptors (Figure 4). A K_D value of 3 ± 1 nM for CGS 21680 was observed with a B_{max} value of 80 ± 6 fmol mg^{-1} protein, similar to the estimate made above. In the case of CPT, the low affinity binding site was no longer evident and all values generally reflected those observed in the striatum at pH 5.5 (compare Tables 2 and 4). The CP66,713-insensitive element was reduced from 40 to 20% which is similar to that seen in the striatum at pH 5.5, having a K_i value of 25 ± 9 (7). The inability of CP66,713 to displace specific binding completely at concentrations of up to 10 μM may be due to the relative

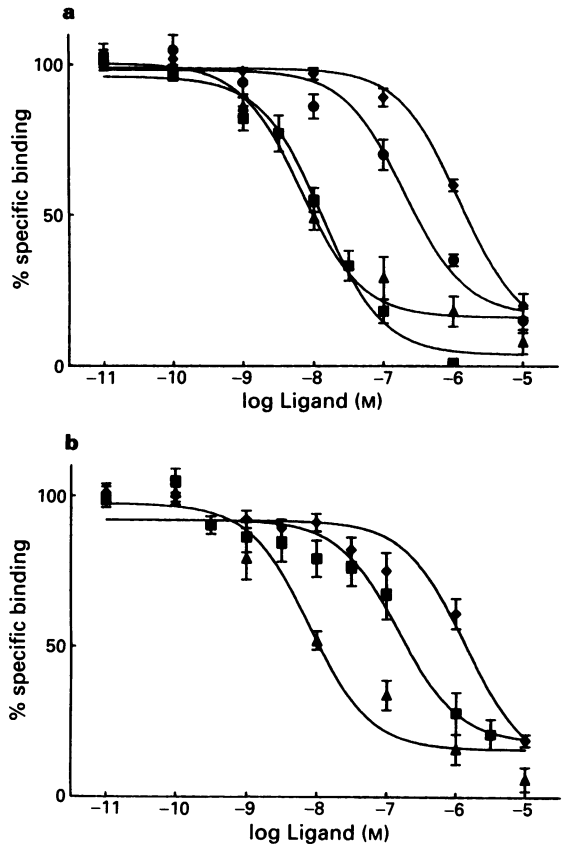


Figure 4 Displacement of 10 nM [^{3}H]-CGS 21680 from cortical membranes at pH 5.5 in the presence of 20 nM DPCPX by adenosine receptor ligands was carried out as described in Methods. The data points represent the mean ± s.e.mean, except when s.e.mean was less than the size of the symbol used. The number of determinations are shown in parentheses: The agonists are shown in (a): NECA (▲, 5); CGS 21680 (■, 8); R-PIA (●, 5); S-PIA (◆, 4), and the antagonists in (b): CGS15943 (▲, 5); CP66,713 (■, 7); CPT (◆, 5). For abbreviations, see text.

Table 4 Inhibition of [^{3}H]-CGS 21680 binding to the rat cortex in the presence of 20 nM DPCPX at pH 5.5

Ligand	K_i *(nM)*
CGS 21680	3.0 ± 1.0 (8)
NECA	1.6 ± 0.3 (5)
R-PIA	42 ± 4.0 (5)
S-PIA	261 ± 23 (4)
CGS15943	1.8 ± 0.6 (5)
CP66,713	25 ± 9 (7)
CPT	233 ± 20 (8)

K_i values represent the mean ± s.e.mean with the number of determinations shown in parentheses. For abbreviations, see text.

insolubility of this compound in aqueous buffer at concentrations above 1 μM (Sarges *et al.*, 1990) which may have been further enhanced by the lower pH of the buffer, as this was not observed to the same extent at pH 7.4.

Discussion

The present paper describes our attempt to determine whether the rat adenosine A_{2A} receptor exhibits different binding characteristics in cortical and striatal membranes. When binding was performed at pH 7.4 the pharmacological profile of the [^{3}H]-CGS 21680 binding site in the striatum was typical of an adenosine A_{2A} receptor i.e. for agonists NECA > CGS 21680 > R-PIA > S-PIA and for antagonists CGS 15943 > CP66,713 > CPT = DPCPX, such findings being consistent with a number of other reports (Jarvis *et al.*, 1989; Wan *et al.*, 1990). Interestingly, when binding in the striatum was performed at pH 5.5, the same A_{2A} profile was observed although there was a significant increase in affinity for this binding site for all the compounds tested with no apparent change in B_{max}. This increase in affinity was probably due to the protonation of the histidine residues in the receptor binding site at low pH (Askalan & Richardson, 1994), since these residues have been shown to be involved in ligand binding to the A_{2A} receptor (Jacobson *et al.*, 1993) and the A_1 receptor (Allende *et al.*, 1993; Van der Wenden *et al.*, 1991). The diversity of the ligand structures experiencing this affinity change suggests that a pH-dependent change in ligand structure was not involved. It is interesting to note that the greatest increase in affinity was for the A_1-selective ligand R-PIA, and that both agonists and antagonists were affected to different extents.

With regard to [^{3}H]-CGS 21680 binding in the cortex, initial experiments revealed low levels of specific binding. In order to maximize the signal, binding was performed at pH 5.5, where specific binding was enhanced by around 50%. Using this methodology, we were able to demonstrate the presence of a [^{3}H]-CGS 21680 binding site in the cortex, with an apparent B_{max} of 117 fmol mg^{-1} protein which corresponds to approximately 25% of that observed in the striatum. This is in accordance with earlier studies where low levels of cortical [^{3}H]-CGS 21680 binding have been reported, although not characterized (Jarvis *et al.*, 1989; Wan *et al.*, 1990). Such low levels of receptor may in part explain the failure of previous workers to detect mRNA in the cortex (Schiffman *et al.*, 1991a,b; Fink *et al.*, 1992).

The agonist binding characteristics of this cortical binding site were as expected for an A_{2A} receptor, although the K_i values were different from those obtained in the striatum under similar conditions (i.e. pH 5.5), which could have reflected a difference in the receptor binding sites in the two brain areas. It was unlikely that this site represented either the A_{2B} or A_3 receptor as neither are reported to bind CGS 21680 with high affinity (Zhou *et al.*, 1992; Yákel *et al.*, 1993). Furthermore it is unlikely that this binding site represented the recently proposed A_4 receptor for which both CGS 21680 and NECA have low affinities (Cornfield *et al.*, 1992). The antagonist profile of the cortical site could however be resolved into two components with the major component (80%) being that of a typical A_{2A} site, with a second compontent (20%) which probably represented binding to the A_1 receptor.

The A_{2A} receptor therefore appears to be present in the cortex, despite previous assertions that it was restricted to the basal ganglia. It has already been shown that the mRNA encoding this receptor is transiently expressed in the developing cortex (Weaver, 1993) and that A_{2A} receptor activation can regulate the release of GABA and glutamate from the ischaemic cortex (O'Regan *et al.*, 1992; Simpson *et al.*, 1992). In addition the A_{2A} receptor regulates neuronal excitability (Sebastiao *et al.*, 1994) and acetylcholine release in the hippocampus (Cunha *et al.*, 1994b). It therefore appears that this receptor may be much more widely distributed than was previously thought.

Simple calculations suggested that the second binding component identified in this paper could be explained by binding of the radiolabel to the A_1 receptor, so accounting for the intermediary characteristics observed. This was further confirmed when cortical binding was repeated in the presence of the 750 fold A_1-selective antagonist, DPCPX yielding a B_{max} value of 80 fmol mg^{-1} protein and resultant K_i values very similar to those obtained in the striatum at pH 5.5. This therefore suggested that the cortical binding site was a typical

(i.e. striatal-like) A_{2A} binding site. Although the striatum has an A_1 receptor density similar to that of the cortex, significant binding of [^{3}H]-CGS 21680 to the A_1 receptor is not observed. This is because the proportion of [^{3}H]-CGS 21680 binding to this receptor in striatal membranes is much lower, due to the 4 to 5 fold greater density of the A_{2A} receptor. The ratio of the K_i values for S-PIA and R-PIA has been used to distinguish between A_1 and A_{2A} receptors (Bruns *et al.*, 1987), with values greater than 20 implying the presence of A_1 receptors. In the striatum at pH 7.4 and 5.5 values of 10 and 13 respectively were observed, indicating the presence of A_{2A} receptors. In contrast, in the cortex a value of 19 was obtained in the absence of DPCPX, perhaps indicating the presence of A_1 receptors. It would be interesting to determine whether N-ethylmaleimide treatment of cortical membranes, which selectively reduces A_1 receptor binding (Ukena *et al.*, 1984), also indicates that a substantial proportion of the [^{3}H]-CGS 21680 binding was to the A_1 receptor.

If the cortical [^{3}H]-CGS 21680 binding can indeed be explained by a combination of A_1 and A_{2A} receptors, then one would expect a biphasic displacement curve with CGS 21680. However this was not apparent (Figure 3), probably because of the relatively low abundance of the A_1 receptor binding under the conditions used (i.e. approximately 20%) and the high K_D of the A_1 receptor for CGS 21680 (approximately 700 nM). More detailed examination of this region of the displacement curve would be required to reveal the A_1 receptor binding site.

The initial characteristics of the cortical binding site described in this paper (i.e. in the absence of DPCPX) have a resemblance to the cortical binding site recently characterized by Johansson *et al.* (1993). Using autoradiography with [^{3}H]-CGS 21680, they reported a K_i value of 47 nM and a B_{max} of 100 fmol mg^{-1} of grey matter which are close to the values obtained in this study (taking into account the effect of pH). They went on to demonstrate an intermediary A_1/A_2 agonist profile leading to the proposal of a novel [^{3}H]-CGS 21680 binding site. Similarly Cunha *et al.* (1994a) showed the existence of a high affinity CGS 21680 binding site sensitive to low (nM) concentrations of DPCPX in the rat cortex and hippocampus. Interestingly this site was the major component of the binding detected by these authors whose assays were performed at pH 7.4. The equivalent site described was not the major component in this paper because of the selective enhancement of A_{2A} receptor affinity for CGS 21680 at pH 5.5.

In addition to the above, characterization of [^{3}H]-CGS 21680 binding in the human brain by James *et al.* (1992) revealed the presence of two binding sites, an abundant striatal specific site typical of an A_{2A} receptor and a less abundant site of intermediary A_1/A_2 profile that was present in low levels in both the cortex and striatum and was not due to the presence of an A_1 receptor. In both this study and the ones by Johannsson *et al.* (1993) and Cunha *et al.* (1994) binding to the cortical site was completely abolished by the addition of Gpp(NH)p. It is possible that the greater susceptibility to Gpp(NH)p in the rat cortex compared to the striatum observed by these workers could be accounted for by the presence of A_1 receptors, which are more sensitive to Gpp(NH)p treatment than A_2 receptors (Nanoff *et al.*, 1991).

In summary, we have demonstrated the presence of a pH-sensitive [^{3}H]-CGS 21680 binding site in the rat striatum and the existence of a similar site of lower abundance in the cortex. The novel binding site recently described in the cortex by other groups can be explained by the binding to the A_1 receptor. This does not however rule out the existence of a binding site with high affinity for both CGS 21680 and DPCPX. Although the present study would tend to suggest that receptor subtypes of the A_{2A} receptor do not exist in the rat brain, the possibility still remains in human brain.

I.P.K. is the recipient of a Glaxo Group Research Training Award.

References

ABBRACCHIO, M.P., CATTABENI, F., FREDHOLM, B.F. & WILLIAMS, M. (1993). Purinoceptor nomenclature: a status report. *Drug Dev. Res.*, **28**, 207–213.

ALLENDE, G., CASADO, V., MALLOL, J., FRANCO, R., LLUIS, C. & CANELA, E. (1993). Role of histidine residues in agonist and antagonist binding sites of A_1 adenosine receptor. *J. Neurochem.*, **60**, 1525–1533.

ASKALAN, R. & RICHARDSON, P.J. (1994). The role of histidine residues in the adenosine A_{2a} receptor ligand binding site. *J. Neurochem.* (in press).

BROWN, S.J., JAMES S., REDDINGTON, M. & RICHARDSON, P.J. (1990). Both A_1 and A_{2a} purine receptors regulate striatal acetylcholine release. *J. Neurochem.*, **55**, 31–38.

BRUNS, R.F., LU, G.H. & PUGSLEY, T.A. (1986). Characterisation of the A_2 adenosine receptors labelled by [^{3}H]-NECA in rat striatal membranes. *Mol. Pharmacol.*, **29**, 331–346.

BRUNS, R.F., LU, G.H. & PUGSLEY, T.A. (1987). Adenosine receptor subtypes. In *Topics and Perspectives in Adenosine Research*, ed. Gerlach E, & Becker, B.F. pp. 59–73. Berlin: Springer-Verlag.

CORNFIELD, L.J., HU, S., HURT, S.D. & SILLS, M. (1992). [^{3}H]2-phenylaminoadenosine ([^{3}H]CV 1808) labels a novel adenosine receptor in rat brain. *J. Pharmacol. Exp. Ther.*, **263**, 552–561.

CUNHA, R.A., JOHANSSON, B., SEBASTIAO, A.M., RIBEIRO, J.A. & FREDHOLM, B.B. (1994a). The binding sites for the adenosine A_{2A} receptor agonist [^{3}H]-CGS 21680 are different in the hippocampus and cerebral cortex and in the striatum of the rat. *Drug Dev. Res.*, **31**, 260.

CUNHA, R.A., MILUSHEVA, E., VIZI, E.S., RIBEIRO, J.A. & SEBASTIAO, A.M. (1994b). Excitatory and inhibitory effects of A1 and A2A receptor activation on the electrically evoked [3H]-acetylcholine release from different areas of the hippocampus. *J. Neurochem.*, **63**, 207–214.

DEBLASI, A., O'REILLY, K. & MOTULSKY, H.J. (1989). Calculating receptor number from binding experiments using same compound as radioligand as competitor. *Trends Pharmacol. Sci.*, **10**, 227–229.

FINK, J.S., WEAVER, D.R., RIVKEES, S.A., PETERFREUND, R.A., POLLACK, A.E., ADLER, E.M. & REPPERT, S.M. (1992). Molecular cloning of the rat A_2 adenosine receptor: selective co-expression with D_2 dopamine receptors in rat striatum. *Mol. Brain Res.*, **14**, 186–195.

FREDHOLM, B.B & DUNWIDDIE, T.V. (1988). How does adenosine inhibit transmitter release? *Trends Pharmacol. Sci.*, **9**, 130–134.

JACOBSON, K.A., VAN GAELEN, P.J.M, JI, X., RAMKUMAR, V., OLAH, M.E. & STILES, G.L. (1993). Molecular characterisation of A_1 and A_{2a} adenosine receptors. *Drug Dev. Res.*, **28**, 226–231.

JAMES, S., XUERUB, J.H., ASKALAN, R. & RICHARDSON, P.J. (1992). Adenosine receptors in post-mortem human brain. *Br. J. Pharmacol.*, **105**, 238–244.

JARVIS, M.F., SCHUTZ, R., HUTCHISON, A.J., DO, E., SILLS, M.A. & WILLIAMS, M. (1989). [^{3}H]-CGS 21680, an A_2 selective adenosine receptor agonist directly labels A_2 receptors in rat brain tissue. *J. Pharmacol. Exp. Ther.*, **251**, 888–893.

JARVIS, M.F. & WILLIAMS, M. (1989). Direct autoradiographic localisation of adenosine A_2 receptors in the rat brain using the A_2-selective agonist [^{3}H]-CGS 21680. *Eur. J. Pharmacol.*, **168**, 243–246.

JOHANSSON, B., GEORGIEV, V., PARKINSON, F.E. & FREDHOLM, B.B. (1993). The binding of the adenosine A_2 receptor selective agonist [^{3}H]-CGS 21680 to rat cortex differs from its binding to rat striatum. *Eur. J.Pharmacol.*, **247**, 103–110.

KIRK, I.P. & RICHARDSON, P.J. (1994). Adenosine A_{2A} receptor mediated modulation of striatal [^{3}H]-GABA and [^{3}H]-ACh release. *J. Neurochem.*, **62**, 960–966.

KIRKPATRICK, K.A. & RICHARDSON, P.O. (1993). Adenosine receptor mediated modulation of acetylcholine release from striatal synaptosomes. *Br. J. Pharmacol.*, **110**, 949–954.

LOWRY, O.H., ROSEBROUGH, N.J., FARR, A.L. & RANDALL, R.J. (1951). Protein measurement with the folin reagent. *J. Biol. Chem.*, **193**, 265–275.

MAYFIELD, R.D., SUZUKI, F. & ZAHNISER, N.R. (1993). Adenosine A_{2a} receptor modulation of electrically evoked endogenous GABA release from slices of rat globus pallidus. *J. Neurochem.*, **60.** 2334–2337.

MOTULSKY, H. (1989). *GRAPH pad In Plot Version 3.0.* San Diego: Graph Pad Software.

NANOFF, C., JACOBSEN, K.A. & STILES, G.L. (1991). The A_2 adenosine receptor: Guanine nucleotide modulation of agonist binding is enhanced by proteolysis. *Mol. Pharmacol.*, **39,** 130–135.

O'REGAN, M.H., SIMPSON, R.E., PERKINS, L.M. & PHILLIS, J.W. (1992). Adenosine receptor agonists inhibit the release of γ-aminobutyric acid (GABA) from ischaemic rat cerebral cortex. *Brain Res.*, **582,** 22–26.

SARGES, R., HOWARD, H.R., BROWNE, R.G., LEBEL, L.A., SEYMOUR, P.A. & KOE, B.K. (1990). 4-Amino [1,2,4] triazolo [4,3-a] quinoxalines. A novel class of potent adenosine receptor antagonists and potential rapid-onset antidepressants. *J. Med. Chem.*, **33,** 2240–2254.

SCHIFFMAN, S.N., JACOBS, O. & VANDERHAEGEN, J.J. (1991). Striatal restricted adenosine A_2 receptor (RDC8) is expressed by enkephalin, but not by substance P neurons: An *in situ* hybridisation histochemistry study. *J. Neurochem.*, **57,** 1062–1067.

SCHIFFMAN, S.N., LIBERT, F., VASSART, G. & VANDERHAEGEN, J.J. (1991). Distribution of adenosine A_2 receptor mRNA in the human brain. *Neurosci. Lett.*, **130,** 177–181.

SEBASTIAO, A.M., CUNHA, R.A., CORREIA DE SA, P., DE MENDONCA, A. & RIBEIRO, J.A. (1994). A_{2A} adenosine receptors in the hippocampus and motor nerve terminals. *Drug Dev. Res.*, **31,** 320.

SHIMADA, J., SUZUKI, F., NONAKA, H., ISHII, A. & ICHIKAWA, S. (1992). (E)-1,3-Dialkyl-7-methyl-8-(3,4,5-trimethoxy-styryl)xanthines: Potent and selective adenosine A_2 antagonists. *J. Med. Chem.*, **35,** 2342–2345.

SIMPSON, R.E., O'REGAN, M.H., PERKINS, L.M. & PHILLIS, J.W. (1992). Excitatory transmitter amino acid release from the ischaemic rat cerebral cortex: Effects of adenosine receptor agonists and antagonists. *J. Neurochem.*, **58,** 1683–1690.

UKENA, D., POESCLA, E., HUTTEMANN, E. & SCHWABE, U. (1984). Effects of N-ethylmaleimide on adenosine receptors of rat fat cells and human platelets. *Naunyn. Schmied. Arch. Pharmacol.*, **327,** 247–253.

VAN CALKER, D., MULLER. M. & HAMPRECHT, R. (1979). Adenosine regulates via two different types of receptor, the accumulation of cAMP in cultured brain cells. *J. Neurochem.*, **33,** 999–1005.

VAN DER WENDEN, E., VAN GALEN, P.J.M., IJZERMAN, A.P. & SOUDIJN, W. (1991). A model for the hydrogen-bonding interactions between adenosine receptor ligands and histidyl residues in the adenosine A_1 receptor binding site, based on AM1 calculations. *J. Mol. Structure*, **231,** 175–184.

WAN, W., SUTHERLAND, G.R. & GEIGER, J.D. (1990). Binding of the adenosine A_2 receptor ligand [^{3}H] CGS 21680 to human and rat brain. Evidence for multiple affinity sites. *J. Neurochem.*, **55,** 1763–1771.

WEAVER, D.R. (1993). A_{2A} adenosine receptor gene expression in developing rat brain. *Mol. Brain Res.*, **20,** 313–327.

WILLIAMS, M., FRANCIS, J., GHAI, G., BRAUNWALDER, A., PSYCHOYOS, S., STONE, G.A. & COSH, W.D. (1987). Biochemical characterisation of the triazoloaminazoline, CGS 15943, a novel, non-xanthine adenosine antagonist. *J. Pharmacol. Exp. Ther.*, **241,** 415–420.

YAKEL, J.L., WARREN, R.A., REPPERT, S.M. & NORTH, R.A. (1993). Functional expression of adenosine A_{2b} receptor in Xenopus oocytes. *Mol. Pharmacol.*, **43,** 277–280.

ZHOU, Q.Y., LI, C., OLAH, M.E., JOHNSON, R.A. & STILES, G.L. (1992). Molecular cloning and characterisation of an adenosine receptor: the A3 receptor. *Proc. Natl. Acad. Sci. U.S.A.*, **89,** 7432–7436.

(Received June 20, 1994
Revised September 27, 1994
Accepted September 30, 1994)

British Journal of Pharmacology (1995) 114, 544–550 © 1995 Stockton Press All rights reserved 0007–1188/95 $9.00

Modulation of Ca^{2+}-dependent currents in metabolically stressed cultured sensory neurones by intracellular photorelease of ATP

S.R. Stapleton, *B.A. Bell, †J.F. Wootton & [1]R.H. Scott

Department of Physiology and *Division of Clinical Neuroscience, St George's Hospital Medical School, Cranmer Terrace, London SW17 0RE, and †Department of Physiology, Cornell University, Ithaca, NY 14853-6401, U.S.A.

1 The whole cell recording technique was used to study high voltage-activated Ca^{2+} currents and Ca^{2+}-activated Cl^- tail currents from cultured neonatal dorsal root ganglion neurones of the rat which were metabolically stressed. The neurones were metabolically stressed with 2-deoxy-D-glucose (5 mM) for 30 min to 3 h. The aim of the project was to examine the actions of intracellular photorelease of ATP on the properties of Ca^{2+}-dependent currents and determine if the effects of metabolic stress could be reversed.

2 The mean duration of Ca^{2+}-activated Cl^- tail currents was significantly increased by metabolic stress and this effect was reversed by intracellular photorelease of approximately 300 μM ATP. Intracellular photolysis of 'caged' photolabile compounds was achieved with a xenon flash lamp.

3 Intracellular photorelease of ATP and adenosine 3':5'-cyclic monophosphate (cyclic AMP) (about 40 μM) also accelerated the inactivation of high voltage-activated Ca^{2+} currents evoked by 500 ms depolarizing step commands from −90 mV to 0 mV. This effect was prevented by intracellular application of the calcineurin (protein phosphatase-2B) inhibitor cyclosporin A (14 nM) and cyclophilin A (50 nM) either applied together or individually. In contrast the protein phosphatase 1 and 2A inhibitor, calyculin A, increased voltage-activated Ca^{2+} currents, but failed to prevent enhanced inactivation induced by intracellular photorelease of ATP. Intracellular photorelease of ATP had no effect on Ca^{2+} currents recorded from control neurones which were not metabolically stressed and supplied with glucose and ATP in the extracellular and patch pipette solutions respectively.

4 In conclusion, intracellular photorelease of ATP increases the decay of Ca^{2+}-activated Cl^- tail currents in metabolically stressed neurones suggesting that the efficiency of intracellular Ca^{2+} buffering was improved. Additionally, an ATP/cyclic AMP-dependent component of high voltage-activated Ca^{2+} current inactivation which is mediated by calcineurin is revealed following photolysis of 'caged' ATP or cyclic AMP in metabolically stressed neurones.

Keywords: Cultured sensory neurones; photoreleased ATP; phosphatase; calcium-activated chloride current; cyclosporin A; calcium current inactivation; 2-deoxy-D-glucose

Introduction

The electrophysiological properties of neurones are profoundly altered by metabolic stress (oxygen/glucose deprivation). Events which develop and lead to neuronal death include changes in membrane potential associated with activation of specific conductances, disturbance of ionic gradients, alterations in the release and uptake of neurotransmitters and reduced efficiency of intracellular Ca^{2+} homeostatic mechanisms. Both *in vivo* and *in vitro* studies have shown that ischaemia/hypoxia and other metabolic insults which result in reduced levels of ATP subsequently lead to raised intracellular Ca^{2+} (Kass & Lipton, 1986; Duchen *et al.*, 1990; Silver & Erecińska, 1990; Dubinsky & Rothman, 1991). The complex changes in electrical properties which also occur are in part due to activation of Ca^{2+}-dependent K^+ conductances (Godfraind *et al.*, 1971; Leblond & Krnjevic, 1989). Additionally, disturbances in Ca^{2+} homeostatic mechanisms can also result in enhancement of Ca^{2+}-activated Cl^- tail currents (Duchen, 1990; Stapleton *et al.*, 1992; 1994).

The aim in this study has been to metabolically stress cultured dorsal root ganglion (DRG) neurones with 2-deoxy-D-glucose (Stapleton *et al.*, 1994) and then investigate the actions of intracellular photorelease of ATP on high voltage-activated Ca^{2+} currents and Ca^{2+}-activated Cl^- tail currents. Calcium-activated Cl^- currents appear not to inactivate but gradually deactivate when intracellular Ca^{2+} declines (Currie *et al.*, 1995; Scott *et al.*, 1995). Therefore as part of the study we have used Ca^{2+}-activated Cl^- tail currents as a physiological index of Ca^{2+} concentration close to the plasma membrane to gain an insight into the ability of cells to handle Ca^{2+} which has entered the cultured neurones through voltage-activated Ca^{2+} channels.

[1] Author for correspondence at the Department of Physiology, St George's Hospital Medical School, Cranmer Terrace, London SW17 0RE.

Methods

Cell culture

Primary cultures of DRG neurones were prepared from 2-day old Wistar rats. The DRG neurones were enzymatically and mechanically dissociated, and then plated on laminin-polyornithine coated cover-slips. The cultures of DRG neurones were maintained for up to 3 weeks at 37°C in humidifed air with 5% CO_2. F14 culture medium (Imperial Laboratories) supplemented with 10% horse serum (Gibco) was used with added penicillin (5000 iu ml^{-1}), streptomycin (5000 μg ml^{-1}), $NaHCO_3$ (14 mM) and nerve growth factor (20 ng ml^{-1}, Sigma). Cell cultures were refed with F14/horse serum mixture containing nerve growth factor (10 ng ml^{-1}) every 7 days. For experiments where metabolically stressed neurones were studied, cells were pretreated with recording medium which contained 2-deoxy-D-glucose (5 mM) for at least 30 min before electrophysiological work was carried out.

Electrophysiology

The whole cell variant of the patch clamp technique was used (Hamill *et al.*, 1981) to study Ca^{2+}-dependent currents in cultured DRG neurones. The neurones were voltage-clamped with an Axoclamp 2A switching amplifier operated at a sampling rate of 20–25 kHz, with low resistance (3–7 MΩ) micropipettes. A pulse generator (Digitimer D4030) provided the timing of voltage command protocols. All experiments were performed at room temperature (approx. 23°C).

Extracellular recording medium and a patch pipette solution which metabolically stressed the cultured sensory neurones were used for most of the experiments (Stapleton *et al.*, 1994). This recording medium contained, in mmol l^{-1}: choline chloride 130, KCl 3.0, $MgCl_2$ 0.6, $NaHCO_3$ 1.0, HEPES 10.0, tetraethylammonium bromide 25.0, 2-deoxy-D-glucose 5.0, $CaCl_2$ 2.0, tetrodotoxin 0.0025. The pH was adjusted to 7.4 with NaOH and the osmolarity to 320 mOsmol l^{-1} with mannitol. The patch pipette solution contained, in mmol l^{-1}: CsCl 140, EGTA 1.1, $MgCl_2$ 2.0, $CaCl_2$ 0.1, HEPES 10.0, the pH was corrected to 7.2 with Tris (1 mM) and the osmolarity to 310 mOsmol l^{-1} again with mannitol. The estimated free Ca^{2+} concentration in the patch pipette solution was 16 nM. A modest amount of EGTA (1.1 mM) was used to buffer the Ca^{2+} in the patch pipette solution; this was necessary to ensure stability and consistency of voltage-activated Ca^{2+} currents and Ca^{2+}-activated Cl^- tail currents under control conditions. A series of control recordings was also made from neurones which were not metabolically stressed. Under these conditions the 'standard' recording medium contained 4 mM glucose in place of 2-deoxy-D-glucose and the patch pipette solution contained 2 mM ATP and sucrose was used to correct the osmolarity of intracellular and extracellular solutions.

Drugs applied to the extracellular environment were dissolved in recording medium and after checking and adjustment of pH where necessary, were applied by low pressure ejection via a micropipette (tip diameter approximately 10 μm) positioned within 100 μm of the cell being recorded. Intracellular drug application was performed by including the drug in the patch pipette solution. After breaking the membrane patch and achieving the whole cell configuration the cultured DRG neurone was then left for 5 min before experiments were started. This period allowed the patch pipette solution to equilibrate with the intracellular environment. The period of equilibration was important when 'caged' compounds were included in the patch pipette solution and subsequently photolysed inside the DRG neurones during the experiments. One mM 'caged' ATP (adenosine-5'-triphosphate, P^3-1-(2-nitrophenyl) ethyl ester) or 100 μM 'caged' cyclic AMP (adenosine-3':5'-cyclic monophosphate P^1-(2-nitrophenyl) ethyl ester: axial isomer) were included in the patch pipette solution in this study. Intracellular photorelease of ATP (~300 μM) and cyclic AMP (~40 μM) was achieved using a xenon arc flash lamp (Hi-Tech Scientific model XF-10) with a Schott UG11 band-pass filter (280–360 nm) fitted. A 200 V lamp discharge (200 V flash) gave 100 mJ of near u.v. light which photolysed 11% and 42% of the 'caged' ATP and the axial isomer of 'caged' cyclic AMP respectively. The estimates of the amount of ATP and cyclic AMP photoreleased in cells were determined by flashing 12 μl samples of 'caged' compound made up in patch pipette solution and analysing the conversion from 'caged' compound to uncaged product by h.p.l.c. (Walker *et al.*, 1988; Currie *et al.*, 1995). The 'caged' compounds were synthesized and characterized by previously published methods (Walker *et al.*, 1988; Wootton & Trentham, 1989).

Calyculin A an octamethyl polyhydroxylated fatty acid and novel highly potent inhibitor of phosphatase-1 and 2A (Ishihara *et al.*, 1989) and the cyclic undecapeptide, cyclosporin A, were used in some experiments. These compounds are hydrophobic and stock solutions were made up in dimethylsulphoxide (DMSO) prior to serial dilution. The final concentration of DMSO applied to cells was 2.5 nM or 0.005% and previous studies have shown that Ca^{2+}-dependent currents are not affected by this concentration of DMSO (Currie & Scott, 1992). Calyculin A appears to be readily able to cross cell membranes and enter cells (Suganuma *et al.*, 1990) and was therefore applied to the extracellular environment. Cyclosporin A complexed with cyclophilin A affects signal transduction by inhibiting serine-threonine protein phosphatase-2B (calcineurin) (Sigal & Dumont, 1992; Walsh *et al.*, 1992). Both cyclosporin A (14 nM) and cyclophilin A (50 nM) were applied to the intracellular environment by inclusion in the patch pipette solution. The stock solution of human recombinant cyclophilin A contained sodium azide, however the final concentration applied was $<0.0006\%$. The calyculin A was purchased from LC laboratories.

Analysis

Net Ca^{2+} currents were evaluated following scaled linear substraction of leakage and capacitative currents. Previously Ca^{2+} current inactivation has been described as a double exponential decay process by Chad & Eckert (1984). As a result in this study the rate of inactivation of voltage-activated Ca^{2+} currents was assessed quantitatively by fitting a double exponential decay curve to the current data between I_{max} (peak current) and I_{end} (current at the end of the voltage step command) during the 500 ms voltage step command. Two time constants of inactivation, τ_1 and τ_2, were derived for each current using the equation:

$$I_{Ca} = a + b\ \exp(^{-t}/\tau_1) + c\ \exp(^{-t}/\tau_2)$$

The curves were fitted after over 100 iterations of a least squares procedure with a variance of less than 1.0×10^{-6} using Cambridge Electronic Design (CED) software.

Ca^{2+}-activated Cl^- tail currents ($I_{Cl(Ca)}$) were assessed by measurement of the current amplitude 20 ms after the end of the voltage step command and by the time taken for the inward current to decay by 63% of the maximal amplitude ($t_{63\%}$). An estimation of the total charge flow (Q) for each tail current was also made by measurement of the area under the tail current decay curve using an integration programme for tail currents of less than 4 s, while for longer tail currents the traces were cut out and weighed. Since there was a wide distribution of tail current total charge flow these values have also been normalised (Q%) to give values as percentages of the response compared to the first voltage step command in each series of 4 currents activated at 1 per min.

All data are given as mean ± standard error of the mean and statistical signficance has been assessed using Student's two-tailed *t* test.

Results

The actions of intracellular photorelease of ATP on Ca^{2+}-activated Cl^- tail currents

In a variety of neuronal preparations including cultured DRG neurones Ca^{2+}-activated Cl^- tail currents can be recorded from a proportion of cells which have been loaded with chloride-based patch pipette solution (Mayer, 1985; Currie & Scott, 1992). The Cl^- tail currents are observed as slowly decaying inward currents which are dependent on Ca^{2+} entry through voltage-activated Ca^{2+} channels. The equilibrium potential for Cl^- under our recording conditions is close to 0 mV so by applying a voltage step command of 90 mV, to neurones voltage clamped at a holding potential (V_h) of −90 mV, voltage-activated Ca^{2+} currents can be activated free from contamination by Cl^- current. However, on stepping back to the V_h of −90 mV there is large driving force for Cl^- which leaves the neurones while Ca^{2+}-activated

Cl^- channels remain opened by the raised intracellular [Ca^{2+}]. Calcium-activated Cl^- tail currents which follow 500 ms high voltage-activated Ca^{2+} currents were found to be progressively prolonged by 2-deoxy-D-glucose ($n = 11$) (Figure 1a). This effect was not observed in control cells ($n = 7$) and was prevented by intracellular application of D-fructose 1,6-diphosphate ($n = 7$) suggesting that it results from metabolic stress induced by inhibition of glycolysis (Stapleton *et al.*, 1994).

The intracellular photolysis of 'caged' ATP has been used in this study to demonstrate that the progressive prolongation of Ca^{2+}-activated Cl^- tail current observed in the presence of 2-deoxy-D-glucose is the consequence of ATP depletion. After entering the whole cell configuration, 5 min equilibration was allowed before 500 ms voltage step commands from a V_h of -90 mV to a V_c of 0 mV were applied. A single initial current was activated and then approximately 300 μM ATP was photoreleased inside the cells by three 200 V flashes. Currents were activated at 1 min intervals for 3 min thereafter. Comparing the sequence of currents activated in seven cells no significant changes in the peak amplitude of voltage-activated Ca^{2+} currents were observed, and the mean amplitude of the Ca^{2+}-activated Cl^- current was also unaltered. Additionally, the mean duration for the tail current to decay to 63% of the maximum value ($t_{63\%}$), did not increase when ATP was photoreleased in metabolically stressed neurones. Photorelease of ATP in DRG neurones prevented increases in $t_{63\%}$ values measured from the first and fourth currents, these values were 5070 ± 1180 ms and 5250 ± 970 ms ($n = 7$) respectively. In several cases the rate of decay of the tail current was increased even when the voltage-activated Ca^{2+} current became larger following intracellular photorelease of ATP (Figure 1b). By comparison the $t_{63\%}$ values increased from 4000 ± 800 ms to 7350 ± 2080 ms ($n = 11$; $P < 0.05$) in metabolically stressed cells in which no ATP was photoreleased (flashed without 'caged' ATP present).

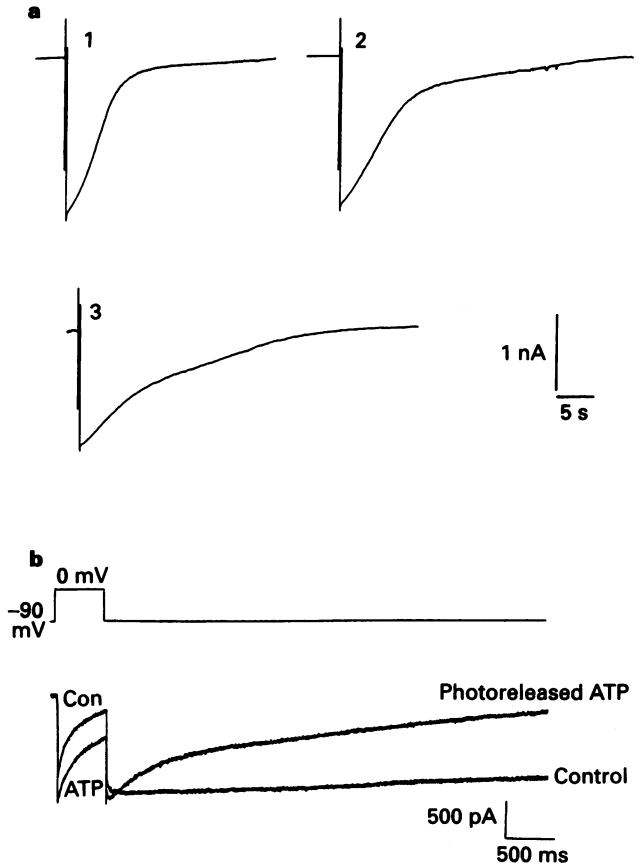


Figure 1 The prolongation of Ca^{2+}-activated Cl^- tail currents by 2-deoxy-D-glucose is reversed by intracellular photolysis of 'caged' ATP. (a) The records show Ca^{2+} currents and long lasting Ca^{2+}-activated Cl^- tail currents evoked in a cultured DRG neurone metabolically stressed by 2-deoxy-D-glucose. The cell was held at -90 mV and depolarized to 0 mV for 500 ms to activate currents (1,2,3) every min. The $t_{63\%}$ values for the successive Cl^- tail currents increased from about 9 s to 14 s and then 20 s. (b) Traces showing the effect of intracellular flash photolysis of 'caged' ATP on a net high voltage-activated Ca^{2+} current after leak subtraction and the accompanying Ca^{2+}-activated Cl^- tail current. The records were obtained from a cultured DRG neurone in the presence of 2-deoxy-D-glucose. The control record (Con) shows a Ca^{2+}-activated Cl^- tail current with a $t_{63\%}$ of 7 s, and a record of the tail current 2 min after photorelease of ATP when the $t_{63\%}$ was reduced to 1.3 s even though the voltage-activated Ca^{2+} current increased, causing a greater Ca^{2+} load to be handled by cellular homeostatic mechanisms.

The mean total charge flow during the tail current was also unchanged in metabolically stressed neurones when 'caged' ATP was photolysed, the values obtained from the first and fourth currents were 5.7 ± 1.3 nC and 4.6 ± 1.6 nC ($n = 7$). When these variable values were normalized, no significant change in the mean percentage charge flow values (Q%) was observed when comparing the first currents with those activated after intracellular photorelease of ATP. This is in contrast to what is observed in cells treated with 2-deoxy-D-glucose alone where significant changes in Q% were seen. The data also strengthen the previous evidence obtained from cells treated with 2-deoxy-D-glucose but supported metabolically by intracellular application of fructose 1,6-diphosphate to bypass the inhibitory effect of 2-deoxy-D-glucose on glycolysis (Stapleton *et al.*, 1994).

The effect of intracellular photoreleased ATP and cyclic AMP on inactivation of calcium currents

During the experiments on the effect of 'caged' ATP on tail currents in the presence of 2-deoxy-D-glucose it was noticed that the photorelease of ATP appeared to increase the rate of inactivation of the high voltage-activated calcium currents. In this part of the study the maximum high voltage-activated Ca^{2+} currents activated from a V_h of -90 mV by 500 ms voltage step commands to potentials were measured. The clamp potential (0 to $+10$ mV) at which the maximum voltage-activated Ca^{2+} current was evoked was determined for all the neurones studied. The increase in the rate of Ca^{2+} current inactivation occurred despite a modest reduction in the I_{max} from an initial current value of -1.13 ± 0.12 nA to -0.80 ± 0.10 nA ($n = 21$) 3 min after photorelease of ATP. A reduction in Ca^{2+} current amplitude might have been expected to slow Ca^{2+}-dependent inactivation (Chad & Eckert, 1984), but ATP was found to decrease signficantly the two time constants of inactivation τ_1 and τ_2 ($n = 21$) reflecting an increase in inactivation rate (Figure 2). These time constants τ_1 and τ_2 were determined for the four successive currents, one activated before the flash and three after intracellular photorelease of ATP. Similarly control cells exposed to 2-deoxy-D-glucose and flashed three times (200 V) but without 'caged' ATP present were also studied. In cells without 'caged' ATP present there was no significant increase in the rate of inactivation with successive steps, whereas in those cells in which ATP was photoreleased both τ_1 and τ_2 became significantly shorter by the fourth voltage step command (Figure 2). These data suggested that the increased rate of inactivation of high voltage-activated Ca^{2+} currents evoked by intracellular photorelease of ATP was not an artifact produced by three 200 V flashes from the xenon flashlamp. Experiments using 'standard' recording solutions to determine the effect of photoreleased ATP on high voltage-activated Ca^{2+} current inactivation in the absence of metabolic stress were performed using an identical protocol. These data demonstrated that the mean τ_2 value was prolonged significantly from 590 ± 190 ms to 760 ± 230 ms by the fourth step, suggesting a slowing of inactivation under

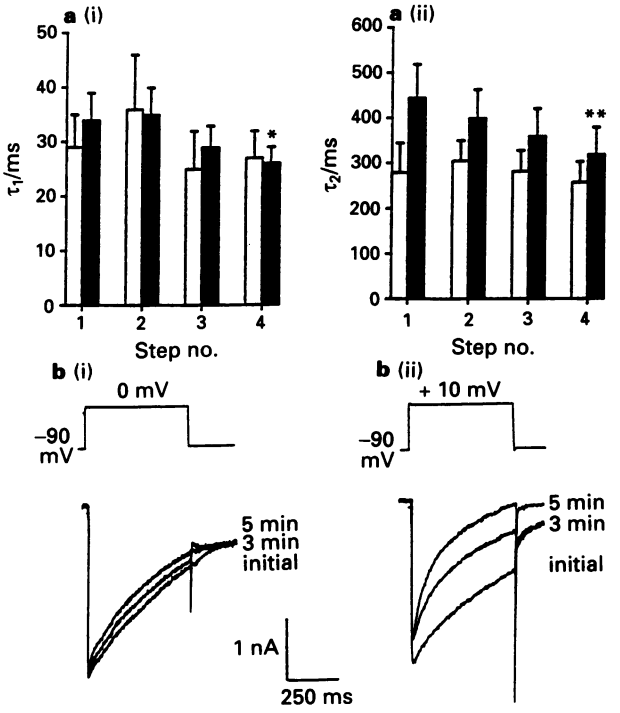


Figure 2 The effect of intracellular photoreleased ATP on inactivation of Ca^{2+} currents recorded in the presence of 2-deoxy-D-glucose. (a) Figures showing the mean ± s.e.mean of the fitted time constants (τ_1 and τ_2) of Ca^{2+} current inactivation for four consecutive 500 ms voltage step commands. The time constants τ_1 (i) and τ_2 (ii) are shown for neurones with no intracellular 'caged' ATP present (open columns, $n = 5$) and after photorelease of about 300 μM ATP (solid columns, $n = 21$). Neither τ_1 nor τ_2 changed significantly when cells were flashed in the absence of 'caged' ATP, however after photorelease of ATP both τ_1 and τ_2 were significantly reduced by the 4th step compared with the 1st step. (b) Traces show high voltage-activated Ca^{2+} currents recorded from a cell with no intracellular 'caged' ATP present (i), and from a cell in which ATP was photoreleased (ii). The initial traces are current records before the cells were flashed, two additional currents activated 3 and 5 min after flashing the cells are also illustrated. The maximum high voltage-activated Ca^{2+} currents were activated at 0 mV and +10 mV in the two cells.

these conditions ($n = 6$; $P < 0.05$). No significant change in the τ_1 was observed under these recording conditions. The metabolic stress produced by 2-deoxy-D-glucose appeared therefore to be an important factor in the apparent ATP-dependent increased rate of Ca^{2+} current inactivation seen under those conditions. Furthermore these data suggested that neither the flashes from the lamp nor the byproducts of the photolysis reaction of 'caged' ATP were responsible for the changes in Ca^{2+} current inactivation seen in the presence of 2-deoxy-D-glucose.

In order to determine if the increased rate of inactivation of high voltage-activated Ca^{2+} currents seen on flash photolysis under conditions of metabolic stress was due to a direct effect of ATP or occurred via an intermediary formed from ATP, further flash photolysis experiments using 'caged' cyclic AMP (40 μM) were carried out. Once again an identical protocol and evaluation was used. Table 1 shows data which demonstrate that in a similar way to the intracellular photorelease of ATP, cyclic AMP was able to cause a significant increase in inactivation rate of Ca^{2+} current after the activation of four currents as reflected by the decreases in τ_1 and τ_2.

These findings suggested that in the presence of 2-deoxy-D-glucose, the restoration of a supply of ATP by flash photolysis increased the rate of Ca^{2+} channel inactivation. Cyclic AMP could also produce the effect under conditions of metabolic stress. However, the effect was not seen under 'standard' recording conditions. Since Ca^{2+} channels are known to require enzymatic phosphorylation for their proper function (Chad & Eckert, 1986; Armstrong & Eckert, 1987), the possibility that inactivation during exposure to 2-deoxy-D-glucose involved dephosphorylation catalyzed by an ATP- or cyclic AMP-dependent protein phosphatase was investigated using various protein phosphatase inhibitors.

The effect of protein phosphatase inhibitors on changes in Ca^{2+} current inactivation induced by intracellular photorelease of ATP

Protein phosphorylation is a cellular mechanism which appears to underlie the regulation of numerous physiological processes including neurotransmitter release, cellular metabolism and the transduction of intracellular second messenger effects (Levitan, 1985; Hemmings *et al.*, 1989; Nairn & Shenolikar, 1992). The regulation of these processes depends upon a balance between substrate phosphorylation, mediated by a variety of protein kinases, and dephosphorylation, produced by the action of protein phosphatases. Serine-threonine protein phosphatases have been classified by Cohen (1989) and include a cyclic AMP-dependent protein phosphatase, PP-1, and a Ca^{2+}-calmodulin-dependent protein phosphatase, PP-2B, otherwise known as calcineurin, which represents up to 1% of total brain protein (Cohen, 1989). One of the most specific substrates for PP-2B appears to be an endogenous inhibitor of PP-1, named inhibitor-1. Thus PP-2B may activate PP-1 by dephosphorylation of this inhibitor, allowing Ca^{2+}-activated signals to alter the actions of cyclic AMP-dependent processes.

Voltage-activated Ca^{2+} channels require phosphorylation for normal function (Armstrong & Eckert, 1987) while the inactivation process may, in part, be mediated by PP-2B, calcineurin (Armstrong, 1989). In the light of the increased inactivation rates of voltage-activated Ca^{2+} currents seen after photorelease of ATP and cyclic AMP, the effects of protein phosphatase inhibitors on Ca^{2+} current inactivation were studied, after the photorelease of ATP.

Inhibition of protein phosphatase-2B (calcineurin)

Cyclosporin A was originally isolated from the fungus *Tolypocladium inflatum*, and it binds to a cytosolic protein, cyclophilin A. Cyclophilin A is one of a class of highly conserved immunophilin proteins, found in all eukaryotic cells (Walsh *et al.*, 1992), which have *cis-trans*-peptidylprolyl isomerase activity, involved in protein folding. However, the cyclosporin-cyclophilin complex appears to affect signal transduction pathways in both lymphocytes and neurones by inhibition of the serine-threonine protein phosphatase-2B, calcineurin with IC_{50}s in the range 40–120 nM (Sigal & Dumont, 1992; Walsh *et al.*, 1992).

Cyclosporin A and cyclophilin A were used to study the effect of inhibition of calcineurin in DRG neurones in the presence of 2-deoxy-D-glucose. The same voltage and flash photolysis protocol was used as previously described. The inactivation rate of high voltage-activated Ca^{2+} currents was again evaluated by fitting a double exponential curve to the currents and obtaining two time constants τ_1 and τ_2. Initial experiments were performed with both cyclosporin A and cyclophilin A, made up in ATP-free patch pipette solution, but with 'caged' ATP (1 mM) present. The data in Table 2 demonstrate that the inactivation time constants were lower under these conditions but that they did not change significantly during the course of the successive currents, suggesting that the ATP-dependent inactivation was slower or prevented in the presence of cyclosporin A and cyclophilin A. In other words, inhibition of calcineurin attenuated the ATP-dependent component of Ca^{2+} current inactivation seen in neurones metabolically stressed by 2-deoxy-D-glucose. This suggested that a PP-2B-mediated mechanism may be involved in the inactivation process under these conditions.

Table 1 Effect of intracellular photoreleased cyclic AMP (40 μM) on Ca^{2+} current inactivation during exposure to 2-deoxy-D-glucose ($n = 11$)

Step No.	I_{max}/nA	I_{end}/nA	τ_1/ms	τ_2/ms
1 (pre-flash) 3 × 200 V flashes	−1.59 ± 0.18	−0.65 ± 0.09	65 ± 10	757 ± 128
1 min	−1.36 ± 0.16	−0.46 ± 0.07	44 ± 5*	585 ± 74
2 min	−1.22 ± 0.16	−0.43 ± 0.06	49 ± 5	584 ± 80
3 min	−1.12 ± 0.15	−0.35 ± 0.06	46 ± 7*	532 ± 67*

*$P < 0.05$ when compared with pre-flash value.
I_{max} and I_{end} are the mean values for the high voltage-activated Ca^{2+} current measured at the peak and at the end of the 500 ms voltage step command respectively.

Table 2 Effect of intracellular cyclosporin A (14 nM) and cyclophilin A (50 nM) on ATP-dependent Ca^{2+} current inactivation during exposure to 2-deoxy-D-glucose ($n = 7$)

Step No.	I_{max}	I_{end}	τ_1	τ_2
1 (pre-flash) 3 × 200 V flashes	−2.25 ± 0.23	−0.75 ± 0.16	39 ± 6	486 ± 92
2	−2.04 ± 0.20	−0.53 ± 0.16	43 ± 6	507 ± 82
3	−1.94 ± 0.20	−0.44 ± 0.15	42 ± 4	468 ± 73
4	−1.95 ± 0.20	−0.46 ± 0.14	38 ± 5	484 ± 71

I_{max} and I_{end} are the mean values for the high voltage-activated Ca^{2+} current measured at the peak and at the end of the 500 ms voltage step command respectively.

As internal controls, experiments using an identical protocol were performed, using either cyclosporin A alone or cyclophilin A alone. Exposure to cyclosporin A alone also attenuated the ATP-mediated Ca^{2+} current inactivation process ($n = 5$). This may imply that the cells were able to provide their endogenous cyclophilin in order to produce the effect on Ca^{2+} current inactivation. However, when cyclophilin A alone was used, the ATP-dependent inactivation was also still seen to be slowed or prevented over the course of the successive steps ($n = 6$). It would appear that under conditions of metabolic stress, (exposure to 2-deoxy-D-glucose), the ATP-dependent increase in inactivation rate of Ca^{2+} current can be reduced by cyclosporin A or by cyclophilin A both when present together and independently. One possible explanation for this may lie in the fact that cyclophilins are ubiquitous proteins which may have an, as yet unidentified, endogenous ligand.

As a result of the above observations we investigated whether an inhibitor of other protein phosphatases altered the ATP-induced inactivation of Ca^{2+} currents in metabolically stressed DRG neurones.

Inhibition of protein phosphatases-1 and 2A: the effects of calyculin A on voltage-activated Ca^{2+} currents

Calyculin A is isolated from the marine sponge *Discodermia calyx* (Kato *et al.*, 1986), and is a highly potent inhibitor of both PP-1 and PP-2A (Ishihara *et al.*, 1989). Low pressure ejection of calyculin A (2.5 nM) for 3–5 min caused a significant increase in the mean amplitude of the Ca^{2+} current when 100 ms voltage step commands were applied to cells held at a V_h of −90 mV and stepped to a V_c of 0 mV, in the presence of recording medium which containing 2-deoxy-D-glucose (Figure 3). The mean increase in I_{max} was by 26% and that in I_{end} was by 30%, and after removal of the pressure ejection pipette the Ca^{2+} current returned to its original level.

In order to assess the contribution of PP-1 to the ATP/cyclic AMP-dependent Ca^{2+} channel inactivation observed in the presence of 2-deoxy-D-glucose (5 mM), the inactivation rates of Ca^{2+} currents were evaluated in the presence of calyculin A (2.5 nM) before and after the photorelease of 'caged' ATP. An identical voltage and flash photolysis protocol was followed to that used in previous experiments. The inactivation rates were again evaluated by fitting a double exponential decay curve to 500 ms high voltage-activated Ca^{2+} currents.

Despite some reduction in the Ca^{2+} current amplitude, the inactivation time constants were reduced significantly by the third min after the photorelease of ATP. In other words, calyculin A failed to inhibit the action of photoreleased ATP on Ca^{2+} current inactivation (Table 3). PP-1 and PP-2A therefore did not appear to play a role in the ATP/cyclic AMP-dependent inactivation seen during exposure to 2-deoxy-D-glucose.

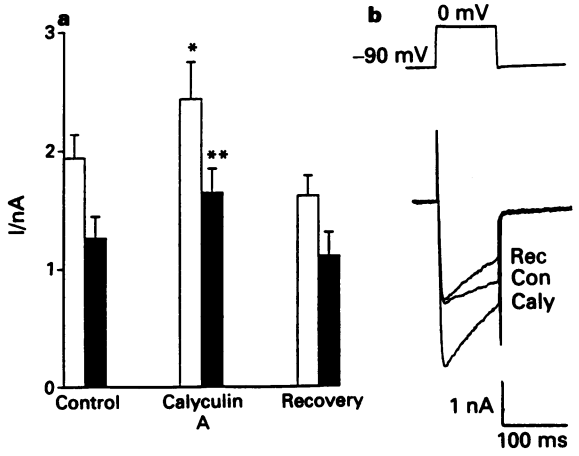


Figure 3 The effect of calyculin A on voltage-activated Ca^{2+} currents recorded in the presence of 2-deoxy-D-glucose. (a) Figure showing the effect of extracellular application of 2.5 nM calyculin A for 3–5 min on high voltage-activated Ca^{2+} currents in the presence of 2-deoxy-D-glucose (5 mM). Both the maximum Ca^{2+} current (open columns) and the Ca^{2+} current measured at the end of the 100 ms voltage step command (solid columns) were increased and returned to control levels 5 min after removal of the pressure ejection pipette. The data are the mean ± s.e.mean for 8 cells. *$P < 0.05$ and **$P < 0.005$ compared with control values. (b) Traces showing the reversible action of calyculin A (2.5 nM) on high voltage-activated Ca^{2+} currents. A 100 ms depolarizing voltage step command from a holding potential of −90 mV to 0 mV activated a calcium current (Con) which was increased by calyculin A (Caly), but recovered (Rec) 5 min after removal of the pressure ejection pipette.

Table 3 Effect of intracellular photoreleased ATP (≈300 μM) on Ca^{2+} current inactivation in the presence of calyculin A (2.5 nM) and 2-deoxy-D-glucose ($n = 6$)

Step No.	I_{max}	I_{end}	τ_1	τ_2
1 (pre-flash) 3 × 200 V flashes	−1.52 ± 0.31	−0.36 ± 0.07	39 ± 7	396 ± 71
2	−1.23 ± 0.29*	−0.29 ± 0.07	33 ± 5	386 ± 54
3	−1.10 ± 0.29**	−0.22 ± 0.04*	31 ± 5	335 ± 46
4	−1.01 ± 0.28***	−0.16 ± 0.05**	28 ± 5*	286 ± 64**

*$P<0.05$, **$P<0.01$, and ***$P<0.001$ when compared with pre-flash values.
I_{max} and I_{end} are the mean values for the high voltage-activated Ca^{2+} current measured at the peak and at the end of the 500 ms voltage step command respectively.

Discussion

As previously reported, cultured DRG neurones can be metabolically stressed with 2-deoxy-D-glucose so that Ca^{2+} homeostatic mechanisms are attenuated as indicated by the slowed rate of the decay of Ca^{2+}-activated Cl^- tail currents (Stapleton *et al.*, 1994). This effect of metabolic stress can be reversed by D-fructose 1,6-diphosphate and intracellular photorelease of ATP. Flash photolysis experiments showed that ATP also increased Ca^{2+} current inactivation.

The intracellular photorelease of cyclic AMP as well as ATP caused an increase in the rate of inactivation of high voltage-activated Ca^{2+} currents in metabolically stressed cultured DRG neurones. Inhibition of PP-1 and PP-2A increased the amplitude of Ca^{2+} currents but did not prevent the change in inactivation rate seen on photorelease of ATP. However, inhibition of PP-2B (calcineurin) was able to prevent this effect.

This finding was in keeping with the known requirement of L-type Ca^{2+} channels to be phosphorylated for their normal function via a cyclic AMP-dependent protein kinase (Armstrong & Eckert, 1987). Since a protein phosphatase mechanism is thought to be involved in Ca^{2+} current inactivation, the effects of calyculin A, an inhibitor of the cyclic AMP-dependent protein phosphatases, PP-1 and PP-2A, was studied in this system. Calyculin A itself was found to enhance Ca^{2+} currents in metabolically stressed DRG neurones. This was in agreement with the finding that calyculin A and okadaic acid, another PP-1 and PP-2A inhibitor increased Ca^{2+} currents in guinea-pig cardiac myocytes (Hescheler *et al.*, 1988) and guinea-pig taenia coli smooth muscle cells (Usuki *et al.*, 1991). However, in some studies a reduction in Ca^{2+} current with calyculin A was observed (Ward *et al.*, 1991), while Obara & Yabu (1993) found an increase in Ca^{2+} currents in guinea-pig intestinal smooth muscle at nanomolar concentrations and higher but inhibition at subnanomolar concentrations. The biphasic response has been attributed to differential effects of calyculin A on PP-1 and PP-2A. Further, in the absence of ATP in the patch pipette solution Obara & Yabu (1993) found no effect of calyculin A or okadaic acid on Ca^{2+} currents (Obara & Yabu, 1993). Both PP-1 and PP-2A modulate the Ca^{2+} channels in these systems but the precise role of each remains to be determined.

Although calyculin A enhanced Ca^{2+} currents in the present study, it did not prevent the ATP-dependent inactivation of Ca^{2+} currents, implying that a PP-1 or PP-2A mediated mechanism was not involved. The possibility of a calcineurin (PP-2B) mediated process was therefore investigated with the cyclosporin A-cyclophilin A complex which inhibits calcineurin. Previously cyclosporin A and cyclophilin together have been shown to reduce desensitization of 5-HT_3 receptors in NG108-15 cells. This has been suggested to involve a Ca^{2+} and calcineurin-mediated process which controls receptor availability (Arbuckle *et al.*, 1993). In our study this complex prevented the ATP-dependent inactivation of Ca^{2+} currents. The Ca^{2+}-calmodulin-dependent protein phosphatase, calcineurin has previously been implicated in the Ca^{2+}-dependent inactivation process, since its perfusion into *Helix* neurones caused a substantial increase in the rate of Ca^{2+} current inactivation (Chad & Eckert, 1986).

Surprisingly, not only could the ATP-dependent inactivation of Ca^{2+} current be prevented by the cyclosporin A-cyclophilin A complex together but also by each component of the complex separately. Cyclophilins are ubiquitous proteins and therefore the endogenous cyclophilins of the DRG neurones may be active when cyclosporin A alone is provided in the patch pipette solution. An explanation for the effect of cyclophilin A alone is more difficult but the exogenous cyclophilin A itself may enhance the activity of endogenous, unidentified cyclophilin ligands.

L-type Ca^{2+} channels appear to exist in three different modes of activation, each mode being characterized by changes in the phosphorylation state of the channel (Hess *et al.*, 1984; Nowycky *et al.*, 1985; Armstrong *et al.*, 1991). It is clear, from recent studies on cardiac myocytes, that the activity of protein kinases and phosphatases plays an important role in the transformation between different kinetic states of the channel (Frace & Hartzell, 1993; Ono & Fozzard, 1993). Calcium channels have several potential phosphorylation sites and each may be regulated by different phosphatases and kinases. The situation in neurones is still less clear, although the same general regulatory mechanisms exist. Whether other high voltage-activated Ca^{2+} currents (N- and P-type currents) in neurones are regulated in a similar fashion and whether multiple kinetic states exist remains to be determined. The results of this study demonstrate a further modulatory pathway, namely ATP-dependent inactivation, which is revealed only on reintroducing ATP or cyclic AMP to cells exposed to metabolic stress when the dynamic balance of phosphorylation and dephosphorylation may have been altered. Since cellular phosphatases are themselves regulated by phosphorylation and dephosphorylation, it is possible that the mechanism underlying the involvement of calcineurin in the ATP-dependent inactivation involves phosphorylation and subsequent activation of an endogenous regulatory component of this phosphatase. Endogenous regulation of PP-1 activity by cyclic AMP has been found to modulate the interaction between Ca^{2+} channels and G-proteins in DRG neurones (Dolphin, 1992). However an additional consideration is that in *Lymnaea* neurones Johnson & Byerly (1993) did not demonstrate Ca^{2+} channel regulation by phosphorylation and suggested that Ca^{2+} channel inactivation may be mediated by an interaction of the channel with components of the cytoskeleton, under regulation by both Ca^{2+} and ATP. A further possibility is that after exposure to metabolic stress the photorelease of ATP may selectively activate a population of Ca^{2+} channels with faster inactivation kinetics than those seen under 'standard' conditions.

In conclusion our data suggests that a consequence of metabolic stress is that calcineurin is less efficient at mediating the Ca^{2+}-dependent inactivation of high voltage-activated Ca^{2+} currents. As a result greater Ca^{2+} entry may occur by this pathway in metabolically stressed neurones when cellular mechanisms for handling intracellular Ca^{2+} loads are compromised. This further raises the possibility that high voltage-activated Ca^{2+} channels play a role in

intracellular Ca^{2+} overload which causes neuronal damage to neurones when metabolism is attenuated.

The authors thank the Wellcome Trust, Nuffield Foundation and London University Central Research Fund for financial support. We also thank Dr A. Hughes for the computer programme used to calculate free calcium concentrations, and Drs R. Ziegler, T.J. Petcher and M. Zurini of Preclinical Research, Sandoz Pharma Ltd. for the very generous gift of cyclosporin A and human recombinant cyclophilin A.

References

ARBUCKLE, J.B., MIEGEL, I., BODDEKE, H.W.G.M. & DOCHERTY, R.J. (1993). Inhibition of calcineurin reduces desensitization of 5-HT_3 receptors in NG108-15 neuroblastoma × glioma hybrid cells. *J. Physiol.*, **473**, 267P.

ARMSTRONG, D.L. (1989). Calcium channel regulation by calcineurin, a Ca^{2+}-activated phosphatase in mammalian brain. *Trends Neurosci.*, **12**, 117–122.

ARMSTRONG, D. & ECKERT, R. (1987). Voltage-activated calcium channels that must be phosphorylated to respond to membrane depolarisation. *Proc. Natl. Acad. Sci. U.S.A.*, **84**, 2518–2522.

ARMSTRONG, D.L., ROSSIER, M.F., SHCHERBATKO, A.D. & WHITE, R.E. (1991). Enzymatic gating of voltage-activated calcium channels. *Ann. NY Acad. Sci.*, **635**, 26–34.

CHAD, J.E. & ECKERT, R. (1984). Calcium domains associated with individual channels can account for anomalous voltage relations of Ca-dependent responses. *Biophs. J.*, **45**, 993–999.

CHAD, J.E. & ECKERT, R. (1986). An enzymatic mechanism for calcium current inactivation in dialysed *Helix* neurones. *J. Physiol.*, **378**, 31–51.

COHEN, P. (1989). The structure and regulation of protein phosphatases. *Annu. Rev. Biochem.*, **58**, 453–508.

CURRIE, K.P.M. & SCOTT, R.H. (1992). Calcium-activated currents in cultured neurones from rat dorsal root ganglia. *Br. J. Pharmacol.*, **106**, 593–602.

CURRIE, K.P.M., WOOTTON, J.F. & SCOTT, R.H. (1995). Activation of Ca^{2+}-dependent Cl^- currents in cultured rat sensory neurones by flash photolysis of DM-nitrophen. *J. Physiol.* (in press).

DOLPHIN, A.C. (1992). The effect of phosphatase inhibitors and agents increasing cAMP-dependent phosphorylation on calcium channel currents in cultured rat dorsal root ganglion neurones: interaction with the effect of G-protein activation. *Pflügers Arch.*, **421**, 138–145.

DUBINSKY, J.M. & ROTHMAN, S.M. (1991). Intracellular calcium concentrations during 'chemical hypoxia' and excitotoxic neuronal injury. *J. Neurosci.*, **11**, 2545–2551.

DUCHEN, M.R. (1990). Effects of metabolic inhibition on the membrane properties of isolated mouse primary sensory neurones. *J. Physiol.*, **424**, 387–409.

DUCHEN, M.R., VALDEOLMILLOS, M., O'NEILL, S.C. & EISNER, D.A. (1990). Effects of metabolic blockade on the regulation of intracellular calcium in dissociated mouse sensory neurones. *J. Physiol.*, **424**, 411–426.

FRACE, A.M. & HARTZELL, H.C. (1993). Opposite effects of phosphatase inhibitors on L-type calcium and delayed rectifier currents in frog cardiac myocytes. *J. Physiol.*, **472**, 305–326.

GODFRAIND, J.M., KAWAMURA, H., KRNJEVIC, K. & PUMAIN, R. (1971). Actions of dinitrophenol and some other metabolic inhibitors on cortical neurones. *J. Physiol.*, **215**, 199–222.

HAMILL, O.P., MARTY, A., NEHER, E., SAKMANN, B. & SIGWORTH, F.J. (1981). Improved patch-clamp techniques for high-resolution current recordings from cells and cell-free membrane patches. *Pflügers Arch.*, **391**, 85–100.

HEMMINGS, H.C., NAIRN, A.C., MCGUINNESS, T.L., HUGANIR, R.L. & GREENGARD, P. (1989). Role of protein phosphorylation in neuronal signal transduction. *FASEB J.*, **3**, 1583–1592.

HESCHELER, J., MIESKES, G., RÜEGG, J.C., TAKAI, A. & TRAUTWEIN, W. (1988). Effects of a protein phosphatase inhibitor, okadaic acid, on membrane currents of isolated guinea-pig cardiac myocytes. *Pflügers Arch.*, **412**, 248–252.

HESS, P., LANSMAN, J.B. & TSIEN, R.W. (1984). Different modes of Ca channel gating behaviour favoured by dihydropyridine Ca agonists and antagonists. *Nature*, **311**, 538–544.

ISHIHARA, H., MARTIN, B.L., BRAUTIGAN, D.L., KARAKI, H., OZAKI, H., KATO, Y., FUSETANI, N., WATABE, S., HASHIMOTO, K., UEMURA, D. & HARTSHORNE, D.J. (1989). Calyculin A and okadaic acid: inhibitors of protein phosphatase activity. *Biochem. Biophys. Res. Commun.*, **159**, 871–877.

JOHNSON, B.D. & BYERLY, L. (1993). A cytoskeletal mechanism for Ca^{2+} channel metabolic dependence and inactivation by intracellular Ca^{2+}. *Neuron*, **10**, 797–804.

KASS, I.S. & LIPTON, P. (1986). Calcium and long-term transmission damage following anoxia in dentate gyrus and CA1 regions of the rat hippocampal slice. *J. Physiol.*, **378**, 313–334.

KATO, Y., FUSETANI, N., MATSUNAGA, S. & HASHIMOTO, K. (1986). Calyculin A, a novel antitumour metabolite from the sponge *Discodermia* calyx. *J. Am. Chem. Soc.*, **108**, 2780–2781.

LEBLOND, J. & KRNJEVIC, K. (1989). Hypoxic changes in hippocampal neurons. *J. Neurophysiol.*, **62**, 1–14.

LEVITAN, I.B. (1985). Phosphorylation of ion channels. *J. Memb. Biol.*, **87**, 177–190.

MAYER, M.L. (1985). A calcium-activated chloride current generates the after-depolarisation in rat sensory neurones in culture. *J. Physiol.*, **364**, 217–239.

NAIRN, A.C. & SHENOLIKAR, S. (1992). The role of protein phosphatases in synaptic transmission, plasticity and neuronal development. *Curr. Opin. Neurobiol.*, **2**, 296–301.

NOWYCKY, M.C., FOX, A.P. & TSIEN, R.W. (1985). Long-opening mode of gating of neuronal calcium channels and its promotion by the dihydropyridine calcium agonist Bay K 8644. *Proc. Natl. Acad. Sci. U.S.A.*, **82**, 2178–2182.

OBARA, K. & YABU, H. (1993). Dual effect of phosphatase inhibitors on calcium channels in intestinal smooth muscle cells. *Am. J. Physiol.*, **264**, C296–C301.

ONO, K. & FOZZARD, H.A. (1993). Two phosphatase sites on the Ca^{2+} channel affecting different kinetic functions. *J. Physiol.*, **470**, 73–84.

SCOTT, R.H., SUTTON, K.G., GRIFFIN, A., STAPLETON, S.R. & CURRIE, K.P.M. (1995). Aspects of calcium-activated chloride currents: a neuronal perspective. *Pharmacol. Ther.*, (in press).

SIGAL, N.H. & DUMONT, F.J. (1992). Cyclosporin A, FK-506, and rapamycin: pharmacologic probes of lymphocyte signal transduction. *Annu. Rev. Immunol.*, **10**, 519–560.

SILVER, I.A. & ERECÍNSKA, M. (1990). Intracellular and extracellular changes of $[Ca^{2+}]$ in hypoxia and ischaemia in rat brain *in vivo*. *J. Gen. Physiol.*, **95**, 837–866.

STAPLETON, S.R., CURRIE, K.P.M., SCOTT, R.H. & BELL, B.A. (1992). Palmitoyl-DL-carnitine has Ca^{2+}-dependent effects on cultured neurones from rat dorsal root ganglia. *Br. J. Pharmacol.*, **107**, 1192–1197.

STAPLETON, S.R., SCOTT, R.H. & BELL, B.A. (1994). Effects of metabolic blockers on Ca^{2+}-dependent currents in cultured sensory neurones from neonatal rats. *Br. J. Pharmacol.*, **111**, 57–64.

SUGANUMA, M., FUJIKI, H., FURUYA-SUGURI, H., YOSHIZAWA, S., YASUMOTO, S., KATO, Y., FUSETANI, N. & SUGIMURA, T. (1990). Calyculin A, an inhibitor of protein phosphatases, a potent tumour promoter on CD-1 mouse skin. *Cancer Res.*, **50**, 3521–3525.

USUKI, T., OBARA, K., SOMEYA, T., OZAKI, H., KARAKI, H., FUSETANI, N. & YABU, H. (1991). Calyculin A increases voltage-dependent inward current in smooth muscle cells isolated from guinea pig taenia coli. *Experienta*, **47**, 939–941.

WALKER, J.W., REID, G.P., MCCRAY, J.A. & TRENTHAM, D.R. (1988). Photolabile 1-(2-nitrophenyl) ethyl phosphate esters of adenine nucleotide analogues. Synthesis and mechanism of photolysis. *J. Am. Chem. Soc.*, **110**, 7170–7177.

WALSH, C.T., ZYDOWSKY, L.D. & MCKEON, F.D. (1992). Cyclosporin A, the cyclophilin class of peptidylprolyl isomerases, and blockade of T-cell signal transduction. *J. Biol. Chem.*, **267**, 13115–13118.

WARD, S.M. VOGALIS, F., BLONDFIELD, D.P., OZAKI, H., FUSETANI, N., UEMURA, D., PUBLICOVER, N.G. & SANDERS, K.M. (1991). Inhibition of electrical slow waves and Ca^{2+} currents of gastric and colonic smooth muscle by phosphatase inhibitors. *Am. J. Physiol.*, **261**, C64–C70.

WOOTTON, J.F. & TRENTHAM, D.R. (1989). 'Caged' compounds to probe the dynamics of cellular processes: synthesis and properties of some novel photosensitive P-2-nitrobenzyl esters of nucleotides. In *Photochemical Probes in Biochemistry*, NATO ASI series C. **272**, 277–296.

(Received July 18, 1994
Revised September 28, 1994
Accepted September 30, 1994)

British Journal of Pharmacology (1995) 114, 551-557 © 1995 Stockton Press All rights reserved 0007-1188/95 $9.00

Secretion of endothelin-1 and endothelin-3 by human cultured vascular smooth muscle cells

Julie C.M. Yu & [1]Anthony P. Davenport

Clinical Pharmacology Unit, University of Cambridge, Addenbrooke's Hospital, Cambridge CB2 2QQ

1 It is generally accepted that endothelial cells secrete endothelin (ET) to the underlying media which mediates the contractile effects of ET. However, there is some evidence that animal vascular smooth muscle cells (VSMCs) also secrete ET. We cultured VSMCs from human vessels representative of a number of different vascular beds to determine whether human VSMCs endogenously secrete ET.

2 VSMCs explanted from adult arterial vessels secrete picomolar quantities of immunoreactive mature ET: coronary artery 226.6 ± 58.8 pM/10^6 cells (n = 7), thoracic aorta 169.5 ± 105.4 pM/10^6 cells (n = 3), left internal mammary artery 102.4 ± 23.1 pM/10^6 cells (n = 3) and saphenous vein 69.4 ± 19.9 pM/10^6 cells (n = 3), as well as from umbilical vein (HUVSMCs) 38.3 ± 4.3 pM/10^6 cells (n = 3). Secretion of immunoreactive big ET-1 was also detected: coronary artery 249.1 ± 59.4 pM/10^6 cells (n = 7), thoracic aorta 120.0 ± 13.4 pM/10^6 cells (n = 3), left internal mammary artery 170.0 ± 68.2 pM/10^6 cells (n = 3), saphenous vein 105.1 ± 30.7 pM/10^6 cells (n = 3) and from umbilical vein 146.3 ± 7.4 pM/10^6 cells (n = 3). Comparable, intracellular levels of immunoreactive big ET-1 and mature ET were also detected in cultured VSMCs.

3 Since enzyme-dispersed VSMCs are thought to be more differentiated and more closely resemble their *in vivo* counterparts, and these enzyme-dispersed VSMCs from human umbilical vein (HUVSMCs) also secreted the greatest levels of immunoreactive peptides, they were characterized further. Reverse transcription-polymerase chain reaction assay demonstrated that HUVSMCs express ET-1 mRNA. High performance liquid chromatography coupled to radioimmunoassay revealed that HUVSMCs secrete ET-1 and ET-3, in addition to big ET-1. However, levels of ET are not altered by 100 μM phosphoramidon, an inhibitor of metalloproteases or by 100 μM pepstatin A, an aspartyl protease inhibitor.

4 In concordance, K_D and B_{max} values for [^{125}I]-ET-1 saturation binding are not altered in HUVSMC cultures incubated for 24 h with 100 μM phosphoramidon (431 ± 218 pM and 31.1 ± 12.7 fmol mg^{-1}; mean ± s.e.mean, n = 3) or 100 μM pepstatin A (381 ± 169 pM and 19.9 ± 7.8 fmol mg^{-1}, n = 3) as compared to controls (355 ± 99 pM and 33.3 ± 9.3 fmol mg^{-1}; n = 3). This observation indicates the absence of an autocrine 'unmasking' effect for ET receptors.

5 HUVSMCs synthesize and secrete immunoreactive ET-1, ET-3 and big ET-1, and possess intracellular levels of immunoreactive mature ET and big ET-1. There is some evidence of common cellular mechanisms between growth factors and vasoconstrictor peptides, suggesting a close relationship between contraction and proliferation. Since the development of various vascular pathologies such as atherosclerosis, hypertension and after vessel injury has been attributed to alterations in the normal growth pattern of VSMCs, the role of ET in these diseases may be of significance.

Keywords: Human vascular smooth muscle; endothelin secretion; endothelin converting enzyme; phosphoramidon; pepstatin A

Introduction

The endothelins (ET-1, ET-2 and ET-3) are 21 amino acid peptides with potent and protracted vasoconstrictor activity (Yanagisawa *et al.*, 1988) which are all expressed in the human cardiovascular system (Plumpton *et al.*, 1993). Endothelins were first isolated from cultures of porcine endothelial cells (Yanagisawa *et al.*, 1988) but endothelins and their precursor have since been shown to be secreted from human endothelial cells, renal epithelial cell lines, endometrial cells, bronchial epithelial cells, and pleural mesothelial cells (Huggins *et al.*, 1993, for review). In the vasculature, it has been postulated that ET-1 and its precursor, big ET-1, are predominantly secreted by endothelial cells to the underlying media. However, it has been observed that rat and rabbit vascular smooth muscle cells (VSMCs) also secrete various isoforms of mature ET (Kanse *et al.*,1991). The induction of ET mRNA and peptide was also demonstrated in human omental VSMCs (Resink *et al.*, 1990).

Mature ETs are generated from big ET precursors by unusual proteolytic processing between Trp 73 and Val 74 with the possible involvement of an 'endothelin-converting enzyme' (ECE). Numerous conflicting theories have arisen regarding the identity of the ECE(s), but there is substantial evidence that the enzyme can be inhibited by phosphoramidon, a metalloproteinase inhibitor. Phosphoramidon blocks both exogenous and endogenous big ET-1 conversion in bovine aortic endothelial cells (Corder *et al.*, 1993) while phosphoramidon studies in rat *in vitro* provides evidence that big ET-1 conversion occurs outside the vessel lumen (Corder & Vane, 1994). The ECE in bovine and porcine smooth muscle also appears to be sensitive to phosphoramidon (Hioki *et al.*, 1991; Matsumura *et al.*, 1990; 1991; Tsukahara *et al.*, 1993). More recently, Murphy *et al.* (1994) compared the ECE potential of two phosphoramidon-sensitive peptidases, endopeptidase-24.11 and bacterial thermolysin. *In vivo* studies also favour a phosphoramidon-sensitive protease as the putative ECE. McMahon *et al.* (1991) demonstrated that phosphoramidon prevents the pressor activity of big ET-1 in both Wistar-Kyoto and spontaneously hypertensive rats. Lastly, big ET-1 conversion was shown to be inhibited by 12 mM phosphoramidon in human umbilical vein endothelial cells (HUVECs) which led to increased specific binding of radiolabelled ET-1 (Fujitani *et al.*, 1992). Thus, it has been

[1] Author for correspondence at: Clinical Pharmacology Unit, University of Cambridge, Box 110, F & G Block, Level 2, Addenbrooke's Hospital, Cambridge, CB2 2QQ.

hypothesized that autocrine ET secretion 'masks' ET receptors, so that inhibition of big ET-1 conversion would reveal more ET-1 receptors in binding studies.

Since it is hypothesized that ET secretion from the endothelium to the underlying media elicits the contractile effects of ET, the aim of our study was to determine whether endogenous secretion of ET occurs in VSMCs cultured from human vessels susceptible to abnormal VSMC function. Vessels representative of a number of different vascular beds were cultured to determine ET secretion in both adult and neonates, whose developing vasculature may be expressing a plethora of genes including the gene for ET, and from both arteries and veins, where the former requires stronger tonic contractions. VSMCs were cultured using the explant method or by enzyme dispersion. Since enzyme-dispersed HUVSMCs produced the highest levels of peptides, and are thought to resemble more closely their *in vivo* counterpart, these were further characterized: ET-1 messenger RNA was detected in HUVSMCs using reverse transcription and polymerase chain reaction. High performance liquid chromatography (h.p.l.c.) coupled to radioimmunoassay (RIA) was used to identify the mature ET isoform secreted, and levels of mature ET secretion were determined in the presence and absence of phospohoramidon, or pepstatin A. Finally, the effect of phosphoramidon and pepstatin A on K_D and B_{max} values for ET-1 binding were determined. A preliminary account of this work has been presented to the British Pharmacological Society (Yu & Davenport, 1994).

Methods

Tissue collection

Untraumatized human umbilical veins were collected within 24–48 h post-parturition from the Rosie Maternity Hospital, Cambridge. Epicardial coronary arteries and thoracic aortae were obtained from heart transplant patients, while left internal mammary arteries and saphenous vein were obtained from patients undergoing bypass surgery, at Papworth Hospital, Cambridge.

Cell culture

Vessels were opened transversely, the endothelium removed by gently scraping the intimal surface with a scalpel blade, and cut into approximately 0.5 cm^2 portions. To obtain HUVSMC cultures by enzyme dispersion, the endothelium was removed from veins of untraumatized human umbilical cords by an initial enzyme dispersion with collagenase type II at 1 mg ml^{-1} (Sigma Chemical, Dorset, U.K.). The endothelial cells (HUVECs) were cultured for subsequent comparison during immunocytochemistry and fluorescence-activated cell sorting. After the removal of endothelial cells, a subsequent enzyme dispersion was performed to obtain smooth muscle cells as previously described (Gimbrone & Cotran, 1975). All VSMC cultures were maintained in complete medium (Medium 199 (Gibco BRL, Paisley, Scotland) supplemented with 50 iu ml^{-1} penicillin, 50 μg ml^{-1} streptomycin, 2.5 μg ml^{-1} amphotericin B) containing 15% heat-treated foetal calf serum (Seralab, Sussex, U.K.). Culture medium was changed two to three times per week. All cell growth occurred in a humidified incubator at 37°C in which the atmosphere was equilibrated with 5% CO_2.

Characterization of VSMC cultures

The cultured VSMCs displayed a 'hill-and-valley' morphology typical of smooth muscle cells. Since HUVSMCs were used for further studies, these cultures were further characterized by immunocytochemistry and fluorescence-activated cell sorting (FACS).

For immunocytochemical studies, HUVECs and HUVSMCs were stained for von Willebrand factor (vWF) (Dako, High Wycombe, Buckinghamshire, U.K.) and for smooth muscle α-actin (Sigma). Secondary antibodies conjugated to fluorescein isothiocyanate (FITC) or the peroxidase anti-peroxidase immune complex method, was employed to visualize the staining patterns. Propidium iodide was used to counterstain nuclei. Immunoreactive (IR) vWF was distributed on endothelial cells in a typical punctate pattern, but endothelial cells did not stain for α-actin. Conversely, IR vWF was not detectable on HUVSMCs while α-actin was distributed as a filamentous network.

FACS was used to confirm that contamination of smooth muscle cell cultures by endothelial cells was not detectable. Single cell suspensions of HUVSMCs and HUVECs were obtained by trypsinization. The cell suspensions were stained for 15 min on ice, with primary rabbit antibodies against human vWF. The cells were washed twice with PBS, centrifuged and re-suspended. The suspensions were then stained for 15 min on ice, with goat anti-rabbit secondary antibodies conjugated to fluoroisothiocyanate. Cells were analysed for fluorescence with FACSort (Becton-Dickinson, Plymouth, U.K.). Results were further analysed using Lysis II (Becton-Dickinson) to determine that less than 1% of HUVSMCs stained for vWF.

Molecular biology

HUVSMCs were grown to confluence in gelatin-coated 75 cm^2 flasks (Galcon, Cowley, Oxford, U.K.). Total RNA was isolated by a guanidinium thiocyanate/isopropanol method with minor modifications (Chomczynski & Sacchi, 1987). Reverse transcription coupled with polymerase chain reaction was carried out as previously described (Nunez *et al.*, 1990). cDNA was generated using 10 μg of total RNA as template for hexanucleotide random primers, in a reaction mixture containing reverse transcription buffer (50 mM Tris-HCl pH 8.3, 10 mM $MgCl_2$, 75 mM KCl, 10 mM dithiothreitol, 0.1 mg ml^{-1} BSA), deoxynucleotides, 38 u human placental ribonuclease inhibitor (Pharmacia Fine Chemicals, Hertfordshire, U.K.), and 32 u cloned murine Maloney leukaemia virus reverse transcriptase (Pharmacia Fine Chemicals). Resulting cDNA (2.5 μl volume) was amplified using two specific human ET-1 primers (sense: 5'-TGC TCC-TGC TCG TCC CTG ATG GAT AAA GAG TGT GTC; anti-sense: 5'-GGT CAC ATA ACG CTC TCT GGA GGG CTT). The reaction mixture contained PCR buffer (Cambio, Cambridge, U.K.), 0.2 mM dNTPs, 25 pmol of each primer, and 1 u of cloned Taq polymerase (Cambio). PCR was performed for 40 cycles, with each cycle consisting of 2 min denaturation at 95°C, 45 s for primer annealing at 60°C and 2.5 min extension time at 72°C, with the final extension occurring for 10 min at 72°C. The PCR products were separated by electrophoresis on a 1% agarose gel and DNA fragment sizes were estimated by reference to a 1 kb DNA molecular weight standard.

Reverse phase high performance liquid chromatography and radioimmunoassay

Supernatants were solid-phase extracted as previously described (Davenport *et al.*, 1990). Briefly, ethyl silica mini-columns (Amprep C2; 500 mg; Amersham International plc, Amersham) were equilibrated by washing with methanol (2 ml). Supernatants collected from confluent cultures of HUVSMCs were acidified by the addition of 2 M HCl (1:0.25 ml, v v^{-1}), clarified by centrifugation for 10 min at 10,000 *g* and loaded onto the column. Each column was washed with 5 ml of 0.1% (v v^{-1}) trifluoroacetic acid and eluted with 0.1% (v v^{-1}) trifluoroacetic acid in 80% methanol. The eluant was dried down under vacuum centrifugation into polypropylene tubes and retained for radioimmunoassay.

To determine secreted levels of big ET-1 and mature ET, and to determine intracellular levels, supernatants of cultures were collected and the cells were washed twice with PBS. Cells were then trypsinized to obtain estimates of cell number in a haemocytometer. Cell membranes were permeabilized with 0.1% Triton X-100. The preparations were spun at 4,000 *g* for 5 min and the resulting supernatants were retained. These supernatants and the culture supernatants were directly radioimmunoassayed for mature ET and big ET-1 as previously described (Plumpton *et al.*, 1992). Briefly, the mature ET antisera were raised against the C-terminus of ET-1 [15-21] and showed 100% cross-reactivity with ET-2 and ET-3. Antisera against big ET-1 was raised against the C-terminus [31-38] and showed <0.007% cross-reactivity with the mature peptides (ET-1, ET-1 and ET-1), big ET-2 and big ET-3. The sensitivity of detection of both assays was 0.4 fmol/tube. The inter- and intra-assay variations were <13% in all cases.

To determine the effect of 100 μM phosphoramidon (Scientific Marketing Ass., Barnet, U.K.) or 100 μM pepstatin A (Sigma) on secretion of mature ET, HUVSMCs were incubated for 12 h in the absence or presence of either inhibitor. Culture medium was collected at designated intervals and directly assayed for big ET-1 and mature ET.

Saturation binding

HUVSMCs were plated onto a collagen-coated Costar 96-well strip plate with low evaporation lid (Cambridge, MA, U.S.A.) and grown to confluence. A Titertek Microplate Washer (ICN/Flow, High Wycombe, U.K.) was used to wash the cells. Saturation binding for HUVSMCs was carried out in the absence and the presence of 100 μM phosphoramidon or 100 μM pepstatin A for 24 h, using [^{125}I]-ET-1 (Amersham International, Little Chalfont, U.K.) as previously described (Davenport *et al.*, 1993). Dissociation constants and receptor density were estimated using EBDA (McPherson, 1983) and an iterative non-linear curve-fitting programme LIGAND (Munson & Rodbard, 1980).

Protein determinations

Protein concentrations of washed cells were estimated after solubilization (0.5 M NaOH and 1% sodium dodecyl sulphate) for 5 min at room temperature. The Bio-Rad Detergent Compatible 96-well microtiter plate method (BioRad Laboratories, Hertfordshire, U.K.) was used with bovine serum albumin as a reference standard.

Statistical analysis

There was no evidence for non-normality of the data using the Shapiro and Francia probability plot correlation test. RIA data and B_{max} values were analysed by one-way analysis of variance followed by Student's *t*-test for comparison of RIA data at each time point, $P < 0.05$. Results are given as mean ± s.e.mean.

Results

Secretion of big ET-1 and mature ET from explanted VSMCs

Cultures of explanted VSMCs from adult human vessels secreted comparable levels of immunoreactive ET: coronary artery 226.6 ± 58.8 pM/10^6 cells ($n = 7$), thoracic aorta 169.5 ± 105.4 pM/10^6 cells ($n = 3$), left internal mammary artery 102.4 ± 23.1 pM/10^6 cells ($n = 3$), and saphenous vein 69.4 ± 19.9 pM/10^6 cells ($n = 3$), as well as from umbilical vein (HUVSMCs) 38.3 ± 4.3 pM/10^6 cells ($n = 3$); each value represents mean ± s.e.mean of *n* different cultures. Secretion of immunoreactive big ET-1 was also detected: coronary

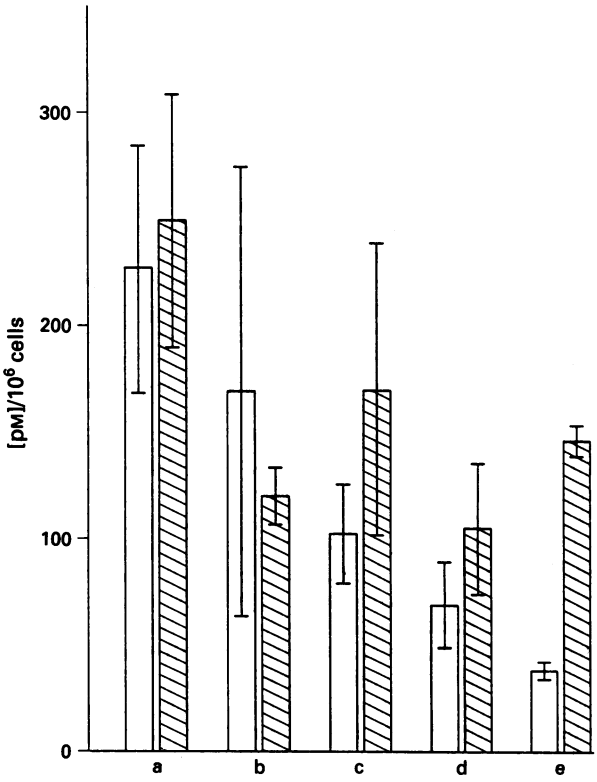


Figure 1 Levels of immunoreactive mature endothelin (ET) (open columns) and immunoreactive big ET-1 (hatched columns) secreted from VSMCs over a 72 h period, as determined by radioimmunoassay in (a) coronary artery, $n = 7$, (b) aorta, $n = 3$, (c) left internal mammary artery, $n = 3$, (d) saphenous vein, $n = 3$ and (e) umbilical vein, $n = 3$. Each value represents mean ± s.e.mean and is standardized to pM per 10^6 cells.

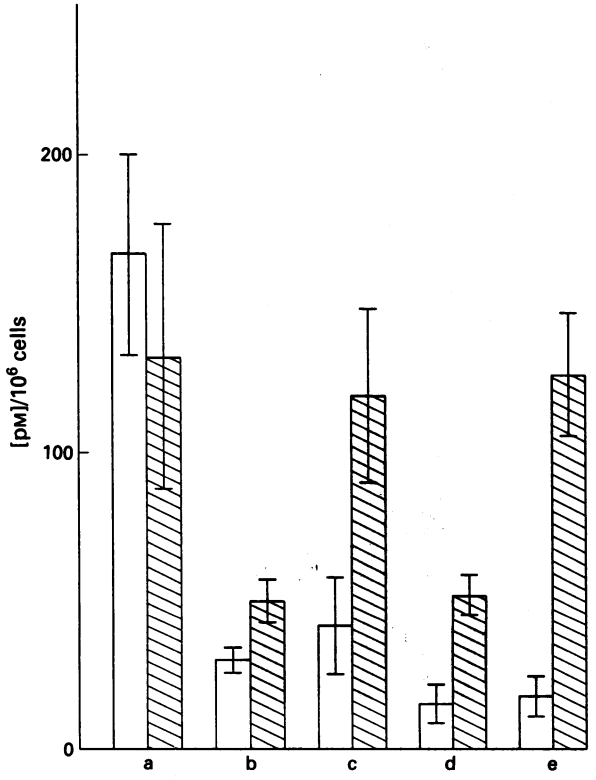


Figure 2 Intracellular levels of immunoreactive mature endothelin (ET) (open columns) and immunoreactive big ET-1 (hatched columns) in VSMCs over a 72 h period, as determined by radioimmunoassay in (a) coronary artery, $n = 7$, (b) aorta, $n = 3$, (c) left internal mammary artery, $n = 3$, (d) saphenous vein, $n = 3$ and (e) umbilical vein, $n = 3$. Each value represents mean ± s.e.mean and is standardized to pM per 10^6 cells.

artery 249.1 ± 59.4 pM/10^6 cells (n = 7), thoracic aorta 120.0 ± 13.4 pM/10^6 cells (n = 3), left internal mammary artery 170.0 ± 68.2 pM/10^6 cells (n = 3), saphenous vein 105.1 ± 30.7 pM/10^6 cells (n = 3) and umbilical vein 146.3 ± 7.4 pM/10^6 cells (n = 3); each value represents mean ± s.e.mean of n different cultures (Figure 1). The ubiquitous secretion of immunoreactive big ET-1 and mature ET from the VSMC cultures indicate that secretion was not restricted to foetal or arterial or pathophysiological SMCs. In comparison to secretion from VSMCs, endothelial cells cultured from umbilical vein secreted higher levels of ET (1469 ± 217 pM/10^6 cells, n = 3) and big ET-1 (564 ± 199 pM/10^6 cells, n = 3); each value represents mean ± s.e.mean. As demonstrated in Figure 2, intracellular irET in addition to irbig ET-1 was detected from all VSMC explant cultures by RIA: coronary artery irET: 166.6 ± 33.5 irbigET-1; 132.2 ± 44.3 pM/10^6 cells (n = 7), thoracic aorta irET: 30.0 ± 4.3 irbigET-1: 50.6 ± 7.5 pM/10^6 cells (n = 3), left internal mammary artery irET: 42.0 ± 16.8 irbigET-1: 119.2 ± 29.2 pM/10^6 cells (n = 3), saphenous vein irET: 15.2 ± 6.5 irbigET-1: 52.5 ± 6.5 pM/10^6 cells (n = 3), and umbilical vein irET: 17.8 ± 6.8 irbigET-1: 126.4 ± 20.7 pM/10^6 cells (n = 3); each value represents mean ± s.e.mean. Comparable intracellular levels of both peptides were also detected within endothelial cells cultured from umbilical vein: ET: 122 ± 35 pM/10^6 cells and big ET-1: 149 ± 62 pM/10^6 cells, n = 3; each value represents mean ± s.e.mean. We noted that for HUVSMCs obtained by enzyme-dispersion, levels of ET and big ET-1 were more abundant (for example n = 1, 657 pM/10^6 cells and 124 pM/10^6 cells, respectively), so these cultures were characterized further.

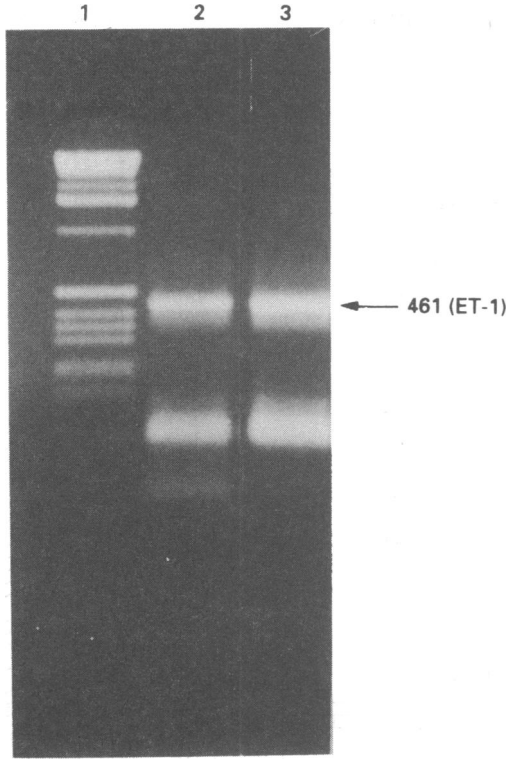


Figure 3 RNA extracted from two separate cultures of human umbilical vein smooth muscle cells was reverse transcribed and amplified by polymerase chain reaction using primers specific for endothelin-1 (ET-1). Product were separated on a 1% agarose gel. Arrowheads in lanes 2 and 3 indicate bands of cDNA from two separate cultures amplified for ET-1, at the expected fragment size (461 base pairs) in comparison to the 1 kb ladder in lane 1. Low molecular weight bands represent primer dimerisation and have been observed previously (Nunez *et al.*, 1990).

Characterization of enzyme-dispersed HUVSMCs

Presence of ET-1 mRNA HUVSMCs expressed RNA for ET-1. Figure 3 indicates bands of ET-1 cDNA from two different HUVSMC cultures, at the expected fragment size (461 base pairs) in comparison to the 1 kb ladder in lane 1. The presence of low molecular weight bands represent dimerisation of primers and has been observed previously (Nunez *et al.*, 1990).

H.p.l.c.-RIA to identify ET isoforms HUVSMCs obtained by enzyme dispersion secreted significant amounts of both mature ET and big ET-1 in a time-dependent manner. Levels of mature irET were nearly double that of big ET-1 by 12 h. High performance liquid chromatography coupled to RIA resolved ET-1, ET-2, ET-3 and big ET-1 with baseline separation, and was validated using both u.v. (214 nm) and RIA detection (10^{-5} M and 10^{-8} M mixtures, respectively) on separate, but batch matched, C_{18} columns. Blank runs showed no evidence of carryover of immunoreactivity from either standard or sample runs. Retention times obtained from u.v. and RIA columns were identical (Figure 4, a and b). ET-3, ET-1 and big ET-1 were detected in supernatants from three separate HUVSMC cultures. Figure 4c demonstrates an example of immunoreactivity from HUVSMC

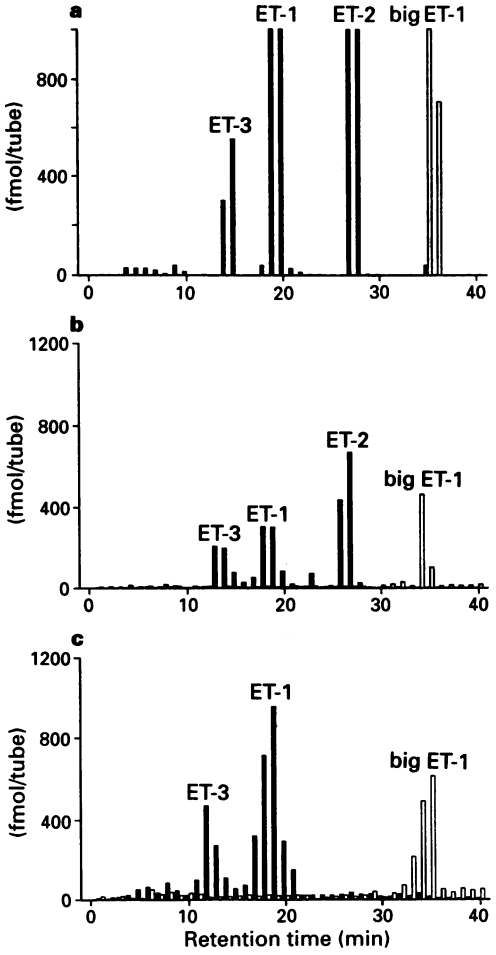


Figure 4 Identification of endothelin (ET) isoforms present in supernatants of enzyme-dispersed human umbilical vein smooth muscle cells (HUVSMCs) using high performance liquid chromatography coupled to radioimmunoassay (RIA). Standard runs on (a) u.v. column (214 nm) and (b) RIA column demonstrate the resolution of mature peptides ET-3, ET-1 and ET-2 respectively, followed by big ET-1. (c) Retention times for supernatants from a representative culture of collagenased HUVSMCs (n = 3) indicate peaks co-eluting with authentic ET-3, ET-1 and big ET-1.

Table 1 Levels of immunoreactive big endothelin-1 (ET-1) and immunoreactive mature ET detected by radioimmunoassay in supernatant of collagenase-dispersed human umbilical vein smooth cells at 4 h intervals over a 12 h incubation period

	Control		*+ Phosphoramidon*	
Time (h)	*irbig ET-1*	*irET*	*irbig ET-1*	*irET*
4	392.9 ± 56.7	470.7 ± 59.0	493.0 ± 78.4	472.5 ± 91.4
8	750.5 ± 64.3	1023.4 ± 132.6	1024.5 ± 106.3	1013.3 ± 193.3
12	991.4 ± 145.6	1699.7 ± 182.4	1288.6 ± 132.6	1205.0 ± 186.2

Each value is expressed as picomol litre^{-1} and represents the mean ± s.e.mean of 3 different cultures with triplicate wells measured for each time-point. In comparison to controls, 100 μM phosphoramidon does not significantly affect secretion of either peptide ($P > 0.05$).

Table 2 [^{125}I]-endothelin-1 ([^{125}I]ET-1) saturation binding of enzyme-dispersed human umbilical vein smooth muscle cells incubated with control medium, or 100 μM phosphoramidon, or 100 μM pepstatin A for 24 h

	n	K_D *[pM]*	B_{max} (fmol mg^{-1})
Control	6	355 ± 99	33.3 ± 9.3
Phosphoramidon	3	431 ± 218	31.1 ± 12.7
Pepstatin A	3	381 ± 169	19.9 ± 7.8

Each value represents the mean ± s.e.mean of 3–6 different cultures. In comparison to controls, 100 μM phosphoramidon or 100 μM pepstatin A did not significantly affect the dissociation constant or receptor density of human umbilical vein smooth muscle cells ($P > 0.05$). The latter observation indicates the absence of an 'unmasking' effect for autocrine ET receptors, which supports the observation that neither phosphoramidon nor pepstatin A affected the conversion of big ET-1.

supernatant co-eluting with authentic ET-3, ET-1 and big ET-1.

Effect of phosphoramidon or pepstatin A on ET secretion

Radioimmunoassay demonstrated that secretion of immunoreactive ET was not inhibited by 12 h incubation with 100 μM phosphoramidon ($n = 3$ different cultures, triplicate wells for each time-point, protein = 75–82 μg per well) (Table 1). Similarly, ET secretion was not affected after incubation with 100 μM pepstatin A for up to 12 h when assayed at time intervals parallel to those of phosphoramidon. For example, at 12 h control cultures secreted 387 ± 57 pM (mean ± s.e.mean of $n = 3$ different cultures) irET, while cultures incubated with 100 μM pepstatin A secreted 352 ± 58 pM (mean ± s.e.mean of $n = 3$ different cultures) irET.

Saturation binding for ET-1 receptors and effect of phosphoramidon or pepstatin A

Saturation binding studies with [^{125}I]-ET-1 indicated that HUVSMCs possess a single population of receptors for ET-1 with a dissociation constant in the picomolar range. K_D and B_{max} values for ET-1 binding were not significantly altered in HUVSMC cultures incubated for 24 h with 100 μM phosphoramidon or 100 μM pepstatin A as compared to controls (Table 2). These results are in concordance with the observations that neither phosphoramidon nor pepstatin A have any effect on ET secretion, indicating that the putative ECE inhibitors failed to 'unmask' ET binding sites.

Discussion

We have shown by specific and sensitive RIAs that cultured human VSMCs are able to synthesise endogenously and secrete immunoreactive mature ET and big ET-1. VSMCs cultured from both adult and neonatal vessels, in addition to cells from both arteries and veins, were able to express ET peptides. There was however, a difference in levels of peptide secretion between VSMCs obtained by the explant method and those obtained by enzyme dispersion. The latter is proposed by Chamley-Campbell *et al.* (1979) to be more differentiated and more closely resemble their *in vivo* counterparts.

Parallel to the findings of Kanse *et al.* (1991) who used cultures of rabbit VSMCs, we have shown in this study that HUVSMCs secrete ET-1, ET-3 and big ET-1. In contrast, messenger RNA for ET-1 and ET-2 only, was detected by reverse transcription-polymerase chain reaction in endothelial cells (O'Reilly *et al.*, 1993). It is thought that expression of ET-1 peptide only, occurs from endothelial cells (Chabrier *et al.*, 1993). However, to exclude the possibility of contamination by endothelial cells, cultures were characterized as smooth muscle by three methods: (a) their 'hill and valley' morphology typical of smooth muscle cell growth; (b) positive staining with antibodies against α-actin and concomitant absence of staining for vWF; (c) confirmation of the absence of vWF by fluorescence activated cell sorting.

The mechanism of ET synthesis was investigated using both phosphoramidon, an inhibitor of metalloproteinases and pepstatin A, an aspartyl protease inhibitor, both of which have been widely used to inhibit the putative endothelin converting enzymes (ECE). We have shown that neither phosphoramidon nor pepstatin A affect endogenous conversion of big ET-1 in HUVSMCs. Consequently, there was no change in receptor density which would have been observed by the 'unmasking' of ET receptors. In cultures of porcine aortic endothelial cells, Ikegawa *et al.* (1991) and Matsumura *et al.* (1992) demonstrated that conversion of both endogenous big ET-1 and exogenously applied big ET-1, is inhibited by phosphoramidon. In HUVECs, conversion of endogenous big ET-1 is also inhibited by phosphoramidon (Plumpton *et al.*, 1994). In contrast, whilst in VSMCs from porcine aorta, Ikegawa *et al.* (1990) showed that phosphoramidon inhibits conversion of exogenous big ET-1, it does not affect endogenous ET-1, production. It appears then, that VSMCs possess an ECE for endogenous ET-1 production which is phosphoramidon-insensitive, while the enzyme for exogenous big ET-1 cleavage is sensitive to phosphoramidon. This is in agreement with our findings. However, we cannot exclude the possibility that the ECE in HUVSMCs is intracellularly located and simply inaccessible to phosphoramidon, since phosphoramidon is a phosphorylated sugar derivative and thought unlikely to enter cells efficiently (Turner *et al.*, 1993). The presence of intracellular immunoreactive ET is of interest and may represent newly generated ET en route to the plasma membrane for secretion.

The precise physiological or pathophysiological significance of ET secretion from human VSMCs is not yet established. In undiseased, intact vessels, such as saphenous vein and left internal mammary artery, we previously employed immunocytochemistry to localize mature ET, big ET-1 and big ET-2 to the cytoplasm of endothelial cells with no detectable staining in medial smooth muscle cells (Howard *et al.*, 1992) suggesting very low levels of ET synthesis, if any, in normal VSMCs. However, Lerman *et al.* (1991) demonstrated the presence of irET in medial VSMCs of atherosclerotic plaques. Since proliferating VSMCs *in vitro* develop cytoskeletal features similar to those observed in normal foetal, or pathological VSMCs (Skalli *et al.*, 1986; Campbell & Campbell, 1990), the use of cultured VSMCs may prove a useful model to study the pathogenesis and progression of vascular diseases. In view of the absence of ET in the media of normal vessels and the presence of ET in atheromatous VSMCs, our report that cultured human VSMCs synthesize and secrete ET suggests that under pathophysiological conditions, VSMCs may 'induce' ET synthesis.

Development of vascular pathologies in established hypertension, arteriosclerosis, and after vessel injury has been attributed to alterations in the normal growth pattern of VSMCs (Folkow, 1990). A close relationship between VSMC proliferation and contraction has been suggested on the basis of recent observations that growth factors and vasoconstrictor peptides exhibit several common cellular mechanisms of action (Berk & Alexander, 1989). However, most vascular pathologies are accompanied by alterations in VSMC function such as hyperplasia, and it is difficult to elucidate whether the induction of ET secretion enhances VSMC growth, or whether ET induction is secondary to VSMC proliferation. It is clear, however, that rapidly proliferating VSMCs also secrete ET. The proliferation of VSMCs and induction of ET could be attributed to the selection of a specific population of cells, or due to a loss of inhibitory factors for ET induction and/or proliferation from the overlying endothelium such as heparin/heparan sulphates, TGF-β, nitric oxide and prostacyclin. Increases in blood flow and shear stress are also known to downregulate induction of preproET-1 mRNA (Yanagisawa *et al.*, 1988) and VSMC proliferation. The absence of flow and shear stress in culture conditions may serve to upregulate ET synthesis from VSMCs and enhance their proliferative rate. The isolation of blood vessels in itself, stimulates a growth response, possibly due to longitudinal and radial collapse of the vascular wall upon withdrawal of transmural pressure (De Mey *et al.*, 1993) which may also contribute to the induction of ET. Regardless of the mechanism, the induction of ET from proliferating VSMCs may serve as a useful model to study the pathogenesis and progression of vascular pathologies whose hallmark is abnormal VSMC phenotype, growth and function.

The authors are grateful to the consultant and staff at Papworth Hospital and the Rosie Maternity Hospital for allowing the collection of vascular tissue. The authors wish to thank Dr M. Wills for his expertise in fluorescence activated cell sorting. Thanks also to M.J. Ashby for sharing his special skills in h.p.l.c. and to Dr C. Plumpton for tissue culture expertise. J.C.M.Y. is a recipient of an Overseas Research Scheme Award, a Cambridge Commonwealth Trust Award, a Raymond and Beverly Sackler Studentship and a Canadian Centennial Scholarship.

References

BERK, B.C. & ALEXANDER, R.W. (1989). Vasoactive effects of growth factors. *Biochem. Pharmacol.*, **38**, 219–255.

CAMPBELL, G.R. & CAMPBELL, J.H. (1990). The phenotypes of smooth muscle expressed in human atheroma. *Ann. NY Acad. Sci.*, **598**, 143–158.

CHABRIER, P.E. (1993). The role of endothelin in the vessel wall. *Ballière's Clin. Haematol*, **6**, 577–591.

CHAMLEY-CAMPBELL, J., CAMPBELL, G.R. & ROSS, R. (1979). The smooth muscle cell in culture. *Physiol. Rev.*, **59**, 1–61.

CHOMCZYNSKI, P. & SACCHI, N. (1987). Single-step method of RNA isolation by acid guanidinium thiocyanate-phenol-chloroform extraction. *Anal. Biochem.*, **162**, 156–159.

CORDER, R., HARRISON, V.J., KHAN, N., ÄNGGÅRD, E.E. & VANE, J.R. (1993). Effect of phosphoramidon in endothelial cell cultures on the endogenous synthesis of endothelin-1 and on conversion of exogenous big endothelin-1 to endothelin-1. *J. Cardiovasc. Pharmacol.*, **22** (Suppl. 8), S73–S76.

CORDER, R. & VANE, J. (1994). Radioimmunoassay evidence that the pressor effect of big endothelin-1 in anaesthetised rats is due to local conversion of endothelin-1. *Br. J. Pharmacol.*, **111**, 225P.

DAVENPORT, A.P., ASHBY, M.J., EASTON, P., ELLA, S., BEDFORD, J., DICKERSON, C., NUNEZ, D.J., CAPPER, S.J. & BROWN, M.J. (1990). A sensitive radioimmunoassay measuring endothelin-like immunoreactivity in human plasma: comparison of levels in patients with essential hypertension and normotensive control subjects. *Clin. Sci.*, **78**, 261–264.

DAVENPORT, A.P., O'REILLY, G., MOLENAAR, P., MAGUIRE, J.J., KUC, R.E., SHARKEY, A., BACON, C.R. & FERRO, A. (1993). Human endothelin receptors characterised using reverse transcriptase-polymerase chain reaction, *in situ* hybridization and sub-type selective ligands BQ123 and BQ3020: evidence for expression of ET_B receptors in human vascular smooth muscle. *J. Cardiovasc. Pharmacol.*, **22** (Suppl. 8), S22–S25.

DE MEY, J.G.R., SCHIFFERS, P.M. (1993). Effects of endothelium on growth responses in arteries. *J. Cardiovasc. Pharmacol.*, **21** (Suppl. 1), S22–S25.

FOLKOW, B. (1990). The structural factor in hypertension. In *Pathophysiology, Diagnosis and Management*. ed. Laragh, J.M. & Brenner, B.M. pp. 565–581. New York: Raven Press.

FUJITANI, Y., ODA, K., TAKIMOTO, M., INUI, T., OKADA, T. & URADE, Y. (1992). Autocrine receptors for endothelins in the primary culture of endothelial cells of human umbilical vein. *FEBS Lett.*, **298**, 79–83.

GIMBRONE, M.A. & COTRAN, R.S. (1975). Human vascular smooth muscle cells in culture. *Lab. Invest.*, **33**, 16–27.

HIOKI, Y., OKADA, K., ITO, H., MATSUYAMA, K. & YANO, M. (1991). Endothelin converting enzyme of bovine carotid artery smooth muscles. *Biochem. Biophys. Res. Commun.*, **174**, 446–451.

HOWARD, P.G., PLUMPTON, C. & DAVENPORT, A.P. (1992). Anatomical localization and pharmacological activity of mature endothelins and their precursors in human vascular tissue. *J. Hypertension*, **10**, 1379–1386.

HUGGINS, J.P., PELTON, J.T. & MILLER, R.C. (1993). The structure and specificity of endothelin receptors: their importance in physiology and medicine. *Pharmacol. Ther.*, **59**, 55–123.

IKEGAWA, R., MATSUMURA, Y., TAKAOKA, M. & MORIMOTO, S. (1990). Evidence for pepstatin-sensitive conversion of porcine big endothelin-1 to endothelin-1 by the endothelial cell extract. *Biochem. Biophys. Res. Commun.*, **167**, 860–866.

IKEGAWA, R., MATSUMURA, Y., TSUKAHARA, Y., TAKAOKA, M. & MORIMOTO, S. (1991). Phosphoramidon inhibits the generation of endothelin-1 from exogenously applied big endothelin-1 in cultured vascular endothelial cells and smooth muscle cells. *FEBS Lett.*, **293**, 45–48.

KANSE, S.M., TAKAHASHI, K., WARREN, J.B., PERERA, T., PORTA, M., GHATEI, M. & BLOOM, S.R. (1991). Production of endothelin by vascular smooth muscle cells. *J. Cardiovasc. Pharmacol.*, **17** (Suppl. 7), S113–S116.

LERMAN, A., EDWARDS, B.S., HALLETT, J.W., HEUBLEIN, D.M., SANDBERG, S.M. & BURNETT, J.C. (1991). Circulating and tissue endothelin immunoreactivity in advanced atherosclerosis. *New Engl. J. Med.*, **325**, 997–1001.

MATSUMURA, Y., IKEGAWA, R., TSUKAHARA, Y., TAKAOKA, M. & MORIMOTO, S. (1990). Conversion of big endothelin-1 to endothelin-1 by two types of metalloproteinases derived from porcine endothelial cells. *FEBS Lett.*, **272**, 166–170.

MATSUMURA, Y., IKEGAWA, R., TSUKAHARA, Y., TAKAOKA, M. & MORIMOTO, S. (1991). Conversion of big endothelin-1 to endothelin-1 by two-types of metalloproteinases of cultured porcine vascular smooth muscle cells. *Biochem. Biophys. Res. Commun.*, **178,** 899–905.

MATSUMURA, Y., TSUKAHARA, Y., KUNINOBU, K., TAKAOKA, M. & MORIMOTO, S. (1992). Phosphoramidon-sensitive endothelin-converting enzyme in vascular endothelial cells converts big endothelin-1 and big endothelin-3 to their mature form. *FEBS Lett.*, **305,** 86–90.

MCMAHON, E.T., PALOMO, M.A. & MOORE, W.M. (1991). Phosphoramidon blocks the pressor activity of big endothelin[1-39] and lowers blood pressure in spontaneously hypertensive rats. *J. Cardiovasc. Pharmacol.*, **17** (Suppl. 7), S29–S33.

MCPHERSON, G.A. (1983). A practical computer based approach to the analysis of radioligand binding experiments. *Comput. Prog. Biomed.*, **17,** 107–114.

MUNSON, P.J. & RODBARD, D. (1980). LIGAND: a versatile computerized approach for characterization of ligand-binding systems. *Anal. Biochem.*, **107,** 220–239.

MURPHY, L.J., CORDER, R., MALLET, A.I. & TURNER, A.J. (1994). Generation by the phosphoramidon-sensitive peptidases, endopeptidase-24.11 and thermolysin, of endothelin-1 and C-terminal fragment from big endothelin-1. *Br. J. Pharmacol.*, **113,** 137–142.

NUNEZ, D.J.R., BROWN, M.J., DAVENPORT, A.P., NEYLON, C.B., SCHOFIELD, J.P. & WYSE, R.K. (1990). Endothelin-1 mRNA is widely expressed in porcine and human tissues. *J. Clin. Invest.*, **85,** 1537–1541.

O'REILLY, G., CHARNOCK-JONES, D.S., CAMERON, I.T., SMITH, S.K. & DAVENPORT, A.P. (1993). Endothelin-2 mRNA splice variants detected by RT-PCR in cultured human vascular smooth muscle and endothelial cells. *J. Cardiovasc. Pharmacol.*, **22** (Suppl. 8), 18–21.

PLUMPTON, C., CHAMPENEY, R., ASHBY, M.J., KUC, R.E., HOSKINS, S.L. & DAVENPORT, A.P. (1992). Identification of endothelin isoforms and proendothelin-1 in the human heart by high performance liquid chromatography and radioimmunoassay. *Br. J. Pharmacol.*, **107,** 279P.

PLUMPTON, C., CHAMPENEY, R., ASHBY, M.J., KUC, R.E. & DAVENPORT, A.P. (1993). Characterization of endothelin isoforms in human heart: endothelin-2 demonstrated. *J. Cardiovasc. Pharmacol.*, **22** (Suppl. 8), S26–S28.

PLUMPTON, C., HORTON, J., KALINKA, K.S., MARTIN, R. & DAVENPORT, A.P. (1994). Effects of phosphoramidon and pepstatin A on the secretion of endothelin-1 and big endothelin-1 in human umbilical vein endothelial cells: measurement by two-site ELISAs. *Clin. Sci.*, **87,** 245–251.

RESINK, T.J., HAHN, A.W., SCOTT-BURDEN, T., POWELL, J., WEBER, E. & BÜHLER, F.R. (1990). Inducible endothelin mRNA expression and peptide secretion in cultured human vascular smooth muscle cells. *Biochem. Biophys. Res. Commun.*, **168,** 1303–1310.

SKALLI, O., BLOOM, W.S., ROPRAZ, P., AZZARONE, B. & GABBIANI, G. (1986). Cytoskeletal remodeling of rat aortic smooth muscle cells in vitro: relationship to culture conditions and analogies to in vitro situations. *J. Submicrosc. Cytol.*, **18,** 481–493.

TSUKAHARA, Y., MATSUMURA, Y., KUNINOBU, K., KOJIMA, T., TAKAOKA, M. & MORIMOTO, S. (1993). Phosphoramidon-sensitive endothelin converting enzyme in cultured vascular smooth muscle cells converts big endothelin-3 to endothelin-3. *Life Sci.*, **53,** 465–471.

TURNER, A.J. (1993). Endothelin-converting enzyme and other families of metalloendopeptidases. *Biochem. Soc. Trans.*, **21,** 697–701.

YANAGISAWA M., KURIHARA, H., KIMURA, S., TOMOBE, Y., KOBAYASHI, M., MITSUI, Y., YAZAKI, Y., GOTO, K. & MASAKI, T. (1988). A novel potent vasoconstrictor peptide produced by vascular endothelial cells. *Nature*, **332,** 411–415.

YU, J.C.M. & DAVENPORT, A.P. (1994). Human vascular smooth muscle cells secrete big ET-1 and mature ET but conversion is not blocked by phosphoramidon. *Br. J. Pharmacol.*, **112,** 167P.

(Received May 9, 1994
Revised September 6, 1994
Accepted October 3, 1994)

British Journal of Pharmacology (1995) 114, 558–562 © 1995 Stockton Press All rights reserved 0007–1188/95 $9.00

Differences between 5-HT_3 receptor antagonists in modulation of visceral hypersensitivity

[1]S.E. Banner & G.J. Sanger

SmithKline Beecham Pharmaceuticals, Coldharbour Road, The Pinnacles, Harlow, Essex, CM19 5AD.

1 Noxious colo-rectal distension was applied in conscious rats by acute balloon inflation and the effects observed as abdominal muscle contraction with the threshold typically between 10–40 mmHg. The effects of 5-HT_3 receptor antagonists on responses to noxious colo-rectal distension were then studied in both normal rats and those pretreated with 5-hydroxytryptophan (5-HTP).

2 Granisetron and ondansetron (10 $\mu g\,kg^{-1}$ and 1 $mg\,kg^{-1}$, s.c.) had no effect on visceromotor thresholds to colo-rectal distension in normal rats.

3 Hypersensitivity of the colo-rectum was achieved by systemic administration of a low dose of 5-HTP (10 $mg\,kg^{-1}$, s.c.) which lowered the distension pressure required to induce the visceromotor reflex; analysis of variance showed a highly significant treatment effect ($F_{1,11} = 84.26$, $P<0.001$).

4 Granisetron, zatosetron, bemesetron and renzapride equi-potently increased the threshold values at which distension evoked a visceromotor reflex after dosing with 5-HTP, with a maximal response 3.6 to 4.2 fold above saline controls, at 10 $\mu g\,kg^{-1}$, s.c. Metoclopramide (10 $\mu g\,kg^{-1}$) also raised the level of distension required to elicit a response. By comparison, tropisetron caused a small, non-significant increase in visceromotor threshold values and only at high doses (1 $mg\,kg^{-1}$), whilst ondansetron and BRL 46470 had no signficant effects at doses up to 10 $mg\,kg^{-1}$.

5 The response to granisetron (10 $\mu g\,kg^{-1}$, s.c.) in 5-HTP-treated rats was unaltered by pre-administration of naloxone (5 $mg\,kg^{-1}$, s.c.).

6 These results suggest that a 5-HT_3-like receptor modulates 5-HTP- evoked visceral hypersensitivity. However, the rank order of antagonist potency does not correlate with their order of potency against the classically defined 5-HT_3 receptor.

Keywords: 5-HT_3 receptors; antagonists; colo-rectal distension; visceral pain; 5-hydroxytryptamine (5-HT)

Introduction

Studies in the anaesthetized rat using acute levels of noxious colo-rectal or duodenal distension have demonstrated both pressor and depressor blood pressure pseudoaffective reflexes (Ness & Gebhart, 1988; Moss & Sanger, 1990). Of these cardiovascular pseudoaffective reflexes, the depressor response was found to be inhibited by the 5-HT_3 receptor antagonists, granisetron and ondansetron, the latter showing only weak activity (Moss & Sanger, 1990; Banner & Sanger, 1991). As a consequence of these findings, granisetron was tested clinically as a potential visceral analgesic agent since pain and related gastrointestinal sensations are one of the diagnostic features of Irritable Bowel Syndrome (IBS; Thompson *et al.*, 1992). Prior & Read (1993) investigated the analgesic potential of granisetron in IBS patients with bowel hypersensitivity and they found that granisetron raised the thresholds for sensations elicited by rectal distension.

Ness & Gebhart (1988, 1990) have described an experimental model using conscious rats, in which a visceromotor reflex is monitored as an indication of noxious levels of colo-rectal distension (CRD). However, using this model Danzebrink & Gebhart (1991) found that the 5-HT_3 receptor agonist, 2-methyl-5-hydroxytryptamine (2-methyl-5-HT) when administered intrathecally was antinociceptive and that its ability to raise visceromotor thresholds was prevented by pretreatment with the selective antagonist, bemesetron. When administered intrathecally, the antagonist alone had no effect on visceromotor thresholds. Similar results were obtained by Glaum *et al.* (1990) in a standard nociceptive model when they used intrathecal 2-methyl-5-HT to inhibit the tail flick reflex in rats and subsequently prevented this response with bemesetron.

The apparently conflicting data obtained with 5-HT_3 receptor antagonists in different experimental models made it necessary to determine if the action of the 5-HT_3 receptor antagonists seen in the anaesthetized rat model and in IBS patients could be obtained in conscious rats. Therefore, the conscious CRD model was modified to study the effect of the antagonists in both normal rats and in rats in which the visceral hypersensitivity of IBS patients was mimicked by systemic administration of the precursor to 5-HT, 5-hydroxytryptophan (5-HTP).

Methods

Male Wistar rats (200–500 g) were fasted individually overnight to promote emptying of the colo-rectum. Under halothane anaesthesia a 6–7 cm long latex balloon was inserted intra-anally to a position approximately 1 cm beyond the ano-rectal verge. The animals were allowed to recover. The cannula from the balloon, which was taped to the tail to prevent expulsion of the balloon, was connected to a pressure transducer linked to a pen recorder and via a 3-way tap to a peristaltic pump. Throughout the procedure the singly housed animals were allowed unrestricted movement. After full recovery the rats were dosed subcutaneously (s.c.) with either, 5-HTP (10 $mg\,kg^{-1}$ and 25 $mg\,kg^{-1}$) or saline vehicle. At 5 min a ramp inflation of the colo-rectal balloon was performed until the visceromotor threshold was observed, within 40 s. This is seen as abdominal muscle contraction and at this point the stimulus was immediately removed by opening the 3-way tap to air until the following inflation. The threshold value was noted from the pen recorder. This inflation procedure was repeated at 5 min intervals. It had previously been found that electromyographic recording and

[1] Author for correspondence.

visualisation of abdominal muscle contraction gave the same results (unpublished observations), which is in agreement with Ness & Gebhart (1988). 5-HT$_3$ receptor antagonists or saline were given s.c. after 3 stable responses to noxious CRD were achieved and within 45 min of 5-HTP dosing. The distensions were then performed at 5 min intervals for a further 30 min. If, at any time, the distension pressure reached 100 mmHg without observation of the visceromotor reflex then that inflation procedure was terminated and the stimulus removed. The experimental procedure was repeated twice in the animals at an interval of at least one week.

Changes in distension pressure were compared with the mean of the predose stable recordings which was taken to be 100%. The maximum effect in the presence of the antagonist at any time point within the 30 min post-dose period was used for the construction of dose effect-curves. The maximum threshold responses in the presence of the antagonists were then compared as a ratio against the maximum response obtained after dosing with saline, this increase being assigned the value of 1.0. The results represent the mean and standard error of the mean and were compared by Student's t test where raw data were analysed. Analysis of variance using a repeated measures design was also used.

5-Hydroxy-L-trytophan, cisapride, morphine sulphate, naloxone hydrochloride were obtained from Sigma, Janssen Pharmaceuticals, Evans Medical and Endo Laboratories Inc. respectively. Granisetron, BRL 46470A (endo-N-(8-methyl-8-azabicyclo [3.2.1] oct-3yl)-2,3-dihydro-3,3-dimethyl-indole-1-carboxamide HCl), bemesetron (MDL 72222), tropisetron (ICS 205-930), metoclopramide, renzapride, ondansetron, quipazine maleate and zatosetron, were synthesized by SB Pharmaceuticals. All drugs were administered s.c. with 0.9% w/v saline as vehicle and at a volume equivalent to 1 ml kg^{-1} body weight.

Results

Visceromotor threshold values in both 5-HTP-treated and vehicle-treated animals lay in the range of 10–40 mmHg. Morphine (10 μg kg^{-1}) was administered to demonstrate that the visceromotor threshold in response to noxious levels of colo-rectal distension could be altered by an analgesic agent. Thus at this dose morphine caused a maximum increase above stable pre-dose control pressures of 153.1 ± 80.8%, $n = 5$, compared to a maximum increase of 18.8 ± 3.1%, $n = 11$, after dosing with saline. At 100 μg kg^{-1} morphine caused the distension pressure to reach the cut off level at which the stimulus was removed.

5-HTP did not demonstrate any antinociceptive properties. Rather, it was found that 5-HTP lowered the threshold to noxious levels of distension. Figure 1 shows that whilst the vehicle had no effect on levels of CRD required to evoke a visceromotor reflex, 5-HTP (10 mg kg^{-1}) reduced the visceromotor threshold, within 10 min, to a minimum of 52.8 ± 4.9% ($n = 13$) of predose values. Analysis of variance using repeated measures showed a highly significant effect with 5-HTP treatment when compared with saline controls ($F_{1,11} = 84.26$, $P<0.001$). As can be seen in Figure 1 there was a time-dependent onset of maximal activity after 5-HTP treatment (treatment × time $F_{11,121} = 6.07$, $P<0.001$). A further lowering of the visceromotor threshold was achieved by increasing the dose of 5-HTP to 25 mg kg^{-1}; the distension pressure then required to elicit a response was only 34.6 ± 9.6% ($n = 5$) of predose control values. However, in separate experiments (not presented here) this higher dose of 5-HTP was found to cause diarrhoea and therefore was not used further. The 5-HTP-induced reduction in visceromotor threshold was not mimicked by the gastrointestinal prokinetic 5-HT$_4$ receptor agonist, cisapride, which had no significant effect on the distension pressures required to evoke a response (data not shown) at 100 μg kg^{-1}. This dose of cisapride is lower than that required to cause a 50% reduction of

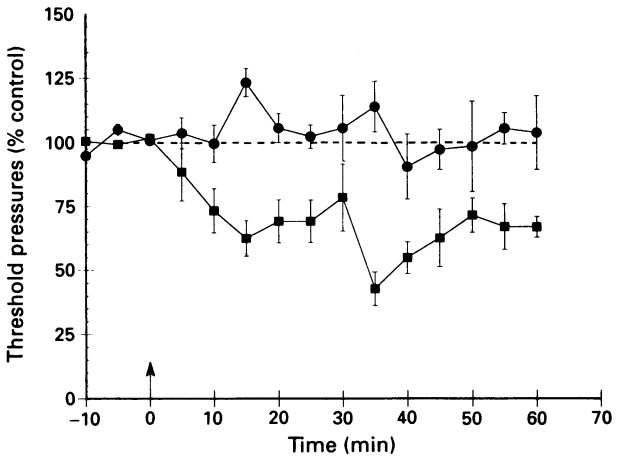


Figure 1 The effect of 5-hydroxytryptophan (■) at 10 mg kg^{-1} s.c. and saline vehicle (●) on threshold pressure values for visceromotor responses evoked by noxious colo-rectal distension, expressed as a % of control values. Points represent the mean ± s.e.mean of 11–13 animals.

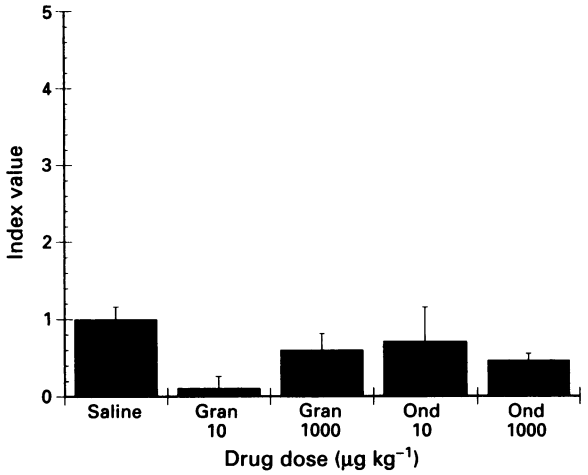


Figure 2 The effect of granisetron (Gran) and ondansetron (Ond) on visceromotor responses to noxious colo-rectal distension in normal rats, expressed as a function of the response to saline (index value of 1.0). Columns represent the mean ± s.e.mean of 6–7 animals.

the 5-HT-evoked Bezold-Jarisch reflex in rats (Dunbar *et al.* 1986).

Granisetron and ondansetron (both at 10 μg kg^{-1} and 1 mg kg^{-1}) in rats which were not pretreated with 5-HTP, did not affect the visceromotor threshold values (Figure 2). However, in rats predosed with 5-HTP (10 mg kg^{-1}), granisetron dose-dependently increased the visceromotor threshold values. The time course of this effect is demonstrated with a dose of 10 μg kg^{-1} in Figure 3. To compare the effects of different doses this effect of granisetron is expressed as an increase in the visceromotor threshold above the maximum percentage increase obtained in a separate groups of rats after dosing with saline (defined as 1.0, Table 1). A maximum 4.2 ± 0.6 fold increase in the pressures required to evoke a response was achieved for granisetron at 10 μg kg^{-1}. Further increases in the dose of granisetron resulted in a partial bell-shaped dose-effect curve, such that at doses up to 10 mg kg^{-1}, granisetron still reduced the hypersensitivity caused by 5-HTP, but to a lesser extent than that obtained with 10 μg kg^{-1} granisetron (Figure 4a). By comparison, ondansetron (10 μg kg^{-1}–10 mg kg^{-1}, Figure 4b) did not cause any increase in the visceromotor threshold values in the presence of 5-HTP. However, other 5-HT$_3$ receptor antagonists acted similarly to granisetron as demonstrated by zatosetron and

the trend shown by bemesetron. Both antagonists were also maximally effective at 10 μg kg^{-1} (Table 1). Table 1 also shows that quipazine at 100 μg kg^{-1} and renzapride at 10 μg kg^{-1} demonstrated good activity, whilst metoclopramide demonstrated weaker visceral analgesic properties. Tropisetron was considerably less potent than the most active antagonists with a tendency to increase at 1 mg kg^{-1}. BRL 46470A was without effect.

A further study was carried out with granisetron, to investigate whether endogenous opioids have a role to play in the action of this compound. Rats were pretreated with 5-HTP (10 mg kg^{-1}) and 5 min later with a dose of naloxone (5 mg kg^{-1}), which had no effect on responses to CRD. When a stable response was achieved, granisetron 10 μg kg^{-1} was administered and found to retain good visceral analgesic activity in the presence of naloxone with a 3.9 ± 0.8 ($n = 6$) fold increase in the drug/saline ratio compared to a 4.2 ± 0.6 fold increase in the absence of naloxone.

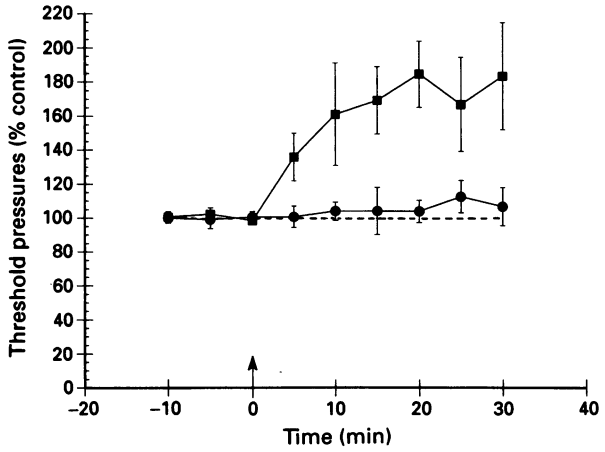


Figure 3 The effect of granisetron 10 μg kg^{-1}, s.c. (■) and saline vehicle (●) on threshold pressure values for visceromotor responses evoked by noxious colo-rectal distension in rats pretreated with 5-hydroxytryptophan, expressed as a % of control values. Points represent the mean ± s.e.mean of 11–16 animals.

Table 1 The effect of 5-HT$_3$ receptor antagonists on colorectal distension in the presence of 5-hydroxytryptophan (5-HTP)

Compound	*Dose* (μg kg^{-1} s.c.)	*Index*	P	n
Granisetron	0.1	1.6 (1.0)		6
	1	2.2 (0.4)	*	6
	10	4.2 (0.6)	***	16
	100	2.9 (0.7)	**	7
	1000	2.2 (0.4)		11
	10 000	2.0 (0.7)		8
Ondansetron	10	1.0 (0.2)		5
	100	0.9 (0.2)		5
	1000	0.4 (0.2)		6
	10 000	1.6 (0.5)		6
Zatosetron	1	2.7 (0.8)		5
	10	3.6 (0.4)	**	6
	100	2.7 (0.6)	*	6
Bemesetron	1	2.8 (0.7)		6
	10	3.7 (1.1)		6
	100	2.6 (0.8)		5
Quipazine	1	2.7 (0.9)		8
	10	3.1 (0.5)	*	6
	100	3.6 (0.8)	*	8
Renzapride	1	2.6 (0.9)		8
	10	3.8 (0.7)	**	8
Metoclopramide	1	1.9 (0.4)		6
	10	2.7 (0.4)	*	6
	100	2.2 (0.7)		7
Tropisetron	10	1.3 (0.3)		4
	100	1.8 (0.7)		5
	1000	2.0 (0.7)		8
	100 000	0.4 (0.8)		7
BRL 46470	1	0.5 (0.4)		5
	10	1.5 (0.3)		6
	100	0.02 (0.3)		6
	1000	0.6 (0.4)		6

Values are mean ± s.e.mean. Maximum post-dose increase in visceromotor threshold values indexed against saline (1.0). Student's t test significance: *$P<0.05$; **$P<0.01$ and ***$P<0.001$.

Discussion

Noxious visceral sensation can be consistently and reproducibly evoked by CRD (Ness & Gebhart, 1988). Analgesia in this model is represented as an increase in the threshold distension pressure above pre-dose stable control values, as demonstrated here by the analgesic, morphine. Although the possibility that morphine may have altered gastrointestinal tone cannot be excluded, distension of the balloon after dosing with 100 μg kg^{-1} caused cut-off levels to be reached prior to nociception, as anticipated with a strongly effective analgesic. Therefore, even with the limitation described, CRD is a useful model for determining the pharmacology of visceral nociceptive mechanisms.

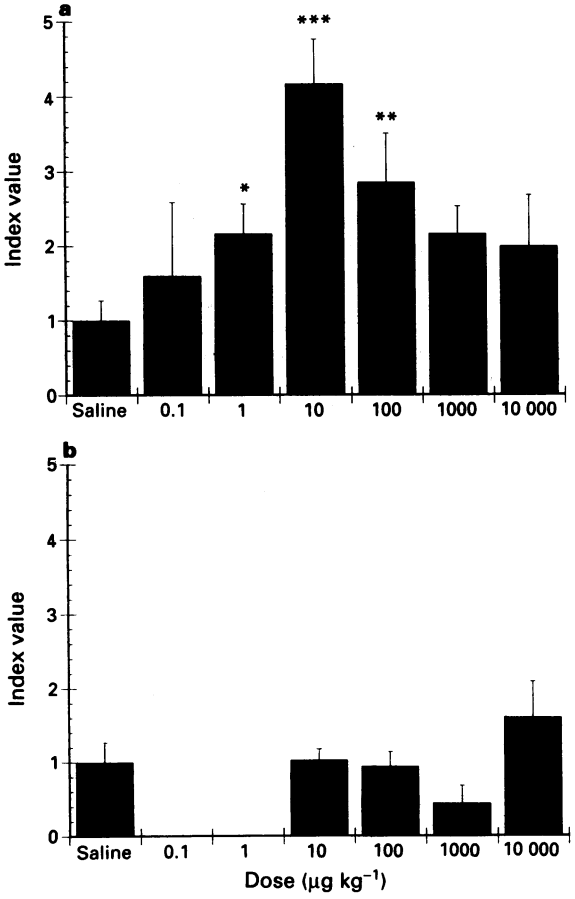


Figure 4 The effect of (a) granisetron and (b) ondansetron on responses to noxious colo-rectal distension in rats pretreated with 5-hydroxytryptophan, expressed as a function of the response to saline (index value of 1.0). Columns represent the mean ± s.e.mean of 5–16 animals; Student's t test significance: *$P<0.05$; **$P<0.01$; ***$P<0.001$.

The clinical study by Prior & Read (1993) demonstrated that the 5-HT$_3$ receptor antagonist, granisetron, increased the thresholds for the perception of sensations elicited by rectal distension in IBS patients with a hypersensitive bowel When it was found that the 5-HT$_3$ receptor antagonists, granisetron and ondansetron, had no effect on normal rats, which is in agreement with Danzebrink & Gebhart (1991), it was considered necessary to sensitize the rat colo-rectum in order to mimic the rectal hypersensitivity that typifies the IBS condition (see Mayer & Raybould, 1990). We found that rather than producing antinociceptive effects that may be expected by the activation of 5-HT-mediated, descending noxious inhibitory control pathways, 5-HTP lowered the visceromotor threshold. This hyperalgesic effect of 5-HTP was dose-dependent and clearly unrelated to the known propulsive motility properties of 5-HTP (Brittain & Collier, 1958) as the effect was not mimicked by the potent prokinetic and 5-HT$_4$ receptor agonist, cisapride. Despite the use of a very low dose of 5-HTP which did not induce diarrhoea, the fact that secretory mechanisms activated by the 5-HT precursor could still affect distension pressures in the colo-rectum cannot be totally dismissed and neither can the potential action of the antagonists at peripheral sensory nerve teminals. However, previous studies which demonstrated that intrathecal administration of granisetron caused complete blockade of blood pressure depressor, pseudoaffective reflexes, which occurred in response to colo-rectal distension in anaesthetized rats, support the hypothesis that at least some of the 5-HT effects may be outside the gut (unpublished observations).

When different 5-HT receptor antagonists were administered after sensitization with 5-HTP, variable effects were observed. Thus, certain structurally distinct antagonists appeared to raise the visceromotor threshold in an approximately equi-potent manner, thereby reducing the hypersensitivity induced by 5-HTP, whilst other antagonists had little or no effect. The former included granisetron, bemesetron and interestingly, metoclopramide. Tropisetron also tended to cause an increase in visceromotor thresholds but with reduced efficacy and at a relatively lower potency. In contrast, the structurally dissimilar compounds, BRL 46470A and ondansetron were found to be inactive. These differences in the ability of the selective 5-HT$_3$ receptor antagonists to produce antinociception in the rat appear to correlate with their clinical efficacy as analgesic drugs. Thus, in pilot studies granisetron has demonstrated its ability to raise the distension pressure required to elicit discomfort in IBS patients (Prior & Read, 1993). In preliminary clinical studies granisetron and bemesetron have been shown to be effective in the treatment of another visceral pain state, that of migraine (Loisy *et al.*, 1985; Couturier *et al.*, 1990; Rowat *et al.*, 1991). Tropisetron demonstrated only partial analgesic activity in migraine patients (Ferrari *et al.*, 1991). Similarly, metoclopramide has also been shown to have a clinical use as an analgesic in a variety of conditions (Hughes, 1977; Grauers *et al.*, 1982; Rosenblatt *et al.*, 1991; Coppola & Yealy, 1992; Kandler & Lisander, 1993). The least potent antagonist in the CRD model, ondansetron, was reported in studies on IBS patients to have variable effects in its ability to treat the associated pain to the extent that some patients complained of increased discomfort (Maxton *et al.*, 1991; Steadman *et al.*, 1990; 1992). A recent study similar to that of Prior & Read (1993) concluded that ondansetron did not alter the increased sensitivity or any index of colonic function, observed in IBS patients (Hammer *et al.*, 1993). Thus, these antagonists differ in their ability to inhibit nociception in man and this may be reflected in the present study.

The analgesic activity or lack of activity, of 5-HT$_3$ receptor antagonists described experimentally tends to correlate with clinical observations but fails to correlate pharmacologically with their ability to antagonize the 5-HT$_3$ receptor defined *in vivo* or *in vivo* in rats. Although, we cannot entirely rule out the possibility that these findings can be explained in terms of pharmacodynamics, against the rat Bezold-Jarisch reflex all antagonists, with the exception of metoclopramide and bemesetron, show good activity. Thus, i.v. ID_{50} values have been reported, ranging form 0.4 $\mu g\,kg^{-1}$ for tropisetron (Donatsch *et al.*, 1984) and 0.7 $\mu g\,kg^{-1}$ for granisetron (Fake *et al.*, 1987) to 3.6 $\mu g\,kg^{-1}$ for ondansetron (see Sanger, 1990) with bemesetron at 39 $\mu g\,kg^{-1}$ (Fozard, 1984) and metoclopramide at 377 $\mu g\,kg^{-1}$ (Fozard & Host, 1982). Furthermore, radioligand binding studies using the mammalian brain have demonstrated that these antagonists exhibit broadly similar K_i values except for metoclopramide (see review by Zifa & Fillion, 1992). Consequently, the findings presented here are suggestive of differences in the nature of the 5-HT$_3$ receptor involved in the mechanisms of visceral nociception. It may be significant that a recent study demonstrated that the release of 5-HT from enterochromaffin cells of guinea-pig isolated small intestine was inhibited by granisetron, bemesetron and tropisetron whilst ondansetron did not modify 5-HT release (Gebauer *et al.*, 1993) indicating potential differences in the actions of 5-HT$_3$ receptor antagonists.

The ability of granisetron to act as an analgesic in the presence of naloxone suggests that the 5-HT involvement in nociception is not modulated by opioid receptors, thereby eliminating one major pathway in nociceptive modulation. As such it can be suggested that this 5-HT$_3$-like receptor facilitates neurotransmission of nociceptive information rather than having a role in noxious inhibitory control.

In conclusion, 5-HT$_3$ receptor antagonists demonstrate a wide range of potency and efficacy for increasing threshold values to noxious colo-rectal distension in 5-HTP treated conscious rats. This model, which defines responses to colorectal hypersensitivity, may mimic conditions seen in the clinic and allow for the development of compounds which exploit potential differences between 5-HT$_3$ receptor antagonists, to address the dysfunction associated with visceral pain.

References

BANNER, S.E. & SANGER, G.J. (1991). The effect of 5-HT$_3$ receptor antagonists on visceral pseudoaffective reflexes. *Serotonin*, 1991, *5-Hydroxytryptamine- CNS Receptors and Brain Function*, 78P.

BRITTAIN, R.T. & COLLIER, H.O.J. (1958). Effects of 5-hydroxytryptamine and 5-hydroxytryptophane on defaecation and propulsion of a charcoal meal in intact mice. *J. Physiol.*, **141**, 14–15P.

COPPOLA, M. & YEALY, D.M (1992). Randomized placebo-controlled evaluation of metoclopramide verses prochlorperazine for the emergency department treatment of migraine. *Ann. Emerg. Med.*, **21**, 1047.

COUTURIER, E.G., HERING, R., FOSTER, C.A., STEINER, T.J. & CLIFFORD, R.F. (1991). First clinical study of the selective 5-HT$_3$ antagonist, granisetron (BRL 43694), in the acute treatment of migraine headache. *Headache*, **31**, 296–297.

DANZEBRINK, R.M. & GEBHART, G.F. (1991). Evidence that spinal 5-HT$_1$, 5-HT$_2$ and 5-HT$_3$ receptor subtypes modulate responses to noxious colo-rectal distension in the rat. *Brain Res.*, **538**, 64–75.

DONATSCH, P., ENGEL, G., RICHARDSON, B.P. & STADLER, P. (1984). ICS 205-930: a highly selective and potent antagonist at peripheral neuronal 5-hydroxytryptamine (5-HT) receptors. *Br. J. Pharmacol.*, **81**, 34P.

DUNBAR, A.V., MCCLELLAND, C.M. & SANGER, G.J. (1986). BRL 24924: a stimulant of gut motility which is also a potent antagonist of the Bezold-Jarisch reflex in anaesthetized rats. *Br. J. Pharmacol.*, **88**, 319P.

FAKE, C.S., KING, F.D. & SANGER, G.J. (1987). BRL 43694: a potent and novel 5-HT$_3$ receptor antagonist. *Br. J. Pharmacol.*, **91**, 335P.

FERRARI, M.D., WILKINSON, M., HIRT, D., LATASTE, X., NOTTER, M. & THE ICS 205-930 MIGRAINE STUDY GROUP (1991). Efficacy of ICS 205-930, a novel 5-hydroxytryptamine$_3$ (5-HT$_3$) receptor antagonist, in the prevention of migraine attacks. A complex answer to a simple question. *Pain*, **45**, 283–291.

FOZARD, J.R. (1984). MDL 72222: a potent and highly selective antagonist at neuronal 5-hydroxytryptamine receptors. *Naunyn-Schmeid. Arch. Pharmacol.*, **326**, 36–44.

FOZARD, J.R. & HOST, M. (1982). Selective inhibition of the Bezold-Jarisch effect of 5-HT in the rat by antagonists at neuronal 5-HT receptors. *Br. J. Pharmacol.*, **77**, 520P.

GEBAUER, A., MERGER, M. & KILBINGER, H. (1993). Modulation by 5-HT$_3$ and 5-HT$_4$ receptors of the release of 5-hydroxytrytamine from the guinea-pig small intestine. *Naunyn-Schmied. Arch. Pharmacol.*, **347**, 137–140.

GLAUM, S.R., PROUDFIT, H.K. & ANDERSON, E.G. (1990). 5-HT$_3$ receptors modulate spinal nociceptive reflexes. *Brain Res.*, **510**, 12–16.

GRAUERS, O., DANNESKIOLD-SAMSOE, P., HASSELGREN, K-H., INGEMANSSON, S. & WESTBERG, R. (1982). Metoclopramide in acute pain caused by gallbladder- or kidney stones. *Scand. J. Gastroenterol.*, **17**, A886.

HAMMER, J., PHILLIPS, S.F., TALLEY, N.J. & CAMILLERI, M. (1993). Effect of a 5-HT$_3$-antagonist (ondansetron) on rectal sensitivity and compliance in health and the irritable bowel syndrome. *Aliment. Pharmacol. Ther.*, **7**, 543–551.

HUGHES, J.B. (1977). Metoclopramide in migraine treatment. *Med. J. Australia*, **2**, 580.

KANDLER, D. & LISANDER, B. (1993). Analgesic action of metoclopramide in prosthetic hip surgery. *Acta Anaesthesiol. Scand.*, **37**, 49–53.

LOISY, C., BEORCHIA, S., CENTONZE, V. (1985). Effects on migraine headache of MDL 72, 222, antagonist at neuronal 5-HT receptors. Double-blind, placebo-controlled study. *Cephalagia*, **5**, 79–82.

MAXTON, D.G., HAIGH, C.G. & WHORWELL, P.J. (1991). Clinical trial of ondansetron, a selective 5-HT$_3$ antagonist in irritable bowel syndrome (IBS). *Gastroenterol.*, **100**, A468.

MAYER, E.A. & RAYBOULD, H.E. (1990). Role of visceral afferent mechanisms in functional bowel disorders. *Gastroenterol.*, **99**, 1688–1704.

MOSS, H.E. & SANGER, G.J. (1990). The effects of granisetron, ICS 205-930 and ondansetron on the visceral pain reflex induced by duodenal distension. *Br. J. Pharmacol.*, **100**, 497–501.

NESS, T.J. & GEBHART, G.F. (1988). Colorectal distension as a noxious visceral stimulus: physiologic and pharmacologic characterization of pseudoaffective reflexes in the rat. *Brain Res.*, **450**, 153–169.

NESS, T.J. & GEBHART, G.F. (1990). Visceral pain: a review of experimental studies. *Pain*, **41**, 167–234.

PRIOR, A. & READ, N.W. (1993). Reduction in rectal sensitivity and postpranidal motility by granisetron, a 5-HT$_3$ receptor antagonist, in patients with irritable bowel syndrome. *Aliment. Pharmacol. Ther.*, **7**, 175–180.

ROSENBLATT, W.H., CIOFFI, A.M., SINATRA, R., SABERSKI, L.R. & SILVERMAN, D.G. (1991). Metoclopramide: An adjunct to patient-controlled analgesia. *Anaesth. Analg.*, **73**, 553–555.

ROWAT, B.M.T., MERRILL, C.F., DAVIES, A. & SOUTH, V. (1991). A double-blind comparison of granisetron and placebo for the treatment of acute migraine in the emergency department. *Cephalagia*, **11**, 207–213.

SANGER, G.J. (1990). New antiemetic drugs. *Can. J. Physiol. Pharmacol.*, **68**, 314–324.

STEADMAN, C.J., TALLEY, N.J., PHILLIPS, S.F. & MULUIHILL, C. (1990). Trial of a selective serotonin type 3 (5-HT$_3$) antagonist ondansetron (GR38032F) in diarrhoea predominant irritable bowel syndrome (IBS). *Gastroenterol.*, **98**, A394.

STEADMAN, C.J., TALLEY, N.J., PHILLIPS, S.F. & ZINSMEISTER, A.R. (1992). Selective 5-hydroxytryptamine type 3 receptor antagonism with ondansetron as treatment for diarrhoea – predominant irritable bowel syndrome – A pilot study. *Mayo Clin. Proc.*, **67**, 732–738.

THOMPSON, W.G., CREED, F., DROSSMAN, D.A., HEATON, K.W. & MAZZACCA, G. (1992). Functional bowel disease and functional abdominal pain. *Gastroenterol. Int.*, **5**, 75–91.

ZIFA, E. & FILLION, G. (1992). 5-Hydroxytryptamine receptors. *Pharmacol. Rev.*, **44**, 401–458.

(Received June 21, 1994
Revised September 8, 1994
Accepted October 10, 1994)

British Journal of Pharmacology

VOLUME 114 (2) JANUARY 1995

SPECIAL REPORTS

M.T. Silva, S. Rose, J.G. Hindmarsh, G. Aislaitner, J.W. Gorrod, P.K. Moore, P. Jenner & C.D. Marsden. Increased striatal dopamine efflux *in vivo* following inhibition of cerebral nitric oxide synthase by the novel monosodium salt of 7-nitro indazole 257

E. Boichot, N. Germain, V. Lagente & C. Advenier. Prevention by the tachykinin NK_2 receptor antagonist, SR 48968, of antigen-induced airway hyperresponsiveness in sensitized guinea-pigs 259

PAPERS

D.E. Hu & T.-P.D. Fan. Suppression of VEGF-induced angiogenesis by the protein tyrosine kinase inhibitor, lavendustin A 262

M. Göthert, M. Hamon, M. Barann, H. Bönisch, H. Gozlan, R. Laguzzi, P. Metzenauer, B. Nickel & I. Szelenyi. 5-HT_3 receptor antagonism by anpirtoline, a mixed 5-HT_1 receptor agonist/5-HT_3 receptor antagonist 269

F. D'Allaire, C. Atgié, P. Mauriège, P.-M. Simard & L.J. Bukowiecki. Characterization of β_1- and β_3-adrenoceptors in intact brown adipocytes of the rat 275

H. Chiao & R.W. Caldwell. Local cardiac effects of substance P: roles of acetylcholine and noradrenaline 283

G. Panagiotidis, B. Åkesson, E.L. Rydell & I. Lundquist. Influence of nitric oxide synthase inhibition, nitric oxide and hydroperoxide on insulin release induced by various secretagogues 289

M.G. Peter & A.P. Davenport. Selectivity of [^{125}I]-PD151242 for human, rat and porcine endothelin ET_A receptors in the heart 297

S.H. Ferreira, B.B. Lorenzetti, M. Devissaguet, D. Lesieur & Y. Tsouderos. S14080, a peripheral analgesic acting by release of an endogenous circulating opioid-like substance 303

A. Chopping & S.E. O'Connor. Presence of vasoconstrictor 5HT_1-like receptors revealed by precontraction of rabbit isolated mesenteric artery 309

P.B.S. Clarke & M. Reuben. Inhibition by dizocilpine (MK-801) of striatal dopamine release induced by MPTP and MPP^+: possible action at the dopamine transporter 315

L. Sautebin, A. Ialenti, A. Ianaro & M. Di Rosa. Modulation by nitric oxide of prostaglandin biosynthesis in the rat 323

Y. Fukuizumi, S. Kobayashi, J. Nishimura & H. Kanaide. Cytosolic calcium concentration-force relation during contractions in the rabbit femoral artery: time-dependency and stimulus specificity 329

L.A. Bishop, V.P. Gerskowitch, R.A.D. Hull, N.P. Shankley & J.W. Black. The use of receptor desensitization to analyse CCK_A and CCK_B/gastrin receptors coupled to contraction in guinea-pig stomach muscle 339

C.S. Barnes & S.J. Coker. Failure of nitric oxide donors to alter arrhythmias induced by acute myocardial ischaemia or reperfusion in anaesthetized rats 349

E.A. Clark & S.J. Hill. Differential effect of sodium ions and guanine nucleotides on the binding of thioperamide and clobenpropit to histamine H_3-receptors in rat cerebral cortical membranes 357

P. Klemm, C. Thiemermann, G. Winklmaier, P.A. Martorana & R. Henning. Effects of nitric oxide synthase inhibition combined with nitric oxide inhalation in a porcine model of endotoxin shock 363

M. Villarroya, L. Gandía, B. Lara, A. Albillos, M.G. López & A.G. García. Dotarizine versus flunarizine as calcium antagonists in chromaffin cells 369

M.K. Pugsley & D.A. Saint. Tonic and use-dependent block of sodium currents in isolated cardiac myocytes by bisaramil 377

H. Sipma, M. Duin, B. Hoiting, A. den Hertog & A. Nelemans. Regulation of histamine- and UTP-induced increases in Ins(1,4,5)P_3, Ins(1,3,4,5)P_4 and Ca^{2+} by cyclic AMP in DDT_1 MF-2 cells 383

D. McHugh & D.J. Beech. Inhibition of delayed rectifier K^+-current by levcromakalim in single intestinal smooth muscle cells: effects of cations and dependence on K^+-flux 391

E.S. Ellis, C. Byrne, O.E. Murphy, N.S. Tilford & G.S. Baxter. Mediation by 5-hydroxytryptamine$_{2B}$ receptors of endothelium-dependent relaxation in rat jugular vein 400

S.A. Douglas, R.M. Edwards, J.D. Elliott & E.H. Ohlstein. *In vivo* pharmacological characterization of the non-peptide endothelin receptor antagonist SB 209670 405

R.E. Santing, Y. Pasman, C.G. Olymulder, A.F. Roffel, H. Meurs & J. Zaagsma. Contribution of a cholinergic reflex mechanism to allergen-induced bronchial hyperreactivity in permanently instrumented, unrestrained guinea-pigs 414

M. Inoue & I. Imanaga. Mechanism of activation of nonselective cation channels by putative M_4 muscarinic receptor in guinea-pig chromaffin cells 419

S.Y. Yuan, J.C. Bornstein & J.B. Furness. Pharmacological evidence that nitric oxide may be a retrograde messenger in the enteric nervous system 428

J.C. Hardwick & R.L. Parsons. Necessity of protein kinase C activity for maintenance of acetylcholine receptor function at snake twitch fibre endplates 433

J.C. Hardwick & R.L. Parsons. Requirement of a colchicine-sensitive component of the cytoskeleton for acetylcholine receptor recovery 442

A. Ishihata & M. Endoh. Species-related differences in inotropic effects of angiotensin II in mammalian ventricular muscle: receptors, subtypes and phosphoinositide hydrolysis 447

M.E.M. Benwell, D.J.K. Balfour & C.E. Birrell. Desensitization of the nicotine-induced mesolimbic dopamine responses during constant infusion with nicotine 454

I. Kimura, K. Dezaki, H. Tsuneki & M. Kimura. Postsynaptic nicotinic receptor desensitized by non-contractile Ca^{2+} mobilization via protein kinase-C activation at the mouse neuromuscular junction 461

K. Yasui & P. Palade. Inhibitory action of SR33557 on L-type calcium current in single ventricular myocytes of rat **468**

B.E. Crack, C.E. Pollard, M.W. Beukers, S.M. Roberts, S.F. Hunt, A.H. Ingall, K.C.W. McKechnie, A.P. IJzerman & P. Leff. Pharmacological and biochemical analysis of FPL 67156, a novel, selective inhibitor of ecto-ATPase **475**

A. Paul, R.H. Pendreigh & R. Plevin. Protein kinase C and tyrosine kinase pathways regulate lipopolysaccharide-induced nitric oxide synthase activity in RAW 264.7 murine macrophages **482**

T. Tokimasa, M. Ito, M.A. Simmons, C.R. Schneider, T. Tanaka, T. Nakano & T. Akasu. Inhibition by wortmannin of M-current in bullfrog sympathetic neurones **489**

B. Ghaleb, J.-L. Dubois-Randé, L. Hittinger, J.-F. Giudicelli & A. Berdeaux. Comparisons of the effects of nicorandil, pinacidil, nicardipine and nitroglycerin on coronary vessels in the conscious dog: role of the endothelium **496**

I. Kodama, R. Suzuki, K. Maruyama & J. Toyama. Electrophysiological effects of SD-3212, a new antiarrhythmic agent with vasodilator action, on guinea-pig ventricular cells **503**

G.J. Southan, C. Szabó & C. Thiemermann. Isothioureas: potent inhibitors of nitric oxide synthases with variable isoform selectivity **510**

M. Parramón, M.P. González & M.J. Oset-Gasque. A reassessment of the modulatory role of cyclic AMP in catecholamine secretion by chromaffin cells **517**

C. Astarie-Dequeker, I. Korichneva & M.-A. Devynck. Different effects of endothelin-3 on the Ca^{2+} discharge induced by agonists and Ca^{2+}-ATPase inhibitors in human platelets **524**

T.J. Williams & D.E. Clarke. Characterization of α_1-adrenoceptors mediating vasoconstriction to noradrenaline and nerve stimulation in the isolated perfused mesentery of rat **531**

I.P. Kirk & P.J. Richardson. Further characterization of [^{3}H]-CGS 21680 binding sites in the rat striatum and cortex **537**

S.R. Stapleton, B.A. Bell, J.F. Wootton & R.H. Scott. Modulation of Ca^{2+}-dependent currents in metabolically stressed cultured sensory neurones by intracellular photorelease of ATP **544**

J.C.M. Yu & A.P. Davenport. Secretion of endothelin-1 and endothelin-3 by human cultured vascular smooth muscle cells **551**

S.E. Banner & G.J. Sanger. Differences between 5-HT_3 receptor antagonists in modulation of visceral hypersensitivity **558**

STOCKTON

BRITISH JOURNAL OF PHARMACOLOGY

The *British Journal of Pharmacology* welcomes contributions in all fields of experimental pharmacology including neuroscience, biochemical, cellular and molecular pharmacology. The Board of Editors represents a wide range of expertise and ensures that well-presented work is published as promptly as possible, consistent with maintaining the overall quality of the journal.

Edited for the British Pharmacological Society by

A.T. Birmingham
(Chairman)

R.W. Horton **W.A. Large**
(Secretaries)

Editorial Board

J.A. Angus *Melbourne, Australia*
M.L.J. Ashford *Cambridge*
G.W. Bennett *Nottingham*
W.C. Bowman *Glasgow*
N.G. Bowery *London*
Alison F. Brading *Oxford*
S.D. Brain *London*
K.D. Butler *Horsham*
M. Caulfield *London*
R. Chess-Williams *Sheffield*
M.K. Church *Southampton*
T. Cocks *Melbourne, Australia*
S.J. Coker *Liverpool*
R.A. Coleman *Ware*
Helen M. Cox *London*
A.J. Cross *London*
V. Crunelli *Cardiff*
T.C. Cunnane *Oxford*
F. Cunningham *London*
A. Dray *London*
J.R. Docherty *Dublin*
J.M. Edwardson *Cambridge*
P.C. Emson *Cambridge*
W. Feniuk *Cambridge*
J.R. Fozard *Basle, Switzerland*
Allison D. Fryer *Baltimore, USA*
Sheila M. Gardiner *Nottingham*
C.J. Garland *Bristol*
L.G. Garland *Beckenham*
A. Gibson *London*
R. W. Gristwood *Cambridge*
D.W.P. Hay *Philadelphia, USA*
P.G. Hellewell *London*
P.E. Hicks *Edinburgh*
S.J. Hill *Nottingham*
S.M.O. Hourani *Guildford*
J.C. Hunter *Cambridge*
C.C. Jordan *Ware*
D.A. Kendall *Nottingham*
P. Leff *Loughborough*
R. McMillan *Macclesfield*
J. Maclagan *London*
C.A. Maggi *Florence, Italy*
Janice M. Marshall *Birmingham*
G. Martin *Beckenham*
W. Martin *Glasgow*
A. Mathie *London*
D.N. Middlemiss *Harlow*
P.K. Moore *London*
R.J. Naylor *Bradford*
C.D. Nicholson *Oss, The Netherlands*
C.P. Page *London*
A.N. Payne *Beckenham*
F.L. Pearce *London*
J.D. Pearson *London*
A.G. Renwick *Southampton*
M.H.T. Roberts *Cardiff*
C. Robinson *London*
G.J. Sanger *Harlow*
M.A. Simmonds *London*
J.M. Sneddon *Sunderland*
P. Sneddon *Glasgow*
K. Starke *Freiburg, Germany*
R.J. Summers *Melbourne, Australia*
P.V. Taberner *Bristol*
J. Tamargo *Madrid, Spain*
C. Thiemermann *London*
M.D. Tricklebank *Harlow*
M.B. Tyers *Ware*
S.P. Watson *Oxford*
K.J. Watling *Boston, USA*
A.H. Weston *Manchester*
B.J.R. Whittle *Beckenham*
Eileen Winslow *Riom, France*
B. Woodward *Bath*
E.H.F. Wong *California, USA*

Corresponding Editors

P.R. Adams *Stony Brook, U.S.A.*
C. Bell *Melbourne, Australia*
F.E. Bloom *La Jolla, U.S.A.*
A.L.A. Boura *Newcastle, Australia*
N.J. Dun *Toledo, U.S.A.*
R.F. Furchgott *New York, U.S.A.*
T. Godfraind *Brussels, Belgium*
S.Z. Langer *Paris, France*
R.J. Miller *Chicago, U.S.A.*
R.C. Murphy *Denver, U.S.A.*
E. Muscholl *Mainz, Germany*
R.A. North *Portland, U.S.A.*
M. Otsuka *Tokyo, Japan*
M.J. Rand *Melbourne, Australia*
S. Rosell *Södertalje, Sweden*
P. Seeman *Toronto, Canada*
L. Szekeres *Szeged, Hungary*
B. Uvnas *Stockholm, Sweden*
P.A. Van Zwieten *Amsterdam, Netherlands*
V.M. Varagič *Belgrade, Yugoslavia*
G. Velo *Verona, Italy*
Wang Zhen Gang *Beijing, China*
M.B.H. Youdim *Haifa, Israel*

Submission of manuscripts: Manuscripts (two copies) should be sent to The Editorial Office, British Journal of Pharmacology, St. George's Hospital Medical School, Cranmer Terrace, London SW17 0RE.

Authors should consult the Instructions to Authors and the Nomenclature Guidelines for Authors in Vol. **114,** 245–255. These Instructions and Guidelines also appear with the journal Index for Volumes **111–113,** 1994. A checklist of the essential requirements is summarised in each issue of the journal, or as the last page of the issue.

Whilst every effort is made by the publishers and editorial committee to see that no inaccurate or misleading data, opinion or statement appears in this Journal, they and the *British Pharmacological Society* wish to make it clear that the data and opinions appearing in the articles and advertisements herein are the responsibility of the contributor or advertiser concerned. Accordingly, the *British Pharmacological Society*, the publishers and the editorial committee and their respective employees, officers and agents accept no liability whatsoever for the consequences of any such inaccurate or misleading data, opinion or statement.

ANTI-HUMAN DOPAMINE D_1 RECEPTOR MONOCLONAL ANTIBODY

Antibody used to localize the D_1 dopamine receptor. The antibody has been used successfully in immunoblotting and immunocytochemistry studies using both transfected cells and rat and human brain.

Levey et al. "Localization of D_1 and D_2 dopamine receptors in brain with subtype-specific antibodies." *Proc. Natl. Acad. Sci. USA* **90**, 8861 (1993); Smiley et al. "D_1 dopamine receptor immunoreactivity in human and monkey cerebral cortex: Predominant and extrasynaptic localization in dendritic spines." *Proc. Natl. Acad. Sci. USA* **91**, 5720 (1994).

Available exclusively from RBI — Cat. No. D-187

RBI also offers a complete listing of adrenergic, dopamine and muscarinic recombinant receptors. Please call or fax for further information as well as a copy of our 1995 Catalog/Handbook.

RBI® **RESEARCH BIOCHEMICALS INTERNATIONAL**

One Strathmore Road, Natick, MA 01760-2447 USA
508-651-8151 • 800-736-3690 • Fax 508-655-1359

Distributors
Australia, Arncliffe • 2-567-5258
Czech Republic, Olomouc • 68-551-7217
Denmark, Roedovre • 44-948822
France, Illkirch • 88-67-14-14
Germany, Köln • 221-497-2034
Israel, Jerusalem • 2-794951
Italy, Milano • 02-5088220
Japan, Tokyo • 03-5684-1622
Korea, Seoul • 2-945-2431
Norway, Oslo • 22-220411
Switzerland, Zurich • 01-312-2124
Taiwan, Taipei • 2-918-1206
United Kingdom, St. Albans • 0727-841414

The *British Journal of Pharmacology* is published by Stockton Press, a division of Macmillan Press Ltd. It is the official publication of the British Pharmacological Society.

Scope The *British Journal of Pharmacology* is published twice a month. It welcomes contribution in all field of experimental pharmacology including neuroscience, biochemical, cellular and molecular pharmacology. The Board of Editors represents a wide range of expertise and ensures that well-presented work is published as promptly as possible, consistent with maintaining the overall quality of the journal

This journal is covered by Current Contents, Excerpta Medica, BIOSIS and Index Medicus.

Editorial Manuscripts (plus two copies) and all editorial correspondence should be sent to: The Editorial Office, British Journal of Pharmacology, St George's Hospital Medical School, Cranmer Terrace, London SW17 0RE, UK. Tel: +44 (0)181 767 6765; Fax: +44 (0)181 767 5645.

Advertisements Enquiries concerning advertisements should be addressed to: Michael Rowley, Hasler House, High Street, Great Dunmow, Essex CM6 1AP, UK. Tel: +44 (0)1371 874613; Fax: +44 (0)1371 872273.

Publisher All business correspondence, supplement enquiries and reprint requests should be addressed to British Journal of Pharmacology, Stockton Press, Houndmills, Basingstoke, Hampshire RG21 2XS, UK. Tel: +44 (0)1256 29242; Fax: +44 (0)1256 810526. Publisher: Marija Vukovojac. Editorial Assistant: Alice Ellingham. Production Controller: Tony Holton.

Subscriptions – EU/Rest of World Subscription price per annum (3 volumes, 24 issues) £620, rest of world £820 (Airmail), £685 (Surface mail) or equivalent in any other currency. Orders must be accompanied by remittance. Cheques should be made payable to Macmillan Magazines and sent to: The Subscription Department, Macmillan Press Ltd, Houndmills, Basingstoke, Hampshire RG21 2XS, UK. Where appropriate, subscribers may make payments into UK Post Office Giro Account No. 519 2455. Full details must accompany the payment. Subscribers from EU territories should add sales tax at the local rate.

Subscriptions – USA USA subscribers call toll free 1-800-221-2123 or send check/money order/credit card details to: Stockton Press, 49, West 24th Street, New York, NY 10010; Tel: 212 627 5757, Fax: 212 627 9256. USA annual subscription rates: $1230 Airmail; $1030 Surface (Institutional/Corporate); $225 (Individual making personal payment).

British Journal of Pharmacology (ISSN 0007–1188) is published twice a month by Macmillan Press Ltd, c/o Mercury Airfreight International Ltd, 2323 Randolph Avenue, Avenel, NJ 07001, USA. Subscription price for institutions is $1030 per annum (surface). 2nd class postage is paid at Rahway NJ. Postmaster: send address corrections to Macmillan Press Ltd, c/o Mercury Airfreight International Ltd, 2323 Randolph Avenue, Avenel NJ 07001.

Reprints of any article in this journal are available from Stockton Press, Houndmills, Basingstoke, Hampshire RG21 2XS, UK. Tel: +44 (0)1256 29242; Fax: +44 (0)1256 810526.

Copyright © 1995 Stockton Press

ISSN 0007–1188

All rights of reproduction are reserved in respect of all papers, articles, illustrations, etc., published in this journal in all countries of the world.

All material published in this journal is protected by copyright, which covers exclusive rights to reproduce and distribute the material. No material published in this journal may be reproduced or stored on microfilm or in electronic, optical or magnetic form without the written authorisation of the Publisher.

Authorisation to photocopy items for internal or personal use of specific clients, is granted by Stockton Press, for libraries and other users registered with the Copyright Clearance Center (CCC) Transaction Reporting Service, provided that the base fee of $9.00 per copy is paid directly to CCC, 21 Congress St., Salem, MA 01970, USA. 0007-1188/95 $9.00+$0.00.

Apart from any fair dealing for the purposes of research or private study, or criticism or review, as permitted under the Copyright, Designs and Patent Act 1988, this publication may be reproduced, stored or transmitted, in any form or by any means, only with the prior permission in writing of the publishers, or in the case of reprographic reproduction, in accordance with the terms of licences issued by the Copyright Licensing Agency.

PREPARATION OF MANUSCRIPTS

Authors are strongly recommended to read the full *Instructions to Authors* and *Nomenclature Guidelines for Authors* (*Br. J. Pharmacol.* 1995, **114,** 245–255) before submitting a manuscript for publication in the *British Journal of Pharmacology*. The manuscript and cover letter should be checked against the following list before mailing.

The original and one copy of the manuscript must be supplied. Manuscripts must be typed in double-line spacing on one side of A4 paper, in type not smaller than 12 characters per inch or 10 point. Both copies to include Tables and a set of labelled Figures. One set of Figures without numbers or letters is also to be included. The text to be arranged in the following subsections:

1. **Title**—To have no more than 150 characters on a separate page, which should also include a Short Title (50 characters maximum) and the name and address of the author for correspondence.

2. **Summary**—To be arranged in numbered paragraphs (Full Papers) or a single paragraph (Special Reports).
   —to include aims, principal results and conclusions.
   —to include Key words (10 maximum) at end of summary.

3. **Introduction**—To contain concise statements of the problem and the aims of the investigation.

4. **Methods**—To have brief but adequate account of the procedures; *full names of drugs* (*including those referred to by manufacturer's code*), sources of drugs and statistical tests to be stated.

5. **Results**—To have no repetition of data in Figures, Tables and text.

6. **Discussion**—Findings and conclusions to be placed in context of other relevant work.
   NB Simple repetition of results and unwarranted speculation are not acceptable.

7. **Acknowledgements**—Sources of support. Sources of drugs not widely available commercially.

8. **References**—All references in the text to be included in the Reference List and *vice versa*. References in alphabetical order with complete citations; Journals publishing 'in press' papers identified.
   References to manuscripts submitted to other journals but not yet accepted are not allowed.

9. **Tables**—Each on a separate page and prepared in accordance with current requirements of the Journal.

10. **Figures**—Both labelled and non-labelled Figures to be prepared in accordance with current requirements of the Journal (see *Instructions to Authors*, 1995, **114,** 245–251) and provided with Figure Number and Authors' names on back (*in pencil*).
    —each legend to be typed on a separate page and carrying keys to symbols.
    —keys to symbols and histograms must not appear on the figures themselves, but in the respective legends.
    —'box style' figures are not in keeping with the Journal style; line drawings etc must have only left-hand and bottom axes.

11. **Manuscripts**—To be accompanied by a declaration signed by each author that
    (a) results are original
    (b) approval of all persons concerned has been given to submit manuscripts for consideration (see also 12b)
    (c) the same material is neither 'in press' (i.e. is in proof or has definitely been accepted for publication) nor under consideration elsewhere. Furthermore it will not be submitted or published elsewhere before a decision has been reached by the Editorial Board of the *British Journal of Pharmacology* and will not be submitted elsewhere if accepted by the *British Journal of Pharmacology*.
    (d) Copyright assignment is included.

12. **Cover letter**—To state clearly
    (a) Corresponding author's full postal address, telephone, telex or Fax number
    (b) where appropriate, that *either* ethical approval has been given for investigation *or* Company or Institutional permission to publish work has been received.

13. **Reminder**—Packaging to be sufficiently robust to protect Figures and to withstand mailing.

Failure to comply with *Instructions to Authors* may lead to substantial delays in processing, review and publication and may even jeopardize acceptance of the manuscript.

NOMENCLATURE

Authors are reminded that accepted receptor and associated terminology is laid out in *Nomenclature Guidelines for Authors*, as published in the *British Journal of Pharmacology, Br. J. Pharmacol.*, 1995, **114,** 253–255.

SPECIAL REPORTS

The purpose of *Special Reports* is to provide rapid publication for **new** and **important** results which the Editorial Board considers are likely to be of special pharmacological significance. *Special Reports* will have publication priority over all other material and so authors are asked to consider carefully the status of their work before submission.

In order to speed publication there is normally no revision allowed beyond very minor typographical or grammatical corrections. If significant revision is required, the Board may either invite rapid re-submission or, more probably, propose that it be re-written as a Full Paper and be re-submitted for consideration. In order to reduce delays, proofs of *Special Reports* will be sent to authors but **essential corrections must reach the Production Office within 48 hours of receipt.** Authors should ensure that their submitted material conforms exactly to the following requirements.

Special Reports should normally occupy no more than two printed pages of the Journal; two illustrations (Figures or Tables, with legends) are permitted. As a guideline, with type face of 12 pitch and double-line spacing, a page of A4 paper could contain about 400 words. The absolute maximum length of the *Special Report* is 1700 words. For each Figure or Table, please deduct 200 words. The manuscript should comprise a Title page with key words (maximum of 10), a Summary consisting of a single short paragraph, followed by Introduction, Methods, Results, Discussion and References (maximum of 10). In all other respects, the requirements are the same as for Full Papers (see current 'Instructions to Authors').

BRITISH JOURNAL OF PHARMACOLOGY VOLUME 114 (2) 1995

SPECIAL REPORTS

M.T. Silva, S. Rose, J.G. Hindmarsh, G. Aislaitner, J.W. Gorrod, P.K. Moore, P. Jenner & C.D. Marsden. Increased striatal dopamine efflux *in vivo* following inhibition of cerebral nitric oxide synthase by the novel monosodium salt of 7-nitro indazole 257

E. Boichot, N. Germain, V. Lagente & C. Advenier. Prevention by the tachykinin NK_2 receptor antagonist, SR 48968, of antigen-induced airway hyperresponsiveness in sensitized guinea-pigs 259

PAPERS

D.E. Hu & T.-P.D. Fan. Suppression of VEGF-induced angiogenesis by the protein tyrosine kinase inhibitor, lavendustin A 262

M. Göthert, M. Hamon, M. Barann, H. Bönisch, H. Gozlan, R. Laguzzi, P. Metzenauer, B. Nickel & I. Szelenyi. 5-HT_3 receptor antagonism by anpirtoline, a mixed 5-HT_1 receptor agonist/5-HT_3 receptor antagonist 269

F. D'Allaire, C. Atgié, P. Mauriège, P.-M. Simard & L.J. Bukowiecki. Characterization of β_1- and β_3-adrenoceptors in intact brown adipocytes of the rat 275

H. Chiao & R.W. Caldwell. Local cardiac effects of substance P: roles of acetylcholine and noradrenaline 283

G. Panagiotidis, B. Åkesson, E.L. Rydell & I. Lundquist. Influence of nitric oxide synthase inhibition, nitric oxide and hydroperoxide on insulin release induced by various secretagogues 289

M.G. Peter & A.P. Davenport. Selectivity of [^{125}I]-PD151242 for human, rat and porcine endothelin ET_A receptors in the heart 297

S.H. Ferreira, B.B. Lorenzetti, M. Devissaguet, D. Lesieur & Y. Tsouderos. S14080, a peripheral analgesic acting by release of an endogenous circulating opioid-like substance 303

A. Choppin & S.E. O'Connor. Presence of vasoconstrictor 5HT_1-like receptors revealed by precontraction of rabbit isolated mesenteric artery 309

P.B.S. Clarke & M. Reuben. Inhibition by dizocilpine (MK-801) of striatal dopamine release induced by MPTP and MPP^+: possible action at the dopamine transporter 315

L. Sautebin, A. Ialenti, A. Ianaro & M. Di Rosa. Modulation by nitric oxide of prostaglandin biosynthesis in the rat 323

Y. Fukuizumi, S. Kobayashi, J. Nishimura & H. Kanaide. Cytosolic calcium concentration-force relation during contractions in the rabbit femoral artery: time-dependency and stimulus specificity 329

L.A. Bishop, V.P. Gerskowitch, R.A.D. Hull, N.P. Shankley & J.W. Black. The use of receptor desensitization to analyse CCK_A and CCK_B/gastrin receptors coupled to contraction in guinea-pig stomach muscle 339

C.S. Barnes & S.J. Coker. Failure of nitric oxide donors to alter arrhythmias induced by acute myocardial ischaemia or reperfusion in anaesthetized rats 349

E.A. Clark & S.J. Hill. Differential effect of sodium ions and guanine nucleotides on the binding of thioperamide and clobenpropit to histamine H_3-receptors in rat cerebral cortical membranes 357

P. Klemm, C. Thiemermann, G. Winklmaier, P.A. Martorana & R. Henning. Effects of nitric oxide synthase inhibition combined with nitric oxide inhalation in a porcine model of endotoxin shock 363

M. Villarroya, L. Gandía, B. Lara, A. Albillos, M.G. López & A.G. García. Dotarizine versus flunarizine as calcium antagonists in chromaffin cells 369

M.K. Pugsley & D.A. Saint. Tonic and use-dependent block of sodium currents in isolated cardiac myocytes by bisaramil 377

H. Sipma, M. Duin, B. Hoiting, A. den Hertog & A. Nelemans. Regulation of histamine- and UTP-induced increases in $Ins(1,4,5)P_3$, $Ins(1,3,4,5)P_4$ and Ca^{2+} by cyclic AMP in DDT_1 MF-2 cells 383

D. McHugh & D.J. Beech. Inhibition of delayed rectifier K^+-current by levcromakalim in single intestinal smooth muscle cells: effects of cations and dependence on K^+-flux 391

E.S. Ellis, C. Byrne, O.E. Murphy, N.S. Tilford & G.S. Baxter. Mediation by 5-hydroxytryptamine$_{2B}$ receptors of endothelium-dependent relaxation in rat jugular vein 400

S.A. Douglas, R.M. Edwards, J.D. Elliott & E.H. Ohlstein. *In vivo* pharmacological characterization of the non-peptide endothelin receptor antagonist SB 209670 405

R.E. Santing, Y. Pasman, C.G. Olymulder, A.F. Roffel, H. Meurs & J. Zaagsma. Contribution of a cholinergic reflex mechanism to allergen-induced bronchial hyperreactivity in permanently instrumented, unrestrained guinea-pigs 414

M. Inoue & I. Imanaga. Mechanism of activation of nonselective cation channels by putative M_4 muscarinic receptor in guinea-pig chromaffin cells 419

S.Y. Yuan, J.C. Bornstein & J.B. Furness. Pharmacological evidence that nitric oxide may be a retrograde messenger in the enteric nervous system 428

J.C. Hardwick & R.L. Parsons. Necessity of protein kinase C activity for maintenance of acetylcholine receptor function at snake twitch fibre endplates 433

J.C. Hardwick & R.L. Parsons. Requirement of a colchicine-sensitive component of the cytoskeleton for acetylcholine receptor recovery 442

A. Ishihata & M. Endoh. Species-related differences in inotropic effects of angiotensin II in mammalian ventricular muscle: receptors, subtypes and phosphoinositide hydrolysis 447

M.E.M. Benwell, D.J.K. Balfour & C.E. Birrell. Desensitization of the nicotine-induced mesolimbic dopamine responses during constant infusion with nicotine 454

I. Kimura, K. Dezaki, H. Tsuneki & M. Kimura. Postsynaptic nicotinic receptor desensitized by non-contractile Ca^{2+} mobilization via protein kinase-C activation at the mouse neuromuscular junction 461

K. Yasui & P. Palade. Inhibitory action of SR33557 on L-type calcium current in single ventricular myocytes of rat 468

B.E. Crack, C.E. Pollard, M.W. Beukers, S.M. Roberts, S.F. Hunt, A.H. Ingall, K.C.W. McKechnie, A.P. IJzerman & P. Leff. Pharmacological and biochemical analysis of FPL 67156, a novel, selective inhibitor of ecto-ATPase 475

A. Paul, R.H. Pendreigh & R. Plevin. Protein kinase C and tyrosine kinase pathways regulate lipopolysaccharide-induced nitric oxide synthase activity in RAW 264.7 murine macrophages 482

T. Tokimasa, M. Ito, M.A. Simmons, C.R. Schneider, T. Tanaka, T. Nakano & T. Akasu. Inhibition by wortmannin of M-current in bullfrog sympathetic neurones 489

B. Ghaleb, J.-L. Dubois-Randé, L. Hittinger, J.-F. Giudicelli & A. Berdeaux. Comparisons of the effects of nicorandil, pinacidil, nicardipine and nitroglycerin on coronary vessels in the conscious dog: role of the endothelium 496

I. Kodama, R. Suzuki, K. Maruyama & J. Toyama. Electrophysiological effects of SD-3212, a new antiarrhythmic agent with vasodilator action, on guinea-pig ventricular cells 503

G.J. Southan, C. Szabó & C. Thiemermann. Isothioureas: potent inhibitors of nitric oxide synthases with variable isoform selectivity 510

M. Parramón, M.P. González & M.J. Oset-Gasque. A reassessment of the modulatory role of cyclic AMP in catecholamine secretion by chromaffin cells 517

C. Astarie-Dequeker, I. Korichneva & M.-A. Devynck. Different effects of endothelin-3 on the Ca^{2+} discharge induced by agonists and Ca^{2+}-ATPase inhibitors in human platelets 524

T.J. Williams & D.E. Clarke. Characterization of α_1-adrenoceptors mediating vasoconstriction to noradrenaline and nerve stimulation in the isolated perfused mesentery of rat 531

I.P. Kirk & P.J. Richardson. Further characterization of [^{3}H]-CGS 21680 binding sites in the rat striatum and cortex 537

S.R. Stapleton, B.A. Bell, J.F. Wootton & R.H. Scott. Modulation of Ca^{2+}-dependent currents in metabolically stressed cultured sensory neurones by intracellular photorelease of ATP 544

J.C.M. Yu & A.P. Davenport. Secretion of endothelin-1 and endothelin-3 by human cultured vascular smooth muscle cells 551

S.E. Banner & G.J. Sanger. Differences between 5-HT_3 receptor antagonists in modulation of visceral hypersensitivity 558

STOCKTON

Typeset by Elite Typesetting Techniques, Eastleigh, Hants
and printed in Great Britain by Unwin Brothers Ltd., The Gresham Press, Old Woking, Surrey